

2013 OPTO

SPIE Photonics West

2–7 February 2013

Technical Summaries

www.spie.org/pw

Conferences & Courses

2–7 February 2013

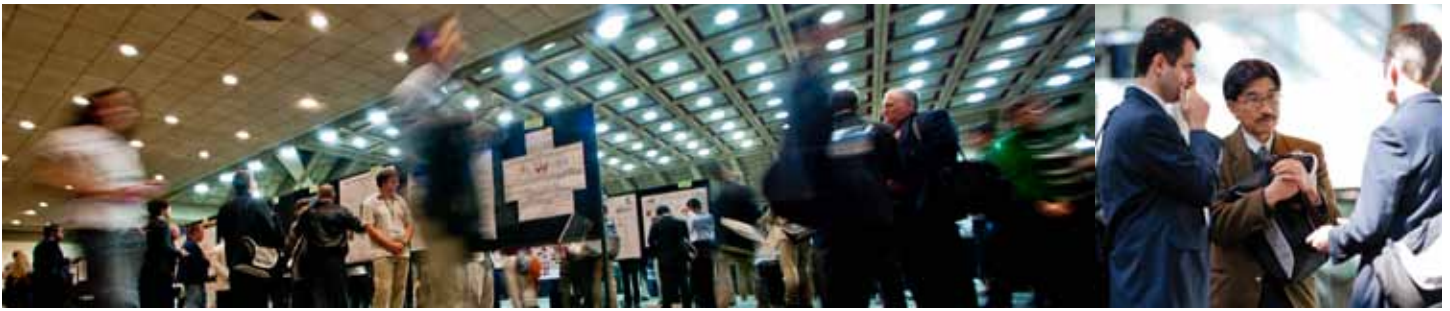
Exhibition

BiOS Expo: 2–3 February 2013

Photonics West: 5–7 February 2013

Location

The Moscone Center
San Francisco, California, USA



OPTO

SPIE Photonics West

Symposium Chair



David L. Andrews
Univ. of East Anglia Norwich
(United Kingdom)

Symposium Cochairs



Alexei L. Glebov
OptiGrate Corp. (USA)



Klaus P. Streubel
OSRAM AG (Germany)

Contents

8619: Physics and Simulation of Optoelectronic Devices XXI	3
8620: Physics, Simulation, and Photonic Engineering of Photovoltaic Devices II	24
8621: Optical Components and Materials X	42
8622: Organic Photonic Materials and Devices XV	57
8623: Ultrafast Phenomena and Nanophotonics XVII	71
8624: Terahertz, RF, Millimeter, and Submillimeter-Wave Technology and Applications VI	87
8625: Gallium Nitride Materials and Devices VIII	99
8626: Oxide-based Materials and Devices IV	123
8627: Integrated Optics: Devices, Materials, and Technologies XVII	141
8628: Optoelectronic Integrated Circuits XV	154
8629: Silicon Photonics VIII	161
8630: Optoelectronic Interconnects XIII	175
8631: Quantum Sensing and Nanophotonic Devices X	186
8632: Photonic and Phononic Properties of Engineered Nanostructures III	212
8633: High Contrast Metastructures II	232
8634: Quantum Dots and Nanostructures: Synthesis, Characterization, and Modeling X	240
8635: Advances in Photonics of Quantum Computing, Memory, and Communication VI	248
8636: Advances in Slow and Fast Light VI	259
8637: Complex Light and Optical Forces VII	268
8638: Laser Refrigeration of Solids VI	279
8639: Vertical-Cavity Surface-Emitting Lasers XVII	283
8640: Novel In-Plane Semiconductor Lasers XII	292
8641: Light-Emitting Diodes: Materials, Devices, and Applications for Solid State Lighting XVII	309
8642: Emerging Liquid Crystal Technologies VIII	327
8643: Advances in Display Technologies III	335
8644: Practical Holography XXVII: Materials and Applications	341
8645: Broadband Access Communication Technologies VII	351
8646: Optical Metro Networks and Short-Haul Systems V	358
8647: Next-Generation Optical Communication: Components, Sub-Systems, and Systems II	364

Click on the Conference Title to be sent to that page

Conference 8619: Physics and Simulation of Optoelectronic Devices XXI

Monday - Thursday 4 -7 February 2013

Part of Proceedings of SPIE Vol. 8619 Physics and Simulation of Optoelectronic Devices XXI

8619-1, Session 1

Photon extraction from semiconductors embedded in metal and coupling to optical fibers

Ikuo Suemune, Jae-Hoon Huh, Tomoya Asano, Xiangming Liu, Nahid A. Jahan, Hideaki Nakajima, Hokkaido Univ. (Japan); Kouichi Akahane, National Institute of Information and Communications Technology (Japan); Natsuko Kobayashi, Hirotaoka Sasakura, Hidekazu Kumano, Hokkaido Univ. (Japan); Masahide Sasaki, National Institute of Information and Communications Technology (Japan)

Photon extraction efficiency (PEE) from semiconductors is generally limited with total internal reflections at the air interface. We have developed methods to embed semiconductor nano pillars in metal and to extract photons generated from quantum dots from one-sided air interface. With FDTD simulations we have shown that thin pillars directly embedded in metal show cut off of guided modes. Replacing thin pillars with nano-cone with the expanded diameter toward the air interface, the simulations predict that PEE more than 90% is possible. The optical coupling of such structures to single-mode fibers was also simulated. With the direct contact of the metal-embedded semiconductor at a cleaved facet of a single-mode fiber, 16% of coupling efficiency was simulated. For the higher coupling efficiency, the control of the far-field of the extracted photons will be necessary. Experimental fabrication of nano-cones and measurements will be also reported.

(submission as a contributed paper in the Special Session on "Highly Efficient Photon Extraction from Semiconductors")

8619-2, Session 1

Selectively grown nanowires for efficient single photon emission and detection (*Invited Paper*)

Michael E. Reimer, Val Zwiller, Technische Univ. Delft (Netherlands)

High efficiency single-photon sources and detectors are required in future quantum information applications such as secure communication and quantum computation. In this work, we demonstrate very efficient single photon emission and detection from selectively grown nanowires with controlled shape and composition. Due to the unprecedented material freedom available during nanowire growth, they are ideal candidates for interfacing remote quantum bits in a large scale quantum computer.

We achieve a high efficiency single-photon source by precisely controlling the quantum dot position perfectly on the nanowire axis and growing a tapered nanowire waveguide around it. Since the quantum dot is on the nanowire axis, excellent coupling of the emitter to the nanowire waveguide mode is obtained. This excellent coupling is accompanied by an increase in the spontaneous emission rate in comparison to no waveguide [1]. In combination with an integrated mirror at the nanowire bottom, we achieve a 24-fold enhancement in the collected single photon flux in comparison to earlier work with no waveguide [2].

Finally, we introduce a novel device concept that allows us to spectrally and spatially isolate the absorption region from the avalanche multiplication region [3]. Here, the absorption region takes place in a single quantum dot, followed by a tunneling event and avalanche multiplication process in the depletion region of the nanowire p-n junction. Due to the large internal gain of both electrons and holes exceeding 10,000, we detect a single photon resonantly absorbed in the quantum dot.

[1] G. Bulgarini, M.E. Reimer et al., Spontaneous emission control of

single quantum dots in bottom-up nanowire waveguides. *Appl. Phys. Lett.* 100, 121106 (2012).

[2] M.E. Reimer, G. Bulgarini et al., Bright single-photon sources in bottom-up tailored nanowires, *Nature Commun.* 3, 737 (2012).

[3] G. Bulgarini, M.E. Reimer et al., Avalanche amplification of a single exciton in a semiconductor nanowire. *Nature Photon.* 6, 455-458 (2012).

8619-3, Session 1

On-chip generation and transmission of single photons (*Invited Paper*)

Sokratis Kalliakos, Toshiba Research Europe Ltd. (United Kingdom); Andre Schwagmann, Toshiba Research Europe Ltd. (United Kingdom) and Univ. of Cambridge (United Kingdom); Ian Farrer, Jonathan P. Griffiths, Geb A. C. Jones, David A. Ritchie, Univ. of Cambridge (United Kingdom); Andrew J. Shields, Toshiba Research Europe Ltd. (United Kingdom)

We discuss the highly-efficient on-chip transmission of quantum light from an integrated source. Under optical excitation, single photons emitted from a semiconductor quantum dot are injected into the propagating mode of a coupled photonic crystal waveguide. In such a system, slow-light effects induce Purcell enhancement of the coupled emitter increasing significantly the single-photon emission rates. Our system exhibits a single-photon emission rate into the propagating mode of 19 MHz with 24% efficiency. The high emission rate together with the coherence properties of the emitted single photons demonstrate the suitability of these systems for on-chip quantum information processing using quantum optical circuits.

8619-4, Session 1

Photonic wires and trumpets for ultrabright single photon sources (*Invited Paper*)

Jean-Michel Gerard, Julien Claudon, Joël Bleuse, Matthieu Munsch, Nitin S. Malik, Commissariat à l'Énergie Atomique (France); Jesper Mørk, Niels Gregersen, Technical Univ. of Denmark (Denmark)

Optimizing the coupling between a localized quantum emitter and a single-mode optical channel represents a powerful route to realise bright sources of non-classical light states. Reversibly, the efficient absorption of a photon impinging on the emitter is key to realise a spin-photon interface, the node of future quantum networks. Besides optical microcavities [1], photonic wires have recently demonstrated in this context an appealing potential [2,3]. For instance, single photon sources (SPS) based on a single quantum dot in a vertical photonic wire with integrated bottom mirror and tapered tip have enabled for the first time to achieve simultaneously a very high efficiency (0.72 photon per pulse) and a very pure single photon emission ($g(2)(0) < 0.01$). Furthermore, photonic wires with an elongated cross-section provide polarization control of the spontaneous emission of embedded emitters [4]. However, the performance of photonic wire SPS with tapered tips is sensitive to minute geometrical details and optimum behaviour is only obtained for ultra-sharp tips. Photonic trumpets, which exploit the opposite tapering strategy, overcome this important limitation. Moreover, they feature a Gaussian far-field emission, a strong asset for most applications. We report on the first implementation of this strategy and demonstrate an ultra-bright SPS (first-lens external efficiency: 0.75 ± 0.1). More generally, photonic trumpets appear as a very promising template to explore and exploit in a solid-state system the unique optical properties of "one-dimensional atoms".

[1] J.M. Gérard et al, *Phys. Rev. Lett.* 81, 1110 (1998)

**Conference 8619:
Physics and Simulation of Optoelectronic Devices XXI**

- [2] I. Friedler et al, Opt Exp 17, 2095-2110 (2009)
 [3] J.Claudon et al, Nature Photon. 4, 174 (2010)
 [4] M. Munsch et al, Phys. Rev. Lett. 108, 077405 (2012)

promising for improving transmitter modules for future long-haul and high-speed optical fiber links.

8619-5, Session 1

Ultrabright solid state sources of indistinguishable single photons (*Invited Paper*)

Pascale Senellart, Olivier Gazzano, Steffen Michaelis de Vasconcellos, Anna Nowak, Christophe Arnold, Isabelle Sagnes, Loic Lanco, Aristide Lemaître, Lab. de Photonique et de Nanostructures (France)

The quantum interference between indistinguishable single photons is the building block of linear quantum computing and long distance quantum communications. Developing solid-state single-photon sources that have simultaneously high brightness and single-photon coherence is an important challenge for the scalability of quantum information processing. Recent years have seen impressive progress in the fabrication of bright sources of quantum light using semiconductor quantum dots in pillar cavities or tapered nanowires. However, until now, high brightness has not been combined with indistinguishability. Indeed, high brightness requires a strong excitation of the quantum system, which in turn leads to dephasing and is detrimental the photon coherence.

In the present work, we report on the fabrication of ultrabright sources of indistinguishable photons using quantum dots deterministically inserted in well-designed pillar cavities. We demonstrate an unprecedented brightness of 78% collected photon per pulse. We study the indistinguishability of the photons as a function of the source brightness and various excitation conditions. We propose a new excitation scheme, which enables to minimize dephasing under high pumping conditions. With this approach, we demonstrate 82% indistinguishability for a brightness of the source as large as 65% photon collected per pulse.

8619-6, Session 2

Differential gain enhancement in a quantum dash laser using strong optical injection (*Invited Paper*)

Luke F. Lester, Univ. of New Mexico (United States); Frédéric Grillot, Telecom Paristech (France); Nader A. Naderi, Vassilios I. Kovanis, Air Force Research Lab. (United States)

The 3-dB modulation bandwidth and linewidth enhancement factor (LEF) of a semiconductor laser both directly benefit from an increased differential optical, which is typically improved through the use of strain, quantum confinement, or p-type doping in the active region of the device. All of these methods have been applied to quantum dot or dash materials to raise the differential gain, but unfortunately these low-dimensional systems have relatively small optical gain. The result is that the laser cavity has to be relatively low-loss, which might make the LEF smaller, but comes at the expense of the modulation bandwidth since the photon lifetime is longer. The challenge is to access the large differential gain available in a quantum dot at a low optical gain value without sacrificing the photon lifetime. Strong optical injection is a possible method to accomplish this goal because it is capable of shifting the laser threshold close to optical transparency. Also, larger differential gains are found at wavelengths blue-shifted from the gain peak. Using this approach and strong injection, more than 50X improvement in the differential gain is shown in an injection-locked QDash Fabry-Perot laser compared to its free-running value. Furthermore, the injection-locked system's 3-dB bandwidth enhancement, flat modulation response profile, and extremely low LEF are investigated using a set of analytical equations derived for the zero-detuning, zero-LEF case. From an applications perspective, the combination of an enhanced bandwidth and a very low α -factor is

8619-7, Session 2

Impacts of Carrier Capture and Relaxation Rates on the Modulation Response of Injection-Locked Quantum Dot Lasers

Cheng Wang, Frédéric Grillot, Jacky Even, Institut National des Sciences Appliquées de Rennes (France)

Quantum-dot (QD) lasers are promising directly modulated laser sources. However, the existences of the wetting layer (WL) and the excited state (ES) are known to cause severe limitations in the modulation bandwidth [1-3]. Injection-locking technique is an attractive approach for improving the modulation characteristics [4-8]. This paper aims to theoretically investigate the impacts of carrier capture and relaxation rates on the intensity modulation (IM) response of injection-locked QD lasers. The model is based on a set of five rate equations: one for the ground state (GS) photons, another one treating the phase difference between the slave and the master lasers while three rate equations are used to describe the carriers in WL, ES and GS, respectively. The modulation transfer function is obtained through a small signal analysis of the differential rate equations. In the free-running case, simulations point out that both large capture and relaxation rates enhance the modulation bandwidth and the peak frequency, while the latter leads to an increase in the peak amplitude as well. For the injection-locking case under the zero or negative detuning condition, both the bandwidth and the peak amplitude increase with larger capture or relaxation rates. Under the positive detuning case, simulations show that large capture rate enhances both the peak frequency and the bandwidth, while the relaxation rate alters the peak frequency without influencing the bandwidth. Finally, this study also demonstrates that the pre-resonance frequency dip can be eliminated with large carrier capture and relaxation rates as well as small linewidth enhancement factor.

8619-8, Session 2

Rate equation analysis of high-speed photon-lifetime-modulated strongly injection-locked semiconductor ring lasers

HemaShilpa Kalagara, Gennady A. Smolyakov, Marek Osinski, Univ. of New Mexico (United States)

A novel method for modulation bandwidth enhancement is presented, involving strongly injection-locked whistle-geometry semiconductor ring laser modulated through photon lifetime. Advantages of photon-lifetime modulation over conventional injection current modulation are confirmed through numerical modeling.

8619-9, Session 2

Extending the direct laser modulation bandwidth by exploiting the photon-photon resonance: modeling, simulations and experiments

Mihail M. Dumitrescu, Antti I. Laakso, Tampere Univ. of Technology (Finland)

Because the carrier-photon resonance (CPR) is related to the carrier and photon lifetimes, there are inherent physical limitations for increasing the direct laser modulation bandwidth as long as it is determined by the CPR. However, the direct modulation bandwidth can be substantially extended by introducing a supplementary high-frequency photon-

photon resonance (PPR). In order to study the PPR we have developed a modified rate-equation model by treating the longitudinal confinement factor as a dynamic variable. According to this model, when the laser has two dominant quasi-phase-locked modes, the modulation transfer function has an additional term with respect to the conventional transfer function. This term induces a supplementary resonance at the frequency difference between the quasi-phase-locked modes. Multi-section distributed feedback lasers with PPR have been designed, fabricated and characterized in the 1.3 and 1.55 μm wavelength ranges. The experiments showed a good agreement with the simulations and proved that the PPR can be systematically and reproducibly be induced at frequencies between 14 GHz and 1.3 THz. The main difficulty in extending the direct laser modulation bandwidth by exploiting the PPR is, however, related to obtaining a relatively flat modulation response between the CPR and PPR. Besides the modified rate equation model, the paper presents simulation studies analyzing the conditions required for obtaining a strong PPR and experimental results confirming the model and simulations. We also discuss the methods that can be used to flatten the modulation transfer function between the CPR and PPR and the possibility to induce the PPR in VCSELs.

8619-10, Session 3

Characteristics of passive mode-locked quantum dot lasers from 20 to 120 C

Jesse K. Mee, Air Force Research Lab. (United States); Mark T. Crowley, David Murrell, Ravi Raghunathan, Luke F. Lester, The Univ. of New Mexico (United States)

Development of an uncooled, compact pulsed source is extremely attractive for applications in high bit rate low energy-per-bit data distribution [1]. Transmitters based on passively mode-locked quantum dot lasers are an excellent choice. Compared to other semiconductor laser materials, GaAs-based quantum dot (QD) lasers possess many unparalleled characteristics, including for example, ultra-low chirp, tunable linewidth-enhancement factors, low lasing threshold current densities, wide gain bandwidth, easily saturated gain and absorption, low differential gain and temperature-insensitive operation [2].

The two-section mode-locked lasers (MLL) used in these experiments were based on a 6 stacks of Quantum Dots in a Well (DWELL) type active regions. Using a segmented contact method [3], we extracted gain and absorption characteristics from 20–120 $^{\circ}\text{C}$ from a multi-section test structure. These measurements served as inputs to a set of analytic expressions which predict the stability of mode-locking over temperature for a device with a given absorber-section length to gain-section length ratio. Using this method, it was previously shown [4] that a shorter absorber length would be favourable for high temp operation. This result is verified for a device with a 0.11 absorber to gain section length ratio. Mode-locking at the fundamental repetition rate was observed from this device up to 110 $^{\circ}\text{C}$ with pulse widths at FWHM being measured pulse FWHM are < 20 ps over the entire temperature range. An in-depth analysis of these measurements provides invaluable insight into the essence of the observed wide temperature operation of these devices.

References:

1. A. Aboketaf, A. W. Elshaari, and S. F. Preble, *Opt. Express* 18, 13529, (2010).
2. M. T. Crowley, N. A. Naderi, H. Su, F. Grillot and L. F. Lester *GaAs-based Quantum Dot Lasers in Semiconductors and Semimetals* 86, Chapter 10: *Advances in Semiconductor Lasers* (New York: Academic, (2012).
3. Y-C Xin, Y. Li, A. Martinez, T. J. Rotter, H. Su, L. Zhang, A. L. Gray, S. Luong, K. Sun, Z. Zou, J. Zilko, P. M. Varangis and L. F. Lester, *IEEE J. Quantum Electron.* 42 725, (2006).
4. M. T. Crowley, D. Murrell, N. Patel, M. Breivik, C-Y Lin, Y. Li, B-O Fimland and L. F. Lester, *IEEE J. Quantum Electron.* 18, 1059, (2011).

8619-11, Session 3

Modeling and characterization of pulse shape and pulse train dynamics in two-section passively mode-locked quantum dot lasers

Ravi Raghunathan, Mark T. Crowley, The Univ. of New Mexico (United States); Frédéric Grillot, Telecom Paristech (France); Jesse K. Mee, Air Force Research Lab. (United States) and Univ. of New Mexico, Albuquerque, NM (United States); Vassilios I. Kovanis, Air Force Research Lab. (United States); Luke F. Lester, The Univ. of New Mexico (United States)

Quantum dot mode-locked lasers (QDMLLs) have generated considerable interest in recent years as promising sources of low energy, low jitter, stable pulses for precision applications such as optical communications and clocking, where identical pulses with a regular shape are sought at a fixed repetition rate. Passive mode-locking is a key technique to generate such pulses, and understanding the output dynamics of passively mode-locked QDMLLs is a key step toward producing output pulses suited to their target applications. In particular, since abrupt transitions in the nonlinear dynamics of the device behavior can influence device performance dramatically, it is essential to acquire physical insight into the different regimes of operation where the output is stable/ unstable, the points at which the device transitions from one regime of operation to another, and output pulse structure typical of each regime of operation.

This paper builds on our previous efforts [1, 2, 3] to better understand the pulse characteristics and mode-locking stability of QDMLLs. To this end, a Delay Differential Equation model [4] seeded with parameters extracted from an actual device is used to model and analyze its dynamical trends, observed experimentally on diagnostic equipment (such as a high speed oscilloscope), including pulse breakup, transitions to harmonic mode-locking and double-pulsing regimes, as well as asymmetry reversal. The insight gained from the model is very promising, not only for critical information about the conditions of device operation that can cause a degradation of pulse quality, but also for pulse-shaping applications such as chirp compensation for optical communications technologies.

References:

1. Usechak, N. G., Xin, Y. -C., Lin, C. -Y., Lester, L. F., Kane, D. J. and Kovanis, V., "Modeling and direct electric field measurements of passively mode-locked quantum-dot lasers," *IEEE J. Sel. Top. Quantum Electron.* 15, 653–660 (2009).
2. M. T. Crowley, D. Murrell, N. Patel, M. Breivik, C. Y. Lin, Y. Li, B. O. Fimland and L. F. Lester, "Analytical modeling of the temperature performance of monolithic passively mode – locked quantum dot lasers", *IEEE J. Quantum Electron.* 18, 1059, (2011).
3. R. Raghunathan, M. T. Crowley, F. Grillot, S. D. Mukherjee, N. G. Usechak, V. Kovanis and L. F. Lester, "Delay differential equation-based modeling of passively mode-locked quantum dot lasers using measured gain and loss spectra", *Physics and Simulation of Optoelectronic Devices XX*, Proc. SPIE 8255, 82551K (2012).
4. A. G. Vladimirov and D. Turaev, "Model for passive mode – locking in semiconductor lasers", *Phys. Rev. A* 72, 033808, (2005).

8619-12, Session 3

Numerical simulation of passively mode-locked fiber laser based on semiconductor optical amplifier

Jingwen Yang, Dongfang Jia, Zhongyuan Zhang, Jiong Chen, Tonghui Liu, Zhaoying Wang, Tianxin Yang, Tianjin Univ. (China)

Passively mode-locked fiber laser (MLFL) has been widely used in many applications, such as optical communication system, industrial production, information processing, laser weapons and medical equipment. And many efforts have been done for obtaining lasers with

**Conference 8619:
Physics and Simulation of Optoelectronic Devices XXI**

small size, simple structure and shorter pulses. In recent years, nonlinear polarization rotation (NPR) in semiconductor optical amplifier (SOA) has been studied and applied as a mode-locking mechanism. This kind of passively MLFL has faster operating speed and makes it easier to realize all-optical integration. In this paper, we had a thorough analysis of nonlinear polarization rotation effect in SOA. And we explained the principle of mode-locking by SOA and set up a numerical model for this mode-locking process. Besides we conducted a Matlab simulation of the mode-locking mechanism. We also analyzed results under different working conditions and several features of this mode-locking process are presented. Our simulation shows that: Firstly, initial pulse with the peak power exceeding certain threshold may be amplified and compressed, and stable mode-locking may be established. After about 25 round-trips, stable mode-locked pulse can be obtained which has peak power of 850mW and pulse-width of 780fs. Secondly, when the initial pulse-width is greater, narrowing process of pulse is sharper and it needs more round-trips to be stable. Lastly, the bias currents of SOA affect obviously the shapes of mode-locked pulses and the mode-locked pulse with high peak power and narrow pulse-width can be obtained by adjusting reasonably the bias currents of SOA.

8619-13, Session 3

Active holographic quantum-well cavities

Hao Sun, David D. Nolte, Purdue Univ. (United States); Eric S. Harmon, LightSpin Technologies, Inc. (United States)

A multiple quantum-well asymmetric Fabry-Perot is reported as a promising new optoelectronic device to produce significant diffraction efficiencies in four-wave mixing holography. It combines the advantages of large excitonic absorption with large carrier density and cavity resonances in a multiple quantum well (MQW) cavity to make dynamic holographic devices. Numerical modeling shows that large absorption or gain in the cavity makes reflection contrast strong, and high mirror reflectivity determines the output intensity. The cavity is highly sensitive to the phase modulation, approaching π phase shifts. Experiments use holographic 1060 nm pump pulses that go through the transparent back mirror and are absorbed by the quantum well, and a tunable 1550 nm laser probes the gratings. The absorption and gain in the quantum wells balance the mirror reflectivity to make the device operate at a low Q near the lasing threshold. Previous work demonstrated that asymmetric Fabry-Perot GaAs reflection modulators produced high diffraction efficiencies, with input diffraction efficiencies approaching 5% [1]. In this paper, we present significant diffraction enhancement of asymmetric Fabry-Perot multiple quantum well devices using InP-based multiple quantum wells operating near 1550 nm wavelengths. The input diffraction efficiencies have been demonstrated larger than 25%. Broad-area InGaAsP microcavity and multiple quantum wells provide a new type of optically-addressed spatial light modulator.

[1] D. D. Nolte, K. M. Kwolek, C. Lenox, and B. Streetman, "Dynamic Holography in a Broad-Area Vertical GaAs microcavity," J. Opt. Soc. Am. B, vol. 18, pp. 257-63, March 2001.

8619-14, Session 4

computational modelling of surface effects in InGaN/GaN quantum disk nanowire LEDs

Friedhard Römer, Marcus Deppner, Bernd Witzigmann, Univ. Kassel (Germany)

The recent progress in the fabrication of InGaN/GaN based LEDs facilitates a successive replacement of incandescent and fluorescent lighting by solid state lighting devices. Actual research on this field focuses on the realization of InGaN/GaN nanowire LEDs which are supposed to overcome some of the limitations of current thin film LEDs such as the high substrate costs and a native true colour emission. The ratio of the surface area to the active volume is much higher in these nano structured LEDs than in thin film LEDs leading to an increased effect of surface states. Their specific effect is hard to capture by a

device characterization, though. Therefore we propose a computational model to analyse surface effects.

Surfaces close to an active region require accurate physical modelling using a surface trap model. Such a model has been implemented in our physics based semiconductor device simulator. This simulator provides a multi scale approach for coupling the carrier transport problem in bulk and low dimensional regions. Quantization effects and luminescence are treated by a multi band kp Schrödinger solver. The simulator aims for self-consistency between the kp Schrödinger problem and the transport problem. The simulation has been calibrated with the characteristics of actual InGaN/GaN thin film LEDs.

Using the simulator we investigate the impact of surface recombination and charges on the performance of InGaN/GaN multi quantum disk nanowire LEDs. These LEDs are attractive for their ability to incorporate high In concentrations in the quantum wells to enable wide band emission. We demonstrate that surface recombination as well as charges have a major impact on the efficiency. Using these results we discuss the effect of surface preparation by overgrowth or etching.

8619-15, Session 4

Optical and electrical properties of large area stacked graphene for use as transparent conducting electrodes

Sheng Chun Hung, Chung Wei Chen, Y. H. Chien, Chia-Yuan Chang, G. C. Chi, National Central Univ. (Taiwan)

Graphene, a monolayer of sp² bonded carbon atoms, has attracted a lot of attention in various research and application area. In this study, we study the optical and electrical properties of stacked CVD grown monolayer graphene.

According to the results of Raman spectrum measurement, the full width at half maximum of G band and 2D band peaks are both smaller than 40 cm⁻¹ and the ratio of 2D/G is larger than 1.5, which means the as grown graphene is monolayer. The average sheet resistivity of as grown graphene, which is measured by Hall measurement system, is about 2000 ohm/sq.

For the optical and electrical properties of stacked multilayer graphene, the transmittance, Raman spectrum, and Hall measurement were taken. The Raman spectrum results shows that the peak positions of G and 2D band didn't shift and the 2D/G ratio were almost the same between one and stacked multilayer graphene. In addition, no shoulders were observed in the 2D peak of Raman spectrum that means there should be no interactions between layers. In the optical transmittance results, the absorption of multilayer graphene is about 3.1%/layer at 555 nm wavelength. The transmittance of three layers graphene is about 90%. In electrical properties, the sheet resistivity of graphene were decreased to 50% with layer number was increased one when the total layer number is smaller than three layers.

8619-16, Session 4

A full band Monte-Carlo study of carriers transport properties of InAlN lattice matched to GaN

Sara Shishehchi, Boston Univ. (United States); Francesco Bertazzi, Politecnico di Torino (Italy); Enrico Bellotti, Boston Univ. (United States)

This work presents a study of the carrier transport properties of InAlN lattice matched to GaN calculated using a full band Monte-Carlo method. III-Nitride materials and their alloys have attracted extensive attention due to their potential applications in semiconductor devices; however, not much theoretical work has been done on AlInN. When the Indium content of AlInN is approximately 17-18%, this alloy is lattice matched to GaN and as a result can be grown strain-free. As a consequence,

**Conference 8619:
Physics and Simulation of Optoelectronic Devices XXI**

AlInN is an attractive semiconductor for applications in electronics and optoelectronic devices. Using the models that we have previously used to study the carrier transport parameters in AlGaIn and GaN, we have evaluated the temperature dependent electron and hole mobilities and drift velocities. Furthermore, we have also evaluated the high-field transport properties and computed the carriers' ionization coefficients. Within the full band Monte-Carlo, the alloy's electronic structure has been computed using the empirical pseudopotential method, including the effect of the compositional disorder. The scattering mechanisms, either wave-vector or energy dependent, have been evaluated using the full details of the electronic structure. Specifically we include: polar-optical phonon, non-polar-optical phonon and acoustic phonon interaction; ionized impurity and alloy scattering. Additionally, electrons and holes impact ionization rates, calculated directly from the full band structure, are also included to calculate the carrier impact ionization coefficients. Due to the complex nature of electronics structure of this alloy, in our model we have explicitly used the quantum transport formalism we have developed to study GaN.

8619-17, Session 4

Simulation of nanoscale ITO top grating of GaN LED

Gabriel M. Halpin, California Polytechnic State Univ., San Luis Obispo (United States); Xiaomin Jin, California Polytechnic State Univ., San Luis Obispo (United States) and Peking Univ. (China); Greg Chavoor, California Polytechnic State Univ., San Luis Obispo (United States); XingXing Fu, Xiang-Ning Kang, Guo Yi Zhang, Peking Univ. (China)

Today's advanced technology allows engineers to fabricate GaN LEDs with various heights, widths, shapes, and materials. Total internal reflection prevents light from escaping the LEDs. The ratio of refractive indices at the boundary, determine the critical angle, or minimum angle at which light completely reflects. A large difference in refractive indices results in a small critical angle and more reflected light. A small difference in refractive indices results in a large critical angle, less light reflected back and more light transmitted into the following medium. Changing the material of the top grating from GaN to ITO increases the critical angle from 23.5 degrees to 28.4 degrees. Additionally, surrounding the chip with an epoxy dome further increases the critical angle to 47.9 degrees. For these reasons, this paper analyzes light extraction enhancement of an ITO to epoxy interface through theoretical simulation. We use FDTD analysis to compare light extraction efficiency for ITO and GaN gratings, optimize ITO grating period, and investigate the effects of an Ag reflection layer, and successfully shows that increasing the critical angle and implementing an Ag reflection layer improves overall light extraction efficiency in simulation. First, increasing the critical angle from 23.5 to 47.9 degrees using an ITO top grating and an Epoxy dome improved light extraction by 40%. Next, in agreement with Peking University's RCWA simulations, increasing the ITO grating period increases light extraction. Finally, we show that light extraction for structures containing Ag reflection layers is highly dependent on sapphire substrate thickness.

8619-18, Session 5

Pseudospectral algorithm for numerical integration of Maxwell's Equations

Gregorio G. Mendoza González, Benemérita Univ. Autónoma de Puebla (Mexico); Juan M. Merlo Ramírez, Tecnológico de Monterrey (Mexico); Arnulfo Luis-Ramos, Luz del Carmen C. Gómez-Pavón, Erwin A. Marti-Panameno, Benemérita Univ. Autónoma de Puebla (Mexico)

The numerical experiment techniques represent a strong toehold in the design and development of nanodevices. Particularly, nanophotonics demands a widespread support to study light propagation and

interaction in low dimensional waveguides and systems. The main characteristic for light evolution description in nanoworld is the needs of numerical integration of Maxwell's Equations (ME). Among others, the Finite Difference Time Domain (FDTD) is one of the most solids algorithms for the description of light behavior for media where the ratio of the characteristic dimension to the radiation wavelength is less or at least equal one. Based on the FDTD method two pseudospectral (PS) algorithms were developed. One so called time domain and the other spectral domain. These PS use the Fast Fourier Transform to evaluate either the spatial or the temporal derivatives, respectively. However, the three approaches above mentioned, require the finite differences support for the propagation derivatives calculation. We present an iterative method for the numerical integration of ME. Analyzing separately the TE and TM waves we solve, in the spatial-frequency domain, the set of coupled first order ordinary differential equations, for both the Electric and Magnetic fields. These solutions provide us with the propagation constants for backward and forward waves. We build up a propagation operator for the iterative solution of the light evolution along nanowaveguides. Our algorithm is successfully tested in two cases, the propagation through the junction of two subwavelength waveguides of different refractive indexes, and for the impedance matching problem.

8619-19, Session 5

Efficient and precise simulation of multiple Mie scattering events using GPUs

Simon Streicher, Hochschule Heilbronn (Germany); Ronald Kampmann, Roman M. Kleindienst, Stefan Sinzinger, Technische Univ. Ilmenau (Germany); Oliver Kalthoff, Hochschule Heilbronn (Germany)

Mie theory describes the scattering of electromagnetic waves on spherical particles whose diameter is close to the wavelength of the incident radiation. A variety of computer algorithms exist to calculate scattering parameters. These are sufficiently exact but computationally slow, so the simulation of radiation transport in a medium can be a time consuming task. To the best of our knowledge only few attempts have been made to adapt algorithms to parallel processors such as programmable graphics adapters.

We have implemented a parallel algorithm to calculate perpendicular and parallel polarized scattered waves, from which other scattering parameters can be derived. This facilitates simultaneous tracking of particular waves in scattering media. Our code can be invoked from scripting languages like Matlab as well as from high-level languages such as C/C++ and is executable also on conventional processors. We tested our approach using Monte Carlo simulations. The results correspond to reference implementations. We have shown that execution time can be reduced significantly compared to sequential approaches.

To validate simulation results we use a high precision measuring device with accuracy of 0.1°. The apparatus detects scattered light emitted from a sphere containing a defined number of scattering objects.

8619-20, Session 5

Light extraction by directive sources within optically dense media.

James R. Nagel, Terahertz Device Corp. (United States)

Light extraction efficiency (LEE) from a light emitting diode is commonly estimated by considering an isotropic radiator within a dense dielectric medium. However, this description is not necessarily accurate for photonic devices with directionally radiating elements. We derive formal expressions for the LEE of a directive radiating source next to a planar dielectric boundary, accounting for any Fresnel reflections by the material interface. These results serve as exact, analytical solutions that can be used to validate numerical simulation and also help to formalize a precise mathematical description of LEE. Four variations are explored, including the isotropic radiator, parallel and perpendicular orientations of

**Conference 8619:
Physics and Simulation of Optoelectronic Devices XXI**

the Hertzian dipole, and Lambertian scattering. For emitters in a GaSb substrate ($n = 3.9$), an isotropic radiator has an LEE of 1.7%, while the parallel dipole is 2.5% and the perpendicular dipole is 0.08%. After correcting for Fresnel reflections, these LEEs can reduce by as much as 36% of the original value.

8619-21, Session 5

Efficient Sensitivity Analysis of Waveguide Structures Using Finite Element Method (FEM)

Mohamed R. Abdelhafez, The American Univ. in Cairo (Egypt); Mohamed H. Bakr, McMaster Univ. (Canada); Mohamed A. Swillam, Univ. of Toronto (Canada) and The American Univ. (Canada)

We discuss a novel finite element method-based technique for estimating accurate sensitivities of the desired response. Our technique utilizes the central adjoint variable method (CAVM) for estimating the response sensitivities. This approach features accuracy comparable to that of the central finite difference (CFD) approximation at the response level. Our approach uses a simple perturbation method to calculate the sensitivity of modal parameters of various waveguide structures with respect to the geometric and material parameters. No additional simulation is required to calculate the response and its sensitivity with respect to all the design parameters.

The accuracy of our approach is illustrated by comparing the results with the second order accurate CFD applied on the response level. Our results show a very good agreement between the CAVM-based sensitivities and those obtained using the expensive central.

8619-22, Session 5

Slow/fast light and nonlinear reflection due to induced dispersion in semiconductor lasers

HemaShilpa Kalagara, Gennady A. Smolyakov, Univ. of New Mexico (United States); Marek Osinski, Univ. of New Mexico (United States)

Nonlinear wave interactions (NWIs) are known to lead to significant perturbations of optical parameters of the active medium in semiconductor laser devices. We consider an anomalous behavior of a subsidiary (probe) wave in presence of a strong (driving) electromagnetic wave, using the two-mode approximation. Depending on the frequency detuning between the two waves, the driving wave can support or suppress the probe wave. This behavior is caused by perturbation of the complex dielectric permittivity produced by the driving wave at frequencies detuned from the driving frequency. The perturbation of permittivity is due to nonlinear scattering of the driving wave from the dynamic interference field formed by the driving and probe waves in the active region of a laser or an optical amplifier. As a result, one can expect unusual behavior of the probe wave, namely, slow or fast propagation and nonlinear back reflection of optical flow. We have shown that critically anomalous dispersion (CAD), where the perturbed group index passes zero, can in principle be achieved. A regime of negative group index corresponds to the group velocity directed opposite to the direction of phase velocity. We consider this regime as a case of nonlinear back reflection. Also, the modified group velocity influences the device performance parameters, such as optical gain, linewidth, and modulation characteristics. In this paper, we numerically determine the conditions necessary for obtaining slow/fast light and nonlinear back reflection in a semiconductor laser.

We have performed three-dimensional finite-element modeling of the group index perturbation, assuming that the driving wave is much stronger than the probe wave. A ridge waveguide laser structure is considered, with the active region consisting of a bulk GaAs/AlGaAs separate-confinement heterostructure (SCH). We have determined

that NWIs are stronger in lasers with bulk active region, compared to quantum-well active regions. The perturbed effective index of the fundamental mode of the ridge waveguide is obtained using full vector analysis of RSoft FemSIM mode solver, with all epitaxial layers taken into account. A subsequent differentiation of the phase index by detuning between the strong and probe wave frequencies gives the perturbed (modified) effective group index.

The size of the CAD loop depends on the initial relaxation rate τ_0 of states involved in the optical transitions, optical confinement factor, and the driving wave intensity. The effect of the critically anomalous dispersion becomes less significant at higher initial relaxation rates, because of broadening of the perturbation spectrum. Limitation at the high-intensity side is caused by the contribution of the stimulated recombination to the relaxation rate. The initial rate depends on the spontaneous radiative recombination and the nonradiative recombination rates. Another high-intensity limitation in practice can be associated with the catastrophic optical damage of the semiconductor structure, although it does not directly play a role in the simulation.

In laser case, the coherent backscattering of the beam should not produce significant problems, except for the correction of the actual value of the optical feedback. In contrast to this, in the optical amplifier the induced backscattering can be a serious source of instability of the operation regime. The nonlinear backscattering can produce laser oscillation in the probe wave (on a higher-shifted frequency). This parasitic lasing in an amplifier is not desirable, as it would produce distortions of the output spectrum and would take power from the driving wave.

In the vicinity of CAD points, one can expect very high group velocities. However, a CAD point is not convenient for laser applications, as the laser spectral line is expected to undergo a significant broadening. The linewidth increases when a CAD point is approached, in proportion to squared value of the group velocity. On the other hand, the superluminal propagation can be of interest, because of a possibility of very high-speed modulation.

8619-23, Session 6

New materials and processes for plasmonic and metamaterial devices (Invited Paper)

Mark D. Thoreson, Alexandra Boltasseva, Paul R. West, Gururaj V. Naik, Naresh K. Emani, Purdue Univ. (United States)

The potential applications for plasmonics and optical metamaterials are truly ground-breaking, but optical losses in the metallic components of these devices drastically limit their use in real, commercial devices. In this talk, we present recent work related to novel processes and materials for fabricating nanophotonic, nanoplasmonic and optical metamaterial devices, including hyperbolic metamaterials. We explain new fabrication processes for unique metamaterial designs, and we propose a path for the incorporation of alternative plasmonic materials in real devices. Several examples of recent, relevant experimental demonstrations are also discussed.

8619-24, Session 6

A Monte-Carlo FDTD approach to modeling ensembles of polydisperse plasmonic nanoparticles

Mikhail A. Kats, Herman Gudjonson, Harvard School of Engineering and Applied Sciences (United States); Kun Liu, Gaoxiang Wu, Siyon Chung, Univ. of Toronto (Canada); Zhihong Nie, Univ. of Maryland, College Park (United States); Eugenia Kumacheva, Univ. of Toronto (Canada); Federico Capasso, Harvard School of Engineering and Applied Sciences (United States)

**Conference 8619:
Physics and Simulation of Optoelectronic Devices XXI**

Experiments in nano-optics frequently feature ensembles of elements with some distribution of geometrical and optical properties; some examples include arrays of lithographically defined plasmonic antennas and colloidal mixtures of nanoparticles. Electromagnetic simulations are frequently employed to model or optimize the optical response of these systems; however, it is frequently non-trivial to account for polydispersity in such ensembles.

We present a Monte-Carlo method of modeling the optical properties of ensembles of polydisperse systems with many degrees of freedom. Random sampling from expected distributions of parameters is combined with finite-difference time-domain (FDTD) simulations to obtain the overall optical response of the polydisperse system.

We demonstrate this approach by modeling the optical extinction spectrum of polydisperse gold nanorods and nanorod chains in solution, and comparing the results to experimental measurements. In these experiments, gold nanorods with a known distribution of lengths and diameters are self-assembled into chains via step-growth polymerization, and this time-dependent process is constantly monitored via repeated extinction measurements.

Our results show that the Monte-Carlo FDTD approach is able to accurately reproduce the time-dependent experimental extinction spectra of the ensemble of nanorod chains. We will discuss the merits of applying this technique to a variety of optical structures, and discuss some of the challenges of such an approach.

8619-25, Session 6

Green's function approach to study plasmonic luminescence enhancement in grated multilayer structures

Toufik Sadi, Jani Oksanen, Jukka Tulkki, Aalto Univ. (Finland)

Surface plasmons (SPs) have recently gained substantial attention due to their sub-wavelength localization and strong interactions in the near-field. Their unique properties are expected to be essential for the next-generation photonic nanodevices, for instance, to improve light extraction in light-emitting diodes (LEDs). We discuss and develop a rigorous and transparent method to model luminescence enhancement and absorption in grated multilayer structures. The method is based on Green's functions, obtained as a perturbative solution to Maxwell's equations, and the fluctuational electrodynamics description of the structures. The model provides an analytical alternative to numerical methods such as finite-element methods and gives insight beyond the numerical solutions, offering a direct means of studying emission and luminescence from the periodic structures.

The model is applied to answer key fundamental questions regarding luminescence enhancement, absorption and reflection in realistic plasmonic GaN light-emitting diode (LED) structures. Two aspects are considered in particular: (i) modeling the reflectometry measurements of grated LED structures to explain and map the interference patterns observed experimentally by our partners, and (ii) modeling the luminescence enhancement in plasmonic structures where the emission takes place in quantum wells in the vicinity of the metallic grating. The results clearly reveal e.g. the SP-related luminescence enhancement in InGaN quantum well structures incorporating periodic silver grating.

8619-26, Session 6

Wideband sensitivity analysis of plasmonic structures

Osman S. Ahmed, Mohamed H. Bakr, Xun Li, McMaster Univ. (Canada); Tsuyoshi Nomura, Toyota Research Institute North America (United States)

We propose the theory of dispersive adjoint variable method (AVM) for plasmonic structures. In this paper we exploited time domain modeling technique (transmission line modeling) for efficient calculation of structure

sensitivity. The theory is developed for general dispersive materials modeled by Drude or Lorentz model. Utilizing the dispersive AVM, sensitivity is calculated with respect to all the designable parameter utilizing at most one extra simulation. This is far more efficient than the regular finite difference approaches with a computational overhead scales linearly with the number of design parameters. A z domain formulation is utilized in this theory to allow for the extension to a general material model [1].

The theory has been successfully applied to a structure of teeth shaped plasmonic resonator where the design variables are the shape parameter (width and thickness) of these teeth. The results are compared to the accurate yet expensive finite difference approach and good agreement is achieved.

[1] Osman S. Ahmed, Mohamed H. Bakr, Xun Li, and Tsuyoshi Nomura, "An adjoint variable method for 2D plasmonic structures," *opt. lett.*, Accepted July 2012, posted 07/12/2012; Doc. ID 167649.

8619-27, Session 7

Metamaterials for visible and near infrared antireflective properties and large surface elaboration

Jean-Baptiste Brückner, Institut Materiaux Nanoelectronique de Provence (France); Judikaël Le Rouzo, Ludovic Escoubas, François R. Flory, Institut Matériaux Microélectronique Nanosciences de Provence (France); Olivier Calvo-Perez, Nicolas Vukadinovic, Dassault Aviation (France); Gérard Berginc, Thales Optronique S.A.S. (France)

We propose three distinctive designs of metamaterials demonstrating antireflective properties in the optical and near infrared region and, simultaneously, a high reflectivity in the mid-infrared.

Since the emissivity is related to the absorption of a material, our structures would then offer a high emissivity in the visible and near infrared. Beyond those wavelengths, the emissivity would be quite low. Usually, such systems find their applications in the field of thermophotovoltaics, where the goal is to convert radiation from the visible up to 2.5 microns into electrons, while limiting the emissivity for the larger wavelengths. A particular interest in the field of optoelectronics is found as well, especially for radar detection.

Here, the major difficulty is to offer a metal thick enough to be considered as mirror across the electromagnetic radiation spectrum that possesses at the same time an anti-reflective character within a range of several microns. Thus, we have summoned the exceptional physical properties of the material patterning [1].

Numerical analysis has been performed on commonly used metamaterial designs [2-4]: a perforated metallic plate, a metallic cross grating and finally a metallic pyramid grating. Through all these three different structures, we have demonstrated the various physical phenomena contributing to a reduction in the reflectivity in the optical and near infrared region. By showing realistic geometric parameters, the structures were not only designed to demonstrate a good optical response but were also meant to be feasible on large surfaces by lithographic methods such as micro contact printing or nano-imprint lithography.

[1] Cai, W. and Shalae, V., [Optical Metamaterials: Fundamentals and Applications], Springer: New York (2009).

[2] Baïda, F. I. and Van Labeke, D., "Light transmission by sub-wavelength annular aperture arrays in metallic films", *Optics Commun.* 209, 17 (2002).

[3] García-Meca, C., Ortuño, R., Salvador, R., Martínez, A., and Martí, J., "Low-loss single-layer metamaterial with negative index of refraction at visible wavelengths", *J. Optics express.* 15, 9320-5 (2007).

[4] Rephaeli, E. and Fan, S., "Tungsten black absorber for solar light with wide angular operation range", *Applied Physics Letters.* 92, 211107 (2008).

8619-28, Session 7

Tailoring infrared absorptance with a one-dimensional structure

Yu-Lung Lo, Nghia Nguyen-Huu, National Cheng Kung Univ. (Taiwan)

A one-dimensional structure based a single-layered aluminum subwavelength grating (SWG) which is easily manufactured using microfabrication technology was numerically investigated via the rigorous coupled-wave analysis and a genetic algorithm. The results show that the studied SWG displays a high spectral absorptance (0.99) and a wide bandwidth (1.4 μm). Moreover, it is also shown that the spectrum is insensitive to the angle of incident light and the grating period, but shifts toward a longer (shorter) wavelength when the grating thickness or grating ridge width is increased (decreased). The absorptance enhancement is evaluated based on the governing equations of the excitations of Wood's anomaly, surface plasmon polaritons, cavity resonance, and magnetic polaritons. The physics origin is also analyzed using the finite difference time-domain method to demonstrate magnetic field and Poynting vector distributions.

8619-29, Session 7

Top-flat and top-patterned cone gratings for mid-infrared antireflective properties

Jean-Baptiste Brückner, Judikaël Le Rouzo, Ludovic Escoubas, François R. Flory, Institut Matériaux Microélectronique et Nanosciences de Provence (France); Gérard Berginc, Thales Optronique S.A.S. (France)

Achieving a broadband antireflection property from material surfaces is one of the highest priorities for those who want to improve the efficiency of solar cells or the sensitivity of photo-detectors. To lower the reflectance of a surface, we have decided to study the optical response of a top-flat cone shaped silicon grating, based on previous work exploring pyramid gratings [1].

Through rigorous numerical methods, such as Finite Different Time Domain or Rigorous Coupled-Wave Analysis, we then designed several structures theoretically demonstrating an antireflective character within the middle infrared region.

From the opto-geometrical parameters such as period, depth and shape of the pattern determined by numerical analysis, these structures have been fabricated using controlled slope plasma etching processes [2-4]. Afterwards, optical characterizations of several samples were carried out. The reflectance of the grating in the near and middle infrared domains has been measured by Fourier Transform Infrared spectrometry and a comparison with numerical analysis has been made. As expected, those structures offer a fair antireflective character in the region of interest. Further numerical investigations led to the fact that patterning the top of the cone could enlarge the antireflective domain to the visible region [5]. Thus, as with the simple cone grating, a comparison of the numerical analysis with the experimental measurements is made.

Finally, diffracted orders are studied and compared between both structures. Those orders are critical and must be limited as one wants to avoid crosstalk phenomena in imaging systems.

Reference citations

- [1] Bouffaron, R., Escoubas, L., Simon, J. J., Torchio, P.; Flory, F., Berginc, G., and Masclat, P., "Enhanced antireflecting properties of micro-structured top-flat pyramids", *Optics express* 16, 19304-9 (2008).
- [2] Grann, E.B., Moharam, M.G. and Pommet, D.A., "Optimal design for antireflective tapered two-dimensional subwavelength grating structures", *J. Opt. Soc. Am. A* 13, 333 (1995).
- [3] Southwell, W.H., "Pyramid-array surface-relief structures producing antireflection index matching on optical surfaces", *J. Opt. Soc. Am. A* 8, 549, (1991).
- [4] Oehrlein, G. S. and Kurogi, Y., "Sidewall surface chemistry in

directional etching processes", *Materials Science and Engineering: R: Reports*, 24, 153-183 (1998).

[5] Escoubas, L., Bouffaron, R., Brissonneau, V., Simon, J.-J., Berginc, G., Flory, F. and Torchio, P., "Sand-castle biperiodic pattern for spectral and angular broadening of antireflective properties", *Optics letters*, 35, 1455-7, (2010).

8619-30, Session 7

Electromagnetic modeling of surface plasmon resonance with Kretschmann configuration for biosensing applications in a CMOS-compatible interface

Arnoldo Salazar, Sergio Camacho-León, Tecnológico de Monterrey (Mexico); Olivier Rossetto, Univ. Joseph Fourier (France); Sergio O. Martínez-Chapa, Tecnológico de Monterrey (Mexico)

Surface Plasmon Resonance (SPR) is a wave phenomenon occurring at an interface between a dielectric and a metal. SPR has applications in label-free biodetection systems, where advances in microfabrication are fostering the development of SPR-based lab-on-chips. By selecting the interface's materials to be compatible with a post-CMOS microfabrication process, this work presents a numerical analysis for the excitation of SPR on a gold-oxide interface using the Kretschmann's configuration. The results obtained reveal that for a gold layer with a thickness of 50nm and using a HeNe laser operating at 633nm as light source, good electromagnetic coupling efficiency is achieved at an angle of 68°. The results are also consistent with the theory based on Fresnel's equations and the physics of surface plasmons propagating on smooth surfaces. Moreover, gold is a material that can be used as substrate for a variety of molecules, antibodies, enzymes, etc. In SPR biosensors, the sample under analysis interacts with immobilized agents on the metal surface producing a change on the refractive index. Our simulations show that a change of $\sim 10^{-4}$ on the surface's refraction index can be detected by observing the change in the SPR angle with this configuration. Finally, the noise and sensitivity characteristics are specified for a suitable CMOS image sensor that would facilitate his integration with all the other components of a SPR biosensor on a single chip, in comparison with the conventional off-chip approach involving an external CCD device that measures the light intensity reflected from the functionalized SPR interface.

8619-31, Session 8

Electrical design of lateral junction photonic crystal lasers (*Invited Paper*)

Jan Petykiewicz, Gary Shambat, Bryan Ellis, Jelena Vuckovic, Stanford Univ. (United States)

The strong light-matter interaction in photonic crystal (PC) nanocavities makes them a promising platform for efficient and compact optical devices. The high quality factors and small mode volumes demonstrated in such cavities lead to large Purcell factors, lowering laser thresholds and increasing the achievable modulation rate [1]. Recently, a number of electrically-controlled GaAs PC nanocavity sources and modulators have been demonstrated using a lateral p-i-n diode geometry [2-6]. Such devices can be fabricated using an electron beam lithography and masked ion implantation process which is versatile and readily adapted to work in new materials [2,6].

Here, we model conduction and free-carrier injection in laterally doped GaAs p-i-n diodes formed in one and two-dimensional PC nanocavities. Finite element Poisson and carrier drift-diffusion simulations in the Sentaurus software suite show that the lateral geometry exhibits high electrical conductivity for a wide range of PC parameters and allows for precise control over current flow, enabling efficient carrier injection despite fast surface recombination.

**Conference 8619:
Physics and Simulation of Optoelectronic Devices XXI**

Simulated current-voltage characteristics show reasonable agreement with experimentally measured curves [2,3,5], and exhibit relatively weak dependence on PC hole radius. Injected carrier densities of $2 \times 10^{16} \text{ cm}^{-3}$ are attained at an operating bias of 1.2 V, showing good agreement with previously published estimates [4]. Thermal simulations using an energy-balance method indicate that the temperature increase during steady-state operation is only 3.3 K in nanobeam resonators and 0.29 K in L3 defect nanocavities. The results affirm the suitability of lateral doping in PC devices and indicate criteria for further design optimization.

- [1] G. Bjork and Y. Yamamoto, IEEE J. Quantum Electron 27, 2386 (1991).
- [2] B. Ellis et al., Nat. Photonics 5, 297 (2011).
- [3] G. Shambat et al., Nat. Commun. 2, 539 (2011).
- [4] G. Shambat et al., Opt. Express 19, 7530 (2011).
- [5] G. Shambat et al., Appl. Phys. Lett. 99, 071105 (2011).
- [6] S. Matsuo et al., Opt. Express 20, 3773 (2012).

8619-32, Session 8

Bloch-wave engineered submicron-diameter quantum-dot micropillars for cavity QED experiments

Niels Gregersen, Technical Univ. of Denmark (Denmark); Matthias Lerner, Julius-Maximilians-Univ. Würzburg (Germany); Stephan Reitzenstein, Technische Univ. Berlin (Germany); Sven Höfling, Julius-Maximilians-Univ. Würzburg (Germany); Jesper Moerk, Technical Univ. of Denmark (Denmark); Lukas Worschech, Martin Kamp, Alfred Forchel, Julius-Maximilians-Univ. Würzburg (Germany)

The semiconductor quantum dot - microcavity pillar system represents an attractive platform for studying fundamental light-matter interaction. Since the coupling depends on the cavity field profile, engineering of the photonic environment is central to obtaining the desired functionality. For strong coupling, the figure of merit is the visibility proportional to Q / \sqrt{V} , where Q and V are the quality factor and the mode volume respectively. A high Q factor and a low V are thus desirable.

Q factors of 165000 have been demonstrated for micropillars with relatively large V. However, for large V, pure dephasing limits the visibility. One should thus choose a Q similar to the dephasing and minimize V by reducing the pillar diameter. However, for the standard micropillar design, poor mode matching between the cavity mode and the DBR Bloch mode limits the Q to about 2000.

In this work we present a novel tapered micropillar design where Bloch-wave engineering is employed to significantly enhance the mode confinement. This optimization is performed by introducing an adiabatically tapered cavity, in which the fundamental Bloch mode experiences an adiabatic transition leading to improved mode matching and suppression of light scattering.

This allows us to demonstrate a record-high vacuum Rabi splitting of 85 micro eV of the strong coupling for an 850 nm diameter pillar incorporating quantum dots with modest oscillator strength ($f \sim 10$) as well as measured Q factors up to 13600, representing a relative improvement of 7 compared to previous state-of-the-art in the submicron diameter regime.

8619-33, Session 8

A photonic nanowire trumpet for interfacing a quantum dot and Gaussian free-space mode

Niels Gregersen, Technical Univ. of Denmark (Denmark); Matthieu Munsch, Nitin S. Malik, Joël Bleuse, Adrien Delga, Commissariat à l'Énergie Atomique (France); Jesper Moerk, Technical Univ. of Denmark (Denmark); Jean-Michel Gérard, Julien Claudon,

Commissariat à l'Énergie Atomique (France)

Optimizing the coupling between a localized quantum emitter and a well defined optical channel represents a powerful route to realise the bright sources of the non-classical light states required in quantum communication and information processing applications. Reversibly, the efficient absorption of a photon impinging on the emitter is key to realise a spin-photon interface, the node of future quantum networks.

In this context, the tailored fiber-like photonic nanowire embedding a single quantum dot has recently demonstrated an appealing potential. This structure features no cavity and relies on a geometrical screening of radiation modes rather than resonant effects to ensure a strong coupling between the quantum dot and the optical waveguide mode. This approach renders the system broadband, a huge practical advantage. However, the device requires a delicate, sharp needle-like taper for efficient outcoupling of light, and the performance of this taper is sensitive to minute geometrical details on the order of 1 degree.

In this work, we demonstrate a new photonic nanowire design, the photonic trumpet, exploiting an opposite tapering strategy based on an inverted conical taper to ensure efficient in- and out-coupling. The trumpet allows for side wall angles above 10 degrees, thus greatly relaxing fabrication tolerances. Moreover, the trumpet features a Gaussian far-field emission, a strong asset for most applications, and is fully compatible with electrical contacting. We report on the first implementation of this strategy and demonstrate an ultra-bright single-photon source with a first-lens external efficiency of 0.75 ± 0.1 .

8619-34, Session 8

All-ZnO-based microcavities for strong exciton-photon coupling and lasing

Simon Halm, Sascha Kalusniak, Sergey Sadofev, Matthias Brandt, Fritz Henneberger, Humboldt-Univ. zu Berlin (Germany)

Semiconductor based microcavities (MCs) have been a subject of extensive research for more than 20 years. They allow to study fundamental aspects of the coupling between light and matter, but have also become of enormous technological importance, e.g., in vertical cavity surface emitting lasers (VCSELs). The usage of (Zn,Mg,Cd)O as an active material is attractive in both respects: with the given band gap tunability, VCSELs emitting in the ultraviolet to green spectral ranges are in principle accessible, and the high oscillator strength and exciton binding energy permit to extent strong exciton-photon coupling phenomena to room temperature (RT) and beyond. However, other than in the GaAs, CdTe or GaN systems, so far only bulk active ZnO layers have been employed in hybrid MCs with dielectric mirrors.

We demonstrate that epitaxial growth of all-monolithic (Zn,Mg)O based MCs containing high optical quality ZnO multiple quantum wells (MQW) as active layers is feasible by molecular beam epitaxy on sapphire substrates. Starting from distributed Bragg reflectors for the wavelength range of 375 – 500 nm with reflectivities higher than 99 %, via monolithic MCs with a quality factor exceeding 1500, we show that VCSEL laser action is obtained at RT [1], which can be tuned between 371 – 387 nm by the MC resonance. Monolithic ZnO-based MCs are also suited to reach the strong coupling regime at cryogenic [2] and room temperature, which is evidenced by the observation of a finite splitting between the lower and upper polariton branches in angle resolved reflectivity and absorption spectroscopy.

References

- [1] S. Kalusniak, S. Sadofev, S. Halm, and F. Henneberger, Appl. Phys. Lett. 98, 011101 (2011).
- [2] S. Halm, S. Kalusniak, S. Sadofev, H.-J. Wünsche, and F. Henneberger, Appl. Phys. Lett. 99, 181121 (2011)

8619-35, Session 9

Self-consistent analysis of thermal blooming in high-power lasers

Joachim Piprek, NUSOD Institute LLC (United States)

High-power broad-area laser diodes often suffer from a widening of the lateral far-field with increasing current. This effect is also referred to as thermal blooming, since self-heating is considered the main cause. The non-uniform temperature profile inside the waveguide leads to a lateral refractive index profile that enhances the index guiding of laser modes (thermal lens). Numerical simulation is a valuable tool to investigate this complex interaction of electronic, thermal, and optical processes; however, a comprehensive numerical analysis has not been published yet. This paper presents the first self-consistent electro-thermal-optical simulation of the thermal blooming effect in broad-area Fabry-Perot lasers. The two-dimensional model includes current and carrier spreading, the highly non-uniform heat power distribution inside the laser, as well as optical anti-guiding effects caused by the non-uniform carrier distribution inside the quantum wells. A previously investigated GaAs-based quantum well laser structure with an emission wavelength near 970nm is used as an example [1]. The calculated results are in good agreement with measurements, including the modal near and far fields. The simulations reveal that thermal blooming is not only caused by the rising order of lateral modes but also by the far field widening of each individual mode with increasing current. The total number of modes affects the far field of each individual mode. Several variations of laser design and mounting are investigated to obtain smaller and more stable far fields.

[1] P. Crump et al., Sem. Science & Technol. 27 (2012) 045001

8619-36, Session 9

Dynamic analysis of high-order quantum dot based laterally-coupled distributed feedback lasers

Akram Akrouf, Kais Dridi, Trevor J. Hall, Univ. of Ottawa (Canada)

Single-mode operation is achieved in laterally-coupled distributed feedback (LC-DFB) lasers by etching the Bragg gratings alongside the ridge waveguide. This approach allows the fabrication of DFB lasers in a single epitaxial growth process. In addition, using high-order grating, more relaxed lithographic tolerances are thus allowed, which induces a major simplification in the fabrication process and enhances the manufacturing yield.

In this work, we present a time-domain coupled model suitable to investigate high-order $\pi/4$ phase-shift grating quantum dot (QD) based LC-DFB laser. First, by integrating the Streifer's coefficients, we include the effects of radiation and evanescent modes, into the time-domain coupled wave equations, and hence we investigate the effect of the radiation modes. Then, via a set of multi-population rate equations coupled with the travelling field propagation equations, population dynamics in the QD region are modeled and the homogeneous and inhomogeneous broadening of respectively the whole QD ensemble and each QD interband transition are properly taken into account in the model. Finally, we consider the coupling between forward and backward electric fields due to the grating via the travelling wave approach.

This approach advances the impact of radiating partial waves in high-order QD-LC-DFB lasers. It is shown that, in particular for third-order rectangular grating, longitudinal spatial hole-burning is highly reduced and high single mode suppression ratio (55 dB) is obtained by finely engineering the grating features.

8619-37, Session 9

Study of the temperature and cavity length effects on threshold current density and wavelength shift in quantum dot lasers

Dmitry Bykov, Bruno Gonzalez, Horacio L. Rivera, Univ. Carlos III de Madrid (Spain); Vitalii Sichkovskiy, Johan Peter Reithmaier, Univ. Kassel (Germany)

The low-cost, integrated and compact terahertz (THz) frequency sources have been intensively considered over the last years. Quantum Dots (QD) dual mode lasers were proposed (A. Biebersdorf et al., Appl. Phys., 36, 2003) as suitable source for millimetre and THz generation, by photomixing, because they present a stable tuning of emission wavelength with temperature, as well as show more advantages in comparison to quantum well (QW) lasers or bulk materials, such as higher density of states, less temperature sensitive, higher differential gain, and natural size distribution enabling tunability over extended wavelength ranges (A. Markus et al., IEEE JSTQE, vol. 9, 2003). As it is known, the threshold current density is exponentially increased when the temperature is increased as well (Y. Cao et al., IEEE PTL, vol. 20, 2008) because more current is necessary to overcome the increased absorption. Furthermore, previous experimental researches also demonstrated that both threshold current and wavelength are shifted by means of cavity length due to its dependence with the total cavity losses (E. M. Pavelescu et al., SST, vol. 23, 2008).

In this paper, we present a theoretical study and its comparison with experimental results of the temperature and cavity length effects on the threshold current density and wavelength on QD lasers. The used model was supported by rate equations and with the dependence of medium gain on temperature and wavelength (B. Gonzalez, H. Lamela et al., SPIE Photonics West, 8255-11, 2012 and E. Dadrasnia et al., SPIE Photonics West, 8255-38, 2012). Theoretical and experimental results seek the development of AlGaAs/GaAs/InGaAs high-power quantum-dot lasers with optimized geometric parameters and stable shifting of these two parameters with temperature and cavity length. For this goal were fabricated QD lasers with cavity lengths of 866 μm , 1316 μm and 1758 μm in a temperature range from 20 to 120 $^{\circ}\text{C}$, in order to get tunable dual mode lasers for THz generation by controlling the temperature.

8619-38, Session 9

Low-temperature characterization of 1.55- μm MQW lasers down to 10 K

Emmanuel Mercado Sotelo, Dipendra Adhikari, Gennady A. Smolyakov, Marek Osinski, The Univ. of New Mexico (United States)

A novel method for modulation bandwidth enhancement is presented, involving strongly injection-locked whistle-geometry semiconductor ring laser modulated through photon lifetime. Advantages of photon-lifetime modulation over conventional injection current modulation are confirmed through numerical modeling.

Long-wavelength semiconductor lasers with multiple structures and carrier confinement mechanisms are characterized from room temperature down to 10K. The temperature dependence of important laser parameters extracted from typical L-I-V-I measurements is presented. The laser threshold current is dramatically reduced at low temperatures, down to a level that can be much lower than the current required to reach the diode saturation voltage. The central wavelength of emission also decreases with temperature implying a significant increase in the active region energy band gap resulting in higher threshold voltages. The difference between increasing saturation and lasing threshold voltages clearly indicates power consumption can be no longer estimated from band gap energy temperature effects alone and predict additional power dissipation in the active region. The diode non-linear V-I relationships at lasing threshold precludes series resistance estimations from sub- and post-threshold measurements and only

**Conference 8619:
Physics and Simulation of Optoelectronic Devices XXI**

saturation voltage criteria remain applicable. Series resistance results are interpreted in terms of different lattice and ionization scattering effects on carrier mobility in both p and n-type carrier transport sections under non-equilibrium conditions. Concentrations and activation energies of dopants are estimated from these considerations. In addition, non-linear behavior greatly improves the sensitivity of differential analysis for the possible determination of active region features. Laser external differential quantum efficiency is improved as temperature drops indicating a significant reduction of non-radiative processes. The low-temperature laser internal efficiency can be estimated by extrapolation. From this and the theoretical temperature dependence of non-radiative processes the optical internal loss can be estimated.

8619-83, Session 9

Two-wavelength switching with a 1310nm-QDot DFB laser

Antonio Hurtado, Ctr. for High Technology Materials (United States) and Univ. of Essex (United Kingdom); M. Nami, Ctr. for High Technology Materials (United States); Ian D. Henning, Michael J. Adams, Univ. of Essex (United Kingdom); Luke F. Lester, Ctr. for High Technology Materials (United States)

We report a first experimental observation of two-wavelength switching and bistability with a 1310nm-Quantum Dot (QDot) Distributed Feedback (DFB) laser subject to external optical injection and operated in reflection. We experimentally demonstrate the switching of the emission wavelength of the QDot laser when an external optical signal is injected into one of the subsidiary longitudinally modes located in the longer subwavelength side of the device's lasing mode. Clockwise nonlinear switching and bistability are attained in all cases for both the emitting and the injected mode of the QDot laser as the injection strength is increased. Moreover, very high on-off contrast ratio is measured in the switching (and bistability) transition of the emission mode of the device. We have also analysed the switching properties of the 1310-QDot DFB laser as a function of the applied bias current and the initial wavelength detuning between the wavelengths of the external signal and that of the device's injected mode. In general, wider bistable loops, higher on-off contrast ratio between output states and higher input power requirements for switching are observed as the applied bias and initial detuning are increased. This diversity of switching behaviors obtained with a 1310 QDot DFB laser under external optical injection, added to the theoretically superior properties of nanostructure lasers, offers exciting prospects for novel uses of these devices in all-optical logic and all-optical switching/routing applications in present and future optical telecommunication networks.

8619-39, Session 10

Amplification and lasing in nanoplasmonics and metamaterials: an overview (Invited Paper)

Ortwin Hess, Imperial College London (United Kingdom)

Nanoplasmonics and optical metamaterials have in the last 10-15 years emerged as a new paradigm in condensed matter optics and nanoscience, offering a fresh perspective to the optical world. They enable the efficient coupling of light fields to the nanoscale, the world of biological or other inorganic molecules [1]. This tight light localisation on truly nanoscopic dimensions ? well below the diffraction limit of light ? enhances its interaction with matter, paving the way for a multitude of classical and quantum nano-optics applications. However, metal optics suffers from inherent dissipative losses and only recently theoretical [2,3] and experimental [4] advancements have shown that it is realistically possible to overcome dissipative losses of nanoplasmonic metamaterials, even in the exotic negative-index regime. If the gain supplied by the active medium is sufficient to overcome dissipative and radiative losses, the structure can even function as a coherent emitter of surface plasmons over the whole ultrathin 2D area, well below the diffraction limit for visible light [5,6].

The talk will give an overview of recent advances in the field of gain-enhanced plasmonics and optical metamaterials and show that these constitute an exciting new frontier in nanophotonics and nanoscience, and are precursors towards active, integrated quantum nano-optics¹. Bringing gain on the nanoscale is anticipated to improve the performance of a host of active nano-components, such as electro-optic modulators and light sources, but also passive ones, such as plasmonic waveguides or sensors featuring intensified plasmonic hotspots for single-emitter spectroscopy.

1. O. Hess, et al., Active nanoplasmonic metamaterials, *Nature Materials* 11, pp. 573-584, 2012. doi:10.1038/nmat3356
2. S. Wuestner, A. Pusch, K. L. Tsakmakidis, J. M. Hamm, and O. Hess, Overcoming losses with gain in a negative refractive index metamaterial, *Phys. Rev. Lett.* 105, p. 127401, 2010. doi:10.1103/PhysRevLett.105.12740
3. J. M. Hamm, S. Wuestner, K. L. Tsakmakidis, and O. Hess, Theory of Light Amplification in Active Fishnet Metamaterials, *Phys. Rev. Lett.* 107, p. 167405, 2011. doi:10.1103/PhysRevLett.107.167405
4. S. Xiao, et al., Loss-free and active optical negative-index metamaterials. *Nature* 466, pp. 735-738, 2010. doi: 10.1038/nature09278
5. A. Pusch, S. Wuestner, J. M. Hamm, K. L. Tsakmakidis, and O. Hess, Coherent Amplification and Noise in Gain-Enhanced Nanoplasmonic Metamaterials: A Maxwell-Bloch Langevin Approach, *ACS Nano* 6, 2420-2431, 2012. doi:10.1021/nn204692x
6. S. Wuestner, et al., Control and dynamic competition of bright and dark lasing states in active nanoplasmonic metamaterials, *Phys. Rev. B* 85, p. 201406(R), 2012. doi: 10.1103/PhysRevB.85.201406

8619-40, Session 10

The physics of plasmonic lasers (Invited Paper)

Rupert F. Oulton, Imperial College London (United Kingdom)

Lasers have recently been scaled in size beyond the diffraction limit of light by using electromagnetic surface excitations of metals. In this talk, I will discuss our approach to constructing "plasmonic" lasers using semiconductor materials and outline potential applications. In particular, I will focus on the physics of plasmonic lasers, which is rich with interesting effects due to the strong interaction of nanoscale light and matter. Such devices could be the most efficient and compact method of delivering optical energy to the nanoscale. There are two benefits: firstly, the efficiently generated (focused) coherent laser field can be extremely intense; and secondly, vacuum fluctuations within the laser cavity are considerably stronger than in free space. Consequently, plasmonic lasers have the unique ability to drastically enhance both coherent and incoherent light-matter interactions bringing fundamentally new capabilities to bio-sensing, data storage, photolithography and optical communications. While there is a great deal of research to do on plasmonic laser systems, this talk highlights the feasibility of nano-scale light sources and the potential to do laser science at the nanoscale.

8619-41, Session 10

Electrically driven plasmonic nanocircuits (Invited Paper)

Mark Brongersma, Geballe Lab. for Advanced Materials (GLAM) (United States)

Metallic nanostructures are well-known for their unparalleled ability to concentrate light into deep subwavelength volumes. This property is derived from the unique optical behavior of metals that allows for collective electron excitations, known as surface plasmons. In this presentation, I will illustrate the use of plasmonic, structures in combination with semiconductor, and dielectric nanostructures in a variety of applications (nanoscale sources, high-speed modulators, and detectors) and discuss their relative strengths and weaknesses.

**Conference 8619:
Physics and Simulation of Optoelectronic Devices XXI**

8619-42, Session 10

Low-threshold semiconductor plasmonic nanolasers (*Invited Paper*)

Shangjr Gwo, Yu-Juang LU, National Tsing Hua Univ. (Taiwan); Jisun Kim, The Univ. of Texas at Austin (United States); Hung-Ying Chen, National Tsing Hua Univ. (Taiwan); Charlotte E. Sanders, Chihhui Wu, Nima Dabidian, The Univ. of Texas at Austin (United States); Chun-Yuan Wang, Ming-Yen Lu, National Tsing Hua Univ. (Taiwan); Wen-Hao Chang, National Chiao Tung Univ. (Taiwan); Lih-Juann Chen, National Tsing Hua Univ. (Taiwan); Gennady B. Shvets, Chih-Kang Shih, The Univ. of Texas at Austin (United States)

Scaling down semiconductor lasers in all three dimensions holds the key to the development of compact, low-threshold, and ultrafast coherent light sources/amplifiers. However, the minimum size of conventional semiconductor lasers utilizing dielectric cavity resonators is limited by the diffraction limit. Recently, it has been proposed and experimentally demonstrated that the use of plasmonic cavities based on metallodielectric structures can break this limit. But it remains to be seen whether one can indeed overcome the high losses in three-dimensional-confined, deep-subwavelength plasmonic cavity with the currently available metals and semiconductor gain materials. In this talk, we report on the use of atomically smooth, epitaxial Ag films grown on Si substrates to fabricate low-loss plasmonic cavities. In particular, by using single shape-controlled InGaN/GaN core-shell nanorods as laser/spaser gain media in the full visible spectrum, we are able to realize spaser-enabled metal-oxide-semiconductor (MOS) nanolasers that can be operated with an ultra-low continuous-wave threshold power (<1 kW/cm²) above liquid nitrogen temperature and well-defined lasing/spasing modes. In these record-semiconductor nanolasers, the record-small cavity and mode volumes are orders of magnitude smaller than the diffraction limit and the feature sizes are comparable with that of the state-of-the-art MOS transistors used in nanoelectronics.

8619-43, Session 11

3D full-wave optical and electronic modeling of organic bulk-heterojunction solar cells: a predictive approach

Wee Shing Koh, Yuriy Akimov, A*STAR Institute of High Performance Computing (Singapore); Wei Peng Goh, A*STAR Institute of Materials Research and Engineering (Singapore) and Nanyang Technological Univ (Singapore)

A predictive approach using 3D full-wave optical and electronic modeling of an organic bulk-heterojunction photovoltaic device (in the configuration Glass/ITO/PEDOT:PSS/P3HT:PCBM/Ca/Ag) is presented. The optical part is modeled by solving 3D frequency domain Maxwell's equations such that the scattering of subwavelength nanostructures can be modeled accurately. The electronic simulation which consists of solving the rate equations to account for the generation and recombination of polarons or charges, and the flow of electrons and holes are assumed to be drift-diffusion in nature. It has to be noted that the both geminate and non-geminate recombination models has been applied to describe polaron recombination and the difference and applicability of both implementations in the model will be presented. The planar model is then calibrated with experimental data such that both the dark and illuminated current-voltage (I-V) curves coincide with simulation results pretty well.

With the aid of the model, we demonstrate the impact of the addition of Ag nanoparticles with subwavelength sizes into the P3HT:PCBM bulk-heterojunction device. We will also illustrate and relate both the optical measure (i.e. optical absorption in the P3HT:PCBM active layer) and the corresponding electrical measure (i.e. I-V behavior) predicted by the simulation model. Localized enhancement in absorbed power due to the presence of the Ag nanoparticles near the active layer (which

leads to enhanced polaron generation) will be demonstrated and its corresponding influence on the electrical characteristics of the organic bulk-heterojunction photovoltaic device will be discussed.

8619-44, Session 11

Study of silicon solar cell top and bottom grating location

Michael J. Marshall, Xiaomin Jin, California Polytechnic State Univ., San Luis Obispo (United States)

This study examines optical power absorption in a silicon solar cell utilizing single and double diffraction gratings at varying locations (depths) within the device. The solar cell under discussion consists of a rectangular top grating, P-type Si, N-type Si, a rectangular bottom grating, and a reflective material on the bottom. We use 3D finite differential time domain (FDTD) simulations to calculate the power at the PN interface at wavelengths ranging from 300nm to 1100nm. Throughout simulation, the structure of the gratings remains unchanged, only its location within the device varies, which is accomplished by varying the thickness of the N and P regions. We take the spectrum of incident solar light and the photo-responsivity of silicon into account to obtain a total weighted power factor, allowing comparison between all simulated cases. We find an increase in weighted power absorption (compared to the no-grating case) ranging from 64% to 102% across all simulated grating locations. Overall, our simulations show that varying the location of the grating(s) changes the amount of power absorbed, and that certain device thicknesses correspond to increased power absorption, which can be used in the solar cell design.

8619-58, Session PWed

Laser beam bending cylindrical gradient curved lens under atmospheric conditions

Remzi Yildirim, Yildirim Beyazit Univ. (Turkey)

We propose that in this experimental study, we add a new feature, "bending" in addition to the widely known basic characteristic of light. This can be the symptoms of sub-atom pieces or particles that we may not notice in relation to the structure of light in the current models of physics. In another perspective, we think that it is a system, which is formed by a flexible symmetric structure made up of photon and sub-atom pieces or particles, different from the known light model of wave and photon. We also think that in this system, the sub-atom pieces or particles, which we cannot know or name as yet, are very effective in the physical structure of light. These pieces or particles, when they are aimed towards the weak point of the flexible structure that forms light, can change the physical structure of the light. We are of the opinion that bending occurs via affecting the weak point of the flexible symmetric structure of the light through the lenses, thereby causing a physical corruption in this flexible symmetric structure. These unknown sub-atom pieces or particles, in some critical situations, have so strong effects as to make the light gain a permanent physical characteristic. Therefore, it is possible that in this case "Asymptotic freedom", "Nucleus Democracy" or "Tuning" theories appear. For this special case, we propose a new term. We call this "Basic Particle Freedom". We defined "Basic Particle Freedom" as the free hand behavior of the same and identical particles in the particle ocean of element,

In this experiment, we just determined the case that we observed. We would like to share and discuss the findings of the experiment with other scientists interested in this issue and look forward to their support, suggestions and criticism.

8619-59, Session PWed

Tailoring coaxial fiber parameters for gain flattening in erbium doped fiber amplifiers

Jyoti Anand, Enakshi K. Sharma, Jagneet K. Anand, Univ. of Delhi South Campus (India)

We propose use of coaxial fibers for gain flattening in an Erbium Doped Fiber Amplifier (EDFA). In coaxial fibers, the rod and tube form two independent waveguides which can be chosen to be single moded and synchronous at a phase matching wavelength $\lambda = \lambda_{ph}$. The fiber parameters are chosen such that phase matching wavelength coincides with the peak of the EDF spectrum, i.e., typically around 1530 nm. A coaxial fiber doped with Erbium ions only in rod can be used for inherent gain flattening as well as gain enhancement. The two waveguides are coupled through their evanescent field and hence, the power launched into the rod waveguide for wavelengths around $\lambda = \lambda_{ph}$, couples back and forth between rod waveguide (which has gain) and tube waveguide, as it propagates along the length. Hence, when a large number of signal wavelengths propagate simultaneously through coaxial EDF, the gain for wavelengths around λ_{ph} (~1530nm) is reduced. The corresponding stimulated emissions by wavelengths around 1530nm are also reduced and hence there is an increase in gain at other wavelengths due to availability of population inversion for those wavelengths. This results in inherent gain flattening as well as an increase in average gain across the 1540-1560nm band. We achieved a gain excursion of ± 1.68 dB over a band of 40nm ranging from 1525nm to 1565nm in comparison to ± 5.36 dB for a single core EDFA.

8619-60, Session PWed

Intensity modulation response of injection-locked quantum cascade lasers

Cheng Wang, Frédéric Grillot, Jacky Even, Institut National des Sciences Appliquées de Rennes (France)

Quantum cascade lasers (QCLs) are promising laser sources for applications in optical communication, imaging and remote sensing [1]. Although the directly modulated bandwidth up to terahertz has been predicted theoretically [2, 3], recent results show that the bandwidth is limited to only tens of gigahertz [4, 5]. It is attractive to employ the injection-locking technique in QCLs, which has already been proved to be an effective approach for improving the modulation characteristics of interband lasers [6, 7]. This paper aims to theoretically study the modulation properties of injection-locked QCLs. Unlike recent theoretical studies [8], the model in this paper takes into account three levels in the QCL structure [9], which are coupled with the injected photons as well as the phase difference between the slave and the master lasers. The modulation transfer function is obtained from a small signal analysis. Calculations show that the modulation bandwidth can be enhanced by increasing the injection strength, while the frequency detuning is found to have little impact on the modulation bandwidth. Both positive frequency detuning as well as large linewidth enhancement factor (LEF) leads to the peak occurrence without exhibiting pre-resonance frequency dip in the modulation response. As opposed to interband lasers, calculations also point out that injection-locked QCLs do not show any unstable regimes in the locking range, while large LEF can enlarge both the locking and the stable regimes. Besides, slow carrier removal rate from the lower subband can well raise the modulation bandwidth at the expense of high threshold current.

8619-61, Session PWed

Numerical modeling method for the dispersion characteristics of single-mode and multimode weakly-guiding optical fibers with arbitrary radial refractive index profiles

Raushan Mussina, David R. Selviah, F. Anibal Fernández, Univ. College London (United Kingdom); Anton G. Tjihuis, Bastiaan P. de Hon, Technische Univ. Eindhoven (Netherlands)

Accurate, reliable and fast numerical modeling methods are required to design the optimum radial refractive index profile for single and multimode fibers to give specific dispersion characteristics without the need for costly experimental work. Such profiles include graded index and multiple concentric cladding layers. In this paper, a new numerical method is introduced which enables the derivatives of the propagation coefficient to be calculated up to the third order of a single mode or multimode weakly guiding optical fiber having an arbitrary radial refractive index profile, which are required to determine the group delay, τ_g , chromatic dispersion, D , and dispersion slope of the fiber. Having expanded the modal fields in terms of Laguerre-Gauss polynomials in the Galerkin method, the new approach offers certain benefits: due to simplicity of the basis functions it is possible to carry out further analytical work on the results such as repeated differentiation of the matrix equation resulting from the Galerkin method to define the first, second and third-order derivatives of the propagation coefficient with respect to wavelength. This avoids the approximation errors inherent in numerical differentiation, giving better accuracy and, at the same time, significantly reducing the computation time. A computer program was developed to demonstrate the proposed method for single and multimode fibers with radially arbitrary refractive index profiles. The paper provides simulation results to validate the approach and compares the simulation results with available experimental and published data.

8619-63, Session PWed

FBG pressure sensor of high pressure electric oil pumps for prestressing

Zhenwu Guo, Fuwei Ge, Guangwei Liu, Weixiang Li, Nankai Univ. (China)

Prestressed concrete structure is getting more and more extensive application in architecture, hydraulic engineering and traffic engineering because of its significant advantages of crack later or not cracks completely. It is an internal stress concrete structure that a certain force relies on prestressing tendons. The effectivity of the prestressing tendon in concrete structure is directly related to the reliability, applicability and viability of the whole concrete structure. So it is a key program to apply accurate prestress to the prestressing tendon. According to the pressure sensing principle of the fiber Bragg grating (FBG), a circular plate diaphragm-based FBG sensor for high pressure electric oil pumps that is the pressure source device of the prestressed concrete structure was presented. To overcome the cross sensitivity of temperature and pressure, two FBGs were integrated in the sensor, one of the FBGs isolated from the pressure is used as temperature compensation grating, it is called temperature-FBG comparing to another FBG called pressure-FBG. The elastic diaphragm was chosen as the pressure sensing element whose distortion displace is proportional to the difference of the two sides' pressure of the diaphragm. A certain stress is applied to the pressure-FBG which is stuck to the center of the diaphragm, and then the reflection wavelength of the pressure-FBG is inverse proportional to load of the diaphragm. The results indicated that the linearity is up to 99.99%, and the pressure sensitivity coefficient is 0.024nm/MPa within the measurement scope of 0-70MPa.

8619-64, Session PWed

Optofluidic-core hi-bi photonic crystal fiber for refractive index sensing

Christos Markos, Univ. of Patras (Greece) and National Hellenic Research Foundation (Greece); Kyriakos G. Vlachos, Univ. of Patras (Greece); George Kakarantzas, National Hellenic Research Foundation (Greece)

In this work, we present a design where an optofluidic channel is embedded in the core of an all-silica highly-birefringent PCF. By modifying the analyte in the hollow channel, the birefringence of the fiber will directly be affected maintaining the index-guidance of the fiber. We have numerically investigated the guiding properties of the proposed structure using the Finite Difference Method (FDM) for different hollow channels ($d_c = 0.8 \mu\text{m}, 1, 1.3, 1.6 \mu\text{m}$) to act as refractive index (RI) sensor. All the calculations performed at C-band. The range of the RI varied from 1.3 - 1.46, providing this way a dynamic range of $\Delta n \sim 0.16$ where analytes with RI higher than silica can be still detected. For the case of $d_c = 1.6 \mu\text{m}$, there is a dramatic change of birefringence over a wide dynamic range of $\Delta n \sim 0.16$, which can be as high as $\sim 0.004/\text{RIU}$ (defined as change in birefringence per RIU) from 1.3-1.42. The main advantage of the presented sensor is that can be used for lower and higher refractive indices than the host material (in this case fused silica) over a wide dynamic range while it can be potentially used for biosensing applications as well. The case of using microstructured polymer optical fiber (mPOF) as the host material will be also discussed and compared to silica PCF.

8619-65, Session PWed

Design of a compact polarization splitter composed of multiple-slotted waveguide and silicon nanowire

Jiayuan Wang, Jinbiao Xiao, Southeast Univ. (China); Xiaohan Sun, Southeast Univ (China)

A compact polarization splitter (PS) based on a directional coupler (DC) composed of vertical multiple-slotted waveguide (MSW) and silicon nanowire is proposed and designed by using a modified three-dimensional full-vectorial beam propagation method. For the vertical MSW, the modal distributions for the quasi-TE modes are strongly confined in the slots and those for the quasi-TM modes are almost spread through the entire core. Therefore, for quasi-TE modes, the effective indexes of the slot waveguides greatly differ from those of the silicon nanowires, while for quasi-TM modes, they can be almost identical. As a result, the coupling of the DC in quasi-TE modes can be almost neglected, and only that in quasi-TM is considered. When light is injected from the input port, the quasi-TE mode passes through without coupling while the quasi-TM mode couples to the cross waveguide as it transmits the coupling length of the quasi-TM mode, leading to a compact PS. Moreover, the condition of the evenly spaced effective indexes like that published earlier is not necessary so that it is easier to determine the structural parameters. In addition, the MSW is utilized in our design rather than single-slotted waveguide because the former can enhance the optical confinement inside the slot regions and thus result in higher birefringence, which then leads to a reduction in length for the present device. To our knowledge, there has no attempt so far to design a PS by using such a waveguide structure. The numerical results show that a PS with a length of $20.5 \mu\text{m}$ in the coupling region is achieved, and the crosstalks are up to -23.3dB and -33.4dB for the quasi-TE and quasi-TM modes, respectively.

8619-66, Session PWed

Polarization engineering in group-III-nitride based ultraviolet light-emitting diodes

Yu-Rui Lin, National Changhua Univ. of Education (Taiwan); Bo-Ting Liou, Hsiuping Institute of Technology (Taiwan); Jih-Yuan Chang, Yen-Kuang Kuo, National Changhua Univ. of Education (Taiwan)

Group III nitrides are promising for several critical applications due to the inherent characteristics of direct and wide bandgap energy. By tuning the compositions of aluminum (Al), gallium (Ga) and indium (In), high degree-of-freedom in designing bandgap energy, lattice constant and polarization is feasible. Especially, group-III-nitride material system is one of the best candidates as the active region for UV and deep UV LEDs. However, the problems regarding the large lattice mismatch of epilayers grown on common sapphire substrate and the corresponding polarization issues still need to be solved. In this study, the polarization engineering in active region is investigated via theoretical investigation. The advantage of quaternary AlInGaN material is discussed. Simulation results show that, through the employment of properly designed quaternary AlInGaN material in active region for UV LEDs, the polarization mismatch between hetero-layers can be efficiently mitigated. Moreover, because of the reduced polarization effect, not only the hole injection efficiency is improved, but also the electron leakage can be suppressed because the effective potential height for electrons is increased. The band diagrams carrier concentrations, radiative and non-radiative recombination rates, and internal quantum efficiency (IQE) are also studied.

8619-67, Session PWed

Plasmonic ring laser cavity with tiny footprint

Xudong Liu, Feifei Shi, Zhaoyu Zhang, Peking Univ. Shenzhen Graduate School (China)

We design a type of plasmonic ring laser which has the footprint smaller than previous published, showing the potential of single-mode operation and being an ultra-compact light source. In this structure, CdS gain medium and Ag substrate are separated by thin MgF₂ layer to mitigate the radiation loss. The short distance between high-index CdS material and silver makes photonic modes of CdS ring hybridize with surface plasmon polaritons (SPPs) of the Ag-MgF₂ interface, which leads to strong light confinement in thin MgF₂ gap region. The surface plasmons of this structure carry high momentum leading to strong feedback at the ring boundary by total internal reflection forming whispering gallery like mode. Finite difference time domain method (FDTD) is used for the calculation. Different plasmonic ring parameters are calculated and optimized. With a 15 nm thick MgF₂ layer, the ring's outer and inner radius can be shrunk to 310 nm and 190 nm with quality factors of 40 at the resonant wavelength of 498 nm. With the MgF₂ thickness decreases and the ring's width fixed, the radius of ring has to decrease to fit with CdS spontaneous emission. When MgF₂ thickness decreases to 10 nm, the outer and inner radius is 250 nm and 130 nm, and the quality factor reduces to 32. FSR of the ring is around 45 nm, which shows a good ability to pick the resonance wavelength from a broadband electromagnetic wave. Their highly confined optical fields can significantly enhance light-matter interactions and getting high Purcell factor.

8619-68, Session PWed

On-line scanned probe microscopy transparently integrated with DualBeam SEM/FIB systems

Aaron Lewis, Hebrew Univ. of Jerusalem (Israel); Anatoly Komissar, Andrey Ignatov, Nanonics Imaging Ltd. (Israel)

A multifunctional scanning probe microscope (SPM) will be described that transparently integrates with a DualBeam SEM/FIB System. This is done without perturbing any of the capabilities of the Dual Beam in terms of detectors, gas injectors, analyzers etc while allowing for a completely exposed probe tip to be imaged online even with immersion objectives at working distances as short as 4 mm.

An additional integral part of the design is electron/ion beam friendly probes with unique characteristics. The functional capabilities of these probes will be described. All such probes are slender, long (>60 microns) with an axial ratio that can be as high as 10:1. All such probes designed for this combination of SPM with SEM/FIB have highly exposed probe tips. This, combined with the Z extent of the AFM imaging provides deep trench capabilities especially important for FIB fabrication. The system allows for standard imaging modalities such as elasticity and data on the relative elasticity of copper on silicon will be presented. Within the class of probes that have been implemented with SEM are probes for nanometric optical near-field imaging (NSOM) and data on GaN wires excited by electron beams will be shown as part of this presentation. Other functionalities existing for such probes exist such as thermal, magnetic and electrical.

Such a combination of SPM with the Dual Beam capabilities of SEM/FIB is in effect a new form of analytical instrument which pertends to be a disruptive technology affecting the potential of electron, ion and even scanned probe applications in fundamental and applied science.

8619-69, Session PWed

Fabrication of nanocomposite by graphene for infrared detection device

Sana M. Baleg, Univ. Teknologi Malaysia (Malaysia)

The novel properties of graphene with plasmonic nanostructures have potential application in enormous optoelectronic devices in recent years. Since it has constant absorption for a wide range of spectrum from visible wavelength range to infrared wavelength range potentially allow its application to detect over broad wavelength operating at height frequencies. Herein, brief review is given on the recent research progress of graphene as the novel ultrafast photodetector and this work focused on some of the main working principle relating to realization of graphene-based device and we will show by combining graphene-based photodetectors with metal nanostructures and laser technique lead to enhance the performed of detecting.

Graphene is the fascinating material in this decade for its peculiar electronic properties and potential use in future electronic devices [1]. It is the newest numbers in two-dimensional (2D) carrier systems. However, it has several shortcomings such as high carrier mobility and Fermi velocity allows ultra-fast operation speed [2,3,4]. Moreover the optical properties of graphene are remarkable constant absorption of 2.3% per monolayer over wide range of spectrum at least from the visible wavelength to near infrared wavelength[5], that make it the ideal photodetector device due to absence of a cut-off wavelength. The photoelectrical response of graphene has been widely investigated both experimentally and theoretically [4]. Responses at wavelength of 0.514, 0.633, 1.55 and 2.4 μm have been reported [6]. However, the maximum possible operation bandwidth of photodetectors is typically restricted by their transit time; the finite duration is typically photogeneration current [7]. The common problem for traditional photodetector is low responsivity[8], the generation and transport photocarrier in graphene differ fundamentally from those in photodetectors that made from conventional semiconductors.

The graphene ultra photodetectors is based on the presence of long-range band-bending caused by charge transfer doping at metal contacts [9]. This is include a Fermi-level relaxed back to the initial doping level[10]. While the photoexcitation in graphene is followed repaired e-h recombination, excitation near to the contacts lead to current because the build in field separate the electrons and holes[11]. It involves depositing on graphene layers different metal contacts one with high and one with low work function, the two different work functions lead to different band-bending generate an internal field that allows photodetection over entire face of the device, and allow large photocurrent to be generate as shown in Figure 1a. In a symmetric device, the simultaneous illumination both contacts produce equal but opposite polarity current and there no net photocurrent. so the improvement design by using different work function electrodes. In the vicinity of contacts, the photodetectors is responsive to incident light and a photo voltage/-current is produced. The working principle of graphene photodetector relies on the making p-n junction by separate the incident light to electron-hole pairs[12]

8619-70, Session PWed

Estimation of amplified spontaneous emission in erbium doped fibers with phase sensitive structures

Amita Kapoor, Rashmi Singh, Univ. of Delhi (India); Enakshi K. Sharma, Univ. of Delhi South Campus (India)

In recent years, wavelength division multiplexing (WDM) has captivated attention due to increasing demand for fiber optic communication. The key device supporting WDM technology is an Erbium doped fiber (EDF) amplifier. An erbium-doped fiber (EDF) behaves as an optical amplifier in the wavelength around 1.53 μm with a bandwidth of about 40 nm, making it a necessary component of all optical communication systems. However EDF has two major disadvantages, non-uniform gain spectrum and amplified spontaneous emission (ASE) which degrades the signal to noise ratio (SNR). Conventionally to estimate ASE noise its power spectra is considered. The total ASE power, at any point z along the fiber is sum of the ASE power from previous sections and the ASE noise power generated locally. This amplified ASE propagates in both directions and is referred to as forward (positive z direction) and backward ASE (negative z direction). This approach completely ignores the fact that ASE generated locally also has a random phase. The phase of the locally generated noise is very important in the analysis of recently proposed gain flattening structures with long period grating (LPG) written in EDF itself. In this paper we propose a method which estimates the ASE taking into consideration the physical mechanism contributing to the generation of ASE. In our approach, ASE at any point z along the fiber is sum of the ASE amplitudes from previous sections and locally generated spontaneous emission with a random phase at each section of the EDF. In order to validate this approach, we have compared the results obtained for the EDF using our approach with those obtained by the standard power coupled equations.

8619-71, Session PWed

EELS investigation of surface plasmon excitation on silver nanowire

Xiuli Zhou, Univ. of Michigan (United States)

We have investigated electronic energy loss induced by electron beam passing close to Ag nanowires. Electron energy loss spectrum (EELS) in terms of the local density of electromagnetic states (LDOS) in the vicinity of nanowire verifies the collective surface Plasmon (SP) resonance excitations. Lower energy excitations between zero loss peak (ZLP) and the silver SP resonance frequency are quantized as resonance modes with energy filtered TEM (EFTEM). The mapping images of the Plasmon field distributions in the defined field on the structures evidences the gradual evolution of the SP resonance.

**Conference 8619:
Physics and Simulation of Optoelectronic Devices XXI**

J M Pitarke's theoretical discussion model on the nano sphere and infinite long nano cylinder are used to understand the energy loss and one theoretical calculation modeling Ag nanowire with light-induced SP excitation is conducted to compare the SP excitation. The data from theoretical analysis and simulation proved the measured EELS. It shows the localized non symmetrical nano structure effect and the electron beam trajectories are important factors to study the EELS, and multipole resonances are the main resonant modes when electron beam is very close to the silver surface or on the edges of the nanowire. The difference between the electron beam-induced resonance and light-induced resonance shows the multipole resonance is dominant because of the highly localized electron beam excitation and dipole resonance is the dominant resonance from the light irradiation. The energy dispersions relation of the resonant modes near the Ag nanowire suggest a good approach to investigate some other coupling effects from the semiconductor Quantum Dots resonance by simply coating them on Ag nanowire.

8619-72, Session PWed

A discrete transmission-matrix method for modeling the distributed feedback arising from continuously varying refractive index profiles

Derek S. Heeger, Robert M. Bunch, Paul O. Leisher, Rose-Hulman Institute of Technology (United States)

Several methods exist for modeling the Fresnel reflectance arising from arbitrary refractive index profiles. In many cases, the calculation can be done analytically; however, a numerical method must be employed for more complicated scenarios. The transmission matrix is an analytic method which is well suited for modeling reflection at abrupt interfaces. In this work, we develop a numerical approach, relying on the transmission matrix method, which can properly model the reflection and transmission properties of a continuously varying index profile. This approach has been applied to high power semiconductor lasers by modeling the built-in distributed feedback arising from the continuously mismatched wave impedance along the cavity length caused by a non-uniform temperature profile.

8619-73, Session PWed

Optimization of AlGaIn/GaN superlattice electron blocking layers by genetic algorithm for high-efficiency GaN-based light-emitting diodes

Dong-yeong Kim, Junhyuk Park, Sunyong Hwang, Jong Kyu Kim, Pohang Univ. of Science and Technology (Korea, Republic of)

The efficiency droop at a high current density is a big challenge for high power applications of GaN-based light-emitting diode (LED). Electron overflow is regarded as one of the dominant causes of efficiency droop. To suppress the electron overflow, p-type AlGaIn electron blocking layer (EBL) is typically used, however, it unlikely blocks electrons efficiently, besides it does suppress hole injection into active region. This is attributed to uncompensated polarization dipole at GaN/AlGaIn interface, which pulls down the energy band, and low p-type doping concentration in typical bulk AlGaIn layers. Various EBL structures were suggested to enhance hole injection efficiency as well as to reduce electron overflow such as AlGaIn EBL with graded Al composition and AlGaIn/GaN superlattice (SL) EBL. However, no systematic effort to find an optimal EBL structure has been made since many parameters should be considered simultaneously for optimization.

In this study, we use a genetic algorithm (GA) to explore optimized AlGaIn/GaN SL-EBL structures for LEDs with high efficiency and low efficiency droop. The GA optimization creates a random population of potential AlGaIn/GaN SL EBL structures with various periods, Al

compositions, thicknesses, and p-doping levels, and then determines the fitness of each EBL against the figure of merit – in this study, combination of efficiency and efficiency droop estimated by a self-consistent Schrodinger and Poisson equation solver -. Then, it replaces a fraction of worst performing EBLs with the genetic offsprings and repeats this until good convergence on the design parameters is achieved. GaInN/GaN multiple quantum well LEDs with the GA-optimized AlGaIn/GaN SL EBLs were grown on c-plane sapphire substrates by metal organic chemical vapor deposition. Improved performances in terms of I-V characteristics, internal quantum efficiency, and efficiency droop behavior of the optimized SL EBL embedded LEDs and their origin will be discussed in detail.

8619-74, Session PWed

Compact polarization rotator based on slotted optical waveguide with buffer layer using surface plasmon polariton

Hong-Seung Kim, Tae-Kyeong Lee, Geum-Yoon Oh, Byeong-Hyeon Lee, Chung-Ang Univ. (Korea, Republic of); Doo Gun Kim, Korea Photonics Technology Institute (Korea, Republic of); Young-Wan Choi, Chung-Ang Univ. (Korea, Republic of)

A novel polarization rotator with asymmetric optical waveguide based on plasmonics is proposed and analyzed for the first time. The polarization rotator using skewing effects at the slotted optical waveguide (SOW) with metal film was designed by 3D-FDTD method. We have analyzed various structures such as a slotted waveguide, a metal-clad optical waveguide with and without buffer layers. A metal film on the waveguide acts to rapidly rotate the optical polarization, because the plasmonic characteristics of a metal film can induce the slow group velocity through the metal-clad optical waveguide. In general, the optical waveguides using plasmonic effects have a large propagation loss. Here, the optical waveguide with a buffer layer is proposed to reduce the propagation loss. The polarization rotator length of 6 μm is among the shortest reported in the waveguide-type polarization rotators. The polarization conversion efficiency of 98.93 % is observed near 1550 nm along with a propagation loss of -0.43 dB. The proposed structure is smaller than previous polarization rotator with asymmetric optical waveguide and is more effective to control polarizations using by plasmonic effects.

8619-75, Session PWed

New method for thermal resistance evaluation of optical components by simple electrical characterisation

Joel Jacquet, Catherine Burcklen, Samuel Spieser, Anthony Philippe, Carl Mugnier, Adrian Iordachescu, Supélec (France)

Semiconductor based components are widely used for active function realization (light source, amplifier, optical receiver,...) and we know that performances of these devices can strongly be affected by temperature variation. Therefore, most of them need to be cooled and an important part of the whole power consumed by the optical module is used by thermo-electronic cooler and associated electronics. Thermal resistance of optical components becomes therefore an important parameter that describes the capacity of the device to dissipate heat.

We propose in this paper to determine experimentally the thermal resistance of any optical components by using a simple electrical characterization of the device. The method has been proposed for thermal resistance determination of electrical components that include a P-N diode junction. The principle is based on V-I characteristic measurements at different temperatures and the use of V(I) junction model as well as signal processing. Preliminary results show that the thermal resistance of an active region alone is much higher than the total thermal resistance that we can measure by other methods.

Analysis of this result shows that this method gives up the possibility to

**Conference 8619:
Physics and Simulation of Optoelectronic Devices XXI**

separate the different contributions to the thermal resistance value. Our method allows the determination of the active region alone. Standard optical measurement based for example on the Fabry Perot modes shift as function of injected electrical power gives the thermal resistance of the whole optical module including the package. Combining both methods allows a better understanding of heat dissipation mechanism in the module.

8619-76, Session PWed

Photon migration and fluorescence resonance energy transfer in CdSe/ZnS quantum dot colloidal systems

Adamo F. Monte, Guilherme A. Alves, Tamiris S. Souza, Arnaldo F. Reis, Djalmir N. Messias, Univ. Federal de Uberlândia (Brazil)

The dynamics of energy spread in material systems plays a fundamental role for optical devices design and many physical studies. Energy Transfer is a very common process in nature responsible for the spread of excitation of energy in several systems. The study of the spatial photon migration as a function of the concentration brings into attention the problem of the energy transfer in quantum dot (QD) embedded systems. By measuring the photon propagation and its spatial dependence it is possible to understand the whole dynamics in CdSe QD systems, and also improve their concentration dependence to maximize energy propagation. Core-shell quantum dots CdSe-ZnS in decane colloidal solutions were used to explore energy transfer phenomena. A confocal microscope was adapted to scan the spatial distribution of emitted luminescence from the sample. The energy migration provided by the luminescence spatial distribution was measured as photon propagation according to the diffusion theory. During the emission and capture processes, the excited states experience spatial migration by photons. We observed that the photon migration length (PML) decreases by increasing the QD concentration, being regarded as a signature of Forster resonance energy transfer (FRET) from the donor QDs to the acceptor QDs. Since we have the PML and its wavelength dependence it is also possible to understand the whole dynamics in the QD embedded systems. These facts demonstrate the great importance of the spatial energy transfer processes besides absorption and capture into the QDs for the improvement of QD-based devices.

8619-78, Session PWed

Rate equation modeling of current injection efficiency in 1.3- μm InAs-InGaAs quantum-dot lasers

Umesh Singh, Univ. of Central Florida (United States); Amit Dikshit, IBM India Private Ltd. (India); Jon M. Pikal, Univ. of Wyoming (United States)

Cavity length vs. inverse of slope efficiency technique is most widely used to extract the injection efficiency in semiconductor lasers which assumes that all the carriers occupy single energy level in the lasers. However, QD lasers contain multiple levels in dots and wetting layer; with intradot capture and relaxation times in picoseconds, which results in the occupation of higher energy levels. In addition to the multiple energy levels, the density of states of each energy level is inhomogeneously broadened, which leads to the broadening of the gain spectrum as a whole. Inhomogeneous broadening is a result of the random size distribution of QDs grown by the self-assembled growth technique. In this work, we present the results of an above threshold multi-level rate equation model developed to understand the effect of inhomogeneous broadening, capture and relaxation time, and gain on the measured low injection efficiencies of InAs-InGaAs based quantum-dot (QD) lasers operating at 1.3 μm .

To study the effect of inhomogeneous broadening on extracted injection efficiency in QD lasers, entire quantum dot ensemble was divided into

energy groups with fixed capture and intradot relaxation times. The model contains the multiple energy levels for each energy group in the dots, as well as levels in the wetting layer. A maximum error of ~ 35 % been simulated between the assumed and extracted injection efficiency using cavity length technique. Therefore, it seems likely, and our model confirms, that the conventional method of extracting the injection efficiency using the cavity length technique may not be accurate for multi-level laser systems.

8619-79, Session PWed

Propagation of a Gaussian pulse in a coaxial optical fiber

Jyoti Anand, Enakshi K. Sharma, Jagneet K. Anand, Univ. of Delhi South Campus (India)

Coaxial fibers have been widely studied as dispersion compensating fibers assuming the excitation and the propagation of only the LP₀₁ supermode which offers a large negative dispersion. However, we note that the coaxial fiber supports both the LP₀₁ and LP₀₂ supermodes and in general both are excited. At a certain wavelength, λ , both the supermodes have the same group velocity and almost equal and opposite group velocity dispersion (GVD). When the coaxial fiber is excited by a Gaussian temporal pulse of spectral spread $\sim 2.5\text{nm}$ and pulse width ($\tau = 1\text{ps}$), from a single mode fiber identical to the rod waveguide of the coaxial fiber, both supermodes are almost equally excited. In each mode each spectral component propagates with its own propagation constant. Due to opposite GVD, the $\pm\Delta\omega$ components of the LP₀₂ mode and $\pm\Delta\omega$ components of the LP₀₁ mode have the same group delay and hence arrive at any distance, z , at the same time. The temporal interference between these components can produce pulses at the beat frequency $\Delta\omega$. The two modes also interfere spatially due to which power oscillates between the rod and tube waveguides of the coaxial fiber. Due to the spatial as well as the temporal interference between the supermodes, the light coupled into a similar output single mode fiber consists of a series of narrow pulses within a broadened Gaussian envelope.

8619-80, Session PWed

Modeling and computation of grating-integrated waveguides in optoelectronic applications

Meng-Mu Shih, Univ. of Florida (United States)

This work presents electromagnetic waveguide models for optoelectronic devices integrated with metallic nano-gratings. The photonic method is utilized to compute the mode-coupling in active and passive devices for wide applications. The guided-wave propagations in devices depend on the diffractive order and mode polarization of light-waves. The eigenvalue systems with Fourier expansions based on light-wave propagations are constructed. A three-dimensionally visualized process of solving the multi-parametric systems is demonstrated. Numerical results show how different structures and materials (organic, semiconductor, metal, hybrid) in gratings and waveguides affect the mode-coupling. Qualitative interpretations of results provide insights into the modeling, computational, and design-for-application issues.

8619-81, Session PWed

Light propagation through AgI nanowires for waveguide applications

Desapogu Rajesh, Univ. of Hyderabad (India)

Nanowire research is an important area in nanoscience and nanotechnology today. Synthesis and characterization of semiconducting nanowires is vital to nanoscience since these materials are essential building units for devices. In this paper we describe the AgI nanowires were synthesized via a simple but effective two step sol-gel process. FESEM, TEM and EDX elemental analysis confirmed the presence AgI nanowire on cover coated glass substrate. As a crucial characterization the SNOM experiments on selected AgI nanowires were performed which confirmed that these could act as potential waveguides for laser light propagation.

8619-82, Session PWed

The photoemission mechanism of multi-alkali cathode

Xiaofeng Li, North Night Vision Technology Co., Ltd. (China)

In this paper, the fluorescent spectrum between multi-alkali cathode with Cs-Sb surface layer and without Cs-Sb surface layer were measured and the phenomena of peak wavelength of the fluorescent spectrum shift to shorter wavelength and intensity of fluorescent spectrum to be become stronger for the multi-alkali cathode with Cs-Sb surface layer were found. This phenomenon shows that in the condition of a multi-alkali cathode with Cs-Sb surface layer, not only the surface work function of multi-alkali cathode has been reduced, but also Na₂KSb structure has been changed. This means that in the conditions of the same wavelength and same incident power irradiation, Na₂KSb with Cs-Sb surface layer could be excited more transition electrons and got higher transition energy levels, so they can escape the multi-alkali cathode surface more easily and have higher probability to access the vacuum. This will lead to higher cathode sensitivity and shows that not only the Cs-Sb surface layer has a surface effect, but also has bulk effects. This effect could be explained by semiconductor band theory. As the Na₂KSb surface was absorbed a layer of Cs-Sb, the distortion of lattice of Na₂KSb surface would be taken place. This would lead to change in energy band structure of Na₂KSb layer. To further increase the sensitivity of multi-alkali cathode, it is need to further improve the performance of Na₂KSb layer in addition to further reduce surface work function of the multi-alkali cathode, so that more transition electrons and higher energy transition levels could be obtained.

8619-84, Session PWed

Basis functions for solution of non-homogeneous wave equation

Sina Khorasani, Sharif Univ. of Technology (Iran, Islamic Republic of); Farhad Karimi, Univ. of Wisconsin, Madison (United States)

In this note we extend the Differential Transfer Matrix Method (DTMM) for a second-order linear ordinary differential equation to the complex plane. This is achieved by separation of real and imaginary parts, and then forming a system of equations having a rank twice the size of the real-valued problem. The method discussed in this paper also successfully removes the problem of dealing with essential singularities, which was present in the earlier formulations. Then we simplify the result for real-valued problems and obtain a new set of basis functions, which may be used instead of the WKB solutions. These basis functions not only satisfy the initial conditions perfectly, but also, may approach the turning points without the divergent behavior, which is observed in WKB solutions. Finally, an analytical transformation in the form of a matrix exponential is presented for improving the accuracy of solutions.

8619-45, Session 12

Design of high sensitive surface plasmon resonance sensor with metallic nanostructure

Byeong-Hyeon Lee, Geum-Yoon Oh, Hong-Seung Kim, Tae-Kyeong Lee, Young-Wan Choi, Chung-Ang Univ. (Korea, Republic of)

Surface plasmon is a collective charge density oscillation on a nano-metallic structure excited by incident light. When in a resonant condition, the incident light is highly absorbed and loses a fair amount of its energy, resulting in a dip in the intensity profile of the reflected light. This phenomenon is called the surface plasmon resonance (SPR). The SPR has been an essential technology in chemical and bio-chemical sensing, pharmaceutical research, and environmental monitoring area. It has many major features, such as high sensitivity, real time detection, and non-labeling. More development of different types of SPR sensors have been done recently, which are comparable to or better than the conventional SPR sensors in terms of sensitivity and compactness.

Localized surface plasmon resonance (LSPR) is collective electron charge oscillation in metallic nano-particles that is excited by light. It exhibits enhanced near field amplitude at a resonant wavelength. The resonant condition of LSPR is very sensitive to the size of nano-particles, the refractive index of dielectric around the nano-particles, and the wavelength of light.

In this paper, we have designed the metallic nano-structures on a conventional SPR sensor to induce the LSPR for an improved sensitivity. We optimized the parameters of nano-structures for the best sensitivity and analyzed the structure using the 3D finite-difference time-domain method for the exact characteristic. More detailed results will be presented.

8619-46, Session 12

Single and multiprobe apertureless thermal imaging of electromagnetic excitation over a wide range of wavelengths

Aaron Lewis, Hebrew Univ. of Jerusalem (Israel); Rimma Dekhter, Sophia Kokotov, Patricia Hamra, Boaz Fleischman, Hesham Taha, Nanonics Imaging Ltd. (Israel)

Near-field optical effects have generally been detected using photodetectors. There are no reports on the use of the temperature changes caused by electromagnetic radiation using thermal sensing probes for scanned probe microscopy. In this paper we apply our development of such probes to monitor the effects of electromagnetic radiation at a number of different wavelengths using the heating caused in a sample by specific wavelengths and their propagation. The paper will catalogue effects over a wide spectrum of wavelengths from the near to mid infrared. The method has been applied from devices to molecules. The thermal sensing probes are based on glass nanopipettes that have metal wires that make a contact at the very tip of a tapered glass structure. These probes are cantilevered and use normal force tuning fork methodology to bring them either into contact or near-contact since this feedback method has no jump to contact instability associated with it. Data will be shown that defines the resolution of such thermal sensing to at least the 32 nm level. In addition the probes have the important attribute of having a highly exposed tip that allows for either optical sensing methodologies with a lens either from directly above or below or heat sensing with a single or additional probe in a multiprobe scanning probe system. With such a system it will be shown that apertureless infrared excitation and detection can be affected and results will be shown on a variety of systems including devices and a suspended carbon nanotube. The approach described in this paper has considerable advantages over purely optical methods for both excitation and detection to which it can be directly compared.

**Conference 8619:
Physics and Simulation of Optoelectronic Devices XXI**

8619-47, Session 12

The design and fabrication of the metallic nano-annular structure on the glass and the study of its optical property

Shu-Sheng Lee, Sheng-En Chen, Yi-Kai Huang, National Taiwan Ocean Univ. (Taiwan)

The substrate is very important for many optical metrologies such as surface-enhanced Raman scattering (SERS) and surface plasmon resonance (SPR). The enhanced or concentrated local electric field on a substrate surface is very helpful to the signal improvement. In this research, the metallic nano-cylinder, the nano-hole, and nano-annular aperture structures on the glass have been simulated by the finite difference time domain method (FDTD) first to understand the localized surface plasmon resonance (LSP) of them. The light was set as the normally incident plane wave polarized X-axis direction because the design idea was to fabricate the metallic nano structure on the glass were not only for SERS detection use but also suitable for surface plasmon resonance (SPR). The design parameters for the nano-annular structure were the inner diameter, outer diameter and the thickness of the metal thin film. Therefore, the metallic nano-cylinder and the nano-hole structures on the glass have been simulated to decide the better range of the inner and outer diameter for the nano-annular aperture structure. The simulations for different inner diameters, outer diameters and thickness of the gold film have been done and the better dimension and film thickness which can induce the largest electric field concentration have been chosen. The vertical and horizontal distances between the nano-structures have been decided by the simulation, too. To fabricate the metallic nano-annular aperture structure on the glass, we used electric beam evaporator to coat 2 nm and 5 nm thick chromium (Cr), and 50nm and 60 nm thick gold (Au) films on SF2 glass substrate, respectively. Then, the different nano-annular aperture structures were successfully patterned on them by using focus ion beam (FIB) to etching gold film surface. The transmission spectrometer has been adapted to measurement the substrate to observe the spectrum and to know the optical property of them. Different concentrations of sodium chloride(NaCl) solutions also have been measured on the different substrates, and the shift of the transmission light wave peak was detected. This showed the metallic nano-annular aperture structure on the glass we designed and fabricated has the potential to be applied for the bio-molecule interaction measurement.

8619-48, Session 12

Development and optimization of an integrated Faraday modulator and compensator design for optical polarimetry

Brandon W. Clarke, Brent D. Cameron, The Univ. of Toledo (United States)

In the past, Faraday based optical polarimetry approaches have shown considerable potential for the measurement of optical activity with application towards the noninvasive measurement of physiological glucose concentration. To date, most reported closed-loop systems incorporate separate Faraday components for modulation and compensation requiring two optical crystals. These systems have demonstrated significant stability and sub-millidegree rotational sensitivities, however, the main drawbacks to this approach are the optical crystals (e.g., terbium gallium garnet) can be quite expensive and often custom fabricated induction coils are required. In this investigation, we propose a new design for the Faraday components capable achieving both modulation and compensation in a single crystal device. The design is more compact and is capable of achieving similar performance with low cost commercially available inductive components. To facilitate prototype optimization, our group has developed a finite element model (FEM) that can simulate various physical parameters such as geometry, inductance, and orientation with respect to the optical crystal in order to minimize power consumption and size while maintaining appropriate

field strength. Performance is comparable to existing nonintegrated approaches and is capable of achieving modulation depths $> 1^\circ$ under similar operating conditions and attaining sub-millidegree linear polarization sensitivity. There is also excellent correlation between the FEM and experimental prototype with operational performance shown to be within 1%. The use of FEM simulations allows for the analysis of a vast range of parameters before prototypes are fabricated and can facilitate custom designs as related to development time, anticipated performance, and cost reduction.

8619-49, Session 12

Gold nanoparticle absorption under a nanoscale tip illuminated by surface-plasmon polaritons

Gazi M. Huda, J. Todd Hastings, Univ. of Kentucky (United States)

This research numerically calculated the optical absorption of gold nanoparticles (AuNP) in proximity to an atomic force microscope (AFM) probe, when illuminated by surface-plasmon polaritons (SPP). Metallic (Au) and dielectric (Si) probes were considered, and the SPP was confined to a gold-air interface. Nanoscale probes localize and enhance the electric field between the apex of the tip and the particle and/or the gold substrate. However, this does not always result in enhanced absorption by the nanoparticle; in fact, under a gold tip, the AuNP's absorption can be dramatically suppressed. Although counterintuitive, this result is consistent with prior work analyzing the effect of a nanoscale tip on nanoparticle absorption under total internal reflection.

Fitting the numerical absorption data with the equation of a driven damped harmonic oscillator reveals that the AFM tip modifies both the driving force (F0), consisting of the free carrier charge (q) and the driving field (E), and the overall damping of the oscillator (?). The change in absorption can be understood in terms of the competition between changes in ? and F0. A change in F0 can be interpreted as a modification of either q or E, while a change in ? arises from additional scattering or absorption introduced by the tip. Introducing the metallic tip increases ? and decreases F0, resulting in reduced absorption. Introducing the dielectric tip increases ?, but also increases F0, resulting in overall absorption enhancement. Therefore, one must consider both ? and F0 to control the absorption of nanoparticles illuminated by SPP.

8619-50, Session 13

Auger recombination in bulk InGaN and quantum wells: a numerical simulation study (Invited Paper)

Enrico Bellotti, Boston Univ. (United States); Francesco Bertazzi, Boston Univ. (United States) and Politecnico di Torino (Italy); Michele Goano, Politecnico di Torino (Italy)

The versatility of III-Nitrides semiconductors has led to their use in an increasing number of technologically important applications. Their ability to operate over a wide spectral range from the infrared to the deep ultraviolet has propelled this material system into the field light emitters and detectors. Along with the experimental activity to fabricate and characterize optoelectronic and electronic devices, a number of significant theoretical efforts are underway to understand the novel properties of this material system. Nitride-based light-emitting diodes (LEDs) hold great promise for lighting applications but their performance is limited at high current densities. Although alternative explanations for the efficiency droop in GaN-based LEDs have proliferated in the last decade, the true origin of droop is not understood. This talk will present an analysis of the non-radiative recombination processes that are relevant in analyzing the quantum efficiency data of III-Nitride based LEDs. Direct (phonon-less) and indirect (phonon-assisted) Auger recombination processes and their impact on the calculated quantum

**Conference 8619:
Physics and Simulation of Optoelectronic Devices XXI**

efficiency of III-Nitrides LEDs will be discussed. The model includes realistic electronic structures computed with the nonlocal empirical pseudopotential method and phonon dispersion relations determined using the linear-response method within density functional perturbation theory. The effects of phonons are formally included by means of a spectral density function accounting for the renormalization of electron propagators. Due to the strong polarization induced electric fields present in GaN-based QWs, Auger coefficient in quantum wells can be potentially different from their bulk counterparts. A preliminary study of Auger transitions in confined structures will be presented.

8619-51, Session 13

Effect of Interband energy separation on the interband Auger processes in III-nitride semiconductors

Chee-Keong Tan, Jing Zhang, Guangyu Liu, Nelson Tansu, Lehigh Univ. (United States)

The efficiency-droop phenomenon in III-Nitride light-emitting diodes (LEDs) remains an important limitation for achieving low-cost and high-power LEDs for solid state lighting. The carrier leakage and interband Auger processes have been narrowed down as most likely possible factors in limiting the efficiency for InGa_N quantum wells (QWs) LEDs. Thus, the availability of intuitive and simple relation for describing the interband Auger in semiconductors are of great relevance in elucidating the physics of efficiency-droop in nitride LEDs.

The interband Auger process in III-Nitride semiconductors is attributed to the recombination of the electron (C1) and hole (H1) in the first subbands accompanied by the excitation of electron from the first conduction subband (C1) to the upper conduction (C2) subband. The interband energy separation (C2-C1) plays a very important role in determining the interband Auger recombination rates in semiconductor. In this work, we developed an analytical relation for describing the statistical probability function for analyzing the interband Auger rate as a function of interband energy separation for semiconductors. Our function indicates that the statistical weight factor is largely affected by the energy band gap, interband separation energy and the material effective masses. The analytical relation describes the interband Auger rates for three different scenarios as follow: (a) bandgap > interband separation energy, (b) bandgap < interband separation energy, and (c) bandgap ≈ interband separation energy. The comparison of interband Auger rates for various III-Nitride semiconductors will be reported.

8619-52, Session 13

Carrier-density-dependent recombination rates in GaInN/GaN QW LED structure with V-defect and threading dislocation

Yong-Hee Cho, Jun-Youn Kim, Jaekyun Kim, Youngsoo Park, Munbo Shim, Sungjin Kim, Samsung Advanced Institute of Technology (Korea, Republic of)

We model carrier-density-dependent radiative and non-radiative recombination rates in the InGa_N/GaN quantum well structure containing V-defect and threading dislocation. It is known that the threading dislocation acts as the non-radiative recombination center, leading to the reduction of carriers which can participate in the radiative recombination. On the other hand, the quantum well structure grown on the sidewalls of V-defect, formed by the strain relying on In/Ga contents and connected with threading dislocation directed along the polar direction, plays a role of the energy barriers to prevent quantum well in-plane charge carriers flowing to the non-radiative recombination center, i.e., the threading dislocation. Therefore, such V-defects can enhance the internal quantum efficiency in the InGa_N/GaN quantum well light emitting diode (LED). However, the explicit model of the V-defect and the threading dislocation coupled to three dimensional electronic states has rarely been studied.

We take into account those defects by including their potentials in a system Hamiltonian. It can describe the electronic states of in-plane quantum well, in which the V-defects and threading dislocations are distributed. Here we show that charged carriers are more distributed away from the threading dislocation by having the V-defect, and it leads to the reduction of carrier losses to the non-radiative recombination and hence the enhancement of radiative recombination rate. Their effects on the recombination rates depend on injected carrier densities. We also take into account mid-gap defect states generated due to n-/p-type dopants, threading dislocations, and the V-defects in the recombination rates.

8619-53, Session 13

Auger recombination and carrier transport effects in III-nitride quantum-well light emitting diodes

Marcus Deppner, Bernd Witzigmann, Friedhard Römer, Univ. Kassel (Germany)

Gallium nitride based LEDs have become a viable technology for general lighting. Despite the progress within recent years, the so-called „efficiency droop“ is still a central issue of nitride-based LED research. Up to now, no widely accepted explanation is available for the reduction of the internal quantum efficiency with increasing injection current.

We report on a novel mechanism contributing to efficiency droop, that combines two of the previously reported effects: Auger recombination and carrier leakage.

A sophisticated Auger model, that takes account of the overlap of the wavefunctions, is extended to model the energy transfer towards the third involved carrier. This carrier is assumed to be expelled from the well and regenerated in the continuum carrier population, where it can contribute to carrier leakage.

A physics-based simulation of a quantum-well LED has been employed to demonstrate the impact of this effect. The computational model consists of a continuity equation for bulk regions, whereas in the quantum-well the energy space is divided into bound well and continuum populations. Carrier capture in and out of the well is mediated by a dynamic scattering mechanism. For the bound carrier population, a 6x6 kp band structure calculation is performed. This Schrödinger solver is iterated self-consistently with the transport simulation.

Depending on the parametrization of the leakage model the Auger coefficient is reduced up to 50% when compared to a standard Auger model, which explains the discrepancy between recently published calculated and experimentally extracted Auger coefficients.

8619-54, Session 14

Hybrid silicon organic high speed electro-optic phase shifter

Soon Thor Lim, Ching Eng Png, Vivek Dixit, A*STAR Institute of High Performance Computing (Singapore)

We study a hybrid silicon organic high speed electro-optic phase shifter based on polymer infiltrated P-S-N (“S” refers to the slot) diode capacitor structure. This optical phase shift is realized based on index perturbation both inside the slot via Pockels nonlinearity and within the silicon ridges via the free carrier effect (carrier depletion) simultaneously. Therefore, the overall EO overlap can be noticeably improved from that which relies on either of the individual NLO effects alone. Additionally, the device speed can be significantly elevated with the introduction of free carriers as they are found to respond faster to the external driving signal than the E-field due to the smaller experienced transient capacitance. According to our numerical results, the combination of the polymer diode capacitor configuration with the low aspect ratio slot waveguide system leads to

**Conference 8619:
Physics and Simulation of Optoelectronic Devices XXI**

a promising method of constructing sub-THz speed optical modulators without sacrificing either modulation efficiency or energy consumption. To be more specific, by optimizing the waveguide geometry in terms of balancing effective index shift and device speed, at least 269 GHz bandwidth can be achieved with a high modulation efficiency of 5.5 V-cm when the diode capacitor is reverse biased by an external radio frequency (RF) voltage signal between the electrodes (optical propagation loss is acceptably low at 4.29 dB). The device figures of merits (FOM) are encouraging when compared to either depletion mode or polymer SWG based designs. These are conservative numerical results, and as will be shown, are grounded in well-understood physical phenomena.

8619-55, Session 14

Memory effect in gated single-photon avalanche diodes: a limiting noise contribution similar to afterpulsing

Davide Contini, Alberto Dalla Mora, Laura Di Sieno, Rinaldo Cubeddu, Alberto Tosi, Gianluca Boso, Antonio Pifferi, Politecnico di Milano (Italy)

In recent years, emerging applications in which a wide dynamic range is crucial have turned the interest towards Single-Photon Avalanche Diode (SPAD), such as diffuse optical imaging and spectroscopy (e.g., functional brain imaging and optical mammography). In these fields, the use of a fast-gated SPAD has proven to be a successful technique to increase the measurement sensitivity of different orders of magnitude. However, an unknown background noise has been observed at high illumination during the gate-OFF time, thus setting a limit to the maximum increase of the dynamic range. In this paper we describe this noise in thin-junction silicon single-photon avalanche diode when a large amount of photons reaches the gated detector during the OFF time preceding the enabling time. This memory effect increases the background noise with respect to primary dark count rate similarly to a classical afterpulsing process, but differently it is not related to a previous avalanche ignition in the detector. We discovered that memory effect increases linearly with the power of light impinging on the detector and it has an exponential trend with time constants far different from those of afterpulsing and independently of the bias voltage applied to the junction. For these reasons, the memory effect is not due to the same trapping states of afterpulsing and must be described as a different process.

8619-56, Session 14

Design optimization of an optically drivable heterogeneous MOSFET with silicon compatibility

Seongjae Cho, Stanford Univ. (United States); Hyungjin Kim, Seoul National Univ. (Korea, Republic of); S. J. Ben Yoo, Univ. of California, Davis (United States); Byung-Gook Park, Seoul National Univ. (Korea, Republic of); James S. Harris Jr., Stanford Univ. (United States)

Optical interconnect is considered for the next-generation interconnect technology as one of the promising copper replacements due to its merits of high bandwidth, low power and latency, and noise immunity. Optical and electronic devices for optoelectronic integrated circuits have been extensively studied, and now, more efforts for the conversion between optical and electrical signals are accordingly required. In this work, a Si-compatible optically driven compound metal-oxide-semiconductor field-effect transistor (MOSFET) is studied by simulation. The suggested optoelectronic device provides a linkage between the optical and the electronic interfaces as a key part of optical interconnects. The optically driven MOSFET device is analogously analyzed into a photodetector and its complementary device, getting

rid of the necessity of receiver circuitry, which greatly improves the integration density and simplifies the fabrication processes. There have been several reports on metal-semiconductor field-effect transistor (MESFET) based on similar approach. However, in our work, by isolating gate from channel, with the MOSFET configuration, the off-state leakage current by Fermi-level pinning between compound semiconductor channel and metal gate is effectively reduced. For maximizing the active area, a bottom gate is formed to modulate the channel and a geometric optimization is performed to suppress dark current and improve Ion/Ioff current ratio. Ge and GaAs are the active materials on Si platform. Both direct-current and alternating-current performances of the optimized device are evaluated.

8619-57, Session 14

Simulations of light beam incident on a gainy slab elicit mechanism of amplified TIR

Tobias S. Mansuripur, Harvard Univ. (United States); Masud Mansuripur, College of Optical Sciences, The Univ. of Arizona (United States)

We theoretically investigate the claim that the total internal reflection (TIR) of light from a transparent medium onto a lower index, semi-infinite gain medium has a reflection amplitude greater than unity. By analyzing the case of a finite thickness gain medium, we demonstrate the importance of the 'round-trip coefficient'--the factor by which the amplitude of a plane wave is multiplied upon traveling one round-trip in the gainy slab--on the qualitative behavior of reflection, both below and above the critical angle. Analytical simulations of a Gaussian beam show that the 'side-tail' of the beam enters the slab before the central part of the beam; when the magnitude of the round-trip coefficient is greater than one, this weak pre-excitation of the amplifying medium gains more during propagation than it loses to transmission at the back facet, and returns to interfere with the central part of the beam at the first interface, giving rise to an amplified reflection of the primary beam. The angle at which the round-trip coefficient exceeds one can be smaller than the critical angle, and appears to be more relevant than the critical angle in determining whether the primary reflection is amplified. Most previous investigations have focused on the behavior of plane waves, which by themselves do not elucidate this behavior. Because the back facet is instrumental in generating the amplified reflection, we argue against the existence of amplified TIR from a semi-infinite medium.

Conference 8620: Physics, Simulation, and Photonic Engineering of Photovoltaic Devices II

Sunday - Thursday 3 -7 February 2013

Part of Proceedings of SPIE Vol. 8620 Physics, Simulation, and Photonic Engineering of Photovoltaic Devices II

8620-1, Session 1

Plasmonic and dielectric enhancement of solar cells (*Invited Paper*)

Kylie Catchpole, The Australian National Univ. (Australia)

We describe recent progress and future prospects for enhancement of solar cells using plasmonic and dielectric structures.

Materials costs are a large component of total module costs for wafer based solar cells. As a result, there is a trend to thin film solar cells, in which the active semiconductor layer is deposited on a cheap substrate such as glass. However, this leads to reduced absorption, particularly for silicon based solar cells because of the indirect band gap of silicon. Therefore there is a need to increase the optical thickness of thin film solar cells, by trapping light inside the cell. The use of nanophotonic structures deposited directly on a planar device is a promising new approach to increasing absorption in thin film solar cells.

Two particularly promising approaches are the use of high index dielectric scattering structures such as TiO₂ and metallic structures based on plasmonic resonances. Recently, we have achieved a doubling of the photocurrent in thin film polycrystalline silicon solar cells, through the use of a combination of plasmonic particles and dielectric scatterers. For thin crystalline silicon cells, a range of particle sizes is advantages in order to scatter over a broad spectral range. By combining a periodic array of metal nanoparticles with a back reflector in a resonant arrangement, nearly 100% of incident light can be diffracted outside the escape cone.

8620-2, Session 1

Excitation of Multiple Surface-Plasmon-Polariton Waves at the Interface of a Metal and Photonic Crystal

Anthony S. Hall, Muhammad Faryad, Greg D. Barber, Akhlesh Lakhtakia, Thomas E. Mallouk, The Pennsylvania State Univ. (United States)

The excitation of multiple surface-plasmon-polariton (SPP) waves at the interface of a metal and a photonic crystal was studied both experimentally and theoretically in the grating-coupled configuration. Each period of the photonic crystal consists of nine layers of dielectric material with varying refractive indexes. The excitation of SPP waves was indicated by the absorbance peaks that are invariant with respect to the total thickness of the photonic crystal. Because of the periodic nonhomogeneity of the photonic crystal, multiple SPP waves of both linear polarization states and phase speeds are excited. SPP waves excited by s-polarized incident light display sharper absorbance peaks than the SPP waves excited by p-polarized incident light. The experimental and theoretical results show the number of p-polarized SPP waves is higher than the number of s-polarized SPP waves excited in the grating-coupled configuration. The effects of the period and the duty cycle of the surface-relief grating on the number of p- and s-polarized SPP waves were also studied. Multiple SPP waves may provide an interesting route to enhancing the efficiency of photovoltaics if incorporated into a thin-film solar cell or planar concentrator system. The configuration studied in the paper is superior to conventional plasmonic concentration schemes because it allows the excitation of SPP waves of both s- and p-polarization states over most of the visible frequency range.

8620-3, Session 1

Improving photovoltaic devices using silver nanocubes

Fouad Hejazi, Shuyu Ding, Yao Sun, Adam Bottomley, Carleton Univ. (Canada); Anatoli Ianoul, Carleton Univ. (Canada); Winnie Ye, Carleton Univ. (Canada)

This paper presents a novel design to enhance the performance of silicon-based thin film solar cells. Solar energy is the cleanest and the most abundant renewable energy source on earth that can be harnessed directly from the sun. To make solar energy technology competitive with the traditional non-renewable energy technologies, the fabrication cost needs to be reduced by a factor of 2 to 5. Thin film solar cells are thin, lightweight and flexible, and the cells could be placed on a variety of surfaces including plastics and fabrics. However, they are lagging behind the dominant bulk silicon solar cell technology with regards to efficiency. The proposed research involves the modeling, fabrication, and testing of innovative designs of silicon-based thin film solar cells. Two design aspects are proposed for improving the efficiency: (a) p-i-n configuration, and (b) an effective light trapping system utilizing plasmonic enhancement effects induced from metallic nanoparticles. The novelty of the proposed solar cell is three-fold. Firstly, the metallic nanoparticles are used as subwavelength scattering elements to couple and trap the light into the absorbing i-region, causing an increase in the effective optical path length in the cell. Secondly, metallic nanoparticles act as subwavelength antenna in which the surface-plasmon-polariton excitation promotes a strong localized field enhancement, increasing the effective absorption in i-region. Thirdly, the metallic nanoparticles are cubic, rather than the traditional spherical geometry, enabling precise control on the resonant wavelengths.

We first present our theoretical findings on the design of the p-i-n solar cells and the locations of the plasmonic metal nanoparticles. Our initial FDTD simulations show that the plasmonic properties of the cubic nanoparticles are far more attractive in terms of efficiency improvement compared to the traditional spherical configuration. After that, we present the experimental fabrication of our silicon solar cells, and the chemical process for the incorporation of the cubic metallic nanoparticles. Finally, we present our preliminary experimental measurements which demonstrate a much improved cell efficiency by increasing the scattering and trapping of light through the plasmonic nanoparticles.

8620-4, Session 1

Efficiency enhancement of amorphous silicon based solar cell due to multiple surface-plasmon-polariton waves

Muhammad Faryad, Akhlesh Lakhtakia, The Pennsylvania State Univ. (United States)

The efficiency of a multi-junction thin-film solar cell backed by a surface-relief grating was studied theoretically using rigorous coupled-wave approach (RCWA). If the partnering semiconductor material is homogeneous, only one surface plasmon-polariton (SPP) wave, that too of p-polarization state, can be excited using the surface-relief grating for a given wavelength of incident light. However, if the partnering semiconductor material is made periodically nonhomogeneous (with appropriate period) normal to the mean grating/semiconductor interface and an appropriate surface-relief grating is selected as a backing metallic layer, it may result in the excitation of multiple SPP waves of both linear polarization states with the same free-space wavelength and the direction of propagation but different phase speeds, degrees of localization to the interface, and different spatial profiles. The effects of multiple SPP waves on the efficiency of thin-film solar cell with practically realizable materials and geometry were studied. The solar cell was made of hydrogenated-amorphous silicon alloys and the spectrum of the incident light was

taken to be AM1.5 solar irradiance spectrum in the wavelength range of 400-1100 nm. The enhancement in the efficiency of the thin-film solar cell depends on the period of the periodicity of the partnering semiconductor material; and the depth, period, and duty cycle of the surface-relief grating.

8620-5, Session 1

On energy transfer in metallicly nanomodified photocells via surface plasmons in metallic nanoparticles: inclusion of nanoparticle size-effect

Witold A. Jacak, Wrocław Univ. of Technology (Poland)

Nowadays more and more effort is made in order to harness solar energy in ecologically and economically efficient manner. Despite the huge progress recently achieved, photovoltaic still needs significant improvements to become competitive with traditional energy sources.

One of the promising techniques to improve properties of solar cells is deposition of nanostructured metallic layers or nanoparticles [1, 2]. Metallic nanocomponents modify electro-optical properties of the system due to collective oscillations of electronic plasma in metal. Noble (gold, silver, also copper) metal nanoparticles are of great importance in photovoltaic [3] because of their strong resonances present in visible range of spectrum.

There are several experimental evidences [4-7] of successful application of metallic nanocomponents in optoelectronics of both types: organic and inorganic. However the effect is very sensitive to factors like: type of system, material, geometrical configuration finally size and shape of nanocomponents. Presence of nanoparticles can enhance or diminish efficiency of solar cell. The photovoltaic enhancement effect is not fully-recognised yet and because of its possible application it is worth to investigate it in details. Below the discussion of some aspects of near field interaction to energy transfer efficiency is given in terms of fully analytical random phase approximation type model of plasmons in spherical geometry. Within this approach The idea of inclusion of indirect interband transitions in semiconductor substrate induced by near-field coupling to plasmons is investigated. Nanosphere with plasmons coupled in near field to semiconductor is not translational invariant system and thus momentum conservation does not hold here, which results in admitting of additional transitions forbidden in an ordinary photo-effect. The effect weakens, however, with the nanosphere radius growth, and analysis of this effect is the topic of the present contribution. The comparison between quantum quasiparticle approach with phenomenological driven oscillator model for strong damped (including over-damped) oscillations in the system is also discussed.

References:

- [1] Green MA, Pillay S. Harnessing plasmonics for solar cells. *Nature Photonics* 2012;6:130-132.
- [2] Atwater HA, Polman A. Plasmonics for improved photovoltaic devices. *Nature. Materials* 2010;9:205-213.
- [3] Zayats AV, Smolyaninov II, Maradudin AA. Nano-optics of surface plasmon polaritons. *Physics Reports* 2005;408:131-314.
- [4] Pillai S, Catchpole KR, Trupke T, Green MA. Surface plasmon enhanced silicon solar cells. *Journal of Applied Physics* 2007;101:093105.
- [5] Derkacs D, Lim SH, Matheu P, Mar W, Yu ET. Improved performance of amorphous silicon solar cells via scattering from surface plasmon polaritons in nearby metallic nanoparticles. *Applied Physics Letters* 2006;89:093103.
- [6] Schaadt DM, Feng B, Yu ET. Enhanced semiconductor optical absorption via surface plasmon excitation in metal nanoparticles, *Applied Physics Letters* 2005;86:063106.
- [7] Kim SS, Na SI, Jo J, Kim DY, Nah YC. Plasmon enhanced performance of organic solar cells using electrodeposited Ag nanoparticles. *Applied Physics Letters* 2008;939:073307.

8620-7, Session 2

Intraband carrier dynamics in InAs/GaAs quantum dots studied by two-color excitation spectroscopy

Yukihiro Harada, Tsuyoshi Maeda, Takashi Kita, Kobe Univ. (Japan)

We have studied the intraband carrier dynamics in InAs/GaAs self-assembled quantum dots (QDs) by using a two-color excitation spectroscopy. InAs/GaAs QDs were embedded in a one-dimensional photonic cavity structure with the resonant energy tuned to the bound-to-continuum intraband transition. An enhancement of the intraband transition probability is required for the high conversion efficiency of the intermediate-band solar cells according to the numerical simulations on the detail balance limit of the efficiency. Two-color excitation was carried out by using a continuous-wave (cw) laser light for the interband transition and a near-infrared pulsed laser light for the intraband transition. The interband photoluminescence (PL) intensity was observed to be drastically decreased just after the pulsed laser excitation. This result indicates that the photogenerated electrons in QDs are pumped out by the intraband transition. The enhancement of the intraband transition using the photonic cavity was demonstrated by a factor of 8. On the other hand, the dip structure in the PL response was followed by a gain. To interpret the results, we proposed a model describing the carrier excitation and relaxation processes in the InAs/GaAs QD system, where the two-photon absorption and the Pauli blocking in QDs are taken into account. According to these calculations, it was found that the intraband carrier relaxation dynamics strongly depends on the cw laser power due to the Pauli-blocking effect. The calculation results well explain the observed cw laser power dependence of the interband PL response.

8620-8, Session 2

Evaluation of micrometer scale lateral fluctuations of transport properties in CIGS solar cells

Amaury Delamarre, Daniel Ory, Myriam Paire, Daniel Lincot, Jean-François Guillemoles, Laurent Lombez, Institut de Recherche et Développement sur l'Énergie Photovoltaïque (France)

Thin films absorbers like CIGS are widely studied in the photovoltaic field due to their potentially high efficiencies and low production costs. However they present complex structures that need to be analyzed in order to increase their performances. Especially they are polycrystalline and have spatial inhomogeneities at the micrometer scale, which may influence the electrical parameters of the cell. In this communication, we study the local transport properties by mean of different techniques.

Firstly, we present results obtained from two setups: a Hyperspectral Imager (HI) and a confocal microscope. Both allow mapping of luminescence spectra emitted by the cell. However the way they operate are strongly different [1,2]: the HI acquires luminescence directly from a large surface contrary to a confocal microscope. Combination of these local and global measurements gives information on local properties like carrier transport, open-circuit voltage and carrier collection. Secondly, using an original setup, we are able to record PLE (Photoluminescence Excitation) and EQE (External Quantum Efficiency) spectra with a micron scale resolution. Spatial variations of absorption and diffusion length are accessible. Attention has been paid to differentiate between fluctuations arising from optical and electrical properties. The local reciprocity relations [3] can thus be analyzed.

- [1] A. Delamarre, L. Lombez, and J.-F. Guillemoles, *Journal of Photonics for Energy* 2, 027004 (2012).
- [2] A. Delamarre, L. Lombez, and J.-F. Guillemoles, *Appl. Phys. Lett.* 100, 131108 (2012).
- [3] U. Rau, *Phys Rev B*, 76, 085303 (2007).

8620-9, Session 2

Characterization of semiconductor devices, wafer and solar cell materials via time-correlated single-photon counting with sub ns time-resolution

Volker Buschmann, Felix Koberling, PicoQuant GmbH (Germany); Samantha Fore, PicoQuant North America Inc. (United States); Hannes Hempel, Friedrich-Schiller-Univ. Jena (Germany); Andrea Knigge, Ferdinand-Braun-Institut (Germany); Christian Kraft, Friedrich-Schiller-Univ. Jena (Germany); Uwe Ortmann, PicoQuant GmbH (Germany); Maurizio Roczen, Helmholtz-Zentrum Berlin für Materialien und Energie GmbH (Germany); Torsten Siebert, Rainer Erdmann, PicoQuant GmbH (Germany)

The characterization of charge carrier dynamics on the pico- to microsecond time-scale via time-correlated single-photon counting (TCSPC) based photo-luminescence measurements is presented as a versatile methodology for analyzing the function and quality of semiconductor systems. This general time-domain technique can be expanded with spectral and spatial resolution for addressing different aspects of multi-component semiconductor systems.

The key parameter in the time-resolved photoluminescence (TRPL) measurements presented in this work is the minority carrier lifetime, which can span several orders of magnitude over the sub-nanosecond to millisecond time scale and shows a strong dependency on impurities and defect sites. The charge carrier dynamics can be assigned to particular materials and sub-structures by spectrally resolving the photoluminescence signal, which allows for an analysis of their function within the architecture of complex systems. In spatially resolved experiments based on raster scanning microscopy, a correlation between the morphology and function of the system as well as the direct observation of diffusion dynamics and transport phenomena are possible.

A multimodal TRPL setup is presented based on pulsed diode lasers and TCSPC with highly sensitive single photon avalanche detectors (SPADs). In order to exemplify the general capabilities, TRPL measurements on a GaAsP quantum well imbedded in an AlGaAs structure and a multi-layer CdTe heterojunction system are discussed.

8620-79, Session 2

Mapping of solar cells optoelectronic properties from luminescence and photocurrent signals (*Invited Paper*)

Laurent Lombez, Institut de Recherche et Développement sur l'Energie Photovoltaïque (France)

No Abstract Available

8620-10, Session 3

Nanophotonics for solar energy harvesting from ultrathin cells (*Invited Paper*)

Mark Brongersma, Geballe Lab for Advanced Materials (GLAM) (United States)

Nanophotonics is an exciting new field of science and technology that is directed towards making the smallest possible structures and devices that can manipulate light. Until recently, it was thought that the fundamental laws of diffraction would preclude much further miniaturization of the micron-scale photonic devices we have today. In this presentation, I will show how semiconductor and metallic nanostructures can mold the flow of light well below the wavelength of light. This ability opens up the opportunity to effectively trap light in

ultrathin solar and photo-electrochemical cells. I will discuss how the individual nanostructures and their non-periodic arrangement on a cell can be optimized to effectively harvest solar energy from such thin cells and across the broad solar spectrum.

8620-11, Session 3

Broadband light trapping in ultra-thin nanostructured solar cells

Clément Colin, Lab. de Photonique et de Nanostructures (France) and Ecole Nationale Supérieure de Chimie de Paris (France); Inès Massiot, Andrea Cattoni, Nicolas Vandamme, Christophe Dupuis, Nathalie Bardou, Lab. de Photonique et de Nanostructures (France); Isabelle Gérard, Univ. de Versailles Saint-Quentin-en Yvelines (France); Negar Naghavi, Jean-François Guillemoles, Institut de Recherche et Développement sur l'Energie Photovoltaïque (France); Jean-Luc Pelouard, Stéphane Collin, Lab. de Photonique et de Nanostructures (France)

Broadband light trapping in very thin semiconductor layers is one of the main issues for the conception of next-generation solar cells. Here, we demonstrate numerically and experimentally that high-efficient broadband optical absorption can be achieved in a very thin semiconductor layer by multi-resonant mechanism.

As a proof of concept, we have numerically studied a model 25 nm-thick GaAs solar cell. This is a 40-fold thickness reduction compared to record GaAs solar cells. We show that a metallic nano-array embedded in a transparent front contact layer leads to multi-resonant light trapping. The origin of the different resonances is analyzed and we predict a short circuit current of $J_{sc}=19\text{mA/cm}^2$ (AM1.5G) and an efficiency of $\eta=18\%$ for this simplified solar cell. The first experimental evidence of these theoretical predictions is presented. A 25 nm-thick GaAs layer has been reported on a gold mirror, and covered by a metallic nanoarray embedded in a ZnO:Al layer. We demonstrate nearly perfect (~90 %) optical absorption over the whole visible spectrum, independent from the incidence angle and light polarization.

We show that similar absorption enhancement is obtained in ultra-thin (100-300nm) solar cells. For this last particular case, we present the latest key experimental fabrication processes for such design: preparation of well controlled 100 nm-thick ClGSe layers on an alternative metallic substrate and nano-imprint lithography for a large scale processing of ClGSe solar cells. First experiments on ultrathin nano-patterned ClGSe solar cells will be presented.

8620-12, Session 3

Silicon solar cell light-trapping using defect mode photonic crystals

Kelsey A. Whitesell, Dennis M. Callahan, Harry Atwater, California Institute of Technology (United States)

Nanostructured active or absorbing layers of solar cells, including photonic crystals and wire arrays, have been increasingly explored as potential options to enhance performance of thin film solar cells because of their unique ability to control light. We show that 2D photonic crystals can improve light trapping by an enhanced local density of optical states and incoupling via optical diffraction, and explore theoretical light-trapping limits for solar cells with patterned absorbing layers. Using FDTD simulations, we demonstrate absorption enhancements in 200nm thick crystalline silicon solar cells of up to 200% from $\eta = 300\text{nm}$ to 1100nm compared to a planar cell with an optimized two-layer anti-reflection coating. We report here a method to further enhance absorption by introducing multiple defects into the photonic crystal. These defects act as local resonators coupled both to each other and to the optical modes arising from the periodic structure of the photonic crystal. Defects of a single size can enhance absorption at the resonant frequency up

Conference 8620: Physics, Simulation, and Photonic Engineering of Photovoltaic Devices II

to 40 times compared to the ordered photonic crystal case. Coupling defects with different resonant frequencies together results in broadband improvements. Highest absorption efficiencies were achieved for hybrid photonic crystals and planar cells where resonant modes with electric fields concentrated in non-absorbing, low-index regions of the photonic crystals are injected into the underlying flat layer where the energy can be absorbed. Our results show that 2D photonic crystals are a viable and rich research option for light trapping in thin film photovoltaics.

8620-13, Session 3

GaAs Thin-Film Single-Junction Solar Cells Integrated with a Reflective Back Scattering Structure

Weiquan Yang, Jingjing Li, Charles Allen, Arizona State Univ. (United States); Hector Cotal, Spectrolab, Inc. (United States); Christopher Fetzer, Spectrolab, Inc. (United States); Shi Liu, Ding Ding, Stuart Farrell, Arizona State Univ. (United States); Nasser Karam, Spectrolab, Inc. (United States); Yong-Hang Zhang, Arizona State Univ. (United States)

We have proposed double-heterostructure GaAs/InGaP thin-film single-junction solar cells integrated with a reflective back scattering structure to increase the light absorption path. The reflective back scattering structure consists of a textured lattice-matched ZnSe layer coated with a reflective mirror. We have designed and fabricated the devices with a GaAs active region of 300 nm, 1000 nm and 1500 nm thick. I-V and EQE are measured under different bias light illuminations and temperatures. The device performances under typical terrestrial condition are obtained. The temperature dependence of Voc and the voltage dependences of the series and shunt resistances are studied to find the type and height of barriers for current transport. The temperature dependence of the ideality factor is studied to obtain information about the trap locations. The voltage dependence of EQE is studied at different wavelengths yielding information about defect distributions and the effects of ZnSe growth and fabrication on minority carrier lifetime. The EQE data is fit using numerical models considering the light reflection, transmission and absorption, and the current transport and recombination. From this information, a relationship of active region thickness to device performance is presented.

8620-14, Session 4

Photon up-conversion as a means for enhancing photovoltaic power conversion efficiency (*Invited Paper*)

Nicholas J. Ekins-Daukes, Roland Piper, Imperial College London (United Kingdom); Tim Schulze, Yuen Y. Cheng, Tyler Troy, Burkhard Fückel, The Univ. of Sydney (Australia); Klaus Lips, Helmholtz-Zentrum Berlin für Materialien und Energie GmbH (Germany); Tim Schmidt, The Univ. of Sydney (Australia)

Molecular approaches to up-conversion have been demonstrated in a number of systems where absorption proceeds via a strong, allowed S₀-S₁ transition followed by efficient inter-system-crossing to a long-lived T₁ triplet state. With the excitation locked into the T₁ state, there is significant time (microseconds) for the excitation to migrate. In most molecular up-conversion schemes, a second molecular species is introduced with a S₁ singlet state located at an energy twice that of the T₁ triplet state. In the event that two molecules in their T₁ state interact, triplet-triplet annihilation (TTA) can take place, resulting in the population of the higher S₁ and associated prompt fluorescence. This process has been shown to be efficient in molecular solutions, where the transport of molecules in their excited T₁ state is physical. In molecular thin-films, the molecules are static, so achieving efficient up-conversion requires sufficient mobility of excited triplets. Results from recent experiments

on up-converting thin-films will be reported to demonstrate the extent to which the mobility of the excitation is critical for efficient up-conversion.

8620-15, Session 4

Rare-earths doped planar 2D-photonic crystals for quantum cutting in solar cells

Thierry Deschamps, Institut des Nanotechnologies de Lyon (France); Antoine Guille, Univ. Claude Bernard Lyon 1 (France); Emmanuel Drouard, Radoslaw Mazurczyk, Regis Orobtcchouk, Cecile Jamois, Alain Fave, Romain Peretti, Institut des Nanotechnologies de Lyon (France); Antonio Pereira, Bernard Moine, Univ. Claude Bernard Lyon 1 (France); Christian Seassal, Institut des Nanotechnologies de Lyon (France)

In silicon-based solar cells, a substantial part of the energy losses is related to the carriers thermalization in the UV-blue range. This issue can be partially circumvented by the down-conversion phenomenon, using a rare-earths doped thin layer deposited on top of silicon solar cells, but the efficiency of this process needs to be increased. We introduce a new concept which combines a rare-earths doped thin layer with a photonic crystal (PC), in order to control the frequency conversion. The doped thin layer is synthesized by pulsed laser deposition and contains Ce³⁺, Pr³⁺ and Yb³⁺ ions incorporated in amorphous CaYAlO₄. The Ce³⁺ ions absorb incident light in the UV range and its emission efficiently sensitizes the upper level of Pr³⁺ around 450 nm. The down-conversion involves energy transfers between Pr³⁺ and Yb³⁺ which allows a “quantum-cutting” process, i.e the emission of two near-IR photons for one blue photon absorbed. On the top of the rare-earths doped layer, a silicon nitride layer is deposited by sputtering. After lithographic lithography and reactive ion etching, this layer is patterned as a planar PC, able to control incident absorption in the UV-blue range, and photon emission in the near-IR range. The PC topographical parameters as well as the layers thicknesses are optimized using Finite-Difference-Time-Domain simulations. In this communication, we will present the design and realization of such PC-assisted quantum-cutting structures, as well as preliminary optical measurements which assess the potentialities of this approach.

8620-16, Session 4

Enhancing absorption in a thin film photovoltaic system with periodic nanostructures obtained by low-cost techniques

Arthur Le Bris, Saint-Gobain Recherche (France) and Ctr. National de la Recherche Scientifique (France); Barbara Brudieu, Saint-Gobain Recherche (France) and Ecole Polytechnique (France) and Ctr. National de la Recherche Scientifique (France); Jérémie Teisseire, Fabien Sorin, Saint-Gobain Recherche (France) and Ctr. National de la Recherche Scientifique (France)

Reducing the absorber thickness in photovoltaic devices has emerged as a promising way to reduce fabrication costs by requiring less material and allowing for faster processing. To obtain an efficient absorption of light in ultra-thin absorbers, a lot of effort is dedicated to finding innovative photon management techniques such as coherent light trapping using diffraction gratings, photonic crystals or plasmonic structures. However, additional processing costs are detrimental to the technology competitiveness, and low cost and scalable fabrication techniques should be targeted.

Here, numerical simulations using a Rigorous Coupled Wave Analysis (RCWA) method are performed to design and optimize a structure combining a Distributed Bragg Reflector (DBR) and a diffraction grating.

Conference 8620: Physics, Simulation, and Photonic Engineering of Photovoltaic Devices II

We consider specifically materials and structures that are compatible with non-vacuum and low temperature fabrication techniques to enable scalable and low cost processes. A DBR is obtained by successive spin coating of sol-gel oxide layers, and it is textured by Nano Imprint Lithography (NIL). The structures that are synthesized are then characterized and their optical properties (reflection, transmission, absorption) are compared with simulations.

The NIL technique is also used to obtain ordered metallic arrays with plasmonic frequencies suitable to enhance absorption in various thin absorbers. Its optical properties are determined and well fitted by RCWA simulations. These light trapping structures can be optimized and could be integrated into inorganic thin film systems, as well as Dye sensitized cells and organic photovoltaics.

8620-17, Session 4

Broadband Light Absorption Enhancement in Thin-Film Solar Cells by Combining Front Dielectric and Back Metallic Gratings

Zhaoyu Zhang, Peking Univ. (China); Siyao Guo, Guangyao Su, Deng Xiao, Peking Univ. Shenzhen Graduate School (China)

A thin-film solar cell structure combining front dielectric grating and back metal grating is proposed to improve light absorption in 300-900 nm wavelength range and the finite element method (FEM) is used to conduct the study. The absorption enhancement at short and long wavelengths of the spectrum comes from different mechanisms. For shorter wavelengths (300-550nm), the front dielectric grating plays a major role while for longer wavelengths (550-900 nm), the interaction of the front dielectric and back metal gratings is the key. The front dielectric grating scatters the incident light into active layer without much energy loss, especially for shorter wavelengths. The back metal grating causes the absorption enhancement at longer wavelengths due to the excitation of surface plasmon polaritons (SPPs) or photonic modes. When these two gratings are combined, a broadband absorption enhancement over the entire spectrum can be realized. Additionally, we observed an interaction between the front dielectric grating and the back metal grating which has a positive effect on increasing field distribution. For better comparison, the flat structure without any gratings is chosen as a standard. In our study, almost over the entire wavelength range, the absorption enhancement of the solar cell with dual gratings is superior to the structures with a front or back grating alone. For wavelengths in the range 300-900 nm, 72% absorptivity is observed for flat Si case, 77% and 75% for front and back grating cases, and up to 82% for dual grating case.

8620-18, Session 5

Six not so easy pieces in intermediate band solar cell research

(Invited Paper)

Antonio Martí, Univ. Politécnica de Madrid (Spain); Elisa Antolín, Univ. Politécnica de Madrid (Spain) and Consejo Superior de Investigaciones Científicas (Spain); Pablo García-Linares, Iñigo Ramiro, Irene Artacho, Esther López, Estela Hernández, Manuel J. Mendes, Alex Mellor, Ignacio Tobías, David Fuertes Marrón, César Tablero, Ana B. Cristóbal, Antonio Luque, Univ. Politécnica de Madrid (Spain)

The concept of "intermediate band solar cell" (IBSC) is, apparently, simple to grasp. Our group proposed it in 1997. However, since the idea was proposed, our understanding has improved and we feel now that we can explain better some concepts than we initially did. We think clarifying these concepts is important, even if they are well-known for the advanced researcher, so that efforts can be driven in the right direction from start. The six pieces this work are: Does a miniband need to be

formed when the IBSC is implemented with quantum dots?; What are the problems of each of the main practical approaches that exist today? What are the simplest experimental techniques to demonstrate whether an IBSC is working as such or not? What is this thing of the absorption coefficient overlap? and Mott's transition? What the best system would be, if any?

8620-20, Session 5

Modification of band alignment at interface of $\text{Al}_x\text{Ga}_{1-x}\text{Sb}/\text{Al}_x\text{Ga}_{1-x}\text{As}$ type-II quantum dots by concentrated sunlight in intermediate-band solar cells with separated absorption and depletion regions

Ara M. Kechiantz, The George Washington Univ. (United States) and National Academy of Sciences of the Republic of Armenia (Armenia); Andrei Afanasev, The George Washington Univ. (United States); Jean-Louis Lazzari, CINaM - Ctr. Interdisciplinaire de Nanoscience de Marseille (France)

We have used $\text{AlGaSb}/\text{AlGaAs}$ material system for studying photovoltaic performance of intermediate band (IB) solar cells composed by type-II quantum dots (QDs) buried "outside" the depletion region in p-doped and in n-doped $\text{Al}_x\text{Ga}_{1-x}\text{As}$ regions of GaAs solar cell. Such cell displays a unique property of quenching recombination activity under concentrated sunlight. Our calculation shows that proper tuning of acceptor doping of $\text{Al}_x\text{Ga}_{1-x}\text{As}$ spacer layer between QDs buried in p-doped region or of donor doping of QDs buried in n-doped region may increase the cell performance by 20% compare to the conventional reference GaAs solar cell.

8620-21, Session 5

Investigation of the design parameters of quantum dot enhanced III-V solar cells

Kristina Driscoll, Mitchell Bennett, Stephen Polly, David V. Forbes, Seth M. Hubbard, Rochester Institute of Technology (United States)

The incorporation of nanostructures, such as quantum dots (QD), into the intrinsic region of III-V solar cells has been proposed as a potential route towards boosting conversion efficiencies with immediate applications in concentrator photovoltaic and space power systems. Necessary to the optimization process of this particular class of solar cells is the ability to correlate nanoscale properties with macroscopic device characteristics. To this purpose, the physics-based software Crosslight has been developed to investigate the design parameters of QD enhanced solar cells with particular focus on the InAs/GaAs system. This methodology is used to study how nanoscale variables, including size, shape and material compositions, influence photovoltaic performance. In addition, device-level engineering of the nanostructures is explored in optimizing the overall device response. Specifically, the effect of the position of the QDs within the intrinsic regions is investigated. Preliminary simulations suggest strategically placing the QDs off-center reduces non-radiative recombination and thereby the dark saturation current, contributing to a marked increase in open circuit voltage and fill factor. The short-circuit current remains unchanged in the high field region resulting in an increase in overall conversion efficiency. To further explore this finding, a series of three samples with the QDs placed in the center and near the doped regions of a pin-GaAs solar cell have been grown using MOCVD with device fabrication and full characterization underway.

8620-22, Session 5

Improving photonic-electronic characteristics in quantum-dot solar cells via lattice strain mechanisms

Wiley P. Kirk, The Univ. of Texas at Arlington (United States);
Jateen Gandhi, Univ. of Houston (United States); Choong-Un Kim, The Univ. of Texas at Arlington (United States)

No Abstract Available.

8620-23, Session 6

Towards high-efficiency triple-junction solar cells with biologically-inspired nanosurfaces *(Invited Paper)*

Peichen Yu, National Chiao Tung Univ. (Taiwan)

Multi-junction solar cells (MJSCs) offer extremely high power conversion efficiency with minimal semiconductor material usage, and hence are promising for large-scale electricity generation. To fully exploit the broad absorption range, antireflective schemes based on biomimetic nanostructures become very appealing due to sub-wavelength scale features that can collectively function as a graded refractive index (GRIN) medium to photons. The structures are generally fabricated with a single-type dielectric material which guarantees both optical design robustness and mechanical durability under concentrated illumination. However, surface recombination and current matching issues arising from patterning still challenge the realization of biomimetic nanostructures on a few micrometer thick epitaxial layers for MJSCs. In this presentation, bio-inspired antireflective structures based on silicon nitride (SiN_x) and titanium dioxide (TiO₂) materials are demonstrated on monolithically grown Ga_{0.5}In_{0.5}P/In_{0.01}Ga_{0.99}As/Ge triple-junction solar cells. The nano-fabrication employs scalable polystyrene nanosphere lithography, followed by inductively-coupled-plasma reactive-ion-etching (ICP-RIE). We show that the fabricated devices exhibit omni-directional enhancement of photocurrent and power conversion efficiency, offering a viable solution to concentrated illumination with large angles of incidence. Moreover, a comprehensive design scheme is also presented to tailor the reflectance spectrum of sub-wavelength structures for maximum photocurrent output of tandem cells.

8620-24, Session 6

On coupling surface texturing and electrical characteristics for improving solar cell efficiency

Vijayakumar Venugopal, Fiat Lux Technologies (United States)

No Abstract Available.

8620-25, Session 6

Simulation and development of subwavelength textured ARCs for CPV applications

Wei Wang, Univ. of Houston (United States); Paul Narchi, Ecole Polytechnique (France); Alexandre Freundlich, Univ. of Houston (United States)

In high X III-V concentrator applications sunlight is focused onto the surface of cell with a wide angular distribution that limits the effectiveness of conventional thin-film AR coatings. Furthermore the

transmission properties are generally degraded non-uniformly over the electromagnetic spectrum which in the case of multi-junction solar cells leads to additional sub-cell current matching related losses. Here, and in an attempt to identify a better alternative to the conventional dual layer ARCs, we have undertaken a systematic analysis of design parameters and angular dependent antireflective properties of dielectric grating formed through the implementation of sub-wavelength arrays of 2D pyramidal and hemispherical textures. The evaluation indicates that through a careful selection of the design and dielectric material these structures can significantly surpass the performance of planar double layer ARCs (i.e. MgF₂/ZnS), and the total number of reflected photons over the 380-2000 nm wavelength range can be reduced to less than 2%. Finally it is shown that the implementation of these structures for a typical 3 or 4 junction solar cells (i.e. inverted metamorphic) and for acceptance angles ranging from 0-60 degrees, reduces total losses of reflected photons for each subcell (and to some extent the resulting current degradation) to less than 4%. Anti-reflection and angular tolerant properties of 2D TiO₂ surface texturing made by nano imprinting technique were simulated and measured in this work. It has been proved that from both simulation and experimental work textured surface surpasses both antireflection and angular tolerant characters of planar ARC, which supplies a potential candidate AR structure for concentrated photovoltaic system.

8620-26, Session 6

Design of broadband omnidirectional antireflection coatings using ant colony algorithm

Xia Guo, Shuai Guo, Bao Lu Guan, Beijing Univ. of Technology (China)

Optimization method which is based on the ant colony algorithm (ACA) is described to optimize antireflection (AR) coating with broadband and omnidirectional characteristics for silicon solar cells incorporated with the solar spectrum (AM1.5 radiation). It's the first time to use ACA for optimizing the AR coatings. In this paper, over 400 nm to 1100 nm, the optimized three-layer step graded-refractive-index (GRIN) AR coating could provide an average reflectance of 2.98% for incident angles from 0 to 80 degree and 6.56% for incident angles from 0 to 90 degree.

8620-27, Session 7

Approaches to future-generation photovoltaics and solar fuels: multiple exciton generation in quantum dots, quantum dot arrays, molecular singlet fission, and quantum dot solar cells *(Keynote Presentation)*

Arthur Nozik, National Renewable Energy Lab. (Viet Nam); Matt Beard, Joey Luther, Justin Johnson, Tavi Semonin, National Renewable Energy Lab. (United States); Josef Michl, Univ. of Colorado at Boulder (United States)

One potential, long-term approach to more efficient future generation solar cells is to utilize the unique properties of quantum dots (QDs) and quantum rods (QRs) and unique molecular chromophores to control the relaxation pathways of excited states to produce greatly enhanced conversion efficiency through efficient multiple electron-hole pair generation from single photons. We have observed efficient multiple exciton generation (MEG) in PbSe, PbS, PbTe, and Si QDs and efficient singlet fission (SF) in molecules that satisfy specific requirements for their excited state energy level structure to achieve carrier multiplication. We have studied MEG in close-packed QD arrays where the QDs are electronically coupled in the films and thus exhibit good transport while still maintaining quantization and MEG. We have developed simple, all-inorganic QD solar cells that produce large short-circuit photocurrents

Conference 8620: Physics, Simulation, and Photonic Engineering of Photovoltaic Devices II

and power conversion efficiencies of about 5% via both nanocrystalline Schottky junctions and nanocrystalline p-n junctions. These solar cells also show for the first time quantum yields (QYs) for photocurrent that exceed 100% in the photon energy regions of the solar spectrum where MEG is possible; the photocurrent MEG QYs as a function of photon energy match those determined via time-resolved spectroscopy. We have also observed very efficient SF in thin films of molecular crystals of 1,3-diphenylisobenzofuran with quantum yields of 200% at the optimum SF threshold of 2Eg (HOMO-LUMO for S0-S1), reflecting the creation of two excited triplet states from the first excited singlet state. Various possible configurations for novel solar cells based on MEG in QDs and SF in molecules that could produce high conversion efficiencies will be presented, along with progress in developing such new types of solar cells. Recent analyses of the effect of MEG or SF combined with solar concentration on the conversion efficiency of solar cells will also be discussed.

8620-28, Session 7

Silicon rich carbide as a conductive substrate for Si QD solar cells

Dongchen Lan, Dawei Di, Gavin J. Conibeer, Xuguang Jia, Lingfeng Wu, ARC Photovoltaics Ctr. of Excellence, The Univ. of New South Wales (Australia)

Silicon quantum dot (Si QD) tandem solar cell is a promising cell structure for realising high efficiency at low cost. The tandem solar cell effectively harnesses energy from the solar spectrum by stacking two or more cells together in the order of descending band gaps. Due to quantum confinement, the band gap of silicon based nanostructures such as Si QDs can be tailored by varying the size of the QDs. Solar cells and light emitting diodes based on Si QDs have been realised in experiments. However, current crowding due to high lateral resistance remains to be a major problem for Si QD devices grown on quartz substrates. Annealed silicon rich carbide (SRC), owing to its electrical conductivity, thermal stability and energy band gap compatible with Si QD cell fabrication, has the potential to overcome this problem. Further, this quasi-transparent thin-film can be used as either substrate or superstrate of a Si QD solar cell and therefore provides flexibility in cell structure design. Here, we investigate the physical, optical and electrical properties of the new material as functions of silicon concentration and doping conditions via a number of characterisation techniques including X-ray diffraction, Raman spectroscopy, ultraviolet-visible-infrared spectroscopy and four-point probe measurement. Some discoveries, including the lower crystallisation temperature of SiC within SRC, are also discussed. The research may provide some insight into the optimisation of annealed SRC as the new conductive material for Si QD solar cell and may boost the final arrival of all-silicon tandem solar cell.

8620-29, Session 7

Non PN junction solar cells using carrier selective contacts (Invited Paper)

Stuart Bowden, Kunal Ghosh, Arizona State Univ. (United States)

A novel device concept utilizing the approach of selectively extracting carriers at the respective contacts is outlined in the work. The dominant silicon solar cell technology is based on a diffused, top-contacted p-n junction on a relatively thick silicon wafer for both commercial and laboratory solar cells. The Voc and hence the efficiency of a diffused p-n junction solar cell is limited by the emitter recombination current and a value of 720 mV is considered to be the upper limit. The value is more than 100 mV smaller than the thermodynamic limit of Voc as applicable for silicon based solar cells². Also, in diffused junction the use of thin wafers (< 50 μm) are problematic because of the requirement of high temperature processing steps. But a number of roadmaps have identified solar cells manufactured on thinner silicon wafers to achieve lower cost and higher efficiency. The carrier selective contact device provides a novel alternative to diffused p-n junction solar cells by eliminating

the need for complementary doping to form the emitter and hence it allows the solar cells to achieve a Voc of greater than 720 mV. Also, the complete device structure can be fabricated with low temperature thin film deposition or organic coating on silicon substrates and thus epitaxially grown silicon or kerfless silicon, in addition to standard silicon wafers can be utilized.

8620-30, Session 8

Advanced multi-junction solar cells for space applications: Analysis and modeling of radiation effects and device performance (Invited Paper)

Raymond Hoheisel, U.S. Naval Research Lab. (United States) and The George Washington Univ. (United States); Matthew P. Lumb, U.S. Naval Research Lab. (United States) and The George Washington Univ. (United States); Scott R. Messenger, U.S. Naval Research Lab. (United States); Maria Gonzalez, Sotera Defense Solutions, Inc. (United States); Christopher G. Bailey, David A. Scheiman, U.S. Naval Research Lab. (United States); Sergey Maximenko, Sotera Defense Solutions, Inc. (United States); Phillip P. Jenkins, Robert J. Walters, U.S. Naval Research Lab. (United States)

The design of advanced space solar cells is motivated by optimizing the performance at not only beginning-of-life (BOL) but also at end-of-life (EOL) mission conditions. To understand, control and ultimately improve the EOL performance, a detailed characterization and simulation of the radiation response is required. The interaction of space particles with the different semiconductor materials in a multi-junction solar cell structure is discussed and the consideration of radiation-induced defects in solar cell device models is presented. Special consideration is given to the EOL performance of novel PV structures. Advanced characterization techniques like EL, EBIC, and CL are discussed to study the impact of space radiation on both optical and electrical semiconductor parameters.

8620-31, Session 8

Modeling of defect tolerance of IMM multijunction photovoltaics for space application

Akhil Mehrotra, Alexandre Freundlich, Univ. of Houston (United States)

Previously we have shown that by optimizing the device design (emitter-base thickness, doping) the efficiency of highly dislocated (or irradiated) single junction and multi junction III-V solar cell can be significantly improved. Here we have evaluated the dependence of efficiency as a function of thicknesses, defects, space-radiation and band gaps for 3 and 4 junction IMM solar cells. Reduction of defects by use of thick sophisticated graded metamorphic buffers in metamorphic or inverted metamorphic solar cells has been a requirement to obtain high efficiency devices. With increase in number of metamorphic junctions to obtain higher efficiencies, these graded buffers constitute a significant part of growth time and cost for manufacturer of the solar cells. Ultrathin IMM devices perform better in presence of dislocations or/and radiation harsh environment compared to conventional thick IMM devices. By optimizing device design we can obtain nearly same EOL efficiencies from highly dislocated InGaAs present in IMM solar cells than defect filtered IMM solar cells. Thickness optimization of the device would result in better defect and radiation tolerant behavior of 0.7eV and 1eV InGaAs sub-cells which would in turn require thinner buffers with higher efficiencies, hence reducing the total device thickness. It is also shown that for an equivalent 1015 cm⁻² 1 MeV electron fluence radiation, very high EOL efficiencies can be afforded with substantially higher dislocation densities (<2x10⁷ cm⁻²) than those commonly perceived as acceptable for IMM devices with remaining power factor as high as 0.85.

8620-32, Session 8

Investigation of carrier removal from quantum dot triple junction solar cells

Christopher Kerestes, David V. Forbes, Mike Welsh, Eli Fernandez, Rochester Institute of Technology (United States); William T. Lotshaw, The Aerospace Corp. (United States); Yong Lin, Benjamin C. Richards, Paul Sharps, Seth M. Hubbard, EMCORE Corp. (United States)

Quantum dot triple junction solar cells (QD TJSCs) have potential for higher efficiency for space and terrestrial applications. Extended absorption in the QD layers can increase efficiency by increasing the short circuit current density of the device, as long as carrier extraction remains efficient and quality of the bulk material remains high. Experimental studies have been conducted to quantify the carrier extraction probability from quantum confined levels and bulk material. One studies present insight to the carrier extraction mechanisms from the quantum confined states through the use of temperature dependent measurements. A second study analyses the loss in carrier collection probability in the bulk material by investigating the change in minority carrier lifetimes and surface recombination velocity throughout the device. Recent studies for space applications have shown response from quantum structures to have increased radiation tolerance. The role strain and bonding strength within the quantum structures play in improving the radiation tolerance is investigated. The combination of sufficiently good bulk material and device enhancement from the quantum confinement leads to temperature dependent measurements that show TJSCs outperform baseline TJSCs near and above 60oC. Insight into the physical mechanisms behind this phenomenon is presented.

8620-33, Session 8

Simulation of radiation effects on solar cells: DLTS vs SRIM for trap data

Marek Turowski, Timothy Bald, Ashok Raman, Alex Fedoseyev, CFD Research Corp. (United States); Jeffrey Warner, U.S. Naval Research Lab. (United States)

We present a predictive computational approach that limits use of DLTS experiments. Three-dimensional NanoTCAD simulations are used for physics-based prediction of space radiation effects in III-V solar cells, and validated with experimentally measured characteristics of a p+n GaAs solar cell with AlGaAs window. The computed dark and illuminated I-V curves as well as corresponding performance parameters matched very well experimental data for 2 MeV proton irradiation at various fluences. We analyze the role of majority vs. minority and deep vs. shallow carrier traps in the solar cell performance degradation. The traps/defects parameters used in the simulations were derived from Deep Level Transient Spectroscopy (DLTS) data obtained at NRL. It was noticed that the degradation caused by deep traps observed in single-trap numerical tests exhibit a very similar trend to the degradation caused by a full spectrum of defect traps, but to a lesser degree. This led to the development of a method to accurately simulate the degradation of a solar cell by using only a single deep level defect whose density is calculated by the Stopping and Range of Ions in Matter (SRIM) code. Using SRIM, we calculated the number of vacancies produced by 2 MeV proton irradiation for fluences ranging from $6E10\text{ cm}^{-2}$ to $5E12\text{ cm}^{-2}$. Based on the SRIM results, we applied trap models in NanoTCAD and performed full I-V simulations from which the amount of degradation of performance parameters (I_{sc} , V_{oc} , P_{max}) was calculated. The physics-based models using SRIM allowed obtaining good match with experimental data.

8620-34, Session 8

Characterization of radiation tolerance and radiative lifetime effects in doping superlattice solar cells

Michael A. Slocum, David V. Forbes, Seth M. Hubbard, Rochester Institute of Technology (United States)

Doping superlattice devices have been pursued in part because of their inherent radiation hardness which results from long lifetimes and minimum diffusion length requirements in the nanometer range. Diffusion length requirements are reduced because of the multiple closely spaced doped layers in the superlattice. Higher doping levels in conjunction with close superlattice spacing result in large electric fields in the range of $5 \times 10^5\text{ V/cm}$ that quickly collect carriers into the majority doped layers. The effect of the alternative solar cell structure will be studied by irradiating multiple device structures with 4.2 MeV alpha particles. Comparisons will be made between doping superlattice devices and single junction p-i-n structures, as well as between varying doping superlattice device designs. Previous work developing a simulation routine to characterize the radiation response for these devices will be extended to confirm the predictive model developed. One of the fundamental aspects of the doping superlattice that increases radiation tolerance is an increase in radiative lifetime due to spatial charge separation. Lifetimes in GaAs have been seen to increase from the nanosecond range to the microsecond range in doping superlattices, and it is believed that this also helps to improve the radiation tolerance. Lifetimes will be measured prior to and following radiation to understand the effect on lifetime in a device structure where the lifetime is not limited by the crystal structure. This work signifies a step forward in understanding the radiation effects of doping superlattice devices, and their potential for high radiation environments.

8620-36, Session 9

Physics of Cu(In,Ga)Se₂ microcells under ultrahigh illumination intensities (*Invited Paper*)

Myriam Paire, Laurent Lombez, Frédérique Donsanti, Marie Jubault, Institut de Recherche et Développement sur l'Energie Photovoltaïque (France) and Ecole Nationale Supérieure de Chimie de Paris (France); Stéphane Collin, Jean-Luc Pelouard, Lab. de Photonique et de Nanostructures (France); Daniel Lincot, Jean-François Guillemoles, Institut de Recherche et Développement sur l'Energie Photovoltaïque (France) and Ecole Nationale Supérieure de Chimie de Paris (France)

In order to develop photovoltaic devices with increased efficiency using less rare semiconductor materials, the concentrating approach was applied on Cu(In,Ga)Se₂ thin film devices. Microscale solar cells down to a few micrometers wide were fabricated [1,2]. They show, at around $\times 475$, an efficiency of 21.3%, thanks to concentrated illumination (532 nm laser), compared to 16% efficiency under non-concentrated illumination. Due to the miniaturization, ultrahigh fluxes can be studied (> 1000), without damaging the device.

We analyse the high concentration regime of these micro-devices. Under ultrahigh light fluxes the collection efficiency of photogenerated carriers decreases on certain devices. We attribute this to the screening of the electric field in the junction under high illumination. Numerical simulations of p-n junctions under intense fluxes corroborate this hypothesis. We built a homemade finite element method program, solving Poisson and continuity equations without resorting to the minority carrier approximation. We study the electric field at a p-n junction as a function of illumination intensity, and highlight the screening phenomena. The influence of the semiconductor doping or recombination intensity on the screening of the electric field is studied.

Cu(In,Ga)Se₂ thin films prove to be appropriate for a use under concentration, leading to significant gains in terms of efficiency and

**Conference 8620: Physics, Simulation, and
Photonic Engineering of Photovoltaic Devices II**

material usage. On these particular devices, ultrahigh illuminations can be used and the electric regime studied.

[1] Paire et al, Appl. Phys. Letters, 98, 26, 264102 (2011)

[2] Paire et al, Energy Environ. Sci., 4, 4972-4977 (2011)

8620-37, Session 9

Optofluidic planar solar concentrator

Volker Zagolla, Eric J. Tremblay, Christophe Moser, Ecole Polytechnique Fédérale de Lausanne (Switzerland)

State of the art solar concentrators use free-space, non-imaging optics to concentrate sunlight. Mechanical actuators keep the focal spot on a small solar cell by tracking the sun's position. Planar concentrators emerged recently that employ a waveguide slab to achieve high concentration by coupling the incident sunlight into the waveguide. We report on the development of an opto-fluidic waveguide coupling mechanism for planar solar concentration. The self-adaptive mechanism is light-responsive to efficiently maintain waveguide coupling and concentration independent of incoming light's direction. By using an array of axicons and lenses, an array of vapor bubbles are generated inside a planar, liquid waveguide, one for each axicon-lens pair. The mechanism uses the infrared part of the solar spectrum on an infrared absorbing medium to provide the energy needed for bubble generation. Visible light focused onto the bubble is then reflected by total internal reflection (TIR) at the liquid-gas interface and coupled into the waveguide. Vapor bubbles inside the liquid are trapped by a thermal effect and are shown to self-track the location of the infrared focus. We show experimental results on the coupling efficiency of a single bubble and discuss the effect of angular coupling. Furthermore the effect of an array of bubbles inside the waveguide (as produced by a lensarray) onto the coupling efficiency and concentration factor is analyzed.

8620-38, Session 9

Self-tracking planar concentrator using a solar actuated phase-change mechanism

Eric J. Tremblay, Damien Loterie, Christophe Moser, Ecole Polytechnique Fédérale de Lausanne (Switzerland)

Due to the fundamental principle of étendue, solar concentrators cannot simultaneously achieve large concentration and a large angular acceptance. Because of this, systems with significant concentration (>10x) require mechanical tracking to keep the optics aligned. We will present the design and proof of principle operation of a self-adaptive (passive) planar solar concentrator capable of self-tracking the sun. Reactive self-tracking is a recent concept based on a combination of micro-tracking and a self-adaptive mechanism which directly uses energy from the sun to align the optics. Small localized changes to the optical arrangement are used to align the concentrating system to the sun's position. With fixed panels this approach is limited in field of view (FOV) by the cosine-theta obliquity and not suitable for full diurnal tracking. However, when combined with inexpensive coarse single-axis tracking, this approach suggests new possibilities for low cost concentrating systems.

The self-tracking concentrator is based on a planar solar concentrator where light from a number of lenses is coupled into a lightguide to combine, mix and transport the light to the concentrator output. The self-tracking mechanism uses a paraffin wax phase-change actuator for in-plane displacement of a transparent elastomer for locally actuated lightguide coupling. This coupling mechanism resembles frustrated total internal reflection. A dichroic long-pass faceted reflector buried in the elastomer allows focused infrared light from the sun to pass through and activate the PCM actuator, while reflecting shorter wavelength light which is efficiently coupled into the lightguide at the location of the focused sunlight.

8620-39, Session 9

Adjustable planar lightguide solar concentrators with liquid-prism structure

Jong-Woei Whang, Meng-Che Tsai, Tsung-Xian Lee, Yi-Yung Chen, National Taiwan Univ. of Science and Technology (Taiwan)

Research interests on sunlight applications are booming in recent years, due to the worldwide green-energy trends. Either using PV cells to store sunlight then convert to electricity, or to use sunlight for direct illumination source are among the many research projects which deserve investigation.

In this research, we focus a design combined the above two features together: direct sunlight illumination, and store the sunlight for later usage. Our design structure is as follows:

1. On the surface of outer layer, we use the liquid-prism structure to guide the visible portion of the sunlight spectrum for indoor lighting, and other bands of light passed to another collection;
2. Combine the micro structure of the solid-state prism and aspheric lens to produce a planar lightguide structure, which compresses the plane light source into line light source, then guide the light into solar cells area;
3. Design a light switch to control the angle of the liquid-prism of outer layer, it guides the visible portion of the sunlight spectrum into solar cells, when it is not used for illumination.

We apply it in the NLIS® developed at NTUST, not only retain the advantages of the static concentrator modules, but also eliminate the complex procedure of transmitting and emitting, reduce the loss and cost of energy transfer.

8620-40, Session 10

Multiscale modeling and interface engineering accelerates efficiency enhancements in non-traditional photovoltaic materials (Invited Paper)

Riley Brandt, Rupak Chakraborty, Katy Hartman, Massachusetts Institute of Technology (United States); Jaeyeong Heo, Harvard Univ. (United States) and Chonnam National Univ. (Korea, Republic of); Yun Seog Lee, Jonathan Mailoa, Sin Cheng Siah, Massachusetts Institute of Technology (United States); Prasert Sinsermsuksakul, Roy Gordon, Harvard Univ. (United States); Tonio Buonassisi, Massachusetts Institute of Technology (United States)

With the exception of cuprous sulfide (Cu₂S), binary Earth-abundant photovoltaic compounds (FeS₂, Cu₂O, SnS...) have record conversion efficiencies of a few percent or less, despite decades of research. It has recently been questioned whether these materials are intrinsically limited, or whether further efficiency improvements are possible with the proper scientific approach. In this presentation, we will present evidence supporting the latter hypothesis, demonstrating how a systematic approach to absorber and buffer layer development can accelerate efficiency improvements in certain Earth-abundant compounds. This systematic approach, mirroring the successes of more traditional semiconductor compounds, features multiscale modeling and interface engineering as cornerstones of a concerted effort to improve device performance. We postulate that this systematic approach to improving device performance may extend to a wider range of Earth-abundant absorber materials, potentially increasing the range of "serious" candidate solar cell materials at a historically high rate.

8620-41, Session 10

Dielectric function of ZnO and ZnO:Al thin films obtained under different oxygen concentration during deposition

Nazim T. Mamedov (Mammadov), Eldar Mammadov, Zakir Chahangirli, Oktay Alekperov, Institute of Physics (Azerbaijan); G. Renou, Negar Naghavi, Daniel Lincot, Jean-François Guillemoles, Institut de Recherche et Développement sur l'Energie Photovoltaïque (France)

ZnO:Al/ZnO stack of submicron thickness is commonly used as a conducting transparent front window in standard CIGSe solar cells. Development of their ultrathin variety is currently on agenda and steps towards realization of CIGSe solar cells with ultrathin absorber are directed not only to thinning of the CIGSe active layer but also to optimum design of the ZnO:Al and ZnO window layers. Optical performance of these layers is of great importance for conversion efficiency since optical losses taking place on the way from top contact to active layer are equal to the product of frequency of the incident light and imaginary part of dielectric function of the stack materials.

In this work ZnO and ZnO:Al thin films obtained on glass substrates have been studied at room temperature by spectroscopic ellipsometry using M-2000 an IR-VASE Woolam ellipsometers with rotating compensator, which allow to continuously access the spectral range from 0.188 to 30 micron.

In a trial to compensate the O₂ deficiency in the intrinsic ZnO, a series of ZnO samples have been prepared under oxygen concentration ranging from 0.5 to 8% and examined by spectroscopic ellipsometry. Significant evolution of the dielectric function with oxygen concentration has then been clearly demonstrated.

ZnO:Al thin films with different resistivity have been prepared by changing oxygen concentration during the deposition. Obvious correlation between resistivity of the obtained samples and free electron absorption related part of their dielectric function has then been disclosed.

Optical transitions responsible for dielectric function of the obtained thin films are analyzed.

8620-42, Session 10

Effects of off-stoichiometry and 2nd phases on Cu₂ZnSn(S,Se)₄ (CZTS) device parameters

E. A. Lund, Michael A. Scarpulla, The Univ. of Utah (United States)

While increasing rapidly, record photovoltaic Cu₂ZnSn(S,Se)₄ (CZTSSe) photovoltaic device efficiencies lag the >20% for the sister chalcopyrite system Cu(In,Ga)(S,Se)₂ (CIGSSe). Understanding the complications of quaternary CZTS or CZTSe layers induced by the more complex phase and defect contents compared to the pseudo-ternary CIGSSe layers will aid in developing CZTSSe as a viable thin film photovoltaic earth-abundant material replacement for CIGSSe. In this paper we model the changes in optoelectronic properties of a Mo/CZTSSe/CdS/i-ZnO/ZnO:Al/Ni/Al resulting from compositional and defect population changes within the absorber layer. Various off-stoichiometric conditions and scenarios of composition fluctuations and defect distributions are investigated within a 1D device simulation model. Compositional variation and the relative instability of CZTS may induce changes in the presence and concentration of a variety bulk and interface defects as well as phase segregation both of structurally-coherent and -incoherent phases. We will show results using defect distributions calculated within our quasi-chemical framework and from scenarios of phase segregation at interfaces or within the absorber layer bulk. These scenarios are modeled and simulated device parameters including J-V curves, VOC, JSC, EQE, and FF and admittance spectroscopy results will be reported for various scenarios.

8620-43, Session 10

GaN micro-domes for broadband omnidirectional antireflection for concentrated photovoltaics

Peng Zhao, Ian V. Kidd, Roger H. French, Hongping Zhao, Case Western Reserve Univ. (United States)

III-nitride (In, Al, Ga-N) semiconductors cover a wide spectral range in solar spectrum from ultraviolet to infrared, which provides a great promise to be used as tandem multi-junction (MJ) cells for the next generation high efficiency concentrated photovoltaics (CPVs). The incident photon energy loss due to reflection and scattering at the interface between semiconductor and free space becomes the bottleneck that limits the total conversion efficiency of the solar cells. The ideal surface anti-reflection coating design should cover a broad spectral region of the solar spectrum and with a wide range of light incidence angles.

Here, we propose to form GaN micro-domes in the range of sub-micron to micron as a broadband omnidirectional anti-reflection structure for MJ solar cells. Comprehensive studies on the effect of the micro-dome sizes and shapes on the frequency-dependent and angle-dependent light collection efficiency will be performed. Our studies by using three-dimensional finite-difference-time-domain method indicate significant enhancement of light collection efficiency is achievable by using the GaN micro-domes for MJ CPVs. Studies also show the significant advantage of the micro-dome shapes on the light collection efficiency especially for light with large incidence angles. The formation of GaN micro-domes is through the reactive ion etching (RIE) of both GaN and the self-assembled silica monolayer microspheres. Preliminary experimental studies indicate the tunability of the GaN micro-dome sizes and shapes by controlling the RIE etching conditions. Characterizations of the angle-dependence and frequency-dependence light collection efficiencies for both GaN micro-domes and flat surface show the similar trend as the simulation.

8620-44, Session 11

Recent progress with chalcogenide thin film solar cells (Keynote Presentation)

Daniel Lincot, Institut de Recherche et Développement sur l'Energie Photovoltaïque (France)

No Abstract Available

8620-45, Session 11

Ultra-thin defect tolerant In-free III-V tandems: simulation and development

Alexandre Freundlich, Akhil Mehrotra, Univ. of Houston (United States)

Development of high quality III-V epitaxial films on inexpensive flexible substrates can be a game-changing enabler toward significantly reducing the cost and increasing the efficiency of thin film solar cells, as it offers the possibility of combining the unsurpassed performance of GaAs based multi-junction technologies (1 sun efficiency >36%) with a conventional roll to roll processing standard of thin film industry as afforded by polycrystalline metallic foil technology. Previously we have shown the possibility of fabrication of single crystalline GaAs epilayers on Ceria-coated (A. Mehrotra et al, 38th IEEE PVSC) and Ge/Ceria-coated (A. Freundlich et al, 35th IEEE PVSC) flexible polycrystalline thin metal foils substrates. While such epilayers have demonstrated minimal residual stresses (as extracted from PL analysis), absence of micro-cracks and antiphase disorder, they however exhibit high dislocation densities in excess of 10⁸cm⁻² which exceed by nearly two order of magnitude

Conference 8620: Physics, Simulation, and Photonic Engineering of Photovoltaic Devices II

defect densities considered as acceptable for the demonstration of conventional high efficiency devices.

Here we theoretically and experimentally demonstrate that through a careful design optimization, and despite these dislocation densities, ultra thin (< micron) dual junction solar cells with practical efficiencies in excess of 25% could be achieved. The study has also attempted to avoid the use of conventional indium-bearing III-V alloys and has focused on III-V semiconductor alloys made with more earth-abundant elements (i.e. Al, Sb, N...). We have evaluated as a function of dislocation densities, the design parameters for devices that comprise a 1.7 eV top AlGaAs solar cell and a 1.25 eV bottom GaAs/GaAs(N)Sb cells. The experimental validation of modeling data was undertaken by the fabrication the proposed thin film subcells on intentionally dislocated buffers. As shown here, and in-line with our modeling results, even for defect densities in excess of 10^{18}cm^{-2} , we were able to fabricate sets of top and bottom cells with open circuits voltages of in excess of 1 and 0.8 volts respectively. A direct extrapolation of these preliminary experimental results already indicate the potential for fabricating thin-film III-V devices on metal foils with 1 sun efficiencies in excess of 16%.

8620-46, Session 11

Lambertian back reflector in Cu(InGa)Se₂ solar cell: optical modeling and characterization

Nir Dahan, Univ. Paris-Sud 11 (France); Zacharie Jehl, Jean-François Guillemoles, Daniel Lincot, Negar Naghavi, Institut de Recherche et Développement sur l'Energie Photovoltaïque (France); Jean-Jacques Greffet, Lab. Charles Fabry (France)

In the past years, reducing the thickness of the absorber layer in CIGSe-based solar cells has become a key issue to reduce the global Indium consumption and thus increased its competitiveness. As the absorber thickness is reduced, less photons are absorbed and consequently the efficiency decreases. It is well known that scattering light in the absorbing layer increases the effective optical length, which results in enhanced absorption. In this study, we have deposited a transparent conductive oxide as a back contact to the cell with a white-paint on the rear surface to diffuse the light back to the cell. A proof of concept device is realized and optically characterized. Modeling scattering by rough surfaces can be done by brute force numerical simulations but does not provide a physical insight in the absorption mechanisms. In our approach, we regard the collimated solar light and its specular reflections / transmissions as coherent. On an irregular surface, part of the collimated light is scattered in other directions. To model this diffuse light, we adopt the formalism of the radiative transfer equation, which is an energy transport equation. Thus, interference effects are accounted for only in the coherent part. A special attention is dedicated to preserving reciprocity and energy conservation on the interface. It is seen that most of the absorption near the energy bandgap of CIGSe is due to the diffuse light and that this approach can yield very significant photocurrent gains below 500 nm absorber thickness.

8620-47, Session 11

Effect of nonhomogeneous intrinsic layer in a thin-film amorphous-silicon solar cell

Akhelsh Lakhtakia, Muhammad Faryad, Mahmoud R. Atalla, The Pennsylvania State Univ. (United States)

The intrinsic layer in an amorphous-silicon solar cell is usually several orders of magnitude thicker than the p- and n-type layers to increase the electron-hole pair generation in the intrinsic layer and to decrease the recombination losses in the p- and n-type layers. We hypothesized that a nonhomogeneous intrinsic layer may trap the incident light better and increase the generation rate of charge carriers. The nonhomogeneity can be introduced by varying the composition of amorphous silicon alloys during chemical vapor deposition. The effect of nonhomogeneity

of various types was studied theoretically on the short-circuit current of a single-junction thin-film amorphous-silicon solar cell. The absorption of light was calculated using the rigorous coupled-wave approach for an AM1.5 solar irradiance spectrum for a wavelength range of 400-1100 nm. An antireflection coating consisting of two layers of homogeneous dielectric materials was also used. The backing metallic layer of the solar cell was taken to be periodically corrugated. The short-circuit current of the solar cell with nonhomogeneous intrinsic layer was found to be higher than the solar cell with a homogeneous intrinsic layer.

8620-48, Session 12

Efficiency gain of quantum-well solar cells by light-trapping structure and sunlight concentration (*Invited Paper*)

Masakazu Sugiyama, Kentaroh Watanabe, Yunpeng Wang, Hassanet Sodabanlu, Hiromassa Fujii, Boram Kim, Kenjiro Miyano, Yoshiaki Nakano, The Univ. of Tokyo (Japan)

Insertion of InGaAs/GaAsP strain balanced multiple quantum wells (MQWs) into a GaAs p-i-n junction extends the absorption edge to a longer wavelength and enhances short-circuit current, with a sacrifice of open-circuit voltage (Voc) due to the carrier accumulation to the ground confinement states of the superlattice. Implementation of the superlattice with ultra-thin GaAsP barriers (approximately 3 nm in thickness) can accelerate carrier escape from the confinement states with the help of tunneling carrier transport, resulting in a reduced degradation in Voc. It has been proved that sunlight concentration improves Voc of the p-i-n cell with the superlattice, in a more strong dependency on the sunlight concentration ratio than the cell with the MQWs with thicker barriers. As a result, the superlattice cell has almost negligible drop in Voc with respect to the p-i-n cell without any quantum wells at a concentration ratio larger than 50, leading to a gain in total conversion efficiency. A possible mechanism behind the improvement in Voc for the superlattice cell is the photocurrent generation via the two-step photon absorption, using the infrared photons having the energy smaller than the absorption edge of the superlattice. To help the absorption of such long-wavelength photons, an optical cavity structure has been implemented. On the backside of a p-i-n cell with the superlattice inside, a textured mirror was fabricated that bends the light propagation direction from the normal to the surface and facilitates multiple total reflection of light inside the cell, resulting in the enhanced photo-absorption by the superlattice.

8620-49, Session 12

Thick-well quantum-structured solar cells

Roger E. Welsler, Magnolia Solar, Inc. (United States)

Quantum-structured solar cells incorporating III-V quantum wells or quantum dots have the potential to revolutionize the performance of photovoltaic devices. Enhanced spectral response characteristics have been widely demonstrated in both quantum well and quantum dot solar cells using a variety of different III-V materials. To fully leverage the extended spectral response of quantum-structured solar cells, new device designs are discussed that can both maximize the current generating capability of the limited volume of narrow band gap material and minimize the unwanted carrier recombination that degrades the voltage output.

High-voltage InGaAs quantum well devices have recently been demonstrated in structures that employ advanced band gap engineering to suppress non-radiative recombination and expose the limiting radiative component of the diode current. Analysis of the dark current in these high-voltage structures offers fresh insights into the physical mechanisms governing recombination in quantum well structures. In addition, interesting trends are observed when comparing the spectral response characteristics of quantum-structured solar cells with varying well thickness. These latest findings have important implications for the design of quantum-structured solar cells, strongly suggesting that

Conference 8620: Physics, Simulation, and Photonic Engineering of Photovoltaic Devices II

high efficiency quantum-structured solar cell designs should include structures incorporating a thick narrow band gap well.

8620-50, Session 12

Modeling of dilute nitride cascaded quantum well solar cells for high efficiency photovoltaics

Gopi Krishna Vijaya, Univ. of Houston (United States); Andenet Alemu, First Solar, Inc. (United States); Alexandre Freundlich, Univ. of Houston (United States)

III-V Dilute Nitride multi-quantum well structures are currently promising candidates to achieve 1 sun efficiencies of >40% with multi-junction design (InGaP/ GaAs/ GaAsN/ Ge). Previously under the assumption of complete carrier collection from wells, we have shown that III-V Dilute Nitride GaAsN multi-quantum well (MQW) structures included in the intrinsic region of the third cell in a 4 junction configuration could yield 1 sun efficiencies greater than 40%. However for a conventional deep well design the characteristic carrier escape times could exceed that of radiative recombination hence limiting the current output of the cell, as has been indicated by prior experiments. In order to increase the current extraction here we evaluate the performance of a cascaded quantum well design whereby a thermally assisted resonant tunneling process is used to accelerate the carrier escape process (<30ps lifetime) and hence improve the photo generated carrier collection efficiency. The quantum efficiency of a p-i-n subcell where a periodic sequence of quantum wells with well and barrier thicknesses adjusted for the sequential extraction operation is calculated using a 2D drift diffusion model and taking into account absorption properties of resulting MQWs. The calculation also accounts for the E-field induced modifications of absorption properties and quantization in quantum wells. The results are then accounted for to calculate efficiencies for the proposed 4 junction design, and indicate potential for reaching efficiencies in excess of this structure is above 42% (1 sun) and above 50% (500 sun) AM1.5.

8620-51, Session 12

Thermal up-conversion in nanostructured GaAs solar cells

Daniel J. Farrell, Hassanet Sodabanlu, Yunpeng Wang, The Univ. of Tokyo (Japan); Ryo Tamaki, The Univ. of Tokyo (Japan); Masakazu Sugiyama, Yoshitaka Okada, The Univ. of Tokyo (Japan); Markus Führer, Louise C. Hirst, Nicholas J. Ekins-Daukes, Imperial College London (United Kingdom)

Up-conversion is a promising route to improve the efficiency of conventional photovoltaics. Below-bandgap photons, which normally remain unabsorbed, can be harvested by an up-converter placed at the rear of a solar cell. The up-converter emits above-bandgap photons towards the solar cell which generates additional photocurrent and boosts conversion efficiency.

Conventional up-conversion is a non-linear phenomena driven by a two-photon absorption process occurring in materials with multiple energy levels, such as rare-earth ions or specially engineered molecular systems. However, because of the nature of these materials it is challenging to utilize them directly with conventional high efficiency III-V solar cells.

Thermal up-conversion is a non-equilibrium process occurring when hot-carriers are confined in nanostructures. In the hot-carrier regime the Fermi-Dirac distribution function overlaps strongly with the excited state energy levels of the nanostructured absorber (e.g. III-V quantum wells or quantum dots). This overlap enables the emission of up-converted light from the excited state.

In this presentation we share our progress towards integrating a thermal up-converter into a nanostructured GaAs solar cell. In the III-V material system it may be possible to enhance the up-conversion efficiency by

positioning the nanostructures in an optical cavity, where the cavity is tuned to accelerate the radiative lifetime of the excited state. We will report on photoluminescence studies which demonstrate the thermal up-conversion effect and investigate the role that optical cavities may play in enhancing the up-conversion efficiency.

8620-52, Session 12

Carrier collection efficiency in multiple quantum well solar cells

Hiromasa Fujii, Yunpeng Wang, Kentaroh Watanabe, Masakazu Sugiyama, Yoshiaki Nakano, The Univ. of Tokyo (Japan)

The present paper proposes Carrier Collection Efficiency (CCE) as a useful evaluation measure to investigate the carrier transport in quantum well solar cells. CCE is defined as the ratio of the carriers extracted as a photocurrent to the total number of the carriers that are photo-excited within the p-n junction area. To estimate CCE, the collected current, $J_c(\lambda, V)$, is firstly calculated by subtracting the dark current from the current under a monochromatic illumination at the wavelength of λ . Since $J_c(\lambda, V)$ is the increment of the current by the irradiation, it can be regarded as the amount of the photo-generated carriers which are actually collected to the external circuit. Generally, $J_c(\lambda, V)$ is saturated at a reverse bias, a phenomenon which can be interpreted as 100 % carrier collection. CCE is then calculated by normalizing the collected current at an arbitrary bias to the saturation value.

This derivation procedure is based on the assumption that the saturation of $J_c(\lambda, V)$ at reverse biases indicates the complete extraction of the photo-excited carriers. We verified this hypothesis by studying the balance between the saturated quantum efficiency at a reverse bias and the absorption fraction in the well region estimated with the reflectance and the transmittance of the device grown on a double-side polished wafer.

Characterization of CCE by changing the irradiation wavelength and the applied bias allows us to uncover the underlying problems in carrier transport that especially emerge under operation of the cells, and gives us appropriate clues to overcome those challenges.

8620-53, Session 13

Drift-diffusion modeling of InP-based triple junction solar cells (*Invited Paper*)

Matthew P. Lumb, The George Washington Univ. (United States) and U.S. Naval Research Lab. (United States); Maria Gonzalez, Sotera Defense Solutions, Inc. (United States); Christopher G. Bailey, Igor Vurgaftman, Jerry R. Meyer, Michael K. Yakes, Joshua Abell, Joseph G. Tischler, U.S. Naval Research Lab. (United States); Raymond Hoheisel, The George Washington Univ. (United States); Paul N. Stavrinou, Markus Fuhrer, Nicholas J. Ekins-Daukes, Imperial College London (United Kingdom); Robert J. Walters, U.S. Naval Research Lab. (United States)

The InP-based multijunction solar cell is a promising candidate for achieving ultra-high efficiencies in an all lattice-matched configuration. Detailed balance limiting efficiency calculations reveal that the InP-based material system offers lattice matched materials with bandgaps within the optimal ranges for terrestrial and space power applications. However, the assumptions in such calculations take no account of the real-world carrier transport and optical properties of the materials, and therefore do not give a realistic estimate of the conversion efficiency of actual solar cell architectures. In this work, we use an analytical drift-diffusion model, coupled with detailed carrier transport and minority carrier lifetime estimates, to make realistic predictions of the conversion efficiency of InP-based triple junction cells. Furthermore, we also use the model to make comparisons with incumbent technologies grown on Ge or GaAs substrates. We evaluate the possible strategies for overcoming the

Conference 8620: Physics, Simulation, and Photonic Engineering of Photovoltaic Devices II

problematic top cell for the triple junction, and compare the performance predictions of the detailed balance approach with the predictions of the more realistic charge transport model. The calculations include optical effects from tunnel junctions and dielectric coating layers, and a network simulation approach for calculating the performance at high concentration.

8620-54, Session 13

FEM-based optical modeling of silicon thin-film tandem solar cells with randomly textured interfaces in 3D

Martin Hammerschmidt, Daniel Lockau, Konrad-Zuse-Zentrum für Informationstechnik Berlin (Germany); Sven Burger, Frank Schmidt, Konrad-Zuse-Zentrum für Informationstechnik Berlin (Germany) and JCMwawe GmbH (Germany); Christoph Schwanke, Simon Kirner, Sonya Calnan, The Helmholtz Zentrum Berlin (Germany); Bernd Stannowski, Bernd Rech, Helmholtz-Zentrum Berlin für Materialien und Energie GmbH (Germany)

Light trapping strategies are one of the key research areas in thin film silicon photovoltaics. Due to the relative poor absorption of silicon as an indirect semiconductor light trapping is of the utmost importance for silicon based solar cells. Especially for multi-junction cells, like amorphous silicon / microcrystalline silicon tandem thin-film solar cells, a specific absorption management is necessary to gain optimum efficiency by balancing subcell currents.

Since the 1980s different randomly rough textured front transparent oxides (TCOs) have been the methods of choice as light trapping strategies for thin-film devices with silicon absorbers. Rigorous simulation of these cells opens up a good way of estimating and optimizing the efficiency of light management textures, because a full theoretical understanding of near field effects of light scattering and trapping by these textured interfaces is very difficult.

Rigorous optical modeling of thin-film solar cells with textured interfaces is numerically challenging. Several groups have investigated this using different methods and approaches. We focus strongly on an error analysis study for the presented simulator to demonstrate the numerical convergence of the method. We are convinced that the numerical error of the underlying model should be thoroughly investigated before any predictions are made.

We employ the finite element method in our simulation approach to obtain rigorous solutions of Maxwell's equations for scattering problems in 3D with the appropriate boundary conditions. We include all layer of a common a-Si/muc-Si tandem cell with realistic material parameters in our model. Our analysis includes a detailed study of the simulated cell performance with grid and finite element degree refinement strategies. This rules out discretization errors in order to obtain reliable simulation results.

8620-64, Session PWed

Tuning up the performance of intermediate band Al_xGa_{1-x}As solar cells by doping of AlyGa_{1-y}Sb Type-II quantum dots and spacer layers between dots

Ara M. Kechiantz, Andrei Afanasev, The George Washington Univ. (United States)

The intermediate band (IB) concept involves into consideration the non-linear effect of resonant two-photon absorption for generation of additional photocurrent in solar cells. Such phenomenon promises 63% conversion efficiency if the IB electronic states assist to the resonant absorption only. However, very often IB-states convert themselves into

recombination centers, which drastically increases the dark current and reduces the open circuit voltage of IB solar cells. We have already shown that IB-states composed by type-II quantum dots (QDs) located outside of the depletion region acquire a unique property of quenching recombination activity by concentrated sunlight. Also alignment of energy bands and a shape of potential barriers surrounding QDs are extremely important for quenching recombination activity of such IB-states. The flexibility, in sense of energy band building and incorporating of type-II QDs, brings AlGaSb/AlGaAs system into a range of attractive materials for IB solar cell designs. In particular, doping of these materials enables to control the shape of potential barriers surrounding type-II QDs located "outside" the depletion region. In this paper we model the effect of such doping on the band alignment and photovoltaic performance of GaAs solar cell with AlyGa_{1-y}Sb type-II QDs buried "outside" (separated from) the depletion region. First we study the effect of acceptor doping of Al_xGa_{1-x}As spacer layer between QDs buried in p-doped region of GaAs solar cell, then the effect of donor doping of QDs buried in n-doped region on performance of IB solar cells.

8620-65, Session PWed

MBE grown dilute nitride quantum well solar cells for high-efficiency photovoltaics

Gopi Krishna Vijaya, Univ. of Houston (United States); Akhil Mehrotra, Univ. of Houston (United States); Manori Gunasekera, Alexandre Freundlich, Univ. of Houston (United States)

III-V Dilute Nitride multi-quantum well structures are currently promising candidates to achieve 1 sun efficiencies of >40% with multi-junction design (InGaP/ GaAs/ GaAsN/ Ge). In other works, we have discussed the design having III-V Dilute Nitride GaAsN multi-quantum well (MQW) structures with resonant tunneling setup in the intrinsic region, in order to improve the response potentially yielding 1 sun efficiencies greater than 40%. Earlier efforts in this direction had yielded samples with considerable incorporation of N at the QW/barrier interface, leading to the formation of traps and reducing the overall quantum efficiency. In this work we discuss the results of the growth of MQW solar cells in MBE, with a modified run-vent system for the RF N-plasma setup aimed at increasing the sharpness of the well-barrier transition, and the change in quality of the quantum wells grown. Results from PL spectroscopy and the IV characteristics are also presented.

8620-67, Session PWed

An innovative static compound parabolic concentrator with prism structure used in natural lighting illumination system

Jong-Woei Whang, Guan-Wei Chen, Yi-Yung Chen, National Taiwan Univ. of Science and Technology (Taiwan)

SunLego® is among many types of light concentrators used to collect sunlight for various purposes. SunLego® has the advantage of high concentrate efficiency and easy to produce. However, its concentration efficiency decreases dramatically when the sunlight incident azimuth angle decreases. Current azimuth tolerance is from negative 30 degree to positive 30 degree.

We proposed an innovative static compound parabolic concentrator (CPC) and it will increase the concentrate efficiency largely. It composes of two primary optical components; one is the innovative CPC on the top to increase incident azimuth angle. The bottom component is the prism structure to increase output fiber coupling efficiency.

We utilize Etendue, edge ray and flow line method to design CPC structure. Regarding to different incident azimuth angles sunlight, we use Taguchi method to optimize the prism structure for high coupling efficiency.

The innovative static CPC structure could approach high incident azimuth angle tolerance that is from negative 50 degree to positive 50 degree.

Conference 8620: Physics, Simulation, and Photonic Engineering of Photovoltaic Devices II

Additional, the coupling efficiency is 2.5 times of SunLego. We proposed a high incident azimuth sunlight tolerance CPC. It provides high output efficiency and a stable output.

8620-68, Session PWed

The hybrid coupling element for light-correcting in Natural Light Illumination Systems (NLIS)

Jong-Woei Whang, Tsung-Xian Lee, Ya-Huei Jhang, Yi-Yung Chen, National Taiwan Univ. of Science and Technology (Taiwan)

Sunlight is the most environmental-friendly energy. Through the Natural Light Illumination Systems (NLIS®), we can guide sunlight indoors to use. However, due to the construction cost of the NLIS®, the most cost is spent on the optical fiber. Therefore we intend to design an element that can re-shape the beam from the SunLego to be narrower, where SunLego® is the building unit of NLIS® for light collection.

The element consists of two functional optical structures: the first structure is to convert light from SunLego to parallel beam, technically, is to convert stray light to parallel. We design the first structure based on free form principle. The second is a fan-shaped structure, which is to reduce the light transmission area, this design is based on the E'tendue principle. The reduction of area means we can use smaller fiber for later light transmission, which is crucial to reduce material cost.

8620-69, Session PWed

Modular design optical light pipe with high efficiency

Jong-Woei Whang, Yi-Hsin Yeh, Yi-Yung Chen, National Taiwan Univ. of Science and Technology (Taiwan)

The best benefit of Natural Light Illumination System (NLIS®) is to reduce energy consumption that compare to traditional lighting system. However, the propagation efficiency will decrease dramatically when there is the long distance propagation in NLIS®.

Therefore, this paper has proposed an innovative modulated guiding structure with high propagation efficiency. The base structure is consisting of two Fresnel lenses and the distance between two lenses is two times of focal length. Furthermore, the light will be focused by first Fresnel lens and diverge as original input again before the second lens due to two times of focal length design. The advantage of the innovative design is to avoid energy loss when propagation.

Based on two times of focal length design method and connecting several base structures in the way of cascading, it could make the structure become modulated. The efficiency of a base module structure will reach above 80%.

We have proposed an innovative modeled structure that is with high propagation efficiency. By the Fresnel lens, the structure has the benefit of low cost and easy to produce that compare to traditional natural light system.

8620-70, Session PWed

Improve GaAs solar cells efficiency by using high-transmittance textured PDMS film

Hau-Vei Han, Hsin-Chu Chen, Chien-Chung Lin, Yu-Lin Tsai, Hao-Chung Kuo, Peichen Yu, National Chiao Tung Univ. (Taiwan)

We demonstrate the GaAs solar cells which utilize the high-transmittance textured polydimethylsiloxane (PDMS) film can outstanding increase the short circuit current density and power conversion efficiency of solar cells. The transmittance of PDMS film is exceeded 90%, which can pass through almost all the light of GaAs Solar cells can be absorbed. We

used a special imprint technology to let the PDMS film possess a highly textured surface. Then we measured the characteristics of textured PDMS film and found out that it has a very excellent Haze performance. The effect of flexible textured PDMS film on the suppression of surface reflection in GaAs solar cells is also investigated. The presented technology provides an inexpensive surface anti-reflection process, which can potentially replace typically complex anti-reflection coating (ARC) layer. The GaAs solar cells with textured PDMS layer can effectively enhance the short-circuit current density from 22.91 to 26.54 mA/cm² and the power conversion efficiency from 18.28 to 21.43 %, corresponding to a 17 % enhancement compared to the one without textured PDMS. The open-circuit voltage (Voc) and the fill-factor (FF) of GaAs solar cells exhibit negligible change, because the textured PDMS film was pasted up on the surface of GaAs solar cells and did not interfere with the diode operation. At the same time, we observed through the EQE measurement that the textured PDMS film not only proved wonderful light scattering effect but also generated more electron-hole pairs in all absorption spectrum range. Finally, through this simple PDMS process, we believe this technology shall be a great candidate for next generation of highly efficient and low-cost photovoltaic devices.

8620-71, Session PWed

Investigation in feasibility of molybdenum as a back contact layer for silicon-based quantum dot solar cells

Ziyun Lin, Ivan Perez-Wurfl, Lingfeng Wu, Xuguang Jia, Tian Zhang, Haixiang Zhang, Binesh Puthen-Veetil, Dawei Di, Gavin J. Conibeer, The Univ. of New South Wales (Australia)

A vertical structure with a back contact layer is suggested for silicon quantum dots (Si QDs) solar cells to overcome the current crowding effect arising from the high lateral resistance in the emitter layer of the existing mesa-structured Si QDs solar cells on quartz substrates (Perez-Wurfl, Hao et al. 2009). Molybdenum (Mo) is widely used as the back contact layer in CIGS solar cells due to its high electrical conductivity, good optical reflectance and chemical stability. This paper will focus on the feasibility of Mo as a back contact layer deposited between a quartz substrate and a sputtered silicon rich oxide (SRO) bilayer structure to obtain a fully vertical Si QDs solar cell. In this structure, the desired previously mentioned electrical and optical properties of the Mo thin film have to be maintained during and after a high temperature annealing process. This high temperature process is unavoidable in this structure as it is required to form the Si QDs. This paper aims to study factors that have impacts on critical properties of the Mo thin films processed in contact with Si and SiO₂ at high temperatures. Characterizations including film thickness, microstructure, sheet resistance and optical reflectance measurements are also performed. Furthermore, interfacial properties between the Mo layer and the upper SRO bilayers are investigated.

8620-72, Session PWed

Miniaturized concentrator arrays as compact angle transformers for light collection and distribution

Roland Bitterli, Toralf Scharf, Franz-Josef HAUG, Ecole Polytechnique Fédérale de Lausanne (Switzerland)

Efficient light management is one of the key issues in modern energy conversion systems, might it be to collect optical power or to redistribute light generated by high power light emitting diodes. One problem maintains: the final size of the elements if high quality of light management is needed. We propose a novel scheme by using miniaturized angle transformers or concentrators that have size of several millimeters. In this size range diffraction effects play rarely a role and the design can be based on classical ray tracing. Dimensions are chosen to allow effective solution for high power light emitting diodes as well as

Conference 8620: Physics, Simulation, and Photonic Engineering of Photovoltaic Devices II

solar cells.

In most solar cell designs, the photocurrent is extracted through a conducting window layer in combination with a silver grid at the front of the device. The trade-off between series resistance and shadowing requires either buried contacts or screen printing of narrow lines with high aspect ratio. We propose an alternate approach where an array of parabolic concentrators directs the incoming light into the cell. The front metallization can thus be extended over the area between the paraboloids without shadowing loss.

High power light emitting diodes are source with certain far field distribution and composed often out of several chips. Applying the concentrator array technology not on the whole source but locally on each chip promises small and effective solutions.

We demonstrate realization of linear and hexagonal arrays of micro-concentration systems, discuss details of application and results of simulation of their optical properties in applications.

8620-73, Session PWed

Improvement in etching rate for epilayer lift-off with surfactant

Fan Lei Wu, Ray Hua Horng, Jian Heng Lu, Kao Yu Cheng, Chun Li Chen, National Chung Hsing Univ. (Taiwan)

In this study, the GaAs epilayer is quickly separated from GaAs substrate by epitaxial lift-off (ELO) process with mixture etchant solution. The HF solution mixes with surfactant as mixture etchant solution to etch AlAs sacrificial layer for the selective wet etching of AlAs sacrificial layer. Addition surfactants etchant significantly enhance the etching rate in the hydrofluoric acid etching solution. It is because surfactant provides hydrophilicity to change the contact angle with enhances the fluid properties of the mixture etchant between GaAs epilayer and GaAs substrate. Arsine gas was released from the etchant solution because the critical reaction product in semiconductor etching is dissolved arsine gas. Arsine gas forms a bubble, which easily displaces the etchant solution, before the AlAs layer was undercut. The results showed that acetone and hydrofluoric acid ratio of about 1:1 for the fastest etching rate of 45 $\mu\text{m} / \text{min}$. The etching rate increases about 4 times compared with pure hydrofluoric acid, moreover can shorten the separation time about 70% of GaAs epilayer with GaAs substrate. The results indicate that etching ratio and stability are improved by mixture etchant solution. It is not only saving the epilayer and the etching solution exposure time, but also reducing the damage to the epilayer structure.

8620-74, Session PWed

ZnO nanowire arrays for photovoltaic and light-emitting devices

Bitu Janfeshan, Siva Sivoththaman, Univ. of Waterloo (Canada)

One dimensional nanostructures of zinc oxide (ZnO) have become increasingly popular due to their unique properties and versatile potential applications in electronic and opto-electronic devices. ZnO is a compound semiconductor with a wide direct band gap of 3.37 eV and large exciton binding energy of 60 meV. It is a conductive and transparent material and, more importantly, its nanostructures have shown UV-blue photoluminescence emission at room temperature. These properties make it an excellent candidate for photovoltaic (PV) and light emitting (LED) devices as active structural component, transparent electrode, or a UV-blue emitter.

In this work, synthesis of ZnO nanowires (NW) by chemical vapor deposition (CVD) and hydrothermal growth methods are reported and PVD and LED device applications discussed. The NW arrays are fully characterized. The morphology of the NWs was studied by SEM and TEM microscopies. The synthesis process leads to a high crystallinity in the ZnO NWs. The optical properties of the NWs were investigated by photoluminescence (PL). The PL studies revealed a high intensity UV-blue emission at 378 nm and a low intensity green emission at 506

nm. The spectra also revealed low point defect concentration in the NWs. Different substrates have been used for the NW growth.

In the second part of the paper, PV and LED device architectures will be presented exploiting the observed properties of the NWs. While the NWs grown on ITO-coated glass wafers can be used to fabricated quantum dot-sensitized solar cells (QDSSC), those grown on GaN layer (as the p-type material) can be used for the LED fabrication. In the case of QDSSCs, the QDs are embedded in the spacing between the NWs. The electroluminescence spectra, I-V characteristics, and incident photon conversion efficiency (IPCE) spectra of the corresponding devices will be presented and discussed.

8620-75, Session PWed

Effect of grain boundary on nanoscale electronic properties of hydrogenated nanocrystalline silicon studied by Kelvin probe force microscopy

Rubana B. Priti, Sandeep Mahat, Venkat Bommisetty, South Dakota State Univ. (United States)

Hydrogenated nanocrystalline silicon (nc-Si:H) based alloys have strong potential in cost effective and flexible photovoltaics. However, nc-Si:H undergoes light induced degradation (LID), which degrades the device efficiency by over 15%. The microstructural processes responsible for the LID are still under debate. Several recent studies suggest that the generation of metastable defects at grain/ grain-boundary (GB) interface enhances density of traps, which limits the charge collection efficiency. Conventional characterization techniques can measure transport properties such as electrical conductivity or carrier mobility averaged over large sample volumes. However, nanoscale characterization tools, such as Scanning Kelvin probe Force Microscopy (KFM), reveal local electronic properties of grains and GBs which may lead to better understanding of microscopic process of metastability. The optoelectronic properties of nc-Si:H films were measured in dark and under illumination to study LID at the nanoscale. The surface potential, surface photovoltage (SP) and charge distribution were measured in as-deposited and photo-degrade samples using a custom-designed scanning probe microscopy tool installed in an environment controlled glove-box. Photodegradation resulted in an increased upward bending of the conduction band edge, suggesting accumulation of photo-generated charges at GBs. This effect is attributed to generation of acceptor like defects (traps) at GBs during illumination. Density of defects will be estimated from grain/GB width and absolute value of band bending.

8620-76, Session PWed

Numerical investigation on the structural characteristics of GaN/InGaN solar cells

Yen-Kuang Kuo, Jih-Yuan Chang, Shih-Hsun Yen, National Changhua Univ. of Education (Taiwan)

Due to the tunable energy bandgap of InGaN alloys ranging from 0.7 eV to 3.4 eV with characteristics of direct bandgap and numerous superior photovoltaic characteristics, it was predicted that high-efficiency multi-junction and full-spectrum-response tandem solar cells could be achieved based solely on the III-nitride material system. The most conventional configuration of III-nitride solar cells is Ga-faceted and p-on-n structures. Additionally, the GaN layer is usually employed to be the base and the p-contact layer of the solar cell. However, it is demonstrated that the huge polarization-induced charges and potential barrier in the hetero-interfaces are harmful for the photogenerated carriers to be collected. The energy conversion efficiency is thus severely degraded, especially when the indium composition is high. To solve these challenges, the elimination or mitigation of the abrupt hetero-interfaces should be efficient. In this study, various kinds of solar cell structures, including the homo-junction structures and the hetero-junction structures with compositional-graded layers are investigated numerically. The structures

Conference 8620: Physics, Simulation, and Photonic Engineering of Photovoltaic Devices II

under various situations of indium composition and degree of polarization are explored systematically. Specifically, the photovoltaic performance, energy band diagrams, electrostatic fields, and recombination rates are analyzed. Then, according to the simulation results, the appropriate solar cell structure which possesses high energy conversion efficiency is proposed.

8620-77, Session PWed

Thin film solar cells based on cavity enhanced grating structure

Guangyao Su, Fangwang Gou, Chuanhong Liu, Siyao Guo, Zhaoyu Zhang, Peking Univ. Shenzhen Graduate School (China)

A cavity enhanced one-dimensional grating structure is proposed to improve the light absorption within the thin film solar cell. Typically, dielectric or metal structure including gratings or particles is integrated in the solar cells for light absorption enhancement. The mechanism includes increasing the surface area/surface angle for light scattering, forming the planar guided modes, forming a cavity within the thin film itself allowing the light trapping. However, the latter two mechanisms are optimized separately. In this paper, we optimize two thicknesses of the cavities and then combine them into a grating structure for better control of the absorption. Due to the large test parameter space, only one-dimensional grating structure is tested with finite element method (FEM). In a unit of proposed grating structure, twosome width parts with different thickness T_a and T_b are combined. To keep the top and back surface flat, the difference in thickness is compensated with indium tin oxide (ITO). Thus two cavities form with top surface of active layer and top surface of ITO. The two cavity resonances result in an absorption enhancement for the different spectrum region. Comparing to the flat thin film solar cells with thickness of T_a and T_b respectively, absorption enhancement factor of 1.17 and 1.13 for the AM 1.5 spectrum is achieved. Noted that this grating structure could be combined with other techniques such as anti-reflection coating, metal and dielectric nano-structures. Furthermore, three or more different thickness could be integrated to get three or more cavity resonance to absorb more light.

8620-78, Session PWed

Use free-form reflector method in lighting coupler

Jong-Woei Whang, Shu Hao Chang, Yi-Yung Chen, National Taiwan Univ. of Science and Technology (Taiwan)

The Natural Light Guiding System (NLIS®) developed at NTUST is designed to guide the outdoor sunshine for indoors illumination. The system can be divided into three subsystems: the light collecting sub-system (LCS), the light transmitting sub-system (LTS), and the light emitting sub-system (LES). These three sub-systems are intimately connected with one another. However, a great deal of energy is wasted during the process of passing the sunlight from the LCS to the LES.

In this research, we design an optical coupler based on a combination of "The Power Index of Energy" and "Free-form" structure to improve the efficiency. Six time periods were selected when the sunlight was the strongest during a day. Six different angles were produced by these six rays of the sunlight. And the six angles of incidence could be derived from the "Equation of Internal Circle." Using this method accompanying with the "Discrete surface" built by "The Power Index of Energy," the "Reflect surface" was formed.

Through the stimulations and analyses of this "Reflect surface" by the optical software, the results showed that the efficiency of the light transmission was improved more than three times comparing to the original system.

8620-55, Session 14

High current generation in dilute nitride solar cells grown by molecular beam epitaxy

Arto Aho, Antti Tukiainen, Ville Polojärvi, Joel Salmi, Mircea Guina, Tampere Univ. of Technology (Finland)

Dilute nitrides, i.e. GaInNAs, are semiconductor compounds that incorporate a small amount of N, typically below 5%, and exhibit extraordinary optical and electrical properties. Most important for solar cell applications is the fact that their band-gap can be engineered to cover the entire range from 1.1 eV to 0.8 eV while preserving lattice matching to GaAs. Thus they are ideal candidates for the development of multijunction solar cells with efficiencies above 40%, the enabler of future concentrated photovoltaic systems.

We review our recent work concerning the molecular beam epitaxy of dilute nitride solar cells. Molecular beam epitaxy enables a high level of control of the growth conditions and alleviates known issues related to epitaxy of dilute nitrides, such as C-doping, ultimately enabling to achieve high quality materials. We focus on discussing the mechanisms linking the epitaxial and annealing conditions to the operation of dilute nitride solar cells for a rather wide range of N compositions. We report operation of a single junction dilute nitride solar cells with a short circuit current density as high as ~ 40 mA/cm² under 1 sun illumination. We also demonstrated a 3-junction GaInP/GaAs/GaInNAs solar cell that exhibited a JSC of ~ 13 mA/cm², an open circuit voltage of ~ 2.52 V, and a fill-factor higher than 80%.

8620-56, Session 14

Dilute phosphide nitride semiconductors as photocathodes for electrochemical solar energy conversion

Vijay Parameshwaran, Xiaoqing Xu, Yangsen Kang, James Harris, H. S. Philip Wong, Bruce Clemens, Stanford Univ. (United States)

A wide variety of semiconductor materials have been investigated for use as photoelectrodes in electrochemical solar energy conversion systems. However, most are not viable for this application due to insufficient bandgap energetics, poor light absorption and charge transport properties, and instability in aqueous media. Dilute phosphide nitride semiconductors, which have the form (Al,Ga,In)P_{1-x}N_x for small x, offer a platform for designing and optimizing photocathode structures that can address all of these issues. Engineering these materials can be achieved through nitrogen incorporation, alloy and bandgap engineering, heterostructure design, and nanostructure synthesis.

In this work, we present results in the synthesis of dilute phosphide nitride thin films and nanowires through metalorganic chemical vapor deposition. High-resolution x-ray diffraction and x-ray photoemission spectroscopy provide evidence of a dilute amount of nitrogen incorporated within heteroepitaxial thin films. Scanning electron microscopy and Auger electron spectroscopy provide evidence of dilute phosphide nanowire growth with both ex-situ gold nanoparticle catalysts and in-situ Group III metal nanoparticle catalysts. Electrochemical testing in aqueous electrolytes provides evidence of photocurrent enhancement and material stability under both monochromatic LED radiation and xenon lamp illumination. Finally, nanostructure and heterojunction modeling with Sentaurus shows optimized architectures that would best incorporate these dilute phosphide nitride materials as photocathodes with respect to light absorption and band diagram energetics.

8620-57, Session 14

Ohmic contacts to n-type GaSb grown on GaAs by the interfacial misfit dislocation technique

Nassim Rahimi, Orlando S. Romero, The Univ. of New Mexico (United States); Daniel M. Kim, Virginia Polytechnic Institute and State Univ. (United States); Nathan B. J. Traynor, SUNY Geneseo (United States); Andrew A. Aragon, Thomas J. Rotter, Ganesh Balakrishnan, Sayan D. Mukherjee, Luke F. Lester, The Univ. of New Mexico (United States)

For high conversion efficiencies, photovoltaic solar cells must absorb the widest solar spectral range possible. GaSb absorbs in the infrared and is therefore extremely useful in multijunction solar cells. However, bulk-grown GaSb is expensive, which limits the cost-benefit for its usefulness in solar power industries. Epitaxial GaSb grown on substantially cheaper GaAs substrates would not only reduce cost but also combine its wide IR absorption spectral range with the high absorption in the visible spectrum for GaAs, thereby providing high efficiencies.

Unfortunately, the lattice constant of GaSb is 7.8% larger than that of GaAs, causing large concentrations of dislocations at the interface. To overcome lattice mismatch, metamorphic or several microns thick strain-relaxing buffer layers of GaSb on GaAs substrates are generally grown. However, metamorphic layers have very low carrier lifetimes and are difficult to dope with n- or p-type dopants for appropriate carrier densities required in multijunction solar cells.

The Interfacial Misfit Dislocation (IMF) technique is used to reduce the thick metamorphic layer to a single monolayer interface, at which nearly all the strain associated with the GaSb-GaAs lattice mismatch is relaxed. Low resistance Ohmic contacts, essential for efficient photovoltaic solar cells, have been fabricated on MBE grown n-GaSb on Si-GaAs by the IMF technique. The IMF interface is highly conductive. Therefore, it is essential that Ohmic contacts do not penetrate to it during annealing, thereby creating vertical shunt paths to the underlying GaAs. Different metallizations and process windows on annealing time and temperature have been investigated to achieve minimal penetration depth while maintaining low Ohmic contact resistances.

8620-58, Session 14

Carrier dynamics in bulk 1eV InGaAsNSb materials and epitaxial lift off InGaP-GaAs layers grown by MOVPE for multi-junction solar cells

Yongkun Sin, Stephen LaLumondiere, William T. Lotshaw, Steven C. Moss, The Aerospace Corp. (United States); Tae Wan Kim, Kamran Forghani, Luke J. Mawst, Thomas F. Kuech, Univ. of Wisconsin-Madison (United States); Rao Tatavarti, Andree Wibowo, Noren Pan, MicroLink Devices, Inc. (United States)

III-V multi-junction solar cells are based on a triple-junction design that consists of an InGaP top-junction, a GaAs middle-junction, and a bottom-junction that employs either a 1eV-material such as dilute nitride or InGaAs layer. Both approaches have a potential to achieve high performance triple-junction solar cells. In addition, it will be beneficial if III-V triple-junction solar cells can significantly reduce weight and can be manufactured cost effectively while maintaining high efficiency. The most attractive approach is to employ full-wafer epitaxial lift off (ELO) technology, which can eliminate the substrate weight and also enable multiple substrate re-usages.

We employed time-resolved photoluminescence (TR-PL) techniques to study carrier dynamics in MOVPE-grown bulk dilute nitride layers lattice matched to GaAs substrates, where carrier lifetime measurements are crucial in optimizing MOVPE materials growth. We studied carrier dynamics in InGaAsN(Sb) layers with different amounts of N

incorporated. Carrier lifetimes were also measured from InGaAsN(Sb) layers at different stages of post-growth thermal annealing steps. Post-growth annealing yielded significant improvements in carrier lifetimes of InGaAsNSb double hetero-structure (DH) samples compared to InGaAsN DH samples possibly due to the surfactant effect of Sb. In addition, we studied carrier dynamics in MOVPE-grown InGaP-GaAs layers grown on GaAs substrates. The structures were grown on top of a thin AlGaAs release layer, which allowed epitaxial layers grown on top of the AlGaAs layer to be removed from the substrate. The GaAs layers had various doping densities and thicknesses. We will present our TR-PL results from both pre- and post-ELO processed InGaP-GaAs samples.

8620-59, Session 14

Improved efficiency of InGaN/GaN multiple quantum well solar cells using CdS quantum dots and distributed Bragg reflectors

Yu-Lin Tsai, Hsin-Chu Chen, Chien-Chung Lin, Kuo-Ju Chen, Hau-Vei Han, National Chiao Tung Univ. (Taiwan); Po-cheng Chen, Jin-Kong Sheu, National Cheng Kung Univ. (Taiwan); Peichen Yu, Hao-Chung Kuo, National Chiao Tung Univ. (Taiwan)

In recent year, InGaN-based alloys have also been considered for photovoltaic devices owing to distinctive material properties which are beneficial for photoelectric conversion. However, the device top layer employs indium tin oxide (ITO) as transparent conductive oxide (TCO), which absorbs UV photons without generating photocurrent. Moreover, the thin quantum-well absorber restricted by the epitaxial challenges has led to insufficient light absorption. In this report, we propose an approach for solving these problems. A hybrid design of InGaN/GaN multiple quantum wells (MQWs) solar cells combined with colloidal CdS quantum dots (QDs) and back-side distributed Bragg reflectors (DBRs) has been demonstrated. In this design, CdS QDs provide a down-conversion effect at the UV regime to avoid absorption of ITO and also function as anti-reflective features. DBRs at the back side can effectively reflect the light back into the absorber layer. Consequently, CdS QDs enhance the external quantum efficiency (EQE) for light with wavelengths shorter than 400 nm, while DBRs provide a broad band enhancement in EQE, especially within the wavelength range of 400 nm ~ 430 nm. CdS QDs effectively enhanced the power conversion efficiency by as high as 7.2%, compared to a reference device without CdS QDs. With the incorporation of DBRs, the enhancement in power conversion efficiency can be further boosted to 14%. We believe that the hybrid design of InGaN/GaN MQWs solar cells with QDs and DBRs offers a viable solution to the attainment of high efficiency InGaN/GaN MQWs solar cells.

8620-60, Session 15

Optical and electrical characteristics of silicon nanocone: Polymer hybrid heterojunction solar cells

Chun-Yao Lee, National Taiwan Univ. (Taiwan); Huai-Te Pan, Yu-Chih Cheng, National Chiao Tung Univ. (Taiwan); Yuh-Renn Wu, National Taiwan Univ. (Taiwan); Peichen Yu, National Chiao Tung Univ. (Taiwan)

Recently, Si/organic hybrid solar cells have been widely studied due to advantages of low-cost materials and room-temperature solution process. In this work, we present the simulation results of hybrid heterojunction solar cells based on a conjugated polymer poly(3,4-ethylenedioxythiophene): poly(styrene sulfonate) (PEDOT:PSS) directly spun-cast on Si nanocones. The conformal surface coverage of the conductive polymer on the optimal Si nanocone structures forms a uniform heterojunction to enhance light absorption and carrier collection, leading to a high power conversion efficiency of over 11% by Yi Cui's group. The device modeling employs a rigorous coupled wave analysis method and a two-dimensional self-consistent Poisson and continuity

Conference 8620: Physics, Simulation, and Photonic Engineering of Photovoltaic Devices II

equations solver, which calculate the optical and electrical properties of hybrid heterojunction solar cells. In addition, the effects of nanocone dimension, doping concentration, band alignment, and back surface field will also be discussed. With the good light trapping ability resulting from sub-wavelength nanostructure and inexpensive processing method, hybrid solar cells based on thin organic/inorganic material are promising alternatives for the attainment of economical green energy resources.

8620-61, Session 15

Carbon nanotube-silicon nanowire inversion layer solar cells

Maureen K. Petterson, Andrew Rinzler, Univ. of Florida (United States)

Research on electrolyte gated carbon nanotube-silicon Schottky solar cells has demonstrated that the electrolyte can laterally extend the depletion layer across the silicon surface, well beyond the nanotube/semiconductor junction, enabling the nanotube film to cover a small percentage of the active area of the solar cell without a decrease in the power conversion efficiency (PCE). In these devices a gate voltage is capacitively coupled to the nanotube film through an electrolyte, simultaneously modulating the Fermi level of the carbon nanotube film and extending the depletion (inversion) layer. This mechanism permits exploitation of an anti-reflective nanostructure, silicon nanowires, which would otherwise be impractical. A silicon nanowire forest etched into the surface of a silicon substrate exhibits excellent broad band light absorption (less than 5% over 400-1100 nm), making it suitable for photovoltaic applications. A thin nanotube film draped across the top of this nanowire forest forms a Schottky junction solar cell having a negligible short circuit current and very low PCE due to the very small junction contact area that exists between the nanotubes and the nanowires and the large number of recombination sites along the Si nanowire sidewalls. Simple addition of the electrolyte immediately increases the device short circuit current to 32.5 mA/cm² while a gate voltage of 1V gives an open circuit voltage of 0.58V, a fill factor of 0.74, and a PCE of 13.9%.

8620-63, Session 15

Enhancement of power conversion efficiency of DSSCs by hybridization of TiO₂ nano-helices array and nanoparticles

Seung Hee Lee, Jong Kyu Kim, Pohang Univ. of Science and Technology (Korea, Republic of)

One-dimensional nanostructures such as an array of TiO₂ nanotubes or nanorods have attracted considerable attention for high performance dye sensitized solar cells (DSSCs) due to their better light scattering and enhanced charge collection efficiency compared to conventional randomly-packed TiO₂ nanoparticles. However, poor dye adsorption ascribed from their relatively low surface area limits the photovoltaic performance of DSSCs.

Here, we fabricated an array of TiO₂ nano-helices by electron-beam oblique-angle deposition technique for improving the performance of DSSCs through considerable light-scattering effect, and enhanced electron transport along the near-single-crystalline TiO₂ nano-helices. In addition, the empty space between TiO₂ nano-helices is filled with TiO₂ nanoparticles in order to overcome the low surface area of the nano-helices array. We fabricated DSSCs with the hybridized TiO₂ nano-helices array and nanoparticles, together with conventional DSSCs with TiO₂ nanoparticles as a reference. The specific surface area and the light-scattering effect were evaluated through dye desorption and light absorption measurement after the dye adsorption process. After the completion of the DSSC fabrication, carrier transport and recombination time were estimated by intensity-modulated photocurrent spectroscopy and intensity-modulated photovoltage spectroscopy (IMPS/IMVS), and the current-voltage characteristics were also acquired for evaluating the

cell performance.

It was found that DSSCs with the hybridized TiO₂ nano-helices array and nanoparticles show enhanced performances such as higher light absorption and power conversion efficiency than the reference, which are attributed to the larger specific surface area, enhanced light scattering by the 3-dimensional nano-helices array, and fast transport time of photo-injected electrons enabled by the near-single-crystalline TiO₂ nano-helices.

8621-1, Session 1

Graphene-enabled silver nanoantenna sensors (*Invited Paper*)

Ertugrul Cubukcu, Jason C. Reed, Hai Zhu, Alexander Y. Zhu, Univ. of Pennsylvania (United States)

Because of its low loss at optical frequencies, silver is the ideal material for plasmonics. However, it is often replaced by a more lossy metal, gold, due to silver's tendency to tarnish and roughen, forming silver sulfide on its surface. This dramatically diminishes its optical properties and renders it unreliable for applications. By passivating the surface of silver nanostructures with monolayer graphene, atmospheric sulfur containing compounds are unable to penetrate the graphene to degrade the surface of the silver. Preventing this sulfidation eliminates the increased material damping and scattering losses originating from the unintentional silver sulfide layer. Because it is atomically thin, graphene does not interfere with the ability of localized surface plasmons to interact with the environment in sensing applications. Furthermore, after 30 days graphene-passivated silver nanoantennas exhibit a 2600% higher sensitivity over that of bare Ag nanoantennas and 2 orders of magnitude improvement in peak width endurance. We also demonstrate that graphene passivated silver nanoantennas exhibit a bulk index sensitivity that is 60% better than that of the gold counterparts while showing no significant signs of degradation. By employing graphene in this manner, the excellent optical properties and large spectral range of silver, aluminum, and copper can be functionally utilized in a variety of nanoscale plasmonic devices and applications.

8621-2, Session 1

Carbon nanotube photonics on silicon (*Invited Paper*)

Laurent Vivien, Nicolas Izard, Adrien Noury, Institut d'Électronique Fondamentale (France); Etienne Gaufres, Univ. de Montréal (Canada); Xavier Le Roux, Institut d'Électronique Fondamentale (France); Richard Martel, Univ. de Montréal (Canada); Masa Tange, Toshiya Okazaki, National Institute of Advanced Industrial Science and Technology (Japan)

The main applications of photonics are optical communications, optical interconnects in microelectronic circuits and biosensing. For these purposes, the development of efficient photonic devices is the key. For several years, silicon-based photonics have generated a growing interest with impressive results on passive and optoelectronic devices. III-V laser on silicon, silicon modulator and germanium detector have been successfully demonstrated. These different used materials and technologies induce some integration issues. To overcome this limitation, we propose to use optoelectronic properties of new materials and especially of semiconducting single wall carbon nanotubes (SWNTs). SWNTs is more and more considered for their future use in microelectronics as electrode or transistor channel. For few years, s-SWNTs are also considered for photonic applications due to their tunable direct band gap in the NIR wavelength range.

s-SWNTs exhibit strong photoluminescence properties at 1.3 μm and 1.55 μm . These advances led to the first demonstration of optical gain in carbon nanotubes of about 180cm⁻¹ at the wavelength of 1.3 μm . This result is a precursor to obtain nanotube-based laser. SWNT have then be integrated in silicon structures to develop a new class of optoelectronic devices. A complete study was carried out which led to the demonstration of the s-SWNTs absorption and emission coupling with evanescent silicon waveguides at a wavelength of 1.3 μm . The emission intensity at the device output was temperature-independent. These results open the door to the development of a new type of silicon photonic devices based on carbon nanotubes.

8621-3, Session 1

PbSe quantum dots grown in a high-index low-melting-temperature glass for infrared laser applications

Pradeesh Kannan, Amol Choudhary, Ben Mills, Vincent Leonard, Dan W. Hewak, Xian Feng, David P. Shepherd, Univ. of Southampton (United Kingdom)

Growing quantum dots (QDs) in glass offers attractive applications, both as a passive medium, such as a saturable absorber, and as an active laser medium, making them an important building block in the field of photonics. Growing QDs in glass further allows a wide range of refractive indices for the host, enabling index matching for minimized Fresnel reflection losses and flexibility in designing integrated guided-wave structures. In this work we developed a high-index ($n \sim 1.76$) and low-melting-temperature lead-zinc-phosphate (PbO-ZnO-P2O5) (PZP) glass containing narrowly size-distributed lead selenide (PbSe) QDs. The QD-doped glasses were characterized by various techniques including thermal analysis, energy dispersive X-ray analysis, transmission electron microscope, absorption and photoluminescence. The melting temperature and glass transition temperature are $\sim 700^\circ\text{C}$ and $\sim 350^\circ\text{C}$ respectively. This low melting temperature prevents the evaporation of PbSe, enabling high concentrations of PbSe to be obtained. Such glass compositions also provide a wide range of host refractive indices to match the index of a specific laser crystal. QDs of radius between 2 and 5.3nm were grown within the glass by controlling the QD growth parameters. The corresponding QD exciton energy was tuned over the infrared spectral region between ~ 0.93 and 2.75 μm . Emission spectra show a Stokes shift of $\sim 200\text{nm}$ for QDs with size 2nm and decreases with an increase in QD size. As a demonstration of the use of QDs in laser applications, the saturation fluence (F_{sat}) of one of the QDs was evaluated and found to be $\sim 2.1\mu\text{J}/\text{cm}^2$ at 1.2 μm .

8621-4, Session 1

Bismuth nano-particle dispersed organic composite for optical components

Naoyuki Kitamura, National Institute of Advanced Industrial Science and Technology (Japan); Kohki Takahashi, Tohoku Univ. (Japan); Kohei Fukumi, National Institute of Advanced Industrial Science and Technology (Japan); Iwao Mogi, Satoshi Awaji, Kazuo Watanabe, Tohoku Univ. (Japan)

Metal nano-particle dispersed transparent organic material is a candidate for advanced photonics applications. If the nano-particle can be oriented in the materials, new optical and electrical functions will be expected. Magnetic orientation is one of interest processes to construct anisotropic structure in composite or homogenous materials and to create new functions related to the structure. Bismuth is a half metal having large anisotropic susceptibility which can be oriented under magnetic fields. Bismuth nano-particles, which have spherical, plate-like or rod-like shapes, were prepared by a polyol process in our recent study. In the present paper, orientation of bismuth particles in a viscous liquid was demonstrated by using in-situ observation system of x-ray diffraction under high magnetic field. We have successfully introduced oriented bismuth nano-particle into the organic polymer by using high magnetic fields up to 8T. The composite showed difference transmittance depending on the direction of propagation of light being parallel or perpendicular to the applied field, indicating an anisotropic nature of the particle. Optical properties such as transmission, reflection and scattering of polarized light in the bismuth nano-particles oriented organic composite were discussed.

8621-5, Session 2

Cherenkov SiPM development

Elena Popova, National Research Nuclear Univ. MEPhI (Russian Federation); Razmik Mirzoyan, Max-Planck-Institut für Physik (Germany); Philippe Bérard, Martin Couture, Henri Dautet, Excelitas Canada, Inc. (Canada)

Excelitas (formerly PerkinElmer Optoelectronics) in Montréal, Canada, together with the MEPhI group in Moscow, Russia, and the Max Planck Institute for Physics in Munich, Germany, has been working on advanced SiPM designs aiming at various applications. While another presentation in this Conference reports on the results of SiPM optimization for PET imaging and analytical applications, we here report on the approach and advancements to arrive at a “Cherenkov SiPM”.

Characteristics of such a SiPM would be a high Photon Detection Efficiency (PDE) in the near UV-blue wavelength range at a very low level of cross-talk and thermal noise. For achieving this goal one needs to operate the SiPM under a relatively high over-voltage that should saturate the Geiger efficiency. Suppression of the cross-talk is important because otherwise it degrades the amplitude and time resolutions of a SiPM. In this report we present our current results and approach to arrive at an optimized SiPM which can be applied in astro-particle physics, high-energy physics experiments as well as in numerous industrial applications.

8621-6, Session 2

Polish-like facet preparation via dicing for silica integrated optics

Lewis G. Carpenter, Christopher Holmes, James C. Gates, Peter G. R. Smith, Univ. of Southampton (United Kingdom)

Preparation of high quality facets for low-loss coupling is a significant production issue for integrated photonics. Usually requiring both lapping and polishing steps, to produce flat surfaces, with low surface roughness, low waviness and be free of chips and cracks. However both lapping and polishing are time consuming (i.e. sample stacking and waxing, plate preparation) and can need constant human attention to ensure consistent quality. Recently, the development of precision dicing saws for the semiconductor industry with diamond impregnated blades has allowed the achievement of optical grade surfaces, in ‘hard-to-cut’ optical materials based on dicing alone. Offering wafer scale facet preparation, under CNC machine control and typically taking only tens of seconds per facet.

In this report we investigate optimisation of optical quality surfaces that can be achieved by correct selection of blade (i.e. diamond size, diamond concentration and diamond bond type), blade rotational speed, sample translation speed and depth of cut. Preliminary results have shown surface roughness as low as tens of nanometers (Sa) in silica-on-silicon, which is characteristic of ductile mode machining. We will discuss machining parameters and blade selection and show appropriate metrology based on AFM and white light interferometry. Combining optimised facets with single mode channel waveguides (1200-1700 nm) and Bragg gratings using direct UV written, allows optical loss to be determined by using a grating based loss measurement technique.

8621-7, Session 2

High-performance parallel nonlinear photonic processor on photorefractive crystal substrate

Ramin Pashaie, Mehdi Azimipour, Univ. of Wisconsin-Milwaukee (United States)

Computation and data processing are inseparable parts of daily life in our today’s modern society. The complexity of our algorithms, and

consequently, the need for higher computational power is continuously growing. To build intelligent systems, run sophisticated search algorithms, simulate multi-dimensional mathematical problems, compute synthetic values in recursive pattern recognition problem, or to predict the destiny of a nonlinear dynamical system, we need processors specifically designed for massive nonlinear calculations. Currently, photonics and electronics are the major enabling technologies to perform signal processing and computation. Nevertheless, the architecture of electronic computers are mostly adapted for serial processing of segmented information. Conversely, parallelism is one of the major advantages of optical signal processing. A novel approach for the invention of new processors is using the inherent properties and quantum structures of materials to perform parallel processing.

In this article, we discuss a new design of a high performance parallel nonlinear processor on the substrate of a doubly doped photorefractive crystal and thin films of bacteriorhodopsin. We develop a set of algorithms to control the nonlinear behavior of the system and realize a variety of nonlinear operations on the surface of these materials.

Combining this new approach with state-of-the-art fast spatial light modulators and CCD cameras that can precisely control and measure exposure, large arrays of nonlinear processing elements can be accommodated in a thin film of such materials. We also discuss the process for optimizing the performance of the material for parallel nonlinear computation by manipulation of the synthesizing parameters.

8621-8, Session 2

High-sensitivity photoacoustic absorption spectroscopy of nonlinear optical materials

Frank Kuehnemann, Niklas Waasem, Fraunhofer-Institut für Physikalische Messtechnik (Germany); Karsten Buse, Fraunhofer-Institut für Physikalische Messtechnik (Germany) and Univ. Freiburg (Germany)

Nonlinear optical materials are important to extend the spectral coverage of existing lasers, mainly through frequency doubling and optical parametric processes.

The need for high output power (as in material processing or analytical applications) leads to increased quality requirements for the non-linear optical components: At high pump light intensities even minor residual absorptions in the bulk material or at surfaces may lead to thermal distortions or material damage.

The paper presents photoacoustic absorption measurements which combine high-sensitivity with broad spectral coverage. This allows one not only to quantify the absorption level but can also assist in the characterization of the materials in terms of optically relevant impurities and imperfections.

In the present study an OPO-based pulsed photoacoustic spectrometer is used which covers the wavelength range between 215 and 2600 nm. Pulse energies up to 100 mJ allow one to record absorption spectra with a sensitivity down to 10 ppm/cm.

The paper will present spectra of nonlinear optical materials relevant for high-power applications as lithium niobate (LiNbO₃) and lithium triborate (LBO). The results are discussed with respect to material impurities and the suitability of individual samples for frequency conversion.

8621-57, Session 2

Er,Ce:Y3Al5O12 crystal properties under UV, VIS, and IR radiation exposure

Pavel H. Muzhikyan, Vahan G. Babajanyan, Radik B. Kostanyan, Ashot G. Petrosyan, Institute for Physical Research (Armenia)

Improving the efficiency of laser active media in the “eye save region” (near 1.5 μm) is of undoubted interest in connection with practically important applications of laser radiation. One of the promising methods to improve the efficiency of optical excitation and lasing characteristics

of crystals is usage of sensitization effect of working impurities with appropriate donor ions. Ce³⁺ ions are good sensitizers for generation near 1.5 μm in the widely used Er³⁺:Y₃Al₅O₁₂ (YAG) crystal due to their dipole-allowed interconfigurational transitions which have intense absorption bands and effective channels of optical excitation energy transfer to the working Er³⁺ ions. This results in significant increase in the optical excitation efficiency near 460 nm wavelength for realization of generation near 1.5 μm wavelength on the YAG:Er³⁺+Ce³⁺ crystal. We investigated the photoluminescence properties of samples made of yttrium-aluminum garnet and doped with the following concentrations of impurity Er³⁺ and Ce³⁺ ions: YAG:Er³⁺(1 at.%)–Ce³⁺(0.12 at.%), YAG:Er³⁺(5 at.%), YAG:Ce³⁺(0.12 at.%), YAG:Er³⁺(5 at.%)–Ce³⁺(0.12 at.%), YAG:Er³⁺(20 at.%)–Ce³⁺(0.25 at.%), YAG:Er³⁺(20 at.%)–Ce³⁺(0.5 at.%), YAG:Er³⁺(20 at.%). The results of investigations of spectral and kinetic characteristics of fluorescent responses to optical excitations, corresponding to absorption bands of Er³⁺ and Ce³⁺ ions, are presented. The emission spectra of these crystals in the visible and IR spectral regions (0.5-1.8 μm), decay time and delay time of the luminescence peak relative to the short exciting pulse off time are investigated. As excitation sources CW and pulsed laser radiations at 446, 457, 532, 808 and 980 nm wavelengths are used. The excitation energy transfer processes from Ce³⁺ to Er³⁺ ions are discussed. Analysis of the obtained results revealed a significant contribution of Ce³⁺ sensitizer ions in the process of population inversion formation between the 4I_{13/2} and 4I_{15/2} levels of Er³⁺ ions in YAG matrix for generation near 1.5 μm. Comparison of experimental results with theoretical estimations obtained on the basis of numerical solutions of kinetic equations showed good agreement, indicating the adequacy of the models used in describing the processes of optical excitation energy redistribution in the impurity subsystem of the material under study.

8621-10, Session 3

Ultra-fast PDLC optical gate

Pavlo A. Molchanov, Ampac Inc. (United States); Anatoliy Glushchenko, Univ. of Colorado at Colorado Springs (United States); Rudolf Lucente, Ampac Inc. (United States); Richard Billmers, RL Associates Inc. (United States); Olha Asmolova, Thomas Curran, Ampac Inc. (United States)

The result of research, design and testing of an ultra-fast polymer-dispersed liquid crystal (PDLC) optical gate with aperture 1.5cm x 1.5cm is presented. The feasibility of 100 nsec gate opening time with crystal clear transmission (better than 1.54 dB) and attenuation in OFF state more than 26 dB (30.4 dB for two serial samples) has been shown. We investigated low molecular weight liquid crystals to determine switching abilities and strategies because aperture switching with liquid crystal can be polarization-independent and have better transmission than with photorefractive materials in the open state. Application of low molecular weight 5CB liquid crystal and different polymer matrixes, ferroelectric nanoparticles, and bipolar pulse driver with 20 nsec rise time has allowed adequate stimulation of samples and a decrease in gate response time from a hundred microseconds to hundred nanoseconds. A test fixture was made that provides consistent interface for evaluating gated samples. Low molecular weight PDLC optical gate provides polarization independence and can be applied for sun light and reflected from water light to protect sensitive sensors and increase signal/noise ratio.

1. M. W. Geis, R. J. Molnar, G. W. Turner, T. M. Lyszczarz, Lincoln Lab, MIT, R. M. Osgood and B. R. Kimball. 30 to 50 ns Liquid-Crystal Optical Switches, DEC, Proc. SPIE 7618: 76180J/1-5.
2. Molchanov, P.A., Contarino, V. M., Concannon, B.M., Asmolova, O. V., Podobna, Y. Y. Nanosecond gated PMT for LIDAR-RADAR applications. Infrared and Photoelectronic Imagers and Detector Devices II. Proceedings of the SPIE, Volume 6294, pp. 62940H (2006).

8621-11, Session 3

An optical pulse width modulation generator based on the injection-locking property of single mode FP-LD

Hoai Tran Quoc, Bikash Nakarmi, Yong Hyub Won, KAIST (Korea, Republic of)

A novel simple optical pulse width modulation generator (OPWMG) based on injection-locking property of a single mode FP-LD (SMFP-LD) has been proposed and experimentally verified. The OPWMG consists of a SMFP-LD (which acts as comparator), an optical sinusoidal wave source (analog input), and a continuous optical beam (control signal). The power required for fully injection-locking the SMFP-LD (all side modes are suppressed) acts as the referent power whereas the combination power of continuous optical beam and analog optical sinusoidal signals work as control signals for changing the duty cycle of the proposed OPWMG. The presence of only continuous optical beam is not sufficient to suppress the dominant mode of SMFP-LD with high ON/OFF contrast ratio; however, the application of additional sinusoidal wave of constant amplitude and frequency, the dominant mode of SMFP-LD can be suppressed for the certain time window. Since, injection-locking power is dependent with the combined power of input injected continuous beam and sinusoidal optical wave, the time window of injection-locking can be varied by changing input beam power which provides different duty cycle of 10% to 60% at the output. Current available schemes for generating PWM signals are in electrical domain, hence, they need to convert electrical signals into optical domain by using expensive O/E converters for application in optical control and signal processing. The proposed OPWMG scheme has several advantages, such as low cost, low power consumption (~0.5 mW) which can be used for various applications where the effect of EMI/EMR is considered as an important factor such as control circuit for high voltage converters in power plant and electrical vehicles.

8621-12, Session 3

Multi-wavelength access gate for WDM-formatted words in optical RAM row architectures

Dimitrios Fitsios, Theonitsa Alexoudi, Christos Vagionas, Ctr. for Research & Technology - Hellas (Greece) and Aristotle Univ. of Thessaloniki (Greece); Amalia Miliou, Aristotle Univ. of Thessaloniki (Greece); George T. Kanellos, Ctr. for Research & Technology - Hellas (Greece); Nikos Pleros, Ctr. for Research & Technology - Hellas (Greece) and Aristotle Univ. of Thessaloniki (Greece)

Optical RAM has emerged as a promising solution for overcoming the "Memory Wall" of electronics, indicating the use of light in RAM architectures as the approach towards enabling ps-regime memory access times. Taking a step further towards exploiting the unique wavelength properties of optical signals, we reveal new architectural perspectives in optical RAM structures by introducing WDM principles in the storage area. To this end, we demonstrate a novel SOA-based multi-wavelength Access Gate for utilization in a 4x4 WDM optical RAM bank architecture. The proposed multi-wavelength Access Gate can simultaneously control random access to a 4-bit optical word, exploiting Cross-Gain-Modulation (XGM) to process 8 Bit and XBit channels encoded in 8 different wavelengths. It also suggests simpler optical RAM row architectures, allowing for the effective sharing of one multi-wavelength Access Gate for each row, substituting the eight AGs in the case of conventional optical RAM architectures. The scheme is shown to support 10Gbit/s operation for the incoming 4-bit data streams, with a power consumption of 15mW/Gbit/s. All 8 wavelength channels demonstrate error-free operation with a power penalty lower than 3 dB for all channels, compared to Back-to-Back measurements. The proposed optical RAM architecture reveals that exploiting the WDM capabilities of optical components can lead to RAM bank

implementations with smarter column/row encoders/decoders, increased circuit simplicity, reduced number of active elements and associated power consumption. Moreover, exploitation of the wavelength entity can release significant potential towards reconfigurable optical cache mapping schemes when using the wavelength dimension for memory addressing.

8621-13, Session 3

Crystal ion sliced lithium niobate for efficient 100 GHz electro-optic modulation

Vincent E. Stenger, James E. Toney, Andrea Pollick, SRICO Inc. (United States); James Busch, SRICO, Inc. (United States); Jon Scholl, Peter Pontius, Sri Sriram, SRICO Inc. (United States)

This paper reports on the status of thin film lithium niobate (TFLNTM) modulator development at SRICO. TFLNTM is formed on various handle substrates using a layer transfer process called crystal ion slicing. Ion slicing is used to produce bulk quality lithium niobate films of any orientation with controlled thickness from sub-micron to 9 microns. The choice of handle substrate is thus driven by the application rather than by lattice matching or other material constraints. Ion slicing technology opens up a vast design space to produce lithium niobate electro-optic modulators that were not possible using bulk substrates or physically deposited films. For broadband electro-optic modulation, TFLNTM is formed on RF friendly quartz substrates to achieve impedance matched operation at up to 60 GHz with a switching voltage of less than 2.5V. Highly compact modulators suitable for heterogeneous large scale photonic integration are implemented by forming photonic crystal (PhC) structures in the TFLNTM waveguide layer. Sub-micron TFLNTM is essential for producing the high aspect ratio and closely spaced hole patterns needed for efficient PhC operation at the industry standard 1550 nm operating wavelength. Applications of the TFLNTM modulator technology include high bandwidth long haul fiber optic links and ultra-compact and sensitive electric field (E-field) probes.

8621-14, Session 3

Development of HgCdTe single-element avalanche photodiode based detectors for low-flux short-wave infrared applications

Kevin Foubert, Johan Rothman, Gilles Lasfargues, Lydie Mathieu, Gautier Vojetta, Quentin Benoît à la Guillaume, Vincent Calvo, CEA-LETI (France); Fabien Gibert, Ecole Polytechnique Fédérale de Lausanne (France); Jérémy Picot-Clemente, Univ. de Bourgogne (France)

Short Wave Infrared (SWIR) HgCdTe electron-initiated avalanche photodiodes (e-APDs) have shown noticeable internal gain (>100) along with a close to constant output signal-to-noise ratio (SNR) [1], [2]. With an upper GHz expected bandwidth (BW), these detectors rank as front-runners for gated low flux applications. Thus, several demonstrations of active imaging using HgCdTe focal plane arrays have been reported [3], [4]. However, only few developments concerning single-elements applications can be found in the literature, whereas these outstanding characteristics would benefit various demanding fields. Indeed, the latter often impose drastic limits in terms of BW, output noise, residual current, and avalanche gain. These are directly defined by the e-APD composition, geometry, operating temperature and the proximity electronics. The challenge is therefore to carefully choose these parameters in order to fulfil the application requirements.

In our laboratory for cooled IR at CEA/LETI-Minatec (France), we address this issue through two photon-starved applications; spectroscopy and LIDAR. On one hand, at 77K, HgCdTe single-element e-APDs allow us to observe the photoluminescence of Ge nanowires in the range 1.5-2.5 μm with a significantly increased SNR along with a reduce pump laser power. One the other hand, we utilize the e-APDs low noise equivalent power at 180K (few fW/rtHz). It enables direct LIDAR detection at moderate BW

(20 MHz) without the need for long time averaging, which is crucial in far field (≥ 5 km) analysis. Finally, the possibility to perform these detectors in the photon counting limit will be discussed in light of our recent results [5].

- [1] J. Rothman et al., J. Electron. Mater., 41 (2012)
- [2] M. A. Kinch, J. Electron. Mater., 39 (2010)
- [3] A. Ashcroft and I. Baker, Proc. SPIE 7660, 76603C (2010)
- [4] J. Rothman et al., Proc. SPIE 7834, 78340O (2010)
- [5] J. Rothman et al., Proc. SPIE, 8375, 83750Y (2012)

8621-15, Session 3

Wide-band performance of a sinusoidal phase mask coronagraph

Qing Cao, Ourui Ma, Fanzhen Hou, Shanghai Univ. (China)

The direct high contrast imaging of exoplanets will play an important role in space exploration. Various coronagraph designs have been proposed to detect those faint objects, which are very close to their nearby stars. High-contrast images have been achieved through numerical simulations and experimental demonstrations. One approach employs modified Lyot concept with phase mask. Four-quadrant phase mask coronagraph, angular groove phase mask coronagraph, vortex phase mask coronagraph, and eight-octant phase mask coronagraph have been designed and discussed. However, wide-band performance is still a challenge.

As we know, low chromatic coronagraph needs less time to image the exoplanets. Therefore, it is desired that the coronagraph mask can be designed efficient for a wide band of wavelengths. We here suggest a sinusoidal phase mask coronagraph, which gives a deep extinction of the star light in wide-band. The mask has alternatively sinusoidal and uniform phase functions in the angular direction. Analytical derivation and numerical tests are both presented. It is shown that the mask has an inner working angle as small as $1.1\lambda/d$, representing a close detection of exoplanets. This property is very similar to other phase mask coronagraphs. The most important point is that a sinusoidal phase mask has a low chromatism, compared with four-quadrant phase mask coronagraph and vortex phase mask coronagraph. With such an advance, the sinusoidal phase mask coronagraph can work in a wide-band. We expect that it could be widely used for direct detection of the earthlike exoplanets.

8621-16, Session 4

New optical fibers for distributed Brillouin sensors (*Invited Paper*)

Ming-Jun Li, Shenping Li, Kevin W. Bennett, Richard S. Vodhanel, Dragan Pikula, Dawn M. Sutherland, Bruce C. Chow, Corning Incorporated (United States)

Distributed sensors based on Brillouin scattering are attractive for structural health monitoring for buildings, bridges, tunnels, dams and pipelines, as well as ships and airplanes. Brillouin sensing systems such as BOTDR and BOTDA have been studied extensively and commercial products are available. However the spatial resolution of such systems is practically limited to 1 m because the natural Brillouin linewidth is given by the phonon lifetime of ~ 10 ns. Another issue is how to discriminate strain and temperature effects. To address these issues, a concept of Brillouin dynamic grating has been proposed and demonstrated using polarization-maintaining fiber or standard single mode fiber. However, the sensing length in this approach is limited to a length shorter than 1 km.

In this paper, we discuss new fiber designs that can improve performance of distributed Brillouin fiber sensors. To increase the optical power before reaching the SBS threshold, we propose to use a design with Brillouin frequency modulation along the fiber. This design allows longer sensing distance. Then we discuss a dual-core fiber design. The two cores have different Brillouin frequency shifts that allow discrimination of strain

and temperature effects. Finally we present a new distributed Brillouin sensing system using few mode fibers. The few mode fiber sensing approach can not only separate the strain and temperature effects, but also increase the spatial resolution and sensitivity. We will discuss fiber design considerations for each fiber design and show actual fiber examples and experimental results.

8621-17, Session 4

High-sensitivity current sensor based on an embedded microfiber loop resonator

Min-Seok Yoon, Oh-Jang Kwon, Hyun-Joo Kim, Young-Guen Han, Hanyang Univ. (Korea, Republic of)

Optical microfiber resonators (OMRs) have been considered as promising devices for wide range of applications including optical filters, highly compact lasers, and optical sensors because of their advantages of low scattering/absorption loss, small size, and direct coupling to input/output fibers. The OMRs are very sensitive to variations in the surrounding refractive index because of the large evanescent field that propagates through the microfiber. Recently, the current sensor based on microfiber knot resonator (MKR) has been proposed. With the assistance of a copper wire that is directly wrapped by the microfiber knot, resonant wavelength of the MKR can be shifted by applying electric current to the copper wire. However, the sensitivity of the current sensor based on MKR with copper support rod was limited because of the low value of thermal-expansion coefficient and electrical resistance of copper support rod. In this paper, we investigate a highly sensitive current sensor based on a microfiber loop resonator (MLR) by wrapping a microfiber on a low refractive index polymer coated nichrome support rod. The resonant wavelength should be shifted because of the thermally induced optical phase shift due to the heat produced by the flow of electric current. The sensitivity of the proposed MLR was measured to be 437.9 pm/A². Since the low refractive index polymer have large thermal expansion coefficient, the sensitivity of the proposed MLR is almost 10 times higher than that of the previous MKR-based current sensor.

8621-18, Session 4

Versatile chemical molecule sensing using multi-wavelength fiber laser based on inter-core interference in twin-core photonic crystal fiber

Bong Kyun Kim, Youngjoo Chung, Jihee Han, Khurram Naeem, Gwangju Institute of Science and Technology (Korea, Republic of)

The studies on photonic crystal fibers (PCFs) have drawn considerable interest and played an important role in various applications. PCFs provide unique optical properties and controllable modal properties because of their flexibilities on manipulation of the transmission spectrum and the waveguide dispersion properties. PCFs are especially useful for optical sensing applications because the micro-structured air channels in PCF can host various types of analytes such as liquids, gases, and chemical molecules. Recently, many studies have focused on the development of PCF-based optical sensors for various gases and chemical molecules. The fiber-based multi-wavelength fiber lasers also have attracted much interest because of their potential applications in wavelength-division-multiplexing (WDM) systems and sensing applications as well as their numerous advantages such as multiple wavelength operation, low cost, and compatibility with fiber optic systems.

In this paper, we propose a new chemical molecule sensing scheme using multi-wavelength fiber laser based on inter-core interference in twin-core photonic crystal fiber. In our proposed multi-wavelength fiber laser, two separated cores are integrated in a single photonic crystal fiber and surrounded by air channels. The anti-symmetrical super-modes participate in inter-core interference, which leads to the formation of twin-core photonic crystal fiber-based wavelength-selective comb filter. Most

of the evanescent waves are localized in the 13 air channels around the two integrated cores, where light-matter interaction takes in place. The presence of chemical molecules in the air channels of TC-PCF leads to perturbation of the inter-core effective index difference between the two propagating core modes and the associated lasing wavelength shift. The sensitivity, the stability, and the potential applications of the proposed fiber laser will be discussed.

8621-19, Session 4

Temperature-insensitive strain sensor based on Mach-Zehnder interferometer with a microfiber

Sung-Jae Kim, Min-Seok Yoon, Hyun-Joo Kim, Young-Geun Han, Hanyang Univ. (Korea, Republic of)

Optical fiber strain sensors have attracted much attention in variety of applications, such as aerospace, civil, power, and process control engineering, because of their many advantages like small size, light weight, and immunity to electro-magnetic wave. Strain sensors using Mach-Zehnder interferometers (MZIs) have been intensively developed because of their advantages such as ease to fabricate and high sensitivity. However, since the MZI-based strain sensors are sensitive to temperature, it should discriminate concurrent sensitivities between temperature and strain. In this paper, we propose and experimentally demonstrate a temperature-insensitive MZI-based strain sensor by using the large evanescent field of a microfiber to mitigate temperature dependence. We deposited a polymer overlay of index matching oil with high negative thermo-optic coefficient on the microfiber. Since the temperature dependence of the microfiber-based MZI is closely related with the diameter of the microfiber, it is possible to suppress the temperature dependence of the MZI. The temperature dependence of the proposed MZI was compensated to be less than 0.01 $^{\circ}\text{C}^{-1}$ by adjusting the diameter of the microfiber. The strain sensitivity was measured -234.54 μm^{-1} in a range from 0 to 3 m.

8621-20, Session 4

Characteristics of arc-induced long-period fiber gratings inscribed in asymmetric adiabatic tapers

Alejandro Martinez-Rios, David Monzon-Hernandez, Guillermo Salceda-Delgado, Centro de Investigaciones en Óptica, A.C. (Mexico)

The characteristics of arc-induced long-period fiber gratings inscribed in the longer transition of asymmetric adiabatic tapers are presented. The tapers dimensions were selected such that a long period fiber grating with 500 μm period and total length around 3 cm could be fabricated on the longest taper transition by periodical application of an electric arc. This resulted in a long period fiber grating inscribed in a variable diameter fiber. Compared to the inscription in non-tapered fibers, the grating inscription in the linear taper transition resulted in deeper notch bands, whose bandwidth and separation increased with the transition slope. Eventually, the longer wavelength band moved out of our measurement range so that a chemical etching was required to bring it back, since this band showed higher sensitivity to external influences such as changes in external refractive index. The sensitivity to external refractive index was measured in a range from 1 to 1.636, which resulted in variations in the notch bandwidth and spectral position.

8621-21, Session 4

Fabrication and applications of visible light long-period fiber grating

Xinwei Lan, Jie Huang, Zhan Gao, Lei Yuan, Hanzheng Wang,

Missouri Univ. of Science and Technology (United States); Qun Han, Tianjin Univ. (China); Hai Xiao, Missouri Univ. of Science and Technology (United States)

Long period fiber gratings (LPFG) are fabricated on the visible light single mode fiber using CO₂ laser point by point irradiation technique. Various sensing parameters, including temperature, strain and refractive index, have been studied based on this new LPFG device. Moreover, by combing visible light LPFG with widely used visible light lasers, many new applications based on optical fiber devices can be explored, such as Raman filters, laser pulse shaping, and inducing nano-particle patterns on optical fiber surface for fiber chemical sensing applications, etc.

Long period fiber gratings (LPFG) are fabricated on the visible light single mode fiber using CO₂ laser point by point irradiation technique. Various sensing parameters, including temperature, strain and refractive index, have been studied based on this new LPFG device. Moreover, by combing visible light LPFG and widely used visible light lasers, many new applications based on optical fiber devices can be explored, such as Raman filters, laser pulse shaping, and inducing nano-particle patterns on optical fiber surface for fiber chemical sensing applications, etc.

8621-22, Session 5

Tailored spectroscopic and optical properties in rare earth-activated glass-ceramics planar waveguides (*Invited Paper*)

Davor Ristic, Istituto di Fotonica e Nanotecnologie (Italy); Thi Thanh Van Tran, Univ. of Sciences (Viet Nam); Belto Dieudonné, Univ. du Maine (France); Armellini Cristina, Istituto di Fotonica e Nanotecnologie (Italy); Simone Berneschi, Museo Storica della Fisica e Ctr Studi e Ricerche Enrico Fermi (Italy) and tuto di Fisica Applicata Nello Carrara (Italy); Andrea Chiappini, Alessandro Chiasera, Stefano Varas, Alessandro Carpentiero, Maurizio Mazzola, Istituto di Fotonica e Nanotecnologie (Italy); Gualtiero Nunzi Conti, Stefano Pelli, Istituto di Fisica Applicata Nello Carrara (Italy); Giorgio Speranza, Fondazione Bruno Kessler (Italy) and Istituto di Fotonica e Nanotecnologie (Italy); Patrice Feron, Ecole Nationale Supérieure des Sciences Appliquées et de Technologie (France); Claire Duverger Arfuso, Univ. du Maine (France); Gilles Cibiel, Ctr. National d'Études Spatiales (France); Sylvia Turrell, Univ. des Sciences et Technologies de Lille (France); Brigitte Boulard, Univ. du Maine (France); Giancarlo C. Righini, Museo Storica della Fisica e Ctr Studi e Ricerche Enrico Fermi (Italy) and tuto di Fisica Applicata Nello Carrara (Italy); Maurizio Ferrari, Istituto di Fotonica e Nanotecnologie (Italy)

Glass ceramic activated by rare earth ions are nanocomposite systems that exhibit specific morphologic, structural and spectroscopic properties allowing to develop interesting new physical concepts, for instance the mechanism related to the transparency, as well as novel photonic devices based on the enhancement of the luminescence. At the state of art the fabrication techniques based on bottom-up and top-down approaches appear to be viable although a specific effort is required to achieve the necessary reliability and reproducibility of the preparation protocols. In particular, the dependence of the final product on the specific parent glass and on the employed synthesis still remain an important task of the research in material science. Looking to application, the enhanced spectroscopic properties typical of glass ceramic in respect to those of the amorphous structures constitute an important point for the development of integrated optics devices, including optical amplifiers, monolithic waveguide laser, novel sensors, coating of spherical microresonators, and up and down converters for solar energy exploitation. This lecture presents a overview of the state of art in glass ceramics focusing the discussion on photonics application, and evidences the capital scientific and technological interest of this kind of two-phase materials.

8621-23, Session 5

Improving Ce³⁺ doped scintillating materials for medical imaging applications

Bruno Viana, Samuel Blahuta, Ecole Nationale Supérieure de Chimie de Paris (France); Vladimir Ouspenski, Compagnie de Saint-Gobain (France); Aurélie Bessière, Ecole Nationale Supérieure de Chimie de Paris (France)

Lu₂(1-x)Y_{2x}SiO₅:Ce (10%at Y) single crystals co-doped with Ca²⁺ and Mg²⁺ were prepared by the Czochralski technique. Co-doping allows significant improvement of the scintillation with a reduction of the afterglow and a large improve of the light yield value. For instance LYSO:Ce codoped with Ca²⁺ and Mg²⁺ led to significantly improved light yield, e.g. 34000 Ph/MeV for LYSO:Ce,Ca instead of 28000 Ph/MeV for standard LYSO:Ce under 137Cs – 662 keV excitation.

Afterglow can be as low as 200ppm at 20ms when Ca²⁺ is used as a co-dopant, which is comparable to commercial Gd₂O₂S:Pr,Ce ceramics performances.

Afterglow reduction with Ca²⁺ co-doping in LSO:Ce was also already reported [1] but to a lower extent : about 700 ppm remain 1s after X-rays are stopped. This new feature could open an interesting area of use of oxy-orthosilicates in the medical imaging field where very low afterglow is required.

In addition, co-doped single crystals were carefully investigated. Using X-ray Absorption Near Edge Spectrometry (XANES) we were able to evidence that a significant part of the Ce ions are stabilized in the Ce⁴⁺ oxidation state in co-doped LYSO:Ce. We presents some possible effects of the Ce³⁺ and/or Ce⁴⁺ doping in theses silicate hosts in term of color, scintillation mechanisms and defect control.

In order to make the correlation between improved scintillation performances and significant Ce⁴⁺ content in co-doped LYSO:Ce, a new mechanism is presented.

[1] Kan Yang, Charles L. Melcher, Philip D. Rack, and Lars A. Eriksson, IEEE Transactions On Nuclear Science 56, 2960-2965 (2009).

8621-24, Session 5

White light emission characteristics of europium doped fluoride materials

Rami R. Bommareddi, Tomeka S. Colón, Alabama A&M Univ. (United States)

Now-a-days many research groups are working on the development of white light emitters. There are some phosphors which emit white light under violet/blue light excitation; for example, tube lights and compact fluorescent lights. There is a parallel effort to develop all solid state white light emitters. Our research effort fits into the latter category. Here we are using europium doped lanthanum fluoride and calcium fluoride crystals for white light emission studies. Eu³⁺ has 7F_j ground manifolds (j = 0 to 6) and 5D_j excited manifolds (j = 0 to 3). The 5D₃ energy level is at 24 355 cm⁻¹, whose energy is close to that of 405 nm diode laser. So, we investigated the luminescence studies of LaF₃:Eu³⁺ under diode laser excitation. Europium doped LaF₃ exhibited bright white light even for a few mW laser power. It emitted photons of several wavelengths in the range 400 to 800 nm. These photons are due to transitions from 5D₃, 5D₂, 5D₁ and 5D₀ levels to different ground manifolds. Europium doped calcium fluoride also exhibited white light emission under 405 nm laser excitation. As expected, its emission wavelengths are different from those of LaF₃: Eu³⁺. On the other hand CaF₂: Eu³⁺ exhibited an intense and broad peak at 426 nm and relatively weaker emission at 590, 615 and 690nm. In spite of its emission having fewer peaks, the material still appeared to be bright white in color. We will discuss in detail the color coordinates of emission.

8621-25, Session 5

Emission efficiency of erbium ions in III-N epilayers

John M. Zavada, National Science Foundation (United States);
Chris Ugolini, I. W. Feng, Ashok Sedhain, Jingyu Lin, Hongxing
Jiang, Texas Tech Univ. (United States)

Rare earth doping of silicon and other semiconductor materials continues to be an active area of research for telecommunication and display applications. In recent years, major advances have been made in rare earth doping of III-Nitride materials due in large part to synthesis by metal organic chemical deposition (MOCVD). However, the emission efficiency of the RE ions in the semiconductor host remains quite very low. In this talk we will present new results concerning the formation energy of optically active erbium (Er) centers in GaN and InGaN epilayers synthesized by MOCVD. Photoluminescence (PL) measurements taken at room temperature show that addition of even small amounts of In significantly reduces the Er emission efficiency at 1.54 microns. To study this behavior, the PL emission intensity for a set of GaN:Er epilayers, grown at different temperatures, was measured. The data were used to establish a value of ~ 1.82 eV as the formation energy of the Er³⁺ centers. This value is > 1 eV lower than the formation energy of nitrogen vacancies in GaN which presumably lead to optical activity. The lower growth temperatures used for synthesis of InGaN epilayers appears to reduce the formation of optically active centers. Implications of these results on light emitting devices and optical waveguide amplifiers based on RE doped nitride epilayers will be discussed.

8621-26, Session 5

Study on SiO₂-Al₂O₃-La₂O₃-glasses for nonlinear and laser applications

Kay Schuster, Doris Litzkendorf, Stephan Grimm, Jens Kobelke,
Anka Schwuchow, Anne Ludwig, Martin Leich, Sylvia Jetschke,
Jan Dellith, Institut für Photonische Technologien e.V. (Germany);
Jean-Louis Auguste, Georges Humbert, Univ. de Limoges
(France)

Crucible melted SiO₂-Al₂O₃-La₂O₃ (SAL) glasses are suitable for two very different applications. With the La₂O₃ content the nonlinear coefficient of the glass can be tuned for nonlinear applications like supercontinuum generation, whereas the partly substitution of La₂O₃ by Yb₂O₃ allow very high Yb-concentration promising for fiber laser applications. The substitution of the typically silica based core by the high melting SiO₂-Al₂O₃-La₂O₃ glass and Yb-doped SiO₂-Al₂O₃-La₂O₃ glass was tested. The glass compositions were optimized in terms of thermal and optical requirements for both, a high La₂O₃ (24 mol%) and Yb₂O₃ (6 mol%) concentration and a good compatibility with a silica cladding. The aluminium concentration was adjusted to about 21 mol% Al₂O₃ and increase the solubility of lanthanum and ytterbium in the glass beyond possible MCVD based techniques. By crucible melting technology we overcome the concentration limits of aluminium and rare earth doping of MCVD (maximum about 6.5 mol% Al₂O₃ and 2.0 mol% RE₂O₃). The glasses have been characterized by dilatometric methods to find transition temperatures from 860 to 880°C and thermal expansion coefficients between 4.1 and 7.0 x 10⁻⁶ K⁻¹. Investigations on thermal properties (thermal diffusivity, heat conductivity) will be shown.

We have achieved a minimum fiber loss of about 0.5 dB/m at 1200 nm for hybrid step index fibers (SAL core, silica cladding). Successful supercontinuum generation between 1025 nm and 1750 nm as well as fiber laser operation at 1060 nm with an efficiency of 41 % has been achieved in such fibers.

8621-27, Session 6

Microresonator-based mid-IR sources (*Invited Paper*)

Ravi K. Jain, Mani Hossein-Zadeh, The Univ. of New Mexico
(United States)

High optical quality (high-Q) whispering-gallery mode (WGM) microresonators are the core of numerous high-performance photonic devices, including ultrasensitive molecular detectors and advanced light sources such as narrowlinewidth lasers and comb generators. For sensing applications, the unique characteristics of such WGM devices appear to be particularly relevant in mid-IR (MIR) regime because of the stronger molecular absorption bands in this spectral region that provide a universal means for their detection. However, nearly all of WGM based passive and active devices are made of silica glass and can only function near-IR regime (NIR) due to rapid increase in absorption of silica glasses above two micron. This technology-gap can be filled by developing high-Q WGM microresonators made of the low-phonon energy glasses developed for MIR applications (such as fluorides, chalcogenides, and tellurides).

In this talk after a brief review of the current state of WGM MIR microresonators and corresponding sources, we present the results of our work on fabrication and characterization of high-Q WGM optical microresonators with MIR relevant ZBLAN, InF₃ and AlF₃ glasses using a simple and reliable method. Intrinsic quality factors in excess of ten million have already been demonstrated in NIR regime and similar or better performance is expected between 2 to 5 microns. Next we discuss our progress toward demonstration of low-threshold and narrow-linewidth MIR lasers using these cavities. At the end potential application of these microresonators in MIR spectroscopy, MIR comb generation, and MIR luminescent sensors will be discussed.

8621-28, Session 6

Microcavity-based cascaded Raman microlaser in air and in buffer

Maria V. Chistiakova, Andrea M. Armani, The Univ. of Southern
California (United States)

The application of microcavity-based microlasers for biodetection is an emerging field. Recent results using rare-earth doped microlasers for nanoparticle detection have demonstrated the viability of this approach. However, rare earth metals are not biocompatible. To solve this challenge, it is necessary to develop a low threshold microlaser using biocompatible materials. In the present work, we demonstrate a cascaded Raman microlaser based on an ultra-high-Q silica microcavity. The laser operates in both air and buffer with sub-mW thresholds in both environments. HEPES buffer was used in the experiments as it is an ideal solution to hold proteins and other molecules of interest.

Using a 770nm pump laser, four emission lines were observed in air at 801, 829, 862, and 895nm with thresholds of 157, 220, 259, and 301 microwatts, respectively. In buffer, two emission peaks appeared at 801 and 827nm with thresholds of 760 and 824microwatts, respectively. As expected, the threshold increased and the slope efficiency decreased as the emission wavelength increased. The increase in the threshold power as the device moved from air to buffer was the result of the increase in optical mode volume, which was modeled using COMSOL Multiphysics. The present work sets the stage for biocompatible microcavity-based microlaser devices that can be used to probe the behavior of biological systems.

8621-29, Session 6

Power consumption of semiconductor optical amplifier

Joel Jacquet, Xunqi Wu, Juliette Pochet, Laurie Pontreau, David

Allioux, Mickael Faugeron, Y. Houzelle, Jean-Louis Gutzwiller, Supélec (France)

Today, the design of any new product must meet new standards related to sustainable development. Furthermore the end of life of the product must be considered during the design step (dismantling, recycling, ...) as well as the power consumption of devices manufactured. This is particularly true in the field of electronics, telecommunications. In these areas, the electrical consumption of the devices becomes an important parameter in the design of optical transmission systems. For a given performance, the component consuming the weakest energy will be preferentially chosen by system manufacturers.

We have measured the gain of a semi-conductor optical amplifier (SOA) at different temperature of the chip and in a varying temperature environment by using oven. The temperature of the oven varies between 20 and 80° as well as the chip temperature. For all measurement, we register the electrical power consumed by the peltier system for the temperature of the chip.

Measurement show an excellent behavior of our SOA when chip temperature increases. A degradation of 8 dB is measured when SOA temperature increases from 20 to 80°C whatever are the current of polarization of SOA or the oven temperature. Electrical power consumption evolution as function of oven temperature has also been investigated. An optimization between gain of SOA and power consumption will be presented.

8621-30, Session 6

On-axis linear-response laser optical beam steerer

Yair J. Mega, Zhenhua Lai, Charles A. DiMarzio, Northeastern Univ. (United States)

Many applications in various fields of science and engineering use steered optical beam. Current methods for beam steering normally use mirrors in order to solve the problem. However, it is an off-axis solution, which essentially increases the total size of the system as well as the its error and complexity. Other applications use a "Risely Prisms" based solution, which is on-axis solution, however it poses some difficulties from an engineering standpoint, and therefore isn't widely used. We present here a novel technique to steer a beam of light on its optical axis with a linear deflection response. We derived the formulation required of the profile of the refractive optical component proposed for performing the beam steering. The functionality of the device was simulated analytically using Matlab, as well as using a ray-tracing software, Zemax, and showed agreement with the theoretical model. We also present some proposed geometries of the several other devices, all based on the same concept, which can be used for higher performance applications such as two-dimensional scanner, video rate scanner etc.

8621-31, Session 6

Polygon mirror scanners in biomedical imaging: a review

Virgil-Florin Duma, Aurel Vlaicu Univ. of Arad (Romania); Adrian G. Podoleanu, Univ. of Kent (United Kingdom)

We review the different applications of polygonal mirror (PM) scanning heads in biomedical imaging, with a focus on OCT (Optical Coherence Tomography). This overview of biomedical optical systems that employ PMs include: (i) TD (Time Domain) OCT setups, where PM can be utilized for generating the modulation function of the system without separate translation stages; (ii) broadband laser sources scanned in frequency, for SS (Swept Source) OCT, with the PM placed in various optical configurations; (iii) FD (Fourier Domain) OCT delay line systems, with PM arrays; (iv) OCM (Optical Coherence Microscopy) system with double PMs; (v) 2D PM plus galvanometer-based scanner (GS) for fast lateral scanning (not only in OCT, but also in confocal microscopy). The stress of the study is placed on SSs, for which the various PM-based setups used

are discussed, in their evolution - from centered to off-axis polygons - and in the race to obtain higher scan speeds to achieve real-time in vivo medical imaging. The parameters, advantages and drawbacks of these different configurations are compared. A necessary comparison is also made with the much faster Fabry-Perot (FP) based SSs. Our approach on PM-based broadband laser sources scanned in frequency, based on simple off-axis polygon configuration, is also presented, and some of its characteristic mathematical functions are analyzed.

8621-32, Session 7

Photodarkening: investigation, mitigation and figure of merit (*Invited Paper*)

Stefano Taccheo, Hrvoje Gebavi, Swansea Univ. (United Kingdom); Benoit Cadier, Thierry Robin, ixFiber SAS (France); Achille Monteville, Olivier Le Goffic, David Landais, David Méchin, Plate-forme d'Étude et de Recherche sur les Fibres Optiques Spéciales (France); Daniel Milanese, Politecnico di Torino (Italy); Lasse Leick, NKT Photonics A/S (Denmark); Tim Durrant, Gooch & Housego Plc (United Kingdom)

In this paper we present the work carried out on photodarkening by LIFT consortium within an EU FP7 project. While the mechanism is not fully understood we will address several aspects of this phenomena. We will first discuss how measurement set-up may influence the measurements. A further point is the investigation of visible emission as well as optical bleaching. Visible emission and bleaching can bring new information on the mechanism of photodarkening and on the type of defects it generates. Finally we will propose a model to evaluate the impact of Photodarkening on laser devices and we will discuss how to define the quality of a active fiber in relationship with photodarkening performance..

8621-35, Session 7

Anomalous dispersive photonic bandgap fiber for ultra short pulse compression

Xuesong Yang, Maggie Y. Chen, Texas State Univ. San Marcos (United States)

In this paper, an anomalous dispersive photonic bandgap fiber is presented with dispersion value around 100 ps/(nm²km) around 1550 nm wavelength region. The photonic bandgap fiber itself serves as the pulse compressor through soliton excitation. The pulse propagation is simulated through solving the nonlinear Schrodinger equation to incorporate the fiber propagation loss and third-order dispersion. Optimum fiber length, compression factor F_c and quality factor of compression Q_c are simulated. One stage pulse compression is demonstrated experimentally based on the fabricated anomalous dispersive photonic bandgap fibers. A FPL-01T femtosecond Erbium doped fiber laser serves as the source pulse. The laser produces optical pulses as short as 0.08 picoseconds in the vicinity of 1550 nm. The output power can be as high as 10 mW average and a 1000 W peak level, with a repetition rate of 19 MHz. The autocorrelator is used to characterize the compressed pulse. The optimum fiber length is confirmed, and compression factor F_c and quality factor of compression Q_c agree with the simulation results reasonably well.

The compressor can be applied to high energy ultra short pulse compression.

8621-36, Session 7

Environmental testing and laser transmission results for ruggedized high-power IR fiber cables

Lynda E. Busse, U.S. Naval Research Lab. (United States);

Frederic H. Kung, Univ. Research Foundation (United States); Catalin Florea, Sotera Defense Solutions, Inc. (United States); Brandon Shaw, U.S. Naval Research Lab. (United States); Ishwar D. Aggarwal, Sotera Defense Solutions, Inc. (United States); Jas S. Sanghera, U.S. Naval Research Lab. (United States)

Mid-IR transmitting glass fiber cables are needed for a wide range of applications, including enabling remote transmission from a centralized laser to outgoing pointers in anti-missile aircraft protection systems, high laser power transmission, and chemical sensing applications. However, the commercial availability of robust, high laser power transmitting fiber cables is limited to few vendors. We will present successful results of high mid-IR laser power transmission as well as mil-spec environmental testing (thermal cycling and vibration testing) of ruggedized, IR-transmitting chalcogenide glass fiber cables. We will also present results of a direct imprinting process to create novel "moth eye" patterned surfaces on the chalcogenide fiber cable ends that significantly reduce the intrinsic reflection loss from about 17% per end to less than 2%. The cables with these imprinted "moth eye" ends show excellent laser damage thresholds near that of the bulk material, unlike previous results obtained for anti-reflection coated fiber ends, that damaged at laser intensities of one-third that of the bulk material. This work has direct impact on the practical utilization of these fiber cables in military system platforms.

8621-37, Session 7

Elastic stability of a dual-coated fiber subjected to thermal and/or mechanical compression

Ephraim Suhir, Univ. of California, Santa Cruz (United States)

The condition of elastic stability of a dual-coated optical-fiber interconnect, when subjected to the thermally induced and/or axial mechanical loading, is established based on a simple, physically meaningful and easy-to-use analytical (mathematical) predictive model. It is shown that the developed model can be also used in flexible (large area) photonics when high-modulus and low-expansion optical nano-fibers are embedded into a high-modulus-and-low-expansion matrix. The problem is reduced to the formalism when a cantilever beam (rod) of finite length lying on a continuous elastic foundation is subjected to a compressive force applied to the rod's free end. Based on the developed model, practical guidelines are suggested for choosing the adequate length of the fiber (rod) and/or its flexural rigidity and/or the physical (mechanical) characteristics of the coating system (the matrix), so that the fiber (rod) remains elastically stable under the action of the axial compressive force and/or the thermally induced compression caused by the thermal contraction mismatch of the fiber (rod) and the coating (matrix) materials. If the fiber (rod) buckles, the functional (e.g., optical or thermal) and/or the structural ("physical") performance of the dual-coated fiber or the flexible (large area) nano-composite might be compromised. Attributes associated with the nano-size, if any, of the fiber (rod) are discussed. The general concept is illustrated by numerical examples.

8621-33, Session PWed

Supercontinuum generation from a multi-ring holes tellurite microstructure fiber pumped with a 2-micron high-power mode-locked fiber laser

Dinghuan Deng, Weiqing Gao, Meisong Liao, Takenobu Suzuki, Yasutake Ohishi, Toyota Technological Institute (Japan)

Supercontinuum (SC) generation from a highly nonlinear tellurite microstructure fiber with multi-ring holes which was fabricated in our laboratory was demonstrated pumped with a 2 micron high power mode-locked fiber laser. The microstructure fiber has a 1.8 μm core surrounded

by four rings of holes. The chromatic dispersion of the fundamental mode of the fiber was measured by a homemade white-light spectral interferometer and calculated by the full-vectorial finite-difference method (FV-FDM) based on scanning electron microscope images. The measured and calculated dispersion could match very well within the whole spectrum range under test. The zero dispersion wavelength (ZDW) of the fiber was measured to be 1358 nm and calculated to be 1390 nm. A 2 μm high power mode-locked fiber laser with a pulse width of about 3.5 picoseconds was used as the pumping source. The maximum output power of the pump could be as high as 1 W at the repetition rate of 30 MHz. Although the pumped wavelength was far away from ZDW, with flat dispersion profile of the fiber on the abnormal dispersion, the SC could be expanded from 650 nm to 2850 nm at the pump power of 500 mW, which was wider than the SC generation pumped with a 1.56 μm femtosecond fiber laser. The comparison of SCs generated by 2 μm picosecond pulses and 1.56 μm femtosecond pulses was also discussed.

8621-34, Session PWed

Analysis of soliton self-frequency shift in ZBLAN fiber as a broadband supercontinuum medium

Xin Yan, Meisong Liao, Takenobu Suzuki, Yasutake Ohishi, Toyota Technological Institute (Japan)

Soliton self-frequency shift (SSFS) is a well-understood phenomenon in fiber-optic communications. SSFS has been investigated in various silica fibers over the past decade to fabricate fiber-delivered, widely frequency-tunable and femtosecond pulse sources. Recently, more attention has been paid to non-silica glasses with wider infrared transmission window, such as tellurite, fluoride and chalcogenide glasses. Heavy metal fluoride (HMF) glasses have drawn significant attention because of their broad transmission window, low optical dispersion, low refractive index, ease of machining and polishing, and small thermal dependence of the optical properties. ZrF₄-BaF₂-LaF₃-AlF₃-NaF (ZBLAN) glass as the most stable HMF glass has been extensively investigated for their ease of fiber drawing. With low transmission loss at mid-infrared region, ZBLAN fibers are attractive for the broadband nonlinear coherent light sources. In this paper, SSFS in ZBLAN is investigated based on Raman gain coefficients and generalized nonlinear Schrödinger equation. We have measured the Raman gain coefficient spectrum and third-order susceptibility $\chi^{(3)}$ of a fluoride ZBLAN glass. The Raman response function and Raman fraction of ZBLAN fibers are obtained from the actual Raman gain spectrum. The enhanced SSFS in the ZBLAN fiber under investigation as compared to the silica fiber is mainly due to the combination of nonlinear coefficient and Raman response function enhancement. Therefore, ZBLAN fiber is promising materials for SSFS. The Raman response function obtained in this study is effective in the simulation of nonlinear optical pulse propagation in ZBLAN fiber and can contribute to analyzing the potential of ZBLAN fiber to nonlinear optics applications.

8621-38, Session PWed

Square-pulse operation in a ring cavity with a single-mode tellurite fiber

Weiqing Gao, Meisong Liao, Hiroyasu Kawashima, Takenobu Suzuki, Yasutake Ohishi, Toyota Technological Institute (Japan)

We demonstrate the square-pulse operation in a ring cavity with a 207 μm single-mode tellurite fiber. The high nonlinearity and birefringence of the tellurite fiber play the key role during the square-pulse formation. The CW operation is obtained when pump power exceeded 80 mW. When the pump power is increased to 140 mW, the single pulse operation with the repetition rate of 689 kHz corresponding to the cavity fundamental frequency is initiated from the ASE noise by the nonlinear polarization rotation (NPR) process. Keeping the pump power at 140 mW and rotating one of the paddles of the polarization controller (PC) toward one direction

in a small scale, the pulse number in one packet increases monotonically from 1 to 11. This process continues until the stable square pulse is formed at last. The stable square pulse has the FWHM of 118 ns and the repetition rate of 689 kHz. It is formed by the nonlinear polarization switching. In our cavity, the tellurite fiber is long enough to make the laser operate in the multibeam-length regime, which could lower the threshold for nonlinear polarization switching and clamp the peak power at a low level. This is advantageous for increasing the pulse width because the pulse duration is determined by the intra-cavity energy and the clamped peak power. When the linear phase delay bias in the cavity is set close to the polarization switching point, the third-order harmonic pulses and multiple packets are also observed under different pump levels.

8621-39, Session PWed

All-solid tellurite-phosphate photonic bandgap fiber

Tonglei Cheng, Toyota Technological Institute (Japan); Meisong Liao, Toyota Technological Institute (Japan); Hoang Tuan Tong, Weiqing Gao, Zhongchao Duan, Takenobu Suzuki, Yasutake Ohishi, Toyota Technological Institute (Japan)

All-solid photonic bandgap fiber (PBGF) has an array of isolated high index rods in a low index cladding and the fiber core is generally a low index area. Light can be guided in a low index core due to the existence of the photonic bandgaps in the two-dimensionally periodical cladding. The guiding mechanism of all-solid PBGF can also be described by use of the antiresonant reflecting optical waveguide (ARROW) model. It can also be used in amplifier and laser, filter, the supercontinuum generation and broadband dispersion compensation.

In the paper, we present an all-solid tellurite-phosphate PBGF with high-index rods in the cladding. The low-index background material is phosphate glass (PZNK) and the high-index rods are made of tellurite glass (TZLB). These two glasses have the same fiber-drawing temperature (about 320 °C). This fiber can be fabricated by stack-and-draw technique and its bandgap characteristic is simulated by the plane-wave method. Due to the tellurite glass exhibits unique optical properties, such as good optical transmission in the mid-infrared, much higher nonlinear index, and easier to form than silica, the tellurite-phosphate PBGFs appear promising for a lot of applications in areas such as fiber lasers and amplifiers for optical communications, wavelength conversion and the modulation of light signal for photonic information technology, fiber sensors for environment, and biomedical applications, etc.

8621-40, Session PWed

Photoluminescence and anti-deliqescence of cesium iodide and its sodium-doped films deposited by thermal evaporation at high deposition rates

Jin-Cherng Hsu, Yueh-Sheng Chiang, Yu-Sheng Ma, Fu Jen Catholic Univ. (Taiwan) and Graduate Institute of Applied Science and Engineering (Taiwan)

Cesium iodide (CsI) and sodium iodide (NaI) are good scintillators due to their high luminescence efficiency. These alkali halides can be excited by ultra-violet or by ionizing radiation. The peak positions of the luminescence for the two halides locate at about 3.69 and 4.24 eV; and, the half-widths at 0.51 and 0.38 eV, respectively. In this study, CsI and its Na-doped films about 8 μm thickness were deposited by thermal evaporation boat without heating substrates at high deposition rates of 30, 50, 70, 90, and 110 nm/sec, respectively. The as-deposited films were sequentially deposited a silicon dioxide film to protect from deliquesce. And, the films were also post-annealed in vacuum at 150, 200, 250, and 300 °C, respectively. We calculated the package densities of the samples according to the measurements of Fourier transform

infrared spectroscopy (FTIR) and observed the luminescence properties by photoluminescence (PL) system. The surfaces and cross sections of the films were investigated by scanning electron microscope (SEM). From the measurements of the crystalline structures, packing densities, and luminescence, we can find the optimal deposition rate of 90 nm/sec and post-annealing temperature of 200 °C in vacuum for the as-deposited cesium iodide and its sodium-doped films.

8621-41, Session PWed

Optical properties of cerium-codoped high-power laser fibers

Sonja Unger, Anka Schwuchow, Sylvia Jetschke, Stephan Grimm, Andy Scheffel, Johannes Kirchhof, Institut für Photonische Technologien e.V. (Germany)

Recently it has been shown that the photodarkening resistivity of ytterbium doped aluminosilicate fibers can be remarkably improved by cerium codoping. This opens up a new way for a laser fiber design and could be used in future to avoid some disadvantages of "Large-Mode-Area" (LMA) fibers on the basis of phosphosilicate glass, which is currently the material of choice for power stable laser fibers.

First investigations have shown that the cerium concentration must be comparable with the ytterbium concentration in order to give the required effect of low photodarkening. Therefore, cerium co-doping influences not only the power stability but also further fiber properties as refractive index, basic optical attenuation, etc., what must be considered in the overall design of the LMA fibers. Up to now, however, little is known about the influence of cerium on these properties.

Here we report on systematical investigations of the influence of cerium co-doping on an optimized fiber design. Fibers with different ytterbium, aluminium and cerium contents have been prepared by MCVD both under reducing and oxidizing conditions in order to study the valency change between trivalent and tetravalent cerium. The comprehensive characterization of the samples includes refractive index, ytterbium absorption cross section, NIR, visible and UV absorption and emission. Typical spectral features in the UV and visible range have been analysed with respect to the presence of Ce³⁺ and Ce⁴⁺. Photodarkening tests have been accomplished in order to correlate the power stability with Ce content and valency state.

8621-42, Session PWed

Research on SNR parameter test system of MCP in vacuum system

Yafeng Qiu, Nanjing Univ. of Science and Technology (China)

The core component of night vision system is Image intensifier. Research and production for the third generation of low light level image intensifier device are in progress in China. Fourth-generation image intensifier imaging mechanism is under Pre-Research. Screen, microchannel plate and the cathode are the main parts of an image intensifier. The important performance parameters such as resolution and signal-to-noise-ratio(SNR) of image intensifier depend on the Comprehensive performances of screen, the microchannel plate and cathode. Noise characteristic of the microchannel plate (MCP) is an important indicator of the evaluation of image intensifiers, while the present theory suggests that MCP is a major noise source of the image intensifier. In order to detect the MCP-generated noise, a vacuum system and designed the test method of the noise factor of MCP have been established. The noise factor of the MCP is measured using the test set-up with microchannel plate MCP signal to noise ratio parameter detection device in the vacuum system. It is can be used to judge the quality of the MCP scientifically. The experiments verify this test system is advanced, and the test results are reliable. This test system Provide a technical to promote the image intensifier research, and experience to testing other parameters or in other areas of research.

8621-43, Session PWed

Fabrication of the reliable (14-18)x1 fiber laser power combiner by the novel double bundling method

Bok Hyeon Kim, Gwangju Institute of Science and Technology (Korea, Republic of); Seon-Ju Kim, Youngkab Yoon, Lighting Solution Technology Co. Ltd. (Korea, Republic of); Swook Hann, Korea Photonics Technology Institute (Korea, Republic of)

Recently, the high power fiber laser has attracted much attention and the laser power combiner is one of the key components for power scaling in the high power laser system. Up to now, several methods have been exploited to develop the combiner and among them the tapered fused bundling (TFB) method becomes one of the most popular and reliable technology.

In the conventional TFB method, the input fibers were bundled with the honeycomb configuration then fused tapered and spliced to the output fiber. In the method, however, the fiber ports configuration was constrained to certain values such as 3x1, 7x1, 19x1, and 35x1 to satisfy the compactness and reliability in the bundling procedure. In this study, we suggest a novel double bundling method to make combiners with the large flexibility in the fiber port configuration. In making the (14-18) x1 combiners, 7 input fibers in the honeycomb stacking configuration was fused bundled and a single layer of secondary 7-11 fibers were stacked outside of the bundle and subsequently tapered and spliced to a output fiber. As a result, (14-18)x1 laser power combiners were made using 105/125 μm input fibers (0.15 NA) and a 200/220 μm output fiber (0.46 NA). In the bundling procedures a LPG torch was used and process parameters such as the gas flow and the tapering length/speed/frequency were optimized. The power transmission efficiency of the combiner was larger than 93% in all ports at the handling power of 100 W.

This work was financially supported by grants from the Regional Industry Development Program (No. 70007226), MKE and by NRF through the Asian Laser Center program of GIST, MEST, Korea.

8621-44, Session PWed

Classical and eclipse optical choppers

Virgil-Florin Duma, Aurel Vlaicu Univ. of Arad (Romania)

The paper presents our advances in optical choppers and applications. An overview of both macroscopic and micro-choppers is done with regard to their constructive and functioning principle. The modulation functions we have studied for classical choppers are pointed out – for top-hat light beam distributions. The eclipse choppers we have introduced are also presented. We study the differences between the modulation functions produced by the classical devices (with rotating wheels with windows with linear margins) and the newly-introduced eclipse choppers – under patent (with windows with circular margins that produce for the circular-shaped section of the laser beam in the plane of the wheel planetary eclipse-like effect – from which the name we have proposed for this type of device). The most convenient (from the technological and from the cost point of view) solution, with wheels with circular holes is highlighted. The advantages and the drawbacks of the various devices are discussed, as well as the sources of errors involved, and methods of correction. Both a theoretical and an experimental approach are considered. The latter is done on a chopper module we have constructed, with chopper wheels we have designed and manufactured. Throughout the study, top-hat laser beams are considered, as some of the most useful in laser manufacturing applications. The perspective of conducting the study on other light beams distributions (e.g., Gaussian) are also pointed out.

8621-45, Session PWed

Upconversion and 1.5 μm - 1.6 μm infrared emission studies of Er³⁺ doped in the low phonon-energy hosts KPb₂Cl₅ and KPb₂Br₅ via 1.5 μm laser excitation

Althea G. Bluiett, T. Searles, T. Jackson, Elizabeth City State Univ. (United States); Ei Ei Brown, U. Hömmerich, Hampton Univ. (United States); S. Trivedi, Brimrose Corp. of America (United States)

To date, Er³⁺ doped solid-state laser materials that can generate stimulated emission in the 1.5-1.6 μm (4I13/2 \rightarrow 4I15/2) range continue to be of interest for eye-safe laser applications and optical communications. Directly pumping the 4I13/2 band of Er³⁺ for the production of 1.5-1.6 μm stimulated emission has been extensively studied in many hosts, such as YAG, for this pumping scheme automatically reduces quantum defect heating. However, it is well understood that the excitation of Er³⁺ through this channel triggers unwanted upconversion, which depletes the 4I13/2 level of Er³⁺ and moreover produces unnecessary heating of the crystal. In this study, we will investigate the upconversion and 1.5-1.6 μm infrared emission of Er³⁺ doped into the low phonon-energy hosts KPb₂Cl₅ and KPb₂Br₅ via 4I15/2 \rightarrow 4I13/2 laser excitation. The advantage of low phonon-energy hosts is that upconversion releases less heat into the host compared to common oxide hosts with higher phonon energies, and therefore thermal issues are reduced (e.g. YAG) [1]. Furthermore, we will explore how the time resolved and spectral emission properties of Er³⁺ varies as a function of Er³⁺-ion concentration, host material, and temperature (77 K – 300 K) in order to ascertain the optimum environment for efficient 1.5-1.6 μm emission and at the same time minimize thermal issues that accompanies upconversion.

[1] R. S. Quimby, N. J. Condon, S. P. O'Connor, S. Biswal, and S. R. Bowman, Opt Mater. 30, 827 (2008).

8621-46, Session PWed

Fluorescence quantum efficiency dependent on the concentration of Nd³⁺ doped phosphate glass

Acácio A. Andrade, Viviane Pilla, Univ Federal de Uberlândia (Brazil); Sidney Lourenço, Univ. Tecnológica Federal do Paraná (Brazil); Anielle Silva, Noelio Dantas, Univ Federal de Uberlândia (Brazil)

Thermal-Lens (TL) for fluorescence quantum efficiency characterizations in a new phosphate glass matrix called PANK doped with Nd were performed. The quantum efficiency studies were accomplish in function of Nd concentrations (0.5-3 x 10²⁰ ions/cm³). In addition, fluorescence quenching was studied by measuring the concentration dependence of the fluorescence lifetime. The PANK matrix glass was suggested, probably first by being host of Nd, due to be transparent in the range of the electromagnetic spectrum ranging from UV to the near infrared, where all the electronic transitions in both absorption and emission occur in accordance with Judd-Ofelt theory.

8621-47, Session PWed

Elastomer based tunable virtual imaged phased array for reconfigurable optical interconnects

Philipp Metz, Christopher Behnke, Martina Gerken, Christian-Albrechts-Univ. zu Kiel (Germany); Jost Adam, Univ. of California, Los Angeles (United States)

As virtual imaged phased arrays (VIPA) offer high dispersion compared to conventional gratings, they have been proposed as building blocks for several photonic devices, including wavelength multipliers, chromatic dispersion compensators, waveform generators and pulse shapers. Here we introduce an elastomer based tunable VIPA, providing an additional degree of freedom for these devices. In particular, we investigate its capability to implement reconfigurable optical interconnects. In a wavelength demultiplexing setup it allows for both compensation of misalignment as well as reconfiguration of a source wavelength to a target channel. It is subject to simple fabrication techniques and promising for wafer-level device integration.

The fabricated VIPA consists of a 170- μm thick polydimethylsiloxane (PDMS) layer sandwiched between two structured silver coatings on a glass substrate. An 80-nm bottom silver coating forms the high reflective mirror of the VIPA, whereas a 40-nm top silver coating forms the VIPA's semi-transparent mirror. Light is coupled into the VIPA through the glass substrate at the edge of the bottom silver coating. The top coating additionally acts as a conductive layer allowing for Joule heating of the PDMS-layer, inducing a high thermal expansion coefficient and a thermo-optic effect. This is utilized for tuning the effective optical resonator cavity. We report a temperature increase of several tens of Kelvins by a power change in the mW regime. This leads to a tuning span of one free spectral range achieved by an effective PDMS layer thickness change of 0.17 %. Both resonance quality and tunability of the device are investigated.

8621-48, Session PWed

Characterization of an SiPM dedicated at analytical, life science and medical imaging

Philippe Bérard, Martin Couture, Frédéric Laforce, Bernicy Fong, Henri Dautet, Excelitas Canada, Inc. (Canada)

Silicon Photomultipliers (SiPMs) with high photon detection efficiency (PDE) in the 400 to 800 nm range and low dark counts are currently being developed in a variety of geometry, microcell size and surface in order to address the needs of the analytical, life science and medical imaging community. This SiPM development platform is based on previous knowledge of low dark count operated avalanche photodiode (APD) in Geiger-mode (SiKTM) that can be found in the Excelitas single photon counting module (SPCM). Low dark counts and low temperature sensitivity are especially important when tilling up SiPMs to form larger area detectors such as typically used block detectors in positron emission tomography (PET). The latest developments include; 1. Optical trenches to suppress cross-talk which allowed us to increase the operating voltage range from 5 to 10 volts above breakdown, 2. Parasitic capacitance was tailored to obtain single photon timing resolution (SPTR) ranging from 200 down to 100 ps FWHM and 3. PDE was improved at shorter wavelengths by optimizing the anti-reflection coating entrance window. A corrected energy resolution of 11.5 % was typically obtained at 511 keV which, with the good timing resolution, makes this SiPM an interesting candidate for time-of-flight (TOF) PET and other application requiring better than 100-200 ps timing resolution. Many aspects of characterization and improvements will be presented and discussed.

8621-49, Session PWed

A novel tellurite-phosphate glass for hybrid microstructured optical fibers

Zhongchao Duan, Hoangtuan Tong, Meisong Liao, Toyota Technological Institute (Japan); Motillon Erwan, Univ. of Rennes (France); Koji Asano, Takenobu Suzuki, Yasutake Ohishi, Toyota Technological Institute (Japan)

A new family of tellurite-phosphate glass was developed in TeO₂-ZnO-Na₂O-P₂O₅ system with the aid of hybrid microstructured optical fiber (HMOF) fabrications. Glass formation in this glass system was determined, compositional dependence of thermal and optical properties

were investigated. HMOFs provide large freedom for the engineering of chromatic dispersion, especially for high nonlinearity fibers made of soft glasses. In this case, the difference of core and cladding glasses (Δn) is a parameter to tailor dispersion of fibers and with various Δn , many special dispersion profiles can be realized in tellurite HMOF. As is well known, tellurite glasses possess high refractive index due to the glass former of TeO₂. In order to vary the refractive index, P₂O₅ was introduced into tellurite glasses. With both TeO₂ and P₂O₅, the refractive index at 1.55 μm can be changed from ~ 1.5 to ~ 2.0 in TeO₂-ZnO-Na₂O-P₂O₅ glass system. Substituting TeO₂ by P₂O₅, the refractive index can be reduced greatly, while the transition temperature doesn't change obviously. From the preparation point of view, softening temperature of glass is another important property for HMOFs. In the present glass system, characteristic temperature of glass, i.e. transition temperature and softening temperature, depends strongly on the content of ZnO and Na₂O. The transition temperature can be varied from 265° to 370° by changing the contents of ZnO and Na₂O. As a result, the refractive index and softening temperature can be changed independently in a large range, which brings large freedom in the fiber design. In the final, Raman spectra and inferred spectra were measured to understand the structural dependence on composition. Using the present glasses, some HMOFs with special dispersion profiles were designed. Tellurite-phosphate glasses with varied refractive index and softening temperature are promising media for hybrid fiber design and preparation.

8621-50, Session PWed

Mechanism of photonic crystal and waveguide effects in ZnO nanorods

Tae Un Kim, Doo Gun Kim, Seon Hoon Kim, Hyun Chul Ki, Korea Photonics Technology Institute (Korea, Republic of); Jin Hyeok Kim, Chonnam National Univ. (Korea, Republic of)

Since photonic crystals (PCs) were reported, there has been a dramatic increase in the number of papers related to nano-scale structures, because of their unique properties, such as presence of bandgap, local field enhancement, anomalous refractive index dispersion. et al.

Among these nano scale PCs materials, ZnO PCs have attracted considerable attention for their wide range of applications because of their outstanding electrical and optical properties. The ZnO nano crystal shows the difference of physical and chemical properties depend upon morphology of nanostructure.

In this study, we have calculated light waveguide effect within ZnO nano rod and photonic crystal effects in arrayed ZnO nano rods by COMSOL and 3D-finite dimension time domain (3D-FDTD) programs. Various ZnO nano photonic crystals were grown by laser interference lithography and hydrothermal method. The propagation and photonic crystal effects in ZnO nanorod was governed by shape of ZnO nanorod and arrangement of ZnO nanorods, respectively.

8621-51, Session PWed

Optical characterization of Er-doped glasses for solar-pumped laser applications

Takenobu Suzuki, Yasuyuki Iwata, Kohei Nogata, Toyota Technological Institute (Japan); Shintaro Mizuno, Hiroshi Ito, Kazuo Hasegawa, Toyota Central R&D Labs., Inc. (Japan); Yasutake Ohishi, Toyota Technological Institute (Japan)

The quantum efficiencies (QEs) of Er³⁺-silicate, tellurite, phosphate and fluoride glasses have been examined under simulated sunlight excitation to elucidate feasibility of the materials for solar-pumped lasers. The Er³⁺-doped glasses exhibited several emission bands in the visible and near-infrared regions. The QE of the whole emission bands was obtained as about 75 % for fluoride glass and about 20 % for silicate glass. The most intensive emission was the 4I13/2⁴I15/2 transition around 1.5 μm under simulated sunlight excitation. The highest QE of the emission band at 1.5 μm was about 35 % for fluoride glass and about 7 % for silicate

glass.

The product of the stimulated emission cross-section and the emission lifetime ?? was about 43×10^{-24} cm²sec for fluoride glass and about 100×10^{-24} cm²sec for silicate glass. These values are about 3-7 times larger than that of Nd-doped glasses. This means that advantage of Er³⁺-doped glasses by the large ?? exceeds the disadvantage that Er³⁺ is the 3-level laser system. Because a solar-pumped fiber laser has been achieved by using Nd-doped fluoride glass as the gain media, the Er³⁺-doped glasses would be candidate as host media of Er³⁺-doped solar-pumped lasers.

8621-52, Session PWed

UV-enhanced silicon avalanche photodiodes

Richard A. Myers, Richard Farrell, Mickel McClish, Radiation Monitoring Devices, Inc. (United States)

There is a need for high quantum efficiency (QE), high speed response light detectors, in the blue and ultraviolet (UV) region of the spectrum (200 to 500 nm). In addition, many applications require miniature, portable, rugged, and field ready detectors, which drive requirements away from photomultiplier tubes and towards solid state devices. For example, medical imaging systems such as PET or CT utilize multiple scintillators that convert nuclear energy to light in the region of 200 to 500 nm. In an outdoor environment, the use of pulsed UV sources (e.g. tripled Nd:YAG lasers at 355 nm) provides an advantage for non-line-of-sight optical communications as well as active targeting and ranging systems through improved eye-safety and reduced interference from solar background. Unfortunately, despite developments in wide-bandgap materials, the highest QE for large area, low noise detectors is limited to 50% at 355 nm, compared to > 90% at the longer wavelengths.

Recently, scientists at RMD have developed a method to improve the QE and bandwidth of our silicon avalanche photodiodes (APDs). This method relies on a modified surface treatment to reduce the probability of charge trapping near the detector's surface. The process also allows us to maintain the high gains (> 1000) and low noise performance characteristic of our standard APD detectors. As a result, we have been able to increase the bandwidth of our silicon APDs and APD arrays to > 200 MHz and improve the QE to > 60%.

8621-53, Session PWed

Fluidic lens of floating oil using jar-shape chamber based on electrowetting

Hyunhwan Choi, KAIST (Korea, Republic of)

Fluidic lens presented in this report has a double-sided curved surfaces and make it possible to control the curvature of the lens surface independently. Primal advantages by using the double-faced fluidic lens is that it can realize the strong dioptric power overwhelming the optical property of conventional adaptive lens, even better than the conventional glass lens. Different from the fact that the conventional liquid lens uses only two electrodes to change the lens curvature by controlling the tilting angle between the actuating liquid and the hydrophobic surface, the proposed lens uses four different electrodes to control the curvatures of both surfaces by changing the tilting angle with the hydrophobic surface and spherical angle from the center and edge of the actuating water. This study presents a liquid lens using electrowetting phenomenon that makes a floating lens in between the actuating fluids. The lens shape has double-sided curved surfaces and is able to implement powerful optical properties such as optical power and ability to change its spherical aberration and chromatic aberration as well. Its optical power ranges from -100 to 100 diopters, which is operating with bias of -30 to 30 volts. The spherical aberration of the lens working by maximum bias voltage is less than 5 μ m in the focal plane. Image through the lens is so clear to see the USAF chart of 25 LP/mm.

8621-54, Session PWed

Optical gain medium for plasmonic devices

Victor A. Rivera, Univ. de São Paulo (Brazil); Yannick Ledemi, Univ. Laval (Canada); Sergio P. Osorio, Fabio A. Ferri, Univ. de São Paulo (Brazil); Younes Messaddeq, Univ. Laval (Canada); Luis A. Nunes, Euclides Marega, Univ. de São Paulo (Brazil)

Nowadays, we can see a great rise of research on nanophotonics based on surface plasmon-polariton, aside the so-called diffraction limit. These concepts rely exclusively on the notion of electromagnetic evanescent waves sustained in the metal-dielectric interface. In this frame, the miniaturization of traditional optical components has been essential for the integration and development of "novel" (traditional) photonic devices for manipulating light at nanoscale, to the aim of processing information with unparalleled operation speeds using subwavelength in photonic devices. Here, we propose a novel substrate for the fabrication of plasmonic devices, which consists of an Er³⁺-doped tellurite glass with embedded silver nanoparticles (NPs). The inclusion of an amplifying response in the medium surrounding the metal particle results in a change in the internal field, i.e., an electric coupling between NP and erbium ion can be achieved. Those NPs, when illuminated by a 976 nm diode laser, yields a localized surface plasmon resonance (LSPR) that stimulates the radiative emission of neighboring Er³⁺ ions in the telecommunication band. This work shows that a gain medium: Er³⁺ ions (amplification function in the telecommunication band) with Ag NPs (luminescence enhancement) can modify the complex parameter $\gamma(\text{neff})$ increasing the polarizability of the samples. That improvement in the luminescence has potential applications for nano-waveguide amplifiers.

8621-55, Session PWed

High near-infrared emission intensity of Er³⁺-doped zirconium oxide films on a Si(100) substrate

Victor A. Rivera, Fabio A. Ferri, Univ. de São Paulo (Brazil); Jose C. Huaman, Marcelo Kawamura, UFSCAR (Brazil); Marcelo A. Pereira, Luis A. Nunes, Maximo S. Li, Euclides Marega, Univ. de São Paulo (Brazil)

High crystalline quality Er³⁺-doped zirconium oxide films were deposited on Si(100) by electron beam evaporation into a vacuum chamber, with 130, 350 and 1300 nm of thickness, and with different erbium oxide concentrations. From those samples, we studied the characteristics of light emission in the telecommunication window before and after thermal treatment in oxygen atmosphere. We obtained a decrease in the intensity of luminescence and the $4I_{13/2}$ lifetime with the increase of the erbium oxide concentration, which is analysed via an energy transfer process. After the thermal treatment at 900 °C the luminescence intensity of those samples was improved in comparison with those before the thermal annealing. On the other hand, the structure environment of the Er³⁺ ion in the thin films before and after annealing were studied by X-ray diffraction, and, together with the measured surface morphology as a function of the thermal annealing in controlled atmosphere, it showed significant changes. This fact indicates that the thermal treatment can modify the crystalline field around the Er³⁺ ions, resulting in a luminescence enhancement and in a subtle blue shift.

8621-56, Session PWed

Low cost CMOS silicon photomultipliers with ultrafast timing

Carl Jackson, Kevin O'Neill, Nikolai Pavlov, Stephen Bellis, SensL (Ireland)

SensL has developed a new Silicon Photomultiplier (SPM) process and

associated products that deliver vastly improved timing and detection capabilities from 300nm to 450nm.

SPM technology is now well established as an alternative to photodetectors such as the PMT, APD and photodiode, with the first SPM-based PET systems currently in FDA (510k) trials in the USA.

SensL has developed a new process based on P-type into N-type silicon wafers and the resulting FB series of SPM feature significant improvements in both PDE and coincidence signal timing. Both the maximum PDE and the wavelength range are improved due to the newly-employed P-on-N structure. In addition, the FB series SPM detectors exhibit extremely fast output pulses (ns rise and fall times) through the fast output architecture SensL has patented. For the first time, picosecond coincidence timing is possible in a technology manufactured in a high volume CMOS foundry.

This combination of high PDE and fast signals leads to excellent timing performance, particularly for applications like time-of-flight PET (ToF PET) that use blue emitting scintillation crystals to make fast coincident timing measurements of 511keV annihilation radiation. Other applications that benefit from this new SPM technology are LiDAR and ranging, hazard and threat detection and biophotonics.

We will present the latest results from the new detectors including gain, PDE, noise, temperature coefficients as well as application specific measurements from large area arrays (64 channels of 6mm SPM pixel) of detectors with dimensions greater than 50mm x 50mm.

8621-58, Session PWed

Improving single-beam thermal lens spectroscopy by wavefront spatial filtering

Carlos Estupiñán-López, Christian Dominguez, UFPE (Brazil); Renato E. de Araujo, Univ. Federal de Pernambuco (Brazil)

The determination of fluorescence quantum yield is an important step on the characterization of novel fluorescent probes. Single-beam thermal lens (SBTL) spectroscopy is a powerful and well established method to evaluate quantum efficiency. In this work, we introduce new detection mode for the SBTL technique improving the sensitivity of the spectroscopic method. Here we explored a wavefront spatial filter to detect only the external fraction of incident laser beam, in contrast with the conventional SBTL. As a wavefront spatial filter we used an opaque circular obstacle in front of the detector in the single-beam thermal lens setup. A spherical lens was used to collect and send the beam to a photodetector. In order to demonstrate the method we used a cw Nd:YAG laser at 532 nm and ethanol solution of Rhodamine 6G in a 1mm quartz cuvette. We show that signal/noise rate on the determination of absolute quantum yield can be enhanced 3,8 times exploring wavefront spatial filter on the single-beam thermal lens technique.

8621-59, Session PWed

A method of distinguishing different types of petrol based on fiber-optic surface plasmon resonance sensor

Dachao Li, Zhu Rui, Peng Wu, Tianjin Univ. (China)

To realize the online, fast, accurate detection for distinguishing different types of petrol in transportation pipelines, a method based on fiber-optic surface plasmon resonance (FO-SPR) sensor is proposed. The calculation and simulation of FO-SPR end-reflection structure were carried out with the parameters of fiber diameter, the length of the sensing area, the gold film thickness and the thickness of chromium layer through fiber theoretical model and SPR principle. The impact of different parameters on sensor performance was analyzed as follows: when the fiber diameter increases, the normalized light intensity increases but curvature radius and attenuation of the SPR curve change small; The normalized light intensity and curvature radius decrease as the length of sensor area increases; When the gold film thickness increases, the

SPR curve has a red shift and a larger curvature radius, the attenuation becomes larger first and then smaller; The impact of chromium layer thickness is little. The optimized structural parameters of FO-SPR were obtained as follows, fiber diameter: 600 μ m, the length of the sensing area: 15mm, gold film thickness: 50nm, the thickness of chromium layer: 3-5nm. According to the optimal parameters, the SPR sensor was manufactured through the vacuum coating technology. A wavelength modulation optical measurement system with the core of SPR sensor was set up. Sample petrol 90#, 93# and 97# and their mixture were measured. The distinguishing of product oil is realized by the refractive index information obtained through the change of resonance wavelength as different petrol has different refractive index. The experiment results show that the measurement method can identify the different types of petrol and their mixture with better degree of distinction and measurement repeatability. It lays the foundation for the identification of mixed product oil in transportation pipelines.

8621-60, Session PWed

Filamentation and supercontinuum generation in tellurite glass

Meisong Liao, Weiqing Gao, Tonglei Cheng, Zhongchao Duan, Xiaojie Xue, Hiroyasu Kawashima, Takenobu Suzuki, Yasutake Ohishi, Toyota Technological Institute (Japan)

Though soft glass such as tellurite or chalcogenide glass is transparent in the range of 3-6 μ m, fiber made of it is difficult to generate supercontinuum (SC) to that range because of the high loss, the wavelength limit of pump source, and the challenges in light-coupling. To circumvent these problems, we developed SC light source by using tellurite bulk glass through filamentation. For this scheme, the optical path length in the glass is very short due to the adopted high pump power, so the negative influence of material loss is reduced greatly. The light-coupling is straightforward, and the coupling efficiency is high. The bulk glass for SC generation is cheap, and can be fabricated easily.

We adopted a pump wavelength of 1600 nm which is comparatively long. Such a long pump wavelength ensures a large energy ratio of the glass's bandgap to the incident photon, so the disadvantage of small bandgap of tellurite glass is reduced, and the two-photon absorption is avoided as well. We have shown that under suitable pump condition, the SC generation by filamentation can cover from visible to 6 μ m. It is the broadest SC generation by tellurite (including glass and fiber). For the suitable pump condition, the glass was free of optical breakdown. If the interface reflections were deducted, the SC conversion efficiency was 87%. The SC conversion efficiency was stable. To the best of our knowledge, this is the first report on filamentation in tellurite glass which has a comparatively small bandgap.

8621-61, Session PWed

Long-period grating in tapered fiber and its equivalent chirped grating for dispersion management

Krishna C. Patra, Sambalpur Univ. (India); Enakshi K. Sharma, Univ. of Delhi South Campus (India)

We have developed the procedure for numerical solution of the multiple coupled mode equations for LPGs in tapered fibers. A given grating period the phase matching condition can be satisfied to a given mode at different wavelengths or at one wavelength to different modes as it propagates through the grating in the fiber. The coupled equations for amplitudes of modes have to be solved numerically and a correction for the change in effective indices of the coupled modes along the grating length needs to be applied. An equivalent slightly apodized chirped grating can be used to manage dispersion.

8621-62, Session PWed

Coupled mode analysis for graded index multi-waveguide systems

Krishna C. Patra, Sambalpur Univ. (India); Sangeeta Srivastava, Univ. of Delhi (India); Enaksh K. Sharma, Univ. of Delhi South Campus (India)

We present the modified scalar coupled mode analysis for the N waveguide diffused channel waveguide directional power coupler. The study simulates the lateral evanescent field coupling in Graded Index Multi-Waveguide Systems. In a two-step procedure, the propagation characteristics of individual waveguides have been obtained first using the completely analytical variational approach. After obtaining the individual waveguide characteristics, the complete scalar coupled mode theory has been developed to obtain the supermodes corresponding to the coupled waveguide configuration. A comparison with the numerically intensive though exact multilayer staircase procedure justifies the use of this simple formulation, especially for repetitive calculations as required for design optimization.

8621-63, Session PWed

Fiber optic sensor based on radio frequency Bragg grating

Jie Huang, Xinwei Lan, Lei Yuan, Hanzheng Wang, Lei Hua, Zhan Gao, Hai Xiao, Missouri Univ. of Science and Technology (United States)

Optical fiber sensors are well known for their advantages, such as small size, light weight, immunity to electromagnetic interference, resistance to chemical corrosion and high temperature survivability. Also, as a transmission line, optical fiber is supreme in terms of transmission loss and cost in comparison with its analog, coaxial cable in the radio frequency domain. These unique features position optical fiber sensors to fulfill the needs of a wide range of sensing tasks. Optical fiber devices have been explored to create microwave photonic processors, including filters, signal generators, mixers, etc. It is proven that the photonic signal processing offers wide bandwidth operation, high resolution, and low noise performance. These unique features stem mainly from the intrinsic excellent properties of optical fiber delay lines. Inspired by the microwave photonic processors, we propose a passive optical fiber sensor that can be interrogated using RF instruments.

An optical fiber radio frequency Bragg grating is proposed in this paper. The period of radio frequency Bragg grating is around tens of millimeters, which is much larger than that of a commercial FBG. A radio frequency modulated laser light is injected into an optical fiber Bragg grating and collected by a photodetector. The reflection spectrum in radio frequency is observed by sweeping the frequency using network analyzer. The Bragg resonance in radio frequency domain can be seen. The proposed radio frequency Bragg grating sensor has a linear response to applied strain change.

8621-64, Session PWed

Yb:CaGdAlO₄:1μm laser with different architectures

Bruno Viana, Ecole Nationale Supérieure de Chimie de Paris (France); Sandrine Ricaud, Lab. Charles Fabry (France); Anael Jaffres, Akiko Suganuma, Pascal Loiseau, Ecole Nationale Supérieure de Chimie de Paris (France); B. Weichelt, M. Abdou-Ahmed, T. Graf, Univ. Stuttgart (Germany); Daniel Rytz, FEE GmbH (Germany); M. Delaigue, Eric Mottay, Amplitude Systèmes (France); Frédéric Druon, Francois Belembois, Patrick Georges, Lab. Charles Fabry (France); Julien DidierJean, FiberCryst (France)

Yb³⁺:CaGdAlO₄ is a near infrared laser material with very high thermal conductivity (> 6.5 W K⁻¹m⁻¹) allowing high-power diode pumping. High gain and broad emission (> 40 nm) allow this matrix to be well suitable for high power and/or ultrafast laser realization and the material is very competitive between other various oxide laser hosts. We recently succeed to improve the optical quality with thermal of annealing in reducing atmosphere after the growth technique by the Czochralski (CZ) process at several ytterbium concentrations. Thermal conductivity is slightly affected by the increase of ytterbium content.

The thin-disk laser design allows the generation and the amplification of ultrashort pulses with very high efficiency, high output power and good beam quality. Laser experiments were performed with about 350 μm-thick Yb³⁺:CaGdAlO₄ crystal with different ytterbium content (2, 3.5 and 5 %). For instance, at about 1 μm, in the case of 2 Yb at. %, thin disk laser has been obtained with a slope efficiency of 41% average power of 30W and optical-to-optical efficiency of 32%.

In the work laser performances will be review for bulk matrix, thin disk configuration and in CW and femtosecond regime. Others configurations such as crystalline fibers will be discussed.

8621-65, Session PWed

Optical properties of porous nano-composites of zinc (hydr)oxide with graphite oxide

S. M. Z. Islam, Taposh Gayen, Mykola Seredych, Teresa Bandosz, Robert Alfano, The City College of New York (United States)

The aim of the research is to determine the key optical properties of zinc (hydr)oxide and the composites of zinc (hydr)oxide with 2% and 5% graphite oxide using three spectroscopic techniques: absorption, fluorescence and photocurrent spectroscopies. The energy gaps obtained from 2.85 eV to 2.95 eV of the composites were smaller than that for zinc oxide (~3.2 eV) and zinc (hydr)oxide (~3.00 eV). The band gap narrowing of the composite materials is due to presence of defects, less confinement, and larger particles. The bonds between zinc (hydr)oxide lattice and the carbon of graphene phase also contribute to this phenomenon.

The determination of the optical band-gap is important because it not only controls the efficiency for solar conversion and the shape of the optical emission spectrum, but also manifests the effect of structural and thermal disorder on the electronic properties of the nanocomposites. The equations used for direct band gap and Urbach tail, where A_{0D} and A_{0U} are constant. E_g is energy gap, E_{op} is optical energy gap.

New classes of optical nano-composite materials that exhibit band gap narrowing have been investigated. The presented results open the possibility of engineering of these materials for myriad of applications, ranging from sensors to energy-harvesting and energy conversion in hybrid solar cells.

Conference 8622: Organic Photonic Materials and Devices XV

Monday - Wednesday 4 -6 February 2013

Part of Proceedings of SPIE Vol. 8622 Organic Photonic Materials and Devices XV

8622-1, Session 1

Liquid fiber photonics for optical networking and testing (*Keynote Presentation*)

Robert A. Norwood, College of Optical Sciences, The Univ. of Arizona (United States)

We have developed a novel integrated platform for liquid photonics based on liquid core optical fiber (LCOF). The platform is created by fusion splicing hollow core optical fiber to standard single-mode optical fiber making it fully integrated and practical. Filling of the hollow core fiber with liquids of interest then becomes straightforward, with the selection of the liquid being based upon the requirements set by the refractive index contrast desired and the wavelength of operation, among other considerations. At 1550nm, the core liquids should generally have a small or vanishing amount of aliphatic hydrocarbon, as overtone absorption from carbon-hydrogen bonds limits propagation lengths to about 10-20cm. Among the compelling applications of this technology are optical networking, optical sensing and optical testing. As examples of optical networking applications, we highlight the use of carbon disulfide in integrated LCOF for ultralow threshold Raman generation (< one nanojoule), inverse Raman scattering based all-optical switching, and narrow linewidth Brillouin lasing. The integrated LCOF platform has further potential for optical testing, owing to the long pathlengths (~ 1m) and availability of state-of-the-art fiber coupled solid state light sources, such as ultrafast fiber lasers, high power broadband incoherent sources and high power semiconductor lasers. This enables high sensitivity measurements of the optical absorption of liquids and solutions, so that weak tail absorption of technologically important dye molecules can be determined. Measurements of the third order nonlinearity of liquids and solutions based on self-phase modulation and parametric frequency generation is demonstrated and discussed as another unique testing capability enabled by LCOF. Future applications of the integrated LCOF platform for ultralow power nonlinear optics include efficient white light generation for displays, mid-IR generation, slow light generation, parametric amplification, all-optical switching and wavelength conversion using liquids that have orders of magnitude larger optical nonlinearities compared with silica glass.

8622-2, Session 1

Next-generation optical interconnect device technology using photonic polymers (*Invited Paper*)

Okihiko Sugihara, Toshikuni Kaino, Tohoku Univ. (Japan)

Photonic polymers play important role for board-level and chip-level optical interconnection. We present recent progress of photonic polymers and waveguide device technologies for next generation integrated optical circuits. High performance photonic polymer is a potential candidate for optical waveguide material, and simple waveguide fabrication and assembly techniques are also required for practical optical modules.

8622-3, Session 1

Use of polymer and organic/inorganic hybrid materials for optical printed circuit board (O-PCB) and VLSI photonics application (*Invited Paper*)

El-Hang Lee, Yong Ku Kwon, Seung-Gol Lee, Beom-Hoan O, Se-Geun Park, Kyong-Hon Kim, Inha Univ. (Korea, Republic of)

This talk presents an overview on our research on the use of polymer and organic/inorganic hybrid materials for the micro/nano-photonics integration and fabrication of optical printed circuit boards (O-PCBs). It discusses on the theory, design, fabrication, and integration of these materials for O-PCBs of generic and application-specific nature. Very large scale integrated (VLSI) micro/nano-photonics chips of various functionalities are integrated on the O-PCBs for diverse applications. An O-PCB consists of two-dimensional array of micro/nano-optical wires made of these materials on a hard or flexible board. VLSI photonic chips use nano-wires and devices made of silicon, semiconductor, and plasmonic metals. The micro/nano-optical devices include: micro-lasers, nano-optical wires, switches, modulators, directional couplers, filters, micro-resonators, photonic crystals, and plasmonic devices. We discuss the scientific and technological characteristics of these materials for the micro/nano-photonics devices to be integrated on the O-PCBs and the VLSI photonic chips. The materials issues include optical refractive indices, transmission windows, losses, birefringence, dispersion, nonlinearity, thermal/mechanical stability, and other optical properties. The integration issues include the compatibility and mismatch problems of these materials for various devices and applications. We will present the detailed examples of these materials and discuss further prospects of these materials for the O-PCB and VLSI photonic applications.

8622-4, Session 1

Flexible, stable, and easily processable optical silicones for low loss polymer waveguides

Brandon W. Swatowski, Chad M. Amb, Sarah K. Breed, David J. Deshazer, W. K. Weidner, Dow Corning Corp. (United States); Roger F. Dangel, Norbert Meier, Bert J. Offrein, IBM Zürich Research Lab. (Switzerland)

Flexible waveguide based optical links are of interest for board-level signal routing, e.g. from a processor to the board-edge. Flexibility, i.e. bendable structures, enables versatile 3D signal routing and is a must for in the box assembly. Photo patternable optical silicone materials have been developed that can be fabricated into flexible polymer waveguides using conventional film processing such as doctor blading and spincoating. Core features can be patterned using non contact photolithography or laser writing methods, subsequently developed in a solvent. Minimal thermal treatment by hotplate or ovens in air are required, with total processing time demonstrated to less than 1 hour. Flexible waveguides designed for multimode applications have demonstrated loss of 0.05 dB/cm at 850 nm, with opportunity to reduce further. These waveguides have proven stable in 85 °C and 85% relative humidity storage conditions in accordance with Telecordia specification GR1221 for greater than 1000 hours to date with no degradation in optical performance. This polymer waveguide system has shown to adhere to both composite rigid substrates and flexible polyimide substrates. The layer stack shows absolutely no curling effects as may be caused by thermal expansion differences. This greatly simplifies post-processing and is an essential property for both thin rigid and especially flexible applications. The flexibility has been demonstrated with static bending to 1 mm radius and dynamic bending of 500 cycles at 5 mm radius. The flexible waveguides have also proven to sustain twisting, which should aid in the assembly of modules.

8622-5, Session 1

Modeling polymer-based hybrid-material photonic waveguides

Meng-Mu Shih, Univ. of Florida (United States)

This work demonstrates numerical modeling for photonic waveguides

**Conference 8622:
Organic Photonic Materials and Devices XV**

with multi-layers of polymer, silicon, and metal. Since the transparency of polymer and silicon in certain wavelength range, the light can be guided for optical applications such as interconnects, communications, or circuits. The built-in gratings with nano periodicity between the polymeric and the metallic layers can stabilize light propagation. Numerical results show how grating depth in polymeric layer and metallic layers, layer thickness, metal types, and mode-polarization can affect the coupling coefficients of such waveguides. Qualitative interpretations based on quantitative calculations can provide insights into the modeling and design of such waveguides.

8622-6, Session 2

THz planar metamaterials as anisotropic sensors for liquid crystal and carbon nanotube

(Invited Paper)

Jeong-Weon Wu, J.H. Woo, E. Choi, Boyoung Kang, E. S. Kim, J. Kim, Y.U. Lee, Ewha Womans Univ. (Korea, Republic of); Tae Y. Hong, Jae H. Kim, Yonsei Univ. (Korea, Republic of); Ilha Lee, Young Hee Lee, Sungkyunkwan Univ. (Korea, Republic of)

THz metamaterials are employed to examine changes in the meta-resonances when two anisotropic organic materials, liquid crystal and carbon nanotubes, are placed on top of metamaterials. In both anisotropic double split-ring resonators and isotropic four-fold symmetric split-ring resonators, anisotropic interactions between the electric field and organic materials are enhanced in the vicinity of meta-resonances. In liquid crystal, meta-resonance frequency shift is observed with the magneto-optical coupling giving rise to the largest anisotropic shift. In carbon nanotube, meta-resonance absorptions, parallel and perpendicular to nanotube direction, experience different amount of broadening of Lorentzian oscillator of meta-resonance. This work opens the application of metamaterials as a sensor for anisotropic materials.

8622-7, Session 2

Polymer cladding silicon-nitride ring resonator for athermal waveguide application

Shiyoshi Yokoyama, Feng Qiu, Feng Yu, Andrew M. Spring, Kazuhiro Yamamoto, Kyushu Univ. (Japan)

We fabricated a ring resonator waveguide of SiN/SiO₂. The waveguide was covered with the chromophore/polymer film in order to demonstrate the temperature independent ring resonator application. To fabricate such an athermal waveguide, both the dimensions of the core and cladding, refractive index, and thermo-optic (TO) coefficients have to be controlled precisely. Silicon nitride has been recently employed in silicon photonics application, with some outstanding performance in nonlinear optical properties and visible-near infrared sensing. To realize on-chip nonlinear optical source or sensors using silicon nitride ring resonator, it is clear that temperature independent resonance is crucial for stable and reliable operation of these devices. Silicon nitride has a refractive index which is lower than silicon but still higher than general polymers in optics. Thus, the compensation of the temperature dependence wavelength shift by using a polymer cladding is possible by considering the TO coefficient of silicon nitride and negative TO coefficient of polymer. In this study, we mixed DR1 chromophore in PMMA as the cladding and are able to control its refractive index and TO coefficient through the process of photo-bleaching. We show that polymer/chromophore covered ring resonator show an enhanced athermal performance with a temperature dependent wavelength shift of 0.018 pm/oC. Such a device is shown to perform with little change in peak wavelength, Q factor, and on/off ratio from room temperature up to 50C

8622-8, Session 2

Dielectric elastomer actuators for adaptive photonic microsystems

Marcus Heimann, Technische Univ. Berlin (Germany); Henning Schröder, Fraunhofer-Institut für Zuverlässigkeit und Mikrointegration (Germany); Sebastian Marx, Klaus-Dieter Lang, Technische Univ. Berlin (Germany)

The various applications in the field of photonic microsystems for Dielectric Elastomer Actuators (DEA) were shown with this research. DEA belong to the class of Electro Active Polymers (EAP) and have the potential to substitute common technologies like piezoelectric actuators. DEAs offers several advantages like compact and variable shapes, large actuation ranges and cost efficient production processes that have to be emphasized. For the market of adaptive photonic microsystems especially area actuators are very suitable. They can be used e.g. as tuneable lens, mirror or grating component and tool for optical fiber alignment. These area actuators have a similar structure like a capacitor. They consist of three layers, two electrode layers on top and bottom and one dielectric layer in the center. The dielectric layer is made of a ductile and prestretched elastomer film. When applying a voltage between both electrode layers the thickness of the dielectric film is compressed and the actuator is displaced in the plane. The use of material compositions like a polymer matrix with graphite, carbon nano particles or carbon nano tube as well as thin metal films for the electrodes were studied. The paper presents results on suitable dielectric and electrode materials, actuator geometries and respective adaptive photonic components. The manufacturing process of area actuators is described in detail. As a basic size of the area actuators 20 times 20 mm² were chosen. Onto the produced area actuators polymer lenses or mirrors were assembled. The deflection of the optical beam path is calculated with optical simulations and measured at the prepared adaptive optical components. Static actuations of about ±15 μm are reached when applying a voltage of 200 V. Also the function of a tuneable beam splitter is demonstrated to show further applications.

8622-10, Session 3

Organic DSTMS crystals for high-field wide bandwidth THz spectroscopy (Keynote Presentation)

Peter Günter, Mojca Jazbinsek, Tobias Bach, Blanca Ruiz, Carolina Medrano, Rainbow Photonics AG (Switzerland)

THz generation using nonlinear optical effects in organic crystals has unique advantages compared to inorganic alternatives: high figures of merit for THz generation using various fs–ns pump laser sources in the infrared, as well as a relatively broad THz frequency range, which is because of the possibility for phase matching between pump optical and the generated THz waves in the region between 0.1–20 THz. Compared to poled polymers, the advantage of organic crystals is the high stability and possibility for relatively large thicknesses (several mm) and therefore high conversion efficiency at the phase-matched conditions. However, most of the efforts in the past have focused only on the generator crystal DAST (4-N,N-dimethylamino-4'-N'-methyl-stilbazolium tosylate), because of the lack of alternative crystals with similarly high figures of merit and possibilities for growth of high-quality single crystals.

We investigate THz interactions using recently developed materials, stilbazolium salt DSTMS (4-N,N-dimethylamino-4'-N'-methyl-stilbazolium 2,4,6-trimethylbenzenesulfonate), which is a derivative of DAST with superior processing and THz figures of merit, as well as phenolic polyene OH1 (2-(3-(4-hydroxystyryl)-5,5-dimethylcyclohex-2-enylidene) malononitrile), which is a hydrogen bonded crystal and an important alternative for stilbazolium salts due to the low absorption at around 1 THz. Best phase-matching properties of these materials for pump optical wavelengths in the range of 800–1600 nm and for THz frequencies in the range of 0.1–12 THz have been determined. We demonstrate efficient generation and detection of very broadband THz pulses (0.1–12 THz)

**Conference 8622:
Organic Photonic Materials and Devices XV**

using these materials, pumped by fs fiber lasers at telecommunication wavelengths.

8622-11, Session 3

Second harmonic generation in non-electrically-poled NLO polymers excited by surface plasmon enhanced electric field

Atsushi Sugita, Kaname Suto, Tomoyuki Sato, Atsushi Ono, Wataru Inami, Yoshimasa Kawata, Shigeru Tasaka, Shizuoka Univ. (Japan)

We will report second harmonics generations (SHG) in nonlinear optical (NLO) polymers excited by surface plasmon (SP) enhanced fields. The surface plasmon polariton was excited in an attenuated total reflection geometry having the Kretschmann configuration. Here, the NLO interactions occurred in the thin films of the NLO polymers, consisting of Disperse Red 1 as guest chromophores and PMMA as host, coated on Ag thin films. Our experimental results indicated that NLO polymers emitted strong SHG signals in the SP resonance conditions. The SHG intensities from NLO polymer coated Ag films were more than 10 times higher than those of the uncoated Ag films. The measurements were conducted for the polymer films with different thickness between 10 and 100 nm. All of the samples with different polymer thickness exhibited the SHG signals at its SP resonance condition that depends on the film thicknesses. The highest SHG conversion efficiency was recorded from the sample with 30 nm film thicknesses. The p-polarized pump beams gave the highest SHG conversion efficiency while the s-polarized ones gave almost no signals. On the other hand, the polarizations of the SH signals were highly oriented in the direction of the p-polarizations. The SP-enhanced field attracts a lot of interests as light sources for sub-diffraction-limit imaging. The SP can be excited only in the regions lower than surface plasma frequencies peculiar to the metals. The present frequency conversion technologies for the SP enhanced fields in the NLO polymers will extend the frequency regions available for the sub-diffraction-limit imaging.

8622-12, Session 3

Nonlinear absorption and frequency upconversion of a salicylaldehyde azine

Amadeu Souza, Márcio A. Alencar, Sílvia Cardoso, UFAL (Brazil); Marcelo Valle, UFSJ (Brazil); Renata Diniz, UFJF (Brazil); Jandir Hickmann, UFAL (Brazil)

In this work, we report on the observation of infrared-to-visible frequency upconversion from salicylaldehyde azine 1 crystals and the determination of its third-order nonlinear response using an open-aperture Z-scan technique. The produced salicylaldehyde azine 1 crystals were characterized by the techniques: ¹H NMR, EI-MS, melting point, X-ray diffraction, UV-VIS-NIR spectrophotometry and a spectrofluorometry. The two-photon fluorescence and nonlinear absorption measurements were performed using a model locked Ti:Sapphire laser, tuned at 793 nm, delivering pulses of 200 fs at a 76 MHz repetition rate. Varying the laser power, we observed that this fluorescence process involves the absorption of two laser photons. For nonlinear absorption measurements, the laser repetition rate was reduced to 1 KHz by means of a pulse picker. A solution of 0.1 M of this crystals in chloroform was employed as the sample which was placed in a 1 mm thick quartz cell. We obtained that this solution presents a nonlinear absorption coefficient 0.39 cm/GW. Using this result, we also calculated the two-photon absorption cross-section of this OM to be 162 GM. Our results demonstrate that this organic crystal presents a huge potential to be exploited in photonic applications such as fluorescence microscopy and optical limiting devices.

8622-13, Session 3

Studies of new organic molecules and hybrid systems for lasing applications (*Invited Paper*)

Jaroslawn Mysliwiec, Adam Szukalski, Lech Sznitko, Wroclaw Univ. of Technology (Poland); Karolina Haupa, Univ. of Wroclaw (Poland)

We present experimental results of studies of new organic compounds and hybrid systems which can be used for amplified spontaneous emission (ASE) and lasing applications.

As molecules we have choose group of derivatives of pyrazole. Synthesized compounds were dissolved in a different solvents and organics matrices. We analyzed luminescence, ASE and lasing of thin films excited by the Nd:YAG nanosecond pulsed laser doubled and tripled in frequency, in function of different excitation pulse energy densities.

We show the light amplification and spectral narrowing of dye doped matrices, low threshold energy density of optical pumping, large gain and low photodegradation (good photostability of chromophores).

8622-14, Session 3

Polarization properties of dye-based random lasers

Sebastian Knitter, Michael Kues, Carsten Fallnich, Westfälische Wilhelms-Univ. Münster (Germany)

We present the first systematic study on the emission polarization of coherent random lasers. Random Lasing (RL) occurs in scattering and amplifying media (e.g., nanoparticles in a dye solution) under intense pumping. Employing a one-shot spectropolarimeter the complete polarization state and degree of polarization could be recovered for individual RL modes. The degree of polarization of RL modes was significantly higher, than for fluorescent or amplified spontaneous emission. A statistical analysis revealed that the mean polarization of RL modes is strongly dependent on the polarization of the pump laser. For linearly polarized pump light, the RL modes were confined to one hemisphere of the Poincaré sphere with the pump polarization in the centroid of the distribution. In contrast, under circular pump polarization, the RL modes covered the entire Poincaré sphere isotropically. This general behavior can be explained, by the dipolar nature of the dye molecules and consequently the dichroism in their absorption momenta. The study also revealed that the spread of mode polarizations under linearly polarized excitation could be significantly narrowed if the mobility of the dye molecules was reduced. Using a highly viscous solvent (e.g., Glycerol) and linear pump polarization, all RL modes could be forced into the same polarization state. A polarimetric coupling of RL modes was detected in these Glycerol samples, which is still under investigation. In conclusion it was shown, that the properties of the amplification medium have a dominant influence on dye-based random lasers and can be used to manipulate the polarization of RL modes.

8622-15, Session 4

Engineering for near-IR biphotonic applications (*Invited Paper*)

Chantal Andraud, Ecole Normale Supérieure de Lyon (France)

Over the past decade, laser sources in the near infrared spectral range (NIR, 1100 -1660 nm) have become widely used in optical telecommunications and laser range finders, which has stimulated the design of new chromophores for NIR two-photon absorption (TPA) based applications, as telecommunication and optical power limiting (OPL) devices.

Since 2005, numerous dyes, e.g. dipolar or quadrupolar polyenes,

**Conference 8622:
Organic Photonic Materials and Devices XV**

?-conjugated oligomers, singlet diradical molecules, cyanine, squaraine, poly(porphyrins), bodipy, among others have been developed, and very large TPA cross-sections have been achieved.

In this presentation, we describe photophysical properties in the NIR spectral range of chromophores belonging to the general family of "cyanine dyes", and present different approaches to tune these features: we show that absorption properties of heptamethine cation are dramatically correlated to the nature of the associated counterion, while photophysical properties of aza-boron-dipyromethene dyes are moved to the NIR thanks to peripheral substitutions. The TPA efficiency of these systems is interpreted in relation with the origin of the generated transition.

Finally, we present TPA related OPL properties of these "cyanine dyes" in relation with excited state absorption, which is shown to be a key phenomenon for the optimization of the OPL process at telecommunication wavelength.

8622-16, Session 4

Water-soluble conjugated polymers for fluorescence biosensors and two-photon biological imaging (*Invited Paper*)

Han Young Woo, Ji-Eun Jeong, Pusan National Univ. (Korea, Republic of)

We demonstrate highly sensitive and selective potassium ion detection against excess sodium ions in water, by modulating the interaction between the G-quadruplex-forming molecular beacon aptamer (MBA) and cationic conjugated polyelectrolyte (CPE). The K⁺-specific aptamer sequence in MBA is used as the molecular recognition element and the high binding specificity of MBA for potassium ions offers selectivity against a range of metal ions. The detection limit of the K⁺ assays is determined to be ~ 1.5 nM in the presence of 100 mM Na⁺ ions, which is ~3 orders of magnitude lower than those reported previously. The successful detection of 5'-adenosine triphosphate (ATP) with the MBA containing an ATP-specific aptamer sequence is also demonstrated using the same sensor scheme. We also report self-assembled polymeric nanovesicles containing cationic a two-photon fluorophore, 1,4-bis[4'-(N,N-bis(6'-trimethylammoniumhexyl)amino)styryl]benzene tetrabromide (C1). The encapsulation of C1 inside the nanovesicles enhances ~ 2-fold the fluorescence quantum yield (?) and two-photon action cross section (?d, ?d is two-photon absorption cross section), and allows internalization into the cells, as revealed by the bright two-photon microscopy (TPM) images of human cervical epithelioid carcinoma (HeLa) cells labeled with the nanovesicles. Moreover, nanovesicles containing a chemotherapeutic drug and a neutral molecule can also be prepared. Furthermore, the C1/vesicular complex is disassembled under acidic conditions, highlighting its potential as a pH-responsive smart nanocarrier for the intracellular drug delivery. These results suggest a new possibility of using nanovesicles as efficient two-photon probes for TPM imaging and possibly as nanocarriers for intracellular drug delivery.

8622-17, Session 4

Two-photon absorption of hydrocarbons at visible wavelengths

Kenji Kamada, National Institute of Advanced Industrial Science and Technology (Japan)

In the last decade a large number of organic compounds have been explored to find efficient two-photon absorption chromophores and to establish the structure-property relationship. Most of them have been studied mainly at NIR wavelength because the NIR two-photon excitation is easily achieved by a Ti:S laser and meets the requirements for the applications for bio-imaging, photodynamic therapy, and optical limiting in telecommunication wavelengths. However, in other applications such as 3D-microfabrication and 3D-optical storage, resolution of the spatial selective excitation is one of the key points and thus excitation with

shorter wavelength is preferable due to the small diffraction limit. Reports on the two-photon absorption properties of organic compounds at visible wavelengths are relatively few, especially for the blue-green wavelengths. It has been thought that there is a trade off between intense two-photon absorption and short wavelength because large π -conjugation system enables a long-distance movement of π -electrons with a small detuning energy from the bathochromic shift of the system. This trade off may work for the lowest-energy two-photon absorption; however, by using two-photon transition to higher excited states, this limitation will be able to overcome.

In this paper, we report the two-photon absorption properties of some organic compounds at visible wavelengths, up to 400 nm. The measurements were performed with the femtosecond open-aperture Z-scan methods. A series of hydrocarbons, phenylethynyl-substituted benzenes, shows moderate (several hundreds GM) or very large (~20000 GM) two-photon absorption cross sections, suggesting such a hydrocarbons can be efficient two-photon absorption chromophores in the wavelength region.

8622-18, Session 4

Modified p-phenylene vinylene platinum (II) acetylides with enhanced two-photon absorption: solution vs solid host

Aleksander K. Rebane, Montana State Univ. (United States); Galyna G. Dubinina, Randy Price, Kirk S. Schanze, Univ. of Florida (United States); Yuriy Stepanenko, Pawel Wnuk, Institute of Physical Chemistry (Poland); Geoffrey Wicks, Mikhail Drobijev, Montana State Univ. (United States)

Organometallic complexes comprising platinum (II) acetylide core linked with different π -conjugated chromophores are promising materials for applications requiring strong nonlinear-optical response. In the dual-mode optical power limiting, the chromophore first undergoes ultrafast two-photon absorption (2PA) in singlet manifold, followed by efficient intersystem crossing (ISC) and subsequent T-T absorption. While the heavy atom facilitates efficient T-T absorption, achieving sufficiently high intrinsic 2PA cross-section value has remained an issue. Here we present a series of linear- and cross-conjugated p-phenylene vinylene platinum (II) acetylides (TPV1-Ph, TP01-TPV2, crossTPV1, crossTPV3) with extended n -conjugated chains and discuss their linear- and nonlinear photophysical properties, including comparison to the properties of the constituting ligand chromophores. Remarkably high femtosecond 2PA cross-section values (up to 104 GM) were obtained for several of the new complexes by both nonlinear transmission (NLT) and two-photon excited fluorescence (2PEF) method. The large 2PA values, especially in crossTPV1 and crossTPV3, span broad range of wavelengths, 570 – 810 nm, which overlaps with maximum wavelength of strong T-T excited state absorption measured by nanosecond transient absorption method. This combination of properties is rendering these compounds efficient dual-mode nonlinear absorbers in the visible to near-IR. Comparison between direct (NLT) and indirect (2PAF) measurement of the 2PA that allows us to elucidate the structure-property relationships both in the solutions as well as in solid samples where the chromophores are incorporated into a polymer host.

8622-19, Session 5

Theory-guided nano-engineering of organic electro-optic materials for hybrid silicon photonic, plasmonic, and metamaterial devices (*Keynote Presentation*)

Larry R. Dalton, Univ. of Washington (United States)

Control of lattice dimensionality is used to enhance electro-optic activity in electrically-poled organic materials [1]. Lattice dimensionality and chromophore acentric order are controlled by incorporating spatially-

**Conference 8622:
Organic Photonic Materials and Devices XV**

anisotropic intermolecular electrostatic interactions at various positions on chromophores exhibiting large molecular first hyperpolarizability or by utilizing polarized laser radiation to introduce a 2-dimensional lattice surrounding the chromophores. Lattice dimensionality is defined experimentally from the ratio of acentric (odd) to centric (even) order parameters with the centric (even) parameters determined by variable angle spectroscopic ellipsometry (VASE) or variable angle polarization referenced absorption spectroscopy (VAPRAS) [2]. Lattice dimensionality is varied from 3-D to nearly 1-D by control of the strength of the anisotropic interactions and the position of the interactions. Steric effects defined by the shape of the core chromophore also are important. The incorporated spatially-anisotropic interactions also influence viscoelasticity behavior including the temperatures of phase transitions to lattices of reduced dimensionality and the material glass transition temperature. Viscoelastic properties are important for materials processing and they define poling conditions. Viscoelastic properties are experimentally defined by shear modulation force microscopy (SM-FM), intrinsic friction analysis (IFA), and dielectric relaxation spectroscopy (DRS), which permit definition of thermodynamic properties associated with intermolecular interactions and the length scale of molecular cooperativity [3]. Optimum poling efficiency and electro-optic activity are observed to correspond to the temperature of maximum entropy reduction defined by IFA. Molecular cooperativity is observed to vary from little more than a nanometer to nearly a micron with increasing strength of incorporated intermolecular interactions. The improvement of electro-optic activity and poling efficiency is particularly important for integrating organic electro-optic materials into silicon photonics, plasmonics, and metamaterial architectures. Recent progress in hybrid electro-optic technology is discussed.

[1] Larry R. Dalton, Stephanie J. Benight, Lewis E. Johnson, Daniel B. Knorr, Jr., Ilya Kosilkov, Bruce E. Eichinger, Bruce H. Robinson, Alex K.-Y. Jen, and Rene M. Overney, "Systematic nanoengineering of soft matter organic electro-optic materials," *Chem. Mater.*, vol. 23, p. 430-445, 2011.

[2] Benjamin C. Olbricht, Philip A. Sullivan, Peter C. Dennis, Jeffrey T. Hurst, Lewis E. Johnson, Stephanie J. Benight, Joshua A. Davies, Antao Chen, Bruce E. Eichinger, Philip J. Reid, Larry R. Dalton, and Bruce H. Robinson, "Measuring order in contract-poled organic electrooptic materials with variable-angle polarization-referenced absorption spectroscopy (VAPRAS)," *J. Phys. Chem. B*, vol. 115, p. 231-241, 2011.

[3] S. J. Benight, D. B. Knorr, Jr., L. E. Johnson, P. A. Sullivan, D. Lao, J. Sun, L. S. Kocherlakota, A. Elangovan, B. H. Robinson, R. M. Overney, and L. R. Dalton, "Nano-Engineering Lattice Dimensionality for a Soft Matter Organic Functional Material," *Adv. Mater.*, vol. 24 (24), p. 3263-3268, 2012.

8622-20, Session 5

**Plastic solar cells with engineered interfaces
(Keynote Presentation)**

Tobin J. Marks, Northwestern Univ. (United States)

The ability to fabricate molecularly tailored interfaces with nanoscale precision can selectively modulate charge transport and molecular assembly at hard matter-soft matter interfaces, and facilitate transport of the "correct charges" while blocking transport of the "incorrect charges." This interfacial tailoring can also control carrier-trapping defect densities at interfaces and stabilize them with respect to physical/thermal decohesion. In this lecture, challenges and opportunities are illustrated for three specific and related areas of research: 1) controlling charge transport across hard matter-soft matter interfaces in electroluminescent devices, 2) controlling charge transport across hard matter-soft matter interfaces in organic photovoltaic cells, 3) controlling charge transport by active layer organization at electrodes. It will be seen that rational interface engineering along with improved bulk-heterojunction polymer structures affords high solar power conversion efficiencies along with greater cell durability.

8622-21, Session 6

Biotronics: recent progress (Keynote Presentation)

James G. Grote, Air Force Research Lab. (United States)

No Abstract Available.

8622-22, Session 6

Multimodal dyes: toward correlative two-photon and electron microscopy (Invited Paper)

Frederic Bolze, Hussein Ftouni, Nicoud Jean-François, Univ. de Strasbourg (France); Leoni Piero, Univ. di Pisa (Italy); Yannick Schwab, Institut de Genetique et Biologie Moleculaire et Cellulaire (France); Jean-Luc Rehspringer, Mafouana Rodrigues Roland, Institut de Physique et Chimie des Matériaux de Strasbourg (France)

Nowadays, many crucial biological questions involve the observation of biological samples at different scales. Thus, optical microscopy can be associated to magnetic nuclear imaging allowing access to data from the cellular to the organ level, or can be associated to electron microscopy to reach the sub cellular level. Our team has worked for 10 years in molecular engineering of two-photon dyes for biological imaging. Using our experience in this field, we shifted to the design of multimodal dyes for correlative imaging with two-photon excited microscopy associated to another imaging modality such as magnetic resonance imaging and electron microscopy. We will describe here new bimodal probes, which can be used as dye in two-photon excited microscopy and contrast agent in scanning and transmission electron microscopy.

First we will described new dyes with small molecular organic systems grafted on metal atoms or clusters (Pt, Au) leading to hybrid organic-inorganic systems. Such systems show good two-photon induced fluorescence and two-photon images of HeLa cells will be presented.

Secondly, we will present new organic fluorescent dyes based on a diketopyrrolopyrrole core, and grafted on iron oxide-silica core shell nanoparticles by peptide bond. Such systems present high two-photon absorption cross sections and good fluorescence quantum yields. These nanoparticles are rapidly internalized in HeLa cells and high quality two-photon images were performed with low laser power.

In conclusion we will present our recent results on correlative light-electron microscopy were two-photon and electron microscopy (both scanning and transmission) images were obtained on the same biological sample.

8622-23, Session 6

All-optical method of sensing the components of the internal local electric field in proteins

Mikhail Drobizhev, J. Nathan Scott, Patrik Callis, Aleksander Rebane, Montana State Univ. (United States)

Knowledge of the local electric fields inside proteins can shed light on different biological problems, including functioning of ionic channels, color vision, and molecular mechanics of enzymes. Here we develop a new method based on the measurements of the one-photon absorption (1PA) and two-photon absorption (2PA) properties of a fluorescent probe that allows quantitative determination of the two projections of the local electric field E on the x - and y - axes of the probe molecular frame. Our method is based on the measurement of one-photon absorption frequency and change of the permanent electric dipole moment upon excitation, d . While the first can be obtained from 1PA spectrum, the

**Conference 8622:
Organic Photonic Materials and Devices XV**

second requires measurements of the 2PA spectrum and cross section, as well as the 2PA polarization ratio in the region of the first electronic 0-0 transition. Several molecular parameters of the fluorophore in vacuum should also be calculated with quantum-mechanical methods. This information is then introduced in the system of two equations: one describing the quadratic Stark shift as a dot product of d and E and another – the absolute value of d squared as a sum of the corresponding projections squared (Pythagorean Theorem). The solution of this system (intersection of two conical sections) provides the components of the field E_x and E_y . We use mCherry fluorescent protein as an example to demonstrate the applicability of the method. We believe that this method implemented in multiphoton microscopes will allow probing electric fields not only in protein solutions, but in living cells.

8622-24, Session 6

Multiscale analysis of THG microscopy from organized media

Emmanuel Beaufrepaire, Maxwell Zimmerley, Pierre Mahou, Delphine Débarre, Marie-Claire Schanne-Klein, Ecole Polytechnique (France)

Nonlinear optical microscopy is a biocompatible avenue for probing ordered molecular assemblies in biological tissues. As in polarized linear microscopy, the nonlinear optical response from ordered systems shows a polarization dependence which can be used to identify and characterize local molecular ordering.

In particular, third-harmonic generation (THG) microscopy is a nonlinear optical modality sensitive to the electronic nonlinear susceptibility $\chi^{(3)}$ of a material. THG microscopy can be used to map $\chi^{(3)}$ spatial variations (i.e. material interfaces), and to probe birefringence, an effect typically encountered in organized media such as the eye cornea[1]. In principle, polarization-dependent THG (P-THG) can therefore be used to probe ordered molecular arrays. However, the orientation, distribution, and nonlinear optical properties of the molecules near the beam focus all affect the experimentally observed far-field intensity. It is therefore imperative to develop a systematic theoretical method which decouples these effects and permits the extraction of orientational information from P-THG images.

We present a multiscale model spanning the molecular (nm) and ensemble (μm) scales for predicting the P-THG signal. We first calculate the electronic hyperpolarizability of a molecule from its structure. From there, we determine the anisotropic $\chi^{(3)}$ for various distributions of the molecule in the array. Using these values, we then perform numerical calculations of the microscope P-THG signal and derive accurate relations between the measured response and orientation parameters.

Finally, we present P-THG images of model systems and biological tissues which corroborate the theoretical results.

[1] Olivier, Opt Express 18(5), 5028-40 (2010).

8622-25, Session 6

Space-charge-limited current in DNA-surfactant complex

I-Ching Chen, Ting-Yu Lin, Yu-Chueh Hung, National Tsing Hua Univ. (Taiwan)

In recent years, deoxyribonucleic acid (DNA) biopolymers have attracted much research attention and been considered as a promising material when being employed in many optoelectronic devices. Since performance of many DNA biopolymer-based devices relies on carrier transport, it is crucial to study the carrier mobility of these DNA-surfactant complexes for practical implement. In this work, we present hole mobility characterization of cetyltrimethylammonium (CTMA)-modified DNA biopolymer by using space-charge-limited current (SCLC) method. Devices were fabricated using a sandwich structure with a buffer layer of MoO_3 to enhance hole injection and achieve ohmic contact

between the anode and the DNA layer. Current-voltage (I-V) curves of the devices were analyzed. A trap-free SCLC behavior can ultimately be achieved and a quadratic dependence in I-V curve was observed. With increasing electric field, a positive field-dependent mobility was demonstrated. The correlation between mobility and temperature was also investigated and a positive relation was found. The characterization results can be further utilized for DNA-based device design and applications.

8622-26, Session 7

Functionalization and linear as well nonlinear optical properties characterization of DNA biopolymer based complexes (Invited Paper)

Ileana Rau, Ana-Maria Manea, Roxana Zgarian, Alexandrina Tane, Aurelia Meghea, Francois Kajzar, Polytechnical Univ. of Bucharest (Romania)

Functionalization of deoxyribonucleic acid (DNA) with different surfactants as well as with photoresponsive molecules will be described and discussed. The DNA-surfactant complexes exhibit better physico-chemical properties as the biopolymer alone. Moreover, depending on the surfactant used, the DNA-surfactant complex can be soluble in a large number of solvents, facilitating its functionalization with nonlinear optical (NLO) chromophores. The linear optical and NLO properties of obtained compounds will be reviewed and discussed

8622-27, Session 7

Inspirations for EO polymer design gained from modeling of chromophore poling by Langevin dynamics (Invited Paper)

Martins A. Rutkis, Andrejs Jurgis, Univ. of Latvia (Latvia)

One of the possibilities to create organic molecular material for NLO applications are polymers with dispersed NLO active chromophores. These molecules must be acentrically ordered by applying an external electric poling field. The NLO efficiency depends on dipole moment, molecular hyperpolarizabilities, concentration of the chromophores and external poling field strength. Calculating, from first principles, the extent of the alignment and via this NLO efficiency has proven to be challenging. One approach to solve this problem is pure analytic statistical mechanics treatment, what could be enhanced by Monte Carlo (MC) statistical mechanical modelling. The chromophore molecules usually have been treated as point dipoles embedded in some kind of realistic molecular shape – prolate spheroid. Another possibility is fully atomistic molecular modelling with classical force field MD methods. This method allows obtain extent of alignment and observing kinetics of poling and relaxation. Unfortunately, in case when host and chromophores are represented at atomistic level, MD approach requires huge amount of computations. One of the solutions is to reproduce the motion of the molecules of interest (chromophores) using Langevin dynamics (LD). This method simulates the effect of molecular collisions and the resulting dissipation of energy that occur in real host, without explicitly including host molecules. In this contribution chromophore load, dipole moment and poling field impact on extent of alignment and poling / relaxation dynamics of model system obtained by LD simulations will be presented. On a basis of these results we would like to come forward with some inspirations for EO polymer design.

8622-28, Session 7

Electro-optic polymer waveguides made by successive coating of cross-linkable EO polymers

Akira Otomo, Isao Aoki, Toshiaki Yamada, Kohei Ota, Rieko Ueda, Toshifumi Terui, Shin-ichiro Inoue, National Institute of Information and Communications Technology (Japan)

There has been growing interest in organic and polymeric electro-optic (EO) materials due to their large EO response and modulation bandwidth. Recent development of EO chromophore produces a significantly large EO coefficient in a poled polymer form, which is higher than 100 pm/V at the telecommunication wavelength. However, the EO polymers in a waveguide form do not show EO activity as large as those in a single layer film. This is due to the mismatch in resistivity between an EO core layer polymer and clad layer materials in a waveguide structure. The clad layer need to have both optical transparency and low resistivity simultaneously because EO polymers show relatively low resistivity which is on the order of 10^7 ohm-m. In addition to that, a clad material and an EO polymer should be resistive in over coating each other. UV curable polymers are often used as a clad material however their resistivity is a few orders larger than the EO polymer. We have synthesized cross-linkable EO polymers which are soluble in common solvents for spin coating but are resistive to them after appropriate heat treatment. These polymers enable us to fabricate multilayer structures such as a waveguide by spin coating one after another. Large enough contrast of refractive index for waveguides can be made by varying chromophore concentration of the EO polymers with similar resistivity. We will discuss EO properties of the waveguides whose core and clad layers are both made by cross-linked EO polymers.

8622-29, Session 7

All-polymer organic EO material modulator for high frequency low drive voltage applications

David L. K. Eng, Stephen T. Kozacik, Benjamin C. Olbricht, Shouyuan Shi, Dennis W. Prather, Univ. of Delaware (United States)

As EO phase modulators become more prevalent components in optical and RF applications, the demand increases for high bandwidth and low drive voltage modulators that can easily be homogeneously integrated. The proposed paper will discuss a device architecture for a phase modulator based on a recently developed organic EO material (OEOM), IKD-1-50 integrated into a PMMA polymer host, using a low-index, photo-curable epoxide resin as the cladding layers all on a Si platform. Designs for both TE and TM waveguide and electrode configurations will be presented from theory and modeling, through fabrication to characterization. The EO material serving as the core of the waveguide is poled using a poling stage and monitoring apparatus with the electrode structures already in place for modulation. Poling procedures have been optimized for this material based on experimentation in simple slab-capacitor characterization devices, and produce in-device r_{33} values that agree with attenuated total internal reflection measurements. The challenges presented by the instability of OEOMs in common processing conditions have been addressed and a very simple fabrication process has been developed using standard photolithography to define an inverted ridge waveguide structure, pattern surrounding electrodes, and prepare usable end facets, without damaging the EO material. Waveguide loss figures and phase modulation characterization results for fabricated and poled devices have been quantified and will be presented. The simplicity of this device architecture on a Si handle allows for integration into various photonic applications. Designs for implementation in antenna array designs and high frequency operation will be discussed.

8622-30, Session 7

Solution phase-assisted reorientation of chromophores

Benjamin C. Olbricht, Stephen T. Kozacik, David L. K. Eng, Dennis W. Prather, Univ. of Delaware (United States)

Organic EO materials, sometimes called EO polymers, offer a variety of very promising properties that have improved at remarkable rates over the last decade, and will continue to improve. However, these materials rely on a "poling" process to afford EO activity, which is commonly cited as the bottleneck for the widespread implementation of organic EO material-containing devices. The Solution Phase-Assisted Reorientation of Chromophores (SPARC) is a process that utilizes the mobility of chromophores in the solution phase to afford acentric molecular order during deposition. The electric field can be generated by a corona discharge in a carefully-controlled gas environment. The absence of a poling director during conventional spin deposition forms centric pairs of chromophores which may compromise the efficacy of thermal poling. Direct spectroscopic evidence of linear dichroism in modern organic EO materials has estimated the poling-induced order of the chromophores to be 10-15% of its theoretical maximum, offering the potential for a many-fold enhancement in EO activity if poling is improved. SPARC is designed to overcome these limitations and also to allow the poling of polymeric hosts with temporal thermal (alignment) stabilities greater than the decomposition temperature of the guest chromophore. In this report evidence supporting the theory motivating the SPARC process and the resulting EO activities will be presented. Additionally, the results of trials towards a device demonstration of the SPARC process will be discussed.

8622-48, Session 7

Transparent electroactive polymer gratings for color and intensity modulation

Xu Yang, Haijin Shin, Thiruvellu Bhuvana, Byeongwan Kim, Eunyoung Kim, Yonsei Univ. (Korea, Republic of)

Recently, the fabrication of polymer nanostructures has attracted considerable attention because of the potential applications in solar cells, light-emitting diodes, electrochromic devices, photodiodes, transistors, and biosensors. Through micromolding in capillaries method (MIMIC), nanostructures of the solution-processable electroactive polymers could be efficiently obtained at low temperature.

In this report, a simple electrochromic (EC) device based on transparent electroactive polymer gratings (EPG) was fabricated. The EC electrode was prepared by the MIMIC process, using yellow color electrochromic polymer and non-color-changing redox polymer. The optics required for EPGs were simpler since they were adjusted to show only zeroth-order diffraction. The refractive index of the electroactive polymer were changed by applying different applied potential. Under the illumination of a white light, various diffraction colors were generated by changing the angle of incidence. On the other hand, at a given angle of incidence, the diffracted color was reversibly modulated by applying electrical potential to control the electrochemical status. In addition, the memory effect of EPGs was also demonstrated by measuring the color and intensity after power was turned off.

8622-31, Session 8

Third-generation organic light-emitting diodes (Keynote Presentation)

Chihaya Adachi, Kyushu Univ. (Japan)

Although typical organic molecules are simply composed of carbon (C), hydrogen (H), nitrogen (N) and oxygen (O) atoms, carbon's unique bonding manners based on sp^3 , sp^2 and sp hybrid orbitals enable very complicated molecular architectures, leading to amazing functions

**Conference 8622:
Organic Photonic Materials and Devices XV**

in a wide variety of creatures and industrial products. In the last two decades, the allure of unlimited freedom of design with organic molecules has shifted a significant part of the research effort on electronics from inorganic into organic materials. In particular, great progress has been achieved in the development of organic light-emitting diodes (OLEDs). The successive progress of 1st generation OLEDs using fluorescent molecules and 2nd generation OLEDs using phosphorescent molecules solidified organic materials as a very attractive system for practical electronics.

In this study, we designed new advanced electroluminescent (EL) molecules composed of only conventional CHN atoms without any precious metals. With proper molecular design, the energy gap between the two excited states, i.e., singlet (S1) and triplet (T1) excited states, are minimized, promoting very efficient spin up-conversion from T1 to S1 states (reverse intersystem crossing (ISC)) while maintaining a rather high radiative decay rate of $>10^6$ /s, leading to a very high fluorescence efficiency. Using these unique molecules, we realized a very high external EL efficiency that is comparable with those of high-efficiency phosphorescence-based OLEDs. Thus, these molecules harvest both singlet and triplet excitons for light emission under electrical excitation through fluorescence decay channels.

8622-32, Session 8

Fabrication of high efficient organic/CdSe quantum dots hybrid OLEDs by spin-coating method

Ashraf Uddin, The Univ. of New South Wales (Australia)

The CdSe quantum dots (QDs) have promising applications in display technology since its luminescence wavelength can be tuned precisely from blue to red by changing the diameter of the core from 2.0 to 7.0 nm. A single self-assembled monolayer of QDs, sandwiched between two organic thin films is necessary to isolate the luminescence processes from charge conduction. The use of QDs for device technology, one of the fundamental issues is how to distribute QDs uniformly on patterned surfaces with precise control of density. In this study, we demonstrate that uniform distribution of QDs with controllable density can be achieved using the conventional spin-coating method. We have fabricated high efficient QD-OLED by spin-coating method. The estimated QDs threshold concentration was found $\sim 9 \times 10^{11}$ cm⁻² for the best performance of QD-OLED. We have investigated the effect of CdSe/ZnS QDs concentration on the electrical and optical properties of QD-OLED. The AFM morphological studies of the hybrid device showed the formation of a disordered QD film as a result of the aggregation of CdSe/ZnS QDs upon phase segregation. The analysis of electroluminescence (EL) and photoluminescence (PL) performance of OLED showed that precise control of the QD concentration is necessary to maximize the coverage of QDs on organic surface which is an important factor in color tuning. The peak energies of the EL and PL showed only small spectral shifts and no significant dependence on the QD-concentration. The QD emission was increased about three times by annealing of QD-OLED.

8622-33, Session 8

Electroluminescence enhancement of polymer light-emitting diodes by volume grating in active layer

Kang Li, Yongkang Gong, Jungang Huang, Juan Martinez, Nigel Copner, Univ. of Glamorgan (United Kingdom); Gene Koch, Lomox, Ltd. (United Kingdom); Antony Davies, Univ. of Glamorgan (United Kingdom); Tao Duan, Yishan Wang, Wei Zhao, Xi'an Institute of Optics and Precision Mechanics (China)

The biggest loss in standard polymer light emitting diodes (PLED) or organic light emitting diodes (OLEDs, small molecule) is absorption of in-plane emissions. In this paper, a detailed experimental and numerical

study of the volume grating effect in active layer on the emission efficiency of PLED is performed. One-dimensional gratings are achieved in liquid-crystalline conjugated polymer, poly(9,9-dioctylfluorene-co-benzothiadiazole) (F8BT) by means of UV laser lithography. A green-emitting liquid crystal (LC) polymer, F8BT, was chosen because it is relatively stable in air and its physical properties have been studied in detail. PLED device structure includes a quartz substrate coated with a 150 nm thick indium-tin-oxide (ITO) layer as the anode, two layers spin coated of 50 nm thick PEDOT:PSS as the hole-transporting material and 80 nm thick F8BT, and vacuum deposited 50 nm thick silver layer as the cathode. A grating structure with period of 220 nm is chosen in F8BT, which enables the control of light propagation in the direction of the grating refractive index alternation. Such volume gratings made in the PLED emitting peak region enhance the vertical light emission to the PLED Sandwich plan structure. Also, difference period of gratings are studied to control the plasmon polariton (SPP) peaks close to the emitting peak. Average 80% enhancement of electroluminescence based on the grating in active layer is achieved between 500 nm to 600 nm with 100 degree viewing angle. The electroluminescence enhancement in relation with grating period and depth is studied to couple out of the waveguide mode by FDTD method and optical waveguide theory.

8622-34, Session 8

High-performance AC electroluminescence from colloidal quantum dot hybrids

Cheolmin Park, Sung Hwan Cho, Yonsei Univ. (Korea, Republic of)

Electroluminescent (EL) devices based on solution-processed printable materials that include fluorescent polymers and, more recently, colloidal semi-conducting quantum dots (QDs) are quite attractive for a variety of emerging mobile applications due to their low production costs and potential for fabrication into flexible, large area, lightweight devices. Tremendous effort has been focused toward the design of emitting⁶ and various functional interlayer, synthetic materials, device architecture, and layering processes including various printing technologies to enhance the performance of such EL devices, progressing them closer to commercial usage.

In addition to conventional EL device architecture in which EL from either the polymer or QDs is in principle achieved by holes and electrons injected from their own ohmic electrodes followed by formation of excitons in the emissive layer that recombine radiatively, new EL devices with different mechanisms for emission have been proposed based on alternating current (AC) electric fields. Although light emission from AC excitation of both fluorescent polymer and colloidal QD films deposited on or inserted between insulators has been reported, these studies have mainly focused on understanding the principles of emission and device performance has remained far from actual implementation. Similar to well established inorganic electroluminescent devices, solution-processible devices are also mechanistically understood as being either solid-state cathode luminescence (SSCL), in which EL is achieved by impact excitation of the emitting layer by bombardment of hot electrons accelerated through an inorganic oxide layer, or field-induced luminescence in which bipolar charges injected from electrodes in an AC field form excitons followed by recombination in the emissive layer.

To enhance brightness and to reduce the driving power of AC EL devices arising from low intrinsic density and mobility of charge carriers of the emitters as well as the high contact resistance between the electrode and emissive material, we have recently employed individually networked single wall carbon nanotubes (SWNTs) dispersed in a fluorescent polymer layer. This nanocomposite resulted in significantly enhanced brightness at several tens of operating volts due to facilitated injection of both holes and electrons into the ambipolar carbon nanotubes from an electrode and subsequent transfer of the carriers to the fluorescent polymer. Great challenge, however, still remains of fine control of emitting color by mixing as well as tuning which is, we believe, one of the most important issues for further development of solution-processible AC driven EL devices. The challenge could be addressed by an organic/inorganic hybrid nanocomposite of two emissive materials, a fluorescent polymer and colloidal QDs, with different emitting energies. Strong

**Conference 8622:
Organic Photonic Materials and Devices XV**

phase-segregation of colloidal QDs embedded in a fluorescent polymer could allow facile color tuning and mixing as a function of the relative composition of the two materials with controlled fluorescence resonant energy transfer (FRET).

Here, we report a robust and efficient route for both color mixing and tuning of field induced EL based on solution-processed colloidal QDs and their hybrids with fluorescent polymers. A novel field-induced EL device was demonstrated containing a thin organic/inorganic hybrid nanocomposite film of colloidal CdSe-ZnS core-shell type QDs blended in a light emitting polymer matrix together with homogeneous incorporation of a small amount of SWNTs which facilitated carrier injection from the electrode and transfer to the emissive layer under the influence of an AC electric field. Cooperative emission of the two light emitting materials due to unique phase segregated microstructure resulted in extremely bright AC EL of approximately 620 cd/m² at an applied voltage and AC frequency of 755 V and 300 kHz, respectively. Furthermore, the hybrid AC EL device (hereafter denoted as HACHEL) which featured an emissive layer composed of a blue poly(9,9-di-n-octylfluorenyl-2,7-diyl) (PFO) polymer and orange QDs exhibited effective color mixing, giving rise to high performance white HACHEL. Our simple device platform afforded facile preparation of the hybrid nanocomposite film by spin coating and enabled fabrication of a reliable AC EL device also capable of color tuning by control of the blend composition.

8622-35, Session 8

Microcavity effect of an OLED heterostructure in a vertical microcavity

Anthony Coens, Mahmoud Chakaroun, Alexis Fischer, Min Won Lee, Azzedine Boudrioua, Lab. de Physique des Lasers (France); Bernard Geffroy, CEA-IRAMIS (France)

For now more than a decade there has been many attempts for demonstrating lasing in an electrically pumped organic diode without success. In the same time, demonstrations of optically-pumped organic laser with lower and lower threshold are reported. It is expected from further progress in laser cavity design to pull the threshold (optical) excitation density down to the level of the state of the art OLED current density. Among the various laser resonators, the concept of an organic active medium embedded in low mode-volume microcavities with a high quality factor would be more favorable to the demonstration of lasing action under electrical pumping in an organic diode. Small volume microcavities can substantially modify the spatial distribution of spontaneous emission of a material placed within the cavity. In the photon mode picture, this can be considered as a reduction of the total number of allowed photonic modes for spontaneous emission. Therefore, the coupling efficiency (the ratio of the number of spontaneously emitted photons coupled to the lasing mode to the total number of spontaneously emitted photons) is increased dramatically in the small mode-volume microcavity lasers. In this work, we theoretically and experimentally investigate organic light emitting diode (OLED) microcavities with different cathode and organic layers thicknesses. The design of the cavities is chosen to realize the smallest possible cavity thickness of $\lambda/2$. The OLED heterostructure is based on a Alq₃/DCM2 guest-host system as an emitting layer whose intrinsic emission shows a peak around 600 nm. The OLED heterostructure is sandwiched between two dielectric multilayer mirrors. The experimental results show that the emission spectrum of the OLED in the microcavity is characterized by a single narrow peak centered at 606 nm with a full width at half maximum (FWHM) of 4 nm whereas the FWHM of a non-cavity OLED or the Alq₃/DCM intrinsic emission is 80 nm. The microcavity devices show also a substantial forward luminance enhancement at the resonance wavelength. The devices with different organic layer thickness were characterized by electroluminescence, reflectance, and transmission measurements and results compared with the optical model. In this article we present a joint experimental and theoretical analysis of the EL emission pattern of the microcavity OLEDs.

8622-36, Session 9

Nanoimprinted polymer solar cell (Keynote Presentation)

Wenchuang Hu, Yi Yang, Kamil Mielczarek, Anvar A. Zakhidov, The Univ. of Texas at Dallas (United States)

The performance of polymer solar cell is greatly determined by the nanoscale morphology and the molecular orientation/crystallinity in the photoactive layer. A vertically bicontinuous and interdigitized heterojunction between donor and acceptor has been considered to be one of the ideal architectures to enable both efficient exciton separation and charge transport. In recent years, nanoimprint lithography has emerged as a novel approach to realize this structure and simultaneously control the heterojunction morphology and polymer chain orientation in organic photovoltaics.

In this work, we will first demonstrate the geometric effect of patterned poly(3-hexylthiophene) (P3HT) nanostructures on chain alignment, charge transport and solar cell performance. Nanoimprint changes the initial edge-on alignment in non-imprinted P3HT thin film to a preferred vertical orientation with an organization height $h \geq 170$ nm and width $60 \text{ nm} \leq w < 210$ nm. Imprinted solar cells show an increase in efficiency with the decrease of nanostructure width and increase of height. Besides P3HT, similar work is extended to a low band gap polymer poly[2,6-(4,4-bis-(2-ethylhexyl)-4H-cyclopenta[2,1-b;3,4-b']-dithiophene)-alt-4,7-(2,1,3-benzothiadiazole)] (PCPDTBT) to study the process window of this technique. Besides active layer patterning, our recent progress on electrode patterning such as poly(3,4-ethylenedioxythiophene) poly(styrenesulfonate) (PEDOT:PSS) will be shown as well. Finally the current challenges and future tasks for nanoimprinted polymer solar cells will be previewed.

8622-37, Session 9

Broadband transparent electrode for flexible polymer solar cells

Juyoung Ham, Sungjun Kim, Gwan Ho Jung, Wanjae Dong, Jong Lam Lee, Pohang Univ. of Science and Technology (Korea, Republic of)

Flexible organic solar cells have strong potential for ease of processing, light-weight portability and a competitive price. Although their potentials have been investigated over the past decade, these efficiencies are yet to be translated to the flexible devices due to the use of brittle electrode. Indium tin oxide is incompatible with processing on flexible plastic substrates owing to high annealing temperature and poor flexibility. Furthermore, low transparency in the short wavelength region can be another drawback because new polymer solar cells developed to better harvest the solar spectrum. Recently, dielectric/metal/dielectric structure of transparent electrode is developed in both organic light-emitting diodes and organic solar cells for alternative ITO. In spite of their competitive price and suitability for large scale fabrication, the DMD have shown a high peak transmission at specific wavelength, but it suffers from a reduced transmission at narrow band width. Also, there is no attempt to enlarge the band width by optimizing both the inner-dielectric and outer-dielectric layers have been conducted in designing a broadband transparent electrodes for opto-electronic devices. Hereby, we suggest that design rules for broadband transparent DMD electrode. Inner dielectric layer with high workfunction overcomes the limitation of low charge extraction efficiency from organic materials to metal. Outer dielectric layer with refractive index ($n = 2.1$) used to obtain the broader spectra. The optimized structure of Ag layer embedded in two dielectrics of Ta₂O₅ and WO₃ could be satisfied zero reflection condition and showed high optical transmittance up to 91% in overall visible range.

**Conference 8622:
Organic Photonic Materials and Devices XV**

8622-38, Session 9

Plasmonic nanoparticle inclusions into polymer photovoltaic films

Christopher E. Tabor, Air Force Research Lab. (United States); Chun-Wan Yen, National Academy of Sciences (United States); Robert C. Wadams, Rutgers The State Univ. of New Jersey (United States); Laura Fabris, Rutgers, The State Univ. of New Jersey (United States); Michael F. Durstock, Air Force Research Lab. (United States)

We demonstrate the inclusion of metallic nanoparticles of systematically varying aspect ratios and optical resonances into organic bulk heterojunction films and the subsequent effect of these particles on device performance. A variety of capping ligands are explored to accomplish a homogenous particles/BHJ composite film. The optical and device performance effects of the particles will be discussed.

8622-62, Session 9

Multilayer hybrid thin film encapsulation for organic electronics

Rakhi Grover, Indian Institute of Technology Delhi (India); Ritu Srivastava, National Physical Lab. (India); Modeeparampil N. Kamalasanan, National Physical Lab. (United Kingdom); Dalip Singh Mehta, Indian Institute of Technology Delhi (India)

Extreme sensitivity of Organic optoelectronic devices towards water vapour and oxygen is the primary cause of their degradation and therefore limiting factor for their commercialization. Thin film Encapsulation (TFE) is an emerging technology especially for flexible and transparent Organic Light emitting diodes (OLEDs). The present work is focussed on an easy to grow, transparent and effective TFE for OLEDs with alternate multilayer structure composed of two organic materials with entirely different morphological properties. TPD (N, N'-diphenyl-N, N'-bis-3-methylphenyl (1, 1'-biphenyl)) is well known to have a very low glass transition temperature. Thin films of TPD are readily crystallized as soon as the thicker films are deposited which is remarkable as the material tends to form crystals resulting in different permeation pathways along the grain boundaries. Another organic film from the TPD family with a Spiro structure exhibits a high glass transition temperature thus imparting very high thermal stability to the material. Thin films of Spiro Meo-TPD are relatively dense and amorphous. These thin films act as planarization layers. Three stacks of alternate films of amorphous and crystalline materials created a complicated path resulting in very long effective diffusion pathways for oxygen and water vapours, increasing the barrier performance. The alternate stacks of these layers are further protected by a barrier coating of MgF₂ (Magnesium Fluoride) which is in direct contact with the ambient atmosphere. Note that a neat MgF₂ layer acts as substantial barrier coating. However, neither a neat MgF₂ layer nor the simple organic alternate multilayer structure can reach the high quality barrier characteristics. Calcium Optical Tests and lifetime tests of OLEDs were carried out. A dramatic reduction in water and oxygen permeation rate and hence a remarkable enhancement in lifetime of OLEDs was obtained by employing this multilayered hybrid geometry.

8622-40, Session 10

Low bandgap polymers for organic thin film transistors and solar cells (*Invited Paper*)

Kwang-Sup Lee, Yun Hyuk Koh, Deepak Chandran, Yi-Seul Han, Sun-Young Nam, Tae-Dong Kim, Hannam Univ. (Korea, Republic of)

'Plastic electronics' has attracted worldwide attention due to their low cost of production and processing. Organic π -conjugated polymers

and small molecules constitute these flexible materials of high interest. They can act as active materials for organic photovoltaic (OPV) cells, organic thin film transistors (OTFTs), light emitting diodes (LEDs), etc. One of the most important properties of these materials influencing their efficiency in thin films devices is the degree of their supramolecular ordering. It controls the fundamental energy transfer processes and the charge carrier pathways. A better supramolecular ordering is obtained when a π - π stacking π -conjugated moieties are used as monomers to prepare the polymer back bone. On the other hand, using electron push-pull monomers will provide an opportunity to tune their bandgaps, which controls their light harvesting properties. Our group has been pursuing to design and synthesize new low bandgap polymers by optimal combination of these properties. We have developed polymers with tuned bandgaps having benzothiadiazole (BTD), diketopyrrolopyrrole (DPP) and bezotriazole (BTZ) as acceptor molecules in combination with various donors which showed power conversion efficiencies of 1-5 % in OPVs, ambipolar behavior and high mobility values up to 1.6 cm²/Vs (p-type) in OFETs.

8622-41, Session 10

Measurement of the electron mobility by local illumination of an organic photoconductive sensor

Wouter Woestenborghs, Patrick De Visschere, Filip Beunis, Kristiaan Neyts, Univ. Gent (Belgium); Arnout Vetsuypens, Barco N.V. (Belgium)

We present a transparent photoconductive sensor consisting of an organic double layer deposited on top of two interdigitated electrodes. The concept is based on the work of John C. Ho et al.. The performance of the sensor is demonstrated with measurements of the current-voltage characteristic and of the spectral response. The shape of the current-voltage plots suggests the presence of a space-charge region.

We present a method to measure the occurrence of the space charge region, by illuminating the photoconductive sensor between the electrodes with a laser line parallel to the electrodes. The local illumination is achieved by coupling the laser line into a microscope and projecting it onto the photoconductive sample. On the sample the line has a width of 1 μ m and a length of 1 mm.

For each position of the local illumination the current through the sensor is measured, with and without laser line at 9V. Figure 1 shows the current as a function of the position of the local illumination. The plot shows that the current is increased for illumination near the cathode.

A simplified model of the photoconductive sensor shows that the electric field above the electrodes is negligible, therefore the current increase for illumination above the cathode is due to diffusion. We will present a way to calculate the electron mobility from the local illumination experiment.

With this contribution we present a method to measure a space-charge region in a photosensitive organic device. From the measurement we show how to calculate the electron mobility.

8622-42, Session 10

Enhanced efficiency in biopolymer nanocomposite light-emitting devices

Yi-Wen Chiu, I-Ching Chen, Yu-Chueh Hung, National Tsing Hua Univ. (Taiwan)

Deoxyribonucleic acid (DNA) biopolymers have shown promise to be utilized in optoelectronic devices owing to several unique features of DNA molecules. In this study, we present the fabrication of DNA-Au nanoparticles (Au NPs) nanocomposite and incorporate it in organic light-emitting devices (OLEDs). DNA biopolymer attributes to a high lowest unoccupied molecular orbital (LUMO) level for electron blocking, whereas Au NPs are the hole traps to retard hole injection. We evaluate the performance of DNA-Au NPs nanocomposite OLEDs comprised of

**Conference 8622:
Organic Photonic Materials and Devices XV**

different concentrations of Au NPs. The results indicate that the utilization of DNA-Au NPs nanocomposite gives rise to higher luminance and higher current efficiency compared to the DNA-based device without Au NPs.

8622-43, Session 10

Effect of inserting hole injection layer 2,3,5,6-tetrafluoro-7,7,8,8-tetracyanoquinodimethane on the life time of organic light-emitting device

Arunandan Kumar, Priyanka Tyagi, Ritu Srivastava, M.N. Kamalsanan, National Physical Lab. (India); Suneet Tuli, Indian Institute of Technology Delhi (India)

In this work, the effect of inserting hole injection layer 2,3,5,6-Tetrafluoro-7,7,8,8-tetracyanoquinodimethane (F4-TCNQ) at ITO/ hole transport layer has been studied on the life time of the organic light emitting device (OLED) by measuring the luminescence and the pixel temperature. Pixel temperature has been measured using an infrared camera. The thickness of F4-TCNQ layer has been varied and the pixel temperature has been measured at different point of times. The results have been compared with the reference device without F4-TCNQ layer. The operating voltage has decreased with the insertion of F4-TCNQ layer. Joule heating inside the device has also been found to be reduced with the insertion of F4-TCNQ layer. It has been observed that with the insertion of 1 nm thick F4-TCNQ layer, the pixel suffers a faster decay and have reduced life time in comparison to the reference device. The rate of joule heating has been found to be increased with time. Further increase in thickness of F4-TCNQ leads to improved lifetime and improved performance of OLEDs in comparison to reference device. These results have been supported by the optical micrograph, which clearly shows the faster degradation of device with the insertion of 1 nm F4-TCNQ layer. The diffusion of F4-TCNQ into other layers with the application of field has been suggested to be the reason for faster degradation.

8622-44, Session 10

Anode and donor engineering of heterojunction small molecule organic solar cell with 4.52% power efficiency

Yung-Chih Cheng, Mau-Kuo Wei, National Dong Hwa Univ. (Taiwan); Chi-Feng Lin, National United Univ. (Taiwan); Tien-Lung Chiu, Yuan Ze Univ. (Taiwan); Shun-Wei Liu, Ming Chi Univ. of Technology (Taiwan); Chin-Ti Chen, Academia Sinica (Taiwan); Jiun-Haw Lee, National Taiwan Univ. (Taiwan)

In this manuscript, an organic solar cell (OSC) with 4.52% in power efficiency based on small molecule organic material and heterojunction structure was demonstrated. Device structure of the OSC is: ITO/4,4',4"-tris-(N-carbazolyl)-triphenylamine (TCTA) (0 or 3 nm)/ boron subphthalocyanine chloride (SubPc) (15 nm)/C60 (55 nm)/ bathocuproine (BCP) (10 nm)/ Al (100 nm). Due to the large energy difference between the highest occupied molecular orbital (HOMO) of subPC (5.6 eV) and lowest unoccupied molecular orbital (LUMO) of C60 (4.5 eV), an OSC with high open circuit voltage (Voc) is theoretical possible. However, to extract the carriers out of the device, the HOMO level should be matched to the workfunction of the ITO. Here, by choosing suitable ITO substrate and plasma treatment, ITO with the workfunction of 5.6 eV was achieved. A thin (3 nm) TCTA layer is further inserted between ITO and subPC to prevent the exciton diffusing from subPC into ITO and hence increase the short circuit current to 6.92 mA/cm². The criteria of the exciton blocking layer include suitable HOMO value (close to workfunction of ITO and HOMO of subPC), and wide bandgap (larger than subPC). However, the insertion of TCTA also results in the increase of serial resistance and hence lower fill factor.

8622-45, Session 11

Janus tectons: a versatile platform for decoupling self-assembled chromophores from metallic substrates (Invited Paper)

André-Jean Attias, David Bléger, Antoine Colas, Amina Bakma, Fabrice Mathevet, David Kreher, Univ. Pierre et Marie Curie (France); Fabrice Charra, Amandine Bocheux, Commissariat à l'Énergie Atomique (France)

In view of the demanding forthcoming applications in nanotechnology, it is of prime interest to create functions out-off the plane and fully exploit the room above the substrate. Accessing the third dimension is so a mandatory step for nanooptics/electronics. Previously we introduced the Janus-like 3D tecton concept. It consists of a dual-functionalized unit presenting two faces linked by a rigid spacer: one face (A) is designed for steering 2D self-assembly, the other one (B) is a functional molecule. The objective is to take advantage of the in-plane self assembling of building blocks lying on face A to control the positioning of out-off plane active unit B, linked to the base by a rigid pillar. Here we present a series of Janus tectons incorporating chromophores ranging from fluorescent dyes to photoswitchable molecules. We will present the optical properties in solution as well as the properties of the self-assembled functional monolayers on HOPG investigated by STM.

8622-46, Session 11

Nanostructured materials and their optical features

Natalie V. Kamanina, S.I. Vavilov State Optical Institute (Russian Federation)

No Abstract Available

8622-47, Session 11

Organic polymer-metal nanocomposites for opto-electronic sensing of chemicals in agriculture

Sergey S. Sarkisov Sr., SSS Optical Technologies, LLC (United States); Michael Czarick III, Brian D. Fairchild, The Univ. of Georgia (United States); Yi Liang, Univ. of Arkansas (United States); Tatiana V. Kukhtareva, Michael J. Curley, Alabama A&M Univ. (United States)

Recent research findings led the team to conclude that a long lasting and inexpensive colorimetric sensor for monitoring ammonia emission from manure in confined animal feeding operations could eventually become feasible. The sensor uses robust method of opto-electronic spectroscopic measurement of the reversible change of the color of a sensitive nano-composite reagent film in response to ammonia. The film is made of a metal (gold, platinum, or palladium) nano-colloid in a polymer matrix with an ammonia-sensitive indicator dye additive. The response of the indicator dye (increase of the optical absorption in the region 550 to 650 nm) is enhanced by the nano-particles (~10 nm in size) in two ways: (a) concentration of the optical field near the nano-particle due to the plasmon resonance; and (b) catalytic acceleration of the chemical reaction of deprotonization of the indicator dye in the presence of ammonia and water vapor. This enhancement helps to make a miniature and rugged sensing element without compromising its sensitivity of less than 1 ppm for the range 0 to 100 ppm. The sensor underwent field tests in commercial broiler farms in Georgia, Alabama, and Arkansas and was compared against a commercial photoacoustic gas analyzer. The sensor output correlated well with the data from the photoacoustic analyzer (correlation coefficient not less than 0.9 and the

**Conference 8622:
Organic Photonic Materials and Devices XV**

linear regression slope after calibration close to 1.0) for several weeks of continuous operation. The sources of errors were analyzed and the conclusions on the necessary improvements and the potential use of the proposed device were made.

8622-49, Session 11

Optical data storage using fluorescence-modulation of silver nanoparticle polymer films

Cory W. Christenson, Case Western Reserve Univ. (United States)

New approaches to optical data storage are needed to maintain pace with the ever-increasing information generated by multimedia, security, and data archival markets. The reflection-based media used in commercial technologies greatly limit the number of writable layers, and only a few of the organic 3D materials proposed in the literature produce a nonlinear response with compact CW laser sources. Such a response is necessary to reduce the destructive read-out and ensure low cross-talk during writing of many layers. To this end, Ag nanoparticles and dye-functionalized Ag nanoparticles have been explored, which exhibit high photostability and have a surface plasmon resonance near the Blu-Ray wavelength of 405 nm. In one technique, the nanoparticles in a polystyrene host are heated using a CW laser, leading to the formation of fluorescent radicals in the film. The process itself exhibits a threshold dependence and the absorption is unchanged under heating to 200°C, allowing large area films to be made by methods such as extrusion. Patterned fluorescent regions have been written in a few layers of a monolithic film as a demonstration. We have also functionalized nanoparticles with a dye/polymer brush. The interaction of the plasmon with the dye will alter the fluorescence, and the photo-induced heating of the nanoparticle suggests a number of possible writing mechanisms such as thermal bleaching and brush diffusion. A combination of materials engineering and scalable film fabrication by co-extrusion could lead to orders-of-magnitude improvement in storage capacity.

8622-9, Session PWed

Wavelength tunable transparent flexible electrodes

Sungjun Kim, Pohang Univ. of Science and Technology (Korea, Republic of); Kihyon Hong, Pohang Univ. of Science and Technology (Korea, Republic of) and Univ. of Minnesota (United States); Juyoung Ham, Bonhyeong Koo, Ilhwan Lee, Kisoo Kim, Jong-Lam Lee, Pohang Univ. of Science and Technology (Korea, Republic of)

Controlling the wavelength of electrodes with desirable region is important in most optoelectronic devices for enhancing their efficiencies. Several flexible transparent electrodes with tunable optical transmittance have been reported. The carbon nanotubes could have wide color variance from 400 to 800 nm by control of diameter of the tubes, but showed low transmittance (~70%) and high sheet resistance (>1,000 Ω/sq). Metal nanostructure with the sub-wavelength nanostructures showed also the optical tunability from 480 nm to 680 nm by control of the diameter, but it showed low transmittance of 50~60%, high cost process. Therefore, it is necessary to develop the wavelength tunable transparent electrodes for flexible optical devices with good optoelectrical performance and simple processability.

Hereby, we demonstrated wavelength controlled flexible transparent electrode by control of refractive index of dielectrics in metal-dielectric multilayer. Through controlling the refractive indices of dielectrics between metal and substrate (wavelength matching layer, WML) from 1.9 to 2.5, the peak wavelength of electrodes could be tuned from 470 nm to 610 nm by adjusting the optical phase thickness of whole electrode, and it showed high transmittance (>85%). In the case of electrodes with tungsten oxide (n=1.9) showed high transmittance (90.5 %) at 460 nm

and low sheet resistance (11.08 Ω/sq), comparable with those of indium tin oxide (86.4 %, 12 Ω/sq). Replacing ITO by WAW to blue OLEDs (λ=460 nm), a high optical transmittance and low sheet resistance were achieved, leading to the enhancement of luminance of devices from 7020 to 7200 cd/m² at 222 mA/cm².

8622-50, Session PWed

Effect of metal ions and pH gradation on PS-b-P2VP lamellar film

Youngbin Baek, DongMyung Shin, Hongik Univ. (Korea, Republic of)

Tunable reflect color characteristics of the devices using photonic gel film were studied. Poly(styrene-b-2-vinyl pyridine) (PS-b-P2VP) lamellar film which has hydrophobic block-hydrophilic block copolymer of 52 kg/mol -b- 57 kg/mol were prepared for photonic gel films. The lamellar structure was 1 dimension photonic crystal. That photonic gel films were swollen by various solutions. Typical swelling solutions are deionized water and alcohols. The reflect color was changed by swelling water which contained a few of metal ions. Likewise, hydrogen ion concentration change was shown similar changing. The photonic gel film which has Ca²⁺ ions was max-reflectance wavelength shifted 653 nm to 451 nm (at DI water condition, maximum concentration of ions). And the photonic gel film which has Cu²⁺ ions was reflectance max-wavelength shifted 653 nm to 516 nm. The more decreased hydrogen ion concentration of swelling solution, the more shifted to short wavelength (789 nm to 593 nm). We can control color of photonic device by changing the condition of swelling solution.

8622-51, Session PWed

Monolithic quasi-solid-state dye-sensitized solar cells based on graphene modified mesoscopic carbon counter electrodes

Yaoguang Rong, Xiong Li, Guanghui Liu, Heng Wang, Zhiliang Ku, Mi Xu, Linfeng Liu, Min Hu, Ying Yang, Hongwei Han, Huazhong Univ. of Science and Technology (China)

We have developed a monolithic quasi-solid-state dye-sensitized solar cell (DSSC) based on graphene modified mesoscopic carbon counter electrode (GC-CE), which offers a promising prospect for commercial applications. Based on the design of a triple layer structure, the TiO₂ working electrode layer, ZrO₂ spacer layer and carbon counter electrode (CE) layer are constructed on a single conducting glass substrate by screen-printing. The quasi-solid-state polymer gel electrolyte employs a polymer composite as the gelator and could effectively infiltrate into the porous layers. Fabricated with normal carbon counter electrode (NC-CE) containing graphite and carbon black, the device shows a power conversion efficiency (PCE) of 5.09% with the fill factor (FF) of 0.63 at 100 mW cm⁻² AM1.5 illumination. When the NC-CE is modified with graphene sheets, the PCE and FF could be enhanced to 6.27% and 0.71, respectively. This improvement indicates excellent conductivity and high catalytic activity of the graphene sheets, which have been considered as a promising platinum-free electrode material for DSSCs.

8622-52, Session PWed

Thermal glass-forming nonlinear optical and holographic properties of “push-pull” type azochromophores with triphenyl moieties containing isophorene and pyranilidene fragments

Elmars Zarins, Riga Technical Univ. (Latvia); Andrejs Tokmakovs,

**Conference 8622:
Organic Photonic Materials and Devices XV**

Zane Kalnina, Univ. of Latvia (Latvia); Valdis Kokars, Riga Technical Univ. (Latvia); Martins Rutkis, Univ. of Latvia (Latvia); Andris Ozols, Peteris Augustovs, Kristine Lazdovica, Valdis Kampars, Riga Technical Univ. (Latvia)

Low molecular mass organic compounds with incorporated triphenyl groups, as well as with electron donating and electron acceptor fragments in their molecules show potential for creating cheap and simple solution processable materials with nonlinear optical properties. Additional insertion of azobenzene fragment in their structures makes them also possible to form holographic volume and surface relief gratings (SRG) after exposure to laser radiation, which could be useful for holographic data storage.

For these purposes polymers are generally used. However their repeated synthesis is complicated and challenging task as in every attempt to obtain the same polymer it will have different physical properties. On the other hand, the synthetic procedure of molecular glasses is more accurate as their physical properties are more defined. Unfortunately, there is still no clear relation between compound structures and physical properties.

In this report we present ten molecular glassy organic compounds with three different fragments as main backbones of the molecules: indene-1,3-dione, isophorene and pyranilidene. Our findings on their structural relation with thermal, glass-forming, nonlinear optical and holographic properties will be discussed.

8622-53, Session PWed

Nonlinear optical studies of Zn Phthalocyanine in the presence of high-energy materials

Soma Venugopal Rao, P. T. Anusha, Univ. of Hyderabad (India); Lingamallu Giribabu, Indian Institute of Commerce and Trade (India); Surya P. Tewari, Univ. of Hyderabad (India)

Most of the high energy materials (HEMs) consist of nitro groups which are highly capable for accepting electrons and are known to act as fluorescence quenchers. This property can be exploited to detect HEMs in liquid phase, solid phase, and vapor phase. The use of conjugate organic compounds, as fluorophore, has proven to be an efficient way to detect such nitro-aromatics¹. The phenomenon of quenching also provides valuable context for understanding the role of excited state lifetimes in allowing fluorescence measurements to detect dynamic processes in solutions or in macromolecules. In this paper, we present the modification in nonlinear optical properties of Zn Phthalocyanine upon the addition of HEM's like RDX, HMX, TNT etc using the picosecond Z-scan technique. These materials can alter the excited state dynamics of the system and the modified molecules are also studied using degenerate and non-degenerate pump probe techniques.

References

1. M. S. Meaney, V. L. McGuffin, "Luminescence-based methods for sensing and detection of explosives" *Anal. Bioanal. Chem.* 2008, 391, 2557-2576.
2. A. Narayanan, O. P. Varnavski, T. M. Swager, T. Goodson III, "Multiphoton Fluorescence Quenching of Conjugated Polymers for TNT Detection" *J. Phys. Chem. C* 2008, 112(4), 881-884.

8622-54, Session PWed

Printing method for organic lighting-emitting device (OLED) lighting

Hyun Chul Ki, Seon Hoon Kim, Doo Gun Kim, Tae-Un Kim, Korea Photonics Technology Institute (Korea, Republic of); Sang Gi Kim, Linkline Inc. (Korea, Republic of); Kyung Jin Hong, Gwangju Univ. (Korea, Republic of); Soon-Yeol So, Mokpo National Univ. (Korea,

Republic of)

Organic Light Emitting Device (OLED) has a characteristic to change the electric energy into the light when the electric field is applied to the organic material. OLED is currently employed as a light source for the lighting tools because research has extensively progressed in the improvement of luminance, efficiency, and life time. OLED is widely used in the plate display device because of a simple manufacture process and high emitting efficiency. But most of OLED lighting projects were used the vacuum evaporator (thermal evaporator) with low molecular. Although printing method has lower efficiency and life time of OLED than vacuum evaporator method, projects of printing OLED actively are progressed because was possible to combine with flexible substrate and printing technology. Printing technology is ink-jet, screen printing and slot coating. This printing method allows for low cost and mass production techniques and large substrates. In this research, we have proposed screen printing for organic light-emitting devices has the dominant method of thick film deposition because of its low cost and simple processing. In this research, the fabrication of the passive matrix OLED is achieved by screen printing, using a polymer phosphorescent ink. We are measured optical and electrical characteristics of OLED.

8622-55, Session PWed

Electro-optic waveguide with conductive chromophore contained polymer cladding

Kazuhiro Yamamoto, Feng Yu, Shiyoshi Yokoyama, Kyushu Univ. (Japan); Akira Otomo, National Institute of Information and Communications Technology (Japan); Kei Yasui, Masaaki Ozawa, Nissan Chemical Industries, Ltd. (Japan)

Polymer electro-optic (EO) waveguides are key component of high performance electro-optic switches. Recently, EO chromophore and host polymer matrix are investigated to get high EO coefficient (r_{33}) and fabricate waveguide structures. To realize high r_{33} , chromophore density in host polymer matrix must be increased. However, in general, high loading density of chromophore result in increasing electrical conductivity of EO materials. It becomes a problem when chromophores are poled in waveguide structure and EO switches are worked at low frequency. In this case, EO material is sandwiched by other cladding materials but usually these materials have low conductivity compared with EO material. It means effective electric field applied to EO material and r_{33} is reduced by cladding material layers.

To improve these difficulties, we proposed new chromophore contained polymer as cladding material of EO waveguide. This polymer without chromophore show the conductivity around 10^{-10} S/m at poling temperature (around 100-140 degree) but addition of EO chromophore (6wt %) increase conductivity to 10^{-7} ~ 10^{-6} S/m. The value is comparable or above to EO materials. In addition, EO chromophore has low absorption at operating wavelength?1310,1550nm?compared with other conductive materials and cross linking of polymer enable us to improve solvent resistivity of the cladding polymer result in expand EO material and solvent selection. We present recent results of EO ridge waveguide with the chromophore contained cladding polymer.

8622-56, Session PWed

Polymer optical fiber for sensing application based on multimode interference

Jie Huang, Xinwei Lan, Hanzheng Wang, Lei Yuan, Zhan Gao, Hai Xiao, Missouri Univ. of Science and Technology (United States)

Fiber optic strain sensors have unique advantages such as high signal-to-noise ratio, light weight, small size and insensitive to ambient electromagnetic field. A series of strain sensors based on optical fibers have been reported and some of them have been commercially available. However, most of the optical fiber based strain sensors are made of fused silica, which may lead to a limited dynamic range of 4000 μ

**Conference 8622:
Organic Photonic Materials and Devices XV**

(0.4%). This will limit their applications, especially in some highly loaded engineering structures, such as bridges, buildings, pipelines, dams, offshore platforms, etc. A fiber optic strain sensor with large dynamic range was highly demanded.

Recently, polymer optical fibers (POFs) as strain-sensing substrates have been attracted much more attentions. Aside from their great optical performance inherited from silica optical fiber, their flexibility and deformability make it possible to sustain a large strain load. Meanwhile, POFs have similar advantages to the conventional silica optical fibers. Since the commercial available single mode POF holds a very high cost currently, multimode POF has increasingly gained attentions. So far, most of the existing strain sensors based on multimode POFs are based on time-domain signal analysis. This paper discusses a novel type of strain sensor which uses multimode POF with the frequency-domain signal interrogation method that has relatively high resolution. A section of POF which serves as a multimode fiber (MMF) is sandwiched in between two silica based single mode fibers (SMFs). The resulted single-mode-multimode-single-mode (SMS) structure has been successfully applied in sensing application based on multimode interference (MMI) theory.

8622-60, Session PWed

Synthesis and properties of a suite of mixed neutral and zwitterionic chromophores for second order nonlinear optics

Andrew Kay, Victoria Peddie, Industrial Research Ltd. (New Zealand); Ayele Teshome, Inge Asselberghs, Koen Clays, Katholieke Univ. Leuven (Belgium)

We report details of the synthesis and the linear and nonlinear optical properties of a series of bi- and tri-chromophores. These compounds contain mixtures of chromophores that have zwitterionic (ZWI) and neutral ground state (NGS) components covalently attached to each other. The neutral ground state moieties are based on dyes with aniline donors - such as Disperse Red 1 - while the zwitterionic components are derived from chromophores with pro-aromatic donors such as 1,4 dihydropyridinylidene. An analysis of the UV-vis and hyper-Raleigh scattering (HRS) results suggests that at the molecular level the embedded constituents should be treated as discrete elements. Consequently their linear and nonlinear optical responses are the sum of the individual subunits and the molecules do not behave as a single, dipolar entity. HRS data obtained at 800 nm shows that a compound containing two ZWI units and one NGS unit has the highest dynamic first hyperpolarizability - 2645×10^{-30} esu - and has a static first hyperpolarizability value of 1450×10^{-30} esu. While UV-vis data obtained in low polarity solvents such as dioxane suggests some aggregation between the individual chromophores does occur, further studies are required to determine how this translates to the macroscopic level - i.e. deployment of the compounds in polymers followed by electric field poling.

8622-63, Session PWed

Effect of interface modification on the injection and transport properties of spiro-TAD

Omwati Rana, Ritu Srivastava, National Physical Lab. (India); M. Zulfequar, Jamia Millia Islamia Univ. (India); Mushahid Husain, Jamia Milia Islamia Univ. (India); Modeeparampil N. Kamalasanan, National Physical Lab. (India)

The charge injection and transport properties of Indium Tin Oxide (ITO)/2,2',7,7'-tetrakis(N,N-diphenylamine)-9,9'-spirobifluorene (spiro-TAD)/Au hole only device have been studied using current density voltage (J-V) measurements. The ITO/spiro TAD interface has been found to be non ohmic. The modification of the ITO/spiro TAD interface by thin layers of F4-TCNQ modify the conduction mechanism from injection limited to bulk limited. The hole current in spiro TAD based hole only device shows RS type thermionic injection from which the barrier height has been calculated, 0.37 eV. The study state J-V characteristics of modified and unmodified interface were compared to the expected JTFSCLC and injection efficiencies were calculated which are 0.9 and 3.4×10^{-3} respectively. This indicates that the modification of the ITO by a strong electron acceptor molecule makes the contact ohmic. The J-V characteristics of the modified hole only device demonstrate the space charge limited current from which the hole mobility of spiro TAD has been calculated to be 1.8×10^{-4} cm²/V-sec which is in good agreement with the value reported from TOF measurement. The combination of the field dependent mobility with the space charge effect provides a consistent description of the hole conduction in spiro TAD films as a function of temperature and thickness. The value of mobility obtained from the present study is comparable with that reported from time of flight measurement. The F4-TCNQ modified ITO substrates were used as hole injection contacts in OLEDs and which show enhanced device current, lower operating voltages and enhanced Luminescence.

Conference 8623: Ultrafast Phenomena and Nanophotonics XVII

Sunday - Wednesday 3 –6 February 2013

Part of Proceedings of SPIE Vol. 8623 Ultrafast Phenomena and Nanophotonics XVII

8623-1, Session 1

THz Raman of hydrophiles and amphiphiles measured by the ultrafast optical Kerr effect (*Invited Paper*)

Steve Meech, Univ. of East Anglia Norwich (United Kingdom)

The effect of solutes on the dynamics of liquid water is widely studied. Here we employ the ultrafast optical Kerr effect to probe waters of solvation in the presence of a range of solutes, from small molecules and ions to proteins. The OKE method provides both picosecond dynamics and low frequency (THz) Raman spectra with high signal-to-noise, and thus permits some new insights into aqueous solvation.

8623-2, Session 1

Ultrabroadband terahertz spectroscopies of biomolecules and water (*Invited Paper*)

Klaas Wynne, David Turton, Univ. of Glasgow (United Kingdom)

We will describe the use of a range of modern spectroscopic techniques—from terahertz time-domain spectroscopy (THz-TDS) to high dynamic-range femtosecond optical Kerr-effect (OKE) spectroscopy [1]—to study the interaction of proteins, peptides, and other biomolecules with the aqueous solvent. Chemical reactivity in proteins requires fast picosecond fluctuations to reach the transition state, to dissipate energy, and (possibly) to reduce the width and height of energy barriers along the reaction coordinate. Such motions are linked with the structure and dynamics of the aqueous solvent making hydration critical to function. These dynamics take place over a huge range of timescales: from the nanosecond timescale of diffusion of water molecules in the first solvation shell of proteins, picosecond motions of amino-acid side chains, and sub-picosecond librational and phonon-like motions of water. We will show that the large range of frequencies from MHz to THz is accessible directly using OKE resulting in the Raman spectrum [2] and by using a combination of techniques including THz-TDS resulting in the dielectric spectrum. Using these techniques, we can now observe very significant differences in the spectra of proteins in aqueous solvent in the 3-30 THz range and more subtle differences at lower frequencies (10 GHz-3 THz).

1. D. A. Turton, C. Corsaro, D. F. Martin, F. Mallamace and K. Wynne, *Phys Chem Chem Phys*, 2012, 14, 8067.
2. D. A. Turton, T. Sonnleitner, A. Ortner, M. Walther, G. Hefter, K. R. Seddon, S. Stana, N. V. Plechkova, R. Buchner and K. Wynne, *Faraday Discuss.*, 2011, 154, 145-153.

8623-3, Session 2

Utilizing THz spectroscopy to characterize biological systems (*Invited Paper*)

Emma Pickwell-MacPherson, Hong Kong Univ. of Science and Technology (Hong Kong, China); Vincent P. Wallace, The Univ. of Western Australia (Australia)

Previous terahertz (THz) studies of skin cancer, breast cancer and liver cirrhosis have suggested that THz spectroscopy has the potential to help determine the extent of disease before and during surgery so as to reduce patient trauma and improve patient survival rates. It was initially thought that changes in water content of the tissue was the main cause of contrast in THz images of cancers but recent findings suggest that other factors such as structural changes may contribute more than 50%. Since proteins are key constituents to support the tissue structure, we have started to investigate protein properties in the THz region with a

view to understanding and improving image contrast. Meanwhile other groups have investigated how nanoparticles could be used to improve image contrast by causing local temperature increases in targeted cells after illumination. The THz properties of water are dependent on temperature and so if diseased areas of tissue can be manipulated to be relatively warmer or colder, THz spectroscopy will be able to detect the differences. Similarly, protein conformation is temperature dependent and the conformation also affects the THz properties. Given that biological tissues are largely composed of water and proteins, we discuss the capabilities of THz spectroscopy for probing temperature and concentration dependent properties of water and proteins.

8623-4, Session 2

Measuring phonons in protein crystals (*Invited Paper*)

Andrea G. Markelz, Gheorghe Acbas, Katherine Niessen, Rohit Singh, Deepu George, Univ. at Buffalo (United States); Edward Snell, Univ. at Buffalo (United States) and Hauptman Woodward Medical Research Institute (United States)

Large scale correlated motions in proteins have been associated with necessary conformational changes during function. The frequencies for these motions have been calculated to lie in the terahertz range and calculations have suggested that for frequencies > 0.5 THz these modes will be underdamped. A number of terahertz spectroscopic studies have been performed on proteins and while these measurements have contributed to fundamental understanding of protein dynamics such as the biological water-protein interface and the protein dynamical transition, the frequency dependent response is smooth without strong features that one could associate with specific structural modes. This smooth glass like response has been associated with the biological water and librational motions of the residue side chains. In this talk we will discuss methods to remove the homogeneous relaxational background through alignment and anisotropic response. THz anisotropy measurements of hen egg white lysozyme give sharp anisotropic features similar to the expected to the anisotropic response calculated using molecular mechanics. The anisotropic features can be associated with specific modes. We will discuss the role of contact forces in these measurements as a function of crystal space group and the possible functional relevance of the observed modes.

8623-5, Session 2

Low-frequency dynamics of proteins, amino acids, and aqueous solutions studied by terahertz time-domain spectroscopy (*Invited Paper*)

Keisuke Tominaga, Naoki Yamamoto, Haruka Iguchi, Atsuo Tamura, Kobe Univ. (Japan)

Theoretical calculations have predicted that collective motions of proteins have characteristic frequencies in the far-infrared region, or the THz region, whose timescales range from sub-picoseconds to picosecond. Since some of these modes include functionally-relevant motions such as open and close movements involving active sites, they are thought to be related to the functions, and thus important for understanding of protein function. THz-TDS has been turned out to be a powerful tool to investigate dynamics in condensed phases such as protein and DNA. Previously, by using a membrane protein, bacteriorhodopsin, we demonstrated that when the protein is hydrated onset of anharmonicity of low-frequency dynamics are observed at around 220 K. The phenomenon, usually called dynamical transition, has been nowadays known to be universally observed among proteins and polypeptides.

**Conference 8623:
Ultrafast Phenomena and Nanophotonics XVII**

However, even today little is known about how the transition is related to the protein physicochemical properties. In this work we investigated temperature and hydration dependence of low-frequency dynamics to clarify relationships between the dynamical transition and protein structures, and its functional states. For those purposes, poly-L-glutamic acid (polyE) and myosin II subfragment1 (S1) were chosen as samples for THz-TDS. We also studied low-frequency spectrum of hydration water molecules around the hydrophobic probe in an aqueous solution by using tetraalkylammonium cation as a probe. The obtained spectrum of hydration water has intensity larger than that of ice and smaller than that of bulk water. This suggests that dynamics of hydration water molecules are partially restricted compared to those of bulk water.

8623-6, Session 3

Sub-cycle multi-THz dynamics: from spin-density waves to polaritons (*Invited Paper*)

Michael Porer, Jean-Michel Menard, Univ. Konstanz (Germany) and Univ. Regensburg (Germany); Kyungwan Kim, Univ. Konstanz (Germany) and Chungbuk National Univ. (Korea, Republic of); Jure Demsar, Alexej Pashkin, Alfred Leitenstorfer, Univ. Konstanz (Germany); Rupert Huber, Univ. Regensburg (Germany) and Univ. Konstanz (Germany)

Ultrashort pulses in the terahertz (THz) spectral range allow us to study and control spin dynamics on time scales faster than a single oscillation cycle of light. In a first set of experiments, we harness an optically triggered coherent lattice vibration to induce a transient spin-density wave in BaFe₂As₂, the parent compound of pnictide superconductors. The time-dependent multi-THz response of the non-equilibrium phases shows that the ordering quasi-adiabatically follows a coherent lattice oscillation at a frequency as high as 5.5 THz. The results suggest important implications for unconventional superconductivity. In a second step, we utilize the magnetic field component of intense THz transients to directly switch on and off coherent spin waves in the antiferromagnetic nickel oxide NiO. A femtosecond optical probe traces the magnetic dynamics in the time domain and verifies that the THz field addresses spins selectively via Zeeman interaction. This concept provides a universal ultrafast handle on magnetic excitations in the electronic ground state.

8623-7, Session 3

Ultrafast mid-infrared spectroscopy of charge- and spin-ordered nickelates (*Invited Paper*)

Giacomo Coslovich, Bernhard Huber, Lawrence Berkeley National Lab. (United States); Wei-Sheng Lee, Stanford Univ. (United States); Yi-De Chuang, Yi Zhu, Lawrence Berkeley National Lab. (United States); Takao Sasagawa, Tokyo Institute of Technology (Japan); Zahid Hussain, Hans A. Bechtel, Michael C. Martin, Robert W. Schoenlein, Lawrence Berkeley National Lab. (United States); Zhi-Xun Shen, Stanford Univ. (United States); Robert A. Kaindl, Lawrence Berkeley National Lab. (United States)

The interplay of charge excitations with spin and lattice degrees of freedom in transition metal oxides leads to novel correlated phases, including high-temperature superconductivity in cuprates. In this context, nickelates represent a particularly interesting system to study charge correlations in antiferromagnetic insulators, since they share chemical and structural similarity to the cuprates yet allow access to carrier correlations without superconductivity at relevant doping levels. In particular, at low temperatures the carriers in nickelates order into static charge and spin stripes on the atomic-scale.

Ultrafast spectroscopy provides the important ability to transiently excite correlated systems into non-thermal phases, and the ensuing relaxation dynamics can provide the ability to distinguish otherwise entangled degrees-of-freedom in the time domain.

We report on the first ultrafast mid-infrared study of charge and spin-ordered nickelates. A strong photo-induced modulation of the optical conductivity is observed on sub-picosecond timescales, indicating the filling and subsequent re-establishment of the mid-infrared pseudogap in the time-domain. The fast timescale of the initial relaxation (about 600 fs) testify the electronic origin of the spectral weight transfer associated with the pseudogap formation.

Further time-resolved measurements of the Ni-O stretching phonon peak resonance show a relatively slow thermalization of the phonon population (on a timescale of about 2 ps). Measuring the ultrafast dynamics of both electronic carriers and phonons yields one of the most reliable estimation of the electron-phonon coupling constant in this material. The surprisingly small value obtained suggests a predominant role of electronic correlations in stabilizing stripe ordering in nickelates.

8623-8, Session 3

Hole Spin relaxation in Ge/SiGe quantum wells

Sangam Chatterjee, Philipps-Univ. Marburg (Germany); Giovanni Isella, Daniel Chrastina, Lab. for Epitaxial Nanostructures on Silicon and Spintronics (Italy) and Politecnico di Milano (Italy); Fabio Pezzoli, Lab. for Epitaxial Nanostructures on Silicon and Spintronics (Italy) and Univ. degli Studi di Milano-Bicocca (Italy); Niko S. Köster, Ronja Woscholski, Philipps-Univ. Marburg (Germany); Christoph Lange, Univ. Regensburg (Germany)

Accessing spin dynamics in solids is key to understanding spin-related processes and to tailoring materials for spin optoelectronics such as spin transistors, and possibly quantum computers. Polarization-resolved spectroscopy has been used in a variety of experiments to measure the circular dichroism which reveals information on the net spin orientation of charge carriers along the optical beam axis.

We take advantage of the indirect nature of Ge to isolate the hole from the electron dynamics. The electrons scatter on a 100 fs timescale from the direct valley where they are optically excited towards the L valleys. Subsequently, the hole populations can be probed virtually independently of the electron dynamics via the same direct transitions to the conduction band. We exploit this mechanism using a polarization-resolved fs-pump-white-light-probe method to determine the hole spin dynamics in a Ge/SiGe quantum well (QW) structure without magnetic bias.

Our analysis of the ultrafast spin dynamics in the QWs at high carrier densities, reveals a spin-dependent band-gap renormalization governed by hole spin exchange processes which shift hole and electron states in energy by 60 μ eV. A heavy-hole spin relaxation time of $\tau_{hh} \approx 2$ ps is determined for a lattice temperature of 10 K, longer than in bulk Ge. We find that these slow dynamics result from a reduced influence of spin mixing in strained Ge QWs, where confinement and strain lift the degeneracy of heavy and light holes.

8623-9, Session 3

Spin relaxation in spin light-emitting diodes: Effects of magnetic field and temperature

Henning Höpfner, Carola Fritsche, Arne Ludwig, Astrid Ludwig, Ruhr-Univ. Bochum (Germany); Frank Stromberg, Heiko Wende, Werner Keune, Univ. Duisburg-Essen (Germany); Dirk Reuter, Andreas D. Wieck, Nils C. Gerhardt, Martin R. Hofmann, Ruhr-Univ. Bochum (Germany)

We report experimental results on the electron spin relaxation length during vertical transport in spin light-emitting diodes (LEDs). Our

**Conference 8623:
Ultrafast Phenomena and Nanophotonics XVII**

devices are GaAs based LEDs with InAs quantum dots in the active region, an MgO tunnel barrier and an Fe/Tb multilayer spin injector with perpendicular magnetic anisotropy, i.e. remanent out-of-plane magnetization, enabling efficient electrical spin injection in magnetic remanence. Additionally, our devices can be operated at room temperature.

A series of samples with different injection path lengths allows us to experimentally determine the spin relaxation length. In combination with operation in magnetic remanence, we are able to determine the spin relaxation length without the influence of external magnetic fields and at room temperature and find it to be 27 nm. Applying an external magnetic field, we find that at 2 T magnetic field strength, this relaxation length almost doubles. This is in quantitative agreement with spin lifetime measurements in GaAs inside magnetic fields.

Temperature control of our samples allows us to measure the temperature dependence of the spin relaxation length. At 200 K, the spin relaxation length doubles to 50 nm and reaches 80 nm at 30 K, in good agreement with theoretic calculations.

Our results show that polarization values obtained with spin-LEDs inside strong magnetic fields and at low temperatures are not comparable to those in remanence and at room temperature. However, the transfer of efficient spintronic devices to such application-enabling settings is absolutely necessary and will be a major challenge considering the enormous differences in spin relaxation.

8623-10, Session 3

Electron spin relaxation dynamics in GaN: influence of temperature, doping density, and crystal orientation

Jan H. Buss, Jörg Rudolph, Sebastian Starsosielec, Arne Schaefer, Ruhr-Univ. Bochum (Germany); Fabrice Semond, Ctr. de Recherche sur l'Hétéro-Epitaxie et ses Applications (France); Daniel Hägele, Ruhr-Univ. Bochum (Germany)

Gallium nitride is not only one of the most attractive materials for optoelectronics, it also bears potential for high power electronics, and spin electronics. Here we present a systematic study of the electron spin lifetime in wurtzite GaN performed by femtosecond-Kerr-rotation spectroscopy. We find that spin lifetimes at room temperature hardly exceed 50 ps [1]. The relaxation is found to be caused by a Rashba effective magnetic field that linearly depends on the electron momentum k . Unlike in cubic semiconductors where the effective magnetic field scales with k^3 , the linear term prevents long spin lifetimes at room temperature. We further evidence an anisotropic spin relaxation tensor by magnetic field dependent measurements, highlighting the peculiarities of spin orbit coupling in wurtzite materials. The presence of a k -linear Rashba term is further corroborated by comparison of spin dynamics with cubic GaN and GaAs. The direct comparison with cubic GaN shows dramatically increased spin lifetimes. As a consequence of the k -linear term, wurtzite GaN shows compared to GaAs a weaker dependence of the spin lifetime both on temperature and doping density. We give a fully analytical description of both effects based on Dyakonov-Perel theory that describes our results quantitatively without any fitting parameter.

[1] B. Beschoten et al., Phys. Rev. B 63, 121202 (2001)

8623-11, Session 4

Tracking the non-equilibrium properties of the insulator-metal transition VO₂ (Invited Paper)

Simon Wall, ICFO - Institut de Ciències Fotòniques (Spain); Daniel Wegkamp, Laura Foglia, Julia Staehler, Martin Wolf, Fritz-Haber-Institut der Max-Planck-Gesellschaft (Germany); Kannatassen Appavoo, Richard Haglund Jr., Vanderbilt Univ. (United States)

Understanding the evolution of the structural and electronic properties of VO₂ during the ultrafast photoinduced transition from the room temperature insulating phase to the metallic conducting phase requires new ways to monitor how macroscopic properties that define the phases evolve on the ultrafast timescale.

We examine the broadband reflectivity changes during the photo-induced phase transition, which allow us to tune our probe energy to be particularly sensitive to the lattice displacements. By analysing the response of the coherent phonons we observe that the lattice potential is modified on an ultrafast timescale dictated by the pump pulse. This is inferred from the ultrafast loss in the coherent phonon spectrum that characterizes the insulating phase. In addition, by performing pump-probe measurements on the transient state of the system, we are able to observe the formation of the metallic state occurs on a different, slower, timescale to the structure change.

Our results show that the photoinduced transition follows a highly non-equilibrium pathway along which the properties that define the insulating phase are lost on a faster timescale than the properties that define the metallic state emerge.

8623-12, Session 4

Ultrafast dynamics in topological insulators (Invited Paper)

Chih Wei Luo, National Chiao Tung Univ. (Taiwan)

Ultrafast dynamics of carrier and phonon in topological insulators $Cu_xBi_2Se_{3-y}$ ($x=0, 0.1, 0.125, y=0, 1$) was studied using femtosecond pump-probe spectroscopy. Two damped oscillations were clearly observed in the transient reflectivity changes ($\Delta R/R$), which are assigned to acoustic and optical (A1g) phonons. According to the red shift of A1g phonon frequency, the Cu atoms in $Cu_xBi_2Se_3$ crystals may predominantly intercalated between pair of the quintuple layers. Moreover, the carrier dynamics in the Dirac-cone surface state is significantly different from that in bulk state. The energy loss rate of carriers in the Dirac-cone surface state was estimated to be 1 meV/ps.

8623-13, Session 4

Two-photon physics with quantum-dot biexcitons (Invited Paper)

Stefan Schumacher, Univ. Paderborn (Germany)

Excitation and de-excitation of biexcitons in semiconductor quantum-dots in a direct two-photon process offers some conceptual advantages over more commonly used cascaded single-photon absorption or emission.

In our recent work we have studied the quantum properties and statistics of photons emitted by a quantum-dot biexciton inside a cavity. In the normal biexciton-exciton cascade, fine-structure splitting between exciton levels is known to degrade polarization-entanglement for the emitted pair of photons. However, we have shown theoretically that the polarization-entanglement can be preserved in such a system through simultaneous emission of two degenerate photons into cavity modes tuned to half the biexciton energy [1].

In my presentation I will give an overview of our work in this area.

[1] S. Schumacher, J. Förstner, A. Zrenner, M. Florian, C. Gies, P. Gartner, and F. Jahnke, Optics Express 20, 5335 (2012).

8623-14, Session 4

Extraction of the light-driven charge-transfer kinetics at the semiconductor surface using pump-probe spectroscopy

Jin Suntivich, Yu-Ting Lin, Kasey Phillips, Eric Mazur, Harvard Univ. (United States)

Solar fuel, which is a type of light-harvesting technology that operates by utilizing sunlight to drive energy-fuel production, has recently received substantial attention due to its ability to form energy-carrying molecules with very high efficiency. Despite these advances, the mechanism for how the photo-excited carriers are transferred from the semiconductor to the catalyst, and then to the reactant is still not well understood. A detailed understanding of how a semiconductor surface converts photon energy to fuel can therefore help further guide the design of a more efficient photocatalytic material for energy and also environmental applications. In this contribution, we use femtosecond laser pulses to study the charge transfer kinetics between titanium dioxide surfaces and a variety of model adsorbates in a pump-probe configuration. By observing the ultrafast optical responses of the semiconductor and reactant, we monitor and postulate the charge transfer pathway to the chemical molecule. We will formulate the observed results using classical electron transfer theory and will discuss the strategy for how to further enhance charge transfer kinetics between titanium dioxide surfaces and energy-carrying molecules.

8623-15, Session 4

Dephasing in Ge/SiGe quantum wells measured by means of coherent oscillations

Kolja Kolata, Niko S. Köster, Alexej Chernikov, Michael J. Drexler, Philipps-Univ. Marburg (Germany); Eleonora Gatti, Lab. for Epitaxial Nanostructures on Silicon and Spintronics (Italy) and Univ. degli Studi di Milano-Bicocca (Italy); Stefano Cecchi, Daniel Chrastina, Giovanni Isella, Lab. for Epitaxial Nanostructures on Silicon and Spintronics (Italy) and Politecnico di Milano (Italy); Mario Guzzi, Lab. for Epitaxial Nanostructures on Silicon and Spintronics (Italy) and Univ. degli Studi di Milano-Bicocca (Italy); Sangam Chatterjee, Philipps-Univ. Marburg (Germany)

In general, all coherent effects in optically excited materials depend crucially on the dephasing of the addressed states. Therefore, knowing the duration of the coherence and understanding dephasing mechanisms are mandatory in order to interpret coherent effects correctly. Both are often summarized in the dephasing time which is used as a phenomenological damping parameter in theoretical descriptions. Ge/SiGe hetero structures as a material system are especially interesting for dephasing studies since they exhibit strong nonlinear coherent responses such as the giant dynamical Stark effect.

We present a dephasing time analysis of the excitonic resonances in Ge/SiGe quantum wells for various lattice temperatures by coherent oscillations spectroscopy (COS).

The results are compared to the linewidths of the excitonic resonances determined by linear absorption measurements. The combination of both techniques provides a distinctive characterization of the contributions from homogeneous and inhomogeneous broadening present in the samples. Exemplary, COS is applied to a series of samples with varying linewidth.

Strikingly, the lowest direct-gap transition in all analyzed samples is dominated by homogeneous broadening over the entire investigated temperature range. This is explained by the fast intrinsic dephasing mechanism of electrons scattering into the lower lying L valleys which leads to intrinsically short dephasing times of merely 300 fs as an upper limit.

8623-16, Session 5

Ultrafast nonlinearities of metallic 3D metamaterials (Invited Paper)

Jeremy J. Baumberg, Silvia Vignolini, Stefano Salvatore, Petros Farah, Ullrich Steiner, Univ. of Cambridge (United Kingdom)

The optical properties of metals have become of extreme interest recently due to the rise of the fields of plasmonics and metamaterials. Engineering metallic nanostructures at sub-wavelength scales has been shown to lead to metamaterials with novel optical properties. Realizing such three-dimensional (3D) metallic architectures for visible wavelengths has proven experimentally challenging, as it requires unit cells and features on the 10nm scale. Our recent breakthrough in fabricating reliable metamaterials on large-scales with unit cells of 50nm and below allows investigation of their modified optical nonlinearities. The nonlinear response of gold gyroid metamaterials is investigated through widely-spectrally-tuneable optical pump-probe pulses of 200fs duration and uses a novel broadband lock-in technique, employing a custom 256-pixel photodiode array switched between different charge banks. Gold gyroids are found to exhibit longer electron-phonon scattering rates as compared to bulk gold due to the dominance of surface scattering, with different spectral signatures. Their optical response based on the transient perturbation of the gold dielectric functions gives a range of new tuning mechanisms and elicits insight into the novel mechanisms governing metamaterial nonlinear optical properties.

[1] J. B. Pendry et al, Phys. Rev. Lett. 76, 4773 (1996)

[2] S. Vignolini et al, Adv. Mater. (2011)

[3] P. Farah et al, Phys. Rev. B 84, 125442 (2011)

8623-17, Session 5

Collective phenomena in photonic metamaterials (Invited Paper)

Stefan Linden, Rheinische Friedrich-Wilhelms-Univ. Bonn (Germany); Fabian B. P. Niesler, Karlsruher Institut für Technologie (Germany); Jens Förstner, Yevgen Grynko, Torsten Meier, Univ. Paderborn (Germany); Martin Wegener, Karlsruher Institut für Technologie (Germany)

Photonic metamaterials do not only possess unusual linear optical properties but are also promising candidates for artificial nonlinear optical media. The general idea is to resonantly excite plasmonic modes in the meta-atoms and to benefit from the resulting local field enhancement. Based on this idea, one could try to create an efficient nonlinear metamaterial by identifying meta-atoms which act as efficient nonlinear oscillators and then to pack these meta-atoms as densely as possible.

Here, we present experiments and numerical calculations which demonstrate that collective phenomena do not only modify the linear optical properties of a metamaterial but also influence its nonlinear optical response. We perform experiments on resonant second-harmonic generation from planar gold split-ring-resonator arrays in which we vary the lattice constant but keep the other sample parameters fixed. By doing so, we can study the influence of the electromagnetic interaction of the metaatoms on the nonlinear response. Surprisingly, we find the strongest nonlinear signals at intermediate lattice constants. This observation can be interpreted as the interplay of dilution effects and near-field changes due to interactions between the meta-atoms. Our interpretation is supported by numerical calculations based on the discontinuous Galerkin time-domain method.

**Conference 8623:
Ultrafast Phenomena and Nanophotonics XVII**

8623-18, Session 5

Enhancement of 3rd-order nonlinearities in nanoplasmonic metamaterials: figures of merit (*Invited Paper*)

Jacob B. Khurgin, Johns Hopkins Univ. (United States); Greg Sun, Univ. of Massachusetts Boston (United States)

A simple analytical theory of plasmonic enhancement of optical nonlinearities in various nanoplasmonic structures is developed. It is shown that in simple structures roughly two-to-three order enhancement of effective third order nonlinear susceptibility can be obtained, while in more complicated arrangements of plasmonic dimers and nanoantennae, enhancement can be as high as four-to-five orders of magnitude. At the same time, if one introduces a more practical figure of merit for nonlinearity, as a maximum attainable phase shift per 10dB loss, this phase shift can never exceed a few degrees, thus making photonic switching in metamaterials all but unattainable. This self-contradictory behavior is caused by a combination of inherently low values of nonlinear susceptibility and large loss in the metal. The conclusion is then that nanoplasmonic metamaterials may enhance weak nonlinearities for various sensing applications, but are rather ineffectual in photonic switching and modulation.

8623-19, Session 5

Active terahertz metamaterials (*Invited Paper*)

Nathaniel Grady, Ranjan Singh, Matthew T. Reiten, Dibakar Roy Chowdhury, Jiangfeng Zhou, Abul K. Azad, Stuart A. Trugman, Quanxi Jia, Antoinette J. Taylor, Hou-Tong Chen, Los Alamos National Lab. (United States)

Metamaterials have enabled the manipulation of electromagnetic wave propagation in unusual ways which are extremely difficult or impossible to realize using naturally occurring materials. The design flexibility and external resonance control through integration of additional active materials facilitate high performance devices with novel functions. We demonstrated a series of metamaterial resonant structures operating at terahertz frequencies. Further integration of semiconductors or complex oxides enabled active terahertz metamaterials, where the resonance strength and frequency were tuned through application of an external stimulus such as temperature, photoexcitation, or electric field. Using strontium titanate single crystal substrate we have been able to continuously tune the resonance frequency of a split-ring resonator array by varying its temperature. Semiconductors were also used as the metamaterial substrate or as part of metamaterial resonant element, in which we can switch the resonance or tuning the resonance frequency in an ultrafast fashion using femtosecond photoexcitation, or conveniently using a voltage bias. Recently we have also demonstrated photo-induced switching of chirality of meta-molecules. The unique properties in high-temperature superconductors facilitate another type of active terahertz metamaterials. When the metamaterial resonant elements are made out of superconducting films, the resonance strength and frequency can be actively tuned by temperature change or photoexcitation. These demonstrations are promising for many applications in active control and manipulation of terahertz waves, a frequency band that is still very challenging using other techniques.

8623-20, Session 5

Optimal second-harmonic generation in split-ring resonator arrays

Yevgen Grynko, Torsten Meier, Univ. Paderborn (Germany); Stefan Linden, Rheinische Friedrich-Wilhelms-Universität Bonn (Germany); Fabian B. P. Niesler, Martin Wegener, Karlsruher Institut für Technologie (Germany); Jens Förstner, Univ. Paderborn (Germany)

Previous experimental measurements and numerical simulations give evidence of strong electric and magnetic field interaction between split-ring resonators in dense arrays. This changes their linear spectra as compared to those of individual SRRs. One can expect that such interactions have also an influence on the second harmonic generation, however their role remains unclear in this case. In this work we apply the Discontinuous Galerkin Time Domain (DGTD) method to simulate the linear and nonlinear optical response from SRR arrays. DGTD has a number of advantages in comparison to other widely used numerical methods and one of them is the capability of handling complex non-linear problems. To calculate SHG emission we use a semi-classical approach and evaluate the hydrodynamic Maxwell-Vlasov model. We study near-field collective effects at different separations and mutual orientations of the constituent SRRs. The simulations show that dense placement of the constituent building blocks appears not always optimal and dipole coupling can lead to a significant suppression of the near fields at the fundamental frequency and, consequently, to the decrease of the SHG intensity.

8623-21, Session 6

Electron-hole recollisions in semiconductors (*Invited Paper*)

Mark S. Sherwin, Ben Zaks, Univ. of California, Santa Barbara (United States); RenBao Liu, The Chinese Univ. of Hong Kong (China); Hunter Banks, Univ. of California, Santa Barbara (United States)

Intense laser fields can rip electrons from an atom and slam them back into it. By using intense terahertz radiation from UC Santa Barbara's Free-Electron Lasers, we have observed an analogous phenomenon for photo-excited electrons and holes in a semiconductor. A trillion energetic electron-hole collisions per second convert a monochromatic near-infrared laser beam at 350 THz (0.8 μm) into a polychromatic near-infrared beam containing up to 11 new frequencies spaced by 1 Terahertz. Implications for the nature of optical excitations in solids and possible applications to optical communications will be discussed.

8623-22, Session 6

Terahertz semiconductor nonlinear optics (*Invited Paper*)

Dmitry Turchinovich, Max-Planck-Institut für Polymerforschung (Germany) and Technical Univ. of Denmark (Denmark)

In this presentation we describe our recent results on semiconductor nonlinear optics, investigated using single-cycle THz pulses. We demonstrate the nonlinear absorption and self-phase modulation of strong-field THz pulses in doped semiconductors, using n-GaAs as a model system. The THz nonlinearity in doped semiconductors originates from the near-instantaneous heating of free electrons in the ponderomotive potential created by electric field of the THz pulse, leading to ultrafast increase of electron effective mass by intervalley scattering. Modification of effective mass in turn leads to a decrease of plasma frequency in semiconductor and produces a substantial modification of THz-range material dielectric function, described by the Drude model. As a result, the nonlinearity of both absorption coefficient and refractive index of the semiconductor is observed. In particular we demonstrate the nonlinear THz pulse compression and broadening in n-GaAs, as well as an intriguing effect of coexisting positive and negative refractive index nonlinearity within the broad spectrum of a single-cycle THz pulse. Based on Drude analysis we demonstrate that the spectral position of zero index nonlinearity is determined by (but not equal to) the electron momentum relaxation rate. Single cycle pulses of light, irrespective of the frequency range to which they belong, inherently have an ultrabroadband spectrum covering many octaves of frequencies. Unlike the single-cycle pulses in optical domain, the THz pulses can be easily sampled with sub-cycle resolution using conventional femtosecond

**Conference 8623:
Ultrafast Phenomena and Nanophotonics XVII**

lasers. This makes the THz pulses accessible model tools for direct observation of general nonlinear optical phenomena occurring in the single-cycle regime.

8623-23, Session 6

Observation of strong and broadband terahertz induced electroabsorption in multiple quantum wells

Chia-Yeh Li, The Univ. of New Mexico (United States); Denis V. Seletskiy, The Univ. of New Mexico (United States) and Air Force Research Lab. (United States); Jeffrey G. Cederberg, Sandia National Labs. (United States); Mansoor Sheik-Bahae, The Univ. of New Mexico (United States)

We report the observation of terahertz-induced electroabsorption (EA) modulation in in multiple quantum well (MQW) structures under normal incidence. Typical samples consist of 180 pairs of 5nm wide GaAs wells, separated by 7.5nm of Al_{0.3}Ga_{0.7}As barriers. To understand the nature of the EA signal, we probe spectro-temporal response of MQW structures in transmission geometry, by detecting THz-induced modulation of a spectrally-resolved probe signal. In this geometry, both terahertz and probe polarizations are perpendicular to the quantum well growth direction. Broadband quasi-single cycle terahertz pulses are generated by two-color laser induced plasma and produce peak fields of ~1MV/cm at the focus, on the MQW. We observe strong (up to 50% modulation of the transmitted probe) and complex response of the MQW to the incident THz radiation. This response is attributed to several mechanisms, including observed qualitative agreement with the two-dimensional Franz-Keldysh signal. This conclusion required full knowledge of the broadband THz waveform, which was measured via air-breakdown coherent detection with controlled Z₂ injection. In addition, MQW exciton transitions were obtained by reciprocity, from the photoluminescence measurements. Multi-parameter studies, including variation of relative polarizations, sample orientation and composition are underway to fully understand all the responsible mechanisms of the EA signal. Finally, a simple THz imaging scheme is presented, utilizing conventional imagers and our MQW structures.

8623-24, Session 6

Envelope and field effects in the nonlinear interaction of broadband terahertz fields and optical pulses in air

Matteo Clerici, Institut National de la Recherche Scientifique (Canada) and Heriot-Watt Univ. (United Kingdom); Daniele Faccio, Heriot-Watt Univ. (United Kingdom); Lucia Caspani, Mostafa Shalaby, Mathieu Giguère, Bruno E. Schmidt, Oded Yaakobi, Institut National de la Recherche Scientifique (Canada); Marco Peccianti, Institut National de la Recherche Scientifique (Canada) and Istituto dei Sistemi Complessi (Italy); François Vidal, François Légaré, Tsuneyuki Ozaki, Roberto Morandotti, Institut National de la Recherche Scientifique (Canada)

Terahertz pulses generated by two-color filamentation in air are characterized by several tens of THz bandwidth and are an intriguing tool for broadband spectroscopy in the far-infrared. Furthermore, their strong spatial and temporal localization may allow for the onset of novel nonlinear optical effects.

A relevant question that arises is how they interact, through the third-order nonlinearity, with optical pulses at more common near-infrared wavelengths (~800 nm).

More specifically, due to the long wavelength, the terahertz pulse may be regarded to as a static field during the interaction with optical pulses, leading to an electric-field induced second-harmonic generation

(EFISH). On the other hand, the short pulse durations, down to few tens of femtoseconds, featuring the pulses generated by air ionization are typically comparable to those of an ultrafast optical field, hence a standard four-wave-mixing behavior may be expected. In this last condition the interaction is insensitive to the instantaneous terahertz electric field and a photon-number conservation law holds.

We have experimentally and numerically investigated the nonlinear interaction of broadband terahertz pulses generated by air-ionization with near-infrared optical fields with comparable duration in air. We show that the aforementioned interaction regimes coexist and can be isolated in the spectrum of the nonlinear wave-mixing product. By recording the wave-mixing spectrogram we show that, in the four-wave-mixing regime the nonlinear product is proportional to the envelope of the terahertz pulse, whereas in the EFISH regime the interaction is sensitive to the instantaneous terahertz electric field and can be exploited for terahertz electric-field detection.

8623-29, Session 7

Photophysics of colloidal graphene quantum dots (Invited Paper)

John A. McGuire, Michigan State Univ. (United States)

We present optical studies of graphene quantum dots (GQDs) with 132 and 168 sp² hybridized C atom cores. For all its potential applications, extended graphene has some limitations on account of its semimetallic nature. Colloidally synthesized graphene quantum dots (GQDs) of the order of 100 sp² hybridized C atoms display size-tunable electronic structure with HOMO-LUMO transitions in the near infrared and visible. Bottom-up synthesis also provides control over the edge structure of GQDs and has allowed us to study GQDs with fully filled electronic bands, i.e., without the partially filled edge states introduced by zigzag edges. These features make colloidal GQDs potentially useful sensitizers for photovoltaics as well as model systems for understanding the combined effects of dimensionality and quantum confinement. From both applied and fundamental perspectives it is important to understand the carrier interactions and dynamics in these systems. We have performed ultrafast (~100 fs) transient absorption and time-resolved emission measurements of GQDs in toluene solution to explore the single- and biexciton interactions and dynamics in these GQDs. We find biexciton interaction energies of the order of 100 meV as well as biexciton Auger recombination to single excitons on sub-picosecond timescales. We also observe unusual excitation-energy dependence of the ratio of singlet emission to triplet emission. We will discuss these results in the context of other sp² hybridized carbon systems and colloidal semiconductor quantum dots and their relevance for photovoltaic applications.

8623-30, Session 7

Theory of ultrafast carrier and phonon dynamics in graphene (Invited Paper)

Andreas Knorr, Torben Winzer, Ermin Malic, Technische Univ. Berlin (Germany)

Graphene is an ideal structure to study the non-equilibrium dynamics of optically generated charge carriers in a two-dimensional material: Its linear energy dispersion and the vanishing bandgap allow scattering processes, such as interband electron-phonon scattering, impact ionization and Auger recombination, typically suppressed in conventional semiconductors. Here, we present microscopic calculations of the coupled coherence and carrier/phonon occupation dynamics after coherent optical excitation for a broad frequency and time range. This allows us to study coherent generation, transient gain and orientational as well as energy relaxation of non-equilibrium charge carriers.

Applying an optical pulse, a highly anisotropic non-equilibrium carrier population is created. The efficient intraband carrier-carrier scattering leads to a redistribution of carriers to energetically lower states already within the first ten femtoseconds. Preferably, the scattering occurs along

**Conference 8623:
Ultrafast Phenomena and Nanophotonics XVII**

the Dirac cone conserving the anisotropy. In contrast, the phonon-induced relaxation processes bring carriers across the Dirac cone, which leads to an isotropic distribution already after 50 fs. Furthermore, our calculations predict a significant contribution stemming from Auger processes. The impact excitation leads to a considerable carrier multiplication - in spite of the competing phonon-induced processes. We clarify also the conditions for transient gain.

After about 100 fs the carriers are completely thermalized resulting in a spectrally broad Fermi distribution. Finally, the intra- and interband scattering via optical and acoustic phonons accounts for energy dissipation and a cooling down of the carrier system on a picosecond timescale.

In particular, the obtained results are in excellent agreement with recent experiments investigating the relaxation dynamics close to the Dirac point and in the infrared spectral range. We give a detailed comparison with experiments.

In summary, the presented theoretical study provides a clear picture of the detailed interplay of electron and phonon relaxation phenomena in graphene.

8623-31, Session 7

Interaction of single-layer CVD graphene with a metasurface of terahertz split-ring resonators

Federico Valmorra, Giacomo Scalari, Curdin Maissen, ETH Zurich (Switzerland); Wangyang Fu, Univ. of Basel (Switzerland); Christian Schoenenberger, Univ. Basel (Switzerland); Jong Won Choi, Hyung Gyu Park, Mattias Beck, Jérôme Faist, ETH Zurich (Switzerland)

The TeraHertz (THz) frequency region is subject of increasing research for both its technological and fundamental importance. Single-layer graphene, already established also as 2-dimensional electronic system, is emerging as an optoelectronic material in the THz range where its intraband absorption frequencies lay.

In such a frame, we study the interaction of single-layer graphene with THz split-ring resonators (SRR) via THz Time-Domain Spectroscopy in the frequency range 100GHz-3.5THz[1]. Large-area single-layer graphene was grown by Chemical Vapour Deposition on copper foil and transferred onto Si/SiO₂ substrate. The metasurface of THz-SRR with periodicity of 60micrometers was deposited onto the graphene and it is constituted by an array of subwavelength gold structures with resonant frequencies of 610GHz for the first LC-mode and 1.26THz for the LC-resonance in the orthogonal polarization. Room temperature measurements show that the presence of the graphene shifts the first LC-resonance of the THz-SRR towards lower energies by 6.5%, decreases the Quality-factor by 13.5% and increases the transmission by 9.8dB. Similar but weaker behaviour is observed for the second LC-resonance, due to the lower electric-field density. The gating of the graphene tends to restore the Q-factor of the resonances by decreasing the intensity of the transmitted light when moving the Fermi level towards the charge neutrality point.

Further investigations in the magnetic field are expected to show strong coupling between the cyclotron transition in the graphene and the photonic modes of the THz-metasurface[2,3].

[1] Papsimakis et al., Optics Express 18, 8353 (2010).

[2] Scalari et al., Science 335, 1323 (2012).

[3] Hagenmueller and Ciuti, arXiv:1111.3550 (2011)

8623-25, Session 8

Ultrafast plasmonics with multi-material metal-based nanoparticles (*Invited Paper*)

Natalia Del Fatti, Anna Lombardi, Paolo Maioli, Aurelien Crut, Fabrice Vallee, Univ. Claude Bernard Lyon 1 (France)

Metal-based multimaterial nanoparticles are very promising for linear and nonlinear ultrafast plasmonic applications. In this context, key aspects are the impact of confinement and material interfacing on their optical, electronic and vibrational properties. We have investigated electromagnetic coupling of silver and gold nanoparticles forming heterodimers, demonstrating a Fano resonance effect due to interaction of the silver surface plasmon resonance with the gold interband transitions in a single dimer. We'll also show that information on the mechanical coupling between the materials forming a multi-material nano-object can be obtained by investigating its vibrational modes with ultrafast spectroscopy.

8623-26, Session 8

Addressing quantum effects in tunneling plasmonics (*Invited Paper*)

Javier Aizpurua, Ruben Esteban, Centro de Fisica de Materiales (Spain); Peter Nordlander, Rice Univ. (United States); Andrei Borissov, Univ. Paris-Sud 11 (France)

Plasmonic nanostructures can be used as canonical building blocks to host and actively participate in a variety of complex physical phenomena such as in non-linear effects, in quantum tunneling or in photoemission processes, to cite a few. We will present a number of examples where a conductive contact between the two arms of a gap-antenna is used for (i) effective control of the near-field oscillations in the loaded antenna, (ii) relating transport and optical properties based on the evolution of the plasmon excitations and (iii) producing optical spectral switch based on the presence of a photoconductive material linking the gap that can sustain a fast and large free-carrier density.

As the control of sub-nanometer separation distances is technological feasible, a classical description of the metal surface, based on the assumption of an abrupt change of the electron density at the surface of the metallic material, fails to correctly describe the optical response of a gap antenna. To account for the effect of the spill-out of the electrons at the surface of the metal, full quantum mechanical calculations have been developed with use of techniques such as time-dependent density functional theory (TDDFT). We present a new method to calculate quantum effects in large plasmonic systems based on parametric inputs derived from simpler full mechanical calculations. With this quantum corrected model (QCM), we bridge a gap between classical and quantum plasmonics.

8623-27, Session 8

Photo-induced ultrafast magnetization dynamics of self-assembled bimetallic nanoparticles (*Invited Paper*)

Makoto Kuwata-Gonokami, The Univ. of Tokyo (Japan)

Strong electric field at a localized surface plasmon resonance in metal nanoparticles enhances optical processes, such as fluorescence, Raman scattering, second- or third-order harmonic generations. In this study, we investigate the effect of plasmon resonance on the ultrafast photo-induced magnetization dynamics of bimetallic nanoparticles. The ultrafast control of magnetization is crucial for advanced magneto-optics applications such as spintronics and high-capacity data storage devices. The rapid demagnetization in ferromagnetic metal by femtosecond laser pulse opened a new field of ultrafast control of magnetization

**Conference 8623:
Ultrafast Phenomena and Nanophotonics XVII**

with light. Thermal excitation of electronic system by the femtosecond laser pulses has been considered to be the prime mechanism of the demagnetization. A direct coherent coupling process between photon field and spin system has also been discussed. Although the mechanism of ultrafast demagnetization has been still strongly debated, it is natural to use the enhanced electric field at plasmon resonance to reduce the operation power for photo-induced demagnetization. Hybridization of ferromagnetic metal/noble metal nanoparticle is a promising candidate to realize it. In this study, we prepared Ag-Co hybrid nanoparticles dispersed in an epitaxial TiO₂ thin film using pulsed laser deposition, and measured the ultrafast magnetization dynamics by time-resolved Faraday effect measurement using the femtosecond pump-probe technique. We observed that Ag nanoparticles with localized surface plasmon resonance enhance light-matter coupling and carrier relaxation resulting in strong demagnetization and few-picoseconds fast recovery.

8623-28, Session 8

Purcell factor of metallic nanoantennas

Philippe Lalanne, Institut d'Optique Graduate School (France)

The spontaneous emission of a quantum emitter is a cornerstone of nano-optics, with the objective to control light absorption and emission at the nanometre scale. At the heart of the engineering lies the emitter-cavity coupling. A figure of merit for this coupling is the famous Q/V ratio introduced by Purcell in 1946. During the last decennia, the Purcell factor has been essentially used to fashion purely dielectric microcavities that confine light at the wavelength scale. Here we completely revisit the Purcell formula to encompass the important case of nanoantennas, the analogues of radio antennas at optical frequencies that have recently emerged for improving light-matter interactions by exploiting the unique properties of metallic nanostructures. We derive a self-consistent formalism capable of analytically handling the coupling between single emitters and the modes of complex nanocavities that include radiative leakage, absorption, material dispersion and multiple resonances.

8623-32, Session 9

fs-PEEM as an ideal probe for ultrafast nano-optics (Keynote Presentation)

Martin Aeschlimann, Technische Univ. Kaiserslautern (Germany)

The high sensitivity and lateral resolution of the time-resolved photoemission electron microscopy technique (TR-PEEM [1]) is used to verify simultaneous spatial and temporal control of nano-optical fields in the vicinity of metallic nanostructures and clusters. This opens a route towards space-time-resolved spectroscopy on nanometer length-scales and femtosecond time-scales [2,3]. We are able to demonstrate that the plasmonic phase coherence of localized excitations on a corrugated silver surface can persist for more than 100 fs and exhibits coherent beats. This was analyzed with a model of coupled oscillators leading to Fano-like resonances in the hybridized dark- and bright-mode response. We introduce a new spectroscopic method that determines nonlinear quantum-mechanical response functions beyond the optical diffraction limit [4]. While in established coherent two-dimensional (2D) spectroscopy a four-wave-mixing response is measured using three ingoing and one outgoing wave, in 2D nanoscopy we employ four ingoing and no outgoing waves. This allows studying a broad range of phenomena not accessible otherwise such as space-time resolved coupling, transport, and nonlocal correlations.

[1] O. Schmidt et al, Appl. Phys. B 74, 223, (2002)

[2] M. Aeschlimann et al, Nature 446, 301 (2007)

[3] M. Aeschlimann et al, PNAS 107 (12), 5329 (2010)

[4] M. Aeschlimann et al, Science 333, 1723-1726 (2011)

8623-33, Session 9

Ultrafast phonon dynamic in plasmonic supracrystal (Invited Paper)

Pierre-Adrien Mante, National Taiwan Univ. (Taiwan); Meng-Hsien Lin, Hung-Ying Chen, Shangjr Gwo, National Tsing Hua Univ. (Taiwan); Chi-Kuang Sun, National Taiwan Univ. (Taiwan)

The assembly of plasmonic materials has recently attracted much interest. Indeed, such a structure could enable the creation of a material with tailor made optical and electronic properties, or with anomalous behavior, such as negative refractive index. Numerous application could therefore be considered, such as optical trapping or waveguiding, super focusing.... To further increase the applications, modulation of the properties has to be achieved. A possible way to achieve this goal is by using acoustic waves. Acoustic waves offer numerous advantages, they can operate at high frequency (up to THz), and they can be remotely controlled.

In this presentation we will discuss the coupling between vibrations and plasmon resonances of artificial crystal made of gold nanoparticles. Thanks to a new layer-by-layer growth method [1], it is possible to fabricate three dimensional crystal-like structures made of nanoparticles with long range ordering. Due to near-field coupling between nanoparticles of the same layer and of different layers, a splitting of the plasmon resonance is observed.

We use ultrafast pump-probe spectroscopy to monitor the different vibrations of this supracrystal thanks to the coupling of phonon and plasmon. Among the detected vibrations, we show that interparticle vibrations, which are similar to optical phonon modes, are extremely sensitive to their environment. We demonstrate that by exciting these vibrations, we are able to modulate the plasmon resonances and to characterize the interparticle bonding. The observation of these vibrations could be useful for the realization of future phonon modulated photonic and plasmonic devices.

[1] M.H. Lin, H.Y. Chen and S. Gwo, J. Am. Chem. Soc. 132, 11259 (2010)

8623-34, Session 9

Nanogap-Enhanced Raman Scattering (NERS) controlled by DNA (Invited Paper)

Yung D. Suh, Korea Research Institute of Chemical Technology (Korea, Republic of)

Since smSERS (single molecule Surface-Enhanced Raman Scattering) was independently reported by S. Nie group and K. Kneipp group in 1997 [1][2], tremendous amount of interest has been shown to this field because Raman spectroscopy can provide molecular fingerprint together with multiplexing capability in bioassay. Regarding to the origin of this smSERS phenomena, so called "SERS hot spot", Nie group argued sharp edges in nanostructure, such as corners of a silver nanorod or even of a single nanoparticle, can play as a hot spot of smSERS, while Kneipp group argued they could observe smSERS signal only from colloidal aggregation in solution. Later on, Brus group and others showed that SERS hot spots, formed at the junction of two nanoparticles, likely play a major role in smSERS [3][4]. Theoretical calculations also support that SERS electromagnetic enhancement factors can approach up to ~10¹¹ when inter-particle spacing reaches down to a few nanometer or less at the junction between two nanoparticle pair. However, formation of these smSERS-active nanostructures with a nano-gap at the SERS hot-spot junction, mostly dimer or colloidal aggregation of Ag or Au nanoparticles adsorbed with Raman active molecules (e.g., Rhodamine 6G), is a random process driven by salt-induced non-specific aggregation. This fact has been a main hurdle for smSERS toward advanced applications.

Based on the idea that controlling this nano-gap between two noble metal nanoparticles is the key to realize reliable smSERS, we have designed a gold-silver nano dumbbell (GSND) and Gold Nanobridged Nanogap Particles (Au-NNP) to exhibit Nanogap-Enhanced Raman

**Conference 8623:
Ultrafast Phenomena and Nanophotonics XVII**

Scattering (NERS) controlled by DNA. As for GSND, two gold nano particles with different sizes were linked to each other by double helix DNA (30mer), with a single Raman dye molecule at the center position, to fix the two at a known gap distance (~10 nm). Then we narrowed the gap down to < 1 nm by standard silver staining method to endow the GSND with single molecule sensitivity. We have successfully detected smSERS signals, as well as typical single molecular blinking and polarization behaviors, from each GSNDs by Nano Raman spectroscopy at the single particle level [5]. As for Au-NNP, hollow spherical gap (~1 nm) between the gold core and gold shell can be precisely loaded with quantifiable amounts of Raman dyes labeled on DNA backbone which is anchored at the gold core and then covered by gold shell [6].

1. S. Nie and S.R. Emory, *Science* 275, 1102 (1997).
2. K. Kneipp, Y. Wang, H. Kneipp, L.T. Perelman, I. Itzkan, R.R. Dasari, and M.S. Feld, *Phys. Rev. Lett.* 78, 1667 (1997).
3. A.M. Michaels, M. Nirmal, and L.E. Brus, *J. Am. Chem. Soc.* 121, 9932 (1999).
4. Y.D. Suh, G.K. Schenter, L. Zhu, and H.P. Lu, *Ultramicroscopy* 97, 89 (2003).
5. D. Lim, K.-S. Jeon, H.M. Kim, J.-M. Nam, and Y.D. Suh, *Nature Materials* 9, 60 (2010)
6. D. Lim, K.-S. Jeon, J.H. Hwang, H.Y. Kim, S.H. Kwon, Y.D. Suh, and J.-M. Nam, *Nature Nanotechnology* 6, 452 (2011).

8623-35, Session 10

Solids in ultrafast and strong optical fields: new phenomena (*Invited Paper*)

Mark I. Stockman, Georgia State Univ. (United States)

This talk will consider phenomena in insulator nanofilms and bulk crystals subjected to strong and ultrafast optical fields with carrier frequency much below the bandgap. Such fields cause adiabatic phenomena such as the Wannier-Stark localization, formation of quantum bouncers at the surfaces, and anticrossings of adiabatic levels. In the dielectric nanofilms subjected to sufficiently slow fields, the anticrossings of the quantum-bouncer levels of the valence and conduction bands is predicted to lead to adiabatic metallization of the solid [M. Durach, A. Rusina, M. F. Kling, and M. I. Stockman, *Metalization of Nanofilms in Strong Adiabatic Electric Fields*, *Phys. Rev. Lett.* 105, 086803-1-4 (2010)]. In the ultrafast optical fields, a combination of the adiabatic and non-adiabatic effects leads to the increased polarizability of the system making it similar to semiconductors or plasmonic metals [M. Durach, A. Rusina, M. F. Kling, and M. I. Stockman, *Predicted Ultrafast Dynamic Metallization of Dielectric Nanofilms by Strong Single-Cycle Optical Fields*, *Phys. Rev. Lett.* 107, 0866021-5 (2011)]. We will also discuss response of a dielectric solid to near-single cycle strong optical fields, where new theoretical and experimental results have been recently obtained [A. Schiffrin, T. Paasch-Colberg, N. Karpowicz, V. Apalkov, D. Gerster, S. Mühlbrandt, M. Korbman, J. Reichert, M. Schultze, S. Holzner, J. V. Barth, R. Kienberger, R. Ernstorfer, V. S. Yakovlev, M. I. Stockman, and F. Krausz, *Optical-Field-Induced Current in Dielectrics*, *Nature* (2012, In print)].

8623-36, Session 10

Photoemission at metallic nanostructures: multiphoton and strong-field dynamics (*Invited Paper*)

Claus Ropers, Univ. Göttingen (Germany)

The photoelectric effect has been a defining problem in modern physics, marking the transition to quantum theory and introducing light quanta over a century ago. Currently, nanostructured cathodes and ultrafast laser sources are spawning new studies of photoemission from surfaces. The nanostructure enhances and confines the optical field and offers a means to further manipulate the process with tailored geometrical properties and applied voltages. At high-intensities, the photoelectric effect becomes

nonlinear, generating high-brightness electron pulses in the multiphoton and field-driven regimes. In the former case, multiple photons are needed to overcome the material's work function, which has been investigated in recent experiments with plasmonic nanotips; such photoelectron sources hold significant promise for imaging and diffraction with high spatiotemporal precision. With increasing intensity, the ponderomotive (quiver) energy grows, rapidly closing channels of low photon number and inducing above-threshold photoemission. This behavior culminates in a transition to the strong-field regime, as observed in experiments and modeled in simulations. Under these conditions, the classical optical field governs the emission and acceleration. While it is difficult to reach deeply into the strong-field regime with visible wavelengths before causing irreversible material damage, it is more readily accessed at longer wavelengths due to the ponderomotive energy scaling. In recent work, we have utilized ultrashort, mid-infrared light pulses to induce electron emission deep in the strong-field regime with acceleration up to hundreds of eV. The field confinement afforded by the nanotip generates novel dynamics in which photoelectrons escape the high-field region in less than a single half-cycle.

8623-37, Session 10

Probing ultrafast electron dynamics in condensed matter with attosecond photoemission (*Invited Paper*)

Stefan Neppel, Max-Planck-Institut für Quantenoptik (Germany); Ralph Ernstorfer, Fritz-Haber-Institut der Max-Planck-Gesellschaft (Germany); Adrian L. Cavalieri, Deutsches Elektronen-Synchrotron (Germany); Elisabeth M. Bothschafter, Max-Planck-Institut für Quantenoptik (Germany); Johannes V. Barth, Dietrich Menzel, Technische Univ. München (Germany); Ferenc Krausz, Max-Planck-Institut für Quantenoptik (Germany); Reinhard Kienberger, Peter Feulner, Technische Univ. München (Germany)

Isolated attosecond ($1 \text{ as} = 10^{-18} \text{ s}$) laser pulses in the extreme ultraviolet (XUV) spectral range [1] allow time domain access to fundamental electronic processes in atoms, molecules and solids. Applied to simple atomic systems, the combination of attosecond XUV pulses with inherently synchronized near-infrared (NIR) laser pulses has enabled the real-time observation of field-induced electron tunneling [2], of the wave packet motion of valence electrons [3], and the discovery of subtle time delays in the photoemission from single atoms [4]. Up to now, time-resolved attosecond spectroscopy of solids was demonstrated only in a single experiment on a tungsten crystal, where a time delay of only 110 as between photoelectrons emitted from the valence band and core levels has been observed [5]. Such high time resolution can be achieved with the attosecond streaking technique, where the XUV-induced one-photon photoemission is initiated by an attosecond XUV pulse and the outgoing electron wave packets are streaked by a waveform-controlled NIR laser field [6]. However, the origin of photoemission time delays, especially in the case of solids, is still highly controversial thereby complicating the interpretation of the ultrafast dynamics encoded in measured time shifts [5,7-10].

In order to shed light on the mechanisms underlying this phenomenon in condensed matter, we performed attosecond streaking experiments on different single crystals and well-defined metal-adsorbate interfaces. We demonstrate the capability of the streaking method for clocking electron emission from solids with a precision of only a few attoseconds. Our results further indicate that, at least for target materials exhibiting a nearly free-electron-like electronic band structure, the measured time delays can be interpreted intuitively as the real-time observation of photoelectrons moving through the solid prior to their escape from the surface. This holds true irrespective of the spatial localization of their initial electronic wave function - in strong disagreement with predictions from full quantum mechanical calculations [8-10]. On the other hand, streaking experiments on the more complex transition metals suggest contributions to time shifts that are beyond ballistic electron propagation.

References:

**Conference 8623:
Ultrafast Phenomena and Nanophotonics XVII**

- [1] M. Hentschl et al. Nature 414, 29 (2001). [6] R. Kienberger et al. Nature 427, 817 (2004).
 [2] M. Uiberacker et al. Nature 446, 627 (2007). [7] C. Lemell et al. PRA 79, 62901 (2009)
 [3] E. Goulielmakis et al. Nature 466, 739 (2010). [8] C.-H. Zhang et al. PRL 102, 123601 (2009).
 [4] M. Schultze et al. Science 328, 1658 (2010). [9] A.K. Kazansky et al. PRL 79, 177401 (2009).
 [5] A.L. Cavalieri et al. Nature 449, 1029 (2007). [10] C.-H. Zhang et al. PRA 84, 065403 (2011).

8623-38, Session 10

Attosecond physics at a nanotip: a new strong-field physics laboratory (*Invited Paper*)

Michael Krüger, Sebastian Thomas, Michael Förster, Lothar Maisenbacher, Max-Planck-Institut für Quantenoptik (Germany); Georg Wachter, Christoph Lemell, Joachim Burgdörfer, Technische Univ. Wien (Austria); Peter Hommelhoff, Max-Planck-Institut für Quantenoptik (Germany)

Attosecond physics is based on the control of electronic matter waves on sub-optical cycle time scales. We have demonstrated that attosecond physics phenomena can be observed at nanoscale metal tips [1, 2]. In particular, experiment and theory show that re-scattering takes place, where an atom is emitted from a tip, propagates away from the tip, only to return to it within a single optical cycle, and elastically scatters off the tip again to gain more energy in the laser field [3]. With few-cycle laser pulses at 800nm we observe time-energy interference of electronic matter wave packets. Last, we show that the tip based system represents a simple laboratory for strong-field physics: Because of the broken symmetry at the tip, only two trajectory classes exist (direct and re-scattered), which can be modeled easily. The simple model is able to describe the spectra surprisingly well [4]. We will discuss the current status of the experiment.

- [1] M. Krüger, M. Schenk, P. Hommelhoff, Nature 475, 78 (2011)
 [2] M. Krüger, M. Schenk, M. Förster, P. Hommelhoff, J. Phys. B. 45, 074006 (2012)
 [3] G. Wachter, Chr. Lemell, J. Burgdörfer, M. Schenk, M. Krüger, P. Hommelhoff, Phys. Rev. B 86, 035402 (2012)
 [4] M. Krüger, M. Schenk, P. Hommelhoff, G. Wachter, Chr. Lemell, J. Burgdörfer, to appear in New J. Physics

8623-39, Session 11

Ultrafast near-field optical control on the nanoscale: impedance matching to quantum systems with optical antennas (*Invited Paper*)

Markus B. Raschke, Univ. of Colorado at Boulder (United States)

Combining plasmonic and optical antenna concepts with ultrafast and shaped laser pulses allows for the precise control of an optical excitation on femtosecond time and nanometer length scales. I will present several new concepts extending tip-enhanced spectroscopy into the nonlinear and ultrafast regime for nano-scale imaging and spectroscopy of surface molecules and nano-solids. Examples include adiabatic nano-focusing on a tip for nano-spectroscopy, spatio-temporal superfocusing and optical control at the 10 nm-10 fs level, and the study of the optical antenna coupled ultrafast free-induction decay in near-field nano-IR spectroscopy of organic nano-structures. I will conclude with an outlook for future directions including the possibility for extreme nonlinear optics, strong light matter interaction, and radiative decay engineering.

8623-40, Session 11

Spontaneous emission control of single emitters by optical antennas (*Invited Paper*)

Kwang-Geol Lee, Hanyang Univ. (Korea, Republic of)

Spontaneous emission plays a central role in the majority of optical phenomena in our world. The rate of this emission process is determined by the radiative decay of the excited state of the emitter. It scales with the second and third powers of the dipole moment. Because optical emitters have nanometer or sub-nanometer extensions, the size of their dipole moments is restricted, giving rise to typical fluorescence lifetimes in the nanosecond regime, which is orders of magnitude longer than an optical cycle. This long lifetime and the correspondingly slow decay limit the optical power that can be extracted. It has been shown that nano-metallic antennas can boost up the fluorescence of an emitter in its near field. Here, we used spherical gold nanoparticles in several different antenna configurations. Especially, with a dimer antenna composed of two spherical gold nanoparticles sandwiching a single molecule we could shorten down the fluorescence lifetime by more than two orders of magnitude. We will discuss how detailed experimental parameters affect on the lifetime change.

8623-41, Session 11

A nanoantenna for nonlinear spectroscopy of a single nano-object (*Invited Paper*)

Markus Lippitz, Max-Planck-Institut für Festkörperforschung (Germany)

Already the linear optical response of a single nanoobject is weak. The nonlinear response is even weaker. We employ a plasmonic nanoantenna to enable nonlinear optical spectroscopy of a single nanoobject. We present antenna-enhanced transient absorption spectroscopy of mechanical breathing oscillations in Au discs and carrier dynamics in CdSe nanowires. Already a simple antenna design leads to an enhancement of the transient signal by one order of magnitude.

8623-42, Session 12

Efficient generation of record-short and record-long wavelengths based on backward and forward parametric interaction in lithium niobate (*Invited Paper*)

Yujie J. Ding, Lehigh Univ. (United States)

In our research, we have generated the shortest wavelengths from periodically-poled lithium niobate in the vicinity of 62.5 microns at the poling period of 7.1 microns. We have demonstrated large enhancements in the output powers from three gratings. We have also efficiently generated far-infrared radiation at the wavelengths centered at 20.8 microns in the vicinity of one of the polariton resonances of lithium niobate. Such an efficient nonlinear conversion is made possible by exploiting phase-matching for difference-frequency generation in lithium niobate. The highest peak power reached 233 W. These wavelengths correspond to the shortest wavelength in the terahertz region and longest wavelength in the mid-infrared/far-infrared regions from lithium niobate, respectively.

8623-43, Session 12

Passively aligned four-wave mixing apparatus for investigating high-intensity laser-matter interactions

Amanda K. Meier, Michael Greco, Colorado School of Mines (United States); Jens Thomas, Friedrich-Schiller-Univ. Jena (Germany); Jeff Squier, Charles G. Durfee, Colorado School of Mines (United States)

We demonstrate a passively stable transient grating arrangement suitable for studies of multi-photon, non-equilibrium ionization dynamics. The ± 1 diffracted orders from a transmission grating are crossed as pump beams to form an index grating that is probed by the zero order. A 4-f imaging system would produce a low intensity image of a grating without relative pulse front tilt between the pumps. To produce an interference pattern that is sufficiently intense to ionize the material, we use two custom fabricated transmission gratings in the form of a single-pass compressor that can accept both ± 1 orders and an off-axis parabola to focus the beams. Our analysis shows that when the grating separation is equal to the mirror focal length, the pulse front tilts are matched across the focal spot. Interfering the two pump beams creates a transient grating with the same groove density as the transmission beam-splitter gratings at the focus. We use a thick window to tilt the 0 order probe beam out of plane, to approach the BOXCARS geometry and to time the chirped zero order with the pumps. This arrangement allows us to distinguish between coherent mixing (BOXCARS signal) and incoherent diffraction from the index grating. By looking for high orders of diffraction from the transient grating, we aim to measure the time evolution of its shape. We have observed several types of mixing signals in a thin semiconductor sample. We acknowledge funding support from AFOSR under grants FA9550-10-1-0394 and FA9550-10-0561.

8623-44, Session 12

Laser pulse propagation in relativistically time-dependent media (*Invited Paper*)

Daniele Faccio, Heriot-Watt Univ. (United Kingdom)

There are a significant number of theoretical predictions regarding unusual quantum effects in the presence of rapidly varying boundary conditions. For example, an oscillating mirror will excite photon pairs from the vacuum state or a flowing medium with a transition from sub to super-luminal flow will emit radiation similar to Hawking emission from a black hole. However, reproducing and studying these effects experimentally is extremely challenging.

We present a generic methodology, based on fundamental light-matter interactions, that is slowly gaining ground in this area of physics and in principle allows us to study the physics of the quantum vacuum in the presence of curved space-times.

Using traditional nonlinear optical phenomena e.g. the Kerr effect, it is possible to create the required curved space-times by adequately focusing intense laser pulses to induce a travelling or oscillating refractive index perturbations within an optical medium. The interaction of a probe pulse with the resulting relativistically time-dependent medium can lead to a variety of unexpected and novel effects. Based on both numerical studies and experimental results, we will discuss effects such as negative frequency generation and amplification at time-dependent boundaries. We shall then discuss the implications of these findings in terms of fundamental studies and analogies with black hole event horizons and dynamical Casimir effects.

8623-45, Session 12

Simultaneous generation and coherent control of terahertz and XUV using two-color laser field

Aram Gragossian, The Univ. of New Mexico (United States); Denis V. Seletskiy, The Univ. of New Mexico (United States) and Air Force Research Lab. (United States); Mansoor Sheik-Bahae, The Univ. of New Mexico (United States)

We demonstrate simultaneous terahertz (THz) and high-order harmonic generation (HHG) in a gas plasma generated by orthogonally polarized two-color excitation using femtosecond pulses centered at 800 nm and its second harmonic at 400 nm. We identify the strong correlation between the XUV and THz radiation under coherent control of the relative phase between the two-color excitation fields.

In the experiment an 800nm beam (3mJ, 1kHz, 35fs) is focused onto a 200 μ m type-I BBO placed inside a vacuum chamber. An adjustable tilt of a 250 μ m fused silica plate, is used to control the relative phase between θ and 2θ beams ($\theta = 2\theta - 2\theta$). Various rare gases are injected after the focal region through a 0.5mm diameter nozzle. An off-axis parabolic mirror (OPM) with a central hole allows for simultaneous detection of both XUV and THz emissions, by reflecting the generated THz out of the vacuum chamber, while transmitting the XUV through the hole. Either a 0.2 μ m aluminum filter or a 500 μ m Si window are used to block residual pump radiation in the relevant detection arms. The spectrum of the generated XUV emission is analyzed using a grazing-incidence spectrometer, while THz radiation is coherently detected using electro-optic sampling in a ZnTe crystal.

A definite correlation between HHG and THz is observed when θ is varied within the 2π range. The starting point for both phenomena is the tunneling ionization. HHG, however, relies on return trajectories of the liberated electrons while –in the most accepted model, a directional macroscopic current ensuing the ionization is responsible for THz generation. Further investigation into this correlation is underway regarding various experimental parameters. These experiments will allow for the more fundamental understanding of the generation processes of XUV and THz radiation using coherently controlled hybrid fields.

8623-46, Session 12

Accessing new types of photocurrents using polarization-shaped excitation pulses

Shekhar Priyadarshi, Klaus Pierz, Mark Bieler, Physikalisch-Technische Bundesanstalt (Germany)

The excitation of exciton resonances in semiconductors with certain polarization-shaped optical pulses reveals the existence of new photocurrents. For resonant excitation of excitons with an optical pulse whose linear polarization is slowly rotating versus time we observe an antisymmetric shift current (ASC) linked to a second-order nonlinear tensor that is antisymmetric in its last two indices. Moreover, for detuned excitation of excitons with elliptically polarized optical pulses whose major axis slowly decreases in time and becomes minor axis we observe an additional symmetric shift current (SSC). Both of these currents vanish for continuous-wave excitation and, thus, differ from previously known SSC.

Experiments are performed on light-hole exciton transitions in (110)-oriented GaAs quantum wells being excited by an orthogonally polarized pulse pair with a variable phase delay (τ) between the two pulses. The shift currents, which result from a spatial shift of the electron charge during excitation, are detected with a standard free-space THz setup. Measuring the THz amplitude versus τ yields THz interferograms, which are even (odd) functions of τ for currents with symmetric (antisymmetric) tensor elements and, thus, provide a tool to distinguish between such currents. A simple Bloch-equations model shows that the ASC occurs for a phase mismatch between orthogonal transition dipole moments. Moreover, analysis of the phase of the THz

**Conference 8623:
Ultrafast Phenomena and Nanophotonics XVII**

interferogram proves the existence of the additional SSC, which arises from the nonlinear frequency dynamics of the coherent polarization induced by detuned excitation of excitons.

8623-47, Session 12

Sub-diffraction quantum interference control of electrical currents in nanodevices

Markus Betz, Sebastian Thunich, Claudia Ruppert, Technische Univ. Dortmund (Germany); Alexander W. Holleitner, Walter Schottky Institut (Germany)

Coherent control utilizing phase-related femtosecond pulse pairs induces currents in bulk semiconductors. Recently, we have extended the concept to single nanostructures. Here we focus on the optoelectronic response of antennas on GaAs. They resonantly enhance current injection and thereby permit deep sub-wavelength control of currents on femtosecond timescales.

8623-48, Session 12

The competing dynamics in an ultimate fast all-optically switched microcavity

Emre Yüce, Georgios Ctistis, MESA+ Institute for Nanotechnology (Netherlands); Julien Claudon, Emmanuel Dupuy, Commissariat à l'Énergie Atomique (France); Klaus J. Boller, MESA+ Institute for Nanotechnology (Netherlands); Jean-Michel Gérard, Commissariat à l'Énergie Atomique (France); Willem L. Vos, MESA+ Institute for Nanotechnology (Netherlands)

There is a fast growing interest to switch the resonance of a cavity on ultrafast time scales. The motivation for this ambitious undertaking lies in future optical information processing to enhance (or even replace) current electronic switches, and also in fundamental electro-dynamics as well as in ultrafast cavity QED. Therefore, it is crucial to identify competing mechanisms during the switching of cavities to lead the switching in a favorable direction; towards sub-picosecond switching.

We demonstrate the ultimate-fast switching of a GaAs-AlAs cavity resonance in the Original (O) telecom band by exploiting the instantaneously fast electronic Kerr effect. We show that the switch-on and switch-off time of the cavity resonance can be achieved within 300 fs and is only limited by the cavity storage time τ_{cav} . We observe that at low pump-pulse energies the switching of the cavity resonance is governed by the instantaneous electronic Kerr effect and is achieved in sub-picosecond time scale. At high pump-pulse energies the free carriers generated in the GaAs start to compete with the electronic Kerr effect and reduce the resonance frequency shift. We have developed an analytic model, which predicts this competition in agreement with the experimental data. We identify the optimal conditions for ultimate fast switching of microcavities with different quality factors to enable reversible switching within the cavity storage time. By exploiting the regime where only the electronic Kerr effect is the main switching mechanism we pave the way to repeated switching at THz rates.

8623-49, Session 13

Terahertz wave-induced optical non-linearity in graphene (Invited Paper)

Koichiro Tanaka, Kyoto Univ. (Japan)

Dc transport properties of graphene have been described by fast carrier scattering process such as LO-phonon scattering, which also make it difficult to clear the ultrafast carrier transport. Thanks to recent advances in terahertz (THz) technologies, we can apply high electric field as large as 100 kV/cm on graphene in the sub-picosecond time duration. In this

study, we focused on near-infrared absorption change that reflects the non-thermal carrier distribution caused by the THz pulse excitation. We found that a considerable number of highly excited carriers are generated in graphene by the intense THz-wave excitation.

8623-50, Session 13

Dynamics of excitons and trions in semiconducting carbon nanotube (Invited Paper)

Makoto Okano, Taishi Nishihara, Yasuhiro Yamada, Yoshihiko Kanemitsu, Kyoto Univ. (Japan)

Because of their utility in fundamental physics and potential applications, optical properties of semiconducting single-walled carbon nanotubes (SWCNTs) have attracted much attention over the past decade. Strong Coulomb interactions between electrons and holes due to one-dimensional quantum confinement cause the formation of stable excitons with huge binding energies. In addition to the bright exciton, even-parity dark excitons, triplet excitons, and trions (charged excitons) are experimentally observed. The underlying dark-exciton and trion states affect PL properties of carbon nanotubes. However, the role of these states in exciton dynamics still remains unclear.

The samples were SWCNTs dispersed in toluene with poly[9,9-dioctylfluorenyl-2,7-diy] (PFO). 2,3,5,6-tetrafluoro-7,7,8,8-tetracyanoquinodimethane (F4TCNQ) was used as a p-type dopant. In doped SWCNTs, new photoluminescence and absorption peaks due to trions appeared below the lowest exciton peak (E11). Here, we discuss recombination dynamics of excitons and trions in undoped and hole-doped nanotubes studied by time-resolved spectroscopy.

We found that the E11 exciton decay time depends strongly on the dopant concentration. The decay time becomes shorter with increasing dopant concentration. This indicates that doped holes strongly affect the exciton relaxation processes. The E11 exciton decay dynamics depend on the excitation energy and the excitation intensity. Auger recombination between excitons and between a hole and an exciton play an important role in exciton decay dynamics. We also observed the slow decay of trions. We will present comprehensive discussions of exciton dynamics in undoped and hole-doped SWCNTs.

Part of this work was supported by KAKENHI (20104006), JST-CREST, and The SEI Group CSR Foundation.

8623-51, Session 13

Ultrafast broadband THz spectroscopy of carbon nanotubes and single-layer graphene

Hyunyoung Choi, Dominik Pfaff, Robert A. Kaindl, Lawrence Berkeley National Lab. (United States)

Carbon nanomaterials such as fullerenes, nanotubes, or graphene exhibit a large variation of electronic and optical properties, linked to the strong charge carrier confinement. Understanding the basic excitations, correlations and carrier dynamics in these materials, in turn, can provide important insight for future applications in optoelectronics and high-speed devices. We report experiments that probe the ultrafast dynamics of photoexcited nanotubes and single-layer graphene using broadband THz pulses. For the experiments, semiconducting (6,5) and (7,5) single-walled carbon nanotubes were embedded in a CMC polymer matrix to yield thin films suitable for broadband THz studies. The induced changes in the THz probe field are measured in the 1-6 THz range after visible or near-IR photoexcitation at the band-edge exciton peaks. We observe the emergence of an induced low-energy oscillator around ~2 THz, revealing an insulating non-Drude response in agreement with low-energy excitations of bound e-h pairs. The response is strongly enhanced at the nanotube E11 and E22 band-edge exciton peaks, underscoring both the excitonic origin and strong semiconducting chirality enhancement of the transient THz conductivity. The dynamics follows a bi-molecular kinetics

**Conference 8623:
Ultrafast Phenomena and Nanophotonics XVII**

due to exciton-exciton annihilation. Moreover, we have carried out the first ultrafast mid-IR-pump, THz probe experiments of exfoliated single-layer graphene. An ultrabroadband THz probe pulse reaching up to 20 THz was used to cover both intra- and interband transitions to map the Dirac fermion distribution functions. We observe transient conductivity changes in single-layer graphene and will discuss its complex spectral response and relaxation dynamics.

8623-52, Session 14

Ultrafast interactions of ultrashort surface plasmon polaritons on plane metal films and in dielectric waveguides (*Invited Paper*)

Carsten Reinhardt, Wei Cheng, Arune Gaidukeviciute, Urs Zywiets, Andrey B. Evlyukhin, Boris N. Chichkov, Laser Zentrum Hannover e.V. (Germany)

We present studies on ultrafast surface plasmon-polariton (SPP) interactions in systems with multiple coherently excited SPP and light beams. The replica of ultrashort laser pulses used for the excitation of SPPs is realized using a Michelson-interferometers. SPPs on thin metallic films are excited by local scattering of the laser light on surface nanostructures consisting of polymeric or metallic ridges [1] and grooves. SPP interaction and scattering effects are investigated by leakage radiation microscopy [2]. The interference of SPPs inside dielectrically-loaded SPP waveguides [3] as well as the interference of SPPs with additional light fields is used for tracking the propagation of ultrashort SPP pulses excited by 60 fs laser pulses at a central wavelength of 800 nm. We present results on SPP autocorrelation, allowing the SPP dispersion and pulse durations to be measured. Furthermore, we demonstrate ultrafast scattering of propagating SPPs on regions of metal films pumped by additional laser pulses. In a time-delay pump-probe experiment it is shown that this SPP scattering occurs on the time scale of the pulse duration. Applications of this effect as ultrafast SPP switches are discussed.

8623-53, Session 14

All-optical modulation in silicon-based nanoplasmonic devices (*Invited Paper*)

Shawn Sederberg, Abdulhakkem Y. Elezzabi, Univ. of Alberta (Canada)

Plasmonic devices offer several properties that are superior to dielectric photonic devices, such as their ability to confine electromagnetic energy to sub-diffraction dimensions and their ability to enhance electromagnetic fields. These properties make all-optical circuitry based on plasmonic waveguides an attractive prospect. Over the last decades, the field of silicon photonics has undergone rapid developments, and a host of devices for routing, filtering, buffering, and modulating electromagnetic signals. Despite these developments, the integration density of silicon photonic waveguide devices is limited by the diffraction limit and radiation losses around sharp bends. While there have been promising demonstrations of passive plasmonic waveguide devices, there have been comparatively few demonstrations of ultrafast active plasmonic devices, an essential component of any plasmonic circuit.

In this work, we explore the possibility of ultrafast active silicon-based plasmonic circuitry. Notably, development of plasmonic circuitry using a CMOS-compatible process would allow for monolithic integration of electronic and plasmonic devices. We present passive waveguiding devices and demonstrate coupling between silicon photonic devices and silicon-based plasmonic devices. Waveguiding around sharp bends is demonstrated using s-bend structures. Ultrafast all-optical modulation is investigated using above-bandgap pump pulses to photogenerate free-carriers, which in turn attenuate a telecommunications signal.

8623-54, Session 14

Supported plasmonic nanocrystals improve the performance of novel fiber-based sensors (*Invited Paper*)

Anatoli I. Ianoul, Jacques Albert, Carleton Univ. (Canada)

In the present work plasmonic properties of metal nanocrystals (gold or silver monocrystalline nanocubes, nanorods or nanocages) deposited on planar substrates or on tilted fiber Bragg grating (TFBG) sensors have been fine tuned to enhance the performance of such novel sensing platforms. Superior refractive index sensitivities of nanocrystal/substrate or nanocrystal/TFBG have been observed and correlated with their plasmonic properties. In addition, surface enhancement of the Raman signal for such sensors was observed. The study proposes a novel fiber based sensing platform utilizing localized surface plasmon resonances.

8623-55, Session 14

Probing ultrafast exciton spin dynamics in self-assembled InGaAs quantum dots

Kai Müller, Timo Kaldewey, R. Ripszam, Johannes Wildmann, Max Bichler, Gerhard Abstreiter, Jonathan J. Finley, Walter Schottky Institut (Germany)

We apply ultrafast pump-probe photocurrent spectroscopy to directly probe exciton spin dynamics in single, self-assembled InGaAs quantum dots. Excitons with well-defined spin configurations are resonantly created using polarized pump pulses and the exciton spin is read-out by spin selective conditional absorption or stimulated emission of probe pulses. We demonstrate a direct mapping of the polarization state of the pulses to the exciton spin Bloch sphere and the readout of the spin projection on arbitrary axis. The precession of the exciton spin due to the finestructure splitting is shown to be fully coherent with coherence times exceeding the exciton lifetime.

8623-56, Session 14

Ultrafast control of light trapping and reciprocity in nanophotonic media

Otto L. Muskens, Thomas Strudley, Univ. of Southampton (United Kingdom); Timmo van der Beek, FOM Institute AMOLF (Netherlands); Erik P. A. M. Bakkers, Technische Univ. Delft (Netherlands); Thomas Wellens, Albert-Ludwigs-Univ. Freiburg (Germany)

Light transport in nanostructured photonic materials is governed by strong multiple scattering, resulting in photonic bands, light trapping, and diffuse transport phenomena. Here, we show ultrafast control over light transport through a spatially and temporally non-uniform pulsed laser excitation. We demonstrate that adiabatic control over light paths can be achieved, which gives rise to reciprocity breaking in the medium [1]. Ultrafast dephasing and reciprocity breaking hold promise for nanophotonic switches, ultrafast nanoscale and random lasers, and control of light trapping and localization.

[1] O. L. Muskens, P. Venn, T. van der Beek, T. Wellens, Phys. Rev. Lett. 108, 223906 (2012)

**Conference 8623:
Ultrafast Phenomena and Nanophotonics XVII**

8623-57, Session 15

Influence of resonator design on ultrastrong coupling between a two-dimensional electron gas and a THz metamaterial

Curdin Maissen, Giacomo Scalari, Federico Valmorra, Christian Reichl, ETH Zurich (Switzerland); Dieter Schuh, Univ. Regensburg (Germany); Werner Wegscheider, Matthias Beck, ETH Zurich (Switzerland); Simone De Liberato, David Hagenmüller, Cristiano Ciuti, Lab. Matériaux et Phénomènes Quantiques, Univ. Paris 7-Denis Diderot and CNRS (France); Jérôme Faist, ETH Zurich (Switzerland)

THz metamaterials have been shown to be a promising candidate for QED experiments, i.e. Ultrastrong coupling has been demonstrated. Modes of split ring resonators (SRRs) have been coupled via the AC-electric field to inter Landau level transitions in two dimensional electron gases (2DEGs).

SRR typically exhibit two distinct electromagnetic modes. One mode consists of an electric field confined in the slit of the resonator, while current in the resonator ring stores the magnetic field. This mode is often called LC-mode, in analogy to the lumped circuit representation, and has a nearly Lorentzian line shape. The other mode is a dipole mode localized physically on the resonator edges. The line shape of this resonance is more sensitive to the actual resonator geometry.

We studied extensively the influence of the resonator geometry on the coupling strength. The resonances studied span the frequency range from 250 GHz to 1.3 THz for the LC type and 0.8 to 2.5 THz for the dipole resonance. The number and position of gaps in the SRR has been varied, putting them both in series as well as in parallel. These modifications influence the mode volume of the LC-mode which changes the coupling strength in two opposite ways. The electric field intensity increases and thus the coupling. However, the number of participating electrons in the 2DEG is reduced which reduces the $N^{0.5}$ coupling enhancement.

In the same way, we have investigated the coupling of the dipole resonance. The largest coupling we measured so far is $\Omega/\omega = 0.58$.

8623-58, Session 15

InGaAs amplifier for loss-compensation in nanoplasmonic circuits

Michael P. Nielsen, Abdul Y. Elezzabi, Univ. of Alberta (Canada)

Surface plasmon polaritons have become a contender for next-generation optical computing with their superior subwavelength modal confinement and nonlinearity over conventional photonics. Gap plasmon waveguides, as known as metal-insulator-metal (MIM) waveguides, have been shown to have one of the best balances in the inherent trade-off between confinement (<200nm) and propagation length (several microns) among plasmonic waveguide geometries. There is great interest in introducing gain into plasmonic systems to compensate for their innate short propagation lengths. To this end, we present an electrically pumped Ag/HfO₂/In_{0.485}Ga_{0.515}As/HfO₂/Ag metal-insulator-semiconductor-insulator-metal (MISIM) amplifier design for loss-compensation in nanoplasmonic interconnects at the telecommunication wavelength of 1.55 μ m. Finite difference time domain simulations utilizing the full rate equations were used to study the signal gain experienced upon transmission through the device. The direct bandgap semiconductor gain medium In_{0.485}Ga_{0.515}As was modelled as a four level laser system with homogeneous broadening. The effect of varying critical amplifier dimensions, namely the HfO₂ spacer layer thickness and the width of the In_{0.485}Ga_{0.515}As core, on the amplifier's performance was studied. A 3 μ m long linear amplifier is shown to be capable of restoring a 500 GHz, 500 fs FWHM pulse train after 150 μ m of propagation through a nanoplasmonic interconnect network without significant pulse distortion at a pump current density of 36.6 kA/cm², or 1 mA total current. A

periodic arrangement of such devices could therefore be used to indefinitely increase the effective propagation length of a signal.

8623-59, Session 15

Switching spontaneous emission in microcavities in the time domain

Henri Thyrrestrup, Alex Hartsuiker, Univ. Twente (Netherlands); Jean-Michel Gérard, Commissariat à l'Énergie Atomique (France); Willem L. Vos, Univ. Twente (Netherlands)

An impressive progress has been achieved in controlling the spontaneous emission rate for emitters in Nanophotonic structures, such as microcavities, photonic crystals and nano-antennas. However, the modification of the emission is stationary in time. Thus, the emission rate is time-independent and the temporal distribution of emitted photons is stochastic and follows an exponential law in the weak coupling regime. Here, we propose to quickly modify the environment of an ensemble of emitters in time, during the time they emit photons. By utilizing fast all optical switching of a microcavity we tune the cavity resonance within tens of picoseconds [JOSA B. 29, A1 (2012)]. This drastically changes the local optical density of states at the emission frequency within the emission lifetime of the emitters. We have theoretically studied an ensemble of two-level sources with a time dependent decay rate and have derived the excited state population and emitted intensity as a function of time for continuous wave and pulsed excitation. We obtain deterministic bursts of dramatically enhanced or inhibited emission intensity within short intervals. Thereby, we control the photon distribution to show behavior that strongly deviates from single exponential decay. This can be used to protect quantum information systems against decoherence and to realize non-Markovian dynamics in cavity quantum electrodynamics.

8623-60, Session 15

Plasmonic slot waveguides with core nonlinearity

Sherif A. Tawfik, Mohamed A. Swillam, The American Univ. in Cairo (Egypt)

Metal-insulator-metal plasmonic waveguides (plasmonic slot waveguides, PSW) are known to offer high propagation lengths and confinement factors and have recently been gaining increasing attention in the literature. We analytically study the interplay between group velocity dispersion and self-phase modulation on ultrafast surface plasmon-polariton (SPP) pulse-reshaping for plasmonic-slot waveguides with nonlinear dielectric core. The analytic investigation of the role of the core nonlinearity on pulse propagation has, to our knowledge, not been investigated in the literature. We analyze the interplay between the core width and the index parameters on pulse broadening and output intensity for a range of wavelengths by using the optimized parameters reported for the empirical Drude-CP model, and for a range of pulse durations. Moreover, PSW performance is monitored by computing the propagation length and confinement factor. We correlate our analytical results with numerical FDTD simulations.

8623-61, Session 15

Evolution of surface plasmon resonance with core thickness in Au/InGaAs slab waveguide hybrid nanostructure

Seunghyun Kim, Chung-Min Lee, Ki-Ju Yee, Chungnam National Univ. (Korea, Republic of)

We report on experimental and theoretical study for spectral position of surface plasmon resonance (SPR) as a function of core thickness

**Conference 8623:
Ultrafast Phenomena and Nanophotonics XVII**

in Au-InGaAs slab waveguide hybrid nano-structure. Slab waveguide covered by metallic sub-wavelength slit array was composed by InGaAs core of 100, 200 and 400 nm thick and InP substrate. Transmission for Au slit array on 100, 200 and 400 nm thick InGaAs was measured at near-infrared region, and the origin of this transmission dips was revealed by numerical simulation. Each one transmission dip of SPR and waveguide mode was observed for 400 nm thick InGaAs while one SPR transmission dips were only observed for 100- and 200 nm thick InGaAs, this transmission dip was generated guiding of photons with specific wavelength in InGaAs core and resonant coupling of photon-SP at interface between Au/InGaAs.

It is interesting that wavelength of the SPR transmission dip becomes shorter as the InGaAs thickness decreases from 400 nm to 100 nm. If InGaAs layer is thin as 100 nm thick, where appreciable extent of SP field intrudes into InP substrate, SP at interface between Au/InGaAs is influenced not only by the dielectric constant of InGaAs but also by the dielectric constant of InP. Thus SPR transmission dip at shorter wavelength with thinner InGaAs layer can be explained by the SP field intrusion into low index substrate region. Our semiconductor-metal hybrid nanostructure can be applied for surface plasmon based ultrafast optical switch.

8623-62, Session 15

Measurements of giant second harmonic generation from vertically-aligned silicon nanowires

Mohamed A. Swillam, Univ. of Toronto (Canada) and The American Univ. in Cairo (Egypt); Mohammadreza Khorasaninejad, Simarjeet Sinai, Univ. of Waterloo (Canada)

In this paper, we present our recent measurement of second harmonic generation (SHG) from silicon nanowires which are vertically aligned. The SHG shows a great enhancement due to the increase of the surface area which breaks the symmetry of silicon lattice and increase the surface SHG. A high SHG is also obtained in counter polarization for both S and P polarization excitation. An enhancement of 80 times is also observed.

This huge enhancement opens the door for novel applications including frequency mixing and frequency generation for various novel nonlinear application of silicon based devices.

8623-63, Session PWed

Wavelength-tuneable GHz repetition rate picosecond pulse generator using an SBS frequency comb

Victor Lambin Iezzi, Sébastien Loranger, Raman Kashyap, Ecole Polytechnique de Montréal (Canada)

We have developed a new system to generate GHz repetition rate tuneable pulses in the picosecond regime at any wavelength by using self-phase-locked Stimulated Brillouin Scattering (SBS). The phase-locked comb at any required wavelength is generated using a single long length of fiber in a ring cavity, seeded by an amplified single frequency CW pump laser. We demonstrate a coherent phase relationship between multiple cascaded Stokes waves in the cavity, which directly lead to a highly stable pulse regime. The coherent pulses in the time domain are in the order of ~ 10 ps. The nature of the fiber leads to a stable SBS frequency shift, which is directly correlated to the repetition frequency and which is in the order of tens of GHz. Since the process is governed by SBS, it is self-starting and has a linear dependence with temperature ($1 \text{ MHz}/^\circ\text{C}$), which could be used for fine adjustments. Such a laser is therefore suitable for high-speed optical clocks and optical communication system, amongst other applications. This system allows the ultra-short pulses to be generated at any wavelength by simply tuning the wavelength of the seed laser. The pump power allows the pulse width to be tuned in steps, by generating additional Stokes orders. The

repetition rate is altered by the choice of fiber cavity or by selection of various Stokes orders.

8623-64, Session PWed

Investigation of saturation in two- and three-photon nano-photonic absorbers

Mary Potasek, Gene Parilov, Simphotek Inc. (United States)

Many techniques in biological and clinical science use multiphoton absorbers. The applications include medical imaging for living cells to diagnostic techniques for disease. Knowing the intrinsic value of the multiphoton absorber coefficients is therefore of the utmost importance. In particular, the laser intensity at which the absorber saturates can determine which absorber is useful for a particular application.

Yet, many traditional investigations of saturation in multiphoton absorbers use an approximate analytical formula that assumes a steady-state approximation. Using a numerical simulation for Maxwell's equations and coupled electron population dynamics, we show that the commonly used analytical formula for determining saturation in multiphoton absorbers is often not correct. Using published experimental data on semiconductor quantum dots, we show that saturation, in fact, does not occur at the laser intensity values predicted for these two and three photon absorbers. We fit experimental transmission data and obtain new absorption values for multiphoton absorbers that accurately reflect their intrinsic values. Because multiphoton absorbers are being used more extensively in medical diagnostics and microscopy, it is important to have accurate values for the two and three-photon absorption coefficients.

8623-65, Session PWed

Ultrafast degenerate pump-probe studies of SI-GaAs and LT-GaAs

Soma Venugopal Rao, P. T. Anusha, Surya P. Tewari, Debasis Swain, Univ. of Hyderabad (India)

Ultrafast switching of photo-conducting antennas (PCAs) made from Low Temperature grown GaAs (LT-GaAs) has proven to be efficient way for the generation of THz with respect to both intensity and spectral bandwidth. This material has unique properties such as the ultrashort carrier lifetime, large resistivity, and relatively good carrier mobility¹. It is epitaxially grown on a semi insulating GaAs (SI-GaAs) substrate. The bandwidth of PCA is limited by the finite carrier lifetime or the momentum relaxation time of carriers in the PC substrates². Therefore, femtosecond/picosecond relaxation times of such non-equilibrium carrier dynamics in semiconductors are important to perceive their application potential and can be measured using ultrafast pump-probe spectroscopy. When a semiconductor is excited with photons of energy greater than its band gap, Eg, electron-hole pairs are created with excess kinetic energy $h\nu - E_g$. This excess energy will then redistribute among the electronic and lattice degrees of freedom until an equilibrium is reached with the surroundings. The relaxation of these electrons and/or the redistribution of the excess energy, initially confined in these excited carriers, is then monitored with a time resolved probe. In this paper we present the measurement of carrier lifetimes of both LT-GaAs and SI-GaAs using picosecond/femtosecond degenerate pump probe experiment at 800 nm/600 nm. The experiments are performed with photon energy ($\sim 1.55 \text{ eV}$) higher than band gap of GaAs. The intensity dependent excitation and dynamics of carriers is also studied.

References

1. J. Zhang, Y. Hong, S.L. Braunstein and K.A. Shore, "Terahertz pulse generation and detection with LT-GaAs photoconductive antenna" IEE Proc.-Optoelectron 2004, 151, 98-101.
2. T. A. Liu, M. Tani, M. Nakajima, M. Hangyo, C. L. Pan, "Ultrabroadband terahertz field detection by photoconductive antennas based on multi-energy arsenic-ion-implanted GaAs and semi-insulating GaAs" Appl. Phys. Lett. 2003, 83(7), 1322-1324.

8623-66, Session PWed

Air-breakdown coherent detection of terahertz using controlled optical bias

Chia-Yeh Li, The Univ. of New Mexico (United States); Denis V. Seletskiy, The Univ of New Mexico (United States) and Air Force Research Lab. (United States); Mansoor Sheik-Bahae, The Univ. of New Mexico (United States)

Detection of broadband terahertz with gas plasma has been previously reported (air break-down coherent detection). Coherent detection (linear with the THz field) requires bias in addition to the EFISH signal. This was accomplished in previous reports under two arrangements. In the first arrangement, high laser intensity provides this bias from either strong 2ω plasma (nitrogen) fluorescence or octave-spanning supercontinuum in order to exceed the EFISH signal, which, detected by itself, is proportional to $|\text{E}_{\text{THz}}|^2$. In the second arrangements, high voltage DC field is applied across the plasma channel, serving the role of the required bias. Here we report a new method where. By adding a Beta barium borate (BBO) before the air plasma, the controlled 2ω generation in BBO fulfills the role of bias field. Unlike in previous works, coherent detection here can be achieved at lower laser intensity. The absence of high intensity and high voltage makes the detection scheme more viable for remote sensing. The dependence of the coherent detection on the injector (BBO) phase-matching conditions will be discussed.

8623-67, Session PWed

Time-resolved Faraday effect in layered structures

Margarita I. Sharipova, Alexander I. Musorin, Artem V. Chetvertukhin, Tatyana V. Dolgova, Andrey A. Fedyanin, Lomonosov Moscow State Univ. (Russian Federation)

Magnetic circular birefringence or Faraday effect is the rotation of polarization plane of linearly polarized light by a magnetic medium. Because of the non-reciprocity of the effect the significant enhancement can be achieved by light interference inside Fabry-Perot resonator with magnetic medium, for example in thin films or photonic crystals and microcavities [1,2]. When short 100-femtosecond pulse goes through a sample with time of its passage comparable with pulse duration, interference between initial and final parts of one pulse is possible, which leads to time dependence of Faraday rotation. Resulting time dynamics depends on interference conditions. For positive interference between different parts of one pulse continuous increasing with time is observed. In case of destructive interference output Faraday effect confirms decreasing intervals in time dependence.

Calculations were made by using transfer matrix formalism in frequency domain and consequent Fourier transform [3]. Experimental detection of Faraday dynamics was performed by using correlation method. Magnetic contribution to correlation function registers with modified set-up, inclusive 1-kOe constant magnet and photoelastic modulator. At the measured interval Faraday rotation decreases with time from 1.2-degree value to practically zero in 30-um-thick magnetic film and slightly increases from 1.1 to 1.3 degrees in microcavity at the position of defect mode. Experimental data are in good agreement with simulation.

[1] M. Inoue et al, J. Phys. D. 39 (2006) 237 R151.

[2] K. H. Chung et al, J. Appl. Phys. 107 (2010) 09A930.

[3] A.V. Chetvertukhin et al, J. Appl. Phys. 111 (2012) 09A944.

Conference 8624: Terahertz, RF, Millimeter, and Submillimeter-Wave Technology and Applications VI

Tuesday - Thursday 5 -7 February 2013

Part of Proceedings of SPIE Vol. 8624 Terahertz, RF, Millimeter, and Submillimeter-Wave Technology and Applications VI

8624-1, Session 2

A powerful new THz photoconductive source driven at 1550 nm (*Invited Paper*)

Elliott R. Brown, Wright State Univ. (United States)

Ultrafast (< 1 ps) photoconductive sources continue to be the workhorse for THz time- and frequency-domain sources and systems. For over a decade, they have been pursued at 1550-nm drive wavelength to take advantage of the affordable laser, amplifier, and fiber-optic component technology. But the 1550-nm photoconductive sources have generally been fabricated from InGaAs-based epitaxial layers on InP substrates with performance inferior to their GaAs-based counterparts driven in the 780-850 nm range, largely because of inferior resistivity and breakdown voltage. This paper addresses a new ultrafast source using GaAs as the epitaxial layer with 1550 nm drive wavelength – the “best of both worlds”. The trick is to utilize a metal-nanocomposite form of GaAs containing a high concentration of ErAs nano-islands. This material had previously been demonstrated as the most powerful THz photoconductive source at 780 nm, and we recently showed that it produces comparable power with 1550-nm-laser drive. The average power from a photoconductive switch is been found to ~100 uW, and the -3-dB bandwidth well above 100 GHz. The physical mechanism has been tentatively identified as extrinsic photoconductivity, although two-photon absorption has not been entirely ruled out. This paper will report the detailed THz performance of the new device, and address the underlying physical mechanism.

8624-2, Session 2

THz imaging using broadband direct detection (*Invited Paper*)

Zachary D. Taylor, Ctr. for Advanced Surgical and Interventional Technology (United States); Nuria Llombart, Univ. Complutense de Madrid (Spain); Priyamvada Tewari, Neha Bajwa, Rahul S. Singh, Martin O. Culjat, Ctr. for Advanced Surgical and Interventional Technology (United States); Elliott R. Brown, Wright State Univ. (United States); Warren S. Grundfest M.D., Univ. of California, Los Angeles (United States)

Research in THz imaging is currently focused on three primary application areas: medical, security, and nondestructive evaluation (NDE). While research in THz security imaging and personnel screening is populated by a number of different active and passive system architectures medical imaging and NDE are dominated by THz time-domain systems. These systems typically employ photoconductive or electrooptic source/detector pairs and can acquire depth resolved data or spectrally resolved pixels by synchronously sampling the electric field of the transmitted/reflected wave. While time-domain is a very powerful scientific technique results reported in the literature suggest that desired THz contrast may not require the volume of data available from time-resolved measurements and that simpler techniques may be more optimal for specific applications. In this talk we discuss a direct detection system architecture operating at a center frequency of ~ 525 GHz that uses a photoconductive source and schottky diode detector. This design takes advantage of radar-like pulse rectification and novel reflective optical design to achieve high target imaging contrast with significant potential for high speed acquisition time and scatter mitigation. Results in spatially resolved hydration mapping and concealed target imaging for both medical and NDE applications are presented and contrast mechanism sensitivity of this technique compared to traditional THz imaging system architectures are discussed.

8624-3, Session 2

Strong optical forces in the mid-IR and terahertz mediated by coupled spoof surface plasmons

David Woolf, Mikhail Kats, Nanfang Yu, Federico Capasso, Harvard Univ. (United States)

The force from surface plasmons on parallel metal surfaces is inherently tied to the dispersive properties of the metal. This severely limits the strength of the force below near-infrared frequencies where the modes are close to the light line. Subwavelength surface structures can significantly modify the dispersive properties of guided modes, such as with so-called “spoof” surface plasmon polaritons (SSPPs). SSPPs are surface plasmon-like waves that propagate along metal surfaces with deeply sub-wavelength corrugations, and whose dispersive properties are determined primarily by the dimensions of the grooves. Two parallel corrugated metallic surfaces separated by a sub-wavelength dielectric gap create a spoof-plasmon analog of the plasmonic metal-insulator-metal (MIM) waveguide that supports “bonding” and “anti-bonding” modes. Such spoof plasmon waveguides are promising for the guiding and manipulation of light from the near-infrared to the terahertz frequency range. We study the dispersion relations of coupled SSPPs and calculate the optical gradient forces generated between the two corrugated surfaces. By changing the groove geometry, attractive and repulsive optical forces can be generated at nearly any frequency, paving the way for opto-mechanical devices at mid-infrared and terahertz frequencies.

8624-4, Session 2

CMOS: Compressive Multi-heterodyne Optical Spectroscopy

Nikhil Mehta, The Pennsylvania State Univ. (United States); Jingbiao Chen, Zhigang Zhang, Peking Univ. (China); Zhiwen Liu, The Pennsylvania State Univ. (United States)

High-resolution optical spectroscopy enables exciting applications such as molecular fingerprinting of gas molecules, identification of drugs and biological species, fine Doppler shift measurements, and evaluation and monitoring of fundamental physical constants. The development of octave spanning frequency comb using a mode-locked laser has opened new opportunities for ultra high resolution optical spectroscopy through multi-heterodyne schemes. However, existing techniques cannot provide continuous frequency coverage within the adjacent modes, unless another frequency comb or a probe laser is swept relative to the source comb across the entire multi-THz optical band, which limits the acquisition speed. To address this problem, we present a general framework for a compressive multiplex multi-heterodyne scheme to achieve ultra-high resolution optical spectroscopy using dynamically encoded laser frequency combs. Our technique maps the multi-THz optical band to a single RF baseband, few GHz across. It provides continuous frequency coverage and can be used for both incoherent and coherent (both amplitude and phase) acquisition. We present proof-of-concept numerical simulations using iterative algorithms based on compressive sensing to take advantage of the sparsity inherent in typical optical spectra of interest, to reduce the number of multiplexed RF measurements. We demonstrate that fewer than 50% RF measurements as compared to the number of comb modes suffice to retrieve a hypothetical 2 THz wide optical spectrum. Our results are consistent with the theoretically expected reduction in the number of measurements for successful retrieval based on sparsity-constrained inversion.

8624-5, Session 3

Microfabrication and cold testing of copper circuits for a 50-watt 220-GHz traveling wave tube (*Invited Paper*)

Colin D. Joye, Alan M. Cook, Jeffrey P. Calame, David K. Abe, U.S. Naval Research Lab. (United States); Khanh T. Nguyen, Edward L. Wright, Beam-Wave Research, Inc. (United States)

A 220 GHz, 50 W vacuum electron traveling wave tube amplifier is nearing completion utilizing an 11.7 kV, 120 mA electron beam with a predicted bandwidth of 15 GHz and small signal gain of 18 dB. The amplifier showcases a novel microfabrication technique employing embedded polymer monofilaments to simultaneously fabricate the circuit and beam tunnel within a UV-LIGA process [1] (U.S. and Foreign Patent Applications filed). The method shows promise for fabricating similar circuits from about 90 GHz to ~1 THz. Beryllia vacuum windows provide over 20 GHz bandwidth with better than -20 dB S11 reflection. The circuits have been completely fabricated and cold tested at the U.S. Naval Research Laboratory. The tube is expected to begin hot testing at the end of 2012 after final assembly and evacuation.

1. C. D. Joye, et al, J. of Micromech./Microeng, Vol. 22, p. 015010, 2012.

* Work supported in part by the U.S. Office of Naval Research and by DARPA. Approved for Public Release, Distribution Unlimited. The views expressed are those of the author and do not reflect the official policy or position of the Department of Defense or the U.S. Government.

8624-6, Session 3

A tunable continuous-wave terahertz generator based on 1.3 μm dual-mode laser diode and travelling-wave photodiode

Han-Cheol Ryu, Namje Kim, Jeong-Woo Park, Sang-Pil Han, Hyunsung Ko, Kiwon Moon, Electronics and Telecommunications Research Institute (Korea, Republic of); Min Yong Jeon, Chungnam National Univ. (Korea, Republic of); Kyung Hyun Park, Electronics and Telecommunications Research Institute (Korea, Republic of)

We demonstrate the tunable continuous-wave (CW) terahertz generator based on the $\pi/4$ phase-shifted 1.3 μm dual-mode laser diode (DML) and travelling-wave photodiode (TWPD). The DML and TWPD operate as an optical beat source and terahertz photomixer, respectively. The laser diodes (LDs) operating at the 1.3 μm can be used in terahertz wireless communication when it is related with an optical access network. Furthermore, the characteristics of LDs operating at 1.3 μm are more suitable as optical beat sources than those of LDs at 1.55 μm because of the high efficiency and better thermal stability of them. The micro-heaters are integrated on top of each DFB LD for mode beat frequency tuning. The fabricated DML was continuously tuned from 230 to 1485 GHz by increasing the temperature of each DFB section independently via integrated micro-heaters. The high-speed TWPD with an InGaAs absorber was designed and fabricated to efficiently generate the photomixing terahertz CW. A complementary log-periodic antenna was integrated with the TWPD to radiate the generated terahertz wave with minimum reflection in the wide frequency range. The feature of the TWPD showed relatively high responsivity and high speed exceeding a RC limitation. The terahertz characteristics of the tunable CW terahertz generator based on the DML and TWPD were measured in a fiber-coupled, homodyne terahertz photomixing system. Our results of the tunable CW terahertz generator show the feasibility of a compact and highly efficient CW terahertz spectrometer and imager.

8624-7, Session 3

Sub-mm/THz wave generation/amplification using Cerenkov-transition based device

Ahmed I. Nashed, Sujeet K. Chaudhuri, Safieddin Safavi-Naeini, Univ. of Waterloo (Canada)

Abstract— Due to the rapid growth of the biomedical and the security applications, the interest in the development of compact and flexible sub-mm/THz radiation sources has grown significantly. In this paper we propose a novel design to address this need. Taking the advantage of the Photonic Crystal (PC) structure, a metallic defected PC, with no axial discontinuities, was designed as a Slow Wave Structure (SWS). This SWS was used in a high power Cerenkov-transition based oscillator/amplifier working in sub-mm/THz frequency regime. The SWS allows electron beams to travel axially in it, facilitating the beam interaction required for the desired signal generation. Two coaxial transitions are used as input and output for the proposed device. The analysis of the proposed device was done using a combined Finite Difference Time Domain (FDTD) / Particle In Cell (PIC) simulation. Using the FDTD thin wire model, coaxial transitions were modeled to feed/extract the input/generated signals. To show the potential of the proposed device, two design examples; one for the amplifier and the other for the oscillator, are presented.

8624-8, Session 3

Room temperature generation of THz radiation in GaN quantum wells structures

Alexandre Penot, Jérémie Torres, Luca Varani, Univ. Montpellier 2 (France); Yvon Cordier, M. Chmielowska, Ctr. de Recherche sur l'Hétéro-Epitaxie et ses Applications (France); Jean-Pierre Faurie, Bernard Beaumont, LUMILOG (France); Pavel Shiktorov, E. Starikov, Semiconductor Physics Institute (Lithuania)

We report on the experimental emission of THz radiation measured by a Fourier Transform Spectrometer from GaN quantum well structures under dc-bias. The different layers of the GaN devices have been grown by molecular beam epitaxy on a iron doped GaN on GaN substrate and consist of a GaN 1 μm -thick buffer, a 1 nm-AlN/ 21 nm-Al_{0.29}Ga_{0.71}N, 3 nm-GaN active layer. This heterostructure is covered by interdigitated Ti/Al ohmic contacts with distance between contacts of 6 to 52 μm . The device under test lays at the focal point of an experimental configuration composed of two parabolic mirrors, a Michelson interferometer and a bolometer.

It is biased by a pulse voltage from 0 to 25 V with a filling factor of and a frequency of 123 Hz. A lock in amplifier is used to improve the signal to noise ratio. After crossing a threshold at 10 V, we observe an emission peak at a frequency around 3 THz that can be tuned by dc-bias. Moreover the power of the peak grows with the applied voltage. The different physical mechanisms that could be at the origin of the observed emission will be discussed at the conference.

8624-9, Session 3

An improved design of THz radiation device with hybrid waveguide structures compatible with latest technique of monolithic integration fabrication

Tianxin Yang, Zhuo Zhang, Xuehui Niu, Dongfang Jia, Mei Sang, Tianjin Univ. (China)

The thickness of core layer in a THz emitting waveguide device based on optical rectification effects in gallium arsenide (GaAs), which we designed before, is about a hundred and more micrometers which is too thick to fabricate by conventional molecular beam epitaxial (MBE) technique.

Conference 8624: Terahertz, RF, Millimeter, and Submillimeter-Wave Technology and Applications VI

The latest emerged direct semiconductor bonding technique makes the fabrication practicable for realizing III-V/Si hybrid integration that are free from lattice-match restrictions required in conventional heteroepitaxy[1]. However it is challenging to etch a second order grating on the surface of GaAs to form a grating coupler for converting the THz guide mode, generated by the optical pump based on optical rectification effects in GaAs, into the radiation. In this paper, to reduce the number of extra processing steps for fabrication, a compact metal grating coupler on the surface of GaAs is design to replace the etching grating. The metal grating is compatible with silicon fabrication technology and it offers a new concept of electromagnetic waves coupling at THz band. For the design of metal grating couplers and optimization, CAivity Modelling FFramework (CAMFR), a two dimensional fully vectorial simulation-tool based on eigenmode expansion and mode propagation with perfectly matched layer (PML) boundary conditions, is a useful tool in visible and near infrared (IR) regions. However CAMFR is not yet ready for dispersive metal with negative real part of permittivity so that it is not adapted at terahertz regions in which electromagnetic waves could propagate in the form of surface plasmon-assisted guided modes in a metal-dielectric surface waveguides (MD-SWGs). Considering of all possible modes, the radiation losses at THz band of the device we designed is simulated to find the optimum structure parameters of the metal grating.

Reference:

[1] Tanabe, K.; Watanabe, K.; Arakawa, Y., III-V/Si hybrid photonic devices by direct fusion bonding, Scientific Reports 2, Article number:349, 2012.

8624-11, Session 4

Terahertz time-domain spectroscopy of organic semiconductors

Daniel M. Hailu, Hany Aziz, Safieddin Safavi-Naeini, Univ. of Waterloo (Canada); Daryoosh Saeedkia, TeTechS Inc. (Canada)

In this paper, we conduct transmission and reflection mode terahertz time-domain spectroscopy (THz-TDS) measurements of organic semiconductors such as ALQ3 and BH2. THz-TDS is effective for determining the purity of the organic semiconductors based on the refractive index and spectral signatures in THz range.

In order to prepare the sample in a custom built sample holder, the powder samples are pressed into pellets of 13 mm diameter and a thickness of 2 mm using a hydraulic press. The organic semiconductor, for example ALQ3 sample, is prepared as a 70% ALQ3 and 30% polyethylene (PE) concentration pellet by mixing ALQ3 and PE. The ALQ3 pellet is measured in a chamber purged with dry nitrogen to avoid the effect of water vapor absorptions in ambient air. The absorption coefficient and index of refraction is measured from the spectra of the THz pulse of reference and THz pulse after transmission through the sample. The THz spectrum is obtained by applying a fast Fourier transform to the THz waveform. Further studies were conducted by reducing the concentration of the organic semiconductor from 70% to 10% ALQ3. We also obtained the spectral signature and absorption coefficient for 50% BH2 50% PE pellet. The spectral signatures of ALQ3 were found to be at 0.868 THz, 1.271 THz and 1.52 THz, while spectral signature of BH2 was found to be at 1.033 THz.

8624-12, Session 4

3D terahertz beam profiling

Pernille K. Pedersen, Krzysztof Iwaszczuk, Andrew Strikwerda, Tianwu Wang, Maksim Zalkovskij, Jonas D. Buron, Peter U. Jepsen, Technical Univ. of Denmark (Denmark)

With the heightened interest in both imaging techniques and nonlinear spectroscopic measurements in the terahertz (THz) regime, it is increasingly important to fully characterize the spatial profile of a generated THz beam. Previous profiling experiments have been carried out with knife-edge scans, apertures, disks, or 2D scanning of

a THz detector, but these methods can be time consuming, difficult, or potentially inaccurate due to the significant affects of diffraction at these wavelengths. However, recent advances in detector arrays have led to the development of THz cameras, allowing for the fast and easy measurement of THz beam profiles, similar to conventional CCD based beam profile measurements at higher frequencies.

In this presentation we demonstrate the characterization of THz beams generated in both air plasma and a LiNbO₃ crystal. In both generation methods, scans are conducted in the propagation direction through the focal point of the THz beam. Measurements as a function of distance are taken with a THz-camera (produced by NEC Corporation), which is an uncooled microbolometer array with sensitivity from 1 to 7 THz and a spatial resolution of 23.5 μm . We will show our latest results on profile scans, visualize the beam scans into a 3D profile, characterize the beams according to their Gaussian parameters, and discuss our results in the context of imaging and nonlinear spectroscopy.

8624-13, Session 4

Imaging at 0.2 and 2.5 terahertz

Arline M. Melo, BR Labs (Brazil); Mauricio A. P. Toledo, Univ. Estadual de Campinas (Brazil); Francisco C. B. Maia, Andre Rocha, Matheus B. Plotegher, BR Labs (Brazil); Daniel Pereira, Flavio C. Cruz, Univ. Estadual de Campinas (Brazil)

TeraHertz imaging is receiving considerable interest due the possibility of looking through objects which are opaque to visible light. Aside from applications in inspection and security, without the risks associated with X-rays, it may also allow the application of several optical techniques to material studies in this spectral region. Progress in the field, especially for real-time or distant imaging, is directly linked to the development of powerful sources and sensitive detectors. Here we report the development and initial results from two Terahertz imaging systems based on monochromatic sources at 0.2 and 2.52 THz. The first is based on a microwave oscillator, whose frequency is amplified and multiplied to 0.2 THz, used in conjunction with a zero-bias detector. The sample is scanned across the beam, and transmission images have been obtained after processing. The second system allows real-time images, and consists of a methanol gas laser emitting at 119 microns (2.52 THz) and a commercial microbolometer camera. We describe the construction and performance of the methanol laser and its tunable CO₂ pump laser, which can emit 20 W at the 9P(36) line. Both lasers incorporate automated operation Labview routines. Due to the high coherence of the laser, this system is particularly suited for diffraction and interference imaging. We also report measurements of the absorption coefficients of common opaque materials, such as printer paper, letter envelope and styrofoam, assuming the Beer law.

8624-14, Session 4

Introducing a 388x284 pixel terahertz camera core

Claude Chevalier, Luc Mercier, François Duchesne, Lucie Gagnon, Bruno Tremblay, Marc Terroux, Linda Marchese, Martin Bolduc, Hubert Jerominek, Alain Bergeron, INO (Canada)

Terahertz is a field in expansion with the emergence of various security needs such as parcel inspection and through-camouflage vision. Terahertz wavebands are characterized by long wavelengths compared to the traditional infrared and visible spectra. From the common perception and using resolving limit defined by the Raleigh criterion, $1.22 \lambda / F\#$, long wavelength would yield to the use of large pixel focal plane arrays. On a system point of view, for a given surveillance distance large pixels yield to the use of long focal lengths to obtain sufficient resolution for useful applications. To maintain a sufficient optical throughput this translates in large optics that increases the volume and cost of a system.

However, it has recently been demonstrated that a 52 μm pixel pitch microscanned down to an efficient sampling pitch of 26 μm could provide

Conference 8624: Terahertz, RF, Millimeter, and Submillimeter-Wave Technology and Applications VI

useful information even using a 118.83 μm wavelength. With this in mind, INO has developed a terahertz camera core based on a 384x288 pixel 35 μm pixel pitch uncooled bolometric terahertz detector. The camera core provides full 16-bit output video rate.

The introduction of this new camera core paves the way to the use of smaller THz optics and the design of more compact systems which should in terms yield to a wider acceptance of the technology. This paper reviews the various characteristics of the cameras as well as the initial performances obtained.

8624-15, Session 4

The terahertz spectroscopic investigation of diflubenzuron and theoretical analysis

Qiang Wang, China Jiliang Univ. (China)

The experimental terahertz (THz) spectrum of diflubenzuron has been obtained by utilizing terahertz time-domain spectroscopy (THz-TDS). We analysis the absorption and refractive spectra of diflubenzuron in the confidence interval in the range of 0.0?1.6THz. The experimental THz spectrum of diflubenzuron consists of seven obvious absorption peaks. To analysis the experimental spectrum, the theoretical simulation spectrum of diflubenzuron are calculated by various solid state density function theory. Then, we analysis the crystal structure changes combined with vibrational frequency of diflubenzuron are. The results show that the solid state simulation is in good agreement with experimental calculation, and the B3LPY density function with 6-31G(d,p) calculation can achieve better results. The observed experimental spectral features of diflubenzuron mainly originate from the bond stretching vibration and the vibration of benzene ring of the symmetry molecule in crystalline cell.

8624-49, Session 4

Precise manipulation of the light properties in the optical domain by the RF technology (Invited Paper)

Tianxin Yang, Tianhe Wang, Zifei Wang, Chunfeng Ge, Dongfang Jia, Zhaoying Wang, Mei Sang, Tianjin Univ. (China)

No Abstract Available

8624-16, Session 5

Millimeter-wave and sub-millimeter-wave vacuum electronics amplifier development at the US Naval Research Laboratory (Invited Paper)

David K. Abe, Jeffrey P. Calame, Igor A. Chernyavskiy, Alan M. Cook, Simon Cooke, Colin D. Joye, Baruch Levush, John A. Pasour, Alexander N. Vlasov, U.S. Naval Research Lab. (United States); Khanh T. Nguyen, Dean E. Pershing, Beam-Wave Research, Inc. (United States); David P. Chernin, SAIC (United States)

We present an overview of the theoretical and experimental research activities at the Naval Research Laboratory in the area of millimeter-wave and sub-millimeter-wave vacuum electronics. Amplifier development ranging in frequency from 30 GHz to 670 GHz at power levels from multi-kilowatts to milliwatts will be described along with electron gun topologies that include single-, multiple-, and sheet electron beams. In addition, we will describe the development of a suite of physics-based, geometry-driven computational tools for electron gun and collector design, and the optimization and analysis of circuit structures for

klystrons and helix, coupled-cavity, and serpentine waveguide traveling-wave tubes.

* Work supported in part by the U.S. Office of Naval Research and by DARPA. Approved for Public Release, Distribution Unlimited. The views expressed are those of the author and do not reflect the official policy or position of the Department of Defense or the U.S. Government.

8624-17, Session 5

Integrated RF photonic devices based on crystal ion sliced lithium niobate

Vincent E. Stenger, James E. Toney, Andrea Pollick, James Busch, Jon Scholl, Peter Pontius, Sri Sriram, SRICO Inc. (United States)

This paper reports on the development of thin film lithium niobate (TFLNTM) electro-optic devices at SRICO. TFLNTM is formed on various substrates using a layer transfer process called crystal ion slicing. In the ion slicing process, light ions such as helium and hydrogen are implanted at a depth in a bulk seed wafer as determined by the implant energy. After wafer bonding to a suitable handle substrate, the implanted seed wafer is separated (sliced) at the implant depth using a wet etching or thermal splitting step. After annealing and polishing of the slice surface, the transferred film is bulk quality, retaining all the favorable properties of the bulk seed crystal. Ion slicing technology opens up a vast design space to produce lithium niobate electro-optic devices that were not possible using bulk substrates or physically deposited films. For broadband electro-optic modulation, TFLNTM is formed on RF friendly substrates to achieve impedance matched operation at up to 100 GHz or more. For narrowband RF filtering functions, a quasi-phase matched modulator is presented that incorporates domain engineering to implement periodic inversion of electro-optic phase. The thinness of the ferroelectric films makes it possible to in situ program the domains under a few tens of applied volts. A planar poled prism optical beam steering device is also presented that is suitable for optically switched true time delay architectures. Applications of the TFLNTM device technologies include high bandwidth fiber optic links, cellular antenna remoting, photonic microwave signal processing, optical switching and phase arrayed RADAR.

8624-18, Session 5

IMDD microwave photonic link modeling using Optsim

Joseph Haefner, Troy Copenhaver II, Jacob Kurka, Jessika West, Christopher Middlebrook, Michael Maurer, Michigan Technological Univ. (United States)

An intensity modulation direct detection RF photonic link using a dual output Mach-Zehnder modulator and a balanced detection scheme has been modeled and simulated. Validation of the model was performed by comparing the optical third-order intercept point, spur free dynamic range, and the gain results to actual provided industry measured output metrics. The model is highly accurate and provides the basis for demonstrating the RF photonics links performance as a function of varied input parameters such as power levels, detector performance, and varied fiber lengths. This allows the system designer to analyze performance parameters that are not possible in a laboratory environment. In addition the designer can analyze the performance of new and improved link designs without having to incur significant fabrication or manufacturing costs associated with prototypes. The link architecture and specific implementation challenges particular to the link are discussed. Performance comparisons are shown between the models to the theoretical calculations as well as to collected experimental data.

Conference 8624: Terahertz, RF, Millimeter, and Submillimeter-Wave Technology and Applications VI

8624-19, Session 5

Toward a widely tunable narrow linewidth RF source utilizing an integrated heterogenous silicon photonic module

Garrett A. Ejzak, David W. Grund Jr., Garrett J. Schneider, Janusz Murakowski, Shouyuan S. Shi, Dennis W. Prather, Univ. of Delaware (United States)

It is possible to generate RF signals from near DC to hundreds of GHz by mixing two lasers together. Through the use of a narrow-linewidth low-frequency oscillator, optical modulator, and injection locking, much higher frequency outputs can be produced that still retain the narrow linewidth of the low frequency oscillator. Here we focus on the design and implementation of an integrated device including photonic sources and modulators to realize the system described above. Specifically, we report on the creation and mixing of two tunable lasers on a silicon platform with a heterogeneously integrated gain medium realized in a III-V material system.

8624-20, Session 6

Towards integrated continuous-wave photomixing terahertz systems

Thorsten Göbel, Dennis Stanze, Ute Troppenz, Jochen Kreissl, Bernd Sartorius, Martin Schell, Fraunhofer-Institut für Nachrichtentechnik Heinrich-Hertz-Institut (Germany)

Within the last years, THz technologies became mature and ready for everyday use. Many applications have been demonstrated, but the industrial breakthrough has yet to come, though.

THz systems at the optical telecommunication wavelength of 1.5 μ m are most suitable to fulfill industry's demand for reliable and reasonable priced systems. Here, cw THz systems profit most from telecom technologies, since all required optical components are available off-the-shelf in high quality and at low price, and no fs-pulse laser is needed.

We present the next evolutionary step for cw THz photomixing: The transition from discrete components to Photonic Integrated Circuits (PICs). This will further increase mechanical stability and decrease size and costs.

Our PIC comprises two DFB-lasers and an optical phase modulator. A unique bidirectional operation technique allows driving THz emitter and detector at the same time and enables full control of the THz signal (amplitude, frequency and phase) via standard electronics, whereas the tuning of the laser wavelength (i.e. the THz frequency) is enabled by integrated heaters.

To evaluate the performance of our solution, we applied a coherent cw THz system i) fully driven by the integrated chip and ii) operated with discrete lasers and standard components. As the results show, both setups feature an identical signal-to-noise ratio, reaching 50dB @ 1 THz for an integration time of 200ms, which is the best reported performance of CW photomixing systems running at 1.5 μ m. Thus, this next generation device has the potential for the realization of low-cost THz systems in the future.

8624-21, Session 6

Widely-tunable opto-electronics oscillators based on a dual frequency laser

Jeremy Maxin, Grégoire Pillet, Loic Morvan, Daniel Dolfi, Thales Research & Technology (France); Khaldoun Saleh, Olivier Llopis, Lab. d'Analyse et d'Architecture des Systèmes (France)

Heterodyning of optical modes of a diode-pumped solid-state dual-frequency laser (DFL) is a simple way to generate optically carried

microwave signals for the distribution of signals in radar systems and the implementation of stable optoelectronic microwave oscillators. We present here the stabilization of the beatnote of an Er,Yb:glass DFL at 1.53 μ m with a double optical frequency locked loop (OFL).

Due to its structure, the DFL can be used as a voltage controlled oscillator (VCO) which generates a widely tunable microwave signal from 0 to 14 GHz by heterodyning its two orthogonally polarized optical modes. The optical beatnote is detected with three different high-speed photodiodes : the first one directly at the laser output, the second and the third one after respectively a short and a long optical fiber delay line (inducing two delays t_1 and t_2). The two delayed microwave signals are summed and then mixed with the first signal. The resulting error signal is injected through a baseband filter to the DFL frequency control input. This combination of two fibers take the advantages of both short and long delay.

With 100 m and 1000 m long optical fibers, the beatnote phase noise reaches a level of 240 dBc/Hz (respectively 290 dBc/Hz), at 10 Hz (respectively 10 kHz) from the carrier. It is a 80 dB improvement compared with the free-running beatnote. Since this architecture does not require an RF filter, this oscillator is tunable from 2 to 9 GHz, limited by the RF components of our frequency discriminator.

8624-22, Session 6

Study of carbon nanotubes using continuous-wave terahertz spectroscopy

Sujitha Puthukodan, Horacio L. Rivera, Univ. Carlos III de Madrid (Spain); Guillaume Ducournau, Jean-François Lampin, Univ. des Sciences et Technologies de Lille (France)

In past few years, Terahertz (THz) spectroscopic studies are making rapid development. Of the many techniques related to THz spectroscopy, Terahertz Time Domain spectroscopy (THz- TDS) is one of the common methods under study (Y. Ueno et al, 2008). Another method is Continuous Wave Terahertz (CW- THz) spectroscopy which is based on photomixing. This method offers advantages of frequency selectivity and much higher frequency resolution than THz- TDS (A. Roggenbuck et al, 2010). The millimeter-wave region of the electromagnetic spectrum is generally taken into consideration from the range of 30 GHz-300 GHz, while terahertz region is considered to be from 0.1 THz -10 THz. This leaves an overlap from 100 GHz- 300 GHz. Compared to THz- TDS, CW THz spectroscopy is compact, fast and relatively low- cost system (N. Karpowicz et al. 2005).

CNTs and graphene structures and their properties have been studied by several means such as photonic emission, microscopy etc. It shows that several physical parameters have characteristic resonant frequencies within THz range. Study of absorption and dispersion properties of the single walled and multi walled CNTs in the frequency range of 0.1 - 2 THz (H. Lamela et al, 2011). Along with other applications, CNTs have also been proposed for a lot of electronic device applications because of their unique properties (J.D. Chudow et al, 2012).

In this work, we like to extend our studies of CNTs using CW THz spectroscopy mainly due to the advantages offered by it. The optical and electrical properties will be studied in three different bands in the lower frequency range i.e. 140- 220 GHz, 220 – 325 GHz and 325- 500 GHz. The advantages offered are very good dynamic range (more than 80 dB) and very good frequency resolution. The work will be done in collaboration with IEMN, University of Lille, France and MNSL, University of Sungkyunkwan, Korea.

8624-23, Session 6

Continuous-wave terahertz reflection imaging of colorectal cancer

Pallavi Doradla, Univ. of Massachusetts Lowell (United States); Karim Alavi, Univ. of Massachusetts Medical School (United States); Cecil S. Joseph, Robert H. Giles, Univ. of Massachusetts

Lowell (United States)

Colorectal cancer is the third most commonly diagnosed cancer in the world. Many studies showed that there is a difference in bound and free water content between normal and cancerous tissue. The terahertz (THz) frequency range, located midway between the microwave and infrared region, is non-ionizing and has the potential to offer intrinsic contrast between normal and cancerous tissue due to its high sensitivity to water content. In this study, we show that continuous wave terahertz imaging offers a safe, noninvasive medical imaging modality for delineating colorectal cancers.

Human normal and cancer affected samples of colorectal tissue have been measured using continuous wave terahertz imaging techniques. Reflection measurements of ≈ 1 mm thick sections of colorectal cancerous tissues, mounted between two z-cut quartz slides, were obtained at a frequency of 584 GHz. A CO₂ pumped Far-Infrared molecular gas laser was used for illuminating the tissue while the reflected signals were detected using a liquid Helium cooled silicon bolometer. Two dimensional THz reflection images of both normal and cancerous colorectal tissues were acquired with a spatial resolution of 0.5 mm. Well contrast has been observed between cancerous and normal tissue at 584 GHz frequency. The resulting images were compared to the sample histology, and showed a correlation between reflection variation and cancerous region. Based on experimental analysis of colorectal tissues by THz imaging, we show that it is possible to distinguish between healthy and cancerous zones. However, the source mechanism behind this contrast is not completely understood. The results will be presented and discussed during SPIE conference.

8624-24, Session 6

Fine structure analysis of nanomaterials by CW terahertz spectroscopy

Anis Rahman, Aunik K. Rahman, Applied Research & Photonics, Inc. (United States); Nick J. Turro, Columbia Univ. (United States)

Terahertz spectrometry offers unique capabilities by exploiting the so called "terahertz gap" (~ 0.1 THz to a few tens of THz). T-ray can penetrate almost all non-metallic objects, thus allows an opportunity to study intrinsic properties of materials in their native environment. For this study a terahertz spectrometer (TeraSpectra, Applied Research & Photonics, Harrisburg, PA 17111) was used. Calibration of the spectrometer and a measurement scheme was carried out by means of the supplied front-end software. The Fourier transform process comprise of a number of different manifestations to suit the versatility of experiments. Further, built-in tools such as Prony frequency spectrum, auto regressive spectrum, and eigen analysis spectrum, allows one to learn details about the molecular properties such as the fine states of Fullerenes, chemical reactions, proteins and detergents in biopharmaceuticals, nanoparticle and ligand properties, label-free DNA hybridization and polymorphism, and others. The molecular motions of Fullerene C60 and Fullerenes encaging H2 and D2 have been investigated in the low wavenumber region. The encaging Fullerenes offer the opportunity of investigating the spin selectivity of the para and ortho H2 species, so that a stronger nuclear spin polarization may be produced. The present study demonstrates that terahertz spectra can clearly distinguish between the pure and encaging Fullerenes. The presence of different absorbance peaks identified by THz spectra suggests that this tool has sensitivity for detecting the spin isomers of H2 and D2 inside C60. Additionally, the increased number of observed peaks indicates that this method can detect the modes not visible in IR or Raman, yielding unique insight into uncharacterized host-guest interactions. Many of the states identified from THz spectra matches with theoretically predicted states of C60 including a number of degeneracies. These results will be discussed.

8624-25, Session 7

Sub-terahertz and terahertz detectors based on plasmon excitation in InGaAs/InP HEMT devices

Nima Nader Esfahani, Air Force Research Lab. (United States) and Solid State Scientific Corp. (United States) and Univ. of Central Florida (United States); Robert E. Peale, Univ. of Central Florida (United States); Walter R. Buchwald, Solid State Scientific Corp. (United States); Joshua Hendrickson, Justin W. Cleary, Air Force Research Lab. (United States)

Plasmons can be generated in the two dimensional electron gas (2DEG) of grating-gated high electron mobility transistors (HEMTs). Since the plasmon frequency at a given wavevector depends on sheet charge density, a gate bias can tune the plasmon resonance. In some cases, plasmon generation results in a resonant change in channel conductance, this effect allows a properly designed HEMT to be used as a voltage-tunable detector or filter. This work describes resonant response of such devices to sub-terahertz and terahertz radiation.

Previously, HEMT devices were fabricated with two grating periods of 10 and 0.5 μm . Large grating period will result plasmon absorptions in millimeter-wave region while the shorter period will shift absorptions to THz frequencies. Different parameters of these devices were obtained from measured IV-Curves and used to predict plasmonic transmission spectrum, this was also measured for THz devices at zero gate bias and strong evidence of plasmon absorptions were reported in frequencies predicted by theory, although clear absorption deeps were masked by low signal levels. Photoresponse of mm-wave device was also investigated previously in the frequency range of 78-103 GHz using backward wave oscillator (BWO) as radiation source.

In this work, we are using high power ultrastable BWO sources operating in range of 40-110 GHz along with wire-grid polarizer to study resonant photoresponse effect of the mm-wave HEMT device in broader frequency range and for different polarizations. We are also using FTIR spectrometer interfaced with an IR-microscope, liquid-He cooled Si-bolometer and cryostat to measure transmission spectra of the THz device for different gate biases. This system provides stronger and more stable Far-IR and THz radiation

8624-26, Session 7

Comparison between the electrical conductivity obtained by four-point probe method and terahertz time-domain spectroscopy in multi-walled carbon nanotubes and graphene for transparent thin-films

Dong-Mok Lee, Sungkyunkwan Univ. (Korea, Republic of); Ehsan Dadrastia, Univ. Carlos III de Madrid (Spain); Seunghyun Baik, Sungkyunkwan Univ. (Korea, Republic of); Horacio L. Rivera, Univ. Carlos III de Madrid (Spain); Mohan-Babu Kuppam, Frédéric Garet, Jean-Louis Coutaz, IMEP-LAHC (France)

Carbon nanotubes (CNTs) and graphene have been considered as an alternative material to Indium-Tin Oxide (ITO) for flexible transparent conductive films since it has unique electrical, optical and mechanical properties (Wu et al., 2004, Bae et al., 2010). CNTs and graphene have been also applied for other electronic devices and materials such as touch screens (Bae et al., 2010), conductive flexible adhesives (Ma et al., 2012), and field-effect transistor (Lee et al., 2010). In order to suggest electronic applications of carbon nanostructures, it is essential to evaluate electrical and optical properties more accurately. Until now, there is no study for electrical conductivity in CNTs and graphene by comparing the dc and terahertz frequency technique measurement.

Conference 8624: Terahertz, RF, Millimeter, and Submillimeter-Wave Technology and Applications VI

The four-point probe has been proven to be a convenient and precise tool for measuring the electrical conductivity of conductive thin-films (Smits, 1958, Chun et al., 2010). Terahertz time-domain spectroscopy (THz-TDS) provides an approach to measuring electric properties of multi-walled carbon nanotubes (MWNTs) thin-films from its electromagnetic absorption and dispersion over the frequency range 0.1-3THz due to the unique CNTs electronics and optical properties in terahertz range (Dresselhaus et al., 2001, Lamela et al., 2011).

In this work, we study the THz-TDS of MWNTs and graphene conductive transparent thin-films in comparison with the electrical conductivity obtained by the four-point probe method. The measured electrical conductivity of those films at terahertz frequency is evaluated with the values obtained by four-point probe method (dc frequency).

8624-27, Session 7

Surface conductivity responses of carbon nanostructures thin-films with contactless terahertz time-domain spectroscopy

Ehsan Dadrastia, Univ. Carlos III de Madrid (Spain); Dong-Mok Lee, Sungkyunkwan Univ. (Korea, Republic of); Horacio L. Rivera, Univ. Carlos III de Madrid (Spain); Seunghyun Baik, Sungkyunkwan Univ. (Korea, Republic of); Mohan-Babu Kuppam, Frédéric Garet, Jean-Louis Coutaz, IMEP-LAHC (France)

The nondestructive and contactless optoelectronic setups that generate and detect coherent terahertz electromagnetic waves like terahertz time-domain spectroscopy (THz-TDS) can characterize the precise absorption and dispersion properties of different materials at high frequencies (Jepsen et al., 2011). Due to the quick fast relaxation time and slow recombination time of carbon nanostructure and graphene, finding the optical and electrical properties using THz-TDS have been the forefronts of researches (Maeng et al., 2012, Liang et al., 2011, Lamela et al., 2011).

The surface conductivity, as outcomes of complex terahertz (THz) transmission, can provide a direct evaluation of the metallic treatment in carbon nanostructure thin-films (Wang et al., 2011). The main ongoing challenge still is getting and comparing the electrical surface conductivity of those carbon nanostructure thin samples in high frequency in order to apply them in the wide range of applications (Ziran et al., 2011).

Deposition of the carbon nanotubes thin-film on a gate insulator with a high dielectric permittivity, such as quartz, has the advantage that it does not degrade the perfect high-speed carrier transport of the carbon nanostructures. In this work, two multi-walled carbon nanotubes (thickness of less than 200nm) and the single-layer graphene (thickness 0.34nm) thin-films are deposited on the high transparent (absorption 8 cm⁻¹ at 2 THz) quartz substrates. We present a reasonable and reliable THz-TDS free contact nondestructive setup by analyzing complex transmission of the reference substrate and samples in order to compare the surface electrical conductivity responses of MWNTs and the single-layer graphene thin-films.

8624-28, Session 7

Frequency, amplitude, and phase measurements of GHz and THz sources using unstabilized THz frequency combs

Heiko Füsler, Mark Bieler, Physikalisch-Technische Bundesanstalt (Germany)

Technological progress at very high frequencies demands for a complete characterization of electromagnetic sources in the GHz and THz frequency range. Here, we demonstrate high-precision frequency measurements and spatially resolved amplitude and phase measurements of an antenna under test (AUT) using a THz frequency comb generated from an unstabilized femtosecond laser. Using this measurement setup, frequencies ranging from DC up to 30 THz (10.6

µm CO₂ laser line) can be detected. Additionally, we analyze electro-optic (EO) and photoconductive (PC) sampling regarding accuracy and invasiveness.

The measurement principle is based on heterodyne detection. The cw emission of the AUT is mixed with a comb line of a THz frequency comb. The latter is generated by rectifying an unstabilized optical comb (15 fs pulse duration, 800 nm central wavelength, 76 MHz repetition rate) employing either a PC switch or EO sampling. The mixing product is analyzed using digital data processing and compared to the mixing signal obtained from a reference antenna simultaneously measured in a second detection setup. The signal from the reference antenna allows us to eliminate the influence of fluctuations of the repetition rate of the optical comb and simultaneously yields a phase reference. Absolute frequency measurements with an accuracy of 9?10⁻¹⁴ as well as relative phase and amplitude measurements with standard deviations of ~1° and ~1%, respectively, are obtained. Comparing the emission pattern of the AUT taken in the near field we find that the invasiveness of EO sampling is considerably reduced as compared to PC sampling.

8624-48, Session PWed

Tunable THz wave transmission using liquid metal based devices

Rongguo Zhou, Jiangtao Cheng, Yuankun Lin, Hualiang Zhang, Univ. of North Texas (United States)

Due to the fact that many physical and chemical systems have specific fingerprints at the THz frequency band, THz technology has drawn a lot of attentions both in academia and industry. As a result of these efforts, many THz devices have been proposed and studied in the past ten years. Among these devices, THz plasmonic device becomes attractive since it offers unique capabilities for manipulating and guiding THz electromagnetic wave propagations. So far, different materials (both metallic and non-metallic materials) have been applied in THz plasmonic devices. However, it is still challenging (yet important) to realize an active control of the THz plasmonic devices. Very recently, liquid metals have been experimentally verified to be a suitable material for THz plasmonics. In this paper, we propose to combine liquid metals with the well developed electro-wetting technique to design tunable THz plasmonic devices. Specifically, the proposed devices will be used to achieve an active control of THz wave transmissions. Different THz plasmonic device configurations will be investigated. By applying electro-wetting controls, the key geometrical parameters of these devices including shapes, dimensions, and tilting angles can be tuned. In this way, different tunable THz plasmonic devices can be realized. For example, by varying the tilting angles, the operating frequency of the proposed THz device can be changed. To provide a design guideline for the proposed devices, systematic studies will be conducted. It is expected that the proposed liquid metal based tunable THz devices will pave the way towards the development of high performance THz systems.

8624-29, Session 8

Fabrication and characterization of suspended graphene membranes for miniature Golay cells (*Invited Paper*)

Elizabeth Ledwosinska, McGill Univ. (Canada); Abdeladim Guermoune, Mohamed Siaj, Univ. du Québec à Montréal (Canada) and Univ. Laval (Canada); Thomas Szkopek, McGill Univ. (Canada) and RQMP (Canada)

The development of miniaturized Golay cell arrays would enable the combination of the high sensitivity of a Golay cell with the imaging capability of focal plane arrays. The critical component of a miniaturized Golay cell is the deflecting membrane, which must simultaneously have a high breaking strength and a low flexural rigidity. Graphene suits this purpose ideally on account of its high strength and atomic thickness, in

Conference 8624: Terahertz, RF, Millimeter, and Submillimeter-Wave Technology and Applications VI

contrast with thicker polymeric membranes. Low flexural rigidity is critical to deflection sensitivity in response to temperature changes of the gas enclosed within a Golay cell scaled to the 10 μm to 100 μm scale. We report here a simple method for mass-fabrication of suspended graphene membranes suitable for focal plane arrays. The technique is based on chemical vapour deposition of graphene on copper, followed by a sacrificial etch of the copper substrate. By this organic-free technique, graphene can be suspended over 10 \times 20 μm apertures in copper thin films free of surface contamination and with high structural integrity. The quality of suspended graphene is verified by Raman spectroscopy, transmission electron microscopy and Auger spectroscopy. The cavities are sealed on the back-side with an indium film, to produce proof-of-principle miniature cells with a flexible, suspended graphene membrane. Atomic force microscopy enables the force versus deflection curve of a graphene-enclosed cell to be characterized. We further report the temperature dependent equilibrium deflection (up to 60°C) of a graphene-enclosed cell by atomic force microscopy measurements taken with heat directly applied to the cell substrate. We conclude our work with a future outlook on the development of practical graphene Golay cell arrays.

8624-30, Session 8

Design and fabrication of an RF GRIN lens using 3D printing technology

Jeffery W. Allen, Bae-lan Wu, Air Force Research Lab. (United States)

Electromagnetic media and metamaterials have been explored in frequency regimes ranging from the acoustic to the visible domain over the past decade. A large part of the design, fabrication and prototyping of such materials has been focused on planar structures and have been demonstrated primarily for certain propagation directions and/or defined polarization. Here we present the design of a focusing Gradient Index (GRIN) lens to operate RF frequencies that is not polarization constrained. We compare theoretical and experimental results from this lens designed to operate at X-band and fabricated using 3D printing technology to implement the effective medium. The lens with radially varying refractive index gradient was designed, optimized and analyzed by conducting full-wave simulations finite-element method based software Ansoft HFSS. The permittivity was estimated by effective medium theory and calculated by HFSS. The optimized design was used to fabricate the GRIN lens with isotropic, inhomogeneous dielectric material. The refractive index was designed to match the theoretical results using mixing ratio of air/voids and a polymer. Further, we used the refractive index profile to predict the rays' trajectories and focus length to compare them to those predicted by the FEM simulations. The field distributions were also analyzed to compare performance of the theoretical design to the fabricated lens and were found to be in good agreement with each other.

8624-31, Session 8

An FBG sensor interrogation technique based on a precise optical recirculating frequency shifter driven by RF signals

Zifei Wang, Tianxin Yang, Dongfang Jia, Zhaoying Wang, Mei Sang, Tianjin Univ. (China)

Fiber Bragg grating (FBG) sensors have numerous advantages to sense multi-physical quantities such as the temperature and strain simultaneously by monitoring the shift of the returned "Bragg" wavelength resulting from changes in these quantities. The fast and easy way to detect the wavelength shift is to use an expensive commercial optical spectrum analyzer (OSA) with high wavelength resolution. Several FBG interrogation systems have been set up using photo detectors instead of an optical spectrum analyzer (OSA) to convert wavelength to time measurements. However, in those systems, it is necessary to use mechanical tuning components, such as Fabry-perot (F-P) tunable filters,

to generate fast-speed wavelength-swept light sources for high-precise FBG interrogation. In this paper, a low-cost and ingenious wavelength-shift detection system, without any mechanical scanning parts, is proposed and demonstrated. The wavelength scanning system is a recirculating frequency shifter (RFS) which consists of an optical amplifier, an FBG sensor and an optical single-sideband (SSB) modulator driven by RF signals at 10 GHz. A gated optical pulse is produced by using another optical modulator, which is driven by square wave signals at hundreds of kHz, to modulate the output port of a narrow bandwidth light resource with a fixed wavelength, λ_0 . The gated pulse enters the RFS with the wavelength, λ_0 , and this wavelength can be shifted by, for example, 10 GHz, or 0.08 nm, equivalently, when the wave goes through the SSB modulator each time. In our wavelength interrogation system, the gated pulse which is assigned to recirculate in the RFS will not be ejected out of the circulations until its wavelength is shifted to the reflective wavelength of the FBG sensor. Afterwards, the gated pulse can be detected by a photo detector when it exits the RFS. The time delay or the number by which the gated pulse circulates in the RFS, can be recorded by a simple electric counter and is used to determine the reflective wavelength of the FBG sensor.

8624-32, Session 8

Enhanced terahertz emission from photoconductive emitters using plasmonic contact electrodes

Christopher W. Berry, Mohammed Reza Hashemi, Mona Jarrahi, Univ. of Michigan (United States)

Photoconductive emitters are one of the most commonly used sources of terahertz radiation. They consist of an ultrafast photoconductor connected to a terahertz antenna. When pumped by a femtosecond laser, an electrical current with terahertz frequency components is generated in the photoconductor and propagates to the terahertz antenna to radiate. To operate efficiently at terahertz frequencies, the majority of the photocarriers should be collected by the photoconductor contact electrodes within a sub-picosecond time scale. Considering the carrier drift velocities of the semiconductors used, only the carriers generated within 100-200 nm from the photoconductor contact electrodes will reach the electrodes within 1 ps. However, the requirements for the photoconductor active area and the capacitive loading to the terahertz radiating antenna impose much larger contact electrode spacings ($> 2 \mu\text{m}$) for conventional photoconductive terahertz emitters. To significantly reduce the photocarrier transport distance to photoconductor contact electrodes while maintaining a low capacitive loading to the antenna, we have employed two separated (not interdigitated) nano-scale plasmonic gratings as the photoconductor contact electrodes. Excitation of surface plasmon waves at the grating-semiconductor interface enables efficient transmission of the optical pump into the nano-scale photo-absorbing semiconductor active regions between the contact electrodes. It also results in a significant optical pump intensity enhancement in close proximity with the photoconductor contact electrodes. We have fabricated and experimentally compared the performance of photoconductive emitters with and without the plasmonic gratings under the same operation conditions and observed up to 50 times higher terahertz power levels when using the plasmonic gratings.

8624-33, Session 8

Organic electro-optic materials as a platform for widely tunable narrow linewidth RF sources

Stephen T. Kozacik, Maciej Murakowski, David Eng, Mathew J. Zablocki, Univ. of Delaware (United States); Ahmed S. Sharkawy, EM Photonics, Inc. (United States); Janusz Murakowski, Benjamin C. Olbricht, Shouyuan S. Shi, Dennis W. Prather, Univ. of Delaware (United States)

Conference 8624: Terahertz, RF, Millimeter, and Submillimeter-Wave Technology and Applications VI

Modern communications and RADAR applications require high frequency narrow linewidth sources. Optical generation of RF signals provides a method of producing sources meeting these specifications. The current state of the art method for generating these systems optically involve the use of two tunable lasers, an electro optic modulator, and a low frequency RF source. The two lasers are injection locked at the RF frequency difference by seeding one of the lasers with a sideband modulated onto the first laser. Organic electro optic materials, leveraging the Pockels effect, allows tunable lasers and electro optic modulators to be realized on a common substrate. Tunable lasers can be achieved by fabricating DBR lasers with either external or internal gain media and a grating formed out of organic electro optic material. By applying a voltage across a grating composed of electro optic material the refractive index can be modified, shifting the reflected wavelength of this grating, resulting in a widely tunable laser peak. An organic phase modulator can be used to generate the necessary sidebands. By utilizing polymer architecture it is possible to fabricate and transition the technology to flexible, conformal substrates.

8624-34, Session 8

Flat pulse-amplitude rational-harmonic-mode-locking fiber lasers with GHz pulse repetition rates

Tianhe Wang, Tianxin Yang, Dongfang Jia, Zhaoying Wang, Mei Sang, Tianjin Univ. (China); Neng Bai, Guifang Li, CREOL, The College of Optics and Photonics, Univ. of Central Florida (United States)

Generating high-speed electrical signals in the sub-millimeter band (hundreds of gigahertz (GHz)) by pure electrical methods is difficult. However, using a simple high-speed response photomixer or photodetector, continuous optical pulse trains (OPTs) with high pulse repetition rate (PRR) can be converted into electrical signals. The rational harmonic mode locking (RHML) in an active mode-locked fiber laser is effective in increasing the output optical PRR a number of times the modulation frequency at which an intracavity optical modulator, i.e., Mach-Zehnder optical modulator (MZOM), is driven by a GHz regime signal. However, the amplitudes of the output OPT in a high order RHML operation are not equalized and flat. The output OPT amplitudes profile is sinusoidal because the MZOM is driven by single frequency GHz sinusoidal-waves. For improving the flatness of the output OPT amplitudes, Ozharar used 1 GHz electrical negative impulse signals to drive the MZOM thus the transmission window of the MZOM is fully open during the most of the modulation cycle [1]. In this paper, a modified RHML technique using standard instrumentation generating 1 GHz electrical square-waves to accomplish RHML in fiber lasers with flat OPT at a PRR up to 12 GHz is presented. Setting the modulation bias voltage to the half-wave voltage of the MZOM and amplitude of the square-wave to the full-wave voltage of the MZOM, the transmission window can be kept fully open except when quickly shutdown at the rising and falling edges of the square-wave. An additional advantage is the PRR in our system is twice Ozharar's system when the same frequencies are applied to the MZOMs.

Reference:

[1] Ozharar, S.; Gee, S.; Quinlan, F.; Lee, S.; Delfyett, P. J.; Pulse-amplitude equalization by negative impulse modulation for rational harmonic mode locking, *Opt. Letts.* 31 (19), 2924-2926, 2006.

8624-35, Session 9

Metamaterial films as narrowband terahertz emitters

Brian T. Kearney, Fabio Alves, Dragoslav Grbovic, Gamani Karunasiri, Naval Postgraduate School (United States)

Continued progress in terahertz (THz) research has emphasized the need

for both improved THz sources and detectors. One simple solution to provide a narrowband THz illumination source is to use metamaterial absorbers as thermal emitters. We present emitters consisting of a 100 nm aluminum layer patterned into squares separated from a ground plane of aluminum by a thin layer of silicon oxide (<2 μm) fabricated using standard microfabrication techniques. These metamaterials were designed to emit in one, two, and three different bands of the 4-8 THz range and demonstrate clearly definable separate peaks with bandwidths of approximately 1 THz. Modifying the multiple band configurations can produce an extended single emission peak if desired. Single band emitters designed for 4.1, 5.4, and 7.8 THz were observed to emit, respectively, 11, 18, and 36 W/m² at 400 °C in accordance with Kirchhoff's law of thermal radiation. Coating a 4-inch wafer with these materials and heating it to 400 °C would produce an estimated 86, 145, and 280 mW of power, respectively. Additionally, emitted power increased linearly with temperature, as expected in the THz region for blackbody curves at temperatures above room temperature. Emissivity of the metamaterial did not change significantly when heated, indicating that the constituent materials did not significantly change their optical or geometric properties. Imaging of these structures with a microbolometer camera fitted with THz optics clearly showed the high emissivity of the metamaterial emitters compared to surrounding aluminum.

8624-36, Session 9

High-sensitivity metamaterial-based bi-material terahertz sensor

Fabio Alves, Dragoslav Grbovic, Brian Kearney, Gamani Karunasiri, Naval Postgraduate School (United States)

We report on the fabrication of a microelectromechanical systems (MEMS) bi-material terahertz (THz) detector integrated with a metamaterial structure to provide high absorption at 3.8 THz. The absorbing element of the sensor was designed with a resonant frequency that matches the quantum cascade laser illumination source, while simultaneously providing structural support, desired thermomechanical properties and optical read-out access. It consists of a periodic array of aluminum squares separated from a homogeneous aluminum (Al) ground plane by a silicon-rich silicon oxide (SiO_x) layer. The absorbing element is connected laterally to two Al/SiO_x microcantilevers (legs) anchored to a silicon substrate, which acts as a heat sink, allowing the sensor to return to its unperturbed position when excitation is terminated. The metamaterial structure absorbs the incident THz radiation and transfers the heat to the legs where the significant difference between thermal expansion coefficients of Al and SiO_x causes the structure to deform proportionally to the absorbed power. The amount of reflecting element bending is probed optically by measuring the displacement of a laser beam reflected on the Al ground plane. Measurement showed that the fabricated absorber has nearly 90% absorption at 3.8 THz. The responsivity and time constant can be controlled by the sensor design and the by the operating pressure. Preliminary results indicate that use of metamaterial absorbers allows for tuning the sensor response to the desired frequency to achieve high sensitivity and speed of operation required in real time THz imaging applications.

8624-37, Session 9

Numerical simulation of terahertz plasmons in gated graphene structures

Akira Satou, Victor Ryzhii, Tohoku Univ. (Japan); Fedir T. Vasko, Vladimir V. Mitin, Univ. at Buffalo (United States); Taiichi Otsuji, Tohoku Univ. (Japan)

Plasmons in graphene have attracted much attention recently for applications to electronic and optoelectronic devices in a wide range of radiation frequency between terahertz (THz) and visible. Especially, they are promising for compact, frequency-tunable terahertz sources and detectors that operate at room temperature, owing to long carrier

Conference 8624: Terahertz, RF, Millimeter, and Submillimeter-Wave Technology and Applications VI

relaxation time up to about 10 ps in clean monolayer graphene and, hence, to weak damping of plasmons even in the THz range.

In this paper, we study THz plasmons in monolayer graphene by numerical simulation. We develop a numerical model based on the quasi-classical Boltzmann equation for electron and hole transport with the Poisson equation for self-consistent electric field. We take into account different scattering mechanisms as collision integrals in the Boltzmann equation. We consider plasmons in different structures: gated graphene with reflective boundaries, graphene transistors with a gate and side contacts, and a periodic grating-gate structure. Also, we compare the approach developed here with the hydrodynamic approach developed previously.

We show that frequencies of plasmons are in the THz range and can be widely tuned by the applied gate voltages. We show that the characteristic damping time of plasmons by acoustic phonon scattering at room temperature is close to 10 ps and it increases as the carrier concentration decreases, due to the energy-dependent momentum relaxation time. Those results suggest that plasmons in graphene are feasible and promising for the realization of the THz devices at room temperature.

8624-39, Session 10

Efficient horn antennas for next-generation terahertz and millimeter-wave space telescopes

Darragh McCarthy, Neil Trappe, Anthony Murphy, Colm Bracken, Stephen Doherty, Marcin L. Gradziel, Cr  idhe O’Sullivan, National Univ. of Ireland, Maynooth (Ireland)

Astronomical observations in the far-infrared are critical for investigation of the early universe and the formation of planets, stars and galaxies. In the case of space telescope receivers a strong heritage exists for corrugated horn antenna feeds for coupling the astronomical signals to the detectors mounted in a waveguide or cavity structure. These have been utilized, for example, in the Planck satellite in both single-mode channels for the observation of the cosmic microwave background (CMB) and the multi-mode channels optimised for the detection of foreground sources. Looking to the demands of next generation space missions it is clear that the development of new alternative solutions for horn antenna structures will be required that are more appropriate for the large arrays envisaged in future projects. Horn antennas will continue to offer excellent control of beam properties for CMB polarisation experiments satisfying stringent requirements on low sidelobe levels, symmetric beams and low cross polarization in large arrays. Similarly for mid-infrared systems multi-mode waveguide structures will give high throughput to reach the required sensitivities.

In this paper we present a computationally efficient approach for modelling and optimising new horn designs. In particular we investigate smooth walled profiled horns with equivalent performance to the corrugated horns traditionally used for CMB measurements and we also report on the design and analysis of multi-mode horn coupled detectors for far-infrared astronomy. We discuss the horn optimisation process and the algorithms available to maximise performance parameters such as low cross polarisation, beam symmetry and high Gaussicity.

8624-40, Session 10

Low-loss waveguides for THz guidance and devices

Azizur Rahman, Christos Themistos, Kejalakshmy Namassivayane, Anita Quadir, City Univ. London (United Kingdom)

Although THz technology is emerging strongly, however, most of the present systems are free space based due to lack of low-loss waveguides. At this frequency range both dielectric and conductive losses of materials are high to design any suitable low-loss waveguides.

Recently, it has been shown that hollow-core metal clad waveguides [1,2] can support THz waves in the low-loss air-core. It is also shown that by optimizing a dielectric layer between the air-core and metal layer, waveguide loss can be minimised. Similarly, it has also been reported that photonic crystal fibres with many hollow air-holes can confine most of the power in the low-loss air region to reduce the overall propagation losses. Instead of a solid core, by incorporating porous core, loss in such waveguides can be significantly reduced. The development of low-loss THz guides is expected to provide impetus on the development of compact THz integrated circuits combining various functional devices.

Design optimization of such low-loss THz waveguides and devices will be presented by using rigorous full vectorial finite element based numerical approaches.

[1] C. Themistos, et al., “Characterization of Silver/Polystyrene (PS)-coated hollow glass waveguides at THz frequency”, *Journal Lightwave Technology*, vol. 25, pp. 2456-2462, 2007

[2] B. M. A. Rahman, et al., “Characterization of plasmonic modes in a low-loss dielectric coated hollow core rectangular waveguide at terahertz frequency”, *IEEE Photonics Journal*, 3, pp.1054-1066, Dec. 2011.

8624-41, Session 10

Ultra-broadband wavelength conversion sensor based upon thermochromic liquid crystals

I-Chun Anderson Chen, North Carolina State Univ. (United States); Dwight L. Woolard, U.S. Army Research Office (United States)

Wavelength conversion (WC) imaging was first introduced in the 1950’s as an alternative method of imaging emissions from infrared sources. It is achieved by converting the IR generated heat on an absorbing medium into a signal in the visible spectrum by using optically active thermotropic monomers. However, poor chemical stability, low thermal responsivity, and large supporting apparatuses made WC devices less attractive than their rapidly advancing semi-conductor counterparts. Today, many more thermotropic materials have emerged and combined with a mature semiconductor industry, have yet been leveraged in realizing the true potential of WC systems. In this work, commercial off-the-shelf screen (COTS) printed thermochromic liquid crystals (TLCs) have been explored to show a temperature coefficient $[\alpha]_{\text{opt}}$ of 10%/deg C at room temperature. This is nearly a two times increase in the highest performing resistive bolometer devices that are available today. And unlike micro-fabricated bolometer imaging arrays, these sensors do not require a capital investment in their fabrication, making them the ideal candidate for low-cost applications or augmenting the existing arsenal of imagers available for laser research groups requiring sensitivity across the visible to GHz spectrum. Results for improving image quality by means of drop-on-demand printing will also be discussed.

8624-42, Session 10

Antenna-coupled heterostructure field effect transistors for integrated terahertz heterodyne mixers

Alessandra Di Gaspare, Istituto di Fotonica e Nanotecnologie (Italy); Valeria Gilliberti, Univ. degli Studi di Roma La Sapienza (Italy) and Istituto di Fotonica e Nanotecnologie (Italy); Roberto Casini, Ennio Giovine, Istituto di Fotonica e Nanotecnologie (Italy); Florestanto Evangelisti, Univ. degli Studi di Roma Tre (Italy); Dominique Coquillat, Wojciech Knap, Univ. Montpellier 2 (France); Sergey Sadofev, Raffaella Calarco, Paul-Drude-Institut für Festkörperelektronik (Germany); Massimiliano Dispenza, Claudio Lanzieri, SELEX Sistemi Integrati S.p.A. (Italy); Michele Ortolani, Univ. degli Studi di Roma La Sapienza (Italy) and Istituto di Fotonica e Nanotecnologie (Italy)

Photonics applications of sub-millimeter waves (0.1-1.0 THz) require the development of a "terahertz camera" which could be used for real-time imaging at a long distance with millimeter-resolution and good penetration through the atmosphere and concealing materials, which cannot be obtained e.g. with infrared imaging and/or with RF metal detectors and body scanners. The use of active materials and device architectures compatible with electronic industrial processes would surely help the development of integrated electronic systems containing terahertz functionalities. High electron mobility transistors (HEMTs) can operate as direct detectors of radiation at frequency well beyond their cutoff frequency of tenths of GHz, due to the plasma wave oscillations at THz frequency present in the high-mobility two-dimensional electron gas which forms the active channel. The direct detection signal is a low-frequency signal proportional to the incoming terahertz radiation power, which is the result of the homodyne mixing of terahertz oscillations in the transistor channel induced by an antenna coupling. In this work we present the realization of a HEMT-based mixer realized on AlGaIn/GaN and AlGaAs/InGaAs heterostructure materials. A novel design enabling the mixing of THz oscillations on the two device ports, hence usable for high-resolution heterodyne spectroscopy, is proposed. Excitation of currents into the HEMT channel with deeply subwavelength dimensions (8x8 microns) was obtained by the on-chip integration of planar bow-tie antennas and a substrate lens. Spectral analysis at 0.18-0.72 THz provided conversion efficiency of the order of 300 V/W and noise equivalent power of 1 nW/Hz^{0.5}.

8624-43, Session 10

Realization of an ultra-broadband voltage pulse standard utilizing time-domain optoelectronic techniques

Mark Bieler, Heiko Fuser, Physikalisch-Technische Bundesanstalt (Germany)

Femtosecond optoelectronic techniques are routinely employed for the generation and detection of ultrashort voltage pulses. However, so far, not much effort has been spent to determine the exact shape of such voltage pulses over a very broad frequency range. For this purpose, i.e., for the realization of a voltage pulse standard, it is essential to (i) fully know the transfer function of the detection and (ii) be able to separate forward and backward propagating signals from each other. Here we report the realization of a voltage pulse standard with frequency components exceeding 500 GHz and a 500 MHz frequency spacing.

Experiments are performed on a 4-mm long coplanar waveguide (CPW) evaporated onto low-temperature-grown GaAs. The ultrashort voltage pulses are generated by focusing a femtosecond laser beam (~800 nm center wavelength) onto a photoconductive gap that is integrated into the CPW. A second laser beam (~1600 nm center wavelength), which is synchronized to the first laser beam, is used to measure the electric field of the voltage pulses by employing the electro-optic effect of the

GaAs substrate. We obtain the transfer function of the EO detection by comparing the EO signal from probe pulses which propagate once and twice through the electric-field region of the voltage pulses. The separation of forward and backward propagating signals is accomplished by measuring the voltage pulses at different positions on the CPW. Our techniques are applicable to any termination of the CPW. As an application example we characterize a coplanar-coaxial microwave probe.

8624-44, Session 11

Electric field sensor based on electro-optic polymer refilled silicon slot waveguide

Xingyu Zhang, The Univ. of Texas at Austin (United States); Amir Hosseini, Omega Optics, Inc. (United States); Ray Chen, The Univ. of Texas at Austin (United States)

Electric field measurements play a crucial role in various scientific and technical areas, including process control, electric field monitoring in medical apparatuses, ballistic control, electromagnetic compatibility measurements, microwave integrated circuit testing, and detection of directional energy weapon attack. Conventional electronic electric field measurement systems currently use active metallic probes, which can disturb the measured electromagnetic field and make sensor sensitive to electromagnetic noise. Photonic electric field sensors, on the other hand, are compact in size and achieve broad bandwidth operation with minimal disturbance to the field to be measured. In this paper, we present the design, fabrication and characterization of an antenna-coupled photonic crystal waveguide (PCW) based electric field sensor. An electro-optic (EO) polymer with a large r_{33} (>100pm/V) is used to refill the PCW slot and air holes. Butterfly-shaped electrodes are used as both poling electrodes and as receiving antenna. The slow-light effect in the PCW is used to increase the effective in-device r_{33} >500pm/V. The slot waveguide is designed for maximum poling efficiency as well as optical mode confinement inside the EO polymer. The antenna is designed for operation at 10GHz.

8624-45, Session 11

Technological customization of uncooled amorphous silicon microbolometer for THz real-time imaging

Stephane Pocas, Pierre Imperinetti, Pierre Brianceau, Jérôme Meilhan, Francois Simoens, Wilfried Rabaud, Agnes Arnaud, CEA-LETI-Minatec (France)

Terahertz uncooled antenna-coupled microbolometer focal plane arrays are being developed at CEA Leti for real time THz imaging and sensing. This detector relies on LETI amorphous silicon bolometer technology that has been deeply modified to optimize sensitivity in THz range. Main technological key lock of the pixel structure is the quarter wavelength cavity that consists in a thick dielectric layer deposited over the metalized CMOS wafer, improving significantly the optical coupling efficiency. Copper plugs connect the microbolometer level down to the CMOS readout circuit (ROIC) upper metal pads through this thick dielectric cavity. This paper explains how we improved the copper vias technology and the challenges we faced to customize the microbolometer while keeping a monolithically above IC technology fully compatible with standard silicon processes. The results show a very good operability and reproducibility of the contact through this thick oxide cavity. These good results permit to realize real time imaging with a good sensitivity to THz frequencies.

8624-46, Session 11

Generation of frequency tunable and broadband THz pulses in the frequency range 1-20 THz with organic electro-optic crystals OH1 and DSTMS

Mojca Jazbinsek, Tobias Bach, Blanca Ruiz, Carolina Medrano, Peter Günter, Rainbow Photonics AG (Switzerland)

Organic electro-optic crystals are efficient THz-wave generators using optical rectification (OR) or difference-frequency generation (DFG) of various fs–ns pump laser sources in the infrared, which is due to their higher second-order susceptibilities compared to inorganics, combined with phase-matching possibilities [1–3]. We investigate THz interactions using recently developed new materials, stilbazolium salt DSTMS*, which is a recently developed material with improved properties as compared to the more commonly used DAST* crystals, as well as phenolic polyene OH1*, which is a novel hydrogen bonded crystal and an important alternative for stilbazolium salts due to the low THz absorption and even better figures of merit for THz wave generation.

Best phase-matching parameters of these materials for pump optical wavelengths in the range of 800–1600 nm and for THz frequencies in the range of 0.1–12 THz have been determined. We demonstrate efficient generation and coherent detection of very broadband THz pulses (0.1–12 THz) using these materials, pumped by fs fiber lasers at telecommunication wavelengths, and show its use for THz time-domain spectroscopy, imaging and material testing. In another set-up, tunable THz waves for remote sensing have been realized using difference frequency generation of the signal and idler wavelengths of a BBO based optical parametric oscillator. THz pulses with frequencies 1–20 THz and a bandwidth of less than 100 GHz are produced via a difference frequency generation (DFG) process by mixing two infrared waves in OH1 and DSTMS.

*DSTMS (4-N,N-dimethylamino-4'-N'-methyl-stilbazolium 2,4,6-trimethylbenzenesulfonate);

DAST (4-N,N-dimethylamino-4'-N'-methyl-stilbazolium tosylate);

OH1 (2-(3-(4-hydroxystyryl)-5,5-dimethylcyclohex-2-enylidene) malononitrile).

[1] X. Zheng et al, J. Nanoelectron. Optoelectron. 2, 1, 2007

[2] I. Katayama et al, Appl. Phys. Lett. 97, 021105, 2010

[3] A. Schneider et al, J. Opt. Soc. Am. B 23, 1822, 2006

8624-47, Session 11

THz emission as a probe for silicon-based multilayer systems

Ulrike Blumröder, Friedrich-Schiller-Univ. Jena (Germany); Patrick Hoyer, Fraunhofer-Gesellschaft (Germany); Gabor Matthäus, Kevin Füchsel, Friedrich-Schiller-Univ. Jena (Germany); Andreas Tünnermann, Stefan Nolte, Fraunhofer-Institut für Angewandte Optik und Feinmechanik (Germany) and Friedrich-Schiller-Univ. Jena (Germany)

We applied THz emission spectroscopy as a non-destructive and contact free method for the examination of silicon surfaces used in the fabrication of solar cell devices. The THz emission is mainly dominated by the acceleration of the photogenerated carriers within the electrical fields present at the silicon surface.

Silicon is still the most established semiconductor for optoelectronic devices and dominates the world market of solar cell materials. Especially nanostructured silicon surfaces are of growing interest in solar cell device fabrication.

We investigated semiconductor-insulator-semiconductor (SIS) solar cells build up on silicon and nanostructured silicon.

It was recently demonstrated that nanostructured silicon surfaces (so called “Black Silicon” (BS)) are capable to generate THz radiation approximately two orders of magnitude higher than unstructured silicon. The THz emission from BS is mainly dominated by the photo-Dember effect as found for moderately doped wafers.

In case of a SIS-system that shows a photovoltaic behavior a pseudo pn-junction is formed at the silicon surface.

In opposite to improperly processed SIS-systems or Black Silicon the acceleration of photogenerated electrons and holes is dominated by the electric potential at the boundary zone which results in a flipping of the THz polarity.

The results can be transferred to other coated silicon surfaces as long as depletion or enhancement zones are present at the semiconductor interface.

Conference 8625: Gallium Nitride Materials and Devices VIII

Monday - Thursday 4 -7 February 2013

Part of Proceedings of SPIE Vol. 8625 Gallium Nitride Materials and Devices VIII

8625-1, Session 1

Application of DERI method to InN/InGaN MQW, thick InGaN and InGaN/InGaN MQW structure growth (*Invited Paper*)

Tomohiro Yamaguchi, Kogakuin Univ. (Japan); Ke Wang, Tsutomu Araki, Ritsumeikan Univ. (Japan); Tohru Honda, Kogakuin Univ. (Japan); Euijoon Yoon, Seoul National Univ. (Korea, Republic of); Yasushi Nanishi, Ritsumeikan Univ. (Japan) and Seoul National Univ. (Korea, Republic of)

We have proposed a new RF-MBE method called DERI (droplet elimination by radical-beam irradiation) for obtaining high-quality InN-based III-nitride films. The DERI method consists of two series of growth processes; metal-rich growth process (MRGP) in the growth under a metal-rich condition and droplet elimination process (DEP) in the growth with consecutive nitrogen radical beam irradiation. This method has realized a reproducible growth, since the appearance and elimination of excess metal can be simply monitored and controlled using in-situ RHEED and laser reflection.

In the growth of InGaN, Ga was preferentially captured from excess Ga/In wetting layer and droplets in MRGP. Then, In was preferentially swept out from the growing InGaN surface. The swept In was eliminated by transforming to InN epitaxially on InGaN in DEP. Repeating this process, InN/InGaN MQW structure was successfully fabricated.

Although phase separation should become a very serious problem for the growth of thick and uniform InGaN, uniform InGaN was successfully obtained without phase separation by keeping constant Ga beam supply even during DEP. When Ga/N* beam supply ratio was changed in DEP from that in MRGP, InGaN/InGaN MQW structure was successfully fabricated. Possible mechanism to explain these successful results including not only thick InGaN film but also InGaN/InGaN MQW will be demonstrated.

This work was partly supported by ALCA project of JST, MEXT through Grant-in-Aids for Scientific Research (A) #21246004 and WCU program of MSE at Seoul National University (R31-2008-000-10075-0). One of the authors (T. Y.) was also supported by TEPCO Memorial Foundation.

8625-2, Session 1

Semipolar GaN growth on patterned sapphire substrates by hydride vapor phase epitaxy (*Invited Paper*)

Kazuyuki Tadatomo, Narihito Okada, Keisuke Yamane, Hiroshi Furuya, Yamaguchi Univ. (Japan)

It is well-known that the commercialized GaN-based LEDs fabricated on a polar c-plane GaN layer are under the quantum-confined Stark effect (QCSE). The QCSE causes band bending in InGaN quantum well and is one of the reasons to decrease the internal quantum efficiency (IQE) especially at long wavelength region and to cause so-called "green-gap problem". The QCSE may be one of the possible suspected origins of "efficiency droop phenomenon" at the high injection current density. To overcome these problems, the GaN-LEDs fabricated on nonpolar or semipolar GaN layer, such as {20-21} plane, have been investigated. Therefore, it is eager to develop the nonpolar and semipolar GaN substrate. However, effective methods to fabricate the substrates with high-quality and large-diameter are still under investigation. This paper presents the growth of thick semipolar GaN layers on patterned sapphire substrates (PSSs) by hydride vapor phase epitaxy (HVPE) to realize a high-quality free-standing GaN substrate with large diameter.

We prepared 2 inch {10-11}, {11-22}, and {20-21} plane GaN layers grown by metal organic vapor phase epitaxy (MOVPE) on n, r, and {22-43} plane PSSs, respectively, as templates for the HVPE growth. The HVPE growth

was performed on these templates at the reactor temperature of 1040°C with the growth rate of approximate 70 $\mu\text{m}/\text{h}$. Dislocation densities of the MOVPE- and the HVPE-grown GaN layers on the PSSs were measured by the plan-view cathodeluminescence (CL). While dark spots of the CL images were linearly aligned in the MOVPE-grown surface, they were distributed on the HVPE-grown surface. The thickness dependence of the dislocation density is well explained by the fitting curves derived from the reference [1]. The reduction rate of the dislocation density of {11-22} and {20-21} planes were lower than that of c-plane. But, the reduction rate of the dislocation density of {10-11} plane GaN layer was drastically decreased over 100- μm -thickness.

In summary, we demonstrated HVPE growth of semipolar GaN layers on the PSS, which has the possibility to realize a large-sized and high-quality semipolar GaN substrate.

Reference:

[1] S.K. Mathis et al., J. Cryst. Growth, 231, (2001) 371.

8625-3, Session 1

Ordering in InGaN, AlInN, and AlGaIn alloys (*Invited Paper*)

Jacek A. Majewski, Michal Lopuszynski, Univ. of Warsaw (Poland)

We present results of theoretical studies that shed light on the longstanding problem of composition fluctuations in nitride alloys. This issue has been debated for a long time, especially in the context of indium clustering, since it is of great importance for performance of optoelectronic devices. However, in spite of intensive experimental and theoretical works, the degree of structural ordering in nitride alloys has not been clarified satisfactorily yet (see, e.g., [1,2] and references therein). First, we analyze short-range [3] and long-range [4] ordering (SRO and LRO, respectively) on the zinc-blende cationic sublattice in bulk nitride ternary alloys, $\text{Ga}_x\text{In}_{1-x}\text{N}$, $\text{Al}_x\text{In}_{1-x}\text{N}$, and $\text{Al}_x\text{Ga}_{1-x}\text{N}$. This comprehensive analysis is based on Monte Carlo calculations within the NVT ensemble (see [5] for details), covers the whole range of concentrations, and temperatures from 873 K up to 1673 K.

It turns out that for In containing alloys (i.e., $\text{Ga}_x\text{In}_{1-x}\text{N}$ and $\text{Al}_x\text{In}_{1-x}\text{N}$), the considerable degree of SRO occurs as quantified by Warren-Cowley short range order parameter $\gamma_{AB}^{(i)}$. For indium atoms on the first and fourth coordination shells, there is a small preference to anti-clustering, whereas on the second and third coordination shells, the small In-In neighboring preference is observed. On the contrary, for $\text{Al}_x\text{Ga}_{1-x}\text{N}$ alloy, any kind of short range order is negligible. Also, we do not observe any long range ordering for all three alloys studied.

However, the nitride alloys in the active regions of optoelectronic devices quite often experience the biaxial strain induced by epitaxial growth on a substrate. We study influence of the biaxial strain on the ordering phenomena focusing on the most relevant technologically $\text{Ga}_x\text{In}_{1-x}\text{N}$ alloy and consider the magnitudes of the biaxial strain in this alloy that would result from the growth on fairly well lattice matched substrates, such as AlN, GaN, InN, ZnO, CaO, and SiC.

It turns out that the for smaller magnitudes of biaxial strain, the ordering of Ga and In atoms on cationic sublattice is qualitatively very similar to the bulk case, (i.e., only weak SRO occurs and there is no LRO). Interestingly, the larger biaxial strain triggers the long-range order. The observed ordering patterns of cations

include the chalcopyrite structure and development of planes parallel or perpendicular to the substrate, which can be considered as a certain mode of phase separation.

References: newline

[1] T. P. Bartel, P. Specht, J. C. Ho, C. Kisielowski, Philos. Mag. textbf{87}, 1983 (2007). newline

[2] C. J. Humphreys, Philos. Mag. textbf{87}, 1971 (2007). newline

[3] S. V. Dudiy, A Zunger, Phys. Rev. B textbf{68}, 41302 (2003). newline

**Conference 8625:
Gallium Nitride Materials and Devices VIII**

[4] L. Bellaiche, A. Zunger, Phys. Rev. B **57**, 4425 (1998). [newline](#)
 [5] M. {L}opuszy{‘n}ski, J. A. Majewski, Phys. Rev. B **85**, 035211 (2012).

8625-4, Session 1

GaN on Si and strain control (*Invited Paper*)

Alois J. Krost, Otto-von-Guericke-Univ. Magdeburg (Germany)

For a long time GaN growth on silicon was considered not being competitive and rather an exotic system as compared to GaN growth on sapphire or SiC. Especially, the cracking issue due to a huge thermal mismatch between GaN and silicon seemed to be a too serious problem for growing device quality layers. Meanwhile GaN-on-Si(111) has become a mainstream technology at least for microwave applications making use of AlGaN/GaN FETs; high voltage, high power GaN-based FETs on Si is one of the hottest topics now. Furthermore, several big companies have announced breakthroughs in GaN-on-Si-based high-power LEDs aimed for general lighting. E.g., Osram Opto1 achieved an optical power of 634 mW at 3.15 V, equivalent to 58% efficiency and prototype white LEDs with 140 lumen at 350 mA with an efficiency of 127 lm/W at 4500 K.

For such application thick, high-quality structures with highly conducting n-type layers are required which is a major challenge because of doping with Si leads to additional thermal stress. The latter can be overcome by Ge-doping instead of Si-doping. An upcoming difficulty for large diameter wafers is the mechanical weakness of Si at high temperature which may lead to plastic wafer deformation.

We show ways to control stresses and strains in GaN heteroepitaxy to achieve crack-free, device-relevant GaN layers on Si. An emerging field is the growth on Si(001) and of semipolar GaN on high-index Si(h11) substrates.

[1] P. Stauss, SPIE Photonics West, San Francisco, 2012

8625-5, Session 1

Crack-free growth of InGaN/GaN quantum-well structures on Si substrate with temperature-graded AlN buffer deposition

Chih-Yen Chen, Yen-Hung Liu, Wen-Ming Chang, Wei-Lun Chung, Chieh Hsieh, Che-Hao Liao, Horng-Shyang Chen, Chih-Chung Yang, National Taiwan Univ. (Taiwan)

Crack-free growth is the first key issue in depositing nitride compounds on Si substrate before various devices can be implemented. Here, we demonstrate the growth of crack-free InGaN/GaN quantum-well (QW) structures on Si (111) substrate based on a novel buffer method of temperature-graded growth of AlN. This buffer effectively produces a thermal compressive stress in the epitaxial layer during high-temperature growth such that it can compensate the tensile stress induced during sample cooling down. By combining with an inter-layer structure of three-period GaN/AlN superlattice, crack-free growths of thick GaN layers and InGaN/GaN QW structures are achieved. The results of Raman scattering show that a larger number of graded temperatures in depositing the AlN buffer layer leads to a weaker residual stress at room temperature. Transmission electron microscopy is used for showing that in a sample of a lower residual stress level, the threading dislocation density is lower. Also the strain state analysis method is used to calibrate the indium contents of the samples with various residual stresses. It is demonstrated that a sample with a weaker residual stress has lower indium content. This trend is consistent with that from X-ray diffraction measurement. Photoluminescence measurement also illustrates different emission characteristics when the residual stresses are different among different samples. A sample of a weaker residual stress has a shorter emission wavelength. However, it has a higher emission internal quantum efficiency.

8625-6, Session 2

Effect of Internally Focused Laser Processing of Sapphire Substrate on Bowing Management for III-Nitride Epitaxy (*Invited Paper*)

Hideo Aida, Namiki Precision Jewel Co., Ltd. (Japan); Hitoshi Hoshino, DISCO HI-TEC EUROPE GmbH (Germany); Hidetoshi Takeda, Namiki Precision Jewel Co., Ltd. (Japan); Chikara Aikawa, Disco Corp. (Japan); Natsuko Aota, Namiki Precision Jewel Co., Ltd. (Japan); Keiji Honjo, Disco Corp. (Japan)

Sapphire is the most common and important substrate for growing epitaxial III-nitride devices such as light emitting diodes (LEDs). However, the substrates often bow during and after epitaxy due to the large mismatch in the lattice constants and thermal expansion coefficients of the sapphire and nitrides. Therefore, the development of a new technique to manage the bowing of the III-nitride/sapphire system is highly desired. There are two main areas in which bowing control is required: controlling the initial bow of the sapphire substrate and reducing the bow after epitaxy.

As one possible approach, we have developed a unique new technique: internally focused laser processing. The wide-range control of the substrate bowing was achieved by inducing volume expansion effects due to the phase change from single-crystalline sapphire to amorphous with the laser treatment. For the initial bow control, a ~250 μm pre-bowed sapphire substrate in any direction (concave or convex) was demonstrated. The effect of the pre-bowed substrate on III-nitride epitaxy was also experimentally verified with an in situ curvature monitoring system during the III-nitride epitaxy. The same technique applied to the substrate after epitaxy successfully flattened the substrate for a subsequent chip-fabrication process. The effect of flattening on the back-thinning process was also experimentally confirmed.

This new approach gives us wide flexibility in the design engineering of epitaxial and device fabrication processes and thus accelerates the realization of larger diameter device processes with III-nitride/sapphire. Details of the technique will be given in this presentation.

8625-7, Session 2

Growth of high quality AlN layer and its polarity control by LPE using Ga-Al flux (*Invited Paper*)

Hiroyuki Fukuyama, Masayoshi Adachi, Mari Takasugi, Tohoku Univ. (Japan); Masashi Sugiyama, Akikazu Tanaka, Sumitomo Metal Mining Co., Ltd. (Japan)

AlN is a promising substrate material for AlGaN-based UV-LEDs, because of its high thermal conductivity and high ultraviolet transmittance, and its small lattice mismatch with AlGaN. The growth of AlN on sapphire substrates should be further improved to satisfy the increasing demand for large-size sapphire substrates. In our group, high-quality AlN thin films were fabricated by nitriding sapphire using the N₂-CO gas mixture¹). Using this nitrided sapphire substrate as a template, we have developed a new liquid phase epitaxy (LPE) process^{2, 3}). In the LPE method, an AlN layer was successfully grown on the nitrided sapphire using a Ga-Al flux at 1573 K. In contrast with other LPE processes, our LPE process does not require high growth temperatures or high pressures.

In recent studies, the FWHM values of (0002) and (10-12) x-ray rocking curve for the LPE AlN layer formed on the nitrided sapphire were 220 and 378 arcsec, respectively. An edge-type threading dislocation was dominant in the AlN layer, and its density was estimated to be as low as 10⁹ cm⁻² from the FWHM values. The convergent-beam electron diffraction (CBED) analysis showed that the LPE layer had Al-polarity, even though the nitrided sapphire layer had N-polarity. Thus, the polarity inversion arose at the interface between the nitrided sapphire layer and the LPE layer. The oxygen partial pressure in the nitrogen gas plays an

**Conference 8625:
Gallium Nitride Materials and Devices VIII**

important role in the polarity inversion in the LPE growth. The details of the polarity inversion will be presented in the conference.

Reference

- [1] H. Fukuyama et al., J. Appl. Phys., 100 (2010) 043905.
- [2] M. Adachi et al., Phys. Stat. Sol. (a), 208 (2011) 1494.
- [3] M. Adachi et al., Mater. Trans., 53 (2012) 1295.

8625-8, Session 2

Role and influence of impurities on GaN crystal grown from liquid solution under high nitrogen pressure in multi-feed-seed configuration

Michał Bockowski, Institute of High Pressure Physics (Poland) and TopGaN Ltd. (Poland)

It is well known that the High Nitrogen Pressure Solution (HNPS) growth method allows obtaining high quality GaN crystals. Recently, the multi-feed-seed (MFS) configuration for this method has been developed. That configuration is based on the conversion of a free-standing HVPE-GaN crystal to the free-standing, pressure grown HNPS-GaN of much higher quality than the seeds. In this paper the role and the influence of impurities such as oxygen, indium, magnesium and beryllium on HNPS-GaN will be presented and discussed in details. The differences in properties of differently doped GaN crystals will be shown.

The crystallization of HNPS-GaN in MFS configuration without an intentional doping results in growth of strongly n-type crystals with free electron concentration increasing in the function of growth temperature (from $2 \times 10^{19} \text{ cm}^{-3}$ for 1300°C to $6 \times 10^{19} \text{ cm}^{-3}$ for 1500°C). Higher concentration ($1 \times 10^{20} \text{ cm}^{-3}$) can be obtained, if indium impurities are added to the gallium solution. High free electron concentration in HNPS-GaN is associated with high oxygen concentration in the material. It will be shown that nitrogen vacancies can also play a crucial role.

The oxygen impurities in the HNPS-GaN crystals can be compensated by magnesium. Then, highly resistive crystals with stable electrical properties against annealing and time are obtained. In this case the crystallization process proceeds on (000-1) GaN surface instead of (0001) surface typical for n-type HNPS-GaN growth. It can be thus suggested that polarity of the GaN seed surface is determined and controlled by the gallium solution and its impurities. Beryllium doping confirms that hypothesis.

8625-9, Session 2

Progress on purity, transparency and thermal conductivity of GaN substrates obtained by ammonothermal method

Marcin Zajac, Roman Doradzinski, Robert Dwilinski, Romuald Stankiewicz, Robert Kucharski, Ammono Sp. z o.o. (Poland); Piotr Wilinski, Ammono Sp. z o.o. (Poland); Andrzej Jezowski, Institute of Low Temperature and Structure Research, Polish Academy of Science (Poland)

The ammonothermal method is regarded as one of the key technologies of bulk GaN substrates manufacturing. It enables growth of large diameter crystals of high crystalline quality and low dislocation density. The current diameter of GaN substrates surpasses 2-inch.

Firstly developed n-type ammonothermal GaN substrates were highly conductive. A material of high crystalline quality, electron concentration of about 10^{19} cm^{-3} and resistivity $10^{-3} - 10^{-2} \text{ } \Omega \cdot \text{cm}$ was achieved. These highly-conductive substrates are excellent for manufacturing of high power laser diodes [1]. However, described advantages of ammonothermal substrates should be combined with high transmission in visible spectral range and high thermal conductivity. The transparency

is crucial especially for light emitting diodes (LEDs) grown on such substrates, since outgoing light is extracted through the substrate and loss of output power related to the substrate absorption should be minimized. Therefore, in this communication, the recent progress on purity, transparency and thermal conductivity of bulk substrates grown by ammonothermal method (in ammonobasic environment) will be presented.

Special innovative technological procedures were applied in order to reduce impurity content, resulting in oxygen concentration of about $5 \times 10^{17} \text{ cm}^{-3}$ and transition metal concentration of about 10^{16} cm^{-3} . Lower concentration of impurities leads to a reduction of free carrier and impurity absorption bands, yielding finally to a decrease by several times of absorption coefficient to very few cm^{-1} at 450 nm (as compared to highly conductive substrates). This higher transparency material has got a lower electron concentration (of the order of 10^{17} cm^{-3}) and the highest thermal conductivity at 300K, which is increasing with a reduce of donor and acceptor content. It should be stressed that dislocation density ($< 5 \times 10^4 \text{ cm}^{-2}$), crystalline properties and resistivity remains at the same level.

To conclude, we present a new type of n-type ammonothermal substrate of low absorption and high thermal conductivity level, especially dedicated for high brightness LED and electronic devices production.

- [1] P. Perlin et al., Appl. Phys. Express 4, 062103 (2011).

8625-10, Session 2

HVPE-GaN growth on ammonothermal GaN crystals

Tomasz Sochacki, Institute of High Pressure Physics (Poland)

The HVPE technology is the most common approach for manufacturing GaN substrates. This technique gives a possibility to crystallize GaN with relatively fast growth rate (even up to $500 \text{ } \mu\text{m/h}$). The HVPE is based on crystallization of GaN from the vapor phase on foreign substrates. The significant differences between the lattice constant and thermal expansion coefficient of the foreign substrate and the HVPE-GaN film leads to lattice bowing and threading dislocation density in the new grown material. Therefore, a good solution seems to use ammonothermal GaN crystals, GaN grown from solution in supercritical ammonia (A-GaN), as seeds for the HVPE crystallization. The quality of A-GaN is very high in terms of flatness, threading dislocation density and uniformity of electrical properties.

In this work, the HVPE crystallization on the A-GaN crystals is described. Preparation of the (0001) surfaces of 1 in. A-GaN crystals is presented. The HVPE growth conditions are demonstrated. Smooth GaN layers of good crystalline quality, up to 1 mm thick, without cracks, and with dislocation density lower than 10^6 cm^{-2} are shown. Some details of mechanism of the HVPE crystallization are discussed. Morphology of the new grown material is shown. An influence of free carrier concentration in the initial substrate on quality, rate and mode of growth by the HVPE is determined. Results of a single and multi-growth run are presented and compared to the homoepitaxial HVPE crystallization on the free-standing HVPE-GaN crystals. All experimental analyzes are based on X-ray diffraction, defect selective etching and photo-chemical etching measurements.

8625-11, Session 3

Luminescence of acceptors in Mg-doped GaN (Invited Paper)

Bo Monemar, Linköping Univ. (Sweden)

Recent photoluminescence (PL) studies show that Mg-doping in GaN produces two separate acceptor states A1 and A2 with different optical signatures. The possible identity of these two acceptors has been discussed 1-3, but not clarified. Structural studies of c-plane and m-plane GaN:Mg layers grown by MOCVD on low defect bulk GaN substrates

**Conference 8625:
Gallium Nitride Materials and Devices VIII**

reveal a high density of nano-size stacking faults (SFs) in such material, induced by the Mg-doping^{4,5}. The interaction of the Mg acceptors with these SFs can explain the presence of two acceptor states, and their optical properties. The following identification is suggested: A1 is the isolated substitutional Mg acceptor, while A2 is the same acceptor interacting with a nearby basal plane SF. Arguments for this: The A1 PL (3.466 eV ABE1 and 3.27 eV DAP) dominates at low Mg doping, where the material is n-type and no SFs are seen (This argues against the suggestion that the 3.27 eV PL is related to a neutral defect state³). The A2 PL (ABE2 PL at 3.454 eV and 3.1 eV DAP) is only strong at high Mg doping, when SFs also exist. A spatial correlation between Mg atoms and the SF has been shown in TEM⁴. The ABE2 PL shows strong broadening, consistent with inhomogeneous broadening with a slight variation of distance to the SF and the size of the SF (local strain broadening). The SFs show characteristic luminescence spectra in CL⁵. The metastability data in PL¹ may be explained in a different way than suggested in Refs 1-3, as related to a deeper metastable non-radiative defect which has no PL signature, but affects the Fermi level position during extended optical excitation¹, e. g. upon annealing. The low temperature PL transient data give strong evidence of exciton transfer from A1 to A2. PL data from Mg-doped samples grown by MOCVD, MBE and HVPE will be compared and discussed.

1. B. Monemar et al, Phys. Rev. Lett. 102, 235501 (2009)
2. S. Lany and A. Zunger, Appl. Phys. Lett. 96, 142114 (2010)
3. J.L. Lyons et al, Phys. Rev. Lett. 108, 156403 (2012)
4. S. Khromov et al, Phys. Rev. B84, 075324 (2011)
5. S. Khromov et al, Appl. Phys. Lett. 100, 172108 (2012)

8625-12, Session 3

The role of Mg in p-type In_xGa_{1-x}N alloys

Mary E. Zvanut, William R. Willoughby, The Univ. of Alabama at Birmingham (United States); Dan D Koleske, Sandia National Labs. (United States)

One approach for lowering the resistance encountered in the p-region of nitride devices is to employ In_xGa_{1-x}N films which yield hole concentrations 10-100 times those found in GaN. However, the role of Mg in hole production remains controversial. The present work uses electron paramagnetic resonance (EPR) spectroscopy to monitor the Mg-related acceptors and Hall measurements to determine hole densities in 0.25-0.44 μm thick In_xGa_{1-x}N:Mg films with x=0.021 to 0.112 and Mg, Si, and O concentration of 3x10¹⁹, 1x10¹⁶, and 1x10¹⁷ cm⁻³, respectively. As expected, the hole concentrations increased from 5-15x10¹⁷ cm⁻³ as the In mole fraction increased. However, unlike GaN:Mg, the number of EPR detected Mg acceptors decreased ten-fold as the hole density increased and was never more than 25% of the total Mg.

The data require that the presently suggested models for hole production in InGaN be modified. For example, although lowering the acceptor activation energy (E_a) adequately accounts for the hole densities, the EPR results indicate that In induces defects which passivate at least 75% of the EPR-active Mg. The defect could be a Mg near neighbor which distorts the local environment and lowers E_a. Alternatively, impurity band formation could account for the missing EPR centers without introducing additional defects; however, this model cannot count for the 25% of the Mg that remains EPR active. In summary, the EPR results indicate that neither isolated acceptors nor band formation adequately explain hole production in InGaN. Rather, additional features such as In-induced passivating centers must be introduced. This work is supported by NSF, DMR-1006163.

8625-13, Session 3

Lattice-matched AlInN/GaN heterostructures: n- and p-type doping and UV-LEDs (*Invited Paper*)

Yoshitaka Taniyasu, NTT Basic Research Labs. (Japan) and Ecole Polytechnique Fédérale de Lausanne (Switzerland); Jean-François Carlin, Antonino Castiglia, Raphaël Butté, Nicolas Grandjean, Ecole Polytechnique Fédérale de Lausanne (Switzerland)

Among III-nitride semiconductors, AlInN is the only ternary alloy that can be grown lattice-matched to GaN. Lattice-matched AlInN/GaN structure should be free from cracks, strain-driven composition inhomogeneities, and strain-related defects, which are limiting the performance of UV/Visible LEDs and LDs when using conventional lattice-mismatched AlGaIn/GaN and InGaIn/GaN structures. In addition, AlInN/GaN structure has a larger bandgap discontinuity and a larger refractive index contrast. Thus, AlInN/GaN structures are expected not only to improve device properties but also to increase the design flexibility for novel III-nitride devices.

In general, undoped AlInN shows n-type conduction with high residual donor concentrations, which is a significant obstacle to the p-type doping as well as to the intentional n-type doping. To reduce the residual donor concentration, we grew AlInN under In-rich condition to benefit from the In surfactant effect. Then, n-type conduction was intentionally controlled by Si doping. On the other hand, we found that one of the compensating defects for Mg acceptors is related to the presence of surface pits. By decreasing the pit density, p-type AlInN was successfully obtained.

We fabricated AlInN/GaN multiple quantum well LEDs. The emission wavelength varied with the GaN well width due to the interplay between quantum size effect and quantum confined Stark effect. At a well width of 2 nm, the LED showed UV emission at a wavelength of approximately 380 nm. These results show that lattice-matched AlInN/GaN is a promising alternative approach to UV-LEDs. Other UV/Visible LEDs and LDs based on lattice-matched AlInN/GaN will be also proposed.

8625-14, Session 3

MOVPE growth of Si doped AlN on trench patterned template

Gou Nishio, Mitsuhsa Narukawa, Hideto Miyake, Kazumasa Hiramatsu, Mie Univ. (Japan)

The effects of Si doping on the structural properties of a high-quality AlN layer grown on a trench-patterned AlN/sapphire by metalorganic vapor phase epitaxy (MOVPE) were systematically studied. With a high Si doping concentration, void formation became much slower than that in undoped AlN film. This phenomenon was attributed to the anti-surfactant effect of Si in the growth process. Moreover, as the Si doping concentration increased, compressive stress was significantly relaxed in Si-doped AlN films. Furthermore, a high Si doping concentration of 1.7x10¹⁸ cm⁻³ was successfully achieved for AlN grown at 1500 °C.

8625-15, Session 4

Defects in nitrides, positron annihilation spectroscopy (*Invited Paper*)

Filip Tuomisto, Aalto Univ. School of Science and Technology (Finland)

In-grown cation vacancies in GaN, AlN and InN are typically complexed with a donor-type defect that may in principle be a residual impurity such as O or H, an n-type dopant such as Si, or an intrinsic defect such as

**Conference 8625:
Gallium Nitride Materials and Devices VIII**

the N vacancy. The cation vacancies and their complexes are generally deep acceptors generating both radiative and non-radiative deep levels in the gap, they compensate for the n-type conductivity, and add to the scattering centers limiting the carrier mobility in these materials. These defects are formed during materials synthesis and device processing steps.

Positron annihilation spectroscopy has been widely applied to identify native vacancy defects in nitrides. In a semiconductor material, positrons can get trapped at negative and neutral vacancy defects, and at negatively charged non-open volume defects given the temperature is low enough. The trapping of positrons at these defects is observed as well-defined changes in the positron-electron annihilation radiation. The combination of experimental techniques with theoretical calculations provides the means to deduce both the identities and the concentrations of the vacancy defects.

The identification of the vacancies and vacancy complexes is based on comparison with irradiated samples where isolated vacancy defects are dominant, while in as-grown materials only vacancy complexes are detected. State-of-the-art theoretical calculations provide significant support for the identification through theoretical modelling of the relevant positron annihilation parameters. Interestingly, the vacancy-donor complexes are different in GaN, AlN and InN, and their importance in determining the opto-electronic properties of the material varies as well.

8625-16, Session 4

Short period InN/nGaN superlattices: experiment versus theory

Tadek Suski, Izabela Gorczyca, Grzegorz Staszczak, Institute of High Pressure Physics (Poland); Xinqiang Wang, State Key Lab. of Artificial Microstructure and Mesoscopic Physics (China); Niels E. Christensen, Axel Svane, Aarhus Univ. (Denmark); Emmanouil Dimakis, Univ. of Crete (Greece); Theodore D. Moustakas, Boston Univ. (United States)

Creation of short-period InN/GaN superlattices is one of the possible ways to perform band gap engineering in blue-green range of the spectrum.

Measurements of photoluminescence and its dependence on hydrostatic pressure are performed on a set of InN/nGaN superlattices with one InN monolayer, and with different numbers of GaN monolayers (n from 1 to 40). We show that the built-in electric field play an important role in these structures. The emission energies measured at ambient pressure, are close to the value of the band gap in bulk GaN, but they are significantly higher than the calculated band gap energies for the $1/n$ superlattices, and also higher than the band gaps calculated for $0.5/n$ and $1.5/n$ superlattices (assuming that the fabricated InN quantum well may contain some Ga atoms due to cation interdiffusion from GaN barriers). The above discrepancies between emission energies and band gap values lead to the conclusion that the optical transitions may be attributed to GaN excitons localized in the InN region.

The pressure dependence of the emission energies, resembles that of the InN energy gap (about 30 meV/GPa), i.e. smaller in magnitude than the pressure dependence of GaN excitons (about 40 meV/GPa), what can again indicate on their localized nature. Interestingly, pressure dependence of photoluminescence resembles rather the pressure dependence of the band gap of $0.5/n$ type superlattice than that of $1/n$ type of superlattice.

Finally, we also consider a possible role of screening of the internal electric fields by free carriers.

8625-17, Session 4

Defect generation and annihilation in GaN grown on patterned silicon substrate

Nobuhiko Sawaki, Shogo Ito, Taihei Nakagita, Hiroyuki Iwata, Aichi Institute of Technology (Japan); Tomoyuki Tanikawa, Masashi Irie, Yoshio Honda, Masahito Yamaguchi, Hiroshi Amano, Nagoya Univ. (Japan)

The presence of stacking faults in III nitrides has often degraded the crystalline quality/device performances. The elimination of basal plane stacking faults has been desired especially in semi-polar and non-polar GaN grown on patterned substrates where coalescence of micro-crystals is the essential. In this paper, the behavior of threading dislocations and stacking faults are studied by TEM analyses in a (1-101) GaN grown on a patterned (001)Si substrate.

Selective MOVPE of GaN was performed on (111) stripe facets of the Si with an AlN buffer layer, and flat (1-101)GaN surface was achieved by coalescence of GaN trapezoids. Cross sectional TEM and HRTEM images showed that threading dislocations are generated at the hetero-interface of GaN/AlN/Si induced by misfit dislocations, while stacking faults are generated when two crystals with different crystal axes coalesce each other. We found some of them are annihilated making a loop, where two stacking faults have been generated at a short distance. This annihilation process might be just the reverse to the generation process induced by dislocation half loop. Under our growth conditions, the growth of wurtzite-phase along the $\langle 0001 \rangle$ axis is more favorable than to the $\langle 000-1 \rangle$ direction. Therefore, the inclusion of cubic-phase will not be relevant. As the result, the pair of stacking faults cannot survive during the crystal growth. Possible trigger to the annihilation event will be in the growth modes on the patterned substrate.

8625-18, Session 4

Nonlinear absorption in InN under resonant- and non-resonant excitation

Hyeyoung Ahn, Min-Tse Lee, Yuan-Ming Chang, National Chiao Tung Univ. (Taiwan); Jin-Long Peng, Center for Measurement Standards, Industrial Technology Research Institute (Taiwan); Shangjr Gwo, National Tsing Hua Univ. (Taiwan)

We report the wavelength-dependent nonlinear absorption (NLA) of InN film grown by molecular beam epitaxy technique on an r -plane sapphire. Due to its narrow band gap, InN can be easily integrated with a fiber laser to achieve compact optical system and it shows large optical bleaching and fast recovery within a few picoseconds at 1550 nm, which exhibits the potential of InN as nonlinear material for all-optical switching at the optical communication spectral range. In order to understand the nonlinear optical properties of InN, it is necessary to identify its NLA process and the corresponding parameters. To do this, the Z-scan measurement was performed for the photon energy of the incident irradiance slightly higher (resonant excitation) or much higher (non-resonant excitation) than the bandgap of InN. Under non-resonant excitation, band-filling effect leads the dominant saturable absorption, while under resonant excitation, reverse saturable absorption processes, such as two-photon absorption (2PA) via a virtual intermediate state or excited state absorption (ESA) by the excited electrons, are available. From the open-aperture Z-scan measurement, we found that InN exhibits more than one nonlinear absorption process simultaneously. Particularly, under relatively weak non-resonant excitation, the transformation from ESA to 2PA was observed as the sample approaches the beam focus. The close-aperture Z-scan signals of InN show valley-peak response, implying that the nonlinear refraction in InN is caused by the self-focusing of the Gaussian laser beam. Using the Z-scan theory, the corresponding nonlinear parameters, such as saturation intensity, 2PA coefficient, and nonlinear refractive index, of InN were estimated.

**Conference 8625:
Gallium Nitride Materials and Devices VIII**

8625-90, Session 4

Simultaneous CL and TEM investigation of defects in GaN of various orientation (*Invited Paper*)

Juergen Christen, Otto-von-Guericke-Univ. Magdeburg (Germany)

The combination of luminescence spectroscopy - in particular at liquid He temperatures - with the high spatial resolution of a scanning transmission electron microscopy (STEM) ($\Delta x < 1$ nm at RT, $\Delta x < 5$ nm at 10 K), provides a unique, extremely powerful tool for the optical nano-characterization of semiconductors. The CL-intensity is collected simultaneously to the STEM signal - typically chemical sensitive HAADF Z-contrast. The TEM acceleration voltage is optimized to minimize sample damage and prevent luminescence degradation under e-beam excitation. In CL-spectral imaging mode, a complete CL spectrum is recorded at every single pixel. Subsequently, by evaluating the complex data matrix $ICL(\lambda, x, y)$, sets of simultaneously recorded monochromatic mappings $ICL(\lambda, i, x, y)$, CL peak wavelength mappings $\lambda_{CL}(x, y)$, local spectrum linescans, local CL spectra, etc. can be processed. Typical results which will be presented include nm-scale correlation of the optical properties and strength and appearance of structural defects in: strain engineering and dislocation reduction by AlN interlayers in GaN-on-Si structures, lattice matched AlInN/GaN distributed Bragg reflectors; minority carrier diffusion lengths of $\tau < 17$ nm, as well as the efficient carrier transfer over > 150 nm into quantum wells are directly measured in STEMCL.

The impact of structural defects like dislocations is directly visualized: Special emphasis is given to the formation and in particular the annihilation and the prevention of basal plane as well as prismatic stacking faults in non- and semi-polar GaN.

8625-92, Session 4

3D atomic scale chemistry of gallium nitride materials and devices studied by atom probe tomography (*Invited Paper*)

George D. W. Smith, M. Müller, Alfred Cerezo, B. Gault, D. W. Saxey, P. A. J. Bagot, M. P. Moody, Univ. of Oxford (United Kingdom); S. E. Bennett, Rachel A. Oliver, Colin J. Humphreys, Univ. of Cambridge (United Kingdom)

Solutions to many fundamental problems of nitride semiconductor devices require understanding of materials behaviour at the atomic level, particularly atomic-scale chemistry. Atom probe tomography provides unique insight into this area. This paper describes our latest work on phase separation in ternary nitrides as a function of layer thickness; the effects of electron beam irradiation on phase stability; chemical segregation at V-type defects; and intermixing at interfaces in MBE-grown device structures. Key results include:

In the case of thick (300nm) layers of In_{0.25}Ga_{0.75}N grown on a GaN buffer layer by MOCVD, composition gradients are found both normal to, and parallel to, the growth interface. As the distance from the substrate increases, there is clear evidence of phase separation, with a morphology indicative of a spinodal decomposition process.

A MOCVD-grown multi-quantum well structure consisting of repeats of 2.4nm of In_{0.18}Ga_{0.82}N and 7.0nm of GaN showed a random statistical distribution of In within the quantum wells in the as-grown condition. After exposure to electron irradiation in a transmission electron microscope, the distribution of In became statistically non-random.

V-defects in InGaN show complex patterns of morphological and chemical changes, including segregation of impurities to the defects.

Analysis of a III-nitride laser diode structure grown by molecular beam epitaxy was used to study the distribution of p-type dopants, the randomness of the In distribution in the InGaN quantum wells, and the extent of intermixing at interfaces. Localised intermixing was found, with

significant top-bottom asymmetry, depending on the growth sequence of the layers.

8625-19, Session 5

High quality factor nanocavities embedding nitride quantum dots (*Invited Paper*)

Christelle Brimont, L2C (France); Thierry Guillet, L2C (France); Diane Sam-Giao, Commissariat à l'Énergie Atomique (France); Delphine Neel, Institut d'Électronique Fondamentale (France); Sylvain Sergent, Ctr. de Recherche sur l'Hétéro-Epitaxie et ses Applications (France); Bruno Gayral, Commissariat à l'Énergie Atomique (France); M.J. Rashid, Commissariat à l'Énergie Atomique (France) and CRHEA-CNRS (France); Fabrice Semon, Ctr. de Recherche sur l'Hétéro-Epitaxie et ses Applications (France); Meletios Mexis, L2C (France); Sylvain David, Xavier Checoury, Philippe Boucaud, Institut d'Électronique Fondamentale (France)

Semiconductors of the III-N family have become the dominant materials for UV to blue-green semiconductor light sources. Besides these conventional light emitters, III-N materials are also attracting candidates to probe light-matter interaction in photon confining structures in the UV and visible ranges. For room temperature operation, nitride quantum dots are promising candidates due to their large radiative efficiency, as shown recently for GaN/(Al,Ga)N QDs grown on Si substrates. However, processing photonic nanostructures with large quality factors with these materials is a real challenge due to the larger scattering losses compared to similar structures in the visible and IR spectral ranges.

In this work, we study the spectroscopy of two types of nanocavities. The first one consists of Al(Ga)N microdisk resonators embedding GaN QDs. We have observed and modelled their optical modes, called whispering gallery modes, with promising quality factors from 1000 to 7000 (Optics Letters, vol. 36 p.2203 - 2011). The second type of nanocavities is photonic crystals obtained by small modifications of a W1 waveguide in an AlN photonic crystal membrane containing QDs. The room temperature photoluminescence of the embedded quantum dots reveals the existence of even-symmetry and odd-symmetry confined cavity modes and guided modes. Cavity mode quality factors up to 4400 at 395nm and 2300 at 358nm are obtained (APL, 100 p.191104 - 2012). These results will be compared to state of the art nitride microdisks and photonic crystal cavities.

8625-20, Session 5

Excitonic Fine-Structure of Quantum Dots Based in Nitrides (*Invited Paper*)

Axel Dr Hoffmann, TU Berlin Servicegesellschaft GmbH (Germany)

Single photon emission of MOCVD grown GaN quantum dots embedded in an AlN matrix was observed for up to 200 K [1] which represents a technological advantage in comparison to the well established system of arsenide quantum dots. In this presentation, we study the fundamental processes of photon emission by excitonic complexes confined in single III-N QDs. Experimental results from time-integrated and time-resolved single-QD spectroscopy are evaluated as well as theoretical results obtained by Hartree-Fock calculations based on realistic eight-band k.p wave functions. The emission properties of excitonic states in QDs are dominated by an interplay of valence-band mixing effects and electron-hole exchange effects within the excitonic states. Furthermore, we demonstrate that single GaN/AlN QDs exhibit a huge exciton brightstate FSS of up to 7meV, larger than in any other QD system. Surprisingly, the FSS increases drastically with increasing emission energy, which is directly opposed to recent observations on InAs/GaAs QDs. To this day single photon emission of GaN quantum dots at room temperature seems

**Conference 8625:
Gallium Nitride Materials and Devices VIII**

to be hindered by a combination of various effects as the excitonic Coulomb interaction with charged defects situated in the vicinity of the GaN quantum dot and a comparably strong exciton-phonon interaction. As a measure of the exciton-LO-phonon coupling strength we determine Huang-Rhys factors between 0.02 and 0.3 by analyzing the intensity ratio of the LO-phonon sidebands with their corresponding single quantum dot related excitonic transition. Furthermore, we give a thorough analysis of the built-in dipole moments of excitonic and multiexcitonic complexes of GaN/AlN quantum dots and substantiate it with experimental survey. Then, we predict a new sort of hybridization state consisting of two semiconductor holes forming a Wigner-crystal in wurtzite GaN/AlN quantum dots, interacting with two additionally confined electrons in their s-shaped ground state orbital within the same quantum dot.

(1) Kako et al., Nature Materials 5, 887 (2006).

8625-21, Session 5

Individual GaN quantum dots imaged by low temperature cathodoluminescence scanning transmission electron microscopy

Frank Bertram, Gordon Schmidt, Markus Mueller, Peter Veit, Juergen Christen, Otto-von-Guericke-Univ. Magdeburg (Germany); Eva Monroy, A. Das, Commissariat à l'Énergie Atomique (France)

We will present our results from nanoscale optical and structural characterization of a III-nitride based QD heterostructure which was grown by plasma-assisted molecular-beam epitaxy (PAMBE). A 1.7 μm thick AlN layer grown on a sapphire substrate using metal organic vapor phase epitaxy serves as template for the subsequent PAMBE growth of a stack of 10 GaN QD layers each embedded in 50 nm thick AlN barriers. Atomic force microscopy of the top uncapped GaN QD layer exhibits a homogeneous QD distribution with a density of 3-4 × 10¹⁰ cm⁻².

The cross-section STEM image clearly shows the AlN-MOVPE/sapphire template and the GaN QD layers. Originating from the AlN-MOVPE/sapphire interface vertically running threading dislocations show up in the high angle annular dark field contrast (HAADF). The comparison of the STEM-HAADF images with the simultaneously recorded panchromatic cathodoluminescence (CL) mappings at 16 K exhibits a spot like luminescence distribution of the upper six QD layers solely. An evidence of QD contrast either in HAADF or CL-intensity images cannot be observed for the first intentionally grown QD layers indicating no formation of QDs. Monochromatic CL-intensity mappings at the same position proof this finding. We observe a broad luminescence band between 325 nm and 385 nm originating from the GaN QD ensemble. Investigating the CL distribution of single QDs, an area of 175 × 175 nm² was scanned in panchromatic mode. The ambipolar carrier diffusion length towards a GaN QD was determined to be 18 nm by measuring a linescan over the spot-like QD emission.

8625-22, Session 5

Raman spectroscopy of GaN and AlGaIn nanowires: from ensemble to single nanowire study (Invited Paper)

Francois Demangeot, Renaud Pechou, Univ. de Toulouse (France); Jiangfeng Wang, Ctr. d'Elaboration de Matériaux et d'Etudes Structurales (France); Ana Cros, Univ. de Valencia (Spain); Bruno Daudin, Rudeesun Songmuang, Commissariat à l'Énergie Atomique (France)

The wide band-gap GaN semiconductor has attracted much attention as a promising material for the development of optoelectronic devices operating in the blue and ultraviolet range. Self-assembled GaN nanowires (NWs) currently are a subject of sustained interest in the scientific community motivated by both their potential applications for

new LEDs, which should take benefit of the improved crystalline quality of those nano-objects, due to a strongly reduced defects density. In addition, the strong interest of the scientific community for these 1D nano-systems, is also related to the new fundamental questions opened by their strongly anisotropic geometry, and to their potential as possible building blocks for future nano-electronic devices. In this context, Raman spectroscopy has been increasingly used to study nitride NWs and several new phenomena have been reported to date with respect to these one-dimensional structures.

In this work, both GaN and AlGaIn Nanowires (NWs) grown by Plasma Assisted Molecular Beam Epitaxy have been investigated experimentally by micro-Raman spectroscopy and theoretically by both elastic and dielectric models.

On one hand, we were interested in NWs ensemble for the study of their statistic and/or collective properties by using non resonant visible laser excitation. Conventional Raman scattering by confined optical phonons of wurtzite structure, i.e. E_{2h} and QLO symmetry optical modes, was measured. In addition, new Raman bands were attributed to the surface optical mode of the nanostructures. This observation has been found in good agreement with the results of a calculation performed using an anisotropy model that takes into account an effective dielectric function. From this experimental observation of surface related vibrations, we gave evidence for original surface effects in the optical phonon physics related to both structural anisotropy of the material and 1D geometry of the NWs. These peculiar effects manifest itself by the apparition of a double band related to surface vibrations in the Raman spectra of self-assembled GaN NWs. We demonstrated that these two modes result from the anti-crossing of two distinct surface phonon branches, occurring at the peculiar case $f=0.4$, f standing for the filling factor value measured independently in the investigated samples. In addition, it has been shown that this double structuration of surface phonon mode has been related to the splitting into two different components, i.e. axial and planar surface-related modes.[1] Moreover, it is also shown that the frequency of surface optical phonons can be used to probe very sensitively the dielectric constant of the exterior medium lying between the as-grown NWs. Indeed, strong red-shift of surface modes frequencies is measured, typically six times larger than the reported data recorded in Raman spectra of GaP microcrystals. This very sensitivity to the dielectric constant of the exterior media makes GaN NWs, but more generally nitrides NWs good candidates for dielectric sensors.

On the other hand, in order to circumvent any averaging effect by a measure of a statistical population of NWs, we focused our attention to detailed resonant micro-Raman analysis of a single GaN and AlGaIn NW. We report the demonstration of an ultra-sensitive Raman probing of single GaN/AlIn nanowires (NWs). The high sensitivity of the Raman scattering by longitudinal optical phonon is achieved by using ultraviolet resonant excitation near the energy band-gap of GaN and AlGaIn. Structural variations within one single nanowire are evidenced very accurately by strong LO phonons shifts in the UV Raman spectra recorded on different regions of the NW. They are tentatively interpreted as a fine probing of structural fluctuations of GaN within the NW, due to the formation of an AlN shell in the bottom part of the NW. The core-shell structure has been confirmed in a statistical way by estimating the average strain in the NWs ensemble thanks to the Raman scattering excited in the visible range. Data have been comprehensively accounted for by considering an axial strain in GaN NW part covered by AlN shell, in the elastic regime, while the top GaN is relaxed.[2] Structural fluctuations were also observed in AlGaIn NWs, where phase separation has been evidenced by our UV Resonant Raman probe at the scale of a single NW. We show that complementary to visible Raman experiments, in which volume information of the different phases is obtained, resonant UV Raman scattering process allows to enhance and to detect minority phases as long as the fundamental transition of their electronic properties coincides with the energy of the exciting laser.

[1] V. Laneuville, F. Demangeot, R. Pechou et al., Phys. Rev. B. 83, 115417 (2011)

[2] J. Wang, F. Demangeot, R. Pechou et al. Phys. Rev. B. 85, 155432 (2012)

**Conference 8625:
Gallium Nitride Materials and Devices VIII**

8625-23, Session 5

Photonic Crystal III-Nitride Nanowire Lasers

Jeremy B. Wright, Sandia National Labs. (United States) and The Univ. of New Mexico (United States); Ganapathi Subramania, Qiming Li, Igal Brener, Ting S. Luk, George T. Wang, Sheng Liu, Sandia National Labs. (United States); Huiwen Xu, Luke F. Lester, The Univ. of New Mexico (United States)

There is great interest in utilizing semiconductor nanowire lasers as low power, compact light sources. Strain relaxation of nanowires allows for a wider composition of alloys leading to a larger range of emission wavelengths. A two-step top-down processing technique was used to fabricate an ordered array of GaN/InGaN nanowires to act as a photonic crystal laser. By lithographically defining the nanowire diameter and spacing it was possible to control the wavelength of the laser emission. The lasing wavelength was tunable from 425-455nm by altering the diameter of the nanowires. Our results indicate a promising approach for wavelength selection in periodic arrays of short-wavelength nanowire devices. Sandia National Laboratories is a multi-program laboratory managed and operated by Sandia Corporation, a wholly owned subsidiary of Lockheed Martin Corporation, for the U.S. Department of Energy's National Nuclear Security Administration under contract DE-AC04-94AL85000.

8625-24, Session 6

Nanolithography for 3-Dimensional Nanostructures: Enhancement of Light Output Power in Vertical Light Emitting Diodes (Invited Paper)

Jong-Lam Lee, Pohang Univ. of Science and Technology (Korea, Republic of)

To successfully replace conventional light sources, the quantum efficiency of LEDs should be further increased. The quantum efficiency is determined using the internal quantum efficiency (IQE) and the light extraction efficiency. Although an IQE of nearly 80 % has been achieved, much room remains for LEE enhancement because most of the generated photons from the active layer remain inside the LEDs due to the total internal reflection at the semiconductor-air interface. In conventional GaN-based LEDs, the photons have a small critical angle of 23.4° due to the large difference in refractive indices between GaN ($n = 2.52$) and air ($n = 1$). Photons within the critical angle are easily emitted into the air; however, other photons that are beyond the extraction angle are internally reflected within the GaN and absorbed by metal electrodes or the active region.

Here, we report several kinds of novel methods to maximize the light extraction efficiency of V-LEDs, developed using SiO₂ nanosphere lithography, nano-imprint lithography, nano-rods, nano template using inverse monolayer colloidal crystals and spontaneously formed nanopyramid with rock-salt structures. The SiO₂ nanosphere lithography demonstrate the novel cone shape nanostructure with controllable side wall angle to maximize the light extraction efficiency of V-LEDs. These achievements are attributed to effective elimination of total internal reflection by angle-controllable nanostructures, which is in good agreement with theoretical calculation using the three-dimensional (3-D) finite-difference time-domain (FDTD) method.

8625-25, Session 6

High efficient InGaN blue LED with embedded nanoporous structure (Invited Paper)

Ta-Cheng Hsu, Wei-Chih Peng, Epistar Corp. (Taiwan)

High-efficiency GaN-based light-emitting diodes (LEDs) with an emitting wavelength of 450nm were demonstrated utilizing nanoporous (NP) GaN structure on sapphire substrates. Unlike the previous patterned sapphire substrates (PSS), the presented substrate has a new morphology that can not only easily enlarge the wafer scale but also generate a void-embedded nanostructural layer to enhance light extraction. Under a driving current of 350 mA, the light output power of an LED with NP GaN structure is enhanced by 2 -fold compared with that of the conventional LED and the performance can compete with the most optimized PSS LEDs. The light output power of the NP GaN devices of 45 mil x 45 mil without and with encapsulate are 455 and 545 mW, respectively. Methods for further enhancement, such as use the size of nanoporous structure on GaN layer were also discussed.

8625-26, Session 6

Low resistivity electrical contacting of porous n-type GaN layers due to reduced workfunction intermetallic seed layers

Oleksandr V. Bilousov, Joan Josep Carvajal Marti, Univ. Rovira i Virgili (Spain); Colm O'Dwyer, Univ. College Cork (Ireland); Xavier Mateos, Francesc Díaz, Magdalena Aguiló, Univ. Rovira i Virgili (Spain)

GaN has received a huge attention in the fabrication of new devices for electronic and optoelectronic applications. In its porous form, GaN has received particular interest due to beneficial optical and electronic properties in light-emitting diodes (LEDs) with high light extraction efficiency, for example. Porous GaN has been typically fabricated by corrosion methods such as (photo)electrochemical and chemical etching techniques. We produced porous GaN through a novel and greener method based on crystal growth through the vapour-solid-solid (VSS) mechanism of nanoporous GaN microparticles by chemical vapour deposition (CVD) without needing any secondary etching or chemical treatment after growth to induce porosity.

Here we present the successful growth in a high surface area and at the same time low resistivity electrical contacting of nanoporous n-type GaN. Nanoporous GaN single crystal microparticles were grown through the direct reaction of Ga and NH₃ in the CVD system using high workfunction Au- and Pt-coated silicon substrates. Au and Pt acted both as catalyst for the synthesis of porous GaN supported by the VSS mechanism and result in the formation of an intermetallic compound at the GaN-Pt(or Au) interface that prevents oxidation of the GaN, and also allows high quality ohmic electrical contacts to the porous n-GaN layers with a significantly reduced Schottky barrier height. Pt(or Au)-Ga intermetallic alloy formation promotes thermionic low-resistance ohmic transport through the porous layer.

8625-27, Session 6

Single-Mode Lasing in Gallium Nitride Nanowires

Huiwen Xu, The Univ. of New Mexico (United States); Jeremy B. Wright, Sandia National Labs. (United States); Antonio Hurtado, The Univ. of New Mexico (United States); Ting S. Luk, The Univ. of New Mexico (United States) and Sandia National Labs. (United States); Jeffery J. Figiel, Sandia National Labs. (United States); Karen Cross, Sandia National Labs. (United States); Ganesh Balakrishnan, Luke F. Lester, The Univ. of New Mexico (United States)

**Conference 8625:
Gallium Nitride Materials and Devices VIII**

States); George T. Wang, Igal Brener, Qiming Li, Sandia National Labs. (United States)

GaN nanowires with large diameter and/or length typically operate as multimode lasers. To achieve single-mode operation, we demonstrate two separate mode-selection techniques to simultaneously suppress multiple longitude/transverse mode oscillation in GaN nanowires. In this paper, a nanowire-pair geometry is firstly introduced to generate single-mode operation. By placing two nanowires side-by-side in contact through nanoprobe manipulation, a coupled cavity is formed. The coupled cavity generates a so-called Vernier effect, which dramatically increases the free spectral range between adjacent resonant modes, giving rise to single-mode operation. We have realized single-mode lasing from coupled nanowires with diameters of about 700nm and lengths of about 8 μ m by this approach. We also demonstrate single-mode lasing by contacting a GaN nanowire, which otherwise exhibits multimode lasing properties, to a gold substrate. The difference in the spatial distribution of different transverse modes causes them to be attenuated differently by the presence of the metal. Simulation by a finite difference time domain method illustrates that high-order transverse modes have much larger attenuation compared with the fundamental mode. Therefore, the nanowire-gold contact generates a mode-dependent loss, which can strongly attenuate higher modes and ensure the single-mode operation. We have realized single-mode lasing from a 300nm diameter nanowire via this approach. Sandia National Laboratories is a multi-program laboratory managed and operated by Sandia Corporation, a wholly owned subsidiary of Lockheed Martin Corporation, for the U.S. Department of Energy's National Nuclear Security Administration under contract DE-AC04-94AL85000.

8625-28, Session 7

GaN Power Devices for Automotive Applications *(Invited Paper)*

Tsutomu Uesugi, Tetsu Kachi, Toyota Central R&D Labs., Inc. (Japan)

In future automobiles, 3 battery systems will be applied to vehicles; which are 14-V low voltage battery for low power sub-systems, 288-V high voltage battery for high power sub-systems like an electric air conditioner or an electric power steering, and 650-V boost-up voltage source for main systems like an inverter or a boost-up DC-DC converter.

In order to reduce exhaust emissions and improve fuel efficiency, we should decrease power consumption not only at main systems but at sub-systems. It is very important to develop high performance power devices for high and low rating voltage. We have developed GaN vertical power devices for main systems and GaN lateral power devices for sub-systems.

We have presented the GaN vertical power devices at Photonics West 2012. Therefore, in we focus on the GaN lateral power devices in this presentation.

Normally-off operation and suppression of current collapse are serious technical issues in GaN lateral power devices.

These two issues are strongly related to interface state between GaN (AlGaN) and a gate or a passivation insulator.

We have investigated Al₂O₃ fabricated by ALD method as the gate and passivation insulators. An interface state density between the Al₂O₃ and GaN was about 1E12/cm². TDDB (Time Dependent Dielectric Breakdown) was 1E7 sec at 150- $^{\circ}$ C and 3MV/cm.

We have studied an effect of NH₃ pre-deposition treatment of the GaN surface to the current collapse characteristics, and found out that this treatment was very effective to suppression of the current collapse.

8625-29, Session 7

Proton irradiation effects on InAlN/GaN high electron mobility transistors *(Invited Paper)*

Fan Ren, Univ. of Florida (United States); Stephen J. Pearton, Univ. of Florida (United States)

The effects of proton irradiation energy on dc and rf characteristics of InAlN/GaN high electron mobility transistors (HEMTs) were investigated. A fixed proton dose of 5×10^{15} cm⁻² with 5, 10 and 15 MeV irradiation energies was used in this study. The HEMT structures were grown with a Metal Organic Chemical Vapor Deposition (MOCVD) system, starting with a thin AlGaIn nucleation layer, followed with a 1.9 μ m low-defect carbon-doped GaN buffer layer, 50 nm undoped GaN layer, 10.2 nm undoped InAlN layer with a 17% of In mole fraction, and capped with a 2.5 nm undoped GaN layer. The samples were all grown on three inch diameter, c-plane sapphire substrates. Hall measurements on the as-grown structures showed sheet carrier densities of 2.1×10^{13} cm⁻² and the corresponding electron mobility of 1000 cm²/V-s. For the dc characteristics, degradation was observed for sheet resistance, transfer resistance, contact resistivity, saturation drain current, maximum transconductance, reverse-bias gate leakage current and subthreshold drain leakage current for all the irradiated HEMTs, however the degree of the degradation was decreased as the irradiation energy increased. Similar trends were obtained for the rf performance of the devices, with ~10% degradation of the unity gain cut-off frequency (f_T) and maximum oscillation frequency (f_{max}) for the HEMTs irradiated with 15MeV protons but 30% for 5 MeV proton irradiation. The carrier removal rate was in the range 660-1240 cm⁻¹ over the range of proton energies investigated.

8625-30, Session 7

Junction temperature measurements and reliability of GaN FETs *(Invited Paper)*

Martin Kuball, Univ. of Bristol (United Kingdom)

Semiconductor electronic devices, such as GaN HEMTs, are being developed and implemented to enable higher powers, and higher operating frequencies than ever possible before. This poses challenges in that devices operate at much higher channel temperatures as well as have to withstand much higher electric fields than standard material device systems, affecting performance and reliability. Recent developments on the accurate determination of channel temperature in GaN HEMTs, impacting device reliability, with <300nm resolution using optical methods will be reported, as well as methodologies to understanding physical mechanisms that affect device reliability, i.e. how a combination of optical and electrical methods can be used, complemented by simulation, to understanding the physics of degradation in GaN HEMTs, such as the role of impact ionization, electronic trap generation at surface and in the channel, surface pitting, and the rise in leakage current during device operation, including the role of dislocations.

8625-31, Session 7

High-sensitivity HFET type photosensors with a p-GaN gate

Mami Ishiguro, Kazuya Ikeda, Masataka Mizuno, Motoaki Iwaya, Tetsuya Takeuchi, Satoshi Kamiyama, Isamu Akasaki, Meijo Univ. (Japan)

Wireless visible-light communication has attracted attention for optical bus in computers, for wireless access in vehicles, and so on. For these applications, the photosensor must have high sensitivity and a high response speed. However, no appropriate devices with high sensitivity in the visible region. In this study, we fabricated high-performance AlGaIn/GaN based HFET-type photosensors with a p-GaN gate for the

**Conference 8625:
Gallium Nitride Materials and Devices VIII**

detection of visible light. After depositing a 20-nm-thick buffer layer at a low temperature, a 3.0- μ m-thick unintentionally doped GaN, a 12-nm-thick unintentionally doped AlGaIn barrier layer, and a 110-nm-thick Mg-doped p-GaN layer with a Mg concentration of 3×10^{19} cm⁻³ were grown. The InN molar fractions in p-GaN was 0.14. After the activation of Mg acceptors to 550°C for 5 min in N₂, mesa isolation was performed by Cl₂ reactive ion etching (RIE). Next, the p-GaN layer was etched by RIE, except for the gate region. Then, Ti/Al/Ti/Au was deposited as the source and drain contacts on the u-AlGaIn. We characterized the monochromatic photosensitivity of this photosensor, for a VDS of 5 V in the case of using a Xe lamp and a spectrometer with a resolution of 6 nm. The photosensitivity of AlGaIn/GaN HFET-type photosensor was over 4×10^5 A/W (@385 nm). The sensitivity of this AlGaIn/GaN HFET-type photosensor with a p-GaN gate far surpassed that of the Si pin photodiodes and Si avalanche photodiode, and was closed to photomultiplier tube.

8625-32, Session 7

Traps and defects in pre- and post-proton irradiated AlGaIn-GaN high-electron mobility transistors and AlGaIn Schottky diodes

Yongkun Sin, Brendan Foran, Stephen LaLumondiere, William T. Lotshaw, Steven C. Moss, The Aerospace Corp. (United States)

AlGaIn-GaN high electron mobility transistors (HEMTs) are promising for high voltage, high power, and high efficiency operation. Study of reliability and radiation effects of AlGaIn-GaN HEMTs is necessary before they are deployed in high reliability satellite systems. A few AlGaIn HEMT manufacturers have recently reported encouraging reliability, but their long-term reliability under high electric field and irradiation still remains a major concern.

We studied traps and defects in MOCVD-grown AlGaIn HEMTs and Al_{0.25}Ga_{0.75}N Schottky diodes on SiC substrates. Our HEMTs consisting of GaN cap, AlGaIn/AlN barrier, and GaN buffer layers had a Schottky gate length of 0.25 μ m, a total gate width of 400 μ m periphery, and SiN_x passivation. Our HEMT structures consisting of undoped AlGaIn barrier and GaN buffer layers grown on an AlN nucleation layer show a charge sheet density of $\sim 1 \times 10^{13}$ /cm² and a Hall mobility of ~ 1500 cm²/Vsec. Electrical characteristics of AlGaIn HEMTs and Schottky diodes were compared before and after they were proton irradiated with different energies and fluences. Current-mode deep level transient spectroscopy and capacitance-mode DLTS were employed to study traps in the AlGaIn-GaN HEMTs and AlGaIn Schottky diodes, respectively before and after proton irradiation. Of two dominant traps identified from pre-stress devices, the ~ 0.5 eV traps showed significant changes in their post-stress characteristics. Focused ion beam was employed to prepare cross-sectional TEM samples for defect analysis using a high resolution TEM. A detailed analysis will be presented along with our understanding on the role that ~ 0.5 eV traps and defects play in degradation processes of the AlGaIn HEMT devices.

8625-33, Session 8

Comparative study of III-nitride vertical-cavity surface-emitting laser diodes and optically-pumped polariton lasers (Invited Paper)

Raphaël Butté, Jacques Levrat, Gatién Cosendey, Georg Roszbach, Marlene Glauser, Antonino Castiglia, Eric Feltin, Jean-François Carlin, Nicolas Grandjean, Ecole Polytechnique Fédérale de Lausanne (Switzerland)

In this talk, we will compare two types of vertical cavity devices emitting coherent light but operating in different regimes. The structures are based on a fairly similar design since they both rely on a semi-hybrid scheme with a bottom crack-free highly-reflective nearly lattice-matched AlInN/(Al)GaN distributed Bragg reflector (DBR) followed by a cavity

with embedded quantum wells followed by a top dielectric DBR. We will first depict the optical and electrical characteristics of recently achieved vertical cavity surface emitting laser diodes [1] that operate in the conventional weak coupling regime – where photon emission is depicted by Fermi's golden rule. Then we will focus on the properties of polariton lasers [2-3] that operate in the so-called strong coupling regime – a nonperturbative regime leading to the formation of novel eigenmodes, cavity polaritons which are composite bosons that spontaneously decay into photons. In this latter case we will more specifically describe the phase diagram leading to polariton condensation [4-5] that is a prerequisite to the understanding of the specificities of polariton lasers with respect to vertical cavity surface emitting lasers.

- [1] G. Cosendey et al., submitted to Appl. Phys. Lett.
- [2] S. Christopoulos et al., Phys. Rev. Lett. 98, 126405 (2007).
- [3] G. Christmann et al., Appl. Phys. Lett. 93, 051102 (2008).
- [4] R. Butté et al., Phys. Rev. B 80, 233301 (2009).
- [5] J. Levrat et al., Phys. Rev. B 81, 125305 (2010).

8625-34, Session 8

Nonpolar and semipolar GaN, optical gain and efficiency (Invited Paper)

Seoung-Hwan Park, Catholic Univ. of Daegu (Korea, Republic of); Doyeol Ahn, The Univ. of Seoul (Korea, Republic of)

Wurtzite (WZ) gallium nitride (GaN)-based light-emitting diodes (LEDs) and laser diodes (LDs) have received much attention in the past few years due to their promising applications such as solid-state lighting, high-density optical storage systems, and laser projection displays. It has been shown that the introduction of biaxial strain into the (0001)-plane of a wurtzite GaN-based crystal does not effectively reduce the effective masses in the transverse direction, unlike in other III-V semiconductors. This is due to the fact that, for a wurtzite layer grown along the (0001) orientation, the strain shifts both the heavy hole (HH) and light hole (LH) bands by almost the same amount and the in-plane effective masses remain almost the same as those in the unstrained case. Also, the (0001) WZ GaN-based QW lasers are found to have higher carrier densities to generate optical gain because these structures have not only a large internal field due to the strain-induced piezoelectric (PZ) and spontaneous (SP) polarizations, but also a heavier hole effective mass than the conventional zincblende (ZB) crystals such as GaAs or InP. The built-in electric fields along the [0001] direction (c axis) cause a spatial separation of electrons and holes which in turn gives rise to restricted carrier recombination efficiency, reduced oscillator strength, and redshifted emission.

Several methods have been proposed in an effort to reduce the effect of the internal field due to polarizations. They include methods using ultrathin In-rich InGaIn well, inserting an AlGaIn δ -layer into the thick InGaIn well, using a quaternary AlInGaIn material, and using non-square QW structures. In addition, the crystal orientation effect has been studied as an additional parameter for band structure engineering. In an effort to overcome these inherent drawbacks of III-V nitride quantum well structures, Ohtoshi et al. investigated theoretically the crystal orientation effects on the valence subband states in GaN QWs and found that heavy hole effective masses for the (10 $\bar{1}$ 0)- and (10 $\bar{1}$ 2)-oriented QWs are significantly reduced when compared with those for the (0001) case. After the pioneering of Ohtoshi et al. various physical schemes are being investigated to overcome these serious imperfections caused by the built-in field effects. Sometime ago, one of the authors and Waltereit et al. independently suggested the use of different crystal orientation to eliminate the internal field and several groups have studied nitride quantum wells on the non-polar crystal orientation to avoid PZ and SP. Another approach to reduce PZ and SP and decrease the hole effective mass is to grow the nitrides on semi-polar plane that is the plane tilted with respect to the (0001) direction. Initially, it was argued that the layers grown on non-polar and semi-polar substrates contain numerous non-radiative recombination centers because it is difficult to achieve a high crystal quality on non-polar or semi-polar planes. However, recent progress includes the finding of polarization crossover in a single

**Conference 8625:
Gallium Nitride Materials and Devices VIII**

InGaN/GaN QW grown on a semi-polar direction, high compositional homogeneity of InGaN QW grown on semi-polar substrate and non-polar m-plane thus shedding the light on the practical applications of QWs grown on non-polar and semi-polar substrates. Considering the rapid growth of non-polar and semi-polar nitride material research, it would be important to have the theoretical studies on both electronic and optical properties taking into account the arbitrary crystal orientation.

In this paper, crystal orientation effects on electronic and optical properties of WZ InGaN/GaN QWs with PZ and SP polarizations are investigated using the multiband effective-mass theory and non-Markovian optical model.

Also, the electron overflow in non-polar InGaN/GaN QW structures with a superlattice (SL)-like electron injector (EI)

layer is investigated as one of mechanisms governing the internal efficiency loss at high current levels.

The band structure of QW with an arbitrary crystal orientation is calculated within the 6-band multiband effective-mass theory. The non-Markovian model of the optical gain and the luminescence for the strained-layer QW is employed taking into account the many-body effects within the Hartree-Fock approximation. Plasma screening, bandgap renormalization and Coulomb enhancement of optical transitions are included in the model.

The average hole effective mass is observed to be greatly reduced with increasing crystal angle. The (0001)-oriented QW structure shows that a hole effective mass increases with increasing In content because the valence-band hole effective mass parameter is reduced with increasing In content. On the other hand, in the case of the non-polar plane, the QW structure with a larger In content has a smaller hole effective mass than that with a smaller In content. This is mainly attributed to the fact that the valence band effective mass parameter along k_y increases with increasing In content. The y -polarized optical matrix element gradually increases with increasing crystal angle and begins to saturate when the crystal angle exceeds about 56° because the internal field of the InGaN/GaN QW structure is gradually reduced with increasing crystal angle and its sign is changed near the crystal angle of 56° . In particular, in the case of non-polar or semipolar plane, the matrix element is dominated by the y -polarization because the states constituting the topmost valence subband near the band edge are predominantly $Y'_{3/2}$ -like for QW structures with larger crystal angle. The optical matrix element decreases with increasing In content, irrespective of the crystal angle.

The optical anisotropy is shown to increase with increasing In content. The increase of the in-plane optical anisotropy at a higher In content is attributed to the fact that the optical intensity for the y -polarization increase while that for the x -polarization decrease with increasing In content. The optical anisotropy of the non-polar a-plane InGaN/GaN QW structure with the well width of 30 nm changes from 0.58 to 0.80 at a carrier density of $2 \times 10^{12} \text{ cm}^{-2}$ in a range of investigated In contents ($x=0.1-0.4$). Also, the QW structure with a thin well width shows a smaller optical anisotropy than that with a thick well width. In the case of (112)-oriented InGaN/GaN QW structure with the well width of 30 nm, the optical anisotropy changes from 0.27 to 0.52 at a carrier density of $2 \times 10^{12} \text{ cm}^{-2}$ in a range of investigated In contents ($x=0.1-0.4$). These results are in good agreement with the experiment data. The optical anisotropies of (112)-plane QW structures are much smaller than those of a-plane QW structures. The well width dependence of the optical anisotropy for (112)-plane QW structure is similar to that for a-plane QW structure.

The electron overflow is shown to decrease with the inclusion of the EI layer. In the case of single EI layer, the thick layer of ≈ 13 nm is needed to reduce electron overflows. On the other hand, the QW structure with the superlattice-like EI layer is more effective in reducing the ballistic and quasiballistic electron transport across the active region, compared with a thick single EI layer in the sense that it will be difficult to obtain a thick single EI layer with a high quality. The electron overflow is shown to decrease with increasing the number of the SL layer.

8625-35, Session 8

True-blue nitride laser diodes grown by plasma assisted MBE on low dislocation density GaN substrates

Henryk Turski, Institute of High Pressure Physics (Poland); Marcin Siekacz, Institute of High Pressure Physics (Poland) and TopGaN Ltd. (Poland); Grzegorz Muziol, Institute of High Pressure Physics (Poland); Marta Sawicka, Institute of High Pressure Physics (Poland) and TopGaN Ltd. (Poland); Szymon Grzanka, Piotr Perlin, Tadeusz Suski, Institute of High Pressure Physics (Poland); Zbigniew R. Wasilewski, Waterloo Institute for Nanotechnology (Canada); Izabella Grzegory, Sylwester A. Porowski, Institute of High Pressure Physics (Poland); Czesław Skierbiszewski, Institute of High Pressure Physics (Poland) and TopGaN Ltd. (Poland)

Future progress of laser displays depends on availability of reliable and efficient laser diodes (LDs) operating in true-blue and green spectral ranges. Development of the new low temperature growth mechanism for nitrides in plasma assisted molecular beam epitaxy (PAMBE) has led to the demonstration of violet LDs (410 nm), which has renewed interest in this technology for long wavelength emitters.

In this work we demonstrate nitride based true-blue LDs, grown by PAMBE on low dislocation density c-plane GaN substrates, operating in continuous wave (CW) mode at wavelengths 450-460 nm. The CW optical power measured for these LDs is 80 mW and lifetime is longer than 3000h (for 10 mW CW optical power). We present a new AlGaIn claddings free design consisting of thick InGaIn waveguides with 8% of In. The key innovation in PAMBE process was to increase the nitrogen flux which improved InGaIn quality and allowed to demonstrate optically pumped lasing from our structures up to 501nm. We show that PAMBE allows to grow (i) InGaIn QWs with very narrow photoluminescence (PL) lines and (ii) high quality thick InGaIn layers used as waveguides, that simplify the LD design. We will discuss the influence of InGaIn waveguides and GaN/AlGaIn claddings to LDs performance. Results presented in this work demonstrate that PAMBE has a potential to become a viable alternative to metal organic vapour phase epitaxy for nitride based LDs fabrication.

8625-36, Session 8

Thin AlGaIn cladding blue-violet InGaIn laser diode with plasmonic GaN substrate

Piotr Perlin, Institute of High Pressure Physics (Poland) and TopGaN Ltd. (Poland); Szymon Stańczyk, Anna Kafar, Institute of High Pressure Physics (Poland); Robert Kucharski, Ammono Sp. z o.o. (Poland); Tomasz Czyszanowski, Technical Univ. of Lodz (Poland); Lucja Marona, Tadek Suski, Institute of High Pressure Physics (Poland); Greg Targowski, TopGaN Ltd. (Poland)

Highly oxygen doped GaN substrate crystals, having a refractive index lowered by a plasmonic effect, offer a possibility of designing strain reduced InGaIn laser diodes of better than conventional manufacturability. Low substrate refractive index prevent an optical mode of the laser diode from leaking out from its waveguide region. Thanks to that we can substantially reduce the thickness of tensile strained bottom AlGaIn cladding layers thus reducing the tendency of epistructure for bowing and cracking. For this study we used very highly doped GaN crystals with the electron concentration close to $1.2 \times 10^{20} \text{ cm}^{-3}$. We show that for our blue-violet laser diodes (emitting wavelength 410-420 nm) the thickness of a bottom AlGaIn cladding of the Al concentration of 8% can be reduced from the standard value of 800 nm down to 400 nm with no observable worsening of the mode confinement of the threshold current value. We performed a measurements of a near-field patterns for these type of plasmonic cladding laser diodes not observing any tendency for the mode leakage. The reduction of AlGaIn thickness leads

**Conference 8625:
Gallium Nitride Materials and Devices VIII**

the reduction of the wafer bowing and dislocation density which can be then kept at the low level of 10^4cm^{-2} . The results are supported by a calculation of mode distribution in the structure containing plasmonic cladding substrates.

8625-37, Session 8

Cathodoluminescence study of degraded InGaN laser diode structures

Lucja Marona, Przemysław Wiśniewski, Piotr Perlin, Tadek Suski, Institute of High Pressure Physics (Poland); Robert Czernecki, TopGaN Ltd. (Poland); Mariusz Płuska, Andrzej Czerwiński, Institute of Electron Technology (Poland)

Cathodoluminescence is an efficient tool to visualize, in the microscale, the details of recombination mechanisms in semiconductor nanostructures. We demonstrate the use of this method to study the degraded InGaN laser diodes. We focus our attention on the laser ridge which is a sole part being stressed by the current flow. We analyze the border line between the stressed and unstressed region looking for the current dependent contrast. From the analysis of the cathodoluminescence images of the degraded devices we can draw the following conclusions:

The degradation occurs uniformly through all the injection area.

We do not observe any type of optical degradation (photon related) which means that the non-injected part of the ridge does not show any damage.

The contrast between the injected and non-injected parts of the ridge increases with the increasing electron beam current in the Scanning Electron Microscope. This observation seems to be surprising if we assume that the sole mechanism of degradation is the generation of new nonradiative recombination centers, because in such a situation the contrast should be smaller at higher excitation. Other mechanisms like an enhanced carrier escape should be also considered.

8625-38, Session 8

Picosecond pulse generation in monolithic GaN-based multi-section laser diodes

Katarzyna A. Holc, Thomas Weig, Wilfried Pletschen, Klaus Köhler, Joachim H. Wagner, Fraunhofer-Institut für Angewandte Festkörperphysik (Germany); Ulrich T. Schwarz, Fraunhofer-Institut für Angewandte Festkörperphysik (Germany) and Freiburg Univ. (Germany)

We develop a monolithic picosecond laser pulse generator, based on the classical design of a group-III-nitride Fabry-Perot laser diode with electrically separated ridge sections. We use two different multi-section design variants, with the absorber section placed either in the center or at the end of the ridge. Profiting from the very low lateral conductivity in the p-type GaN top contact layer, we implement the multi-section concept just by etching off small sections of the top metallization on the ridge.

The physical mechanism underlying short pulse generation within such system strongly depends both on the reverse bias applied to the absorber and the forward current in the gain section. Varying the applied reverse bias affects both the differential optical gain and the carrier lifetime in the absorber section through changes in the internal piezoelectric fields. In consequence we can distinguish between different modes of operation. For moderately long carrier lifetimes the absorber stabilizes relaxation oscillations in the GHz frequency range and self-pulsation occurs, of relatively long duration. With increasing reverse bias, and thus decreasing carrier lifetime we observe a transition to self-Q-switching. Applying driving pulses a few nanoseconds in length we achieved single pulse operation with pulse duration of 7 ps. Finally, at large enough negative bias, the carrier life time in the absorber is so short that the laser diode operates in a passive self-mode-locking regime with

a repetition rate of 87 GHz and pulse duration of 5 ps for a cavity length of 570 μm .

8625-39, Session 9

Intersubband spontaneous emission from GaN-based THz quantum cascade laser (Invited Paper)

Wataru Terashima, Hideki Hirayama, RIKEN (Japan)

We studied on terahertz-quantum cascade lasers (THz-QCLs) using III-Nitride semiconductors, which are promising materials for the realization of the unexplored frequency range from 5 to 12 THz and the higher temperature operation on THz-QCLs, because these compounds have much higher longitudinal optical phonon energies ($> 18 \text{ THz}$) than those of conventional GaAs-based materials ($\sim 9 \text{ THz}$). Firstly, we showed clearly that it is possible to design a GaN-based quantum cascade (QC) structure which operates in the THz range in which population inversion can be obtained, by performing numerical calculations based on a self-consistent rate equation model. Secondly, we succeeded in the stack of QC structure with a large number of periods and the drastic improvement of structural properties of QC structure, by introducing a new growth technique named "a droplet elimination by thermal annealing (DETA)" in which utilized the differences of the properties between metal (Al, Ga) and Nitride (AlN, GaN) into molecular beam epitaxy. Finally, we for the first time successfully observed spontaneous electroluminescence due to intersubband transitions with peaks at frequencies from 1.4 to 2.8 THz from GaN/AlGaIn QCL devices fabricated with using the DETA technique grown on a GaN substrate and a metal organic chemical vapor deposition (MOCVD)-AlN template on a sapphire substrate. In this paper, we demonstrate recent achievements on the quantum design, fabrication technique, and electroluminescence properties of GaN-based QCL structures.

8625-40, Session 9

Vertical cavity surface emitting terahertz lasers based on GaN (Invited Paper)

Alexis Kavokine, Univ. Montpellier 2 (France)

Polariton lasers based on GaN/AlGaIn optical microcavities have been recently demonstrated. In these lasers condensates of mixed light-matter quasiparticles (exciton-polaritons) containing up to 10000 particles can be created. These condensates can stimulate terahertz optical transitions from 2p exciton states. These transitions are optically allowed and polarised in plane of the structure, so that terahertz emission goes away across the Bragg mirrors in vertical geometry. Pumping of 2p excitons may be achieved by resonant optical two-photon pumping provided by commercial red semiconductor LEDs. We discuss also bosonic cascade terahertz laser scheme providing the internal quantum efficiency of over 700%.

8625-41, Session 9

Latest developments in AlGaInN laser diode technology

Stephen P. Najda, TopGaN Ltd. (Poland); Piotr Perlin, Tadek Suski, Lucja Marona, Michal Bockowski, Institute of High Pressure Physics (Poland); Mike Leszczynski, TopGaN Ltd. (Poland); P. Wisniewski, Robert Czernecki, Grzegorz Targowski, Institute of High Pressure Physics (Poland)

The latest developments in AlGaInN laser diode technology are reviewed. The AlGaInN material system allows for laser diodes to be fabricated over a very wide range of wavelengths from u.v., i.e. 380nm, to the visible,

**Conference 8625:
Gallium Nitride Materials and Devices VIII**

i.e., 530nm, by tuning the indium content of the laser GaInN quantum well. Advantages of using Plasma assisted MBE (PAMBE) compared to more conventional MOCVD epitaxy to grow AlGaInN laser structures are highlighted. Ridge waveguide laser diode structures are fabricated to achieve single mode operation with optical powers of >100mW in the 400-420nm wavelength range with high reliability. High power operation of AlGaInN laser diodes is demonstrated with a single chip, AlGaInN laser diode 'mini-array' consisting of a 3 stripe common p-contact configuration at powers up to 2.5W cw at 410nm. Low defectivity and highly uniform GaN substrates allow arrays and bars of nitride lasers to be fabricated. Packaging of nitride laser diodes is substantially different compared to GaAs laser technology and new processes & techniques are required to optimize the optical power from a nitride laser bar. Laser bars of up to 5mm with 20 emitters have shown optical powers up to 4W cw at ~410nm with a common contact configuration. An alternative package configuration for AlGaInN laser arrays allows for each individual laser to be individually addressable allowing complex free-space and/or fibre optic system integration within a very small form-factor.

8625-42, Session 9

Room-temperature optically pumped AlGaInN multiple-quantum-well lasers operating at 260nm grown by metalorganic chemical vapor deposition

Russell D. Dupuis, Zachary Lochner, Xiaohang Li, Jae-Hyun Ryou, Tsung-Ting Kao, Shyh-Chiang Shen, P. Douglas Yoder, Mahbub Satter, Georgia Institute of Technology (United States); Alec Fischer, Fernando Ponce, Arizona State Univ. (United States)

In the past few years, efforts have been made to realize compact, efficient semiconductor-based coherent light sources in the UVC spectral region. While UVC injection lases have not yet been demonstrated due to the many materials issues involved in the growth of high-quality and electrically conducting III-N wide-bandgap n- and p-type layers, optically pumped lasers operating in this spectral region have been reported. In particular, coherent UV light emission and laser operation of III-N quantum-well heterostructures at 300K have been demonstrated and reported in the deep-UV (240-270nm) spectral range using optical or electron-beam pumping. For example, recently Wunderer, et al. have reported optically-pumped UV laser operation of an Al_xGa_{1-x}N-Al_yGa_{1-y}N three-quantum-well heterostructure grown by metalorganic chemical vapor deposition (MOCVD) at ~267nm with a pumping threshold ~126 kW/cm². These structures were grown on bulk (0001) AlN substrates.

We report here the metalorganic chemical vapor deposition (MOCVD) growth of UVC optically pumped lasers at ~257nm. These structures were grown by low-pressure MOCVD on a vicinal (0001) bulk AlN substrate and typically had a three-quantum-well active region structure with ~5.5nm QW barriers and ~2.8nm QWs. After growth, the wafer was thinned to ~70 μm and bars were cleaved with facets oriented along the m-plane. The cavity length was varied between ~0.7 and 1.2 μm. No facet coatings were applied to the cleaved facets. The samples were mounted without heat sinking and excited using the 248nm emission from a KrF laser or a 193nm ArF laser operating at a repetition rate of 100 Hz. Pulsed laser operation at room-temperature (300K) operation of optically pumped Al_xGa_{1-x}N-Al_yGa_{1-y}N (x=0.66, y=0.53) multiple-quantum-well (MQW) heterostructures operating at ~257nm by photopumping at a threshold of ~1.9 MW/cm². Other similar III-N MQW structures have been grown and lased at ~260nm wavelengths. We will describe the growth conditions, device structures, and 300K laser results in detail in this paper.

8625-43, Session 9

Tunable light source with GaN-based violet laser diode

Masaki Omori, Naoki Mori, Norihiro Dejima, Nichia Corp. (Japan)

GaN based violet Laser Diode has been applying for the industrial market with unique high potential characters. It has possibility Replacing Gas lasers, Dye Lasers, SHG lasers and Solidstate Lasers and more. Diode based laser extreme small and low costs at the high volume range. In addition GaN Laser has high quality with long lifetime and has possibility to cover the wide wavelength range as between 375 to 520nm. However, in general, diode based laser could only lase with Longitudinal Multi Mode. Therefore applicable application field should be limited and it was difficult to apply for the analysis.

Recently, Single Longitudinal Mode laser with GaN diode has also been accomplished with external cavity by Nichia Corporation. External cavity laser achieved at least much higher than 20dB SMSR. The feature of installing laser is that Laser on the front facet with AR coating to avoid chip mode lasing. In general, external cavity laser has been required precision of mechanical assembly and Retention Capability. Nichia has gotten rid of the issue with Intelligence Cavity and YAG Laser welding assembly technique. This laser has also been installed unique feature that the longitudinal mode could be maintained to Single Mode lasing with installing internal functional sensors in the tunable laser.

This tunable laser source could lock a particular wavelength optionally between 390 to 465nm wavelength range. As the results, researcher will have benefit own study and it will be generated new market with the laser in the near future.

8625-44, Session 10

Growth, characterization, and fabrication of regularly patterned nanorod LED array (*Invited Paper*)

Che-Hao Liao, Wen-Ming Chang, Yu-Feng Yao, Chia-Ying Su, Chih-Yen Chen, Chieh Hsieh, Hao-Tsung Chen, Horng-Shyang Chen, Charng-Gan Tu, Yean-Woei Kiang, Chih-Chung Yang, National Taiwan Univ. (Taiwan)

With the nano-imprint lithography and the pulsed growth mode of metalorganic chemical vapor deposition, a regularly-patterned, c-axis nitride nanorod (NR) array of quite uniform geometry with simultaneous depositions of top-face, c-plane disc-like and sidewall, m-plane core-shell InGaN/GaN quantum well (QW) structures is formed. The differences of geometry and composition between these two groups of QW are studied with scanning electron microscopy, cathodoluminescence, and transmission electron microscopy (TEM). In particular, the strain state analysis results in TEM observations provide us with the information about the QW width and composition. It is found that the QW widths are narrower and the indium contents are higher in the sidewall m-plane QWs, when compared with the top-face c-plane QWs. Also, in the sidewall m-plane QWs, the QW width (indium content) decreases (increases) with the height on the sidewall. The observed results can be interpreted with the migration behaviors of the constituent atoms along the NR sidewall from the bottom. The cross-sectional sizes of the GaN NRs and QW NRs of different heights and different hexagon orientations between different hole patterns, including different hole diameters and pitches, are demonstrated. The cross-sectional size of the GaN NRs is controlled by the hole diameter and has little to do with the NR height and pitch. On the other hand, the cross-sectional size of the QW NRs is mainly determined by the NR height and is slightly affected by the hexagon orientation.

**Conference 8625:
Gallium Nitride Materials and Devices VIII**

8625-45, Session 10

Prospect of GaN light-emitting diodes grown on glass substrates (*Invited Paper*)

Jun-Hee Choi, Yun Sung Lee, Chan Wook Baik, Ho Young Ahn, Kyung Sang Cho, Sun Il Kim, Sungwoo Hwang, Samsung Advanced Institute of Technology (Korea, Republic of)

We report the enhanced electroluminescence (EL) of GaN light-emitting diodes (LEDs) on glass substrates by controlling GaN crystal morphology, crystallinity, and device fabrication. Depending on the degree of epitaxy, we could control three different GaN morphologies; randomly oriented GaN polycrystals, nearly single-crystalline pyramid arrays, and fully single-crystalline pyramid arrays. At proper growth temperature, GaN crystallinity was improved with increasing the GaN crystal size irrespective of the GaN crystallographic orientation, as determined by spatially-resolved cathodoluminescent spectroscopy. All the different GaN morphologies were further fabricated into LEDs to investigate their EL characteristics. The optimized GaN LEDs on glass composed of the nearly single-crystalline GaN pyramid arrays currently exhibited excellent microscopic EL uniformity and a luminance of about 2700 and 1150 cd/m² at the peak wavelength of 537 and 480 nm, respectively. We expect in the future that the GaN LEDs on glass substrates would be used for low-cost, large-sized lightings.

8625-46, Session 10

Surface plasmon enhanced high efficiency LEDs (*Invited Paper*)

Seong-Ju Park, Gwangju Institute of Science and Technology (Korea, Republic of)

Light-emitting diodes(LEDs) have drawn much attention due to their application to display and solid-state lighting. However, the external quantum efficiencies of LEDs are still low to realize the high efficiency LEDs. In this talk, surface plasmons in metal nanostructures are demonstrated to increase the internal quantum efficiency of multi-quantum wells and transmittance of transparent conducting layer of LEDs. The electrical and optical properties of surface plasmon enhanced blue-, green-, and NUV-LEDs and their enhancement mechanism will be presented.

8625-47, Session 11

Progress in the development of a-plane nonpolar GaN LED grown on r-plane sapphire substrate (*Invited Paper*)

Hyung-Gu Kim, Kyu-Hyun Bang, Young-Hak Chang, Jina Jeon, Eun-Jeong Kang, Sangwook Byun, Sukkoo Jung, Yoon-Ho Choi, Jeong-Soo Lee, LG Electronics Inc. (Korea, Republic of); Jung-Hoon Song, Kongju National Univ. (Korea, Republic of); Jun Seok Ha, Chonnam National Univ. (Korea, Republic of)

Wide bandgap GaN-based non-polar and semi-polar GaN light emitting diodes (LEDs) have recently received much interest due to the potential to eliminate the influence of large polarization-related electric field, which are reported to have detrimental influence on internal quantum efficiency and efficiency-droop [1-3]. However, performance of non-polar LEDs on sapphire substrates has not been competitive to c-plane based LEDs, mainly due to inferior material quality of GaN epitaxial layers which consist of high density of threading dislocations and basal plane stacking faults. Consequently, only LEDs fabricated on high quality GaN substrates have shown competitive results to that of c-plane LEDs to date [4,5].

In this study, we report on realization of high-brightness a-plane GaN LEDs grown on r-plane sapphire substrate with light output powers

reaching above 10mW at a current of 20mA. The LED structures consisted of a high quality n-type GaN underlying layer, a single InGaN quantum well active layer, and a p-type GaN layer. In some cases, a patterned-epitaxial-lateral-overgrowth (PLOG) structure, with hexagon shaped SiO₂ selective masks, was employed to improve crystalline quality of underlying GaN layer.

Various characterization methods were used to verify crystalline improvements of GaN layers. Cathodoluminescence measurement showed strong luminescence intensity and reduced density of dark spots. X-ray rocking curve having full width at half maximum values as low as 387 and 336 arcsec were obtained along c-axis and m-axis, respectively. Finally, preliminary results of non-polar vertical LEDs will also be presented. To our best knowledge this is the first report on non-polar vertical LEDs from sapphire substrates.

[1] A. Chakraborty, B. A. Haskell, S. Keller, J. S. Speck, S. P. DenBaars, S. Nakamura, and U.K. Mishra, *Appl. Phys. Lett.* 85, 5143 (2004).

[2] X.Ni, J. Lee, M. Wu, X. Li, R. Shimada, U. Ozgur, A.A. Baski, H. Morkoc, T. Paskova, G. Mulholland, and K.R. Evans, *Appl. Phys. Lett.* 95, 101106 (2009).

[3] S.C. Ling, T.C. Lu, S.P. Chang, J.R. Chen, H.C. Kuo, and S.C. Wang, *Appl. Phys. Lett.* 96, 231101 (2010).

[4] Y. Zhao, J. Sonada, I. Koslow, C. Pan, H. Ohta, J. Ha, S. P. Denbaars, and S. Nakamura, *Jpn. J. Appl. Phys.* 49, 070206 (2010).

[5] C.C. Pan, S. Tanaka, F. Wu, Y. Zhao, J.S. Speck, S. Nakamura, S.P. DenBaars, and D. Feezell, *Appl. Phys. Express* 5, 062103 (2012).

8625-48, Session 11

Excitation dependency of polarized light emission from nonpolar InGaN quantum wells

Lukas Schade, Ulrich T. Schwarz, Fraunhofer-Institut für Angewandte Festkörperphysik (Germany); Tim Wernicke, Ferdinand-Braun-Institut (Germany); Jens Rass, Simon Ploch, Technische Univ. Berlin (Germany); Markus Weyers, Ferdinand-Braun-Institute (Germany); Michael Kneissl, Technische Univ. Berlin (Germany)

Light emitting diodes based on nonpolar InGaN quantum wells (QWs) emit polarized light due to the character of the valence band at the Γ -point, the large energy distance (2 to 3 times kBT at room temperature) between the two topmost valence subbands, and asymmetric in-plane strain. At high excitation, occupation of states by charge carriers has to be described by Fermi distribution (in contrast to Boltzmann approximation). This results in a decrease of the polarization ratio with increasing excitation density. Bandfilling together with homogeneous and inhomogeneous broadening causes a minimum in the dependency of linewidth and a shift of the peak energy position with carrier density.

We observe these effects experimentally by polarization-resolved micro-photoluminescence spectroscopy of undoped violet nonpolar QWs and pulsed electroluminescence from nonpolar LEDs, both at room temperature and 10 K. The experiments are analyzed in terms of emission properties: intensity, spectral broadening and energy position. The transition from the Boltzmann to the Fermi-Dirac regime is observed experimentally by a decrease of the polarization degree in the high charge carrier density regime.

In addition a model based on the effective mass approximation was designed to describe the specific emission properties of nonpolar InGaN QWs. A quantitative comparison with the experiment allows deriving the total charge carrier density in the system, the energetic distance of the subbands in strained non-polar InGaN QWs, and the impact of inhomogeneous broadening and Fermi-statistics on peak energy and linewidth of the partially polarized emission.

8625-49, Session 11

Effects of local structure on optical properties in green-yellow InGaN/GaN quantum wells

Jongil Hwang, Toshiba Corp. (Japan); Rei Hashimoto, Shinji Saito, Shinya Nunoue, Toshiba Corp. (Japan)

Light output power of nitride-based c-plane LEDs decreases significantly above wavelength of 530 nm because of the degradation of the crystal quality and increase of the quantum confinement Stark effect (QCSE). With increase in the In composition to fabricate the LED with wavelength above 530 nm, the degradation of crystal quality may occur depending on the local structure that may affect the magnitude of the QCSE.

In order to evaluate the effect of change of the local structure as well as the crystal quality, we have investigated wavelength dependence of internal electric field (F) and photoluminescence (PL) intensity of multiple quantum wells with the wavelength above 530 nm grown by metal-organic chemical vapor deposition. The F was evaluated from theoretical calculation with the F as a parameter fitting to the experimental PL peak shift depending on the excitation power. The measurements were performed for several structures varying the well widths and adding InGaN or AlGaIn layer.

This analysis revealed that the F increased monotonically with increasing the wavelength. The analysis also shows that the PL intensities were enhanced in some structures although the wavelength dependence of the F scarcely changes, showing that the local structural change dominantly affects the crystal quality rather than the QCSE. This indicates that internal efficiency of the LEDs can be enhanced through improvement of the crystal quality by optimizing the layer structure. Utilizing one of the local structures, we obtained a c-plane LED with the light output power 5.8 mW at wavelength of 551 nm.

8625-50, Session 11

Influence of hole injection layer and electron blocking layer on carrier distributions in III-nitride visible light-emitting diodes

Russell D. Dupuis, Jeomoh Kim, Mi-Hee Ji, Jae-hyun Ryou, Md. Mahbub Satter, P. Douglas Yoder, Georgia Institute of Technology (United States); Kewei Sun, Reid K. Juday, Alec M. Fischer, Fernando Ponce, Arizona State Univ. (United States)

We report on the behavior of electron and hole transport and resulting distributions of carriers in III-nitride-based LEDs in relation to the effect of hole injection layers and electron blocking layers (EBLs). In order to study the transport of carriers and resulting distributions for radiative recombination, we employed a triple-wavelength (TW)-emitting multiple-quantum-well active region which has different In content in each $\text{In}_x\text{Ga}_{1-x}\text{N}$ QW. The emission of TW-LED structures was characterized from fabricated LEDs. In the case of the LEDs with higher In mole fraction in p- $\text{In}_x\text{Ga}_{1-x}\text{N}$, emission from QW1 becomes stronger. This gradually increased EL intensity of QW1 compared to QW2 and QW3 for the LEDs with increasing indium mole fraction in p- $\text{In}_x\text{Ga}_{1-x}\text{N}$ layer indicates that more holes can be transported to the lower QW by hole injection layers. The EL spectrum of the TW-LED without an EBL showed the highest emission peak at QW3, one closest to the p-type layer, and gradually decreased in QWs with increasing distance from the p-GaN layer. For the TW-LED with an InAlN EBL, QW2 has the highest emission peak intensity among the three QWs even at low injection current and the emission from QW1 is also much higher than that of the TW-LED without an EBL. We will compare characteristics of TW-LEDs employing InAlN and AlGaIn EBLs in comparison to one without EBLs and employing various p- $\text{In}_x\text{Ga}_{1-x}\text{N}$ layers in order to distinguish the carrier transport and distribution in the active region. The carrier dynamics and related efficiency droop behavior will be further discussed.

8625-51, Session 11

Metal middle layers for improving thermal stability of Ag reflector for high-power GaN-based light-emitting diode

Tae-Yeon Seong, Woong-Sun Yum, Joon-Woo Jeon, Korea Univ. (Korea, Republic of)

For efficient light extraction, GaN-based vertical-geometry LEDs require Ga-polar reflectors with high reflectance and low contact resistance. Ag is the most frequently used reflector because of its reasonable electrical property. However, Ag only reflector experiences thermal instability when annealed above 300°C in air. Thus, a variety of different approaches, such as the use of interlayers, capping layers, or Ag alloys, have been adopted so as to enhance the thermal property. In this work, we investigated the effect of 5-nm-thick metal middle layers on the electrical and thermal properties of Ag contacts. The metal middle layers were used to serve as a capping layer for the bottom Ag layer and as an interlayer for the superjacent Ag layer. The performance of LEDs fabricated with Ag/metal/Ag reflectors is also investigated and compared to those with Ag only reflectors. It is shown that the 5-nm-thick metal middle layers suppress agglomeration by forming metal-oxide. The Ag/metal/Ag contacts exhibit a contact resistivity of $\sim 10^{-5} \text{ } \Omega\text{cm}^2$ and reflectance of 80 – 75% at 440 nm when annealed at 500 °C, which are much better than those of Ag only contacts. Blue LEDs fabricated with the 500°C-annealed Ag/metal/Ag contacts yield a lower forward voltage at an injection current of 20 mA than that of LEDs with the 500 °C-annealed Ag only contacts. The LEDs with the 500 °C-annealed Ag/metal/Ag contacts exhibit $\sim 29\%$ higher output power (at 20 mA) than LEDs with the 500 °C-annealed Ag only contacts.

8625-52, Session 11

InGaN-based multi-double heterostructure light-emitting diodes with electron injector layers

Fan Zhang, Xing Li, Shopan A. Hafiz, Serdal Okur, Vitaliy Avrutin, Ümit Özgür, Hadis Morkoç, Virginia Commonwealth Univ. (United States)

For high efficiency at high current injection InGaN light emitting diodes (LEDs) necessitate active regions that can mitigate the aggravating electron overflow. Multi double-heterostructures (DHs), 3D active regions separated by low energy barriers, provide an optimum solution as they can accommodate a larger number of states compared to multiple quantum wells (MQWs). However, as the material degrades with increasing thickness, carrier cooling has to be partially achieved before the active region using electron injector layers with stepwise or gradually increased In content. Using electroluminescence (EL) efficiency measurements supported by simulations active regions and electron injectors were optimized to minimize the electron overflow and the associated efficiency drop at high injection levels. For a single 3 nm DH LED, the electron overflow was nearly eliminated by increasing the two-step staircase electron injector layer thickness from 5+5 nm to 20+20 nm. Temperature and excitation density dependent photoluminescence spectroscopy allowed determination of the material quality and the internal quantum efficiency of different device structures.

8625-70, Session PWed

Reducing threading dislocations in GaN grown on (111) Si by double GaN island growth method

Cheng Lung-Chieh, Liu Hsueh-Hsing, National Central Univ. (Taiwan); Chen-Zi Liao, Industrial Technology Research Institute

**Conference 8625:
Gallium Nitride Materials and Devices VIII**

(Taiwan); Lee Geng-Yen, National Central Univ. (Taiwan); Chyi Jen-Inn, National Central Univ. (Taiwan) and Research Ctr. for Applied Sciences, Academia Sinica (Taiwan)

In recent years, growing GaN on (111) silicon substrates has been considered a competitive approach to achieve low-cost optical and power GaN devices. One of the key issues is the 17% lattice constant mismatch between GaN and silicon substrate, resulting a dislocation density as high as 10^{10} cm⁻². Several methods have been proposed to reduce the dislocation density, including multi-epitaxial-lateral-overgrowth (multi-ELO), AlGaIn/GaN superlattice and patterned substrate. Although the multi-ELO method could reduce dislocation density significantly, it still needs an extra regrowth process. In this work, we develop a growth method, which produces an in situ multi-island structure, to lower dislocation densities without any regrowth process. Scanning electron microscope images show that while the GaN islands in the first island structure are formed randomly due to the in situ SiNx mask, the islands in the second structure are selectively grown on the area between the islands of the first GaN island structure because the second SiNx mask is preferentially deposited on top of the GaN islands. This self-aligned double island structure results in reduced dislocation density in the topmost GaN layer. Accordingly, the full width at half maximum of the (102) x-ray rocking curve of GaN is reduced from 1073 arcsec to 783 arcsec. As revealed by atomic force microscopy, the etch-pit density of the GaN grown on double island structure is reduced from 6.7×10^9 cm⁻² to 2.6×10^9 cm⁻².

8625-71, Session PWed

Thermal properties of InGaIn laser diodes and arrays.

Szymon Stanczyk, Anna Kafar, Institute of High Pressure Physics (Poland) and Gdansk Univ. of Technology (Poland); Grzegorz Targowski, Przemek Wiśniewski, Irina Makarowa, Tadek Suski, Piotr Perlin, Institute of High Pressure Physics (Poland)

Junction temperature of an operating laser diode determines many critical parameters of these devices. These are: the value of threshold current, the maximum power achievable and finally the device lifetime.

In our work, in order to measure the junction temperature we applied a comparison method based on an assumption, that short pulse (< 200 ns) operation does not introduce self heating in laser junction. We measured several current voltage characteristics under pulsed bias and at chosen temperatures, stabilized by a thermo-electric cooler. A comparison of those characteristics with that measured at room temperature and under DC conditions provided us with a junction temperature vs. electric power dependence. Based on those results we also calculated the thermal resistivity of measured devices.

We studied the dependence of thermal properties on number of emitters: a single emitter laser diode, mini laser array (3 emitters) and large laser array (10 emitters). We also studied two laser diodes with different substrate thickness (50 μm and 120 μm).

The results show, that large laser array exhibits an order of magnitude smaller thermal resistivity than single emitter. This reduction is proportional to the increase of the device surface. That implies that the primary factor determining thermal resistance of the device is the chip's surface meaning that a limiting factor is here a heat transfer between the chip and the heat sink. The measurements connected with the change of substrate thickness showed that this modification has no influence on thermal properties which should be linked to an outstanding substrate thermal conductivity.

8625-72, Session PWed

Nonradiative recombination due to point defects in GaInN/GaN quantum wells induced by Ar implantation

Torsten Langer, Hans-Georg Pietscher, Heiko Bremers, Uwe Rossow, Dirk Menzel, Andreas Hangleiter, Technische Univ. Braunschweig (Germany)

In this contribution, we quantitatively investigate nonradiative recombination due to point defects. We experimentally estimate an average hole capture coefficient of Ar implantation induced point defects of about 2×10^{-12} cm²/s in GaInN/GaN single quantum wells.

The samples were grown via metalorganic vapor phase epitaxy and implanted with argon (doses: 1×10^{12} to 1×10^{13} 1/cm²) afterwards in order to generate point defects (e.g. vacancies). The thermal stability of the defects has been analyzed using rapid thermal annealing (RTA) at 800°C. We measure the carrier recombination times via temperature-dependent time-resolved photoluminescence spectroscopy using selective excitation of the quantum wells (QW) at three different stages before and after implantation as well as after RTA.

A significant reduction of carrier lifetimes in the QW is observed for implantation doses of 1×10^{12} 1/cm² and higher due to nonradiative recombination at implantation defects whereas the radiative lifetimes remain unchanged. We find a partial recovery of the nonradiative lifetimes after RTA proving an elimination of some defects. A comparison of the lifetimes at the three different stages allows us to distinguish between the nonradiative recombination times at defects that are curable (e.g. displaced atoms in the vicinity of a corresponding vacancy) and persistent ones. While the curable defects show rather low activation energies (about 10 meV), they are higher (approx. 50 meV) for the persistent defects. Hole capture coefficients are determined using the measured nonradiative lifetimes and simulated (SRIM) defect densities. Furthermore, we have evidence that defects in the barriers strongly contribute to carrier losses in the QW.

8625-73, Session PWed

Influence of growth interruption on performance of nitride-based blue LED

Kazuki Aoyama, Meijo Univ. (Japan); Atsushi Suzuki, Tsukasa Kitano, EL-SEED Corp. (Japan); Naoki Sone, Koito Manufacturing Co., Ltd. (Japan); Satoshi Kamiyama, Tetsuya Takeuchi, Motoaki Iwaya, Isamu Akasaki, Meijo Univ. (Japan)

In general nitride-based light-emitting diodes (LEDs), a p-AlGaIn electron block layer (EBL) is commonly used to suppress carrier overflow from an active layer. However, determination of growth condition for p-AlGaIn EBL is quite difficult because it must be placed at neighbor of the GaInN/GaN multi-quantum well (MQW) active layer. The MQW has to be grown at lower temperature (800°C or lower) in N₂-ambient, while the high quality p-AlGaIn EBL should be grown at higher temperature (more than 1,000°C) in H₂-ambient. Due to this mismatched growth condition, growth interruption is generally applied in the growth sequence.

Two kind of blue LEDs were prepared; one was grown with growth interruption between MQW active layer and p-AlGaIn EBL, and another was grown without the growth interruption. In latter case, the growth temperature and ambient were changed during the progress of top GaN barrier layer. There are no significant differences in current versus voltage characteristics of two samples. However, in light output versus current characteristics, 1.4 times higher light output was observed in the LED grown without the growth interruption. This result implies that a kind of defect related non-radiative recombination center is induced during the growth interruption of LED growth.

8625-74, Session PWed

Design and geometry of hybrid white light-emitted diodes for efficient energy transfer from the quantum well to the nanocrystals

Oleksii Kopylov, Roza Shirazi, Technical Univ. of Denmark (Denmark); M. Mikuli?, Beata Kardynal, Forschungszentrum Jülich GmbH (Germany)

We study light emission from patterned GaN/InGaN light-emitting diode, designed for light colour conversion via non-radiative exciton energy transfer from the electrically driven diode to the colloidal nanocrystals. For this work standard LED wafers, grown using MOCVD on sapphire substrate with 10 pairs of InGaN/GaN MQWs with quantum well (QW) thickness of 2.5 nm and GaN barrier of 11 nm, were used. Mesas with diameter of 300 μm were made in order to define diode dimensions and provide p- and n-GaN for contacts. In order to put nanocrystals closer to QWs mesa was patterned by etching holes of different diameters. We show that the patterning is necessary to increase the coupling between these two layers. We have shown that devices fabricated with holes pattern for colour conversion with non-radiative energy transfer to nanocrystals have good electrical properties and exhibit clear exciton diffusion towards surface which is needed for the colour conversion scheme. The device has turn on voltage at 2.2V and patterning didn't result in a leaking current. That confirms that surface damage, caused by ICP etching, was successfully removed by post-etching treatment in HCl. Varying the pattern parameters of the light-emitting diode, such as the diameter of holes and distances between them, one can control the overall colour conversion rate in order to achieve good quality of a white light. By having 27% of excitons to be converted into red light emission we can achieve warm white light and 11% will go for cold white.

8625-75, Session PWed

Influence of free-standing GaN substrate on ultraviolet light-emitting-diodes by atmospheric-pressure metal-organic chemical vapor deposition

Chen Yu Shieh, National Central Univ. (Taiwan); Ching-Hsueh Chiu, Po-Min Tu, National Chiao Tung Univ. (Taiwan) and Advanced Optoelectronic Technology Inc. (Taiwan); Zhen Yu Li, Hao Chung Kuo, National Chiao Tung Univ. (Taiwan); Gou Chung Chi, National Central Univ. (Taiwan) and National Chiao Tung Univ. (Taiwan)

We reported the influence of free-standing (FS) GaN substrate on ultraviolet light-emitting-diodes (UV LEDs) by atmospheric-pressure metal-organic chemical vapor deposition (APMOCVD). The Raman spectrum showing the in-plane compressive stress of the GaN epitaxial structures grown on FS GaN substrate revealed the relation between the crystal quality and the carrier localization degree in multi-quantum wells (MQWs). High resolution X-ray diffraction (HRXRD) analysis results show that the $\text{In}_{0.025}\text{Ga}_{0.975}\text{N}/\text{Al}_{0.08}\text{Ga}_{0.92}\text{N}$ MQWs grown on FS GaN substrate has higher indium mole fraction than Sapphire at the same growth conditions. The higher indium incorporation is corresponding with the red-shift 6 nm (387 nm) of the room temperature photoluminescence (PL) peak. The full widths at half maximum (FWHM) of omega-scan rocking curve in (002) and (102) reflectance on FS GaN substrate (83 arcsec and 77 arcsec) was narrower than UV LEDs grown on sapphire (288 arcsec and 446 arcsec). This superior quality may attribute to homoepitaxial growth structure and better strain relaxation in the FS GaN substrate. An anomalous temperature behavior of PL in UV LEDs designated as an S-shaped peak position dependence and W-shaped linewidth dependence indicate that exciton/carrier motion occurs via photon-assisted tunneling through localized states, what results in incomplete thermalization of localized excitons at low temperature. The Gaussian broadening parameters of carrier localization was about

16.98 meV from the temperature dependent photoluminescence (TDPL) measurement. The saturation temperature from the TDPL linewidth of UV LEDs on FS GaN substrate at about 175 K represents a crossover from a nonthermalized to thermalized energy distribution of excitons.

8625-76, Session PWed

Numerical analysis of using superlattice-AlGaIn/InGaIn as electron blocking layer in green InGaIn light-emitting diodes

Fang-Ming Chen, National Changhua Univ. of Education (Taiwan); Bo-Ting Liou, Hsiuping Univ. of Science and Technology (Taiwan); Yi-An Chang, Jih-Yuan Chang, Yih-Ting Kuo, Yen-Kuang Kuo, National Changhua Univ. of Education (Taiwan)

III-nitride-based light-emitting diodes (LEDs) have demonstrated excellent performance in visible region of the spectrum for potential applications in general illuminating, full-color displays, back-lightings, and medical applications. From the view point of numerical simulation for obtaining high-brightness LEDs, it had been pointed out that the use of high-bandgap AlGaIn layer on top of the active region is to block the electrons from escaping to the p-layers and hence the electronic leakage current is suppressed. However, the electron blocking layer (EBL) may also act as a potential barrier for the holes in the valence band, which is detrimental for the injection of holes into the active region. To solve this problem, the solutions of grading Al content in AlGaIn EBL, using polarization-matched AlInGaIn and superlattice-AlGaIn/GaN EBLs are presented to improve the hole injection efficiency. In this study, the effect of using superlattice-AlGaIn/InGaIn as EBL in green InGaIn LEDs is numerically investigated. In contrast to the conventional AlGaIn and superlattice-AlGaIn/GaN EBLs, the use of superlattice-AlGaIn/InGaIn as EBL is presented to provide better optical and electrical output performance. The output power of the green InGaIn LED with superlattice-AlGaIn/InGaIn EBL is enhanced by a factor of 19% when compared to that with conventional AlGaIn EBL at 100 mA. The improvement is mainly attributed to the enhanced hole transport and injection efficiency into the active region. The energy band diagrams, carrier distribution, and radiative recombination rate distributed in the quantum wells of the active region are discussed in detail.

8625-77, Session PWed

Role of nonequivalent atomic step edges in the growth of InGaIn by plasma-assisted molecular beam epitaxy

Henryk Turski, Institute of High Pressure Physics (Poland); Marcin Siekacz, Marta Sawicka, Institute of High Pressure Physics (Poland) and TopGaN Ltd. (Poland); Zbig R. Wasilewski, Univ. of Waterloo (Canada); Sylwester Porowski, Institute of High Pressure Physics (Poland); Czeslaw Skierbiszewski, Institute of High Pressure Physics (Poland) and TopGaN Ltd. (Poland)

Growth of high quality InGaIn with indium concentrations of more than 20%, essential for long wavelength emitters, is still challenging. The advantage of plasma assisted molecular beam epitaxy (PAMBE) over metal-organic vapor phase epitaxy (MOVPE) is considerably lower growth temperatures that is required for high quality InGaIn growth. Therefore it is highly interesting whether PAMBE technology can be useful for high In content structures required for true-blue and green emitters.

In this work we study the mechanism of indium incorporation into InGaIn layers in PAMBE. The layers were grown at In-rich regime, which is beneficial for low temperature growth of InGaIn in PAMBE. We found that both Ga and N fluxes influence composition and morphology of grown layers. We explain this effect by the different kinetics of neighboring atomic steps that are present at the surface of wurtzite InGaIn. Based on experimental data obtained for structures grown using different Ga and N fluxes, we present a phenomenological model of InGaIn growth,

**Conference 8625:
Gallium Nitride Materials and Devices VIII**

which accounts for temperature, nitrogen and gallium flux dependencies on indium incorporation. We will discuss the model predictions for the maximum In content of InGaN layers and show its usefulness in the growth of devices such as continuous wave true-blue laser diodes.

8625-78, Session PWed

Diffusion-assisted current spreading for III-nitride light-emitting applications

Pyry Kivisaari, Jani Oksanen, Jukka Tulkki, Aalto Univ. School of Science and Technology (Finland)

Large-area LEDs and LED structures based on nanowires have recently received increasing amounts of attention as a potential way to increase the output power and efficiency of GaN LEDs. In these structures, however, the challenges related to current transport become highlighted due to the typically large lateral distances between contacts and the difficulties in properly doping and contacting the free ends of the nanowires. We study a slightly unconventional approach based on bipolar diffusion to spread carriers in these structures. In the studied 2D and 3D structures the active region is located outside the traditional pn junction.

We present simulation results on how the carrier spreading, distribution, and recombination depend on the details of the structure. In addition to numerical simulations we present analytical calculations of the diffusion current equation to 1D test structure, propose selected diffusion-assisted nanowire and quantum well structures, and show that the diffusion-assisted injection concept has significant potential in optoelectronic applications. According to our initial results, the proposed structures enable e.g. bipolar charge injection to quantum wires through only one end leaving the other end completely free. In addition to nanowire LEDs, they possibly enable fabricating effective large-area LED matrices and efficient solar cells.

8625-79, Session PWed

Structural and optical characterizations of GaN-based green LEDs growth using TiN buffer layer

Chen Yu Shieh, National Central Univ. (Taiwan); Zhen Yu Li, Hao-Chung Kuo, National Chiao Tung Univ. (Taiwan); Gou Chung Chi, National Central Univ. (Taiwan) and National Chiao Tung Univ. (Taiwan)

We reported the structural and optical characterizations of GaN-based green light-emitting diodes growth using TiN buffer layer. The purpose of grown GaN-based green LEDs on TiN nano-masks layer was produced the naturally hexagonal pattern structure on the surface of undoped-GaN. Then the dislocations of grown InGaN/GaN MQWs green LED structure on uGaN/TiN/sapphire was produced horizontal staking faults by epitaxial lateral overgrowth. Cross-section transmission electron microscope showed that the dislocation density of green LEDs was decreasing from $5 \times 10^8/\text{cm}^2$ to $7 \times 10^7/\text{cm}^2$. And the dislocations in the green LEDs structure were reproduced. The full widths at half maximum of omega-scan rocking curve in (002) and (102) reflectance on GaN-based green LEDs were 334 and 488 arcsec. As the injection current increases from 5 mA to 40 mA, the electroluminescence peak wavelength of the GaN-based green LEDs shifts from 508 nm to 481 nm blue-shifted for 27 nm. The measured forward voltages at an injection current of 20 mA was 4.9 V for GaN-based green LEDs from the current-voltage characteristics. Due to the In mole fraction of GaN-based green LEDs on uGaN/TiN/sapphire increasing, the strain and phase separation increase, the multiple quantum wells structure quality and device performances of GaN-based green LEDs can decay. It was produced the yellow band that the wavelength was 551 nm from room temperature photoluminescence measurement. Meanwhile cross-section transmission electron microscope observed V-defects from multiple quantum wells structure of green LEDs.

8625-80, Session PWed

Temperature-dependent external quantum efficiencies of bulk ZnO and GaN

Nils Rosemann, Philipps-Univ. Marburg (Germany); Melanie Pinnisch, Bruno K. Meyer, Justus-Liebig-Univ. (Germany); Sangam Chatterjee, Philipps-Univ. Marburg (Germany); Martin Eickhoff, Justus-Liebig-Univ. (Germany); Stefan Lautenschläger, Justus-Liebig-Univ. Giessen (Germany)

Currently, GaN-based materials are probably considered to be the most promising candidates for efficient solid-state UV-emitters. However, ZnO has to be considered as an alternative system. Both material classes have many similar characteristics, e.g., a wurzit crystal structure, large exciton binding energies, and strong phonon coupling. While this does not necessarily hold true for their respective down-sides, as they both have own challenges. ZnO to date still lacks uncontested claims of p-type doping while the realization of high-power devices in GaN remains a large challenge due to the “droop”.

In order to better quantify the potential of both materials we investigate two series of bulk layers by temperature-dependent absolute photoluminescence spectroscopy. The samples are mounted inside a He-closed cycle cryostat equipped with a 2” diameter integrating sphere. The 325nm line of a HeCd laser at 1mW is used for excitation and a compact spectrometer equipped with a Si charge-coupled device camera is used for detection. Generally, all samples display a strong decrease of the overall external quantum efficiency (EQE) with increasing temperatures. At first glance the GaN-samples appear superior as they show a less significant decrease of the EQE towards room temperature. The situation changes when looking at selected spectral regions. A clear quenching of the near-edge emission of GaN is found. Intriguingly, an EQE of about 30% is found in the range of deep defects which is virtually independent of the lattice temperature. The ZnO samples EQE, however, is still dominated by the near-edge emission even at room temperature.

8625-81, Session PWed

Microwave performance of AlGaN/AlN/GaN-based single and coupled channels HFETs

Romualdo A. Ferreyra, Xing Li, Fan Zhang, Congyong Zhu, Natalia Izyumskaya, Cemil Kayis, Vitaliy Avrutin, Ümit Özgür, Hadis Morkoç, Virginia Commonwealth Univ. (United States)

In this work we compare electronic transport performance in HFETs based on single channel (SC) GaN/Al_{0.30}GaN/AlN/GaN (2nm/20nm/1nm/3.5µm) and coupled channel (CC) GaN/Al_{0.285}GaN/AlN/GaN/AlN/GaN (2nm/20nm/1nm/4nm/1nm/3.5µm) structures. Current gain cutoff frequency, for SC (11.6 GHz) is lower than CC (14.8 GHz), additionally, the maximum drain current, IDmax, is higher in the CC HFET than in the SC HFET. For both HFETs, maximum occurs near bias point where maximum transconductance (gm,max) is achieved; VGS = -2.75 V and VDS = 12 V and VGS = -2.5 V and VDS = 8 V for SC and CC HFETs, respectively. Therefore, both HFETs can operate at the high frequencies while delivering high ID, as the pinch-off voltage (Vpo) is ~ -3.75 V. This is in contrast with reports by other groups where is attained at VGS closer to Vpo, and therefore, at lower ID/IDmax ratios and low gm. Results are consistent in that CC HFET delivers higher IDmax because of the higher electron mobility (µ) and higher carrier density (ns) in the channel. As saturation drain current, IDsat, is attained at electric fields (~40KV/cm) lower than the critical electric field, Ecr, (~150KV/cm for GaN) the higher in CC HFETs can be attributed, mainly, to a higher µ, which is in agreement with the Hall measurements.

**Conference 8625:
Gallium Nitride Materials and Devices VIII**

8625-82, Session PWed

Linewidth reduction of site-controlled InGaN quantum dots by surface passivation

Chu-Hsiang Teng, Lei Zhang, Hui Deng, Univ. of Michigan (United States); Pei-Cheng Ku, Univ. of Michigan (United States)

Indium gallium nitride (InGaN) semiconductor quantum dots are an attractive candidate for scalable room temperature quantum photonics applications owing to the large exciton binding energy and large oscillation strength. Previously, we reported single photon emission from site-controlled InGaN dot-in-wire structures fabricated by e-beam lithography and dry etching. However, large homogeneous linewidth and abnormally long radiative lifetime were thought to be linked to the nearby charge centers. These charge centers can limit the excitation rate of excitons in the quantum dots, result in spectral diffusion, and contribute to the excessive non-radiative recombinations at high temperature. The linewidth of a single quantum dot is on the order of tens of meV at low temperature and increases and saturates at 150 K. Moreover, time-resolved PL rendered 3.5 ns lifetime, while the second order correlation measurement showed 200 ps lifetime. The inconsistency further confirmed the presence of surface charge centers acting as a carrier reservoir. In this work, approaches to reducing InGaN quantum dot emission linewidth were investigated. These include the passivation of surface states (mainly nitrogen vacancies) and passivation of InGaN active region against oxidation. Nitrogen vacancies were successfully passivated by ammonium sulfide ((NH₄)₂Sx) treatment, and the emission linewidth of a single quantum dot was reduced by 5 meV. Furthermore, the linewidth broadening with an increasing temperature was suppressed in the temperature range from 9 K to 95 K in this study. Satellite emission peak believed to be associated with the nitrogen vacancy was observed for un-passivated quantum dots. The satellite peak was 55 ~ 80 meV away from the main InGaN emission peak and was eliminated after sulfide passivation.

8625-83, Session PWed

Recombination dynamics in non-polar m-plane GaN investigated by polarization- and time-resolved photoluminescence

Serdal Okur, Virginia Commonwealth Univ. (United States); Kestutis Jarasiunas, Vilnius Univ. (Lithuania); Jacob Leach, Tanya Paskova, Kyra Technologies, Inc. (United States); Vitaliy Avrutin, Hadis Morkoç, Ümit Özgür, Virginia Commonwealth Univ. (United States)

The carrier recombination dynamics in non-polar m-plane GaN were investigated by excitation and temperature dependent time-resolved photoluminescence (TRPL) measurements. By easily probing polarization states parallel and perpendicular to the c-axis, polarization-resolved photoluminescence (PRPL) allowed separation of exciton and free carrier contributions to radiative recombination at low temperatures as emission resulting from free carrier recombination has no preferred polarization whereas that due to excitons is strongly polarized along the a-axis of wurtzite GaN. The radiative recombination at temperatures below 150K was mainly from free and donor bound excitons, while it was dominated by free carriers with further increase in temperature due to exciton dissociation and with increasing excitation density due to screening of excitons. Theoretical temperature dependence of radiative lifetime (~ T^{3/2}) was used to extract the exciton recombination lifetime from the radiative recombination rates measured using TRPL. At an excitation density of 4 μJ/cm² exciton recombination lifetime (free and donor bound excitons mixture) was nearly constant at 1.5 ns below 150K, but decreased rapidly above 150K. In this work, it was shown that by

combining TRPL and PRPL spectroscopy techniques the excitonic nature of radiative recombination at different temperatures can be identified.

8625-84, Session PWed

Gallium nitride distributed feedback nanowire lasers

Jeremy B. Wright, Sandia National Labs. (United States) and The Univ. of New Mexico (United States); Qiming Li, Igal Brener, Ting S. Luk, George T. Wang, Sandia National Labs. (United States); Huiwen Xu, Luke F. Lester, The Univ. of New Mexico (United States)

Compact, single-mode, coherent light sources are highly desirable in many photonic applications. For many of these applications it is desirable to have single-mode emission. Nanowire lasers can fill this role, but it is difficult to implement modal control due to the small scale of these devices. A single GaN nanowire was coupled to a dielectric grating acting as external distributed feedback and providing control over modal behavior. Nanowires were placed by dry-transfer onto a silicon nitride grating structure. Nanowires were randomly oriented on the grating structure and then optically pumped at room temperature. We observed a direct relationship between the number of transverse/longitudinal lasing modes and the relative misalignment of a nanowire to the grating. Further study was performed by intentionally adjusting the orientation of single nanowires via a piezo-electric driven probe in a scanning electron microscope. Single-mode emission was observed for all nanowires at full nanowire/grating alignment. Sandia National Laboratories is a multi-program laboratory managed and operated by Sandia Corporation, a wholly owned subsidiary of Lockheed Martin Corporation, for the U.S. Department of Energy's National Nuclear Security Administration under contract DE-AC04-94AL85000.

8625-85, Session PWed

GaN-based vertical cavity lasers with all dielectric reflectors and polar and nonpolar crystal orientations

Fan Zhang, Serdal Okur, Shopan Hafiz, Vitaliy Avrutin, Ümit Özgür, Hadis Morkoç, Virginia Commonwealth Univ. (United States)

Polar c-plane and nonpolar m-plane GaN-based vertical cavity structures were investigated for lasing in both weak and strong coupling regimes. For c-plane, epitaxial lateral overgrowth technique allowed the use of both top and bottom all dielectric reflector stacks without substrate removal and the fabrication of the active region containing InGaN multiple quantum wells entirely on the nearly defect-free laterally grown wing regions to avoid nonradiative centers caused by extended and point defects. The second lateral overgrowth step ensured current conduction only through defect-free active region that is at the center of the emission window. The c-plane VCSEL structures so developed exhibited clear cavity modes under electrical injection albeit having low Q factors (~110). Under optical excitation lasing was observed with Q values over 1200 above an excitation threshold of ~4uJ/cm². Vertical cavity structures with bottom AlN/GaN DBRs and top dielectric DBRs were also fabricated on freestanding c-plane and m-plane GaN substrates and the cavity polariton effects investigated. Polariton dispersion obtained from angle-resolved photoluminescence and reflectivity measurements revealed the strong coupling regime in these structures, which will pave the way for high efficiency and low-threshold vertical cavity lasers.

8625-86, Session PWed

Depth distribution of carrier lifetimes in semipolar GaN grown by MOCVD on patterned Si substrates

Natalia Izyumskaya, Serdal Okur, Fan Zhang, Vitaliy Avrutin, Ümit Özgür, Virginia Commonwealth Univ. (United States); Sebastian Metzner, Christopher Karbaum, Frank Bertram, Jurgen Christen, Otto-von-Guericke-Univ. Magdeburg (Germany); Hadis Morkoç, Virginia Commonwealth Univ. (United States)

Large internal electric fields in polar wurtzite structures, which have been the technological basis for the development of GaN-based devices, lead to spatial separation of electron and hole wavefunctions in active regions of light-emitting diodes (LEDs) and lasers (so-called quantum confined Stark effect), reducing light emission efficiency and causing a blue shift with increased injection. Therefore, the possibility to reduce or even completely eliminate internal electric fields has fueled substantial interest in nonpolar and semipolar GaN structures. At present, a good understanding of electrical and optical properties of nonpolar and semipolar GaN is lacking. Recently, we have demonstrated that optical quality of (1-101)GaN grown by metal-organic chemical vapor deposition (MOCVD) on patterned Si(001) substrates is comparable to that of c-plane GaN films grown on sapphire [1] and studied dependence of optical properties of the semipolar GaN on MOCVD growth conditions [2].

In this contribution we report on optical properties of semipolar (1-101) GaN layers and GaN/InGaN LED structures grown on patterned (001) Si substrates. Photon energies and intensities of emission lines from steady-state PL as well as carrier decay times from time-resolved PL (TRPL) were correlated with the distributions of extended defects studied by spatially resolved cathodoluminescence (spatio-CL) and near-field scanning optical microscopy (NSOM). To gain insight into the contribution from surface recombination to carrier dynamics in polar c-plane and semipolar (1-101) GaN, we have studied TRPL with different excitation wavelengths (from 280 to 355 nm) providing different excitation depths.

[1]. N. Izyumskaya et al., Proc. SPIE, vol. 7939, pp. 79391W-1 – 79391W-9 (2011).

[2]. N. Izyumskaya et al., “Effect of MOCVD growth conditions on the optical properties of semipolar GaN on Si patterned substrates”, Proc. SPIE, vol. 7939, pp. 79391W-1 – 79391W-9 (2011).

8625-87, Session PWed

Investigation of microwave and noise properties of InAlN/GaN HFETs after electrical stress: role of surface effects

Congyong Zhu, Fan Zhang, Romualdo A. Ferreyra, Xing Li, Cemil Kayis, Vitaliy Avrutin, Ümit Özgür, Hadis Morkoç, Virginia Commonwealth Univ. (United States)

In 18.5%Al/81.5%N/GaN HFETs on sapphire substrates were subjected to on-state-high-field electrical stress for up to 20 hours. The current gain cutoff frequency f_T showed a constant increase from ~2.5 GHz to ~5 GHz after stress, which was consistent with the decreased gate lag and the decreased phase noise. Extraction of small-signal circuit parameters revealed that the increase of f_T originates from the decreased gate-source (C_{gs}) and gate-drain (C_{gd}) capacitances as well as the increased small-signal transconductance (g_m). All these observations are consistent with the diminishing of the gate extension (“virtual gate”) through the creation of long time-constant electron trap states around the gate area.

8625-88, Session PWed

Atomic structure and optical properties of GaN surfaces with polar (000-1), nonpolar (1-100) and semi-polar (20-21) crystal orientations

Oleksandr Romanyuk, Petr Jiricek, Josef Zemek, Pingo Mutombo, Institute of Physics of the ASCR, v.v.i. (Czech Republic); Tania Paskova, North Carolina State Univ. (United States)

The atomic surface structure and optical properties of the commercially available GaN substrates with polar (000-1), non-polar (1-100), and semi-polar (20-21) surface plane alignment have been investigated. Several surface treatment procedures have been performed: the (1x1) surfaces have been prepared by circles of nitrogen and argon ion sputtering and by surface annealing under ammonia, hydrogen and combination of both fluxes environment. The surface quality was monitored by x-ray photoelectron spectroscopy (XPS) and x-ray photoelectron diffraction (XPD) measurements. The Ga/N concentration ratio on a surface and surface quality were found significantly influenced by the surface treatment procedures.

The surface polarity of polar GaN substrates was evaluated by quantitative low-energy electron diffraction (LEED) and was confirmed by XPD measurements. The optical constants of the GaN surfaces have been determined by reflection electron energy loss spectroscopy (REELS) measurements for a wide frequency range.

Ab initio calculations of the electronic band structure have been carried out for the (1x1) terminated surfaces. Density of states (DOS) of the valence bands has been correlated with the angle-resolved ultraviolet photoelectron spectroscopy (ARUPS) measurements on polar and non-polar GaN. Surface states at the top of the valence band have been localized.

8625-89, Session PWed

Mode-polarization effect on the mode-coupling in gallium-nitride-based semiconductor-metal lasers

Meng-Mu Shih, Univ. of Florida (United States)

This work demonstrates the theoretical modeling in order to compute the mode-coupling in the grating-assisted semiconductor lasers. The metallic corrugated grating layer is adjacent to the gallium-nitride multi-layer quantum-well laser. The photonic method is utilized in the computational process for the periodic waveguide structure. Numerical results show how the mode-coupling can be affected by structural parameter such as grating depth, period and layer thickness and by material parameters in semiconductor and metallic layers. The modified model further shows how mode-polarization can affect the mode-coupling. Physical interpretations of numerical results can provide more insights into the modeling and design of such lasers.

8625-53, Session 12

Semipolar GaN-based optoelectronic structures on large area substrates (*Invited Paper*)

Ferdinand Scholz, Dominik Heinz, Robert A. R. Leute, Tobias Meisch, Junjun Wang, Univ. Ulm (Germany)

Green light emitting diodes based on group-III nitrides still suffer from fairly low performance as compared to shorter wavelength blue emitters. One possible reason is the lattice mismatch induced strain of the GaInN quantum wells in the active region in such devices having a comparably

**Conference 8625:
Gallium Nitride Materials and Devices VIII**

large In content. This causes the formation of huge piezoelectric fields within the GaInN quantum wells separating electrons and holes locally and hence reducing their recombination probability. By changing the main epitaxial growth direction from the conventional polar c-direction into less polar crystal directions, the internal fields can be strongly reduced. We currently study some hetero-epitaxial approaches which can be easily applied to large size sapphire wafers. In this review, we will describe such approaches which make use of the well-established growth of GaN in c-direction eventually leading to semipolar device structures. In the first approach, GaInN quantum well structures are grown on semipolar side facets of selectively grown GaN stripes with triangular cross-section. By decreasing the size and distance of such stripes to sub-micrometer dimensions, they can be embedded into n- and p-doped planar cladding layers. Moreover, we have used inclined c-plane side-facets prepared by etching grooves into adequately oriented sapphire wafers as nucleation sites for GaN. After coalescence of these striped nitride structures, they form large area planar semipolar nitride surfaces on which again LED structures can be grown. The formation of the commonly observed defects like dislocations and stacking faults was reduced by various methods leading eventually to excellent structural properties.

8625-54, Session 12

First-principles studies of Auger recombination in InGaN (*Invited Paper*)

Emmanouil Kioupakis, Univ. of Michigan (United States); Daniel Steiauf, Qimin Yan, Chris G. Van de Walle, Univ. of California, Santa Barbara (United States)

Auger recombination is an important nonradiative recombination mechanism that reduces the efficiency of optoelectronic devices at high power. Predictive first-principles calculations based on density functional can provide theoretical insight into the nature of Auger recombination in semiconducting materials. We will discuss the results of our first-principles studies of direct and indirect Auger recombination in InGaN alloys. We will show that indirect Auger recombination mediated by electron-phonon coupling and alloy scattering is particularly strong and can explain the efficiency droop of nitride LEDs. We will present our computational methodology and compare our results with other theoretical studies and experiment.

8625-55, Session 12

Investigation of droop-causing mechanisms in GaN-based devices using fully microscopic many-body theory

Jörg Hader, College of Optical Sciences, The Univ. of Arizona (United States) and Nonlinear Control Strategies Inc. (United States); Jerome V. Moloney, The Univ. of Arizona (United States) and Nonlinear Control Strategies Inc. (United States); Stephan W. Koch, Philipps-Univ. Marburg (Germany)

Many models have been suggested as possible explanation for the efficiency droop in GaN-based devices. Generally, these models are based on rate equations in which the underlying microscopic properties are described using macroscopic parameters that are used as adjustable parameters like radiative and Auger constants. This gives these models a high flexibility that allows obtaining good fits with experimental data. However, it also makes it questionable whether they represent the underlying physics correctly.

Here, we use fully microscopic many-body models to calculate carrier losses due to radiative and direct and indirect Auger processes. These models have been shown to be able to determine the losses quantitatively correct without requiring additional fit parameters. Thus, they allow reducing the amount of adjustable parameters to a minimum which allows for stringent tests of proposed droop models.

Using the microscopic modeling we test some of the most frequently proposed droop mechanisms. It is shown that Auger losses are too small and have a wrong temperature dependence. Models that assume that the droop is solely due to carrier (de)localization have to assume unreasonable localization parameters, especially at elevated densities and temperatures. And, using the calculated radiative losses, one finds that one cannot explain experiments in which electrical AND optical pumping has been used assuming droop models that consider only carrier injection/transport phenomena. On the other hand, no contradicting evidence is found for a model that assumes density-activated defect-recombination as droop cause for low to intermediate pump powers and injection/transport phenomena at higher pump levels.

8625-56, Session 12

Analysis of nonradiative carrier recombination process by extracting nonradiative current component in InGaN light-emitting diodes

Kyu-Sang Kim, Sangji Univ. (Korea, Republic of); Il-Gyun Choi, Dong-Pyo Han, Joo-Sun Yun, Jong-Ik Lee, Dong-Su Shin, Jong-In Shim, Hanyang Univ. (Korea, Republic of)

Nonradiative carrier recombination process depending on current injection level has been investigated in InGaN/GaN light-emitting diodes (LEDs). In general, the ideality factor of current-voltage (I-V) curves in LEDs has been known to have a close relation to the carrier transport and recombination. The ideality factor could be extracted from Shockley equation, which has been usually fitted by two kinds of equivalent circuit model both consisting of diode and resistor. However, it is difficult to extract the exact nonradiative recombination mechanisms from the ideality factor just by fitting I-V curve, because the radiative/nonradiative recombination current ratio of total current would vary on its current injection level. In this study, therefore, we investigate the nonradiative recombination mechanism by proposing new equivalent circuit model and extracting the radiative and nonradiative current component from I-V curve using IQE characteristics. We separated radiative current and nonradiative current from I-V and IQE by low temperature dependent electroluminescence (TDEL) measurement and then analyze dominant nonradiative mechanism in IQE droop from the ideality factor variation. As a result, we could know that the dominant nonradiative mechanism of LEDs is changed over from either Shockley-Read-Hall recombination or a tunneling current at low current density, subsequently to carrier overflow at high current density, thereby, IQE droop.

8625-57, Session 12

Comparative investigation of induced electroluminescence in InGaN/GaN light-emitting diodes with open- and short-circuit conditions

Seung-Hyuk Lim, Yong-Hoon Cho, KAIST (Korea, Republic of)

Group III-nitrides have been widely used in optoelectronic devices. The optical properties of InGaN quantum wells (QWs) on c-GaN (polar) are governed by quantum confined Stark effect (QCSE), which is caused by the polarization itself. Due to asymmetry in the wurtzite structure, the group III nitrides have strong internal spontaneous polarization. Additionally, the strain due to huge lattice mismatches causes additional piezoelectric polarization and interface charges. These large electrostatic fields in the [0001] orientation result in a QCSE and poor electron-hole overlap. Because emission efficiency of LEDs is strongly dependent on QCSE, the research on QCSE of nitrides is very significant. To investigate QCSE, external biased photoluminescence (PL) has been widely studied. However, when uniformly excited light-emitting diodes (LEDs) is left in an open circuit, the voltage gradually increases as excess electrons and holes accumulate on the n-type and the p-type sides, respectively. This forward voltage results in emission called induced electroluminescence

**Conference 8625:
Gallium Nitride Materials and Devices VIII**

(EL). In this work, we report on the relation between induced EL and QCSE in LEDs with open- and short-circuit. Spatial-resolved PL, time-resolved PL and external biased PL experiments were used on a variety of LEDs (e.g., blue LEDs with and without electron blocking layer, patterned substrate, and so on) with open- and short- circuits. Lifetime and induced bias were measured to distinguish PL and induced EL. We systematically studied the carrier dynamics of LEDs with open- and short- circuit condition.

8625-58, Session 12

Changes in the Mg profile and in dislocations induced by high-temperature annealing of blue LEDs

Matteo Meneghini, Nicola Trivellini, Marina Berti, Tiziana Cesca, Andrea Gasparotto, Univ. degli Studi di Padova (Italy); Anna Vinattieri, Univ. degli Studi di Firenze (Italy); Franco Bogani, Univ. degli Studi di Firenze (Italy); Dandan Zhu, Colin Humphreys, Univ. of Cambridge (United Kingdom); Gaudenzio Meneghesso, Univ. degli Studi di Padova (Italy); Enrico Zanoni, Univ. degli Studi di Padova (Italy)

The injection and recombination efficiency of InGaN/GaN LEDs can be influenced by the high temperatures used during the growth of the devices. In particular, to improve the fabrication process, it is very important to study how high temperatures can modify the magnesium profile, and the properties of dislocations.

This paper reports on an extensive analysis of the effects of high temperature annealing on the properties of InGaN-based LED structures. The study is based on time-resolved photoluminescence (TR-PL), SIMS, and RBS-Channeling measurements, carried out before and after a series of annealing tests at 800 °C and 900 °C, in N₂ atmosphere. The analyzed samples are LEDs with five-fold MQW structure, grown on sapphire, and emitting in the blue spectral region.

Results indicate that high temperature annealing may induce: (i) an increase in carrier lifetime, which corresponds to a decrease in the non-radiative recombination rate; (ii) an increase in the efficiency of the GaN NBE emission and the blue spectral peak; (iii) a decrease in Mg-related luminescence bands, located at 3.2 eV. This result indicates a decrease in the Mg concentration in the p-type material, which is confirmed by SIMS characterization. (iv) a diffusion of Mg towards the active region of the LEDs, detected by SIMS measurements. (v) a re-arrangement of the dislocations, detected by RBS-channeling measurements, that can partly explain the reduction of non-radiative recombination measured after stress (point (i) and (ii)).

These results are of fundamental interest for the optimization of the fabrication process for high-efficiency LEDs.

8625-59, Session 13

Development of 260 nm band deep-ultraviolet light-emitting diodes on Si substrates (Invited Paper)

Takuya Mino, RIKEN (Japan) and Panasonic Corp. (Japan); Hideki Hirayama, RIKEN (Japan); Takayoshi Takano, Kenji Tsubaki, RIKEN (Japan) and Panasonic Corp. (Japan); Masakazu Sugiyama, The Univ. of Tokyo (Japan)

Deep-ultraviolet (DUV) light-emitting diodes (LEDs) have a wide range of potential applications such as sterilization, water purification, medicine and biochemistry. In recent years, the external quantum efficiency (EQE) and the performance of AlGaIn-based DUV LEDs on sapphire substrates have increased markedly by improvement of crystalline-quality of high Al-content AlGaIn layer and optimization of LED structure. On the other hand, DUV LED fabricated on Si substrate is very promising as a low-cost

DUV light-source in near future. However, DUV LEDs on Si substrates with wavelength shorter than 350 nm have been hardly reported until now. This is because AlN layer on Si has always suffered from cracking by the large mismatch of lattice constant and thermal expansion coefficient between AlN and Si. In this paper, DUV LEDs on Si were realized by reduction of cracks and threading dislocation density (TDD) of AlN templates, using a combination of NH₃ pulsed-flow growth method and epitaxial lateral overgrowth (ELO) method. ELO-AlN templates were successfully coalesced on trench-patterned substrates with the stripes along <10-10> direction of AlN. The 4- μ m-thick ELO-AlN templates were crack-free, because voids formed by ELO process relaxed the tensile stress in the AlN layer. Furthermore the AlN templates showed low-TDD. The full width at half maximum values of (0002) and (10-12) x-ray rocking curves were 780 and 980 arcsec, respectively. DUV LEDs fabricated on the high-quality ELO-AlN/Si showed single peak emission at 256-278 nm in electroluminescence measurement. It is expected to realize the low-cost DUV LEDs on Si substrates using ELO-AlN templates.

8625-60, Session 13

Studies of hole transport in Mg-doped AlGaIn layers for deep-ultraviolet light emitters

Suk Choi, Bowen Cheng, Zhihong Yang, Clifford Knollenberg, Mark Teepe, Thomas Wunderer, Christopher Chua, John Northrup, Noble Johnson, Palo Alto Research Center, Inc. (United States)

AlGaIn epilayers with Al composition higher than 50% are required for the realization of high-performance nitride-based light-emitting devices operating in the deep ultraviolet (DUV) region ($\lambda < 300$ nm), with their wide bandgap, UV transparency, and high optical confinement effect. In DUV light emitters, the growth of p-type AlGaIn layers have been a major challenge because of the dramatic increase of Mg-acceptor thermal activation energy in AlGaIn with increasing Al composition. Mg-doped AlGaIn superlattice structures that utilize polarization fields to reduce Mg acceptor energy level have been reported as an alternative method to improve p-type doping efficiency of AlGaIn layers. However, the existence of a large energy barrier in these structures severely degrades hole mobility and layer conductivity in the vertical direction, which makes these structures less useful in actual device structures. We have explored a number of designs for the p-layer for DUV light emitters and will report the results.

The studies were conducted with p-layers of AlGaIn grown on bulk AlN substrates. Van der Pauw devices were fabricated for variable-temperature Hall-effect measurements. The AlGaIn p-layers show very small effective dopant activation energies in the range of 20 meV. This is to be compared to that for p-type GaN (146 meV) or AlGaIn (323 meV). The results indicate that the acceptors in our AlGaIn structure are activated via an athermal process. AlGaIn p-n junction devices were grown on bulk AlN to confirm high vertical conductivity of the p-layer structure. Current-voltage and four-wire measurements on the p-n junction devices revealed that our p-layer provides higher conductivity, smaller voltage drop, and higher current drive compared to standard homogeneous AlGaIn p-layer with similar average Al composition. A UV test diode employing our p-layer displayed DC-mode current injection level of 550 mA, which is equivalent to 11 kA/cm².

8625-61, Session 13

High optical power ultraviolet superluminescent InGaIn diodes

Anna Kafar, Institute of High Pressure Physics (Poland) and Gdansk Univ. of Technology (Poland); Szymon Stanczyk, Grzegorz Targowski, Przemek Wisniewski, Mike Leszczynski, Tadek Suski, Piotr Perlin, Institute of High Pressure Physics (Poland)

Conference 8625: Gallium Nitride Materials and Devices VIII

Superluminescent diodes are semiconductor devices which emit a narrow light beam of very low time coherence. This kind of devices are of great use for applications such as optical coherence tomography or pico-projectors.

The epitaxial structure of such devices is identical to that of a laser diode. The suppression of light resonance in the diode is realized by specific shape of defined waveguide. In presented work we chose to apply a bent waveguide in a shape of letter "j". This geometry provides a light reflection from the rear facet (straight end) and low reflection from the bended end. We fabricated devices with various bending angles (from 4.75° to 8°) and two waveguide lengths: 1000 and 1500 μm. To optimize the device performance, for chosen 1500 μm long devices we applied anti-reflection coating at the front facet and high-reflection coating at rear facet.

Under pulsed operation the devices emit optical power up to 500 mW in the ultraviolet region (395 nm) at room temperatures. The measured spectra are smooth and show no tendency for lasing with increasing of current. The optical spectrum has width of 4 to 5 nm even at high current densities (about 35 kA/cm²). Emitted optical power was very sensitive to the device temperature. This effect limited the maximum optical power obtained in CW operation to between 10 and 30 mW. With better packaging scheme better performance in CW regime should be achieved.

8625-62, Session 13

mechanism for in-situ measurement of GaN luminaire chip temperatures

Daren A. Lock, Univ. of Surrey (United Kingdom); Simon Hall, National Physics Lab. (United Kingdom); Andrew Prins, Stephen J. Sweeney, Univ. of Surrey (United Kingdom)

LED based lamps on the market today are expensive due to the complex packaging required to dissipate the heat generated. This also limits their performance and lifetime due to degradation of the phosphor or individual LED chips in the case of RGB sources. There is a strong commercial imperative to develop in-situ technology to measure, and ultimately compensate for the thermal environment of a luminaire. This paper will describe a chip based temperature measurement system for use in commercial luminaires, utilising the luminaire pump LED chips themselves to determine the temperature.

The large Stoke's shift in GaN green and blue emitting LEDs, enables a blue LED emitter to be utilised as a pump to induce a photocurrent within the devices. Measurements have shown that we can excite both the green and blue emitters on the absorption edge resulting in a rise in open circuit voltage (Voc) with increasing temperature. From these measurements we have been able to plot the junction temperature of a device in quasi-cw mode with a good correlation to its measured forward voltage junction temperature.

Running two banks of RGB LEDs in opposing duty cycles would enable the active blue pumps to generate a photocurrent within the off state devices and hence, using on-board control electronics, it should be possible to compensate for ambient temperature fluctuations to ensure uniform illumination from the luminaire.

8625-63, Session 14

Preparation of high-quality AlGaIn and its application for electron-beam-excitation ultraviolet light source (*Invited Paper*)

Hidetomi Miyake, Mie Univ. (Japan); Fumitsugu Fukuyo, Mie Univ. (Japan) and Hamamatsu Photonics K.K. (Japan); Shunsuke Ochiai, Kazumasa Hiramatsu, Mie Univ. (Japan); Harumasa Yoshida, Yuji Kobayashi, Hamamatsu Photonics K.K. (Japan)

AlGaIn alloy has attracted significant attention for deep-ultraviolet (UV) light-emitting diodes (LEDs) is actively carried out. However, the emission efficiency of LEDs with wavelength less than 260 nm is rather low, partly

due to the high resistivity of p-AlGaIn and the low quality of the AlGaIn template. To improve the crystal quality of AlGaIn, many methods have been proposed, such as growth on GaN and the use of low-temperature buffer layer technology. We have recently obtained high-quality crack-free AlGaIn layers for all AlN molar fractions by using an AlN/sapphire template.

In this study, we performed the growth of Si-doped AlGaIn and AlGaIn/AlGaIn multiple-quantum wells (MQWs) on by low-pressure MOVPE. We fabricated a the Si-doped Al_{0.60}Ga_{0.40}N / Al_{0.75}Ga_{0.25}N MQWs with thickness of 600 nm after sequentially depositing an Al_{0.85}Ga_{0.15}N buffer layer, Al_{0.80}Ga_{0.20}N buffer layer and Si-doped Al_{0.75}Ga_{0.25}N buffer layer on the AlN/sapphire templates. We evaluated samples with different well thicknesses of 1.0, 1.5 and 3.0 nm, with constant barrier thickness 7 nm and a total MQWs thickness of 600nm. The peak intensity of the CL spectra was greatest at a well thickness of 1.5 nm, so that optimum well thickness was 1.5nm. We also evaluated samples with different barrier thicknesses of 3, 7, 11 and 15 nm with here optimized well thickness of 1.5 nm, and a total MQW thickness of 600 nm. The highest peak intensity was observed at a barrier thickness of 7 nm, so that optimum barrier thickness was 7 nm. A prototype ultraviolet-light-source tube was fabricated with an AlGaIn film used as a target for electron-beam (EB) excitation.

We confirmed that the deep-UV light output power was 16 mW at a wave length of 256 nm with the EB input power of 2W at 10kV, and that the conversion efficiency was 1% at the EB input power of 1W.

8625-65, Session 14

X-ray detectors based on GaN (*Invited Paper*)

Jean-Yves Duboz, Eric Frayssinet, Sebastien Chenot, Ctr. de Recherche sur l'Hétéro-Epitaxie et ses Applications (France); Jean-Luc Reverchon, Alcatel-Thales III-V Lab. (France); Mourad Idir, Soleil (France)

The potential of GaN for X-ray detection in the range from 5 to 22 keV has been assessed. The absorption coefficient has been measured as a function of photon energy. Schottky diode detectors have been fabricated and tested under polychromatic X-ray illumination and under monochromatic irradiation from 5 to 22 keV in the Soleil synchrotron facility. Some parasitic effects related to the electrical activation of defects by high energy photons and to the tunnel effect in lightly doped Schottky diodes have been evidenced and modeled. These effects disappear in optimized detectors. The measured spectral response is found to be very consistent with the spectral absorption coefficient. The sensitivity of GaN Schottky diodes is evaluated and found to be slightly below the one of Si detectors at 15 keV. The use of such detectors for fabricating 2D arrays will be discussed.

8625-67, Session 14

Electroabsorption and refractive index modulation induced by intersubband transitions in GaN/AlN heterostructure waveguides

Anatole Lupu, Institut d'Electronique Fondamentale (France); Salam Sakr, Univ. Paris-Sud 11 (France); Yulia Kotsar, Commissariat à l'Énergie Atomique (France); Maria Tchernycheva, Isac Nathalie, Univ. Paris-Sud 11 (France); Eva Monroy, Commissariat à l'Énergie Atomique (France); François Julien, Univ. Paris-Sud 11 (France)

We present the determination of the index variation in the GaN/AlN heterostructures related to the population/depletion of the quantum wells fundamental state leading to the intersubband (ISB) absorption variation in the spectral domain around 1.5 μm. The experiments were performed using wide-strip waveguide structure. It is shown that the

Conference 8625: Gallium Nitride Materials and Devices VIII

determination of the refraction index in a wide-strip structure is possible when the waveguide is multimode in the vertical direction with a small number of higher order modes. The variation of the refractive index is then deduced from the shift of the position of the beating interference maxima of different order modes. The obtained index variation with bias from complete depletion to full population of the quantum wells is around -0.005. This value is similar to the typical index variation achieved in InP and is an order of magnitude higher than the index variation obtained in silicon. The remarkable feature is that maximum index variation is obtained at the wings of the ISB transition line where absorption is reduced with respect to the peak value. This index variation mechanism opens prospects for the realization of ISB phase modulators by inserting the active region in a Mach-Zehnder interferometer. The preliminary results on the design, fabrication and characterization of such Mach-Zehnder interferometers for phase modulator application are presented.

8625-68, Session 14

Avalanche photodiodes with cutoff wavelengths below 280nm based on AlGaIn grown by pulsed MOCVD

Puneet Suvarna, Jeffrey M. Leathersich, Pratik Agnihotri, F. Shadi Shahedipour-Sandvik, Univ. at Albany (United States); L. Douglas Bell, Shouleh Nikzad, Jet Propulsion Lab. (United States)

AlGaIn based photodetectors provide numerous advantages over currently available UV detectors. They can achieve solar blindness without the use of filters, have high quantum efficiency and are radiation hard. Visible blind GaN based Avalanche Photodiodes (APDs) have seen significant development over the years, however numerous challenges in material quality and device design need to be addressed for the realization of Al_xGa_{1-x}N (x>.4) photodetectors with cutoff wavelength in the solar blind regime below 280nm and capable of sustaining avalanche breakdown with high reliability.

The lack of readily available bulk AlN substrates and epitaxy issues make the growth of high Al composition AlGaIn extremely challenging. In this work we employ a newly developed pulsed MOCVD technique to epitaxially grow AlGaIn-based APDs on UV transparent double side polished sapphire substrates. The transparency of the substrate is critical to solar blind UV detectors due to the use of lower bandgap GaN as the p-layer. AFM, high resolution XRD and Hall measurements are used for characterizing the quality and structure of the layers.

Physics based simulation using Sentaurus TCAD is employed to evaluate and optimize various device designs. Vertical mesa photodiodes of diameters ranging from 20 to 240 microns are fabricated and characterized. The relationship of the various performance metrics for solar blind APDs namely dark current, gain, responsivity, cutoff wavelength and noise to layer structure, template quality, and device design will be presented.

8625-69, Session 14

High voltage GaN-based photoconductive switches for pulsed power and RF synthesis applications

Jacob H. Leach, Robert Metzger, Edward Preble, Keith R. Evans, Kyma Technologies, Inc. (United States)

Switches are at the heart of all pulsed power and directed energy systems, which find utility in a number of applications. At present, those applications requiring the highest power levels tend to employ spark-gap switches, but these suffer from relatively high delay-times (~10-8 sec), significant jitter (variation in delay time), and large size. That said, optically-triggered GaN-based photoconductive semiconductor switches (PCSS) offer a suitably small form factor and are a cost-effective, versatile solution in which delay times and jitter can be extremely short. Furthermore, the optical control of the switch means that they are

electrically isolated from the environment and from any other system circuitry, making them immune from electrical noise, eliminating the potential for inadvertent switch triggering. Our recent work shows great promise to extend high-voltage GaN-based PCSS state-of-the-art performance in terms of subnanosecond response times, very high di/dt, very high dV/dt, low on-resistance, and high blocking voltages. In this work, we discuss these recent findings, suggest possible physical models for the GaN photoconductivity, and additionally propose several device topologies for various pulsed power and synthesis applications.

8625-91, Session 14

AlN-based technology for deep UV and high-power applications (*Invited Paper*)

Zlatko Sitar, HexaTech, Inc. (United States) and North Carolina State Univ. (United States); Baxter Moody, S. Craft, Raoul Schlessler, Rafael F. Dalmau, Jinqiao Xie, Seiji Mita, HexaTech, Inc. (United States); T. Rice, J. Tweedy, J. LeBeau, Lindsay Hussey, Ramon Collazo, B. Gaddy, D. Irving, North Carolina State Univ. (United States)

For the first time in history of III-nitrides, the availability of low defect density (<10³ cm⁻²) native AlN substrates offers an opportunity for growth of AlGaIn alloys and device layers that exhibit million-fold lower defect densities than the incumbent technologies and enable one to assess and control optical and electrical properties in absence of extended defects. Epi-ready AlN wafers are fabricated from AlN boules grown by physical vapor transport at temperatures between 2200 and 2300°C. Gradual crystal expansion is achieved through a scalable, iterative re-growth process in which the high crystal quality is maintained over many generations of boules.

Despite the excellent crystal quality, below bandgap optical absorption bands in the blue/UV range affect the UV transparency of wafers. We use density functional theory (DFT) to develop a model to understand the interplay of point defects responsible for this absorption. We show a direct dependence of the mid-gap absorption band with the carbon concentration within the AlN.

Low defect density AlN and AlGaIn epitaxial films are grown upon these wafers that exhibit superior optical properties in terms of emission efficiency and line width and can be doped with an efficiency that is several orders of magnitude higher than possible in technologies using non-native substrates. UV LED structures and Schottky diodes were fabricated on these materials that exhibit low turn-on voltages and breakdown fields greater than 10 MV/cm.

This presentation will review state-of-the-art of AlN-based technology and give examples of potential applications in future devices and contrast these with other wide bandgap technologies.

Conference 8626: Oxide-based Materials and Devices IV

Sunday - Wednesday 3 –6 February 2013

Part of Proceedings of SPIE Vol. 8626 Oxide-based Materials and Devices IV

8626-1, Session 1

Thickness dependence of mobility and concentration in highly conductive ZnO

David C. Look, Wright State Univ. (United States); Kevin D. Leedy, Arnold M. Kiefer, Bruce B. Claflin, Air Force Research Lab. (United States)

Thin films of highly conductive ZnO and other TCOs nearly always show a strong thickness (d) dependence of mobility (μ) and concentration (n), especially for $d < 100$ nm. We quantitatively explain $\mu(d)$ and $n(d)$ by assuming a constant donor concentration N_D and a depth(z)-dependent acceptor concentration $N_A(z) = N_{A\text{-bulk}} + N_{A\text{-interface}} \exp(-z/z_0)$, yielding $n(z) = N_D - N_A(z)$, and $\mu(z) = F(N_D, N_{A\text{-bulk}}, N_{A\text{-interface}}, T, z)$ [1]. The quantities $\mu(d)$ and $n(d)$ are obtained through integrations over z of well-known functions involving $\mu(z)$ and $n(z)$, set up in MathCad. The NA profile is based on the observation that large, acceptor-like defects, e.g. dislocations, often decrease rapidly from the substrate ($z = 0$) to the surface ($z = d$). We hypothesize that the acceptor nature of the large defects in highly-doped ZnO is due to decoration by Zn vacancies (V_{Zn}), which have already been shown to be dominant acceptors in our Ga-doped ZnO layers [1]. For Ga-doped ZnO layers grown on Al₂O₃ by pulsed laser deposition in pure Ar at 200°C, with $d = 19 - 420$ nm, we get: $N_D = 1.6 \times 10^{21}$ cm⁻³, $N_{A\text{-bulk}} = 1 \times 10^{20}$ cm⁻³, $N_{A\text{-interface}} = 7 \times 10^{20}$ cm⁻³, and $d_0 = 35$ nm. In short, this model suggests that $[Ga] = 1.6 \times 10^{21}$ cm⁻³, uniformly distributed; $[V_{Zn}]_{\text{bulk}} = 1 \times 10^{20}$ cm⁻³, uniformly distributed; and $[V_{Zn}]_{\text{int}} = 7 \times 10^{20}$ cm⁻³, falling off rapidly toward the surface with a fall-off constant of about 35 nm.

1. D.C. Look et al, Phys. Rev. B 84, 115202 (2011).

8626-2, Session 1

Graphene versus oxides for transparent electronics applications (*Invited Paper*)

Vinod E. Sandana, Graphos (France)

Due to their combination of good electrical conductivity and optical transparency, Transparent Conducting Oxides (TCOs) are the most common choice for transparent electronics applications. In particular, transparent electrodes in a range of opto-electronic devices, such as LEDs, LCDs, touch screens and solar cells typically employ Indium Tin Oxide (ITO). However, Indium has some significant drawbacks including toxicity issues (which are hampering manufacturing), an increasing rarefaction (due to market growth [1]) and resulting price increases. Thus alternative materials solutions are actively being sought. This review will compare the performance and perspectives of graphene with respect to TCOs for use in transparent conductor applications.

[1] JRC European Commission Report: « Critical Metals in Strategic Energy Technologies, Assessing Rare Metals as Supply-Chain Bottlenecks in Low-Carbon Energy Technologies » (2011)

8626-3, Session 1

Impact of degenerate n-doping on the absorption edge in transparent conducting oxides (*Invited Paper*)

Andre Schleife, Lawrence Livermore National Lab. (United States); Claudia Rödl, Karsten Hannewald, Friedhelm Bechstedt, Friedrich-Schiller-Univ. Jena (Germany)

In order to facilitate the development of next-generation display devices or modern solar cells, material performance is critically important. A combination of high transparency in the optical spectral range and

high electrical conductivity under ambient conditions is attractive, if not crucial, for many applications. Transparent conducting oxides, such as zinc oxide, have large potential in this context, since doping, e.g. with aluminum or indium, renders these materials conductive even though they have wide fundamental band gaps.

While the doping-induced presence of free electrons in the conduction bands can increase the conductivity up to values desired for technological applications, it is, however, expected to impact the optical properties at the same time. For instance, variations of the band gap, effective electron mass, and optical-absorption onset have been reported. In this talk we discuss the different effects that are relevant for an accurate description of the absorption edge. Based on parameter-free electronic-structure calculations, as a powerful complement to modern experimental techniques, we illustrate: (i) The Pauli blocking of the lowest optical transitions. The influence of the degenerate electron gas on the screening of the electron-electron interaction, causing (ii) a narrowing of the quasiparticle band gap and (iii) a reduction of the excitonic effects near the absorption edge. (iv) Free-carrier inter-band absorption and the role it plays for different materials.

In the second part, strategies are presented to take into account the interesting physics related to these effects within an ab-initio framework. We developed a technique [1] that captures, in addition to quasiparticle and excitonic effects, also the Pauli blocking and the Fermi-edge singularity near the optical-absorption onset. It is applied to compute the optical band gap and the optical-absorption spectrum of heavily n doped zinc oxide over a wide range of free-electron concentrations, leading to predictive agreement with experiment. Furthermore, we discuss whether electron doping induces an excitonic Mott transition or triggers the evolution of Wannier-Mott excitons into Mahan excitons. Part of this work was performed at LLNL under Contract DE-AC52-07A27344.

[1] A. Schleife, C. Rödl, F. Fuchs, K. Hannewald, and F. Bechstedt; Phys. Rev. Lett. 107, 236405 (2011)

8626-4, Session 1

Application of highly conductive ZnO to plasmonics

Monica S. Allen, Jeffery W. Allen, Brett R. Wenner, Air Force Research Lab. (United States); David C. Look, Wright State Univ. (United States); Kevin D. Leedy, Air Force Research Lab. (United States)

Plasmonics combines attractive features in nanoelectronics and optics enabling highly integrated, dense subwavelength optical components and electronic circuits which will help alleviate the speed-bottleneck in important technologies such as information processing and computing. The wide application of plasmonic devices hinges on practical demonstrations with low losses at standard optical wavelengths such as near infrared, visible, telecom, etc. Conventional plasmonic devices, based on noble metals, suffer from large losses in these frequency regimes and are difficult to compensate completely by simply adding gain material. Transparent conducting oxides (TCOs) such as ZnO are good alternatives to metals for plasmonic applications in the optical regime since they exhibit high conductivity and relatively small negative real permittivity values necessary for practical plasmonic devices. Ga-doped ZnO layers were grown on Al₂O₃ at 200 C by pulsed laser deposition in Ar ambient. For a thickness of about 400 nm, the electrical properties, determined by the Hall effect, were: $\rho = 1.8 \times 10^{-4}$ ohm-cm; $\mu = 29$ cm²/V-s; and $n = 1.2 \times 10^{21}$ cm⁻³. These values of μ and n were used to predict optical properties through the Drude dielectric function: $\epsilon(E) = \epsilon_{\text{inf}}(1 - eD) = \epsilon_{\text{inf}}[1 - E_p^2/(E^2 + E_\mu^2)]$ where $E_p^2 = (e^2 n/m^* \epsilon_{\text{inf}} \epsilon_{\text{vac}})/2$ is the plasmon resonance energy and $E_\mu = (e^2/m^* \mu)$ is a conveniently defined energy involving μ . Reflection measurements confirmed the Hall-effect predictions by increasing rapidly at $E = E_p$. The optical and electrical material properties were used to design insulator-metal-insulator (in our case, Al₂O₃-TCO-air) waveguides for long range plasmons using full-wave electromagnetic

**Conference 8626:
Oxide-based Materials and Devices IV**

models. The simulated models were used to predict the behavior of ZnO and other TCO films as well as optimize the device geometry to maximize propagation length of the plasmon mode while simultaneously minimizing losses.

and doping level to characterization of diffusion mechanisms. Aspects of analytical performance with regards to sensitivity, quantification, repeatability and sample throughput will be discussed.

8626-5, Session 2

Stability of dopant concentration in heavily doped ZnO (Invited Paper)

Bruce B. Claflin, Kevin D. Leedy, Air Force Research Lab. (United States); David C. Look, Wright State Univ. (United States) and Wyle Labs. (United States) and Air Force Research Lab. (United States)

Recent interest has focused on the use of group III elements (Al, Ga, and In) in heavily doped ZnO as an alternative to Sn-doped In₂O₃ (ITO) for transparent conductive oxide (TCO) applications such as electrodes for solar cells or touch screens. It is known [1] that these group III metals will segregate in the near surface region when ZnO is annealed at temperatures above 900 °C; however, it is not clear if a similar surface accumulation of these dopants or mixed oxide phases are present in as-grown films, especially for highly doped samples. In this work, X-ray photoelectron spectroscopy (XPS) is used to determine the composition as a function of depth for heavily Ga doped ZnO films before and after etching with acetic acid. These films were grown by pulsed laser deposition (PLD) using a target with 3 wt% Ga₂O₃ in ZnO. In addition, the electrical properties of these films are determined from temperature-dependent Hall-effect measurements. The as-grown film contains ~10% Ga in the surface region and has a Zn:O ratio of ~1:1 with a room temperature sheet resistance $R_{sh} = 4.3 \text{ Ohm/sq}$ ($R = 1.9E-4 \text{ Ohm-cm}$) and sheet carrier density $n_{sh} = 5.0E16 \text{ cm}^{-2}$ ($n = 1.1E21 \text{ cm}^{-3}$). The surface concentration of Ga in the etched sample decreases to ~2% and the Zn:O ratio increases to ~1.4:1 which suggests preferential etching occurs, perhaps along grain boundaries. The room temperature sheet resistance for the etched sample increased to $R_{sh} = 27.8 \text{ Ohm/sq}$ while the sheet carrier density decreased slightly to $n_{sh} = 3.8E16 \text{ cm}^{-2}$. Interesting dependence of composition on depth will be discussed.

[1] D. C. Look, B. Claflin, and H. E. Smith, Appl. Phys. Lett. 92, 122108 (2008).

8626-6, Session 2

Multidimensional depth profile analysis of oxide layers by plasma profiling techniques, GD OES and PP TOFMS (Invited Paper)

Patrick Chapon, Agnes Tempez, Sébastien Legendre, HORIBA Jobin Yvon S.A.S. (France)

Plasma Profiling Techniques provide direct measurement of the chemical composition of materials as a function of depth, with nanometre resolution and the capability to measure both thin and thick layers.

These techniques rely on the fast sputtering of a representative area of the material of interest by a high density ($10^{14}/\text{cm}^3$) and low energy plasma.

The unique characteristics of this plasma allow very fast erosion (2-10nm/s) with minimum surface damage (as the incident particles have an average energy of about 50eV) and it has been shown that it can be used advantageously for sample preparation in SEM.

When coupled to a high resolution optical system, the resulting technique is called RF GDOES and is well established – an ISO document is in preparation on oxide films - when coupled to ToF MS detection, it is named Plasma Profiling Time of Flight Ion Mass Spectrometry. Both instruments feature an advanced pulsed RF source allowing the measurements of conductive and non conductive layers.

Various applications will be presented ranging from thin film analysis for composition, contamination detection, surface area measurements

8626-7, Session 2

Optical and electrical properties of aluminum-doped ZnO bulk crystals grown by the hydrothermal technique (Invited Paper)

Buguo Wang, Matthew Mann, Bruce B. Claflin, David C. Look, Air Force Research Lab. (United States)

Bulk ZnO crystals were grown by the hydrothermal technique with Al₂O₃ added to the solution in an attempt to obtain Al-doped ZnO crystals. Al and In codoped ZnO crystals were also grown hydrothermally. Adding Al₂O₃ to the growth solution significantly reduces the ZnO growth rate and affects the crystal quality; however, the resulting crystals are highly conductive, similar to In and Ga doped ZnO crystals as we reported previously, with a resistivity approaching 0.01 ohm-cm revealed by Hall-effect measurements. Photoluminescence spectra at 4 K show AlO-bound-exciton and InO-bound-exciton peak energies of 3.3609 eV and 3.3584 eV for the Al- or Al/In-codoped crystals, respectively; these energies are slightly higher than the literature values, evidently due to compressive strain. Absorption and reflection spectra were also measured. Detailed growth characteristics, optical and electrical properties of Al-doped, and Al/In-codoped ZnO bulk crystals will be presented in this paper.

8626-9, Session 2

Enhancement (100 times) of photoluminescence in pulsed laser deposited ZnO thin films by hydrogen ion implantation

Saurabh Nagar, Subhananda Chakrabarti, Indian Institute of Technology Bombay (India)

Owing to its wide bandgap (3.37eV) and a large exciton binding energy (60meV), fabrication of ZnO based optoelectronic devices is a very active research area. Hence, enhancing the photoluminescence of the ZnO films will be important to achieve higher efficiency optoelectronic devices. Hydrogen ion implantation (Energy = 50keV, Dose = $5 \times 10^{12} \text{ cm}^{-2}$) have been performed on Pulsed Laser Deposited ZnO thin films deposited at 650°C. The samples were subsequently subjected to Rapid Thermal Annealing at 750°C, 800, 850°C and 900°C for 30 seconds in oxygen environment. X-ray Diffraction study confirms deposition of highly oriented <002> ZnO films for all the samples. However, the peaks for the samples are not at the same position due to the strain induced during implantation and subsequent annealing. Low temperature photoluminescence (8K) spectra of the samples revealed the presence of peaks of donor-bound exciton (D⁰X) and free-exciton (FX) at 3.36eV and 3.37eV respectively. Deep level defect peak around 2.5eV was also observed in the samples but the intensity of these peaks was substantially weaker than the near band edge (NBE) peaks verifying the high quality of the films. Moreover, the integrated PL peak intensity of the NBE show that the luminescence gets considerably enhanced as the samples are implanted (4 times) and subsequently annealed (up to 100 times) when compared with the as-deposited sample. Thus, implanting hydrogen ions maybe a good way to enhance the photoluminescence and thus efficiency for ZnO based devices. DST, India is acknowledged.

8626-75, Session 2

Prospects on lanthanide-doped wide band gap oxides (*Invited Paper*)

M. J. Soares, J. Rodrigues, Armando J. Neves, Fernanda Madalena Costa, Teresa Monteiro, Univ. de Aveiro (Portugal)

Wide band gap oxide media including 4fⁿ ions attracts a considerable attention in the context of photonics and bio-photonics applications due to the electromagnetic widespread spectral range covered by the intraionic radiative relaxation of the trivalent charged lanthanide ions.

Converting ultraviolet commercial light into visible luminescence continues to raise interest for the solid state light market, justifying the demand for new and efficient phosphors with wide spectrum coverage and improved thermal quenching behavior. New materials and methods have been thoroughly investigated for the desired purposes.

In this work we report on laser processing for the growth of oxides media such as ZrO₂ and ZnO hosts. The transparent crystalline materials in-situ doped with different amounts of lanthanide ions are explored in order to enhance the room temperature ions luminescence by selective pumping the samples with blue and ultraviolet photons. Simultaneously, the same doped hosts were processed at nanoscale envisaging the enhancement of the ions radiative recombination.

The crystalline quality of the grown material was characterized by X-ray diffraction (XRD) and Raman spectroscopy. Samples morphology and grain size was analyzed by transmission electron microscopy (TEM).

Spectroscopic studies of the doped hosts were performed by photoluminescence (PL) and photoluminescence excitation (PLE) spectroscopy. The temperature dependence of the optical features was analyzed and discussed.

8626-10, Session 3

MOCVD growth of ZnO nanowire arrays for advanced UV detectors (*Invited Paper*)

Tariq Manzur, Naval Undersea Warfare Ctr. (United States); John Zeller, Naval Undersea Warfare Ctr. (United States) and Magnolia Optical Technologies, Inc. (United States); Ashok Sood, Magnolia Optical Technologies, Inc. (United States); Mehdi Anwar, Univ. of Connecticut (United States)

Zinc oxide (ZnO) is a biocompatible and versatile functional material that exhibits both semiconducting and piezoelectric properties, and also has a diverse group of growth morphologies. Bulk ZnO has a bandgap of 3.37 eV that corresponds to emissions in the solar blind ultraviolet (UV) spectral band (240-280 nm). We have grown highly ordered vertical arrays of ZnO nanowires using a metal organic chemical vapor deposition (MOCVD) growth process. This growth process has distinct advantages over other methods that require incorporation of metal catalysts as seed layers, which can introduce undesired defects to the structure that decrease crystal quality. For the MOCVD nanowire growth, diethylzinc (DEZn) was used as zinc precursor and nitrous oxide (N₂O) as the oxygen precursor, with nitrogen (N₂) as the carrier gas. The nanowires were grown on p-Si (100), SiO₂, GaN, and m-plane sapphire substrates. The structural and optical properties of the grown vertically aligned ZnO nanowire arrays were characterized by scanning electron microscopy (SEM), X-ray diffraction (XRD), and photoluminescence (PL) measurements. The unique diffraction pattern for ZnO (002) concurred with the SEM inspection indicating vertical orientation of the nanowires. UV detectors based on ZnO nanowires offer high UV sensitivity and low visible sensitivity for applications such as missile plume detection and threat warning. Compared to the photomultiplier tubes (PMTs) prevalent in current missile warning systems, the nanowire detector arrays are expected to exhibit low noise, extended lifetimes, low power requirements, and can be coupled with microlens arrays to further improve their sensitivity for UV detector applications.

8626-11, Session 3

Persistent photoconductivity and transient recovery of Al:ZnO:Al planar structures

James C. Moore, Laura R. Covington, Coastal Carolina Univ. (United States)

We have investigated the photoconductivity and transient response of polycrystalline ZnO films grown using a thermal oxidation technique. Zinc-metal films were grown on c-plane sapphire substrates via non-reactive dc sputter deposition at room temperature with subsequent thermal annealing at 300°C, 600°C, 900°C, and 1200°C. Metal-semiconductor-metal (MSM) Al:ZnO:Al planar ultraviolet (UV) photodetectors were fabricated via sputter deposition of aluminum contacts. Decreasing photoconductivity is seen for increasing annealing temperature, which is consistent with photoluminescence (PL) studies showing a similar decrease in the green-to-UV emission ratio. As-grown photodetectors annealed at low temperature (300°C) over 9 hours demonstrated a responsivity of ~100 mA/W. We also present a phenomenological model of photoconductivity transients in which transient recoveries are fitted with a linear combination of two exponential decays. The primary fast drop in photoconductivity involves a recombination of free electron-hole pairs coinciding with free excitation relaxation. The slower portion of the decay, in which the persistence of the photocurrent is an order of magnitude longer than the fast, can be explained by the slow absorption/desorption process of electrons that must overcome a high-energy barrier with holes at surface oxygen states.

8626-12, Session 3

Study of Photoresponsivity in Optoelectronic Devices Based on Single Crystal α -Ga₂O₃ Epitaxial Layers

Ray-Hua Horng, National Chung Hsing Univ. (Taiwan); Parvaneh Ravadgar, National Cheng Kung Univ. (Taiwan)

α -Ga₂O₃ epitaxial layers are promising semiconductor oxides for their optoelectronic applications in deep ultraviolet (wavelength between 200 to 290 nm) region. However, single crystal growth and point defects such as oxygen and gallium vacancies still remain as the main problems through the high performance of α -Ga₂O₃-based devices. Crystalline quality of α -Ga₂O₃ epitaxial layers and presence of donors and acceptors defects, providing free electrons and holes, successively, are known for their direct relationships with photoresponsivity of their optoelectronic devices.

We could develop single crystal α -Ga₂O₃ epitaxial layers on c-axis (0001) sapphire substrates using chemical vapor deposition (MOCVD) technique which is essential for mass productions. However, optimization of many MOCVD growth parameters, including low growth temperature (450 °C) left uniform single crystal α -Ga₂O₃ epitaxial layers but at the same time it introduces many oxygen and gallium vacancies inside the epitaxial layers. Post annealing, up to 800 °C, doesn't affect the crystalline structure of α -Ga₂O₃ epitaxial layers; explored by x-ray diffraction, while dramatically decreases the dark current and improves photoresponsivity studied by fabrication of metal-semiconductor-metal photodetectors on α -Ga₂O₃ samples. Significant decrease in dark current (~5 orders in magnitude) and considerable improvement in photoresponsivity are attributed to their defects reduction. It is suggested that post annealing single crystal α -Ga₂O₃ epitaxial layers provides enough energy for both types of vacancies (O and Ga) to find and heal each other, increasing the device performance with minimum effect on crystalline structure.

Conference 8626:
Oxide-based Materials and Devices IV

8626-13, Session 4

Photon detectors based on oxide heterostructures and superlattices

Hanns-Ulrich Habermeier, Max-Planck-Institut für Festkörperforschung (Germany)

A new class of thermoelectric thin film material is described, characterized by anisotropic Seebeck tensors which is also referred to as atomic layer thermopile (ALT). Early studies revealed that in YBa₂Cu₃O₇ thin films there appears a voltage when shining light pulses onto the surface of films which is of thermoelectric origin. Originally, only layered high T_c superconductor oxides have been regarded as suitable ALT materials, however, a similar effect was discovered in quasicubic LaCaMnO₃ thin films thus opening a new avenue for material systems other than high T_c superconductors for such experiments.

Recently, research revealed that there are quite a number of complex transition metal oxides which demonstrate ALT properties, such as manganites, cobaltates and nickelates. In this contribution we explore the application potential of the concept of ALT for thermoelectric as well as photon sensing devices and pay special attention to designing novel materials with enhanced thermoelectric figures of merit. Furthermore concepts based on ALT materials are developed guiding to thin film thermoelectric power generation devices.

8626-14, Session 4

Properties of high-density two-dimensional electron gases at Mott/band insulator interfaces (Invited Paper)

Susanne Stemmer, Pouya Moetakef, Daniel Ouellette, Univ. of California, Santa Barbara (United States); James R. Williams, David Goldhaber-Gordon, Stanford Univ. (United States); S. James Allen, Univ. of California, Santa Barbara (United States)

Two-dimensional electron gases at oxide interfaces have attracted significant attention because they can exhibit unique properties, such as strong electron correlations, superconductivity and magnetism. In this presentation, we will discuss emergent phenomena at interfaces between band insulators, such as SrTiO₃, and strongly correlated (Mott) materials, such as the rare earth titanates (RTiO₃, where R is a trivalent rare earth ion). A fixed polar charge exists at these interfaces because of a polar discontinuity at the interface. This interfacial charge can be compensated by a two-dimensional electron gas. We report on intrinsic electronic reconstructions, of approximately 1/2 electron per surface unit cell at a prototype Mott/band insulator interface between GdTiO₃ and SrTiO₃, grown by MBE. The sheet carrier densities of all GdTiO₃/SrTiO₃ heterostructures containing more than one unit cell of SrTiO₃ are approximately 1 electron per surface unit cell (or 3 × 10¹⁴ cm⁻²), independent of layer thicknesses and growth sequences. We will report on electron correlation effects, such as magnetism, in the extremely high carrier density SrTiO₃ quantum wells that can be obtained using these interfaces. We will present measurements of quantum (Shubnikov-de Haas) oscillations that provide insights into the nature of the two-dimensional electron gas and into subbands that are derived from the Ti d-states and report on phenomena due to extreme carrier confinement.

8626-15, Session 4

Recent progress in highmobility electron gas at MgZnO/ZnO heterointerfaces (Invited Paper)

Yusuke Kozuka, Joseph Falson, The Univ. of Tokyo (Japan); Denis Maryenko, RIKEN (Japan); Atsushi Tsukazaki, Soichiro Teraoka, Akira Oiwa, Seigo Tarucha, Masashi Kawasaki, The Univ. of Tokyo (Japan)

Oxide heterointerfaces have provided a variety of physical properties as a representative example of high-mobility electrons at LaAlO₃/SrTiO₃ interfaces, where coexistence of superconductivity and magnetism was recently proposed. MgZnO/ZnO two-dimensional electron gas (2DEG) is another intriguing system, exhibiting the highest electron mobility of ~ 750,000 cm²/Vs among oxides. So far, we have demonstrated 2DEG at MgZnO/ZnO shows several quantum phenomena originating from large electron correlation. For instance, four times enhancement of spin susceptibility was observed in a dilute carrier density. In this study, we focused on spin-orbit interaction and spin relaxation of 2DEG at the MgZnO/ZnO interfaces as another characteristic property of ZnO because long spin coherence time was anticipated owing to the weak spin-orbit interaction and low nuclear spin concentration. Here we used electrically detected electron spin resonance to investigate spin properties in MgZnO/ZnO 2DEG. The result indicated one order of magnitude weaker Rashba effect than that of typical III-V high-mobility 2DEGs such as in GaAs/AlGaAs or GaN/AlGaN. The spin relaxation time was also estimated as ~ 25 ns, which was somewhat shorter than that in Si/SiGe heterostructures (~ 100 ns), but longer than that of GaAs/AlGaAs (~ 7 ns), reflecting the strength of spin-orbit interactions. Our result indicates ZnO 2DEG is another promising candidate for spintronic applications.

8626-16, Session 4

Controlling electronic orbitals in complex oxide heterostructures

John W. Freeland, Argonne National Lab. (United States)

Functional oxides based on the transition metal series display a wide spectrum of remarkable electronic properties including magnetism, superconductivity and metal-insulator transitions. These novel properties arise from the interaction between the charge, orbital, spin, and lattice degrees of freedom. The key to controlling these properties lies in the ability to control the underlying structure. By using epitaxial growth to strain oxide crystal structures, thin film synthesis offers novel route to control oxide structure in ways not attainable in the bulk counterparts. This allows one to access new regions of phase-space to explore emergent states not present in bulk form. Extending this to ultrathin heterostructures then offers the ability to harness dimensionality as an additional knob to control the interactions of strongly correlated electrons. Here I will highlight our recent work on complex oxide heterostructures focused on using strain and confinement to manipulate orbital configurations in nickelates[1-4] and cuprates[5-6].

Work at Argonne is supported by the U.S. Department of Energy, Office of Science, under Contract No. DE-AC02-06CH11357.

- [1] J. Liu et al. Phys. Rev. Lett. 109, 107402 (2012)
- [2] J. Liu et al. Phys. Rev. B 83, 161102 (2011).
- [3] J. Chakhalian et al. Phys. Rev. Lett. 107, 116805 (2011).
- [4] J.W. Freeland et. al. Europhysics Letters 96, 57004 (2011).
- [5] J. Chakhalian, J.W. Freeland et. al. Nature Physics 2, 244 (2006).
- [6] J. Chakhalian, J.W. Freeland et. al. Science 318, 1114 (2007).

8626-17, Session 4

Access to a buried phase in manganite by field effect carrier control (Invited Paper)

Takafumi Hatano, RIKEN (Japan); Yasushi Ogimoto, Fuji Electric Co., Ltd. (Japan); Naoki Ogawa, Zhigao Sheng, Masao Nakamura, Masaki Nakano, RIKEN (Japan); Shimpei Ono, Central Research Institute of Electric Power Industry (Japan); Masashi Kawasaki, The Univ. of Tokyo (Japan); Kenjiro Miyano, National Institute for Materials Science (Japan); Yoshihiro Iwasa, Yoshinori Tokura, The Univ. of Tokyo (Japan)

**Conference 8626:
Oxide-based Materials and Devices IV**

The mutual interactions among charge-spin-orbital degrees of freedom in strongly-correlated electron systems make a rich variety of orderings which have been controlled by external stimuli such as magnetic field, light and pressure. However, electric-field effect, which is of critical importance for electronics applications, has been left to be investigated because of insufficient strength of electric field attainable by conventional solid dielectrics in field-effect geometry. In this work, we demonstrate electric-field control of electronic phases in perovskite manganite thin films by using electric-double-layer transistors (EDLTs) which can accumulate hundred times larger charges than conventional field-effect transistors.

We fabricated EDLT with Pr_{0.5}Sr_{0.5}MnO₃ (PSMO) thin films which show ferromagnetic metal (FM) to antiferromagnetic insulator (AFI) transition at low temperature. Since this AFI phase can be converted to an FM phase by a small amount of carrier doping, this system is a good candidate for realization of electric-field control of electronic phases. In PSMO, we realized a field induced AFI to FM transition, and found a particularly stable insulating phase which corresponds to a charge/orbital ordered insulating (COOI) phase in between FM and AFI phases. This COOI phase has been missed in previous bulk studies since this phase is stable in extremely narrow region of doping level. Fine tuning of gate voltage in EDLT allowed us to access to this buried phase.

8626-18, Session 4

Towards non-silicon technologies: growth and characterisation of complex oxides for multiferroic and resistive memory applications
(Invited Paper)

Donald A MacLaren, Univ. of Glasgow (United Kingdom)

Transition metal oxide (TMO) heterostructures are at the forefront of microelectronics materials research, not least because they may provide a route to 'beyond Moore' devices. Their promise derives from the remarkable large range of functionality - both intrinsic to the material and emergent at interfaces - which ranges from insulating to superconducting and even multiferroic behaviour. Individually, these functionalities enable, for example, scalable, non-volatile data-storage; in combination, multifunctional TMO structures may enable entirely new device architectures. Nevertheless, these properties are intimately related to structural perfection and achieving reproducibly the required structural perfection remains a challenge, even in those systems where the structure-function relationship is well understood.

I will describe recent progress in Glasgow towards the optimised deposition of TMOs for multiferroic and resistive random access memory applications. Pulsed laser deposition (PLD) is found to be almost ideal, having wide applicability, giving excellent control over thin film stoichiometry and, in combination with in-situ electron diffraction, allowing monolayer precision in deposition. By optimising deposition parameters including the laser profile and background gas pressure, epitaxial growth of TMO heterostructures is feasible, with minimal interfacial mixing or roughness. Ex-situ scanned probe microscopy and transmission electron microscopy are essential to assess basic structural parameters. Most excitingly, recent advances in electron energy loss spectroscopy enable chemical analysis of the thin films right down to the atomic scale: this is particularly important in understanding the chemical and electronic properties of interfaces and will be essential in developing next-generation devices.

8626-19, Session 5

MOCVD growth and characteristics of ZnO-based LEDs
(Keynote Presentation)

Seong-Ju Park, Gwangju Institute of Science and Technology (Korea, Republic of)

No Abstract Available

8626-20, Session 5

Engineering light-emitting diodes with inexpensive materials: Integrating ZnO and Si into solid state lighting
(Invited Paper)

Can Bayram, Devendra Sadana, IBM Thomas J. Watson Research Ctr. (United States); Ferechteh Teherani, David Rogers, Nanovation (France); Yinjun Zhang, Simon Gautier, Chu-Young Cho, Erdem Cicek, Zahra Vashaei, Ryan McClintock, Manijeh Razeghi, Northwestern Univ. (United States)

Growing world population and increasing energy demand call for energy savings in every aspect of our lives. With about 20% of annual energy being consumed for lighting (a \$120 Billion industry with general lighting covering about 75% of it), environmental-friendly alternatives to existing lighting technologies are under investigation for energy savings. Solid state lighting based on light emitting diodes (LEDs) is the most promising candidate capable of fulfilling the lighting demand without trade-off in lighting quality.

Emerging LED lighting is based on gallium nitride (GaN) technology and has the potential to reduce energy consumption by nearly one half while enabling significant carbon emission reduction. However, benefiting at most from light emitting diodes requires a wide-scale adoption. This necessitates reducing a single LED device cost currently dominated by the substrate (i.e. sapphire) and the epitaxy (i.e. GaN).

In this talk, we will be discussing the advantages and challenges of integrating Si and ZnO into GaN-based light emitting diodes. Silicon (Si) and zinc oxide (ZnO), being the most scalable and earth-abundant materials, can be great substitutes in current LEDs for the costly substrate and epitaxy. Engineering such hybrid devices may reduce the cost significantly but comes with additional hurdles necessitating new technological breakthroughs. We will focus on engineering light emitting diodes with such inexpensive materials and look into novel concepts targeted for solid state lighting.

8626-21, Session 5

Near UV ZnO LED coupled to QD based phosphors

Guido Faglia, Camilla Baratto, Elisabetta Comini, Isabella Concina, Giorgio Sberveglieri, Univ. degli Studi di Brescia (Italy) and Institute of Acoustics O. M. Corbino, CNR (Italy)

Nearly all white LEDs sold today use a blue GaN/InGaN LED plus a yellow phosphor. This is fine for many applications (e.g., displays, lighting in cars), but the quality of light is probably not good enough for home lighting, for which a warmer white light containing some red light is desirable: a better route to higher quality white light might be to use a near-UV LED plus red, green, and blue phosphors.

A candidate to develop near-UV LEDs is ZnO: vertically aligned ZnO nanowires (NWs) with diameter ranging from 20 to 200nm have been deposited on p-GaN, growth is hexagonal and NWs are tapered at the end. Growth of metal oxide nano-crystals is based on the combined Vapour-Phase (VP) and Vapour-Liquid-Solid (VLS) growth mechanism, which consists in two steps: (i) thermal evaporation of bulk metal oxides and (ii) following condensation.

The high quantum yield (QY) and high degree of color (size) tuning reported for quantum dots (QDs) make them an obvious target of investigation for white LEDs. The use of QDs for color shifting of the UV light into the visible with high QY is of interest not only for their high efficiency but because they minimize light scattering and can be uniformly dispersed in either epoxy or silicone. We carried out preparation and characterization of both core-shell and doped QDs, prepared by using the well-established hot injection approach, to be integrated with the near-UV ZnO based LEDs.

We acknowledge OSRAM Opto Semiconductors GmbH Regensburg for providing GaN and ORAMA project FP-NMP-2009-LARGE-3 NMP-

**Conference 8626:
Oxide-based Materials and Devices IV**

2009-2.2-1, Grant Agreement 246334: "Oxide Materials for Electronics Applications" for partial financial support.

8626-22, Session 5

CdxZn1-xO epilayers grown on MgZnO for red to violet emission (*Invited Paper*)

Andrés Redondo-Cubero, Univ. Técnica de Lisboa (Portugal) and Univ. de Lisboa (Portugal); Matthias Brandt, P. Schäfer, Fritz Henneberger, Humboldt-Univ. zu Berlin (Germany); Nuno Franco, Eduardo Alves, Univ. Técnica de Lisboa (Portugal); Joana Rodrigues, Teresa Monteiro, Univ. de Aveiro (Portugal); Katharina Lorenz, Univ. Técnica de Lisboa (Portugal) and Univ. de Lisboa (Portugal)

CdxZn1-xO ternaries are very promising compounds for visible and UV optoelectronics [1]. Utilizing low-temperature molecular beam epitaxy (MBE), the low equilibrium solubility limit (4 %) of CdO in ZnO related to the different crystallographic structures (rocksalt versus wurtzite, respectively) could be overcome, allowing the growth of phase-pure wurtzite alloys up to a Cd concentration of about 40 %. The use of appropriate substrates provides a possibility to further improve structural perfection of the ternaries. While most of previous work is based on sapphire, we analyze here the structural and optical properties of CdxZn1-xO epilayers grown on MgZnO.

The layers were grown by MBE with O excess at very low temperatures (150 °C) with a CdO molar fraction varied from x=0.1 to x=0.4. The MgO concentration of the MgZnO template is ~8 at. %. X-ray diffraction (XRD) reciprocal space maps signify a near-pseudomorphic growth mode along the total film thickness of 270 nm for low (x=0.12) and plastic relaxation for high CdO contents (x=0.25 and x=0.38). For the intermediate composition (x = 0.16), multiple peaks in the XRD spectra indicate structural inhomogeneities. Depth profiles extracted from Rutherford backscattering spectrometry were used to determine whether such features are due to compositional gradients or due to phase separation. Near-pseudomorphic and relaxed layers exhibit slight compositional gradients along the growth direction with increasing CdO concentration towards the surface (e.g. from x=0.107 in the first 100 nm to x=0.126 in the shallower region in the near-pseudomorphic sample), whereas no significant compositional variations took place in the sample with x=0.16. Ion channelling measurements reveal that the multiple XRD peaks occur as a result of a gradual variation of the strain state of the wurtzite film during the growth and not due to the presence of cubic inclusions (also analyzed in XRD pole figures). Photoluminescence measurements showed near band-edge emission ranging from 2.0 eV (red) to 2.7 eV (violet), confirming the potential of MBE growth at low temperature on MgZnO.

[1] S. Kalusniak et al., *Laser & Photon Rev.* 3, 233 (2009).

8626-23, Session 5

Photonic devices on paper (*Invited Paper*)

Magnus Willander, Linköping Univ. (Sweden)

In this talk I will present some of our results from chemical growth of inorganic (ZnO) crystalline nanostructures on paper substrates. Nanowires and nanotubes are grown. The nanowires were processed to white LEDs with CRI up to 95. Then the nanotubes were tested regarding the piezoelectric effect and for generating voltage and current. This opens the possibility to drive the LEDs from mechanical energy from the paper.

The second part deals with printing the grown nanowires on a paper substrate. Again LEDs were fabricated, with the intention to deposit large areas with LEDs. Also on the paper contacts and interconnection lines were made by a simple pencil drawing on the paper on which the nanowires then were printed. This graphitic circuitry worked excellent as metal electrodes. In this way a UV-detector was fabricated.

Finally, I will also compare the paper substrates results with our other results on other different types of flexible substrates like cotton and plastic substrates.

8626-24, Session 5

New emissive ZnO-graphene hybrid quantum dots (*Invited Paper*)

Won Kook Choi, Dong-Ick Son, Korea Institute of Science and Technology (Korea, Republic of)

A simple solution method was used to prepare emissive hybrid quantum dots consisting of a ZnO core wrapped in a shell of single-layer graphene. In ZnO-graphene quasi core-shell QDs, a strain of $\approx 0.8\%$ imposed on bent graphene by analyzing the splitting 26 cm^{-1} of subband (G_+ , G_-) in Raman measurement creates a mid infrared bandgap opening of 250 meV. Two blue emissions of 406 nm and 432 nm are observed in photoluminescence (PL) of ZnO-graphene quasi core-shell QDs besides near-band edge ultraviolet emission 379 nm. By a simple model calculation with density functional theory (DFT) as implemented in Gaussian package on graphene and graphene oxide (GO), it is revealed that the lowest unoccupied molecular orbital (LUMO) level of graphene splits into 3 levels with oxygen attachment indicated as LUMO, LUMO+1 and LUMO+2 in oxide density of state (DOS). Considering the partial density of states (PDOS) of oxygen, LUMO and LUMO+2 have definite contributions of s orbital from the oxygen state, however LUMO+1 does not. By the selection rule ($\Delta l = \pm 1$), the new PL features in ZnO-Graphene QD can be understood as the electron transition via two unoccupied levels, LUMO and LUMO+2 of GO to ZnO O2p valence level. In this study, it was found that graphene bonded with ZnO could shift from the UV emission center 378 nm of ZnO to blue emission by electron-transfer and static quenching.

8626-25, Session 6

Active glass ceramics for photonic applications (*Invited Paper*)

Setsuhisa Tanabe, Jumpei Ueda, Kyoto Univ. (Japan); Takayuki Nakanishi, Hokkaido Univ. (Japan)

This talk will overview novel glass ceramics we have developed for photonic applications ; solid-state lighting, persistent phosphor, optical amplifier and photovoltaic applications.

Reference

- [1] S.Tanabe, S.Fujita, A.Sakamoto, S.Yamamoto, "Glass ceramics for solid-state lighting", in "Advances in Glass and Optical Materials", (Eds. S. Jiang, The American Ceramic Society, Westerville, 2006) pp.19-25.
- [2] S.Tanabe, "Active glass and ceramic materials for green photonics", International Congress on Glass 2010, (Salvador, Sept. 2010).
- [3] S.Nishiura, S.Tanabe, "Properties of transparent Ce:YAG ceramic phosphors for white LED", *Opt. Mater.* 33, (2011) 688-691.
- [4] T.Nakanishi, S.Tanabe, "Novel Eu²⁺-activated glass ceramics precipitated with green and red phosphors for high power white LED", *IEEE. J. Select. Top. Quant. Electron.* 15, (2009) 1171-1176.
- [5] J.Ueda, S.Tanabe, "Preparation and Optical Property of Glass Ceramics Containing Ruby Crystals", *J. Am. Ceram. Soc.* 93[10], (2010) 3084-3087.
- [6] T.Nakanishi, Y.Katayama, J.Ueda, T.Honma, S.Tanabe, T.Komatsu, "Fabrication of Eu: SrAl₂O₄-based glass ceramics using frozen sorbet method", *J. Ceram. Soc. Jpn.* 119[7], (2011) 609-615.

8626-26, Session 6

Control of the point defects in oxide materials to enhance functionalities in imaging

Bruno Viana, Aurélie Bessière, Didier Gourier, Ecole Nationale Supérieure de Chimie de Paris (France); Thomas Maldiney, Cyrille Richard, Daniel Scherman, UPCI (France)

In medical imaging, careful control of the doping and point defects should be realized to optimize the optical properties. Doping ions and defects could for instance offer a non radiative route which gives rise to a decrease of the luminescence intensity or lead to traps. When these traps are thermally released, they populate the excited state of an emitting centre, leading to additional emission.

First, one can find a great interest for materials with a long afterglow luminescence, also called persistent luminescence for various applications (emergency signing, luminous painting, and lighting sources). This concept was recently used for the development of new medical imaging called optical imaging. In such system, oxides-nanoparticules of persistent luminescent materials could present emission lasting for hours and this allows to follow in vivo and in real-time the biodistribution of these fluorescent nanoprobables. In that case, effort is done to improve the optical response and increase the afterglow.

Second, if in some oxide based material for medical imaging such afterglow is deleterious should be suppressed. This is the case for instance when fast medical imaging is required in X-Rays scans and positron emission tomography (PET). Effects on structural properties of the mixed oxides could be done and addition of various dopants could either enhance or eliminate the luminescence properties.

8626-27, Session 6

Photocatalytic properties of TiO₂ nanotubes

Andreas Pfuch, INNOVENT e.V. (Germany); Frank Guell, Univ. de Barcelona (Spain); Tina Toelke, INNOVENT e.V. (Germany); Susanta K. Das, Indian Institute of Technology Guwahati (Germany); Hamza Messaoudi, Max-Born-Institut für Nichtlineare Optik und Kurzzeitspektroskopie (Germany); Enda McGlynn, Dublin City Univ. (Ireland); Wolfgang Seeber, Friedrich-Schiller- Univ. Jena (Germany); Ruediger Grunwald, Max-Born-Institut für Nichtlineare Optik und Kurzzeitspektroskopie (Germany)

TiO₂ is well known as a low-cost, highly active photocatalyst of good environmental compatibility. Recently it was found that TiO₂ nanotubes promise to enable for high photocatalytic activity (PCA). In our experiments, we studied the photocatalytic activity and spectroscopic properties of TiO₂ nanotube arrays formed by the anodization of Ti. The PCA efficiency related to the decomposition of methylene-blue was measured. To obtain reliable data, the results were calibrated by comparing with standard materials like Pilkington Activ™ which is a commercially available self cleaning glass. The studies included a search strategy for finding optimum conditions for the nanotube formation and the investigation of the relationship between PCA and annealing temperature. TiO₂ nanotubes of different shapes and sizes were prepared by anodization of Ti foil in different electrolytes, at variable applied voltages and concentrations. The coated samples were dipped in methylene blue solution and, after storing in dark, irradiated with UV-light. The resulting photo-dissociation of methylene-blue was detected by UV-VIS spectroscopy. In particular, the absorption at a wavelength of 664 nm was measured. For optimized material, an enhancement factor of 2 in comparison to Pilkington Activ™ was found. Furthermore, femtosecond-laser induced photoluminescence and nonlinear absorption of the material were investigated. A further enhancement of the PCA by UV and femtosecond laser post-processing and the study of PCA properties of other types of TiO₂ nanostructures are currently under progress.

8626-28, Session 7

Waveguiding and confinement of light in semiconductor oxide microstructures (Invited Paper)

Bianchi Mendez, Teresa Cebriano, Iñaki López, Emilio Nogales, Javier Piqueras, Univ. Complutense de Madrid (Spain)

(Invited talk)

Interest on the control of light at the nano- and microscale has increased in the last years because of the incorporation of nanostructures into optical devices. In particular, semiconductor oxides microstructures emerge as important active materials for waveguiding and confinement of light from UV to NIR wavelengths. Obtention of high quality and quantity of nano- and microstructures of semiconductor oxides with controllable morphology and tunable optical properties is an attractive challenge in this field. In this work, we will show the influence of dopants on the morphology and luminescence properties in gallium oxide and antimony oxide microstructures obtained by a thermal evaporation method. Several morphologies have been obtained, such as nanowires, nanorods or branched nanowires as elongated structures, but also triangles, microplates or pyramids [1,2]. Light waveguide experiments were performed with both oxides which have wide band gap and a rather high refractive index. Some of the synthesized microstructures have been found to act as optical cavities and resonant modes were observed. In particular, photoluminescence results showed the presence of resonant peaks in the PL spectra of single Sb₂O₃ triangles and rods, single Ga₂O₃ microwires and microplates, which suggest their applications as optical resonators in the visible range.

[1] I. López, E. Nogales, B. Méndez and J. Piqueras, Appl. Phys. Lett. 100, (2012) 261910.

[2] T. Cebriano, B. Méndez and J. Piqueras, Materials Chemistry and Physics <http://dx.doi.org/10.1016/j.matchemphys.2012.06.024>.

8626-29, Session 7

Modification of fiber facet reflection with a ZnO nanowire array

Igor V. Melnikov, Dmitry G. Gromov, Moscow Institute of Electrical Engineering and Technical Univ. (Russian Federation); Andrey E. Mironov, Moscow Institute of Electrical Engineering and Technical Univ. (Russian Federation) and Univ. of Illinois at Urbana-Champaign (United States); Pavel B. Novozhylov, Michael Y. Nazarkin, Andrey A. Machnev, Moscow Institute of Electrical Engineering and Technical Univ. (Russian Federation)

The small uniform diameter ≤ 100 nm along with low absorption and large refractive index in the visible of wide-gap semiconductor nanowires have opened several avenues for pursuing sub-wavelength optical devices. Among others, ZnO continues to be of particular interest, not only for studies of fundamental solid-state physics but for application to optical waveguides. The practical implementation of ZnO nanowires requires a detailed understanding of coupling external light into the guiding modes of the nanowire whose diameter is much smaller than the corresponding vacuum wavelength. This report presents measurements of broadband light propagating through a single-mode optical silica fiber that has an end facet modified by a deposited array of ZnO nanowires.

The procedure exploited to create an array of ZnO nanowires on a tip of a single-mode optical fiber is based on a standard technological procedure. In order to provide required level of the surface quality, the magneto-sputtering of 300-nm ZnO film is executed immediately after the fiber (SMF-28 Corning) cleaving. This film works as a catalyst for ZnO nanowires to grow and also provides proper adhesion and ordering for the structure to be created in the next step, where low-temperature chemical deposition is used to create an array of ZnO nanowires. In the solution, there is a concentration of 0.01 M of Zn(NO₃)₂·6H₂O and 0.4 M of NaOH, and pH of this solution is equal to 13.2. The solution is kept

**Conference 8626:
Oxide-based Materials and Devices IV**

for ten minutes a water bath heated to 80°C, and the end facet of the fiber is immersed into it afterwards and kept there for twenty minutes, correspondingly. The fiber with ZnO nanowires grown on its end facet, is cleaned in a deionized water and then air-dried. The length of the nanowire is equal 800 nm, diameter varies from 40 to 50 nm, and surface density is 5x10¹⁰ cm², correspondingly.

In the next step, the transmission and reflection spectra of the fiber that comprises a bundle of ZnO nanowires grown on its cleaved facets, are studied using experimental setup as follows. The output of the Er³⁺-broadband source MPB EBS-7210 is launched into one piece of SMF-28 followed by a circulator and another length of the SMF-28 that has ZnO nanowires on its facet and is connected by means of an adapter to the optical spectrum analyzer AQ6370 by Yokogawa. The circulator is introduced into the set-up in order both reflection and transmission spectrum to be analyzed simultaneously.

The reflection and transmission spectra are measured for the clean cleaved facet, facet with 300-nm seeding layer of ZnO on its cleaved surface, and with ZnO nanowires grown on this cleaved facet, correspondingly, and the reflection spectrum read a profound asymmetry in the reflection spectrum that does not match the transmission one hence making a temptation to claim an observation of surface polaritons excited along the ZnO nanowires. Further basic measurements that are again the spectral measurement but with tilt and variable spacing introduced between the nanowires and collecting fiber confirm this assumption.

In conclusion, measurements of the transmission and reflection spectra of the single-mode optical fiber that end facet is modified by a disordered (but yet controllable) array of ZnO nanowires, exhibit spectral asymmetry of the reflection due to the excitation of surface polaritons that propagate along the surface of the nanowire. The behavior reported here is of interest for the implementation of new sub-wavelength optical waveguides.

8626-30, Session 7

Applications of nanosecond laser annealing to fabricating p-n homo junction on ZnO nanowires

Tetsuya Shimogaki, Taihei Ofuji, Norihiro Tetsuyama, Kota Okazaki, Mitsuhiro Higashihata, Daisuke Nakamura, Hiroshi Ikenoue, Tanemasa Asano, Tatsuo Okada, Kyushu Univ. (Japan)

Zinc oxide (ZnO) is one of the most promising semiconductor materials for optoelectronic applications in particular ultra violet light emitting diode (UV-LED). In addition, the one-dimensional ZnO crystals are quite attractive as building blocks for light emitting devices like laser and LED, because of their high crystallinity and light confinement properties. However, a method for the realization of the stable p-type ZnO has not been well established. In our study, we have investigated the effect of the nanosecond laser irradiation to the ZnO nanocrystals as an ultrafast melting and recrystallizing process for realization of the p-type ZnO. Fabrication of the p-n homo junction along ZnO nanocrystals has been demonstrated using P⁺ ion implantation and ns-laser annealing. Rectifying I-V characteristics attributed to p-n junction were observed from the measurement of electrical properties. In addition, Sb laser doing using the nanosecond laser have also been investigated. In this presentation, optical, structural, and electrical characteristics of the P⁺ ion implanted ZnO nanocrystals activated by the laser annealing and the Sb-doped ZnO nanocrystals by laser doping technique will be discussed.

8626-31, Session 7

Lasing characteristics of optically-pumped single ZnO micro/nanocrystal

Kota Okazaki, Tetsuya Shimogaki, Koshi Fusazaki, Mitsuhiro Higashihata, Daisuke Nakamura, Tatsuo Okada, Kyushu Univ. (Japan)

Zinc Oxide (ZnO) has a wide band-gap energy of 3.37 eV and a large exciton binding energy of 60 meV which is considerably larger than the thermal energy at room temperature (26 meV), and therefore, the efficient exciton emission in ultraviolet (UV) region can be expected. ZnO has considerably similar characteristics and several advantages compared to Gallium Nitride (GaN), including the larger exciton binding energy than that of GaN (28 meV) and abundant natural resources. In addition, environmental load of ZnO is very less than that of GaN because of the scarce resources of Ga. Therefore, ZnO is a promising material in UV emission devices replacing GaN. Especially, ZnO micro / nanocrystals are quite attractive as the building blocks for the efficient ultraviolet optoelectronic devices.

We have investigated lasing characteristics from an optically-pumped single ZnO nanowire and nanosheet by spectra observation, and it was considered that those ZnO nanocrystals could be a promising UV laser medium. Recently, lasing from a single ZnO micro / nanosphere made by a simple ablation method of ZnO target was also observed. In this presentation, we report the lasing characteristics of an optically-pumped single ZnO nanowire, nanosheet and micro / nanosphere studies by the micro-fluorescence spectroscopy. It was found that the ZnO micro / nanosphere showed a good light confinement property due to the whispering-gallery mode lasing. The micro-cavity lasing characteristics will be discussed.

8626-32, Session 8

Influence of defects in ZnO nanomaterials on the performance of dye-sensitized solar cell and photocatalytic activity (*Invited Paper*)

Mu Yao Guo, The Univ. of Hong Kong (Hong Kong, China); Alan Man Ching Ng, South Univ. of Science and Technology of China (China) and The Univ. of Hong Kong (Hong Kong, China); Fang Zhou Liu, Yu Hang Leung, Ka Kan Wong, Annie Ng, Yip Hang Ng, Gang Wang, Aleksandra B. Djurić, Wai Kin Chan, The Univ. of Hong Kong (Hong Kong, China)

ZnO as a wide band gap semiconductor is of significant interest for various applications, including dye-sensitized solar cells (DSSC) and photocatalytic degradation of organic pollutants. For DSSC, although the performance of ZnO-based devices is generally inferior to TiO₂-based ones, it shown a potential to improve due to its high electron mobility. While the relationship between the material and the device performance are complicated, many studies have been focused on morphologies and surface area of the nanomaterials. The studies of the effect of the material properties such as the types and concentrations of native defects on the DSSC performance have been scarce. For photocatalytic degradation of pollutants, many reports showed ZnO has a higher or similar efficiency compared to the commonly used TiO₂. Reports have also pointed out the important role of native defects of ZnO in its photocatalytic activity. Nevertheless, the effect of the type and location of the defects has been contradictory in the literature indicating that there is a complex relationship.

Therefore, we will discuss the effect of ZnO native defects on the dye adsorption, charge transport and hence the DSSC performance. We will also discuss their influence on reactive oxygen species (ROS) generation and photocatalytic dye degradation. As photoluminescence (PL) is a common methodology in studying native defects of ZnO, the relationship between PL, DSSC performance and photocatalytic properties will also be investigated. Preliminary results showed a higher overall PL intensity would result in a better device performance and higher photocatalytic

Conference 8626:
Oxide-based Materials and Devices IV

activities.

8626-33, Session 8

ZnO:Al with tuned properties for photovoltaic applications: thin layers and high-mobility material (*Invited Paper*)

Florian Ruske, Mark Wimmer, Robert Rößler, Sebastian Neubert, Stefan Kämpfer, Bernd Rech, Helmholtz-Zentrum Berlin für Materialien und Energie GmbH (Germany)

Transparent conducting oxides (TCOs) are used as front contacts in various solar cell layouts. While for all applications the general requirement is to eliminate absorption while maximizing conductivity, further limitations apply regarding for instance maximum film thickness or the deposition process.

In the case of a-Si:H/ μ c-Si:H thin film solar cells, the main focus lays on the optimization of the surface morphology for efficient light trapping and on a minimization of optical absorption losses within the TCO layer. In order to achieve high conductivities while retaining low absorption in the near infrared spectrum it is mandatory to increase carrier mobility instead of carrier concentration. Recently we introduced a post-deposition annealing procedure which allows for the maximization of carrier mobility and a control of carrier concentration in ZnO:Al films. This results in a significant reduction of optical losses in the NIR spectral range and is also accompanied by a reduction of absorption in the sub-bandgap region. These improvements could also be proven in the spectral response of tandem cells deposited on treated TCO films.

Amorphous/crystalline silicon heterojunction solar cells require high optical and electrical quality TCO films at low film thickness (< 100 nm), which further have to be deposited at moderate substrate temperatures below 200 °C. Different TCO materials and sputtering technologies were compared in order to fulfill the requirements with a focus on the thickness dependence of material properties. In the case of a-Si/c-Si heterojunctions the effect of the TCO deposition method on the underlying a-Si/c-Si interface was investigated.

8626-34, Session 8

Laser crystallization of high-mobility aluminum-doped ZnO (AZO) thin films (*Invited Paper*)

Gary Cheng, Purdue Univ. (United States)

Highly conductive and transparent alumina-doped ZnO (AZO) thin films (250 nm) are deposited at room temperature using pulsed laser deposition (PLD) and direct pulsed laser recrystallization (DPLR). Morphological characterizations show that the AZO films undergo recrystallization and growth during DPLR, which leads to less internal imperfections in AZO films and hence better film conductance. Electrical-optical characterizations show that DPLR results in significant improvement of in conductivity, hall mobility, carrier concentration density and transmission from UV to NIR regions. Decrease in carrier concentration density in AZO film is observed. Compared with PLD, DPLR processed AZO films also possess smaller band gap which leads to broader solar spectrum acceptance

8626-35, Session 8

Design of oxide structured films for dye-sensitized photovoltaic solar cells

Thierry Pauporté, Ecole Nationale Supérieure de Chimie de Paris (France)

Interest in the study of dye-sensitized nanocrystalline metal oxide solar cells (DSSCs) has grown considerably in recent years from both fundamental and applied viewpoints. We will present results on the chemical and electrochemical design of ZnO nanostructures for DSSC application. We have developed the growth of a large variety of structured films : nanoparticulate porous films, nanoporous films prepared by electrodeposition with or without a structure directing agent dissolved in the deposition bath and arrays of ZnO nanorod or nanowires. The developed deposition techniques are versatile and the morphological, structural, optical and electrical properties of these layers could be finely tuned by changing the deposition conditions. In a second step we have worked on the combination of these structure to optimized their use in DSSC. Electrodeposited nanowires are good electron pathways, very well-contacted to the FTO substrate because electrons are exchanged upon the growth process, however their developed surface is small. We have then electrodeposited a secondary ZnO porous phase epitaxially grown on the ZnO nanowires. It was prepared at low-temperature without any template and presented a distribution of pore sizes which favored the electrolyte penetration in the photoanode and the redox shuttle diffusion in the cell. The efficiency of DSSCs prepared from hierarchical structures made of wires covered by the porous layer was drastically improved compared to pure nanowires or porous nanostructured layers. The various cells have been studied by J-V curves and impedance spectroscopy measurements and their performance will be discussed.

8626-36, Session 8

Comparison of chemical and laser lift-off for the transfer of GaN to alternative substrates

David J. Rogers, Nanovation (France); Abdallah Ougazzaden, Georgia Tech-Lorraine (France); Ferechteh H. Teherani, P. Bove, Nanovation (France); K. Pantzas, Georgia Tech-Lorraine (France); Tarik Moudakir, Gaëlle Orsal, Supélec (France); Mohamed Abid, Georgia Tech-Lorraine (France); Gilles Patriarche, Lab. de Photonique et de Nanostructures (France); Simon Gautier, Supélec (France); Ryan McClintock, Manijeh Razeghi, Northwestern Univ. (United States)

p-n junctions of (In)GaN are widely used in wide-bandgap opto-electronic devices. Such devices usually require high materials quality which is obtained via epitaxial growth on single crystal substrates, such as sapphire. For many end applications, however, it would be preferable to avoid inherent substrate constraints such as poor thermal/electrical conductivity and relatively high cost levels.

In this work, we compare two processes for transferring GaN from sapphire to glass substrates. The first involves laser-lift-off and thermo-metallic bonding and the second involves chemical lift-off using sacrificial ZnO templates and direct wafer bonding.

Conference 8626:
Oxide-based Materials and Devices IV

8626-37, Session 9

Residual stresses, stoichiometry, and clamped thermal expansion in LiNbO₃ and LiTaO₃ thin films (*Invited Paper*)

Samuel Margueron, Ctr. National de la Recherche Scientifique (France); Ausrine Bartasyte, Univ. de Lorraine (France); Valentina Plausinaitiene, Abrutis Adulfas, Tomas Murauskas, Vilnius Univ. (Lithuania); Pascal Boulet, Sylvie Robert, Jerome Gleize, Univ. de Lorraine (France); Virgaudas Kubilius, Zita Saltyte, Vilnius Univ. (Lithuania)

LiNbO₃ and LiTaO₃ are the two of the most important crystals, being the equivalent in the field of optics, nonlinear optics and optoelectronics to silicon in electronics. Thus, the studies about epitaxial ferroelectric LiNbO₃ and LiTaO₃ thin films are of great interest because of their potential application as elements in static random access memories, high dielectric constant capacitors, acoustic delay lines, microwave tunable devices, and optical waveguides. Although LiNbO₃ and LiTaO₃ films have been fabricated by different techniques, many electrical and electro-optical properties reported are not comparable for those of LiNbO₃ and LiTaO₃ single-crystals. Thus, the degradation of physical properties in thin films can be explained by the difficulty to control and to measure the Li concentration within the film.

In this work, high quality epitaxial LiTaO₃ and LiNbO₃ films, consisting of single phase, were deposited by pulsed-injection MOCVD – a method providing the digital control of the film deposition. The twin structure of the films has been studied in details by means of XRD. The indirect methods, used to estimate Li concentration in the single crystals, cannot be applied directly due to the presence of strain, size effects or other defects in the films, which influences also the structural, optical and other physical properties. Thus, the indirect method for estimation of nonstoichiometry of LiNbO₃ and LiTaO₃ films, based on Curie temperature and dampings of Raman modes and taking into account secondary effects, was developed. Furthermore, the effects of strain and Li stoichiometry on the thermal expansion and phase transitions of LiNbO₃ and LiTaO₃ films were studied. The clamping by the substrate induced the decrease/increase of the thermal expansion of the film lattice parameters by several times.

This paper has been accepted and is under minor revision for publication in Applied Physic Letters.

8626-38, Session 9

Electric-field induced bulk phase transition in VO₂ (*Invited Paper*)

Masaki Nakano, RIKEN (Japan); Keisuke Shibuya, National Institute of Advanced Industrial Science and Technology (Japan); Daisuke Okuyama, Takafumi Hatano, RIKEN (Japan); Shimpei Ono, Central Research Institute of Electric Power Industry (Japan); Masashi Kawasaki, Yoshihiro Iwasa, Yoshinori Tokura, The Univ. of Tokyo (Japan)

The field-effect transistor (FET) enables electrical switching through precise control of the number of electrons in a channel material by external voltage. This simple but unique feature is essential for information processing technology, as well as for fundamental scientific research regarding external control of the state of matter as successfully demonstrated in electric-field control of ferromagnetism and superconductivity. However, such electric-field effect is in principle a local effect, where an active channel is limited at the topmost surface within a nanometer scale due to the fundamental electronic screening effect, precluding electrostatic control of bulk phases. Here, we show that this conventional picture is no longer valid for some class of materials having inherent collective interactions between electrons and lattices. We fabricated FETs based on VO₂ thin films with electrolyte as a gate dielectric layer, and found that the electrostatically induced carriers

at a channel surface drive all preexisting localized carriers of 10²² cm⁻³ even inside a bulk to motion, leading to bulk carrier delocalization over structural phase transition. This non-local switching of bulk phases is achieved by applying just around 1 V, and moreover, a novel non-volatile memory like character emerges in a voltage-sweep measurement, which is basically operable at room temperature. These observations are apparently distinct from those of conventional FETs based on band insulators, broadening the concept of electric-field control further to macroscopic phase control.

8626-39, Session 9

Ion beam synthesis of nanothermochromic diffraction gratings with giant switching contrast at telecom wavelengths

Johannes Zimmer, Achim Wixforth, Helmut Karl, Hubert Krenner, Univ. Augsburg (Germany)

The metal-insulator transition (MIT) of vanadium dioxide (VO₂) has been studied in great detail over the past 50 years, showing both electronic and structural phase transition. We fabricated nanothermochromic diffraction gratings of VO₂ nanocrystals by high-dose ion implantation in a SiO₂ matrix to realize switchable optical devices. In contrast to bulk material, which exhibits the MIT at 68°C, when heated from the insulating phase to the metallic phase, such synthesized VO₂ nanocrystals show a broad thermal hysteresis down to room temperature [1]. Here, we present two routes to define and synthesize switchable gratings based on the strong variation of the optical constants at the MIT [2]. We defined these gratings either directly by spatially selective ion beam synthesis (DS) or by site-selective deactivation (SD) of the MIT. For DS gratings vanadium and oxygen were implanted through lithographically metal masks. Afterwards, nanoclusters with a diameter of ~95nm form during an annealing step. In contrast, the SD gratings were structured in a cold process, by introducing defects in already synthesized nanocrystals, which inhibit the MIT into the metallic state. We observe high switching contrasts in diffraction efficiencies, exceeding more than a factor of three for DS and one order of magnitude for SD gratings. This switching is most pronounced at the telecom wavelengths with a maximum at 1550nm [2].

[1] R. Lopez et al., Appl. Phys. Lett. 85, 1410–1412 (2004).

[2] J. Zimmer et al., Appl. Phys. Lett. 100, 231911 (2012).

8626-40, Session 10

The effects of deposition conditions and annealing temperature on the performance of gallium tin zinc oxide thin film transistors (*Invited Paper*)

Shanthi Iyer, Tanina Bradley, Robert Alston, Ward Collis, Olanrewaju Ogedengbe, North Carolina A&T State Univ. (United States); Jay S. Lewis, Garry Cunningham, RTI International (United States)

In this work the performance of bottom gate thin film transistors (TFTs) with transparent amorphous gallium tin zinc oxide (GSZO) active layers fabricated by radio frequency sputter deposition using a single GSZO target on SiO₂/Si wafers will be presented. Trap density, defect creation and oxygen chemisorption were found to play a critical role in determining the operational characteristics of the device, all of which can be controlled by the oxygen incorporation and substrate temperature during deposition, along with the post-deposition annealing. In addition device instability, with respect to the electrical stress and optical illumination, can be suppressed by suitably tailoring these parameters. TFTs which are normally “on” exhibiting a drain current (I_D) of 10⁻⁶ A, threshold voltage (V_T) of -3 V, and on/off current ratio (I_{on}/I_{off}) of 10⁶ was achieved. The best characteristics for the initially “off” device

**Conference 8626:
Oxide-based Materials and Devices IV**

demonstrated a typical ID of 10-7 A, VT of 3 V, and Ion/off of 106 with 9% oxygen flow on a 50 μm x 50 μm device. A stable TFT has been achieved under electrical stress for 2% oxygen flow exhibiting VT as low as ~0.5 V for 3hr stress under a gate bias of 1.2 and 12 V, with good optical stability. Further the differences in the C-V characteristics of the TFT displayed at low and high frequency can be successfully correlated to the relevant device parameters.

8626-41, Session 10

TiO2 thin film transistor by atomic layer deposition

Ali K. Okyay, Feyza Oruc, Furkan Cimen, Bilkent Univ. (Turkey)

There is a rapidly growing interest in low-temperature metal-oxides since the initial demonstration of functional electronic devices for low cost and flexible applications. Among these, ZnO has been intensively investigated as a channel material. ZnO is a wideband semiconductor with high optical transparency in the visible wavelengths, therefore, allowing transparent circuits. There are reports on RF sputtered, solution processed and atomic layer deposited (ALD) ZnO layers used in thin film electronic devices. TiO2 is also a wideband semiconductor with a higher energy gap than ZnO, however, there are limited reports on low temperature TiO2 based TFTs. Recently, TiO2 based TFTs were demonstrated by ablation from an anatase polymorph target by an excimer laser which is not a suitable technique for large-area low-cost electronics. ALD technique, on the other hand, offers low temperature growth, large area uniformity, precise thickness control, highly conformal deposition and scalability to roll-to-roll processes. To the best of our knowledge, we report, for the first time, ALD-TiO2 channel TFTs.

The fabricated devices exhibit n-type FET behavior and the threshold voltage is extracted as -1.85 V. The maximum on-to-off ratio of 100 is observed for a device with a gate length and width 40 μm and 50 μm, respectively. Sub-threshold slope is extracted from I-V measurements to be 2.5 V/decade. This is the first demonstration of a proper TiO2 FET in the literature.

8626-43, Session 11

Growth of single and multilayer sesquioxide crystal films for lasing applications via pulsed laser deposition

Katherine A. Sloyan, Robert W. Eason, Univ. of Southampton (United Kingdom); Sebastian Heinrich, Günter Huber, Univ. Hamburg (Germany)

Sesquioxides, materials of the form RE2O3 (RE: rare earth), are of great interest for lasing applications. These materials offer high thermal conductivities, are mechanically stable, can easily be doped with various rare earth ions and are optically isotropic. Members of the sesquioxide family have the same crystal structure but differing refractive indices, and hence are ideal candidates for multilayer as well as single film growth. Sesquioxides can be challenging to grow from the melt, however, due to their high melting points (>2400 °C).

Pulsed laser deposition (PLD) is a simple and versatile thin film fabrication technique that should be suited to sesquioxide growth, providing the required high growth temperatures (≥900 °C) can be achieved. We present the growth via PLD of doped and undoped scandia, lutetia and yttria thin films on 10x10 mm2 c-cut sapphire substrates. An excimer laser ablated ceramic targets in an oxygen gas pressure of 8x10-2 mbar. Substrates were heated to ~1000 °C via CO2 laser to obtain (222)-orientated crystal films whose thicknesses ranged from ~2 to ~10 μm, with thicker film growth currently under investigation. Particulate densities are low (<10^4/cm2); scattering and hence propagation losses are therefore expected to be much lower than in previous reports [1]. Lutetia and yttria films have also been grown on lutetia and yttria substrates respectively.

Emphasis has been placed on the growth of Yb:lutetia for lasing applications. Single- and cladged multilayer samples will be presented, along with the results of lasing experiments.

[1] Kahn et al, Opt. Express 17(6) (2009)

8626-44, Session 11

Atomic force microscopy based morphological, electric, and photoelectric characterization of ZnO (Invited Paper)

Christian Teichert, Montan Univ. Leoben (Austria)

ZnO is a versatile and multifunctional material with potential applications in photovoltaics and electronics as well as actuators. Here, we employ atomic-force microscopy (AFM) based techniques to study the morphological, electrical, and optoelectric properties of upright standing ZnO nanorods on the one hand and polycrystalline ZnO films in multilayer varistors on the other hand.

We have demonstrated that - against the intuition - AFM is applicable to study the morphology of individual freestanding ZnO nanorods [1], and conductive atomic-force microscopy (C-AFM) allow to characterize the electric properties of these nanostructures [2]. C-AFM measurements under simultaneous light irradiation - so called photoconductive AFM revealed a persistent photoconductivity which can be addressed to photo-excitation of charge carriers localized at defect states [3].

In the case of polycrystalline ZnO in multilayer varistors we employed C-AFM [4] and KPFM to explore the electrical properties of the grain boundaries.

This work has been supported by FWF Austria under projects P19636 and by FFG (Austria) under Bridge Project # 824890. Contributions by A. Andreev, I. Beinik, G. Brauer, X.Y. Chen, A. Djurić, M. Hofstätter, Y. Hou, Y. F. Hsu, M. Kratzer, A. Nevosad, M. Schloffler, and P. Supancic are acknowledged.

REFERENCES

- [1] G. Brauer, et al., Nanotechnology 18 (2007) 195301
- [2] I. Beinik, et al., J. Appl. Phys. 110 (2011) 052005.
- [3] I. Beinik, et al., submitted to Beilstein J. Nanotechnol., Nov. 2012.
- [4] M. Schloffler et al., J. Eur. Ceram. Soc. 30 (2010) 1761.

8626-50, Session 11

Fabrication of single crystalline ZnO microspheres by laser ablation in superfluid helium

Shinya Okamoto, Satoshi Ichikawa, Yosuke Minowa, Masaaki Ashida, Osaka Univ. (Japan)

Recently, nano and micro-structured material has been of great interest due to their potential application. In particular, microspheres have attracted much attention as high Q microcavities and micro objects manipulated by light. However, it has been difficult to fabricate semiconductor microspheres.

ZnO is a unique semiconductor with wide direct band gap and it has received a great deal of attention as ultraviolet and visible photonic devices. So far, fabrication techniques of ZnO nano and microwires have been widely developed because ZnO has hexagonal wurtzite structure. On the other hand, we successfully fabricated ZnO microspheres with typical diameter in the range of several nm to 3 μm by laser ablation in superfluid helium and observed efficient lasing due to three dimensional light confinement at room temperature. Then, the detailed microstructures of fabricated ZnO microspheres were characterized using a transmission electron microscope (TEM). From the result of TEM observation, the fabricated ZnO particles was found to have extremely good sphericity without faceted structures which are characteristic of usual ZnO crystals. In addition, we clarified from the electron diffraction

**Conference 8626:
Oxide-based Materials and Devices IV**

the isolated ZnO microspheres are single crystals with ZnO bulk crystal structure. Moreover, the ZnO microspheres have good crystalline quality even at their surfaces although even single crystalline ZnO microwires have thin amorphous layer at their surface in some cases. This novel fabrication method of single crystalline semiconductor should be applicable to different promising materials such as TiO₂, GaN, and CdSe, because the method does not depend on their lattice structures.

8626-46, Session 12

Crystallization effect on rare-earth activated biocompatible glass-ceramics (Invited Paper)

Rolindes Balda, Univ. del País Vasco (Spain); Daniel Sola, Centro de Fisica de Materiales (Spain); Jose Ignacio Peña, Univ. de Zaragoza (Spain); Joaquín M. Fernández, Univ. del País Vasco (Spain)

Eutectic structures are a paradigm of composite materials with a fine microstructure whose characteristics are controlled by the solidification conditions. The favorable conditions of eutectic mixtures to produce glasses with a low number of components are also remarkable from the point of view of their photonic applications. A good optical quality glass can be produced by fast directional solidification of the CaSiO₃/Ca₃(PO₄)₂ eutectic system. This system presents two non-conventional and interesting properties: firstly, the degenerated lamellar structure of the system favors the biological transformation of the tricalcium phosphate phase into hydroxiapatite, giving rise to a biological material with a microstructure similar to that of human bone. Secondly, it is possible to form an eutectic glass of this composition with excellent optical properties.

In this work we report the influence of the crystallization stage of the host matrix on the spectroscopic properties of rare-earth ions in CaSiO₃/Ca₃(PO₄)₂ eutectic glass-ceramics grown by the laser floating zone. This technique allows to grow rods and fibers at different growth rates directly from ceramic precursors as well as to incorporate doping ions. The microstructural analysis shows that a growth rate increase leads the system to a structural arrangement from three (two crystalline and one amorphous) to two phases (one crystalline and one amorphous). The crystalline phases correspond to apatite-like and Ca₂SiO₄ structures. Site-selective laser spectroscopy of rare-earth ions allows to distinguish between crystalline and amorphous environment for the rare-earth ions and to correlate the spectroscopic properties with the microstructure of these eutectics.

8626-47, Session 12

Defects study of MOCVD-grown β -Ga₂O₃ films

Parvaneh Ravadgar, National Cheng Kung Univ. (Taiwan); Ray-Hua Horng, National Chung Hsing Univ. (Taiwan); Hui-Ping Pan, Shu-De Yao, Peking Univ. (Taiwan)

β -Ga₂O₃ is a wide bandgap (4.5 – 4.9 eV) semiconductor oxide opening its way through many applications in optoelectronic technology. Many studies are reported on fabrication and device efficiency of β -Ga₂O₃ and almost all of them mentioned about presence of different defects, disturbing device performance. Here, we tried to focus on defect study of single crystal β -Ga₂O₃ films fabricated by metal organic chemical vapor deposition (MOCVD). Relatively low temperature (~450 °C) along with other growth parameters allows fabricating of MOCVD single-crystal β -Ga₂O₃ films. At the same time many defects are found, affecting the related device performance. A comprehensive understanding of defects is important not only for improving attributed device performance, but even it may introduce some un-known potential of single-crystal β -Ga₂O₃ films, recommending novel devices.

The resistivity of samples is examined under harsh thermal conditions. The crystalline structure of samples checked by x-ray diffraction (XRD)

remains almost unchanged up to 800 °C. Rutherford backscattering spectrometry (RBS) applied to investigate the ratio of oxygen to gallium reveals no specific vacancy. But, cross-sectional transmission electron microscopy (TEM) exposes many defects in the form of vacancies and interstitials. The harmony between RBS and TEM suggests a balance between vacancies and interstitials.

Optical properties of samples were probed by cathodoluminescence (CL) measurements at room temperature under 2 and 10 KeV applied voltage to track different depth of films. A comparison between results of CL at different depth is found to be very appreciable to study the chemistry of β -Ga₂O₃ at both of surface and bulk.

8626-48, Session 12

Nonlinear optical photonic crystal waveguide with TiO₂ material

Koji Uchijima, Tomohiro Kita, Hirohito Yamada, Tohoku Univ. (Japan)

Enhancement of nonlinear optical effect using slow light effect in TiO₂ photonic crystal (PhC) waveguide was demonstrated. Titanium dioxide (TiO₂) has attractive properties such as high linear and nonlinear refractive indices and wide bandgap for applying nonlinear optical devices. We have been studied channel waveguides with TiO₂ as the submicron size core and demonstrated their possibility as nonlinear optical devices. In this study, we analyze the TiO₂ PhC waveguide and demonstrate the enhanced nonlinearity using slow light effect.

8626-49, Session 12

Optimizing anatase-TiO₂ deposition for low-loss planar waveguides

Lili Jiang, Christopher C. Evans, Orad Reshef, Eric Mazur, Harvard Univ. (United States)

Advances in laser and fiber-optic technology expand the capacity of existing communications networks. Electronic switching and routing becomes very inefficient at future data rates, leading us to ask if we can design photonic devices capable of switching and routing data completely in the optical domain. Among the candidate materials for photonic devices, titanium dioxide (TiO₂) combines a high optical nonlinearity with extended transparency from 400 nm to the infrared and low two-photon absorption for wavelengths longer than 800 nm.

Sustaining high optical intensities remains as a critical challenge for the development of TiO₂-based devices. My project explores TiO₂ deposition parameters to understand the dominant source of propagation losses in our films and achieve higher quality, lower-loss films. We deposit anatase-TiO₂ films using reactive sputtering of titanium metal in an oxygen environment. To characterize the physical and optical properties of our films, we use ellipsometry and prism coupler to measure their thickness and planar optic losses. Raman spectroscopy and scanning electron microscopy (SEM) provide information on the crystalline phase and granularity. The resulting films are polycrystalline and display differing grain sizes and orientations, depending on deposition parameters in reactive sputtering.

By pairwise correlating film morphology, optic loss and the deposition parameters, we have developed an understanding of the effect of changing oxygen flow rate, deposition pressure, power and temperature on the physical and optical properties of the films. We also identify a deposition procedure for anatase-TiO₂ optic devices with losses down to 2dB/cm while maintaining a reasonable deposition rate.

Conference 8626:
Oxide-based Materials and Devices IV

8626-42, Session PWed

Inkjet-printed indium zinc oxide nonvolatile memory thin-film transistors with organic ferroelectric gate InsulatorSoon-Won Jung, Bock Soon Na, Jae Bon Koo, In-Kyu You,
Electronics and Telecommunications Research Institute (Korea,
Republic of)

Thin-film transistor (TFT) with nonvolatile memory function can be one of the key devices to realize highly-functionalized large-area electronic systems such as active-matrix display panel and various sensor applications. These memory TFTs have features of a mechanical flexibility and/or a transparency in the visible range. For these fields, the employment of solution-based process is very desirable, because it provides us many advantages of simpler process, lower cost, and higher throughput compared to the conventional vacuum-deposition-based methods. The memory transistor composed of ferroelectric gate insulator and oxide semiconducting channel is a good approach. Because a relatively high crystallization temperature required for the sol-gel-driven oxide ferroelectric films such as $\text{Pb}(\text{Zr,Ti})\text{O}_3$ may restrict the scopes of process window and applications, the use of ferroelectric copolymer is more acceptable. A typical ferroelectric copolymer of poly(vinylidene fluoride-trifluoroethylene) [P(VDF-TrFE)] can be formed by means of a simple spin-coating method and crystallized at a lower temperature of around 140 °C. Although the P(VDF-TrFE) has been employed with various organic semiconductor to fabricate such memory transistors, the change of the active channel into the oxide semiconductor can be a good choice in obtaining higher mobility and better stability in device behaviors. However, the combination of spin-coated P(VDF-TrFE) ferroelectric gate insulator with the solution-processed oxide semiconducting channel have been seldom attempted for the promising candidate of embeddable nonvolatile memory device for large-area electronics, although there have been only a few reports on the memory transistors using sputtered or atomic-layer deposited (ALD) ZnO active layers. In this paper, we present the memory transistors fabricated using the inkjet printed active channel and P(VDF-TrFE) gate insulator(GI).

8626-51, Session PWed

Development of tellurium oxide and lead-bismuth oxide glasses for mid-wave infrared transmission opticsBeiming Zhou, Charles F. Rapp, John K. Driver, Michael J. Myers,
John D. Myers, Kigre, Inc. (United States); Jonathan T. Goldstein,
Air Force Research Lab. (United States); Rich Utano, Shantanu
Gupta, Fibertek, Inc. (United States)

Heavy metal oxide glasses exhibiting high transmission in the Mid-Wave Infra-Red (MWIR) spectrum are often difficult to manufacture in large sizes with optimized physical and optical properties. In this work, we researched and developed improved tellurium-zinc-barium and lead-bismuth-gallium heavy metal oxide glasses for use in the manufacture of fiber optics, optical components and laser gain materials. Two glass families were investigated, one based upon tellurium and another based on lead-bismuth. Glass compositions were optimized for stability and high transmission in the MWIR. Targeted glass specifications included low hydroxyl concentration, extended MWIR transmission window, and high resistance against devitrification upon heating. Work included the processing of high purity raw materials, melting under controlled dry Redox balanced atmosphere, fining, casting and annealing. Batch melts as large as 4 kilograms were sprue cast into aluminum and stainless steel molds or temperature controlled bronze tube with mechanical bait. Small (500g) test melts were typically processed in-situ in a gold coated platinum crucible. Our group manufactured and evaluated over 100 different experimental heavy metal glass compositions during a two year period. A wide range of glass melting, fining, casting techniques and experimental protocols were employed. MWIR glass applications

include remote sensing, directional infrared counter measures, detection of explosives and chemical warfare agents, laser detection tracking and ranging, range gated imaging and spectroscopy. Enhanced long range mid-infrared sensor performance is optimized when operating in the atmospheric windows from ~ 2.0 to 2.4 μm , ~ 3.5 to 4.3 μm and ~ 4.5 to 5.0 μm . High refractive index heavy metal glasses may provide other unique properties besides high MWIR spectral transmission. For example, tellurite glass fibers provide nonlinear properties capable of stimulated Raman amplification. Lead-bismuth glasses exhibit high non-resonant optical nonlinearity capable of Faraday effect optical switching. We began this work with a tellurium-zinc-barium ($65\text{TeO}_2\text{-}13\text{ZnO-}10\text{BaO-}7\text{Li}_2\text{O}$) glass composition. It was chosen for its excellent stability with respect to crystallization. Work on lead bismuth glasses began with a Dumbaugh composition ($57.2\text{PbO-}25\text{Bi}_2\text{O}_3\text{-}17.8\text{Ga}_2\text{O}_3$) The heavier the metal and the weaker the M-O bond, the further the glass phonon edge is moved out. The long wavelength transmission limit of a glass is usually determined by the multiphonon absorption edge. This multiphonon edge is determined by the highest energy vibration of the glass host and may be increased through the use of compositions that include heavy metal oxides as the glass former. For the common glass forming oxides, the multiphonon edge and infrared transmission increase in the order $\text{B}_2\text{O}_3 < \text{P}_2\text{O}_5 < \text{SiO}_2 < \text{GeO}_2 = \text{Al}_2\text{O}_3 < \text{TeO}_2 < \text{Bi}_2\text{O}_3$. A significant absorption generally begins about 1 to 2 microns before the "cutoff" wavelength. The shape of this absorption edge is greatly affected by other components in the glass. Small amounts of an ion with a high charge and/or light weight can affect the transmission at shorter wavelengths. Dry tellurite oxide glass samples based on $\text{TeO}_2\text{-BaO-ZnO}$ manufactured during this study provided high transmission out to 4.5 microns. This compares with a theoretical cutoff wavelength of 6.5 microns. Partially dry $\text{PbO-Bi}_2\text{O}_3\text{-Ga}_2\text{O}_3$ glasses showed (after removing the water bands from the spectra) an infrared wavelength transmission cutoff of 7.0 microns. Our first goal was to develop highly stable $\text{TeO}_2\text{-BaO-ZnO}$ (TBZ) glass compositions exhibiting low liquidus temperatures and high spectral transmission in the MWIR. Well stabilized glasses show a high resistance to crystallization during the glass casting, quenching and annealing processes. Candidate glass compositions did not include light weight or highly charged ions such as Nb^{5+} or W^{6+} that can contribute to a shorter IR absorption edge wavelength. Work began with melting small 100 and 200g TBZ glass compositions in uncontrolled air atmosphere. One test melt composition (PbBiGa_1) did not include tellurium. Compositions were initially batched, melted and fined in-situ in Pto crucibles and later in Auo/Pto crucibles. A TA Instruments Q10 Differential Scanning Calorimeter (DSC) was used to measure transition (Tg) crystallization (Tx) and fluidity (Tf) temperatures. The DSC curves provided us with quantitative evidence for glass stability. Glasses were prepared and analyzed by DSC for their tendency to crystallize. Heating and cooling rates of 20, 5 and 1 oC / min were used on the different glasses.

8626-52, Session PWed

Synthesis and characterization of core/shell (ZnO/gamma-Fe₂O₃) structured nanoparticlesNoureddine Jouini, Imen Balti, Lab. de Physique des Lasers
(France); Laila Samia Smiri, Univ. of Carthage (Tunisia); Pierre
Rabu, Institut de Physique et Chimie des Matériaux de
Strasbourg (France); Eric Gautron, Philippe Leone, Institut des
Matériaux Jean Rouxel (France); Bruno Viana, Ecole Nationale
Supérieure de Chimie de Paris (France) and Univ. Pierre et Marie
Curie (France) and Collège de France (France)

Recently, core-shell nanoparticles have received intensive attention because of their biomedical and biological potential applications including magnetic separation and detection of cancer cells, bacteria and viruses [1,2]. These heterostructured core/shell systems provide the possibility for multiple properties. Herein, core-shell ZnO/gamma-Fe₂O₃ nanoparticles were prepared via a simple method using forced hydrolysis of acetate metallic salts in a polyol medium. Two types of morphologies can be easily obtained: (i) quasi-spherical ZnO core 20 nm in diameter coated with a continuous shell with 3 nm in length, (ii)

**Conference 8626:
Oxide-based Materials and Devices IV**

rod-like ZnO decorated with γ -Fe₂O₃ nanoparticles. The ZnO nanorods are 80 nm in diameter and 400 nm in length. The maghemite (γ -Fe₂O₃) nanoparticles with 5 nm in diameter are strongly bonded to ZnO, well separated from each other and form a monolayer on the surface of ZnO nanorods. In both systems, coating ZnO by γ -Fe₂O₃ inhibits the surface defects and thus enhances the UV luminescence. The two systems present a superparamagnetic behaviour with blocking temperature depending on the morphology: the decorated ZnO nanorods present a blocking temperature around 6 K whereas this temperature is significantly higher (300 K) for spherical core-shell nanoparticles.

8626-53, Session PWed

The effect of moisture on negative bias stability of oxide TFTs

Yong Han, Xiaoli Nan, Haitao Dai, Shu Guo Wang, Xiao Wei Sun, Tianjin Univ. (China)

Transparent oxide based thin film transistors (TFTs) have attracted much attention recently due to their excellent electrical and optical characteristics for advanced display applications. In particular, amorphous indium gallium zinc oxide (a-IGZO) TFTs are intensively investigated in active matrix displays as they can simultaneously offer high mobility, high optical transparency with low temperature processing. Although a-IGZO TFTs have shown good performance, they still suffer from reliable problems. In general, the reliability of a-IGZO TFTs influenced by positive/negative bias, light illumination condition and the temperature has been investigated extensively. There are few papers, however, to consider the adsorption of water on the reliability of a-IGZO TFTs. In this paper, we will focus on the variation of the field effect mobility, threshold voltage and the sub-threshold swing in different humid environment. First the output characteristic curve and transfer characteristic curve of the a-IGZO TFTs will be measured under different humidity. Subsequently, the field effect mobility and threshold voltage will be calculated from the measured transfer curves. Meanwhile, the sub-threshold swing is extracted from the linear portion of the log plot of the drain-source current (IDS) versus the gate-source voltage (VGS). In addition, the contact interfaces between a-IGZO and source/drain electrodes is investigated as well because these interfaces strongly affect the performances of the device.

8626-54, Session PWed

The influences of deposition conditions on a-IGZO TFTs and the investigation of stability

Xiaoli Nan, Yong Han, Haitao Dai, Shu Guo Wang, Xiao Wei Sun, Tianjin Univ. (China)

Transparent amorphous oxide semiconductors (TAOSs) like amorphous In-Ga-Zn-O (a-IGZO) have drawn considerable attention as a promising material for channel layers in thin film transistors (TFTs) for high-resolution active-matrix flat-panel displays (AMFPD) and active matrix organic light-emitting diode (AMOLED). In comparison with amorphous Si:H and Poly-Si TFTs, a-IGZO materials can achieve high field-effect mobility, spectra transmission in visible range with low processing temperature. However, a-IGZO TFTs generally suffer from stability problems, which refer to the variation of threshold voltage (V_{th}) and degradation of mobility upon prolonged operation.

In this paper, we report the fabrication of highly stable bottom-gate a-IGZO TFTs with rational performance by optimizing deposition conditions (such as the gas-flow rate of O₂ : Ar and deposition pressure etc) and O₂ plasma treatment on the SiO_x gate insulator. Experimental results show that the O₂ plasma post-treatment on the SiO_x gate insulator can improve the device stability under a gate bias stress and illumination conditions because the surface modification may result in the creation of a stable interlayer. Meanwhile, the less O₂ ratio can increase the mobility of devices due to the higher density of the oxygen vacancy lead to higher carrier concentration. We also discussed the

effects on device performance with different film thickness and annealing temperature, respectively. In comparison with thick film, thin film enhances the switching behavior greatly, since the thinner film, the lower number of free carriers and then easier depletion.

8626-55, Session PWed

Various post-annealing treatments on aluminum doped zinc oxide films fabricated by ion beam co-sputtering

Jin-Cherng Hsu, Yu-Yun Chen, Yueh-Sheng Chiang, Heng-Ying Cho, Fu-Jen Catholic Univ. (Taiwan)

Aluminum doped zinc oxide (AZO) films with the aluminum concentration of 1.5 at.% were fabricated by co-sputtering dual metallic targets, Al and Zn, under the oxygen partial pressure of 1.3×10^{-4} torr. The total pressure was kept at 2.3×10^{-4} torr during the deposition. The poly-crystalline structure, optical property and conductivity of the films were investigated by XRD, UV-VIS-IR spectrometer and Hall effect measurement, respectively. The more intense ZnO crystallinity of (002), larger grain size, smaller d-spacing and highest carrier concentrations were observed on the as-deposited AZO film which had the lowest resistivity of $7.8 \times 10^{-4} \Omega \cdot \text{cm}$. Comparing the AZO films post-annealed in air, in vacuum and in hydrogen ambiance, the structures processed in vacuum and hydrogen ambiance remained the good ZnO crystallinity in the film resulting from the oxygen deficient state of the films after post-annealing processes. The better thermal stability of resistivity was observed in the films post-annealed in hydrogen ambiance due to the formation of the shallow donor in the film.

Furthermore, the resistivity increased as the temperature of post-annealing in air increasing. When the as-deposited film were post-annealed at temperature of 400 oC, the resistivity was about more than two orders of magnitude than that of the as-deposited film resulting from the decrease of the donor concentration and mobility in the AZO film. The variation of the carrier concentration in the AZO film also shifted the energy band gap. However, the average visible transmittance of all AZO films in this study was above 80 % regardless of the deposition and post-annealing conditions.

8626-56, Session PWed

Effects of O₂ plasma post-treatment on ZnO:Ga thin films grown by H₂O-thermal ALD

Yueh-Lin Lee, Jia-Hao Chuang, Tzu-Hsuan Huang, Chong-Long Ho, Meng-Chyi Wu, National Tsing Hua Univ. (Taiwan)

Transparent conducting oxides have been widely employed in optoelectronic devices using different deposition methods such as sputtering, thermal evaporator, and e-gun evaporator technologies. In this work, thermal- and plasma-mode atomic layer deposition (ALD) of gallium doped zinc oxide (GZO) thin films were grown on glass substrates at various deposition temperatures from 200? to 350?. ALD-GZO thin films were constituted as a layer-by-layer structure by stacking zinc oxides and gallium oxides. Diethylzinc (DEZ), triethylgallium (TEG) and H₂O/O₂ were used as zinc, gallium precursors and sources of oxygen, individually. GZO films were prepared by thermal-mode ALD (TM-ALD) and plasma-mode ALD (PM-ALD) using H₂O and O₂ as the oxidant, respectively. The effects of each deposition condition on the growth rates, the surface morphology, the electrical and optical properties of Ga doped ZnO films were investigated. The characteristics of ALD-GZO films exhibited a smooth surface, low resistivity, high carrier concentration, and good optical transmittance in both the visible range and infrared region. The results indicate that the transparent conducting GZO films fabricated in this study are suitable for the applications of optoelectronics and photonics such as light emitting diodes (LEDs) and infrared photodetectors (IR-PDs).

8626-57, Session PWed

Current-voltage characteristics of n-AlMgZnO/p-GaN junction diodes

Kuang-Po Hsueh, Po-Wei Cheng, Yi-Chang Cheng, Vanung Univ. (Taiwan); Jinn-Kong Sheu, Yu-Hsiang Yeh, National Cheng Kung Univ. (Taiwan); Hsien-Chin Chiu, Hsiang-Chun Wang, Chang Gung Univ. (Taiwan)

This study investigates the current-voltage (I-V) characteristics of n-AlMgZnO/p-GaN junction diodes. A 200-nm-thick p-GaN layer used in this study was grown by MOCVD. The Ohmic contacts on p-GaN were formed by evaporating a Ni (50 nm)/Au (50 nm) metal stack and subsequently annealing at 500 °C for 5 minutes in oxygen ambient. Afterward the Al-doped Mg_xZn_{1-x}O (AMZO) films were deposited by rf sputtering method using a 4 inch ZnO/MgO/Al₂O₃ (76/19/5 wt %) target and lifted off. The AMZO mesa size was 100 μm x 100 μm. The AMZO samples were then annealed at 700, 800, 900, and 1000 C in nitrogen ambient for 60 seconds, respectively, in a rapid thermal annealing system (RTA). Finally, Cr (50 nm)/Au (150 nm) was deposited by evaporating on top of the AMZO layer to provide an n-type contact.

The Hall measurement and the x-ray diffraction pattern are measured to study the AMZO/GaN films. XRD result is shown that the diffraction angles of the annealed AMZO films remain the same as the GaN without shifting.

The breakdown voltage in forward bias and the leakage current in reverse bias were also analyzed on these n-AlMgZnO/p-GaN junction diodes which the AMZO films were annealed at different temperatures. Based on these findings, the n-AlMgZnO/p-GaN junction diode is feasible for GaN-based heterojunction bipolar transistors.

8626-58, Session PWed

ZnO nanorods on V-doped AZO thin films

Yen-Ju Wu, Yu-Shan Wei, Chih-I Hsieh, Cheng-Yi Liu, National Central Univ. (Taiwan)

In this study, ZnO nanorods (NRs) were prepared on the AZO and V-doped AZO substrates by the hydrothermal method. The solution of the hydrothermal method is 1:1 molar concentrations of Zn(NO₃)₂•6H₂O and hexamethylenetetramine (C₆H₁₂N₄). AZO and V-doped AZO thin films were deposited on quartz substrates by sputter and annealed under various annealing temperatures and ambient. According to the preliminary results, vertically aligned ZnO NRs arrays grew on the AZO and V-doped AZO thin films. XRD and SEM analysis on the ZnO NRs indicate that the diameters and growth directions of ZnO NRs depend on the crystallinity and surface atomic structure of the AZO and V:AZO substrates. The diameter of the ZnO NRs on the AZO substrate is larger than that on the V:AZO substrates. In addition, the growth direction of ZnO NRs on the V:AZO substrate is not vertical to the substrate. Instead, the growth direction of ZnO NRs on the V:AZO substrate is very random. We believe that the above discrepancies are due to the differences in the microstructure of the AZO and V:AZO substrates. Using XRD and SEM, we found that, with the V dopants in the V:AZO, the grains size of the V:AZO would be smaller than that of the AZO thin film. Also, we found that the preferred orientation of the (002) growth direction of ZnO NRS would decrease with V doping. In this talk, we will discuss the detail mechanism of ZnO formation on the AZO and V:AZO substrates. Also, we will correlate the ZnO NRs growth with the microstructures of AZO and V:AZO substrates.

8626-59, Session PWed

Electrodeposited ZnO nanowire-based light-emitting diodes with tunable emission from near-UV to blue

Thierry Pauporté, Oleg Lupan, Bruno Viana, Ecole Nationale Supérieure de Chimie de Paris (France)

Nanowires (NWs)-based light emitting diodes (LEDs) have drawn large interest due to many advantages compared to thin film based devices. Markedly improved performances are expected from nanostructured active layers for light emission due to good light extraction. The use of wires avoids the presence of grain boundaries and then limits the non-radiative recombinations. An electrochemical deposition technique has been developed for the preparation of ZnO-NWs based light emitters. Nanowires of high structural and optical quality have been epitaxially grown on p-GaN single crystalline films substrates and the heterojunction has been integrated in LED devices. The fabricated LED exhibited high brightness and low-threshold emission voltage. Moreover, it has been shown that the wires acted as waveguides that favored the directional light extraction. CdCl₂ or CuCl₂ were used as an additive in the deposit bath for ZnO doping. The doping could be tuned by changing their concentration in the bath and yielded to a bandgap narrowing. LEDs prepared with the doped nanowires exhibited low-threshold emission voltage and the single electroluminescence emission peak was shifted from ultraviolet to violet-blue spectral region compared to pure ZnO/GaN LEDs. The emission wavelength could be tuned by changing the Cd or Cu atomic concentration in the ZnO nanomaterial. The shift, due to the bandgap reduction, will be discussed, including insights from DFT computational investigations: the bandgap narrowing has two different origin for Zn_{1-x}Cd_xO and Zn_{1-x}Cu_xO.

8626-60, Session PWed

P-type ZnO films by phosphorus doping using plasma immersion ion-implantation technique

Saurabh Nagar, Subhananda Chakrabarti, Indian Institute of Technology Bombay (India)

ZnO has been a subject of intense research in the optoelectronics community owing to its wide bandgap (3.3eV) and large exciton binding energy (60meV). However, difficulty in doping it p-type posts a hindrance in fabricating ZnO-based devices. In order to make p-type ZnO films, phosphorus implantation, using plasma immersion ion-implantation technique (2kV, 900W, 10μs pulse width) for 30 seconds, was performed on ZnO thin film deposited by RF Magnetron Sputtering (Sample A). The implanted samples were subsequently rapid thermal annealed at 700°C and 1000°C (Samples B and C) in oxygen environment for 30 seconds. Low temperature (8K) photoluminescence spectra reveal dominant donor-bound exciton (D^oX) peak at 3.36eV for samples A and B. However, for Sample B the peaks around 3.31eV and 3.22eV corresponding to the free electron-acceptor (FA) and donor to acceptor pair peaks (DAP) are also observed. A dominant peak around 3.35eV, corresponding to acceptor bound exciton (A^oX) peak, is detected for Sample C alongwith the presence of FA and DAP peaks around 3.31eV and 3.22eV. Moreover, the deep level peak around 2.5eV is higher for Sample B which may be due to implantation and acceptor related defects. However, for Sample C, the deep level peaks are very weak compared to the near band edge peaks confirming that these peaks are mainly due to intrinsic defects and not related to acceptors. These results clearly show us a promising way to achieve p-type ZnO films using phosphorus doping. DST, India is acknowledged.

**Conference 8626:
Oxide-based Materials and Devices IV**

8626-61, Session PWed

Synthesis and optical characterization of Gd₂O₂S:Tb nanoparticles for high-energy photon detection

Gabriela Palestino, Univ. Autónoma de San Luis Potosí (Mexico); Luis Hernández-Adame, Univ. Autónoma de San Luis Potosí (Mexico); Francisco Javier Medellín-Rodríguez, Univ. Autónoma de San Luis Potosí (Mexico); Antonio Méndez-Blas, Benemérita Univ. Autónoma de Puebla (Mexico); Roger Vega-Acosta, Univ. Autónoma de San Luis Potosí (Mexico)

In the last decades, a large number of materials based on rare earth ions have been studied due to its main characteristic of luminescence after the absorption of particles or high energy photons. In this work, Terbium-doped gadolinium oxysulfide (Gd₂O₂S:Tb) nanoparticles have been synthesized by hydrothermal precipitation of urea. On the reaction, we observed the influence of some variables as the temperature of solutions, the reaction time and the stirring velocities, are factors that play a key role on the crystal growth, modifying the morphology and the particle size that were inspected by TEM analysis. Furthermore a DLS studies were carried out to determine the particle surface energy in a wide range of pH, showing that basic solutions increase the surface energy to avoid agglomerations and sedimentations of the particles. Moreover, the photoluminescent properties of the material were evaluated as response at the UV light to obtain the energy levels related with the emission mechanism that showed a main peak at 544 nm. Besides, we found that the rare earth host lattice of the particles and doped-ions concentration is essential to obtain a strong visible photoluminescence that were evaluated experimentally and theoretically using a system of rate equations in order to determine the dynamics of the energy level populations.

Acknowledgments: FAI C12-FAI-03-94.94, Bilateral program project No. 122017, CONACYT for the scholarship 270040, Dr. Jaime Ruiz García (IF-UASLP) and Dr. Ángel Gabriel Rodríguez Vázquez (IICO-UASLP) for the DLS and FT-IR techniques.

8626-62, Session PWed

Impact of growth conditions on ZnO homoepitaxial films on ZnO substrates by plasma-assisted molecular beam epitaxy

Ming Wei, Ryan C. Boutwell, CREOL, The College of Optics and Photonics, Univ. of Central Florida (United States); Winston Schoenfeld, CREOL, The College of Optics and Photonics, Univ. of Central Florida (United States) and Univ. of Central Florida (United States)

ZnO thin films were epitaxially grown on Zn-polar (0001) ZnO substrates by plasma-assisted molecular beam epitaxy. Surface root mean square (rms) roughness below 0.3 nm was achieved on a large range of growth temperature by growing on ZnO substrates with 0.5 degree miscut angle toward to [1-100] axis. Surface treatment with acid etching and ozone exposure was required to remove contamination such as silica residual and carboxyl and carbonate groups on the surface. Removal of these surface impurities reduces the likelihood of extrinsic defect migration into the epitaxial films. High growth temperature (> 640°C) and oxygen rich conditions were required for films with terrace steps, but resulted in a very low growth rate (~30nm/h) and low photoluminescence (PL) lifetimes of lower than 50 ps. With moderate growth temperature (~610°C), higher growth rate and higher PL lifetime with up to 398ps were achieved. Deflection plates were used for the oxygen plasma to reduce high oxygen flux etching of the surface. Oxygen deflection also provided more neutral oxygen, resulting in a higher growth rate and less defects in the films. Oxygen impurities used for plasma generation were also studied. Low-purity oxygen (4N5) gave some satellite peaks in (0002) X-ray diffraction scan. With high purity oxygen (6N), good crystalline quality was evident

in X-ray rocking curves with full width at half maximum (FWHM) of (0002), (10-12) and (20-21) peaks less than 30 arc sec. Narrow FWHM indicates low threading dislocations, which were confirmed by cross sectional transmission electron microscopy.

8626-63, Session PWed

Thin film field effect transistor and ferroelectric memory

Armen R. Poghosyan, Natella R. Aghamalyan, Tigran A. Aslanyan, Ruben K. Hovsepyan, Institute for Physical Research (Armenia)

We report the preparation and investigation of heterostructures based on ferroelectric crystals and semiconductor films. The ferroelectric field effect transistor with high transparency for visible light and high field-effect mobility of the charge carriers has been fabricated using ZnO:Li films as a transistor channel. The possibility of use of ferroelectric field effect transistor based on ZnO:Li films as bistable element for information writing has been shown. Two methods of the non-destroying information readout are proposed. In the first method the spontaneous polarization sign is defined from ZnO:Li|LaB6 junction's saturation current. In the second method the spontaneous polarization sign is defined as a response of the drain current to the weak signal, sent to the control gate of the ferroelectric field-effect transistor. A large value of the stored electrical energy makes it possible to reach enormous information recording density with high signal/noise ratio.

8626-64, Session PWed

Metal-dielectric electronic phase transitions in transparent zinc oxide thin films

Armen R. Poghosyan, Natella R. Aghamalyan, Tigran A. Aslanyan, Yevgenia A. Kafadaryan, Ruben K. Hovsepyan, Silva I. Petrosyan, Institute for Physical Research (Armenia)

Metal-dielectric electronic phase transitions in wide gap ZnO semiconductors have been studied. The influence of defect complex caused by oxygen vacancy and interstitial zinc atom on the metal-dielectric transition is considered. The peculiarities of this transition in ZnO films doped by donor or acceptor impurity and the influence of mentioned defect complex on the charge carrier transfer mechanism were investigated. The control parameter of this transition is the concentration of Zn interstitial atom. The films with high concentration of Zn interstitial atom have high conductivity of metallic type. Air annealing leads to conductivity decreasing and to change of conductivity temperature dependence from metallic type to semiconductor (dielectric) one.

8626-65, Session PWed

ZnO based optical modulator in the visible wavelengths

Ali K. Okyay, Levent Aygun, Feyza Oruc, Bilkent Univ. (Turkey)

ZnO based transparent thin film transistors are extensively investigated recently due to their potential of replacing amorphous Si thin film transistors. Also, UV (ultra-violet) detecting properties of ZnO photodiodes are attracting increasing attention. Phototransistors with ZnO channel layer deposited by high temperature RF magnetron sputtering system are demonstrated in the literature. However, such a high temperature process is not suitable for flexible low cost substrates. Atomic layer deposition (ALD) technique can be used to deposit highly conformal ZnO films at low temperatures with unmatched large-area uniformity. In this work, we demonstrate an ALD based ZnO thin-film optical modulator with electrically tunable photo response in the visible spectrum.

**Conference 8626:
Oxide-based Materials and Devices IV**

ZnO based three-terminal devices are fabricated on 14-nm-thick ZnO grown by ALD technique at $T < 100^\circ\text{C}$. A controlling gate-terminal is used to modulate the absorption in the ZnO layer. This is verified by photocurrent measurements and UV-VIS transmission characterization. Spectral measurements in the visible region show that the absorption of sub-bandgap photons can be controlled by the applied voltage at the gate terminal.

8626-66, Session PWed

Surface modified-ZSM-5 zeolite-coated long period fiber grating for ammonia detection in water

Zhan Gao, Xinwei Lan, Jie Huang, Hanzheng Wang, Lei Yuan, Missouri Univ. of Science and Technology (United States); Xiling Tang, Junhang Dong, Univ. of Cincinnati (United States); Hai Xiao, Missouri Univ. of Science and Technology (United States)

A surface modified ZSM-5 zeolite-coated long period fiber grating (LPFG) sensor was developed and tested for direct measurement of ammonia solution. The sensor was prepared by growing continuous zeolite thin films on the optical fiber grating region through in situ hydrothermal crystallization. The ammonia concentration in water was measured by monitoring the LPFG resonance wavelength shift caused by molecular sorption into the zeolite cavity. Because the nanoporous hydrophilic ZSM-5 zeolite possesses the ability to effectively concentrate the ammonia molecules by physical adsorption, high sensitivity was achieved. To further enhance the sensitivity and selectivity for ammonia detection, the ZSM-5 zeolite was modified through the ammonium ion exchange and the subsequent calcination to form acidic ZSM-5 (H-ZSM-5). The H-ZSM-5 coated LPFG is capable of quantifying ammonia concentrations in low ppm level without sample pre-concentration and rigorous control of operating conditions.

In this paper, the LPFG fabrication process, the zeolite thin film synthesis, the surface modification of zeolite thin films and the experiment setup will be presented in detail. The mechanism for the enhancement of sensitivity and selectivity will be discussed. The material characterization information, including SEM images, EDS spectrum, XRD spectrum and Raman spectrum will be provided.

8626-67, Session PWed

Effect of transition metal oxide anode interlayer in bulk heterojunction solar cells

Annie Ng, Xiang Liu, Aleksandra B. Djurić, The Univ. of Hong Kong (Hong Kong, China); Alan Man Ching Ng, South Univ. of Science and Technology of China (China); Wai Kin Chan, The Univ. of Hong Kong (Hong Kong, China)

Organic solar cells have been attracting increasing interests over the past decade because of their promising properties such as high mechanical flexibility, low cost and light weight. Glass/ITO/PEDOT:PSS/P3HT:PCBM/Al is the conventional device architecture for bulk heterojunction (BHJ) solar cells with the power conversion efficiencies (PCE) up to around 3-4%. However, for long term practical applications, it is necessary not only to be able to obtain outstanding PCE but also to improve the stability of the devices for commercialization. It was reported that PEDOT:PSS layer likely absorbs water due to its highly hygroscopic properties which results in device degradation. Therefore, replacement of PEDOT:PSS with metal oxides is one of the strategies to increase the device stability. In this work, we considered solution processing and/or vapor deposition methods for depositing metal oxides, such as tungsten oxide (WO₃), nickel oxide (NiO), vanadium oxide (V₂O₅, V₂O₃) and molybdenum oxide (MoO₃). We also examined the effect of different metal oxide layer on the P3HT:PCBM solar cell performance and the morphology of the metal oxide and polymer films was examined by SEM and/or AFM. The results are discussed in detail.

8626-68, Session PWed

Effect of sheet resistance, transmittance, and morphology of ITO electrode on polymer solar cells characteristics

Xiang Liu, Annie Ng, Aleksandra B. Djurić, The Univ. of Hong Kong (Hong Kong, China); Alan Man Ching Ng, South Univ. of Science and Technology of China (China); Wai Kin Chan, The Univ. of Hong Kong (Hong Kong, China)

As a promising power source, polymer solar cells continue attract most research interest due to their environmentally friendly processing, relatively low cost and highly flexible properties. In particular, the poly(3-hexylthiophene):[6,6]-phenyl-C61-butyric acid methyl ester (P3HT:PCBM) based bulk heterostructure has been the most studied system with the power conversion efficiency (PCE) typically around 3-4%. However, for a further application, increasing effort is being made to achieve a higher efficiency, such as introducing a light trapping structure, while in this case, the ability of depositing highly conductive and transparent ITO bottom electrode on the light trapping structure is a key issue to obtain the best performance of solar cells, which are critically process dependent. In this work, we fabricated the ITO electrode by radio frequency (RF) sputtering, and considered the effects of the deposition condition as substrate temperature, RF power, argon flow, and substrate rotation speed to achieve the lowest possible electrical resistivity and the optimized highest transparency in the visible range. Meanwhile, the sheet resistance, transmittance and the surface morphology of sputtered ITO were examined and the using of optimized deposition condition for ITO fabrication on glass and glass/Bragg Reflector substrates in P3HT:PCBM solar cells were detected. The results are discussed in detail.

8626-73, Session PWed

Mg and N doping of ZnO thin films grown by PLD

David J. Rogers, Nanovation (France)

No Abstract Available

8626-74, Session PWed

Optical, microstructural, vibrational, and theoretical studies of p-type SrCu₂O₂-based and BaCu₂O₂-based transparent conductive oxides and alloys

Jacky Even, L. Pedesseau, Olivier Durand, Institut National des Sciences Appliquées de Rennes (France); Mircea G. Modreanu, Tyndall National Institute (Ireland); Guido Huyberegts, FLAMAC (Belgium); B. Servet, Guy Garry, Thales Research & Technology (France); Odette Chaix-Pluchery, Institut National Polytechnique de Grenoble (France)

Transparent conducting metal oxides (TCO) are unusual semiconducting materials displaying transparency to visible light. TCO materials are used for electrostatic shielding, antistatic screens, transparent heating devices, solar cells and even organic light emitting diodes. However, most TCOs are n-type, while p-type TCOs are scarce. SrCu₂O₂ is a leading candidate as a p-type transparent conductive oxide. In this paper, we report theoretical calculations and experimental studies on the vibrational, optical and microstructural properties of both bulk and thin films of polycrystalline undoped SrCu₂O₂ obtained by pulsed laser deposition (PLD). Barium doping of the SrCu₂O₂ by substitution of Sr atoms is also reported. The simulated crystal structures of both SrCu₂O₂ (SCO) and BaCu₂O₂ (BCO) materials, obtained through a state-of-the-art implementation of the Density functional theory, are compared with

**Conference 8626:
Oxide-based Materials and Devices IV**

experimental X-ray diffraction data of undoped and Ba-doped SrCu₂O₂ bulk materials. Raman spectra of both SCO and BCO materials are simulated from the derivatives of the dielectric susceptibility and a symmetry analysis of the optical phonon eigenvectors at the Brillouin zone center is proposed. Good agreement with Raman scattering experimental results is demonstrated. Measurements of the optical bandgaps are reported from spectroscopic ellipsometry.

8627-1, Session 1

Ultrafast laser inscription: a new platform for photonic devices (*Invited Paper*)

Ajoy K. Kar, Heriot-Watt Univ. (United Kingdom)

A focussed ultrashort laser pulse can modify the local refractive index of certain materials, significant research has been expended into using ultrafast lasers to fabricate integrated optical devices. Integrated optical waveguides – the optical analogue of wires – can be simply fabricated by translating the sample in the path of such short optical pulse trains, which effectively amounts to fabricating the desired optical circuit in a controlled way in the linear and nonlinear optical materials. This direct-write approach offers several key benefits over conventional fabrication techniques. It neither requires use of expensive clean room facilities, nor involves complex film deposition and subsequent etching processes. This technology can also yield 3D structures, unachievable through any other technologies.

In my talk I will present how the ultrafast laser inscription technology can be used to develop components like switches, splitters/combiners, amplifiers and lasers. I will also describe how all-optical devices could be monolithically integrated into a substrate in the form of optical integrated circuits for unique biophotonic applications.

8627-2, Session 1

Optical spectrum control circuit with flat pass band characteristics using a high-resolution arrayed-waveguide grating

Tatsuhiko Ikeda, Keio Univ. (Japan); Takayuki Mizuno, Hiroshi Takahashi, NTT Photonics Labs. (Japan); Hiroyuki Tsuda, Keio Univ. (Japan)

Optical signal processing based on time-to-space conversion is very useful and can be applied to various functions in optical communication system. We designed and fabricated an arrayed-waveguide grating (AWG) type high-resolution optical spectrum control circuit using silica planer lightwave circuit (PLC) technology. Input optical signal is spectrally decomposed by the AWG and then each phase is controlled by the tunable phase shifters individually and again synthesized to the output signal with different waveforms. In order to obtain flat pass band characteristics that are required for optical signal processing, the number of channel waveguides in the circuit is set to be twice as many as the number of arrayed waveguide in the AWG. The spectral phase and amplitude of an optical signal can be arbitrarily controlled. Therefore, it works as a tunable band-pass filter or a tunable dispersion compensator.

The center frequency of the AWG is 193.35 THz. The free spectral range (FSR) is 150 GHz and the central 100-GHz bandwidth of the FSR can be controlled with 1.67-GHz resolution. The number of arrayed waveguides is 45, and the number of channel waveguides is 90. We obtained flat pass band characteristics with ripple of 2.5 dB or below with the fabricated device by controlling tunable phase shifters. We also obtained 25-dB extinction ratio, and the tunable band-pass filter function is confirmed.

8627-3, Session 1

Design and fabrication of EO polymer-clad one-dimensional silicon photonic crystal nanowire modulators

Shin-ichiro Inoue, Akira Otomo, National Institute of Information and Communications Technology (Japan)

Ultra-compact and fast silicon-based modulators with low drive voltage

are one of the most critical components for enabling high-speed optical interconnects of such on chip networks. The fast light modulation in silicon with free-carrier injection is intrinsically limited by the carrier lifetime, which allowed modulation up to around 30 GHz. On the other hand, an organic electro-optic (EO) polymer can provide much higher modulation speeds in excess 100 GHz, and EO coefficients that are much higher than that of lithium niobate (~30 pm/V). We have recently demonstrated a novel EO polymer with donor-modified phenyl vinylene thiophene vinylene bridge chromophores, exhibiting high EO coefficients ($r_{33} > 150$ pm/V), thus enabling EO operation with low drive voltage. Furthermore, EO polymers can be infiltrated into silicon nano-structure. This allows combining the highly EO characteristics of polymers with the high-index silicon nano-photonic devices fabricated in CMOS technology that have the potential to considerably cut costs for large-scale optoelectronic integration. In this study, for the first time, we demonstrated Mach-Zehnder EO modulators fabricated from one-dimensional (1D) silicon photonic crystal (PhC) nano-wires combined with our novel EO polymer exhibiting large electro-optic properties. The high index contrast of the combination of a silicon nano-wire with a surrounding cladding of EO polymer provides strong optical confinement and slow light properties, rivaling the best 2D-PhC while maintaining an ultra-compact device footprint. We reveal a direct relationship between the observed EO responses and the numerically designed slow light modulation properties in the EO polymer-clad 1D silicon PhC nano-wire modulators.

8627-4, Session 1

Single- and double-energy N⁺ - irradiated planar and channel waveguides in eulytine and sillenite type BGO crystals

István Bányász, Wigner Research Ctr. for Physics of the H.A.S. (Hungary); Stefano Pelli, Istituto di Fisica Applicata Nello Carrara (Italy); Zsolt Zolnai, Miklós Fried, Research Institute for Technical Physics and Materials Science (Hungary); Simone Berneschi, Enrico Fermi Ctr. for Study and Research (Italy) and Istituto di Fisica Applicata Nello Carrara (Italy); Tivadar Lohner, Research Institute for Technical Physics and Materials Science (Hungary); Gualtiero Nunzi Conti, Istituto di Fisica Applicata Nello Carrara (Italy); Giancarlo C. Righini, Enrico Fermi Ctr. for Study and Research (Italy) and Istituto di Fisica Applicata Nello Carrara (Italy)

Bismuth germanate is a well known scintillator material. It is also used in nonlinear optics, e.g. for building Pockels cells, and can also be used in the fabrication of photorefractive devices. Formation of planar waveguides in Bi₄Ge₃O₁₂ (eulytine) crystals by implantation of He⁺ ions of the 1 - 2 MeV energy range was reported by Mahdavi et al. [1]. Preliminary results in fabricating planar waveguides in both eulytine and sillenite (Bi₁₂GeO₂₀) type bismuth germanate crystals using MeV energy N⁺ ions were first reported by Bányász et al. [2]. Yang et al. formed planar waveguides in Bi₄Ge₃O₁₂ crystals via irradiation with 17 MeV C⁵⁺ and O⁵⁺ ions at relatively low fluences [3].

In the present work planar and channel optical waveguides were designed and fabricated in eulytine (Bi₄Ge₃O₁₂) and sillenite (Bi₁₂GeO₂₀) type bismuth germanate crystals using single- and double-energy irradiation with N⁺ ions in the 2.5 MeV < E < 3.5 range. Choice of irradiation energies and fluences were based on previous experiences in N⁺ ion beam fabrication of planar [4,5] and channel [6] waveguides in Er-doped tungsten-tellurite glass.

Planar waveguides were fabricated via scanning a 2 mm x 2 mm beam over the waveguide area. Channel waveguides were irradiated through a thick photoresist mask. Typical fluences were between 1 x 10¹⁵ and 2 x 10¹⁶ ions/cm².

Multi-wavelength m-line spectroscopy and spectroscopic ellipsometry

**Conference 8627:
Integrated Optics: Devices, Materials, and Technologies XVII**

were used for the characterisation of the ion beam irradiated waveguides. Waveguide structures obtained from the ellipsometric data via simulation were compared to N^+ ion distributions calculated using the Stopping and Range of Ions in Matter (SRIM) code.

M-lines could be detected up to a wavelength of 1310 nm in the planar waveguide fabricated in sillenite type BGO, and up to 1550 nm in those fabricated in eulytine type BGO. Post-irradiation thermal annealing was used to reduce propagation losses in the waveguides.

Functionality of the channel waveguides was checked by end-fire coupling.

- [1] S. M. Mahdavi, P. J. Chandler and P. D. Townsend, J. Phys. D: Appl. Phys., vol.22, p. 1354 (1989)
- [2] I. Bányász, et al., IOP Conf. Ser.: Mater. Sci. Eng., vol. 15 , p. 012027 (2010)
- [3] J. Yang, C. Zhang, F. Chen, Sh. Akhmedaliev, and Sh. Zhou, Appl. Optics, vol. 50, p. 6678 (2011)
- [4] S. Berneschi, et al., Optical Engineering, vol. 50, p. 071110 (2011)
- [5] I. Bányász, et al., IEEE Photonics Journal, vol. 4, p. 721 (2012)
- [6] S. Berneschi, et al., Applied Physics Letters, vol. 90, p. 121136,(2007)

8627-5, Session 2

Ultra-low power CMOS photonic interconnects (*Invited Paper*)

Ashok V. Krishnamoorthy, Oracle (United States)

We will motivate the need for photonic interconnects directly to CMOS computing and memory chips, present a vision for a photonically-interconnected macrochip, and review the progress in photonic component integration toward this vision.

8627-6, Session 2

III-V/silicon photonic integrated circuits for communication and sensing applications (*Invited Paper*)

Gunther Roelkens, Shahram Keyvaninia, Stevan Stankovic, Yannick De Koninck, Univ. Gent (Belgium); Martijn Tassaert, UGent (Belgium); Pauline Mechet, Univ. Gent (Belgium); Thijs Spuesens, UGent (Belgium); Nannicha Hattasan, Alban Gassenq, Univ. Gent (Belgium); Muhammad Muneeb, Eva Ryckeboer, UGent (Belgium); Samir Ghosh, Roel G. Baets, Dries Van Thourhout, Univ. Gent (Belgium)

Silicon-based photonic integrated circuits are gaining considerable importance for a variety of applications, from telecommunications to sensors. The interest in this technology stems mostly from the expectation that the maturity and low cost of CMOS-technology can be applied for advanced photonics products. Other driving forces for silicon photonics include the design richness associated with high refractive index contrast as well as the potential for integration of photonics with electronics. Building laser sources and other opto-electronic devices on integrated silicon circuits is a long-sought goal, on one hand in order to complete the functionality of the integrated circuit but on the other hand also as a manufacturing approach for opto-electronic devices on large wafers in CMOS-fabs. In terms of device performance the most successful approach to date is the heterogeneous III-V on silicon laser. In this device thin layers of III-V semiconductors are bonded to silicon. The laser cavity gets its gain from the III-V layers but couples its output light into a silicon waveguide. Often part of the cavity structure is implemented by means of patterning in silicon, thereby taking advantage of the resolution and accuracy of lithography tools in CMOS fabs. In that sense these III-V/silicon lasers take the best of two worlds.

Different types of integrated laser sources on a silicon platform will be

discussed, with a focus on emission at 1.3 μ m and 1.55 μ m. Besides communications, we will also elaborate on our first steps in the field of photonic integration for the short-wave and mid-infrared, for sensing applications.

8627-7, Session 2

Design and experimental characterization of an InP photonic integrated circuit working as a receiver for frequency-modulated direct-detection microwave photonic links

Javier S. Fandiño, Iñigo Artundo, Pascual Muñoz, Univ. Politècnica de València (Spain); José Capmany Franco, Univ. Politècnica de Valencia (Spain)

Thanks to its high bandwidth and low loss, microwave photonic links (MPL) have emerged as a promising technology for the transmission of analog microwave signals over long distances, such as in distributed wireless networks and military aircraft communications. However, the need for even higher overall system linearity has spurred much research on new system architectures beyond the traditional IM-DD scheme. Among them, Frequency Modulated - Direct Detection (FM-DD) MPLs show up as a cost-effective alternative, where the inherent inearity of phase modulators teams up with a simple detection scheme, which exploits the phase to intensity modulation effect in a properly designed optical filter. In this paper, the steps followed in the design of an InP photonic integrated circuit (PIC) working as a receiver for a FM-DD MPL are presented. The PIC consists of a thermally tunable, integrated, optical ARMA filter which acts as a frequency discriminator, along with an on-chip high-bandwidth balanced photodiode, and was manufactured using a generic InP technology platform under the EuroPIC EC FP7 project. Multiple SiN thermo-optic heaters allow for the fine tuning of the filter response, providing an effective way to compensate for manufacturing deviations. A complete experimental characterization of the optical filters is provided, including both amplitude and phase response, and the results are compared with the corresponding design values.

8627-8, Session 2

Low-voltage broadband electro-absorption from Ge/SiGe QWs on silicon

Elizabeth H. Edwards, Edward Fei, Theodore I. Kamins, James S. Harris, David A. B. Miller, Stanford Univ. (United States)

The adoption of Si photonics technology hinges on meeting power efficiency requirements, compatibility with integrated photonic platforms and, for compatibility with telecommunications, C band (1530-1565nm) wavelength operation. The design and epitaxial growth of Ge films on Si substrates is complicated by the large difference in lattice constant (4%) and thermal expansion coefficient. Here we show, using a new Ge/SiGe QW epitaxy design, that electroabsorption contrast greater than 5 dB (3dB) over a wavelength range of 1449 - 1580nm is possible with only 1V (0.4V) drive. The record thin form factor of this epitaxy expands the tool kit of Si-based photonic modulators, enabling thinner waveguides, microdisks, and photonic crystals.

8627-10, Session 3

Optofluidic fiber optic

Genni Testa, Gianluca Persichetti, Romeo Bernini, Consiglio Nazionale delle Ricerche (Italy)

We present an integrated tunable optofluidic liquid core-liquid cladding (L2) optical fiber. The device is based on a novel three-dimensional hydrodynamic focusing scheme that permits to obtain a tunable circular

liquid core located in the center of the channel regardless of the flow rate ratio of the cladding and core liquids. The hydrofocusing effect is achieved, in a very simple way, simultaneously in both directions in a single step by combining a central channel with two pairs of deeper channels orthogonally connected to it. This circular geometry permits a more simple control of the optical property of the beam and the input and output coupling with standard optical fiber. This is a very important for application where high quality beam M2 are required. The device consists of two-layers Polymethylmethacrylate (PMMA) microfluidic structures bonded together. The fluidic microchannels were fabricated by high precision micromilling of two 3mm-thick pieces of PMMA. Fluidic channels and groove for the optical fiber have been realized by utilizing $127 \pm 12.7 \mu\text{m}$ diameter milling tools. With these channel dimension, standard optical fiber for exciting the liquid fiber can be inserted into the channels, resulting in a self-aligned optical configuration where the core of the input fiber is centred with the core of the hydrodynamically induced liquid fiber. A liquid core with a tunable diameter ranging from 45.3 to $11.2 \mu\text{m}$ has been successfully obtained.

8627-11, Session 3

Low cross-talk glass integrated polarization splitter

Francois Parsy, Institut National Polytechnique de Grenoble (France) and IMEP-LAHC (France); Elise Ghibaudo, Univ. Joseph Fourier (France) and IMEP-LAHC (France); Damien Jamon, François Royer, Univ. Jean Monnet Saint-Etienne (France) and LT2C (France); Jean Emmanuel Broquin, Institut National Polytechnique de Grenoble (France) and IMEP-LAHC (France)

We propose and demonstrate a novel integrated polarization splitter realized by ion-exchange on glass. The design consists of an asymmetrical Y-junction exploiting shape birefringence and working at a wavelength of $1.55 \mu\text{m}$. The TM branch has low modal birefringence whereas the TE branch exhibits high birefringence and a TM cutoff wavelength below the working wavelength. This waveguide thus acts as a passive polarization filter based on radiation which drastically enhances the performances of the branch in terms of polarization extinction ratio. The final device is particularly suited as building block for integrated components needing high quality linear polarization and a reference arm such as optical isolators.

The fabrication process involves two photolithographic steps with one alignment, and two silver/sodium ion-exchange steps which require precise control of the temperature and exchange duration.

We measured the performances of the fabricated device on the $1.50 - 1.60 \mu\text{m}$ wavelength range by injecting linearly polarized light at an angle of 45° with the principal axes of the waveguide. The peak values were respectively -18.3 dB and -38.2 dB for the TE and TM cross-talks, and 36.3 dB and 20.2 dB for the TE and TM extinction ratios at a wavelength 1540 nm . Performances over 15 dB are obtained over a 15 nm bandwidth. We fully analyzed the losses of the device. Component losses of 5.6 dB were measured for both TE and TM modes respectively.

8627-12, Session 3

Numerical study on the reduction of bend losses in sharp bends by metallic layers

Mustafa Akin Sefunc, T. Dubbink, Markus Pollnau, Sonia M. García-Blanco, Univ. Twente (Netherlands)

Surface plasmon polaritons have drawn significant attention in recent years thanks to their capability of confining the electromagnetic field to the dielectric/metal interface. Furthermore, embodying metallic layers within an optical waveguide is advantageous for thermo-optical or electro-optical devices, such as modulators and switches. However, the high confinement comes at the cost of high propagation losses due to the highly absorptive nature of metals at visible and near-IR wavelengths.

In order for plasmonic waveguides to find a widespread use in integrated optics, an advantage over dielectric waveguides needs to be found that justifies their utilization.

In this work, we show that plasmonic waveguides allow for sharper bends than their dielectric counterparts, resulting in 90° bends with smaller loss. By adding a thin metallic layer underneath the waveguide core, the calculated bend losses ($\text{dB}/90^\circ$) are reduced with respect to the bend losses of the equivalent dielectric structure without the metallic layer for a range of radii from $50 \mu\text{m}$ to $1 \mu\text{m}$. More than 2-fold reduction of bend losses is observed in TE-polarization with a more modest decrease for TM-modes. The mechanism for the reduction of bend losses is different for each polarization. For TM-modes it can be explained by the higher confinement of the mode to the metal layer. For TE-modes the metal layer is believed to act as shield preventing the field to leak into the substrate. A physical model permitting full understanding of these effects as well as the fabrication of the devices is currently under way.

8627-13, Session 3

Filters of radial polarization formed by periodically focusing microsphere-chain waveguides

Arash Darafsheh, The Univ. of North Carolina at Charlotte (United States); Anatole Lupu, Institut d'Électronique Fondamentale (France); Vasily N. Astratov, The Univ. of North Carolina at Charlotte (United States)

We show that microsphere-chain waveguides have strongly polarization-dependent attenuation properties that can be used for developing efficient filters of radial polarization. We show that along with a special case of periodically focused modes (PFMs) with TM polarization in chains of spheres with index $n = \sqrt{3}$ which propagates in such structures without losses, similar periodic modes exist in a broad range of indices from 1.4 to 2.0 . For each n such generalized PFMs have various radial extents in the regions between the neighbouring focused beams. We study polarization-transmission properties of such modes and demonstrate that for 10-sphere long chains with $n = 1.68 - 1.80$ they have total propagation losses smaller than 1 dB . Using light sources with different directional properties we show that chains of spheres can be used as efficient polarization components with additional focusing capability.

8627-14, Session 4

Integrated InP based mode-locked lasers and pulse shapers (*Invited Paper*)

Erwin A. Bente, Saeed Tahvili, Valentina Moskalenko, Sylwester Latkowski, Technische Univ. Eindhoven (Netherlands); Mike J. Wale, Technische Univ. Eindhoven (Netherlands) and Oclaro Technology Plc (United Kingdom); Pascal Landais, Dublin City Univ. (Ireland); Julien Javaloyes, Univ. de les Illes Balears (Spain); Meint K. Smit, Technische Univ. Eindhoven (Netherlands)

In this paper we will present recent results obtained in the area of monolithically integrated modelocked semiconductor laser systems using generic InP based integration platform technology operating around 1550 nm . Standardised components defined in this technology platform can be used to design realise short pulse lasers and optical pulse shapers. This makes that the devices can be realised on wafers that contain many other devices. In the area of short pulse laser we will report on work done on designs studies based on measured optical amplifier and saturable absorber performance data. This work has the goal to establish a library of widely applicable laser designs. These include components for e.g. wavelength control. An important boundary condition is that the laser can be located anywhere on the InP chip. In the area of pulse shaping we report on a 20 channel monolithic pulse shaper capable of phase and amplitude control in each channel. Special

**Conference 8627:
Integrated Optics: Devices, Materials, and Technologies XVII**

attention is given to the calibration of the phase modulator and amplifier settings. Pulse compression and manipulation of pulse from modelocked semiconductor lasers is demonstrated using a 40 GHz quantum dash modelocked laser.

8627-15, Session 4

Integrated pulsed lasers realization for LIDAR applications

Hana Ouslimani, Lionel Bastard, Jean Emmanuel Broquin, IMEP-LAHC (France)

High power Q-switched Ytterbium lasers with nanoseconds pulse durations offer applications in various areas such as in industrial manufacturing, nonlinear optics or optical sensors like LIDAR systems. This latest application employs either pulsed laser sources for time of flight measurement, or continuous laser sources with a narrow linewidth for Doppler measurement.

To achieve Doppler measurements with high peak power, we propose to develop a laser source with a narrow linewidth, operating in pulse regime. Moreover, this kind of Doppler velocimeter could be used in aircraft. To endure in this environment, the device should be insensitive to vibrations. This leads to foster integrated technologies. The challenge is then to integrate on the same device a saturable absorber as passive modulator and a Bragg grating for narrow linewidth.

In this paper, a fully integrated passively Q-switched DFB laser made in glass integrated optics technology is designed, realized and investigated.

The laser, operating at a 1030 nm wavelength, is formed by an ion-exchanged single mode waveguide realized in an Ytterbium doped phosphate glass. The feedback is provided by a DFB structure: Bragg grating with a 340 nm periodicity is realized by photolithography and dry etching on the glass surface. The Q-switched behavior is obtained by hybridizing the saturable absorber on the waveguides so that it interacts with the evanescent part of the guided field. The saturable absorber we use is a bis(4-dimethylaminodithiobenzil)nickel (BDN) dye incorporated in a polymeric film.

8627-16, Session 4

An AWG-based multi-wavelength laser grown by MOCVD

Xilin Zhang, Chen Ji, Ruikang Zhang, Dan Lu, Baojun Wang, Lingjuan Zhao, Hongliang Zhu, Wei Wang, Institute of Semiconductors (China)

Multi-wavelength lasers?MWLs?play an important role in instrument testing, sensing, and wavelength division multiplexing (WDM) networks. In this paper we present a monolithically integrated multi-wavelength laser grown on indium phosphide (InP). The device consists of an arrayed waveguide grating(AWG) with an array of semiconductor optical amplifiers (SOAs) connected to its demultiplexed ports and a common output waveguide connected to its multiplexed port. Reflections at the common output facet and at the individual waveguide facets from the SOAs form the extended laser cavities. These components have been fabricated on a single chip using an active/passive integration technology in InP. In this case, the multiplexer is used as an inter-cavity wavelength filter that sets the operating wavelengths of a Fabry-Perot laser. The multiplexer spatially separates the different wavelengths such that they can be individually controlled by current injection in the appropriate optical amplifier, while at the same time all the wavelengths are available in a single output waveguide. An important advantage of such phased array MWLs is that, the mutual wavelength spacing of the channels is still accurate even if the central wavelength of the AWG is not at the design wavelength due to fabrication errors or wafer inhomogeneities. Our devices generate wavelengths around 1.55 μm with a side mode suppression ratio of over 20dB in all eight channels. The channel spacing is 1.4-1.6 nm, which is close to our design (1.6nm).

8627-17, Session 4

Analysis of the light coupling between nano-waveguides made of tellurite glasses

Jhonattan Córdoba Ramírez, Hugo Enrique Hernandez Figueroa, Univ. Estadual de Campinas (Brazil); Ferney O. Amaya, Univ. Pontificia Bolivariana (Colombia); Jorge D. Marconi, UFABC (Brazil); Hugo L. Fragnito, Univ. Estadual de Campinas (Brazil)

This paper presents a study (simulations) of coupling losses between adjacent waveguides made of tellurite glasses. These waveguides are designed to perform parametric amplifiers (PAs).

PAs have some advantageous characteristics over the other optical amplifiers: they have broadband amplification bandwidth (depending on the dispersive characteristics of the waveguide), other all-optical functionalities, and can work at ultra-high bit rates (Pbit/s). PAs are based on the nonlinear phenomena of phase matched four-wave mixing between a strong pump and a weak signal.

The parametric gain increases with the waveguide length, the pump power and the nonlinear coefficient of the waveguide. The best alternative to maximize the parametric gain is to reduce the pump power as much as possible, increasing the waveguide length and/or the nonlinear coefficient of the waveguide. The latter parameter can be enhanced by increasing the nonlinear refractive index of the material (n_2) or by reducing the waveguide effective area.

Here we perform waveguides made of tellurite because these glasses have an n_2 that goes up to $30 \times 10^{-19} \text{ m}^2/\text{W}$. On the other hand, the waveguide length can be increased by using an Archimedean spiral design. This geometry allows obtaining long waveguides (~1 m) within a small area.

Using the Finite Element Method we study the separation distance between adjacent waveguides in order to obtain coupling lengths higher than the waveguide length (total losses $< 2\text{dB/m}$).

The waveguide dimensions are optimized to obtain a monomode waveguide (in our case a TE mode), and with dispersive characteristics to perform PAs (around ~1550 nm).

8627-18, Session 5

Spectroscopy-on-chip applications of silicon photonics (Invited Paper)

Roel G Baets, Ananth Subramanian, Ashim Dhakal, Shankar K. Selvaraja, Katarzyna Komorowska, Frederic Peyskens, Eva Ryckeboer, Nebiyu A. Yebo, Gunther Roelkens, Nicolas Le Thomas, Univ. Gent (Belgium)

In recent years silicon photonics has become a mature technology enabling the integration of a variety of optical and optoelectronic functions by means of advanced CMOS technology. While most efforts in this field have gone to telecom and datacom/interconnect applications, there is a rapidly growing interest in using the same technology for sensing applications, ranging from refractive index sensing to spectroscopic sensing. In this paper the prospect of silicon photonics for absorption, fluorescence and Raman spectroscopy on a chip will be discussed. To allow spectroscopy in the visible and near infrared the silicon photonics platform is extended with siliciconitride waveguides.

8627-19, Session 5

Glass integrated optic Fourier transform spectrometer in the spectral bandwidth 700-1000nm: process improvement

Amélie Creux, Alain Morand, Pierre Benech, IMEP-LAHC (France); Bruno Martin, Resolution Spectra Systems (France); Gregory Grosa, IMEP-LAHC (France); Cédric Cassagnettes, Denis Barbier, Teem Photonics S.A. (France); Etienne P. Le Coarer, Institut de Planétologie et d'Astrophysique de Grenoble (France)

Today spectrometers are used to analyse optical light emitted, reflected or scattered. To decrease their cost, compact spectrometers are now developed. A compact Fourier Transform spectrometer based on a leaky loop (LLIFTS) was already developed in the near infrared domain. It is realized in integrated optics with only one lithography step and without moveable parts. The principle of the LLIFTS is related to the two beam interferometer principle. The light radiated along the bend waveguide is coupled in a planar waveguide to confine vertically the optical field. The overlap of the two beams, due to each arm of the bend, creates an interference pattern at the end of the component, measured directly on a linear camera. An inverse Fourier Transform provides the optical spectrum. The shape and the contrast of the interference pattern are controlled by the evolution of the gap, the distance between the bend and the planar waveguide.

To extend the applications of this component in the metrology domain for example, a development of the LLIFTS was demonstrated in the visible domain. The fabrication process of the component for the visible domain was improved to obtain an interferogram well contrasted from 780 to 850nm. Moreover measurements will be shown to clearly observe the behaviour of the leaky loop depending on the wavelength, the radius of the bend and the gap.

8627-20, Session 5

Multiplexed selective detection and identification of TCE and xylene in water by on-chip absorption spectroscopy

Wei-Cheng Lai, The Univ. of Texas at Austin (United States); Swapnajit Chakravarty, Omega Optics, Inc. (United States); Yi Zou, Ray T. Chen, The Univ. of Texas at Austin (United States)

We demonstrate an on-chip photonic crystal (PC) device for selective detection and identification of xylene and TCE in water by near-infrared absorption spectroscopy. The device consists of a 1x4 multimode interference (MMI) power splitter with PC slot waveguides on each arm. Light guided by the PC waveguide (PCW) propagates with low group velocity at wavelengths near the guided mode transmission band edge. In addition, electric field intensity of the propagating mode is confined and enhanced by the narrow low index slot at the center of the PCW. The combined effect leads to enhanced optical interaction with analytes that infiltrate the slot. Devices are coated with hydrophobic poly-dimethyl-siloxane (PDMS) which extracts volatile organic compounds (VOCs) from water by solid phase micro-extraction. PDMS fills the etched holes of the PC pattern and the slot at the center of the PCW. Transmission spectrum of the PC slot waveguide on each arm is measured in the presence and absence of VOC in water. VOC absorbance is determined from the difference in transmission. We successfully detected 100ppb xylene in water with a 300 microns long silicon PC slot waveguide by near-infrared absorption signatures. Xylene and TCE have distinct absorbance peaks at 1674nm and 1646nm respectively. Both xylene and TCE have absorbance minima at 1632nm. PC slot waveguides on each arm are designed so that light propagates with high group index at above wavelengths. Selectivity is achieved by measuring absorbance at known wavelengths above. Experimental results will be presented.

8627-21, Session 5

Integrated slot waveguide sensor on glass for chemical analysis in a hostile environment

Elsa Jardinier, Davide Bucci, Jean Emmanuel Broquin, IMEP-LAHC (France); Laurent Couston, Fabrice Canto, Alastair Magnaldo, Commissariat à l'Énergie Atomique (France)

The current will of reducing environment hazards and increasing people safety in the context of nuclear waste reprocessing has led the nuclear industry to develop miniaturized techniques for analysis. Miniaturization will not only reduce effluent volumes and response times but will also allow on-line measurements and eventually reduce costs.

Absorption spectroscopy is a tool of choice for the measure of traces concentrations (below 10⁻⁵ M). However, when decreasing the dimensions, the sensitivity is decreased as well and one needs to maximize both the light confinement inside the fluid and the fluid/light interaction length.

In this context, we present a new integrated optical sensor based on a glass slot waveguide structure, for absorption spectroscopy in a hostile environment. Made of borosilicate glass, it is indeed particularly suited for working with acid and nuclearized solutions.

The slot waveguide is made by bonding two ion-exchanged glass wafers, one of them being etched by reactive ion etching to make a 100 nm-deep fluidic channel. Simulation results by beam propagation methods showed that typical confinement factors higher than 2 % could be achieved inside the fluid over a 500nm bandwidth; surmounting evanescent wave performances in terms of confinement efficiency and independence over the chemical surroundings, and suggesting that relevant absorption spectra could be plotted.

Concentration measurements and absorption spectra of neodymium in nitric acid are being performed. An improved sensor including low bending-loss spiral-like waveguides, increasing the fluid/light interaction length and hence the absorption sensitivity is under study.

8627-22, Session 5

Sensing explosives with suspended core fibers: identification and quantification using Raman spectroscopy

Georgios Tsiminis, The Univ. of Adelaide (Australia); Fenghong Chu, Shanghai Univ. of Electric Power (China); Nigel A. Spooner, The Univ. of Adelaide (Australia) and Defence Science & Technology Organisation (Australia); Tanya M. Monro, The Univ. of Adelaide (Australia)

This works demonstrates the use of suspended core optical fibers as a platform for explosives detection using Raman spectroscopy. This is, to the best of our knowledge, the first use of an in-fibre detection scheme based on Raman. This architecture combines small sampling volumes with long light-analyte interaction lengths, resulting in identification of minute quantities of explosives in solutions. In addition, the Raman signature of the solvent is used as an internal calibration standard to allow quantification of the detected molecule. Our results show detection of sub-microgram amounts of hydrogen peroxide (H₂O₂) in aqueous solution, a molecule difficult to detect as it lacks the nitroaromatic units, characteristic of trinitrotoluene (TNT) based explosives, which are usually targeted by traditional optical methods such as fluorescence. The same platform without any modifications can also be used to identify and quantify comparable amounts of 1,4-dinitrobenzene (DNB), a substitute molecule for TNT. These results highlight the capability of suspended-core fibers as small, cost-efficient and low-volume explosives sensors and their potential for use in the field. Furthermore, this flexible platform can be used for additional sensing schemes such as fluorescence detection, resulting in enhanced explosives detection photonic systems.

8627-23, Session 6

On-chip whispering-gallery-mode microlasers and their applications for nanoparticle sensing (*Invited Paper*)

Sahin Kaya K. Özdemir, Lina He, Jiangang Zhu, Obi Kenechukwu, Faraz Monifi, Woosung Kim, Lan Yang, Washington Univ. in St. Louis (United States)

Whispering-Gallery-Mode (WGM) resonators are emerging as an excellent platform to study optical phenomena resulting from enhanced light-matter interactions due to their superior capability to confined photons. The monolithic fabrication process to achieve ultra-high-Q WGM resonators without the need to align multiple optical components as requested in traditional design of resonators based on precise arrangement of mirror is especially attractive. Here we explain how to process a layer of thin film doped with optical gain medium, which is prepared by wet chemical synthesis, into WGM structures on silicon wafer to achieve arrays of ultra-low threshold on-chip microlasers. We can adjust the dopant species and concentration easily by tailoring the chemical compositions in the precursor solution. Lasing in different spectral windows from visible to infrared was observed in the experiments. In particular, we investigated nanoparticle sensing applications of the on-chip WGM microlasers by taking advantages of the narrow linewidth of lasing mode and mode-splitting phenomena arising from interactions of nano-scale objects with high-quality WGMs. It has been found out that a nanoparticle could split a lasing mode in WGM resonator; subsequently a beatnote can be generated by photomixing the two split lasing modes in a photoreceiver, which, in turn, can be used as a signal to detect the nanoparticle. We have demonstrated detection of virions, dielectric and metallic nanoparticles by monitoring the changes in self-heterodyning beatnote of the split lasing modes. The built-in self-heterodyne interferometric method achieved in the monolithic microlaser provides an ultra-sensitive self-referencing sensing scheme.

8627-24, Session 6

Controlling the mode volume in high-Q microcavities with high-refractive index coatings

Ashley J. Maker, Brian A. Rose, Andrea M. Armani, The Univ. of Southern California (United States)

Developing optical resonators with high quality factors, small mode volumes, and high refractive index contrast is important for many integrated optics and communications applications. High quality factors and small mode volumes are especially desirable to maximize the circulating intensity and Purcell factor for laser applications. However, controlling an optical resonator's mode volume and refractive index contrast can be difficult as they depend primarily on the inherent material properties of the resonator. One approach to reduce mode volume and control refractive index contrast is to apply high refractive index polymer coatings. However, polymer coatings are not compatible with all fabrication processes and not as robust as silica and silicon.

Recently, we developed and characterized high refractive index silica films containing small amounts of titanium dopant. The silica films are fabricated using a sol gel method with methyl triethoxysilane (MTES) and tetraethyl orthosilicate (TEOS) precursors. Depending on the amount of titanium added, the refractive index of the resulting film can be tuned from 1.44 to 1.62, as measured by spectroscopic ellipsometry. By spin coating these high index silica films onto silica toroid resonators, we experimentally and numerically obtain a significant reduction in mode volume while maintaining high quality factors. Additionally, the presence of the high refractive index coating allows tuning of the circulating light's position, shape, and interaction with the coating. Therefore, these high refractive index films offer a useful and more robust method to optimize the properties of optical devices for communications and integrated optics applications.

8627-26, Session 6

Ge/SiGe quantum well resonator modulators

Elizabeth H. Edwards, Ross M. Audet, Edward Fei, Gary Shambat, Stanford Univ. (United States); Rebecca K. Schaevitz, Corning West Technology Ctr. (United States); Theodore I. Kamins, James S. Harris, David A. B. Miller, Stanford Univ. (United States)

The strong electroabsorption modulation possible in Ge/SiGe quantum wells promises efficient, CMOS-compatible integrated optical modulators. We demonstrate surface-normal asymmetric Fabry-Perot and microdisk resonator modulators employing Ge quantum wells grown on silicon. We have experimentally measured modulation contrast of 4.8 dB over a 1V swing with 2V bias for the surface normal device and modulation speeds >3GHz. Thin epitaxy was developed for microdisk modulators. The microdisks were tested at AC and DC using a fiber-probe measurement technique.

8627-36, Session 6

wavelength-dependent vertical integration of nanoplasmonic circuits utilizing coupled ring resonators

Michael P Nielsen, Abdulhakem Y. Elezzabi, Univ. of Alberta (Canada)

To become a competitor to replace CMOS-electronics for next-generation data processing, signal routing, and computing, nanoplasmonic circuits will require an analogue to electrical vias in order to enable vertical connections between device layers. Vertically stacked nanoplasmonic nanoring resonators formed of Ag/Si/Ag gap plasmon waveguides were studied as a novel 3-D coupling scheme that could be monolithically integrated on a silicon platform. The vertically coupled ring resonators were evanescently coupled to 100 nm x 100 nm Ag/Si/Ag input and output waveguides and the whole device was submerged in silicon dioxide. 3-D finite difference time domain simulations were used to examine the transmission spectra of the coupling device with varying device sizes and orientations. By having the signal coupling occur over multiple trips around the resonator, coupling efficiencies as high as 39% at telecommunication wavelengths between adjacent layers were present with planar device areas of only 1.00 μm^2 . As the vertical signal transfer was based on coupled ring resonators, the signal transfer was inherently wavelength dependent. Changing the device size by varying the radii of the nanorings allowed for tailoring the coupled frequency spectra. The plasmonic resonator based coupling scheme was found to have quality (Q) factors of upwards of 30 at telecommunication wavelengths. By allowing different device layers to operate on different wavelengths, this coupling scheme could lead to parallel processing in stacked independent device layers.

8627-27, Session 7

Mapping nanoscale chemical and optoelectronic properties by multidimensional plasmonics-based nanospectroscopic imaging

Jim Schuck, The Molecular Foundry (United States)

An ongoing challenge to understanding matter at the nanoscale is the difficulty in carrying out local optical spectroscopy. On a fundamental level, this should be possible by squeezing light beyond the diffraction limit. Optical-antenna-based geometries have been designed to address this 'nanospectroscopy imaging' problem by transforming light from the far-field to the near-field, but unfortunately with serious limitations on sensitivity, bandwidth, resolution, and/or sample types. Here we discuss a plasmonics strategy that overcomes these limitations based on a device geometry capable of efficiently coupling far-field light to the near-field and vice-versa without background illumination, and more significantly, doing so over a wide range of wavelengths. This structure enables the expansion of nano- and nonlinear-optics beyond their current niche roles in nanoscience. Here, ~40 nm resolution hyperspectral imaging of InP nanowires is performed via excitation and collection through the scan-probes based on this device, revealing optoelectronic structure along individual indium phosphide nanowires that is not accessible with other existing methods. We map the influence of local trap states within individual nanowires on carrier recombination rates and energies with resolution well below the diffraction limit, i.e. at the length scales relevant to critical processes in nanomaterials. I will finish by discussing the integration of luminescent upconverting nanoparticles (UCNPs) into plasmonic systems as a way of both probing fundamental plasmonic properties and enhancing UCNPs performance.

8627-28, Session 7

Tilted Bragg grating-based optical components within an integrated planar platform

Helen L. Rogers, Christopher H. Holmes, Keith R. Daly, Lewis G. Carpenter, James C. Gates, Giampaolo D'Alessandro, Peter G. R. Smith, Univ. of Southampton (United Kingdom)

Tilted Bragg gratings (TBGs) within fibers have been extensively investigated and demonstrate a wide range of practical applications, including devices for sensing and the excitation of surface plasmons. Previously, by exploiting a planar geometry, we have fabricated gratings for the excitation of surface plasmons in gold, via an integrated waveguide based TBG.

TBGs can also act as effective polarizers in fibre, with greater than 30 dB polarization dependent extinction, through coupling one of the linearly polarized core modes into the cladding modes. We demonstrate the fabrication of TBGs in a planar platform, allowing integrated functionality to be combined with these versatile components.

A direct grating writing method allows inscription of waveguides and Bragg gratings into a planar silica-on-silicon platform. A pair of interfering focused UV beams allow Bragg grating planes to be defined at a focal spot which is translated within a photosensitive glass core layer. Translation of the sample at an angle allows grating planes to be defined with tilt relative to the core guiding direction.

The gratings allow controlled coupling between the forward-propagating core mode, the backward-propagating core mode and the cladding modes. We have achieved TBGs which couple better than -20 dB from the forward propagating core mode into other modes, even for angles as small as 5°.

We will present recent results and modelling of the coupling of tilted Bragg gratings as a function of angle and period within our silica-on-silicon substrate. This allows investigation of TBG applications within an integrated platform.

8627-29, Session 7

Phase modulated direct UV grating writing technique for ultrawide spectrum planar Bragg grating fabrication

Chaotan Sima, James C. Gates, Helen L. Rogers, Paolo L. Mennea, Christopher H. Holmes, Mikhail N. Zervas, Peter G. R. Smith, Univ. of Southampton (United Kingdom)

Direct UV Grating Writing (DGW) is an attractive technique for simultaneously fabricating integrated Bragg grating devices in a silica-on-silicon platform, yielding losses as low as 0.03dB/cm. Previously, an Acousto-Optical Modulator has been used for writing planar Bragg gratings; in this new work we demonstrate a new phase modulation fabrication technique that offers improved performance.

We report a novel phase control DGW method using an Electro-Optical Modulator for planar Bragg grating fabrication. We phase modulate one laser beam in a focusing interferometer as a photosensitive silica-on-silicon sample is translated under the spot to give a moving fringe pattern that allows high quality Bragg gratings and waveguides to be fabricated in a single step. This new approach has allowed us to achieve a 1mm long uniform Bragg grating with ~70% reflectivity and a 1.4nm 3dB bandwidth; while a 3mm long grating has 100% top flat reflectivity and a 1.22nm 3dB reflection bandwidth – refractive index changes of up to 0.001 can be achieved. Since there is neither laser power reduction nor writing speed variation, the method offers significantly faster writing speeds. The simplified optical layout offers greater laser power on sample and furthermore the design coding is simplified. By applying Gaussian apodisation to the grating design we can achieve sidelobe suppression of >15dB. Using grating detuning and this new phase control method we have shown that Bragg gratings can be written from 1200nm to 1900nm on a single chip under software control and with less than 3dB variation across a 250nm bandwidth.

8627-30, Session 7

Nanoscale and multifunctional Bragg-grating structures for photonic applications

Aju S. Jugessur, The Univ. of Iowa (United States)

The applications of Bragg-grating concepts in a multitude of photonic device functionalities are well established [1, 2], in particular, in the design of planar and chip-based miniature device components for dense photonic integrated circuits. In many situations, the Bragg-grating structures are designed to act as a broad or narrow band-pass filter [3] or as a multichannel coupled defects filter [4], optical waveguide and also, as an integrated microfluidic optical sensor [5, 6]. In addition, Bragg-grating concepts are very useful in tailoring the filter response of optical filters [7]. In this work, Bragg-grating concepts are applied in several different scenarios with applications ranging from Bragg optical sensors and Bragg-slot waveguide to one-dimensional photonic crystal microcavities. In addition, Bragg-grating structures integrated with slot waveguide [8] with and without a microcavity are shown to be very promising candidates for label-free optical sensing applications with sensitivity as high as 500nm/RIU. The Bragg-grating structures are designed using 2D/3D Finite Domain Time Difference modeling and fabricated using Electron beam lithography and reactive ion etching on silicon on insulator material. Figures (1) to (3) show the micrographs of the fabricated devices that are designed to function as a Bragg-slot optical waveguide, Bragg-grating waveguide and Bragg microcavity optical filter, respectively. This work demonstrates the versatility of Bragg-grating structures for multiple device functionalities through design for a wide range of devices applications in several scientific and technological areas.

[1] Michael J. Strain and M. Sorel, IEEE J. Quantum Electronics, Vol 46, 774-782, 2010

[2] R. Zengerle and O. Leminger, J. Lightwave Technol. 13, 2354-2358, 1995

**Conference 8627:
Integrated Optics: Devices, Materials, and Technologies XVII**

- [3] A. S. Jugessur, P. Pottier and R. M. De La Rue, Electronics Letters, 39, 367-369, 2003
- [4] H. T. Hsu, M. H. Lee, T. J. Yang, Y. C. Wang and C. J. Wu, Progress in Electromagnetic Research, Vol. 117, 379-392, 2011
- [5] W. C. L. Hopman, P. Pottier, D. Yudistira, J. V. Lith, P. V. Lambeck, R. M. De La Rue, A. Driessen, H. J. W. M. Hoekstra, Select. Topics in Quant. Electron. 11, 11-16, 2005
- [6] A. S. Jugessur, J. Dou, J. S. Aitchison, R. M. De La Rue and M. Gnan, Microelectron. Eng., 86, 1488-1490, 2009
- [7] A. S. Jugessur, P. Pottier and R. M. Delarue, Optics Express, Vol. 12, 1304-1312 2004
- [8] C. A. Barrios, Sensor 9, 4751-4765, 2009

8627-31, Session 7

A transpose optical interconnect utilising metamaterial Luneburg waveguide lenses for switch fabric on-a-chip applications

Hamdam Nikkhah, Trevor J. Hall, Univ. of Ottawa (Canada)

Recently there have been a number of demonstrations of transparent optical switch elements on a silicon photonics integration platform. Published implementations are restricted to modest port counts but simulations provide confidence that dimensions up to 1x64 is feasible. It is timely thereby to consider large dimension switch fabrics for these switch elements. A major challenge is the large number of crossovers which introduce insertion loss and crosstalk. This challenge has been addressed by some innovative free-space optical interconnection architectures but free-space implementations suffer from stringent alignment tolerances. Given the loss of one dimension, planar implementations of similar architectures do not scale as well. Nevertheless, a switch fabric on a chip merits serious consideration given the nano-scale features and precision of contemporary fabrication procedures.

A simulation study of a waveguide-lens based approach to planar switch fabrics is reported. An optical transpose interconnection architecture utilising micro-lenses in free-space is first described and its principles of operation explained in terms of transformations of optical phase-space. This system is shown to almost meet the fundamental minimum volume required for an optical interconnection and is capable of near zero insertion loss and crosstalk. The architecture is mapped to a planar implementation by the substitution of propagation in a slab-waveguide for free-space propagation and Luneburg lenses for the micro-lenses. Results show the careful approximation of the graded index of the Luneburg lens by a metamaterial introduces minimal additional crosstalk. Advantageously, the patterning of the metamaterial region within the slab-waveguide requires only a single etch step.

8627-25, Session PWed

Fabrication of transparent and flexible all-polymer microring resonators and its application to ultrasound imaging

Kyu-Tae Lee, Tao Ling, Hyung Won Baac, Young Jae Shin, L. Jay Guo, Univ. of Michigan (United States)

Microring resonators have been implemented in a variety of fields ranging from optical filters and lasers to chemical and biological sensors. Polymer microring resonators have been studied extensively for ultrasonic and biochemical sensing applications in the past. One of the significant issues still to be addressed is the temperature stability, especially when higher power is coupled into the microring. In order to compensate the thermal effect, polymer microring resonators should be fabricated on a polymer substrate. This approach can also produce transparent polymer microring resonators, which can enable all-optical ultrasound transducers. In this work, a transparent and flexible all-polymer microring resonator fabricated by a nanoimprint technique is demonstrated. A polymer microring resonator is fabricated on a silicon substrate coated with a water soluble polymer used as a release layer between the silicon substrate and the polymer waveguide. Dissolving the release layer allows the polymer microring to be separated from the silicon wafer, resulting in a transparent and flexible polymer microring resonator. The fabrication and application of such transparent microring device for ultrasound imaging will be presented at the conference.

8627-42, Session PWed

AWG-parameters: A new software tool to design arrayed waveguide gratings

Dana Seyringer, Fachhochschule Vorarlberg (Austria)

A new software tool and its application in the design of optical multiplexers/demultiplexers based on arrayed waveguide gratings (AWG) is presented. The motivation for this work is the fact that when designing AWGs a set of geometrical parameters must be first calculated from input design parameters as:

- 1) Technological parameters: refractive indices of the core/cladding (n_{eff} , n_{out}) and waveguide size (w).
- 2) AWG type parameters: number of output waveguides - channels (Num), channel spacing (df) and AWG centre wavelength, λ_{bda} .
- 3) Transmission parameters: any AWG is designed to achieve expected transmission parameters like adjacent/non-adjacent channel crosstalk (Cr , $CRaW$) or channel uniformity (Lu). These parameters define the performance of AWG and also determine its suitability for a particular application.

From these parameters the AWG geometrical parameters like length of the couplers (L_f), minimum waveguide separation between input/output waveguides (dx) and between arrayed waveguides (dd) have to be calculated. These parameters are responsible for correct AWG demultiplexing properties and therefore have to be calculated very carefully. They create the input for AWG layout that will be then simulated using commercial photonics design tools. It is important to point out that there is a strong relation between geometrical and input design parameters, particularly transmission parameters. However, most of the commercial photonics design tools do not support this fundamental calculation.

The tool was already applied in various AWG designs (including very high DWDM AWGs) and also technologically verified. We will show that simulated and measured transmission characteristics feature very good agreement.

**Conference 8627:
Integrated Optics: Devices, Materials, and Technologies XVII**

8627-43, Session PWed

Finite-element analysis of tapered segmented waveguides

Ruth E. Rubio, Hugo Enrique Hernandez Figueroa, Univ. Estadual de Campinas (Brazil)

We present the results of the theoretical study and two dimensional frequency domain finite-element simulation of tapered segmented waveguides. The application that we propose for this device is that of the mode filter, to eliminate higher order modes that can be propagated in a multimode semiconductor waveguide. We demonstrate that by reducing the taper functions for the design of a segmented waveguide we can filter higher order modes at pump wavelength in WDM systems and at the same time low coupling losses between the continuous waveguide and the segmented waveguide. We obtained the cutoff wavelength as a function of the duty cycle of the segmented waveguide to show that we can in fact guide the fundamental mode.

On a silicon on insulator platform (using silica and SU-8) at pump wavelength of 820nm we have 4 guided modes. By reducing the duty cycle to 0.6 the segmented waveguide cannot guide the higher order mode but only the fundamental mode.

For the two-dimensional Finite-element method analysis a new Comsol Multiphysics module is proposed. Its contribution is the inclusion of the anisotropic perfectly matched layer that is more suitable for solving periodic segmented structures and other discontinuity problems and also the Magnetic Field formulation.

8627-44, Session PWed

Calculation of defect modes in index contrast of Al_xGa_{1-x}As waveguides

Latef M. Ali, Farah A. Abed, Erbil Technical Institute (Iraq)

In this paper we used a theoretical and numerical investigation model to calculate the defect modes, penetration depth and effective indices for Al_xGa_{1-x}As planar optical waveguides at a wavelength of 1550 nm. Newton-Raphson method was used to find the radiation modes and its wavenumber. It was found that the change in the refractive index of Al_xGa_{1-x}As optical waveguide is responsible of scattering effects and radiation towards the substrate.

8627-45, Session PWed

Integrated surface plasmon resonance resonator sensor using silicon-on-insulator

Geum-Yoon Oh, Chung-Ang Univ. (Korea, Republic of); Doo-Gun Kim, Seon Hoon Kim, Hyun Chul Ki, Tae Un Kim, Korea Photonics Technology Institute (Korea, Republic of); Hong-Seung Kim, Tae-Kyeong Lee, Byeong-Hyeon Lee, Young-Wan Choi, Chung-Ang Univ. (Korea, Republic of)

The phenomenon of surface plasmon resonance (SPR) was first observed in an attenuated total reflection mirror devised by Kretschmann and Otto. These resonance characteristics have been employed as a real-time monitor of the surface interactions in a medium of interest. One of the most promising detection methods in biosensors, they are based on the detection of the SPR because this method allows one to monitor binding events in real-time without labeling. Different types of SPR sensors have been developed recently, which are comparable to or better than conventional SPR sensors in terms of sensitivity, compactness, and cost. We have analyzed and optimized the triangular resonator sensor structure with an extremely small SPR mirror. Since the SPR mirror is embedded in a resonator structure, the phase change of the SPR can be accumulated resulting in a huge peak shift regarding the resonance peak. In regards to the design of ultra-sensitive biosensors, we need to make a

thorough investigation and analysis of the optical properties of the silicon on insulator-based triangular resonator structure. For the application of SPR on a mirror facet, the angle needs to be larger than the critical angle of the TIR. More detailed results will be presented.

8627-47, Session PWed

Maximizing the intensity in TiO₂ waveguides for nonlinear optics applications

Orad Reshef, Christopher C. Evans, Harvard Univ. (United States); Jonathan D. B. Bradley, Massachusetts Institute of Technology (United States); Eric Mazur, Harvard Univ. (United States)

Titanium dioxide (TiO₂) represents an attractive candidate for nonlinear optical devices due its high transparency, large refractive index, and large Kerr nonlinearity. Using electron beam lithography and a liftoff procedure, we can structure both amorphous TiO₂ as well as polycrystalline anatase thin films to create photonic devices that exploit the material's properties in order to do nonlinear optics. Nonlinear optics benefit from long interactions, necessitating large intensities along long waveguide lengths. For this reason, waveguide losses need to be minimized. We study the effects of mask materials and annealing procedures on waveguide propagation losses. We also study a variety of taper structures and optimize the insertion losses of these waveguides. For short pulses, dispersion becomes an important parameter. For nano-scale structures such as ours, it can be tailored by changing the waveguide geometry. We present finite element simulations and experiments that demonstrate the dispersion engineering that was necessary to maintain high pulse intensity, as well as some nonlinear measurements that demonstrate the benefits of these optimizations. These techniques can readily be applied to other novel photonic devices.

8627-48, Session PWed

Integrated-optic polarization controllers based on polymer waveguide

Jun-Whee Kim, Su-Hyun Park, Woo-Sung Chu, Min-Cheol Oh, Pusan National Univ. (Korea, Republic of)

Integrated-optic polarization controller based on polymeric waveguide technology, which has drawn considerable attention through the demonstration of various functional devices is demonstrated. The polymer waveguide polarization controllers consist of three birefringence modulators sections and 45°-inclined quarter-wave plates inserted between them. By virtue of the design flexibility of organic materials, a novel polymer material with high birefringence has been synthesized and utilized for demonstrating birefringence modulators (BMs) in which the difference in phase retardation for TE and TM guided modes could be controlled through the thermo-optic effect. The polarization controllers are fabricated by following well-established polymer waveguide device fabrication procedures such as spin-coating, photolithography, and oxygen dry etching. The birefringence modulator with significant polarization dependence by incorporating birefringent polymer exhibits the birefringence modulation in proportion to the heating power. Thin-film quarter-wave plates are fabricated by using a reactive mesogen with a birefringence of 0.137 at visible wavelengths, and inserted between the birefringence modulators to produce static phase retardation and polarization coupling. To measure the device performance, a 1550 nm DFB laser is connected to a PM fiber pigtailed polarizer in order to precisely define the input polarization adjusted to TE. By applying a 6.85 V (230 mW) triangular AC signal and a DC signal of up to 3.3 V on another birefringence modulator, it was possible to generate arbitrary polarization states covering the entire surface of the Poincaré sphere.

8627-49, Session PWed

Near-infrared tunable lasers based on flexible polymeric Bragg reflection waveguide devices

Chi-Hun Sung, Kyung-Jo Kim, Nam-Seon Son, Jun-Whee Kim, Min-Cheol Oh, Pusan National Univ. (Korea, Republic of)

Flexible polymer waveguide with an imbedded Bragg grating is incorporated to form an external cavity lasers operating at near infrared wavelength. The third-order Bragg grating and oversized rip waveguide structure were designed by using the effective index method and the transmission matrix method. The polymer waveguide is fabricated using low-loss fluorinated polymer materials with refractive indices of 1.462 and 1.435 for the core and the cladding layers, respectively. The third-order Bragg reflection grating imbedded in a polymer waveguide is optimized to produce an appropriate reflection spectrum for NIR-ECL with a center wavelength of 840 nm. The spectral response of the fabricated tunable Bragg reflector device was characterized by using an SOA with a center wavelength of 838.8 nm and a 3-dB bandwidth of 55.7 nm. The output spectrum of the external cavity laser exhibited a side mode suppression ratio of 35 dB. The lasing spectrum exhibited 20-dB bandwidth of 0.2 nm and 3-dB bandwidth of 0.05 nm. For the wavelength tuning experiment, the flexible polymer device was attached on a motorized precision stage. When the compressive strain imposed, the peak was moved by 7.6 nm to shorter wavelength of 830.7 nm. On the other hand, by imposing the tensile strain, the peak was moved by 24.0 nm to longer wavelength of 862.4 nm. The wavelength peak position was almost linearly proportional to the imposed strain, and the efficiency of wavelength tuning by the imposed strain was 0.9 pm/??.

8627-50, Session PWed

Single-chip integration of polymer waveguide variable optical attenuators and optical switches

Guanghao Huang, Jun-Whee Kim, Min-Cheol Oh, Pusan National Univ. (Korea, Republic of)

In modern WDM optical communication systems, data traffic over the internet is daily growing, so there are strong demands on highly integrated optical components. Variable optical attenuator (VOA) arrays are used with optical switches in cascaded form in ROADM system. Though the two devices based on polymer waveguide technology are commercialized in these days, it is still not viable to integrate the two array devices on a single chip due to the significant crosstalk between them. The light radiated from VOA is guided in the planar waveguide and it hardly escape from the planar waveguide structure, so they could be coupled into the adjacent channels and forms crosstalk to deteriorate the transmission capability. Self-assembled microsphere array is imbedded in a core layer in this work in order to reduce the crosstalk. Because of the large index contrast in the polymer waveguide, causing strong diffraction of the planar guided modes toward the surface normal directions. Depending on the size and period of the microsphere, the diffraction efficiency is simulated based on 2D FDTD method. The PLC waveguide is fabricated by a conventional lithography, a dry etching for optimum size of microsphere, and an UV curing process. By measuring the diffraction efficiency of the sample with different lengths of microsphere area, the sample exhibits cladding mode attenuation efficiency of 23 dB/cm. Consequently the light radiated from VOA was diffracted by the microsphere, then the crosstalk could be decreased to -50 dB.

8627-51, Session PWed

Impact of thermal oxidation, surface chemistry, and porous silicon morphology on sensing performance

Silvia Soria, Istituto di Fisica Applicata Nello Carrara (Italy); Irina A. Kolmychek, Denis A. Kopylov, Sergey E. Svakhovskiy, Tatyana V. Murzina, Lomonosov Moscow State Univ. (Russian Federation); Francesco Baldini, Ambra Giannetti, Sara Tombelli, Simone Berneschi, Gualtiero Nunzi Conti, Istituto di Fisica Applicata Nello Carrara (Italy)

Porous silicon photonic crystalline structures were studied as optical sensors for different proteins. Periodic porous silicon (P-Si) structures were fabricated by electrochemical etching of p-type Si <100>. The layers were formed parallel to the surface of the silicon plate with macropores (70-90 nm) in layers of low and high porosity, respectively. We studied P-Si based microcavities (MC), with MC layers of high and low porosity, between Bragg mirrors composed of several layers (15 to 20) with alternating porosity. After the fabrication, we tested different thermal oxidation procedures in order to minimize the baseline drift in the sensor response.

We have measured the temporal baseline drift of samples soaked in phosphate buffered saline buffer for different thermal oxidation procedures: 1 step annealing at low temperature (20 min at 400°C); 3 step annealing (20 min at 400°C, 30 min in a ramp of 400°C to 900°C, and 3 min at 900°C); 2 step annealing (20 min at 400°C and 10 min at 900°C). Finally, we have optically verified antibody-antigen interactions a shift in the reflectivity spectrum of P-Si MC.

8627-52, Session PWed

Simulating the coupling effects occurring in arrayed waveguide grating (AWG) using the finite difference beam propagation method (FD-BPM)

Maria Cristina F. de Toledo, Univ. de São Paulo (Brazil)

The purpose of this work is to analyze by simulation the coupling effects occurring in Arrayed Waveguide Grating (AWG) using the finite difference beam propagation method (FD-BPM).

Conventional FD-BPM techniques do not immediately lend themselves to the analysis of large structures such as AWG. Cooper et al [1] introduced a description of the coupling between the interface of arrayed waveguides and star couplers using the numerically-assisted coupled-mode theory. However, when the arrayed waveguides are spatially close such that there is strong coupling between them, coupled-mode theory is not adequate. On the other hand, Payne [2] developed an exact eigenvalue equation for the super modes of a straight arrayed waveguide which involve a computational overhead. In this work, an integration of both methods is accomplished in order to describe the behavior of the propagation of light in guided curves. This new method is expected to reduce the necessary effort for simulation while also enabling the simulation of large and curved arrayed waveguides using a fully vectorial finite difference technique.

References:

[1] M.L. Cooper, S. Mookherjea, "Numerically-assisted coupled-mode theory for silicon waveguide couplers and arrayed waveguides", *Optics Express* 17 (2009) 1583.

[2] F.P. Payne, "An analytical model for the coupling between the array waveguides in AWGs and star couplers", *Optical and Quantum Electronics* 38 (2006) 237

8627-32, Session 8

Compact antennas for launching surface plasmons (*Invited Paper*)

Philippe Lalanne, Institut d'Optique (France)

Controlling the launching efficiencies and the directionality of surface plasmon polaritons (SPPs) and their decoupling to freely propagating light is a major goal for the development of plasmonic devices and systems. Here, we report on the design and experimental observation of a highly efficient unidirectional surface plasmon launcher composed of eleven subwavelength grooves, each with a distinct depth and width [Nano Lett. 11, 4207 (2011)]. We additionally show that a single two-mode slit in a thin metal film can be used to dynamically control the direction in which surface plasmons are launched. This is achieved by varying the phase between different coherent beams that are incident on the slit [Opt. Express 20, 15326 (2012)]

8627-33, Session 8

Plasmonic modulator based on thin metal-semiconductor-metal waveguide with gain core

Viktoriia E. Babicheva, Irina V. Kulkova, Radu Malureanu, Kresten Yvind, Andrei V. Lavrinenko, Technical Univ. of Denmark (Denmark)

Ultra-compact and ultra-fast modulators are among the main requirements for modern photonic integrated circuits. Their potential applications range from direct laser modulation to on-chip optical routing and computation. A surface plasmon polariton modulator supplemented with a loss-compensation mechanism provides such possibilities. We focus on plasmonic modulators with a gain core to be implemented as an active nanodevice in photonic integrated circuits. In particular, we theoretically analyze metal-semiconductor-metal (MSM) waveguides with the InGaAsP-based active material layers. A MSM waveguide enables a high effective index of the propagating mode and, therefore, effective modulation. The modulation is achieved by changing the gain of the core that results in different transmittance through the waveguide. Bulk semiconductor, quantum wells and quantum dots arranged in either horizontal or vertical layout, are considered as the core of the MSM waveguide. The designs address also practical aspects like n- and p-doped layers and barriers and feasible levels of gain. We optimize the structure by considering thin (up to 20 nm) metal layers. A thin single metal layer supports an asymmetric mode with a high propagation constant. Implementing such layers as the waveguide claddings allows to achieve several times higher effective indices than in the case of a waveguide with thick (>50 nm) metal layers. In turn, the high effective index leads to enhanced modulation speed. We show that a MSM waveguide with electrical current control of the gain incorporates compactness and deep modulation along with a reasonable level of transmittance.

8627-34, Session 8

Metal-dielectric metamaterials for guided wave optics applications

Natalia Dubrovina, Xavier Le Roux, Institut d'Électronique Fondamentale (France); Sylvain Blaize, Univ. de Technologie Troyes (France); André de Lustrac, Institut d'Électronique Fondamentale (France); Gilles Lérondel, Univ. de Technologie Troyes (France); Anatole Lupu, Institut d'Électronique Fondamentale (France)

We report experimental and modeling results for the behavior of metallic metamaterials (MMs) in a guided wave configuration aimed to investigate the potential for silicon photonics applications in the near-infrared ($\lambda \approx 1.5 \mu\text{m}$). Our approach consists in considering a composite guiding structure made of metamaterial layer over a high index slab waveguide, as for instance silicon in our case. In such a configuration only the evanescent tail interacts with the MMs layer which acts essentially as a perturbation. Its role is to modify the effective index of the composite waveguide structure. Such a solution allows to significantly reduce the propagation losses since the main part of the electromagnetic energy do not interact directly with the metallic part of the metamaterial. Our numerical simulations show that an array of gold coupled cut wires over a slab waveguide leads to a significant variation of the slab effective index in the vicinity of the resonance. The experimental results for the MM resonance behavior are found to be in a good agreement with modeling. The undertaken approach shows that dispersion and guiding properties of photonic waveguides can be carefully controlled with planar metallo-dielectric MMs, paving thus the way for new optical functionalities. The ability to control the energy flow in a silicon waveguide based on the interaction of the evanescent tail with the MMs layer constitutes a real opportunity to design a novel class of photonic devices.

This work was supported by the French National Research Agency (ANR Metaphotonique, contract number 7452RA09) and the Champagne-Ardenne region.

8627-35, Session 8

Metal nanoridge surface plasmon waveguides

Zeyu Pan, Junpeng Guo, The Univ. of Alabama in Huntsville (United States); Richard Soref, Univ. of Massachusetts Boston (United States); Walter R. Buchwald, Solid State Scientific Corp. (United States)

Propagating two-dimensional surface plasmon waveguide modes supported by silver nanoridges with either flat-tops, triangular or elliptical cross sections are investigated. Mode field profiles, dispersion relations, propagation distances, and figures-of-merit are calculated for these silver nanoridge waveguide structures. It is found that there is only one guided mode associated with the nanoridge. This mode is shown to be a quasi-TEM mode with the longitudinal field components one order of magnitude smaller than the transverse field components. The quasi-TEM nature of this mode reveals that free electron oscillations located at the top of the nanoridge is the main contributor to the tightly confined nature of this plasmon mode. It is also found that as the width of the nanoridge decreases, the ridge mode becomes more tightly confined to the ridge top. When the triangle height of the triangular nanoridge or the curvature of the elliptical nanoridge is large, the nanoridge plasmon mode profile approaches a wedge plasmon mode. The triangular and elliptical cross section nanoridge waveguides, if designed properly, can support tightly confined surface plasmon modes with longer propagation distances and higher figures-of-merit than flat-top nanoridge plasmon waveguides of similar width. The optimal elliptical nanoridge waveguide is obtained when the elliptical waveguide cross section approaches that of a semicircular cross section, and the optimal triangular nanoridge waveguide is obtained when the top wedge angle is approximately 120 degree.

8627-39, Session 8

Equivalent circuit model for plasmonic slot waveguide networks

Mohamed A. Swillam, Univ. of Toronto (Canada) and The American Univ. in Cairo (Egypt); Charles Lin, Amr S. Helmy, Univ. of Toronto (Canada)

Plasmonic slot waveguide (PSW) provides the unique ability to confine light within a few nanometers and allows for near perfect transmission through sharp bends as well as efficient light distribution between orthogonally intersecting waveguides. These features motivate the utilization of PSW for various nanoscale on-chip applications. The challenge associated with designing PSW functional devices is the absorption loss that limits the propagation length to $\sim 10 \mu\text{m}$. This calls for network-based devices based on engineered interference within a compact two-dimensional integrated PSW junction structures. The interference can lead to feedback and resonance effects, providing rich functionalities while reducing the footprint of the optical circuitry to only a few micrometers.

Finite difference time domain (FDTD) method is commonly utilized for modeling plasmonic devices. This technique is, however, inefficient as it requires extremely fine grid to model the surface plasmons and careful manipulation of the boundary condition to avoid spurious reflections. Furthermore, the computational resource required scales drastically as the complexity and dimension of the network increases.

In this paper, we present our recent equivalent circuit model that is capable of modeling the response of PSW network consists of arbitrary combinations waveguide junctions with similar accuracy as FDTD. This model is independent of FDTD-extracted parameters and provides means for rapid design optimization and tolerance analysis of proposed network devices. This efficient model is demonstrated to be scalable and allows for the formulation of closed-form transmission responses for PSW networks, thereby opening the door for the incorporation of plasmonics circuits into electronic CAD software.

8627-37, Session 9

Efficient design of photonic-integrated circuits (PICs) by combining device- and circuit- level simulation tools

Cristina Arellano, Igor Koltchanov, Andre Richter, VPIsystems GmbH (Germany); Sergei Mingaleev, VPI Development Ctr. (Belarus); Jan Pomplun, Sven Burger, Frank Schmidt, JCMwave GmbH (Germany)

Photonic Design automation (PDA) can play a part in the continuously development of photonic integrated circuits (PICs). Simulation techniques might be significantly complex because of several factors as the large diversity of photonic components, the broad frequency ranges of optical signals that require usage of advanced signal representations, or the presence of very different time scales. To properly handle such diversities, modern photonic circuit simulators are based on segmentation of the modeled PIC into building blocks ("PIC elements").

In previous works we have addressed the modeling of fully passive PICs, based on the description of PIC elements in terms of frequency-dependent scattering-matrices. Lately we presented a new method for efficient modeling of hybrid large-scale PICs that aids pure time-domain simulations, so called, time-and-frequency domain modeling (TFDM).

Although these device-level approaches cover a large field of applications, traditional photonic simulation techniques based on solving the Maxwell equations might be preferred for modeling specific PIC elements within the PIC design, in order to reach higher level of geometrical details and as a gate to foundry specifications.

In this contribution we present a solution for co-simulation within a circuit-level simulator and a full 3D simulator that implements frequency-domain finite element method (FEM) for solving photonic

devices with any geometry. In this procedure, the layout of wire and slab wires is designed in the FEM-based simulator and an accurate calculation of waveguide parameters is performed. The results are shared with the circuit-level simulator, which is used to design and optimize the device topology.

8627-38, Session 9

Efficient optimization of nanoplasmonic devices using space mapping

Pouya Dastmalchi, Georgios Veronis, Louisiana State Univ. (United States)

We show that the space-mapping algorithm, originally developed for microwave circuit optimization, can enable the efficient optimization of nanoplasmonic devices. Space-mapping utilizes a physics-based coarse model to approximate a fine model accurately describing a device. The main concept in the algorithm is to find a mapping that relates the fine and coarse model parameters. If such a mapping is established, we can then avoid using the direct optimization of the computationally expensive fine model to find the optimal solution. Instead, we perform optimization of the computationally efficient coarse model to find its optimal solution, and then use the mapping to find an estimate of the fine model optimal. In this paper, we demonstrate the use of the space mapping algorithm for the optimization of metal-dielectric-metal plasmonic waveguide devices. In our case, the fine model is a full-wave finite-difference frequency-domain (FDFD) simulation of the device, while the coarse model is based on the characteristic impedance and transmission line theory. We show that, if we simply use the coarse model to optimize the structure without space mapping, the response of the structure obtained substantially deviates from the target response. On the other hand, using space mapping we obtain structures which match very well the target response. In addition, full-wave FDFD simulations of only a few candidate structures are required before the optimal solution is reached. In comparison, a direct optimization using the fine FDFD model in combination with a genetic algorithm requires hundreds of full-wave FDFD simulations to reach the same optimal.

8627-40, Session 9

Robust optimization of 2x2 multimode interference couplers with fabrication uncertainties

Sameer Rehman, Matthijs Langelaar, Fred van Keulen, Technische Univ. Delft (Netherlands)

The performance of integrated photonic devices is strongly dependent on the capabilities of the fabrication process. If fabrication uncertainties are not incorporated at the design stage they can severely degrade performance. In this paper, we propose a novel design-for-manufacture strategy for integrated photonics which specifically addresses the commonly encountered scenario in which probability distributions of the uncertainties are not available, however their bounds are known. To illustrate our approach, we robustly minimize the imbalance of a 2x2 multimode interference (MMI) coupler on Silicon-on-Insulator (SOI). The length and width of the MMI coupler design are used as design variables, while the actual fabricated design geometry can vary within an uncertainty range given by limitations of the fabrication process. By minimizing the maximum realizable value of the imbalance w.r.t. the uncertainty set, we can find an optimum whose performance is relatively immune to fabrication variations. Instead of applying this robust optimization directly on a computationally expensive simulation model of the MMI coupler, we construct a cheap surrogate model by uniformly sampling the simulated MMI coupler at different values of the design variables and interpolating the resulting imbalance values using a Kriging metamodel. By applying robust optimization on the constructed surrogate, the global robust optimum can be found at low computational cost. The proposed method can similarly be applied to find robust

Conference 8627:
Integrated Optics: Devices, Materials, and Technologies XVII

designs of other photonic devices. However, for robust optimization of higher dimensional problems, uniform sampling across the design domain is inefficient, therefore a more efficient strategy is required.

8627-41, Session 9

Equivalent step-index model of multifilament core fibers

Ron Spittel, Adrian Lorenz, Sylvia Jetschke, Matthias Jäger, Hartmut Bartelt, Institut für Photonische Technologien e.V. (Germany)

Multifilament core (MFC) fibers are characterized by a microstructured core consisting of a number of (identical) circular waveguides in a usually hexagonal lattice. Due to the absence of radial symmetry, such fibers need to be simulated numerically, e.g. using a finite-element-method (FEM).

We present a model for the description of such MFC fibers by substituting the microstructured core with a circular equivalent step-index (ESI) core with an effective radius and refractive index. We show that the latter is given by the fundamental space-filling mode (FSM), which is the solution of Maxwell's equations in an infinite extended lattice of filaments.

We use an approximate semi-analytical approach, which is based on the transformation of the hexagonal into a circular unit cell to obtain an analytical expression for dispersion equation of the FSM which we then solve numerically. By introducing an equivalent core radius, we define the numerical aperture and the V-parameter of MFC fibers and calculate the eigenmodes of the ESI fiber.

Finally, the results from the ESI model using the presented dispersion equations are compared with highly accurate numerical simulations of the MFC fibers done with a commercial FEM. We show that the presented ESI model of MFC fibers is highly accurate for the prediction of the numerical aperture and V-parameter. Also, the fundamental mode, its effective index, effective mode area and bend loss can be predicted with very high precision.

The presented model is therefore a very convenient and extremely time-saving tool for the design and analysis of such fibers.

8628-1, Session 1

Integrated silicon photonics for on-chip optical interconnects (*Invited Paper*)

Zhen Peng, Marco Fiorentino, Zhihong Huang, Raymond G. Beausoleil, Janet Chen, Hewlett-Packard Labs. (United States)

The progress made in low-power consumption silicon photonic devices has positioned on-chip optical interconnects as a promising replacement for copper wires to address the bottlenecks in the communication bandwidth and energy consumption of datacenters. Integrated silicon photonics utilizing dense wavelength division multiplexing (DWDM) technology provides considerable advantages in both performance and costs. In this paper, first we present our progress in developing CMOS-compatible device technologies for high-performance short-range interconnects applications, and then report on our attempt at large-scale integration to form a complete on-chip DWDM link.

Our focus in device physics has been on maximizing energy efficiency of each component in a DWDM system perspective. We have reported silicon microring modulators using free carrier injection operating at 6Gbps consuming 45 fJ/bit. In the receiver, mainly we adopt germanium p-i-n photodetectors at the drop port of a silicon microring filter. At the same time we are looking into silicon defect detectors enhanced by a microring resonant cavity.

By integrating silicon microring modulators and linear germanium drop detectors, we will attempt to form a 32-channel DWDM array with an 80 GHz channel spacing. We will examine the power budget contribution from components such as wavelength trimming caused by wafer thickness uniformity and fabrication imperfections, modulation using carrier injection, and wavelength synchronization at the drop detector end. A doped silicon wire will be integrated as a heater around the microring modulator and the passive drop filter to bring resonances into compliance. This on-chip DWDM system will be controlled by a CMOS driving circuit with feedback control loop flip-chip bonded to the photonics wafer.

8628-2, Session 1

Towards low energy consumption and high-speed silicon-based circuits (*Invited Paper*)

Laurent Vivien, Delphine Marris-Morini, Papichaya Chaisakul, Mohamed-Said Rouifed, Institut d'Électronique Fondamentale, CNRS (France); Leopold Virot, Institut d'Électronique Fondamentale, CNRS (France) and CEA-LETI (France) and STMicroelectronics (France); Melissa Ziebell, Gilles Rasigade, Nicolas Abadia, Eric Cassan, Institut d'Électronique Fondamentale, CNRS (France); Jacopo Frigerio, Giovanni Isella, Daniel Chrastina, Lab. for Epitaxial Nanostructures on Silicon and Spintronics (Italy) and Politecnico di Milano (Italy); Jean-Michel Hartmann, CEA-LETI (France); Charles Baudot, Frederic Boeuf, STMicroelectronics (France); Jean-Marc Fedeli, CEA-LETI (France)

Silicon-based photonics has generated a strong interest in recent years, mainly for optical telecommunications and optical interconnects in integrated circuits. The main rationales of silicon photonics are the reduction of photonic system costs and the increase of the number of functionalities on the same chip combining photonics and electronics.

Recent advances in silicon photonics for high speed optical link will be presented. High speed optical modulators are mainly based on carrier depletion effect in pin diode. 40Gbit/s modulator with low insertion loss and high extinction ratio has been already achieved. Such a device suffers from high voltage swing and then high energy consumption which is prohibited for datacom applications. Indeed, energy consumption should be lower than 100fJ/bit and the voltage swing below 1.5V (breakdown voltage of Si transistor). Among new concepts to reach these

specifications, promising electro-absorption modulation results have been obtained using quantum confined stark effect in Ge/SiGe quantum wells. Indeed, 23GHz and high extinction ratio have been demonstrated in waveguide configuration. The energy consumption has been reduced down to 100fJ/bit under 1V swing.

For light detection, bulk Ge embedded in lateral pin photodiode and integrated at the end of the Si waveguide, using butt-coupling configuration has demonstrated reliable detection characteristics. Bandwidth over 50GHz under zero-bias, with internal responsivity as high as 0.8A/W at a wavelength of 1.55 μm have been measured. 40Gb/s open eye diagram were obtained under zero-bias, showing the possibility to get low power ultra-fast receivers in bulk Ge platform.

8628-3, Session 2

Towards a comprehensive silicon-photonics platform (*Invited Paper*)

Michael Watts, Massachusetts Institute of Technology (United States)

Silicon photonics has been developed by a number of groups around the world establishing excellent individual device characteristics, from ultralow power silicon modulators to high-bandwidth germanium photodetectors and tunable filters with flat pass-bands and sharp, high-order roll-offs. However, demonstrations of systems of silicon photonic devices have been rare. Moreover, despite promises of integration with CMOS electronics, such demonstrations have been similarly rare and no common integration strategy has been determined. Here, we consider silicon photonics as a whole and what challenges remain toward implementing a successful platform capable of addressing a wide-range of applications as well as what options exist for integration with CMOS.

Additionally, in order for systems of silicon photonic devices to reliably yield accurate models indicative of yielded components need to be developed and placed within a common simulation environment linking photonics with electronics. We discuss previous and on-going results in silicon photonic components with an emphasis on generating a library of silicon photonic components capable of not only modulating and detecting data, but switching, filtering, and coherently combining, and modifying the polarization state of the electromagnetic wave on chip. It is our belief that with an extensive library of components that can be accurately modeled, silicon photonics will be applied to an increasing number of applications not previously envisioned.

In this talk, we aim to bring together the challenges of integration and modeling to effectively address silicon photonics as a whole, highlighting equally the opportunities and the challenges that remain.

8628-4, Session 2

Very low power and footprint-integrated photonic modulators and switches for ICT (*Invited Paper*)

Lars Thylén, Royal Institute of Technology (Sweden) and Hewlett Packard Labs. (United States); Petter Holmstrom, Lech Wosinski, Royal Institute of Technology (Sweden)

No Abstract Available.

8628-5, Session 3

Silicon, silica, and germanium photonic integration for electronic and photonic convergence (*Invited Paper*)

Hiroshi Fukuda, Tai Tsuchizawa, Hidetaka Nishi, Rai Kou, Tatsuro Hiraki, Nippon Telegraph and Telephone Corp. (Japan); Kazumi Wada, Yasuhiko Ishikawa, The Univ. of Tokyo (Japan); Koji Yamada, Nippon Telegraph and Telephone Corp. (Japan)

Future datacommunications and telecommunications systems require densely integrated low-power and low-cost photonic devices with high functionality. Silicon photonics is one of the key technologies for meeting these requirements. Various types of photonic devices have already been developed. However, it is still very difficult to install silicon photonic devices in practical telecommunications systems because the requirements for telecommunication systems are quite severe. In particular, insertion losses and polarization dependence are serious issues.

To solve these problems, we have developed a low-loss photonic platform in which silicon photonic wire waveguides with a germanium active layer and a silica waveguide with high refractive index contrast are monolithically integrated. The silicon waveguide with the germanium layer is mainly used for dynamic and active devices, which require a small footprint and fast operation.

This paper describes our recent progress with the integration of silicon photonic devices, including germanium photodiodes, silicon variable optical attenuators, and silica arrayed waveguide gratings. We also have integrated an arrayed waveguide grating and photodiode array monolithically and successfully mounted multi-channel transimpedance amplifiers and limiting amplifiers on the integrated photonic device using flip-chip bonding technology.

8628-6, Session 3

Photonic integrated circuits applications based on silica and polymer waveguides (*Invited Paper*)

Tomoyuki Izuwara, Junichiro Fujita, Reinald Gerhardt, Bin Sui, Wenhua Lin, Boris Grek, Enablence (United States)

We report on current applications and future development of photonics integrated circuits (PICs) based on silica and polymer waveguide technology. The PICs of these material platforms include devices for optical networks such as arrayed waveguide gratings, optical switches, tunable PICs, variable optical attenuator, etc. Our subsystem modules contain devices from both platforms based on the unique advantages of each material. To support ever-increasing demand for larger capacity and higher speed, the network node design became complex consisting of many of these devices. Here, the driving forces for integration are the cost and space saving. Examples of higher integration design and performance are presented.

8628-7, Session 3

Silicon hybrid nanoplasmonic waveguides and devices (*Invited Paper*)

Sailing He, Daoxin Dai, Joint Research Ctr. of Photonics (China)

Surface plasmon (SP) waveguides can break the diffraction limit and thus enable nano-scale optical waveguiding and light confinement. This has become a promising candidate to achieve photonic integrated circuits (PICs) with an ultrahigh integration density. The problem for conventional nano-plasmonic waveguides is that the propagation distance is usually limited to the order of several micrometers due to the

large intrinsic loss. Recently, hybrid plasmonic waveguides have been proposed and attracted much attention as a good option to realize a nano-scale light confinement as well as a relatively long propagation distance. Furthermore, the hybrid plasmonic waveguides offer a way to transfer and process both photonic and electronic signals along the same plasmonic circuit, which is desirable in order to combine the advantage of both photonics and electronics for high-speed signal processing and an easy realization of active components. This makes it interesting to realize various functional elements by using hybrid plasmonic waveguides. In this paper, we give a review for our recent work on silicon hybrid nano-plasmonic waveguides and devices. First, several types of silicon hybrid nano-plasmonic waveguides are presented and compared. The potential of realizing micro-scale light propagation distance with nano-scale light confinement is present. Then the design and fabrication of several important basic elements are demonstrated, including directional coupler, Y-branch. Since optical cavities have been used very widely in many applications as a versatile element for photonic integrated circuits, our theoretical and experimental work on silicon hybrid plasmonic sub-micron-disk/ring is also presented.

8628-8, Session 4

Scaling hybrid-integration of silicon photonics in freescale 130 nm to TSMC 40nm-CMOS VLSI drivers for low-power communications (*Invited Paper*)

John E. Cunningham, Oracle (United States)

Within the Ultrapformance Nanophotonic Intrachip Communication (UNIC) program at Oracle, we have been aggressively developing active nanophotonic devices (modulators, detectors, WDM components), circuits, that target ultimate operation of Si photonic links at 15 Gbps and 300 fJ/bit energy consumption. These links are envisioned to operate between computing elements in a large array of chips called a "Macrochip." We present our recent developments in packaging and integration technologies for a macrochip.

8628-9, Session 4

Nanoscale SOI silicon light source design for improved efficiency

Petrus J. Venter, Univ. of Pretoria (South Africa) and INSiAVA (Pty) Ltd. (South Africa); Monuko du Plessis, Univ. of Pretoria (South Africa); Alfons W. Bogalecki, INSiAVA (Pty) Ltd. (South Africa)

Silicon-on-insulator (SOI) is becoming an important technology platform in nanometer scale CMOS integrated circuits. The platform offers a number of distinct advantages over bulk CMOS for materialising silicon light sources based on hot carrier luminescence. This work describes the design of nanoscale silicon structures for enhanced light emission with improved power efficiency, which allows the use of SOI light sources in short-haul optical communication links with extended possibilities for other applications.

It has been shown experimentally that reducing the dimensions of the active material results in an improvement of electroluminescent power emitted from forward-biased pn-junctions. Previously published results show a similar trend for light sources based on hot carrier luminescence. Building on our previous work in SOI light sources, multiple finger-like junctions are manufactured in an arrayed fashion for coupling into large diameter core optical fibers for CMOS optical communications up to a few hundred meters. The manufacturing methodology and associated challenges are discussed for the scaling down of device dimensions and difficulties in realizing the structures are investigated. The optical power characteristics are discussed as well as the spectral nature of emission

along with the advantages and disadvantages thereof.

This work compares different architectures of light sources that were implemented, where a comparison is drawn between previous SOI devices as well bulk CMOS. We believe the improved SOI light sources are fully compatible with modern CMOS technologies based on SOI and may provide such technologies with a much needed light source as part of the circuit designer's toolkit.

8628-10, Session 4

Electrons to photons and RF signals in advanced mobile devices (*Invited Paper*)

Louay A. Eldada, Amprius, Inc. (United States)

We describe leading-edge silicon-nanowire-based rechargeable lithium ion batteries that enable the generation of high-intensity light and high-power RF signals for extended periods of time. These high volumetric energy density batteries address the demanding electrical power requirements of high-resolution ultra-bright displays and high-power-consumption antennas in next-generation 4G LTE cellular data communication smartphones, tablets and laptop computers.

8628-25, Session PWed

Structure-dependent optical characteristics of one-dimensional photonic crystal hydrogenated amorphous silicon waveguides

Dong Wook Kim, Heung Sun Jeong, Kyong Hon Kim, Inha Univ. (Korea, Republic of); Sang Chul Jeon, Sang Hyun Park, Dong Eun Yoo, Ki Nam Kim, National Nanofab Ctr. (Korea, Republic of); El-Hang Lee, Inha Univ. (Korea, Republic of)

Slow light representing the low group velocity of light in a high-group index medium has become an important field of research. Recently it has been demonstrated that the photonic crystal waveguides with periodic structures deliver a high-group index and thus provide slow-light enhanced optical nonlinear effects. In addition, several other candidate technologies, such as coupled resonators, one-dimensional (1-D) gratings or holes, or two-dimensional (2-D) photonic crystals (PhCs) formed in optical fibers or waveguides, have been studied for the slow light. The increased interaction of the light beam with the waveguide materials due to its reduced group velocity within the periodic structures allows the nonlinear optic devices short even for low optical pump powers.

Typically the 1-D periodic structured optical waveguides provide the wavelength-selective properties with high quality factors in a free spectral range (FSR) and the slow light characteristics due to large group indices near the band-edge region. Most PhC waveguide structures exhibit a wide spectral band-gap region, i.e., a wavelength region where no light can propagate, and wide transmission bands beside it. The band-gap wavelength region depends on the structural characteristics of the 1-D PhCs, such as the lattice constant and hole diameter. The transmission spectral profiles of the transmission bands are similar to the interference pattern of Fabry-Perot (FP) filters.

In this paper we report on the experimentally measured optical characteristics in 1-D PhC waveguides made of hydrogenated amorphous silicon with various device structures and compare them with numerically simulated results.

8628-26, Session PWed

Active switching using three-dimensional photonic crystal waveguide

Choloong Hahn, Nali Yoo, Cha-Hwan Oh, Hanyang Univ. (Korea, Republic of)

Photonic crystals have a photonic band gap property, especially the three dimensional photonic crystals have complete photonic band gap, so the photonic crystals can stop propagation of wave in all direction. The three dimensional photonic crystal used in this research is an inverse opal structure. This inverse opal structure has complete band gap, hence embedded channel into the inverse opal structure can guide wave propagation. The photonic crystal was fabricated by using the flow-controlled vertical deposition (FCVD) method two times. In the FCVD method, the colloidal flow is controlled by the atmospheric pressure. Firstly, an opal structure was fabricated by using the FCVD method. The opal structure was used as a template for inverse opal structure. After opal structure fabrication, inverse opal structure was fabricated by using the infiltration method into the opal template. The waveguide structure was fabricated by three steps. First, the bottom layer of waveguide was constructed by the inverse opal fabrication process mentioned above. Second, the guiding channel was fabricated with a photo resist by the spin coating and photo lithography methods on the bottom layer. In this process, we could form arbitrary waveguide pattern we want by choosing the patterning mask. And the last, top layer of waveguide with inverse opal structure was constructed upon the patterned layer. Anisotropic polymer was also tried as a guiding channel material by which we could demonstrate an active optical switch by writing and erasing the channel pattern, because the anisotropic polymer has rewritable property.

8628-11, Session 5

Integrated nanophotonic devices based on plasmonics (*Invited Paper*)

Anatoly V. Zayats, King's College London (United Kingdom)

A variety of plasmonic and Si-photonic waveguiding geometries has recently been proposed to act as possible optical interconnects. In this context, plasmonics which is dealing with surface electromagnetic excitations in metallic structures, provides a great deal of flexibility in photonic integration since with surface plasmons the problem of light manipulation can be reduced from three to two dimensions. The electromagnetic field enhancement effects associated with surface plasmons and specific to them field confinement near metal interfaces result in the strong sensitivity of plasmonic mode to dielectric surroundings, thus facilitating all-optical and electronic control of their propagation. Moreover, utilizing more complex arrangements of plasmonic nanostructures such as plasmonic crystals and metamaterials complete control over surface plasmon dispersion can be achieved. In this talk we will overview plasmonic approaches for achieving subwavelength guiding and manipulation of optical signals. Generation, detection, amplification and modulation of plasmonic signals in the integrated circuitry will also be discussed.

8628-12, Session 5

Computer aided simulation of large-scale high-density photonic integrated circuits (*Invited Paper*)

Wei-Ping Huang, McMaster Univ. (Canada)

No Abstract Available.

8628-13, Session 5

All-silicon and epitaxial hybrid III-V-on-silicon photodetectors for on-chip optical interconnection applications (*Invited Paper*)

Andrew W. Poon, Shaoqi Feng, Yu Li, Yu Geng, Kei May Lau, Hong Kong Univ. of Science and Technology (Hong Kong, China)

Photodetectors are critical building blocks for on-chip optical interconnection applications. In this paper we will review two different approaches to photodetectors on silicon photonic chips, namely all-silicon and epitaxial hybrid III-V-on-silicon photodetectors, both for the 1550nm wavelengths.

Previously, some of us have demonstrated all-silicon microcavity-enhanced photocurrent generation for sub-bandgap 1550nm wavelengths using linear surface-state absorption upon relatively low optical power and nonlinear two-photon absorption upon relatively high optical power. The microcavity was integrated with a p-i-n diode and photocurrent was read out, with orders of magnitude enhancement at the cavity resonance wavelengths. Here, we will report our latest demonstration of such all-silicon microresonator-enhanced linear and nonlinear photodetectors in a host of microresonator-based devices including (i) interferometric-coupled microring resonators and (ii) high-order-coupled microring resonators. Such devices enable tailored wavelength channel filtering and routing while photodetecting simultaneously. We will also report the measured bandwidths of such linear and nonlinear photodetectors, and show the feasibility study of high-speed signal photodetection.

We will also report our latest progress in developing hybrid III-V-on-silicon InGaAs p-i-n photodetectors that are epitaxially grown on patterned silicon-on-insulator substrates by metalorganic chemical vapor deposition using metamorphic growth of a GaAs buffer and an InP template. The photodetector is butt-coupled to a silicon waveguide. Most recently, we demonstrated a 20 μ m \times 20 μ m photodetector with a responsivity of 0.17 A/W at 1550nm wavelength upon -1V bias voltage, a dark current of 2.5 μ A, a 3dB bandwidth of 9 GHz and an open eye diagram at 10Gb/s data rate upon -4V bias voltage. In this paper, we will report an improved photodetector using a reduced device footprint.

8628-14, Session 5

All-optical logic gates and wavelength conversion via the injection-locking of a Fabry-Perot semiconductor laser

Evan Harvey, Michael C. Pochet, Timothy Locke, Air Force Institute of Technology (United States); Nicholas G. Usechak, Air Force Research Lab. (United States)

This work investigates the implementation of all-optical logic gates based on optical injection locking (OIL). All-optical inverting, NOR, and NAND gates are experimentally demonstrated using two distributed feedback (DFB) lasers, a multimode Fabry-Perot laser diode, and an optical band-pass filter. The DFB lasers are externally modulated and represent logic inputs into the cavity of the multimode Fabry-Perot slave laser. The master lasers' wavelengths are correlated to the longitudinal modes of the Fabry-Perot slave laser and their optical power is used to modulate the injection conditions in the Fabry-Perot slave laser. The optical band-pass filter is used to select a Fabry-Perot mode that is suppressed or passed given the logic state of the injecting master laser signals. When the input signal(s) is (are) in the on state, injection locking, and thus the suppression of the non-injected Fabry-Perot modes, is induced, yielding a dynamic system that can be used to implement photonic logic functions. The inverting logic case can also be used as a wavelength conversion mechanism — a key component in advanced wavelength-division multiplexing networks. As a result of this experimental investigation, a more comprehensive understanding of the locking parameters concerning injecting multiple lasers into a multi-mode cavity and the logic transition time is achieved. The performance of optical logic

computations and wavelength conversion has the potential of ultrafast operation, limited primarily by the photon decay rate in the slave laser.

8628-15, Session 6

Nonlinear, ultrafast, and quantum optics in photonic integrated circuits (*Invited Paper*)

Chee Wei Wong, James F. McMillan, Tingyi Gu, Jiangjun Zheng, Pin-Chun Hsieh, Serdar Kocaman, Xiujian Li, Ying Li, Junlin Liang, Matthew D. Marko, Nan Shi, Andrzej Veitia, XinAn Xu, Zhenda Xie, Jinghui Yang, Columbia Univ. (United States)

We describe nonlinear, ultrafast, and quantum interactions of photons in engineered chip-scale photonics crystals and nanophotonics. First, we describe the strong control of dispersion and localization in photonic crystal structures, such as recent observations on superlattices with zero phase delay, disordered localized modes, optical analog to electromagnetically-induced transparency, and ultrahigh-Q optical resonators. Second, we report on studies in nonlinear optics through the tight field confinement and long photon lifetimes in mesoscopic structures. We highlight a few examples such as femtosecond soliton generation and pulse compression, graphene-silicon regenerative oscillations and four-wave mixing, and parametric oscillations in chip-scale cavity optomechanics. Third, we describe our efforts on nonclassical optics on-chip. Examples include observations of strong exciton-photon polaritons in solid-state cavity quantum electrodynamics, single and correlated photons on-chip for dense quantum information processing

8628-16, Session 6

Integrated quantum photonics (*Invited Paper*)

K. Aungskunsiri, Damien Bonneau, J. Carolan, E. Engin, D. Fry, J. P. Hadden, Pruet Kalasuwan, J. Kennard, S. Knauer, T. Lawson, E. Martin-Lopez, Jasmin Meinecke, Guillermo Mendoza, Alberto Peruzzo, Kostantinos Poullos, N. Russell, A. Santamato, Pete Shadbolt, Joshua W. Silverstone, A. Stanley-Clark, Matthaeus Halder, J. Harrison, D. Ho, P. Jiang, Anthony Laing, Mirko Lobino, Jonathan C. F. Matthews, Brian R. Patton, A. Politi, María Rodas Verde, Univ. of Bristol (United Kingdom); P. Zhang, Univ. of Bristol (United States); Xiao-Qi Zhou, Martin J. Cryan, John G. Rarity, Mark G. Thompson, Siyuan Yu, Jeremy L. O'Brien, Univ. of Bristol (United Kingdom)

Quantum information science aims to harness uniquely quantum mechanical properties to enhance measurement and information technologies, and to explore fundamental aspects of quantum physics. Of the various approaches to quantum computing [1], photons are particularly appealing for their low-noise properties and ease of manipulation at the single qubit level [2,3]. Encoding quantum information in photons is also an appealing approach to quantum communication, metrology (eg. [4]), measurement (eg. [5]) and other quantum technologies [6]. However, the implementation of optical quantum circuits with bulk optics has reached practical limits. We have developed an integrated waveguide approach to photonic quantum circuits for high performance, miniaturization and scalability [7]. Here we report high-fidelity silica-on-silicon integrated optical realizations of key quantum photonic circuits, including two-photon quantum interference and a controlled-NOT logic gate [8]. We have demonstrated controlled manipulation of up to four photons on-chip, including high-fidelity single qubit operations, using a lithographically patterned resistive phase shifter [9]. We have used this architecture to implement a small-scale compiled version of Shor's quantum factoring algorithm [10], demonstrated heralded generation of tunable four photon entangled states from a six photon input [11], a reconfigurable two-qubit circuit [12], and combined waveguide photonic circuits with superconducting single photon detectors [13]. We describe complex quantum interference behavior

in multi-mode interference devices with up to eight inputs and outputs [14], and quantum walks of correlated particles in arrays of coupled waveguides [15]. Finally, we give an overview of our recent work on fundamental aspects of quantum measurement [16,17,18] and nonlinear [19,20] photon sources, fast manipulation of single photons [21].

- [1] T. D. Ladd, F. Jelezko, R. Laflamme, Y. Nakamura, C. Monroe, and J. L. O'Brien, *Nature* 464, 45 (2010).
- [2] J. L. O'Brien, *Science* 318, 1567 (2007).
- [3] R. Okamoto, J. L. O'Brien, H. F. Hofmann and S. Takeuchi *Proc. Natl. Acad. Sci.* 108, 10067 (2011)
- [4] T. Nagata, R. Okamoto, J. L. O'Brien, K. Sasaki, and S. Takeuchi, *Science* 316, 726 (2007).
- [5] R. Okamoto, J. L. O'Brien, H. F. Hofmann, T. Nagata, K. Sasaki, S. Takeuchi, *Science* 323, 483 (2009).
- [6] J. L. O'Brien, A. Furusawa, and J. Vuckovic, *Nature Photon.* 3, 687 (2009).
- [7] A. Politi, M. J. Cryan, J. G. Rarity, S. Yu, and J. L. O'Brien, *Science* 320, 646 (2008).
- [8] A. Laing, A. Peruzzo, A. Politi, M. R. Verde, M. Halder, T. C. Ralph, M. G. Thompson, and J. L. O'Brien, *Appl. Phys. Lett.* 97, 211109 (2010).
- [9] J. C. F. Matthews, A. Politi, A. Stefanov, and J. L. O'Brien, *Nature Photon.* 3, 346 (2009).
- [10] A. Politi, J. C. F. Matthews, and J. L. O'Brien, *Science* 325, 1221 (2009).
- [11] J. C. F. Matthews, A. Peruzzo, D. Bonneau, and J. L. O'Brien, *Phys. Rev. Lett.* 107, 163602 (2011).
- [12] P. J. Shadbolt, M. R. Verde, A. Peruzzo, A. Politi, A. Laing, M. Lobino, J. C. F. Matthews, J. L. O'Brien, *Nature Photon.* 6, 45-49 (2012).
- [13] C. M. Natarajan, A. Peruzzo, S. Miki, M. Sasaki, Z. Wang, B. Baek, S. Nam, R. H. Hadfield, and J. L. O'Brien, *Appl. Phys. Lett.* 96, 211101 (2010).
- [14] A. Peruzzo, A. Laing, A. Politi, T. Rudolph, and J. L. O'Brien, *Nature Comm.* 2, 224 (2011).
- [15] A. Peruzzo, M. Lobino, J. C. F. Matthews, N. Matsuda, A. Politi, K. Poulios, X.-Q. Zhou, Y. Lahini, N. Ismail, K. Worhoff, Y. Bromberg, Y. Silberberg, M. G. Thompson, and J. L. O'Brien, *Science* 329, 1500 (2010).
- [16] A. Laing, T. Rudolph, and J. L. O'Brien, *Phys. Rev. Lett.* 102, 160502 (2009).
- [17] X-Q Zhou, TC Ralph, P Kalasuwan, M Zhang, A Peruzzo, BP Lanyon, and JL O'Brien, *Nature Comm.* 2 413 2011.
- [18] A. Crespi, M. Lobino, J. C. F. Matthews, A. Politi, C. R. Neal, R. Ramponi, R. Osellame, J. L. O'Brien, *Appl. Phys. Lett.* 100, 233704 (2012).
- [19] C. Xiong, et al. *Appl. Phys. Lett.* 98, 051101 (2011).
- [20] M. Lobino, et al, *Appl. Phys. Lett.* 99, 081110 (2011).
- [21] D Bonneau, M Lobino, P Jiang, CM Natarajan, MG Tanner, RH Hadfield, SN Dorenbos, V Zwiller, MG Thompson, JL O'Brien *Phys. Rev. Lett.*; 108, 053601 (2012).

8628-17, Session 6

Infrared metamaterial diffractive optics (Invited Paper)

Stéphane Larouche, Duke Univ. (United States)

Metamaterials offer a control of the optical properties at the unit cell level, making them a great candidate for graded optics. Devices with complex graded optical properties have been demonstrated at lower frequencies, but are more difficult to realize in the optical range. Indeed, metals are absorbing at optical wavelengths and the dimensions of the unit cells require sophisticated lithography techniques. This presentation will present the development of a range of metamaterial unit cells operating at 10.6 microns and producing an arbitrary refractive index between 2.0 and 5.1. These metamaterials can be fabricated using focused electron

beam lithography, a fairly slow approach which limits the total number of metamaterial layers that can be fabricated. Diffractive optics, which have a limited thickness, are a great application for metamaterials, as well as a stepping stone toward more complex structures. Those possibilities are demonstrated through the fabrication and characterization of a blazed diffraction grating and a phase hologram.

8628-18, Session 7

Light from germanium tin heterostructures on silicon (Invited Paper)

Erich Kasper, Univ. Stuttgart (Germany); Martin Kittler, IHP GmbH (Germany) and Brandenburgische Technische Univ. Cottbus (Germany); Michael Oehme, Univ. Stuttgart (Germany); Tzanimir Arguirov, IHP GmbH (Germany) and Brandenburgische Technische Univ. Cottbus (Germany)

Germanium and germanium tin alloys of low tin content are promising materials for light emitting devices on silicon substrates. Germanium(Ge) is like silicon(Si) an indirect semiconductor but the direct transition is only 136 meV higher in energy than the indirect one. This energy difference is further reduced by adding small contents of tin(Sn). The direct bandgap energies and the indirect ones decrease with higher atomic number as shown in the following table.

The comparison shows that the direct transition energy shrinks much stronger than the indirect one expecting a direct bandgap group IV semiconductor at about 10 % Sn content GeSn.

In this paper we report about epitaxial growth, device processing and optical characterization. The direct optical transition is the dominant one even at small Sn contents, the peak position shifts to the infrared from 1550nm to more than 1700nm dependant also on the elastic strain status.

8628-19, Session 7

Heterogeneous optoelectronic integration using locally polymerized imprinted hard mask

Avantika Sodhi, Samuel J. Beach, Luis Chen, Univ. of California, Santa Barbara (United States); Matt Jacob-Mitos, Jonathan E. Roth, Aurion, Inc. (United States); Luke Theogarajan, Univ. of California, Santa Barbara (United States)

This paper presents a novel technique for the integration of Complementary Metal-Oxide Semiconductor (CMOS) chip with Photonic Integrated Circuit (PIC). This proposed technique is demonstrated by integrating a PIC comprising of 2X2 optical switches and a CMOS header processor, implemented in the IBM 130nm CMOS technology. The processor configures the switch fabric on the PIC allowing for the design of ultra-fast low-power optical packet switching. An innovative CMOS chip based imprinted hard mask technique, utilizing a heat curable Polydimethylsiloxane (PDMS), allows for accurate microfabrication of wafer-scale sockets. The fabricated sockets in the PIC are at-most 9um larger than the chip on all sides. Accurate alignment between chips is achieved by using bottom side contact lithography printer to pattern alignment marks on the backside of the chip, making the process insensitive to chip size variations. Independent temperature control of the arm and the stage in the flip-chip bonder enables localized polymerization of PDMS to form imprinted hard mask for integration of PIC with more than one CMOS chip, enabling seamless multichip integration. The horizontal gap and the vertical displacement between the chip and the PIC were 7 and 0.5 um respectively. Electrical connections between the CMOS chip and the PIC were patterned and tested both electrically and optically. These measurements show that the functionality of the PIC and the CMOS chip were not affected by the integration process.

8628-20, Session 7

InP-PD integration on silica-based PLC for QPSK receiver (*Invited Paper*)

Mikitaka Itoh, NTT Photonics Labs. (Japan)

No Abstract Available.

8628-21, Session 7

Fabrication of high-efficiency heterogeneous Si/III-V integration and optical vertical interconnect access

Doris K. Ng, Jing Pu, Qian Wang, Kim-Peng Lim, Yongqiang Wei, Yadong Wang, Yicheng Lai, Seng-Tiong Ho, A*STAR - Data Storage Institute (Singapore)

Silicon nanophotonic platform based on a silicon-on-insulator(SOI) substrate enables dense photonic integration due to transparency for light propagation and ultra-high refractive index contrast for light confinement. The usual heterogeneous integration scheme makes use of evanescent field of propagating optical mode in SOI nano-waveguide to interact with the optical gain medium in a III-V bonded layer[1–3]. Here, we consider a different heterogeneous integration platform in which light is basically confined in the III-V bonded layer and coupled to the silicon nanophotonic layer through an optical vertical interconnect access. This design have higher light energy confinement and a short optical vertical interconnect access[4]. We present the fabrication of this heterogeneous Si/III-V integration and vertical optical interconnect access which consist of passive silicon nanophotonic device processing, III-V semiconductor layer bonding on the silicon substrate, and fabrication and alignment of III-V nano-devices on top of the passive nano-devices. To ensure optimal performance, three critical fabrication process modules and their transition towards the next fabrication stage: 1)obtaining maximum bonded areas during direct wafer bonding of SOI strip nano-waveguides with the III-V gain medium, 2)precise alignment of III-V nano-devices on top of the passive SOI strip nano-waveguides and 3)vertical sidewall etch profile from the etching of Si and III-V devices. The device fabricated is characterized through Si/III-V waveguide propagation loss and coupling efficiency of the optical vertical interconnect access. The realization of this heterogeneous Si/III-V integration platform will open up enormous opportunities for photonic system on silicon through integrating various active and passive devices.

References

- [1] A. W. Fang, H. Park, O. Cohen, R. Jones, M. J. Paniccia, and J. E. Bowers, “Electrically pumped hybrid AlGaInAs-silicon evanescent laser”, *Optics Express*, Vol. 14 (20), 9203 (2006)
- [2] Y. D. Wang, Y. Q. Wei, Y. Y. Huang, Y. M. Tu, D. K. T. Ng, C. W. Lee, Y. N. Zheng, B. Y. Liu, and S. T. Ho, “Silicon/III-V Laser with Super-Compact Diffraction Grating for WDM Applications in Electronic-Photonic Integrated Circuits”, *Optics Express* 19, 2006-2013 (2011).
- [3] Yunan Zheng, Doris Keh-Ting Ng, Yongqiang Wei, Yadong Wang, Yingyan Huang, Yongming Tu, Chee-Wei Lee, and Seng-Tiong Ho, “Electrically-Pumped Heterogeneously Integrated Si/III-V Evanescent Lasers with Micro-Loop Mirror Reflector”, *Applied Physics Letters* 99, 011103 (2011).
- [4] Qian Wang, Doris Keh-Ting Ng, Yadong Wang, Yongqiang Wei, Jing Pu, Payam Rabiei, and Seng Tiong Ho, “Compact High-efficiency Heterogeneous Si/III-V Integration and Optical Vertical Interconnect Access”, *Optics Express* 20, 16745 (2012).

8628-22, Session 8

Analysis of high-bandwidth low-power microring links for off-chip interconnects (*Invited Paper*)

Noam Ophir, Keren Bergman, Columbia Univ. (United States)

Performance scalability of computing systems built upon chip multiprocessors are becoming increasingly constrained by limitations in power dissipation, chip packaging, and the data throughput achievable by the interconnection networks. In particular, today's systems based on electronic interconnects suffer from a growing memory access bottleneck as the speed at which processor-memory data can be communicated out of the chip package is severely bounded. Silicon photonics provide a CMOS-compatible solution for integrating high bandwidth-density off-chip optical I/O which can overcome some of these packaging limitations while adhering to pJ/bit-scale power efficiency requirements. Microrings in particular pose an attractive option for realizing optical communication functionalities due to their low footprint, low power dissipation, and inherent WDM-suitability due to their wavelength-localized operation. We analyze a terabit-per-second scale microring-based optical WDM link composed of current best-of-class devices. Our analysis provides quantitative measures for the maximal achievable bandwidth per link that could be reasonably realized within several years. We account for the full optical power budget to determine the achievable bandwidth as well as to enable a power consumption analysis including transmit and receive circuitry, photonic-device power dissipation, and laser power. The results highlight key device attributes that require significant advancement and point out the need for improvements in laser wall-plug efficiencies to provide sub-pJ/bit scale optical links.

8628-23, Session 8

Tunable InP ring resonator filters

Anna Tauke-Pedretti, Gregory A. Vawter, Erik J. Skogen, Gregory M. Peake, Mark Overberg, Charles Alford, David Torres, Florante Cajas, Sandia National Labs. (United States)

Optical channelizing filters with narrow linewidths are of interest for optical processing of microwave signals. Fabrication tolerances make it difficult to exactly place the optical resonance within the approximate 1 GHz tolerance required for many applications. Therefore, efficient tuning of the filter resonance is essential. In this paper we present a tunable ring resonator filter with an internal integrated semiconductor optical amplifier (SOA) fabricated on an InP-based platform. The ring resonance is tuned over 37 GHz with just 0.2 mA of current injection into a passive phase section. The use of current injection is more efficient than thermal tuning using heaters making them useful for low-power applications. The single active ring resonator has a Q of 129,000 with a linewidth less than 1.5 GHz and shows greater than 16 dB of extinction between on and off resonance. The effects of SOA internal ring gain on extinction and linewidth will be shown. We will show agreement between our experimentally demonstrated devices and simulations. The simulations are then expanded to optimize SOA design for low signal to noise ratios and large dynamic range. The integration of the active and passive regions are done using quantum well intermixing and the resonators utilize a buried heterostructure waveguides. The fabrication process of these filters is compatible with the monolithic integration of DBR lasers and high speed modulators enabling single chip highly-functional photonic integrated circuits for the channelizing of RF signals.

8628-24, Session 8

Integrated nanodisk plasmonic laser: design and simulation

Qian Wang, A* STAR - Data Storage Institute (Singapore)

A nanoplasmonic laser with a deep sub-wavelength physical size can have various applications, for example, in intra-chip optical interconnection, near field optical sensing, and high density data storage. An integrated nano-disk plasmonic laser on silicon substrate is considered in this paper. It uses the III-V semiconductor as the gain medium, which is compatible with current photonic integration technology and has a much smaller foot-print as compared to the existing nanoplasmonic laser structure, e.g., Fabry-Perot cavity based. To design and simulate this integrate nanodisk plasmonic laser, we developed a comprehensive but fast simulation approach with body-of-revolution finite-difference-time-domain incorporating with the Drude model for the metal and multi-level/multi-electron model for the gain medium. This simulation approach can provide a temporal and three-dimensional spatial electromagnetic simulation of the lasing performance.

With this simulation platform, we designed a nanodisk plasmonic cavity having a resonance wavelength ~ 1450 nm through analysing the impact of different geometry parameters, like the radius, the thickness of top cladding layer, and thickness of silicon dioxide interlayer used for bonding the III-V semiconductor on silicon substrate. With this designed nanodisk plasmonic cavity and a proper gain medium which can provide maximal gain at the resonant wavelength of the nanodisk cavity, a semiconductor nanodisk plasmonic laser with a radius of 100 nm and height of 300 nm (200 nm multiple quantum wells and barriers, and 100 nm thick) is numerically demonstrated. Simulation results give the mode profile, lasing spectrum and the relationship between pumping and emitting power of the laser.

8629-2, Session 1

Controlled photonic manipulation of proteins and other biological materials (*Invited Paper*)

David Erickson, Cornell Univ. (United States)

The ability to controllably handle the smallest materials is a fundamental enabling technology for nanoscience. Conventional optical tweezers have proven useful for manipulating microscale objects but cannot exert enough force to manipulate dielectric materials smaller than about 100 nm. Here, we have developed a new form of photonic crystal "nanotweezer" that can trap and release on-command Wilson disease proteins, quantum dots, and 22-nm polymer particles with a temperature rise less than ~0.3 K, below the point where unwanted fluid mechanical effects will prevent trapping or damage biological targets. Commercial aspects of the system will also be discussed.

8629-3, Session 1

Silicon photonics for functional on-chip optical tweezers devices and circuits (*Invited Paper*)

Hong Cai, Jia W. Wang, Andrew W. Poon, Hong Kong Univ. of Science and Technology (Hong Kong, China)

Pioneered by A. Ashkin and colleagues in the 1970s and 1980s, the technique of optical tweezers utilizing optical force to trap and precisely control micron-sized particles has been successfully applied in the biological sciences. In recent years, extending the optical tweezers technique for on-chip applications using optical near field of planar optical devices has been attracting a lot of research interests. Among various integrated photonics technology platforms, silicon photonics offer the key merits of strong optical surface fields in a compact footprint, along with mature fabrication processes for integrating photonic, electronic and fluidic devices on the same silicon chip. Therefore, silicon photonics technology is one promising candidate to develop functional on-chip optical tweezers devices for lab-on-a-chip applications. In order to further enhance the optical near field for trapping and to enrich the functionalities for such kind of optical manipulation devices, a number of research groups have recently proposed and demonstrated various waveguide-based and micro/nano-resonator-based optical manipulation devices, in which particles and even biological systems are optically manipulated using the enhanced optical fields in structures such as slot-waveguides and resonance-enhanced optical fields in resonators upon certain laser wavelengths.

In this paper, we will review our progress in developing various microparticle optical manipulation devices on silicon-nitride-on-silica substrates. On the waveguide-based optical manipulation front, we will review our progress in microparticle splitters using multimode-interference-based power splitters and planar optical tweezers using waveguide junctions. On the microresonator-based optical manipulation front, we will review our progress in microring-based microparticle add-drop devices and microdisk-based microparticle trapping devices. The combination of silicon photonic waveguide- and microresonator-based particle manipulation devices enables a wide selection in device designs and flexibility in choosing the operation wavelengths, and thus promise functional on-chip optical-tweezers devices and circuits.

8629-4, Session 1

Ring-resonator based SOI biosensors (*Invited Paper*)

Peter Bienstman, Sam Werquin, Cristina Lerma Arce, Univ. Gent (Belgium); Daan Witters, Robert Puers, Jeroen Lammertyn, KULeuven (Belgium); Tom Claes, Elewout Hallynck, Jan-Willem

Hoste, Daan Martens, Univ. Gent (Belgium)

In this presentation, we will discuss our latest progress in the field of silicon photonics biosensing, including a sensor based on a Vernier cascade of ring resonators with integrated spectrum analyser for cheap readout. Also, TE/TM resonators will be discussed, which can be used to determine the thickness and the refractive index of bilayers separately, and which therefore can be used to measure conformational changes in molecules. We also report on the integration of these types on sensors with a droplet-based microfluidic system, as well as on active techniques to compensate the peak splitting in ring spectra based on interferometric approaches.

8629-5, Session 1

Monolithic silicon interferometric optoelectronic devices for label-free multi-analyte biosensing applications (*Invited Paper*)

Konstantinos Misiakos, Eleni Makarona, Alex Salapatas, Ioannis Raptis, Aimilia Psarouli, Sotirios E. Kakabakos, Panayiota Petrou, National Ctr. for Scientific Research Demokritos (Greece); Marcel Hoekman, LioniX BV (Netherlands); Remco Stoffer, Phoenix B.V. (Netherlands); Kari Tukkiemi, VTT Information Technology (Finland); Gerhard Jobst, Jobst Technologies GmbH (Germany)

Despite the advances in optical biosensors, more progress is needed before they become commercially available for point of need determinations. Two are the main challenges: the inherent inability of most sensors to integrate the optical source in the transducer chip, and the need to specifically design the optical transducer per application. In this work, the development of a radical interferometric biochip is demonstrated based on a monolithic optocoupler array fabricated by standard Si-technology and suitable for multi-analyte detection. In the all-silicon array of transducers, each optocoupler has its own excitation source but all ten of them share a common detector. The light emitting devices (LEDs) are silicon avalanche diodes biased beyond their breakdown voltage and emit in the VIS-NIR part of the spectrum. The LEDs are coupled to individually functionalized optical interferometric waveguides all converging to a single detector for multiplexed operation. The integrated nature of the basic biosensor scheme and the ability to functionalize each transducer independently allows for the development of miniaturized optical transducers tailored towards multi-analyte tests. Encapsulation with an appropriate microfluidic system allowed for the easy delivery of the samples and ensured the facile contact with the external low-noise electronic components. The proposed device can be used interchangeably for the monitoring of a plethora of bio/chemical interactions becoming thus a versatile analytical tool. The interferometric biochip was successfully applied in bioassays and binding in a real-time and label-free format was tested with sensitivities down to 10 pM.

8629-6, Session 2

Bioinspired optofluidic lasers for DNA and protein detection (*Invited Paper*)

Xingwang Zhang, Univ. of Michigan (United States); Qiushu Chen, Univ of Michigan (United States); Mike Ritt, Sivraj Sivaramakrishnan, Xudong Fan, Univ. of Michigan (United States)

Optofluidic lasers combine the advantages of microfluidics and laser technology. Unlike traditional lasers, optofluidic lasers obtain the optical feedback from microfluidic channels with gain media (e.g., dyes) inside. Due to the small size of microfluidic channels, optofluidic lasers own unique capabilities in terms of handling liquid of pL~ μ L volumes. Therefore, there is currently a great deal of interest in adapting optofluidic lasers for compact laser light sources and micro-total-analysis systems. Here, we use two examples to demonstrate the feasibility of using

optofluidic lasers to sensitively detect DNA and protein. In the first example, the optofluidic laser is used to detect small conformational change in DNA Holliday junctions. The DNA Holliday junction has four branched double-helical arm structures, each of which is conjugated with Cy3 or Cy5 as the donor/acceptor pair. The conformational changes of the Holliday junction lead to the changes of fluorescence resonance energy transfer (FRET) between the donor and the acceptor. Using the optical feedback provided by the optofluidic laser, we are able to achieve nearly 100% wavelength switching. The FRET signal generated by the optofluidic laser is about 16 times more sensitive to DNA conformational changes than the conventional method. The second example is concerned with fluorescent proteins. By placing 4 μM of yellow fluorescent protein (YFP) inside the optofluidic laser cavity, we demonstrate lasing emission from YFP with a threshold of only 2 $\mu\text{J}/\text{mm}^2$. This work will potentially open a door to study protein-protein interactions via the sensitive intra-cavity laser detection method.

8629-7, Session 2

Biosensors based on nanoscale porous silicon waveguides and silicon photonic crystals (*Invited Paper*)

Sharon M. Weiss, Vanderbilt Univ. (United States)

Porous materials offer several advantages for chemical and biomolecular sensing applications. In particular, for optical sensing, pores allow target analyte to penetrate into the region of the structure where guided modes propagate, increasing the interaction between the target analyte and peak regions of the electric field and therefore increasing the detection sensitivity of the sensor. Moreover, porous materials possess a very large reactive surface area to facilitate the capture of target molecules, and they have the capability to selectively filter out contaminant molecules by size. This presentation will focus on the fabrication, functionalization, and sensing performance of porous silicon waveguides and silicon photonic crystal microcavities where we consider the air holes in the silicon photonic crystal lattice and defect region to be pores. Issues of efficient molecule infiltration and capture inside porous materials, binding kinetics in porous media, the influence of pore size on small molecule detection sensitivity, and how appropriate design can enable both an increase in quality factor and an increase in available surface area for sensing will be discussed.

8629-8, Session 2

Label-free silicon photonic biosensors for use in clinical diagnostics (*Invited Paper*)

Sahba Talebi Fard, The Univ. of British Columbia (Canada); Shon A. Schmidt, Univ. of Washington (United States); Samantha M. Grist, Jonas Flueckiger, Wei Shi, Xu Wang, The Univ. of British Columbia (Canada); Daniel M. Ratner, Univ. of Washington (United States); Lukas Chrostowski, Valentina Donzella, The Univ. of British Columbia (Canada)

Silicon photonics devices are poised to revolutionize biosensing applications, specifically in medical diagnostics. Optical sensors are being created, specifically optimized for target biomarkers of interest, to improve clinically-relevant diagnostic assays. There are numerous approaches in designing such sensors such as improving the devices performance, increasing the interaction of light with the analyte, and matching the characteristics of the biomolecules by using architectures that complement the biosensing application. Using e-beam lithography and standard foundry processes, we have investigated TM and TE disk and ring resonators, with TM devices providing potential for higher sensitivity and large-particle sensing capabilities due to the increased penetration distance of light into the analyte. In addition, devices such as slot-waveguide Bragg grating sensors have shown high sensitivities and high quality factors and may present advantages for specific biosensing applications. These devices have been investigated for wavelengths

around both $\lambda=1550$ nm (conventional wavelength window in fiber-optic communication) and $\lambda=1220$ nm, where the water absorption is greatly decreased, offering improved limits of detection. Using reversibly bonded PDMS microfluidic flow cells, the performance and bio-detection capabilities of these devices have been characterized. Comparing binding performance across these sensors will help determine which is most appropriate for accurately sensing each biomolecule of interest in complex media. The most promising sensors for each application will then be identified for further study and development. This paper will discuss the sensors comparative advantages for different applications in biosensing and provide an outlook for future work in this field.

8629-9, Session 2

Nanofluidic chips for DNA detection (*Invited Paper*)

Anders Kristensen, Rodolphe Marie, Jonas N. Pedersen, Christopher J. Lüscher, Kristian H. Rasmussen, Lasse H. Thamdrup, Anil H. Thiisted, Johan Eriksen, Henrik K. Flyvbjerg, Technical Univ. of Denmark (Denmark)

The entropic confinement of DNA in nanofluidic devices – where the DNA is localized and stretched but not tethered to a surface – is a powerful tool for manipulating single DNA molecules. In particular, measuring physical or genomic properties such as sequence mapping of single molecules is made possible by confining DNA in nanochannels and imaging by fluorescence microscopy. Loading a human sample, e.g. from a cell culture is a major step toward realizing the potential of a nanofluidic Lab-on-a-Chip for genomics. In particular, extracting and visualizing long DNA molecules would be highly desirable for the mapping of long range features on the genome. We address this challenge by extracting DNA through proteolysis of metaphase chromosomes on the chip and DNA manipulation activated by light induced local heating (LILH). We present a nanoimprinted polymer chip with a thin near-infrared absorber layer that enables light-induced local heating (LILH) of liquids inside micro- and nanochannels. An infrared laser spot and corresponding hot-spot could be scanned across the device. A single chromosome was immobilized in a hydrogel plug formed by a hot-spot, and protease K was introduced in the microfluidic channel for DNA extraction in the plug. Large temperature at gradients at the hot-spot yielded thermophoretic forces, which were used to manipulate and stretch individual DNA molecules confined in nanochannels.

8629-10, Session 3

Ultracompact polarization diversity components for future large-scale photonic integrated circuits on silicon (*Invited Paper*)

Daoxin Dai, Zhejiang Univ. (China)

Various silicon nano-photonic waveguides make silicon photonics very promising to realize large-scale photonic integrated circuits (PICs) for the future optical network-on-chip. The giant birefringence of silicon nano-photonic waveguides makes that silicon nano-PICs usually have severe polarization-dependent issue. Polarization-diversity technology is a well-known general solution to solve this problem. The key devices for polarization-diversity circuits include polarizers, polarization-beam splitters (PBSs), as well as polarization rotators, which are also very important for many other applications, e.g., coherent optical communications, and polarization (de)multiplexing systems. On the other hand, the giant birefringence of silicon nano-photonic waveguides also helps achieve ultracompact polarization-handling devices. In this paper, we give a review for our recent work on ultrasmall polarizers, PBS, as well as polarization rotators on silicon. First, small TE-passed silicon polarizer is presented by utilizing the mode hybridization effect in a straight shallowly-etch silicon-on-insulator (SOI) ridge waveguide. Second, three types of ultrasmall PBSs based on silicon-on-insulator (SOI) nanowires are proposed and their design rules are given. These PBSs are based on

asymmetrical evanescent coupling systems, e.g., a directional coupler with nano-slot waveguide and SOI strip nanowire, a bent directional coupler, and a three-waveguide coupler. Such asymmetrical evanescent coupling systems are presented as a better option than a symmetrical coupling system when used for realizing small PBSs because of the larger bandwidth, smaller foot-print and larger fabrication tolerance. Thirdly, a novel concept for an ultracompact polarization splitter-rotator is proposed by utilizing mode evolution in an adiabatic taper and the evanescent coupling in an asymmetrical directional coupler. The mechanism of the mode evolution in an adiabatic taper and the taper design is also discussed.

8629-11, Session 3

Deeply etched MMI-based components on 4 μm thick SOI for SOA-based optical RAM cell circuits

Matteo Cherchi, Sami Ylinen, Mikko Harjanne, Markku Kapulainen, Timo Aalto, VTT Technical Research Ctr. of Finland (Finland); George T. Kanellos, Foundation for Research and Technology-Hellas (Greece); Dimitrios Fitsios, Foundation for Research and Technology-Hellas (Greece) and Aristotle Univ. of Thessaloniki (Greece); Nikos Pleros, Aristotle Univ. of Thessaloniki (Greece)

We present novel deeply etched functional components, fabricated by multi-step patterning in the frame of our 4 μm thick Silicon on Insulator (SOI) platform based on singlemode rib-waveguides and the previously developed rib-to-strip converter. These novel components include Multi-Mode Interference (MMI) splitters with any desired splitting ratio, wavelength sensitive 50/50 splitters with pre-filtering capability, multi-stage Mach-Zehnder Interferometer (MZI) filters for suppression of Amplified Spontaneous Emission (ASE), and MMI resonator filters. These novel building blocks enable functionalities otherwise not achievable on our SOI platform, and make it possible to integrate optical RAM cell layouts, by resorting to our technology for hybrid integration of Semiconductor Optical Amplifiers (SOAs). Typical SOA-based RAM cell layouts require generic splitting ratios, which are not readily achievable by a single MMI splitter. We present here a novel solution to this problem, which is very compact and versatile and suits perfectly our technology. Another useful functional element when using SOAs is the pass-band filter to suppress ASE. We pursued two complimentary approaches: a suitable interleaved cascaded MZI filter, based on a novel suitably designed MMI coupler with pre-filtering capabilities, and a completely novel MMI resonator concept, to achieve larger free spectral ranges and narrower pass-band response.

Simulation and design principles are presented and compared to preliminary experimental functional results, together with scaling rules and predictions of achievable RAM cell densities.

When combined with our newly developed ultra-small light-turning concept, these new components are expected to pave the way for high integration density of RAM cells.

8629-12, Session 3

Bend-size reduction on the SOI rib waveguide platform

Timo Aalto, Matteo Cherchi, Mikko Harjanne, Sami Ylinen, Markku Kapulainen, VTT Technical Research Ctr. of Finland (Finland)

The minimum bending radius of optical waveguides is typically the most important parameter that defines the footprint and cost of a photonic integrated circuit. In optical fibers and in planar waveguides with equally large mode fields ($\sim 10 \mu\text{m}$) the bending radii are typically in the cm-scale. The main advantage of using a high index waveguide core with

a thickness below 1 μm is the ability to realise single-mode bends with bending radii of just a few micrometers.

In this paper we first discuss the dependence of the minimum bending radius on the size and shape of silicon-on-insulator (SOI) waveguides. Then we present simulation and measurement results from advanced waveguide bends and mirrors that have been integrated with 4-10 μm thick single-mode SOI waveguides. The results are compared with those achieved with other waveguides, including sub- μm SOI waveguides. We show that multi-step patterning and novel designs allow the reduction of the bending radius by up to three orders of magnitude while also reducing the bending losses by approximately one order of magnitude when compared to traditional rib waveguide bends on 4 μm SOI. This allows to use the μm -scale SOI waveguides for making almost as compact photonic integrated circuits as those based on sub- μm SOI waveguides. As a highlight of our effort in footprint reduction we present a novel concept for turning light 90° or 180° with an effective bending radius down to 1.5 μm and a bending loss down to 0.05 dB per bend.

8629-13, Session 3

Fabrication of low-loss silicon nanophotonic waveguide for photonic device integration

Doris K. T. Ng, Kim-Peng Lim, Qian Wang, Jing Pu, Kun Tang, Yicheng Lai, Chee-Wei Lee, Seng-Tiong Ho, A*STAR - Data Storage Institute (Singapore)

Silicon-on-insulator platform can enable multifunctional photonic system on chip based on sub-micron light confinement and III-V semiconductor heterogeneous integration. As the basic building block, the silicon nanophotonic waveguide requires low-loss propagation for high-performance ultra-compact photonic device. Commonly reported nano-waveguides uses Poly-MethylMethAcrylate(PMMA)[1] or hydrogen silsesquioxane(HSQ)[2] as a direct mask for Si nano-waveguides fabrication, which are not suitable in the case of heterogenous III-V semiconductor integration on silicon as direct[3-4] or interlayer bonding[5] of Si with III-V compound is required. For high quality bonding, most Si on the passive device region should remain to serve as a sturdy platform for bonding. A negative mask like HSQ will not be able to achieve this as most Si areas will be removed after the waveguides are formed. Also, the high temperature plasma during Si etching will overheat the resist mask, causing stubborn residues of burnt resist on the Si surface after etching. This will greatly affect the bonding results. Hence, for application of III/V integration on Si towards high power Si photonics integrated devices, a hard mask is required for fabrication of Si nano-waveguides. We experimentally study SiO₂ grown by two different methods (thermal oxidation and PECVD) to be used as hard masks for Si nano-waveguides fabrication and study their effects on propagation loss. Si nano-waveguides fabricated using thermally grown SiO₂ as hard mask exhibit a lower loss compared to having PECVD SiO₂ as hard mask. Combined with wet chemical cleaning at 330C, the loss reduction is brought further down to around 1 dB/cm.

References

- [1] Yurii A. Vlasov, and Sharee J. McNab, "Losses in single-mode silicon-on-insulator strip waveguides and bends", Optics Express, Vol. 12, 1622 (2004)
- [2] M.Gnan, S. Thoms, D. S. Macintyre, R. M. De La Rue and M. Sorel, "Fabrication of low-loss photonic wires in silicon-on-insulator using hydrogen silsesquioxane electron-beam resist", Electronics Letters, Vol. 44, No. 2 (2008)
- [3] Y. D. Wang, Y. Q. Wei, Y. Y. Huang, Y. M. Tu, D. K. T. Ng, C. W. Lee, Y. N. Zheng, B. Y. Liu, and S. T. Ho, "Silicon/III-V Laser with Super-Compact Diffraction Grating for WDM Applications in Electronic-Photonic Integrated Circuits", Optics Express 19, 2006-2013 (2011).
- [4] Yunan Zheng, Doris Keh-Ting Ng, Yongqiang Wei, Yadong Wang, Yingyan Huang, Yongming Tu, Chee-Wei Lee, and Seng-Tiong Ho, "Electrically-Pumped Heterogeneously Integrated Si/III-V Evanescent Lasers with Micro-Loop Mirror Reflector, Applied Physics Letters 99, 011103 (2011).
- [5] Yadong Wang, Doris Keh-Ting Ng, Qian Wang, Jing Pu, Chongyang

Liu, and Seng-Tiong Ho, "Low Temperature Direct Bonding of InP and Si₃N₄-coated Silicon Wafers for Photonic Device Integration", Journal of The Electrochemical Society, Vol. 159, H507 (2012).

8629-14, Session 4

Integration of silicon photonics into electronic processes (*Invited Paper*)

Jason S. Orcutt, Rajeev J. Ram, Vladimir Stojanovic, Massachusetts Institute of Technology (United States)

Front-end monolithic integration has enabled photonic devices to be fabricated in bulk and thin-SOI CMOS as well as DRAM electronics processes. Utilizing the CMOS generic process model, integration was accomplished on multi-project wafers that were shared by standard electronic customers without requiring in-foundry process changes. Simple die or wafer-level post-processing has enabled low-loss waveguides by the removal of the substrate within photonic regions. The custom-process model of the DRAM industry instead enabled optimization of the photonic device fabrication process and the potential elimination of post-processing requirements. Integrated single-crystalline silicon waveguide loss of ~3 dB/cm has been achieved within a 45nm thin-SOI CMOS process that is currently used to manufacture microprocessors. A fully monolithic photonic transmitter including a pseudo-random bit sequence (PRBS) generating digital backend was also demonstrated within this process. The constraints of zero-change integration have limited achieved polysilicon waveguide loss to ~50 dB/cm with commercially available bulk CMOS processes. Custom polysilicon deposition and processing conditions available for DRAM integration have also led to the demonstration of ~6 dB/cm loss waveguides suitable for integration within electronics processes utilizing bulk silicon starting substrates. An overview of required process features, device design guidelines and integration methodology tradeoffs will be presented. Relevant device metrics of area and energy efficiency as well as achievable photonic device performance will be presented within the context of monolithic front-end integration within state-of-the-art electronics processes. Applications of this research towards the implementation of a computer system utilizing photonic interconnect for core-to-memory communication will also be discussed.

8629-15, Session 4

Ion beam irradiation induced fabrication of vertical coupling photonic structures

Haidong Liang, Vanga S. Kumar, Jianfeng Wu, Mark Breese, National Univ. of Singapore (Singapore)

Two layer vertical coupling photonic structures can be directly fabricated on a standard SOI wafer using a combination of reactive ion etching (RIE) and proton beam irradiation followed by electrochemical etching. The top layer structures are defined by RIE on the device layer, which is the same process used for normal two dimensional photonic structure fabrication, while the bottom layer structures are defined by proton beam irradiation on the substrate. Light coupling between the structures in the two layers has been demonstrated via vertical coupling waveguides. According to simulations, the coupling efficiency mainly depends on the thickness of the two layer structure and the gap between them. In this process, the thickness of the top layer structures is fixed by the device layer thickness of the SOI wafer, which is typically 200-300 nm. The gap depends on the thickness of the oxide layer of the SOI wafer, and it can be shifted due to the natural bending of the top layer structures. The bottom layer structure thickness can vary due to different energies of proton beam. Furthermore we show the fabrication of tapered bottom waveguides, which are thin at the coupling region for higher coupling efficiency, and thick at the end for easily coupling light from an optical fiber or a focused lens.

8629-16, Session 4

Highly efficient DBR in silicon waveguides with eleventh order diffraction

Harish Sasikumar, Deepa Venkitesh, Bijoy K. Das, Indian Institute of Technology Madras (India)

The Distributed Bragg Reflectors (DBRs) play a major role in implementing the wavelength-selective functionalities in integrated optics. Due to the recent advances of silicon photonics and CMOS electronics in SOI platform, various types of DBR structures are being investigated for integrated optical couplers, filters, (de-) multiplexers, Fabry-Perot micro-cavities and laser resonators. The first-order diffraction gratings in SOI waveguide require surface relief grating period of ~ 225 nm for a reflection peak at ~ 1550 nm. Fabrication of such sub-micron gratings with uniform periodicity over a length of several mm is really a challenging issue.

Here we report the demonstration of an eleventh order Bragg grating ($\Lambda \sim 2.5 \mu\text{m}$, $\lambda \sim 1565$ nm, $L \sim 5$ mm) on the surface of single-mode rib waveguides. The DBRs and waveguide structures were separately defined by conventional photolithography and subsequent reactive ion etching processes. Waveguide end-facets were polished suitably for optical characterization. The characterizations were carried out using a tunable laser source (tuning resolution ~ 1 pm) in our free-space waveguide coupling setup. The DBRs showed a typical reflectivity of 85% and FWHM ~ 2.5 nm. Higher reflectivity and narrower spectral response can be achieved by increasing the grating length further. It is worth mentioning that the waveguide loss has been increased (~ 0.5 dB/mm) because of the enhanced surface roughness during the Reactive Ion Etching (RIE) process for grating fabrication. It can be reduced if conventional RIE is replaced by ICP RIE.

8629-17, Session 4

Experimental demonstration of 2D photonic crystal, triangular lattice, small angle, low loss Y-Splitter at microwave frequencies

Deepak Kaushal, Robert C. Gauthier, Carleton Univ. (Canada)

A Photonic crystal is a low loss periodic dielectric medium that prevents the flow of light in certain directions for specified frequencies. The availability of low loss waveguide bends in photonic crystal structures makes possible numerous integrated optic devices. The method proposed in this presentation consists of introducing a dielectric shift equivalent to a sheer displacement along a segment of the PhC waveguide and results in a double bent waveguide. The degree of sheer determines the waveguide deflection angle and can extend up to several degrees. As a result of the sheer, the input and output segments of the waveguides are laterally offset relative to each other but remain parallel. Theoretical analysis is performed using FDTD and PWM and predicts low loss bends in the both the square and triangular arrays composed of high dielectric rods in an air background. Micro-fabrications of complex photonic crystal are quite difficult to achieve but models can easily be constructed in the microwave regime at much larger length scale of centimeters. Experiments are performed in the microwave regime using an array of alumina rods in air over the 2 to 14 GHz range. In particular detailed experiments were performed for the TM polarization for triangular lattice in order to obtain information on bend loss versus sheer displacement and waveguide offset angle and show that low losses are achievable for deflection up to 20 degrees. Additional experimental results indicate that low loss Y splitter can also be produced using the same technique and can find applications in integrated optical waveguide devices such as optical sensors, switching and Mach-Zehnders.

8629-18, Session 4

Mid-infrared photonics devices in SOI (*Invited Paper*)

Goran Z. Mashanovich, Milos Nedeljkovic, Univ. of Southampton (United Kingdom); Milan M. Milosevic, Univ. of Surrey (United Kingdom); Youfang Hu, Taha M. Ben Masaud, Ehsan Jaberansary, Xia Chen, Univ. of Southampton (United Kingdom); Michael J. Strain, Marc Sorel, Univ. of Glasgow (United Kingdom); Anna C. Peacock, Harold M. H. Chong, Graham T. Reed, Univ. of Southampton (United Kingdom)

The mid-infrared wavelength region (3-20 μm) offers several application areas. In this paper we present silicon photonics devices designed for the 3-4 μm wavelength region including waveguides, MMIs, ring resonators, Mach-Zehnder interferometers, and multiplexers. The devices are based on silicon on insulator (SOI) platform. We show that 400-500 nm high silicon waveguides can have the propagation loss as low as ~ 4 dB/cm at 3.8 μm . We also demonstrate MMIs with insertion loss of 0.2 dB, high extinction ratio asymmetric Mach-Zehnder interferometers, and SOI ring resonators and multiplexers. This combined with our previous results reported at 3.4 μm confirm that SOI is a viable platform for the 3-4 μm region and that low loss mid-infrared passive devices can be realised on it.

8629-19, Session 4

Silicon slot waveguides and their rigorous characterizations

Azizur Rahman, David Leung, Namassivaye Kejalakshmy, City Univ. London (United Kingdom); Long To, City Univ. of Hong Kong (Hong Kong, China)

When the dimensions of an optical waveguide are much smaller than the operating wavelength, unique materials and structural dependent properties can be observed [1] and these recently have been receiving much attention [2]. In this regard, silicon has been particularly attractive as the low-cost and mature CMOS fabrication technology widely used in the electronics industry can be exploited. The strong discontinuity of high index contrast of silicon allows light confinement in low-index region. The access of high field intensity in the low-index region allows design of highly efficient optical sensors and various nonlinear photonic devices. A rigorous H-field based full-vectorial modal analysis has been carried out, which can more accurately characterize the abrupt dielectric discontinuity of a high index contrast optical waveguide. As a result, the full-vectorial H and E-field and the Poynting vector profiles can be shown in detail. Design of vertical slots supporting TE modes and horizontal slots supporting TM modes, and novel photonic devices incorporating such slots will be presented. Results for novel cross-slot will also be presented.

1] D M H Leung, et al., Rigorous modal analysis of silicon strip nanoscale waveguides, *Optics Express*, vol. 18, pp.8528-8539, 2010.

2] D M H Leung, et al., Numerical analysis of asymmetric silicon nanowire waveguide as compact polarization rotators, *IEEE Photonics Journal*, vol.3, p.381-389, June 2011.

8629-1,

Group IV photonics for the mid infrared

Richard Soref, Univ. of Massachusetts Boston (United States)

This talk outlines the challenges and benefits of applying silicon-based photonic techniques in the 2 to 5 μm mid-infrared (MIR) wavelength range for chem.-bio sensing, medical diagnostics, process control, environmental monitoring, secure communications, signal processing, and more. On-chip passive and active components, mostly waveguided,

will enable opto-electronic CMOS and photonic integrated circuits for MIR system-on-a-chip applications such as spectroscopy and lab-on-a-chip.

Active heterostructures employing Si, Ge, SiGe, GeSn and SiGeSn are key for laser diodes, photodetectors, LEDs, switches, amplifiers, and modulators that provide totally monolithic foundry integration, while a variety of III-V semiconductor MIR devices offer practical hybrid integration on Si PICs.

8629-20, Session 5

How will photonic integrated circuits develop? (*Keynote Presentation*)

Michael W. Haney, Univ. of Delaware (United States)

No Abstract Available.

8629-21, Session 6

Integrated silicon photonic devices for high-speed and low-power optical signal processing (*Invited Paper*)

Linjie Zhou, Xiaomeng Sun, Jingya Xie, Liangjun Lu, Zhi Zou, Yanyang Zhou, Lili Sun, Jianping Chen, Shanghai Jiao Tong Univ. (China)

We present micro-resonator based integrated silicon photonic devices for high-speed and low-power optical signal processing. Three resonator configurations corresponding to different resonance tuning mechanisms are used to realize active tuning. First, we investigate an active microdisk resonator whose resonance wavelength is tuned by the interleaved p-n junctions embedded along the disk rim. Forward and backward biases of the p-n junctions results in blue- and red-shift of the whispering-gallery modes of the microdisk. Due to its miniature size, the active microdisk resonator can be used as a high-speed and low-power optical filter or modulator. Second, we investigate a Mach-Zehnder interferometer (MZI) coupled microring resonator. High-speed push-pull electrodes are integrated in the MZI coupler, leading to a fast tuning of the resonance extinction ratio. As the coupling strength is changed instead of the resonance wavelength, the device can be used to implement unchirped modulation or low-dispersion optical delay. The third structure that we investigate is cascaded self-coupled optical waveguide (SCOW) resonators. Due to the mutual feedback between the SCOW resonators, the cascaded SCOW resonators can exhibit coupled-resonance-induced-transparency (CRIT) with a narrow resonance peak appearing in a broad opaque wavelength window. The CRIT peak can be tuned by an intrinsic thermal-heater made by the connection waveguide between the SCOW resonators. The CRIT effect can be used to implement optical delay and ultra-narrow band optical filters.

8629-22, Session 6

Reconfigurable 3D photonic crystal structure

Robert C. Gauthier, Carleton Univ. (Canada)

Several integrated optical circuits include photonic crystal based waveguides as key structures for light guidance and manipulation. Once the optical circuit fabricated, the performance and operation is dictated by "external" effects imposed on the propagated light (thermal, carrier injection, non-linearity, ...). In this presentation we explore the possibility of directly altering the waveguide configuration in a photonic crystal through a MEMS based equivalent of interdigitated fingers. One of the photonic crystals is formed from high dielectric rods in air while the other photonic crystal is composed of holes in the high dielectric substrate. The interdigitated nature of the proposed structure comes about by locating the rod and hole structure such that the rods fit inside the holes

and positioned through a flip chip configuration. The level of intrusion of the rods in the holes (overlap region) can be controlled through mechanical means. In the overlap region, the filling fraction is larger and defines a layer similar to that of a suspended membrane. Defects in one or both photonic crystals can be used to define resonators and waveguides and control over the level of meshing makes this waveguide structure reconfigurable. The presentation is focused on the theoretical aspects of the proposed design keeping in perspective current manufacturing limitations of 3-D optical circuits. The intent is to consider complimentary photonic crystals with square, triangular and higher order rotational symmetries such as the 8-fold and 12-fold quasi-crystals. Due to the free standing nature of the overlap region, the structure can be easily interfaced with optical fiber and other waveguides.

8629-23, Session 7

[λ]-size silicon-based modulator (Invited Paper)

Volker J. Sorger, The George Washington Univ. (United States) and Univ. of California, Berkeley (United States); Noberto D. Lanzillotti-Kimura, RenMin Ma, Univ. of California, Berkeley (United States); Xiang Zhang, Univ. of California, Berkeley (United States) and Lawrence Berkeley National Lab. (United States)

Electro-optic modulators have been identified as the key drivers for optical communication. With an ongoing miniaturization of photonic circuitries, an outstanding aim is to demonstrate an on-chip, ultra-compact, electro-optic modulator without sacrificing bandwidth and modulation strength. While silicon-based electro-optic modulators have been demonstrated, they require large device footprints of the order of millimeters as a result of weak non-linear electro-optical properties. The modulation strength can be increased by deploying a high-Q resonator, however with the trade-off of significantly sacrificing bandwidth. Furthermore, design challenges and temperature tuning limit the deployment of such resonance-based modulators. Recently, novel materials like Graphene have been investigated for electro-optic modulation applications with a 0.1 dB per micrometer modulation strength, while showing an improvement over pure silicon devices, this design still requires devices lengths of tens of micrometers due to the inefficient overlap between the Graphene layer and the optical mode of the silicon waveguide. Here we experimentally demonstrate an ultra-compact, Silicon-based, electro-optic modulator with a record-high 1dB per micrometer extinction ratio over a wide bandwidth range of 500 nm in ambient conditions. The device is based on a plasmonic Metal-Oxide-Semiconductor (MOS) waveguide, which efficiently concentrates the optical modes' electric field into a nanometer thin region comprised of an absorption coefficient-tuneable Indium-Tin-Oxide (ITO) layer. The modulation mechanism originates from electrically changing the free carrier concentration of the ITO layer. The seamless integration of such a strong optical beam modulation into an existing silicon-on-insulator platform bears significant potential towards broadband, compact and efficient communication links and circuits.

8629-24, Session 7

Silicon-organic hybrid devices (Invited Paper)

Luca Alloatti, Dietmar Korn, Joerg Pfeifle, Robert Palmer, Christian Koos, Wolfgang Freude, Juerg Leuthold, Karlsruher Institut für Technologie (Germany)

Silicon-organic hybrid (SOH) devices combine silicon waveguides with a number of specialized materials, ranging from third-order nonlinear molecules, to second-order nonlinear polymers, and liquid-crystals. Second-order nonlinear materials allow building high-speed and low-voltage electro-optic modulators, which are key components for future silicon-based photonics transceivers. We review our recent advances in high-speed data transmission experiments performed with SOH slot waveguides. Second-order nonlinear materials, moreover, allow creating

nonlinear waveguides for sum- or difference-frequency generation and lowest-noise optical parametric amplification. These processes are exploited in a large variety of applications, like the emerging field of on-chip generation of mid-IR wavelengths, and operate at pump powers significantly smaller than their third-order counterparts. In this work, we present the first SOH waveguide suited for second-order nonlinear processes. We show that our device can achieve 14 dB/cm amplification assuming a conservative $\chi^{(2)}$ -nonlinearity of 230 pm/V and a CW pump power as low as 20 dBm. By using liquid-crystal claddings instead, we show experimentally that phase shifters with record-low power consumption and ultra-low voltage-length product of $V\pi L = 0.085$ Vmm can be obtained when operated at optimum bias point.

8629-25, Session 7

40 Gb/s low-loss self-aligned silicon optical modulator

Melissa Ziebell, Delphine Marris-Morini, Gilles Rasigade, Univ. Paris 11 (France); Jean-Marc Fédéli, CEA-LETI (France); Eric Cassan, Laurent Vivien, Univ. Paris 11 (France)

In the near future, copper will not be able to keep up with the increasing demands of interconnect density, complexity, bandwidth and speed. Silicon photonics has the rationale of integrating electronic and photonic circuits on a same chip to provide high performance optical interconnects that carry more data and use less power. Among all the photonics devices, a high-speed and efficient silicon modulator is one of the most challenging components to design. As classical electro-optic effects used in III-V semiconductors or in Lithium-Niobate is weak in pure silicon, free-carrier concentration variation have been greatly studied in the last years. Refractive index change in silicon is then induced either by carrier accumulation, injection, or depletion.

We present the experimental results of an all-silicon optical modulator based on carrier depletion in a lateral PIPIN diode. By embedding a p-doped slit in the intrinsic region of the PIN diode, the best compromise between the effective index variation in the middle of the waveguide and the optical loss is obtained. The PIPIN design of the active region guarantees a reduction of optical loss as a large part of the waveguide is unintentionally doped. Phase modulation was changed to intensity modulation by integrating PIPIN diodes in both arms of a Match-Zehnder Interferometer. Self-aligned fabrication was used to define the active region accurately, and to guarantee maximum modulation efficiency. At 40 Gbit/s, the modulator provided a 6.6 dB extinction ratio, simultaneously with a 6 dB insertion loss at the operation point.

8629-26, Session 7

Waveguide integrated silicon avalanche photodetectors

Jason J. Ackert, Kyle Murray, Edgar Huante-Ceron, McMaster Univ. (Canada); Paul E. Jessop, Wilfrid Laurier Univ. (Canada); Andrew P. Knights, McMaster Univ. (Canada)

Avalanche photodetectors integrated with silicon waveguides suitable for use with wavelengths around 1550nm are currently realized with germanium [1]. Such devices produce excellent responsivity but require increasing fabrication complexity and suffer from high noise. We will present results from monolithic silicon avalanche photodetectors incorporated into a silicon waveguide. An all-silicon solution exhibits low noise, while having the significant advantage of a simple fabrication procedure. The detectors are composed of a p-i-n junction across a rib waveguide. Infrared absorption is increased by lattice defects, introduced to the intrinsic region with ion implantation. The structure of these detectors is similar to previous monolithic silicon devices; however no avalanche behaviour has previously been reported [2].

Initial measurements of a 200 μ m long detector show a responsivity of 0.2 A/W and a dark current of 20 nA with a reverse bias of 25 V. While at 10 V reverse bias the same device shows a responsivity of .01 A/W

with a dark current of 3 nA. We expect imminent measurements of more absorbent devices to show higher responsivity.

Upcoming work will examine the frequency response of the detectors. In addition, we will present work on the integration of these detectors with ring resonators, which offer very low noise and an excellent minimum detectable power.

References

1. S. Assesfa, F. Xia and Y. Vlasov "Reinventing germanium avalanche photodetector nanophotonic on-chip optical interconnects" *Nature* 464, 80-84 (2010).
2. D.F. Logan, P. Velha, M. Sorel, R.M. De La Rue, A.P. Knights and P.E. Jessop "Defect-enhanced Silicon-on-Insulator Waveguide Resonant Photodetector with High Sensitivity at 1.55 μm " *IEEE Photon. tech. Letters*, 22(20), 1530-1532 (2010).

8629-27, Session 7

Accurate high-speed eye diagram simulation of silicon-based modulators

Ching Eng J. Png, Vivek Dixit, Soon Thor Lim, A*STAR Institute of High Performance Computing (Singapore); Er Ping Li, A*STAR - Data Storage Institute (Singapore)

In recent years, high speed silicon optical modulators have garnered significant research interest, along with rapid performance improvements. A large number of such reported devices operate with multiple Gb/s regime, typically in excess of 10Gb/s. These devices rely largely on the carrier depletion effect commonly embedded into, but not entirely limited to, Mach-Zehnder Interferometers (MZI). A key factor to determine the performance of such devices, especially in GO/NO GO test is the high-speed eye diagram which reveals key information such as rise/fall times, extinction ratios, and jitter characteristics. However, in order to achieve realistic eye diagrams, actual fabricated device details such as topology and carrier induced losses must be encapsulated in the simulations.

Here, we accurately evaluate the performance of a silicon-based MZI device by simulating the eye diagram based on its inherent electrical and subsequent optical modeling of individual silicon depletion modulators. This methodology directly takes into account the characteristics of a modulated optical beam, constituting electrical parameters such as capacitance, conductance, and transitioning times to model time response, to obtain effective complex refractive index from optical simulations of the phase shifter arms of the MZI. In turn this simulates the phase change and resultant loss induced by each arm. This methodology is suitable for interferometer-based optical devices and has been applied to silicon-based depletion modulators at 10-, 40-Gb/s and demonstrated good agreement with experimental data. This development enables rapid design iterations with full accuracy and can be extended to other optical devices such as detectors and ring resonators.

8629-28, Session 7

Interferometric switching in CROW based reconfigurable optical device for routing application

Mattia Mancinelli, Paolo Bettotti, Univ. degli Studi di Trento (Italy); Jean-Marc Fédéli, CEA-LETI (France); Lorenzo Pavesi, Univ. degli Studi di Trento (Italy)

Silicon photonic routers based on Coupled Resonator Optical Waveguides (CROW) for interferometric switching are explored. A novel switching device based on two bus interferometric CROW resonant structures is experimentally investigated. A signal is split along two arms: the relative phase is controlled by a local heater. The two signals are input in the input and add ports of a CROW. The CROW is fabricated on a SOI wafer by deep-UV lithography. CROW with 2,4,6, 8 cascaded resonators are studied. It is demonstrated that depending on the phase of the two

input signals, the CROW behaves as a reconfigurable interleaver or as a splitter. This device extends the functions of the add-drop filter with a wide-range of switching behaviours which might lead to new interesting applications.

8629-29, Session 8

Low-loss high-speed silicon Mach-Zehnder modulator for optical-fiber telecommunications (*Invited Paper*)

Kensuke Ogawa, Kazuhiro Goi, Hiroyuki Kusaka, Yoshihiro Terada, Fujikura Ltd. (Japan); Tsung-Yang Liow, Xiaoguang Tu, Guo-Qiang Lo, Dim-Lee Kwong, A*STAR Institute of Microelectronics (Singapore); Vivek Dixit, Soon Thor Lim, Ching Eng J. Png, A*STAR Institute of High Performance Computing (Singapore)

Mach-Zehnder (MZ) modulators are essential for high-speed long-haul optical-fiber telecommunications, and have been extensively used in modulation formats such as on-off keying (OOK) and phase-shift keying (PSK). The MZ modulators driven in push-pull mode allow high-quality signal modulation without frequency chirping. Lithium-niobate (LN) MZ modulators have been most commonly applied to the long-haul optical-fiber telecommunications.

Silicon MZ modulators have the advantages of small footprint, monolithic integration and low fabrication cost. We have achieved extinction ratio higher than 10 dB in 32-Gb/s OOK and Q-factor as high as 20 dB in 20-Gb/s binary PSK (BPSK) with total optical loss as low as ~11 dB using a Si MZ modulator with reduced series resistance. The Si MZ modulator is comparable with LN MZ modulators in the high-speed performance in OOK and BPSK. Further reduction in total optical loss of the Si MZ modulator is desired to achieve modulator performances fully comparable with those of LN MZ modulators.

High-speed characteristics of the Si MZ modulator are presented, based on eye diagrams in OOK at 10-32 Gb/s and constellation diagrams in BPSK at 10-20 Gb/s. Error-free transmission in 80-km single-mode optical-fiber link using the Si MZ modulator is confirmed and dispersion penalty is compared with that of a LN MZ modulator. New designs are exploited to the Si MZ modulator for the total optical loss lower than 10dB. Dopant profiles, for example, are optimized to reduce phase-shifter optical loss due to free-carrier absorption while phase-shifter efficiency is maintained.

8629-30, Session 8

Graphene optical modulator (*Invited Paper*)

Ming Liu, Univ. of California, Berkeley (United States)

Graphene, a single sheet of carbon atoms in a hexagonal lattice, has attracted increasing interests because of its intriguing electrical and optical properties. What will be graphene's role in optical communication? In this talk I will introduce the progress in graphene optical modulator, which represent a totally new mechanism for optical modulation. Instead of changing the refractive index in silicon, we use graphene as an active layer and change its absorption coefficient by turning on/off the interband transitions. This tuning is realized through shifting the Fermi level by simply a back gate. In this way, we can operate the optical modulator at a relatively high speed (1.2 GHz) over a broad range (1.3 to 1.6 μm), while keep the smallest footprint (~0.17 dB/ μm). More details of the device will be discussed in the talk.

8629-31, Session 8

Silicon photonic modulators: theory, application, and recent advances (*Invited Paper*)

Michael R. Watts, Massachusetts Institute of Technology (United States)

Silicon photonic modulators have progressed significantly over the past decade. Recent results have enabled modulators with drive voltages as low as 1V while maintaining error-free operation at data-rates exceeding 10Gb/s while consuming as little as 3fJ/bit. Yet, many challenges remain. In Mach-Zehnder modulators, reducing the device length is key to achieving low power results. In resonant modulators, control over the resonant wavelength is required. And, in germanium-on-silicon modulators, achieving broadband operation remains elusive. As a result, to date, there appears to be little agreement in the community over which modulator type will be chosen. Yet, the application space appears to be expanding, with applications extending from datacom and telecom to microwave photonics and remote sensing. The silicon integration platform is proving to be a useful platform across a wide variety of applications.

In this talk, we review the theory of operation of silicon and germanium-on-silicon modulators, discuss recent results, integration with CMOS, and highlight the challenges that remain for each modulator type.

8629-32, Session 9

Optical modulation using the silicon platform (*Invited Paper*)

Frederic Y. Gardes, David J. Thomson, Graham T. Reed, Univ. of Southampton (United Kingdom); Kapil Debnath, Liam O'Faolain, Thomas F. Krauss, Univ. of St. Andrews (United Kingdom); Leon J. Lever, Rob W. Kelsall, Zoran Ikonc, Univ. of Leeds (United Kingdom); Maksym Myronov, David R. Leadley, The Univ. of Warwick (United Kingdom)

Optical modulation in silicon has experienced dramatic improvements over the last 7 years, with ever increasing data rates of 40 Gb/s and above. However, the next generation of optical interconnects will have to match the demands of on chip interconnects and commit to micrometre size real estate with sub volt operation and power requirements in the order of femtojoule per bit. Here we describe the work that led to the fabrication of novel devices using the plasma dispersion effect in silicon with size going from the millimetre range to a few microns producing a range of high-speed optical phase modulation whilst retaining a high extinction ratio. We also describe the work on Ge/SiGe quantum confined Stark effect devices for electroabsorption modulation, in which we have used strain engineering to target the commercially significant 1.3- μ m communications 'window'.

8629-33, Session 9

Simulation and experimental studies of diffusion doped p-i-n structures for silicon photonics

Sakthivel P., Nandita Dasgupta, Bijoy K. Das, Indian Institute of Technology Madras (India)

Single-mode silicon rib waveguides with p+-i-n+ diode structures are widely used for Electro-Optic Modulators (EOMs) and Variable Optical Attenuators (VOAs). These are found to be the key components for realizing active integrated optical circuits on SOI platform. However, the device performances are highly controlled by the waveguide geometry, doping profile parameters, and the mode of operation (injection/

depletion). Most of the investigated devices so far are based on single-mode photonic wire waveguides with ion implanted step-type dopant profiles.

In this paper, we are going to present detailed studies on diffusion doped p-i-n waveguide EOMs and VOAs which can be fabricated by conventional microelectronics technologies. We have optimized the device parameters using various design and process simulators like RSoft BPM, Medici, and TSuprem4. The fabrication processes have been optimized for both EOMs & VOAs. The fabricated large cross-section waveguide devices have been investigated in terms of diode characteristics, waveguide losses, forward current dependent attenuation, and figure of merit ($V\pi$ -L) of p-i-n phase modulators at an operating wavelength of $\lambda \sim 1550$ nm for TM-polarized light. The typical attenuation of VOA has been measured to be 17.5 dB/cm for a forward bias current of ~ 130 mA, whereas, the figure of merit of phase modulators is ~ 0.23 V-mm. These experimental results show close agreement to our simulation studies. Further investigations on waveguide loss reduction, polarization and wavelength dependencies, performance of MMI based MZI modulator structures, etc. are in progress. They will be reported during the conference.

8629-34, Session 9

A low-power electro-optic polymer clad Mach-Zehnder modulator for high-speed optical interconnects

Bruce A. Block, Shawa M. Liff, Mauro J. Kobrinsky, Miriam R. Reshotko, Ricky J. Tseng, Ibrahim Ban, Peter Chang, Intel Corp. (United States)

Electro-optic (EO) polymer cladding modulators are an option for low-power high-speed optical interconnects on a silicon platform. EO polymers have inherently high switching speeds[ref 1] and have shown 40 Gb/s operation in EO polymer clad ring resonator modulators (RRM) [ref 2-4]. In EO polymer clad RRM, the modulator's area is small enough to be treated as a lumped capacitor; the capacitance is sufficiently low that the modulation speed is limited by the bandwidth of the resonator. A high Q resonator is needed for low voltage operation, but this can limit the speed and/or require precise control of the resonator's wavelength, necessitating power consuming heaters to maintain optimal performance over a large temperature range. Mach Zehnder modulators (MZM), on the other hand, are not as sensitive to temperature fluctuations, but typically are relatively long and must employ power consuming terminated travelling wave electrodes. In this paper, a novel MZM design is presented using an EO polymer clad device. In this device, the electrodes are broken into three short parallel segments and the waveguide folds around them. The segments of the electrode length are designed to provide good signal integrity up to 40 Gb/s without termination. The electrodes are driven by a single drive voltage and provide push-pull modulation. Modulators were designed and fabricated with both silicon nitride and Si waveguides and demonstrated at high speed (20 GHz). A $V\pi$ *L as low as 3 Vcm is measured on initial devices. An optimized device could provide a $V\pi$ *L less than 1 Vcm enabling devices with 1 V drive voltages, ~ 100 fF total device capacitance and less than 2 dB optical insertion loss.

References:

- 1 D. Chen, H. R. Fetterman, A. Chen, W. H. Steier, L. R. Dalton, W. Wang, and Y. Shi, "Demonstration of 110 GHz electro-optic polymer modulation," Appl. Phys. Lett. 70, 3335-3337 (1997).
- 2 Block BA, Younkin TR, Davids PS, Reshotko MR, Chang P, Polishak BM, Huang S, Luo J, Jen AK. "Electro-optic polymer cladding ring resonator modulators" Opt Express. 2008 Oct 27;16(22):18326-33.
- 3 Young, Ian A.; Block, Bruce; Reshotko, Miriam; Chang, Peter; , "Integration of nano-photonics devices for CMOS chip-to-chip optical I/O," Lasers and Electro-Optics (CLEO) and Quantum Electronics and Laser Science Conference (QELS), 2010 Conference on , vol., no., pp.1-2, 16-21 May 2010
- 4 Chang, P.L.D.; Mohammed, E.M.; Block, B.A.; Reshotko, M.R.; Young, I.A.; , "Optical I/O for chip-to-chip interconnects on CMOS platform,"

Optical Fiber Communication Conference and Exposition (OFC/NFOEC), 2011 and the National Fiber Optic Engineers Conference, vol., no., pp.1-3, 6-10 March 2011 rconnects

8629-35, Session 9

Polarization-independent and dispersion-free integrated optical MZI in SOI substrate for DWDM applications

Karthik Uppu, Bijoy K. Das, Indian Institute of Technology Madras (India)

Polarization dependencies and dispersions are the two major bottlenecks in waveguide based silicon photonic devices for various applications – especially in DWDM systems. In this paper, we present the design and experimental demonstration of a 2nd integrated optical MZI that shows both polarization-independent and dispersion-free response over a wide wavelength range (C+L optical band) in SOI platform - for the first time to our knowledge. The entire device footprint (W²L) is ~ 0.8 mm ² 5.2 mm; which is comprised of optimally designed single-mode waveguides (for input/output and interferometer arms) and a pair of MMI based 3-dB power splitters. To monitor the wavelength dependent performance, unbalanced arm lengths (L ~ 3037 μ m, L+ Δ L ~ 3450 μ m) were introduced to construct the MZI. The differential arm length (Δ L) has been specifically chosen to provide alternate ITU channel transmission peaks at both the output ports alternatively. Accordingly, the fabricated device separates 100 GHz DWDM channel wavelengths alternatively into two output ports and is nearly insensitive to the polarization of the guided light. We have observed a uniform channel extinction of ~ 10 dB (~ 6 dB) at both ports with a 3-dB bandwidth of ~ 110 GHz (~120 GHz) for TM (TE) polarization over the wavelength range of 1520 nm to 1600 nm. The lower extinction for TE polarization is due to its relatively higher bending loss in the longer arm of the MZI. This can be adjusted by introducing identical bends in both the arms.

8629-36, Session 10

Hybrid silicon free-space source with integrated beam steering (*Invited Paper*)

Jonathan K. Doylend, Martijn J. R. Heck, Jock T. Bovington, Jon D. Peters, Michael L. Davenport, John E. Bowers, Univ. of California, Santa Barbara (United States)

Free-space beam steering using optical phase arrays are desirable as a means of implementing Light Detection and Ranging (LIDAR) and free-space communication links without the need for moving parts, thus alleviating vulnerabilities due to vibrations and inertial forces. Implementing such an approach in silicon photonic integrated circuits is particularly desirable in order to take advantage of established CMOS processing techniques while reducing both device size and packaging complexity.

In this work we demonstrate a free-space diode laser together with beam steering implemented on-chip in a silicon photonic circuit. A waveguide phased array, surface gratings, a hybrid III-V/silicon laser and an array of hybrid III/V silicon amplifiers were fabricated on-chip in order to achieve a fully integrated steerable free-space optical source with no external optical inputs, thus eliminating the need for fiber coupling altogether. The chip was fabricated using a modified version of the hybrid silicon process developed at UCSB, with modifications in order to incorporate diodes within the waveguide layer as well as within the III-V gain layer. One-dimensional beam steering across a 12 \times field of view with \pm 0.3 \times accuracy and 1.8 \times 0.6 \times beam width was achieved, with background peaks suppressed 7 dB relative to the main lobe within the field of view for arbitrarily chosen beam directions.

8629-37, Session 10

Second-harmonic generation in strained silicon

Eleonora Luppi, Univ. of California, Berkeley (United States); Elena Degoli, Univ. degli Studi di Modena e Reggio Emilia (Italy) and Istituto di Nanoscienze (Italy); Matteo Bertocchi, Univ. degli Studi di Modena e Reggio Emilia (Italy) and Ecole Polytechnique Palaiseau (France) and European Theoretical Spectroscopy Facility (France); Valerie Veniard, Ecole Polytechnique (France) and European Theoretical Spectroscopy Facility (France); Stefano Ossicini, Univ. degli Studi di Modena e Reggio Emilia (Italy) and Istituto di Nanoscienze (Italy)

Silicon photonics meets the electronics requirement of increased speed and bandwidth with on-chip optical networks. All-optical data management requires nonlinear silicon photonics. In silicon only third-order optical nonlinearities are present owing to its crystalline inversion symmetry.

Introducing a second-order nonlinearity into silicon photonics by proper material engineering would be highly desirable. We show through first-principles calculations [1,2] that in strained-bulk Si a sizable second-order nonlinearity at optical wavelengths is possible. In particular, the best situation is observed when the stress is biaxial and the resulting strain has an inversion in sign resulting in an alternation of compressive and tensile strain. These theoretical calculations supported and confirmed the experimental observed second-harmonic generation in a silicon waveguide strained by silicon nitride overlayers [3]. The combination of strained Si with suitable photonic design can lead to nonlinear Si devices that may compete with devices based on conventional nonlinear materials but with the huge advantages connected with Si photonic integrated circuits, which are potentially compatible with mass manufacturing.

[1] E.Luppi, H. Hübener and Valérie Vénierd, J. Chem. Phys. 132, 241104 (2010) .

[2] E. Luppi, H. Hubener, M. Bertocchi, E. Degoli, S. Ossicini, V. Veniard, MRS Proceedings 1370, 11-1370 (2011).

[3] M. Cazzanelli, F.Bianco, E. Borga, G. Pucker, M. Ghulinyan, E. Degoli, E. Luppi, V. Vénierd, S. Ossicini, D. Modotto, S.Wabnitz, R. Pierobon and L. Pavesi, Nature Materials 11, 148-154 (2012).

8629-38, Session 10

A novel type of ultra-compact lateral-current-injection III/V photonic device integrated on SOI for electronic-photonic chip application

Jing Pu, Qian Wang, A*STAR - Data Storage Institute (Singapore); Seng-Tiong Ho, A*STAR - Data Storage Institute (Singapore) and Northwestern Univ. (United States)

An on-chip light source plays a determinant role in the realization of integrated photonic chips for optical interconnects technology. The key properties for such on-chip lasers are low power consumption, small footprint, as well as coupling the light efficiently to the silicon optical waveguide layer. In this paper, we propose a novel approach to integrate an ultra-compact Lateral-Current-Injection (LCI) laser on silicon-on-insulator (SOI) platform by direct wafer bonding techniques. The proposed LCI device consists of separate confinement heterostructure (SCH) layer, multiple quantum wells (MQWs), and a bonding interfacial layer with a total thickness of 250 nm which is ~10 times thinner than the vertical current injection laser bonded on silicon. The proposed LCI laser integrated on the typical 200 nm thick silicon nanophotonic layer has a confinement factor in the active region larger than 30%. The p+ and n+ regions for the LCI device are formed by ion implantation. In order to transfer light efficiently between III/V and silicon waveguide, an optical vertical interconnect access is designed through tapering the III/V

and silicon waveguide simultaneously in the same direction. Benefiting from the ultra-thin III/V layer, a tapering region as short as 4 μm can give ~100% coupling efficiency between the III/V and silicon layers.

In summary, we propose an ultra-thin LCI III/V device on silicon with an ultra-compact optical vertical interconnect access. The proposed structure has better light confinement (30%) in the active region and efficient light transfer (100%) between III/V and silicon.

8629-39, Session 10

Role of electron and hole transport processes in conductivity and light emission of silicon nanocrystal field-effect transistors

Laura Cattoni, Oleksiy Anopchenko, Andrea Tengattini, Univ. degli Studi di Trento (Italy); Joan Manel Ramirez, Federico Ferrarese Lupi, Yonder Berencén, Blas Garrido, Univ. de Barcelona (Spain); Jean-Marc Fédéli, CEA-LETI (France); Lorenzo Pavesi, Univ. degli Studi di Trento (Italy)

We investigate light emission from silicon four-terminal field-effect transistors (FETs) with silicon nanocrystals in the gate oxide and semitransparent polycrystalline silicon gate. We compare it with light emission from two-terminal light-emitting devices with the same active material. The gate oxide layer of ~45 nm thick is deposited by low pressure chemical vapor deposition using standard microelectronic processes of a CMOS line and a size-controlled multilayer approach of silicon nanocrystal growth. The nanocrystal size and tunneling barrier width are controlled by the thickness of silicon-rich silicon oxide and stoichiometric silicon oxide sub-layers, respectively. The silicon nanocrystals are characterized by means of spectrally and time resolved photoluminescence, high resolution TEM, and x-ray photoelectron spectroscopy. To elucidate the process of electron and hole transport through silicon nanocrystal arrays, their relative contribution into FET conductivity and radiative exciton recombination, n- and p-type FETs are fabricated; 'dark' conductivity, conductivity under light illumination, capacitance, and electroluminescence under direct and pulsed injection current are studied. The results of this study will help to develop practical optoelectronic, photonic, and resistive memory devices via accurate modeling and engineering of charge transport and exciton recombination in silicon nanocrystal arrays.

8629-40, Session 11

Hole system heating by ultrafast interband energy transfer in optically excited Ge/SiGe quantum wells

Kolja Kolata, Niko S. Köster, Philipps-Univ. Marburg (Germany); Sebastian Imhof, Technische Univ. Chemnitz (Germany); Stefano Cecchi, Daniel Chrastina, Giovanni Isella, Politecnico di Milano (Italy); John E. Sipe, Univ. of Toronto (Canada); Angela D. Thränhardt, Technische Univ. Chemnitz (Germany); Sangam Chatterjee, Philipps-Univ. Marburg (Germany)

Germanium is considered as a promising candidate for adding optical functionality to Si. Passive and active components have been realized, including electrically-injected lasers. However, the nature of the carrier dynamics in this indirect-band-gap system is profoundly different from established optoelectronic materials like GaAs. Here, we investigate the hole scattering and cooling dynamics in Ge/SiGe quantum wells on a picosecond time scale. Time-resolved pump-probe experiments show an efficient scattering process between the electron and hole systems in the L- and Gamma-valley, respectively. The Ge quantum wells are excited 10 meV above the band edge and probed with a white-light supercontinuum at cryogenic temperatures. After optical excitation, the electrons scatter from the Gamma-valley into the lower lying L-valleys within a few hundreds of fs. At later times, only the hole system is

probed by the optical pulses as photons can only access vanishing momenta. We observe a hot hole system with a temperature far beyond what is expected from the excess energy of the excitation. Then it cools down towards the lattice temperature on a picosecond time scale. The additional heating of the hole system in the Gamma-valley is caused by an efficient energy transfer from the electrons in the L-valley mediated by Coulomb-interaction. The dependencies on excitation energy as well as carrier density support this explanation. Our findings are corroborated by theoretical semiconductor Bloch equations calculations of the absorption spectra for various hole-system carrier-densities and temperatures.

8629-41, Session 11

Experimental demonstration of novel heterogeneously integrated III-V on Si microlaser

Yannick De Koninck, Univ. Gent (Belgium); Alexandre Bazin, Fabrice Raineri, Rama Raj, Lab. de Photonique et de Nanostructures, CNRS (France); Gunther Roelkens, Roel G. Baets, Univ. Gent (Belgium)

We present experimental results regarding a novel type of heterogeneously integrated III-V on silicon microlaser based on resonant mirrors. The laser consists of an active III-V waveguide with passive silicon grating cavities underneath both facets. The light is confined to the III-V waveguide and evanescently couples into a silicon cavity as it approaches a facet. Because the grating cavities are resonant at the desired laser wavelength, power builds up inside the passive cavities and couples back into the III-V waveguide. The light that couples back co-directionally to the incident light will interfere destructively with the fraction of light in the III-V waveguide that did not couple into the silicon cavity. The light coupling back counter-directionally to the incident light provides the feedback in the III-V waveguide required to establish laser operation. This approach provides strong reflection in a narrow wavelength range and over a short optical path-length. Moreover, all the critical patterning is done in the silicon layer, where processing technology is very mature.

We report the first experimental demonstration of such a laser based on resonant mirrors. The device measures only 55 μm by 2 μm and consists of a 260 nm thick III-V layer on top of a 220 nm thick silicon waveguide with 70 nm deep corrugations. The silicon and III-V layers are separated by 250 nm. The device is optically pumped in a pulsed regime and shows single-mode room-temperature lasing at 1508 nm.

8629-42, Session 11

Temperature-dependent external quantum efficiency of Ga(NAsP) quantum wells

Nils Rosemann, Björn Metzger, Philipps-Univ. Marburg (Germany); Bernardette Kunert, Philipps-Univ. Marburg (Germany) and NAsP III/V GmbH (Germany); Kerstin Volz, Philipps-Univ. Marburg (Germany); Wolfgang Stolz, Philipps-Univ. Marburg (Germany) and NAsP III/V GmbH (Germany); Sangam Chatterjee, Philipps-Univ. Marburg (Germany)

Silicon is the basis for many integrated circuits, microelectronic devices, and even optoelectronic components such as waveguides as well as detectors. However, despite the high quantum efficiencies reported for light-emitting diodes it is generally not considered useful as an active medium for lasers due to the indirect nature of its bandgap. The demand for a laser integrated to Si has kindled research on various approaches, like Raman-or nanocrystal-based concepts both native to silicon or hybrid integration. Alternatively, quaternary alloys with direct band-gap based on GaP can be integrated quasi-lattice matched to Si. Recently, electrically pumped lasing has been achieved for this material system [Appl. Phys. Lett. 99, 071109, (2011)].

In order to investigate the remaining challenges such as low-temperature operation and still comparatively large laser thresholds we investigated a series of Ga(NAsP)/GaP multiple quantum well (MQW) samples by temperature-dependent absolute photoluminescence spectroscopy. The results are compared to a standard laser material, a high-quality (GaIn)As/GaAs MQW. The samples are mounted inside a 2" diameter integrating sphere in a He-closed cycle cryostat. A diode laser at 786nm is used for excitation and a compact spectrometer equipped with a Si charge-coupled device camera covering a wavelength-range from 665 to 1100nm is used for detection. At low temperatures, the reference sample outperforms the Ga(NAsP) structures by a factor of two. At room temperature, however, the EQE of both material systems are comparable for our experimental conditions.

8629-43, Session 11

Room temperature electrically pumped silicon nano-light source at telecommunication wavelengths

Abdul Shakoor, Univ. of St. Andrews (United Kingdom); Roberto Lo Savio, Univ. degli Studi di Pavia (Italy); Paolo Cardile, Univ. degli Studi di Catania (Italy); Simone L. Portalupi, Dario Gerace, Univ. degli Studi di Pavia (Italy); Karl Welna, Univ. of St. Andrews (United Kingdom); Simona Boninelli, Giorgia Franzò, Francesco Priolo, Univ. degli Studi di Catania (Italy); Thomas F. Krauss, Univ. of St. Andrews (United Kingdom); Matteo Galli, Univ. degli Studi di Pavia (Italy); Liam O'Faolain, Univ. of St. Andrews (United Kingdom)

The need for higher data processing speeds and bandwidth has accelerated silicon photonics research over last decade. Significant progress has been made, but a suitable room temperature native light emitter is still missing. Such a device would also need to be electrically pumped, operate at sub-bandgap wavelengths and exhibit a narrow emission line. Here, we demonstrate a possible contender, based on light emission from hydrogen defects that have been incorporated into the silicon matrix by plasma treatment. The enhanced emission is then coupled to a photonic crystal nanocavity and we demonstrate both optically and electrically pumped emission with a very narrow linewidth (0.5nm), which is tunable over the entire telecommunication range. The spectral power density of the emission is 0.8mW/nm/cm², which is the highest value ever reported from any silicon nano emitter. In fact, this is the first demonstration of a room temperature electrically pumped silicon nanolight source at telecommunication wavelengths. The source could be used for biological sensing, optical interconnects and other applications in silicon photonics. We also discuss possibilities for further enhancing the emission, which could lead to the demonstration of electrically pumped silicon lasing action at telecommunication wavelengths.

8629-44, Session PWed

Bulk silicon as photonic dynamic visible-to-infrared scene converter

Volodymyr K. Malyutenko, Viacheslav V. Bogatyrenko, Oleg Y. Malyutenko, V. Lashkaryov Institute of Semiconductor Physics (Ukraine)

Experimental prototypes of Si-based fast (frame rate >1 kHz) large-scale (scene area >16 cm²) broad band ($\lambda=3-12 \mu\text{m}$) contactless dynamic infrared (IR) scene projector are presented. IR movie ($\lambda_{\text{out}} > hc/E_g$, Eg- is the bandgap energy) appears in the scene as a result of conversion of dynamic black-and-white ($\lambda_{\text{in}} < hc/E_g$) scenario projected at a scene kept at T>300 OC. Light down conversion (LDC) process comes as a result of free carrier generation in a bulk Si scene followed by local modulation of its emissivity (and thermal emission power output) in the spectral band of free carrier absorption. Experimental setup, IR

movie, figures of merit of LDC photonic process, and its advantages in comparison to other projecting technologies are discussed.

8629-45, Session PWed

Responsivity measurements of N-on-P and P-on-N silicon photomultipliers in the continuous wave regime

Gabriele Adamo, Diego Agrò, Salvatore Stivala, Antonino Parisi, Costantino Giaconia, Alessandro Busacca, Univ. degli Studi di Palermo (Italy); Massimo C. Mazzillo, Nunzio Delfo D. Sanfilippo, Pier Giorgio G. Fallica, STMicroelectronics (Italy)

We report the electrical and optical comparison, in continuous wave regime, of two novel classes of silicon photomultipliers (SiPMs) fabricated in planar technology on silicon P-type and N-type substrate respectively. Responsivity measurements have been performed with an incident optical power from sub picowatts to several nanowatts and on a broad spectrum, ranging from UV to near infrared (820nm).

N-on-P SiPM responsivity shows a flat response (about 5e9 mA/W), biasing at 5.4V above the breakdown voltage (BV=28.2V), corresponding to an incident optical power ranging up to 11 pW, before decreasing at higher power. The P-on-N SiPM responsivity exhibits a similar trend, but the flat region ranges up to about 60 pW with a value of 7e8 mA/W, biasing at 7.7V above the BV (the same of the N-on-P device). Our responsivity measurements, carried out in the abovementioned spectral range, point out a peak at 654nm for the N-on-P SiPM and a peak at 406nm for the P-on-N.

In the N-on-P device, photons are absorbed within the first micron, thus directly in the depletion layer, and this gives rise to a remarkable responsivity in the blue range. The responsivity peak is in the red range, thanks to the contribution of the electrons photogenerated in the P-doped epitaxial layer. Light in the near infrared range penetrates deeper into the substrate, reducing the probability of reaching the depletion layer due to the higher recombination. Vice versa, the P-on-N device shows a responsivity peak in the blue since the lower hole diffusivity with respect to electrons.

8629-46, Session PWed

Hybrid integrated III-V/SOI waveguides forward coupling phase matching engineering using Bragg gratings: fundamental and applications

Anatole Lupu, Institut d'Électronique Fondamentale (France)

We address the problematic of co-propagative evanescent coupling interactions between fast and slow modes in a system of hybrid integrated III-V/SOI waveguides. The considered approach exploits the dispersive properties of a Bragg grating (BG) in the vicinity of its own photonic band-gap. It is shown that the change of the waveguide dispersion induced by the BG can be successfully used to achieve an additional phase matching condition, resulting then in a single or dual transmission band operations. When the initial phase matching and the Bragg wavelengths coincide, the dual transmission bands become identical and their position symmetrical with respect to the BG wavelength. It is evidenced that this operation regime turns out to be of particular interest for switching or amplitude modulation applications.

The use of a simplified model with linear wavelength dispersion for the waveguides effective index provides an analytical description for the general III-V/SOI coupler behavior. It is shown that the optimal operation is achieved with only one Bragg grating distributed along one of the two waveguides. Different device behaviors are predicted according as the grating is placed along the III-V or SOI waveguides.

Theoretical predictions from the analytical model are verified using a coupled mode theory four-wave model. A numerical validation of the

results of coupled mode theory is performed for selected examples using the free available software CAMFR based on an eigenmode propagation method. The considered design is shown to be compatible with existing III-V/SOI hybrid integration technology.

8629-47, Session PWed

Anomalous localization modes in Bragg-grating based on high index-difference waveguide

Tomohiro Kita, Koji Uchijima, Hirohito Yamada, Tohoku Univ. (Japan)

We observed photonic band-gap disappearance on Bragg-grating wavelength filters with Si photonic-wire waveguides, and studied the physical mechanism with theoretical and numerical analyses. This is a unique phenomenon observed in channel waveguides with very high index-contrast between the waveguide core and cladding materials. The photonic band-gap disappearance was observed in structures where two different optical field distributions of standing wave degenerate.

8629-48, Session PWed

All-optical single resonance control using silicon-based Ring-Assisted Mach-Zehnder Interferometer (RAMZI)

Yule Xiong, Carleton Univ. (Canada); Winnie N. Ye, Carleton Univ. (Canada)

CMOS-compatible microring resonators (MRR) based active devices have attracted significant attention for their ability to confine and manipulate light on a compact SOI platform. Active modulation of the MRR is typically achieved by changing the intensity response. As an alternative to intensity modulation, the phase modulation of the MRR can be converted into intensity modulation of a Mach-Zehnder interferometer (MZI) by means of a ring-assisted Mach-Zehnder interferometer (RAMZI) structure. We theoretically demonstrate selective control of the transmission of a single resonance of silicon RAMZI by optically controlling the intracavity loss of the side-coupled silicon ring using inverse Raman scattering (IRS). The RAMZI structure improves the modulation robustness against fabrication deviations by using the over-coupled rather than the single critical coupling condition for the MRR, without compensating the modulation performance. In silicon, the IRS produces optical loss with bandwidth of 105 GHz at the anti-Stokes wavelength, which blueshifts 15.6 THz from the control light. For our proposed RAMZI structure, the IRS induced loss is spectrally wider than the linewidth of the side-coupled ring but narrower than the free spectral range (FSR), guaranteeing a single resonance selectivity. When the control light pulse of 200 ps switches from "off" (zero) to "on" (20pJ), the transmission of the anti-Stokes resonance transfers from -17.20 dB to -0.33 dB. The corresponding modulation bandwidth is around 2.5 GHz. Compared with the standalone MRR, the RAMZI structure is less sensitive to the fabrication deviations. The proposed structure provides the potential to multichannel all-optical routers on a CMOS compatible platform.

8629-49, Session PWed

Silicon nanomembrane based photonic crystal waveguide true-time-delay lines on a glass substrate

Harish Subbaraman, Omega Optics, Inc. (United States); Xiaochuan Xu, Ray T. Chen, The Univ. of Texas at Austin (United States)

In this paper, we present the fabrication and demonstration of silicon nanomembrane based photonic crystal waveguide true-time-delay lines on a glass substrate. The photonic crystal waveguides are designed to provide large time delay values within a short length. Continuously tunable time delay is achieved by wavelength tuning, which utilizes the strong dispersion of the photonic crystal waveguides. In order to fabricate the devices, large area (> 2cm x 2cm), defect-free silicon nanomembranes are first transferred onto a glass substrate with an SU-8 bottom cladding layer using a bonding technique. The designed photonic crystal waveguides, along with 17.1 μm x 10 μm subwavelength grating (SWG) couplers, consisting of a periodic array of subwavelength scale rectangular holes, are fabricated at the input and output of the waveguides in order to enable efficient light coupling from and to a fiber. The grating couplers provide a peak coupling efficiency of 37%, with 1-dB and 3-dB bandwidths of 27nm and 57nm, respectively. Photonic crystal tapers are implemented at the strip-photonic crystal waveguide interfaces, which lowers the coupling loss and enables operation closer to the band edge, thus providing larger time delay values. A large time delay of 58ps per millimeter length of the true-time-delay line is achievable within a wavelength tuning range of 20nm. Such a demonstration opens vast possibilities for a whole new range of high performance, light-weight and low power photonic crystal waveguide based photonic components on other rigid and flexible substrates.

8629-50, Session PWed

Low power consumption in silicon photonics tuning filters based on compound ring resonators

Carmen Vázquez García, Univ. Carlos III de Madrid (Spain); Salvador Vargas, Univ. Tecnológica de Panamá (Panama); Pedro Contreras Lallana, Univ. Carlos III de Madrid (Spain)

Last developments in integrated optics, specially in silicon photonics make affordable an increment in the integration scale and systems complexity. Platforms based on Silicon on Insulator (SOI) allow to develop optics and electronics functions on the same chip. Developments in this area are fostered by the need of optical interconnects, either on chip as off chip, for improving processor performance in terms of speed, footprint and power consumption capabilities. International Roadmap for Semiconductors (ITRS) foresees a saturation in power dissipation by 2022 [ITRS]. From those data Miller [Miller, 2009] estimates that new systems should be able to consume energies below e 170fJ/bit in 2022, for clock processor speeds of 14.3 GHz (on-chip) and 67.5 GHz (off-chip). But even optical devices should be improved to reach those values. As part of those new silicon photonics devices we proposed compound structures, with novel tuning capabilities, which can be implemented with state of the art SOI technology. Special attention is given to evaluate power consumption of those configurations based on manufactured devices reported in literature [Dong et al, 2009] and to compare single rings and compound configurations consumption. Designs are based on CMOS compatible processes [Orcutt...Ram, 2011] for allowing massive production for cutting costs. The proposed devices are based on multireflection configurations within ring resonators [Vargas, Vázquez, 2007] [Vázquez et al, 2003] [Vargas, Vázquez, 2010] and PIN configurations are used for achieving device tuning. Ring resonators allow developing compact devices with lower energy consumption and the multireflections further reduce the consumption.

If finally, optical interconnects based on ring resonators succeeded, a reduction in each single device consumption should imply a big total reduction. Nowadays, a strategic topic at global level is trying to reduce carbon footprint related to CO2 emission related to human actions. For specifically, Information and Communications Technologies (ICT) contribute in an increasing way to those emissions, because of electricity needed to make all related devices to be operative. It is estimated that by 2020, ICT consumption will be around 3% of total [Feng et al, 2011]; with more than 60% of that consumption to data center, network equipments and PC [Pickavet et al, 2009]. Another relevant data is that, only in USA, 1.5% of total electricity consumption in 2006 in the country was devoted to data center operation [Miller, 2009]. The increase interest for those

matters have led to implementation of a consortium GreenTouch [GT], headed by Alcatel Lucent Bell Labs for trying to reduce in 1/1000 data center consumption. Optical interconnects and optical technologies have to much to say for trying to reach that goal. And one those technologies are developed they can be applied to other sectors such as home and access networks. Thinking about environmental impact, that means a greater success, because at networks levels, if consumption per user is considered, W/user, the largest consumption is in home networks and access networks with a weight 100 times greater [Feng et al, 2011]. Just for giving some data, ring resonators have higher optical confinement and modulators based on ring resonators in SOI have energy consumptions below 50fJ/bit [Dong et al, 2009] [Xu et al, 2005]. Those ring resonators can be used in the future to send traffic between different offices, or rooms in the same building [Koonen et al, 2011].

References

[ITRS], <http://www.itrs.net/Links/2007ITRS/ExecSum2007.pdf>.
 [Miller, 2009] D. A.B. Miller, Device Requirements for Optical Interconnects to Silicon Chips Proceedings of the IEEE, Vol. 97, No. 7, 1166-1185, July 2009.
 [Dong et al, 2009] P. Dong, S. Liao, D. Feng et al Low V_{pp} ultralow-energy, compact, high-speed silicon electro-optic modulator Opt. Express, 17 (25), 2009.
 [Orcutt ...Ram, et al. 2011] Orcutt, J.S, Anatol Khilo, A., Holzwarth, C. W., et al. J. R. Ram, 2011. Nanophotonic integration in state-of-the-art CMOS foundries. Optics Express, 19: 2335-2346.
 [Vargas, Vázquez, 2007] S. Vargas, C. Vázquez, "Synthesis of Optical Filters Using Sagnac Interferometer in Ring Resonator" IEEE Photonics Tech. Lett., Vol. 19,23, 1877, 2007.
 [Vázquez et al, 2003] C. Vázquez, S. Vargas, J.M. S. Pena, P. Corredera "Tunable Optical Filters Using Compound Ring Resonators for DWDM" IEEE Photonics Technology Letters 15 (8), 1085 - 1087, 2003.
 [Vargas, Vázquez, 2010] Salvador Vargas, Carmen Vázquez "Synthesis of optical filters using microring resonators with ultra-large FSR" Opt. Express 18, 25936-25949 (2010).
 [Feng et al, 2011] K. Feng, G. Keiser, S. Lee Power consumption in hybrid access and home networking network. Optical Fiber Conference 2011 JWA17.pdf.
 [Pickavet et al, 2009] M. Pickavet, W. Vereecken, S. Demeyer et al Worldwide Energy Needs for ICT: the Rise of Power-Aware Networking IEEE ANTS 2008 conf., 15-17 December 2008, (India).
 [GT] <http://www.eweekurope.co.uk/news/news-it-infrastructure/alcatel-lucent-vows-to-boost-network-efficiency-1000-fold-2985>.
 [Koonen et al, 2011] Koonen et al. A look into the future of in-building networks: Roadmapping the fiber invasion, 41-46, POF 2011 Bilbao (Spain) Conference Proceedings – DATACOM & NETWORKS I, 2011.
 [Xu et al, 2005] Q. Xu, B. Schmidt, S. Praham and M. Lipson "Micro-scale silicon electro-optic modulator", Nature, 2005.

8629-51, Session PWed

Demonstration of silicon nanomembrane based photonic crystal waveguide PIN modulators on unusual substrates

Xiaochuan Xu, The Univ. of Texas at Austin (United States); Harish Subbaraman, Amir Hosseini, Omega Optics, Inc. (United States); David N. Kwong, Ray T. Chen, The Univ. of Texas at Austin (United States)

Silicon photonics has received considerable attention during the past few decades, and has shown potential for a myriad of applications. In recent years, there has been a rapid growing interest for transferring silicon nanomembrane based electronic and photonic devices onto unusual substrates to obtain special characteristic, e.g. flexibility, and at the same time preserve distinguished performance. Several achievements have been reported, but so far, transferring active silicon photonic devices is still a vacancy. In this paper, we present the transfer

of silicon nanomembrane based photonic crystal PIN modulator onto glass and flexible substrates. The modulator is first fabricated on a 2cm² silicon-on-insulator chip with 250 nm single crystal silicon layer and 3 μm buried oxide layer through electron beam lithography and ion implantation, and afterwards transferred onto glass and flexible substrates through adhesive bonding and deep silicon etching. After the transfer, the electrodes are formed by photolithography and electron evaporation. Due to the large coefficient of thermal expansion mismatch between the adhesive and silicon, the process is tailored to keep the temperature below 90°C. The testing results show GHz bandwidth with low V_π. This demonstration shows the possibilities of integrating high performance silicon based optoelectronic devices on unusual substrates, which could significantly broaden the expanse of silicon electronics and photonics.

8629-52, Session PWed

Silicon nanocrystal density effects in sensitizing erbium atoms

Quamrul Huda, Univ. of Alberta (Canada)

Sensitization of erbium through silicon nanocrystals and the resulting luminescence at 1.54 μm were studied in detail. Silicon nanocrystals were shown to work as the gateway for energy transfer to erbium atoms. Excitation rate of silicon nanocrystals by the incident photon flux, and the subsequent transfer of energy to erbium atoms were modelled. Effects of energy back transfer processes through co-operative up conversion and Auger related processes were incorporated. The effective sensitization range of Si-nc to erbium was found to be a crucial parameter in determining the density of erbium atoms that would remain in excited state at a certain flux incidence. Realization of population inversion condition was shown to depend on erbium and nanocrystal related parameters, as well as their incorporation densities. Based on three dimensional spatial considerations, it was shown that, larger fraction of incorporated erbium, although optically active, may reside outside the range of Si-nc influence. An erbium fraction on the order of 1% was estimated to be excitable through silicon nanocrystals for a Si-nc incorporation density of 10¹⁸/cm³. It was also shown with a statistical approach that silicon nanocrystal excitation in the vicinity of erbium atoms can occur at multiple times during the decay lifecycle of an erbium atom. The probability of Si-nc being excited at every alternate cycles of excitation increases from small fractions to percentage levels for incident flux levels above 10¹⁸/cm²-s. Occurrence of multiple excitation of Si-nc is correlated with the deteriorating effects in Er sensitization at higher flux incidence.

8629-53, Session PWed

Modeling silicon-based photonic periodic waveguides

Meng-Mu Shih, Univ. of Florida (United States)

This work utilizes the photonic method to model silicon-based photonic periodic waveguides for computing coupling coefficients. Such waveguides can have applications such as optical interconnects, communications, or integration. The refractive index contrast between the silicon and silicon-dioxide layers can help confine the modes inside the waveguides. Shiny metal gratings with specific nano period are embedded into the waveguides to make the light-guiding stable. Numerical results show how parameters such as grating geometry, grating materials, layer thickness, and mode polarization can affect the mode-coupling coefficients of waveguides. Physical interpretations with discussion can provide insights into the theoretical modeling and numerical results.

8629-54, Session PWed

A highly accurate engineering of silicon integrated microring resonators based on the nanofabrication technique

Mikhail Erdmanis, Aalto Univ. (Finland)

Optical microring resonators manifest fundamental building blocks in photonic integrated circuits. They provide an opportunity to realize narrow-band optical filters, switches, as well as various high-sensitivity sensing schemes. As a result, there is a great activity on optimization of both the operation properties such as, e.g., free spectral range and quality factor, and the fabrication techniques. Nowadays, when the use of large-scale manufacturing techniques based on UV lithography has been adapted for microring resonators, a fine control of the key parameters becomes more and more crucial.

In this work we present our theoretical and experimental study on the fine engineering of a silicon integrated microring resonator spectral response. The resonators are formed by the 460-520nm wide nanostripe waveguides fabricated by optical lithography. In order to fine-tune the device, we apply various nanometer-thick highly uniform dielectric overlayers. Consequently, the mode propagation constant and the decay length of evanescent field in transverse direction are significantly changed, resulting in a modified optical length of the resonator and the coupling coefficient. In addition, the method provides an opportunity to alter the total losses per trip, what, in combination with the controllable coupling coefficient itself, gives means to facilitate the critical coupling condition in a precise way.

8630-1, Session 1

Chip-to-board interconnects for high-performance computing (*Invited Paper*)

Markus B. K. Riestler, Maris TechCon Technology and R & D Consulting (Austria); Sönke Steenhusen, Ruth Houbertz-Krauss, Fraunhofer-Institut für Silicatforschung (Germany)

Super computing is reaching out to the ExaFLOP, which creates fundamental challenges for the way that systems are built. The governing topic is the reduction of power used for operating the systems, and eliminating the excess heat generated from the system. Current thinking sees optical interconnects on most levels to be a solution to many of the challenges.

Taking this concept to the next level, the introduction of optical links into High Performance Computing (HPC) will allow scaling the technology to larger volumes. As volumes increase, manufacturability will be of increasing importance. Solutions are needed that allow the introduction of optical functions as components, much like the well known Surface Mount Technology used for electrical components.

The challenges introducing optical links into level 1 packaging are manifold, and encompass materials, process and testing. The technical solutions are competing on manufacturability, as they are trying to replace existing designs proven in the marketplace. Therefore, the requirements of the commercial side – technical and non-technical – need to be well understood before a successful implementation can be anticipated.

The paper shows the main challenges and potential solutions to this challenge and proposes a fundamental paradigm shift in the manufacturing of optical links for the level 1 interconnect (chip package).

8630-2, Session 1

Performance methodologies of a modular miniature photonic turn connector

Alan Ugolini, Eric Childers, DJ Hastings, Dirk Schoellner, Jillcha Wakjira, US Conec Ltd. (United States)

A novel multi-fiber photonic turn connector provides direct connection to newly emerging miniature embedded parallel optic modules, allowing perpendicular mating to the printed circuit board. The usage of the connector as a module interface and the implementation of a TIR lens based system rather than a traditional polished fiber connector requires new procedures and guidelines for performance certification and visual inspection. These new performance methodologies will be presented in this paper.

The performance of the ferrule and housing connector system is predicated on its ability to couple power between the module and the fiber bi-directionally. To minimize the need for application specific module based test stations, a common test platform has been developed. The paper will present a new insertion loss test called the Interposer Test; this test can be used to screen a modular photonic turn connector for its prospective in-situ module performance without the need for vendor-specific modules. Test implementation will be discussed, and stability and repeatability results of this test method presented.

Visual inspection criteria has been developed and implemented based on Interposer performance. The lensed ferrule has a 180 μm spot diameter, collimated beam. Relative to traditional multi-mode fiber with a 50 μm core diameter and large exit angle, the new connector is less sensitive to debris or scratches. Experiments were conducted to determine the change in loss as a function of dig diameter and scratch width. Data will be presented to show how the induced defects affected the connector performance.

8630-3, Session 1

Development of low-cost polish-less optical multifiber backplane connector

Tsuyoshi Aoki, Hidenobu Muranaka, Shigenori Aoki, Fujitsu Labs., Ltd. (Japan); Katsuki Suematsu, Mitsuhiro Iwaya, Masato Shiino, Furukawa Electric Co., Ltd. (Japan)

High-speed over 25 Gbps data-rates interconnect between LSIs are required in next-generation servers or supercomputers. Optical interconnect technology has attracted much attention in terms of its advantages such as wide transmission bandwidth, low energy consumption, and so on.

Especially optical interconnect at the backplane level is considered as a promising technology in the near future. Last year, a prototype optical mid-plane for a blade server has been reported by Fujitsu Lab. and Furukawa Elec. 2000-fiber-channels and optical connectors were installed on the mid-plane. For the practical use of it, reducing the costs of passive components is one of the important issues. And, development of low-loss and low-cost optical connectors is thought to be indispensable.

In this research, we designed and fabricated a prototype novel low-cost optical multifiber backplane connector including no-polish multimode fibers. The injection-molded ferrule has a structure which can be elastically deformed by applying compressive forces. At the same time the fibers are bucking inside it. Employing this structure, the length variation in cut fibers is cancelled. And, the ferrule has 12- or 24-fiber-guide holes and guide-pin holes which can be mated to conventional MT-type ferrules. Low connecting losses between optical waveguides in PMT ferrules and fibers in the novel ferrules were achieved by their PC contact. And, the losses are almost equal to that between the PMT ferrules and polished MT ferrules. After the ferrules accommodated in prepared housing were mated 200 times, the connector showed good durability and kept PC contact.

8630-4, Session 1

Graded-index core polymer optical waveguide circuit fabricated using a microdispenser for high-density on-board optical interconnects

Kazutomo Soma, Takaaki Ishigure, Keio Univ. (Japan)

For the rapid performance increase of super computers in these years, high-density optical interconnection technologies are highly expected. Here, multimode polymer parallel optical waveguides (PPOWs) integrated on printed circuit boards (O-PCBs) is one of the feasible solutions. Particularly, densely-aligned waveguide circuits on PCBs are anticipated, and thus we have proposed to form graded-index (GI) circular cores into a planar waveguide, because GI-core exhibits superior properties to conventional step-index (SI)-core counterparts for high-density alignment. Recently, we proposed an innovative fabrication method of GI-circular core PPOWs: “the Mosquito method” that utilizes a microdispenser. In the Mosquito method, a thin hollow needle is directly inserted in a cladding polymer (a silicone resin) layer before curing, and another viscous silicone resin before curing is dispensed from the needle into the cladding with horizontally scanning the needle to draw GI cores.

In this paper, we experimentally demonstrate that a 5-cm long, 40- μm core diameter, and 250- μm pitch GI-circular core PPOWs (12 channels) fabricated by the Mosquito method show an inter-channel crosstalk of approximately -50 dB, almost 10 dB lower than that of a typical SI PPOW with square cores. Furthermore, we fabricate GI-core PPOW circuits in which bent waveguides are involved, by applying the Mosquito method, and we also introduce 3-dimensional GI-core waveguides obtained by a combination of vertical and horizontal needle scan. We will show the experimental results in the on-site presentation and proceeding. We believe that the Mosquito method will open the way for great advantage in high-density on-board optical interconnects.

8630-5, Session 1

Active or passive fiber-chip-alignment: approaches to efficient solutions

Gunnar Böttger, Henning Schröder, Rafael C. Jordan, Fraunhofer-Institut für Zuverlässigkeit und Mikrointegration (Germany)

High precision approaches for active and passive assembly and alignment on optoelectronic microbenches that have been realized at Fraunhofer IZM for various material systems and different scales, will be presented.

The alignment and reliable mounting of optical subcomponents such as laser and photo diodes, microlenses and microprisms require far higher mounting and alignment accuracies than for micro-electronic parts. When connecting from chip level to single mode optical fibers, even higher precisions are called for (typically <100 nm). Assembly and alignment commonly is performed on specialized lab equipment, consuming a lot of time, and with limited possibilities of automatization.

To introduce a higher degree of automatized production, like it has become standard in large volume electronics, one can choose either active or passive alignment processes – or possibly a combination of both. We will present examples of micro-optic benches and optical interconnections that include alignment structures for passive alignment – where the accuracy lies in the components to be assembled, and mounting takes place on a less accurate machine (“fit into place”). But there is also a lot of progresses on optical “pick and place” machines that realize a flexible and fully automated active alignment using vision systems and activated components of less cost in an industrial environment.

Fraunhofer IZM has a strong background in developing, integrating and testing microelectronic systems, including reliability and sustainability. Given the inclusion of more and more optical components into microsystems, we enhance or convert state-of-the-art assembly machines and procedures previously only used in the electronics world.

8630-6, Session 2

Photonic integration in InP for optical interconnects (*Invited Paper*)

Valery I. Tolstikhin, OneChip Photonics Inc. (Canada)

Optical interconnects are increasingly becoming both a solution to and a bottleneck of new generation data processing and storage systems. Their key component, an optical engine, is required to transmit and receive data at a very high (aggregate) bit rate, while being power, space and cost efficient far beyond requirements typical for telecom transceivers. This is hardly achievable without photonic integration, but will work only with functionally suitable and cost efficient PICs. This talk will provide an overview of an original approach, termed Multi-Guide Vertical Integration, which responds to the challenge. Being a regrowth-free PIC technology in InP, it allows for every required functionality, while enabling for unprecedented cost efficiency. The talk will describe the technology fundamentals and report on development of the 100G+ transmitter and receiver PICs for optical interconnects.

8630-7, Session 2

Multi-stacked silicon wire waveguides and couplers toward 3D optical interconnects (*Invited Paper*)

JoonHyng Kang, Nobuhiko Nishiyama, Yuki Atsumi, Tomohiro Amemiya, Shigehisa Arai, Tokyo Institute of Technology (Japan)

No Abstract Available

8630-8, Session 2

Hybrid polymer optical waveguides written by two-photon processing for 3D interconnects

Sönke Steenhusen, Ruth Houbertz-Krauss, Timo Grunemann, Fraunhofer-Institut für Silicatsforschung (Germany)

As the performance of microprocessors is constantly increasing according to Moore’s law, the data flow from and to the processors becomes a predominant bottleneck in the performance of future supercomputers and data centers. Besides the bandwidth limitation of electrical interconnects, power consumption is the main driver for the introduction of optical interconnects from long distance communications to shorter length-scales like the inter-chip level.

However, the implementation of optical interconnects at board level requires materials which are compatible with standard PCB assembly processes and, particularly, technologies which can be easily incorporated into the manufacturing chain.

Optical waveguides written in a multifunctional inorganic-organic hybrid polymer (ORMOCER®) using two-photon absorption (TPA) processes are investigated. TPA allows a strong confinement of photoreactions like the local boost of the refractive index by focussing femtosecond laser pulses into the ORMOCER® material. Thus, it is feasible to create optical waveguides connecting optoelectronic components along arbitrary paths in 3D space in a single process step. Since waveguides are written after the PCB assembly, alignment tolerances are not a critical factor for the manufacturing of a functional device.

TPA fabrication of 3D single mode waveguides at 1310 nm and 1550 nm in bulk ORMOCER® samples and in layers casted on PCBs is demonstrated. In order to maximize the waveguide’s performance, the impact of the applied laser parameters (wavelength, pulse energy, repetition rate) on optical losses and on the contrast in refractive index is investigated. Furthermore, the influence of the waveguides’ radius of curvature on the transmitted light is evaluated.

8630-9, Session 2

Board-to-board optical interconnects using molded polymer waveguide with 45-degree mirrors and inkjet-printed micro-lenses as proximity vertical coupler

Xiaohui Lin, The Univ. of Texas at Austin (United States); Amir Hosseini, Omega Optics, Inc. (United States); Xinyuan Dou, The Univ. of Texas at Austin (United States); Harish Subbaraman, Omega Optics, Inc. (United States); Ray T. Chen, The Univ. of Texas at Austin (United States)

No Abstract Available

8630-10, Session 3

Monolithically integrated Germanium receivers for optical interconnects (*Invited Paper*)

Solomon Assefa, William M. J. Green, Marwan H. Khater, Swetha Kamlapurkar, Huapu Pan, Clint L. Schow, Alexander Rylyakov, Carol Reinholm, Edward Kiewra, IBM Thomas J. Watson Research Ctr. (United States); Steven M. Shank, IBM Corp. (United States); Yurii A. Vlasov, IBM Thomas J. Watson Research Ctr. (United States)

Monolithic integration of deeply-scaled silicon optical components with CMOS analog and mixed signal circuits has high potential to

provide cost-effective and low-power optical interconnects for various applications for Ethernet links in new generation datacenters, optical backplanes in servers, and extensive parallelism in high-performance computing systems [1]. This talk will discuss recent progress in monolithically integrated Germanium receivers for optical interconnects. Monolithic integration of electronic and nanophotonics components was performed at the IBM using 200 mm SOI wafers (SOITEC) having a 220 nm silicon device layer on top of a 2 μ m BOX [2,3]. Several processing modules have been added to a standard CMOS processing flow at the front-end of the line. The Germanium waveguide photodetectors were fabricated by utilizing a rapid melt growth (RMG) technique wherein the Ge was melted and crystallized during the source-drain anneal step [4]. After completion of the monolithic integration with CMOS, receivers operating up to 25Gbps have been demonstrated.

1. Y. Vlasov, "Silicon CMOS-Integrated Nano-Photonics for Computer and Data Communication Beyond 100G," IEEE Comm. Mag., February 2012.
2. S. Assefa et al., "CMOS Integrated Silicon Nanophotonics: Enabling Technology for Exascale Computational Systems", in Proc. Optical Fiber Communication Conference 2011, paper OMM6
3. W.M.J. Green et al., "CMOS integrated silicon nanophotonics – enabling technology for exascale computational systems," SEMICON 2010, available at www.research.ibm.com/photronics
4. S. Assefa et al, "CMOS-integrated high-speed MSM germanium waveguide photodetector," Opt. Express 18, 4986 (2010).

8630-11, Session 3

Compact optical modulators with Si photonic crystals *(Invited Paper)*

Toshihiko Baba, Hong C. Nguyen, Yokohama National Univ. (Japan)

Mach-Zehnder optical modulators are the key in Si photonics because of their high-speed E/O conversion and a wide working spectrum. So far, pn-doped Si rib waveguides on the carrier depletion mode have been mainly used as phase shifters at an operating speed higher than 10 Gbps. However, the device length dominated by the phase shifter is usually longer than millimeters due to the limited index change of the carrier depletion. This length is already much shorter than commercial LN modulators but further shorter devices are desired for large-scale integration toward the high-capacity parallel data transmission and for simplifying an electrical issue of E/O phase matching. A promising solution is to use slow light. It enhances the phase sensitivity against the index change in proportion to the group index n_g . In particular, the enhancement and a wide spectrum can be balanced by engineering slow light in photonic crystal waveguides (PCW). Compared with rib-type devices, n_g of optimized PCWs is 10 times larger, allowing 10 times shorter devices even with a working wavelength range wider than 10 nm. Actually the length can be further shortened to less than 100 μ m at 10 Gbps or higher speed operation, which might be due to the reduced electrical issue. Note that such devices consisting of Si photonic crystal (typical hole diameter of 200 nm) and silica overlaid are fabricated by a standard CMOS process, and the loss penalty related with the PCW is almost negligible.

8630-12, Session 3

2D silicon-based surface normal vertical cavity photonic crystal waveguide array for high-density optical interconnects

JaeHyun Ahn, Harish Subbaraman, Swapnajit Chakravarty, Emanuel Tutuc, Ray T. Chen, The Univ. of Texas at Austin (United States)

No Abstract Available

8630-13, Session 3

Toward 3D plasmonic circuits: controlled coupling to multilevel plasmonic circuits

Mohamed El Sherif, Osman S. Ahmed, Mohamed H. Bakr, McMaster Univ. (Canada); Mohamed A. Swillam, The American Univ. in Cairo (Egypt)

We propose a surface plasmon multilevel coupler based on the orthogonal junction coupling technique between silicon nano-wire and plasmonic slot waveguides (PSWs). It couples light of different polarizations from a silicon nanowire into multilevel plasmonic networks. Two orthogonal PSWs are employed to guide each polarization to its respective port. The proposed structure splits the polarizations and allows for simultaneous processing at different horizontal layers. Our device overcomes inherent polarization limitation in plasmonic structures by providing multilevel optical signal processing. This ability of controlling polarization can be exploited to achieve 3-D multilevel plasmonic circuits and polarization controlled chip to chip channel. Our device is of a compact size and a wide band operation. The device utilizes both quasi-TE and quasi-TM polarizations to allow for increased optical processing capability. The crosstalk is minimal between the two polarizations propagating in two different levels. We achieve a -4.5 dB transmission efficiency at a wavelength of 1.55 μ m for the different polarizations in the respective ports. A transmission efficiency of -21 dB is achieved in the subsidiary port. We analyze and simulate the structure using the FDTD method. The proposed device can be utilized in integrated chips for optical signal processing and optical computations.

8630-14, Session 4

Optical transceivers for interconnections in satellite payloads *(Invited Paper)*

Mikko Karppinen, Veli Heikkinen, Kari Kautio, Jyrki Ollila, Antti Tanskanen, VTT Technical Research Ctr. of Finland (Finland)

Current trends in satellite payloads show a rapid increase in data traffic and processing. For instance, the throughput of next generation digital telecom satellites will exceed terabits per second of data, and the novel instruments, such as high-resolution cameras and synthetic aperture radars, call for high-speed communications on board the satellites. This motivates to investigate switching from electrical to photonic interconnects, to save in mass and volume while enabling high-bit-rate performance. For instance, the European Space Agency promotes the development of the "SpaceFibre" data link standard for spacecraft onboard communications and the studies on the high-throughput optical interconnects for the onboard processors of the telecom payloads.

We have developed optical transmitters and receivers for intra-satellite applications. The components integrate 850-nm VCSELs and photodiodes with transceiver ICs and multimode fibers, enabling to meet the high integration density and low power requirements. The lightweight metal-ceramic packaging results in high reliability and robustness for the harsh spacecraft environments, including mechanical vibration and shock, wide temperature range, and radiation. The low-temperature cofired ceramic substrates of the optical subassemblies include also structures for the passive optical alignment.

The developed components include the 6.25 Gbps "SpaceFibre" transceiver for onboard communications and a parallel optical transceiver, for instance, for board-to-board interconnects. The latter is a 10 Gbps/channel full-duplex quad transceiver. Its hermetic package integrates 4-channel VCSEL and photodiode arrays and a fiber-ribbon pigtail.

Furthermore, inter-chip optical interconnects were studied targeting to bring the optical interfaces close to the onboard processor ICs. Co-packaging of the ICs with multichannel optical interconnect subassemblies was presented.

8630-15, Session 4

Dynamic polymer ribbon couplers for card-to-backplane optical interconnects

Guomin Jiang, Sarfaraz Baig, Michael R. Wang, Univ. of Miami (United States)

Optical interconnects have been extensively researched for high-speed computing systems because of the speed limitations and drawbacks of electrical data buses. Most of optical interconnect architectures are based on point-to-point link topologies, resulting in higher cost per link and lower energy efficient. A shared bus topology can effectively multicast signals to all plug-in cards. But most of them set a fixed power distribution to each link after device fabrication. They are not energy efficient since they consume optical single power even when the cards are not plugged into the backplane. We reported early dynamic array waveguide evanescent couplers for multi-card backplane optical interconnect. One drawback of the approach is that the waveguide cores must be exposed in air for coupling purpose that may subject to dust and handling damage. In this paper, we present flexible polymeric waveguides with dynamic optical coupler array fabricated by vacuum assisted microfluidic technique for card-to-backplane optical interconnect applications. A dynamic optical coupler on backplane consists of an evanescent coupler with two straight multimode polymer waveguides and a 45° micro-mirror. It can couple a backplane waveguide interconnect beam to an interconnect waveguide on a plug-in card. Each card can receive necessary optical signal power from the backplane waveguide by adjusting the coupling efficiency of each dynamic coupler. All the interconnect waveguides are embedded. This technique offers a low-cost and highly repeatable fabrication of flexible polymer waveguides for optical interconnects.

8630-16, Session 4

Demonstration of an optical multi-Gbps board-to-board interconnection including integrated FPGA-based diagnostics

Anton Kuzmin, Dietmar Fey, Friedrich-Alexander-Univ. Erlangen-Nürnberg (Germany); Ulrich Lohmann, Jürgen Jahns, FernUniv. in Hagen (Germany); Hannes Bauer, MICROSENS GmbH & Co. KG (Germany)

We present an optoelectronic parallel multi-Gbps board-to-board interconnection and demonstrate its performance by interconnecting high performance FPGAs. In order to communicate over short distances, the approach of integrated high speed optoelectronic transceiver in combination with ribbon fiber bundles and novel 3D fiber matrices is used. This approach offers the potential for complex interconnectivity, scalability and yet compact size. In addition, we consider the optical performance and the fabrication of this novel fiber-matrix component.

In particular, we show the prototype of a 3D fiber-matrix for board-to-board interconnection with a total number of up to 144 internal optical channels. The 4 activated bidirectional optical multimode links work at 850 nm wavelength, each with a data rate of 8.5 Gbps. The data rate is generated by using high performance FPGAs, additionally this components perform diagnostics of the optical link in the view of BER and eye-width. This diagnostics can further be used for optimization of the optical link parameters with the goal to minimized the power consumption of the complete optical data communication.

The complete setup is demonstrated using a multi-core system separated into two FPGAs. The same connectivity level is achieved between the cores in the different chips as within a single FPGA. The demonstrated distributed layout of the components is of interest, for example, for communication in high-performance embedded computing systems, which have a widely distributed design. Finally, examples for potential applications of such optical networks are shown with specific focus on data centers and avionic optical interconnection.

8630-17, Session 4

A regenerative optical backplane demonstrator for board-level optical interconnects

Nikolaos Bamiedakis, Aeffendi H. Hashim, Richard V. Penty, Ian H. White, Univ. of Cambridge (United Kingdom)

Multimode polymer waveguides are a promising candidate for use in high-speed short-reach board-level optical interconnects as they can be cost-effectively integrated onto conventional printed circuit boards (PCBs) and allow board assembly with automated pick-and-place tools. Moreover, passive optical architectures are attractive for use at the backplane level as they are intrinsically simpler to implement and don't rely on the use high-performance optical switches which typically exhibit large power consumptions and high manufacturing costs. As a result, a multi-channel regenerative optical bus architecture that relies on the use of PCB-integrated polymer waveguides and low-cost optoelectronic regenerator units has been proposed in order to form a cost-effective high-performance optical backplane. The proposed architecture allows arbitrary number of electrical cards to be connected onto the shared optical bus and is scalable to larger numbers of communication channels. In this paper, we present a proof-of-principle optical backplane demonstrator comprising two polymeric bus modules and a prototype 3R regenerator, all formed on low-cost FR4 substrates. The demonstrator enables interconnection between 6 electrical cards over 4 optical channels, with each channel operating at 10 Gb/s. All links on the backplane operate with a power margin greater than 2 dB, achieving error-free (BER<10⁻¹²) communication between all cards at an aggregate data rate of 40 Gb/s (4x10 Gb/s). The system design, details of the optical and electrical layers of the opto-electronic boards, as well as the demonstrator fabrication and assembly are described. Finally, the static and dynamic characterisation of the on-board optical links is presented.

8630-18, Session 5

Optics vs copper: from the perspective of Thunderbolt interconnector technology (Invited Paper)

Hengju Cheng, Intel Corp. (United States)

Interconnect technology has been progressed at very fast pace for the past decade. The signaling rates have steadily increased from 100Mb/s to 25Gb/s. In every generation of technology evolution, optics always seems to take over at first, however, at the end, the cost advantage of copper wins over. Because of this, optical interconnects are limited to longer distance links where the attenuation in copper cable is too large for the integrated circuits to compensate. Optical interconnect has also long been viewed as the premier solution in compared with copper interconnect due to the cost. With the release of Thunderbolt technology, we are entering a new era in consumer electronics that runs at the 10Gb/s line rate (20Gb/s throughput per connector interface). Thunderbolt interconnect technology includes both active copper cables & active optical cables as the interconnect media which have very different physical characteristics. In order for optics to succeed in consumer electronics, several technology hurdles need to be cleared. For example, the optical fiber cables need to handle the consumer abuse. Also, the optical engine used in the active optical cable needs to be physically small without changing the looks & feels of the consumer cable/connector itself. Most importantly, the cost of optics needs to come down significantly to effectively compete with the copper solution. In this talk, two interconnect technologies are compared & discussed on the relative cost, power consumption, form factor, density, & future scalability. Depends on the usage models & the next generation optical technology evolution, this perpetual copper vs. optics debate can have a very different conclusion.

8630-19, Session 5

An all-silicon optical PC-to-PC link utilising USB

Marius E. Goosen, Antonie C. Alberts, INSiAVA (Pty) Ltd. (South Africa); Petrus J. Venter, Monuko du Plessis, Univ. of Pretoria (South Africa); Pieter Rademeyer, INSiAVA (Pty) Ltd. (South Africa)

CMOS has unrivalled integration potential and is currently the dominant technology for integrated circuits. Hot carrier luminescent light sources provide a way to create light in a standard CMOS process, potentially enabling cost effective optical communication between CMOS integrated circuits. This work targets a realworld integrated solution of an all-silicon optical link, connecting two PCs via a USB port while transferring data optically between the devices.

An electronically modulated silicon light emitter array is implemented in a standard 0.35 μm CMOS technology with no post-processing and is mechanically aligned to a 1 mm diameter core plastic optical fiber. The optical data is received via a commercially available silicon avalanche photodiode. For demonstration purposes the data rate was limited to 1 Mb/s resulting in a BER of approximately 10⁻⁴. However, data rates exceeding 10 Mb/s have already been demonstrated in previous work with raw bit streams.

In this paper we present an all-silicon PC-to-PC optical link capable of transferring data between two PCs at a rate not exceeding 1 Mb/s using an all-silicon optical link. The communication between the PCs is realised via the popular USB-port. The USB data is converted into three serial bit streams, data is then transmitted in two half duplex channels, with the clock being transmitted separately. Custom PC terminal software is utilised for controlling the optical data links and facilitating the data transfer. Such an optical communication system could find application in high noise environments where data fidelity, range and cost is a concern.

8630-20, Session 5

Active optical cable-based high-resolution long-distance VGA extenders

Jin-Geun Rhee, Iksu Lee, Heejun Kim, Sungjoon Kim, Terawave Inc. (Korea, Republic of); Hoik Kim, Yeon-Wan Koh, FIBERPRO, Inc. (Korea, Republic of); Jiseok Lim, Chur Kim, Jungwon Kim, KAIST (Korea, Republic of)

Remote transfer of high-resolution video information finds more applications in detached display applications for large facilities such as theaters, sports complex, airports, and security facilities. Active optical cables (AOCs) provide a promising approach for enhancing both the transmittable resolution and distance that standard copper-based cables cannot reach. In addition to the standard digital formats such as HDMI, the high-resolution, long-distance transfer of VGA format signals is important for applications where high-resolution analog video ports should be also supported, such as military/defense applications and high-resolution video camera links.

In this paper we present the development of a high-resolution (up to UXGA, 1920x1200), long-distance (>1 km) VGA extenders without signal degradations based on AOC techniques. We employed asynchronous serial transmission and clock regeneration techniques, which enables lower cost implementation of AOC-based VGA extenders by removing the necessity for clock transmission and large memory at the receiver. Two 2.5 Gbps transceivers are used in parallel to meet the required the maximum video data rate of 4 Gbps. As the data are transmitted asynchronously, 24-bit pixel clock time stamp is employed to regenerate video pixel clock accurately at the receiver side. In parallel to the video information, stereo audio, digital display control, and RS-232 control signals are transmitted as well.

We will further show potential applications of the developed system for security monitoring systems, video camera links, and bio-sensors.

8630-21, Session 5

An optical interconnect for large-scale systems (Invited Paper)

William B. Dress, Lightfleet Corp. (United States)

A switchless, optical-interconnect module comprised of a set of multicast channels is based on an earlier free-space, optical broadcast interconnect designed for tight computing clusters is introduced. The design presented here has 32 single-mode input fibers and 32 single-mode output fibers. Messages in the form of modulated light beams form the inputs to the system. Internally, each input beam undergoes an optical splitting followed by an optical-to-electrical conversion so that a filtering process examining the packet header may direct the packet to the appropriate exit buffer where the electrical data are re-converted to optical data and sent out on the appropriate output fiber(s). Any particular input may appear on any one of the outputs, none of the outputs, all of the outputs, or a subset of the outputs depending on the destination encoded in the message header. The result is an interconnect that is inherently point-to-point, multicast, and broadcast, with decisions as to which made internally in the interconnect based on the addressing mode. This enables, among other features, a single-send multicast.

Certain regular interconnect topologies for large-scale systems are reviewed with the goal of implementation using a network of the optical modules described above as network nodes. Each network node has connections to other such nodes as well as to endpoints which may be servers, high-performance computers, or storage devices. Two key parameters are diameter (which is related to the latency between nodes) and bandwidth. Trade-offs between diameter and bandwidth or diameter and scalability are assessed. The goal this section is to indicate how a fabric topology based on identical distribution modules may be evaluated.

Finally, the problems of fabric management are discussed, contrasting the global control of message traffic in a switched system with the purely local routing in a network of optical-distribution modules. Message forwarding ("routing") in the optical-distribution fabric depends on gating choices at each node made during the filtering process mentioned above. This method operates across interconnects at all scales, from the small enterprise with a few end nodes to large installations with thousands of end nodes. In addition, the method allows adaptive routes to be chosen at the local level, ensuring that optimal route through even the largest of fabrics in the presence of high-volume network traffic is taken. The method also allows re-routing and self-healing in the case of loss of connections or nodes. Examples are given for particular topologies (tree, fat tree, multi-dimensional torus, and modifications of the Clos interconnect).

8630-22, Session 6

Multimode multiplexing on a silicon chip (Invited Paper)

Michal Lipson, Cornell Univ. (United States)

We design and demonstrate an integrated multimode waveguide platform with minimal inter-modal crosstalk on silicon based on a bend designed using computer-optimized transformation optics as well as resonant structures as add/drop mode multiplexers.

8630-23, Session 6

Power-efficient hybrid III-V / SOI external cavity lasers for high-density Si-photonics interconnect platform (*Invited Paper*)

Aaron J. Zilkie, Bhavin J. Bijlani, Pegah Seddighian, Saeed Fatholouloumi, Wei Qian, Daniel C. Lee, Roshanak Shafiiha, Dazeng Feng, Kotura, Inc. (United States); Jonathan Luff, Kotura Inc. (United States); John E. Cunningham, Xuezhe Zheng, Ashok V. Krishnamoorthy, Oracle (United States); Mehdi Asghari, Kotura, Inc. (United States)

We have been engaged in development of a complete suite of low-power and high-density technologies for a 3-micron SOI WDM optical interconnect transceiver and transport platform. We will present latest results on our hybrid laser technology showing hybrid lasers that have wall-plug-efficiencies of 9.5% at powers > 6 mW.

8630-24, Session 6

Scaleable optical transmitter based on cascaded nanoresonator modulators and multiwavelength laser with ultralow switching energies

Liam O'Faolain, Kapil Debnath, Thomas F. Krauss, Univ. of St. Andrews (United Kingdom); Fred Y. Gardes, Graham T. Reed, Univ. of Southampton (United Kingdom); Andreas G. Steffan, u?t Photonics AG (Germany)

Integration density, low switching energy and channel scalability are the major requirements for the deployment of photonics technologies in data communications. Current approaches are based on multiple lasers and spatial channels [1] but the ability to use Wavelength Division Multiplexing (WDM) techniques is crucial for exploiting the available bandwidth. Here, we experimentally demonstrate a new interconnect architecture based on cascaded photonic crystal nanoresonators driven by a frequency comb laser that offers a compelling solution to these challenges.

A silicon nitride waveguide provides the data bus and its low propagation loss is ideal for the on-chip routing of light. The relatively large core also provides efficient coupling (<3dB) from the comb laser. The photonic crystal (PhC) modulators are coupled to the bus waveguide using a novel k-vector matching technique. Each cavity has a resonance wavelength that matches a line of the comb laser's spectrum, allowing efficient modulation of each channel without the need for complex multiplexing/demultiplexing elements. The small mode volume of the PhC cavity enables very low switching energies (<1fJ/bit) and a very large free spectral range (>100nm) [2] while the vertically coupled approach minimises the silicon area consumed by the photonic elements, thus freeing up space for electronic circuitry. This approach has genuine potential for the realisation of energy efficient terabit on-chip interconnects.

[1] IEEE Journal of Solid-State Circuits 44, 301-313 (2009)

[2] Optics Express 17, 22505-22513 (2009)

8630-26, Session 7

High-power flip-chip-bonded silicon hybrid laser for temperature-control-free operation with micro-ring resonator-based modulator (*Invited Paper*)

Shinsuke Tanaka, Seok-Hwan Jeong, Tomoyuki Akiyama, Shigeaki Sekiguchi, Teruo Kurahashi, Yu Tanaka, Ken Morito,

Fujitsu Labs., Ltd. (Japan)

A Si-based, large-scale optical I/O chip is a key device for a large-bandwidth, low-cost optical interconnection employed in high-performance computing systems. For these Si I/O chips, a significant improvement in energy cost is strongly expected, hence, the use of micro-ring-resonator (MRR) based modulator is assumed to be a promising approach. In order to handle a narrow and temperature-dependent operation bandwidth of the MRR-based modulator, we have proposed a novel Si transmitter which uses a cascaded MRR MZ modulator and MRR-based Si hybrid laser. The Si hybrid laser is an external cavity laser integrating a InP SOA and a Si mirror chip comprising of a MRR and DBR. The SOA is flip-chip bonded to the Si mirror chip utilizing a precise flip-chip bonding technology. The fabricated Si hybrid laser exhibited a low threshold current of 9.3mA, a high output power of 15 mW, and a large wall-plug efficiency of 7.6% at 20 C. In addition, the device maintained a stable single longitudinal mode lasing and low RIN level of <-130 dB/Hz for 20-60 degree C. We also fabricated a proto-type of proposed Si transmitter integrating a cascaded MRR MZ modulator and MRR-based Si hybrid laser. The 20-MRR cascaded MZ modulator exhibited a 1-nm operation bandwidth using a relatively low-Q MRR design. The modulator was driven with a 10Gb/s PRBS signal. For a temperature range of 25 to 60 C, the lasing wavelength exhibited a red-shift of 2.5nm, nevertheless, we confirmed clear eye openings without adjusting the operating wavelength of the modulator.

8630-27, Session 7

Progress on energy efficient and high bit rate VCSELs for optical interconnects spanning nanometers to a kilometer (*Invited Paper*)

James A. Lott, Philip Moser, Dieter Bimberg, Technische Univ. Berlin (Germany)

We report our progress on the development of energy efficient vertical cavity surface emitting lasers (VCSELs) with small spectral widths for ≥ 25 Gb/s per channel optical interconnects for heterogeneous photonic integrated circuits with near-zero optical spans, high performance computing systems with ultrashort (micrometers to millimeters) and very short (centimeters) light-guided interconnect paths, active optical cables with plug-and-play distances of up to a few meters, and for data centers with interserver optical fiber interconnect distances up to about a kilometer.

8630-28, Session 7

Philips' VCSEL and photodiode arrays for parallel optical interconnects

Roger King, Steffan Intemann, Stefan Wabra, Philipp Gerlach, Michael Riedl, Martin Grabherr, Philips Technologie GmbH U-L-M Photonics (Germany)

Philips as one of the first volume manufacturers of FDR active optical components successfully sells VCSEL and photodiode products into the very fast growing FDR InfiniBand™ interconnect market. In this work we review the influence of fabrication variations on VCSEL characteristics. It is shown that FDR VCSEL manufacturing reached a maturity level.

As Philips has shipped tens of millions of small diameter single-mode VCSEL into consumer-type applications like e.g. VCSEL-based mice we analyzed a scenario where FDR optical interconnects are based on consumer-type single-mode rather than on multimode VCSELs. Test results indicate, that employment of small-diameter VCSELs reduces the power consumption of the optical transmitter significantly while the reliability of the transmitter will not deteriorate.

VCSEL and photodiodes for the next EDR (26Gbps) InfiniBand™ generation are currently being developed at Philips. This work presents the status of the EDR optical component development.

8630-29, Session 7

Substrate induced effects in photonic crystal thermo-optic devices on a silicon-on-insulator platform

Weiwei Song, Manjit Chahal, George K. Celler, Yogesh Jaluria, Wei Jiang, Rutgers, The State Univ. of New Jersey (United States)

We study the influence of the substrate on a photonic crystal thermo-optic device on a silicon-on-insulator (SOI) platform. In most theoretical or numeric studies, substrate induced effects are considered small. Silicon substrate thicknesses on the order of tens of microns, which are significantly thinner than the values in real SOI devices, are often used in finite element simulations to reduce simulation time. In this work, we show that the artificially reduced substrate thickness in simulations could lead to significant underestimate of the substrate effect in such thermo-optic devices. We calculate the temperature rise in a thick substrate semi-analytically. The results agree well with finite element simulations. The substrate's contribution to the thermo-optic effect is obtained as a function of various physical parameters such as the heater length, buried oxide thickness, and substrate thickness. The upper limit of the contribution of the substrate is evaluated. It is shown that for some applications such as long delay lines, the upper limit can be as high as 10% for an optimized design and 20~30% for some common designs. As such, the substrate's contribution cannot be neglected in those applications where high accuracies are needed for signal delay. Approaches to reducing the substrate effect will be discussed. The advantages of membrane-based devices will also be shown.

8630-30, Session 8

Design principles and realization of electro-optical circuit boards (*Invited Paper*)

Felix Betschon, Tobias Lamprecht, Markus Halter, Stefan Beyer, vario-optics ag (Switzerland)

The manufacturing of planar optical polymer waveguides is based to a large extent on established technologies. First electro-optical circuit board (EOCB) products with embedded polymer waveguides are currently produced in series. The range of applications within the sensor and data communication segments is growing with the increasing level of maturity. EOCBs require design flows, processes, and techniques compatible to existing printed circuit board (PCB) manufacturing and appropriate for optical signal transmission. A key aspect is the precise and automated assembly of active and passive optical components to the optical waveguides.

This work gives an insight into the design principles of EOCBs on the basis of realized examples.

After a short introduction into the build-up and the manufacturing of EOCBs the design flow is described. Based on the required optical signal properties at the end of the optical transmission line, one designs the planar optical elements (waveguides, splitters, couplers), defines the optical coupling approach and the light emitting devices. This includes optical simulation of the key components. This phase already requires co-design of the optical and electrical domain using novel design flows.

The actual integration of an optical system into a PCB is shown in the last part. The optical layer is thereby laminated to the purely electrical circuit board using a conventional PCB-lamination process to form the EOCB. The precise alignment of the various electrical and optical layers is thereby essential. Electrical vias are then generated, penetrating also the optical layer, to connect the individual electrical layers. Finally, the board has to be tested electrically and optically.

8630-31, Session 8

Low-loss 45-degree mirror on GI-core polymer optical waveguide for optical PCB

Masaki Nakano, Takaaki Ishigure, Keio Univ. (Japan)

Optical interconnect technologies are drawing extra attention particularly in high-performance computers (HPCs) and core routers. Specifically, optical printed circuit boards (OPCBs) on which multimode polymer optical waveguides are integrated have been strongly anticipated to realize high-speed on-board interconnects. On the OPCBs, the surface mount technique is applied to laser and photo-detector (PD) chips, and the output/input light from/to those devices needs to be perpendicularly bent to utilize the waveguides on the OPCB. Hence, current trends are in perpendicular light path conversion by 45-degree reflector mirrors formed at waveguide ends.

In this paper, we theoretically demonstrate that graded-index (GI) core waveguides can dramatically reduce the mirror loss, compared to conventional step-index (SI) core waveguides. First, by utilizing a ray-trace simulation we developed, we calculate the optical loss at the reflector mirrors formed on both SI and GI waveguides with different waveguide numerical apertures. From the calculated results for the mirrors near the PD, it is found that since the output light (NFP) from SI-core is uniformly spread in whole core area, after the reflection at the mirror, the diverged rays reflected at the periphery of the core do not reach the PD, resulting in the dominant optical loss. On the contrary, GI waveguide exhibits approximately 2-dB lower mirror loss than SI waveguide, because the output light from GI cores is concentrated to the core center. Furthermore, in this paper, the mirror-loss advantage in GI-core waveguide is also experimentally confirmed. Hence, the GI-core waveguides are promising components for on-board interconnects.

8630-32, Session 8

24-ch microlens-integrated no-polish connector for optical interconnection with polymer waveguides

Takashi Shiraishi, Takatoshi Yagisawa, Fujitsu Labs., Ltd. (Japan); Tadashi Ikeuchi, Osamu Daikuhara, Fujitsu Ltd. (Japan); Kazuhiro Tanaka, Fujitsu Labs., Ltd. (Japan)

Recently, studies have been carried out concerning optical interconnection using polymer waveguides. Generally, a PMT optical connector is used for connection of the waveguides. However, it is expensive because assembly requires polishing and a long time for thermal hardening of the adhesive.

We propose a new 24-ch polymer waveguide connector for cost-effective assembly for joint to a MT connector. The connector consists of a transparent thermoplastic resin that has two rectangular slits on one side for alignment of the waveguide films and integrated microlens arrays on the other side for coupling to the MT connector.

Two 12-ch waveguide films were cut to a 3-mm width. The thickness of each waveguide film was controlled at 100 micrometers. The waveguide films were inserted into the slits until they touched the bottom face of the slit. Ultraviolet curing adhesive was used to achieve a short hardening process. The expanded beam in the transparent material is focused by the microlens arrays formed on the connector surface. This lens structure enables assembly without the need for a polishing process.

We designed the lens for coupling between a step-index 40-micron rectangular waveguide and a graded-index 50-micron fiber. We achieved low-loss optical coupling by designing a way to provide asymmetric magnification between the horizontal and vertical directions in order to compensate the asymmetric Numerical Aperture of the waveguide.

The measured coupling losses from/to waveguide to/from fiber were 1.1 dB and 0.5 dB, respectively. The total losses are as small as that of a Physical Contact connection.

8630-33, Session 8

Rigorous calculation of optical modes and their interference induced power distribution in arbitrary numbered coupled slab waveguides

Guiru Gu, Xuejun Lu, Univ. of Massachusetts Lowell (United States)

No Abstract Available

8630-34, Session 9

Polymer-based optical interconnects using nanoimprint lithography (*Invited Paper*)

Arjen Boersma, Peter Harmsma, Sjoukje Wieggersma, TNO Science and Industry (Netherlands)

The increasing request for higher data speeds in the information and communication technology leads to continuously increasing performance of microprocessors. This has led to the introduction of optical data transmission as a replacement of electronic data transmission in most transmission applications longer than 10 meters. However, a need remains for optical data transmission for shorter distances inside the computer. This paper gives an overview of the Joint European project FIREFLY, in which new polymer based single mode waveguides are developed for integration with VCSELs, splitters and fibers that will be manufactured using multi-layer nanoimprint lithography (NIL). Innovative polymers, new applications of nano-technology as well as new methods for light in- and out coupling and the integration of all these new components are the technical ingredients of this ambitious project.

New polymers: developments in siloxane based polymers will be discussed that reduce the optical loss at datacom and telecom wavelengths. These new polymers can already be processed using processes such as direct laser writing.

New production processes: the implementation of the new polymers in multi-layer NIL will be assessed. Polymer cladding and core is structured at micrometer scale to create dense networks of single mode waveguides. The NIL process is a suitable technique for mass production.

Integration: new concepts will be presented that will optimize the coupling of the components and reduce the optical losses that arise in coupling the lasers to waveguides, waveguides to fibers, and in 45° or 90° bends.

8630-35, Session 9

Embedded planar glass waveguide optical interconnect for data centre applications (*Invited Paper*)

Richard C. Pitwon, Xyratex Technology Ltd. (United Kingdom); Henning Schroder, Fraunhofer-Institut für Zuverlässigkeit und Mikrointegration (IZM) (Germany); Lars Brusberg, Fraunhofer-Institut für Zuverlässigkeit und Mikrointegration (Germany); Jasper Graham-Jones, Plymouth Univ. (United Kingdom); Kai Wang, Xyratex Technology Ltd. (United Kingdom)

Interconnect speeds within data storage systems will increase to over 24 Gb/s by 2016 thereby severely impacting cost and performance in future data centres. Electro-optical printed circuit board technology (EOCB) based on integrated planar polymer optical waveguides has been the subject of research and development for many years to provide a cost viable, fully integrated system embedded optical interconnect solution, however a number of constraints of this technology have yet

to be overcome. Current polymer waveguides are limited to step-index profiles, which places a dispersion limit on how far optical signals can be conveyed along a waveguide. Furthermore, due to higher optical absorption at the longer telecommunication wavelengths, the deployment of polymer waveguides is usually restricted to 850 nm signals.

We present a promising technology for large panel EOCB based on holohedrally integrated glass foils. The planar multimode glass waveguides patterned into these glass foils have a graded index structure, thereby giving rise to a larger bandwidth length product compared to their polymer waveguide counterparts and lower absorption at the longer telecom wavelengths. This will allow glass waveguide based EOCBs to support the future bandwidth requirements inherent to large scale data centre subsystems while not incurring the same dispersion driven penalties on interconnect length or loss dependence on wavelength.

To this end glass foil structuring technologies have been developed that are compatible with industrial PCB manufacturing processes. Established processes as well as new approaches were analysed for their eligibility and have been applied to the EOCB process.

8630-36, Session 9

Hybrid polymers for data and telecom applications

Sönke Steenhuisen, Ruth Houbertz, Fraunhofer-Institut für Silicatforschung (Germany); Zarah Falk, Benedikt Stender, Julius-Maximilians-Univ. Würzburg (Germany); Gerhard Sextl, Fraunhofer-Institut für Silicatforschung (Germany)

During the last two decades, low-cost materials such as polymers for data and telecom applications have been intensively investigated. In order to serve as advanced packaging material, from an industrial point of view emphasis has also to be on cost reduction either for the materials, the processes, or for both. Materials are searched for which enable processing and integration from an nm up to a cm scale on the one hand, and the fabrication of either multi- or single-mode waveguides on the other hand.

A material class which fulfills these requirements is the material class of inorganic-organic hybrid polymers such as ORMOCER®s. Their properties can be intrinsically tailored by catalytically controlled hydrolysis/polycondensation reactions using alkoxysilane precursors, resulting in storage-stable resins consisting of organically functionalized oligomers. Upon synthesis, functional organic groups are introduced into the material which allow photochemical and/or thermal cross-linking.

(Photo-)patterning can be carried out from an nm up to a cm scale, employing a variety of different micro- and nanopatterning methods in order to generate micro- and nano-optical components such as waveguides, gratings, and lenses. The material and processing properties directly influence the resulting structure and, thus, the physical performance of the fabricated elements. The combination of chemically designed low-cost materials with tunable material parameters such as low optical absorption, tunable refractive index, good processability, and high chemical, thermal and mechanical stability, is very attractive for (integrated) optical applications.

8630-37, Session 9

Compact silicon oxynitride waveguides on silicon chips for optical delay line applications

Lianghong Yin, Rutgers, The State Univ. of New Jersey (United States); Ming Lu, Brookhaven National Lab. (United States); Leszek Wielunski, Jun Tan, Weiwei Song, Yicheng Lu, Wei Jiang, Rutgers, The State Univ. of New Jersey (United States)

We investigate silicon oxynitride (SiON) waveguides for long optical delay lines on a silicon chip. With the choice of a moderately low

refractive index contrast, a balance can be achieved between compact waveguide cross-section and low loss. SiON thin films with varying nitrogen concentrations are deposited using a plasma enhanced chemical vapor deposition (PECVD) system with varying NH₃ gas flow. The material composition and refractive index are characterized by Rutherford Backscattering Spectrometry and ellipsometry. Interestingly, under our deposition conditions, the refractive index of a SiON film has an almost linear dependence on ratio of the NH₃ flow rate versus the overall flow rates of all gases although the dependence of SiON refractive index on the NH₃ flow rate is not linear. High temperature annealing is performed after waveguide fabrication so as to simultaneously remove light absorbing bonds in the materials and smooth the sidewall roughness at the core-cladding interface. A meter-long SiON waveguide is demonstrated on a centimeter scale chip. With excellent compatibility with silicon photonics, SiON waveguides studied here can potentially be used for delay lines of an on-chip switchable delay network for phased array antennas. The stronger confinement achieved in the smaller waveguide cross-section will offer advantages for high-density integration of such delay lines including potential 3D integration by transfer printing. Lastly, the reduced SiON waveguide cross-section may also help reduce the power consumption of active (e.g. thermo-optic) SiON devices.

8630-38, Session 9

Low loss polycrystalline silicon waveguides and devices for multilayer on-chip optical interconnects

David N. Kwong, Amir Hosseini, John Covey, Yang Zhang, Xiaochuan Xu, Ray T. Chen, The Univ. of Texas at Austin (United States)

We have investigated the feasibility of multimode polysilicon waveguides to demonstrate the suitability of polysilicon as a candidate for multilayer photonic applications. Solid Phase Crystallization (SPC) with a maximum temperature of 1000°C is used to create polysilicon on thermally grown SiO₂. We then measure the propagation losses for various waveguide widths on both polysilicon and crystalline silicon platforms. We find that as the width increases for polysilicon waveguides, the propagation loss decreases similar to crystalline silicon waveguides. The difference in loss between the two platforms for a given waveguide width is due to the scattering from the polysilicon grain boundaries, which excites higher order modes. Depending on the waveguide width, these modes either propagate as higher order modes or are lost as radiation modes. Due to their different propagation constants, the presence of higher order modes is confirmed using sub-wavelength grating couplers. At a waveguide width of 10µm, polysilicon and crystalline silicon waveguides have propagation losses of 0.56dB/cm and 0.31dB/cm, respectively, indicating there is little bulk absorption from the polysilicon. This propagation loss is the lowest for polysilicon demonstrated to date. Modal and polarization scrambling in multimode waveguides by polysilicon grain boundary scattering are investigated using a sub-wavelength grating coupler and discussed. These results vindicate the use of polysilicon waveguides of varying widths in photonic integrated circuits.

8630-39, Session 10

Open foundry processes for silicon photonics (Invited Paper)

Michael Hochberg, Univ. of Delaware (United States)

Over the last ten years, it has become possible to build fairly complex integrated optical systems at telecommunications wavelengths on electronics-compatible silicon substrates. The OpSIS project is focused on developing and sharing processes suitable for creating large-scale integrated photonic systems-on-chip. This talk will provide an update on the status of and technical capabilities of these publicly-accessible manufacturing processes, a description of our work on improving

photonic design flows, and an overview of some of the emerging applications being explored in the OpSIS processes.

8630-40, Session 10

Silicon photonics for advanced optical communication systems (Invited Paper)

Zhiping Zhou, Peking Univ. (China)

No Abstract Available

8630-41, Session 11

Low power SOI-CMOS photonic links (Invited Paper)

Ivan Shubin, Xueze Zheng, Glenn Li, Hiren Thacker, Ying Luo, Jin Yao, Jin Lee, Kannan Raj, Ashok V. Krishnamoorthy, John E. Cunningham, Oracle (United States)

We demonstrate a highly efficient tunability of the photonic modules composed of arrays of high-speed ring modulators and mux-demux filters. Both SOI CMOS photonic and Si bulk electronic circuits are manufactured in their respective state-of-the-art manufacturing technologies and are hybrid-interconnected to showcase links with high bandwidth density and low sub-pJ/bit energy.

8630-42, Session 11

Integrated high speed hybrid silicon transmitters (Invited Paper)

Sudha Srinivasan, Yongbo Tang, Sid Jain, John E. Bowers, Univ. of California, Santa Barbara (United States)

No Abstract Available

8630-43, Session PWed

Ultracompact high conversion-efficiency polarization rotator based on silicon nanowire

Seung Beom Kang, Electronics and Telecommunications Research Institute (Korea, Republic of)

Silicon photonics can provide an attractive platform for future cost-effective optical communications, where optical components on silicon-on-insulator (SOI) are compatible with mature silicon IC fabrication processes. Silicon waveguides, which are basic platform for most of silicon photonic devices, have large structural birefringence that causes polarization-mode dispersion, polarization-dependent loss, and polarization-dependent wavelength characteristics. As a result, the polarization sensitivity becomes a major problem in silicon photonic waveguide due to the random polarization state in optical fibers. This makes silicon photonic devices less compatible with the optical fibers necessary to connect them to the outside world in practical applications. Therefore, the polarization handling and high-efficiency fiber coupling becomes important issue in silicon photonics technology.

In this work, we investigate high-efficiency polarization splitter and rotator coupled with a inverted-tapered mode-size converter at the input/output port on SOI for polarization transparent coupling system with optical fibers. The polarization rotator is based on an 18µm-long off-axis double-core structure employing SiN_x second core. The fabricated polarization splitter shows the polarization extinction ratio of ~15dB and excess loss of ~1 dB. The polarization rotator exhibits high polarization-conversion efficiency of ~80 %, and the excess loss is about 1 dB. We discuss

improvement in transmission through polarization transparent coupling system and in over-all efficiency in coupling with optical fibers.

8630-44, Session PWed

Broadband thermo-optic switch based on a W2 photonic crystal waveguide

Kaiyu Cui, Xue Feng, Yidong Huang, Qiang Zhao, Zhilei Huang, Wei Zhang, Tsinghua Univ. (China)

Compact, broadband, low power consumption and CMOS compatible optical switches are essential elements for network-on-chip. The smallest size of broadband optical switches reported up to now is still larger than 80 μm with bandwidth of 11 nm [1] or 18 nm [2], where both Mach-Zehnder interferometer and photonic crystal waveguide (PCW) are used. Recently, we have proposed a novel approach for optical switches, which relies on the defect mode coupling in photonic band gap. Based on the unique operating principle, the mode coupling strength can be flexibly controlled by proper designing the PCW. Low power consumption (9.2 mW) and high extinction ratio (17 dB) have been obtained with a 16- μm -long double-slot PCW [3], however its bandwidth needs to be extended.

In this work, broadband switching functionality around the telecommunication wavelength is demonstrated by an 8 μm \times 17.6 μm W2 PCW with integrated titanium/aluminum microheater on its surface. Bandwidth up to 24 nm (1557–1581 nm) is achieved, while the extinction ratio is in excess of 15 dB over the entire bandwidth. What's more, the switching speed is measured by AC modulation. Response time for this thermo-optic switch is 11.0 \pm 3.0 ns for rise time and 40.3 \pm 5.3 ns for fall time, respectively.

8630-45, Session PWed

Vertically integrated double-layer on-chip crystalline silicon nanomembranes based on adhesive bonding

Yang Zhang, Xiaochuan Xu, The Univ. of Texas at Austin (United States); Amir Hosseini, Omega Optics, Inc. (United States); David N. Kwong, Ray T. Chen, The Univ. of Texas at Austin (United States)

Silicon photonics is considered one of the solutions for low energy and high bandwidth on-chip interconnects. However, single layer photonic component counts cannot exceed 10000 in silicon Photonic Integrated Circuits (PICs). In addition, silicon photonic devices require over 1 μm thick oxide cladding layers for optical isolation, which compromise electronic performance if both photonic and electronic devices are integrated on single-layer silicon-on-insulator (SOI) platform.

Vertical integration of multiple layers of electronic and photonic components can resolve the problem of limited real estate on a single layer. In this paper we demonstrate a 3D photonic integration scheme based on crystalline silicon. Crystalline silicon is advantageous over reported deposition-based silicon materials including polysilicon, amorphous silicon and silicon nitride, in terms of electrical and optical properties. We develop a low-temperature process using SU-8 based adhesive bonding and etch-back to fabricate vertically stacked, double-layer crystalline silicon nanomembranes. A single-layer PIC fabricated on SOI and a bare SOI chip are bonded together, followed by removal of the bare SOI chip's silicon substrate using mechanical polishing and deep silicon etching, and buried oxide layer using wet etching, to form a silicon nanomembrane as a platform for additional photonic layer. Silicon PIC can be fabricated on the bonded silicon nanomembrane layer using the same fabrication process as single-layer silicon PIC. Single-mode waveguide propagation loss is characterized on the bonded silicon nanomembrane layer. Subwavelength grating couplers are designed and fabricated for both fiber-to-chip coupling and inter-layer coupling between bottom and top layers.

8630-46, Session PWed

Beam form control in polymer photonic crystals and its impact on optical interconnect devices

Jun Tan, Weiwei Song, Wei Jiang, Rutgers, The State Univ. of New Jersey (United States)

Polymer photonic crystals usually have low index contrast, thus sometimes they do not provide adequate index perturbation to maneuver a light beam effectively as a whole. As such, different part of an optical beam in a polymer photonic crystal may act disjointedly, causing significant beam divergence or even dissociation of the beam form. This problem can be particularly severe for a narrow beam. In this work, the condition for a well-collimated beam in a polymer photonic crystal is studied based on a generalized form of the dynamic theory of X-ray diffraction. The collimation condition is found to depend on the beam width and the pertinent Fourier component of the dielectric function. To illustrate the application of this collimation condition, an ultra-compact photonic crystal device is designed to deflect a light beam at a wide-angle. The input and output of this optical device can be directed to typical polymer waveguides on the same chip. Although polymer photonic crystal devices tend to operate below the lightline, low optical loss can be achieved by a short propagation distance (\sim 5 micron) in the device region. The device is tolerant to structural parameter deviation and has a wide bandwidth. Such polymer photonic devices are attractive in optical interconnects applications due to their compact size, low cost and flexible form.

8630-47, Session PWed

Silicon Schottky-type plasmonic-crystal modulators

Jong-Bum You, Wook-Jae Lee, Kyung Mook Kwon, Kyoungsik Yu, KAIST (Korea, Republic of)

We theoretically study the optical modulation at telecommunication wavelengths using one-dimensional plasmonic crystal cavities containing metal-semiconductor Schottky junctions capable of highly efficient and very fast operation. The plasmonic crystal cavities consist of metal-covered periodic corrugations in dielectric waveguide with center defects and outer mirrors. The surface plasmon polariton (SPP) modes are strongly confined with a relatively high Q-factor of \sim 500 by the clear SPP mode gap appeared far below the fundamental TE mode gap. Detailed analyses of the proposed modulators show that the resonant SPP modes can be efficiently modulated by the free carrier depletion of the reverse-biased Schottky junction. Although it is limited only to uni-carrier operation, we can achieve large change of effective index up to \sim 1.8E-3 (\sim 1E-3) for P-type (N-type) semiconductor with doping concentration of \sim 3.9E18 (\sim 4.1E18) and metal work function of 5 eV (4.2 eV) for -4 V bias. Such large index modulation results from the high confinement factor (20%–25%) of the SPP energy into the carrier depletion region near the metal surface. When applying bias voltage of -2 V for out-of-line coupling scheme, we obtain modulation depth of \sim 2.5 dB and low insertion loss of \sim 1 dB on a compact device footprint of only \sim 5 μm^2 . Moreover, large modulation bandwidth can be realized by low optical Q-factors and electrically uni-carrier operation. Such uni-carrier operation allows us to selectively employ faster carriers (electrons) than slower carriers (holes). All of these features would be promising for realizing future sub-micrometer size optical modulators with high speed, low-power operation.

8630-48, Session PWed

Subwavelength grating couplers for efficient light coupling into silicon nanomembrane based photonic devices

Harish Subbaraman, Omega Optics, Inc. (United States);
Xiaochuan Xu, John Covey, Ray T. Chen, The Univ. of Texas at
Austin (United States)

In this paper, we demonstrate the utilization of a subwavelength grating (SWG) coupler for efficient coupling of light into silicon nanomembrane (SiNM) based photonic devices developed on other rigid/flexible substrates such as glass, plastic etc. A periodic array of subwavelength scale rectangular holes are designed to form the artificial material. Compared with conventional grating structures, the subwavelength grating structure enables single step fabrication on a silicon nanomembrane platform. The single step process not only reduces fabrication complexity, but it also allows for the grating couplers to be simultaneously fabricated along with other photonic devices. Our designed $17.1 \mu\text{m} \times 10 \mu\text{m}$ grating couplers, consisting of a periodic arrangement of $0.345 \mu\text{m}$ long, $0.090 \mu\text{m}$ wide air holes spaced $0.390 \mu\text{m}$ apart, are fabricated at the input and the output of 8 mm long, $2.5 \mu\text{m}$ wide silicon nanomembrane waveguides on a glass substrate. A high coupling efficiency of 39.17% is achieved at a wavelength of 1555.56 nm . The 1-dB and 3-dB bandwidths of the fabricated grating couplers are measured to be 29 nm and 57 nm , respectively. Peak efficiency variation of 0.26 dB is observed from a measurement of 5 grating pairs. Coupling efficiency can further be improved with an improved SiNM transfer process. Such high efficiency coupling into silicon nanomembrane waveguides fabricated on a foreign substrate such as glass opens limitless possibilities for the development and integration of high performance nanomembrane based photonic device on a variety of rigid and flexible substrates.

Conference 8631: Quantum Sensing and Nanophotonic Devices X

Sunday - Thursday 3 -7 February 2013

Part of Proceedings of SPIE Vol. 8631 Quantum Sensing and Nanophotonic Devices X

8631-93,

Monolithic QCL design approaches for improved reliability and affordability (*Keynote Presentation*)

Kwok Keung Law, Naval Air Warfare Ctr. Weapons Div. (United States)

Many advances have been made recently in mid-wave infrared and long-wave infrared quantum cascade lasers (QCLs) technologies, and there is an increasing demand for these laser sources for ever expanding Naval, DOD and homeland security applications. We will discuss in this presentation a portfolio of various Naval Air Warfare Weapons Division's current and future small business innovative research programs and efforts on significantly improving QCLs' performance, affordability and reliability.

8631-2, Session 1

Stabilisation of terahertz quantum cascade lasers to frequency combs: coherent imaging and characterization of the frequency noise spectral density (*Invited Paper*)

Stefano Barbieri, Marco Ravano, Univ. Paris 7-Denis Diderot (France); Giorgio Santarelli, Lab. National de Metrologie et d'Essais (France) and Univ. Pierre et Marie Curie (France) and Observatoire de Paris (France); Vishal Jagtap, Christophe Manquest, Carlo Sirtori, Univ. Paris 7-Denis Diderot (France); Suraj P. Khanna, Edmund H. Linfield, Univ. of Leeds (United Kingdom)

The stabilization of THz QCLs to near-IR frequency combs based on fs-mode-locked fiber lasers was developed during the last few years [1-4]. This technique exploits the sampling (electro-optic or photoconductive, see Refs. [1,2]) of the radiation field emitted by the QCL using the mode-locked pulses from a fs-laser. Owing to the extreme ratio between the THz carrier and the sampling rate (i.e. the fs-laser repetition rate) the THz waveform is heavily undersampled, giving rise, in the frequency domain, to a series of beatnotes that are heterodyne replicas of the QCL emission frequency, thus preserving its amplitude and phase. The lowest frequency beatnote lies between dc and half the sampling rate, which is of the order of 100MHz. Therefore it can be fed into standard RF electronics and used for different purposes.

On the one hand it can be used to control the QCL frequency and phase-lock it to the fs-laser repetition rate thus eliminating the phase jitter between the two sources. Sub-Hz beatnote linewidths have been demonstrated with this technique, allowing the coherent accumulation of the QCL signal over long integration times and the achievement of high signal to noise ratios [4]. In this work we will show how this technique can be used for a proof of principle demonstration of coherent imaging using a QCL emitting on a single mode at 2.5THz. We demonstrate an imaging system with a noise detection limit of 1pW/Hz, and a rise time of 100ns.

In the second part of this work it will be shown how the heterodyne replica of the QCL emission frequency can be demodulated using a tracking oscillator allowing the measurement of the laser frequency noise spectral density. We find that the latter is strongly affected by the level of optical feedback, and obtain an intrinsic linewidth of ~230Hz, for an output power of 2mW [6].

[1] S. Barbieri, P. Gellie, G. Santarelli, L. Ding, W. Maineult, C. Sirtori, R. Colombelli, H. E. Beere, and D. A. Ritchie, "Phase-locking of a 2.7-THz quantum cascade laser to a mode-locked erbium-doped fibre laser", *Nature Phot.* 4, 636 (2010).

[2] Ravano, C. Manquest, C. Sirtori, S. Barbieri, G. Santarelli, K. Blary, J.-

F. Lampin, S. P. Khanna, and E. H. Linfield, "Phase-locking of a 2.5 THz quantum cascade laser to a frequency comb using a GaAs photomixer" *Opt. Lett.* 36, 3969 (2011).

[3] S. Barbieri, M. Ravano, P. Gellie, G. Santarelli, C. Manquest, C. Sirtori, S.P. Khanna, H. Linfield, A.G. Davies, "Coherent sampling of active mode-locked terahertz quantum cascade lasers and frequency synthesis", *Nature Photon.* 5, 306 (2011).

[4] M. Ravano, P. Gellie, G. Santarelli, C. Manquest, P. Filloux, C. Sirtori, J.-F. Lampin, G. Ferrari, S. P. Khanna, and E. H. Linfield, H. E. Beere, D. A. Ritchie, and S. Barbieri "Stabilisation and mode-locking of THz quantum cascade lasers" accepted for publication on *IEEE J. Sel. Top. Quantum Electron.* (July 2012).

[5] S. Barbieri, J. Alton, J. Fowler, H. E. Beere, E. H. Linfield, and D. A. Ritchie, "2.9 THz quantum cascade lasers operating up to 70 K in continuous wave", *Appl. Phys. Lett.* 85, 1674 (2004).

[6] M. Ravano, S. Barbieri, G. Santarelli, V. Jagtap, C. Manquest, C. Sirtori, S. P. Khanna, and E. H. Linfield, "Measurement of the intrinsic linewidth of terahertz quantum cascade lasers using a near-infrared frequency comb", submitted to *Opt. Expr.* (August 2012)

8631-3, Session 1

Quantum-limited linewidth in THz quantum cascade lasers (*Invited Paper*)

Miriam S. Vitiello, Consiglio Nazionale delle Ricerche (Italy); Luigi Consolino, CNR- Istituto Nazionale di Ottica and LENS (Italy); Saverio Bartalini, Andrea Taschin, CNR, Istituto Nazionale di Ottica and LENS (Italy); Alessandro Tredicucci, NEST, CNR, Istituto Nanoscienze and Scuola Normale Superiore (Italy); Massimo Inguscio, CNR, Istituto Nazionale di Ottica and LENS (Italy) and Univ. degli Studi di Firenze (Italy); Paolo De Natale, CNR, Istituto Nazionale di Ottica and LENS (Italy)

In the conventional laser theory, the intrinsic laser linewidth (LW) is governed by the standard Schawlow-Townes (ST) formula.

In a quantum cascade laser (QCL), environmental effects such as temperature, bias-current fluctuations or mechanical oscillations are expected to significantly affect the LWs. This means that any experimental LW measurement is mainly dominated by the extrinsic noise and therefore exceeds the ST limit by far. A clear understanding of the physical effects playing a role in the device LW, of its ultimate lower limit, as well as of its dependence on the gain media architecture and on the waveguide geometry, particularly crucial in the far-infrared, is actually still lacking.

I'll report on the recent development of a sophisticated experimental technique to investigate the spectral purity of a 2.5 THz QCL via the measurement of its frequency-noise power spectral density. The latter provides, for each frequency, the amount of noise contributing to the spectral width of the laser emission by deriving the laser emission spectrum over any accessible time scale. It also allows calculating the LW reduction achievable using a frequency-locking loop, once its gain/bandwidth characteristics are known. Experimental evidence of LW values approaching the quantum limit has been reported. Despite the broadening induced by thermal photons, the measured LW results narrower than in any other semiconductor laser. Performing noise measurements with unprecedented sensitivity levels, we highlight the key role of the gain medium engineering demonstrating that properly designed semiconductor-heterostructure lasers could unveil the mechanisms underlying the laser intrinsic phase-noise, revealing the link between the device properties and its quantum-limited LW.

**Conference 8631:
Quantum Sensing and Nanophotonic Devices X**

8631-4, Session 1

Dynamical stability in terahertz quantum cascade lasers subjected to strong optical feedback

Lorenzo Columbo, Francesco Paolo Mezzapesa, CNR-IFN UOS Bari (Italy); Massimo Brambilla, Maurizio Dabbicco, Univ. degli Studi di Bari (Italy) and CNR-IFN UOS Bari (Italy); Simone Borri, CNR-IFN UOS Bari (Italy); Gaetano Scamarcio, Univ. degli Studi di Bari (Italy) and CNR-IFN UOS Bari (Italy)

The intrinsic stability of continuous wave (CW) emission in Terahertz Quantum Cascade Lasers (THz-QCL) subjected to strong optical feedback is theoretically predicted and experimentally demonstrated. We simulate the THz-QCL dynamics in presence of optical re-injection with a set of semiconductor rate equations with delay (Lang-Kobayashi model). Our numerical results show the absence of coherence collapse due to undamped relaxation oscillations (moderate feedback regime) and of any other CW instability linked to “external cavity modes” competition (strong feedback regime) for parameters typical of unipolar semiconductor lasers such as MIR-QCL and THz-QCL. In particular we highlight the role played by the high value of the photon to carrier lifetime ratio (>10) and the small value of the Henry factor (~ 0.5) in determining this “ultra-stability”. The experimental results obtained with a THz-QCL subjected to strong optical feedback in a quasi self-imaging configuration confirm the theoretical predictions. In particular we verified that CW emission is stable for a feedback level at least ~ 100 times larger than the feedback threshold causing coherence collapse in bipolar diode lasers in the same geometrical configuration.

We believe that this evidence has both a fundamental importance, allowing for a better understanding of QCL dynamics, and a great impact on those applications where THz-QCL works as source and detector in compact self-aligned set-ups, e.g. imaging, high precision spectroscopy and sensing.

8631-97, Session 1

Widely-tuned room-temperature terahertz quantum cascade laser sources (Invited Paper)

Quan-Yong Lu, Neelanjan Bandyopadhyay, Steven Slivken, Yanbo Bai, Manijeh Razeghi, Northwestern Univ. (United States)

We demonstrate room temperature terahertz (THz) quantum cascade laser (QCL) sources with a broad spectral coverage based on intracavity difference-frequency generation. Dual mid-infrared (mid-IR) active cores based on the single-phonon resonance scheme are designed with a THz nonlinearity specially optimized for the high operating fields that correspond to the highest mid-infrared output powers. Integrated dual-period distributed feedback (DFB) gratings with different grating periods are used to purify and tune the mid-IR and THz spectra. Two different phase matching schemes are used for THz generation. The first is the collinear modal phase matching scheme, wherein the wafer is grown on a $n+$ InP substrate. Room temperature single mode operation THz emission with frequency tuning range from 3.3 to 4.6 THz and THz power up to 65 mW at 4.0 THz are realized. The mid-IR to THz power conversion efficiency is 23 $\mu\text{W}/\text{W}^2$. The second is the $\chi^{(2)}$ phase-matching scheme, wherein the wafer is grown on a semi-insulating InP substrate, and device's facet is polished into 20-30 degrees for THz extraction. Room temperature single mode emissions from 1.0 to 4.6 THz with a side-mode suppression ratio and output power up to 40 dB and 32 μW are obtained, respectively. The mid-IR to THz power conversion efficiency is 50 $\mu\text{W}/\text{W}^2$.

To further boost the THz power and efficiency for the $\chi^{(2)}$ phase-matched THz device, a THz diffraction grating is patterned on the backside of semi-insulating InP substrate to extract the THz light from the whole cavity and a epi-down mounting of the $\chi^{(2)}$ THz device to a patterned submount are performed and demonstrated. Room temperature surface emission of an epi-down mounted $\chi^{(2)}$ THz

device with surface emitting power of 35 mW, and total powers of 75 mW from surface and edge emissions with THz total power conversion efficiency of 150 mW/W^2 at 3.4 THz are demonstrated.

Unlike the previous epi-up mounted devices, there is no significant thermal issue for the epi-down mounted devices, and the substrate can be increased arbitrarily by wafer bonding to enhance the THz outcoupling area and efficiency, which is of great importance to the long-cavity devices with potential high THz power outputs. On the other side, the THz anti-reflection coating (such as polyethylene coating) can further increase the THz outcoupling efficiency by about 30%. In the near future, THz output power with THz conversion efficiency above 1 mW and 1 mW/W^2 in the range of 1.0 to 5 THz will be realized.

8631-5, Session 2

Phase-locking of surface-emitting THz quantum cascade laser arrays

Gangyi Xu, Yacine Haloua, Raffaele Colombelli, Institut d'Électronique Fondamentale (France); Suraj P. Khanna, Lianhe Li, Edmund H. Linfield, Giles Davies, Univ. of Leeds (United Kingdom); Harvey Beere, David Ritchie, Univ. of Cambridge (United Kingdom)

We first report high-power, single-mode surface-emission THz quantum cascade (QC) lasers by using graded photonic heterostructure resonators. We then discuss the prospects to develop phase-locked arrays of these devices.

As an initial result, a very robust approach to phase-lock second-order distributed feedback (DFB) THz QC laser arrays (pairs in this case) is demonstrated. Each device contains two parallel and identical DFB lasers linked by two semicircular rings, forming a race-track ring resonator. Both the DFB laser and semicircular ring arms employ a metal-metal waveguide geometry. The measured laser emission spectra and far-field beam patterns demonstrate that single-mode surface-emission is realized and the laser pairs are always phase-locked, regardless the length of semicircular ring (LSR).

The laser pairs are in-phase locked when $\text{LSR} \sim (m \pm 0.25) \cdot \lambda$, and change abruptly to an out-of-phase behavior when $\text{LSR} \sim (m + 0.5 \pm 0.25) \cdot \lambda$, where m is an integer and λ is the wavelength in the waveguide. The robustness of the concept stems from the fact that the emission wavelength is determined by the DFB structure only, while the ring resonator sets the phase character. Details of this mechanism will be discussed during the talk. The light-current-voltage measurements show that phase-locked laser pairs have similar performances (threshold, power, maximum operation temperature) to the case when two DFB lasers are separated but pumped simultaneously.

This approach can be extended to phase-lock more DFB lasers, and arrays of graded photonic heterostructure devices, representing a solution for coherent terahertz sources with simultaneously high power, high operating temperature and directional beam pattern.

8631-6, Session 2

Cavity-enhanced optical frequency comb spectroscopy (Invited Paper)

Bryce J. Bjork, JILA (United States); Adam J. Fleisher, Jun Ye, Univ. of Colorado at Boulder (United States) and JILA (United States)

Optical sensing techniques can potentially provide quick and unambiguous identification of chemical compounds present in an unknown sample when high spectral resolution is achieved at fast acquisition time. Optical frequency combs, which can cover a large portion of the electromagnetic spectrum (from the mid-infrared to the extreme ultraviolet), not only provide the desired high spectral resolution, but also have the added advantage of an inherently broad spectral

Conference 8631: Quantum Sensing and Nanophotonic Devices X

bandwidth and massively parallel detection channels. When coupled to an enhancement cavity and analyzed with one of several novel detection schemes, frequency comb spectroscopy has proven to be a powerful tool for trace detection down to the part-per-billion level in industrial and biological samples, as well as accurate measurement of hundreds of molecular lines recorded simultaneously under atmospheric conditions. We will present examples of recent advances in broadband ion spectroscopy, quantum-noise-limited comb spectrometry, and massively parallel measurement performed under one millisecond.

8631-7, Session 2

Reflection-absorption infrared spectroscopy of thin films using an external cavity quantum cascade laser

Mark C. Phillips, Ian M. Craig, Thomas A. Blake, Pacific Northwest National Lab. (United States)

The technique of Reflection-Absorption InfraRed Spectroscopy (RAIRS), or alternatively InfraRed Reflection Absorption Spectroscopy (IRRAS), is used to measure absorption spectra by reflecting a beam off a substrate at a high angle of incidence (near grazing). RAIRS is routinely used with Fourier Transform InfraRed (FTIR) spectroscopy to measure absorption spectra of thin films or monolayers of adsorbed chemicals on surfaces. However, FTIR-based techniques often require long integration times and/or low spectral resolution to measure the weak absorption features from monolayer coverages of chemicals. Here, we present experimental demonstrations using a broadly tunable external cavity quantum cascade laser (ECQCL) to perform RAIRS measurements of thin layers and residues on surfaces. The ECQCL source allows rapid measurements with low noise, high spectral resolution, and a tuning range sufficient to capture multiple absorption features of solids and adsorbed chemicals.

RAIRS at an 84 degree angle of incidence was performed over the 7.1-7.9 μm tuning range of the ECQCL. Experiments were performed on residues of the explosive compounds PETN, RDX, TNT, and tetryl deposited on gold substrates. The ECQCL-RAIRS technique was used to acquire low-noise spectra in a one-second acquisition time. In addition, monolayers of a fluorinated alkane thiol and a thiol carboxylic acid in varying relative surface coverages were measured. With a six-second acquisition time, an absorbance noise of $6\text{E}-4$ was obtained, enabling rapid measurement of weak absorption features. The ECQCL-RAIRS spectra were compared with polarization-modulation RAIRS spectra acquired using a FTIR spectrometer.

8631-8, Session 2

A field-deployable compound-specific isotope analyzer based on quantum cascade laser and hollow waveguide

Sheng Wu, California Institute of Technology (United States) and Power Environmental & Energy Research Institute (United States); Andrei Deev, California Institute of Technology (United States)

Hollow waveguide (HWG) has long been recognized as an alternative optical absorption sample cell platform for IR sensing and chemical analysis due to the obvious advantage, i.e. small sample volume and thus fast response time. First used in Gas Chromatography (GC) as an online Infrared sensor in the earlier 80's[1], and conventional wisdom in spectroscopy often treat HWG as free space optics and multimode, therefore expect signal to noise level to be inferior.

We first demonstrated that Quantum Cascade lasers could have orders higher coupling efficiency into small bore long HWG than blackbody light sources, and when coupled with capillary GC, the online sensor has potential performance to match Mass Spectroscopy sensors[2]. Here, we give a detailed account of our latest research and development in the past 5 years on this platform. First, we show that HWG could support single mode transmission and even act as single mode filter to filter out

high order modes, and it has superior signal to noise ratio compared to free space or multipass cells when conducting precise measurements. Then, we show that the sensor system, when integrated with GC and online combustion unit, could realize 0.3 per mil accuracy for measuring $12\text{C}/13\text{C}$ ratio for a Gas Chromatography (GC) peak lasting as short as 5 seconds with carbon molar concentration in the GC injection less than 0.5%. Calibration and operating maintenance are much relieved in this system, making it fully field deployable and able to perform similar tasks as the cumbersome GC-IRMS system.

1. Griffiths, P.R., J.A. De Haseth, and L.V. Azarraga, Capillary GC/FT-IR. Analytical Chemistry, 1983. 55(13): p. 1361A-1387A.

2. Wu, S., et al., Hollow waveguide quantum cascade laser spectrometer as an online microliter sensor for gas chromatography. Journal of Chromatography A, 2008. 1188(2): p. 327-330.

8631-9, Session 2

Progress toward mid-IR chip-scale integrated-optic TDLAS gas sensors (*Invited Paper*)

Michael B. Frish, Physical Sciences Inc. (United States); Raji Shankar, Irfan Bulu, Ian Frank, Harvard Univ. (United States); Matthew Laderer, Richard Wainner, Mark Allen, Physical Sciences Inc. (United States); Marko Loncar, Harvard Univ. (United States)

We are building prototype chip-scale low-power integrated-optic gas-phase chemical sensors based on mid-infrared (3-5 μm) Tunable Diode Laser Absorption Spectroscopy (TDLAS). TDLAS is able to sense many gas phase chemicals with high sensitivity and selectivity. Novel gas sensing elements using low-loss resonant photonic crystal cavities or waveguides will permit compact integration of a laser source, sampling elements, and detector in configurations suitable for inexpensive mass production. Recently developed Interband Cascade Lasers (ICLs) that operate at room temperature with low power consumption serve as monochromatic sources to probe the mid-IR molecular spectral transitions. Practical challenges to fabricating these sensors include: a) selecting and designing the high-Q micro-resonator sensing element appropriate for the selected analyte; b) coupling laser light into and out of the sensing element; and c) device thermal management, especially stabilizing laser temperature with the precision needed for sensitive spectroscopic detection. This paper describes solutions to these challenges.

8631-10, Session 3

Hole-mask colloidal nanolithography for large-area low-cost metamaterials and sensing applications (*Invited Paper*)

Harald Giessen, Jun Zhao, Stefano Cataldo, Univ. Stuttgart (Germany); Frank Neubrech, Ruprecht-Karls-Univ. Heidelberg (Germany); Bettina Frank, Univ. Stuttgart (Germany); Chunjie Zhang, Paul V. Braun, Univ. of Illinois at Urbana-Champaign (United States)

Plasmonic nanostructures are tremendously important for applications in the visible and near-IR range. The various applications include surface enhanced Raman spectroscopy (SERS), surface enhanced infrared absorption (SEIRA) spectroscopy, localized surface plasmon resonance (LSPR) sensors for liquid and gas, narrow resonances using plasmon-induced transparency (PIT), and local field concentration in oligomers for creation of hot spots. Recently, resonantly antenna-enhanced SERS and SEIRA methods have been introduced. LSPR sensing using Fano resonances in complex metallic nanostructures has been also studied by many groups, however, usually on small-area samples fabricated by e-beam lithography. In order to bring these advances into chemistry and chemistry labs and allow for a plethora of applications, large-area low-

Conference 8631: Quantum Sensing and Nanophotonic Devices X

cost fabrication is required.

Here we present an elegant solution to this problem, introducing a low-cost simple fabrication method for different complex plasmonic nanostructures with cm² of defect-free areas: hole-mask colloidal nanolithography followed by tilted angle metal evaporation. We manufacture metallic split-ring-resonator (SRR) metamaterial nanoantennas with different SRR geometries and hence a set of different resonance frequencies to demonstrate easy adjustability to the desired vibrational frequencies for SEIRA spectroscopy. SEIRA sensing down to a monolayer sensitivity was observed both for normal as well as deuterated ODT.

At the same time, our manufacturing method represents an elegant method to produce large-area and low-cost asymmetric double SRRs metamaterials that can be utilized for liquid refractive index LSPR sensors, using narrow Fano resonances. Additionally, we demonstrate large-area bi-metallic plasmonic oligomers for gas sensing.

8631-11, Session 3

Nanoantenna-based thermoplasmonic infrared detector

Ertugrul Cubukcu, Fei Yi, Hai Zhu, Univ. of Pennsylvania (United States)

We developed a plasmonic thermomechanical sensor for detection of the infrared (IR) radiation. The temperature sensitive element of the thermal detector is a gold / silicon nitride bilayer structure embedded with a plasmonic nanoantenna absorber. The plasmonic nanoantenna absorber converts the IR power into heat and causes the temperature of the bilayer structure to increase. The bilayer structure is integrated into a fiber optic Fabry – Perot interferometer to read out the mechanical deflection of the bilayer structure caused by its temperature increase. We designed the nanoantennas absorber to have a peak absorption close to 50% at a wavelength of 6 μ m. The thickness of the bilayer structure is optimized to reach the maximum deflection. The fiber optic Fabry Perot interferometer is also carefully designed to have a large sensitivity such that the noises from the optical read out system are minimized. The thermal detector is limited by the thermal fluctuation noise and the theoretical noise equivalent power of 15pW/(Hz) at 6 μ m. Experimentally we achieved a minimum detectable power of 5nW/sqrt(Hz)

8631-12, Session 3

Plasmonics for infrared detection and imaging (*Invited Paper*)

Riad Haidar , ONERA (France)

The current trend towards compact, cost-effective and multi-purpose infrared opto-electronic systems brings the need for new conception tools and technological means. In this frame, subwavelength and plasmonic concepts open promising avenues: at a first level, for the conception of high-efficiency and compact optical elements arrays (i.e., polarizer, filter, or lens arrays) that can be brought in the vicinity of focal plane arrays, inside the confined volume of the camera; at a second level, for the integration of optical functions within the pixel of detection; and at a third level, for the enhancement of the opto-electronic properties of the elementary infrared detector. I will draw an overview of recent advances and realizations done in our lab.

8631-13, Session 3

Differential Fano interference spectroscopy of subwavelength hole arrays for mid-infrared mass sensors

Michele Ortolani, Istituto di Fotonica e Nanotecnologie (Italy)

and Univ. degli Studi di Roma La Sapienza (Italy); Odeta Limaj, Fausto D'Apuzzo, Univ. degli Studi di Roma La Sapienza (Italy); Valeria Giliberti, Univ. degli Studi di Roma La Sapienza (Italy) and Istituto di Fotonica e Nanotecnologie (Italy); Alessandra Di Gaspare, Francesco Mattioli, Roberto Leoni, Istituto di Fotonica e Nanotecnologie (Italy); Simona Sennato, Fabio Domenici, Federico Bordi, Stefano Lupi, Univ. degli Studi di Roma La Sapienza (Italy)

We experimentally and numerically studied mid-infrared mass sensors based on the wavelength shift of Surface Plasmon Polariton resonances upon solid substance deposition on subwavelength hole arrays in a thin metal film. We developed an analytical model of the optical transmission which describes the Fano interference between the Bethe continuum (transmission of radiation through a single hole of subwavelength diameter) and the different Surface Plasmon Polariton resonances (the extraordinary transmission peaks). Best-fitting by our analytical model of the differential transmission signal measured above and after deposition provides a sensitivity down to few molecular monolayers. The electric field profile of each Surface Plasmon Polariton mode has been numerically calculated by three-dimensional electromagnetic simulations with nanometer-scale meshing in order to explain the different sensitivity values found for the different SPP lines. Sensor calibration was performed on thin polymer films and an example of real application is then provided by measuring the optical density of phospholipid membrane complexes with thickness in the range 2-10 nm. The design of a compact sensing system operating in the narrow wavelength range of a single SPP resonance with an external-cavity tunable Quantum Cascade Laser is discussed.

8631-14, Session 3

Tailoring MSM structures for IR photodetection

Matthieu Duperron, Daivid Fowler, Jérôme Le Perchec, Salim Boutami, Giacomo Badano, François Boulard, Olivier Gravrand, Gerard Destefanis, Roch Espiau de Lamaestre, CEA-LETI-Minatec (France)

Throughout recent decades, Metal-Semiconductor-Metal (MSM) cavities have been proposed to enhance IR photodetection. The interest in those structures stems from the highly localized nature of the resonantly excited electromagnetic (EM) near field, which is promising for low pixel size and high angular acceptance imagery [J. Le Perchec et al, Appl. Phys. Lett.94, 181104 (2009); D. Fowler et al, submitted to Appl. Phys. Lett.].

We have investigated various approaches for tuning the light coupling to these cavities using numerical calculations and temporal coupled mode theory as a common interpretation basis. Firstly, we will show that diffractive coupling to periodically arranged vertical MIM cavities can give rise to a hybrid cavity/waveguide mode, whose transverse localization can be tuned. The resulting grating is shown to also serve as an efficient coupling structure for absorption within a thin semiconducting region positioned nearby. We will then discuss the extremely localized mode that can be generated by loading a patch antenna with an absorbing semiconductor, forming a horizontal MSM cavity. In this case, we show how the resulting coupling efficiency depends on the geometric configuration of the cavity. The presence of an absorbing medium is shown to have a strong impact on the critical coupling condition, leading to an optimized geometry that significantly differs from that derived for their use as passive radiating/receiving antenna. Finally, owing to the highly localized character of the EM field, such MSM cavities are shown to exhibit a spectral sorting capability [J. Le Perchec et al, Appl. Phys. Lett.100, 113305 (2012)].

**Conference 8631:
Quantum Sensing and Nanophotonic Devices X**

8631-17, Session 4

Lateral mode competition in broad-ridge quantum cascade lasers (*Invited Paper*)

Nader A. Naderi, Chi Yang, Michael L. Tilton, Gregory C. Dente, Ron Kaspi, Air Force Research Lab. (United States); Stanley Tsao, Selamnesh Nida, Manijeh Razeghi, Northwestern Univ. (United States)

Currently, intersubband quantum cascade lasers are viable candidates for various applications requiring mid-infrared sources. To date, narrow-ridge devices have demonstrated lateral mode control while being necessarily limited in peak power. For scaling to higher powers, significant progress has been made in broad-ridge quantum cascade lasers, demonstrating output powers up to 120 watts, but at the expense of greatly reduced on-axis intensity in the far-field. Furthermore, in a promising set of observations, near- and far-field studies have shown that as the ridge and injection contact widths are increased, the lasers near-field can become spatially coherent across the output facet while forming a lateral standing wave across the ridge width. In turn, the lasing lateral far-field forms a dual-lobed pattern that can remain relatively stable with fixed divergence angles for both lobes. Additionally, each lobe is near the diffraction-limited width allowed by the ridge guide. This data suggests nearly single lateral mode behavior in some of these devices.

In this study, we have experimentally and theoretically investigated the impact of ridge width and injection contact width on the lateral-mode competition in several classes of broad-ridge quantum cascade lasers. While other parameters, such as the ridge side-wall surface quality, also play a role, we have limited our parameter study to ridge and contact widths. In each case, we will quantify the lateral mode competition with near- and far-field intensities, as well as near-field spatial coherence measurements. Combination of good lateral-mode discrimination and lateral spatial coherence is promising for improving brightness in broad-ridge devices.

8631-18, Session 4

Broadly-tunable high-resolution CW lasers based on QC devices: new benchmarks and applications (*Invited Paper*)

Leigh Bromley, Michael Pushkarsky, Alexander Dromaretsky, Timothy Day, Daylight Solutions Inc. (United States)

The need for high-resolution, continuously tunable lasers in the mid-infrared (IR) has driven a generation of source development including color-center lasers, Pb-salt diodes, and difference frequency systems. Quantum cascade (QC) devices are now bringing this performance to the mid-IR with more power and less complexity than earlier technologies. Studies have shown[1] that the intrinsic linewidth of QC lasers is below 1 kHz, more than sufficient for the most demanding mid-IR high-resolution spectroscopy experiments. This paper covers development of broadly-tunable CW lasers that make significant advances in the linewidth and noise floor requirements relevant to high-resolution studies. Recent work on enhancing the performance specifications of QC-based broadly tunable CW lasers is presented, with new frequency and amplitude noise benchmarks. Applications are discussed that require this CW performance, and the future of high-resolution capabilities with QC lasers is considered.

1. Bartalini, S., et al., Observing the Intrinsic Linewidth of a Quantum-Cascade Laser: Beyond the Schawlow-Townes Limit. *Physical Review Letters*, 2010. 104: p. 083904-1 - 083904-4.

8631-19, Session 4

Quantum cascade lasers optimized for low dissipation and broad gain

Stéphane Blaser, Tobias Gresch, Romain Terazzi, Antoine Muller, Alpes Lasers SA (Switzerland)

The state-of-the-art of commercially available quantum-cascade (QC) lasers at Alpes Lasers will be reviewed. High-resolution spectroscopy requires tunable single frequency light sources with very narrow linewidth (< 3.5 MHz); this can be achieved using QC lasers operating in continuous-wave (CW) mode. For small packaged systems, like in TO3-can, a low dissipation of the laser is crucial. In this direction, we report on the design and fabrication of distributed-feedback (DFB) QC lasers which have a low electrical dissipation below 1 W [1]. This could be achieved by a new active-region design together with a low doping-density in the active region and by reducing the device dimensions significantly. In comparison to state-of-the-art high-power mid-IR QC lasers, the dissipation is lower by one order of magnitude.

On the other hand, broadband QC gain regions are very appropriate for operation in external cavity systems and Alpes Lasers have developed a range of broadband designs to this end. Moreover, broad gain material can also be considered for the fabrication of DFB lasers on a large range of frequencies with the same epitaxial material. This approach is especially efficient when processing of full wafers is performed. In this direction, broadband QC lasers composed of three different cascade designs based on the bound-to-continuum structure [2] will be presented. These lasers allow to cover the range from 6 to 12.9 μ m.

[1] B. Hinkov et al. "Single-mode quantum cascade lasers with power dissipation below 1W", *Electronics Lett.* 48 (11), 646 (2012).

[2] J. Faist, et al. "Quantum-cascade lasers based on a bound-to-continuum transition", *Appl. Phys. Lett.* 78, 147 (2001).

8631-21, Session 4

Dual section quantum cascade lasers with wide electrical tuning (*Invited Paper*)

Steven Slivken, Neelanjan Bandyopadhyay, Stanley Tsao, Selamnesh Nida, Yanbo Bai, Quanyong Lu, Manijeh Razeghi, Northwestern Univ. (United States)

While external cavity quantum cascade lasers (QCLs) have shown very broad tuning capability (several hundred cm^{-1}), they are fairly complicated optomechanical devices. On the other hand, tuning of traditional single element distributed feedback (DFB) QCLs has proven to be extremely limited, with a tuning range of $\sim 5 \text{ cm}^{-1}$ at room temperature. It is desirable to develop a technology that is compact and robust like a DFB laser, but with the broad tuning capability of an external cavity device.

Towards this end, we are developing multi-section QCLs with the same size, but much wider electrical tuning than a traditional DFB laser. In this talk I will show how we have dramatically extended the monolithic tuning range of high power quantum cascade lasers with high side mode suppression. This includes individual laser element tuning of over 40 cm^{-1} . These lasers are capable of room temperature continuous operation with high power ($> 100 \text{ mW}$) output. The eventual goal is to realize an extended array of such laser modules in order to cover a similar or broader tuning range than can be realized with an external cavity device. No external optical components will be required for operation, which may provide a cost effective solution for mass production.

**Conference 8631:
Quantum Sensing and Nanophotonic Devices X**

8631-22, Session 4

Mid-IR wavelength tunable quantum cascade lasers

Chung-en Zah, Feng Xie, Abdou Diba, Catherine Caneau, Lawrence C. Hughes, Herve P. LeBlanc, Sean Coleman, Ming-Tsung Ho, Corning Incorporated (United States)

We review the approaches to realize widely wavelength tunable mi-IR lasers for sensing of multiple gases and complex molecules, and the challenges. Wavelength tuning mechanism and limitation are discussed. The performance of monolithic wavelength tunable quantum cascade lasers is presented including the characteristics of sampled-grating distributed Bragg reflectors (SGDBR) quantum cascade lasers with a wide wavelength tuning from 4.48 to 4.69 μm (100cm^{-1}) using the Vernier effect of two wavelength combs of front and back SGDBRs with small difference in the wavelength spacing.

8631-100, Session 4

Continuous-wave room-temperature operation of $[\lambda] \sim 3 \mu\text{m}$ quantum cascade laser

Neelanjan Bandyopadhyay, Yanbo Bai, Stanley Tsao, Selamnesh Nida, Steven Slivken, Manijeh Razeghi, Northwestern Univ. (United States)

Quantum Cascade Lasers (QCLs), operating in continuous wave (CW) at room temperature (RT) in 3-3.5 μm spectral range, which overlaps the spectral fingerprint region of many hydrocarbons, is essential in spectroscopic trace gas detection, environment monitoring, and pollution control. A 3 μm QCL, operating in CW at RT is demonstrated. This initial result makes it possible, for the most popular material system (AlInAs/GaInAs on InP) used in QCLs in mid-infrared and long-infrared, to cover the entire spectral range of mid-infrared atmospheric window (3-5 μm).

To accommodate large intersubband separation between upper and lower laser level in the active region, In_{0.79}Ga_{0.21}As/In_{0.11}Al_{0.89}As strain balanced superlattice, which has a large conduction band offset, was grown. Composite barriers (In_{0.11}Al_{0.89}As /In_{0.4}Al_{0.6}As), were used in the injector region, to reduce the tensile strain and eliminate the need of extremely high compressively strained GaInAs, whose pseudomorphic growth is very difficult.

In RT pulsed mode operation, threshold current density of 1.97 kA/cm², and characteristic temperature (T₀) of 102 K, are obtained. The maximum CW optical power at RT is 2.8 mW. The 3 μm is the shortest reported wavelength QCL operating in CW at RT.

8631-23,

Issues in nanophotonics: coupling and phase in resonant tunneling (*Keynote Presentation*)

Raphael Tsu, The Univ. of North Carolina (United States)

Modern Nano electronics involves the use of heterojunctions in forming energy steps based on band-edge alignments in effecting quantum confinements. When the electron mean-free-path exceeds couple of periods, man-made quantum states appeared, mimicking natural solids with sharpness determined by the degree of coherence dictated by a relatively long mean-free-path. When a single quantum well is involved, the structure is represented by resonant tunneling. This process can further be extended to 3D (3-dimension), however, thus far only few systems have been found possible, mostly involving InAs, or InN. However, the real problem lies in I/O, making contact to a single quantum dot, seems to be impractical on account of making contact in Nano scale regime. However, the issue with impedance matching, is the most important aspect for efficient devices, whether as detectors, or as

generator in frequencies between THz to visible light. As size shrinks to Nano-regime, even the wavelength of IR is too large for effective coupling to the quantum dots without some sort of coupling such as the use of Fabry-Perrot mirrors, which is in fact unsuited for quantum dots, unless these dots are arranged in an array, which in fact defeating the purpose of going to quantum dots, except the density of states for the quantum dots is more or less represented by delta functions, typically a Gaussian. There is another important issue, RPA, Random Phase Approximation, coined by Bohm and Pines for overwhelming majority of physical interactions representable by the neglect of phase. For example, phase arrays depend on phase relationships between individual elements, or in this case, dots, identical to a dielectric function used to represent interaction with light. However, all phase array antennas cannot work with RPA for transmission and receiving. Similarly, meta-materials and photonic crystals utilize dielectric functions, or simply designed with the use of RPA. Therefore, it is important that RPA should be taken into consideration in the design of quantum photonic systems, particularly, I/O and coupling are considered. Lastly, we must look into response time. For example, resonant tunneling has been routinely numerically computed using the time dependent Schrodinger equation, which is roughly correct for a Gaussian pulse for I/O near resonance. When an input photon energy is different from a Gaussian, the build-up time, and decay time are quite different using the time dependent Schrodinger equation. Moreover, if the input light is not a plane wave with infinite wave train and incident at an angle to the structure, time dependent computation must be adopted, particularly when impedance matching is used. Why these issues do not surface in the semiconductor lasers? In semiconductor lasers only light needs to satisfy boundary conditions, while here, light and electrons both need to satisfy boundary conditions. Lastly, quantum entanglement should not be taken seriously as an issue of quantum sensing, because the real world has unavoidable fluctuations.

8631-24, Session 5

Multi-color QWIP FPAs for hyperspectral thermal emission instruments (*Invited Paper*)

Alexander Soibel, Edward M. Luong, Jason M. Mumolo, John Liu, Sir B. Rafol, Sam A. Keo, William R. Johnson, Dan Wilson, Cory J. Hill, David Z. Ting, Sarath Gunapala, Jet Propulsion Lab. (United States)

Infrared focal plane arrays (FPAs) covering broad mid- and long-IR spectral ranges are the central parts of the spectroscopic and imaging instruments in several Earth and planetary science missions. To be implemented in the space instrument these FPAs need to be large-format, uniform, reproducible, low-cost, low 1/f noise, and radiation hard. Quantum Well Infrared Photodetectors (QWIPs), which possess all needed characteristics and have a great potential for implementation in the space instruments, however a standard QWIP has only a relatively narrow spectral coverage. A multi-color QWIP, which is comprised of two or more detector stacks can be used to cover the spectral range of interest.

We will discuss our recent work on development of multi-color QWIP for Hyperspectral Thermal Emission Spectrometer instruments. We developed QWIP comprising of two stacks centered at 9 and 10.5 μm , and featuring nine grating regions optimized to maximize the responsivity in the individual subbands across the 7.5-12 μm spectral range. The demonstrated 1024x1024 QWIP FPA exhibited excellent performance with operability exceeding 99% and noise equivalent differential temperature of less than 15 mK across the entire 7.5-12 μm spectral range.

8631-25, Session 5

Modulation transfer function measurements of QWIP and superlattice focal plane arrays (Invited Paper)

Sarath Gunapala, David Z. Ting, Sir B. Rafol, Alexander Soibel, Arezou khoshakhlagh, C. Hill, John K. Liu, Jason M. Mumolo, Sam A. Keo, Jet Propulsion Lab. (United States)

Long wavelength Complementary Barrier Infrared Detector (CBIRD) based on InAs/GaSb superlattice material is hybridized to recently designed and fabricated 320 x 256 pixel format two-color read out integrated circuit. The n-type CBIRD was characterized in terms of performance and thermal stability. Modulation Transfer Function (MTF) and Minimum Resolvable Temperature Difference (MR?T) are system level performance metrics. MR?T is a subjective measurement of focal plane array (FPA) image using trained human observers. It requires a stable differential temperature between background and a four bar target that will produce a unity signal-to-noise ratio on the display monitor as a function of target spatial frequency. This measures thermal sensitivity as function of spatial resolution defines by the four bar target with aspect ratio of 7:1. The period of the four bar target is varied and the spatial frequency is estimated for each four bar target. At small spatial frequency the horizontal MR?T (HMR?T) and vertical MR?T (VMR?T) are slightly lower than the Noise Equivalent Temperature Difference (NE?T) value. At higher spatial frequency it requires a larger temperature difference to generate a contrast between the four bar targets and background. Positive and negative contrast was measured and difference temperature was average to eliminate the offset. The four bar target becomes difficult to resolve below Nyquist frequency in both the vertical and horizontal direction even after moving the target slightly to compensate for the phasing effect and raising the temperature of the background. It is observed that only three bars are apparent instead of four and two of the bars merge into one at frequency close to Nyquist. The measured horizontal and vertical MTF(f)/MTF(f=0) at Nyquist frequency based on pixel pitch, a, ($= 1/2a$, $a = 30 \text{ ?m}$) ~ 16.67 cycles/mm is about ~ 0.49 and ~ 0.52 , respectively. In conclusion, we have demonstrated LWIR InAs/GaSb superlattice FPA based on n-CBIRD device structure, which has peak quantum efficiency of 54% and mean dark current density of $5 \times 10^{-5} \text{ A/cm}^2$ at 78K. Furthermore, we will report the NE?T, Noise Equivalent Irradiance (NEI), and MR?T of this FPA.

8631-26, Session 5

Dark current in GaAs/AlxGa1-xAs quantum well infrared detectors

Vaidya Nathan, Air Force Research Lab. (United States)

It is not clear whether the tunneling current in QWIPs depends just on the energy corresponding to motion perpendicular to the plane of the quantum well or on the total energy. In order to get a quantitative assessment of the contribution of energy corresponding to motion in the plane of the quantum well to the dark current we use the following approach. We calculate the dark current in GaAs/Alx Ga1-xAs quantum well infrared detectors for both tunneling dependent dependent only on Ez, and tunneling dependent on the total energy, and compare the results to experimental data. Comparison of theoretical results with experimental data at 40K shows that motion in the plane of the quantum well plays a significant role in determining the tunneling dark current. Corrections are made to Levine's original formula. Variation of the dark current with barrier width and doping density is systematically studied. It is shown that increasing the barrier width and/or decreasing the doping density in the well do not always reduce the dark current.

8631-27, Session 5

A bowtie optical antenna coupled quantum dot infrared photodetector with high operating temperature

Jarrold Vaillancourt, Applied NanoFemto Technologies (United States); Xuejun Lu, Univ. of Massachusetts Lowell (United States)

Antennas are key components for transmitting and receiving electromagnetic waves in the RF, microwaves and millimeter spectrum regimes. In this paper, we report a bowtie optical antenna enhanced quantum dot infrared photodetector (QDIP) for middle wave infrared (MWIR) and longwave infrared (LWIR) photodetection with a high operating temperature of 300 K. The bowtie optical antennas show a clear E-field concentration effect at the small detection area. An over 10 times photodetectivity (D^*) enhancement by the bowtie antennas is experimentally demonstrated. High photodetectivities (D^*) of over 1010 $\text{cm}^2/\text{Hz}/\text{W}$ are obtained for a large bias voltage range from -5 V to +2 V. A high operating temperature of over 300 K is also achieved.

8631-28, Session 5

Dual-gated L-QDIPs for tunable infrared detection

Christian P. Morath, Dustin Guidry, David A. Cardimona, Air Force Research Lab. (United States); Yagya Sharma, Sanjay Krishna, Ctr. for High Technology Materials (United States)

Dual-gated Lateral-Quantum Dot Infrared Photodetectors (L-QDIPs), with the potential for a tunable internal spectral response, were investigated. L-QDIPs consist of self-assembled InAs quantum dots buried in InGaAs/GaAs single or double well structures that are in-turn tunnel-coupled to a second, adjacent AlGaAs/GaAs quantum well. Photoexcited electrons from the quantum dots are expected to tunnel over to the second well where they are then swept out via a laterally applied bias voltage. Tunneling of the photocurrent is in part directed by the depletion field from a narrow, pinch-off gate on top of the device, which is applied vertically. A second, bottom pinch-off gate can be considered to block the lateral dark current in the second quantum well. Under a proper biasing arrangement, this detector architecture is expected to exhibit the ability to tune to select infrared wavelengths, as well as operate with reduced dark current and unity photoconductive gain in the second well. Here, L-QDIPs with top and bottom pinch-off gates to block lateral transport in each layer are investigated. The architecture, operating principles and conditions, and preliminary results of I-V, photocurrent and spectral absorption are all discussed.

8631-29, Session 6

Mid- infrared semiconductor laser based trace gas sensor technologies

for environmental monitoring and industrial process control (Invited Paper)

Rafal Lewicki, Mohammad Jahjah, Yufei Ma, Frank K. Tittel, Rice Univ. (United States); Przemyslaw Stefanski, Jan Tarka, Wroclaw Univ. of Technology (Poland)

This talk will focus on recent advances in the development of sensors based on infrared semiconductor lasers for the detection, quantification and monitoring of trace gas species and their applications in atmospheric chemistry and industrial process control. The development of compact trace gas sensors, in particular based on quantum cascade (QC) permit the targeting of strong fundamental rotational-vibrational transitions in the mid-infrared, that are one to two orders of magnitude more intense than overtone transitions in the near infrared. The architecture

**Conference 8631:
Quantum Sensing and Nanophotonic Devices X**

and performance of three sensitive, selective and real-time gas sensor systems based on mid-infrared semiconductor lasers will be described [1]. A QEPAS based sensor capable of ppbv level detection of CO, a major air pollutant, was developed. We used a 4.61 μm high power CW DFB QCL that emits a maximum optical power of more than 1W in a continuous-wave (CW) operating mode [2]. For the R6 CO line, located at 2169.2 cm^{-1} , a noise-equivalent sensitivity (NES, 1 σ) of 2 ppbv was achieved at atmospheric pressure with a 1 s. acquisition time. Furthermore, high performance (> 100 mW) 5.26 μm and 7.24 μm CW TEC DFB-QCLs (mounted in high heat load (HHL) packages) based QEPAS sensors for atmospheric NO and SO₂ detection will be reported [3, 4]. A 1 σ minimum detection limit of 3 ppb and 100 ppb was achieved for a sampling time of 1 s. using interference free NO and SO₂ absorption lines located at 1900.08 cm^{-1} [3] and 1380.94 cm^{-1} [4] respectively.

References

- [1] Rice University Laser Science Group website: <http://ece.rice.edu/lasersci/>
- [2] M. Razeghi, Y. Bai, S. Slivkin, S.R. Davish, SPIE Opt. Engineering 49 111103-1 (2010).
- [3] L. Dong, V. Spagnolo, R. Lewicki, F.K.Tittel, Optics Express 19, 24037-24045 (2011).
- [4] P. Waclawek, R. Lewicki, E.t.H. Chrysostom, F. K.Tittel and B. Lendl, 2012 CLEO Post-deadline Paper Session May 10, 2012.

8631-30, Session 6

Advanced sensors for Earth-sciences applications (Invited Paper)

David M. Sonnenfroh, Krishnan Parameswaran, Physical Sciences Inc. (United States); John Bruno, Maxison Technologies (United States); Kevin Repasky, Montana State University (United States)

The proliferation of unmanned aerial systems (UASs) is enabling new measurement capabilities for Earth science research with enhanced spatial and temporal coverage. These aircraft range from airplanes to helicopters, balloons, kites, and dropsondes. With the need to make multiple measurements from a given platform with limited payload resources, advanced sensors that provide high measurement performance in a small footprint and with minimal power are required. Sensor development strategies capitalize on concurrent advances in device characteristics, including optical output power efficiency and stability.

This talk will review a few of our sensor development efforts, highlighting how design elements meet specific sensor measurement needs. One example is a lightweight, low-power absorption photometer for CO₂. Our sensor was conceived as a high performance sensor for UASs and a means to push technology to small payloads for balloons. This mid-IR LED-based sensor provides sub ppmv precision in a package that is < 2 kg and 0.2 cu ft. Another example is an air quality sensor for manned spacecraft. New high efficiency quantum cascade laser designs enable this low power consumption sensor for CO to provide early warning of fire. A third example is a compact lidar being developed in collaboration with Montana State University for continuous ambient water vapor profiling via differential absorption. This sensor requires a narrow bandwidth, stable frequency laser source. The lidar transmitter is a MOPA design comprised of a near-ir tunable diode laser amplified by a tapered semiconductor optical amplifier. The receiver uses an avalanche photodiode to count returning backscattered photons.

8631-31, Session 6

Atmospheric and environmental sensing by photonic absorption spectroscopy (Invited Paper)

Weidong Chen, Univ. du Littoral Côte d'Opale (France); Tao Wu,

Univ. du Littoral Côte d'Opale (France) and Anhui Institute of Optics and Fine Mechanics (China) and Nanchang Hangkong Univ. (China); Weixiong Zhao, Univ. du Littoral Côte d'Opale (France) and Anhui Institute of Optics and Fine Mechanics (China); Gerard Wysocki, Princeton Univ. (United States); Xiaojuan Cui, Univ. du Littoral Côte d'Opale (France) and Anhui Institute of Optics and Fine Mechanics (China); Christophe Lengignon, Rabih Maamary, Eric Fertein, Univ. du Littoral Côte d'Opale (France); Cécile Coeur, Univ. du Littoral Côte d'Opale (France); Andy Cassez, Univ. du Littoral Côte d'Opale (France); Yingjian Wang, Weijun Zhang, Xiaoming Gao, Wenqing Liu, Fengzhong Dong, Anhui Institute of Optics and Fine Mechanics (China); George Zha, The Hong Kong Polytechnic Univ. (China); Xu Zheng, The Hong Kong Polytechnic Univ. (Hong Kong, China); Tao Wang, The Hong Kong Polytechnic Univ. (China)

Chemically reactive short-lived species play a crucial role in tropospheric processes affecting regional air quality and global climate change. Contrary to long-lived species (such as greenhouse gases), fast, accurate and precise monitoring of atmospheric chemical composition changes of such species represents a real challenge due to their short life time (~1s for OH radical) and very low concentration in the atmosphere (down to 106 molecules/cm³, corresponding to 0.1 pptv at standard temperature and pressure).

We report on our recent progress in instrumentation developments for spectroscopic sensing of trace reactive species. Modern photonic sources such as quantum cascade laser (QCL), distributed feedback (DFB) diode laser, light emitting diode (LED), difference-frequency generation (DFG) are implemented in conjunction with high-sensitivity spectroscopic measurement techniques for : (1) nitrous acid (HONO) monitoring by QCL-based long optical pathlength absorption spectroscopy and LED-based IBBCEAS (incoherent broadband cavity-enhanced absorption spectroscopy); (2) DFB laser-based hydroxyl free radical (OH) detection using WM-OA-ICOS (wavelength modulation off-axis integrated cavity output spectroscopy) and FRS (Faraday rotation spectroscopy); (3) nitrate radical (NO₃) and nitrogen dioxide (NO₂) measurements with IBBCEAS approach.

Applications in field observation and in smog chamber study will be presented.

The main techniques available for routine atmospheric measurements of OH, NO₃ and HONO are overviewed, in comparison with the emerging photonic technologies. Spectroscopic sensing offers the unique advantage of absolute quantitative assessments without any sample preparation (usually needed for non spectroscopic analytical methods), which allows one to minimize sampling induced artifacts and chemical interference, and permits for significant improvement in measurement accuracy.

8631-32, Session 6

Part-per-trillion level detection of SF₆ using a single-mode fiber-coupled quantum cascade laser and a quartz enhanced photoacoustic sensor

Vincenzo Spagnolo, Politecnico di Bari (Italy); Pietro Patimisco, Univ. degli Studi di Bari (Italy); Simone Borri, CNR-INF UOS Bari (Italy); Gaetano Scamarcio, Univ. degli Studi di Bari (Italy); Bruce E. Bernacki, Pacific Northwest National Lab. (United States); Jason M. Kriesel, Opto Knowledge Systems, Inc. (United States)

The detection and quantification of trace chemical species in the gas phase is of considerable interest in a wide range of applications. In combination with quantum cascade lasers (QCLs), quartz enhanced photoacoustic spectroscopy (QEPAS) offers the advantage of high sensitivity and fast time-response. Enhanced versatility of such sensor systems can be obtained via optical fiber delivery and coupling.

Conference 8631: Quantum Sensing and Nanophotonic Devices X

We report here on a QEPAS sensor based on an external-cavity fiber-coupled QCL emitting at 10.54 μm . We designed and realized the mid-infrared hollow waveguide fiber and coupler optics in order to ensure single-mode QCL beam delivery to the QEPAS sensor. SF₆ was selected as the target gas. SF₆ is an invisible, non-hazardous, inert gas, and an extremely efficient absorber of infrared radiation, making it one of the most effective known greenhouse gases. Thanks to the fast vibrational-translation relaxation rate of SF₆, we can operate our sensor at low pressure (75 Torr) where the quartz tuning fork is characterized by a high quality factor (~ 22000). Stepwise concentration measurements were performed to verify the linearity of the QEPAS signal as a function of the SF₆ concentration, which ranged from 10 ppm down to 9 ppb concentration. To determine the best achievable detection sensitivity of the sensor we performed an Allan variance analysis, measuring and averaging its response. We reached a minimum detection sensitivity of 50 parts per trillion in 1 s at a QCL power of 18 mW, corresponding to a record normalized noise-equivalent absorption for QEPAS of $2.7 \cdot 10^{(-10)} \text{ W} \cdot \text{cm}^{(-1)} \cdot \text{Hz}^{(-2)}$.

8631-37, Session 6

Infrared scattering scanning near-field optical microscopy using an external cavity quantum cascade laser for nanoscale chemical imaging and spectroscopy of explosive residues

Ian M. Craig, Mark C. Phillips, Matthew S. Taubman, Pacific Northwest National Lab. (United States); Erik E. Josberger, Markus B. Raschke, Univ. of Colorado at Boulder (United States)

Infrared scattering scanning near-field optical microscopy (s-SNOM) is an apertureless superfocusing technique that uses the antenna properties of a conducting atomic force microscope (AFM) tip to achieve infrared spatial resolution below the diffraction limit. The instrument can be used either in imaging mode, where a fixed wavelength light source is tuned to a molecular resonance and the AFM raster scans an image, or in spectroscopy mode where the AFM is held stationary over a feature of interest and the light frequency is varied to obtain a spectrum. In either case, a strong, stable, coherent infrared source is required. Here we demonstrate the integration of a broadly tunable external cavity quantum cascade laser (ECQCL) into an s-SNOM and use it to obtain infrared spectra of microcrystals of chemicals adsorbed onto gold substrates and to chemically map and identify individual microcrystals.

Residues of explosive compounds PETN, RDX, TNT, and tetryl were deposited onto gold substrates. s-SNOM experiments were performed in the 1260-1400 cm^{-1} tuning range of the ECQCL, corresponding to the NO₂ vibrational fingerprint region. Chemical imaging with fixed wavelength tuned to a molecular resonance allows mapping of species distributions in mixed samples with a lateral resolution of $\sim 25\text{nm}$. Vibrational infrared spectra are then collected on individual chemical domains with a collection area of $\sim 500\text{nm}^2$. Spectra are compared to ensemble averaged far-field infrared reflection-absorption spectroscopy (IRRAS) results.

8631-38, Session 6

Precision measurement of motion using localised evanescent fields

Robin M. Cole, Warwick Bowen, Queensland Quantum Optics Lab. (Australia); Anna Swan, Boston Univ. (United States)

Microscopy has long been utilized to image and track motion with a resolution around the wavelength scale, and recent progress has produced SNOM microscopes which can beat the diffraction limit by an order of magnitude. We show that a SNOM probe can be used to characterize not only static objects, but also those in motion, with extremely high resolution in the axial direction. Such systems have

significant relevance in the area of quantum optomechanics. Our modeling predicts that zero-point motion resolving measurement should be possible, allowing the generation of mechanical squeezing and optomechanical entanglement.

To demonstrate the principle of motion sensing using SNOM, we simulate the transmission of a SNOM probe interacting with a silica nanoparticle located at the probe apex. The transmission drops as the particle moves out of the evanescent field, since the air gap between SNOM aperture and particle increases thus reducing coupling to the far field. The non linear dependence of transmission with particle position is due to the exponentially decaying nature of the evanescent field, and provides the gradient necessary to measure very small changes in axial position of the particle. By taking the maximum gradient of the transmission and choosing an incident optical power of order milliwatts we yield a sensitivity of order 10-13 m/Hz^{1/2} in the particles axial position.

This system can be realized experimentally by supporting a particle on a lightweight membrane (e.g. graphene), forming a new type of optomechanic system. Finally we present recent progress towards experimentally demonstrating this system.

8631-33, Session 7

Gallium nitride on silicon for consumer and scalable photonics (*Invited Paper*)

Can Bayram, Kuen-Ting Shiu, Yu Zhu, Cheng-Wei Cheng, Devendra K. Sadana, IBM Thomas J. Watson Research Ctr. (United States); Zahra Vashaei, Erdem Cicek, Ryan McClintock, Manijeh Razeghi, Northwestern Univ. (United States)

Gallium Nitride (GaN) semiconductor technology is unique as (1) GaN electronics (e.g. high electron mobility transistors) outperform conventional electrical devices in terms of performance thanks to high critical electric field and high saturation velocity, and (2) GaN photonics (e.g. visible light emitting diodes) enable high efficiency deep ultraviolet to near-infrared devices thanks to composition-independent direct-bandgap. However, without environmental-friendly and cheap mass-production scheme to sustain world-wide need, GaN semiconductor technology cannot be adopted in large scale and the benefits will be limited to laboratory experiments and niche applications.

Recently, GaN-based visible light emitting diodes (LEDs) have driven the interest of the community for general lighting applications that has driven the wide-scale metalorganic chemical vapor deposition (MOCVD) installation for LED growths. Despite the expanding infrastructure, the LED adoption as a lighting source is hindered by the cost of the conventional substrate choice: Sapphire. Silicon, with almost a century long know-how, is the most scalable and cost effective substrate for LED volume production. This; however, requires addressing the material issues related to lattice- and thermal-mismatch of gallium nitride with silicon. Conventional gallium nitride growth efforts focus on silicon (111) substrates enabling a bulk epitaxial growth scheme. However, silicon (100) substrates are more interesting due to integration of gallium nitride devices with already-established silicon-based CMOS technology.

In this talk, we will be addressing the integration of gallium nitride with silicon. We will detail the challenges and advantages of GaN on Si approach, and present a novel CMOS-compatible scheme enabling high quality gallium nitride - silicon (100) integration. As emerging GaN semiconductor technology targets consumer devices, our approach fulfills the need for the development of such devices on more available and cheaper silicon substrates. Our work also promise novel device concepts such as on-chip GaN-Si photonics thanks to the direct bandgap of gallium nitride.

**Conference 8631:
Quantum Sensing and Nanophotonic Devices X**

8631-34, Session 7

Monolithic tunable single source in the mid-IR for spectroscopy (*Invited Paper*)

Mathieu Carras, Alcatel-Thales III-V Lab (France); Grégory Maisons, Bouzid Simozrag, Virginie Trinité, Alcatel-Thales III-V Lab. (France); Mickael Brun, CEA-LETI-Minatec (France); G. Grand, CEA-LETI (France); Pierre Labeye, Sergio Nicoletti, CEA-LETI-Minatec (France)

In order to detect a complex molecules or a set of simple molecules, one need a source with a small linewidth and tunable over a few tens of wavenumbers. Monolithic tuneable sources are very appealing for spectroscopy applications because of the compactness, the robustness and the usability. A single DFB QCL has a limited tuneability, the two main leverages being the temperature and the current. Recently, arrays DFB lasers working at different wavelengths with interesting full tuning properties were proposed in the litterature. Since each laser has a different output facet, their use in commercial systems is not straightforward. We first show our ability of producing such a device at different wavelengths of interest for spectroscopy using our metal grating approach (patent III-V Lab). In order to be usable the output of different laser sources can be combined together by the use of a multiplexer providing that suitable materials stack for core/cladding fabrication is available. A viable way to apply this configuration to the Mid-IR while still using microelectronics compatible materials is to develop passive photonics devices on a stack based on semiconducting materials, such as for example SiGe/Si. The use of SiGe/Si stack is currently explored by CEA-LETI and III-V Lab. We show the results of this development. The first step is to achieve low losses guiding over the MIR range. We will present the set up for losses measurements based on Fabry-Perot fringes measurements. We have been able to achieve as low as 1.5dB/cm at 5.65 μ m.

8631-35, Session 7

Integrated thin-film GaSb-based Fabry-Perot lasers: towards a fully integrated spectrometer on a SOI waveguide circuit

Nannicha Hattasan, Alban A. Gassenq, Univ. Gent (Belgium); Laurent Cerutti, Jean-Baptiste Rodriguez, Eric Tournié, Univ. Montpellier 2 (France); Gunther Roelkens, Univ. Gent (Belgium)

Several interesting molecules have their absorption signature in the mid-infrared. Spectroscopy is commonly used for the detection of these molecules, especially in the short-wave infrared (SWIR) region due to low water absorption. Conventional spectroscopic systems consist of a broadband source, detector and dispersive components, making them bulky and difficult to handle. Such systems cannot be used in applications where compact footprint and low power consumption is critical, such as portable gas sensors and implantable blood glucose monitors.

Silicon-On-Insulator (SOI) offers a compact, low-cost photonic integrated circuit platform realized CMOS fabrication technology. On the other hand, GaSb is an excellent material for SWIR lasers and detectors. Integration of GaSb active components on SOI would thus result in a compact and low power integrated spectroscopic system.

In this paper, we report the study on thin-film GaSb Fabry-Perot lasers integrated on a carrier substrate. The integration is achieved by using an adhesive polymer (DVS-BCB) as bonding agent. The lasers operate at room temperature at 2.02 μ m. We obtain a minimum threshold current of 48.9mA in the continuous wave regime and 27.7mA in pulsed regime. This yields a current density of 680A/cm² and 385A/cm², respectively. The thermal behavior of the device is also studied. The lasers operate up to 35 °C, with a 323 K/W thermal impedance, which is due to the high thermal impedance of the bonding layer. Preliminary results of integrated lasers on SOI are reported. Our work brings fully integrated, mid-infrared GaSb sensor systems on SOI a significant step closer to reality.

8631-102, Session 7

Ultraviolet light-emitting diode on Si substrate

Yinjun Zhang, Simon Gautier, Chu-Young Cho, Ryan McClintock, Manijeh Razeghi, Northwestern Univ. (United States)

No Abstract Available

8631-39, Session 8

Monodisperse carbon nanomaterials in electronic, optoelectronic, sensing, and energy conversion technologies (*Invited Paper*)

Mark C. Hersam, Northwestern Univ. (United States)

Recent years have seen substantial improvements in the structural, chemical, and electronic monodispersity of carbon nanomaterials, leading to improved performance in a variety of device applications. This talk will highlight our latest efforts to exploit monodisperse carbon nanomaterials in electronic, optoelectronic, sensing, and energy conversion technologies. For example, high purity semiconducting single-walled carbon nanotubes (SWCNTs) allow the fabrication of thin-film field-effect transistors with concurrently high on-state conductance and on/off ratio and/or high frequency operation exceeding 150 GHz. Using dielectrophoretic assembly, arrays of individual SWCNT transistors can also be realized with high yield. Similarly, high performance digital circuits can be fabricated from semiconducting SWCNT inks via aerosol jet printing. Beyond transistors, semiconducting SWCNTs have been utilized for light-emitting optoelectronic devices or chemical sensors, while metallic SWCNTs are well-suited as transparent conductors in organic photovoltaics. This talk will also explore the utility of solution-processed graphene for high-frequency transistors, charge blocking layers in organic photovoltaics, and supports for photocatalytic production of solar fuels.

8631-40, Session 8

Nano photoconductive switches for microwave applications (*Invited Paper*)

Charlotte Tripon-Canseliet, Univ. Pierre et Marie Curie (France); Salim Faci, Conservatoire National des Arts Métiers (France); Didier Decoster, Univ. des Sciences et Technologies de Lille (France); Antoine Pagies, IEMN (France); Soon Fatt Yoon, Nanyang Technological Univ. (Singapore); Kin Leong Pey, SUTD (Singapore); Jean Chazelas, Thales Airborne Systems (France)

Emerging 1D and 2D nano materials such as nanodots, nanowires, nanotubes and nanoribbons become potential technical solutions to overcome the performances bottleneck of conventional microwave photoconductive switches.

Such new materials offer new opportunities for the confinement of light/matter interaction and exhibit interesting energy band diagram in an optical wavelength spectrum covering visible to NIR. Strong material interests stays for the generation of very high local density of carriers in contrast with a high dark resistivity, in association with a high carrier mobility. These challenges can be reached today thanks to nanotechnology processes with a high compatibility constraint with submicrometer light coupling solutions and microwave devices and circuits technologies. Modeling and design tools dedicated to photoconductive effect description at nanometer scale, for its implementation in passive and active components must be set up in order to exalt this effect for microwave signal processing functionalities such as switching, generation, amplification and emission over a large frequency bandwidth.

**Conference 8631:
Quantum Sensing and Nanophotonic Devices X**

This paper will report on latest demonstrations of high performance photoconductive switches for high frequency applications and review state-of-the-art research work in this area.

8631-41, Session 8

Ultra-short channel field effect transistors based on Ge/Si core/shell nanowires (*Invited Paper*)

Binh-Minh Nguyen, Los Alamos National Lab. (United States); Yang Liu, Sandia National Labs. (United States); Wei Tang, Univ. of California, Los Angeles (United States); S. T. Picraux, Los Alamos National Lab. (United States); Shadi A. Dayeh, Los Alamos National Lab. (United States) and Univ. of California, San Diego (United States)

Transport in one-dimensional semiconductor structures possesses unique properties such as ballistic effect, which attract great attention for both basic research and device applications. However, observing ballistic transport and making use of it are normally obstructed by the difficulties achieving high material quality and minimizing detrimental perturbations from surface processes.

In this work, Ge/Si concentric nanowires are utilized as a platform for studying hole ballistic transport in 1D channels and to demonstrate ballistic and high performance field effect transistors (FETs). The nanowire structure consists of a Ge core and a higher bandgap Si shell in order to spatially confine holes inside the core of the nanowire, thus minimizing surface scattering and trapping effects. Advanced material growth of Ge/Si core/shell nanowires with abrupt doping and composition interfaces were achieved with chemical vapor deposition allowing for high quality materials with long carrier mean free path, to the extent that it can be observable, and deployable in electronic devices. Single nanowire devices were fabricated on a 50nm thick SiN TEM membrane using a gate-last approach. Nickel contacts were deposited using ebeam lithography and ebeam metal evaporation prior to 10nm HfO₂ gate dielectric deposition. TEM was utilized for in-situ thermal treatment of the germanidation/silicidation reaction with nickel electrodes in order to achieve sub-100 nm channel lengths. Finally, titanium/gold gate contacts were deposited precisely on top of the ultra-short unsilicided channel. Preliminary results show that these 20 nm-in-diameter Ge/Si heterostructure FETs exhibit sub-threshold swings of 140 mV/decade with a maximum trans-conductance of 6?S at 100mV VDS.

8631-42, Session 8

Tailoring of optical properties of porous nanocolumnar structures and their device applications by oblique angle deposition (*Invited Paper*)

Jae Su Yu, Jung Woo Leem, Kyung Hee Univ. (Korea, Republic of)

Recently, the modification of refractive index profile of semiconductors has attracted great interest for applications in optical and optoelectronic devices. The oblique angle deposition (OAD) technique was developed to have the capability of efficiently forming three-dimensional nanostructures. The morphological properties of deposited nanocolumnar films can be controlled by simply changing the tilt angle during the deposition process. Additionally, their optical properties, including refractive index and absorption coefficient, can be modified by the incorporation of porosity within the film due to the atomic self-shadowing effect. The reflectance can be also designed by a graded refractive index profile, which results in an efficient antireflective surface structure. The porous films can be easily applied to the devices by the OAD process to improve the device performance.

In this presentation, we reported the controlled growth and optical

properties of porous nanocolumnar structures (e.g., silicon, germanium, indium tin oxide, zinc oxide, zinc sulfide, etc.) by the OAD method using an e-beam evaporation system. The antireflective coatings, graded refractive index films, and distributed Bragg reflectors were applied to various devices such as solar cells, light emitting diodes, sensors, and vertical cavity surface emitting lasers. The characteristics of the fabricated devices were measured. These results suggest that the tailoring of optical properties by a simple OAD technique is very promising for optical and optoelectronic device applications.

8631-43, Session 8

THz oscillations and soft parametric resonances for hot carriers in graphene (*Invited Paper*)

Jean-Pierre Leburton, Univ. of Illinois at Urbana-Champaign (United States)

We investigate the onset of current oscillations induced by hot carriers interacting with high-energy optic phonons ω_{op} in graphene during the transient regime once the electric field is turned-on at room temperature. We show that the oscillations only take place for a specific range of constant electric fields within a voltage and sample length window, and is the direct consequence of the interplay between the electric force and the randomizing nature of deformation potential optic phonons in the linear band structure of graphene. Within this range of parameters the effect is predicted to manifest in damped terahertz oscillations of the carrier drift velocity and average energy .

When an oscillating (AC) electric field is superimposed to a DC field F , the current oscillations are modified by the presence of the AC field, and its amplitude exhibits a soft resonance at the about half of the natural oscillation frequency $\omega_F = 2\omega_{Fv}$ of the carriers in the presence of the DC field. This type of behavior is however different from normal parametric resonance that would occur at $2\omega_F$. In addition the resonance is rather soft with a Q-factor $Q > 1$, as the system is strongly dissipative. Another interesting feature is the dephasing between current and AC field that shows a minimum as a function of the AC field frequency at low damping that softens to become monotonic at high damping for all AC field strengths. Applications for THz sources and detectors will be discussed.

8631-1,

On the foundational equations of the classical theory of electrodynamics: applications to optomechanical sensors and actuators (*Keynote Presentation*)

Masud Mansuripur, College of Optical Sciences, The Univ. of Arizona (United States)

In this presentation, I will describe an approach to a complete and consistent theory of classical electrodynamics based on Maxwell's macroscopic equations, Poynting's postulate, Abraham's linear and angular momentum densities, and the Einstein-Laub equations of force and torque densities. The ideas find application in the areas of optical tweezers and opto-mechanical sensors, as well as optically-driven micro- and nano-mechanisms and actuators.

8631-44, Session 9

Large-area CMOS SPADs with very low dark counting rate

Danilo Bronzi, Federica A. Villa, Simone Bellisai, Politecnico di Milano (Italy); Simone Tisa, Micro Photon Devices S.r.l. (Italy);

Conference 8631: Quantum Sensing and Nanophotonic Devices X

Alberto Tosi, Giancarlo Ripamonti, Franco Zappa, Politecnico di Milano (Italy); Sascha Weyers, Daniel Durini, Werner Brockherde, Uwe Paschen, Fraunhofer-Institut für Mikroelektronische Schaltungen und Systeme (Germany)

We designed and characterized Silicon Single-Photon Avalanche Diodes (SPADs) fabricated in a standard 0.35 μm CMOS technology, achieving state-of-the-art low Dark Counting Rate (DCR), very large diameter, and extended Photon Detection Efficiency (PDE) in the Near Ultraviolet. So far, different groups fabricated CMOS SPADs in scaled-technologies, but with many drawbacks in active area dimensions (just a few micrometers), excess bias (just few Volts), DCR (many hundreds of counts per second, cps, for small 10 μm devices) and PDE (just few tens % in the visible range).

The novel CMOS SPAD structures with 50 μm , 100 μm , 200 μm and 500 μm diameters can be operated at room temperature and show DCR of 100 cps, 2 kcps, 20 kcps and 90 kcps, respectively, even when operated at 6V excess bias. The PDE peaks to 55% at about 400 nm and slowly decreases to 40% at 500 nm, 20% at 650 nm and is still 5% at 800 nm. The photon timing response reaches 77 ps for the 10 μm SPADs and is still 120 ps for the larger ones.

Because of the excellent performances, these large CMOS SPADs are exploitable in monolithic SPAD-based arrays with on-chip CMOS electronics, e.g. for time-resolved spectrometers with no need of microlenses (thanks to high fill-factor). Instead the smaller CMOS SPADs, e.g. the 10 μm devices with just 3 cps at room temperature and 6 V excess bias, are the viable candidates for dense 2D CMOS SPAD imagers and 3D Time-of-Flight ranging chips.

8631-45, Session 9

Low afterpulsing and narrow timing response InGaAs/InP Single-Photon Avalanche Diode

Alberto Tosi, Fabio Acerbi, Michele Anti, Franco Zappa, Politecnico di Milano (Italy)

We designed, fabricated and tested a new planar InGaAs/InP Single-Photon Avalanche Diode (SPAD). By optimizing design and fabrication processes, we obtained low afterpulsing and very good timing jitter, with very fast tail. The detector has a separate absorption, charge and multiplication structure, with double p-type Zn diffusion into n-type InP for defining the p-n high-field avalanche junction. The SPAD can be operated at temperatures achievable with thermo-electric coolers mounted in compact packages (like TO-8). When operated in gated mode with 5 V excess bias, the 25 μm active area diameter InGaAs/InP SPAD reaches good performance at 225 K: i) photon detection efficiency of 40% at 1 μm and 25% at 1.55 μm ; ii) dark count rate below 100 kcps (counts per second); iii) low afterpulsing allowing to set a hold-off time as short as 1 μs , corresponding to 1 Mcps; iv) timing jitter less than 90 ps (full width at half maximum) and time constant of decaying tail of just 30 ps.

Overall this new planar InGaAs/InP SPAD can be exploited in many near-infrared (up to 1.7 μm) applications where low light, wide dynamic range waveforms must be acquired, e.g. in Time-Correlated Single Photon Counting (TCSPC) measurements or Time-of-Flight LIDAR applications for eye-safe 3D ranging.

8631-46, Session 9

A 48-pixel array of single photon avalanche diodes for multispot single molecule analysis

Angelo Gulinatti, Ivan Rech, Politecnico di Milano (Italy); Piera Maccagnani, Istituto per la Microelettronica e Microsistemi (Italy); Massimo Ghioni, Politecnico di Milano (Italy) and Micro Photon Devices S.r.l. (Italy)

In this paper we present an array of 48 Single Photon Avalanche Diodes

(SPADs) specifically designed for multispot Single Molecule Analysis. The detectors have been arranged in a 12x4 square geometry with a pitch-to-diameter ratio of ten in order to minimize the collection of the light from non-conjugated excitation spots. In order to explore the trade-offs between the detectors' performance and the optical coupling with the experimental setup, SPADs with an active diameter of 25 and of 50 μm have been manufactured. The use of a custom technology, specifically designed for the fabrication of the detectors, allowed us to combine a high photon detection efficiency (peak close to 50% at a wavelength of 550nm) with a low dark count rate compatible with true single molecule detection.

In order to allow easy integration into the optical setup for parallel single-molecule analysis, the SPAD array has been incorporated in a compact module containing all the electronics needed for a proper operation of the detectors.

8631-47, Session 9

Comparison of SiPM and PMT as detectors for a spectrophotometry system

Roberto Pagano, Salvatore Lombardo, Domenico Corso, Consiglio Nazionale delle Ricerche (Italy); Giuseppina Valvo, Beatrice Carbone, Angelo Piana, Massimo Cataldo Mazziolo, Nunzio Delfo Sanfilippo, Pier Giorgio Fallica, STMicroelectronics (Italy); Sebania Libertino, Consiglio Nazionale delle Ricerche (Italy)

Silicon Photomultipliers are new pixelated solid state photon-detectors able to compete with traditional Photomultiplier Tubes in those applications where ultra-low light detection is required wishing low power consumption, magnetic shielding and low volume occupancy. In this work we present the electrical and optical characterization of different active area SiPMs produced by the STMicroelectronics showing a very low DC. Data are compared with those of a traditional PMT. The SiPM has been tested in a spectrophotometry system using a known light source and the spectrum obtained was compared with that obtained using a traditional PMT.

8631-48, Session 9

Monolithic time-to-digital converter chips for time-correlated single-photon counting and fluorescence lifetime measurements

Bojan Markovic, Davide Tamborini, Simone Bellisai, Andrea Bassi, Antonio Pifferi, Federica A. Villa, Giorgio Michele Padovini, Alberto Tosi, Politecnico di Milano (Italy)

We present a high performance Time-to-Digital Converter (TDC) chip that provides 10 ps timing resolution, 160 ns dynamic range and a Differential Non-Linearity (DNL) better than 1.5% LSB_{rms} within a compact 6 cm x 6 cm x 8 cm module. The instrument reaches high timing-precision of 15 ps_{rms} (i.e. 36 psFWHM) and is an outbreak for developing compact arrays for Time-Correlated Single-Photon Timing (TCSPC), Time-of-Flight (TOF) and Positron Emission Tomography (PET) instrumentation.

The TDC module provides two connectors for the START and STOP input pulses, an USB 2.0 link for PC interfacing and a 5 V DC power supply plug. The module is composed by three electronic boards, for timing, FPGA processing and power supply. The core of the timing board is the application-specific monolithic TDC chip fabricated in a 0.35 μm CMOS technology. It contains the two independent START / STOP channels and the global electronics for synchronization and data read-out.

The USB 2.0 link allows easy setting of acquisition parameters and fast download of acquired data; TCSPC and TOF data visualization and storing is performed through an user-friendly software interface. The chip opens the way to monolithic arrays of TDCs, requested in a wide range of applications such as: Fluorescence Lifetime Imaging (FLIM), Time-

**Conference 8631:
Quantum Sensing and Nanophotonic Devices X**

of-Flight (TOF) ranging measurements, time-resolved Positron Emission Tomography (PET), single-molecule spectroscopy, Fluorescence Correlation Spectroscopy (FCS), Diffuse Optical Tomography (DOT), Optical Time-Domain Reflectometry (OTDR), quantum optics, etc. In particular, we show the application of the device to fluorescence lifetime spectroscopy of different fluorophores, showing the advantages of concurrent high dynamic range and good timing resolution.

8631-49, Session 9

InGaAs/InP SPAD photon-counting module with auto-calibrated gate-width generation and remote control

Alberto Tosi, Alessandro Ruggeri, Andrea Bahgat Shehata, Adriano Della Frera, Carmelo Scarcella, Politecnico di Milano (Italy); Simone Tisa, Andrea Giudice, Micro Photon Devices S.r.l. (Italy)

We present an advanced photon-counting module based on InGaAs/InP SPAD (Single-Photon Avalanche Diode) for detecting photons up to 1.7 μm . The module exploits a novel architecture for generating and calibrating the gate width, along with other functions (such as module supervision, counting and processing of detected photons, etc.).

The gate width, i.e. the time interval when the SPAD is ON, is user-programmable in the range from 500 ps to 1.5 μs , by means of two different delay generation methods implemented in a FPGA (Field-Programmable Gate Array): i) for delays up to 65 ns (with 100 ps steps) the delay is introduced by means of multiplexers and adders; ii) for longer delays (up to 1.5 μs , with 1 ns steps) a fine-tuned ring oscillator and counters are employed. In order to compensate chip-to-chip delay variations, an auto-calibration circuit picks out the combination of delays that most approaches the selected gate width.

The InGaAs/InP module accepts asynchronous and aperiodic signals and introduces very low jitter (less than 0.1% FWHM – Full-Width at Half-Maximum - of the generated delay, with a minimum value of 10 ps). Moreover the photon counting module provides other new features like a microprocessor for system supervision, a touch-screen for local user interface, and an Ethernet link for remote control. Thanks to the fully-programmable and configurable architecture, the overall instrument provides high system flexibility and can easily match all requirements set by many different applications requiring single photon-level sensitivity in the near infrared with very low photon timing jitter.

8631-50, Session 10

Challenges for ultimate HOT quantum IR detectors (*Invited Paper*)

Olivier Gravrand, Wala Hassis, Johan Rothman, CEA-LETI-Minatec (France)

The high operating temperature detection (HOT) is becoming one the main challenges in future IR quantum detection. Indeed, working at high temperature is very interesting from the system point of view because of cryo-machine considerations: The system gains in power consumption but also in cooler reliability and lifetime which means low exploitation costs. Hence the SWAP approach (Size Weight And Power) requires a total revision of the detection blocs, both from the detector and the cryo-cooler point of view. This paper aims at reviewing the different challenges brought by HOT detection on the detector part, exploring the different material candidates for HOT detection. Then the different current sources and their consequences will be discussed, focussing on the HgCdTe, which is the best known material system today. Focal plane arrays (FPA) implications in terms of pixel operability (mandatory for high quality imagery) will also be reviewed, with a special emphasis on noise features at high operating temperature. Last but not least, more futuristic structures and designs (involving light concentration) will be discussed at the end.

8631-51, Session 10

InAs/InAsSb type-II superlattice infrared nBn photodetectors and their potential for operation at high temperatures

Oray O. Cellek, Zhao-Yu He, Zhiyuan Lin, Ha Sul Kim, Shi Liu, Yong-Hang Zhang, Arizona State Univ. (United States)

Type-II superlattice (T2SL) infrared photodetectors are theoretically expected to offer higher operating temperatures than those made of HgCdTe. InAs/InAsSb T2SL structures, namely Ga-free T2SL, have minority carrier lifetimes an order of magnitude longer than that for conventional InAs/Ga(In)Sb T2SLs in the long wavelength infrared (LWIR) band at 77 K. The bandgap of these structures can be tuned from mid-wave infrared (MWIR) to very long-wave infrared (VLWIR) bands. Ga-free T2SL has simpler MBE growth procedure since group-V elements are not completely changed at the interfaces. Two other significant differences of Ga-free T2SL different from InAs/Ga(In)Sb T2SL devices is the longer superlattice period with lower wavefunction overlap at the same bandgap. In addition, the hole miniband states in the valance band are less coupled. An InAs/InAsSb T2SL nBn device with cut-off wavelength of 13.2 micrometers is characterized. It is observed that lower wavefunction overlap results in lower device absorption quantum efficiency, and weakly coupled hole miniband states result in low hole velocity. However, the device dark current is extremely low, below the Rule-07 limit defined for HgCdTe infrared photodetectors. The dark current activation energy is measured to be equal to the absorber bandgap from 250 K down to background limited operation (BLIP) temperature. Dependence of the device characteristics such as dark current, quantum efficiency, BLIP temperature and operating bias on the device design parameters will be discussed.

8631-52, Session 10

High operation temperature of HgCdTe photodiodes by bulk defect passivation (*Invited Paper*)

Paul Boieriu, Silviu Velicu, Ramana Bommena, Chris Buurma, Caleb Blisset, EPIR Technologies, Inc. (United States); C. Grein, Sivananthan Laboratories, Inc. (United States) and Univ. of Illinois at Chicago (United States); Sivalingam Sivananthan, EPIR Technologies, Inc. (United States); Ping Hagler, Missile Defense Agency (United States)

Spatial noise and the loss of photogenerated current due to material non-uniformities limit the operability of longwave infrared (LWIR) HgCdTe detector arrays at elevated temperatures. Reducing the electrical activity of defects is equivalent to lowering the density of defects, thereby allowing detection and discrimination at longer ranges. Infrared focal plane arrays (IRFPA) in other LWIR applications will also benefit from detectivity and uniformity improvements. Larger signal-to-noise ratio permits either improved accuracy of detection/discrimination when an IRFPA is employed under current operating conditions, or provide similar performance with the IRFPA operating under less stringent conditions such as higher system temperature, increased system jitter or damaged ROIC wells. Bulk passivation of semiconductor with hydrogen continues to be investigated for its potential to become a tool for the fabrication of high performance devices. Inductively coupled plasmas have been shown to improve the quality and uniformity of semiconductor materials and devices. The retention of the benefits following various aging conditions is discussed here.

**Conference 8631:
Quantum Sensing and Nanophotonic Devices X**

8631-56, Session 10

Noise in InAs/GaSb type-II superlattice photodiodes

Robert H. Rehm, Andreas Wörl, Martin Walther, Fraunhofer-Institut für Angewandte Festkörperphysik (Germany)

Over the last few years, InAs/GaSb superlattice (SL) infrared (IR) detectors have shown tremendous progress both in the mid-wavelength (MWIR, 3-5 μm) and in the long-wavelength (LWIR, 8-12 μm) atmospheric windows. Favorable fundamental properties like, e.g., a widely adjustable bandgap, a high quantum efficiency and low dark current render the InAs/GaSb SL material into an attractive alternative to CdHgTe or InSb-based devices, which are widely used for high-performance IR detectors and imagers in the industry today. Recently, various groups have made use of the InAs/GaSb/AlSb materials family remarkable flexibility to engineer device concepts with advanced bandstructures that have significantly pushed the electrooptical performance.

Besides their ultimate performance, however, a sufficient understanding of many fundamental aspects of InAs/GaSb SL IR-detector devices is still lacking. In this study, we have focused on the noise behavior of InAs/GaSb SL homojunction pin-photodiodes with a dark current limited by Shockley-Read-Hall (SRH) processes in the space charge region, i.e., a generation-recombination (g-r) limited behavior. While the characterization of LWIR devices is comparatively straight-forward due to their higher dark current, noise measurements on small-sized MWIR devices require a much more sophisticated experimental set-up. Our analysis of a large set of MWIR diodes shows that the experimental noise data does not match the predictions of the commonly assumed shot noise expression for g-r-limited diodes. An additional noise contribution is observed, when the transition rate via SRH-states, or, in other words, the inverse carrier lifetime, is increased. We will show a theoretical noise model, which is in good agreement with the experimentally observed noise.

8631-98, Session 10

High performance bias-selectable dual-band short-/mid-wavelength infrared photodetectors based on type-II InAs/GaSb/AlSb superlattices

Anh Minh Hoang, Guanxi Andy Chen, Abbas Haddadi, Manijeh Razeghi, Northwestern Univ. (United States)

Active and passive imaging in a single camera based on the combination of short-wavelength and mid-wavelength infrared detection is highly needed in a number of tracking and reconnaissance missions. Due to its versatility in band-gap engineering, Type-II InAs/GaSb/AlSb superlattice has emerged as a candidate highly suitable for this multi-spectral detection.

In this paper, we report the demonstration of high performance bias-selectable dual-band short-/mid-wavelength infrared photodetectors based on InAs/GaSb/AlSb type-II superlattice with designed cut-off wavelengths of 2 μm and 4 μm . Taking advantages of the high performance short-wavelength and mid-wavelength single color photodetectors, back-to-back p-i-n-n-i-p photodiode structures were grown on GaSb substrate by molecular beam epitaxy. At 150 K, the short-wave channel exhibited a quantum efficiency of 55%, a dark current density of $1.0 \times 10^{-9} \text{ A/cm}^2$ at -50 mV bias voltage, providing an associated shot noise detectivity of 3.0×10^{13} Jones. The mid-wavelength channel exhibited a quantum efficiency of 33% and a dark current density of $2.6 \times 10^{-5} \text{ A/cm}^2$ at 300 mV bias voltage, resulting in a detectivity of 4.0×10^{11} Jones. The operations of the two absorber channels are selectable by changing the polarity of applied bias voltage.

8631-99, Session 10

Effect of gating technique on the type-II InAs/GaSb long-wavelength infrared photodetectors

Guanxi Andy Chen, Anh Minh Hoang, Simeon Bogdanov, Shaban Ramezani Darvish, Manijeh Razeghi, Northwestern Univ. (United States)

Surface leakage has been a limiting factor for the long-wavelength infrared (LWIR) Type-II superlattice photodetector. The gating technique, which creates a metal-insulator-semiconductor (MIS) structure on the mesa sidewall, has been demonstrated its ability to effectively suppress surface leakage in the mid-wavelength infrared (MWIR). However, this technique requires very high gate biases to be applied, and has not been transferred to the long-wavelength infrared region because for small band gap active regions, the surface leakage in LWIR P+-?-M-N+ T2SL heterostructure photodetector is more severe and the leakage phenomenon might be more complicated.

In this paper, we demonstrated that, by applying gating technique, surface leakage generated by SiO₂ passivation in long-infrared Type-II superlattice photodetector is eliminated, and different surface leakage mechanisms are disclosed. By reducing the SiO₂ passivation layer thickness, saturated gated bias is suppressed to -4.5 volt. At 77K, the dark current density of gated device at saturated gate bias is reduced by more than 2 orders of magnitude, with 3071 $[\omega\text{cm}^2]$ resistance-area product at -100mV. With quantum efficiency of 50%, the 11 μm 50% cut-off gated photodiode exhibits a specific detectivity of 7×10^{11} Jones, and the detectivity stays above 2×10^{11} Jones from 0 to -500mV operation bias.

8631-57, Session 11

Towards the production of very low defect GaSb and InSb substrates: bulk crystal growth, defect analysis and scaling challenges (Invited Paper)

Rebecca Martinez, Sasson Amirhaghi, Brian Smith, Andrew Mowbray, Mark J. Furlong, Wafer Technology Ltd. (United Kingdom); Patrick J. Flint, Gordon Dallas, Greg Meshew, John Trevethan, Galaxy Compound Semiconductors, Inc. (United States)

In this paper we describe the crystal growth and bulk characterisation of mono-crystalline InSb and GaSb substrates suitable for use in the epitaxial deposition of infrared detector structures. Results will be presented on the production of single crystal 4"-5" InSb and GaSb ingots grown by the Czochralski (Cz) technique. Bulk material quality will be assessed by defect recognition microscopy (DRM) and X-Ray Diffraction (XRD). Scaling challenges associated with the production of 6" InSb and GaSb will be discussed.

8631-58, Session 11

Mid-IR distributed-feedback interband cascade lasers (Invited Paper)

Chul S. Kim, U.S. Naval Research Lab. (United States); Mijin Kim, Sotera Defense Solutions, Inc. (United States); Joshua Abell, William W. Bewley, Charles D. Merritt, Chadwick L. Canedy, Igor Vurgaftman, Jerry R. Meyer, U.S. Naval Research Lab. (United States)

We demonstrate a significant improvement in the performance of distributed-feedback (DFB) interband cascade lasers (ICLs) operating

**Conference 8631:
Quantum Sensing and Nanophotonic Devices X**

in a single spectral mode in the range 3.7-3.8 μm . The first-order DFB grating was fabricated by depositing a high-index Ge layer on top of the relatively thin superlattice n-cladding and then patterning the Ge layer to expose the cladding. The top-cladding thickness was adjusted to provide sufficient coupling at the expense of additional loss from the overlap of the optical mode with the top metallization. Narrow ridges of 7.4 μm width were fabricated, covered with a 6- μm -thick electroplated Au layer, and mounted epitaxial-side-up. At $T = 45^\circ\text{C}$, lasing in a single mode was observed for periods between 519 and 534 nm. One DFB ridge with 534 nm pitch and high-reflection-coated (HR)/uncoated facets provided single-mode emission from 20°C to 75°C , with a maximum tuning range of 21.5 nm at the fixed current of 130 mA. The maximum tuning range with current at fixed temperature was 10 nm at 60°C . The side-mode suppression ratio was estimated to exceed 30 dB. The maximum single-mode output for a device with HR/anti-reflection (AR) coatings was 27 mW at 40°C , and it exceeded 1 mW at 80°C . The minimum power required to operate an HR/uncoated device at 20°C was 90 mW. We anticipate that similar performance characteristics should be attainable at wavelengths ranging from below 3 to at least 5.6 μm , considering that the lasing threshold depends only weakly on emission wavelength.

8631-59, Session 11

Low threshold interband cascade lasers
(Invited Paper)

Sven Höfling, Robert Weih, Adam Bauer, Alfred Forchel, Martin Kamp, Julius-Maximilians-Univ. Würzburg (Germany)

Interband Cascade lasers (ICLs) have proven to be very promising semiconductor heterostructure lasers to cover the spectral range between 3 to 5 μm and beyond. Compared to their intraband counterpart cascade lasers, the quantum cascade lasers, ICLs have attracted yet much less scientific and commercial attention, and many design aspects have not yet been completely optimized. Nevertheless, continuous wave operation at room temperature can be rather routinely obtained with ICL devices. We will report quantum-engineering approaches aiming either at the optimization of the ICL performance or on obtaining ICLs with certain tailored device properties. Based on the developed epitaxial material, single mode emitting devices operating in continuous wave mode at room temperature have been fabricated and their properties make them well suited for highly sensitive gas detection.

8631-60, Session 11

InAs-based dilute nitride materials and devices for the mid-infrared spectral range
(Invited Paper)

Anthony Krier, Martin de la Mare, Lancaster Univ. (United Kingdom); Qian Zhuang, Lancaster Univ (United Kingdom); Peter J. Carrington, Lancaster Univ. (United Kingdom); Amalia Patane, The Univ. of Nottingham (United Kingdom)

There is continuing interest in InAsN dilute nitride alloys for the development of optoelectronic devices operating in the technologically important (2-5 μm) mid-infrared spectral range. In this work we report on InAsN and InAsNSb alloys grown by MBE on InAs and GaAs substrates and LEDs containing ten InAsNSb quantum wells. By careful attention to growth conditions, device quality material can be obtained for N contents up to ~3% with band gap reduction which follows the band anti-crossing model. The onset of plastic deformation occurs when $N > 0.4\%$ and carrier mobility was observed to decrease with increasing N, although not as severely as in GaAsN. Photoluminescence and photoreflectance measurements show localization effects arising from compositional modulation, and the spin-orbit split-off energy (so) is seen to become larger than the bandgap (E_0) for $N > 0.5\%$ in these alloys. These effects combine to give improved temperature quenching behaviour as the N content increases.

We successfully fabricated the first InAsNSb/InAs dilute nitride mid-infrared LEDs which exhibit electroluminescence up to room temperature consistent with e-hh1 and e-lh1 transitions within type I quantum wells in good agreement with calculations. Comparison of the electroluminescence with that of type II InAsSb/InAs reveals more intense emission at low temperature and an improved temperature quenching up to T=200 K where thermally activated carrier leakage becomes important and further increase in the QW band offsets is needed.

8631-61, Session 11

Mid-infrared external cavity lasing through suppression of Fabry-Perot oscillation

Quamrul Huda, Univ. of Alberta (Canada); John Tulip, Boreal Laser, Inc. (Canada); Wolfgang Jaeger, Univ. of Alberta (Canada)

An external cavity lasing system at 2.4 μm involving an InGaAsSb Fabry-Pérot gain chip was developed and characterized. A Littrow configuration was used to achieve a tuning range of about 100 nm. Continuous, mode-hop free tuning was observed with variation of grating angle. Threshold current of the lasing chip varied from 100 mA down to 70 mA for lasing in Fabry-Pérot (FP) and external cavity (ECL) modes, respectively. Dependence of threshold current on the lasing wavelength was observed. A mathematical model was developed to explain the threshold current variations, and also to determine the gain profile of the active medium. The tuning range was found to depend on the semiconductor gain profile and also on the intensity of optical feedback through the collimation-dispersion system. Drifting of wavelength, as observed in intra cavity semiconductor lasers, was not observed for drive currents of up to 400 mA in regions close to the gain peak. Single mode ECL lasing could be sustained in this range at a significantly weaker optical feedback. Traces of FP lasing were, however, observed at currents in the range of 100-200 mA for wavelengths in the shoulder regions of the gain profile. In these cases, an increase of drive current resulted in mode hopping to multi-mode FP lasing. Our results confirm the competing nature of FP lasing with that of ECL mode of lasing. The onset of multi-mode FP lasing, and eventual hopping to these modes, were correlated with the gain profile, drive current, and the optical feedback.

8631-63,

Room temperature GaN-based spin polarized emitters
(Keynote Presentation)

A. G. Melton, The Univ. of North Carolina at Charlotte (United States); B. Kucukgok, UNC Charlotte (United States); Zhiqiang Liu, UNC (United States) and R&D Ctr. for Semiconductor Lighting (China); N. Dietz, Georgia State Univ. (United States); N. Lu, UNC Charlotte (United States); Ian T. Ferguson, The Univ. of North Carolina at Charlotte (United States)

Wide bandgap dilute magnetic semiconductors have recently been of interest due to theoretical predictions of room temperature ferromagnetism in these materials. In this work Ga_{1-x}Gd_xN thin films were grown by metalorganic chemical vapor deposition. These films were found to be ferromagnetic at room temperature and electrically conducting. However, it was only materials produced using TMHD₃Gd, which contains oxygen, that showed strong ferromagnetism; material grown using Cp₃Gd, which does not contain oxygen, did not show ferromagnetic behavior. Ga_{1-x}Gd_xN films grown with these two different metalorganic precursors are summarized. The first successful demonstration of Ga_{1-x}Gd_xN-based spin-polarized LED with 14.6% degree of polarization at 5000 Gauss is detailed.

**Conference 8631:
Quantum Sensing and Nanophotonic Devices X**

8631-64, Session 12

The Micro-OPO: an alternative for ultra-compact largely tuneable mid-infrared sources (*Invited Paper*)

Myriam Raybaut, Jean-Baptiste Dherbecourt, Jean-Michel Melkonian, A. Godard, Michel Lefebvre, ONERA (France); Emmanuel Rosencher, ONERA (France) and Ecole Polytechnique (France)

Optical parametric oscillators (OPO) are ideal coherent optical sources spanning the 3 to 12 μm range, which is of paramount importance for applications such as chemical lidar for the detection of green house gas pollutant (NO_x, CO_x,...). Until recently, OPOs were rather bulky devices with footprints in the m² (including the pump source) which precluded a large use of such devices. Important improvements occurred in recent years which lead to a drastic decrease of the footprint down to matchbox sizes. Among these improvements, we shall emphasize:

- periodically poled or oriented materials such as PPLN or OP-GaAs
- new phase matching scenarios such as Fresnel or cavity phase matching
- doubly resonant structures harnessing the Vernier effect.

We will describe how these devices are intrinsically single mode and display low threshold power. Moreover, recent developments of micro-cavity based OPOs will be also presented.

8631-65, Session 12

Fabrication and characterization of lateral polar GaN structures for second harmonic generation (*Invited Paper*)

Marc Hoffmann, North Carolina State Univ. (United States); Michael D. Gerhold, U.S. Army Research Office (United States); Ronny Kirste, Anthony Rice, Christer-Rajiv Akouala, North Carolina State Univ. (United States); Jinqiao Q Xie, HexaTech (United States); Seiji Mita, HexaTech, Inc. (United States); Ramon Collazo, Zlatko Sitar, North Carolina State Univ. (United States)

Lateral polar homo-structures (LPS) fabricated in Al_xGa_{1-x}N grown via MOCVD on sapphire, can be used as quasi phase matching structures for second harmonic (SH) generation to realize efficient, coherent UV light sources. These structures are obtained by a periodic inversion of the nitride to change the sign of the non-linear optical coefficient. We fabricated high quality GaN and AlN thin films having 5-50 μm wide stripes of Ga- and N-polar domains. A flat surface, with steps lower than one quarter wavelength, is critical to avoid scattering. Typically, a growth rate difference can be observed when simultaneously growing Ga- and N-polar domains adjacent to each other as in a LPS, with a higher growth rate observed for the Ga-polar domains. The structures are defined by using reactive-ion etching of an AlN nucleation layer to achieve polarity control. The etching of the AlN nucleation layer has no significant effect on the nucleation of the material. Also, individually grown Ga- and N-polar films do not indicate any intrinsic growth rate difference, suggesting a mass transport limited growth. Nevertheless, growth of the LPS depends on the Ga-supersaturation during growth. Controlling the supersaturation leads from a Ga- to N-polar dominated growth, with an optimum condition to obtain a flat surface also for AlN LPS. Therefore, the material transport from one domain to the other is connected with supersaturation. Following this, we were able to fabricate alternately poled waveguides, which were characterized optically for refractive index and conversion efficiency.

8631-66, Session 12

Non-linear frequency mixing in THz quantum cascade lasers (*Invited Paper*)

Carlo Sirtori, Univ. Paris 7-Denis Diderot (France); Pierrick Cavalié, Julien Madeo, Jerome Tignon, Sukhdeep S. Dhillon, Ecole Normale Supérieure (France)

Non-linear processes in semiconductor optoelectronic devices are excellent candidates to perform all-optical frequency shifting, a process that mixes two electromagnetic fields oscillating at different frequencies. Non-linear frequency mixing of a near-infrared probe in presence of a terahertz (THz) beam provided by a free electron laser systems has been previously demonstrated using enhanced resonant nonlinearities of quantum wells. In this work, we demonstrate intracavity frequency mixing using the resonant and non-resonant nonlinearities of a THz quantum cascade (QC) laser.

Both nonlinearities are provided by the GaAs crystal. The non-resonant nonlinear susceptibility arises from the zincblende asymmetry and has been tested using telecom wavelengths at 1.3 and 1.5 μm . When the frequencies of the injected photons approach the gap energy, thus using approximately 0.8 μm wavelength, the resonance with the transitions across the gap increases enormously the nonlinear susceptibility and the conversion efficiency gets as high as 0.2% and is limited by the linear absorption of the pump. In this case the no phase-matching is needed, as the conversion occurs within a coherence length.

These processes can be of interest to precisely shift near infrared lasers, particularly for telecom routing. Moreover, they can also be applied, in principle, to mid-infrared QC lasers which are today a very robust technology operating room temperature with watt level power.

8631-67, Session 12

Mid-wave infrared and terahertz quantum cascade lasers based on resonant nonlinear frequency mixing (*Invited Paper*)

Augustinas Vizbaras, Brolis Semiconductors, Inc. (Lithuania); Karun Vijayraghavan, The Univ. of Texas at Austin (United States); Frederic Demmerle, Walter Schottky Institut (Germany); Min Jang, The Univ. of Texas at Austin (United States); Gerhard Boehm, Ralf Meyer, Walter Schottky Institut (Germany); Mikhail A. Belkin, The Univ. of Texas at Austin (United States); Markus C. Amann, Walter Schottky Institut (Germany)

GaInAs/AlInAs/InP quantum cascade lasers (QCLs) have established themselves as most reliable and versatile semiconductor laser sources in the mid-infrared wavelength region. Due to the presence of unique molecular absorption lines, in combination of water-free atmospheric transmission windows, this spectral range is of particular importance for applications in the fields of sensing, medical, material processing and homeland security. Being compact, electrically pumped and able to operate at room-temperature, QCLs are ideal choice for wavelengths between 3.5 – 12 microns. However, wavelengths above and below are more challenging to obtain.

In our work, we use intracavity nonlinear frequency mixing in mid-infrared QCLs to extend the spectral coverage for GaInAs/AlInAs/InP devices. We demonstrate that passive nonlinear structures, consisting of coupled quantum wells can be grown on top of the mid-IR QCL active region. Such nonlinear structures can be designed to possess a resonant nonlinear response for the pump frequency. Such concept, in combination with quasi-phase-matching technique can be used for efficient short-wavelength lasing by second-harmonic generations. We demonstrated room-temperature lasing down to 2.6 micrometer. For long-wavelengths, particularly THz frequencies, a novel waveguide concept was introduced. Here, we used a leaky THz waveguide concept, for a difference-frequency generation device. Phase matching was

**Conference 8631:
Quantum Sensing and Nanophotonic Devices X**

achieved by Cherenkov phase-matching scheme. This concept led to ultra-broadband THz emission at room-temperature (1.2-4.5 THz) with pulsed output powers as high as 14 μ W.

8631-68, Session 12

Recent developments in high-power two-wavelength vertical external-cavity surface-emitting lasers *(Invited Paper)*

Mahmoud Fallahi, Chris Hessenius, Michal Lukowski, College of Optical Sciences, The Univ. of Arizona (United States)

Vertical external-cavity surface-emitting lasers (VECSEL) have proven to be a reliable source for multi-watts high-brightness emission in a wide range of fundamental operating wavelengths from \sim 700nm to over \gg m. Large area optical-pumping has allowed high-brightness cw output powers in the tens of watts without compromising on beam quality. Access to the intra-cavity's high circulating power has allowed efficient watt-level generation of blue-green and yellow by second harmonic generation. Long-wavelengths generation is similarly achievable by difference frequency generation (DFG). Efficient long-wavelength difference frequency generation requires high intracavity power with two stable wavelengths having desired separation. In this talk I will first present some of the recent developments in intra-cavity nonlinear wavelengths generation. I will then present our new approach based on T-cavity two-chip VECSEL configuration for tunable two-wavelength generation. Our first experimental results show two-wavelength generation with separation tuning of over 17nm and total output power of 12W. The latest results on multi-watts two-wavelength emission with orthogonal polarization will be discussed. Our approach is particularly suitable for tunable type-II nonlinear conversion for new wavelengths generation.

8631-36, Session 13

Near-field investigations of active plasmonic devices *(Invited Paper)*

Yannick De Wilde, Institut Langevin (France)

Near-field scanning optical microscopy can be used to map the optical contrast between different nanomaterials, or to image the near-field distribution due to purely evanescent fields confined at the surface of devices or waveguides. We have developed a mid-infrared NSOM which allows one to probe the near-field at the surface of quantum cascade lasers while they are in operation. These devices have been used for the electrical generation of surface plasmon polaritons (SPPs). We will describe the near-field characterization of various types of such generators of SPPs, and show how surface patterning of the metallic waveguides enables one to enhance dramatically the spatial confinement of the SPPs. We will also discuss the extension of these kinds of studies to SPPs generators operating at the telecom wavelengths using laser diodes, and discuss the possibility to use NSOM to probe the local density of electromagnetic modes (EM-LDOS) on various plasmonic systems.

Our research on active plasmonic devices based on semi-conductor lasers is the result of a close collaboration with R. Colombelli, A. Bousseksou, D. Costantini, G. Xu, from Institut d'Electronique Fondamentale for device fabrication, modelling and far-field characterization, and with L. Greusard, A. Babuty, R. Rungsaawang, I. Moldovan-Doyen, F. Peragut from Institut Langevin for near-field characterization. Near-field thermal emission studies of the EM-LDOS in the mid-infrared have been performed in collaboration with K. Joulain (Institut P²), J.-J. Greffet (Laboratoire Charles Fabry-IOGS), P.-O. Chapuis (Centre de thermique de Lyon) for theoretical modelling, and A. Babuty for experiments. The near-field investigations of the EM-LDOS at shorter wavelength are the result of a collaboration with V. Krachmalnicoff, E. Castanié, D. Cao, A. Cazé, R. Pierrat, and R. Carminati, from Institut Langevin.

8631-69, Session 13

Emission in patch plasmonic nano-antennas *(Invited Paper)*

Agnes Maitre, Cherif Belacel, Univ. Pierre et Marie Curie (France); Benjamin Habert, Florian Bigourdan, François Marquier, Jean-Paul Hugonin, Institut d'Optique Graduate School (France); Xavier Lafosse, Lab. de Photonique et de Nanostructures, CNRS (France); Laurent Coolen, Catherine Schwob, Univ. Pierre et Marie Curie (France); Clementine Javaux, Benoit Dubertret, Ecole Supérieure de Physique et de Chimie Industrielles (France); Jean-Jacques Greffet, Institut d'Optique Graduate School (France); Pascale Senellart, Lab. de Photonique et de Nanostructures, CNRS (France)

Plasmonic nano-antennas provide broadband spontaneous emission control by confining light on highly sub-wavelength volumes. This property is promising to fabricate efficient single photon sources with spectrally broad emitters like defects in diamonds or colloidal quantum dots. Although spontaneous emission acceleration ensuring large coupling to the mode has been evidenced in antennas, this property has not been combined with high emission directionality.

Here, we control both the spontaneous emission rate and radiation pattern of nanocrystals in a plasmonic antenna. We use a patch antenna, consisting in a thin gold microdisk 30 nm above a thick gold layer. The small 30 nm separation between the disk and the gold film provide a large confinement of the electromagnetic field. The emitters are clusters of colloidal nanocrystals which are located inside the dielectric layer. A deterministic positioning of each antenna on an emitter is provided by an optical in situ lithography technique for quantum dots in micropillars. The emitters are shown to radiate through the entire patch antenna in a highly directional mode. The average cluster lifetime is reduced by a factor ranging from 5 to 15, which is consistent with an acceleration of spontaneous emission by a factor 70 for dipoles perpendicular to the layers. These measurements are in good agreement with our theoretical calculations. Our work demonstrates the potential of plasmonic patch antennas to fabricate efficient single photon sources.

8631-70, Session 13

Micro- and nano-fabrication of metamaterial and plasmonic structures by laser processing *(Invited Paper)*

Alberto Piqué, Nicholas A. Charipar, Matthew A. Kirleis, Kristin M. Metkus, Heungsoo Kim, Ray C. Y. Auyeung, Scott A. Mathews, U.S. Naval Research Lab. (United States)

Non-lithographic processes are ideally suited for the fabrication of arbitrary periodic and aperiodic structures needed to implement many of the metamaterial and plasmonic designs being proposed. Of the numerous non-lithographic techniques currently in use, laser-based processes offer numerous advantages since they can be applied to virtually any material over a wide range of scales. Furthermore, laser direct-write techniques are true enablers for the development of novel designs such as conformal plasmonic structures or graded metamaterial constructs. This presentation will show examples of metamaterial and plasmonic structures developed at the Naval Research Lab using laser direct-write processes, and discuss the benefits of laser processing for these applications.

8631-71, Session 13

nanophotonic cavity enhanced IR photodetectors (*Invited Paper*)

Roch Espiau de Lamaestre, Daivid Fowler, Salim Boutami, Matthieu Duperron, Jérôme Le Perchec, Giacomo Badano, François Boulard, Olivier Gravrand, Gerard Destefanis, CEA-LETI-Minatec (France)

By promoting the control of photons at the subwavelength scale, the emergence of nanophotonics has triggered the development of infrared photodetectors with enhanced performances and functionalities, such as higher operating temperatures or hyperspectral imaging. The use of photonic cavities has proven very useful to achieve these goals. Their enhanced electromagnetic field together with spatial localization of light allows a decrease of the active region size, hence the dark current, while preserving significant quantum efficiency. Moreover these features naturally come along with a spectral signature that can be useful for monitoring thermal or chemical contrasts.

Starting from the well-known concepts of resonant cavity enhanced photodetectors, where the cavity effect is generated by some multi-layered stack comprising the active semiconductor, we will discuss the interest in going to the subwavelength scale, and the way to achieve high confinement using nanostructured metals. We will emphasize here the required compromise between the desirable confinement and the ubiquitous use of electrical passivation layers, by discussing two distinctive kinds of nanophotonic cavities. Firstly, plasmonic TM modes such as the ones supported by MSM structures [J. Le Perchec et al, Appl. Phys. Lett.94, 181104 (2009)] will be shown to provide an unmatched level of confinement. Then, we will introduce a new nanophotonic TE cavity design [D. Fowler et al, submitted to Appl. Phys. Lett.] where a similar electromagnetic confinement level is observed, but with the advantage of a minimal electric field at the metal-semiconductor interfaces.

8631-72, Session 13

GaSb-based all-semiconductor mid-IR plasmonics (*Invited Paper*)

Thierry Taliercio, Vilianne Ntsame Guilengui, Laurent Cerutti, Jean-Baptiste Rodriguez, Eric Tournié, Univ. Montpellier 2 (France)

Surface plasmon polaritons, generated at the interface between a metal and a dielectric, present actually a great interest because of their potential applications in the fields of metamaterial or metasurfaces, enhanced photonic devices properties, nanophotonics integrated circuits and nano-bio-photonics. All these applications rely on the use of gold resonators. Because of the need to integrate plasmonic functionalities to semiconductor devices and to keep high field exaltation at the metal/dielectric interface for mid-IR applications, it is really attractive to use highly doped semiconductors. By changing the doping level of the semiconductor, it is possible to adjust its plasma frequency to reach the Mid-IR range and to control the magnitude of its permittivity for a better control of the local electromagnetic field. We propose experimental study of strip arrays of doped and encapsulated in undoped semiconductors. The samples consist of a layer of 50 or 100 nm of lattice-matched InAsSb (Si at 10^{20} cm^{-3}) grown by Molecular Beam Epitaxy (MBE) on a GaSb substrate. InAsSb arrays are realized by holography and wet and/or dry etching. The typical grating period is 540 nm and the width of InAsSb ribbon varies from 90 to 210 nm. The encapsulating layer of GaSb is performed by MBE on the InAsSb grating. Reflectance experiments realized by varying the angle of the incident light and its polarization allowed identifying localized surface plasmon (LSP). By changing the doping level, we adjust the plasma frequency and by adjusting the geometry of the lamellar arrays, we modify the resonances of the LSP.

8631-74, Session 14

Infrared spectral filters based on guided-mode resonance with subwavelength structures (*Invited Paper*)

Emilie Sakat, Grégory Vincent, ONERA (France); Petru Ghenuche, Nathalie Bardou, Stéphane Collin, Fabrice Pardo, Jean-Luc Pelouard, Lab. de Photonique et de Nanostructures (France); Riad Haïdar, ONERA (France)

We present an experimental and theoretical study of bandpass filters based on guided mode resonances in metal-dielectric structures. The devices consist of subwavelength gold gratings deposited on a free-standing silicon nitride layer (SiN_x) that behaves as a waveguide. The eigenmodes of the waveguiding layer are excited by the grating diffracted waves.

We fabricated such structures for a demonstration in the infrared with 1D or 2D gratings (square or rectangular patterns). These filters exhibit a high efficiency: the experimental transmission peak reaches ~ 79% in either case, which represents an eight-fold enhancement of the geometrical transmission. Highly resolved spectral and angular transmission measurements reveal Fano-type resonances, and show that the angular sensitivity of the structures strongly depends on the rotation axis of the sample. We explain this particular behavior with an analytical model based on the guided mode resonance mechanism. It highlights also the similarities between 2D and crossed-1D structures.

A variety of filters is obtained: polarizing filters with 1D grating, polarization independent filters with 2D square patterns gratings and tunable filters when used in combination with a polarizer for 2D rectangular patterns. Transmission peak and FWHM (Full Width at Half Maximum) can be tuned by simply changing the grating period and the slits size. The high flexibility of polarization and spectral behaviors allows adapting these filters to various applications such as sensing, dense wavelength division multiplexing networks or multispectral imaging.

[1] E. Sakat et al., Opt. Lett., 36, 3054-3056, (2011)

[2] E. Sakat et al., Opt. Express, 20, 13082-13090, (2012)

8631-75, Session 14

Ultrastrong optical modulation in waveguides by conducting interfaces

Farhad Karimi, Sharif Univ. of Technology (Iran, Islamic Republic of); Sina Khorasani, Georgia Institute of Technology (United States)

In this paper, we perform an in-depth study of a novel electro-optic phenomenon suggested earlier by the authors [J Opt A 3(5) 380] in optical waveguides. We show that it is possible to achieve a very strong optical modulation effect in slab waveguides fabricated on the standard III-V InAlGaAs compound platform. The electro-optic effect is obtained by controlling the density and population of the electron and hole states in the well layer. The additional phase shift contributed to the reflection phase of the guided electromagnetic wave constitutes an ultrastrong source of optical modulation and phase control.

First, we present the design of the Quantum Well based on InAlGaAs alloys, with the primary transition energy of 799meV, corresponding to the communication wavelength of 1.55 microns. By exploiting the envelope function approximation, we derive the wavefunction of electrons and holes, their eigen-energies, and the dipole moment of electron-hole transitions. For finding the wavefunction of holes and their eigen-energies, we use the Luttinger Hamiltonian. Next, we calculated the electrical susceptibility of a three level quantum system (as a model for Quantum Well), by using optical Bloch equations. We obtain the phenomenological optical Bloch equations, which explain the spontaneous emissions and atomic collisions. We notice the interaction of a guided electromagnetic field with the Two-Dimensional Electron Gas (2DEG) formed in the Quantum Well, which its quantum mechanical

**Conference 8631:
Quantum Sensing and Nanophotonic Devices X**

Optical Conductivity is here also found. The optical conductivity of 2DEG can be controlled by controlling the populations of electrons and hole energy levels. At last, we design a slab waveguide in which a guided wave with the wavelength of 1.55 micron experiences a strong interaction with the designed 2DEG. We calculate the propagation constant of the wave in the waveguide with conducting interfaces, by exploiting the Modified Transfer Matrix Method, and show that the changes in the propagation constant of the wave and the conductivity of the 2DEG have a fairly linear relationship.

Finally, we estimate that a Mach-Zehnder configuration based on this optical modulator, will have a very compact size of around 50 microns (to be compared with the millimeter sizes in comparable devices).

8631-76, Session 14

Fabrication of high-quality large-area plasmonic oligomers by angle-controlled colloidal nanolithography

Jun Zhao, Univ. Stuttgart (Germany); Sven Burger, Konrad-Zuse-Zentrum für Informationstechnik Berlin (Germany); Bettina Frank, Harald Giessen, Univ. Stuttgart (Germany)

Plasmonic structures with a structure size of around 100 nm are tremendously important for applications in the visible and near-IR range. Surface-enhanced Raman scattering substrates, localized surface plasmon resonance sensors, narrow resonances using plasmonic induced transparency, and local field concentration in oligomers to create hot spots are among those applications.

Key issues in the design and manufacturing of such structures are small gaps in the range of sub-20 nm, sharp edges, and narrow resonances. For applications, large fabrication areas in the range of cm² and low manufacturing costs are crucial. Electron beam lithography is common in research labs, however, the high cost, its low yield, and problems with lift-off in structures in the sub-20 nm range call for reliable alternatives.

Here, we present a method that fulfils these requirements. Utilizing shadow angle lithography with a polar and azimuthal rotation axis [1] and shutter control together with monolayers of polystyrene spheres we create reproducibly homogeneous structures in the 50 nm range with 10 nm gaps over areas of cm².

We fabricated monomers, dimers, trimers, quadrumers, and pentamers with 100 nm nanospheres and measured their transmittance spectra by FTIR microscopy. The spectra show well modulated resonances which depend sensitively on the incident polarization. We can attribute the various collective modes to the different features of the spectra and observe even hybridization effects. This confirms the high quality of our fabrication method.

Further directions of this manufacturing method include different metals, stacking, and large area biosensors.

8631-103, Session 14

Nanostructured photonic and plasmonic materials for enhanced resonant light absorption (Invited Paper)

Koray Aydin, Northwestern Univ. (United States)

No Abstract Available

8631-73, Session 15

Transport properties related to spin-orbit interaction (Invited Paper)

Henri-Jean Drouhin, Ecole Polytechnique (France); Federico Bottegoni, Ecole Polytechnique (France) and Politecnico di Milano (Italy); Alberto Ferrari, Politecnico di Milano (Italy); Hoai T. Nguyen, Vietnamese Academy of Science and Technology (Viet Nam); Jean-Eric Wegrowe, Ecole Polytechnique (France); Guy Fishman, Univ. Paris-Sud 11 (France)

The notions of probability current and of spin current play central roles when dealing with transport properties. The notion of spin current is known to be complicated due to the existence of source terms. However, even the notion of probability current raise a number of questions in systems described by an effective Hamiltonian which contains cubic or higher order momentum terms. In previous papers, we have shown that including spin-orbit interaction induces drastic changes in the properties of the related current operators and implies revisiting the boundary conditions satisfied by the wave functions.[1-5] We have given a systematic construction of the probability-current operator J , based on an effective Hamiltonian written as a p-power series expansion and we have proposed an extension of the envelope function technique to comply with current conservation. We have put into light the simple structure of the extra terms. In the present paper, we relate these new current operators to several transport currents involving charge, spin, and angular momentum. We discuss transport properties of model systems in this context and we connect the results to phenomenological thermokinetics descriptions. This provides practical tools which are valuable for spin engineering of heterostructures.

[1] S. Richard, H.-J. Drouhin, N. Rougemaille, and G. Fishman, J. Appl. Phys. 97, 083706 (2005).

[2] T. L. Hoai Nguyen, H.-J. Drouhin, J.-E. Wegrowe, and G. Fishman, Phys. Rev. B 79, 165204 (2009).

[3] H.-J. Drouhin, G. Fishman, and J.-E. Wegrowe, Phys. Rev. B 83, 113307 (2011).

[4] F. Bottegoni, H.-J. Drouhin, G. Fishman, and J.-E. Wegrowe, J. Appl. Phys. 111, 07C305 (2012).

[5] F. Bottegoni, H.-J. Drouhin, G. Fishman, and J.-E. Wegrowe, Phys. Rev. B 85, 235313 (2012).

8631-78, Session 15

Structural and optical properties of (In,Ga)As/GaP quantum dots and (GaAsPN/GaPN) diluted-nitride nanolayers coherently grown onto GaP and Si substrates for photonics and photovoltaics applications (Invited Paper)

Olivier Durand, Cédric Robert, Institut National des Sciences Appliquées de Rennes (France); Tra Nguyen Thanh, Samy Almosni, Institut National des Sciences Appliquées de Rennes (France); Thomas Quinci, Institut National des Sciences Appliquées de Rennes (France) and Institut National de l'Énergie Solaire (France); Jitesh Kuyyalil, Institut National des Sciences Appliquées de Rennes (France); Charles Cornet, Antoine Létoublon, Institut National des Sciences Appliquées de Rennes (France); Christophe Levallois, Jean-Marc Jancu, Jacky Even, Laurent Pédesseau, Mathieu Perrin, Institut National des Sciences Appliquées de Rennes (France); Nicolas Bertru, Institut National des Sciences Appliquées de Rennes (France); A. Sakri, Institut National des Sciences Appliquées de Rennes (France); Nathalie Boudet, G2Elab (France); Anne Ponchet, Ctr. d'Elaboration de Matériaux et d'Etudes Structurales

**Conference 8631:
Quantum Sensing and Nanophotonic Devices X**

(France); P. Rale, Ecole Nationale Supérieure de Chimie de Paris (France); Laurent Lombez, Jean-Francois Guillemoles, Institut de Recherche et Développement sur l'Energie Photovoltaïque (France); Xavier Marie, Institut National des Sciences Appliquées de Toulouse (France); A. Balocchi, Univ. de Toulouse (France); P. Turban, Sylvain Tricot, Institut de Physique de Rennes (France); Mircea Modreanu, Tyndall National Institute-University College Cork, Lee Maltings, Prospect Row (Ireland); Slimane Loualiche, Institut National des Sciences Appliquées de Rennes (France); Alain Le Corre, Institut National des Sciences Appliquées de Rennes (France)

Lattice-matched GaP-based nanostructures grown on silicon substrates is a highly rewarded route for coherent integration of photonics and high-efficiency photovoltaic devices onto silicon substrates. We report on the structural, optical and electronic properties of selected MBE-grown nanostructures on both GaP substrates and GaP/Si pseudo-substrates. As a first stumbling block, the GaP/Si interface growth has been optimised thanks to a complementary set of thorough structural analyses. Photoluminescence and time-resolved photoluminescence studies of self-assembled (In,Ga)As quantum dots grown on GaP substrate demonstrate a proximity of two different types of optical transitions interpreted as a competition between conduction band states in X and Γ valleys. Structural properties and optical studies of GaAsP(N)/GaP(N) quantum wells coherently grown on GaP substrates and GaP/Si pseudo substrates are reported. Our results are found to be suitable for light emission applications in the datacom segment. Then, possible routes are drawn for larger wavelengths applications, in order to address the chip-to-chip and within-a-chip optical interconnects and the optical telecom segments. Finally, results on GaAsPN/GaP heterostructures and diodes, suitable for PV applications are reported.

8631-79, Session 15

Short-wave infrared colloidal quantum dot photodetectors on silicon

Chen Hu, Alban A. Gassenq, Yolanda Justo, Univ. Gent (Belgium); Sergii Yakunin, Wolfgang Heiss, Johannes Kepler Univ. Linz (Austria); Zeger Hens, Gunther Roelkens, Univ. Gent (Belgium)

Many molecules that we want to detect in our environment have bands of absorption lines in the short-wave infrared (SWIR). Traditional high-sensitivity photodetectors used in these spectroscopic systems are discrete components based on quantum-confined epitaxial materials. Solution-processed colloidal quantum dots offer an alternative way to realize this functionality, either as discrete components or integrated on photonic integrated circuits. The wavelength range of operation can easily be modified through size tuning of the quantum dots. Meanwhile, a cost-effective material synthesis and deposition technique can lead to their wide deployment.

In this paper, both PbS and HgTe colloidal quantum dots are explored for SWIR photodetectors. The colloidal dots are synthesized in solution, with organic ligands around the dots keeping them stable in solution. However, to achieve efficient carrier transport between the dots in a film, these long organic ligands are replaced by shorter, inorganic ligands. In this paper we report uniform, ultra-smooth colloidal QD films without cracks realized by dip-coating and corresponding ligand exchange on a silicon substrate. Metal-free inorganic ligands, such as OH⁻ and S²⁻, are investigated to facilitate the charge carrier transport. Both PbS and HgTe-based quantum dot photoconductors were fabricated on interdigitated gold electrodes. For PbS-based detectors a responsivity of 200A/W is measured at 1.5 μ m, due to the large internal photoconductive gain. The cut-off wavelength of these devices is at 2.2 μ m. HgTe quantum dot photodetectors with a cut-off wavelength of 2.8 μ m were also obtained. The realization of these devices on silicon photonic integrated circuits will also be discussed.

8631-80, Session 15

Optoelectronic properties of hexagonal boron nitride epilayers (Invited Paper)

X. K. Cao, Texas Tech Unive. (United States); S. Majety, J. Li, Jingyu Lin, Hongxing Jiang, Texas Tech Univ. (United States)

Hexagonal boron nitride (hBN) possesses extraordinary physical properties including high temperature stability, dielectric strength, optical absorption, negative electron affinity, neutron capture cross section and corrosion resistance. Its energy band gap is comparable to AlN (6 eV). Moreover, hBN is a material with a very low dielectric constant, but having a very high dielectric strength. Due to its layered structure and similar lattice constants to graphene, hBN is also highly suitable for use as a template in graphene electronics and as a gate dielectric layer and provides an ideal platform to study fundamental properties of layer-structured materials. Hexagonal BN epilayers have been synthesized by metal organic chemical vapor deposition and their band-edge photoluminescence (PL) properties, dielectric strength, optical absorption, and potential as a deep UV (DUV) emitter and detector material have been studied. These MOCVD grown epilayers exhibit highly efficient band-edge PL emission lines centered at around 5.5 eV at room temperature. The results represent a remarkable improvement over the optical qualities of hBN films synthesized by different methods in the past. It was observed that the emission of hBN is more than two orders of magnitude higher than that of high quality AlN epilayers. Polarization-resolved PL spectroscopy revealed that hBN epilayers are predominantly a surface emission material, in which the band-edge emission with electric field perpendicular to the c-axis is about 1.7 times stronger than the component along the c-axis. This is in contrast to AlN, in which the band-edge emission is known to be polarized along the c-axis. Based on the graphene optical absorption concept, the estimated band-edge absorption coefficient of hBN is about 7×10^5 /cm, which is more than 3 times higher than the value for wurtzite AlN (2×10^5 /cm). The dielectric strength of hBN epilayers exceeds that of AlN and is greater than 4.4 MV/cm based on the measured result for an hBN epilayer released from the host sapphire substrate. The hBN epilayer based DUV detectors exhibit a sharp cut-off wavelength around 230 nm, which coincides with the band-edge PL emission peak and virtually no responses in the long wavelengths. Mg doped hBN epilayers grown on insulating AlN templates were p-type with an in-plane resistivity of about 2.3 Ω cm. Diode behavior in the p-n structures of p-hBN/n-AlxGa1-xN (x=0.62) has been demonstrated. These results represent a major step towards the realization of hBN based practical devices.

8631-94, Session 15

Thermal conductivity tensor of semiconductor layers using two-wire 3-omega method

Chuanle Zhou, Northwestern Univ. (United States); Gregor Koblmüller, Max Bichler, Gerhard Abstreiter, Walter Schottky Institut (Germany); Matthew Grayson, Northwestern Univ. (United States)

Superlattice materials have extensive applications in infrared devices, such as type II InAs/GaSb superlattice (T2SL) for long wavelength (LWIR) and midwave (MWIR) infrared frequency detectors and InAs/GaSb type-II W superlattice (WSL) for high-power interband cascade lasers and long-wavelength infrared photodiodes. These devices perform best at low temperatures or room temperature, and the performance tends to degrade rapidly with increasing temperature. So it is important to know thermal conductivity of the active region and cladding layer which determines the temperature distribution in the optical devices.

The 3-omega method is widely used for thermal conductivity measurements in such nanostructured materials. This method [Cahill, Rev. Sci. Instrum. 61 (2), 802 (1990)] uses a metal stripe deposited on top of the thin film serving as both heater and thermometer. For the out-of-plane thermal conductivity measurement, the stripe is much

**Conference 8631:
Quantum Sensing and Nanophotonic Devices X**

wider than the thin film thickness so the heat flow is mostly vertical. On the other hand, for the in-plane thermal conductivity measurement [T. Borca-Tasciuc, G. Chen, Rev. Sci. Instrum. 72, 2139 (2001)], a stripe of width less than the thin film thickness is deposited, so the heat flow has a significant in-plane component. By comparing the temperature difference induced by the wider stripe and the thinner stripe, one can calculate the out-of-plane and in-plane thermal conductivity ratio. We report our measurement of the in-plane and the out-of-plane thermal conductivity tested in AlGaAs/GaAs SLs and discuss preliminary data in the InAs/GaSb type-II W SL, both active and cladding layers.

8631-90, Session PWed

Investigation of temperature dependence on heterojunction bipolar light-emitting transistors embedded InGaAs/GaAs quantum wells

Tzu-hsuan Huang, Heng-Jui Chang, Kuo-Min Huang, Shao-Yen Chiu, Yueh-Lin Lee, National Tsing Hua Univ. (Taiwan); Wei-Jiun Hong, National Tsing Hua University (Taiwan); Chong-Long Ho, Meng-Chyi Wu, National Tsing Hua Univ. (Taiwan)

A analytical study of the temperature dependence of current gain and Ideality factor in InGaAs/GaAs quantum well (QW) heterojunction bipolar light emitting transistors (HBLT's). In order to utilize the radiative recombination, the structure of HBT embedded two quantum wells in the base region which can improve the radiation efficiency. Compare with the convention HBT, the temperature dependence of current gain increases 42.5% with increasing temperature from 350K followed by a decrease towards 300K in InGaAs/GaAs quantum well HBLT's. Variation of gain with temperature is very different than what is normally seen in HBT adding another advantage in favor of the HBLT. The base-current ideality factor for the two studied device is close, revealing that the space-charge recombination dominates the overall base current. On the other hand, the high output power is 962 mW at 88 mA on passivation of HBLT. It is that can be as significant as that of electronic integration.

8631-91, Session PWed

Nanostructured enhanced chemical sensing surfaces for mid-IR molecular absorption

Andrea Dunbar, Ctr. Suisse d'Electronique et de Microtechnique SA (Switzerland); Edward Threlfall, Photon Design (United Kingdom); Rolf Eckert, Ctr. Suisse d'Electronique et de Microtechnique SA (Switzerland); Silvia Angeloni, CSEM SA (Switzerland); Ross P. Stanley, Ctr. Suisse d'Electronique et de Microtechnique SA (Switzerland)

Chemical sensing using nanostructured metallic surfaces at mid-IR wavelengths have the advantage that metal losses are lower than in the visible and that infra-red wavelengths allow detection in the the fingerprint region of molecules removing the need for markers. Although a substantial body of work exists on surface enhanced infrared spectroscopy and plasmonic enhanced infrared spectroscopy this work has not yet made an impact in industry. The main problems are reproducibility, reliability and quantitative enhancements. To overcome these, it is necessary to understand and control the enhancement effects. Several sources of enhancement are possible with structured or roughened surfaces: increased number of molecules due to increased surface area, improved overlap between the molecule and the optical field, and concentration of the field. It remains a challenge to show systematic and comparative quantitative data.

Here we present work analysing the absorption of monolayers of thiols and of perfluorooctyltrichlorosilane (FOTS). FOTS is deposited using molecular vapour deposition and deposits as a conformal monolayer; it is often used as an anti-stiction layer. We investigate the effect of distance

to the surface, roughness which increases the surface area and gives rise to SEIRA and plasmonic enhanced detection. We show that to obtain reproducible, quantitative data of the enhancements is non-trivial, and that there remain great challenges to move the potential enhancements to a commercial domain.

8631-92, Session PWed

The response properties of NbN superconductor nanowire for multi-photon

Lin Kang, Yu Zhou, Labao Zhang, Pei-Heng Wu, Nanjing Univ. (China)

This paper studies the response properties of NbN superconductor nanowire for multi-photon in with superconductor single photon detectors (SSPD). We have measured the NbN nanowire device's DC characteristics and detection probability for single and multi-photon light pulse signal under at the temperature of 3.5 K in experiments. The measured results shown that the superconducting transition current of superconductor nanowire will decrease as the light irradiation intensity increase. The photon number detected by SSPD was derived from the slope of detection probability versus the light intensity. We found that the detected photon number was increased when the superconducting nanowire bias current was reduced. Moreover, based on quantum optics and hotspot theory, we analyzed the mechanism of the multi-photon response of superconducting nanowire semi-quantitatively. This result may be benefit for understanding of SSPD and developing the SSPD with the capability of resolving photon number.

8631-96, Session PWed

High-speed InGaAs/InP single-photon avalanche photodiode with tunable gating frequency

Yixin Zhang, Xuping Zhang, Shun Wang, Nanjing Univ. (China)

Single photon detection is the key technique for applications that require measurements of extremely weak optical signal. InGaAs/InP single photon avalanche photodiode (SPAD) is the most practical device for single photon detection at telecommunication wavelength since it is compact, non-cryogenic and of low energy consumption. Nowadays, most high speed SPAD works under gated Geiger mode. Although this method can reduce the dark count and afterpulse probabilities, strong spike noise is generated due to charging and discharging on the junction capacitance of SPAD. The spike may bury these weak avalanche pulses which will decrease the detection efficiency. Traditionally, complex electronics components are needed to suppress the spike. The gating frequency is basically fixed after the electronic components are settled. In this paper, we proposed a high speed SPAD at 1.5 μm that enables the user to freely tune the gating frequency within a designated range. Our design features a spike-cancellation circuit which generates cancellation signal from direct digital synthesizer (DDS). Mean suppression ratio of 50dB can be achieved automatically over the whole tunable frequency range. All the components can be integrated within a package of 15cm²15cm²6cm which is quite suitable for in-field application. The compact and flexible of the proposed technique has been experimental demonstrated and proved. At 253K, detection efficiency of 13% is obtained with 1.5⁻¹-5 per gate dark count probability and 3% afterpulse probability for 250MHz gating frequency.

**Conference 8631:
Quantum Sensing and Nanophotonic Devices X**

8631-77,

Advanced PV technologies: challenges and opportunities (*Keynote Presentation*)

Devendra K. Sadana, IBM Thomas J. Watson Research Ctr. (United States)

The PV industry can be divided into four main categories: (i) crystalline Si (multi and single crystal), (ii) thin film (a-Si:H, CdTe, CIGS, and CZTS), (iii) CPV and (iv) space. The latter two categories utilize high efficiency multi-junction III-V solar cells. There is intense competition among the first three types of PV industry to demonstrate lowest cost solution and achieve grid parity. The target cost to achieve grid parity per DOE's Sunshot initiative is \$1/W by 2017 for a fully installed system without any subsidies. Meeting such an aggressive cost target requires innovations at every aspect of the PV system including module, inverter, BOS, and installation.

This presentation will first give a high level overview of various PV technologies and will then focus on innovative approaches to enhance cell efficiency while reducing the material cost. The breakthrough spalling technique which allows controlled release of Si, Ge, and III-V films from a brittle substrate (semiconductor or non-semiconductor) will be discussed. The application of spalling in substrate reuse as well as in enabling thin and flexible PV products will be emphasized.

8631-81, Session 16

Quantum-dot micropillars for parametric THz emission (*Invited Paper*)

Silvia Mariani, Alessio Andronico, Ivan Favero, Sara Ducci, Yanko Todorov, Carlo Sirtori, Univ. Paris 7-Denis Diderot (France); Martin Kamp, Julius-Maximilians-Univ. Würzburg (Germany); Julien Claudon, Jean-Michel Gérard, Univ. Joseph Fourier (France) and Commissariat à l'Énergie Atomique (France); Tianwu Wang, Peter U. Jepsen, Technical Univ. of Denmark (Denmark); Giuseppe Leo, Univ. Paris 7-Denis Diderot (France)

We report on the design, fabrication and optical investigation of AlGaAs microcavities for THz Difference Frequency Generation (DFG) between Whispering Gallery Modes (WGMs), where the pump and DFG wavelengths ($\lambda \approx 1.3 \mu\text{m}$ and $\lambda \approx 75\text{-}150 \mu\text{m}$, respectively) lie on opposite sides of the Reststrahlen band. For the pump modes, we demonstrate CW lasing of quantum-dot layers under electrical injection at room temperature. We control the number of lasing WGMs via vertical notches on the pillars sidewalls, providing a selection mechanism for funneling the power only to the modes contributing to DFG. In parallel with the optimization of the pump lasers and in order to validate design and material parameters before the DFG experiments, we have performed linear measurements on two sets of passive samples. For the telecom range, the micropillars have been integrated with waveguides for distributed coupling and characterized via transmission measurements. In the THz range we have measured reflectivity spectra on 2D arrays of identical cylinders. In both cases, we demonstrate a good agreement between experimental results and simulations. On a more speculative note, we numerically show that etching a hole along the pillar axis can facilitate phase matching, while single-lobe far field pattern can be obtained for the THz mode by micro-structuring the metallic ground plane around the microcavity. Finally, we suggest a real-time fine-tuning mechanism for the forthcoming active devices.

We acknowledge the financial support of the European Union FP7 FET program, under the TREASURE project (grant number: 250056).

8631-82, Session 16

Electronic temperature in phonon-photon-phonon terahertz quantum

cascade devices with high-operating temperature performance

Gaetano Scamarcio, Pietro Patimisco, Maria V. Santacroce, Pasquale Tempesta, Univ. degli Studi di Bari (Italy); Vincenzo Spagnolo, Politecnico di Bari (Italy); Miriam S. Vitiello, Lab. NEST (Italy) and Scuola Normale Superiore di Pisa (Italy); Emmanuel Dupont, Saeed Fatholouloumi, Sylvain R. Laframboise, National Research Council Canada (Canada); Seyed G. Razavipour, Zbigniew Wasilewski, Dayan Ban, Univ. of Waterloo (Canada); H. C. Liu, Shanghai Jiao Tong Univ. (China)

We report on the experimental measurements of subband electronic (T_e) and lattice temperatures (T_L) of THz QCLs with active region scheme based on phonon scattering assisted injection and extraction [1]. Three devices have been investigated, differing for doping region and number of quantum wells composing the active region. The employed experimental approach is based on a microprobe band-to-band photoluminescence, already successfully utilized for the investigation of THz QCLs based on different active region schemes. Differently from what typically observed before, our results demonstrate smaller electronic temperature increases with respect to the lattice one. Below the alignment all the subbands share the same electronic temperatures, which results slightly higher than the lattice one (~ 5 K). Above alignment, while the ground state subband electronic temperature remains close to the lattice one (only ~ 5 K difference in the T_L range 200K - 250K), the T_e of the injection subband increases slightly more and for the higher dissipated power of 6 W, and a corresponding $T_L = 250$ K, we observed a difference of ~ 20 K (25 K) with respect to the ground state T_e (T_L). The observed T_e increase is much smaller than what previously observed in THz QCLs (for example in resonant phonon THz QCL scheme we observed more than 100 K difference between T_e and T_L for 3 W of dissipated power).

References:

[1] E. Dupont et al., "A phonon scattering assisted injection and extraction based terahertz quantum cascade laser", J. Appl. Phys. 111, 073111 (2012).

8631-83, Session 16

Far-infrared InAs/AlSb quantum cascade lasers (*Invited Paper*)

Roland Teissier, Michael Bahriz, Guillaume Lollia, Alexei N. Baranov, Univ. Montpellier 2 (France); Adel Bousseksou, Raffaele Colombelli, Univ. Paris-Sud 11 (France)

Up to now the development of QCLs in the InAs/AlSb material system was essentially focused on short wavelengths close to $3 \mu\text{m}$ or even below. We present in this contribution our work exploring the potential of InAs-based quantum cascade lasers to operate in the far infrared up to the THz spectral region. The main motivation for the development of long wavelength InAs-based QCLs is to exploit the small electron effective mass in InAs, $0.023m_0$ compared with $0.067m_0$ in GaAs which leads theoretically to stronger optical gains of intersubband transitions an improved performances.

We developed a process for the fabrication of double metal waveguide (DM) in structures grown on InAs substrates, suitable for long wavelength and THz lasers. We designed and fabricated far infrared InAs/AlSb quantum cascade active regions using molecular beam epitaxy. A first important result is the demonstration of DM QCLs emitting from $16 \mu\text{m}$ up to $\lambda = 21 \mu\text{m}$ ($\nu = 15$ THz). The possibility of efficient light extraction from these lasers is also studied.

**Conference 8631:
Quantum Sensing and Nanophotonic Devices X**

Active regions designed for emission in the other side of the Reststrahlen band, in the 2 to 4 THz range, will also be presented. We demonstrated that the low residual doping levels required for limiting optical loss can be achieved, and show evidence of selective injection in the excited state of a THz active region based on the LO-phonon depopulation scheme.

This work is supported by French ANR with the project DELTA (ANR 2011 Nano 020).

8631-84, Session 16

Room-temperature nanowire terahertz photodetectors

Lorenzo Romeo, Scuola Normale Superiore di Pisa (Italy); Dominique Coquillant, Univ. Montpellier 2 (France); Leonardo Viti, Daniele Ercolani, Lucia Sorba, Scuola Normale Superiore di Pisa (Italy); Wojciech Knap, Univ. Montpellier 2 (France); Alessandro Tredicucci, Lab. NEST (Italy); Miriam S. Vitiello, Univ. degli Studi di Roma La Sapienza (Italy)

Terahertz technology has become of large interest over the last few years for its potential in non-invasive imaging applications, high resolution spectroscopy and tomography. In this context, the development of a breakthrough solid-state technology for compact and reliable high power THz sources as well as for fast and high-temperature THz detectors is highly desired.

Semiconductor nanowires (NWs) represent an ideal building block for implementing rectifying diodes or plasma-wave detectors that could be well operated into the Terahertz, thanks to the typical attofarad-order capacitance achievable in NW structures. Despite the strong effort in developing these nanostructures for a new generation of complementary metal-oxide semiconductors (CMOS), memory and photonic devices, never before their potential as radiation sensors into the Terahertz has been explored.

We report on the development of NW-based field-effect transistors operating as high sensitivity Terahertz detectors in the 0.3 – 2.8 THz range. By feeding the radiation field of both an electronic THz source and a quantum cascade laser (QCL) at the gate-source electrodes with a wide band dipole antenna, we record a photovoltage signal corresponding to responsivity values up to ≈ 100 V/W, with impressive noise equivalent power levels $< 6 \times 10^{-11}$ W/√Hz at room temperature and a wide modulation bandwidth. The potential scalability to even higher frequencies and the technological feasibility of realizing multi-pixel arrays coupled with QCL sources make the proposed technology highly competitive for a future generation of THz detection systems.

8631-85, Session 16

Rapid screening and identification of illicit drugs by IR absorption spectroscopy and gas chromatography (Invited Paper)

Sandro Mengali, Nicola Liberatore, Domenico Luciani, Roberto Viola, Consorzio CREO (Italy); Giancarlo Cardinali, Ivan Elmi, Consiglio Nazionale delle Ricerche (Italy); Antonella Poggi, Stefano Zampolli, Istituto per la Microelettronica e Microsistemi (Italy); Elisa Biavardi, Enrico Dalcanale, Univ. degli Studi di Parma (Italy); Federica Bonadio, Institut de Police Scientifique, Université de Lausanne, Batochime (Switzerland); Olivier Delemont, Pierre Esseiva, Francesco Saverio Romolo, Univ. de Lausanne (Switzerland)

Analytical instruments based on IR Absorption Spectroscopy (IRAS) and Gas Chromatography (GC) are today available only as bench-top instrumentation for forensic labs and bulk analysis. Within the DIRAC

project funded by the European Commission, we are developing an advanced portable sensor, that combines miniaturized GC as its key chemical separation tool, and IRAS in a Hollow Fiber (HF) as its key analytical tool, to detect and recognize illicit drugs and key precursors, as bulk and as traces.

The HF-IRAS module essentially consists of a broadly tunable EC-QCL, thermo-electrically cooled MCT detectors, and an infrared hollow fiber at controlled temperature. The hollow fiber works as a miniaturized gas cell, that can be connected to the output of the GC column with minimal dead volumes. Indeed, the module has been coupled to GC columns of different internal diameter and stationary phase, and with a Vapour Phase Pre-concentrator that selectively traps target chemicals from the air.

The presentation will report the results of tests made with amphetamines and precursors, as pure substances, mixtures, and solutions. It will show that the sensor is capable of analyzing all the chemicals of interest, with limits of detection ranging from a few nanograms to about 100-200 ng. Furthermore, it is suitable to deal with vapours directly trapped from the headspace of a vessel, and with salts treated in a basic solution.

When coupled to FAST GC columns, the module can analyze multi-components mixes in less than 5 minutes.

8631-15, Session 17

Broadband-tunable external-cavity quantum cascade lasers for the spectroscopic detection of hazardous substances (Invited Paper)

Stefan Hugger, Fraunhofer-Institut für Angewandte Festkörperphysik (Germany); Frank Fuchs, Fraunhofer-Institut für Angewandte Optik und Feinmechanik (Germany); Jan Jarvis, Michel Kinzer, Quankui K. Yang, Rachid Driad, Rolf Aidam, Joachim Wagner, Fraunhofer-Institut für Angewandte Festkörperphysik (Germany)

Broadband tunable external cavity quantum cascade lasers (EC-QCL) have emerged as attractive light sources for mid-infrared (MIR) “finger print” molecular spectroscopy for e.g. detection and identification of chemical compounds. Compared to Fourier Transform Infrared (FTIR) spectrometers EC-QCLs offer the advantage of a much higher spectral brightness as well as a collimated low-divergence output beam, enabling e.g. stand-off detection schemes.

Imaging MIR backscattering spectroscopy using EC-QCLs for wavelength-selective illumination has been shown to be a promising technique for stand-off detection of traces of explosives. Recording the backscattered light with a MIR camera at each illumination wavelength, the MIR backscattering spectrum can be extracted for each point within the laser illuminated area. This way, contaminated areas can be clearly identified on the basis of characteristic finger print backscattering spectra. To achieve a high selectivity, a large spectral coverage is a key requirement. Using a MIR EC-QCL with a tuning range of 300 cm⁻¹, traces of different explosives such as TNT, PETN and RDX residing on different background materials like painted metal sheets, cloth and polyamide, could be detected and clearly identified. Due to their high spectral brightness, EC-QCLs are ideally suited also for the spectroscopic detection of contaminants in water. Due to the high background absorption in water, FTIR spectroscopy is limited to an absorption path length of ~ 10 μm. Here we realized an EC-QCL based measurement system with an extended single-pass optical path length of 100 μm, which allowed sensitive detection of contaminants in water even when using uncooled pyroelectric detectors.

**Conference 8631:
Quantum Sensing and Nanophotonic Devices X**

8631-16, Session 17

QCL: Creating new frontiers of infrared spectroscopy

Frederick G. Haibach, Erik R. Deutsch, Alexander Mazurenko, Jim Ye, Block Engineering, LLC (United States)

Modern practice of infrared spectroscopy is almost synonymous with the use of “FTIR.” Instruments that serve as tunable light sources or tunable detectors have fallen by the wayside as the performance of interferometers complements incandescent sources. Many of the published advantages of interferometers rely on the limitations of the incandescent source. Recent advances in interferometers seek to recapture of the applications where dispersive instruments proved to have superior performance. Step-scan was the most prominent of these advances. The dominance is now so complete, that many modern practitioners of infrared spectroscopy have experience with other spectroscopic instrument designs only peripherally through terahertz, near-infrared or UV-vis.

Quantum cascade lasers (QCLs) make it possible to take advantage of both laser properties and widely tunable infrared. The four advantages that QCLs provide over incandescent sources are: (1) orders of magnitude higher spectral radiance, (2) nearly diffraction-limited source size, (3) collimated light and (4) inherently greater than 100:1 polarization. Pulsed mode operation makes it possible to obtain operation across hundreds of wavenumbers in a single unit. Other properties, such as scan rates in milliseconds, miniaturization, low power consumption and ultrahigh resolution spectroscopy depend on the laser packaging.

These advantages enable spectroscopy that is difficult or impossible to do well with incandescent sources. Standoff absorbance measurements, efficient fiber and ATR coupling, microscopy and measurements on high-absorbance materials have now become possible without compromising effectiveness. Direct measurements are now possible that were not previously achievable, or required extensive work around. Examples and performance of these types of spectroscopy will be discussed.

8631-20, Session 17

Same-frequency detector and laser utilizing bi-functional quantum cascade active region

Benedikt Schwarz, Peter Reininger, Herman Detz, Tobias Zederbauer, Aaron M. Andrews, Technische Univ. Wien (Austria) and Technische Univ. Wien (Austria); Werner Schrenk, Oskar Baumgartner, Hans Kosina, Technische Univ. Wien (Austria); Gottfried Strasser, Technische Univ. Wien (Austria) and Technische Univ. Wien (Austria)

We demonstrate a bi-functional quantum cascade device, operating at room-temperature that detects at the same wavelength as it coherently emits. With this multipurpose device we go a significant step towards monolithic integrated photonic circuits and sensors by generating and detecting light on the same chip with the same epilayer material. Apart from typical real world applications, like chemical sensing and spectroscopy, this structure offers new ways to study the physics of optical couplings, by switching between detection/absorption (0kV/cm), transparency and gain (58kV/cm).

A commonly designed quantum cascade laser can act as a photovoltaic detector, but at a significant lower wavelength. This shift is because the detectors optical transition occurs between the upper laser level and an extraction level, not the lower laser level. However, due to this intrinsic energy-shift and the poor extraction efficiency it is neither possible to reach room-temperature detection nor to match the emission wavelength.

We have recently developed a quantum cascade device optimizer based on a highly efficient semi-classical Monte-Carlo simulator. This design framework gives us the flexibility we need to develop bi-functional intersubband devices. Our structure was fabricated from the lattice matched InGaAs/InAlAs material system. We have compensated the

intrinsic energy-shift by reducing the coupling of the lasers extraction levels and by down-shifting the upper level at zero bias via precise coupling adjustments. Additionally, we provide efficient electron injection/extraction to/from the upper level when used as laser/detector. With this design procedure we were able to achieve room-temperature operation for both emission and detection at $\lambda=6.7\mu\text{m}$.

8631-86, Session 17

CW DFB RT diode laser based sensor for trace-gas detection of ethane using novel compact multipass gas absorption cell

Mohammad Jahjah, Rafal Lewicki, Frank K. Tittel, Rice Univ. (United States); Karol Krzempek, Przemyslaw Stefanski, Wroclaw Univ. of Technology (Poland); Stephen So, David Thomazy, Sentinel Photonics (United States)

Development of a continuous wave (CW), thermoelectrically cooled (TEC), distributed feedback (DFB) laser diode based spectroscopic trace-gas sensor for ultra-sensitive and selective ethane (C₂H₆) concentration measurements at $\sim 3.36\mu\text{m}$ will be reported. The sensor platform used tunable laser diode absorption spectroscopy (TDLAS) and wavelength modulation spectroscopy (WMS) as the detection technique [1]. A CW TEC DFB GaSb based laser diode operating at 9.5 °C was used as an excitation source. TDLAS was performed with an ultra-compact 57.6 m effective path length innovative multipass gas absorption cell capable of 459 passes between two spherical mirrors separated by 12.5 cm. For an interference free C₂H₆ absorption line located at 2976.8 cm⁻¹ a 1? minimum detection limit of 130 pptv with a 1 second lock-in amplifier time constant was achieved. A new state-of-the-art integrated electronic control and data acquisition module was implemented that allowed further significant size reduction without loss of sensor performance. Allan variance measurements indicated long term reliable operation of the ethane sensor platform, essential for the detection of hydrocarbon species as well as in non-invasive medical exhaled breath analysis associated with asthma and lung cancer.

References:

[1] K. Krzempek, R. Lewicki, L. Naehle, M. Fischer, J. Koeth, S. Behahsene, Y. Roulard, L. Worschech, F.K. Tittel, “Continuous wave, distributed feedback diode laser based sensor for trace gas detection of ethane.” Appl Phys B 106: 251-255 (2012)

8631-87, Session 17

Quantum cascade laser based standoff photoacoustic detection of explosives using ultra-sensitive microphone and sound reflector

Xing Chen, Dingkai Guo, Fow-Sen Choa, Univ. of Maryland, Baltimore County (United States); Chen-chia Wang, Sudhir Trivedi, Brimrose Corp. of America (United States); Jenyu Fan, AdTech Optics, Inc. (United States)

Photoacoustic spectroscopy is a highly sensitive sensing technique. Parts-per-billion detection sensitivity has been achieved for on-site measurements. However, chemicals such as explosives will require an as far-away as possible standoff detection distance due to safety concerns. Recently, we have demonstrated standoff photoacoustic detection of isopropanol vapor for more than 40 feet distance using a quantum cascade laser and an electrets microphone. Since explosive chemicals such as TNT have very low vapor pressure, in this work we focus on solid phase TNT standoff detections. In our experiment, a quantum cascade laser with an emission wavelength near 7.35 μm is used. The laser is operated under pulsed condition with a repetition rate of $\sim 1\text{ kHz}$ and pulse width of 250 μs . When the laser beam is focused on the TNT sample, photoacoustic signal is generated through solid to air heating

**Conference 8631:
Quantum Sensing and Nanophotonic Devices X**

coupling. An ultra-sensitive microphone is placed close to the TNT sample and detects the photoacoustic signal. The detection distance can be increased up to 8 inches with the one-inch diameter size microphone. To further increase the distance, a sound reflector with diameter of 2 feet is added to the system. With the help of sound reflector, amplifiers and filters, standoff detection distance is extended to 8 feet. The detected photoacoustic signal is proportional to laser pulse energy and inversely proportional to the detection distance. We also study the standoff photoacoustic detection theory in solid matters in open environment. Our experimental measurements are in good agreement with the theoretical model.

8631-62, Session 18

Tunable excitation of mid-infrared optically pumped semiconductor lasers (*Invited Paper*)

Linda J. Olafsen, Jeremy Kunz, Baylor Univ. (United States); Andrew P. Ongstad, Ron Kaspi, Air Force Research Lab. (United States)

While conventional semiconductor lasers employ electrical injection for carrier excitation, optically pumped semiconductor lasers (OPSLs) have demonstrated high output powers and high brightness in the mid-infrared. An important consideration for optically pumped lasers is efficient absorption of the pump beam, which can be achieved through increasing the number of periods in the active region, by placing the active region in a cavity with an optical thickness of twice the pump wavelength between distributed Bragg reflectors (Optical Pumping Injection Cavity), or by periodically inserting the active quantum wells into an InGaAsSb waveguide designed to absorb the pump radiation (Integrated Absorber). A tunable optical pumping technique is utilized by which threshold intensities are minimized and efficiencies are maximized. The near-IR idler output of a Nd:YAG-pumped optical parametric oscillator (10 Hz, ~4 ns) is the tunable optical pumping source in this work. Results are presented for an OPSL with a type-II W active region embedded in an integrated absorber to enhance the absorption of the optical pump beam. Emission wavelengths range from 4.64 μm at 78 K to 4.82 μm at 190 K for optical pump wavelengths ranging from 1930-1950 nm. The effect of wavelength tuning is demonstrated and compared to single wavelength pumping (1940 nm) at a higher duty cycle (20-30%). Comparisons are also made to other OPSLs, including a discussion of the characteristic temperature and high temperature performance of these devices.

8631-88, Session 18

Single QCL-based sensor measuring the simultaneous displacement of independent targets

Lorenzo Columbo, Francesco Paolo Mezzapesa, CNR-IFN UOS Bari (Italy); Massimo Brambilla, Maurizio Dabbicco, Gaetano Scamarcio, Univ. degli Studi di Bari (Italy) and CNR-IFN UOS Bari (Italy)

We propose an all-optical sensing technique, based on feedback interferometry in a quantum cascade laser (QCL), to measure the collinear displacement of independently moving targets. The common-path geometry and the laser self-mixing scheme, where the QCL acts as the source and the detector, both allows for an extremely compact and self-aligned differential interferometer. The QCL is collimated and directed into an asymmetric cavity composed of a low- and a high-reflectance, front and rear surface, respectively. The radiation back reflected by the two surfaces couples into the QCL and the occurring power modulation is detected as the voltage variations at constant-current. The self-mixing fringes due to the independent displacement of each surface are detected with relative amplitude depending only on the surfaces reflectivity ratio. The experimental results are in excellent agreement with the numerical simulations based on the Lang-Kobayashi semiconductor

rate equations for multiple external cavities. The high stability of the QCL against optical feedback allows for virtually perfect common-mode rejection and sub-wavelength sensitivity of the differential motion of the two surfaces. Hence, MIR-QCLs resonantly tuned to an absorption line of a chemical filling the cavity could be used to detect the thermal expansion of the cavity when a flexible membrane replaces front surface. In the same configuration THz-QCL could be used to detect pressure deformations due to flow variations in cavities not probed by visible light for microfluidics applications.

8631-89, Session 18

Toward on-chip mid-infrared chem/bio sensors using quantum cascade lasers and substrate-integrated semiconductor waveguides

Xiaofeng Wang, Markus Sieger, Boris Mizaikoff, Univ. Ulm (Germany)

State-of-the-art sensing platforms increasingly take advantage of miniaturized and integrated optical technologies ideally providing direct access to molecule-specific information. With point-of-care and personalized medicine becoming more prevalent, detection schemes that do not require reagents or labeled constituents facilitate on-site analysis close to real-time.

However, decreasing the analytically probed volume may adversely affect the analytical figures of merit such as the signal-to-noise-ratio, the representativeness of the sample, or the fidelity of the obtained analytical signal. Consequently, the guiding paradigm for the miniaturization of diagnostic devices should be creating sensing platforms that should be as small as still useful, rather than as small as possible by smartly taking advantage of integrated optics.

Mid-infrared (MIR; 3-20 μm) sensor technology is increasingly adopted in bioanalytics due to the inherent molecular specificity enabling discriminating constituents at ppm-ppb concentration levels in condensed and vapor phase media. Recently emerging strategies capitalize on innovative substrate-integrated waveguide technologies such as hollow waveguides and planar semiconductor waveguides in combination with highly efficient broadly tunable quantum cascade lasers, thereby facilitating miniaturized yet robust MIR diagnostic platforms for label-free bioassays and for breath diagnostics [1-6].

- [1] C. Charlton, et al., Applied Physics Letters, 86, 194102/1-3 (2005).
- [2] C. Charlton, et al., Analytical Chemistry, 78, 4224-4227 (2006).
- [3] C. Young, et al., Sensors and Actuators B, 140, 24-28 (2009).
- [4] S.-S. Kim, et al., IEEE Sensors, 10, 145-158 (2010).
- [5] A. Wilk, et al., Anal. Bioanal. Chem., 402, 397-404 (2012).
- [6] X. Wang, et al., Analyst, 137, 2322-2327 (2012).

8631-95, Session 18

Recent advances in GaSb-based structures for mid-infrared emitting lasers: spectroscopic study (*Invited Paper*)

Grzegorz Sek, Marcin Motyka, Filip Janiak, Krzysztof Ryczko, Jan Misiewicz, Wroclaw Univ. of Technology (Poland); Adam Bauer, Matthias Dallner, Robert Weih, Sven Hoefling, Alfred Forchel, University of Wuerzburg (Germany); Sofiane Belahsene, Guilhem Boissier, Yves Rouillard, University of Montpellier 2 (France)

Applications related to the sensing of hazardous and environmentally relevant gasses drive the growing demands with respect to all the sensor components, requiring cheap, compact and fast laser sources. However, in many cases the respective devices able to emit in the ranges of the maximal absorption, which for many gasses falls into the mid infrared

**Conference 8631:
Quantum Sensing and Nanophotonic Devices X**

range are not commercially available. The target range, which is usually about 3-5 μm , and beyond into the longer wavelengths, can be reached by using several approaches, starting from short wavelength quantum cascade lasers, through common type I quantum-well-based laser diodes, up to the so called interband cascade laser, all possible to be fabricated various material systems.

There will be reviewed the optical properties of such kind of active regions with a special focus on InGaAsSb/InAlGaAsSb type I QWs and InAs/InGaAsSb type II QWs, both grown on GaSb substrates, and the related current challenges with respect to the device characteristics. This will cover such issues as the band offsets importance, and its sensitivity to the layers composition, the active transition oscillator strength versus various structure parameters and external factors as temperature or electric field, and the predominating carrier loss mechanisms. For that a combination of several spectroscopic techniques have been used, both emission-like (photoluminescence) and absorption-like (modulated reflectivity spectroscopy) supported by the energy level calculations employing a multiband kp model. Eventually, the potential for further material optimization and prospects for the improved device performances will be given.

8631-53, Session 19

InAs/GaSb superlattice pin photodiode: choice of the SL period to enhance the temperature operation in the MWIR domain
(Invited Paper)

Philippe Christol, Rachid Taalat, Marie Delmas, Jean-Baptiste Rodriguez, Univ. Montpellier 2 (France); Edouard Giard, Isabelle Ribet-Mohamed, ONERA (France)

Important progresses have been obtained the last past years on the performances of mid-wavelength infrared (MWIR) InAs/GaSb superlattice (SL) photodiodes. These improvements were obtained by the use of particular device designs using nBn, C-BIRD or pMp structures, neither by the choice of the InAs/GaSb SL period while the SL period composition governs the material properties of the active zone material. In this communication, we studied the influence of the SL period (thickness and periodicity) on the performances of MWIR pin photodiodes, fabricated by MBE on p-type GaSb substrate. These SL structures are made of symmetrical or asymmetrical SL period designs and exhibited cut-off wavelength between 4.5 μm and 5.5 μm at 80K. Experimental measurements carried out on several SL pin photodiodes show the superiority of the asymmetrical SL structure composed of 7 InAs monolayers (MLs) and 4 GaSb MLs in terms of dark current and quantum efficiency. As a result, the 7/4 SL diode exhibits at 77K (5 μm cut-off) dark current density values as low as 40nA/cm² and R0A product greater than 1.7x10⁶ Ohm.cm² at 77K, one decade over the value obtained by equivalent symmetrical 8/8 SL diode. This result obtained demonstrates the strong influence of the SL period design on the performances, and then on temperature operation, of MWIR SL photodiodes.

8631-54, Session 19

Radiation tolerance of type-II strained layer superlattice based interband cascade MWIR detector

Vincent M. Cowan, Christian P. Morath, Air Force Research Lab. (United States); Stephen Myers, Nutan Gautam, Sanjay Krishna, Ctr. for High Technology Materials (United States)

Infrared (IR) detectors operated in the space environment are required to have high performance while being subjected to a variety of radiation effects. Sources of radiation in space include the trapped particles in the Van Allen belts and transient events such as solar events and galactic cosmic rays. Mercury cadmium telluride (MCT)-based IR detectors are

often used in space applications because they have high performance and are relatively tolerant of the space environment; in contrast, the CMOS-based readout-integrated circuit is often far more susceptible to radiation effects than the detector materials themselves. However, inherent manufacturing issues with the growth of MCT have led to interest in alternative detector technologies including type-II strained-layer superlattice (T2SLS) infrared detectors employing interband cascade architectures. Much less is known about the radiation tolerance properties of these SLS-based detectors compared to MCT. Here, the effects of 63 MeV protons on variable area, single element, InAs/GaSb T2SLS detectors utilizing an interband cascade architecture are considered. The device employs a seven-stage cascade region, where each stage contains an MWIR absorber, graded T2SLS transport region, and an interband tunneling region. When semiconductor devices are irradiated with protons with energies of 63 MeV the protons are capable of displacing atoms within their crystalline lattice. The radiation effects on these detectors are characterized by dark current and quantum efficiency measurements prior-to and following a single irradiation step with a dose of 500 kRad(Si).

8631-55, Session 19

Ga-free InAs/InAsSb type-II superlattice: its past, present, and future
(Invited Paper)

Yong-Hang Zhang, Arizona State Univ. (United States)

This talk will review the past research on Ga-free InAs/InAsSb type-II superlattices and their growth, structural and electronic properties. Then it will focus on the latest processes in MBE growth, the study of structural and optical properties, and device fabrication. The highlights of the talk will be the measured very long carrier lifetimes as well as the demonstration of nBn detectors with a record low dark current at 77 K for wavelengths beyond LWIR band.

Conference 8632: Photonic and Phononic Properties of Engineered Nanostructures III

Sunday - Thursday 3 -7 February 2013

Part of Proceedings of SPIE Vol. 8632 Photonic and Phononic Properties of Engineered Nanostructures III

8632-1, Session 1

Wetting in color: From photonic fingerprinting of liquids to optical control of liquid percolation (*Invited Paper*)

Ian B. Burgess, Wyss Institute for Biologically Inspired Engineering (United States); Bryan A. Neger, Kevin P. Raymond, Wyss Institute for Biologically Inspired Engineering (United States) and Univ. of Waterloo (Canada); Alexis Goulet-Hanssens, Thomas A. Singleton, McGill Univ. (Canada); Mackenzie H. Kinney, Wyss Institute for Biologically Inspired Engineering (United States) and Univ. of Waterloo (Canada); Christopher J. Barrett, McGill Univ. (Canada); Marko Loncar, Harvard Univ. (United States); Joanna Aizenberg, Wyss Institute for Biologically Inspired Engineering (United States) and Harvard Univ. (United States)

We provide an overview of our recent advances in the manipulation of wetting in inverse-opal photonic crystals. Exploiting photonic crystals with spatially patterned surface chemistry to confine the infiltration of fluids to liquid-specific spatial patterns, we developed a highly selective scheme for colorimetry, where organic liquids are distinguished based on wetting. The high selectivity of wetting, upon which the sensitivity of the response relies, and the bright iridescent color, which disappears when the pores are filled with liquid, are both a result of the highly symmetric pore structure of our inverse-opal films. The application of horizontally or vertically orientated gradients in the surface chemistry allows a unique response to be tailored to specific liquids. While the generic nature of wetting makes our approach to colorimetry suitable for applications in liquid authentication or identification across a broad range of industries, it also ensures chemical non-specificity. However, we show that chemical specificity can be achieved combinatorially, using an array of indicators that each exploit different chemical gradients to cover the same dynamic range of response. Finally, incorporating a photo-responsive polyelectrolyte surface layer into the pores, we are able to dynamically and continuously photo-tune the wetting response, even while the film is immersed in liquid. This in situ optical control of liquid percolation in our photonic-crystal films allows us to manipulate and study disorder in these systems in a controlled way, and may also provide an error-free means to tailor indicator response, naturally compensating for batch-to-batch variability in the pore geometry.

8632-2, Session 1

Funneling single photons into ridge-waveguide photonic integrated circuits

Sartoon Fattah poor, Leonardo Midolo, Technische Univ. Eindhoven (Netherlands); Thang Hoang, Technische Univ. Eindhoven (Netherlands); Lianhe Li, Edmund Linfield, Univ. of Leeds (United Kingdom); Tian Xia, Frank W. M. van Otten, Technische Univ. Eindhoven (Netherlands); Andrea Fiore, Technische Univ. Eindhoven (Netherlands)

The generation, manipulation and detection of single photons enable quantum communication, simulation and potentially computing protocols. However scaling to several qubits requires the integration of these functionalities in a single chip. To this aim, efficient coupling of the emission from single quantum dots in photonic crystal cavities to low-loss ridge-waveguide (RWG) circuits is needed. This is usually hampered by the large mode mismatch between the two systems. In this work the emission of a photonic crystal (PhC) cavity realized on a GaAs/AlGaAs membrane and pumped by quantum dots has been effectively coupled and transferred through a long RWG (~1mm). By using a self-

aligned fabrication technique involving a continuous tapering in both the horizontal and the vertical direction, transmission values (fiber-in, fiber-out) around 0.1 and 0.02% for RWG and coupled PhC waveguide-RWG have been achieved, respectively. This corresponds to about 1.5% coupling efficiency between the center of the PhC waveguide and the single-mode output fiber, a value much higher than what is achieved by top collection. It further shows that around 45% of the light in the PhC waveguide is coupled to the RWG. The emission from quantum dots in the cavity has been clearly identified by exciting from the top and collecting the photoluminescence from the cleaved facet of the device 1mm away from the cavity. This enables the efficient coupling of single photons to RWG and detector circuits, and additionally allows using the cavity as in-line filter to isolate single excitonic lines in integrated experiments with on-chip detectors.

8632-3, Session 1

Slow-light-enhanced surface plasmonic resonance in photonic crystal slot waveguide

Dihan Md. Nuruddin Hasan, Alan X. Wang, Oregon State Univ. (United States)

Localized surface plasmons (LSPs) play significant roles in versatile applications including biomedical sensing, optical tweezers, and light trapping for photovoltaic devices. Despite high enhancement of the electric field has been achieved by LSPs using different metallic nanostructures, further improvement is still desirable to reduce the power dissipation of active photonic devices and to enhance the sensitivity of plasmonic sensors. In this work, we numerically demonstrate significant electric field enhancement from an Ag nanoparticle (NP) and a nanoparticle array that are placed inside a one-dimensional (1-D) slotted photonic crystal waveguide (PCW) with advanced optical coupling structures using optical mode converters and impedance tapers. The slotted PCW structure is based on Si₃N₄ and exhibits a 33 nm transverse-magnetic (TM) bandgap starting from 638 nm wavelength. Using a Gaussian-shape light source operating close to the photonic band-edge, we demonstrate 7x enhancement of the electric field due to slow-light effect. In the meanwhile, we observe that the wavelength of the peak electric field red-shifts 2 nm because of the phase retardation of nanoparticle to the guided-mode of the slotted PCW. To maximize the electric field enhancement, the photonic impedance tapers are optimized using an exponential distribution of the air hole periodicity with a modulation factor of F to gradually manipulate the group index. A significant improvement of 83% of electric field enhancement has been achieved through such optimization as higher optical power is coupled into the slow-light slotted PCW for optical wavelengths close to the band edge.

8632-4, Session 1

Efficient single-photon frequency conversion using a Sagnac interferometer

Matthew Bradford, Jung-Tsung Shen, Washington Univ. in St. Louis (United States)

We present a quantum nanophotonic scheme to achieve efficient single-photon frequency conversion. This mechanism is essential for integrated nanophotonics, as it can provide access to frequency regimes in which no single-photon sources are currently available. Moreover, such a device could be used as the basis of a photonic frequency-shift-keyed quantum information scheme. The proposed scheme uses a Sagnac interferometer to exploit quantum interference between two transition pathways in a three-level quantum dot.

In the proposed scheme, an input photon induces a complete population state transfer on the Lambda-type quantum dot, causing a frequency

Conference 8632: Photonic and Phononic Properties of Engineered Nanostructures III

shift in the outgoing photon. This scheme can be used for either spectral down-conversion or up-conversion, depending on the initialization of the quantum dot. The Sagnac interferometer is used to put the input photon into a superposition of counterpropagating states which interfere at the quantum dot, providing the necessary quantum interference to make the process efficient. Additionally, the mechanism can be switched on and off by modulating the index of one branch of the interferometer, thereby switching between constructive and destructive interference at the quantum dot. We note that on-chip integration of Sagnac interferometer geometry has been experimentally realized.

We have developed a real-space theoretical approach and a computationally efficient pseudospectral numerical method to investigate the full spatiotemporal dynamics of the scattering process. It is shown that the efficiency of the frequency-conversion process approaches unity in the ideal case, and is greater than 80% even in the presence of realistic dissipation.

8632-5, Session 1

High-speed high-sensitivity carbon nanotube-based composite bolometers

Trevor J. Simmons, Rensselaer Polytechnic Institute (United States); Gustavo Vera-Reveles, Univ. Autónoma de San Luis Potosí (Mexico); Gabriel Gonzalez, Tecnológico de Monterrey (Mexico); Hugo Navarro-Contreras, Univ. Autónoma de San Luis Potosí (Mexico); Francisco J. Gonzalez, Univ. Autónoma de San Luis Potosí (Mexico)

In this work films of horizontally aligned single-walled carbon nanotubes were thermally and electrically characterized in order to determine the bolometric performance. Studies were conducted on semiconducting carbon nanotubes, metallic carbon nanotubes, and a mixture. An average thermal time constant of $\tau = 420 \mu\text{s}$ along with a temperature coefficient of resistance of $\text{TCR} = -2.94\% \text{ K}^{-1}$ were obtained for the mixture of semiconducting and metallic carbon nanotubes. The maximum voltage responsivity and detectivity obtained were $R_v = 230 \text{ V/W}$ and $D^* = 1.22 \times 10^8 \text{ cm Hz}^{1/2}/\text{W}$ respectively. These values are higher than the maximum voltage responsivity (150 V/W) and maximum temperature coefficient of resistance ($1.0\% \text{ K}^{-1}$) previously reported for carbon nanotube films at room temperature. The maximum detectivity was obtained at a frequency of operation of 1.25 kHz . It was found that indeed semiconducting carbon nanotubes exhibited the largest TCR, but the values varied significantly. It was found that the mixture of metallic and semiconducting carbon nanotubes yielded the most repeatable TCR values, despite these being somewhat less than the semiconducting carbon nanotubes alone. The morphology of the composite was also examined, and the alignment of the carbon nanotubes across micron-scale fissures proved important to obtaining optimal results. Higher TCR values were obtained when applying a heat flow model to the data obtained, and sudden small changes in temperature show TCR values approaching $10\% \text{ K}^{-1}$. These values are far higher than any previously reported carbon nanotube bolometers, and are competitive with present state-of-the-art commercial technologies.

8632-6, Session 2

Optical absorption enhancement in three-dimensional simple cubic woodpile nanostructures for thin film solar cell applications

Ping Kuang, Shawn-Yu Lin, Rensselaer Polytechnic Institute (United States)

Three-dimensional (3D) photonic crystals possess photonic bandgaps that prohibit the propagation of light in certain wavelength range in all three directions in space. A layer-by-layer woodpile structure can exhibit a full 3D photonic bandgap. It is also of great interest to utilize

photonic crystals for photon management and visible light trapping. In order to control optical light in the visible wavelength range, the physical dimensions of the structures have to be in nanoscale. A recent theoretical study showed that 3D photonic structures could greatly enhance the light trapping and absorption in thin film photonic crystal structures due to strong resonances by parallel interface refraction (PIR). Here, we report on four-layer simple cubic woodpile photonic crystal structures successfully fabricated with hydrogenated amorphous silicon (a-Si:H) and its enhanced absorption over an unpatterned a-Si:H thin film. Optical measurements show the absorption of the woodpile structures are increased from 60% to above 90% in the shorter wavelength range (400 - 600 nm), and the peaks at wavelength 700nm and 800nm have enhancement of 5-10 orders of magnitude when compared to a 600 nm a-Si:H thin film. The 4L samples are 600, 700, and 800 nm in total thickness. However, due to the 50% HSQ filling, the equivalent volume material is only around half that of 600 nm a-Si:H thin film. Therefore, the structure has enhanced absorption while using half of the active material with enhanced absorption.

8632-7, Session 2

Large area selective emitters/absorbers based on 2D tantalum photonic crystals for high-temperature energy applications

Veronika Rinnerbauer, Yi Xiang Yeng, Jay J. Senkevich, John D. Joannopoulos, Marin Soljacic, Ivan Celanovic, Massachusetts Institute of Technology (United States)

Metallic two-dimensional photonics crystals (PhCs) are highly promising as high-performance selective thermal emitters and absorbers for solid-state high-temperature ($>1000\text{K}$) thermal-to-electrical energy conversion schemes including thermophotovoltaic (TPV), solar-thermophotovoltaic, solar-thermal and solar-thermochemical systems.

We report highly selective emitters based on high-aspect ratio 2D photonic crystals (PhCs) fabricated on large area (5 cm diameter) polycrystalline tantalum substrates, suitable for high-temperature operation. As an example we present an optimized design for a selective emitter with a cut-off wavelength of $2 \mu\text{m}$, matched to the bandgap of an InGaAs PV cell, achieving a predicted spectral selectivity of 56.6% at 1200K.

We present a fabrication route for these tantalum PhCs, based on standard microfabrication processes including Deep Reactive Ion Etch (DRIE) of tantalum by an SF₆ based Bosch process, achieving high-aspect ratio cavities ($> 6:1$). Interference lithography was used to facilitate large area fabrication, maintaining both fabrication precision and uniformity, with a cavity diameter variation of less than 2% across the substrate. The fabricated tantalum PhCs exhibit strong enhancement of the emittance at wavelengths below cut-off wavelength, approaching that of blackbody, and a steep cut-off between high and low emittance spectral regions. Moreover, detailed simulations and numerical modeling show excellent agreement with experimental results. We have also characterized high temperature emission as well as the stability of the nanoscale structures and the optical properties as a function of operation temperature and time. We propose a surface protective coating, which acts as a thermal barrier coating and diffusion inhibitor, and its conformal fabrication by atomic layer deposition.

8632-8, Session 2

Real-time tailoring of the spectral shape of infrared transmission filters using anti-resonant anomalies

Thomas Estruch, Julien Jaeck, Sophie Derelle, ONERA (France); Fabrice Pardo, Lab. de Photonique et de Nanostructures (France); Jérôme Primot, Riad Haïdar, ONERA (France)

For the past twenty years, far-field optics of subwavelength gratings has

Conference 8632: Photonic and Phononic Properties of Engineered Nanostructures III

been the subject of numerous studies, particularly for spectral filtering purposes [Collin: Phys. Rev. Lett. 104, 027401 (2010), Haïdar: Appl. Phys. Lett. 96, 221104 (2010)]. As specifications require high transmission filters with quasi perfect extinction out of the transmission band we have been focussing on dual metallic grating structures [Chan: Opt. Lett. 31, 516 (2006), Cheng: Physical Review B 78, 075406 (2008)]. Indeed, in addition to the high transmission amplitude, under certain conditions, this structure exhibits a quasi perfect extinction out of the transmission band [Babicheva: AIP Conference Proceedings, vol. 1291 (2010), Estruch: Optics letters 36, 3160 (2011)]. We have recently unraveled the multiple wave mechanisms ruling the behaviour of this dual structure: more precisely, we used Mason's formalism with Signal Flow Graphs [Estruch: Optics express, To be published (2012)] to highlight the influence of the lateral shift between the gratings. This simple method is particularly useful to study resonant systems and it is a powerful tool to validate the understanding of the spectral behaviour of an optical structure. Following this theoretical work, an experimental bench has been set up to study the near field interaction between subwavelength gratings in the infrared range. To be able to tailor in real-time the transmission shape of the filtering device, the two subwavelength gratings are driven completely free into space by using piezoelectrical actuators. This allows control of the lateral and longitudinal distances between the gratings with nanometric resolution. Thus, we design a filtering structure with the transmission resonance flanked by resonant anomalies which father high rejection efficiency out of the transmission band. The realized structure is a very good candidate for multispectral imaging spectrometry with practical use in gas detection and identification.

8632-9, Session 2

Plasmonic photonic-crystal slab as an ultrasensitive and robust optical biosensor

Alexander V. Baryshev, Toyohashi Univ. of Technology (Japan); Alexander M. Merzlikin, Institute for Theoretical & Applied Electromagnetics (Russian Federation); Mitsuteru Inoue, Toyohashi Univ. of Technology (Japan)

To detect lower abundance proteins in analytes, when detecting diseases at early stages, highly sensitive, reliable diagnostic approaches are necessary. Optical sensors where refractive index sensing is achieved by dispersion of surface plasmon resonance (SPR) are widely applied for detecting tiny variations in biological analytes. Another effective approach to high-resolution sensing is usage of the Bloch surface wave resonance (SWR) excited on a surface of dielectric multilayer (1D photonic crystals, PhC). The binding event is well detectable only in close vicinity of the sensor surface since the SPR-generated near field is pinned to it and is not extended into an analyte. That is why, for probing negligible changes within an analyte, sensors with (i) higher sensitivity and (ii) allowing screening an extended volume can be of great value. Both (i) and (ii) might be satisfied by conventional SWR-based sensors. However, the experimental accuracy for SWR excitation must be extremely high, and the maximum response is observed close to the total internal reflection (TIR) condition. Can the mentioned above limitations of the optical sensors be solved while keeping their advantages? Apparently, a sensor with a new functioning principle is necessary to satisfy the mentioned issues which will have (iii) a larger qualitative robustness—a sensor with high performance margins at lower requirements to structural parameters and measurement tolerance.

In this work we demonstrate sensing performances of a structure comprising a 1D PhC and a plasmonic layer of a thin gold film (the PPhC sensor). The analysis was done for the p polarization. Results showed that the PPhC slab is an ultrasensitive optical biosensor that surpasses the sensitivity of the SPR-based sensors and performance margins of the conventional SWR-based ones.

8632-10, Session 2

Sunflower photonic quasicrystals

Yufeng Liao, Haitao Dai, Yang Yang, Shu Guo Wang, Xiao Wei Sun, Tianjin Univ. (China)

Gradient index structures ?GISs? have attracted much attention in recent years, which have potential applications in invisibility cloaks and an optical black hole etc.. However, it is difficult to fabricate GISs with continuous index distribution in practical. Therefore, Graded photonic crystals (GPCs) were developed to mimic the continuous GISs by means of discrete periodic structures. Very recently, graded dodecagonal photonic quasicrystals were designed to focus light similar with Luneburg lens. Simulated results showed that graded quasicrystals could exhibit better focusing property in compared with the graded photonic crystals with square lattice. In this paper, we present one planar graded photonic quasicrystals based on spiral structures (SGPQs) or sunflower structures to mimic Luneburg lens focusing the incident plane wave. The radius of individual cylinder of the SGPCs was determined by the index profile of Luneburg lens based on Maxwell-Garnett effective medium theory. The focusing features of the SGPQs were investigated by means of finite difference time domain (FDTD) methods. Numerical results show that the SGPQs-based Luneburg lens can focus the light more tightly and efficiently in comparison with graded photonic crystals. As we all know, the spiral structure is determined by the Golden angle. We thereby study the focusing properties of SGPQs with different generating angle to optimize the focusing behavior of the proposed devices.

8632-11, Session 3

Optoelectronic silicon-based nanostructures (Invited Paper)

Axel Scherer, Sameer Walavalkar, Andrew Homyk, Se-Heon Kim, Aditya Rajagopal, California Institute of Technology (United States)

Over the past decades, silicon photonic technology has enabled applications ranging from data communications to biomedical sensing. Its low absorption losses in the near infrared leads to low-loss waveguides, yet light emitters and detectors can be designed in silicon by careful control over the device geometry. Here we describe examples of geometric control at the nanoscale and demonstrate new functions in silicon optoelectronic devices.

8632-12, Session 3

Plasmonic nanoscale energy converters: hot carrier and plasmoelectric energy generation (Invited Paper)

Harry A. Atwater Jr., Matthew T. Sheldon, California Institute of Technology (United States); Ana M. Brown, Stanford Univ. (United States); Andrew J. Leenheer, Prineha Narang, California Institute of Technology (United States)

Recently consider attention has turned towards finding a silver lining in the cloud of plasmonics—extracting energy from the inevitable optical losses resulting from plasmon decay. In this paper, we assess the limits to energy conversion efficiency via hot electron injection across a rectifying junction from localized plasmon decay. We also describe a method for generation of DC electrical power from resonant optical absorption in plasmonic nanostructures, which we term the “plasmoelectric effect”. Power conversion results from the dependence of the plasmon resonance frequency on electron density. Electrically connecting two metallic nanostructures with resonant absorption maxima at distinct frequencies, and irradiating both structures with an intermediate frequency, induces electron transport from the high frequency plasmonic resonator to the low frequency resonator. This

process is entropically driven by an increase of the absorbed incident radiation, which results from the shifted plasmon resonances induced by the new charge density configuration.

8632-13, Session 3

2D-photonic crystals for record solar cell efficiency (*Invited Paper*)

Eli Yablonovitch, Owen Miller, Vidya Ganapati, Gregg Scranton, Univ. of California, Berkeley (United States)

Solar cell technology is changing. New efficiency records are being set, currently 28.8% efficiency in a single junction cell. It is known that solar cells should not simply be plane parallel slabs, but that they are optimized when there is a surface texture on at least one surface. This permits light trapping inside the cell. Within geometrical optics, it was long ago shown that a random texture already achieves the theoretical limit; $4n^2 \sim 50X$ internal path length enhancement. Indeed, light trapping is used in virtually all solar panels within the \$30B/year solar cell industry in the world today. Future generation solar cells will be thin films, less than one-wavelength thick, firmly within the regime of physical optics, not geometrical optics. In physical optics, no scientific limit is known for the light-trapping path-length enhancement, nor do we know the optimal surface texture. Thus we need to find the optimal surface shape for thin film solar cells within the paradigm of "Inverse Design" and mathematical "Shape Optimization". Once the ideal surface texture is mathematically determined, it is expected that all future generations of solar cells will adopt that shape.

8632-14, Session 3

Light trapping, strong exciton-photon coupling, and BEC in photonic band gap materials (*Invited Paper*)

Sajeev John, Univ. of Toronto (Canada)

Photonic band gap (PBG) materials [1,2] are artificial periodic dielectric microstructures capable of trapping light in three-dimensions [3] on sub-wavelength scales without absorption loss. This enables very strong coupling of light to matter where desired, including effects such as bound states between excitons and photons [4,5] and exceptional coherent optical control of the quantum state of quantum dots [6].

I describe how a semiconductor quantum well sandwiched by 3D PBG materials above and below can provide very strong coupling between excitons and band edge photons and at the same time avoid radiative recombination decay [7]. Using a simple model, I discuss the nature of Bose-Einstein condensation of these long-lived exciton-photon bound states and crossover from a coherent to anti-bunched state with lowering of temperature or confinement area [8].

References

1. S. John, Physical Review Letters 58, 2486 (1987)
2. E. Yablonovitch, Physical Review Letters 58, 2059 (1987)
3. S. John, Physical Review Letters 53, 2169 (1984)
4. S. John and J. Wang, Phys. Rev. Lett. 64, 2418 (1990)
5. S. John and S. Yang, Physical Review Letters. 99, 046801 (2007)
6. X. Ma and S. John, Physical Review Letters 103, 233601 (2009)
7. S. Yang and S. John, Physical Review B 75, 235332 (2007)
8. S. Yang and S. John, Physical Review B 84, 024515 (2011)

8632-15, Session 4

Genetic algorithm design and phase mask holography of 3D photonic crystals and metamaterials (*Invited Paper*)

Paul V. Braun, Univ. of Illinois at Urbana-Champaign (United States)

A few years ago, we demonstrated the use of elastomeric binary diffractive phase masks to form 3-D holographic micro- and nano-structures in photosensitive polymers. Laser radiation passing through the phase mask creates a three dimensional distribution of intensity in the photosensitive layer through its thickness, which can be developed yielding a 3-D replica of the intensity distribution. Using a genetic algorithm (GA) based phase mask approach makes possible the design of phase masks for nearly arbitrary 3-D structures. First, the surface relief profile and the incident polarization are encoded into a binary representation called a "chromosome". Then, a random population of these chromosomes is generated and each chromosome is assigned a "fitness" score. Here, fitness quantifies how closely a given chromosome produces the desired target structure. Chromosomes having superior fitness are selected to "reproduce" and "mutate" with greater frequency, providing the necessary driving force toward improved phase mask designs over several generations. Importantly, the manufacturability of the phase mask can be included as part of the fitness factor. The optical response of the resulting structure can also be used as part of the fitness factor, with the only complication the time required to simulate the optical properties of every structure which at least to date has limited this approach to simple dielectric structures. To date, two different structures using the GA design approach have been targeted: rod-connected diamond (fcc) and spiral (hexagonal). An excellent match of experiment and theory has been observed.

8632-16, Session 4

Fiber based holographic lithography for fabrication of period tunable two-dimensional photonic crystal templates

Kai Shen, Michael R. Wang, Univ. of Miami (United States)

Photonic crystals have attracted lots of research and development interests due to the novel properties of controlling the behavior of electromagnetic waves. The fabrication of photonic crystals can be performed by a number of techniques including multi-photon laser direct writing, electron-beam lithography, self-assembly of colloidal particles, and holographic lithography. Considering the cost issue and large area fabrication, holographic lithography using multi-beam interference, special prisms and Lloyd's mirror has shown its advantages since it can produce defect-free nanostructures over large area in one exposure fabrication. However, holographic lithography suffers the difficulty in multi-beam alignment. The beam alignment can be time consuming and critical every time when we want to change the nanostructure periods and patterns, or we need to order lots of prisms to meet different requirements. A fiber based holographic lithography system is introduced to simplify the multi-beam alignment since it greatly reduces the number of beam splitting and mirror components. Both manual and computer controlled beam alignments have demonstrated its effectiveness in fabricating various photonic crystals templates. Furthermore, through carefully adjusting the polarizations of output lights, it can realize artificial metamaterials, which can be used for negative refraction, super-resolution imaging, planar slab lensing, etc.

8632-17, Session 4

Free-standing monolithic LiNbO3 photonic crystal slabs

Jun Deng, Vanga S. Kumar, Hongwei Gao, National Univ. of Singapore (Singapore); Ching Eng J. Png, A*STAR Institute of High Performance Computing (Singapore); Ning Xiang, Andrew A. Bettiol, Aaron J. Danner, National Univ. of Singapore (Singapore)

2D photonic crystal (PC) structures have been widely studied for future photonic integrated circuits applications; in particular, air-bridge PC slabs can be used for tunable filters, sensors and optical MEMS. However, such PC slabs are very difficult to realize on bulk LiNbO3, which is a

widely used dielectric material in integrated and nonlinear optical devices because of its large electro-optic coefficients and transparency range. Our ability to form such structures as reported here is thus important not only for traditional photonics applications, but for potential quantum optical information processing. The main challenges are the well-known dry etching problems and the impact of conical PC holes on photonic crystal properties which inevitably arise when ion beam techniques are used. In this work, however, we demonstrate a monolithic approach to fabricate free-standing LiNbO₃ PC slabs. Ion implantation is first applied to form a buried lattice-damage layer at a specified depth in bulk LiNbO₃. Photonic crystal slabs are then made with FIB milling followed by wet etching. A high etching rate of 100 nm/min for the implanted layer has been obtained. The fabricated results show PC slabs with controllable thickness a large underlying air gap with thickness > 1 μm (between slabs and substrate). A vertical PC profile has been achieved because the bottoms of the milled cones were truncated by the air gap, with a measured slope angle of the hole sidewalls at 89 degree. Numerical simulation and free-space illumination measurements of the reflectance and transmission spectrum over a broadband wavelength on both visible and infrared range are performed to analysing the properties of various PC slabs. The free-standing LiNbO₃ structures make them easily incorporated into MEMS and show potential applications for tunable optical filters, sensors, and quantum optics applications where high quality, single crystal LiNbO₃ is needed. The authors acknowledge Grant # R263000690112 under the Singapore Ministry of Education's Academic Research Fund.

8632-18, Session 4

Spectroscopic ellipsometry study of novel nanostructured transparent conducting oxide structures

Akram Amooali Khosroabadi, Palash Gangopadhyay, Robert A. Norwood, College of Optical Sciences, The Univ. of Arizona (United States)

Various optical constants including effective thickness, effective refractive index and extinction coefficient of an array of nanostructured transparent conducting electrodes (nsTCO) have been measured using spectroscopy ellipsometry. Ellipsometry spectra of the nanostructured samples show several interesting features compared to their planar counterparts. Several Cauchy-like dispersion layers together with Lorentzian oscillators within the effective medium approximation regime have been shown to efficiently model the optical properties of the nsTCOs. The top dispersive layer is modeled by mixing laws in order to incorporate the void (spacing between the pillars) and the pillars. Structural parameters, such as pitch, diameter and height of the pillars in nsTCOs can be controlled efficiently using our novel nanoimprinting approach and we show that the optical properties and ellipsometric behavior are strongly influenced by the dimensions of the pillar structures. Using the structure obtained by fitting the ellipsometric data, reflection spectra of the nsTCO structure alone can be simulated for different input polarizations of light, s and p. Where there is a sharp peak in the ellipsometry spectra, we see a peak in reflection spectra of p polarized light as well. Reflection spectra of the nsTCOs have also been simulated for different incidence angles of input light and show that with increased incident angle, the reflection of p polarized light increases over the s-polarized light. Further, there is more reflection of p polarized light at shorter wavelengths. The penetration depth of the light into the samples is on the order of a few microns. Higher order derivatives of the obtained dielectric constants of the structures, enable us to probe the electronic transitions of the nsTCOs as well.

8632-19, Session 5

Optomechanical and optoacoustic phenomena in microstructured silica fibers (Invited Paper)

Anna Butsch, M. S. Kang, Tijmen G. Euser, Philip S. Russell, Max Planck Institute for the Science of Light (Germany)

The talk will report on optomechanical and optoacoustic interactions in microstructured silica fibers. First, novel aspects of an optomechanically induced nonlinearity, occurring in a new type of optical fiber - the “dual-nanoweb” fiber with two ultra-thin closely spaced glass membranes (webs) – will be covered. Light guided in this structure can exert attractive or repulsive optical gradient forces between the webs, causing them to be pushed together or pulled apart. The elastic deflection of the webs is, in turn, coupled to the electromagnetic field distribution and results in a nonlinear change in the effective refractive index within the fiber. This optomechanical nonlinearity can exceed the Kerr effect by many (up to 8) orders of magnitude, and in contrast to previously reported cavity-based optomechanical devices it does not rely on the optical resonances, it is optically broadband [1]. Furthermore, it allows the formation of stable self-trapped optical modes that represent a novel kind of optical soliton. The first successful fabrication of a guiding dual-nanoweb fiber, in which the optomechanical nonlinearity is experimentally measured, will be reported [2]. Another type of light-matter effect, to be discussed in the talk, is optoacoustic interactions via electrostriction in the micron-sized core of a photonic crystal fiber. It will be shown that coherent optically-driven acoustic waves, tightly guided in the core, can facilitate in-fiber dynamic optical isolation and all-optical switching, thus providing a new functionality that is beneficial in various types of all-optical systems [3].

References:

- [1] A. Butsch, C. Conti, F. Biancalana and P. St.J. Russell, “Optomechanical self-channeling of light in a suspended planar dual-nanoweb waveguide,” *Phys. Rev. Lett.* 108, 093903 (2012).
- [2] A. Butsch, M. S. Kang, T. G. Euser, and P. St.J. Russell, “Strong optomechanical nonlinearity in dual-web fibre,” *Frontiers in Optics Conference*, San Jose, paper PDPC3 (2011).
- [3] M. S. Kang, A. Butsch, and P. St.J. Russell, “Reconfigurable light-driven opto-acoustic isolators in photonic crystal fibre,” *Nature Photonics* 5, 9, 549 (2011).

8632-20, Session 5

Modeling loss and backscattering in a hollow-core photonic-bandgap fiber using strong perturbation theory

Kiarash Zamani Aghaie, Michel J. F. Digonnet, Shanhui Fan, Stanford Univ. (United States)

Surface roughness is the dominant source of loss and backscattering in hollow-core photonic-bandgap fibers (PBFs). Prediction of these characteristics is a complicated problem that requires calculation of a large number of fiber modes with a high accuracy, knowledge of the roughness statistics, and using coupled-mode theory to compute coupling from the fundamental mode to other modes. In previous studies, we and others used a model of the fiber’s permittivity profile that neglected structural deformations on the first two rows of cladding holes, which led to errors in the predicted fields of the fiber modes. The accuracy was further limited by the use of weak perturbation theory to compute mode coupling, which fails due to the high index contrast between the air holes and the silica membranes. Earlier investigations also assumed that the surface roughness had either the statistics of frozen surface-capillary waves, the ideal thermodynamic limit, or unproven statistics.

In this work, we improve on these earlier approaches by utilizing (1) a new permittivity-profile model that includes the structural deformations present in the first two rows of cladding holes, measured with a scanning

Conference 8632: Photonic and Phononic Properties of Engineered Nanostructures III

electron microscope; (2) strong perturbation theory; (3) reasonable roughness statistics that accounts for the cylindrical shape of the air holes and the finite thickness of the membranes, and consistent with physical measurements reported by others. With this new model, we predict values of the loss and of the backscattering coefficient for NKT Photonics' HC-1550-02 hollow-core fiber in reasonable agreement with measured values.

8632-21, Session 5

Guided-mode based Faraday rotation spectroscopy within a photonic bandgap fiber

Florian V. Englich, The Univ. of Adelaide (Australia); Michal Grabka, Jagiellonian Univ. in Krakow (Poland); David G. Lancaster, Tanya M. Monro, The Univ. of Adelaide (Australia)

Microstructured optical fibers provide a unique environment for new compact sensing of gases as they offer advantages including long optical pathlengths, strong confinement of high power light and extremely small sample volumes compared to free-space gas sensing architectures. Here we investigate the interaction of a modulated magnetic field with guided light to detect a paramagnetic active gaseous medium within a hollow-core photonic bandgap fiber (HC-PCF). This novel fiber-optic approach to Faraday Rotation Spectroscopy (FRS) demonstrates the detection of molecular oxygen at 762.309 nm with nano-liter detection volume. By using a differential detection scheme for improved sensitivity, guided-mode FRS spectra were recorded for different coupling conditions of the light (i.e., different light polarization angles) and various gas sample pressures. The observed FRS signal amplitudes and shapes are influenced by the structural properties of the fiber, and magneto-optical properties of the gas sample including the magnetic circular birefringence (MCB) and the magnetic circular dichroism (MCD). A theoretical model has been developed to simulate such FRS signals, which are in good agreement with the observed experimental results and provide a first understanding of guided-mode FRS signals and dynamics of the magneto-optical effects inside the optical fiber. The results show that microstructured optical fibers can offer a unique platform for studies concerning the propagation of light in linearly and circularly birefringent media.

8632-22, Session 5

Soft glass film deposition in silica solid and hollow core photonic crystal fiber

Christos Markos, National Hellenic Research Foundation (Greece); Kyriakos G. Vlachos, Univ. of Patras (Greece); Thomas Vassiliadis, Vasilios Dracopoulos, Foundation for Research and Technology-Hellas (Greece); George Kakarantzas, National Hellenic Research Foundation (Greece); Spyros N. Yannopoulos, Foundation for Research and Technology-Hellas (Greece) and Univ. of Patras (Greece)

We experimentally demonstrate a novel method which allows deposition of solution-based soft-glass films (chalcogenide) inside the holes of commercially available solid and hollow core photonic crystal fiber (PCF). Two different concentrations of amorphous solution amine-based/As₂S₃ chalcogenide glass were synthesized and infiltrated in PCFs using capillary forces. The solvent evaporation led to nanoscale film thickness formation in the silica capillaries of solid and hollow core PCFs. One main advantage of the method is that the annealing process provides control of the refractive index of the formed glass films. The PCFs employed in our experiments were ESM-12, LMA-5 as solid-core and HC-1550-04 as hollow-core. The transmission spectra recorded using supercontinuum source indicating ARROW guidance in the solid core PCFs whereas the bandgap guidance in the hollow core fiber remained. In order to confirm the structural properties of the formed As₂S₃ glass films in all cases, scanning electron microscopy (SEM) and Raman scattering

measurements were employed. The proposed deposition method provides the ability to enhance significantly the nonlinearity in an all-silica PCF in a simple and cost effectiveness manner. Furthermore, multi-material deposition in the holes of the PCF is experimentally feasible using the suggested approach

8632-23, Session 6

Room-temperature high-performance laser diodes from 3 μm to 300 μm (*Invited Paper*)

Manijeh Razeghi, Northwestern Univ. (United States)

Due to continuous perfection of heterostructure design, material growth, device fabrication, and thermal management, we have recently significantly extended the wavelength coverage of InP based quantum cascade lasers. At the short wavelength side, room temperature continuous wave operation has been achieved down to 3 μm. At the long wavelength side, we have realized a room temperature laser source emitting around 300 μm, based on intracavity difference frequency generation. These demonstrations pave the way of realizing an ultra-broadband gain medium using a single material system.

8632-24, Session 6

Nonlinear optics with nW optical powers in photonic crystals (*Invited Paper*)

Sonia Buckley, Kelley Rivoire, Arka Majumdar, Jelena Vuckovic, Stanford Univ. (United States)

We demonstrate enhanced nonlinear frequency conversion in photonic crystal cavities in GaP or GaAs. We first show resonantly enhanced second harmonic and sum frequency generation in GaP L3 photonic crystal cavities and photonic crystal waveguides. Novel photonic crystal designs, allowing resonances broadly spaced in frequency, can further enhance these nonlinear processes. We demonstrate such a design fabricated in (111)-oriented GaAs. These nonlinear frequency conversion elements can be integrated with quantum emitters. We combine this frequency conversion interface with a single InAs quantum dot to produce a fast single photon source that is optically triggered at telecommunications wavelength. We also demonstrate high signal-to-noise quasi-resonant excitation of InP quantum dots via excitation with intra-cavity generated second harmonic. These frequency conversion techniques are critical for applications including light sources at wavelengths that are difficult to access with existing lasers, IR upconversion-based detectors, and photonic quantum interfaces between quantum emitters and fiber-optic networks.

8632-25, Session 6

Spontaneous emission control of single quantum dots by electrostatic tuning of a double-slab photonic crystal cavity

Leonardo Midolo, Francesco Pagliano, Thang B. Hoang, Tian Xia, Frank W. M. van Otten, Technische Univ. Eindhoven (Netherlands); Lian H. Li, Edmund H. Linfield, Univ. of Leeds (United Kingdom); Matthias Lerner, Sven Höfling, Julius-Maximilians-Univ. Würzburg (Germany); Andrea Fiore, Technische Univ. Eindhoven (Netherlands)

Quantum photonic integrated circuits (QPICs) operate at the single photon level and provide a platform for quantum computation and for the study of quantum electrodynamics phenomena. Fast and efficient on-chip single photon sources can be realized using photonic crystal cavities (PCCs) coupled to single semiconductor quantum dots (QDs). However, to compensate the natural spectral inhomogeneity of self-

Conference 8632: Photonic and Phononic Properties of Engineered Nanostructures III

assembled QDs and the unavoidable fabrication imperfections, the real-time tuning of a PCC is essential. Moreover, QPICs applications require an independent control of many cavities at low temperatures.

Nano-electro-mechanical systems have been proposed as a viable solution for the continuous wavelength tuning of a PCC on a chip. In this work we demonstrate the mode tuning of a two-dimensional PCC fabricated on a double GaAs slab and the alignment to single excitonic lines. The tuning is achieved by modulating the inter-membrane distance by applying electrostatic forces across a p-i-n diode under reverse bias. The double-slab structure allows us to completely isolate the QD region from the actuator while keeping a small device size. We present the operation of the device at low temperatures ($< 10\text{K}$) and we demonstrate Purcell effect via the electromechanical control. The spontaneous emission rate of single dots has been modified by over a factor of ten, tuning the cavity reversibly between on- and off-resonant conditions over a 13 nm range with $< 5\text{ V}$ reverse bias. The coupling to ridge waveguides has also been investigated towards the realization of scalable and controllable integrated single photon sources.

8632-26, Session 6

Remote control of spontaneous emission using coupled cavity quantum electrodynamics

Chaoyuan Jin, Eindhoven Univ. of Technology (Netherlands); Milo Y. Swinkels, Robert Johne, Thang B. Hoang, Leonardo Midolo, René P. J. van Veldhoven, Andrea Fiore, Technische Univ. Eindhoven (Netherlands)

The dynamic tuning of the cavity characteristics within the emitter's lifetime is needed to control the timing and waveform of the emitted photons. In practical applications, it requires a "remote" control scheme which produces large changes in the local density of states at the emitter's position but does not affect the emitter-cavity interaction with local perturbations. By implementing a novel concept based on coupled cavity quantum electrodynamics (CCQED), we demonstrate the remote all-optical control of the spontaneous emission of quantum dots using coupled photonic crystal cavities. By thermo-optically tuning a Fabry-Perot cavity in resonance with a target cavity, the Q-factor and the local density of states experienced by emitters in the target cavity are modified, leading to a change in the spontaneous emission rate. A theoretical analysis of the CCQED system shows that the spontaneous emission rate change can be even higher than the Q-factor change due to a reduction of the vacuum field at the emitter's position when the two cavities are brought in resonance. Both the weak and strong coupling regimes of two cavities have been observed experimentally and the spontaneous emission decay rate has been modulated by more than a factor of three with remote optical control. This represents the first demonstration of the all-optical remote control of cavity quantum electrodynamics and an important step towards dynamic control, which can be achieved by replacing the thermo-optic tuning with ultrafast carrier injection.

8632-27, Session 6

Strongly inhibited spontaneous emission of semiconductor quantum dots in 3D photonic band gap crystals

Elahe Yeganegi, Ad Lagendijk, Allard P. Mosk, Willem L. Vos, Univ. Twente (Netherlands)

Control over spontaneous emission has many applications ranging from miniature lasers and light-emitting diodes, to single-photon sources for quantum information. It is known that emission rate of light sources is controlled by their environment, notably by photonic crystals. In certain three-dimensional crystals, there is a frequency range for which light is not allowed to propagate in any direction, called the photonic band gap.

We have fabricated high-quality inverse woodpile photonic crystals from monocrystalline silicon using CMOS-compatible methods.

We have performed time-resolved spontaneous emission experiments of PbS semiconductor quantum dots in three-dimensional silicon photonic band gap crystals at near-infrared frequencies (See PRL. 107. 193903, (2011)).

We observe that the emission rate is strongly modified by the photonic crystal. We observe strong inhibition in the band gap with a maximum of 18X, which is robust to dipole orientations and positioning in the unit cell. In time dependent data we find evidence for novel finite-size behavior.

8632-28, Session 7

Effective dynamic properties of micro-architected composites: theory and applications (*Invited Paper*)

Siaouche Nemat-Nasser, Ankit Srivastava, Univ. of California, San Diego (United States)

There has been a considerable amount of recent research in the fields of phononics and acoustic metamaterials. In this paper we discuss the explicit form of the effective dynamic Willis constitutive relation which emerges equivalently both from ensemble averaging and field averaging of the field variables. These effective constitutive parameters are central to the idea of metamaterials. We elaborate upon the existence and emergence of coupling in the dynamic constitutive relation and further symmetries of the effective tensors. Finally we present theoretical considerations and experimental results within the context of applying the homogenized parameters for practical applications like impedance matching and transformational acoustics.

8632-29, Session 7

Adaptive acoustic metamaterials through nonlinear interactions (*Invited Paper*)

Massimo Ruzzene, Georgia Institute of Technology (United States)

Metamaterials consist of engineered microstructural assemblies that exhibit superior properties in comparison to less-composed or naturally-occurring materials. Their unusual wave properties include band-gap behavior, response directionality, left-handedness, and negative acoustic refraction, among others. These features, and their application for the design of acoustic filters, waveguides, logic ports, and ultrasonic transducer arrays, motivate the investigation of elastic wave propagation in micro-structured media.

The presentation illustrates the directional properties of periodic media, as defined by their ability to direct waves in preferential direction. Such properties are first illustrated on simple spring-mass systems, and subsequently demonstrated in complex structural lattices operating in linear and nonlinear deformation regimes. Lattices that undergo topological changes resulting from structural instabilities are discussed as examples of adaptive metamaterials. Specifically local instabilities are investigated as effective means to provide the considered periodic assemblies with adaptive bandgaps and wave steering characteristics.

8632-30, Session 7

Comprehensive enhancement of the thermoelectric figure-of-merit using phononic crystals and low-dimensional materials (*Invited Paper*)

Charles M. Reinke, Sandia National Labs. (United States);

Conference 8632: Photonic and Phononic Properties of Engineered Nanostructures III

Mehmet F. Su, The Univ. of New Mexico (United States); Byung-II Kim, Sandia National Labs. (United States); P. Hopkins, Univ. of Virginia (United States); D. Goettler, Z. Leseman, The Univ. of New Mexico (United States); Roy H. Olsson III, Sandia National Labs. (United States); Ihab El-Kady, Sandia National Labs. (United States) and The Univ. of New Mexico (United States)

In this paper, we describe the enhancement of the three parameters of the thermoelectric figure-of-merit (ZT) simultaneously using nanostructured phononic crystals (PnCs) and low-dimensional metallic structures. Most published research on improvement of ZT ($ZT = \frac{S^2 \sigma}{T \kappa}$, where S , σ , and κ are the Seebeck coefficient, electrical conductivity, and thermal conductivity, respectively) has largely focused on only one of its components, with the hope that the other two remain favorable. However, due to the interdependent nature of the three components, efforts to reduce κ by incoherent phonon scattering inadvertently create electron scattering with a corresponding reduction in σ , and efforts to increase σ via doping typically decrease in S in accordance with the Mott relationship.

Our approach for circumventing these issues uses PnCs and metallic nanostructures to decouple the components of ZT. PnCs are a periodic arrangement of elastic scattering centers embedded in a homogeneous background matrix that create a controllable redistribution of the phononic density of phonon states (DOS), making them particularly attractive for modifying phonon propagation, and hence thermal transport, in semiconductor materials. In addition, several studies have shown that the S of a material can be enhanced when its electrons are confined in a quantum well, such as in metallic surface states, or a quantum dot, such as metallic nanoparticles, while the metallic inclusions increase the σ of the PnC. Thus, combining such metallic structures with PnC patterning can result in a comprehensive increase in all three components of ZT, resulting in planar, scalable materials with applications in active cooling and waste heat recovery.

Sandia National Laboratories is a multi-program laboratory managed and operated by Sandia Corporation, a wholly owned subsidiary of Lockheed Martin Corporation, for the U.S. Department of Energy's National Nuclear Security Administration under contract DE-AC04-94AL85000.

8632-35, Session 7

Cavity optomechanics and the Casimir force: dynamics and applications

David Woolf, Pui-Chuen Hui, Harvard Univ. (United States); Alejandro Rodriguez, Harvard Univ. (United States) and Massachusetts Institute of Technology (United States); Eiji Iwase, Waseda Univ. (Japan); Mughees Khan, Ray Ng, Harvard Univ. (United States); Steven G. Johnson, Massachusetts Institute of Technology (United States); Federico Capasso, Harvard School of Engineering and Applied Sciences (United States); Marko Loncar, Harvard Univ. (United States)

The gaps separating mechanically oscillating elements and their surroundings are getting increasingly smaller, bringing into play effects such as the Casimir force, which can lead to device failure but can also contribute to interesting new dynamics. Here we present a versatile optomechanical structure fabricated with novel stress management techniques to control the membrane-substrate separation, which can act as an active sensor or reconfigurable element in a chip-based nano-mechanical system. The geometry consists of a two-dimensional, defect-free photonic crystal membrane suspended above a Silicon-on-Insulator substrate, built from a single wafer. The membrane-substrate separation is tunable through engineering of the support structure, and we have thus far been able to achieve separations as small as 100 nm. At these separations the Casimir force significantly perturbs the static and dynamic device behavior, introducing mechanical nonlinearity and bistability. Our devices support photonic modes which can generate strong attractive and repulsive optical forces for actuation and combating stiction while minimizing the impact of two-photon absorption on device

behavior. By controlling the separation, we are able to explore for the first time in a double membrane Si-based system the optomechanical and photo-thermal-mechanical dynamics in conjunction and isolation, measuring the strongest repulsive optomechanical coupling in any geometry to date, and paving the way toward an integrated Casimir-mechanical oscillator.

8632-31, Session 8

Phoxonic crystals: tailoring the light-sound interaction at the nanoscale (*Invited Paper*)

Alejandro Martínez, Univ. Politècnica de València (Spain)

Phoxonic crystals are periodic structures affecting simultaneously the propagation of light (photons) and sound (phonons) of similar wavelengths. For instance, by introducing periodicity of the order of the micron on semiconductor membranes, a phoxonic band gap for near infrared light and sound at GHz frequencies appears [1]. The insertion of defects can give rise to the simultaneous localization of photons and phonons in cavities and waveguides [2]. Moreover, new structures can be tailored to enhance the light-sound interaction in such small volumes. In this work, the last advances in phoxonic crystal structures (including the so-called optomechanical cavities [3]) will be reviewed. Techniques to inject light and sound in phoxonic structures will be described. Future possible applications of phoxonic crystals, ranging from ultrasensitive sensing to all-optical information storage, will finally be introduced.

[1] Y. Pennec, B. Rouhani, E. El Boudouti, C. Li, Y. El Hassouani, J. Vasseur, N. Papanikolaou, S. Benchabane, V. Laude, and A. Martinez, "Simultaneous existence of phononic and photonic band gaps in periodic crystal slabs," *Opt. Express* 18, 14301–14310 (2010).

[2] Vincent Laude, Jean-Charles Beugnot, Sarah Benchabane, Yan Pennec, Bahram Djafari-Rouhani, Nikos Papanikolaou, Jose M. Escalante, and Alejandro Martinez, "Simultaneous guidance of slow photons and slow acoustic phonons in silicon phoxonic crystal slabs," *Opt. Express* 19, 9690-9698 (2011)

[3] M. Eichenfield, R. Camacho, J. Chan, K. J. Vahala, and O. Painter, "A picogram- and nanometre-scale photonic-crystal optomechanical cavity," *Nature* 459 (7246), 550–556 (2009).

8632-32, Session 8

Optomechanics with photonic crystals in diamond and silicon (*Invited Paper*)

Marko Loncar, Harvard Univ. (United States)

I will present a versatile optomechanical structure fabricated using novel stress management techniques that allow us to suspend a two-dimensional defect-free silicon photonic-crystal membrane above a Silicon-on-Insulator (SOI) substrate with a gap that's tunable to below 200 nm. Our devices are able to generate strong attractive and repulsive optical forces over a large surface area which is of interest for control of stiction (Casimir force).

Owing to its excellent mechanical, optical and thermal properties, diamond is promising material for realization of opto-mechanical devices. In addition to applications in force and mass sensing, diamond nano-mechanical and optical resonators would be suitable for sensing in harsh environments, bio-medicine, magnetometry, and so on. However, fabrication of devices in single crystal diamond substrates is challenging. We have recently developed an angle-etching technique suitable for realization of free-standing single-crystal diamond nano structures, and used it to realize high-Q optical and mechanical nano-resonators.

8632-33, Session 8

Metallic-pillar-based phononic crystal structures for radio frequency applications

Reza Pourabolghasem, Saeed Mohammadi, Ali A. Eftekhar, Ali Adibi, Georgia Institute of Technology (United States)

No Abstract Available

8632-34, Session 8

Electrostatically-tunable high-Q and low-mode-volume one-dimensional photonic crystal resonators

Mehdi Miri, Georgia Institute of Technology (United States) and Sharif Univ. of Technology (Iran, Islamic Republic of); Ali A. Eftekhar, Majid Sodagar, Ali Adibi, Georgia Institute of Technology (United States)

One Dimensional Photonic Crystal (1D PhC) based resonators due to their ultra-high quality factor and low modal volume, have been subject of many studies. Here we present such a cavity with quality factor as high as 700,000 and mode volume as low as $0.158 (\lambda / 2n)^3$. The optical cavity is made by modulating the band gap of a 1D PhC structure. The PhC itself is formed by perforating rectangular air holes in a silicon slot waveguide. The presented structure can be used in different applications such as sensing, optical modulation, and opto-mechanics. As an example of these applications we propose the wideband mechanically tunable optical cavity in which the mechanical displacement is achieved by electrostatic forces. Our consistent optical and mechanical simulations show that more than 60 nm wavelength change is achievable by applying less than 1 Volt corresponding to mechanical displacement of 30 nm. Compared to previously reported results the proposed structure has up to seven times higher tuning sensitivity (30 nm wavelength change at 1550 nm for 10 nm mechanical displacement). This higher sensitivity can be attributed to the fact that in our structure field is mainly confined in the air slot, and also the structure has relatively lower weight.

8632-36, Session 9

Conformal transformation of photonic crystal structures

Marco Zocca, Matthijs Langelaar, Fred van Keulen, Technische Univ. Delft (Netherlands)

A photonic integrated circuit features a number of mode-matching sections and propagation bends, all of which occupy significant chip area, and generally introduce optical power losses and back-reflections. Local distributed reflectors such as resonant photonic crystals are a possible route to in-plane loss engineering where tight propagation bends or high field confinement are required by design.

As recent theoretical results suggest, locally-periodic patterns of the dielectric constant can give rise to electromagnetic bandgaps, even if long-range (ideal) periodicity is not fulfilled. A conformal transformation of such structures is expected to preserve the center frequency of the photonic bandgap by enforcing equivalence of their optical lengths. The scattering structure of the deformed propagation medium is preserved by a corresponding modification of the local dielectric permittivity, as prescribed by Fermat's principle; it is to note that conformal dielectric metamaterials have so far been only demonstrated in the subresonant regime.

We present an algorithm to map a reference diffracting structure along an arbitrary boundary, and numerically characterize some photonic device features realized with it. The deformed lattice patches produced have been found to explain well the geometries that were conceived with a heuristic reasoning in previous literature.

Applications we consider include an enhanced channel waveguide bend, a modal adapter between fast- and slow-light waveguides and novel geometries of integrated photonic microcavities.

8632-37, Session 9

Mapping the absolute electromagnetic field strength of individual field components inside a photonic crystal

Thomas Denis, Bob Reijnders, Joan H. H. Lee, Univ. of Twente (Netherlands); Peter J. M. van der Slot, Willem L. Vos, Klaus J. Boller, Univ. Twente (Netherlands)

Photonic crystals allow an unprecedented control of the emission of light. This most intriguing capability of photonic crystals is due to shaping of the local radiative density of electromagnetic states (LDOS) inside the crystal. The field strength of the Bloch modes inside the photonic crystal at the locations of an emitter, such as a quantum dot, determine the magnitude of the LDOS. However, all real photonic crystals suffer inevitably from unpredictable non-periodic local deviations both due to fabrication errors and, also fundamentally, due to thermodynamical arguments. Such deviations cannot effectively be included into any kind of numerical calculations to date. A measurement is the only way to analyze the electromagnetic field inside a real photonic crystal. Common measurement techniques, such as near-field scanning optical microscopy are restricted to probe local fields outside the crystal near its surfaces while the field deep inside the crystal cannot be mapped.

We present a method to map the absolute electromagnetic field strength inside photonic crystals. We apply the method to map the electric field component E_z of a two-dimensional photonic crystal slab at microwave frequencies. The slab is placed between two mirrors to create a resonator and a subwavelength spherical scatterer is scanned inside the resonator. The resonant Bloch frequencies shift depending on the electric field at the scatterer position. By measuring the frequency shift in the reflection and transmission spectrum versus the scatterer position we determine the field strength. Excellent agreement is found between measurements and calculations without any adjustable parameters.

8632-38, Session 9

A theory of extraordinary optical transmission in aperture arrays

Ross P. Stanley, L. Andrea Dunbar, Rolf Eckert, Ctr. Suisse d'Electronique et de Microtechnique SA (Switzerland)

Extraordinary Optical transmission (EOT) in all its forms has been widely studied since the seminal paper by Ebbesen. The wealth of observations and systems studied has led to a wide range of models for EOT. Most of EOT phenomena have been explained on a case by case basis but their lacks a single approach which unites all EOT phenomena.

Our approach to explain EOT is to apply the techniques of thin film optics. Analytical solutions for the Fresnel equations of a generalized aperture array are derived. As in the usual thin film approach, the optical admittance of each layer is an essential element in the Fresnel coefficients and governs their behaviour. The admittance of the external medium can be treated in the metamaterial approach and it is dominated by the overlap integral between the incident wave and the mode in the aperture.

The progression to a complete system via the Fabry-Perot equations is a natural extension. As a consequence, the regimes of high and low transmission for metal aperture arrays fall naturally out of the model giving a unified view of EOT. In addition the transmission mechanisms find their analogues in thin films, i.e. Brewster angle, Fabry-Perot and waveguide resonances, frustrated total internal reflection and evanescent waveguide coupling. Some of these mechanisms are well-known for hole and slit arrays, while others have been observed only very recently.

8632-39, Session 9

Photonic quasi-crystals in Fourier and Fourier-Bessel space

Scott R. Newman, Robert C. Gauthier, Carleton Univ. (Canada)

Photonic crystals that are aperiodic or quasi-crystalline in nature have been the focus of research due to their complex spatial distributions, resulting in high order rotational symmetries. It is the presence of the high rotational orders that have made aperiodic photonic crystals desirable structures. Recently we proposed aperiodic patterns that were rotationally symmetric while being random in the radial direction. The structures are designed by segmenting the circular design space, randomly populating one segment, and repeating that segment about a center of rotation. Studying the symmetries and geometrical attributes of aperiodic structures is typically performed in reciprocal Fourier space by examining the distribution of the Fourier coefficients. This allows the translational symmetry to be directly extracted and the rotational nature to be interpreted. Instead we propose comparing the typical Fourier analysis with the use of a Fourier-Bessel space. The Fourier-Bessel approach expands the dielectric layout in cylindrical coordinates using exponential and Bessel functions as the angular and radial basis functions. The coefficients obtained in this fashion directly provide the rotational symmetries that are present. This work will examine both the Fourier and Fourier-Bessel distributions of the proposed structures in order to explore the strengths and weaknesses of both techniques. The Fourier-Bessel coefficients will also be used in Maxwell's equations to solve for the stationary states that are supported.

8632-40, Session 9

Optical metrology for random distribution of nanoparticles on multilayer films with cluster effects

Yia-Chung Chang, Academia Sinica (Taiwan); Huai-Yi Xie, National Taiwan Univ. (Taiwan)

We develop a theoretical method to describe optical properties of randomly distributed Au nanoparticles and clusters on multilayer films. In an early work, the finite-element Green's function method has been applied to a system of random distributed nanoparticles without clusters. However, we find this theoretical method does not account for some features observed in the low frequency spectra of ellipsometric measurements, which are attributed to plasmonic resonances associated with Au nanoparticle clusters. By using scalar spherical harmonic basis functions rather than cylindrical basis functions we improved the finite-element Green's function code both in efficiency and accuracy when applied to nanospheres. Furthermore, we develop a theoretical scheme to describe optical scattering from the randomly distributed nanoparticles with clustering effect by using a combination of randomly distributed nanoparticles, nanoparticle clusters, dimmers of nanoparticles, and vacant patches. The calculated ellipsometric spectra of the combined system can adequately describe the experimental data for the whole frequency range.

We have used a set of basis functions made of products of spherical harmonics and spherical Bessel functions with radial component of the wave vector which satisfies the Maxwell's equation inside the metallic sphere. The set of basis functions leads to fast convergent results for light scattering from isolated or coupled nanospheres. For isolated nanospheres, our calculated results for near fields are in excellent agreement with those obtained by the Mie theory. Hence this efficient and accurate theoretical method can be applied to randomly distributed metallic nanoparticles, dimmers, and clusters and study their plasmonic effects.

8632-41, Session 9

Femtosecond direct laser writing of permanent and stable second-harmonic generation properties in silver-containing glass

Gautier Papon, Arnaud Royon, Nicolas Marquestaut, Univ. Bordeaux 1 (France); Marc Dussauze, Institut de Chimie de la Matière Condensée de Bordeaux (France); Yannick G. Petit, Institut de Chimie de la Matière Condensée de Bordeaux (France) and Univ. Bordeaux 1 (France); Thierry Cardinal, Institut de Chimie de la Matière Condensée de Bordeaux (France); Lionel S. Canioni, Univ. Bordeaux 1 (France)

Silver-containing zinc phosphate glasses are good candidates for femtosecond Direct Laser Writing (DLW). We have demonstrated that 3D structuring in this glass by femtosecond laser irradiation at the TW/cm² level, leads to an intense and permanent electric field induced second-harmonic generation (EFISHG) and fluorescence emission from the structured zone. Different silver concentrations and glass matrix compositions have been investigated.

We have studied three-dimensional spatial and spectral aspects, as well as polarization dependence of the EFISHG process, to characterize the amplitude and orientation of the embedded electric field resulting from direct laser writing. We will present the mechanisms of formation of the laser-induced space charge distribution during the writing process, as well as the subsequent stability of such EFISHG structure under UV illumination and temperature constraint below the glass transition temperature.

This work reports experimental and numerical aspects, including the rich physical phenomena (multiphoton ionization, cumulative effects and local heating, heat diffusion, photochemical reactivity and chemical diffusions of species), to explain the formation of the space charge distribution.

We also report on correlative microscopy imaging of both fluorescence and EFISHG emission properties of structured lines induced by DLW in the silver-containing glass. We show clear spatial correlation between these two emissions, even if they show significantly different spatial profiles. Fluorescence emission is associated to the silver cluster production which is locally stabilized by the electric potential modification resulting from the space charge distribution. We used fluorescence and nonlinear induced properties as contrast mechanisms for high potential 3D high-density data storage [1-6].

8632-42, Session 10

Holographic plasmonic couplers for vortex beams and non-diffracting surface waves *(Invited Paper)*

Patrice Genevet, Harvard School of Engineering and Applied Sciences (United States); Jiao Lin, Harvard School of Engineering and Applied Sciences (United States) and A*STAR Singapore Institute of Manufacturing Technology (Singapore); Jean Dellinger, Benoit Cluzel, Frédérique A. De Fornel, Univ. de Bourgogne (France); Mikhail A. Kats, Federico Capasso, Harvard School of Engineering and Applied Sciences (United States)

The work presented in this contribution is based on the principle of holography with surface waves. Holography is originally an imaging technique that consists of scattering an incident laser beam from an optically recorded interference pattern (the hologram) such that the scattered light reconstructs the three dimensional image of an object. The hologram is therefore the coupler that achieves phase matching between a complex beam, the object, and a reference beam.

From this observation, we created scattering interfaces to couple surface plasmon polaritons from incident beams with complicated wavefronts like

Conference 8632: Photonic and Phononic Properties of Engineered Nanostructures III

those carrying orbital angular momentum, such as vortex beams[1].

We have integrated these holographic plasmonic interfaces into commercial silicon photodiodes, and demonstrated that such devices can selectively detect the orbital momentum of light.

This holographic approach is very general and can be used to create couplers able to excite cosine-Gauss surface waves, the 2D analogue to the Bessel beams, which propagate without diffraction[2].

Experimental near-field scanning optical microscope results on non-diffracting SPP are compared with our theoretical calculation and show perfect agreement. The ballistic propagation of our non-diffracting solution represents a major advantage compared to existing non-diffracting Airy beams which tend to bend during propagation.

[1] P. Genevet, L. Jiao, M.A. Kats, and F. Capasso submitted (2012).

[2] L. Jiao, J. Dellinger, P. Genevet, B. Cluzel, F. De Fornel and F. Capasso, Phys. Rev. Lett. 109, 093904 (2012)

8632-43, Session 10

Plasmonic mode engineering with template self-assembled nanoclusters

Jonathan A. Fan, Harvard Univ. (United States) and Univ. of Illinois at Urbana-Champaign (United States); Li Sun, Harvard Univ. (United States); Kui Bao, Rice Univ. (United States); Jiming Bao, Univ. of Houston (United States); Vinothan N. Manoharan, Harvard Univ. (United States); Peter Nordlander, Rice Univ. (United States); Federico Capasso, Harvard School of Engineering and Applied Sciences (United States)

In contrast to electronics, which features elements in the nanometer regime, the size of optical components has been inherently limited by the wavelength of light. Recent demonstrations of metallic nanostructures that support plasmons have pushed over this boundary. Plasmons are collective oscillations of free electrons driven by electromagnetic waves. When light is coupled to isolated metallic nanostructures, localized surface plasmon resonances (LSPR) are excited which create unique near- and far-field properties.

Plasmonic nanoparticle assemblies can serve as a platform in which optical modes, optical resonance wavelengths and near-field intensity distributions can be precisely tailored by the number, position and shape of nanoparticles in a cluster. These metallic nanostructures have traditionally been fabricated with lithographic techniques whose planar nature limits the type of structures that can be achieved. One alternate technique that can overcome some of the limitations of lithography is templated self-assembly (TSA), which is a bottom up method that allows for the construction of large arrays of particle clusters based on a pre-designed template.

In this report, we show that a broad range of plasmonic nanoshell clusters can be assembled onto lithographically-defined elastomeric substrates with relatively high yields using TSA. We assemble and measure the optical properties of three cluster types: heptamers which demonstrate Fano resonance dips, linear chains that work as linear antennas, and rings of nanoparticles which exhibit strong magnetic properties. The assembly of plasmonic nanoclusters on an elastomer paves the way for new classes of reconfigurable plasmonic devices and optical metamaterials that can be transfer-printed onto various substrate mediums.

8632-44, Session 10

Large-area fabrication of broadband absorbing tapered nanoresonators

Alex F. Kaplan, Lingjie Guo, Univ. of Michigan (United States)

Plasmonic metal-insulator-metal (MIM) nanoresonators with high angle tolerance and near-perfect light absorption properties have been

demonstrated over a wide spectral range for various applications. Recent work has attempted to generate tailored, broadband absorption utilizing these structures for applications such as improved solar cell efficiency, infrared emitters, and thermal photovoltaics. This has primarily been attempted by confining multiple resonators on the substrate surface with overlapping absorption spectra in a sub-wavelength region, but this technique can be limited in terms of achievable bandwidth and scalability¹.

Tapered, multi-layer nanoresonator structures have been proposed to achieve angular tolerant broadband absorption by stacking these resonators on top of one another in the vertical direction². Using standard etch processes to achieve these high aspect-ratio structures can run into issues with material choice, masking, and by-product removal. This work reports a simple and scalable method to fabricate tapered structures on the nanoscale by taking advantage of linewidth reduction that occurs naturally in evaporation processes^{3,4}. Nanoimprint lithography is used to generate broadband absorbers over large areas, with the first experimental results demonstrated at visible and IR wavelengths. This tapered deposition method can also be applied to create a wide variety of large-area, tapered nanostructures for applications such as solar cell back reflector layers and recently reported hyperbolic metamaterials⁵.

References

1. Y. Cui, J. Xu, K.H. Fung, Y. Jin, A. Kumar, S. He, and N.X. Fang Appl. Phys. Lett., 99, 253101 (2011).
2. Y. Cui, K.H. Fung, J. Xu, H. Ma, Y. Jin, H. Se, and N.X. Fang Nano. Lett., 12, 1443 (2012).
3. A.F. Kaplan and L.J. Guo, ACS Nano (under review).
4. D.N. Hill, J.D. Lee, J.K. Cochran, and A.T. Chapman J. Mater. Sci., 31, 1789 (1996).
5. X. Yang, J. Yao, J. Rho, X. Yin, and X. Zhang, Nature Photonics doi: 10.1038/NPHOTON.2012.124 (2012).

8632-45, Session 10

Characterization of dielectric and plasmonic resonances in periodic arrays of Au-coated Si nanopillars

Francisco J. Bezares, Joshua D. Caldwell, James P. Long, Orest J. Glembocki, Ronald W. Rendell, Jeffrey Owrutsky, Blake S. Simpkins, U.S. Naval Research Lab. (United States); Richard Kasica, National Institute of Advanced Industrial Science and Technology (United States); Loretta Shirey, U.S. Naval Research Lab. (United States)

Periodic Arrays of Au-coated Si nanopillars have shown great potential for the development of novel device components to be used in photonic applications. Although much effort has been aimed at the study of their optical properties and the identification of the mechanisms that govern such properties, the nature and modal characteristics of the resonant modes inherent to these systems has not been established unambiguously. Here, we will present results obtained from bright field reflection and μ -Raman measurements on Au-coated as well as uncoated periodic arrays of Si nanopillars with varying diameter and pitch which, when compared to Finite-Difference Time Domain and Finite-Element Method simulations, give unique insight into the different resonances observed in the optical spectra of such systems. For instance, our data shows that 1) dielectric as well as plasmonic resonances play a major role in the far-field optical properties of these structures 2) both localized and propagating surface plasmon modes contribute to the large enhancements of the electromagnetic field throughout the area of the arrays and 3) the presence of propagating plasmonic modes on the Au film between the nanopillars results in a more prominent variation in the dispersive behavior of the observed plasmonic modes.

8632-47, Session 10

High-performance broadband absorber in visible by engineered dispersion and geometry of metal-dielectric-metal stack

Peng Zhu, Harbin Institute of Technology (China); L. Jay Guo, Univ. of Michigan (United States)

Recently the absorption properties of metamaterials have attracted much interest and a variety of structures have been studied. Due to their inherent dependence on plasmon resonance the majority of them are only able to absorb a narrow band of light. However, achieving a broadband absorption, especially in visible range, is important for the energy harvesting applications. Several broadband absorbers have been proposed recently, which either possess sophisticated structures, or involve high aspect ratio tungsten gratings, leading to difficult and costly fabrication limiting their potential for large scale applications. In this work we have designed and experimentally demonstrated a new broadband plasmonic light absorber in visible frequency. Taking the advantage of the special dispersion relation of coupled plasmon in our structure, the absorber exhibits ultra flat and highly efficient absorption when compared with previous reports, in addition to being fabricated in large areas with relative low cost by nanoimprint lithography. This broadband absorber consists of a three-layer nano-patterned metal-insulator-metal (MIM) structure. Two examples are designed for better understanding of the principle. Cu and Si₃N₄ are used as the metal and insulator in the MIM stack. Top and bottom Cu layers are patterned gratings. The simulation results shows a nearly 100% from 400 nm to 550 nm for structure-I and the whole visible range for structure-II. Experiments confirm an ultra flat average absorption greater than 80% and the profile of spectra agree with simulated results well. The robustness of the design with angle insensitive absorption characteristics is desirable for the applications in thin-film thermal emitters and photovoltaic devices.

8632-48, Session 11

Enhanced light-matter interactions with engineered photonic-plasmonic nanostructures (Invited Paper)

Luca Dal Negro, Boston Univ. (United States)

The ability to design and manipulate light-matter interactions at the nanoscale is central to the rapidly growing field of nanophotonics. Efficient strategies for electromagnetic field localization and intensity enhancement are essential requirements for the design and engineering of novel optoelectronic components that leverage resonantly enhanced optical cross sections at the nanoscale, such as optical nano-antennas, plasmon-enhanced biosensors, photodetectors, light sources, and on-chip nonlinear optical elements.

Fascinating new scenarios emerge when coupling photonic resonances with localized surface oscillations of conduction electrons supported by metal-dielectric nanostructures, known as Localized Surface Plasmons (LSPs). Analogously to the coupling of atomic and molecular orbitals in solid state and quantum chemistry, LSPs resonances of individual nanoparticles couple by sub-wavelength near-field interactions enhancing the intensity of incident electromagnetic fields over nanoscale spatial regions referred to as “electromagnetic hot-spots”. However, when engineered into arrays of nanostructures separated over distances comparable or larger than the wavelength of light, individual LSPs additionally couple by radiative electromagnetic interactions (i.e., diffractive coupling and multiple light scattering), giving rise to collective photonic-plasmonic modes largely tunable by the array geometry.

In this talk, I will present our work on the design, nanofabrication and engineering of coupled photonic-plasmonic arrays of metal-dielectric nanostructures for active nanophotonics device applications. In particular, I will discuss the optical response of complex arrays of metallic nanoparticles with Fourier spectral features that interpolate in a tunable fashion between periodic crystals and disordered random

media, referred to as Deterministic Aperiodic Nano Structures (DANS). These structures, modeled by rigorous multiple scattering theory, give rise to characteristic scattering resonances and localized mode patterns enhancing the intensity of optical near-fields over broad frequency spectra and planar optical chips. Specifically, I will focus on the novel opportunities provided to optical biosensing, broadband and multi-band nano-antennas, nanoscale light sources, and thin-film solar cells. Finally, I will discuss our work on the generation and manipulation of structured light carrying Orbital Angular Momentum (OAM) with resonant arrays of metallic nanoparticles, which is relevant to emerging device applications in singular optics, secure optical communication, classical and quantum cryptography.

8632-49, Session 11

Optically characterized nanogaps for dramatic electric field enhancement

Jesse Theiss, Stephen B. Cronin, The Univ. of Southern California (United States)

We successfully fabricate arrays of metallic nanoparticle pairs with 1-2 nanometer separation using a combination of electron beam lithography and an angle evaporation technique. The “nanogap” samples are fabricated on thin silicon nitride membranes to enable high resolution transmission electron microscope (HRTEM) imaging of the specific nanoparticle separation and geometries. Plasmonic resonances of the dimer pairs are characterized by dark field scattering microscopy in the visible to near IR part of the electromagnetic spectrum (~450 – 1000nm). Collimated white light is focused onto the membrane sample at a high incident angle using an oil immersion dark field condenser setup, and scattered light is collected through a microspectrometer with a cooled CCD detector. A spatial pinhole filter and low fabrication density isolate each scattering spectrum to an individual nanoparticle dimer that can be directly correlated with its physical geometry through HRTEM imaging. The polarization dependence of the plasmon resonance frequency observed in the scattering spectra demonstrates the strong plasmonic coupling of the closely-spaced dimer. We observe a significant upshift in the measured resonance frequency when polarization matches the common axis of the two nanoparticles. Our FDTD simulations validate the experimental resonances and the upshifting behavior in the lower order dipolar-like plasmon mode of the NP dimers. The simulations also demonstrate high localized field enhancement for practical use in areas such as surface-enhanced Raman spectroscopy.

8632-50, Session 11

Field enhancement in linear and triangular oligomers of plasmonic nanoparticles

Salvatore Campione, Univ. of California, Irvine (United States); Sarah M. Adams, Regina Ragan, Univ. of California, Irvine (United States); Filippo Capolino, Univ. of California, Irvine (United States)

Near-field plasmonic coupling and local field enhancement in metal nanoarchitectures, such as arrangements of nanoparticle clusters, have application in many technologies, including medical diagnostics, solar cells, and sensors. Strong signal enhancement and reproducibility for surface enhanced Raman scattering (SERS) is achievable using a non-lithographic fabrication process, thereby producing SERS substrates having high performance at low cost. This fact has inspired us to perform thorough investigations of field enhancement capabilities in oligomers of plasmonic nanoparticles with spherical shape. First, we estimate via full-wave simulations the field between the nanospheres in several oligomer systems, i.e., linear dimers, trimers, and quadrumers, and trimers with various angles (60°, 90°). To have a broader picture of the field enhancement values, we compare the results to a standard hexagonal close-packed (HCP) configuration with same structural dimensions. We also analyze the effect of tightness in the field enhancement and the role of the gap between nanoparticles. Among all the configurations analyzed,

the linear oligomers are found to provide the largest field enhancement values. For this reason, we then focus on the linear oligomers and theoretically predict their resonance frequency location when they are composed of one (monomers), two (dimers), three (trimers) and four (quadrumers) nanoparticles by means of closed-form formulas. These results show that ad-hoc clusters of nanoparticles can be designed and fabricated to obtain larger field enhancement than with the HCP structure and this paves the way for extremely large SERS enhancements.

8632-51, Session 11

Plasmonic-photonic-fluidic hybrid structures for on-chip sensing and spectroscopy applications

Maysamreza Chamanzar, Siva Yegnanarayanan, Zhixuan Xia, Ali Adibi, Georgia Institute of Technology (United States)

We present our recent results on the design, fabrication, and characterization of a novel class of on-chip sensors for sensing and spectroscopy applications. These hybrid plasmonic-photonic-fluidic structures are made of gold plasmonic nanoparticles, SiN photonic waveguides, and PDMS microfluidic channels. Light is first guided in the waveguides and is then coupled efficiently to the LSPR modes of plasmonic nanoresonators. The target molecules of interest flowing in the integrated microfluidic channels are then detected by the plasmonic nanoresonators. The sensing performance of this hybrid sensing system will be demonstrated. We will also demonstrate the possibility of spectral domain spectroscopy by implementing different plasmonic nanoresonators working at different wavelengths.

8632-52, Session 12

Deep subwavelength focusing using optical nanoantenna with enhanced characteristics for near and far field applications

Mohamed A. Swillam, Univ. of Toronto (Canada) and The American Univ. in Cairo (Egypt); Mohamed A. Nasr, The American Univ. in Cairo (Egypt)

Extra-ordinary optical transmission through a sub-wavelength aperture was discovered more than a decade ago. A single sub-wavelength aperture surrounded by a finite array of grooves on a thin metallic film is a design used by many authors to show sub-wavelength focusing. Here, we introduce a modified version that, to the best of our knowledge, gives best results of this design in terms of the peak power and the full width at half maximum FWHM in the near field as well as the far field of the lens. Numerical simulations using Finite-Difference Time-Domain (FDTD) method coupled with perfectly matched layer (PML) boundary conditions verify that the proposed metallic lens can give a near(far) field focal point 125 nm(1.39 μ m) away from lens with FWHM of 245(299) nm at incident wavelength of 760(610) nm with power enhancement of at least 2 times over the unmodified design. The dependence of this resonant focusing ability with a certain geometrical parameter defining the modified structure is extensively analyzed in the visible range of spectrum. Such a focusing plasmonic device has potential practical applications like NSOM and FSOM due to the simplicity in its design and fabrication and due to superior results in near and far fields of the lens.

8632-53, Session 12

Thermal imaging in gold nanoantennas using heterodyne holography

Ariadna Martinez Marrades, Institut Langevin (France); Pascal Desfonds, Institut Langevin (France); Nathalie Bardoux, Lab. de Photonique et de Nanostructures (France) and Ctr. National de la Recherche Scientifique (France); Stéphane Collin, Lab. de Photonique et de Nanostructures (France); Gilles Tessier, Institut Langevin (France) and Ecole Supérieure de Physique et de Chimie Industrielles (France)

Charge oscillation in metallic plasmonic devices is the source of Joule heating, which can be extremely localized, especially in modulated regime, where the modulated component of the heating is confined in the vicinity of the source. Controlling heating in such structures is a major challenge in nanoscience.

Here, we use a non-contact, full field imaging method based on digital heterodyne holography using low power, phase-modulated probe beams. With a low heterodyne frequency compatible with a slow CCD camera, it allows the 3D characterization of the scattering properties of the sample. At higher frequencies, it can also measure variations in the light scattered by the structures as a result of refractive index changes related to the local heating induced by the modulation of a high power excitation beam. A Green function - based analytical approach allowed us to show that the recorded signals are directly proportional to the temperature increase.

A variety of nanodisc chains with different disc numbers, spacings and diameters as well as nanorod pairs were fabricated on glass substrates by e-beam lithography, either in a positive configuration where the gold structures are deposited on glass, or in a negative configuration, where the structures are holes in a uniform gold layer. While the Babinet principle predicts analogies between the optical properties of these complementary structures, their thermal properties differ depending on the localization of the electronic oscillation which induces Joule heating in the metal.

8632-54, Session 12

Platinum optical nano-antenna fabricated by electron beam induced deposition

Eun-Khwang Lee, Jung-Hwan Song, Min-Kyo Seo, KAIST (Korea, Republic of)

There has been a variety of fabrication methods suggested for the construction of nano-scale structures. Among them, electron beam induced deposition (EBID) has come in to the spotlight for its distinct advantages; easy manipulation of size, real-time view and highly precise fabrication due to its scanning electron microscope (SEM) basis. Despite the superior merits, it has mostly held a secondary position in various manufacturing processes working as a nano-welder for carbon nanotubes and a precise tuner for a photonic crystal resonator. Also, it was employed to support a backbone for a keen-edged atomic force microscope tip. However, there was little research precedent about the optical characteristics of EBID-made nanostructures as a functional device.

In this study, the fabrication of a platinum optical nano-antenna, operating over a broad range of light, was demonstrated by the EBID equipped with the precursor gas, $[(CH_3)_3(CH_3C_5H_4)Pt]$. The initial acceleration voltage was 30 kV with 100 μ A emission current. Controlling a deposition length with the magnification of the SEM, rod-shaped antennas with the length of 1-2 μ m were deposited along the x- or y-axis on a silica substrate. They showed the fixed width around 150 nm and a variation of the height according to deposition time and the magnification

The optical characteristics of the Pt nano-rods were under scrutinized with polarization-resolved dark-field (DF) microscope. Even under unpolarized white illumination, they showed distinctive radiations strongly

Conference 8632: Photonic and Phononic Properties of Engineered Nanostructures III

polarized along the rod axis. This was distinguished from the general property of dielectric rods, indicating an indirect evidence of SPP current. By the reciprocating motion of the current within a structure, a multi-lobe radiation pattern can be spotted. This expected result was observed in the Fresnel region with a 532-nm and 660-nm laser with the dependence of the number of lobes on the rods length.

To achieve a conclusion that our EBID antennas having plasmonic characteristics, detailed research is further needed since the Pt purity was not 100 %. Energy dispersive X-ray spectroscopy (EDX) based-verification of a free-standing Pt wire showed the Pt atomic percentage is about 32 % compared to carbon and oxygen after oxygen plasma ashing. Using diverse techniques including annealing or plasma treatment, we expect the composition can be improved.

8632-55, Session 12

New plasmonic materials in visible spectrum through electrical charging

Jiangrong Cao, Canon U.S.A., Inc. (United States); Rajesh Balachandran, Manish Keswani, Krishna Muralidharan, The Univ. of Arizona (United States); Slimane Laref, The Univ. of Arizona (United States); Richard W. Ziolkowski, The Univ. of Arizona (United States); Keith Runge, The Univ. of Arizona (United States); Pierre A. Deymier, Srinu Raghavan, The Univ. of Arizona (United States); Mamoru Miyawaki, Canon U.S.A., Inc. (United States)

Due to their negative permittivity, plasmonic materials have found increasing number of applications in advanced photonic devices and metamaterials, ranging from visible wavelength through microwave spectrum. In terms of intrinsic loss and permittivity dispersion, however, the limitations on available plasmonic materials are becoming a serious bottleneck preventing practical applications of a few novel nano-photonic device and metamaterial concepts in visible and near-infrared spectra.

To overcome this obstacle, efforts have been made and reported in literature to engineer new plasmonic materials exploring metal alloys, superconductors, graphene, and heavily doped oxide semiconductors. Though promising progress in heavily doped oxide semiconductors was shown in near-infrared spectrum, there is still no clear path to engineer new plasmonic materials in visible spectrum that can outperform existing choices noble metals, e.g. gold and silver, due to extremely high free electron density required for high frequency plasma response.

This study demonstrated a path to engineer new plasmonic materials in visible spectrum by significantly altering the electronic states in existing noble metals through high density charging/discharging and its associated strong local bias field effects. A density functional theory model revealed thin gold films (up to 7 nm thick) optical property in visible spectrum can be altered significantly, in terms of both plasma frequency (up to 12%) and optical permittivity (more than 50%). These corresponding effects were observed in our experiments on surface plasmon resonant on a gold film electrically charged via a high density double layer capacitor induced in a chemically non-reacting electrolyte.

8632-56, Session 13

Plasmonic and photonic structures for nanoparticle trapping, color filtering, and single molecule SERS (*Invited Paper*)

Kenneth B. Crozier, Harvard Univ. (United States)

Plasmonic and photonic nanostructures present opportunities for the optical manipulation of micro- and nanoparticles. In this presentation, I highlight recent work performed by my research group on the trapping of micro- and nanoparticles with nanostructures supporting localized and propagating surface plasmons, and with silicon photonics. Displays, image sensors, and a wide variety of optical measurement systems all

make use of color filters. Color filters usually have only one fixed output color. The development of color filters whose color output is controllable would find many applications. In this presentation, I also highlight my group's recent work on a novel color filter, termed a chromatic plasmonic polarizer (CPP), which maps polarization state of white light to output color. Raman scattering provides a powerful means for identifying molecules through their vibrational spectra. Applications of Raman scattering, however, face the challenge of weak signals that arise from the Raman scattering cross sections of most molecules being very small. One approach to mitigate this, employed in surface enhanced Raman scattering (SERS), has been to use metallic nanostructures to enhance the Raman signal. In this presentation, I will highlight recent work from my group in high performance SERS substrates, including those with single molecule sensitivity.

8632-57, Session 13

Effect of non-conformality gold deposition on SERS related plasmonic effects

Swe Z. Oo, Univ. of Southampton (United Kingdom); Martin D. B. Charlton, Univ. of Southampton (United Kingdom)

Recently, a comprehensive three dimensional computational model based on Rigorous Coupled Wave Analysis (RCWA) has been developed to investigate the properties of surface plasmons resident on metal coated arrays of inverted pyramidal pits used for SERS sensing applications in the form of 'KlariteTM'

This simulation tool allows the identification of a variety of dispersive features including propagating and localized surface plasmons as well as simple diffraction according to the influence of geometrical features.

In this paper, we investigate the influence of non-conformality of gold over the internal surfaces of the inverted pyramidal pits on plasmon dispersion. Modeling reveals very strong changes in plasmon behavior as a function of gold layer conformality.

Dependent upon conformality of the gold coating we find that the nano-textured metallic surface can behave either as an efficient broadband mirror-like reflector or as an efficient broadband, wide angle absorber at infrared wavelengths. Creation of a broadband wide angle absorbing surface such as this has important implications for photovoltaic cells. For sensing applications, understanding the effect of metal layer conformality on plasmon dispersion gives clear insight into how to further improve SERS enhancement factor.

8632-58, Session 13

Extraordinary plasmon-quantum dot coupling for enhanced infrared absorption

Rajeev V. Shenoi, James A. Bur, Rensselaer Polytechnic Institute (United States); Danhong Huang, Air Force Research Lab. (United States); Shawn-Yu Lin, Rensselaer Polytechnic Institute (United States)

The use of metallic nanostructures for enhanced transmission and near field phenomena have been a topic of extensive research. Here, we present integration of active media, consisting of InAs quantum dots (QD) embedded in quantum wells, with 2 dimensional metallic hole arrays (2DHA) leading to a strong interaction. Resonant surface plasmons, excited at the metal-semiconductor interface, are coupled with intersubband transitions of the quantum dots. The presence of a low-loss absorber within the enhanced near field region of 2DHA leads to an enhancement of photoresponse. The parameters of 2DHA were designed to overlap with absorption peaks of QDs. We present techniques of fabrication, accurate characterization of enhancement and efforts to optimize the 2DHA-QD coupling. Over an order of magnitude enhancement in photoresponse is observed due to spectral matching of intersubband absorption of quantum dots to that of 2DHA resonance, optimal placement of QD within the structure, and improved

interaction lengths due to lateral propagation. This enhancement is also accompanied by significant narrowing of linewidth and the ability to tune the resonance by varying the 2DHA parameters. A hexagonal lattice with periodic circular holes on a thin gold film is used as the 2DHA. With further optimizations, these structures have significant applications in the mid-wave infrared (3-5 μm) and long-wave infrared (8-12 μm) regions for multispectral and polarization sensitive sensing.

8632-59, Session 13

Low-power plasmon-soliton waves in feasible in realistic nonlinear chalcogenide planar structures

Gilles Renversez, Aix-Marseille Univ. (France) and Institut Fresnel (France); Wiktor Walasik, Aix-Marseille Univ. (France) and ICFO - Institut de Ciències Fotòniques (Spain); Virginie Nazabal, Univ. de Rennes 1 (France); Mathieu Chauvet, Univ. de Franche-Comté (France) and FEMTO-ST (France); Yaroslav V. Kartashov, Institute of Spectroscopy (Russian Federation)

Several works have been recently published about self-sustained solutions that combine soliton and plasmon features in metal/nonlinear dielectric structures[Feigenbaum07,Davoyan09,Bliokh09].

Actually, the first description of 1D nonlinear plasmon-soliton waves propagation along metal/nonlinear dielectric interfaces was given more than 30 years ago[Ariyasu85,Stegeman84,Maradudin83,Mihalache86] though a different terminology was used to describe such states. In these structures, the nonlinear stationary solution is made of a spatial soliton part coupled with a plasmonic wave.

Nevertheless, up to now no experimental results have been published on the issue of plasmon-soliton coupling. The main reason is that, for the previously proposed structures, the nonlinear refractive index change required for the formation of plasmon-soliton waves is too high compared with the one attainable for real materials or, equivalently, the peak power is too high when one uses realistic values of nonlinear coefficients of integrated optics conventional materials[.

In the present work, we describe for the first time planar structures made of conventional materials supporting a low peak power (around 1 GW/cm^2) nonlinear solutions that combine a soliton profile with a measurable plasmonic field. In its current form, it is made of a chalcogenide glass coated with silica and gold films.

It is worth mentioning that structures similar to the ones we propose have already been fabricated even if it was not in the framework of soliton-plasmon studies and that optical solitons have already been observed in chalcogenide planar waveguide for peak power around 2 GW/cm^2 [Chauvet09]. Furthermore, the configuration we propose can be made suitable for sensor applications since the decaying part of the plasmon field can be located at a metal/air or at a metal/water interface.

In our case, the structure is designed to make the plasmon field at the interface between the metal layer and the external dielectric medium recordable using near field optics measurements, and to allow its generation and control by beams with low peak intensities.

A vector approach is required to study such nonlinear waves that include a plasmon part. In our work we expand the 1D vector model used for 3-layer symmetric configurations made of a finite thickness metal layer embedded in semi-infinite nonlinear dielectric regions to study the propagation of nonlinear waves in a 4-layer configuration.

This 4-layer model is required so as to describe our 3-layer structure coupled with a semi-infinite external medium.

We found out that to couple in the same wave a pronounced soliton with a plasmon that extends in a linear low-index external medium the studied nonlinear dielectric/linear dielectric/metal structure is needed. During our talk, we will also present results obtained for the same structures but with a finite element method that allows us to test some of the hypothesis done within the 1D model described above. The extension to the 2D case will also be discussed in this framework.

8632-60, Session 13

Angle independent nearly perfect absorbers by light funneling effect

Yi-Kuei R. Wu, Univ. of Michigan (United States); Andrew E. Hollowell, Univ. of Michigan (United States) and Sandia National Labs. (United States); Jay Guo, Univ. of Michigan (United States)

Plasmonic structures have been used for many applications in the visible regime, such as photovoltaics, color filters, and index biosensors. These structures have led to high coupling efficiencies through excitation of SPPs via grating coupling. However, they are inherently angle-dependent. This angle dependence prevents integration into practical applications such as the fields of dispersive concentrated photovoltaics, nanocavity emitters, miniature hyperspectral imaging, high sensitivity biosensors, and color filters for high resolution displays. To address this issue, we investigated angle independent and widely tunable light absorbers with nearly perfect absorption at specific wavelength ranges. This work describes the analytical and numerical design principles as well as experimental confirmation of metallic nanostructures for wavelength tunable and angle independent optical absorbers. The simulations and experiments show more than 96% absorption at the designed absorption band across the entire visible range. The proposed metallic nanostructures are additionally able to achieve wide-angle tolerance up to 90° . We further studied the angular-response absorption and obtain an optimal periodicity based on the momentum matching consideration. We further discuss field confinement induced through subwavelength periodic effects and light funneling into nano-groove structures. These metallic nano-grooves with high field confinement and angle-robust plasmonic resonance provide a guideline for future plasmonic devices operating independent of incident angles of light.

8632-61, Session 13

Nanoscale interference patterns of gap-mode multipolar plasmonic fields

Keiji Sasaki, Akio Sanada, Yoshito Tanaka, Hokkaido Univ. (Japan)

Arbitrary spatial distributions of the electric field of light are formed through the interference of individual wavenumber mode fields with appropriate amplitudes and phases, while the maximum wavenumber in the far field is limited by the wavelength of light. In contrast, localized surface plasmons (LSPs) possess the ability to confine photons strongly into nanometer-scale areas, exceeding the diffraction limit. In particular, gap-mode LSPs produce single-nanometer-sized, highly intense localized fields, known as hot spots. The strongly increased intensities and high spatial gradients of hot spot fields are applicable for single molecule trapping using strong radiation pressure, the acceleration of anomalous excited state dynamics that break the long wavelength approximation, the enhancement of exciton-photon couplings, such as vacuum Rabi splitting, and other fields. However, the details of the spatial distributions of LSP fields within hot spots have not been investigated theoretically or experimentally to date. In this paper, we show the nanoscale spatial profiles of the LSP fields within hot spots of a gold nanodisk dimer system, which exhibit complicated fine structures, rather than single peaks. The nanopatterns are created by constructive and destructive interferences of dipolar, quadrupolar, and higher-order multipolar plasmonic modes, which can be drastically altered by controlling parameters of the excitation optical system. Realization of nanoscale field manipulation would prove crucial to studies of the light-matter interactions in plasmonic nanospaces as well as to the development of future nanophotonic devices.

8632-75, Session PWed

Numerical analysis and the effective parameter retrieval of helical metamaterials

Hsiang-Hung Huang, Yu-Chueh Hung, National Tsing Hua Univ. (Taiwan)

Research on chiral metamaterial has drawn much attention in recent years. By virtue of chirality, for example, it has been shown that chiral metamaterials can achieve negative refractive index without great energy dissipation. In this report, we applied effective parameter retrieval technique to study the material properties of helical metamaterial. The retrieval procedure yields electromagnetic parameters through employing finite-difference time-domain (FDTD) method under periodic boundary condition. We numerically obtain several electromagnetic parameters of the structure and show that the resonance properties and the index of refraction of the helical metamaterial have strong relationship with its circular dichroism. The optical properties of the structure are also discussed, which provides general design guidelines for engineering functional chiral metamaterials.

8632-76, Session PWed

Design and fabrication of active spectral filter with metal-insulator-metal structure for visible light communication

Kensuke Murai, National Institute of Advanced Industrial Science and Technology (Japan); Yasushi Oshikane, Takaya Higashi, Fumihiko Yamamoto, Motohiro Nakano, Haruyuki Inoue, Osaka Univ. (Japan)

Visible light communication with LED is an important ICT technology for the ubiquitous network society. However visible light communication has the speed limit in the conventional blinking LED method. Therefore an active spectral filter would be useful in order to input information signals onto the LED spectrum. Plasmonic spectral filter based on a metal-insulator-metal (MIM) structure is one of the candidates of such active filter.

We have designed the MIM structure for the visible light communication by the calculation of the optical reflection. The metal should be the plasmonic material such as gold or silver. The MIM structure shows the very narrow absorption dip as functions of the wavelength and the incident light. However very precise thicknesses of the metal and the insulator layers are requested for the designed structure. For example, the thickness of the metal layer (M1) decides the depth of the absorption dip. And the thickness and the flatness of the insulator layer decide the spectral position and the spectral width of the absorption dip, respectively. Since the absorption dip had been decided by the underneath layers, real-time monitoring of the MIM structure would be required in order to see the thickness and the flatness of the deposition of each layer.

We will explain our progress of fabrication of the MIM structures with the vacuum deposition technique and compare their absorption properties with the theoretical prediction.

8632-77, Session PWed

Effect of V-shape on the light transmission of subwavelength slits in metallic thin films

Otávio Silva de Brito, Fabio A. Ferri, Univ. de São Paulo (Brazil); Victor A. G. Rivera, Instituto de Física de São Carlos (Brazil); Sergio P. A. Osório, Euclides Marega Jr., Univ. de São Paulo (Brazil)

Currently, the focused ion beam milling (FIB) technique is a commonly

used approach to fabricate nanostructures because of its unique advantages of one-step fabrication, nanoscale resolution, and no material selectivity, etc. However, the FIB technique also has its own disadvantages. Regarding the process of fabrication of the corrugations and subwavelength apertures, nowadays, there is a major problem: the V-shaped structuring. In this work, we discuss the influence of V-shape on the optical transmission of subwavelength slits designed in Ag and Au thin films possessing different thicknesses. The effect of different cone angles (ratio between the widths at the incidence plane and at the exit plane) originated from the V-shaped slits was also considered. We have performed computational simulations carried out with COMSOL Multiphysics® to investigate the slits optical transmission. In most cases, the subwavelength slits were illuminated with 488.0 nm (for Ag) and 632.8 nm (for Au) wavelength light sources typical of Ar ion and HeNe lasers, respectively. The radiation was directed into the sample surface in TM polarization (magnetic H-field component parallel to the long axis of the slits). The origin of the slits transmission is attributed to plasmonic surface excitations. Our simulation results demonstrated that different cone angles originated from the V-shaped subwavelength slits generate different influences on the beam propagation. The width variation affects the optical transmission intensity significantly. Hopefully, exploring the influence on the light propagation behaviour through subwavelength apertures via theoretical simulations can provide a better understanding of the beam propagation phenomena for future studies.

8632-78, Session PWed

Resonant near-infrared emission of Er³⁺ ions in plasmonic arrays of subwavelength square holes

Victor A. G. Rivera, Univ. de São Paulo (Brazil) and Univ. Laval (Canada); Yannick Ledemi, Mohammed El-Amraoui, Younes Messaddeq, Univ. Laval (Canada); Euclides Marega Jr., Univ. de São Paulo (Brazil)

Periodic nanostructure arrays consisting of square holes were fabricated with a Focused Gallium Ion Beam on a gold or silver thin film deposited onto the surface of an Er³⁺-doped tellurite glass. The nominal dimensions of the square elements are approximately 200?200 nm², separated by 1.0 ?m, such that we have arrays of 15?15, 10?10 and 5?5 ?m² dimensions. The nanostructures were vertically illuminated with a diode laser at 405 nm. The Er³⁺ luminescence spectrum in the near-infrared was measured in the far-field via the micro-luminescence technique. The excitation and emission of the Er³⁺ ions were obtained through of the so-called extraordinary optical transmission of excitation/emission light respectively via those square arrays. In this way, metallic nanostructures sustaining surface plasmons can excite and change the emission properties of locally excited quantum systems such as the Er³⁺ ions. Additional contributions on the emission spectra were achieved due to the influence of the metal film type (silver or gold), film thickness, i.e., the resonant properties from the plasmonic nanostructures can strongly influence the Er³⁺ ions (quantum system). We present a systematic quantum mechanical experiment that shows the quantum plasmonic properties of these nanostructure arrays on the erbium ions, with direct applications to understanding and exploiting for the nanophotonic devices.

8632-79, Session PWed

Absorption capabilities of hyperbolic materials

Caner Guclu, Salvatore Campione, Filippo Capolino, Univ. of California, Irvine (United States)

Composite hyperbolic materials (HMs) are uniaxial anisotropic materials with iso-frequency hyperbolic wavevector dispersion diagram shown to provide field focusing in subwavelength spots, to act as superlenses, to enhance the spontaneous emission of sources positioned close

Conference 8632: Photonic and Phononic Properties of Engineered Nanostructures III

to the HM, and to lead to low reflectance when the HM surface has been corrugated. Here we use a spatial spectrum approach to show theoretically that a HM acts as a super absorber for scattered fields generated by a nanoparticle near its surface. The use of spectral theory enables us to carefully analyze the power emitted by elementary dipoles or small objects located close to HMs for their several physical parameters including, but not limited to, sources' distance from the HM, materials, shapes, and power spectra. This in turns allows us to state that the nanoparticle's scattered fields will be enhanced by the presence of the HM and mainly directed into the HM, and hence there almost totally absorbed. These physical properties are of key importance and allow us to foresee broadband wide-angle absorption when scattering is created at the HM surface, by either purposely roughening a HM surface or, equivalently, locating many nanoscatterers at the HM surface. This work leads to possible innovative methods to absorb energy at microwaves as well as millimeter-wave, infrared, and optical frequencies, since HM fabrication using composite materials is simple and does not require unfeasible material parameters.

8632-80, Session PWed

Anderson localized optical fibers

Salman Karbasi, Univ. of Wisconsin-Milwaukee (United States); Karl W. Koch, Corning Incorporated (United States); Arash Mafi, Univ. of Wisconsin-Milwaukee (United States)

Anderson localization occurs because of the wave interference in a highly scattering medium. In order to observe Anderson localization in an optical system, the scattering should be strong enough so that the mean free path of the photons becomes of the order of the wavelength; this condition is relaxed in two dimensional systems as shown by De Raedt et al, in 1989. Transverse Anderson localization of light was first experimentally observed by Schwartz et al, in a photorefractive crystal with refractive index contrast in the order of 5×10^{-4} . Here, we present the first observation of transverse Anderson localization in an optical fiber: the disordered fiber is composed of PMMA and PS with refractive indices of 1.49 and 1.59, respectively. The disordered polymer fiber is composed of 40,000 8-inch strands of PMMA (200 μ m diameter) and 40,000 8-inch strands of PS (200 μ m diameter), which are randomly mixed and drawn to the square fiber with the side width of 250 μ m. The 633nm He-Ne laser is coupled to the disordered optical fiber using butt-coupling method. The CCD camera monitors the near-field intensity at the end tip of the disordered fiber using a 40x objective. The experimental results are confirmed with simulations. The clear trace of localization can be observed from the exponential decays of the tail of intensity, which is averaged over 100 different near-field measurements on 20 samples. We show, both theoretically and experimentally, that the mean localization radius at the wavelength of 405nm is smaller compared with the mean localization radius at 633nm. We have successfully tested Anderson localization in disordered optical fiber segments as long as 60-cm.

8632-81, Session PWed

On-chip superfocusing of surface plasmon using metal-coat tapered optical fiber pairs with nano-gap structures

Kazuhiro Yamamoto, Shiyoshi Yokoyama, Kyushu Univ. (Japan); Akira Otomo, National Institute of Advanced Industrial Science and Technology (Japan)

Surface plasmons are coupled waves of electron oscillation and electromagnetic field at interfaces between metals and dielectrics and localize at the boundary with nanoscale distribution. So, by using surface plasmons, one can construct integrated optical systems to overcome the diffraction limit of light.

Recently, special electromagnetic modes in tapered metal structures, called "superfocusing modes", are important in this research area, owing

to high field concentration effect due to increasing of wavenumber of surface plasmons along the taper.

Metal-coat tapered optical fibers are commonly used as the probes of near-field microscopy and are suitable for fabrication of these cone-shaped superfocusing devices. Furthermore, when these probes are arranged face to face with nano-scale gap, the electric fields in nano-gap effectively enhanced. In this presentation, we show the fabrication processes and numerical analysis of these metal cone structures consist of tapered optical fiber pairs.

The fabrication processes are below. First, optical fibers are mounted on silicon V-groove substrates with through-hole. Next, the fibers are milled by focused ion beam (FIB) for nano-gap formation. Finally, the fibers are tapered by wet etching using buffered hydrofluoric acid and are coated with gold by sputtering. We obtained several hundred nm gapped tapered optical fiber pairs with 12 degree of taper angle. In addition, we present the method of reducing nano-gap size and controlling the taper angles, and numerical analysis of superfocusing behavior in these structures. We believe that these structures can be applied to the electrical-optical integrated devices and the nano-scale sensing.

8632-82, Session PWed

Mid IR invisibility cloak through manual rolling

Hemi H. Gandhi, Philip A. Munoz, Mathias Kolle, Eric Mazur, Harvard Univ. (United States)

Although many designs for invisibility cloaks have been proposed, very few have been demonstrated due to fabrication challenges. The major difficulty is construction of three-dimensional metamaterial structures with sub-wavelength features. We investigate a novel and simple cloak fabrication method, which leverages 2D photolithography to achieve 3D structures through rolling. Meta-atoms are patterned on polymer sheets, which can be rolled into an Archimedean spiral geometry. To facilitate the rolling process, thin film polymers are floated onto a water basin and manually rolled around an optical fiber. High rolling fidelity is achieved. We present FDTD simulations and metrology characterizations of a mid-IR cloak composed of split ring meta-atoms, fabricated through this rolling method. The ease, simplicity, and low cost of this new fabrication method may enable the realization of previously theorized cloak designs.

8632-62, Session 14

Metamaterial based nanobiosensors and nanophotodetectors (*Invited Paper*)

Ekmel Özbay, Bilkent Univ. (Turkey)

In this talk, we will review our recent work on metamaterial based nanobiosensors and nano-photodetectors. We will first explain how split ring resonator (SRR) structures can be used for bio-assay applications that can improve the assay time and sensitivity. The proof-of-principle demonstration of the ultrafast bioassays was accomplished by using a model biotin-avidin bioassay. Introduction of SRRs resulted in an increase of 35x in detection speeds, while the detection sensitivity improved by 100x. We also present a label-free, optical nano-biosensor based on the Localized Surface Plasmon Resonance (LSPR) effect that is observed at the metal-dielectric interface of silver nano-cylinder arrays located periodically on a sapphire substrate by E-Beam Lithography (EBL), which provides high resolution and flexibility in patterning. Firstly, the size and period dependency of the LSPR wavelength was studied. Secondly, the surface functionalization studies were carried out on an array with a selected size and period. Finally, the concentration dependency of the LSPR shifts was observed by changing the avidin concentrations to be sensed in the target solution. The sensing mechanism is based on the detection of refractive index change, due to the binding of biotin that is immobilized on the silver nano-cylinders to the avidin in the target solution, by observing the shifts in the LSPR wavelength. Our results show that such a plasmonic structure can be successfully applied to bio-sensing applications and extended to the detection of specific bacteria species. The integration of plasmonic structures with solid state

Conference 8632: Photonic and Phononic Properties of Engineered Nanostructures III

devices has many potential applications. It allows the coupling of more light into or out of the device while decreasing the size of the device itself. Such devices are reported in the VIS and NIR regions. However, making plasmonic structures for the UV region is still a challenge. Here, we report on a UV plasmonic antenna integrated metal semiconductor metal (MSM) photodetector based on GaN. We designed and fabricated Al grating structures. Well defined plasmonic resonances were measured in the reflectance spectra. Optimized grating structure integrated photodetectors exhibited more than eightfold photocurrent enhancement.

8632-63, Session 14

Strong coupling between metamaterial resonators and AIAs nano layers

Sheng Liu, Alexander Benz, John L. Reno, Igal Brener, Sandia National Labs. (United States)

We investigate a system consisting of a series of split ring resonators (SRRs) on top of a GaAs wafer with a thin active AIAs layer. By matching the resonance of the SRR with the AIAs phonon energy, two narrow transparency windows are observed. The first transmission peak at $\sim 27.7 \mu\text{m}$ is due to the strong coupling between the metamaterial and the AIAs transverse optical phonon that opens a transparency window. This is confirmed by observing an anti-crossing behavior when the fundamental metamaterial resonance is tuned across the phonon band of AIAs. The second transmission peak at $\sim 24.7 \mu\text{m}$ is located around the AIAs longitudinal optical phonon energy where the AIAs permittivity has a zero crossing. According to the field-continuity boundary conditions, at the wavelength corresponding to zero permittivity, the electric field is greatly enhanced in the AIAs layer. Simulations confirm the strong enhancement of the electric field intensity within the AIAs layer compared to the electric field in GaAs.

This work was performed, at the Center for Integrated Nanotechnologies, a U.S. Department of Energy, Office of Basic Energy Sciences user facility. Sandia National Laboratories is a multi-program laboratory managed and operated by Sandia Corporation, a wholly owned subsidiary of Lockheed Martin Corporation, for the U.S. Department of Energy's National Nuclear Security Administration under contract DE-AC04-94AL85000. #158883

8632-64, Session 14

Mid-infrared metamaterials strongly coupled to intersubband transition

Alexander Benz, Sandia National Labs. (United States); Salvatore Campione, Univ. of California, Irvine (United States); Young Chul Jun, John F. Klem, Michael B. Sinclair, Eric A. Shaner, Sandia National Labs. (United States); Filippo Capolino, Univ. of California, Irvine (United States); Igal Brener, Sandia National Labs. (United States)

Optical metamaterials (MM) in the mid-infrared (MIR) spectral range have recently caused tremendous research interest. Their designable frequency response makes them ideal candidates for filters across the entire spectral range from 3 to 15 μm . The resonance frequency is defined purely by the geometry of the structure. One of the big challenges still remains the electrical tunability of the spectral characteristics.

Here, we present experimentally the strong light-matter coupling of a MM mode and an intersubband transition in the MIR range. We use a conventional two-dimensional metallic meta-surface processed on top of a semiconductor heterostructure designed with an intersubband transition (IST) near $\lambda = 10 \mu\text{m}$. Both structures, the MM and ISTs, were optimized for maximum interaction. The MM rotates the incoming polarization in the near-field making it compatible with the IST selection rules. When the metamaterial resonance and quantum-well transition become similar in energy, the two lines anti-cross with a characteristic

splitting of $\sim 3.6 \text{ THz}$, corresponding to 15% of the central frequency. The quantum-well properties can be easily manipulated by an applied bias. This is the first crucial step towards an all electrically tunable MIR filter.

This work was performed, in part, at the Center for Integrated Nanotechnologies, a U.S. Department of Energy, Office of Basic Energy Sciences user facility. Sandia National Laboratories is a multi-program laboratory managed and operated by Sandia Corporation, a wholly owned subsidiary of Lockheed Martin Corporation, for the U.S. Department of Energy's National Nuclear Security Administration under contract DE-AC04-94AL85000. #158883

8632-65, Session 14

Harmonic generation, optical multistability, and nonlocal effects in near-zero permittivity metamaterial slabs near the pseudo-Brewster angle

Domenico de Ceglia, The AEgis Technologies Group, Inc. (United States); Salvatore Campione, Univ. of California, Irvine (United States); Maria A. Vincenti, The AEgis Technologies Group, Inc. (United States); Filippo Capolino, Univ. of California, Irvine (United States); Michael Scalora, U.S. Army Aviation and Missile Command (United States)

The interest in near-zero permittivity (NZP) materials was originally motivated by the possibility of controlling the directivity of antennas and achieving perfect couplers through electromagnetic tunneling in subwavelength, low permittivity regions. More recently, NZP materials, typically referred to as epsilon-near-zero (ENZ) materials, have been indicated as effective platforms to enhance nonlinear phenomena, such as harmonic generation, optical bistability, and soliton excitation. The goal of this work is to first analyze field enhancement phenomena in engineered NZP metamaterial slabs made of periodically displaced nanocylindrical plasmonic shells. An active medium embedded in the core of the shells induces a damping compensation mechanism near the zero crossing point of the real part of the effective permittivity of the ensemble, so that both the real and the imaginary parts of the effective metamaterial permittivity approach zero. The effective near-zero permittivity condition causes a strong inhibition of reflection at the effective pseudo-Brewster angle of the metamaterial slab, which in turn allows strong field enhancements within the engineered slab. This strong field enhancement leads to significant boosting of nonlinear processes. The ability of this structure to improve the conversion efficiency of second harmonic generation arising from the metallic nanoshells and lower the threshold of optical multistability phenomena is then investigated. Finally we discuss the role of nonlocal effects induced by the free-electron gas pressure in the metallic nanoshells.

8632-66, Session 14

Realizing effective magnetic field for photons by controlling the phase of dynamic modulation

Kejie Fang, Zongfu Yu, Shanhui Fan, Stanford Univ. (United States)

In quantum field theory, a charged particle is defined by its capability to couple to an associated gauge field. In the case of electrons, such a gauge field is the magnetic field. Applying magnetic field to electrons provides some of the most important fundamental breakthroughs in science, including the discoveries of integer and fractional quantum Hall effects that lies at the heart of much of the modern condensed matter physics.

Photons are neutral particles. There is therefore no naturally occurring magnetic field that couples to a photon. Nevertheless, building upon recent breakthroughs in designing artificial photonic materials, we show

Conference 8632: Photonic and Phononic Properties of Engineered Nanostructures III

that one can in fact achieve an effective magnetic field in dynamically modulated photonic lattices. By harmonically modulating the coupling constants between the resonators in the photonic lattice, photons undergo an interband transition and acquire a non-reciprocal phase when hopping between different modes of the resonators. If such a modulation has a spatial phase distribution that resembles a gauge field distribution, photons experience an effective magnetic field that is equivalent to the case of electrons under real magnetic field.

As an unambiguous demonstration of such an effective magnetic field, we present first-principle numerical evidences of a Lorentz force for photons, and a photonic quantum Hall effect with a topologically-protected one-way edge state. Moreover, we show that such a lattice can be achieved both in optical and in microwave frequency ranges using existing technologies.

8632-67, Session 15

Symmetry breaking in optical metamaterials (Invited Paper)

Xiang Zhang, Univ. of California, Berkeley (United States)

No Abstract Available

8632-68, Session 15

Ultra-thin tunable perfect absorber

Mikhail A. Kats, Deepika Sharma, Jiao Lin, Patrice Genevet, Romain Blanchard, Zheng Yang, Harvard School of Engineering and Applied Sciences (United States); M. Mumtaz Qazilbash, The College of William & Mary (United States); Dmitri N. Basov, Univ. of California, San Diego (United States); Shriram Ramanathan, Federico Capasso, Harvard School of Engineering and Applied Sciences (United States)

Perfect absorbers generally comprise relatively complex structures consisting of either wavelength-scale asymmetric Fabry-Perot cavities or plasmonic metamaterials. We show that perfect absorption can be achieved with a single lossy dielectric layer of thickness much smaller than the incident wavelength on an opaque substrate by utilizing the nontrivial phase shifts at interfaces between lossy media. This resonator design is implemented with an ultra-thin (~75 nm) vanadium oxide (VO₂) layer on sapphire, temperature tuned in the vicinity of its insulator-to-metal phase transition, leading to 99.75% optical absorption at $\lambda = 11.6 \mu\text{m}$. The design of such devices benefits from critical coupling, a phenomenon which facilitates efficient power transfer to a resonator. The absence of lithography in device fabrication, its structural simplicity, and its immunity to small variations in material composition enable large area applications. Furthermore, the large tuning capabilities (from ~80% to 0.25% in reflectivity, corresponding to an on/off ratio of more than 300) are promising for modulators, thermal emitters, and bolometers. Both experimental data obtained using a mid-infrared spectroscopy and analytical calculations using the transfer matrix formalism will be presented in support of our conclusions.

8632-69, Session 15

Microscroll invisibility cloak

Philip A. Munoz, Eric Mazur, Harvard Univ. (United States)

We present a design for a self-assembled cylindrical invisibility cloak, based on strained-induced rolling. Here, a 2D slab metamaterial is patterned by electron beam lithography on a compressively strained InGaAs thin film. The metamaterial is composed of an array of periodically spaced silver nanorods embedded in a polymer background. The anisotropic effective permittivity of the slab is defined by on the aspect ratio and pitch of the nanorods, and is modeled by Effective

Medium Theory and the Finite Difference Time Domain method (FDTD). The strained film is released from the substrate by wet etching, and the film strain relaxes, causing the combined metamaterial/thin-film to curl into a tight roll. The rolling radius is modeled by continuum strain theory and confirmed by experiment. Resulting microscroll has an anisotropic and radially-dependent effective permittivity, which is inherited from the original slab metamaterial. Depending on the nanorod spacing in the metamaterial layer, we can tune the radial dependence of the permittivity. This design can be used to realize a variety of transformation optical devices with cylindrical symmetry. In particular, we analyze the case of a TE cylindrical invisibility cloak with reduced parameters using FDTD.

8632-70, Session 15

Theoretical and experimental investigation of hybrid broadband terahertz metamaterial absorber

Mohammad Hokmabadi, Univ. of Alabama (United States); David S. Wilbert, Patrick Kung, Seongsin M. Kim, Univ. of Alabama (United States)

Among electromagnetic spectrum, terahertz region has been paid less attention due to the lack of appropriate devices that works well in this area. But recently growing interest has been focused to design devices with functionality in terahertz region because of potential terahertz applications in biomedical imaging, material optical parameters determination and astronomical radiation detection. One of the major terahertz devices that can revolutionize terahertz research is terahertz metamaterials absorber. A lot of efforts have been made in designing terahertz absorbers with different specifications including polarization independent, narrow band, multiband and broadband absorbers. In this work, we propose a novel structure that broadens bandwidth of terahertz metamaterials absorber with a little decrease in absorption strength. Our structure takes benefit of multiband absorber by making the bands close enough to each other but in a multilayer pattern to decrease the negative interact between rings and corresponding resonances. The structure has been composed of multilayer metal copper concentric rings, followed by polyimide as the spacer and a copper plane to reflect selective frequencies toward the absorber. Ring layers are tightly stacked from each other so that the destructive interaction of rings has been decreased compared to the case when rings are all on the same plane. Also the whole structure is symmetric along the axis of wave propagation so that it is insensitive to the polarization direction. Measured results of fabricated sample are in good agreement with simulated results which shows our design and simulation works well in practice.

8632-71, Session 16

Surface plasma wave enhanced infrared detection

(Invited Paper)

Steven R. J. Brueck, Seung Chang Lee, Sanjay Krishna, The Univ. of New Mexico (United States)

Surface plasma waves (SPW) offer an attractive enhancement for infrared photodetectors. We demonstrate strong enhancement in the detectivity (100%) for both top-surface metal photonic crystal (holes in a Au film) and back surface corrugated metal films on quantum-dot infrared photodetectors (QDIPs). The corrugated metal film is particularly attractive for incorporation in a standard focal plane array processing sequence. The first fully operation SPW focal plane array camera is demonstrated. The long term vision is to encode both spectral and polarization information in a FPA readout greatly increasing the information content of infrared cameras.

Conference 8632: Photonic and Phononic Properties of
Engineered Nanostructures III

8632-72, Session 16

Passive and active metamaterial based ultrathin optical filters and switches (*Invited Paper*)

Koray Aydin, Northwestern Univ. (United States)

By engineering localized resonances, it is possible to control the way light interacts with optical materials and design functional devices with enhanced optical functionalities. In recent years, plasmonics and optical metamaterials have received wide attention from scientific community to their unparalleled ability to confine light into subwavelength dimensions.

In this talk, I will discuss routes to design narrowband transmission and absorption filter utilizing metallic nanostructures with unique localized and delocalized resonances. Recently, we have obtained high-Q optical metamaterial cavities reaching ~ 1000 , which is quite impressive for coupled resonators made of lossy metallic structures. I will describe narrow-band optical absorbers with subwavelength thickness (~ 80 nm). Besides designing passive metamaterial filters, one could realize reconfigurable, dynamic optical metamaterials that change their optical properties when exposed to an external stimuli. I will present frequency-tunable, hybrid infrared metamaterials, in which a dynamic optical response is achieved via a thermally induced phase transition in vanadium dioxide (VO₂) nanostructures. I will also present how the mechanical actuation of flexible polymers can be used to control the nanoscale distances between coupled metallic resonators, in turn enabling frequency-tunable, compliant optical metamaterials. Such reconfigurable nanophotonic materials significantly enhance the infrared reflection signal from a C-H vibrational mode, and could find use in biochemical sensing and environmental screening applications. At the end of my talk, I will outline a strategy to obtain electrically-tunable optical metamaterials using oxide-based material systems.

8632-73, Session 16

Fano-resonant metamaterials for ultra-sensitive spectroscopy and Stokes polarimetry in the infrared (*Invited Paper*)

Gennady B. Shvets, The Univ. of Texas at Austin (United States)

Metamaterials exhibiting Fano interference are emerging as a powerful platform for sensing minute amounts of materials, in some instances as small as a single molecular or atomic monolayer. The basic physical reason for that is their highly spectrally-selective response and very high optical intensity concentration near resonance. We will describe three major applications of Fano-resonant metamaterials: (1) spectroscopy of single atomic and molecular layers, (2) sub-diffraction imaging of nanoscale objects using polarization spectro-tomography, and (3) polarization state detection using strongly asymmetric plasmonic and semiconductor-based structures. In part (1), IR spectroscopy of protein monolayers and single-layer graphene will be discussed. The future role of graphene for making rapidly tunable metamaterials will be discussed, and first experimental data demonstrating lossless blue-shifting of infrared metamaterial resonances will be presented. In part (2), I will discuss how strong Fano interference between "dark" nanoparticle labels such as quantum dots, and much larger "bright" plasmonic nanoparticles enables sub-diffraction imaging. We will discuss several approaches to increasing the spectral selectivity of metamaterials by reducing radiative

losses and Ohmic losses. To achieve these goals, all-semiconductor metamaterials will be described and supporting experimental data presented. Such metamaterials can be used for highly efficient polarization manipulation such as circular polarization conversion. In addition, the possibility of developing ultra-thin Stokes polarimetry using low-symmetry Fano-resonant metamaterials will be discussed.

8632-74, Session 16

Metamaterial-based imaging for potential security applications (*Invited Paper*)

David Shrekenhamer, Willie J. Padilla, Boston College (United States)

New innovative imaging techniques have been gaining interest in the past few years that allow for shorter acquisition times and offering potential advantages in imaging applications, especially in infrared (IR) and terahertz (THz) regimes where there are potential uses in security applications. One promising approach involves metamaterial-based devices that are controllable both dynamically and spatially to act as direct platform for these techniques to be implemented across the electromagnetic spectrum. In our research, we utilize metamaterial perfect absorbers (MPAs) which completely absorb incident electromagnetic energy and implement them so as to demonstrate the imaging capabilities of these types of devices. We have created pixelated arrays of MPAs that acts as a spatial light modulator (SLM). This acts as an innovative substitute for digital micromirror devices (DMDs), which are spectrally featureless and have set frequency limits.

8633-1, Session 1

High contrast gratings: physics and applications (*Invited Paper*)

Connie J. Chang-Hasnain, Univ. of California, Berkeley (United States)

High contrast gratings can be designed to exhibit various extraordinary properties, ranging from broadband reflector, transmission window, lens, beam splitters, to high-Q resonator. In this talk, we will discuss the physics of 1D and 2D high contrast gratings (HCGs) and a set of design rules for various device applications.

8633-2, Session 1

Double photonic crystal vertical-cavity surface-emitting lasers (*Invited Paper*)

Pierre Viktorovitch, Ecole Centrale de Lyon (France); Corrado Sciancalepore, Ecole Centrale de Lyon (France) and CEA-LETI (France); Badhise Ben Bakir, CEA-LETI (France); Xavier Letartre, Christian Seassal, Ecole Centrale de Lyon (France)

Vertical-cavity surface-emitting lasers (VCSELs) emitting in C-band using a double set of one-dimensional Si/SiO₂ photonic crystals as compact, flexible, and power efficient mirrors have been realized within a mass-scale fabrication paradigm by employing standard 200-mm microelectronics pilot lines. High fabrication yields obtained thanks to the state-of-the-art molecular wafer bonding of III-V alloys on silicon conjugate excellent device performances with cost-effective high-throughput production, indicating strong perspective industrial potential. Consequently, double photonic crystal VCSELs constitute a robust high-performance building block for the follow-through of both silicon and VCSEL photonics.

8633-3, Session 1

Physics of high contrast gratings: a band diagram insight

Weijian Yang, Connie J. Chang-Hasnain, Univ. of California, Berkeley (United States)

High contrast grating (HCG) is a single layer of periodic subwavelength grating composed of a high-refractive-index material surrounded entirely by low-index materials. Various extraordinary properties have been demonstrated, such as ultra broadband high reflectivity ($R > 0.99$, $??/? > 35\%$) and high quality-factor resonance ($Q > 10^7$). A phase selection rule and HCG supermode formalism for surface-normal incidence have been established to explain these phenomena.

It is natural to question if the extraordinary properties of HCG can be obtained with the more general case of oblique incidence. It is also interesting to examine HCG properties as the incident angle approaching 90 degree and the HCG looks more and more like a 1D photonic crystal (PhC). Here, we generalize the theoretical modelling to arbitrary incidence angle, and unveil the HCG band diagram with HCG supermode formalism. In the reflection spectrum, the HCG supermode resonances manifest themselves as full transmission as in a Fabry-Perot resonance or, most peculiarly, as sharp transient from high to low reflections as in a Fano resonance. These resonances signify the photonic bands in the band diagram. The band diagram calculated with HCG supermode formalism provides insight into the band structure, and is consistent with the one calculated by finite-difference time-domain method (FDTD) for 1D PhC. We show, for the first time, HCG and PhC can be unified in the same theoretical architecture. They differentiate themselves by operating at different regimes in the band diagram. The supermode formalism provides a powerful tool to study both HCG and PhC.

8633-4, Session 2

Is the Wood anomaly a plasmonic phenomenon? (*Invited Paper*)

Philippe Lalanne, Institut d'Optique Graduate School (France); Haitao Liu, Nankai Univ. (China)

At a microscopic level, the electromagnetic properties of subwavelength metallic surfaces are due to two kinds of elementary distinct waves, surface plasmon polariton and the quasi-cylindrical wave [Nature 452, 728 (2008)]. These waves are launched on the metal surface by the scattering of the incident field on the subwavelength indentations. We review the fundamental properties that govern these waves and discuss their impacts in the Wood anomaly of metallic gratings [Philos. Mag. 4, 396 (1902)], a phenomenon historically attributed to surface plasmon polaritons since Fano's work [J. Opt. Soc. Am. 31, 213 (1941)].

8633-5, Session 2

Demonstration of a slow light high contrast metastructure cage waveguide (*Invited Paper*)

Weimin Zhou, Gerard Dang, Monica Taysing-Lara, U.S. Army Research Lab. (United States); Connie J. Chang-Hasnain, Univ. of California, Berkeley (United States)

We have developed a new type of 3D cage-like high-contrast metastructure waveguide in order to pursue both "slow-light" and low-loss properties, for providing a long time-delay or a high Q cavity in chip-scale integrated OE circuits. Normal waveguides always have a high loss when used in a slow-light region. A 2D computational model indicates that there is a zero-slope, slow-light region on the dispersion curve with very little propagation loss in a planar waveguide formed by two high contrast gratings (HCG) which suggests that it is also possible in a 3D waveguide case. We have successfully developed a nano-fabrication technique for this 3D cage-like waveguide, formed by 4 HCGs, with a square-hollow-core, on a Si wafer. Several waveguides were made with differing dimensions such as, a 2 μm core, 625 nm period HCG with 1.5 μm high and 40% Si-to-Air duty cycle for 1550 nm operating wavelength. We have performed experimental measurements for both waveguide propagation loss and group velocity as a function of wavelength on these waveguides. The cut-back method was used for loss measurements with waveguide lengths between 26 and 3 mm. Preliminary results indicate that there are $< 2\text{dB/cm}$ low-loss regions. For group velocity measurement, we used a short laser pulse to detect the time delay of the propagation in the waveguide and without the waveguide. We have confirmed a group velocity of about 30% of the speed of the light. We have also developed a fabrication technique for a larger 3D cage waveguide for THz sensor application.

8633-6, Session 2

Three-dimensional hollow-core waveguide based on high-contrast grating

Tianbo Sun, Stephen A. Gerke, Weijian Yang, Univ. of California, Berkeley (United States); Philippe Lalanne, Institut d'Optique Graduate School (France); Weimin Zhou, U.S. Army Research Lab. (United States); Connie J. Chang-Hasnain, Univ. of California, Berkeley (United States)

Hollow-core waveguides (HCWs) have received much attention recently for their special properties at the wavelength regime where conventional solid-core waveguides encounter a large absorption loss and nonlinearity. High reflectivity mirrors are essential to realize low-loss HCW. High-contrast sub-wavelength gratings (HCGs) have been reported to achieve a broadband high reflectivity. It consists of a single layer of

sub-wavelength grating with high-refractive-index (e.g. semiconductor), surrounded by low-index materials (e.g. air or oxide). HCG has been demonstrated as a broad bandwidth high reflection mirror both at normal incident angle and glancing angle. These enable novel hollow-core waveguide with HCG as high performance reflectors.

We present two types of HCG-HCWs: longitudinal type (gratings run parallel to the light propagation direction) and cage type (gratings run parallel to the light propagation direction perpendicular to the propagation). We study the relations between these two types of waveguides. The HCWs are designed with intuitive guideline from ray optics and further simulated with finite-difference time-domain (FDTD) method. A fundamental waveguide mode with propagation loss lower than 0.1dB/cm is achieved with a waveguide core size $5\mu\text{m} \times 6\mu\text{m}$. The simulated k - k diagram shows the promising operation region where slow-light can be obtained.

8633-7, Session 2

Fabrication technique development for 3D high-contrast-metastructure cage waveguides

Monica Taysing-Lara, Gerard Dang, Weimin Zhou, U.S. Army Research Lab. (United States)

We report on our fabrication technique development for a new type of 3D cage-like high contrast metastructure waveguide formed by four high contrast gratings (HCGs), with square hollow-core, on a Si wafer. Several processing methods were developed and compared. The goal is to select a relatively simple and practical technique that has better fabrication precision and uniformity as well as CMOS compatibility and low cost for Si-based OEIC. All of these methods involve creating a 2D mask on the top surface of a SOI wafer, then, performing a self aligned dry etch for a deep trench in which we vary the width of trench moving in the vertical direction. This allows a complete undercut in the core region under the HCG and incomplete undercut that creates the vertical posts to form the 2 vertical HCGs, as well as the bottom HCG, therefore forming the 3D cage-like hollow-core waveguide. The first method uses modified Bosch etch cycles to control the width of the trench and under cutting. The second and third methods use modified "SCREAM" method which uses SiO₂ and polymer, respectively, to coat a portion of the uniform deep trench and conduct an isotropic etch to undercut the uncoated portion. Using these different methods, we have produced a series of waveguides with different dimensions from a 625 nm to a 100 μm HCG period for different operating wavelength from 1550nm to 300 μm . We will discuss the pro and cons of these methods from our experimental results.

8633-8, Session 3

Speed enhancement in VCSELs employing grating mirrors (*Invited Paper*)

Il-Sug Chung, Jesper Mørk, Technical Univ. of Denmark (Denmark)

High-index-contrast grating (HCG) mirrors employed in vertical-cavity surface-emitting lasers (VCSELs) provide two photonic parameters that can be engineered to enhance the direct modulation speed: They are the modal volume and the photon life time of the VCSEL cavity. Compared to conventional distributed Bragg reflectors (DBRs), HCG mirrors have very small penetration depth. Thus, employing a HCG mirror or double HCG mirrors may lead to 2-3 times smaller modal volume than VCSELs with conventional DBRs, resulting in considerable speed enhancement. The photon life time of a VCSEL cavity is decided by the mirror and internal losses as well as the roundtrip propagation time within the cavity. In conventional VCSELs with DBRs, the reflectivity of a top mirror is reduced to get a higher mirror loss and a resultant shorter photon life time, even though this may increase the threshold current. Or the cavity length is reduced to have a shorter roundtrip time for obtaining a shorter photon life time. In VCSELs with HCG mirrors, the reflection delay time

of HCG mirrors can be controlled while keeping the mirror reflectivity high. Controlling the reflection delay time to very low value provides another freedom to control the frequency response. In the talk, physical comparison with conventional VCSELs will be presented in details.

8633-9, Session 3

VCSELs with a high-index-contrast grating for space division multiplexing

Qijiang Ran, Il-Sug Chung, Technical Univ. of Denmark (Denmark)

Space division multiplexing (SDM) is a method to use typically six different transverse modes in a few-mode fiber (FMF) to increase transmission bandwidth. So far, spatial phase plates have been used to generate higher order modes from a Gaussian-profile laser output. In this paper, a novel light source structure for SDM is proposed and numerically investigated. This light source is a vertical-cavity surface-emitting laser (VCSEL) structure employing a high-index-contrast grating (HCG) as a light-emitting mirror. The reflectivity of the HCG mirror is spatially modulated between 99.5% and 97%, following the field intensity of each transverse mode of the VCSEL cavity. The transmission phase of the HCG mirror is kept spatially constant throughout the reflectivity-modulated HCG region. In this way, a specific transverse mode of interest can be selectively excited and emitted as output. The reflectivity modulation is obtained by varying the duty cycle and/or period of the grating. The coupling efficiency to a FMF is as high as 80%. Compared to the phase plate approach, the HCG-integrated VCSEL approach can be a much more compact and cheaper alternative. In the talk, the device structure and methodology will be discussed in detail.

8633-10, Session 3

A three-dimensional and vectorial optical solver for HCG tunable VCSELs

(*Invited Paper*)

Pierluigi Debernardi, Renato Orta, Politecnico di Torino (Italy)

High Contrast Gratings (HCG) have become a hot research topic, because of their new functionalities at very small volume: one major application is in tunable devices, where the light HCG (compared with much heavier Bragg stacks) allows faster tunability.

However no 3D VCSEL model capable to account for HCG has been reported so far. HCG design is therefore mainly based on 1D simulations. For realistic structures usually FDTD is the most popular approach, with its well known computation drawbacks.

VELM model, the well established VCSEL electromagnetic solver developed in the last ten years in our group, has now been upgraded to rigorously handle HCG layers.

The efficiency of the tool is fully preserved, and a full set of HCG VCSEL modes can be computed in minutes on an ordinary desktop.

Examples of results will be given for a 1550nm emitting single mode tunable VCSEL, by discussing the higher single mode performance of HCG compared to DBR based devices.

8633-11, Session 3

Fano resonances GaN-based high contrast grating surface-emitting lasers

Tzeng-Tsong Wu, Shu-Hsien Wu, Tien-Chang Lu, Hao-Chung Kuo, Shing-Chung Wang, National Chiao Tung Univ. (Taiwan)

Sub-wavelength high contrast grating (HCG) structures has been recently researched and applied to vertical cavity surface-emitting lasers (VCSELs) and surface-emitting high-quality factor (Q) resonators.

In this report, GaN-based HCG-SELs with AlN/GaN distributed Bragg reflectors (DBRs) were realized at room temperature by optical pumping. Instead of the undercut structure, the AlN/GaN DBRs can play a role as the low refractive index layer. The HCG structure was designed and the reflectivity spectra were calculated by rigorous coupled-wave analysis (RCWA). The asymmetric resonance reflectivity spectra supported by Fano resonance can lead the high Q factor of about 530. GaN-based HCG-SELs with AlN/GaN distributed Bragg reflectors (DBRs) were fabricated by e-beam lithography (EBL) and inductively coupled plasma (ICP) dry etching. The low threshold condition and lasing wavelength of GaN-based HCG-SELs were observed to be 17.7 μ J/cm² by optical pumping at room temperature. When it was below the threshold condition, the photoluminescence (PL) results showed the Fano resonance asymmetric spectra and the Q factor was calculated to be about 400. Besides, laser characteristics such as degree of polarization (DOP) and divergence angle were also measured to be 73% and 12 degrees. Finally, the band diagram and mode pattern were calculated by plane wave expansion (PWE) and finite element method (FEM). The experimental results could be confirmed by the simulation ones.

8633-12, Session 4

Metallic metastructures for THz optoelectronics: high power extraction surface-emitting lasers and sub-diffraction-limit resonators (*Invited Paper*)

Raffaele Colombelli, Institut d'Électronique Fondamentale (France)

We discuss recent trends in THz optoelectronics relying on metallic meta-structures: strategies for high-power emission from THz quantum-cascade (QC) lasers, and the quest for extremely sub-wavelength resonators/lasers. On the first topic, we report high-power, single-mode surface-emission from THz QC lasers using novel "photonic heterostructure" resonators. Peak output powers larger than 100 mW at 20K (60 mW at 78K) are obtained. On the second topic, we demonstrate semiconductor resonators with sub-wavelength dimensions in all three dimensions of space. The maximum confinement achieved is $\eta_{eff}/9$, where η_{eff} is the wavelength inside the material (or $\lambda/30$, if the free space wavelength is considered).

8633-13, Session 4

Novel diffraction properties of high-contrast gratings (*Invited Paper*)

Bala Pesala, CSIR Madras Complex (India)

High-Contrast Gratings (HCG's) have been shown to have interesting reflection, transmission, phase and resonance properties. However, the diffraction properties of HCG's haven't been fully explored so far. Here, we present unique diffraction properties of subwavelength HCG's such as steep angle diffraction into the substrate and high diffraction efficiency with large spectral bandwidth. Steep angle diffraction into the substrate is a direct consequence of subwavelength grating period. Further, high index contrast results in high diffraction efficiency over a large spectral bandwidth. These properties are useful for various applications such as color shifting structures that exhibit different colors at various viewing angles, light concentrators for solar photovoltaic, solar thermal and day lighting applications and light couplers in integrated optics.

8633-14, Session 5

Super-high resolution beam steering based on Bragg reflector waveguides with high-contrast metastructures (*Invited Paper*)

Fumio Koyama, Xiaodong Gu, Tokyo Institute of Technology (Japan)

A beam-steering device has been a key element for various sensing and imaging applications. We proposed a novel beam steering device based on a Bragg reflector waveguide. A steering angle of over 60 degrees and a number of resolution points over 1,000 can be expected for a few mm long device with a low loss high-contrast Bragg reflector waveguide. One- λ thick core is sandwiched by two high-contrast quarter wavelength stack mirrors. A slow-light mode can propagate laterally in such a structure with a low propagation loss thanks to high-contrast DBRs. We could see a large angular dispersion of over 1°/nm for radiated light from the surface. Thanks to the large angular dispersion, we are able to realize beam-steering of the radiated light by tuning the wavelength of incident light. We could obtain a continuous steering angle of more than 60° by wavelength tuning of 40nm. The divergence angle is below 0.04° for all wavelengths. Considering the steering range and sharp beam divergence, we successfully achieved a number of resolution points of over 1,000. To our knowledge, it is the highest number among all other beam steering devices without a mechanical scanner. We will discuss super-high resolution beam steering from an ultra-low loss Bragg reflector waveguide with high-contrast metastructures. Also, high contrast sub-wavelength grating offers additional freedom to control the in-plane phase and reflectivity in Bragg reflector waveguides, which may enable us to control the far-field pattern profile for higher resolutions.

8633-15, Session 5

Optical phased array using single crystalline silicon high contrast grating for beamsteering (*Invited Paper*)

Byung-Wook Yoo, Univ. of California, Berkeley (United States); Trevor K. Chan, Univ. of California, Davis (United States); Mischa Megens, Tianbo Sun, Weijian Yang, Yi Rao, Univ. of California, Berkeley (United States); David A. Horsley, Univ. of California, Davis (United States); Connie J. Chang-Hasnain, Ming C. Wu, Univ. of California, Berkeley (United States)

In this paper, we present single crystalline silicon optical phased array using high-contrast-grating (HCG) for two dimensional beamforming and beamsteering at 0.5 MHz. Since there are various applications on beamforming and beamsteering such as 3D imaging, optical communications, and light detection and ranging (LIDAR), it would be of great interest to develop ultrafast optical phased array. However, the beamsteering speed of optical phased arrays using liquid crystal and electro-wetting is typically limited at tens of milliseconds. Optical phased array using micro-electro-mechanical systems (MEMS) technologies can reportedly actuate in the submegahertz range, but generally requires metal coating that causes thermally induced stress. A novel MEMS-based optical phased array herein consists of electrostatically driven 8 \times 8 HCG pixels fabricated on a silicon-on-insulator (SOI) wafer. The HCG mirror is designed to have 99.9% reflectivity at 1550 nm wavelength without any reflective coating that MEMS mirror usually needs. The size of HCG mirror is 20 \times 20 μ m² so that the mass is only 139 pg, which is much lighter than traditional MEMS mirrors. The 8 \times 8 optical phased array has a total field of view of $\pm 10^\circ \times 10^\circ$ and a beam width of 2°. The maximum phase shift regarding the actuation gap defined by 2 μ m buried oxide layer of a SOI wafer is 1.7 π at 20 V. The response time of HCG pixels is measured to be microseconds.

8633-16, Session 5

High-speed optical phased array using two-dimensional high-contrast grating all-pass filters

Weijian Yang, Tianbo Sun, Yi Rao, Trevor K. Chan, Mischa Megens, Byung-Wook Yoo, Univ. of California, Berkeley (United States); David A. Horsley, Univ. of California, Davis (United States); Ming C. Wu, Connie J. Chang-Hasnain, Univ. of California, Berkeley (United States)

Optical phased arrays have enabled free-space beam steering for a wide range of applications, such as imaging, display and sensing. A chip-scale and high-speed optical phased array is of particular desire. It matches the high-integration-density, small-footprint, low-power-consumption and high-speed requirement of advanced applications such as optical circuit switching, light detection and ranging (LIDAR) etc. Several phase tuning mechanisms have been demonstrated for optical phased arrays, such as electro-mechanical, electro-optic, and thermo-optic effect. However, most of them are relatively low speed at a few kHz to tens of kHz.

In this paper, we demonstrate a novel 8x8 optical phased array based on two-dimensional high-contrast grating all-pass filters with high speed (0.626 MHz) micro-electro-mechanical actuation. Each array element is an all-pass filter (APF) with a two-dimensional high-contrast grating (HCG) as a highly reflective top reflector and a distributed Bragg reflector (DBR) as the bottom reflector. Highly efficient phase tuning is achieved by actuating the HCG to tune the cavity length of the APF across the Fabry-Perot resonance. The ultrathin HCG further ensures a high tuning speed. Compared with a one-dimensional HCG, the two-dimensional HCG can be actuated more uniformly, especially at high frequency. The symmetric design overcomes the polarization sensitivity of the one-dimensional HCG. Beam steering is experimentally demonstrated by creating a near-field reflection phase pattern with different applied voltages on individual pixels. Bandwidth > 1 MHz can be achieved by further optimization of the MEMS structure.

8633-17, Session 5

Tunable optical beaming with subwavelength metallic gratings sandwiched in asymmetric dielectric layers

Zhonghua Wang, Anshi Xu, Peking Univ. (China)

We propose a novel tunable optical beaming mechanism based on a dielectric-metal-dielectric-metal (DMDM) structure. The upper dielectric layer is of a denser medium while the lower dielectric layer is of a less dense one. When surface plasmon polaritons (SPPs) propagating along the MDM waveguide impinge upon periodic subwavelength slits milled in the upper optically thick metal film, an off-axis directional beaming effect is generated with a radiation angle of the plasmonic critical angle (PCA) in the denser medium. Controlling the permittivity of the less dense medium sandwiched between two metal layers, the value of the PCA varies and the off-axis beaming with dynamic radiation direction tuning can be realized. The conditions and physical origins of the beaming effect with a radiation angle of the PCA are clarified. With the denser medium of refractive index 2.3 and the less dense one of refractive index varying from 1 to 2, the radiation angle of the beaming can be tuned from 25.8 degree to 60.4 degree. As the PCA is independent of the grating period, fill factor, thickness, the operating wavelength and the refractive index of the material filled in the slits, the proposed tunable beaming mechanism has large fabrication tolerances and can be easily achieved.

8633-18, Session 6

Flat optics with optical antenna metasurfaces (Invited Paper)

Federico Capasso, Harvard School of Engineering and Applied Sciences (United States)

Conventional optical components rely on gradual phase shifts accumulated during light propagation to shape light beams. New degrees of freedom in optical design are attained by introducing in the optical path abrupt phase changes over the scale of the wavelength. For example a two-dimensional array of plasmonic resonators in form of V-shape antennas with spatially varying phase response and sub-wavelength separation can imprint such phase discontinuities on propagating light¹. In this paper, I review the research of my group on the optical response of such antenna arrays and on a new class of flat optical components ("metasurfaces") based on the latter¹⁻⁻⁴. To demonstrate the versatility of metasurfaces, we show the design and experimental realization of a number of flat optical components: (a) metasurfaces with a constant interfacial phase gradient that can beam light into arbitrary directions in the half space; (b) optical antenna arrays with giant birefringence and widely tailorable optical anisotropy; (c) metasurfaces with anisotropic optical responses that can create light beams of arbitrary polarization over a wide wavelength range and (d) metasurfaces with spiral phase distribution that create optical vortex beams that carry orbital angular momentum. The talk will conclude with an overview of related research by other groups.

- [1] N. Yu, et al. Science 334, 333 (2011)
- [2] F. Aieta, et al. Nano Letters 12, 1702 (2012)
- [3] M. Kats et al. PNAS 109, 12364 (2012)
- [3] P. Genevet, et al. Appl. Phys. Lett. 100, 13101 (2012)

8633-19, Session 6

Applications of amorphous silicon grating lenses (Invited Paper)

David Fattal, Sonny Vo, Zhen Peng, Marco Fiorentino, Ray Beausoleil, Hewlett-Packard Labs. (United States)

High contrast gratings provide a way to realize ultra-thin lenses with a moderate feature aspect ratio amenable to mass fabrication. In this talk, I will review our efforts to manufacture such lenses using amorphous silicon, a high index material that can be deposited on a wide variety of substrate by PECVD. I will present the performance of such lenses in the visible and near-IR spectrum and talk about some potential industrial applications.

8633-20, Session 6

Aberration-free ultra-thin flat lenses and axicons at telecom wavelengths based on plasmonic metasurfaces

Francesco Aieta, Patrice Genevet, Mikhail A. Kats, Nanfang Yu, Zeno Gaburro, Federico Capasso, Harvard School of Engineering and Applied Sciences (United States)

The concept of optical phase discontinuities provides a different path for designing flat lenses. In this approach, the control of the wavefront is achieved by tailoring the phase shifts experienced by light as it scatters off an optically-thin array of subwavelength-spaced resonators comprising a metasurface. We experimentally demonstrated light focusing in free space at telecom wavelength $\lambda = 1.55 \mu\text{m}$ using 60nm-thick gold metasurfaces. We fabricated two flat lenses of focal distances 3cm and 6cm and a flat axicon with an angle $\theta = 0.5^\circ$ (which corresponds to a glass plano-convex axicon with base angle 1°). Our experiments

are in excellent agreement with numerical simulations and show the expected focusing properties of the fabricated devices; furthermore the measured profiles display the difference between the Airy patterns generated by the lenses and the Bessel beam created by the axicon. Our calculations also point to the possibility of achieving focusing with numerical aperture as high as $NA = 0.77$.

We note that the phase distribution created from a conventional spherical lens focuses the light to a single point only in the limit of paraxial approximation; a deviation from this condition introduces monochromatic aberrations. In our case, the hyperboloidal phase distribution imposed at the interface produces a wavefront that remains spherical even for non-paraxial conditions. This enables high NA focusing without aberrations.

8633-21, Session 6

1550-nm silicon-on-insulator Planar lenses using high-contrast gratings

Tianbo Sun, Weijian Yang, Fanglu Lu, Connie J. Chang-Hasnain, Univ. of California, Berkeley (United States)

High Contrast Grating (HCG) is an array of high index material fully surrounded by low index medium. We demonstrated broadband reflector and high-Q resonator using periodic HCGs. Also, chirped HCG can be designed for lens purpose, utilizing the fact that HCG resonance is strongly localized. Due to the period and duty cycle change along x axis (grating period direction), plane wave incidence will have different reflection phase at different x. By constructing reflection phase front, we can design different HCG planar lens for focusing or diverging purposes, which will have potential use in CCD lens array, on-chip beam forming and confocal cavity, etc.

To test the HCG lens concept experimentally, three different reflection lenses are fabricated and examined in experiment: 2D lens with $NA \sim 0.025$, 1D cylinder lens with $NA \sim 0.1$ and 2D negative lens. The devices are fabricated on SOI wafer (450nm Si layer sitting on 1um oxide and Si substrate) with photo-lithography and one-step etching, so potentially can be fabricated in large scale. Images of reflected beam spots at different positions are recorded, from which beam profile can be reconstructed and then compared with simulation results. Focal length and lens dispersion for different types of lens are also investigated. Good agreement between theory prediction and experiment is achieved, which strongly indicates the validity of our theory and design algorithm. The reflection of the lens is also measured for the communication spectra (1530nm ~ 1565nm). 90% in reflection is a little bit lower than the expected 97%, probably due to the dimension variation in fabrication.

8633-22, Session 7

High-contrast gratings for high-precision metrology (Invited Paper)

Stefanie Kroker, Thomas Käsebieer, Ernst-Bernhard Kley, Friedrich-Schiller-Univ. Jena (Germany); Andreas Tünnermann, Friedrich-Schiller-Univ. Jena (Germany) and Fraunhofer-Institut für Angewandte Optik und Feinmechanik (Germany)

Experiments in the field of high-precision optical metrology are crucially limited by thermal noise of the optical components such as mirrors or beam splitters. Amorphous coatings are found to be a main source for these thermal fluctuations. In this contribution we present approaches to realize coating free optical components based on resonant high contrast gratings (HCGs) made of crystalline silicon. It is shown that beside classical cavity mirrors the concept of HCGs can also be used for reflective cavity couplers. Therefore, a large angular tolerance of the HCG reflectors has to be ensured. We propose two different approaches in order to enhance the angular bandwidth of conventional HCGs. The first makes use of stacking HCGs whilst the second benefits from polarization effects in HCGs with two-dimensional periodicity. For reflective beam splitters these angular broadband reflectors can be combined with either additional superposed lateral (grating duty cycle, ridge positions) or

transversal (grating thickness) modulations to provide the subwavelength structures with diffraction orders. The diffraction efficiency can therewith be tuned with the strength of the modulation. We compare the advantages and challenges of these HCG reflectors with distributed Bragg reflectors made of crystalline AlxGa1-xAs coatings for applications in optical metrology.

8633-23, Session 7

High-contrast grating mirrors for radiation-pressure optomechanics (Invited Paper)

John R. Lawall, National Institute of Standards and Technology (United States); Utku Kemiktarak, Mathieu Durand, National Institute of Standards and Technology (United States) and Joint Quantum Institute (United States)

High-contrast subwavelength diffraction gratings offer a novel platform for cavity optomechanics, in which the mechanical dynamics of a mirror is coupled by means of radiation pressure to the optical field inside a cavity. By fabricating diffraction gratings in silicon nitride membranes, we realize a mechanically compliant mirror that is far less massive than one obtained with a conventional quarter-wave stack, with a far higher mechanical quality factor. We have used these gratings as the end mirror of a Fabry-Perot cavity with a finesse $F > 2000$, enabling high-sensitivity readout of the mechanical motion of the gratings, along with the ability to control their dynamics via the radiation pressure of the intracavity field. We are able to optically cool hundreds of mechanical modes of the membranes simultaneously, reaching effective temperatures in the vicinity of 1 K. Alternatively, we are able to overcome the intrinsic mechanical damping of the membrane with optomechanical gain, creating a "phonon laser." The nonlinear dynamics of the oscillating system exhibits the threshold behavior and mode competition observed in a conventional optical laser, as well as hysteresis associated with the pump power. We observe birefringence in the cavity and are attempting to compensate it.

We are aiming to improve the optomechanical performance of these devices by further reducing the mass, optical losses, and mechanical losses. Finally, we are experimenting with coupled optomechanical systems, in which the high-contrast grating is used to couple two optical cavities.

8633-24, Session 7

Experimental realization of high-contrast grating based broadband circular polarizer (Invited Paper)

Ekmel Özbay, Bilkent Univ. (Turkey)

We report the fabrication and experimental characterization of a broadband circular polarizer, which is composed of two-dimensional and binary silicon based high-contrast gratings. An experimental bandwidth was measured to be 33%, which is in reasonably good agreement with the theoretically calculated bandwidth of 42%. Within this wavelength range, the conversion efficiency was measured to be larger than 0.9.

8633-25, Session 7

Omnidirectional antireflective mechanism based on buried nano-antennas

Ali Kabiri, Harvard School of Engineering and Applied Sciences (United States); Emad Girgis, Harvard Univ. (United States); Federico Capasso, Harvard School of Engineering and Applied Sciences (United States)

Reflection occurs when light passes the interface of two media with different refractive indices. While reflection is a natural phenomenon, it

is an unwanted loss process in many applications such as solar cells and photo-detectors. Dielectric interface coatings, surface texturing and patterning and adiabatic index matching are among many methods which have been investigated in literature. In general, so far, techniques in producing antireflection are narrowband, angle or polarization dependent. Here, we propose a new technique that highly suppresses the reflection of the electromagnetic wave from a medium over a wide range of incident angles. A periodic structure of nanoantennas is buried inside the incident medium to create a nanoscale vertical cavity at the interface in order to reduce the reflection. To create omnidirectional antireflection, nano-antennas can be designed to be polarization-independent. The novel technique relies on impedance matching mechanism produced by thin layer of nanoantennas array buried in an incident medium. Sample structures have been fabricated to operate at mid-infrared, and the reflection of less than 0.5% is achieved. The fabrication process is based on ebeam nanolithography. In this experiment, the host medium is crystalline Silicon. Proper holes for depositing gold are etched on the Silicon. The structure finally is covered by amorphous Silicon using CVD technique to a calculated thickness to leave the gold nanoantennas at a certain depth inside the medium. The reflection is measured using Fourier Transform Interferometer. Experimental and numerical data are compared, and results are in good agreement.

8633-26, Session 8

Anomalous reflectivity and absorptivity of metastructures combined with metal and dielectric (*Invited Paper*)

Yufei Wang, Anjin Liu, Wanhua Zheng, Institute of Semiconductors (China)

We present a polarization-insensitive subwavelength grating reflector based on a semiconductor-insulator-metal structure. The polarization-insensitive characteristic originates from the combined effect of the TM-polarized high-reflectivity high-index-contrast subwavelength grating and the TE-polarized metallic (Au) subwavelength grating with the addition of the insulator layer. The overlapped high reflectivity (>99.5%) bandwidth between the transverse electric polarization and the transverse magnetic polarization is 89 nm. Additionally, we also study an Au-ITO multilayer grating. The novel thin metal and transparent dielectric ten-pair multilayer structure has the one-way absorption at 1550 nm, which provides potential application value in signal procession and engineering thermal radiation.

8633-27, Session 8

A polychromatic approach to far field superlensing with microwave, sound, and light (*Invited Paper*)

Fabrice Lemoult, Mathias Fink, Geoffroy Lerosey, Institut Langevin (France)

In this talk I will show how the use of time dependent and broadband wavefields, in conjunction with metamaterials, allows to beat the diffraction limit from the far field for imaging or focusing purposes. I will introduce the idea of resonant metalens, first demonstrated in the microwave domain, and explain its principles. In particular, I will show how the concept of time reversal can be utilized to focus in this metamaterial based lens and from the far field, onto focal spots much smaller than the diffraction limit. I will then prove the generality of the approach by demonstrating its transposition to the acoustic domain. Then I will present our latest theoretical and numerical results obtained using a resonant metalens made out of plasmonic nanorods in the visible part of the spectrum. I will show that this lens allows, using polychromatic light, to focus light with far field time reversal onto spots as small as 1/30th of the wavelength in the visible. Finally I will prove that our approach can also be used in order to image from the far field and with a subwavelength resolution and could lead to real time sub-diffraction imaging systems.

8633-28, Session 9

High-index contrast gratings for silicon photonic integrated circuits (*Invited Paper*)

Gunther Roelkens, Univ. Gent (Belgium); Diedrik Vermeulen, Acacia Communications Inc. (United States); Yanlu Li, Univ. Gent (Belgium); Muhammad Muneeb, Nannicha Hattasan, Eva Ryckeboer, UGent (Belgium); Yannick Deconinck, Dries Van Thourhout, Roel G. Baets, Univ. Gent (Belgium)

Silicon photonics is being consolidated as a high-performance platform for integrated photonic functionality. The high index contrast available on the platform allows the realization of ultra-compact waveguide circuits. This however also makes the efficient coupling to a silicon waveguide circuit difficult. However, high index contrast grating structures can provide an efficient way to interface a silicon photonic integrated circuit with an optical fiber or free-space (beam steering). In this paper we elaborate on the different grating coupler structures for high efficiency, polarization-independent and multi-wavelength band fiber-to-chip coupling. The use of these structures for wafer-scale testing of photonic integrated circuits is demonstrated. Special care is taken to avoid parasitic back reflections from the grating towards the silicon waveguide circuit, since this can perturb its operation. The fabrication of sub-wavelength grating structures with advanced CMOS fabrication technology is presented. In a second part of the paper the use of high contrast gratings for the realization of III-V/silicon single wavelength lasers is described. Using resonant grating structures as wavelength selective feedback elements implemented in the silicon waveguide layer and patterned using advanced CMOS fabrication tools, allows realizing compact edge-emitting III-V lasers, with maximum optical confinement in the III-V.

8633-29, Session 9

Transfer printed photonic crystal nanomembrane lasers for integrated silicon photonics (*Invited Paper*)

Weidong Zhou, The Univ. of Texas at Arlington (United States); Zhenqiang Ma, Univ. of Wisconsin-Madison (United States); Hongjun Yang, Semerane, Inc. (United States)

The creation of silicon based light sources has been a major research and development effort world-wide. The availability of a practical on-chip silicon lasers will enable a new generation integrated photonic and electronic components and systems. We proposed and demonstrated a membrane reflector surface-emitting laser on silicon, based on multi-layer semiconductor nanomembrane stacking via stamp transfer printing processes, and photonic crystal Fano resonance membrane reflectors. In this talk, I will review the design, fabrication, and characterization of this new type of membrane lasers. Principles of Fano resonance photonic crystal structures will be discussed, along with the demonstrated photonic devices including filters, reflectors, spectrally-selective detectors, and lasers. The potentials and prospects of nanomembrane materials and transfer printing processes will also be discussed, for applications in silicon photonics, flexible electronics and optoelectronics.

The work was supported by US ARO (W911NF-09-1-0505) and by US AFOSR STTR programs (FA9550-09-C-0200 and FA9550-11-C-0026). The Si nanomembrane work was partially supported by an AFOSR MURI program (FA9550-08-1-0337).

8633-30, Session 9

Optical multiplexer based on vertical coupler using high contrast

Li Zhu, Weijian Yang, Connie J. Chang-Hasnain, Univ. of

California, Berkeley (United States)

As the bandwidth demands of super computers and data centers grow faster and faster, the ultra-high speed data communication with high energy efficiency for rack-to-rack, board-to-board or even chip-to-chip networks becomes urgently desired. The optical interconnect is the key technology to sustain such growth. Within such network system, the on-and-off chip coupling is necessary. In addition, the wavelength multiplexing technology will further improve data speed and make the whole system more compact.

In this paper, we propose an optical multiplexer based on a vertical coupler. The vertical coupler is a two dimensional high contrast metastructure locating on top of a cross junction of various waveguides. Light propagating in each waveguide has a different wavelength, corresponding to an individual data channel. At the cross junction, they will be coupled out of the chip plane into an optical fiber or other free space optics. Utilizing the resonance nature of the high contrast metastructure, the coupling efficiency can reach 87% with 34nm 3dB bandwidth for a 4-channel configuration. The cross talk between different waveguides can be optimized to be smaller than 1%. Because the phase and field of the high contrast metastructure are strongly determined by the local high index structure, it is also possible to tailor the metastructure into different shape while keeping the constant periodicity and duty cycle. By creating different symmetries, such multiplexer can be adjusted to fit different numbers of channels.

8633-31, Session 10

Cavity-resonator-integrated guided-mode resonance filters (*Invited Paper*)

Shogo Ura, Kyoto Institute of Technology (Japan); Kenji Kintaka, National Institute of Advanced Industrial Science and Technology (Japan); Junichi Inoue, Kenzo Nishio, Yasuhiro Awatsuji, Kyoto Institute of Technology (Japan)

A cavity-resonator-integrated guided-mode-resonance filter (CRIGF) consisting of a grating coupler and a pair of distributed-Bragg-reflectors on a thin-film dielectric waveguide has been recently proposed and investigated to provide a narrow-band reflection spectrum for an incident wave of a small beam width from the free space. Newly developed analysis model is discussed with performance simulation. Integration of curved gratings for a small aperture CRIGF is reported with design and experimental work. Integration of a two-dimensional grating coupler and two crossed resonators is also demonstrated for polarization-independent CRIGF.

8633-32, Session 10

Angular sensitivity of guided mode resonant filters in classical and conical mounts (*Invited Paper*)

David W. Peters, Robert R. Boye, Shanalyn A. Kemme, Sandia National Labs. (United States)

The angular sensitivity of guided mode resonant filters (GMRF) is well known. While at times useful for angle tuning of the response, this sensitivity can also be a major detriment as angular changes of tenths of a degree can shift the wavelength response in a narrow bandwidth device by an amount greater than the width of the resonance peak. We identify geometries where the resonance is more angularly stable, demonstrating high reflectivity at the design wavelength for several degrees in both azimuth and inclination angular directions with virtually no change in lineshape of the response.

The investigation of GMRFs in both classical and conical mounts through simulation using rigorous coupled wave analysis reveals that there are preferred mounts for greater angular tolerance. We simulate a grating at telecom wavelengths using a design that we have previously fabricated.

The identical grating placed in different mounts can exhibit angular tolerances that differ by well over an order of magnitude (60x). The most commonly used classical mount has a much more sensitive angular tolerance than does the conical mount. The lineshape of the resonant response shows only negligible changes across the angular band. The angular band for the sample grating is simulated to be several degrees in the conical mount as opposed to a tenth of a degree in the classical mount. We could thus expand the application space for narrow-band GMRFs into areas where angular tolerance cannot be controlled to the degree that we have believed required in the past.

8633-33, Session 10

Modeling and fabrication of angular dependent Si high-contrast grating mirror for transverse mode control of VCSELs

Junichi Kashino, Hayato Sano, Akihiro Matsutani, Takahiro Sakaguchi, Fumio Koyama, Tokyo Institute of Technology (Japan)

We carried out the modeling and experiment of angular dependent high contrast grating (HCG) for the transverse mode control of vertical-cavity surface emitting lasers (VCSELs). HCG mirrors offer the highly incident angular dependence of reflectivity. We proposed the use of the engineered angular dependence of HCG for the transverse-mode control of VCSELs. We have performed a numerical simulation by using RCWA to increase the incident angular dependence for various grating parameters. The optimized angular dependent HCG functions as a sharp spatial frequency filter. High-order modes can be filtered out with excess losses larger than that of a fundamental mode. We have showed a possibility of single-mode VCSELs with a large active area of 15 μ m in diameter. Also, we fabricated amorphous HCG mirrors using nanoimprint lithography. Nanoimprint lithography is a powerful tool for making large area sub-wavelength scale optical devices with high-throughput fabrication. We fabricated amorphous Si sub-wavelength HCG patterns on SiO₂ for 980 nm VCSELs by using Cl₂-based ICP dry etching. A vertical etching profile and a smooth etched surface were obtained. We fabricated large area (7mm x 7mm) a-Si HCG with good uniformity in the entire sample. We measured the reflection characteristic of fabricated HCG mirrors including the angular dependence. We will discuss the single mode behavior of proposed HCG-VCSELs.

8633-34, Session 10

Tunable resonant-cavity-enhanced photodetector with double high-index-contrast grating mirrors

Supanee Learthanakhachon, Kresten Yvind, Il-Sug Chung, Technical Univ. of Denmark (Denmark)

A novel hybrid III-V/Si tunable resonant-cavity-enhanced photodetector (RCE-PD) is proposed and numerically investigated. The detector can provide a tuning wavelength range of 100 nm with an absorption efficiency higher than 70 %, and a full-width-at-half-maximum detection bandwidth less than 0.4 nm. This broad tuning range and narrow detection bandwidth has a potential to enable innovative wavelength division multiplexing (WDM) system design and to replace a spectrometer in gas sensing systems. The photodetector structure consists of an InP high-index-contrast (HCG) subwavelength grating mirror, an air gap, an active region including InGaAs quantum wells (QWs) for light absorption, and a Si HCG mirror made in the Si layer of a silicon on insulator wafer. No anti-reflection layer is included to extend the cavity to include the air gap for a larger tuning range. The detection wavelength can be tuned by moving the InP HCG mirror suspended in the air via either electrostatic or piezoelectric actuation. The resonant cavity structure and QWs are designed to detect transverse magnetic (TM) polarized light around 1550 nm wavelength and are feasibly scalable to detect other wavelengths as well as un-polarized light. In numerical simulations, the rigorous coupled wave analysis (RCWA) method is used to calculate reflection and

transmission coefficient of HCG mirrors and the transfer matrix method (TMM) is used to estimate the light absorption in QWs, considering the standing wave effect. In the talk, cavity design issues such as the effective cavity length, thickness of the air gap, and penetration depth into HCGs will be discussed with respect to broader tuning range and narrower detection bandwidth.

mask photolithography, reactive ion etching and a hydrofluoric acid etch to achieve well-defined suspended Si gratings. Polarization-dependent Fourier transform infrared (FTIR) spectroscopic analysis in reflectance mode shows reflectance greater than 85% between 8.5 and 11.5 μm with strong polarization dependence. Simulations of the grating's optical response using measured dimensions exhibit strong agreement with the experimental results.

8633-35, Session 10

Asymmetric direction selective filter elements based on high-contrast gratings

Stefan Steiner, Fraunhofer-Institut für Angewandte Optik und Feinmechanik (Germany); Stefanie Kroker, Thomas Käsebier, Ernst-Bernhard Kley, Friedrich-Schiller-Univ. Jena (Germany); Andreas Tünnermann, Friedrich-Schiller-Univ. Jena (Germany) and Fraunhofer-Institut für Angewandte Optik und Feinmechanik (Germany)

We present novel filter elements with an asymmetric angle dependent transmission based on high contrast gratings. Asymmetric transmission means a diverging efficiency for light incident from positive or negative angles. Our approach provides the realization of asymmetric direction selective filters by using blaze-like grating structures whose are combined with subwavelength high contrast gratings respectively grating periods in the resonance domain. Those gratings are known for their very selective behavior concerning wavelength, polarization and direction of the incident light. The special characteristics of those gratings enable the realization of filter elements with a high optical performance and efficiency. We also discuss the possibility of an additional selectivity of the polarization state of the incident light. Likewise, the transmission characteristics of those filters are tuneable by means of varying geometric grating parameters such as duty cycle and period. Amorphous silicon is used as high index layer, which is a suitable material due to its very high refractive index n of larger than 3.6 at 850 nm wavelength. This fact permits novel filter elements, which offer large tolerances with respect to design parameter deviations. Filter elements based on silicon technology can easily be integrated into existing micro electrical systems and without extensive adaptation. Thus low fabrication costs are feasible. Our approach provides the possibility of multifunctional filter elements which can be easily integrated in conventional fabrication techniques in semiconductor industry.

8633-36, Session 10

Suspended Si/air high-contrast subwavelength gratings for long-wavelength infrared reflectors

Justin Foley, Jamie D. Phillips, Univ. of Michigan (United States)

Long-wavelength infrared (LWIR, 8-12 μm) imaging is of primary importance for a number of defense, surveillance, and scientific applications. Conventional infrared imaging, however, produces monochromatic images without wavelength specificity; through color filter incorporation better object discrimination is possible. Fabry-Perot etalons are an effective filtering technique but production of conventional low loss distributed Bragg reflectors are difficult to fabricate in the LWIR due to layer thickness requirements. High index-contrast subwavelength gratings (HCGs) are promising candidates for producing broadband, low loss, reflectors in the LWIR and only require two thin film layers. Incorporation of these reflectors into Fabry-Perot etalons has potential to enable multi- or hyperspectral imaging for enhanced military surveillance. Previous work on LWIR reflectors using a Si/SiO₂ based HCG has demonstrated a field response dominated by infrared absorption, limiting its utility in LWIR applications. To circumvent the loss attributed to SiO₂, a suspended Si structure has been analyzed. Using finite element analysis software to simulate the field response of linearly polarized light, a design has been optimized for TM polarization. Grating fabrication has been performed using silicon-on-insulator (SOI) substrates, single

Conference 8634: Quantum Dots and Nanostructures: Synthesis, Characterization, and Modeling X

Monday - Wednesday 4 -6 February 2013

Part of Proceedings of SPIE Vol. 8634 Quantum Dots and Nanostructures: Synthesis, Characterization, and Modeling X

8634-1, Session 1

Selective control of blinking and polarization of single-photon emission in colloidal semiconductor nanocrystals (*Invited Paper*)

Alberto Bramati, Univ. Pierre et Marie Curie (France)

Core/shell colloidal semiconductor nanocrystals are very efficient single photon emitters at room temperature [1, 2]. However in such structures, the competition between radiative and non-radiative recombination channels induces photoluminescence fluctuations between on and off states known as blinking [3].

Shell engineering is a suitable strategy to control recombination paths and has been used to produce almost non-blinking nanocrystals [4], although accompanied by undesired increasing of multi-excitonic emission probability [5].

Here we show that, using asymmetric core/shell nanoparticles (dots-in-rods) with a spherical CdSe core surrounded by a rod-like CdS shell [6, 7] blinking effects, multi-excitonic emission and polarization of the emitted photons can be separately controlled by tuning shell dimensions. This allows an unprecedented capability in radiative channels engineering, making dot-in-rods "state of the art" blinking-free sources of polarized single photons on-demand.

[1] C. Murray, D. Norris, M. G. Bawendi, *Journal of the American Chemical Society* 1993, 115, 8706.

[2] P. Michler, A. Imamoglu, M. D. Mason, P. J. Carson, G. F. Strouse, S. K. Buratto, *Nature* 2000, 406, 968.

[3] M. Nirmal, B. Dabbousi, M. Bawendi, J. Macklin, J. Trautman, T. Harris, L. Brus, *Nature* 1996, 383, 802.

[4] B. Mahler, P. Spinicelli, S. Buil, X. Quélin, J. P. Hermier, B. Dubertret, *Nature materials* 2008, 7, 659.

[5] Y. S. Park, A. Malko, J. Vela, Y. Chen, Y. Ghosh, F. García-Santamaría, J. Hollingsworth, V. Klimov, H. Htoon, *Physical Review Letters* 2011, 106, 187401.

[6] D. V. Talapin, R. Koeppel, S. Götzinger, A. Kornowski, J. M. Lupton, A. L. Rogach, O. Benson, J. Feldmann, H. Weller, *Nano letters* 2003, 3, 1677.

[7] L. Carbone, C. Nobile, M. De Giorgi, F. Della Sala, G. Morello, P. Pompa, M. Hytch, E. Snoeck, A. Fiore, I. R. Franchini, *Nano letters* 2007, 7, 2942.

8634-2, Session 1

Teleportation with electrically-generated entangled light (*Invited Paper*)

R. Mark Stevenson, Toshiba Research Europe Ltd. (United Kingdom); J. Nilsson, K. H. A. Chan, Toshiba Research Europe Ltd. (United Kingdom) and Univ. of Cambridge (United Kingdom); J. Skiba-Szymanska, Martin B. Ward, Anthony J. Bennett, Toshiba Research Europe Ltd. (United Kingdom); C. L. Salter, Toshiba Research Europe Ltd. (United Kingdom) and Univ. of Cambridge (United Kingdom); Ian Farrer, David A. Ritchie, Univ. of Cambridge (United Kingdom); Andrew J. Shields, Toshiba Research Europe Ltd. (United Kingdom)

Teleportation can allow reliable logic operations in massively parallel optical quantum computers, and the formation of secure quantum networks. Previous teleportation demonstrations employ laser driven sources which produce random numbers of entangled photon pairs, complicating deployment of useful quantum information technology. We present teleportation of single photonic qubits facilitated by individual pairs of electrically generated entangled photons. Our entangled

light source is based on a semiconductor quantum dot integrated within a light-emitting-diode. The unique single-photon nature of our photonic teleporter together with its electrical operation will help reduce complexity of future quantum information technology.

8634-3, Session 1

Engineering CdSe/CdS dot-in-rod nanocrystals as novel single photon source and as versatile gain material for lasing application

Gabriele Rainò, IBM Zürich Research Lab (Switzerland); Iwan Moreels, Univ. Gent (Belgium); Thilo Stoefler, IBM Zürich Research Lab. (Switzerland); Raquel Gomes, Zeger Hens, Univ. Gent (Belgium); Rainer F. Mahrt, IBM Zürich Research Lab. (Switzerland)

Colloidal semiconductor quantum nanostructures attract considerable interest due to their potential application in the field of photonics and quantum communication.

Hetero-nanostructures like CdSe/CdS offer new prospects to tailor their optical properties as the small conduction band offset (~ 0.3 eV) allows tuning of the electron delocalization from type-I towards quasi type-II. Indeed, the energy of the quantized levels and their radiative rates can be controlled by adjusting the core size and the shell thickness [1].

In the present work, we use precisely engineered colloidal CdSe/CdS dot-in-rod hetero-nanostructures to demonstrate amplified spontaneous emission (ASE) within a thin film of colloidal Qdots with exceptional low lasing threshold (~100µJ/cm²) which is almost constant over a wide temperature range. Indeed, by determining a T₀ of at least 350 K, we demonstrate that colloidal CdSe/CdS Qdot-in-rod gain materials could enable temperature-insensitive lasing, pivotal for miniaturized and integrated laser sources [2].

Colloidal nanocrystals are also considered as a room-temperature-triggered single-photon source. However, the strong confinement of the charge carriers increases the electron-hole exchange interaction, resulting in a complicated band-edge exciton fine structure. The electron-hole wavefunction manipulation allows us to deliberately tune the exciton fine-structure splittings, well beyond what can be obtained by quantum confinement alone. In particular, samples with small core and/or thick-rod diameters exhibit a strongly reduced fine-structure splitting resulting from a reduced electron-hole exchange interaction [3].

The exciting tuning capabilities of colloidal quantum dots start to extend beyond simple wavelength tuning by size, and enable real quantum engineering of the energy levels.

References

[1] G. Rainò et al., *ACS Nano*, 5, 4031–4036, 2011.

[2] I. Moreels, G. Rainò et al., *Advanced Materials*, 2012, DOI: 10.1002/adma.201202067.

[3] G. Rainò et al., *ACS Nano*, 6, 1979–1987, 2012.

8634-4, Session 1

Fiber-coupled single photon sources based on photonic crystal cavities

Byeong-Hyeon Ahn, Chang-Min Lee, Hee-Jin Lim, Yong-Hee Lee, KAIST (Korea, Republic of)

Recently, several single photon sources are developed with semiconductor quantum dots (QDs) having discrete energy levels like atoms. However, high refractive index of semiconductor materials makes photons from QDs to stay inside the materials, which degrades collection

Conference 8634: Quantum Dots and Nanostructures: Synthesis, Characterization, and Modeling X

of single photons. To solve this problem, people use various structures such as vertical photonic nanowire, or photonic crystals with engineering emission profile. In these cases, an objective lens with high numerical aperture (NA) is required. In a view of practical point, fiber coupling of single photons is indispensable to transfer long distance without loss.

In this study, we demonstrate single photon source with the integration of photonic crystal (PhC) and curved microfiber in a cryostat at low temperature (~10K). Photons from QDs in the semiconductor material are directly coupled to the curved-microfiber. Optical fiber is tapered as heated, stretched, and curved with a curvature of ~100 μm and a diameter of ~1 μm . It is put into the cryostat with PhC and is controlled by XYZ stage from outside. We can attach and detach the curved-microfiber to the PhC patterns and find a QD emitting strong light through the fiber. This method collects photons very efficiently. 3D finite-difference time-domain (FDTD) method predicts a coupling efficiency over 60%. We expect the integrated system can be a new platform for the efficient single photon source based on low density quantum dot PhCs.

8634-5, Session 1

Systematic investigation of the temperature behavior of InAs/InP quantum nanostructure passively mode-locked lasers

Kamil KLAIME, Rozenn Piron, Institut National des Sciences Appliquées de Rennes (France); Frederic Grillot, Institut National des Sciences Appliquées de Rennes (France) and Telecom ParisTech (France); Madhoussoudhana Dontabactouny, Slimane Loualiche, Alain Le Corre, Institut National des Sciences Appliquées de Rennes (France); Kresten Yvind, Technical Univ. of Denmark (Denmark)

Monolithic mode-locked lasers (MLLs) have been the centre of interest for a large range of photonic applications. Due to their short pulse and high frequency repetition rate, MLLs are well suited for low-cost applications such as high bit rate optical telecommunications or optical interconnects [1,2]. In the scope of uncooled applications, evaluation of the mode-locking stability with temperature is required. In this paper, this investigation is conducted over a wide temperature range assuming two sections InAs/InP quantum nanostructures (QN) passively MLLs. Devices under study contain five InAs QN layers either grown on InP(100) (quantum dashes (QDashes)) or on InP (311)B (quantum dots (QDs)). At first, gain and loss spectra are extracted with the segmented contact method (SCM) as a function of current density, over absorber bias voltage and temperature for the QN material comprising the device [3]. Measured values extracted from the SCM are then incorporated into an analytical model [4,5], which is used to predict the mode-locking temperature-dependence both for various laser's geometries and for different kind of QN (QDashes and QDs). Calculated stability maps show that for QDs (QDashes respectively), 2% of L_a/L_g (2% to 18% respectively) associated to a gain current density larger than 10 kA/cm^2 (7.5 kA/cm^2 respectively) can preserve good mode-locking conditions until 45°C. To this end, the results point out that QDash nanostructure can offer a much broader stability range over temperature, which is of first importance for the next generation of InAs/InP MLLs used in datacom and telecom applications.

8634-6, Session 2

Influence of low energy H- ion implantation on the electrical and material properties of quaternary alloy (In_{0.21}Al_{0.21}Ga_{0.58}As) capped InAs/GaAs n-i-n QDIPs

Arjun Mandal, Hemant Ghadi, Indian Institute of Technology Bombay (India); Keshav L. Mathur, Sardar Vallabhbhai

National Institute of Technology (India); Arindam Basu, N. B. V. Subrahmanyam, P. Singh, Bhabha Atomic Research Ctr. (India); Subhananda Chakrabarti, Indian Institute of Technology Bombay (India)

Due to the 3-D confinement of carriers, self-assembled InAs/GaAs quantum dot infrared photodetectors (QDIPs) have its promising applications in the field of night vision, medical diagnosis, environmental monitoring from space etc. InAs/GaAs based n-i-n QDIPs were grown over semi-insulating GaAs (100) substrates by solid source molecular beam epitaxy (SSMBE); 2.7 ML QDs were capped with a combination of 30Å quaternary (In_{0.21}Al_{0.21}Ga_{0.58}As) and 250Å GaAs layers. Both the QD and combination capping were repeated for 8 periods. With the purpose of its application in space and to study the effects of different ions on QDIPs, the heterostructures were further implanted with 50 KeV H- ions of fluence varying between 8E11 to 2E13 ions/cm². The devices were fabricated by conventional photolithography, wet etching and metal evaporation technique. At both positive and negative bias of 0.02 V, symmetric dark current density of 13.2 A/cm² at 77K for as-grown sample, decreased monotonously to 2.7E(-2) A/cm² for the sample implanted with 2E13 ions/cm² fluence. Activation energy of 76.3 meV and 84.8 meV, calculated for unimplanted sample from temperature dependent photoluminescence and electrical measurements respectively, gradually enhanced to the value of 210.5 meV and 154 meV with the increase of fluence upto 2E12 ions/cm²; both the activation energies decreased with further increase in fluence. Thus, the sample, implanted with H- ions of fluence 2E12 ions/cm² exhibited the best confinement. This is probably the first report about the effects of H- ions on the electrical and material properties of InAs/GaAs QDIPs. DST, India is acknowledged.

8634-7, Session 2

Effect of excited states in quantum dots on the modulation bandwidth of a quantum dot laser

Yuchang Wu, Virginia Polytechnic Institute and State Univ. (United States); Robert A. Suris, Ioffe Physico-Technical Institute (Russian Federation); Levon V. Asryan, Virginia Polytechnic Institute and State Univ. (United States)

In present-day semiconductor lasers, a 2-D active region (quantum well) is used. In quantum dot (QD) lasers, an ultimate case of a 0-D active region is realized. While a discrete energy spectrum of carriers in QDs enables lasing with low threshold and high temperature-stability, the potential of QD lasers for high-frequency direct modulation of the optical output by electric current needs to be clarified. As shown earlier, the modulation bandwidth of a QD laser is strongly controlled by the carrier capture delay from the optical confinement layer (OCL) into QDs [L.V. Asryan, Y. Wu, R.A. Suris, Appl. Phys. Lett. 98, 131108 (2011)] and by the internal optical loss in the OCL [Y. Wu, R.A. Suris, L.V. Asryan, Appl. Phys. Lett. 100, 131106 (2012)]. In this work, we study the effect of excited states in QDs on the modulation response of a QD laser. The small-signal analysis of rate equations is used for free carriers in the OCL, carriers confined in the ground- and excited-states in a QD, and photons. The modulation bandwidth is calculated as a function of the carrier relaxation time from the excited state to the ground state in a QD. Our analysis shows that, under the conditions when the carrier capture from the OCL to the lasing ground state is mediated through the nonlasing excited state, the excited-to-ground state relaxation delay is one more key factor strongly limiting the modulation bandwidth of a QD laser.

8634-29, Session 2

Biexciton binding energy and polar exciton-LO-phonon interaction as probe of the built-in fields in GaN/AlN QDs

Andrei Schliwa, Gerald Hönig, J. Settker, Gordon Callsen, J. Brunnermeier, Christian Thomsen, Technische Univ. Berlin (Germany); Satoshi Kako, Yasuhiko Arakawa, The Univ. of Tokyo (Japan); Axel Hoffmann, Technische Univ. Berlin (Germany)

In this contribution we discuss theoretically two strongly interrelated experimental observations recently found in c-plane GaN/AlN quantum dots (QDs): (i) the anti-binding to binding transition of the biexciton relative to the (mono)exciton, and (ii) the strong polar exciton-LO-phonon interaction and its variation with the exciton energy.

(i) Excitons and biexcitons confined in semiconductor quantum dots are ideal sources for single and pairs of entangled photons. GaN/AlN QDs - in addition - have shown their ability of temperature stable single photon emission up to 200 K [1] and are therefore most promising candidates for room temperature stable single photon emitters. Beyond, tuning exciton and biexciton energy in resonance, thus achieving color coincidence, is of large importance for

- QDs in microcavities, where both emission lines need to match the cavity-mode, and

- photon entanglement achieved by photon time reordering, requiring biexciton and exciton having identical emission energies [2].

C-plane GaN/AlN are plagued by huge internal built-in fields causing a small electron-hole overlap leading to long excitonic life times and strongly blue-shifted higher order excitonic complexes such as the biexciton. Hence, it was a welcome but nevertheless surprising experimental result of Simeonov et al. [3], who found a sign change of the biexciton binding energy upon QD-size. Yet, theoretical investigations so far failed to reproduce this finding without assuming artificially reduced polarization fields within the QDs.

Here, we calculate the biexciton binding energy, varying independently QD height and -width using strain dependent 8-band-kp theory taking fully into account the effects of spontaneous polarization and piezoelectricity. Coulomb interaction is included via the configuration interaction model based on Hartree-Fock iterated wavefunctions. This way we can carefully separate self-consistency effects from correlation. The latter turned out to be of largest importance for the understanding of the anti-binding - binding transition of the biexciton since we calculated correlation energies in excess of 65 meV for the biexciton, a magnitude larger than typically found InGaAs/GaAs QDs. Clarifying the influences of crucial QD parameters on correlation energies allows the control of relative emission energies in GaN/AlN QDs in order to realize photon entanglement by time reordering and a more efficient use of single-QD micro-cavities.

(ii) Recently, strong exciton-LO-phonon interaction for epitaxial GaN/AlN quantum dots (QD) was observed experimentally by analyzing the LO-phonon sidebands of single-QD excitonic peaks.

Depending on the exciton energy, ranging from 3 eV to 4.5 eV, values of the Huang-Rhys parameter S between 0.3 and 0.02 were deduced. Since the polar coupling strength (described by S) for an exciton is proportional to the squared absolute value of the Fourier transformed difference of the probability densities of the electron and hole, S provides a measure for the electron-hole separation. GaN/AlN QDs are well known for their strong intrinsic piezo- and pyroelectric fields along the c-axis, giving rise to excitonic charge separation analogous the quantum confined Stark effect. As this charge separation is known to be dependent on the QD height, it should be mirrored by a variation of the parameter S . Here, we calculate the Huang-Rhys parameter for the ground-state exciton as function of size and composition using a strain dependent 3D implementation of the eight-band k-p model taking into account piezo- and pyroelectric effects in the adiabatic approximation.

We discuss the interrelation of QD size, built-in fields, exciton energy, biexciton-binding energy, electron-hole dipole-moment, and Huang-Rhys parameter S .

[1] S. Kako et al., Nature Materials 5, 887 (2006)

[2] J. E. Avron et al., Phys. Rev. Lett. 100, 120501 (2008)

[3] D. Simeonov et al., Phys. Rev. B 81, 241309 (2010)

8634-8, Session 2

Molecular beam epitaxial growth and characterization of InGaN/GaN dot-in-a-wire nanoscale heterostructures: towards ultrahigh-efficiency phosphor-free white light-emitting diodes (Invited Paper)

Zetian Mi, Hieu P. T. Nguyen, Shaofei Zhang, Kai Cui, Mehrdad Djavid, McGill Univ. (Canada)

One of the grand challenges for future solid state lighting is the development of high efficiency, phosphor-free white light emitting diodes (LEDs). In this context, we have investigated the molecular beam epitaxial (MBE) growth and characterization of nanowire LEDs on Si, wherein intrinsic white-light emission is achieved by incorporating self-organized InGaN quantum dots in defect-free GaN nanowires on a single chip. Such devices can exhibit, for the first time, nearly zero efficiency droop and significantly enhanced internal quantum efficiency (up to ~57%) at room-temperature.

Catalyst-free InGaN/GaN nanowire LED heterostructures are grown on Si(111) substrates by MBE. The device active region contains 10 vertically coupled InGaN/GaN quantum dots with In compositions varied in the range of ~10-50% to achieve white-light emission. In addition, each quantum dot layer is modulation doped p-type using Mg. A p-doped AlGaIn electron blocking layer is also incorporated between the active region and the p-GaN. Compared to the undoped nanowire LEDs, the p-doped devices can exhibit significantly enhanced internal quantum efficiency (~57%) at room-temperature, due to the improved hole injection and transport process. Through detailed studies of the current- and temperature-dependent electroluminescence emission, we have further confirmed that electron overflow can be effectively prevented with the incorporation of a p-doped AlGaIn electron blocking layer. The devices can exhibit virtually no efficiency droop for injection current up to ~2,200 A/cm².

Work is currently in progress to achieve further improved performance by utilizing core-shell-based nanowire heterostructures and by transferring the devices on transparent substrates.

8634-9, Session 2

Quantum dots formed by annealing strained-flat epilayers

Haeyon Yang, Casey M. Clegg, South Dakota School of Mines and Technology (United States)

We present self-assembly of InGaAs quantum dots formed by in-situ annealing. Strained-but-flat InGaAs epilayers were grown by Molecular Beam Epitaxy (MBE) at low temperatures. Annealing induces transition of the flat epilayers into quantum dots. Conventional annealing at an elevated temperature resulted in smaller quantum dots than those formed by the typical Stranski-Krastanov growth mode at the annealing temperature. Even smaller quantum dots were observed by ultra-high vacuum Scanning Tunneling Microscope (STM) when the flat epilayers were irradiated by interferential high power laser pulses that create nanoscale thermal modulations in-situ on the surface at near room temperature. STM images indicate that self-assembled dots are formed due to the irradiation and the dot density modulates sinusoidally with a periodicity similar to that of the interference. The comparison of the morphology, size and distribution of size of the QDs will be presented.

Conference 8634: Quantum Dots and Nanostructures: Synthesis, Characterization, and Modeling X

8634-10, Session 2

Strain engineered Volmer-Weber-like growth of epitaxial InAs dots on GaAs (001)

Alexandre Freundlich, Manori V. Gunasekera, Univ. of Houston (United States)

Formation of self-assembled quantum dots (SAQD) of InAs on GaAs has been shown to follow the Stranski-Krastanov growth mode. In this mode, subsequent to the growth of a highly strained 2D InAs epilayer, a critical thickness (~1.5ML) is reached where the elastic relaxation of strain leads to the nucleation of 3D elongated islands/SAQDs over a thin 2D InAs wetting layer (WL). These SAQDs are generally bounded by {136} and {137} facets and exhibit large asymmetries along the <110> directions. The poor aspect ratio (height/base~0.1) and the presence of the wetting layer in these SAQDs affect detrimentally their 0D phononic and electronic properties.

In this study and within the framework of InAs/GaAs system we demonstrate the possibility of obtaining high/aspect ratio self-assembled dots that nucleate directly on (Al)GaAs spacers that isolates them the wetting layers. We have carefully monitored the strain anisotropies, their evolution and onsets of 2D-3D transitions by in-situ RHEED and have found that should the growth of InAs be interrupted prior to the 2D-3D transition and a carefully engineered spacer layer of (Al)GaAs be introduced, the subsequent growth of InAs results into the spontaneous formation of high aspect ratio dots without the formation of cumbersome wetting layer. Post growth TEM and AFM observations confirm these finding and reveal that these dots, unlike their conventional counterparts, are highly symmetrical along the <110> directions and exhibit high aspect ratio with low index facets. TEM analyses also confirm that these properties are preserved after the subsequent capping of dots by (Al)GaAs.

8634-11, Session 2

Atomic structure of InGaAs/GaAs quantum dots in a GaP matrix

Holger Eisele, Christopher Prohl, Andrea Lenz, Dominik Roy, Josephine Schuppang, Mario Daehne, Gernot Stracke, Andre Strittmatter, Udo W. Pohl, Dieter Bimberg, Technische Univ. Berlin (Germany)

Due to the comparably low lattice mismatch, GaP is a promising material for the direct integration of optical III-V-semiconductor applications into silicon-based technology. Hence, the development of epitaxially grown quantum dots on GaP(001) substrates for opto-electronic devices is an interesting new task. Furthermore, In(Ga)As/GaP quantum dots are also promising for new nano-memory cells due to an expected high hole localization energy at the quantum dots, as compared with InAs/GaAs quantum dots, resulting in reasonable long storage times. In order to understand the growth of quantum dots in this new material system, we analyzed InGaAs/GaAs/GaP nanostructures at the atomic scale using scanning tunnelling microscopy (XSTM).

The investigated sample was grown by metal organic vapor phase epitaxy (MOVPE) on a GaP(001) substrate. It contains a stack of three layers, each consisting of nominally 3.0 monolayers (ML) GaAs, followed by 2.0 ML of In_{0.25}Ga_{0.75}As. The thin GaAs interlayer prior to InGaAs deposition was used to encourage the Stranski-Krastanov growth mode for quantum dot formation.

The high-resolution XSTM images show quantum dots, being confined by a truncated pyramidal shape. A wetting layer being connected to the quantum dot at its base is present, clearly demonstrating a Stranski-Krastanov growth mode. The average quantum dot base length is found to be 12 nm, and the height is up to 10 ML. A statistical analysis leads to a high quantum dot density of $2.4 \times 10^{11} \text{ cm}^{-2}$ within the sample. Even though the strain energy in this system is relatively high as compared with the InGaAs/GaAs system, no structural defects, such as e.g., dislocation or nano-void formation, could be found.

8634-12, Session 3

Spectroscopy and dynamics of plasmonic metal nanorods (*Invited Paper*)

Jeff Owrutsky, Ryan E. Compton, Blake S. Simpkins, James P. Long, Joshua D. Caldwell, U.S. Naval Research Lab. (United States)

Several methods were used to fabricate and characterize the optical properties of metal nanorods and periodic arrays of nanoantennas. Template synthesis using electrodeposition into nanoporous membranes produces high aspect ratio (>50) metal nanorods of numerous metals, including Pd, Pt, Co, Fe, Al, and Ni as well as Au, Ag, and Cu. Steady-state spectra demonstrate longitudinal surface plasmon resonance bands in the mid infrared for all the metals, which is consistent with expectations based on the metal optical constants and analytical models of the extinction. Ultrafast transient absorption was used to characterize their optical response which includes coherent acoustic oscillations. Their dephasing depends on the templates and the nanorod length. Also, electron beam lithography was used to produce 550 nm and 1100 nm long rectangular nanoantennas on silicon and sapphire in square periodic arrays to investigate different coupling regimes as a function of pitch or element spacing. Asymmetric resonance bands in the near and mid infrared were observed in reflection and analyzed using a Fano-type resonance lineshape. As the array pitch is reduced, spectral narrowing and blue shifting of the nanorod longitudinal band is observed due to coupling. At the smallest pitches, the bands broaden and redshift due to the onset of another coupling regime. The studies demonstrate that the antenna resonance wavelength depends on both its length and the substrate index but the coupling transitions depend primarily on the length and less on the substrate index.

8634-13, Session 3

Using confocal microscopy to characterize nanoplasmonic structures responsible to light excitation

Mariana T. Carvalho, Univ. de São Paulo (Brazil); Marcel T. Bezerra, Univ. Federal de Pernambuco (Brazil) and Univ. de São Paulo (Brazil); Euclides Marega Jr., Ben-Hur B. Borges, Univ. de São Paulo (Brazil); Frederico D. Nunes, Univ. Federal de Pernambuco (Brazil) and Univ. de São Paulo (Brazil)

The optical properties of nanostructured metallic nano-films have been extensively studied in last few years. It was observed, for a wide variety of structures, an enhancement in the transmission which is explained as resulting from surface plasmon polaritons (SPP) waves propagating in the interface between the metallic film and the surrounding dielectric and/or substrate. This work analyses how a confocal microscope can characterize a nanoplasmonic structure, considering what is or not possible to do. With the confocal microscope nanostructures were observed and data obtained about SPP wave transmission through them for different laser wavelengths (405-633nm). Here is presented the results for a concentric array of circular gaps in a 180nm Au-film, fig (1). The circular channels are 80nm wide with diameters: $d_1=2.5$, $d_2=5.0$, $d_3=7.5$ and $d_4=10$ (dimensions in μm). The fig.(2) shows the images obtained from the top for: upper figure - no polarizer and the other with a polarizer perpendicularly oriented to the electric field of the incident wave. In the first case a two petals rose radiation profile is observed and a four petals rose with polarizer. They are explained describing each channel as a source of radiation formed by two electric systems. One electric dipole of length d aligned to applied field associated to a loop-antenna having a current dependent on the radial angle. The radiation profiles are presented in fig.(2) with the figures. This model is going to include interference among the emitted fields.

**Conference 8634: Quantum Dots and Nanostructures:
Synthesis, Characterization, and Modeling X**

8634-14, Session 3

Probing light-matter interactions at the nanoscale with a deterministically-positioned single quantum dot

Chad Ropp, Zachary Cummins, Sanghee Nah, John T. Fourkas, Benjamin Shapiro, Edo Waks, Univ. of Maryland, College Park (United States)

The interactions between quantum emitters and plasmonic nanostructures are important for a wide variety of applications in quantum optics and nanophotonics. Plasmonic nanostructures localize electromagnetic fields to nanoscale regions of space where single emitters can be precisely placed to exploit enhanced optical nonlinearities and improved light-matter interactions. These enhanced interactions have application in fields such as biological sensing, quantum communication, and the realization of optical logic. In this talk, we will discuss our recent work on nano-manipulation of single colloidal quantum dots (QDs) for deterministic coupling to plasmonic nanostructures as well as for nanoscale probing of light matter interactions. We will describe our approach for QD manipulation based on microfluidics and fluid chemistry, which allows for positioning of a single QD with 50 nm accuracy. Specific results illustrating the interactions between a single QD that is deterministically coupled to a silver nanowire (AgNW) will be presented. Near-field interactions are measured as a function of the QD's spatial position relative to the AgNW and quantified by both measuring the power coupled into the AgNW mode as observed by the radiated light from the wire ends as well as directly from a measure of the QD lifetime. As a result, we will show that our probing technique can be used to image the plasmonic mode of the AgNW with as fine as 15 nm resolution to reveal features such as the profile of the evanescent field decay away from the wire and optical interference along the wire's length.

8634-15, Session 3

High-efficiency quantum dot light-emitting diodes in conjunction with various metal nanoparticle structures

Hyun-Chul Park, Yong-Hoon Cho, Song-Mei Li, Isnaeni ., KAIST (Korea, Republic of)

We present our experimental results that the hybrid quantum dot (QD) light-emitting diode (LED) structure combined with metal nanoparticles (MNPs) which can provide extreme field concentration, enhancing light-matter interactions significantly. The quantum yield of QD-LED is enhanced via coupling of the emitter with localized surface plasmons of different shape of MNPs. The proposed hybrid structures in our work consist of a monolayer of colloidal CdSe/ZnS QD, Au layer, Ag layer, and multiple polyelectrolyte layers which are the spacers to ensure the separation distance between QDs and metal nanoparticles to avoid quenching the emission of QDs by MNPs. The maximum enhancement of the QD emission can be obtained when the distance is approximately 10 nm. This hybrid structure was placed on top of a blue InGaN/GaN LED chip to obtain color down-conversion LED structure. We find that the QD emission enhancement depends on different shapes of the Ag nanocrystal layer, due to the spectral overlap between the blue LED emission and surface plasmon resonance spectrum of the Ag nanocrystal. As a result, we find that the quantum yield of the QD-MNP-LED structures increased compared to the QD-LED itself. The emission enhancement using different shapes of metal nanoparticles can be achieved by the product of the field enhancement and Purcell effect, which are contributions from Ag and Au nanostructures, respectively. From the outcome of this research, it is possible to produce high efficiency QD-LED devices.

8634-16, Session 4

Non-blinking semiconductor nanocrystals: suppression of nonradiative Auger processes (Invited Paper)

Alexander L. Efros, U.S. Naval Research Lab. (United States)

Colloidal nanocrystals randomly turn their photoluminescence (PL) "off" and "on" under continuous light illumination, despite intensive research efforts aimed at suppressing this phenomenon. Today there is a consensus that the blinking is caused by extra electrons or holes that repeatedly charge, and then neutralize, the NC. When a charged NC is excited by a photon the additional energy is not re-emitted as PL, but instead triggers a process known as "non-radiative Auger recombination" during which this energy is acquired by an extra electron or hole. The rate of Auger recombination is orders of magnitude faster than the rate of radiative recombination that produces PL in neutral NCs. As a result, PL is completely suppressed, or "quenched," in charged NCs.

Recently, the soft-confinement (CdZnSe/ZnSe) nanocrystals have been grown that show complete absence of single molecule photoluminescence blinking [1]. Other remarkable photophysical properties these nanocrystals exhibit include unique multi-peaked photoluminescence spectra, and unusually short photoluminescence lifetimes. These properties are consistent with the novel observation of charged exciton recombination in colloidal nanocrystals, and thus are quite unlike any of the typical nanocrystals currently being studied.

We will explain why Auger processes are so efficient in standard NCs and how they have been recently suppressed in the non-blinking NCs [2].

[1] X. Wang, X. Ren, K. Kahen, M. A. Hahn, M. Rajeswaran, S. Maccagnano-Zacher, J. Silcox, G. E. Cragg, Al. L. Efros, and T. D. Krauss, *Nature* 459, 686 (2009)

[2] G. E. Cragg and Al. L. Efros, *NanoLetters* 10, 313 (2010).

8634-17, Session 4

Energy transfer in monodisperse quantum dot solids in the presence of self-organized array of metallic nanoparticles

Seyed M. Sadeghi, Robert G. West, The Univ. of Alabama in Huntsville (United States)

We examined the emission of colloidal CdSe/ZnS quantum dots when were deposited on especial substrates containing self-organized arrays of gold nanoislands with sizes monotonously reduced from the centers of these substrates to their sides. These substrates were fabricated using thermal evaporation in the presence of a special mask followed by annealing. We used such substrates as plasmonic templates to investigate spectral changes of emission of quantum dots and interdot energy transfer between them under controlled degrees of plasmonic effects. Our results showed how these processes were influenced by different amounts of plasmonic field enhancement and Forster energy transfer from the quantum dots to the metallic nanoparticles. For larger metallic nanoparticles we observed significant broadening and red shift in the emission spectra of the quantum dots, while as the nanoparticles become smaller the spectra became narrow, similar to those in the absence of any metallic nanoparticles. Including the impact of the heat generated by the metallic nanoparticles, we analyzed these results in terms of the interdot energy transfer from the quantum dots with smaller sizes to those with larger sizes within the monodisperse distribution. The results suggest how metallic nanoparticles can lead to enhancement of interdot energy transfer in monodisperse quantum dots, and how this process needs to be considered to explain the spectral changes of the quantum dot emission when they are close to the metallic nanoparticles.

8634-18, Session 4

Control of photophysical and photochemistry of colloidal quantum dots via metal and metal-oxide coated substrates

Seyed M. Sadeghi, Ali Nejat, The Univ. of Alabama in Huntsville (United States)

A main feature of colloidal quantum dots is that when they are irradiated, their fluorescence can change significantly. Previous research has shown that substrates can have significant impacts on such a process. This includes photoejection of electrons from such quantum dots into the deep trap states of their substrates, which can enhance their emission via suppression of their photoionization. In this contribution we study how deposition of extremely thin layer of gold and chromium oxide (about 1 nm) on glass substrates can significantly modify the way irradiation changes the fluorescence of CdSe/ZnS quantum dots. The extremely small thickness of such layers did not lead to significant reflection or absorption of light and the effect of the heat was very small. Our results show that the gold layer tends to shield the quantum dots from the substrate, preventing photo-induced fluorescence enhancement caused by the Coulomb barrier formed via migration of electrons into substrate. Additionally, in this case the emission of the quantum dots did not show any broadening, but rather shows a slight red shift which remained nearly unchanged with irradiation time. In the case of chromium oxide, however, we observed significant broadening and blue shift, indicating the fact that such oxide can enhance photo-oxidation of colloidal quantum dots significantly. In the case of quantum dots on glass we observed a slight amount of blue shift and broadening, suggesting limited amount of photo-oxidation.

8634-19, Session 4

Effects of multi shell passivation on the thermal stability of the quantum dots

Hyosook Jang, Shinae Jun, Eunjoo Jang, Samsung Advanced Institute of Technology (Korea, Republic of)

Recent advances in the synthesis of high quality quantum dots (QDs) have increased the chances of the commercialization in the QD light-emitting devices. The critical requirements for the device applications are high efficiency and stability during the device fabrication and operation. Particularly, since the light-emitting diodes (LEDs) generate intensive heat, the thermal stability of the QDs becomes very important for the device efficiency and lifetime. It has been generally known that the energy band gap and the quantum efficiency (QE) are dependent on the temperature.[1] Here, we disclose that the multi shell passivation improves QDs' thermal stability effectively as well as the luminescence efficiency. The CdSe/CdS/ZnS multi shell passivated QDs were prepared by step-wise coating process and the thickness of each shell layer was controlled elaborately. As the QDs have thick shells [2] with more than 7 monolayers, they showed 100% of QE and maintain the luminescence intensity even at 95°. Low temperature photoluminescence (PL) and transient PL are being currently studied intensively. The temperature-dependent optical properties of the various passivation structures and their applications to the LEDs will be discussed in the presentation.

[1] G. W. Walker, V. C. Sundar, C. M. Rudzinski, A. W. Wun, M. G. Bawendi, and D. G. Nocera, *Appl. Phys. Lett.* 2003 83 3555.

[2] J. Lim, S. Jun, E. Jang, H. Baik, H. Kim, and J. Cho, *Adv. Mater.* 2007 19 1927.

8634-20, Session 5

Buried-stressor concept for quantum dot site-control (Invited Paper)

Andre Strittmatter, Technische Univ. Berlin (Germany)

The epitaxial growth of single quantum dots was previously relying on surface patterning methods on a nanometer scale. Not only are such methods limited to small areas as the underlying patterning process is time-consuming but also degrades the surface patterning the optical quality of QDs. Moreover, a second nm-resolution fabrication step with is needed when such site-controlled QDs shall be integrated into pn-junction devices to be used as on-demand single photon emitters.

All these challenges have been mastered using buried stressors which allow for precise alignment of QDs within vertically defined current injection paths of pn-junction LEDs. By tailoring the size and shape of the stressor quantum dots chains, cluster or single QDs can be nucleated above the stressor. Scaling the stressor to sub- μm dimensions single quantum dots become individually accessible for electrical excitation. Thus, the fabrication process electrically-driven single photon sources becomes scalable onto practically un-limited wafer size with high-yield. Most importantly, electro-luminescence of devices employing such site-controlled quantum dots exhibit excitonic emission complexes linewidths (<30 μeV) smaller than the fine-structure splitting of the exciton state. Such high optical properties are pre-requisite for the use of such single photon devices in quantum optic experiments.

8634-21, Session 5

GaAs/GaSb(001) nanostructures at the atomic scale

Andrea Lenz, Josephine Schuppang, Technische Univ. Berlin (Germany); Alban Gassenq, Thierry Taliercio, Eric Tournie, Univ. Montpellier 2 (France); Mario Daehne, Holger Eisele, Technische Univ. Berlin (Germany)

The development of III-V semiconductor devices has been concentrated on the compressively-strained material systems, such as InGaAs/GsAs or GaSb/GaAs. In contrast, the Ga(In)As/GaSb(001) material system may act as the model system for tensile-strained nanostructures, being promising for near-to-mid infrared applications. In order to understand the growth process we study the atomic structure of GaAs depositions with varying layer thicknesses by cross-sectional scanning tunneling microscopy.

The sample was grown using molecular beam epitaxy with cracker cells, evaporating As₂ and Sb₂. It contains four layers with nominally 1 ML, 2 ML, and 3 ML GaAs, grown at 500 °C with a rate of 0.5 ML/s. Prior to each GaAs layer a 5 s growth interruption was applied, but not afterwards.

Within the resulting GaAs/GaSb layers small agglomerations formed with a high density (10¹¹ cm⁻² range), independent of the deposited amount of GaAs. No persistent wetting layer is found. In the case of 1 ML and 2 ML GaAs deposition, the size along growth direction extends over 8 ML. The agglomerations for 1 ML and 2 ML GaAs are of similar size. In the case of 3 ML GaAs deposition, larger nanostructures develop with base lengths of about 10 nm, and heights of about 10–12 ML. However, no well-defined shape of these nanostructures, especially no flat bottom boundaries were observed. This is in contrast to the compressively-strained InGaAs/GaAs or GaSb/GaAs systems, always exhibiting a sharp and flat interface at their base. From these result we consider a different growth mode for GaAs/GaSb.

**Conference 8634: Quantum Dots and Nanostructures:
Synthesis, Characterization, and Modeling X**

8634-22, Session 5

Efficient Ga(As)Sb quantum dot emission in AlGaAs by GaAs intermediate layer

Thomas H. Loeber, Johannes Richter, Johannes H. Strassner, Carina Heisel, Christina Kimmle, Henning Fouckhardt, Technische Univ. Kaiserslautern (Germany)

Ga(As)Sb quantum dots (QDs) are grown in AlGaAs/GaAs by the Stranski-Krastanov mode. In the recent past we achieved Ga(As)Sb QDs in GaAs with an extremely high dot density of $9.8 \times 10^{10} \text{ cm}^{-2}$ by optimization of growth temperature, Sb/Ga flux pressure ratio, and coverage. Additionally, the QD emission wavelength could be controlled precisely with these growth parameters between 876 and 1035 nm.

Here we report an increase in the photoluminescence (PL) intensity of the QDs grown in AlGaAs barriers. Growth parameters and layer composition are varied. The aluminium content is varied between 0 and 90%. Reflectance anisotropy spectroscopy is used as in-situ growth control to determine growth rate, layer thickness, and AlGaAs composition.

Ga(As)Sb QDs, directly grown in AlGaAs emit no PL signal, even with a very low part $X = 0.1$. With additional around 10 nm thin GaAs intermediate layers between the Ga(As)Sb QDs and the AlGaAs barriers PL signals are detected. Samples with 4 QD layers and AlGaAs/GaAs barrier layers in between are grown. The thickness and composition of the barriers are changed. Depending on these values the intensity of the PL signal is even up to 4 times higher compared to simple GaAs barriers, the best case known up to now. With these results efficient Ga(As)Sb QD lasers can be realized. Our index-guided edge emitting broad area lasers operate in cw mode @ 93 K, emit optical powers of more than $2 \times 50 \text{ mW}$ and show a differential quantum efficiency of 53% with a threshold current density of 528 A/cm^2 .

8634-23, Session 5

Data analysis procedure for near infrared time-resolved emission experiments

Elahe Yeganegi, Univ. Twente (Netherlands); Allard P. Mosk, Willem L. Vos, Univ. Twente (Netherlands)

Spontaneous emission is a process of fundamental interest. Its control is relevant to many applications especially in the near-infrared telecom bands. Time resolved emission experiments are essential to understand the decay dynamics of spontaneous emission.

Unfortunately, however, photon detection in the near infrared ($>1100 \text{ nm}$) is much more difficult than in the visible range due to a low signal to noise ratio. In the near infrared the time-resolved emission histograms are measured on large background of dark counts, due to low intrinsic emission rate and a high detector background. Estimation of the correct background level in the case of low signal to background ratio is of key importance for getting the correct decay time. Therefore we discuss a statistical analysis of time-resolved measurements. Estimating the correct background value is solved by using maximum likelihood estimation. This powerful method allows us to extract the parameters of simultaneous best fit to the background measurement and the desired decay curves. Data are included (discarded) if the decay curves are fit assuming a dark rate that lies inside (outside) the statistical credibility interval. We illustrate our method with PbS quantum dots decay curves in suspension and in 3D photonic band gap crystals.

8634-24, Session 5

Unveiling structural properties of self-assembled quantum dots using RHEED

Manori V. Gunasekera, Alexandre Freundlich, Univ. of Houston (United States)

A better understanding of structural properties and growth kinetics of self-assembled Stranski-Krastanov quantum dots is necessary for applying dot potential in optical and electronic applications. In fact, Reflection high energy electron diffraction (RHEED) technique as a real time in-situ diagnostic tool reveals the ability of monitoring quantum dot evolution without limitation of reliability. We have recently demonstrated theoretically and experimentally, the ability of RHEED tool in quantitative analysis such as extracting average dot size, facet orientation and average dot density and real time monitoring of dot size during growth. As an extended study, in this work we present the experimental evidence on onset epitaxial quantum dot average shape in other words facet orientation evolution. We have monitored a sharp transition of chevron angle of (002) diffraction spot near the onset of dot formation at two growth temperatures 4400 C and 4800 C . The evolutions are in agreement with transition of quantum dot shape from shallower bounded facets to steeper low index bounded facets. Based on the home-made theoretical modeling data of RHEED patterns along $[1 -1 0]$ and $[1 -3 0]$ azimuths we propose a structure for quantum dots which is terminated by low index facets. The geometries of simulated RHEED images are consistent with experimental observations. Further, in this work we present the evidences of dot shape asymmetries in chevron angles we have seen during formation of QDs.

8634-25, Session 5

Doped semiconductor nanocrystals

Latha Nataraj, Aaron Jackson, Lily Giri, Mark Bundy, U.S. Army Research Lab. (United States)

Low-dimensional semiconductor structures such as nanocrystals are highly promising for various applications in electronics. The intentional addition of small amounts of foreign materials, known as dopants, provides an easy mechanism to control the behavior of semiconductors as their electronic, optical, and magnetic properties are considerably modified. Therefore, significant research is underway to explore the influence of dopants on semiconductor nanocrystals. Doped nanocrystals have been shown to provide better conductivity for thin conducting films, improved emission characteristics for lasers, protection for photovoltaic devices from photooxidation due to prolonged exposure, and serve as less harmful alternatives to toxic fluorescent dyes in bio-imaging, to name a few advantages. However, the process of doping such nanocrystals is extremely challenging due to their nanoscale sizes. In addition, the introduction of even a few atoms of the dopant into the nanocrystal that contains just a few hundred atoms could result in a degenerate material or compromise the crystal structure. Some strategies such as remote doping and substitutional doping have led to progress in achieving doping in these nanocrystals and heavily doped nanocrystals have been obtained with p- and n-type dopants incorporated. However, such processes involve complex chemical synthesis processes and in some cases, do not provide consistently successful results. Many questions still remain unanswered. In this work, we present a simple, low-cost mechanism for consistently obtaining doped semiconductor nanocrystals through mechanical milling techniques and study their properties.

**Conference 8634: Quantum Dots and Nanostructures:
Synthesis, Characterization, and Modeling X**

8634-26, Session PWed

Stability of lead sulfide colloidal quantum dot films on GaAs

Joanna Wang, Bruno Ullrich, Gail J. Brown, Howard E. Smith, Lawrence Grazulis, Air Force Research Lab. (United States)

The stability of colloidal PbS quantum dot (QD) films deposited on various substrates including glass and GaAs was studied. These QD films were fabricated using a novel supercritical fluid (SCF) CO₂ process to completely remove the solvent containing the oleic ligand capped PbS QDs and leave a close-packed film on the substrate. For comparison, a solution deposition and drying process was also used to create QD films from the same solution. Over a period of months, the QD film sample was retested after being left unprotected in air under ambient conditions. Despite exposure to 532 nm laser excitation and cooling to cryogenic temperatures, the photoluminescence remained stable between early tests. However, after a two year period the PL spectrum did exhibit a blue shift in energy and a lower intensity. The shift to higher energy for the QD emission indicates oxidation of the PbS, which shrinks the active QD volume and pushes the confined states to higher energy. To track potential changes to the QDs over time, x-ray photoelectron spectroscopy, transmission electron microscopy, x-ray diffraction, optical absorption, and atomic force microscopy, were employed. The PbS QD films on GaAs and glass have good adherence, despite the lack of a polymer matrix, and with the SCF CO₂ deposition process the films have very uniform substrate coverage without the typical "coffee ring" pattern of standard solution deposition processes. The PbS QD film stability is important for fabrication of devices, such as light emitters, under ambient conditions.

8634-27, Session PWed

Energy transfer in mixtures of quantum dots of different sizes studied by thermal lens technique

Djalmir N. Messias, Vanessa M. Martins, Adamo G. Monte, Acacio A. Andrade, Univ. Federal de Uberlândia (Brazil)

Energy transfer in mixtures of CdSe/ZnS quantum dots, QD, of different sizes were studied through the Thermal Lens, TL, technique. It was possible to obtain the energy transfer quantum efficiency, ETQE, and the individual luminescence quantum efficiency, LQE. The QD (labeled from C1 to C4) have nominal sizes of 3.2 nm, 2.6 nm, 2.4 nm and 1.9 nm, respectively. The mixtures were prepared diluting the QD in a decane solution obeying 300 ?l of C1 + 300 ?l of Cj (j= 2, 3, 4). The measurements were performed with the excitation beam at 405 nm and, for TL, the probe beam at 632 nm. Following a rate equation treatment it was possible to write a theoretical model for the heat generated in the mixture. This model, which strongly depends on the LQE and ETQE, was used to analyze the TL results. As, in the mixture, both QD emit simultaneously when excited, the individual LQE were determined in a separated experiment. For samples of different sizes and same concentration the LQE increases as the QD sizes decreases, which is an evidence of stronger quantum confinement. Finally, for the mixed samples and using the model, it was observed an ETQE decreases when Cj has its size decreased. A similar behavior was found by using conventional photoluminescence measurements. As a next step we intend to vary the excitation wavelength, for TL measurements, in order to achieve LQE and ETQE in the same experiment. This way, similar systems could be studied with same approach.

8634-28, Session PWed

Demonstration of multi-spectral In(Ga)As/GaAs-based quantum dot infrared photo detectors with quaternary (InAlGaAs) capping operate at low bias voltage

Sourav Adhikary, Indian Institute of Technology Bombay (India); Yigit Aytac, A.G. U. Perera, Georgia State Univ. (United States); Subhananda Chakrabarti, Indian Institute of Technology Bombay (India)

The quantum dot infrared photodetector (QDIP) is an emerging technology for advanced imaging. Blessed with the unique property of three dimensional confinements of carriers, such detectors are predicted to have intrinsic sensitivity to normal incident radiation, longer excited state life-time and reduced dark current. Multi-spectral (MS) and hyper-spectral (HS) imaging technologies are favored as they extend the boundary of applications of the device. We report multi-spectral performance of MBE grown InGaAs/GaAs (device A) and InAs/GaAs (device B) based photodetector with In_{0.21}Al_{0.21}Ga_{0.58}As (30Å) quaternary capping at 77K. Quaternary layer acts as a surface driven phase separation alloy which helps to produce defect free QDs in the active region as well as to reduce the dark current of the device. Low-temperature (77K) photoluminescence (PL) experiment reveals the existence of only ground state emission peak at 1.09eV for sample A, while other sample contains ground state emission peak at 1.18eV and 1st excited state emission peak at 1.25eV. Spectral response (SR) measurement of device A shows the presence of a strong photocurrent peak at 10.2µm along with a weak peak at 8.5µm at -0.4V bias voltage at 77K temperature. Device B exhibits a broad range of photocurrent response (covering MWIR and LWIR region) with two intense peaks at 5.6µm and 13.8µm along with a couple of weaker peaks at 8.5µm and 16.7µm at very low (-0.2V) bias voltage. DST India is acknowledged.

8634-30, Session PWed

3D nanopillar optical antenna avalanche detectors

Pradeep N. Senanayake, Chung-Hong Hung, Alan Farrell, Univ. of California, Los Angeles (United States); David Alejandro Ramirez, The Univ. of New Mexico (United States); Joshua N. Shapiro, Univ. of California, Los Angeles (United States); Chi-Kang Li, Yuh-Renn Wu, National Taiwan Univ. (Taiwan); Majeed Hayat, The Univ. of New Mexico (United States); Diana L. Huffaker, Univ. of California, Los Angeles (United States)

We demonstrate a nanopillar (NP) device structure for implementing plasmonically enhanced avalanche photodetector arrays with thin avalanche volumes (~ 310 nm x 150 nm x 150 nm) 1. A localized 3D electric field due to a core-shell PN junction in a NP acts as a multiplication region, while efficient light absorption takes place via Surface Plasmon Polariton Bloch Wave (SPP-BW) modes due to a self-aligned metal nanohole lattice. Avalanche gains of ~ 216 at 730 nm at -12 V are obtained. We show through capacitance-voltage characterization, temperature-dependent breakdown measurements and detailed device modeling that the avalanche region is on the order of the ionization path length, such that dead-space effects become significant. This work presents a clear path towards engineering dead space effects in thin 3D-confined multiplication regions for high performance avalanche detectors for applications in telecommunications, sensing and single photon detection.

Monday - Thursday 4 -7 February 2013

Part of Proceedings of SPIE Vol. 8635 Advances in Photonics of Quantum Computing, Memory, and Communication VI

8635-1, Session 1

Fluorinated nanodiamonds for charge detection in cells and biological systems *(Invited Paper)*

Miloš Nesladek, IMEC (Belgium)

Recently, fluorescent nanodiamond (fND) particles, containing nitrogen - vacancy color centers were used for medical monitoring as cellular markers. fNDs cover a wide span of applications ranging from quantum computing and photonics to biology and nanomedicine [1]. Here we concentrate on fND particles with specific termination for cancer diagnostics. While recently FRET diagnostics using fND as a donor has been demonstrated [2], in our work we propose a new method based on the electric field detection, developed by biomolecular interactions in cell environment at the fND surface. This principle can be used for fND of sizes to about 50 nm as intracellular nano-sensor with high sensitivity, based on the charge transfer between neutral (NV0) or negatively-charged (NV-) centers [3]. To operate such devices in cells, a specific fND size and surface terminations are required. Apart of the discussed size effects, we have developed a method to terminate fND with high proportion of functional Fluor groups. We study photoluminescence, including quantum size phenomena that can be chemically controlled [3]. We applied the developed fNDs on various cells types such as IC21 cells and report on fND specific interactions with cell environment. fND fractions of 8-10 nm, 10-20 nm, 20-50 nm and 80-120 nm were functionalised with three types of surface termination (H, OH, F). We attached charged molecules or biomolecules such as PEI of different molecular weight polymers at fND surface and interacted with si-RNA. Based on the strong size dependence of PL NV-/NV0 ratio could be precisely tuned. We model NV-/NV0 luminescence and discuss its stability. Finally we applied this system for sensing of si-RNA in IC21 cells.

[1] Vadyan N. Mochalin Nature Nanotechnology 7, 11-23 (2012)

[2] J. Tisler et al, ACS NANO, 5, 2011

[3] Petrakova et al, Adv.Func.Mater. (2012)

8635-2, Session 1

High-brightness fluorescent nanodiamonds for biolabeling applications *(Invited Paper)*

Huan-Cheng Chang, Academia Sinica (Taiwan)

Containing high density ensembles of negatively charged nitrogen-vacancy (NV-) centers as built-in fluorophores, fluorescent nanodiamonds (FNDs) are finding increasing use in optical bioimaging. However, issues related to the brightness and conjugability of the particles with proteins for specific labeling applications remain to be solved. This work explores the possibility of increasing the density of NV- in nanodiamonds using nitrogen-rich type Ib diamond powders and high-energy ion irradiation. An increase of the fluorescence intensity with the density of neutral, atomically dispersed nitrogen was observed for diamonds with [N0] = 100 - 200 ppm and good crystallinity. The increase has enabled practical applications of FNDs as biolabels. To illustrate the usage of these particles, 100-nm FNDs were conjugated either with bovine serum albumin (BSA) modified with carbohydrate for hepatic targeting or with streptavidin through a polyethylene glycol (PEG) spacer to acquire targeting specificity for HepG2 or C7 and MCF-7 cells. We demonstrated in this work the promising applications of these bright FND bioconjugates in vitro. The potential use of the nanoscale diamond material for long-term single particle tracking in vivo is discussed.

8635-3, Session 1

Upconverting fluorescent nanoparticles for biodetection and photoactivation *(Invited Paper)*

Kai Huang, WenKai Li, Muthu Kumara Gnanasammandhan Jayakumar, Yong Zhang, National Univ. of Singapore (Singapore)

Fluorophores including fluorescent dyes/proteins and quantum dots (QDs) are used for fluorescence-based imaging and detection. These are based on 'downconversion fluorescence' and have several drawbacks: photobleaching, autofluorescence, short tissue penetration depth and tissue photo-damage. Upconversion fluorescent nanoparticles (UCNs) emit detectable photons of higher energy in the short wavelength range upon irradiation with near-infrared (NIR) light based on a process termed 'upconversion'. UCNs show absolute photostability, negligible autofluorescence, high penetration depth and minimum photodamage to biological tissues. Lanthanide doped nanocrystals with near-infrared NIR-to-NIR and/or NIR-to-VIS and/or NIR-to-UV upconversion fluorescence emission have been synthesized. The nanocrystals with small size and tunable multi-color emission have been developed. The emission can be tuned by doping different upconverting lanthanide ions into the nanocrystals. The nanocrystals with core-shell and multi-shell structure have also been prepared, to improve the upconversion efficiency and to tune the emission color. The surfaces of these nanocrystals have been modified to render them water dispersible and biocompatible. They can be used for ultrasensitive interference-free biodetection because most biomolecules do not have upconversion properties. UCNs are also useful for light based therapy with enhanced efficiency, for example, photoactivation.

8635-4, Session 1

Rare-earth doped nanoparticles as fluorescent tags for biological applications

Zameer Ul Hasan, Temple Univ. (United States)

No Abstract Available

8635-5, Session 2

Nanodiamond imaging: molecular imaging with optically-detected spin resonance of nitrogen-vacancy centers in nanodiamonds *(Invited Paper)*

Alex Hegyi, Eli Yablonovitch, Univ. of California, Berkeley (United States)

Nanodiamond imaging is a new molecular imaging modality that takes advantage of nitrogen-vacancy (NV) defects in nanodiamonds to image the distribution of nanodiamonds within a living organism with high sensitivity and high resolution. Nanodiamond is a nontoxic material that is easily conjugated to biomolecules, such that the distribution of nanodiamond within a living organism can be used to elicit physiological information. Unlike the tracers used in other molecular imaging modalities such as positron emission tomography (PET) and single photon emission computed tomography (SPECT), nanodiamonds are stable and thus allow longitudinal imaging of the same organism over a long time span. Unlike fluorescence-based molecular imaging that has a resolution degraded by photon scattering, the resolution of nanodiamond imaging is defined by the strength of a magnetic gradient.

To form an image, a magnetic field-free region is created, such as exists halfway between two identical magnets with north poles facing

Conference 8635: Advances in Photonics of Quantum Computing, Memory, and Communication VI

each other. Optical excitation pumps the NVs into a bright fluorescence state, and microwaves transfer them to a dark state, but only for those NVs within the field-free region and resonant with the microwaves. By rastering the field-free region across the sample, the changes in fluorescence yield the nanodiamond concentration. Images of nanodiamond phantoms within chicken breast have been recorded with a prototype system. By modifying the nanodiamond particles and enhancing the imaging system, it should be possible to approach 100 μm resolution and to increase the sensitivity to a 10 nanomolar carbon concentration per root Hz in a mm³ voxel.

8635-6, Session 2

The diamond bionic eye (*Invited Paper*)

Steven Prawer, Univ. of Melbourne (Australia)

Retinal prosthetic devices for the blind are already a reality. In developing these devices the limits of physical, electronic and medical scientific fields are being tested. Of critical concern for retinal implant devices containing microelectronics is the ability to generate long lasting, high density, hermetic electrical feedthroughs in a biocompatible encapsulation material. This has previously proven difficult to achieve using standard materials and methods. Here, we present and characterise a high density, hermetic electrode array, entirely fabricated from diamond. Furthermore, we show that the electrochemical characteristics of the nitrogen incorporated ultra nanocrystalline diamond feedthroughs are suitable for the feedthroughs to be used directly as neural stimulation electrodes. Stimulation efficacy was demonstrated by surgically positioning electrically active diamond electrode arrays against the retina of a cat in vivo. During stimulation, recordings were taken from the visual cortex showing cortical responses from low current stimulation pulses. In all cases the charge densities required to evoke cortical responses were well within electrochemical safe limits. The results demonstrate that diamond is suitable not only as an encapsulation material but also as a promising biocompatible neural stimulation interface.

8635-7, Session 3

Highly-enriched 28Si: a 'semiconductor vacuum' allowing optical readout and control of electronic and nuclear spin qubits (*Invited Paper*)

Mike L. W. Thewalt, Simon Fraser Univ. (Canada)

Highly enriched 28Si is a remarkable new material, in which many optical transitions are much sharper than in natural Si, often by more than an order of magnitude. This allows us to use optical probes to study and manipulate the electronic and nuclear spins of impurities in 28Si, an approach which was thought to be impossible in solid state systems due to their inherently broad spectral linewidths. We use these new methods to study the electronic and nuclear spins of donor impurities in 28Si, beginning with the ubiquitous donor 31P. This is a prime candidate for Si-based quantum computing schemes, and our new methods enable us to study samples with extremely dilute concentrations, so donor interactions can be minimized. As a result we have measured a nuclear spin coherence time for 31P of over 180 seconds - by far a record for any solid state system.[1]

These optical methods are now being extended to the study of the nuclear spin lifetime and coherence time for ionized 31P in 28Si, since ionized donors play a role in a number of potential Si-based quantum computing proposals. We are also extending this work to the study of other donors in 28Si, in particular the deepest Group V donor 209Bi. In addition to a hyperfine coupling much larger than that of the other Group V donors, 209Bi has a large $I=9/2$ nuclear spin, resulting in a very rich hyperfine space which may be put to advantage.

1. M. Steger et al., Science 336, 1280 (2012).

8635-8, Session 3

"Listening" to the intrinsic spin fluctuations of holes coupled to nuclear spin baths in InGaAs quantum dots (*Invited Paper*)

Scott A. Crooker, Los Alamos National Lab. (United States)

Single electron or hole 'central' spins confined in III-V semiconductor quantum dots (QDs) are promising candidates for solid-state qubits. Although confinement suppresses momentum-dependent spin relaxation pathways, it enhances the hyperfine coupling between the central spin and the dense spin bath of $\sim 10^5$ lattice nuclei comprising the QD. These hyperfine interactions dominate decoherence and spin relaxation of the central spin at low temperatures. Although essential for understanding decoherence and relaxation in many quantum systems, the problem of how single central spins interact with a surrounding nuclear spin bath is highly nontrivial due to the many-body nature of the couplings involved. Different theoretical models yield widely varying timescales and dynamical response functions (exponential, power-law, Gaussian, etc).

Here we demonstrate alternative methods for revealing the timescales and functional form of bath-induced spin relaxation by passively "listening" to the tiny, intrinsic random fluctuations of central spins (holes in singly-charged (In,Ga)As QDs) while they remain in thermal equilibrium. The technique uses sensitive optical magnetometers based on Faraday rotation, and an efficient digital spectrum analyzer.

Because spin correlations are revealed in the spectral domain, this approach is well-suited to determine slow dynamical response functions with accuracy sufficient to achieve a novel understanding of coupled spin-bath systems. In contrast with theoretical predictions, the measured spin noise reveals exponential dynamics with long (400 ns) spin correlation timescales at B=0. Using small (100 G) magnetic fields to suppress a dominant hole-nuclear interaction channel, even longer timescales of order 5 microseconds are demonstrated [2]. Concomitantly, the spin noise spectrum evolves from Lorentzian to power-law lineshape, indicating a crossover from exponential to very slow, inverse-log dynamical response of the central hole spins. These noise signals actually increase as the probed volume shrinks, suggesting possible routes towards non-perturbative, sourceless magnetic resonance of few-spin systems.

[1] S. A. Crooker et al., Phys. Rev. Lett. 104, 036601 (2010)

[2] Yan Li et al., Phys. Rev. Lett. 108, 186603 (2012)

8635-9, Session 3

Optical generation and electrical control of valley polarization in atomically thin semiconductor (*Invited Paper*)

Xiaodong Xu, Univ. of Washington (United States)

Electronic valleys are energy extrema of Bloch bands in momentum space. The valley degree of freedom has recently attracted resurgent interest for exploitation in new modes of electronic and photonic device operation, largely due to the arrival of atomically thin two-dimensional electronic systems. In these materials, a pair of valleys exist at the corners of the Brillouin zone which are equivalent by time-reversal and may be distinguishable by their magnetic moment (m) and Berry curvature (?) as long as inversion symmetry is broken. As a result, charge carriers in the two valleys can be distinguished by their different response to optical and electric fields, providing the basis for valley-dependent operations. Here, we report optical generation and electrical control of valley polarization using MoS₂ field-effect transistors. In single layer MoS₂ devices, we demonstrated the generation of valley polarization through optical pumping techniques. Due to the built-in structural inversion asymmetry, the degree of polarization does not depend on perpendicular electric fields in single layers. In contrast, we show that the valley polarization in bilayers can be switched on and continuously tuned from -15% to 15% as a function of gate voltage. Bilayer MoS₂ is structurally inversion-symmetric, and electrical tuning of

Conference 8635: Advances in Photonics of Quantum Computing, Memory, and Communication VI

valley polarization is driven by inversion symmetry breaking induced by the gate electric field. Our results demonstrate the constraint imposed by inversion symmetry on Berry-phase related properties. Our work also points to an optoelectronic means to manipulate valley degrees of freedom for new photonics in truly two-dimensional systems.

8635-10, Session 3

Ultrafast optical control of individual electron and hole spin qubits: entanglement between a single quantum dot electron spin and a downconverted 1560-nm single photon *(Invited Paper)*

Kristiaan De Greve, Peter McMahon, Leo Yu, Jason Pelc, Chandra Natarajan, David Press, Na Young Kim, Eisuke Abe, Stanford Univ. (United States); Dirk Bisping, Sebastian Maier, Christian Schneider, Martin Kamp, Sven Hoefling, Julius-Maximilians-Univ. Würzburg (Germany); Robert Hadfield, Heriot-Watt Univ. (United Kingdom); Alfred Forchel, Julius-Maximilians-Univ. Würzburg (Germany); Martin Fejer, Yoshihisa Yamamoto, Stanford Univ. (United States)

Individual spins in self-assembled InAs quantum dots are interesting candidate-qubits in view of their natural light-matter interface and potential for ultrafast, all-optical control (Press, Ladd et al, Nature 456, 218 (2008); Press, De Greve et al, Nat. Phot. 4, 367 (2010); De Greve, McMahon et al, 7, 872 (2011)). In this work, we will show how both individual electron and hole spins can be coherently manipulated using picosecond modelocked laser pulses, and how an all-optical spin-echo technique can be implemented that decouples slow, shot-to-shot variations in the environment. While the dephasing and decoherence mechanisms for electrons and holes are intrinsically different, similar qualitative results are obtained, except for dynamic nuclear polarization effects that affect the controllability of electrons.

In addition, we demonstrate telecom-wavelength (1560 nm) conversion of single photons emitted from the trion state of an electron-charged quantum dot, again using ultrafast optical pulses. By mixing a short, coherent 2.2 μm pulse with the ~ 900 nm single photon emitted from the trion state in a PPLN waveguide, a 1550 nm photon is transmitted, conditional on exact overlap of the 900 nm single photon with the picosecond 2.2 μm pulse. In combination with a superconducting nanowire detector, this provides an effective and picosecond-resolution 1550 nm single-photon detector. We show how this ultrafast detection can be used to measure high-fidelity entanglement between a quantum dot spin and a telecom wavelength single photon, which should allow for long-distance spin-spin entanglement upon quantum interference of the 1550 nm photons in a Hong-Ou-Mandel setup.

8635-11, Session 4

Electron spin resonance of nitrogen-vacancy centers in optically trapped nanodiamonds *(Invited Paper)*

Viva R. Horowitz, Benjamín J. Alemán, David J. Christle, Andrew N. Cleland, David D. Awschalom, Univ. of California, Santa Barbara (United States)

The nitrogen-vacancy (NV) color center in diamond is gaining significant interest for applications in nanoscale sensing. The optical addressability of the magnetically sensitive spin states and the ability to coherently control these states at room temperature makes this system an exciting candidate for spin-based magnetometry.

Using an optical tweezers apparatus, we have demonstrated three-dimensional position control of nanodiamonds in solution with simultaneous optical measurement of electron spin resonance (ESR) [1].

Despite the motion and random orientation of NV centers suspended in the optical trap, we observe distinct peaks in the measured ESR spectra that are qualitatively similar to the same measurement of NV centers in bulk diamond. Accounting for the random dynamics of the trapped nanodiamonds, we model the ESR spectra observed in an externally applied magnetic field to enable dc magnetometry in solution. We estimate the dc magnetic sensitivity based on variations in ESR line shapes to be approximately $50 \mu\text{T}/\sqrt{\text{Hz}}$ at 500 μT . This technique enables three-dimensional mapping of magnetic fields in solution and may provide a pathway to spin-based sensing in fluidic environments and biophysical systems, such as the interiors of living cells, that are inaccessible to existing scanning probe techniques.

[1] V. R. Horowitz, B. J. Alemán, D. J. Christle, A. N. Cleland, and D. D. Awschalom, Proc Natl Acad Sci USA (In press, 2012). arXiv:1206.1573 [cond-mat.mtrl-sci].

8635-12, Session 4

A spin qubit coupled to a photonic crystal cavity

Timothy M. Sweeney, Samuel G. Carter, U.S. Naval Research Lab. (United States); Mijin Kim, Sotera Defense Solutions, Inc. (United States); Chul Soo Kim, Dmitry Solenov, Sophia E. Economou, Thomas L. Reinecke, Lily Yang, Allan S. Bracker, Daniel Gammon, U.S. Naval Research Lab. (United States)

Central to the goal of quantum information research is the development of a scalable light-matter quantum interface that can reversibly map quantum states between photon and long-lived matter states. Photonic crystal membranes provide an optical architecture in which the interaction of photons with an optically active matter qubit can be controlled through the introduction of optical cavities and waveguides. Charge neutral quantum dots are commonly integrated into photonic crystal architectures and are useful for sources and switches, but do not demonstrate long-lived coherences. The integration of charged quantum dots into a photonic crystal environment can lead to a spin-photon quantum interface, where it is the much longer lived spin of the electron instead of an exciton that serves as a qubit.

We demonstrate optical spin initialization and coherent control of an electron in a quantum dot that is embedded in and coupled to a 2D photonic crystal membrane cavity. The photonic crystal membrane is incorporated into an asymmetric NIP diode that allows for charging of an InAs quantum dot via an applied bias. Resonant laser spectroscopy performed in a transverse magnetic field reveals optical initialization of the electron spin. Furthermore, with the introduction of detuned control pulses, we perform coherent rotations of the electron spin state. These studies demonstrate several essential accomplishments toward a spin-photon interface.

8635-13, Session 4

Microring resonator-based diamond opto-thermal switch: a building block for a quantum computing network

Zhihong Huang, Hewlett-Packard Labs. (United States); Andrei Faraon, Hewlett-Packard Labs. (United States) and California Institute of Technology (United States); Charles M. Santori, Victor Acosta, Raymond G. Beausoleil, Hewlett-Packard Labs. (United States)

Diamond, embedded with nitrogen-vacancy (NV) centers, is an ideal test bed for integrated quantum networks due to its excellent optical and spin properties. Previously, many research groups have demonstrated NV based quantum optic experiments and nanophotonic resonant structures. In a diamond photonic network, while NV emitted photons couple to an optical waveguide, an optical switch constitutes an important functional

Conference 8635: Advances in Photonics of Quantum Computing, Memory, and Communication VI

block that can switch optical signal from one channel to another. In this work, we demonstrate a diamond opto-thermal switch that couples two waveguides and a microring resonator (10 μ m-diameter) on a 200nm-thick diamond membrane. Quality factors of $Q=3000$ are measured with free spectral range of $FSR=2.4$ nm and linewidth of 0.2nm. The switching is achieved through variation in the refractive index of ring resonator produced by changing its temperature locally. By heating the microring from 300 to 400K, 0.4nm switching range can be achieved. In addition, the small footprint of the microring opto-thermal switch is suitable for large scale integration.

8635-14, Session 4

NV centre emission in a substrate-free low-index environment

Faraz A. Inam, Macquarie Univ. (Australia); Michael D. W. Grogan, Boston Univ. (United States) and Univ. of Bath (United Kingdom); Mathew Rollings, Univ. of Bath (United Kingdom); Torsten Gaebel, Stefania Castelletto, Jana M. Say, Carlo Bradac, Macquarie Univ. (Australia); Tim A. Birks, William J. Wadsworth, Univ. of Bath (United Kingdom); James R. Rabeau, Micheal Steel, Macquarie Univ. (Australia)

With in-built advantages (high quantum efficiency and room temperature photostability [1]) for deployment in quantum technologies as a bright on-demand source of single photons, diamond NV centre is the most widely studied optical defect in diamond. Despite significant success in tuning its spontaneous emission [2], the fundamental understanding of its emission remains incomplete. Studying NV emission from nanodiamonds (NDs) on a glass substrate, we recently pointed out a disparity between the measured and calculated decay rates (assuming near unity quantum efficiency) [3]. This indicates the presence of some strong non-radiative influences from factors most likely intrinsic to ND itself [3]. In an attempt to obtain a cleaner picture of the NV emission, here we remove the substrate contributions to the decay rates by embedding our NDs inside silica aerogel, a substrate-free environment of effective index $n \sim 1.05$.

Nanodiamond doped aerogel samples were fabricated using the "two-step" process [4]. Time-resolved fluorescence measurement on ~ 20 centres for both coverslip and aerogel configurations, showed an increase in the mean lifetime ($\sim 37\%$) and narrowing of the distribution width ($\sim 40\%$) in the aerogel environment, which we associate with the absence of a air/coverslip interface near the radiating dipoles [3]. FDTD calculations showed the strong influence of the irregular ND geometry on the remaining distribution width. Finally a comparison between measurements and calculations provides an estimate of the quantum efficiency of the ND NV emitters as ~ 0.7 (see Fig.1). This value is apparently consistent with recent reports concerning the oscillation of the NV center between negative and neutral charge states [5].

Figure 1. Contours of total life time enhancement as a function of quantum efficiency and radiative enhancement . Blue dot: coverslip, Red: aerogel. The error-bars indicate one standard deviation uncertainties.

[1] Kurtsiefer C, Mayer S, Zarda P, and Weinfurter H 2000 Stable solid-state source of single photons Physical Review Letters 85 290-3

[2] Aharonovich I, Greentree A D, and Prawer S 2011 Diamond photonics Nat Photon 5 397-405

[3] Inam F A and et al. 2011 Modification of spontaneous emission from nanodiamond colour centres on a structured surface New Journal of Physics 13 073012

[4] Grogan M D W, Heck S C, Xiao L M, England R, Maier S A, and Birks T A 2012 Control of nanoparticle aggregation in aerogel hosts Journal of Non-Crystalline Solids 358 241-5

[5] Waldherr G, Beck J, Steiner M, Neumann P, Gali A, Frauenheim T, Jelezko F, and Wrachtrup J 2011 Dark States of Single Nitrogen-Vacancy Centers in Diamond Unraveled by Single Shot NMR Physical Review Letters 106 157601

8635-15, Session 4

Three-dimensional quantum photonic elements based on nanodiamonds in laser-written 3D microstructures

Andreas W. Schell, Humboldt-Univ. zu Berlin (Germany); Johannes Kaschke, Joachim Fischer, Karlsruher Institut für Technologie (Germany); Rico Henze, Janik Wolters, Humboldt-Univ. zu Berlin (Germany); Martin Wegener, Karlsruher Institut für Technologie (Germany); Oliver Benson, Humboldt-Univ. zu Berlin (Germany)

Single photons in passive optical microstructures are key elements for quantum optical technology. Promising single-photon sources are nitrogen vacancy centers (NV centers) in diamond. However, they are difficult to integrate directly in optical structures, since diamond is hard to process. One way to circumvent this problem is to use nanodiamonds. They can be coupled to photonic structures either deterministically by means of nanomanipulation or randomly by spin-coating.

Here, we present a novel approach where we build photonic microstructures with coupled nanodiamonds in a single production step. Two-photon direct laser writing (DLW) is used to produce nearly arbitrary three dimensional (3D) structures from a photoresist mixed with a solution of nanodiamonds.

We demonstrate the power of our approach by building waveguide-coupled disk resonators from the resist. Single-photon emission from NV centers inside these resonators as well as coupling to the waveguides is realized. Moreover, NV centers in laser-written waveguides are shown to be waveguide-coupled single-photon source with good collection efficiency.

Our new technique of 3D DLW using a photoresist containing photostable NV quantum emitters opens the way for a variety of future experiments: The shape of possible structures is nearly unlimited, different photostable single photon emitters may be used, and even on-demand 3D writing around located single emitters is feasible.

8635-16, Session 5

Photonic quantum computing (*Invited Paper*)

Jeremy L. O'Brien, Univ. of Bristol (United Kingdom)

No Abstract Available.

8635-17, Session 5

Large-scale cluster entanglement in the optical frequency comb: new developments (*Invited Paper*)

Olivier Pfister, Univ. of Virginia (United States); Nicolas Menicucci, The Univ. of Sydney (Australia); Moran Chen, Pei Wang, Univ. of Virginia (United States)

No Abstract Available.

Conference 8635: Advances in Photonics of Quantum Computing, Memory, and Communication VI

8635-18, Session 5

Polar-activation of noisy optical quantum channels

Laszlo Gyongyosi, Sandor Imre, Budapest Univ. of Technology and Economics (Hungary)

In this work a new phenomenon called polaractivation is introduced. Polaractivation of optical quantum channels is based on quantum polar encoding and the result is similar to the superactivation effect — positive capacity can be achieved with zero-capacity quantum channels. The polar coding is a revolutionary channel coding technique, which makes it possible to achieve the symmetric capacity of a noisy communication channel. The method can be extended to quantum channels to construct capacity-achieving codes. The superactivation enables the use of zero-capacity quantum channels for communication, however it has many limitations on the quantum channels.

Polaractivation has many advantages over the superactivation: it is limited neither by any preliminary conditions on the quantum channel nor on the maps of other channels involved in the joint channel structure. The proposed polaractivation is based on the channel polarization effect and on our special coding scheme. We define the encoding and decoding mechanism for the polaractivation of optical quantum channels and give the efficiency of the proposed scheme. We also prove that polaractivation works for the private classical capacity and the quantum capacity of optical quantum channels and these capacities are all polaractive. We also show the conditions for the polaractivation of zero-error capacities of optical quantum channels.

8635-19, Session 5

Protecting entanglement from decoherence using weak quantum measurement (*Invited Paper*)

Yong-Su Kim, Jong-Chan Lee, Osung Kwon, Yoon-Ho Kim, Pohang Univ. of Science and Technology (Korea, Republic of)

Decoherence, often caused by unavoidable coupling with the environment, leads to degradation of quantum coherence. For a multipartite quantum system, decoherence leads to degradation of entanglement and, in certain cases, entanglement sudden death. Tackling decoherence, thus, is a critical issue faced in quantum information, as entanglement is a vital resource for many quantum information applications including quantum computing, quantum cryptography, quantum teleportation, and quantum metrology. Here, we propose and demonstrate a novel scheme to protect entanglement from decoherence. Our entanglement protection scheme makes use of the quantum measurement itself for actively battling against decoherence and it can effectively circumvent even entanglement sudden death.

8635-20, Session 5

High numerical aperture diffractive optical elements for neutral atom quantum computing

Amber L. Young, Shanalyn A. Kemme, Joel R. Wendt, Tony R. Carter, Sally Samora, Sandia National Labs. (United States)

The viability of neutral atom-trapping based quantum computers is dependent upon scalability for the realization of a many-qubit system. Diffractive optical elements (DOEs) enable the manipulation of light to collect signal or deliver a tailored spatial trapping pattern in a small package. DOEs have an advantage over refractive micro-optics since they do not have measurable surface sag, enabling significantly larger numerical apertures (NA) accessible with a smaller optical component. The smaller physical size of a DOE also allows the micro-lenses to be

placed in vacuum with the atoms, reducing aberration effects that would otherwise be introduced by the cell walls. The larger collection angle accessible with DOEs enable faster quantum computation speeds.

We have designed an array of DOEs to be used for collecting the fluorescence emission of trapped neutral atoms; we compare these DOEs to several commercially available refractive micro-optics. The largest DOE is able to collect over 20% of the atom's radiating sphere whereas the refractive micro-optic is able to collect just 8% of the atom's radiating sphere.

8635-21, Session 6

Optical detection of a single rare-earth species in a crystal (*Invited Paper*)

Roman L. Kolesov, Kangwei Xia, Rolf Reuter, Rainer Stoehr, Andrea Zappe, Univ. Stuttgart (Germany); Jan Meijer, Ruhr-Univ. Bochum (Germany); Philip R. Hemmer, Texas A&M Univ. (United States); Jörg Wrachtrup, Univ. Stuttgart (Germany)

In the quest for solid-state quantum-enhanced sensors and quantum information devices, rare-earth and transition metal ions doped in crystalline hosts have long been prized because of their free-ion-like properties and high quality-factor (Q) optical transitions. These high Q transitions have already demonstrated exceptionally long storage times, long-range conditional two-qubit gates, and quantum entanglement storage. However until now the inability to detect the quantum states of single dopant ions has prevented these promising quantum systems from reaching their full potential. Here, we demonstrate detection of a single photostable Pr³⁺ ion in yttrium aluminum garnet (YAG) nanocrystals with high contrast photon anti-bunching. This was accomplished by using a second photon to convert excited state population of the high Q optical transition into ultraviolet (UV) fluorescence. The fact that the observed UV fluorescence originates from Pr³⁺ ions in YAG is proven by recording its excitation spectra along with their dependence on the polarization of the excitation laser beam. We also demonstrate a possibility of on-demand creation of Pr³⁺ ions in a YAG single crystal by ion implantation. These results enable a whole new class of quantum information devices since rare earth ions provide optically addressable nuclear spins with exceptional coherence properties. Furthermore, having an atomic size photostable UV emitter which can be introduced into any medium and activated by visible light opens a door to nanoscale optical engineering for technological and biological applications.

8635-22, Session 6

Solid-state photon-echo quantum memory for quantum repeaters (*Invited Paper*)

Wolfgang Tittel, Erhan Saglamyurek, Neil Sinclair, Hassan Mallahzadeh, Jeongwan Jin, Joshua A. Slater, Daniel Oblak, Univ. of Calgary (Canada); Mathew George, Raimund Ricken, Wolfgang Sohler, Univ. Paderborn (Germany)

Quantum repeaters promise to extend quantum communication such as quantum key distribution beyond its current distance limit of around 200 km. They rely on the distribution of entanglement over the entire transmission channel by means of entanglement swapping across subsections. To synchronize this procedure in adjacent subsections, quantum repeaters must incorporate quantum memories - devices that allow storing (entangled) quantum states until needed. We report on the storage and recall of members of time-bin entangled pairs of photons, generated by means of spontaneous parametric down-conversion of short laser pulses in a non-linear crystal, in a thulium-doped lithium niobate waveguide cooled to cryogenic temperature. More specifically, we show that the amount of entanglement that characterizes the two-

Conference 8635: Advances in Photonics of Quantum Computing, Memory, and Communication VI

photon state before and after storage remains unaffected by the temporal transfer of one photon's quantum state into collective atomic excitation. Furthermore, we demonstrate two-photon interference with attenuated laser pulses (a precursor to entanglement swapping) with visibility close to the theoretical maximum, regardless whether none, one, or both pulses have previously been stored. Finally, we show multi-mode storage of many photons in ten different frequency channels followed by read-out on demand. Our results constitute important steps to building quantum repeaters and, more generally, quantum networks.

8635-23, Session 6

Rephasing spontaneous emission in a rare-earth ion-doped Solid (*Invited Paper*)

Matthew J. Sellars, Sarah E. Beavan, Kate Ferguson, The Australian National Univ. (Australia); Morgan P. Hedges, Univ. of Calgary (Canada)

Here we present experimental work on generating correlated streams of photons using a rare-earth ion doped crystal; $\text{Pr}^{3+}:\text{Y}_2\text{SiO}_5$. This is achieved using photon echo techniques to rephase coherence in an atomic ensemble which was created when a spontaneous emission event occurred [1]. With single photon detection, this rephased amplified spontaneous emission (RASE) protocol can be used to generate correlated single-photon states, with intermediate storage and on-demand recall of one photon of the pair. This has applications in developing a quantum repeater protocol to extend the range of quantum communication links [2]. The experimental demonstration was enabled by applying a four-level photon echo sequence, allowing for spectral and spatial discrimination of the single-photon fields from the coherent emission following the bright rephasing pulses [3]. A correlation between spontaneous emission and its echo was verified, although the signal to noise ratio was insufficient to verify a non-classical degree of correlation. Progress towards demonstrating non-classical behavior utilizing a moderate finesse cavity to enhance direct transitions from the excited to ground states will also be reported.

[1] P. M. Ledingham, W. R. Naylor, J. J. Longdell, S. E. Beavan and M. J. Sellars, "Nonclassical photon streams using rephased amplified spontaneous emission", *Phys. Rev. A.*, 81, 012301, (2010)

[2] L. M. Duan, M. D. Lukin, J. I. Cirac, and P. Zoller, "Long-distance quantum communication with atomic ensembles and linear optics," *Nature*, 141, 413-148 (2001)

[3] S. E. Beavan, P. M. Ledingham, J. J. Longdell, and M. J. Sellars, "Photon echo without a free induction decay in a double- Λ system", *Opt. Lett.*, 36, 1272-1274, (2011)

8635-24, Session 7

Cavity-aided atomic spin squeezing for quantum-enhanced metrology (*Invited Paper*)

Mark A. Kasevich, Onur Hosten, Nils Engelsen, Rajiv Krishnakumar, Stanford Univ. (United States)

We use a dual-wavelength cavity, resonant at both 780 nm and 1560 nm, with a finesse of ~ 150000 . A few 10^4 Rubidium atoms are trapped at the anti-nodes of the 1560 nm mode, and probed by the 780 nm mode. The commensurate wavelength relationship allows identical coupling of the probe light to all atoms, eliminating decoherence issues associated with inhomogeneous coupling, and allowing the generation of completely symmetric spin-squeezed states that can be released into free-space as input states, e.g., for atom interferometry. The trapping light is frequency stabilized to the 4 kHz wide cavity, and the probe is generated via frequency doubling. The low-level frequency noise on the probe (50 mHz/rtHz from 200 Hz to 10 kHz) permits detection of cavity frequency shifts caused by a single atom. Measurements are accomplished by homodyne detection which includes a heterodyne part that stabilizes the phase at shot-noise level (5 $\mu\text{rad}/\text{rtHz}$).

8635-25, Session 7

Optimal detuning for writing warm-atomic-vapor quantum memory in the presence of collisional fluorescence and four-wave mixing

Igor Vurgaftman, Mark Bashkansky, U.S. Naval Research Lab. (United States)

The use of atomic vapor cells with buffer gas for quantum memory using the DLCZ (Duan-Lukin-Cirac-Zoller) protocol is limited by the simultaneous presence of collisional fluorescence and the four-wave mixing noise due to transitions from the ground state induced by the read beam. An elegant solution to suppress the latter was proposed recently by P. Walther et al., *Int. J. Quantum Inform.* 5, 51 (2007). In that approach, the Rb-87 atoms are pre-pumped to the $F = 2$, $m_F = 2$ substate, and circularly polarized write and read photons are employed, so that there is no allowed final state for the four-wave mixing process in question. We show that the technique is fundamentally limited by the cancellation of the Raman matrix elements for the transitions involving the $F = 1$ and $F = 2$ excited states that becomes more pronounced as the write beam is detuned from resonance. The cancellation is shown to occur for both the D1 and D2 lines of any stable or long-lived alkali isotope with an arbitrary nuclear spin. Experimental evidence for the cancellation is also presented. On the other hand, we show theoretically and experimentally that the detuning cannot be made arbitrarily small, since in that limit, the collisional fluorescence noise due to the presence of the buffer gas dominates the Stokes signal. We determine the optimal detuning for real detectors with dark counts and discuss the implications for atomic-vapor-based quantum-memory schemes with reduced noise.

8635-26, Session 7

Experimental demonstration of adaptive quantum state estimation (*Invited Paper*)

Ryo Okamoto, Hokkaido Univ. (Japan) and The Institute of Scientific and Industrial Research (Japan); Minako Iefuji, Satoshi Oyama, The Institute of Scientific and Industrial Research (Japan); Koichi Yamagata, Osaka Univ. (Japan); Hiroshi Imai, Univ. degli Studi di Pavia (Italy); Akio Fujiwara, Osaka Univ. (Japan); Shigeki Takeuchi, Hokkaido Univ. (Japan) and The Institute of Scientific and Industrial Research (Japan)

Quantum theory is inherently statistical. This entails repetition of experiments over a number of identically prepared quantum objects, for example, quantum states. Such an estimation procedure is important for quantum information, and is also indispensable to quantum metrology. In applications, one needs to design the estimation procedure in such a way that the estimated value of the parameter should be close to the true value (consistency), and that the uncertainty of the estimated value should be as small as possible (efficiency) for a given limited number of samples. In order to realize these requirements, Nagaoka[1] advocated an adaptive quantum state estimation (AQSE) procedure, and recently Fujiwara proved the strong consistency and asymptotic efficiency for AQSE[2].

In this talk, we report the first experimental demonstration of AQSE using photons. The angle of a half wave plate (HWP) that initializes the linear polarization of input photons is estimated using AQSE. A sequence of AQSE is carried out with 300 input photons, and the sequence is repeated 500 times for four different settings of HWP. The statistical analysis verifies the strong consistency and asymptotic efficiency of AQSE. We will also discuss how this method is useful for efficient quantum state tomography.

This work was supported in part by quantum Cybernetics project, Grant-

Conference 8635: Advances in Photonics of Quantum Computing, Memory, and Communication VI

in-Aid from JSPS, JST-CREST project, Q FIRST Program of JSPS, Special Coordination Funds for Promoting Science and Technology, the GCOE programs, and the Research Foundation for Opto-Science and Technology.

[1] H. Nagaoka, Proc. 12th Symp. on Inform. Theory and its Appl. 577 (1989).

[2] A. Fujiwara, J. Phys. A: Math. Gen, {bf 39} 12489 (2006).

8635-27, Session 7

Entropy, information, and compressive sensing in the quantum domain (*Invited Paper*)

John C. Howell, Gregory Howland, James Schneeloch, Univ. of Rochester (United States)

It may seem somewhat surprising that information is governed by uncertainty. Put another way, if we know what someone is going to tell us, then there would be no need for listening. The uncertainty of that communication, entropy, is a measure of the information gained. In this presentation, I will discuss some basic concepts of entropy along with some of our recent experiments on studies of entanglement entropy and quantum imaging using compressive sensing. Lastly, I will present results on recent studies of quantum noise on compressive signals. These experiments will be couched in the ideas of entropy and the information gained as a function of the number of photons. Compressive sensing has a wide range of possible application including imaging through obscurants, hyperspectral imaging, and high resolution single pixel imaging in otherwise difficult regions of the spectrum to image. These concepts are crucial in understanding compressive sensing as a sensing paradigm. Based on these ideas, I will present details of a novel compressive sensing Lidar system.

8635-28, Session 9

Multi-bit-per-photon QKD system based on encoding in orbital-angular-momentum states of light (*Invited Paper*)

Robert W. Boyd, Univ. of Ottawa (Canada) and Univ. of Rochester (United States); Jonathan Leach, Univ. of Ottawa (Canada); Omar Magaña Loaiza, Mehul Malik, Mohammad Mirhosseini, Brandon Rodenburg, Zhimin Shi, Mahmudur Siddiqui, Colin O'Sullivan, Univ. of Rochester (United States)

We have constructed a free-space quantum key distribution (QKD) system in which each photon carries more than one bit of information. We achieve this result by encoding in the orbital-angular-momentum (OAM) states of light. These states reside in an infinite-dimensional Hilbert space, and thus there is in principle no limit to how much information can be carried by an individual photon. An appropriate linear combination of these states forms a basis mutually unbiased with respect to the OAM basis; the use of two bases is required to ensure security of the QKD protocol. Our procedure makes use of weak coherent states carrying on average less than one photon per pulse. Security can be ensured by use of a decoy state protocol. We encode transverse spatial information onto each transmitted pulse through use of a spatial light modulator. Our detection procedure makes use of a "mode sorter" that can discriminate individual photons based on their transverse mode structure. In this presentation, we will be particularly concerned with presenting new results on the optimum design of a mode sorter and on quantifying the influence of atmospheric turbulence on the integrity of the QKD protocol.

8635-29, Session 9

Quantum key distribution with Fibonacci states (*Invited Paper*)

Alexander V. Sergienko, Boston Univ. (United States); David S. Simon, Stonehill College (United States) and Boston Univ. (United States); Nate Lawrence, Jacob Trevino, Luca Dal Negro, Boston Univ. (United States)

Quantum cryptography and quantum key distribution (QKD) have been the most successful applications of quantum information processing. We describe a fundamentally different approach to high-capacity, high-efficiency QKD by exploiting the interplay between cross-disciplinary ideas from quantum information and light scattering of aperiodic photonic media. We propose both a unique type of entangled-photon source and a new physical mechanism for efficiently sharing keys. The new source produces entangled photons whose orbital angular momenta (OAM) are in a superposition of Fibonacci numbers. Combining entanglement with the mathematical properties of Fibonacci sequences leads to a new way of realizing the physical conditions necessary for implementation of the no-cloning principle, which in turn leads to a new QKD protocol. This Fibonacci protocol allows secure generation of long keys from few photons. Unlike other protocols, reference frame alignment and active modulation of production and detection bases are unnecessary, since security does not require use of non-orthogonal polarization measurements.

The Fibonacci protocol has several additional advantages: (i) If Eve intercepts Bob's photon, that alone is not enough to determine the key, since it is the pump value that provides the key, and that pump value can not be determined from the value of Bob's photon alone. (ii) Randomized OAM values are produced in a completely passive manner, without need for active switching of holograms or measurement bases, as required by other approaches, greatly speeding up key generation rates. (iii) Fibonacci coding can be more efficient than binary coding for some purposes.

8635-30, Session 9

The orbital angular momentum of spatially complex modes

(*Invited Paper*)

William N. Plick, Mario Krenn, Sven Ramelow, Robert Fickler, Anton Zeilinger, Institut für Quantenoptik und Quanteninformation (Austria)

Beyond the familiar Hermite-Gauss and Laguerre-Gauss stable light modes exist a whole zoo of spatially complex light fields. We present a theoretical analysis of orbital angular momentum of several novel light modes, revealing several compelling features including: non-monotonic behavior as spatial parameters are varied, stable beams with fractional orbital angular momentum, modes for whom both quantum mode numbers differ but the orbital angular momentum is the same, and modes where the local orbital angular momentum can be controlled in complex ways according to the desires of the experimenter.

We use the Ince-Gauss modes (which are the natural solutions to the paraxial wave equation in elliptic coordinates) and the so-called "Maverick" modes (stable beams which are found by physical experimentation) as test beds to investigate the connections between beam stability, phase singularities, optical vortices, and the concept of topological charge - with emphasis on the diverse potential applications to atom trapping, metrology, quantum key distribution, and quantum communication and informatics in general.

**Conference 8635: Advances in Photonics of
Quantum Computing, Memory, and Communication VI**

8635-31, Session 9

Mode structure reconstruction with multiphoton statistics

Elizabeth A. Goldschmidt, National Institute of Standards and Technology (United States); Fabrizio Piacentini, Istituto Nazionale di Ricerca Metrologica (Italy); Sergey V. Polyakov, National Institute of Standards and Technology (United States); Giorgio Brida, Ivo P. Degiovanni, Marco Genovese, Istituto Nazionale di Ricerca Metrologica (Italy); Alan L. Migdall, National Institute of Standards and Technology (United States); Ivano Ruo Berchera, Istituto Nazionale di Ricerca Metrologica (Italy)

A single photon is often defined as a single excitation of a particular spatio-temporal mode of the electromagnetic field. It is thus not surprising that a range of fundamental properties of a light field depend on its underlying mode structure. Moreover, mode structure engineering is vital for obtaining sources that produce indistinguishable single photons, a paramount problem of scalable quantum information. When dealing with states of light, quantum or classical, understanding the underlying mode structure is of utmost importance. It turns out that many sources of classical and nonclassical light produce light in multiple modes simultaneously, and the shape of those modes, in transverse momentum, spectrum, temporal extent, and polarization, varies from source to source. Thus, full characterization of the mode structure involves separate measurements in spatial, temporal, frequency and polarization domains, requiring a range of instrumentation. An important property of multi-mode states, however, is that the collective statistics of multi-mode light can depend on the number and occupation of modes of all degrees of freedom. We propose and implement a new tomographic method that uses just the photon number statistics of a source to gain information about its underlying mode structure. We experimentally demonstrate a successful mode reconstruction of mixed states with multi-mode pseudo-thermal light and single-mode poissonian light. We mix up to three modes and measure the multi-mode result on a photon number-resolving detector (a detector tree with four avalanche diodes). We use the detected photon number distribution to reconstruct the underlying mode structure of the source.

8635-32, Session 9

Spectral properties of ultra-broadband entangled photons generated from chirped-MgSLT crystal towards monocycle entanglement generation

Akira Tanaka, Ryo Okamoto, Hokkaido Univ. (Japan) and The Institute of Scientific and Industrial Research (Japan); Hwan Hong Lim, National Institute for Materials Science (Japan); Shanthi Subashchandran, Masayuki Okano, Hokkaido Univ. (Japan) and The Institute of Scientific and Industrial Research (Japan); Labao Zhang, Lin Kang, Jian Chen, Pei-Heng Wu, Nanjing Univ. (China); Toru Hirohata, Hamamatsu Photonics K.K. (Japan); Sunao Kurimura, National Institute for Materials Science (Japan); Shigeaki Takeuchi, Hokkaido Univ. (Japan) and The Institute of Scientific and Industrial Research (Japan)

Compressing the temporal correlation of two photons down to monocycle regime (3.5fs, center wavelength: 1064nm) harnesses quantum metrological applications such as enhancement in the axial resolution (<1.0? μ m) of quantum optical coherence tomography as well as quantum information-theoretic benefits that increases available modes for WDM-based multi-frequency QKD network and novel optical non-linear experiments. For this aim, the two photon state must be essentially ultra-broadband in frequency domain coexisting with being ultra-short in time domain. In this report, we have succeeded in the generation and the detection of ultra-broadband, frequency-entangled two photon states via

type-0, non-collinear and cw-pumped (532nm) spontaneous parametric down conversion (SPDC) in four PPMgSLT crystals having different chirping rates of their poling periods in 1st-order QPM conditions. Firstly, we measured one-photon spectra by using an NbN meander-type superconducting single photon detector and InP/GaAs photomultiplier tubes with a photon counter and a laser line Bragg tunable band pass filter. Thanks to the broadband sensitivity of both detectors in near-infrared wavelength range, we observed the maximal SPDC bandwidth of 820nm among four samples. For this spectrum, we calculated and found that it can in principle achieve 1.2cycle temporal correlation by appropriate phase compensation if we employ non-collinear sum frequency generation to measure the temporal correlation of two photon state. Moreover, in order to demonstrate frequency correlation experiment we will discuss several detection strategies to measure coincidences in the presence of wavelength-dependent optical elements.

8635-33, Session 10

Controlling rare-earth fluorescent states in lightly-doped nanoparticles (Invited Paper)

Aras Konjhdzic, Temple Univ. (United States)

No Abstract Available

8635-34, Session 10

Quantum memory in a rare-earth doped crystal: from multiple to single excitation regime (Invited Paper)

Elizabeth A. Goldschmidt, Joffrey Peters, Sergey V. Polyakov, Alan L. Migdall, Joint Quantum Institute (United States)

Robust, long-lived quantum memories are important components of many quantum information protocols. We report on the progress of our efforts toward demonstrating a quantum memory on a long-lived spin transition in a solid state material. We demonstrate coherent generation, storage, and retrieval of multiple excitations on a long-lived spin transition in a rare-earth ion-doped crystal via spontaneous Raman scattering - an enabling step toward realizing a solid-state quantum repeater. We use this intermediate result to study the temporal dynamics of the process and determine the necessary components for entering the single excitation regime, a requirement for a practical quantum memory. In particular, these results demonstrate the need for a high-contrast, tunable, ultra-narrow spectral filter (<1MHz FWHM at 606 nm) to progress to the single excitation regime. We use spectral hole-burning and the dc Stark effect in the same rare-earth material to implement a narrow, switchable filter.

8635-35, Session 10

Towards broadband time separated entanglement using rephased amplified spontaneous emission (Invited Paper)

Jevon J. Longdell, Patrick M. Ledingham, William R. Naylor, Univ. of Otago (New Zealand)

Amplified spontaneous emission (ASE) a ubiquitous optical phenomenon. It is used to make high brightness broadband incoherent light sources for many applications as well as being an important noise source in optical amplifiers and source of inefficiency in lasers. While these are all usually thought of incoherent processes recent theoretical work has highlighted that the output light is entangled with degrees of freedom in the amplifier. This is important in the case of optical amplifiers made of rare earth ion dopants at cryogenic temperatures. The long coherence times of these ions make it possible to coherently recall the amplifier degrees of

Conference 8635: Advances in Photonics of Quantum Computing, Memory, and Communication VI

freedom at a later time as light using rephasing pulses.

We present experimental studies of the rephased amplified spontaneous emission (RASE) using thulium ions in YAG using shot noise limited balanced heterodyne detection. First an inverting pi pulse is applied to the sample resulting in ASE, this is followed by a second pi pulses resulting in an 'echo' of the ASE. The ASE and its echo showed coherent correlations and we saw evidence of entanglement.

We will also present theoretical work looking at RASE within an optical resonator and show the potential for perfect entanglement between the ASE and its echo.

8635-36, Session 11

Message-passing and stochastic architectures for nanophotonic information processing (*Invited Paper*)

Dmitri S. Pavlichin, Hideo Mabuchi, Stanford Univ. (United States)

Nanophotonic systems will involve many interacting components subject to quantum fluctuations and other noise of microphysical origin. Graphical models offer a framework in which to understand the computational power of such systems in a way that naturally incorporates many variables interacting in a structured way. Iterative message-passing algorithms for graphical models can additionally capture the stochastic dynamic evolution of photonic systems mediated by coherent fields coupled to internal degrees of freedom. Message-passing algorithms have emerged as an important tool for handling large problems of inference and optimization, so exploiting the analogy to photonic systems may lead to a fast, low-power implementation.

Starting from the master equation in Lindblad form we show that the evolution of a photonic circuit can be understood in terms of a message-passing scheme. We demonstrate an application of this approach by describing an iterative decoder for low-density parity check (LDPC) codes using familiar objects (such as atomic emitters coupled to cavities, waveguides and coherent sources) and analyze its performance for several codes. We also construct a similar circuit for classical and quantum error correction.

8635-37, Session 11

Nonlinear optics at the few-photon level in Rb-filled photonic band-gap fiber (*Invited Paper*)

Alexander L. Gaeta, Cornell Univ. (United States)

No Abstract Available.

8635-38, Session 11

Low photon number nonlinear optics with a single quantum dot in a cavity (*Invited Paper*)

Edo Waks, Ranojoy Bose, Univ. of Maryland, College Park (United States); Deepak Sridharan, Intel Corp. (United States); Glenn S. Solomon, National Institute of Standards and Technology (United States)

Quantum dots coupled to photonic crystals present a promising material platform for achieving strong nonlinear optical effects. Recently, it has been shown that by embedding a single quantum dot (QD) in the high field region of photonic crystal cavities it becomes possible to achieve strong light-matter interactions at the single photon/single atom level. These unprecedented interaction strengths open up the possibility for creating nonlinear optical effects with a small number of photons. In this talk, we will discuss our work on coupling indium

arsenide QDs to photonic crystal structures for creating nonlinear optical interactions at low photon numbers. We will describe recent experimental demonstrations of giant optical Stark shifts with only 10 photons of energy using a strongly coupled cavity-QD system, as well as a demonstration of all-optical switching with only 150 photons of control energy. Methods for achieving these nonlinearities in a highly compact planar device structure will also be described.

8635-39, Session 12

All-optical integrated RAMs based on nanocavities (*Invited Paper*)

Masaya Notomi, Kengo Nozaki, Akihiko Shinya, NTT Basic Research Labs. (Japan); Shinji Matsuo, NTT Photonics Labs. (Japan); Eiichi Kuramochi, NTT Basic Research Labs. (Japan); Tomonari Sato, NTT Photonics Labs. (Japan); Hideaki Taniyama, NTT Basic Research Labs. (Japan)

Photonic-crystal nanocavities have enabled various nanophotonic devices having nonlinear optical functions, which can operate with ultralow power and be densely integrated in a tiny chip. In this talk, we will focus on optical bistable devices, especially for all-optical random-access memories (RAMs) based on nanocavities, and discuss potential impacts of this technology for future ICT.

8635-40, Session 12

Ultra-low power nonlinear optics in optical nanostructures (*Invited Paper*)

Kelley Rivoire, Hewlett-Packard Labs. (United States)

Optical nanocavities, by localizing light into sub-cubic optical wavelength volumes, can enhance nonlinear optical processes, while simultaneously shrinking the device footprint, reducing the operating power, and providing an on-chip platform. In this talk, I will describe photonic crystal cavities in III-V semiconductors as a platform for scalable and ultralow power nonlinear optical devices and discuss the potential for operation in the few-photon regime.

8635-41, Session 12

Ultra-low power all-optical switching with a single quantum dot in a photonic-crystal cavity (*Invited Paper*)

Michal Bajcsy, Arka Majumdar, Stanford Univ. (United States); Dirk Englund, Stanford Univ. (United States) and Columbia Univ. (United States); Jelena Vuckovic, Stanford Univ. (United States)

We study the dynamics of the interaction between two weak light beams mediated by a strongly coupled quantum dot-photonic crystal cavity system. We first perform all-optical switching of a weak continuous-wave signal with a pulsed control beam, and then demonstrate switching between two weak pulsed beams (40 ps pulses). In both cases, we observe an increase of the system's transmission when the signal and the control light overlap inside the cavity. This is achieved with average number of photons inside the cavity being less than one. We theoretically analyze the low-power optical nonlinearity of our experimental system and present numerical simulation results showing both the detailed temporal behavior and the time-integrated energy transmission through the cavity. Our results show that the quantum dot-nanocavity system enables fast, controllable optical switching at the single-photon level.

8635-42, Session 12

Coupling of quantum fluctuations in a two-component condensate (*Invited Paper*)

Collin M. Trail, Barry Sanders, Univ. of Calgary (Canada)

We model frozen light stored via electromagnetically induced transparency quantum-memory techniques in a Bose-Einstein condensate. The joint evolution of the condensate and the frozen light is typically modeled using coupled Gross-Pitaevskii equations for the two atomic fields, but these equations are only valid in the mean-field limit. Even when the mean-field limit holds individually for each atomic-field component, coupling between the neglected fluctuations of the two components could lead to a breakdown of the mean-field approximation even if it is a good approximation for each species individually. We solve and test the effect of coupled quantum fluctuations on coherent nonlinear evolution of the frozen light pulse to see whether this two-species condensate could enable nonlinear quantum optical phenomena.

Our analysis commences with a full second-quantized Hamiltonian for a two-component condensate. The field operators are broken up into a mean-field and a quantum fluctuation component. The quantum fluctuations are truncated to lowest non-vanishing order. The transformation diagonalizing the second-quantized approximate Hamiltonian is described by coupled differential equations that are solved with a power series expansion. We compare the consequent dynamics with the mean-field evolution given by the two-component Gross-Pitaevskii equation.

8635-43, Session 13

Semiconductor sources of photon pairs (*Invited Paper*)

Gregor Weihs, Univ. Innsbruck (Austria) and Univ. of Waterloo (Canada); Rolf Horn, Univ. of Waterloo (Canada); Payam Abolghasem, Bhavin J. Bijlani, Dongpeng Kang, Amr S. Helmy, Univ. of Toronto (Canada)

We demonstrate efficient photon pair generation for quantum communication using all-semiconductor approaches. In an AlGaAs Bragg-reflection waveguide we employ spontaneous parametric down-conversion to produce photon pairs at telecommunication wavelengths [1]. The various phase-matching solutions present in our device can be used to create time-bin or polarization entanglement. This approach can lead to a fully integrated photon pair source with the pump laser, active and passive optical devices all on a single semiconductor chip.

In our second implementation we use resonant two-photon excitation of a single InAs/GaAs quantum dot to deterministically trigger a biexciton-exciton cascade. We demonstrate Rabi oscillations, Ramsey interference and all-optical coherent control of the quantum dot resulting in single and paired photons with a high degree of indistinguishability and the potential to generate single time-bin entangled photon pairs.

Finally we explore the quantum interface between quantum dot qubits and photonic qubits originating from a pulsed spontaneous parametric down-conversion Sagnac source of polarization entangled photon pairs, which has exceptionally high fidelity, tangle and brightness.

This work was funded in part by the ERC (project EnSeNa), FWF (M-1243), PFC@JQI, CIFAR, CFI, NSERC, ERA, and OCE.

[1] R. Horn, P. Abolghasem, B. J. Bijlani, D. Kang, A. S. Helmy, and G. Weihs, A monolithic source of photon pairs, *Phys. Rev. Lett.* 108, 153605 (2012).

8635-44, Session 13

Semiconductor source of entangled photons at room temperature

Adeline Orioux, Andreas Eckstein, Univ. Paris 7-Denis Diderot (France); Aristide Lemaître, Lab. de Photonique et de Nanostructures (France); Pascal Filloux, Thomas Coudreau, Perola Milman, Univ. Paris 7-Denis Diderot (France); Arne Keller, Institut des Sciences Moléculaires d'Orsay (France); Ivan Favero, Giuseppe Leo, Sara Ducci, Univ. Paris 7-Denis Diderot (France)

In these last years, a great deal of effort has been devoted to the miniaturization of quantum information technology on semiconductor chips. In the context of photon pair sources, the bi-exciton cascade of a quantum dot has been used to demonstrate the generation of entangled states. With respect to this process, spontaneous parametric down-conversion in semiconductor waveguides allows room temperature and telecom wavelength operation, which are two key issues for applications.

We present a source consisting of a multilayer AlGaAs waveguide grown on a GaAs substrate and then chemically etched to achieve lateral confinement in a ridge. The structure design is such that a pump beam (around 775 nm), impinging on the surface of the waveguide with an incidence angle θ , generates two counterpropagating orthogonally polarized beams (around 1550 nm). The waveguide core is surrounded by distributed Bragg reflectors to enhance the pump field within the device.

We demonstrate the direct emission of polarization entangled photons by pumping the device with two symmetric angles of incidence corresponding to frequency degeneracy and performing a quantum tomography measurement. Most common entanglement witnesses are satisfied and a raw fidelity of 0.8 to a Bell state is obtained. These results open the route to the demonstration of other interesting features of our device such as the generation of hyper-entangled states via the control of the frequency correlation degree through the spatial and spectral pump beam profile. This work opens the route to a new generation of completely integrated devices for quantum information.

8635-45, Session 13

A novel method for single photon generation: Incoherent photon conversion in selectively infiltrated hollow-core photonic crystal fibers

Tim Schröder, Humboldt-Univ zu Berlin (Germany); Ping Jiang, China Univ. of Petroleum (China); Michael Barth, Humboldt-Univ. zu Berlin (Germany); Vladimir Lesnyak, Nikolai Gaponik, Alexander Eychmüller, Technische Univ. Dresden (Germany); Oliver Benson, Humboldt-Univ. zu Berlin (Germany)

We suggest a conceptually new method for the creation of single photons and present a novel experimental scheme for its implementation. The method is based on a complementary approach to single photon generation via a single photon emitter. Instead of pumping a single emitter with an ensemble of photons, the emission of a bright and stable single photon source is applied to pump an ensemble of emitters.

The scheme is applied to realize a novel, stable, non-blinking, room temperature infrared single photon source. In the particular implementation presented here, visible single photons from a defect center in diamond are converted to the near infrared. The theoretical conversion efficiency was estimated to be 26 %.

With selectively infiltrated hollow-core photonic crystal fibers equipped with colloidal quantum dots a total conversion efficiency of 0.1% could be realized in a first proof-of-principle experiment. This is still large compared to simply focusing and collecting with high-NA objectives, estimated to be at least an order of magnitude lower. Furthermore, the approach overcomes limitations of photo-stability of quantum dots by relying on an ensemble of quantum dots and addressing them individually with low light powers.

**Conference 8635: Advances in Photonics of
Quantum Computing, Memory, and Communication VI**

With improvements by two orders of magnitude, which are experimentally feasible, as well as visible photon sources approaching 10 Mcts/s, the generation rate of single photons in the infrared could be as high as several 100 kcts/s, much higher than existing true single photon sources in the infrared.

8635-46, Session 13

Waveguide superconducting single-photon autocorrelators for quantum photonic applications

Dondu Sahin, Technische Univ. Eindhoven (Netherlands); Alessandro Gaggero, Istituto di Fotonica e Nanotecnologie (Italy); Giulia Frucci, Johannes P. Sprengers, Saeedeh Jahanmirinejad, Cobra Research School (Netherlands); Francesco Mattioli, Roberto Leoni, Istituto di Fotonica e Nanotecnologie (Italy); Johannes Beetz, Matthias Lermer, Martin Kamp, Sven Höfling, Julius-Maximilians-Univ. Würzburg (Germany); Rosendo Sanjines, Ecole Polytechnique Fédérale de Lausanne (Switzerland); Andrea Fiore, Cobra Research School (Netherlands)

Quantum photonic integrated circuits including single-photon sources, linear circuits and detectors on the same chip could allow scaling quantum simulation and processing to the level of tens of qubits. Recently, we demonstrated waveguide single-photon detectors (WSPDs) based on superconducting NbN nanowires on GaAs ridge waveguides, showing 19.7% quantum efficiency 60 ps jitter and ~100 MHz count rate at 1300 nm, for TE-polarized light [1]. In this contribution we show that combining two electrically-separated nanowires on the same ridge waveguide provides an extremely compact single-photon autocorrelator, which replaces a bulky Hanbury-Brown and Twiss experiment for the measurement of the second-order correlation function $g(2)(t)$. The two wires are patterned onto a 1.85 μm -wide and 30-100 μm -long GaAs/AlGaAs ridge waveguide with the same technology previously used in our WSPDs, and connected to two separate contact pads. The response of each wire is made polarization-independent by an improved waveguide design. For each wire, we measured a device quantum efficiency of >2% at 1300 nm for a 30 μm -long waveguide, and by correlating the electrical outputs of the two wires we obtain the $g(2)(t)$ of the probe laser beam. Progress on the integration of this autocorrelator with an on-chip, quantum-dot-based single-photon source will also be reported, in view of the demonstration of a fully-integrated antibunching experiment.

References:

[1] J. P. Sprengers et. al, "Waveguide superconducting single-photon detectors for integrated quantum photonic circuits", Appl. Phys. Lett. 99, 181110 (2011)

8635-47, Session 13

Squeezing of radiation in coherent anti-stokes hyper Raman scattering

Partha S. Gupta, Indian School of Mines (India)

Squeezing of the electromagnetic field, which is a purely quantum mechanical phenomenon has attracted considerable attention owing to its low-noise property with applications in high quality telecommunication. This quantum effect is expected to manifest itself in optical processes in which the nonlinear response of the system to the radiation field plays an important role. Squeezing has been either experimentally observed or theoretically predicted in a variety of nonlinear optical processes such as harmonic generation, multi-wave mixing processes, Raman, hyper-Raman etc. Later the notion of amplitude squeezing of quantized electromagnetic field have been introduced in various nonlinear optical processes. The effect of squeezing of radiation in coherent anti-stokes hyper Raman scattering (CAHRS) is investigated under the short-time scale based on a fully quantum mechanical approach. In an idealized model CAHRS, the interaction is looked upon as a process involving absorption of two pump photons and emission of stokes photon, which is followed by absorption of two more pump photons and subsequent emission of an anti-Stokes photon at different frequency. The coupled Heisenberg equations of motion involving real and imaginary parts of the quadrature operators are established and solved under short-time scale. The occurrence of amplitude squeezing effects in both the quadrature of the radiation field in the fundamental mode is investigated using required conditions of squeezing. The results obtained may pave way to obtain desired degree of squeezing through different higher-order nonlinear optical processes.

8636-1, Session 1

Slow light in SNAP coupled microresonators *(Invited Paper)*

Misha Sumetsky, OFS Labs. (United States)

Attenuation of light primarily caused by surface roughness and also insufficient fabrication precision became a major bottleneck for applications of the lithographically fabricated chains of coupled microresonators for slowing and manipulating of light. Recently we have developed a new photonic fabrication platform, Surface Nanoscale Axial Photonics (SNAP) which enables fabrication of super-low loss miniature photonic circuits with angstrom precision, i.e., at least an order of magnitude better than the precision achieved in the photonic fabrication technologies developed so far. In this presentation we demonstrate long chains of coupled SNAP microresonators, exhibiting sub-angstrom uniformity, investigate their transmission spectrum and group delay characteristics both experimentally and theoretically.

8636-2, Session 1

EIT analogs using orthogonally polarized modes of a single whispering-gallery microresonator *(Invited Paper)*

Albert T. Rosenberger, Oklahoma State Univ. (United States)

The throughput of a single fiber-coupled whispering-gallery microresonator, such as a fused-silica microsphere, can exhibit behavior analogous to electromagnetically induced transparency and absorption (EIT, EIA). These effects enable slow and fast light, respectively, in the form of pulse delay or advancement. Two different methods can be used to realize this behavior; in both methods, the key feature is the use of two co-resonant orthogonally polarized whispering-gallery modes of very different quality factor (Q). The first method relies on intracavity cross-polarization coupling when only the lower-Q mode is driven, and the second on a simple superposition of orthogonal throughputs (in the absence of intracavity coupling) when the two modes are simultaneously driven. We refer to the behavior observed using the first method as coupled-mode induced transparency and absorption (CMIT, CMIA), and the behavior of the second method as co-resonant polarization induced transparency and absorption (CPIT, CPIA). In both cases, polarization-sensitive detection of the throughput is used, and the EIT/EIA analog features are observed on the same polarization component as that of the linearly polarized input. For both methods, a combination of temperature and strain tuning can be used to achieve many different instances of co-resonance between a TE (transverse electric) mode and a TM (transverse magnetic) mode of the microresonator, from which a case with very different Q values can be chosen. For the second method, for example, this choice, with both modes strongly overcoupled, results in CPIT with a pulse delay approximately equal to the pulse width.

8636-3, Session 1

Targeted design of low-loss CROW waveguides for slow light applications *(Invited Paper)*

Michelle L. Povinelli, The Univ. of Southern California (United States)

No Abstract Available

8636-4, Session 1

Compact coupled resonators for slow-light sensor applications *(Invited Paper)*

Michel J. F. Digonnet, Stanford Univ. (United States)

No Abstract Available

8636-5, Session 1

Resonant multimode photonic structures on-chip *(Invited Paper)*

Michal F. Lipson, Cornell Univ. (United States)

No Abstract Available

8636-6, Session 2

Slow light and optically detected ultrasound *(Invited Paper)*

Philip R. Hemmer, Texas A&M Univ. (United States)

Recently, slow light has found use as a high-performance filter for optically-detected ultrasound imaging. Specifically a combination of spectral hole burning and slow light in a crystal of praseodymium doped yttrium silicate was shown to enable optical detection of ultrasound from deep inside highly scattering tissue phantoms. In this talk I will discuss the advantages of using slow light for optical ultrasound detection compared to other optical filtering techniques, especially others involving time-delay. I will also discuss future prospects for optical imaging deep inside real tissues using slow light.

8636-7, Session 2

Slow light through tightly-coupled light waves and acoustic waves in nanoscale waveguides *(Invited Paper)*

Zheng Wang, The Univ. of Texas at Austin (United States); Wenjun Qiu, Massachusetts Institute of Technology (United States); Peter Rakich, Yale Univ. (United States); Heedeuk Shin, Sandia National Labs. (United States); Hui Dong, The Univ. of Texas at Austin (United States)

Intense sound-light interaction in nanoscale optical waveguides allows for efficient and coherent photon-phonon conversion, leading to a reduction in the propagation of coherent information storage by 5 orders of magnitude reduction. We will discuss the general framework to calculate Stimulated Brillouin Scattering (SBS) gain via the overlap integral between optical and elastic eigen-mode. By applying this method to a silicon rectangular waveguide, we demonstrate how the optical force distribution and elastic modal profiles jointly determine the magnitude and scaling of SBS gains in both forward and backward SBS processes. Given the wide range of elastic phonon modes available in silicon waveguides, we demonstrate that the coupling between distinct optical modes can excite elastic modes with all possible symmetries.

8636-8, Session 2

Slow light in dye-doped chiral liquid crystals
(Invited Paper)

Stefania Residori, Institut Non Linéaire de Nice Sophia Antipolis (France); Dong Wei, Institut Non Linéaire de Nice Sophia Antipolis (France) and Xiamen Univ. (China); Umberto Bortolozzo, Institut Non Linéaire de Nice Sophia Antipolis (France); Jean-Pierre Huignard, Jphopto (France)

Applications in precision interferometry (see, e.g., [1,2]) have been driving interests in slowing down the group velocities of light pulses. An efficient scheme to obtain slow light and even stopped light is to use beam coupling in a nonlinear optical medium. Different mechanisms have been proposed, for example, four wave mixing in hot atomic rubidium vapors [3], beam coupling using Brillouin scattering in optical fibers [4], two-wave mixing in photorefractive crystals [5] and in liquid crystals [6]. Here, we demonstrate slow light and stopped light in chiral dye doped liquid crystals. We employ a medium that combines a nematic liquid crystal with methyl-red and chiral agents [7]. When a circularly polarized pump and a pulse beam interact in the cell, the output pulse is delayed and by switching on/off the pump beam we observed stopped light with a storage time of the order of eight times the response time of the medium. In this case the slow light effect is given by photo-isomerization of the dye molecules, which induces an absorption strongly dependent on the frequency detuning between the pump and signal beam.

- [1] Z. Shi and R.W. Boyd, Phys. Rev. Lett. 99, 240801 (2007).
- [2] M.S. Shahriar, G.S. Pati, R. Tripathi, V. Gopal, & M. Messall, Phys. Rev. A 75 053807 (2007).
- [3] R. M. Camacho, P. K. Vudiyasetu, and J. C. Howell, Nature Photonics 3, 103 (2009).
- [4] L. Thevenaz, Nature Photonics 2, 474 (2008).
- [5] E. Podivilov, B. Sturman, A. Shumelyuk, and S. Odoulov, Phys. Rev. Lett. 91, 083902 (2003).
- [6] S. Residori, U. Bortolozzo, and J. P. Huignard, Phys. Rev. Lett. 100, 203603 (2008).
- [7] D. Wei, A. Iljin, Z. Cai, S. Residori, and U. Bortolozzo, Opt. Lett. 37, 734 (2012).

8636-9, Session 2

Observation of slowed light and darkness through a ruby window

Emma Wisniewski-Barker, Graham Gibson, Sonja Franke-Arnold, Univ. of Glasgow (United Kingdom); Robert W. Boyd, Univ. of Rochester (United States); Miles J. Padgett, Univ. of Glasgow (United Kingdom)

The speed of light can be slowed dramatically by various non-linear or resonant processes. One simple process for slowing light is self-pumped coherent population oscillations, in which the propagating pulse itself drives a non-linear absorption within ruby or similar materials, giving a group index on the order of a million, causing propagation velocities of hundreds of meters per second. We explored the interesting effects that self-pumped, slow light and the consequent increased transmission time lead to in an interferometer. In addition to increasing the transmission time, the slowing of the light within the material also results in massive photon drag, such that a spinning of the medium rotates the transmitted image. We introduce a glass coverslip halfway into the beam to create a phase discontinuity in the center of the beam. The phase discontinuity shows that, despite the effect being driven by the pulse, the dark intensity zeros within the image are also shifted. This effect cannot be explained by invoking only absorption, a time-dependent reshaping of

the light pulse, and bleaching. We conclude that, just as it is possible to slow high-intensity light, it is possible to slow darkness within the surrounding optical field. These experiments demonstrate the principle of optical storage and suggest interesting applications in optical memory, optical processing, and interferometry.

8636-10, Session 2

Progress towards the demonstration of a superluminal DPAL ring laser

Joshua Yablon, Shih Tseng, Selim M. Shahriar, Northwestern Univ. (United States)

No Abstract Available.

8636-11, Session 2

Slow light for integrated photonics (Invited Paper)

Jesper Mørk, Sara Ek, Yaohui Chen, Mikkel Heuck, Kresten Yvind, Technical Univ. of Denmark (Denmark)

No Abstract Available.

8636-12, Session 3

Tunable lossless slow and fast light in a four-level N-system (Invited Paper)

Irina Novikova, Eugeny E. Mikhailov, The College of William & Mary (United States); Logan Stagg, The Univ. of North Carolina at Asheville (United States); Simon Rochester, Rochester Scientific, LLC (United States); Dmitry Budker, Univ. of California, Berkeley (United States)

We investigate the propagation of a weak probe laser field in a medium of warm Rb atoms, controlled with two strong resonant pump fields tuned to the D1 and D2 optical transitions to form an N-scheme arrangement. We have shown theoretically that four-wave mixing has a profound effect on the probe-field group velocity and absorption, allowing the probe-field propagation to be continuously tuned from superluminal to slow-light regimes with amplification. We have also identified the experimental conditions for observation of such tunable slow-to-fast light regime (continuously through the point of zero group index) with positive probe-field gain, and demonstrated that the spectral range corresponding to the zero group index can be tuned by controlling the power of one of the pump laser.

8636-13, Session 3

A comprehensive study of light shift in optical Ramsey interference for estimating the performance of a rubidium vapor cell atomic clock (Invited Paper)

Gour S. Pati, Zachary Warren, Delaware State Univ. (United States); Selim M. Shahriar, Northwestern Univ. (United States)

Precision navigation and timing requirements are important factors continuously driving the advancements in vapor cell clock technologies towards higher accuracy and frequency stability. Pulsed coherent population trapping and Raman-Ramsey interference in alkali vapor constitute a practically competitive scheme for developing such a technology. Here, we will present results to demonstrate the efficacy

of pulsed operation for significantly reducing the light shift in a Raman-Ramsey rubidium clock (RR-RC). We will also discuss our recent efforts to develop a comprehensive theoretical model to calculate the light shift in a multi-level atomic system formed in D1 line excitations in 87Rb atoms. Furthermore, we will present experimental results from our investigations of a prototype RR-RC, and its metrological performance to get an estimate of the long-term frequency stability.

8636-14, Session 3

Integration of nanophotonic devices with alkali vapors for on chip manipulations of light propagation (*Invited Paper*)

Uriel Levy, The Hebrew Univ. of Jerusalem (Israel)

No Abstract Available.

8636-15, Session 3

Dispersion enhancement in atom-cavity and coupled cavity systems (*Invited Paper*)

David D. Smith, NASA Marshall Space Flight Ctr. (United States); Krishna Myneni, U.S. Army Research, Development and Engineering Command (United States); Hongrok Chang, The Univ. of Alabama in Huntsville (United States)

No Abstract Available.

8636-16, Session 4

Ultranarrow transmission resonances, slow and backward light in room-temperature 4He^* (*Invited Paper*)

Rupamanjari Ghosh, Jawaharlal Nehru Univ. (India)

No Abstract Available.

8636-17, Session 4

Fast light and quantum correlations in atomic vapor (*Invited Paper*)

Ulrich Vogl, Ryan T. Glasser, Paul D. Lett, National Institute of Standards and Technology (United States)

We recently demonstrated optical pulses with large negative group velocities using a scheme based on four-wave-mixing in rubidium vapor. Both the probe and the generated conjugate pulses can experience anomalous dispersion, and we have demonstrated a maximum group advancement of 64% relative to the input pulse width. The four-wave-mixing scheme allows us to send whole images through a fast light medium, and we have analyzed the arrival of spatially-encoded information in the system. We are currently investigating the transport of quantum correlations that are shared by the probe and conjugate modes when sent through fast light media.

8636-18, Session 4

Title to be determined

Uriel Levy, The Hebrew Univ. of Jerusalem (Israel)

No Abstract Available.

8636-19, Session 4

Atomic-vapor photonic microcells (*Invited Paper*)

Fetah Benabid, Univ. of Bath (United Kingdom)

No Abstract Available.

8636-20, Session 4

Versatile all-fiber slow-light assisted sensor (*Invited Paper*)

Mikel Bravo Acha, Univ. Pública de Navarra (Spain); Xabier Angulo-Vinuesa, Sonia Martin-López, Consejo Superior de Investigaciones Científicas (Spain) and Univ. de Alcalá (Spain); Manuel Lopez-Amo, Univ. Pública de Navarra (Spain); Miguel González-Herráez, Univ. de Alcalá (Spain)

We present theoretical and experimental results on a slow-light assisted all-fiber configuration that can be used for efficient sensing of a variety of parameters (pressure, displacement, ...). The sensor is based on a lossy ring resonator tuned close to the critical coupling regime. We show that the sensitivity can be strongly enhanced in this working regime. Sensitivity enhancements are theoretically and experimentally demonstrated.

8636-21, Session 4

Light trapping with THz field in a photonic crystals

Igor V. Melnikov, National Research Univ. of Information Technologies, Mechanics and Optics (Russian Federation)

No Abstract Available.

8636-22, Session 5

The solid-state ring laser gyro: current and future trends (*Invited Paper*)

Sylvain Schwartz, Thales Research & Technology (France); Thomas Lauprêtre, Fabienne Goldfarb, Fabien Bretenaker, Lab. Aimé Cotton, Univ Paris-Sud 11, CNRS (France); Rupamanjari Ghosh, Jawaharlal Nehru Univ. (India); Iacopo Carusotto, Univ. degli Studi di Trento (Italy)

We will report our latest achievements towards a high performance solid-state ring laser gyro using a diode-pumped Nd-YAG crystal as the gain medium. We will then discuss the possibility of using a similar device to test the proposal by Shariar and coworkers to increase gyro performance with fast light. This discussion will be supported in particular by the recent results obtained at Laboratoire Aimé Cotton with electromagnetically induced transparency in metastable helium.

8636-23, Session 5

Brillouin fast-light fiber laser super-sensor
(Invited Paper)

Jacob Scheuer, Omer Kotlicki, Tel Aviv Univ. (Israel); Selim M. Shahriar, Northwestern Univ. (United States)

We present a comprehensive study of the properties of a superluminal fiber laser based super-sensor employing Brillouin gain. Exact analytical expressions for the required parameters and the sensitivity enhancement are derived. The dependence of the sensitivity enhancement on the measured phase shift is found to be highly nonlinear, rapidly increasing at smaller quanta. The minimal detectable shift due to shot noise is found to be smaller by 8 orders of magnitude compared to conventional laser sensors. The tradeoffs between the attainable sensitivity enhancement, the cavity dimensions and the impact of the cavity roundtrip loss are studied in detail providing a set of design rules for the optimization of the super-sensor.

8636-24, Session 5

Slow light, fast light, and their applications
(Tutorial Presentation)

Robert W. Boyd, Univ. of Ottawa (Canada)

For the past decade or more, the optical physics community has been intrigued by the related phenomena of slow and fast light [1]. These names refer to situations in which the group velocity of light (roughly, the velocity at which light pulses propagate through a material system) is very much different from the vacuum speed of light c . Several of the early stunning demonstrations of slow and fast light made use of cryogenic systems or atomic media. More recently, it has been realized that extreme values of the group velocity can also be realized in room-temperature solid-state materials, which tend to be far more suited for practical applications. In this presentation, we first review some of the physical mechanisms that can be used to induce slow- and fast-light effects in room temperature solids [2-5] and describe the variety of propagation effects that can thereby be observed [1, 3, 6]. We then turn to a discussion of various applications that can be enabled by use of slow light effects. These examples include buffering and regeneration for telecommunication [7], the development of tunable delay lines for the steering of light beams in laser radars [8], the development of spectrometers with enhanced spectral resolution [9,10], and the use of slow light for optical memories [11,12].

8636-25, Session 5

Two-ring Mach-Zehnder interferometer for biochemical sensing
(Invited Paper)

Yundong Zhang, Jing Zhang, Qinghai Song, Jingfang Wang, Ping Yuan, Harbin Institute of Technology (China)

Photonic microresonators have a great potential in the highly sensitive sensors due to ultrahigh quality factor and microscale mode volumes. Vollmer et al proposed that whispering-gallery-mode (WGM) microresonators have been a powerful method to achieve label-free detection for ultrasensitive biochemical sensors. New label-free optical techniques have been developed to realize portable, inexpensive and high resolution devices to detect biomolecules with very low concentrations. Generally, the refractive index (RI) could be affected by biochemical molecules to the resonators surface or by the surrounding medium that serves as waveguide cladding. Small changes in the refractive index could be detected by monitoring the resonant wavelength shift. This method generally needs a large dynamic spectrum range for the sensor. However, the spectral resolution is usually lower in low concentration detection than that in high concentration detection. As an alternative, the RI detection also can be made by measuring the output

intensity changes at a fixed wavelength. The latter method has higher sensitivity for detecting very small changes by virtue of the large slope sensitivity of the spectrum. In this letter, we investigate a two-ring Mach-Zehnder interferometer (2RMZI) device. It exhibits a sharp asymmetric Fano line shape, in which slope between zero and unity transmission is greatly enhanced compared with conventional symmetric line shape. The device allows for measuring a refractive index change down to 10^{-9} refractive index units (RIU) by adjusting its structural parameters. Additionally, it shows better performance than that in a single ring Mach-Zehnder interferometer (1RMZI) device, which measures a RI change to 10^{-6} (RIU). As a result, the two-ring Mach-Zehnder interferometer device is one of the most promising devices for biochemical sensor.

8636-26, Session 5

Fast-light enhanced integrated on-chip laser gyroscope for rotation sensing

Sisheng Deng, Zhisong Xiao, Hao Zhang, Long Zhao, Anping Huang, Beihang Univ. (China)

We propose a configuration consisting of several passive ring resonators named as fast-light enhanced ring resonator composed by silicon waveguide, coupled to an active ring laser for introducing anomalous dispersion. And a straight waveguide is coupled to the last resonator used as the output port.

Theoretical analysis indicates that the introduced anomalous dispersion, or the so-called fast-light effect allows the frequency shift to be improved as large as one order of magnitude due to Sagnac effect when the structure is rotated, compared to a standard ring-laser gyroscope (RLG) with the same size, namely having the same rotational sensitivity compared to a standard ring-laser gyroscope with tenfold size as that of the proposed structure, since the Sagnac frequency shift is proportional to the optical path of the system. This can be valuable for reducing device size and consumption.

In this paper, the enhanced sensitivity is calculated with respect to rotation rate, it comes out to be that sensitivity gets relatively higher enhanced under lower rotation rate. Moreover the impact of passive ring resonator number is also discussed and deduced, which manifests that only odd number of passive rings will produce effective anomalous dispersion, thus improve the rotational sensitivity.

The configuration proposed here will have broad prospect in realizing highly integrated on-chip laser gyroscope for rotation sensing.

8636-27, Session 6

Slow and stopped-light lasing in active nanoplasmonic metamaterials
(Invited Paper)

Ortwin Hess, Imperial College London (United Kingdom)

No Abstract Available.

8636-28, Session 6

Slow light, plasmonics, and metamaterials: how do they relate?
(Invited Paper)

Jacob B. Khurgin, Johns Hopkins Univ. (United States)

Slow light, plasmonics and metamaterials are all areas of interest in optics in which significant progress has been made in the last decade. In this talk a connection between the fields is made and it is shown that many of the salient features of electromagnetic field propagation in structured metal-dielectric systems, such as large energy concentration, enhanced nonlinearity and modified effective index can be explained as slow light phenomena. Comparison is made between slow light in plasmonic structures and other methods of obtaining slow light in pure dielectric media. It is shown that the differences between the slow light in various

media are mostly related to the different forms in which the energy gets stored in them. Finally, figures of merits for practical use of various slow light media, including plasmonic and metamaterials, are derived and analyzed.

8636-29, Session 6

Dispersion tailored slow metamaterials for enhanced emission and nonlinearity (*Invited Paper*)

Meir Orenstein, Technion-Israel Institute of Technology (Israel)

No Abstract Available.

8636-30, Session 6

Reciprocal and non-reciprocal slow light propagation using metamaterials (*Invited Paper*)

Gennady B. Shvets, Chihhui Wu, Alexander Khanikaev, The Univ. of Texas at Austin (United States)

The ability to slow down light to extremely slow group velocities v_g compared with the vacuum light speed c while maintaining high coupling efficiency is one of the most dramatic manifestations of controlled light manipulation in optics. Apart from its fundamental significance, it has long-reaching technological applications, including enhanced nonlinear effects due to the energy density compression by as much as $c=v_g$; pulse delay and storage for optical information processing [3]; optical switching, and even quantum optics. Most approaches to obtaining slow light rely on the phenomenon of Electromagnetically Induced Transparency (EIT) [4]. EIT and its analogs have been demonstrated in several media, including cold and warm gases.

More recently, there is a growing interest in light slowing using electromagnetic metamaterials which enable engineering electromagnetic resonances with almost arbitrary frequencies and with resonance symmetries. For example, the EIT phenomenon has been emulated in metamaterials possessing two types of resonances: a “dark” one which is not directly coupled to the incident electromagnetic field, and a “bright” one which is strongly coupled to the incident field. If the frequencies of these resonances are very close to each other, then they can become strongly coupled by a slight break of the metamaterial’s symmetry. From a practical standpoint, achieving an exact equality between frequencies of the dark and bright resonances may be difficult. Therefore, it is desirable to find alternative approaches to producing slow light.

In this talk we describe a new technique to producing slow light which relies on the newly-discovered phenomenon of double-Fano resonance. We demonstrate that light propagation through a birefringent medium can be dramatically slowed down when the medium supports three electromagnetic modes: (a) two propagating modes of different polarizations strongly which are both strongly coupled to the incident electromagnetic field, and (b) a “dark” (non-propagating) electromagnetic wave which is decoupled from the incident electromagnetic field. If the frequency of the “dark” mode coincides with that of the propagating modes, then a simple symmetry breaking coupling all three modes with each other results in a dramatic slowing down of light. This phenomenon can be understood as a double Fano resonance: coupling of a single discrete state (“dark” mode) to the two sets of continuum states (two propagating modes of different polarization states).

A specific implementation of such slow-light structures using metallic antennas will be described. We utilize the phenomenon of double-Fano resonance to generate photonic propagation band that are spectrally broad, yet contain embedded narrow-band slow-light segments. Various applications will be outlined, and the possibility of obtaining “one-way” slow light using ferrites or nonlinear materials will be discussed.

8636-31, Session 7

Rapidly reconfigurable atomic photonic crystal (*Invited Paper*)

John C. Howell, Univ. of Rochester (United States)

No Abstract Available.

8636-32, Session 7

CMOS-process-compatible photonic crystal slow light devices (*Invited Paper*)

Toshihiko Baba, Yokohama National Univ. (Japan)

Photonic crystal waveguides with some optimum design generate dispersion-engineered wideband slow light, which is suitable for short optical pulses and high speed signals to slow down. A recent important progress is that complex waveguide structures can be fabricated by CMOS-compatible process. Once they are listed on recipe of the process, we can integrate slow light with other functions of standard Si photonics devices on a chip. Slow light is applicable to delay tuning and enhancement of light-waveguide interaction. The former allows MUX/DMUX and retiming of short pulses, flexible coherent receivers, and fast optical correlators, and the latter, compact modulators and nonlinear devices. The thermal tuning of the device achieves a tunable delay of nearly 100 ps tuning range as well as more than 100 resolution points. A symbol-rate-variable DQPSK receiver at 14 - 18 Gbps and a correlator with 1 kHz repetition have been demonstrated with the tunable slow light. The slow-light-based MZI modulator at 10 Gbps is downsized up to 50 microns. Nonlinearities such as TPA and FWM are easily observed in several hundred micron devices. The TPA-induced carriers are applicable to nonlinear photodiodes suitable for correlators, ultrafast delay tuning free from the carrier lifetime and retiming of disordered optical pulse train. All of these devices are demonstrated with a reasonable fiber-to-fiber insertion loss thanks to the Si photonics technology.

8636-33, Session 7

Electrically-controlled photonic crystal slow light device and its application to optical correlator

Norihiro Ishikura, Ryo Hayakawa, Ryo Hosoi, Mizuki Shinkawa, Hong C. Nguyen, Naoya Yazawa, Toshihiko Baba, Yokohama National Univ. (Japan)

Lattice-shifted photonic crystal waveguides (LSPCWs) are effective for generating wide-band on-chip slow light at room temperature. In this study, we integrated the LSPCW with multi-heaters using CMOS-compatible process, and demonstrated electrically-tunable slow light. Seven heaters were placed on each side of the LSPCW with air slots for thermal isolation. On-demand temperature distributions were formed by controlling each heating power independently. When the heating powers were optimized, a clear delay peak of slow light corresponding to the flat photonic band of the LSPCW was observed, which suggests that fabrication errors in the air-hole diameters were less than 5 nm and related band fluctuation was well compensated by the heating. When a linear temperature distribution was added to this condition, the delay was reduced up to 54 ps. When a quadratic distribution was added, the group delay dispersion was generated in the range from -10.2 to 17.5 ps/nm. We applied the tunable delay to the delay scanning in optical correlator. Here, output pulse were compressed to 0.6 ps through self-phase modulation and dispersion compensation in external fibers, and its delay was tuned in range of 17 ps. At a scanning frequency of 100 Hz, which is >10 times faster than that of conventional mechanical delay scanners, pulse lengths of 0.3 - 6 ps were measured with a >95% accuracy. We are also fabricating all on-chip optical correlator consisting of this slow light delay scanner and two-photon-absorption photo-diodes.

8636-34, Session 7

Narrow band phase sensitive amplifiers and optical comb generators based on slow light propagation in fibers and photonic crystal waveguides (*Invited Paper*)

Gadi Eisenstein, Technion-Israel Institute of Technology (Israel)

No Abstract Available.

8636-35, Session 7

Nonlinear-induced ultrafast slow-light tuning in photonic crystal waveguide

Keisuke Kondo, Mizuki Shinkawa, Yohei Hamachi, Yuji Saito, Yoshiaki Arita, Toshihiko Baba, Yokohama National Univ. (Japan)

We have developed lattice-shifted photonic crystal slow light waveguide (LSPCW) fabricated by using Si CMOS process, and demonstrated the thermally-induced delay tuning and enhanced nonlinear effects with short optical pulses. This presentation shows the ultrafast delay tuning using the nonlinear effects. The LSPCW with the index chirping generates two types of slow light; one is dispersion-compensated (DC) slow light and the other is low-dispersion (LD) slow light. The former arises from the shift of a flat photonic band in the chirped structure, and its delay changes with the chirp profile. The latter arise from the straight photonic band with a small slope, which spatially compresses optical pulses and enhances nonlinear effects. The nonlinearity of the LD slow-light pulse (control pulse) can modify the chirp profile and changes the delay of DC slow-light pulse (signal pulse). In the nonlinear process, the two photon absorption occurs first, leading to the carrier plasma effect. It reduces the index and blue-shifts the pulse wavelength through the dynamic tuning and cross-phase modulation when the control pulse overlaps with the signal pulse. Consequently, the delay of the signal pulse is reduced by up to 10 ps. Since such delay tuning becomes remarkable only when two slow-light pulses overlap in the waveguide, the switching time of the delay is not limited by the carrier decay but the overlap duration shorter than 10 ps. Based on this mechanism, we succeeded in tuning the delay of one target pulse in a pulse train with a 12 ps interval.

8636-36, Session 8

Quantum state tomography of slow and stored light (*Invited Paper*)

Andrew M. Dawes, Noah Holte, Hunter Dasonville, Pacific Univ. (United States)

Quantum information can be transferred from a beam of light to a cloud of atoms and controllably released at a later time. This process forms the basis of many important quantum memory devices that are fundamental to the future of quantum information science, quantum computing, and quantum communication. Prior experiments have stored light in a variety of systems, including cold atom clouds, warm atomic vapor, solid state materials, and optical fibers. To extend these successful investigations, the goal of our research program is to carry out a full characterization of the quantum states of stored-and-retrieved multimode light.

We apply techniques developed for quantum state reconstruction to experimental stored-light systems. The result will be a more complete understanding of the quantum state of light before and after storage. Prior detection schemes cannot distinguish between losses in the retrieval process and losses in the detection process. In particular, single-mode detection suffers from losses if the spatial mode chosen by the detector differs from the spatial mode carrying the retrieved light. Array detectors measure all spatial modes simultaneously. This capability will be used to maximize the number of retrieved photons and allows for computation and optimization of the retrieved spatial mode. Array

detection therefore recovers more information on the quantum state of light than previous methods. Array detection is also used to compare multiple retrieved modes, and to explore correlations between modes. The importance of this new information is that it reveals fundamental properties of the quantum memory process.

8636-37, Session 8

EIT-based optical memory in NV-diamond (*Invited Paper*)

Victor Acosta, Hewlett-Packard Labs. (United States)

No Abstract Available.

8636-38, Session 8

Towards scalable photonics via quantum storage (*Invited Paper*)

Joshua Nunn, Univ. of Oxford (United Kingdom); Nathan K. Langford, Royal Holloway Univ. (United Kingdom); Tessa F. M. Champion, Michael R. Sprague, Patrick S. Michelberger, Ka Chung Lee, Univ. of Oxford (United Kingdom); XianMin Jin, Shanghai Jiao Tong Univ. (China); Duncan G. England, William S. Kolthammer, Marco Barbieri, Ian A. Walmsley, Univ. of Oxford (United Kingdom)

Single photons are a vital resource for optical quantum information processing. Efficient and deterministic single photon sources do not yet exist, however. To date, experimental demonstrations of quantum processing primitives have been implemented using non-deterministic sources combined with heralding and/or postselection. Unfortunately, even for eight photons, the data rates are already so low as to make most experiments impracticable. It is well known that quantum memories, capable of storing photons until they are needed, are a potential solution to this 'scaling catastrophe'. Here, we analyze in detail the benefits of quantum memories for producing multiphoton states, showing how the production rates can be enhanced by many orders of magnitude. We identify the quantity ηB as the most important figure of merit in this connection, where η and B are the efficiency and time-bandwidth product of the memories, respectively. We go on to review our progress in implementing the most broadband memory to date, with $B > 1000$, in room-temperature cesium vapour. We consider the noise properties for single photon storage and the integration of the memory using waveguides.

8636-39, Session 8

Optical nanofibers for quantum photonic circuit (*Invited Paper*)

Kohzo Hakuta, The Univ. of Electro-Communications (Japan)

No Abstract Available.

8636-40, Session 8

Single-photon optical precursor (*Invited Paper*)

Shengwang Du, Hong Kong Univ. of Science and Technology (Hong Kong, China)

Wave-particle duality provides a complementary nonclassical picture for describing a single photon, the quanta of light. However, the propagation of a single photon through a slow or fast light medium has been studied only in a very few limited experiments due to the difficulty in generating single photons with controllable waveforms. The optical precursor refers

to the propagation of the front of a step optical pulse, which always travels at c , the speed of light in vacuum, in any dispersive medium. This wave property, was first predicted by Sommerfeld and Brillouin in 1914 basing on classical electromagnetic wave propagation, and is of great interests because it is linked to Einstein's causality. Here, we report the direct observation of optical precursors of heralded single photons with step- and square-modulated wave packets passing through cold atoms, whose optical property can be varied from slow light to fast light. Using electromagnetically induced transparency and the slow-light effect, we separate the single-photon precursor from the delayed main wave packet. The front of the single-photon precursor, which travels at c , is the fastest part of the entire photon wave packet, even in a superluminal medium. The speed of a single photon does not follow the group velocity. Our results show that there is no probability for a single photon moving faster than c , and the causality holds for a single photon in any dispersive medium. Our observation is important to the understanding of the transmission speed limit of quantum information.

8636-41, Session 8

Measurement of the velocity of a quantum object: a role of group velocity

Yuri Rostovtsev, Univ. of North Texas (United States)

We have analyzed the process of measurement of velocity of a quantum object taking into account the spread of the position due to its wavefunction. By considering wavepacket dynamics during the process of measurement, we show that the measured velocity can be higher than the speed of light in vacuum. We demonstrate that possible errors of measurement of velocity of the quantum object depends on the distance.

8636-42, Session 8

Slow and fast light propagation of quantum optical fields under the conditions of multi-photon resonances in a coherent atomic vapor

Irina Novikova, The College of William and Mary (United States); Gleb Romanov, Travis Horrom, Eugeny E. Mikhailov, The College of William & Mary (United States)

We investigate weak optical probe pulse propagation in a resonant Λ and N -interaction schemes, and investigate the role of the four-wave mixing on classical and quantum properties of the probe field. In particular, we focus our attention on two configurations. In the first case we take into account the off-resonant coupling of the strong field to the signal field ground state. Such configuration is relevant for EIT-based slow light and quantum memory. In the second configuration the additional control field is derived from an independent laser, and it is tuned to a different optical resonance from the ones forming an original Λ system. Such interaction scheme allows realization of tunable slow and fast light, and was considered with regards to enhancement of optical gyroscopes performance.

We demonstrate that in both cases the four-wave mixing (FWM) has a profound effect on signal field group velocity and absorption profile, and may even lead to gain. We present both semi-classical and fully quantum treatments for propagation of both signal and newly generated Stokes fields that include accurate description of their quantum noise. In particular, we analyze the case of a quadrature-squeezed signal field, and demonstrate that vacuum fluctuations of the Stokes field couple into the signal field through the FWM process and degrades the squeezing. The severity of this degradation grows with optical depths of an atomic medium, setting an additional practical limits for the experiments.

8636-43, Session 9

Distortion in a linear slow light system (Tutorial Presentation) (Invited Paper)

Luc Thevenaz, Ecole Polytechnique Fédérale de Lausanne (Switzerland)

No Abstract Available.

8636-44, Session 9

Slow light in lossy and amplifying periodic media (Invited Paper)

N. Asger Mortensen, Technical Univ. of Denmark (Denmark)

No Abstract Available.

8636-45, Session 9

Group velocity dispersion engineering (Invited Paper)

Daniel Gauthier, Yunhui Zhu, Joel Greenberg, Nor A. Husein, Duke Univ. (United States)

We investigate the creation of a strongly dispersive material with large chirp and small group delay via SBS in a highly-nonlinear fiber. This is in contrast to previous SBS experiments, which have typically focused on the creation of a slow light material with minimal dispersion and chirp. We are able to obtain giant tunable dispersion up to ± 100 ns². We study experimentally and theoretically this system and characterize its performance. The results demonstrate the possibility of opening up Fourier pulse shaping techniques in the ns region.

8636-46, Session 9

Deterministic crisis at the origin of extreme events (Invited Paper)

Jorge R. Tredicce, Univ. de la Nouvelle-Calédonie (New Caledonia); Jose Rios Leite, Univ. Federal de Pernambuco (Brazil); Cristina Masoller, Jordi Zamora-Munt, Univ. Politècnica de Catalunya (Spain); Stephane Barland, Institut Non Linéaire de Nice Sophia Antipolis (France); Bruno Garbin, Univ. de Nice Sophia Antipolis (France); Massimo Giudici, Institut Non Linéaire de Nice Sophia Antipolis (France)

Devastating extreme events occur in many natural systems, and a lot of work has focused on predicting and understanding their origin. In laser systems, extreme events occur as ultrahigh intensity pulses capable of producing catastrophic optical damage. We have recently shown that optically injected semiconductor lasers display two deterministic chaotic regimes: one in which extreme intensity pulses, considered rogue waves, are frequent, and one in which they are almost inexistent. Here we show that an external crisis can generate these extreme events, and that they have some degree of predictability. In addition, we show that that noise strongly affects their probability of occurrence. Our results have a significant impact as they contribute to a better understanding of the mechanisms capable of triggering and controlling optical rogue waves. This can improve the reliability and reduce the degradation of optically injected lasers, and will also enable new experiments to test if these mechanisms are also involved in other natural systems where rogue waves have been observed.

8636-47, Session 9

Information theory for the design and analysis of slow light systems (*Invited Paper*)

Mark A. Neifeld, The Univ. of Arizona (United States)

This presentation will review recent results concerning the application of an information theoretic formalism to optical systems for slow and fast light. Theoretical results that bound the information capacity of linear slow light systems will be presented. The formalism will also be applied to an experimental system which employs Brillouin gain to realize broadband all-optical delay.

8636-48, Session 10

Enhanced sensing in a double-Raman superluminal active ring laser (*Invited Paper*)

Tony Abi-Salloum, Widener Univ. (United States)

No Abstract Available.

8636-49, Session 10

Detecting Coriolis force via slow light (*Invited Paper*)

Yuri Rostovtsev, Sankar Davuluri, Univ. of North Texas (United States)

We have suggested a technique of measuring Coriolis force based on enhanced dragging of the light by slow light media. Possible applications and experiments are discussed.

8636-50, Session 10

Superluminal enhancement in a SOA ring laser cavity (*Invited Paper*)

Sean M. Spillane, Los Gatos Research, Inc. (United States); Selim M. Shahriar, Northwestern Univ. (United States)

No Abstract Available.

8636-51, Session 11

Wide band optical switch via an incoherently pumped fast light medium (*Invited Paper*)

M. Suhail Zubairy, Texas A&M Univ. (United States)

No Abstract Available.

8636-52, Session 11

Implementing and exploiting synthetic magnetic field in photonic systems: towards robust delay lines and isolators (*Invited Paper*)

Mohammad Hafezi, Joint Quantum Institute (United States)

Topological properties can lead to phenomena that are insensitive to perturbations. The hallmark of such behavior is the robust and quantized conductance and the edge state transport in quantum Hall systems. Although such effects are associated with charged particles

in two dimensions, subject to a magnetic field, similar behaviors can be simulated for photons by synthesizing an artificial magnetic field. Here, we theoretically and experimentally investigate how quantum spin Hall Hamiltonian (i.e., spin-orbit without time-reversal symmetry breaking) can be created using coupled resonator optical waveguides (CROW) in two dimensions and analyze the application of such systems as an optical delay line. Furthermore, we describe a new approach for on-chip optical non-reciprocity which makes use of strong optomechanical interaction in microring resonators. For different configurations, this system can function either as an optical isolator or a coherent non-reciprocal phase shifter which can implement quantum Hall Hamiltonians (with time-reversal symmetry breaking).

In our photonic approach to the quantum spin Hall physics, we consider a two dimensional CROW to simulate a 2D magnetic tight-binding Hamiltonian with degenerate clockwise and counter-clockwise modes. For certain frequency band, the transport is carried out by robust chiral edge states. In the experimental implementation of our model, we use SOI technology to form the two dimensional array of resonators. The photonic chips are fabricated on SOI wafers with a top Si layer thickness of 220 nm on a μSi buried oxide (BOX) layer and an infrared camera is used to image the state of the system by measuring the scattered light from the resonators.

This research was partially supported by the U.S. Army Research Office MURI award W911NF0910406 and the National Science Foundation through the Physics Frontier Center at the Joint Quantum Institute.

8636-53, Session 11

Tunable storage of optical data packets modulated in spectrally efficient formats (*Invited Paper*)

Thomas Schneider, Deutsche Telekom AG (Germany)

In optical telecommunications the modulation of the phase of the carrier will be increasingly used in the near future. If the amplitude of the carrier stays constant and just the phase changes, the nonlinear influence of the fiber transmission is much lower. Furthermore, a combined amplitude and phase change offers the possibility to dramatically increase the optical data rate in the communications networks. In an all-optical network optical buffers are required. However, most of the buffers which were presented up to now can just store or delay amplitude modulated signals. Here the storage of optical phase modulated data packets with a possible delay-bandwidth product of several thousand bits will be shown. The so called Quasi Light Storage (QLS) method is applied to store phase modulated data packets. The background will be reviewed and the latest results in the all-optical storage of signals modulated with highly efficient modulation formats will be presented.

8636-54, Session 11

Cavity lifetime control by slow-light and nonlinear effects (*Invited Paper*)

Patricio Grinberg, Philippe Hamel, Lab. de Photonique et de Nanostructures (France); Maia Brunstein, Ctr. National de la Recherche Scientifique (France); Kamel Bencheikh, Alejandro Yacomotti, Ariel Levenson, Lab. de Photonique et de Nanostructures (France); Yannick Dumeige, Ecole Nationale Supérieure des Sciences Appliquées et de Technologie (France)

We show both theoretically and experimentally that the lifetime of an active semiconductor photonic crystal nanocavity is enhanced thanks to the combination of two cooperative effects: slow light propagation based on coherent-population-oscillation effect and optical bistability.

8636-55, Session 11

**Slowing light down by low magnetic fields:
pulse delay by transient spectral hole-burning
in ruby** (*Invited Paper*)

Hans Riesen, The Univ. of New South Wales Canberra (Australia);
Aleksander K. Rebane, Montana State Univ. (United States);
Alex Szabo, National Research Council Canada (Canada); Ivana
Carcellera, The Univ. of New South Wales Canberra (Australia)

No Abstract Available.

8636-56, Session 11

**Nonlinear switching with frozen light in
modulated waveguides** (*Invited Paper*)

Nadav Gutman, The Univ. of Sydney (Australia); Andrey A.
Sukhorukov, The Australian National Univ. (Australia); Falk
Eilenberger, Friedrich-Schiller-Univ. Jena (Germany); Martijn de
Sterke, The Univ. of Sydney (Australia)

We predict that nonlinear waveguides which support frozen light by the
inclusion of a degenerate photonic band edge, where the dispersion
relation is locally quartic, exhibit a tunable, all-optical switching response.
The thresholds for switching are orders-of-magnitude lower than at
regular band edges. By adjusting the input condition, bistability can be
eliminated, preventing switching hysteresis.

8636-57, Session 11

**Linear and nonlinear optics in photonic
crystals: from all-photonic management of
the speed of light to laser accelerator** (*Invited
Paper*)

Igor V. Melnikov, National Research Univ. of Information
Technologies, Mechanics and Optics (Russian Federation)

No Abstract Available.

8637-1,

Quantum optomechanics

Markus Aspelmeyer, Vienna Ctr. for Quantum Science and Technology, Univ. of Vienna (Austria)

Massive mechanical objects are now becoming available as new systems for quantum science. Quantum optics provides a powerful toolbox to generate, manipulate and detect quantum states of motion of such mechanical devices – from nanomechanical waveguides of some picogram to macroscopic, kilogram-weight mirrors of gravitational wave detectors. Recent experiments, including laser-cooling of micro- and nanomechanical resonators into their quantum ground state of motion, and demonstrations of the strong coupling regime provide the primary building blocks for full quantum optical control of mechanics, i.e. quantum optomechanics. This new frontier opens fascinating perspectives both for various applications and for unique tests of the foundations of quantum physics.

8637-2,

Light in a twist: optical angular momentum

Miles J. Padgett, Univ. of Glasgow (United Kingdom)

In 1992 Allen et al. recognized that light beams could carry an orbital angular momentum in addition to the photon spin. This twist can be created using lenses, or holograms encoded onto liquid crystal displays. Both whole beams and single photons can carry this twist, or transfer it to particles causing them to spin. I will introduce the underlying properties and discuss a number of manifestations of orbital angular momentum. These will highlight how optics still contains surprises and opportunities for manipulation, imaging and communication in both the classical and quantum worlds.

8637-3, Session 1

Group symmetry and the total angular momentum of light (*Invited Paper*)

Giovanni Milione, The City College of New York (United States); Daniel A. Nolan, Corning Incorporated (United States); Stefan Evans, Joseph L. Birman, Robert R. Alfano, The City College of New York (United States)

Group symmetry plays an important role in describing complex light. Most recently we prescribed $SU(2)$ group symmetry to the higher order states of polarization of vector light beams, such as radial and azimuthal polarization where the $SU(2)$ to $SO(3)$ homomorphism reveals the intimate relationship of vector light beams to light's total angular momentum Eigen states, circular polarized optical vortices, through a higher-order Poincare sphere. An immediate consequence is the prediction and experimental verification of a new geometric phase proportional to light's total angular momentum referred to as the higher-order Pancharatnam-Berry phase. In this presentation an overview of the foundation and applications of the higher-order Poincare sphere and higher-order Pancharatnam-Berry phase will be given. In a strong mathematical analogy to quarks, it will be shown the higher-order Poincare sphere serves as an isospin subgroup within a total angular momentum of light flavour symmetry consisting of the orbital Poincare sphere proposed by Padgett and the conventional Poincare polarization sphere. As encoding information in the N -dimensional state space of light's total angular momentum forms the basis of increasing information capacity in future optical communications the higher-order Poincare sphere may serve as a ubiquitous tool.

8637-4, Session 1

Measurement of orbital angular momentum in the focal region of a high-numerical aperture beam

Daryl C. Preece, Timo A. Nieminen, Halina Rubinsztein-Dunlop, The Univ. of Queensland (Australia)

It is well known that Laguerre Gaussian (LG) beams carry l per photon of orbital angular momentum in paraxial propagation. This angular momentum is caused by the helical structure of the beams wavefronts (here l is related to the winding number of these wavefronts). Such beams have been used for various purposes. However, perhaps the most direct way that their angular momentum can be seen is in the rotation of tiny microscopic objects. Many experiments have shown how various micro-mechanical systems can be rotated by the torques, which these beams exert.

Circularly polarized beams also carry angular momentum, in this case the angular momentum is intrinsic in the beam. Gaussian beams with circular polarization can rotate birefringent objects such as Vaterite microspheres. In order to transfer momentum to objects such as microscopic particles both LG beams and circularly polarized beams create a dipole moment in the material through which they travel. However, when beams are highly focused as they are in most optical trapping experiments, it is difficult to differentiate between the spin and orbital components of the field. Though several experiments have been performed to show the spin and orbital components of the beam changes when it is highly focused, these experiments often do not take direct measurements at the focal region. We present the result of experiments to determine spin to orbital ratio at different points in the focal region of a highly focused light beam and discuss theoretical implications.

8637-5, Session 1

Intensity correlation between fractional incoherent vortices

Eduardo Jorge da Silva Fonseca, Alcenisio Jesus-Silva, Jandir M. Hickmann, Univ. Federal de Alagoas (Brazil)

Light possessing integer or fractional vortex has been widely studied in coherent systems where the phase is well-defined. However, partially coherent systems, where statistics are required to quantify the phase, can also present optical vortex in the correlation function, so-called coherence vortices. These are pairs of points where the spectral degree of coherence, a two-field correlation function, vanishes. In fact, coherence vortices involving correlation between beams with integer topological charge have unveiling a new research field. But, for fractional TC no work has been reported, to the best of our knowledge.

In this work, we explore various fundamental aspects of coherence vortex using intensity correlation, also known as fourth-order field correlation: i) strong vortices correlation - the value of the equivalent topological charge obtained in the intensity correlation follows a correlation rule such that this value is bound to the topological charge associated to each incoherent beam; ii) stability of a coherence fractional vortices - a precise signature of an integer vortex was observed in the intensity correlation from two incoherent beams with each beam possessing fractional vortices; iii) non-localized azimuthal phase - a well-defined amount of orbital angular momentum (OAM) was observed in the intensity correlation when two incoherent beams possessing OAM were diffracted by different objects, the information of azimuthal phase was recovered of a distributed object. Our findings were supported by the theoretical analyses of the correlation function using the Gaussian-Schell correlator.

8637-6, Session 1

Multipole polarization-state patterns in Poincare beams

Enrique J. Galvez, Brett Rojec, Kevin McCullough, Colgate Univ. (United States)

We present a method for generating multipole polarization-state patterns in optical beams as a class of Poincare modes. In our previous work we showed that a variety of polarization patterns can be obtained via the superposition of two Laguerre-Gauss modes in orthogonal polarization eigenstates [1,2]. This work extends the study to include superpositions of a pair of beams in polarization eigenstates, with each beam of the pair itself in a superposition Laguerre-Gauss modes. This results in a richer varieties of Poincare modes not studied before. We present a class of modes that have dipole, quadrupole and hexapole patterns in their polarization profiles. The modes that we prepare also have all the varieties of polarization singularities. We prepare optical beams in mode superpositions using spatial light modulator as part of a polarization interferometer. The modes are diagnosed by nulling individual polarization components. This work was funded by NSF and US Air Force grants.

1. E.J. Galvez, S. Khadka, W.H. Schubert and S. Nomoto, "Poincare-beam patterns produced by nonseparable superpositions of Laguerre-Gauss and polarization modes of light," *Appl. Opt.* 51, 2925-2934 (2012).
2. E.J. Galvez and S. Khadka, "Poincare modes of light," *Proc. SPIE* 8274, 82740Y 1-8 (2012).

8637-7, Session 1

Directions in optical angular momentum

David L. Andrews, Matt M. Coles, Univ. of East Anglia Norwich (United Kingdom)

For a plane electromagnetic wave, where the electric and magnetic fields are precisely disposed in the transverse plane and the Poynting vector is parallel to the propagation vector, it is well known that the classical text-book analysis of angular momentum density gives a vanishing result for any longitudinal component. In particular, under these assumptions, a circularly-polarized wave (or photon) might be construed to have no angular momentum in the propagation direction. Of course this is untrue; indeed it is the basis of Beth's famous measurement of spin angular momentum for circularly polarized light that a torque is exerted about the beam axis. This presentation reviews some of the calculational aspects, and the associated physics, involved in a resolution of the issue. In particular it is shown unnecessary to artificially impose on the beam a transverse intensity profile, vanishing at infinity, to resolve the matter. For optical beams of arbitrary structure, promotion of the electromagnetic fields, and associated potentials, to operator form gives non-zero values to each of the commonly deployed electromagnetic measures of physical significance; with a quantum optical formulation, results are cast in terms of Hermitian operators and duly relate to physical observables. Thus, not only energy and angular momentum, but also measures of chirality such as the 'Lipkin zilch', acquire a consistent physical interpretation.

8637-8, Session 2

The flatland of pulling light: tractor beam, light escalator, and controversy (Invited Paper)

Cheng-Wei Qiu, National Univ. of Singapore (Singapore)

Recently tractor beam which can pull the object has been receiving intensive attention. In this presentation, we will first unveil the fundamental physics and origin of the general pulling force by using multiple beams and even a single gradientless beam. Nevertheless that cannot be called a "tractor beam" per se, as long as the light pulling effect is ultrasensitive to the object's material and size, a perturbation of which will ruin pulling effect. We therefore investigate the universality

condition for Bessel beam to be a material-independent and size-independent tractor beam in dipolar regime. These universal pulling effects and conditions are discussed in association with insight on modified far-field scattering, scattering resonances, and induced polarizabilities. Interestingly, it is found that acoustic pulling force exhibits only size independence, owing to the acoustic scattering theory in contrast to the light scattering counterpart.

It is still too stringent or farfetched to achieve pulling light with nonparaxial Bessel beam in practice. Hence we propose an insightful schematic to transform normal plane waves into a light escalator, which can change the sign of the optical force on the object and gear it up and down using light. A non-magnetic levitating "train" can thus be possible then. Last but not least, we will present some intriguing controversies on which formalism to be adopted in calculation of optical forces, particularly in the presence of pulling force and metamaterials. The findings pave the way for the realistic engineering, rectification and application of pulling light for novel optical micromanipulation.

8637-9, Session 2

Self-trapping and back-action effects in hollow photonic crystal cavity optical traps

Nicolas Deschannes, Ulagalandha Perumal Dharanipathy, Zhaolu Diao, Mario Tonin, Romuald Houdré, Ecole Polytechnique Fédérale de Lausanne (Switzerland)

Since the first demonstration of optical trapping in the 1980s, progresses in nanofabrication have enabled the emergence of a variety of on-chip trapping techniques aimed at lower trapping powers, smaller system footprints, and manipulation of nanometer sized particles. Behind all these advances lies the ability to confine large electromagnetic fields in very small volumes required to exert large field gradients and the associated optomechanical forces.

Properly designed photonic crystal defects, which we refer to as hollow cavities, have a large fraction of the optical field located in air. Such a highly localized and resonant field can be exploited to realize optical traps exhibiting specific features linked to the resonant nature of the optical field like back-action effects.

We present the first experimental demonstration of an integrated hollow photonic crystal cavity, which selectively traps sub-wavelength particles with unprecedented low powers. The optofluidic chip is fabricated with the aid of state-of-the-art silicon technology and soft-lithography. Optical trapping of 250 and 500 nm particles is achieved over trapping times of up to ten minutes and estimated optical powers of the order of 100 μ W. The dynamic perturbation of the cavity eigenmode by the trapped particle is investigated. In particular, we demonstrate the existence of two trapping regimes that derive from the resonant nature of the trap namely back-action trapping regime and self-trapping regime. 3D numerical simulations supporting our experimental observations are presented. Single particle sorting, analysis as well as advanced spectroscopy are immediate areas that could benefit from this advancement.

8637-10, Session 2

Calculation of the force acting on a micro-sized particle with optical vortex array laser beam tweezers

Kuo Chun-Fu, Shu-Chun Chu, National Cheng Kung Univ. (Taiwan)

Optical vortices possess several special properties, including carrying optical angular momentum (OAM) and exhibiting zero intensity. Vortex array laser beams have attracts many interests due to its special mesh field distributions, which show great potential in the application of multiple optical traps and dark optical traps. Previously study developed an Ince Gaussian Mode (IGM)-based vortex array laser beam [Opt. Express 16, 19934 (2008)]. This study develops a simulation model based

on the discrete dipole approximation (DDA) method for calculating the resultant force on a micro-sized spherical dielectric particle that situated at the IGM-based vortex laser beam waist.

Before using the DDA code for the studying, we have verified the simulation code accuracy by comparing its numerical results with analytical results of Mie theory, i.e., the resultant force on a micro-sized spherical dielectric particle due to an incident plane wave. In this study, we calculate the resultant force on micro-sized spherical dielectric particles of different sizes that situated at the IGM-based vortex laser beam waist. The relation between the resultant force and the size of the particle has been discussed. Numerical results show that how many particles could be trapped by an IGM-based vortex laser beam is depended on relation between the trapped particle size and the vortex array beam size. Numerical results suggest that the IGM-based vortex laser beams could be used in the application of multiple optical traps while the trapped particles' sizes are smaller than 100nm.

8637-11, Session 2

Three-dimensional photophoretic micromanipulation

Christina Alpmann, Michael Esseling, Patrick Rose, Cornelia Denz, Westfälische Wilhelms-Univ. Münster (Germany)

Holographic optical tweezers are a well-established tool with implementations which have introduced enormous flexibility for the manipulation of transparent dielectric particles. The manipulation of absorbing matter, however, is typically handicapped due to its high absorption leading to strong scattering forces which cannot be counterbalanced by optical gradient forces. To overcome this shortcoming, optically induced thermal gradients on the particle's surface can be used. These photophoretic forces are orders of magnitude stronger than typical forces in optical tweezers, strong enough to stably trap absorbing matter in air. As absorbing matter is repelled from regions of high light intensity, light fields with a hollow intensity distribution have to be tailored, opposed to optical tweezers, where regions of high light intensity attract dielectric particles. So-called optical bottle beams have already been proposed in different static configurations, while we implemented dynamic holographic optical bottle beams. They are capable of trapping multiple absorbing particles simultaneously and manipulating them in all three dimensions independently. We present the dynamic repulsion of absorbing matter and estimate necessary intensity levels. The three dimensional trajectories are followed by two microscopes that image the transverse and one perpendicular plane with respect to the direction of light propagation. A high-speed camera is implemented to observe the light matter interaction. Our findings go beyond photophoretic solid particle manipulation by including fluidic particles. They are of interdisciplinary interest e.g. in the field of aerosol research and build the basis for a transfer into a variety of optical trapping schemes.

8637-12, Session 2

Characterization of optically trapped magnetic particles by external magnetic field: Effect of anionic surfactant as trapping medium

Vivek S. Jadhav, Univ. of Pune (India) and The AU-KBC Research Ctr. (India) and Trinity College Dublin (Ireland); Gauri R. Kulkarni, Univ. of Pune (India); B. M. Jaffar Ali, Pondicherry Univ. (India)

Metal particles are thought to be poor candidate for optical trapping. In this study, we demonstrate stable optical trapping of magnetic particles including metallic Fe and determine the trapping efficiency at various concentration of anionic surfactant solution (SDS), and at varying intensity gradient of trapping laser. Here, different numerical aperture of the focusing objective lens defines intensity gradient. We consider

the strength of the optical trap at a given laser intensity as strength of applied magnetic field just sufficient to dislodge the particle from the trap. For this purpose, we have modified the single beam gradient trap system to include the magnetic field at focal point of the sample. We have determined the trapping efficiency of Fe and Fe₂O₃ particles. It is seen that the trapping efficiency increases with increase in the SDS concentration. Further the trapping efficiency seems to be dependent on the numerical aperture of the objective lens used. We thus conclude that metallic particles can be stably trapped using objective lens of low numerical aperture and their strength can be further modulated as a function of concentration of anionic surfactant solution.

8637-42, Session 2

Complete azimuthal decomposition of optical fields

Angela Dudley, Igor Litvin, Filippus S. Roux, Andrew Forbes, CSIR National Laser Ctr. (South Africa)

By using digital holograms, we present a simple technique for performing a complete azimuthal decomposition of an arbitrary laser mode. The match-filter, used to perform the azimuthal decomposition, is bounded by an annular ring, allowing us to conduct a scale-independent decomposition on our selected mode. This technique therefore requires no prior knowledge of the mode structure, the mode phases, or the amplitude distribution. A basis comprising of the angular harmonics is used to express the spatial distribution of the selected mode in terms of spatially dependant coefficients. We use this to infer directly from the measured weightings of the azimuthally decomposed modes and their phase-delay measurements, the intensity of the selected field, its phase, and its orbital angular momentum (OAM) density. We illustrate the concept by executing a full decomposition of two examples: a superposition of two Bessel beams, with relative phase differences, and an off-axis vortex mode. We show a reconstruction of the amplitude, phase and OAM density of these fields with a high degree of accuracy.

8637-50, Session 2

Principal states and vortex modes in optical fiber for spatial communications

Daniel A. Nolan, Corning Incorporated (United States); Giovanni Milione, Robert R. Alfano, The City College of New York (United States) and Graduate Ctr. of the City Univ. of New York (United States)

Using SU(N) group theory, we develop a formalism to superimpose N vortex modes and form N orthogonal principal states in fiber. These principal states provide a means to overcome the detrimental effects of mode coupling that occur in optical communications links. This formalism reduces to the Jones matrix eigenanalysis when N equals 2, which has been studied extensively to characterize polarization mode dispersion. Specifically we use the 4 vortex modes of the LP₁₁ modal group to establish the principal states and we graphically display them using the higher order Poincare sphere, HOPS.

For polarization mode dispersion and N = 2, we require 3 Pauli spin matrices and consequently 3 mux demux components to generate the Principal states. For N = 3, we use the 8 Gell Mann matrices and 8 components. For N = 4 as is the case for 4 the vortex modes of the LP₁₁ modal group, we require 15 generators and 15 physical components, since these systems scale as N²-1. The LP₁₁ modal group includes the HE₂₁ horizontal and vertical vortex modes as well as the transvers electric and transverse magnetic vortex modes.

We describe in some detail a link with 3 and separately one with 4 principal states, which are superimposed from the vortex mode and show schematically the active and passive components required to multiplex and demultiplex the principal states.

8637-13, Session 3

Dynamic optics for high-resolution microscopy and photonic engineering (*Invited Paper*)

Martin Booth, Univ. of Oxford (United Kingdom)

Dynamic optical devices, like deformable mirrors or spatial light modulators, have many uses in enhancing the performance of high resolution optical systems. We have applied these methods to adaptive correction of specimen-induced aberrations in microscopes for biological imaging, enabling improved image quality and resolution in thick specimens. We have also developed techniques for aberration correction and beam shaping for laser micro/nanofabrication in transparent substrates, leading to more precise fabrication of photonics structures and waveguide circuits up to hundreds of micrometres inside materials. We also present dynamic methods for parallel laser fabrication, enabling faster operation with hundreds of individually controllable foci.

8637-14, Session 3

Shaping the light transmission through a multimode waveguides: complex transformation analysis and applications

Tomáš ?i?már, Kishan Dholakia, Univ. of St. Andrews (United Kingdom)

We present a powerful approach towards full understanding of laser light propagation through multimode optical fibres and control of the light at the fibre output. Transmission of light within a multimode fibre introduces randomization of laser beam amplitude, phase and polarization. We discuss the importance of each of these factors and introduce an experimental geometry allowing full analysis of the light transmission through the multimode fibre and subsequent beam-shaping using a single spatial light modulator. We show that using this approach one can generate an arbitrary output optical field within the accessible field of view and range of spatial frequencies given by fibre core diameter and numerical aperture, respectively, that contains over 80% of the total available power. We present applications of these approaches in biophotonics and imaging. We show the confinement and manipulation of a number of microparticles using the output field of the multimode fibre. We demonstrate the modalities of bright-field and dark-field imaging and scanning fluorescence microscopy at acquisition rates allowing observation of dynamic processes such as Brownian motion of mesoscopic particles. Furthermore, we show how such control can realise a new form of mode converter and generate various types of advanced light fields such as propagation-invariant beams and optical vortices. These may be useful for future fibre based implementations of super-resolution or light sheet microscopy.

8637-15, Session 3

Beacon guided digital phase conjugation through multimode fibers

Salma Farahi, Ioannis N. Papadopoulos, Demetri Psaltis, Christophe Moser, Ecole Polytechnique Fédérale de Lausanne (Switzerland)

Unlike single mode optical fibers, multimode fibers offer a large number of degrees of freedom corresponding to the number of propagation modes in the fiber and thus allow a higher peak power to be transmitted through. This feature, however, does not come without a cost, as the propagated field is coupled to the different modes and finally gets scrambled.

Digital phase conjugation can compensate for the scrambling of light in a multimode fiber but needs a beacon, an optical field that will get coupled

in the fiber and propagate. The speckled output after propagation, is holographically recorded and its phase is extracted and assigned onto an SLM device that is used to generate the optical phase conjugate field. The phase conjugate field is directed towards the fiber output and comes into focus at the fiber input. The presence of a real time beacon field would enable the implementation of a highly flexible multimode fiber focusing mechanism.

For this propose we propose and experimentally demonstrate the use of a double-clad fiber, in which a first beam propagates through the single mode core. At the distal end of the single mode fiber core, the beam is reflected or scattered by a surface generating a beacon light source. The reflected or scattered light field is coupled back in the multimode cladding. By propagating a phase conjugated field through the fiber cladding a focus is generated at the beacon source location. In this configuration, the excitation and phase conjugation process are done from the same side of the fiber.

8637-16, Session 3

The role of propagation invariant light modes in single and multi-photon imaging

Tom Vettenburg, Heather I. C. Dalgarno, Tomáš ?i?már, Frank J. Gunn-Moore, Kishan Dholakia, Univ. of St. Andrews (United Kingdom)

Our understanding of beam propagation has undergone a revolution in the last decade. One of the cornerstones of wave theory, diffraction, can be obviated to a certain degree by the special class of propagation invariant or 'non-diffracting' beams. These can be decomposed in terms of wavevectors such that they proffer the ability to 'self-heal' or repair when partially blocked by obstacles. Such propagation invariant beams are characterized by a prominent transverse structure of numerous side-lobes, carrying an important fraction of the energy. While this transverse structure does not hinder applications in areas ranging from filamentation, to trapping, and photoporation, it does influence the imaging capability of such light fields. Nevertheless, the propagation invariance in particular is attractive for imaging applications. Recently it was shown that a light sheet created with a Bessel beam enables high resolution imaging of large sample volumes. To overcome the contrast reduction of the Bessel beam's transversal structure one must rely on two-photon excitation or multiple sample exposures, giving up one of the key benefits of light sheet microscopy, minimal photo-bleaching. We demonstrate that light sheet microscopy with an Airy beam has no such restrictions, simplifying its implementation and extending its applicability. Moreover, unlike competing techniques, high contrast and resolution is readily obtained in a single scan without multiple illuminations, whilst the high resolution sample volume is extended by an order of magnitude. We show how the asymmetry in its transverse profile lies at the heart of these unique properties. We compare and contrast the use of the Airy beam and Bessel beam for both single and two-photon excitation.

8637-17, Session 3

Optical twistors: wavefront encoded Helico-Conical beams

Jesper Glückstad, Technical Univ. of Denmark (Denmark)

It is well-known that wavefronts encoded with a helical phase profile correspond to photons having orbital angular momentum. A Laguerre-Gaussian beam is a typical example where its helical phase defines a phase-singularity at the optical axis and forms a vortex-shaped transverse intensity profile. We have previously proposed a unique wavefront encoded light beam where both phase and amplitude express a helical profile as the beam propagates in the far field. We have coined this type of beam as Optical Twistors and demonstrated their capacity to induce spiral motion of particles trapped along the path of each twister. Unlike Laguerre-Gaussian beams, the far field projection of an optical twister maintains a high photon concentration even at higher values of

topological charge of the encoded phase. Optical Twisters have therefore profound applications to fundamental studies of light and atoms such as in quantum entanglement of the orbital angular momentum, toroidal traps for cold atoms and for optical manipulation of microscopic particles.

8637-18, Session 3

Vortex birth at Fraunhofer plane

Eduardo Jorge da Silva Fonseca, Alcenisio Jesus-Silva, Jandir M. Hickmann, Univ. Federal de Alagoas (Brazil)

In 1992, Allen et al. [1] showed that Laguerre-Gaussian beams may possess orbital angular momentum (OAM). These OAM light beams are characterized by two integer indices p , radial index, and m , azimuthal index. The latter is so called topological charge (TC), characterizes by transversal phase dependence. Recently, there has been significant interest in optical vortices with fractional topological charges. In a pioneer paper, Berry showed that the birth of a vortex within the beam occurs as the fractional phase step reaches and passes a half-integer value [2]. This result was experimentally confirmed by [3]. A triangular aperture was aligned over the beam at the plane where the vortex should be born, and the intensity of the field transmitted by this aperture was observed in the Fraunhofer zone. It was shown that only for fractional values greater or equal to half-integer value of m , a new row of lobes developed for a well defined triangular truncated optical lattice [4].

Here, we present that, at the Fraunhofer plane of the fractional TC beam, it is not possible to characterize the birth of a vortex as an event that occurs only for greater or equal to half-integer value of m . But the vortex is born at $m = n + z$, with n an integer number and z a small fraction number that defines the birth of a vortex.

[1] L. Allen et al., PRA 45, 8185 (1992).

[2] M.V. Berry, J. Opt. a-Pure Appl. Op. 6, 259 (2004).

[3] A. Mourka et al., Opt. Express 19, 5760 (2011).

[4] J.M. Hickmann et al., PRL 105, 053904 (2010).

8637-19, Session 4

Patterned multiphoton excitation deep inside scattering tissue (*Invited Paper*)

Valentina Emiliani, René Descartes Univ. (France) and INSERM (France); Eirini Papagiakoumou, René Descartes Univ. (France) and INSERM (France); Aurélien Bègue, René Descartes Univ. (France) and INSERM (France); Osip Schwartz, Ben Leshem, Dan Oron, Weizmann Institute of Science (Israel)

Light is the tool of the 21st century in neuroscience. New photosensitive tools such as caged compound or optogenetics actuators and reporters offer the possibility to monitor and control neuronal activity from the sub-cellular to the integrative level. This ongoing revolution has motivated the development of new optical methods for light stimulation. Among them, it has been recently demonstrated that a promising approach is based on the use of wavefront shaping to generate optically confined extended excitation patterns. This was achieved by combining the technique of temporal focusing with different approaches for lateral light shaping including low numerical aperture Gaussian beams, holographic beams and beams created with the generalized phase contrast method. What is needed now is a precise characterization of the effect of scattering on these different methods in order to extend their use for in depth excitation.

Here we present a theoretical and experimental study on the effect of scattering on the propagation of wavefront shaped beams. Results from fixed and acute cortical slices show that temporally focused spatial patterns are extremely robust against the effects of scattering and this permits their three-dimensional confinement for depths up to 550 μm .

8637-20, Session 4

MEMS axicons for nondiffracting line shaping of ultrashort pulses

Alexander Treffer, Susanta K. Das, Martin Bock, Max-Born-Institut für Nichtlineare Optik und Kurzzeitspektroskopie (Germany); Jens Brunne, Ulrike Wallrabe, Albert-Ludwigs-Univ. Freiburg (Germany); Ruediger Grunwald, Max-Born-Institut für Nichtlineare Optik und Kurzzeitspektroskopie (Germany)

For a growing number of applications in nonlinear spectroscopy, micro- and nano-machining, optical data processing, metrology or medicine, an adaptive shaping of ultrashort pulsed, ultrabroadband laser beams into propagation-invariant linear focal zones (light blades) is required. One example is the femtosecond laser high-speed large area nanostructuring with moving substrates and cylindrical optics we reported about recently. Classical microoptical systems, however, distort the temporal pulse structure of few cycle pulses by diffraction and dispersion. The temporal pulse transfer can be improved with innovative types of reflective MEMS axicons based on two integrated rectangular mirrors, tilted by a piezoelectric bending actuator. In contrast to pixelated liquid-crystal-on-silicon (LCoS) based devices, cutoff frequencies in multi-kilohertz range, a purely reflective setup and continuous profiles with larger phase shift are realized which enable for shaping extended propagation-invariant zones at a faster and more robust operation. Additionally, a fixed phase offset can be part of the structure. Here, the performance of a prototype of linear mechanically tunable MEMS axicon is demonstrated by generating a pseudo-nondiffracting line focus of variable diameter and depth extension from a femtosecond laser pulse. The temporal transfer of 6-fs pulses of a Ti:sapphire laser oscillator is characterized with spectral phase interferometry for direct electric-field reconstruction (SPIDER) and spatially resolved nonlinear autocorrelation. Spatial and temporal self-reconstruction properties were studied. The application of the flexible focus to the excitation of plasmon-polaritons and the self-organized formation of coherently linked deep sub-wavelength laser-induced periodic surface structures (LIPSS) in semiconductors and dielectrics is reported.

8637-21, Session 4

A method to calculate arbitrary linear polarized laser beam evolutions in GRIN lenses

Ko-Fan Tsai, Shu-Chun Chu, National Cheng Kung Univ. (Taiwan)

Gradient-index (GRIN) lens is an important optical component, which has high numerical aperture value and good imaging property. The propagation properties of several beams in GRIN lenses are discussed by researchers via the approaches of Fractional Fourier transform (FrFT) or ABCD Matrix, such as Hermite-Gaussian beams, Laguerre-Gaussian beams, Ince-Gaussian beams, Helmholtz-Gauss (HzG) beams and etc. This study treated the GRIN lenses system as a simplified optical system and then used the Fresnel-Kirchhoff integration to describe the field propagation. The method can calculate arbitrary linear polarized laser beam evolutions in GRIN lenses.

This study compared two approaches in details. The first approach is the well-known FrFT approach that treats the GRIN lens as a single lens equivalent optical system of Fractional Fourier transform (FrFT). The second approach is the proposed method, which treats a GRIN lens as the combination of multiple thin phase sheets. Numerical results show that the FrFT approach can calculate the field at any single plane in a GRIN lens fast. However; when the GRIN lens gradient constant grows larger, the inaccuracy of the FrFT method will also grow larger; while with the same situation, the proposed multiple-phase-sheet approach can still find the field evolution in GRIN lenses with a good precision. Besides, not only the GRIN lenses with the quadratic index distribution, the proposed method can calculate field propagation in most mediums with index distribution of slowly variation. The discussions of this study will be useful to researchers who study in GRIN lens optical systems.

8637-22, Session 4

Arbitrary femtosecond highly non-paraxial accelerating beams

Amaury Mathis, Francois Courvoisier, Luc Froehly, Maxime Jacquot, John M. Dudley, FEMTO-ST (France) and Univ. de Franche-Comté (France)

Accelerating beams such as Airy beams exhibit a curved trajectory of their point of maximum intensity and can exhibit diffraction-free behaviour. They have recently attracted tremendous interest for diverse applications in both linear and nonlinear optics. However, in most previous studies the deviation angles have been confined to the paraxial regime which prevented high focussing conditions. We have recently shown direct spatial shaping of Gaussian beams to produce nonparaxial circular beams, but the intensity distribution along the trajectory was not maximal in the nondiffracting regime. Here, we report the generation of femtosecond accelerating beams from the Fourier plane of high-numerical aperture microscope objectives. We generate accelerating beams with radius of curvatures as small as 80 μm , <2 μm main lobe width and deviation angles exceeding $\pm 40^\circ$. Excellent agreement is observed between experimental and numerical results. We clarify the links between accelerating beams, caustics and catastrophe optics. We show how this allows the direct calculation of the phase mask to generate arbitrary trajectories even if thick optics are used. We numerically show that polarization can be spatially controlled along the propagation. We also demonstrate both numerically and experimentally intensity control along the beam trajectory.

8637-23, Session 5

Orbital angular momentum of photons, atoms, and electrons (*Invited Paper*)

Sonja Franke-Arnold, Univ. of Glasgow (United Kingdom)

Electric field modes that carry orbital angular momentum allow access to and manipulation within an arbitrary-dimensional state space. These modes, interesting for optical applications in quantum communications and computation, have recently been discovered for electron microscopy.

Here we demonstrate the efficient transfer of intensity and phase structure of OAM modes from near infrared pump light to blue light generated in a four-wave mixing process in a rubidium vapour. The method is based on the conservation of OAM in four-wave mixing. Pumping with more complicated light profiles excites spatial modes in the blue that depend strongly on phase-matching, thus demonstrating the parametric nature of the mode transfer. Due to the narrow resonances of the atomic transitions the process is highly frequency dependent. These results have implications on the inscription and storage of phase-information in atomic gases.

Not only light, but all electro-magnetic fields may have an azimuthal phase dependence with associated OAM, and vortex beams have recently been predicted and demonstrated for electrons in transmission electron microscopy. We predict a Faraday effect for electron vortices, based on the different dispersion of right and left handed vortices in a magnetic field. Unlike optical Faraday rotation, which is associated only with polarisation, the electron effect depends on the total angular momentum comprising both spin and orbital angular momentum. Our consideration showcases similarities and differences between optical and electronic vortices. The electron Faraday effect should allow the extremely sensitive investigation of magnetic samples and of the experimental apparatus itself.

8637-24, Session 5

Production of two-photon cluster states in polarization and spatial modes

Enrique J. Galvez, William H. Schubert, Michael A. Senatore,

Colgate Univ. (United States)

We have undertaken the task to produce photon pairs in entangled states of polarization and any desired pair of spatial modes [1]. These constitute 4-qubit states. Photon pairs in polarization-entangled states are produced via spontaneous parametric down-conversion. These photons are in an entangled spatial multimode state. In our method we project the spatial modestate of the photons into their respective fundamental spatial mode by use of single-mode fibers. Thereafter, the pairs are relaunched into free space and sent to polarization interferometers, where new desired spatial modes are encoded by spatial light modulators. The goal is to create a linear or box cluster state. The work is ongoing. Challenges include the reduction of signal in spatial filtering, and decohering processes. This work was funded by NSF and US Air Force grants.

1. E.J. Galvez, "Proposal to produce two and four qubits with spatial modes of two photons," Proc. SPIE 8274, 82740G 1-5 (2012).

8637-25, Session 5

Down-converted bi-photons in a Bessel-Gaussian basis

Filippus S. Roux, Melanie McLaren, CSIR National Laser Ctr. (South Africa); Miles J. Padgett, Univ. of Glasgow (United Kingdom); Andrew Forbes, CSIR National Laser Ctr. (South Africa); Thomas Konrad, Univ. of KwaZulu-Natal (South Africa)

The OAM or spiral bandwidth indicates the dimensionality of the entangled state that is produced by the spontaneous parametric down-conversion process. Normally this bandwidth is determined by modulating the signal and idler beams with helical phase functions with opposite azimuthal indices on the spatial light modulators in the signal and idler beams, respectively. We added an additional binary Bessel function to the helical phase, thereby specifying the radial dependence of the mode to be Bessel-Gaussian (BG) modes. This come down to a post selection process, which is known to have the ability to increase entanglement. The result is a modification to the shape of the OAM spectrum, which leads to a higher dimensionality for the quantum states. Using these transmission functions we performed EPR type experiments to test the entanglement. We also performed state tomography measurements for up to eight dimensions to determine the density matrix for the higher dimensional quantum state. The result indicate that, in addition to an increase in the dimensionality, the resulting post selected states have higher entanglement.

8637-26, Session 5

The generation of entangled matter waves

Wolfgang A. Ertmer, Bernd Luecke, Manuel Scherer, Jens Kruse, Oliver Topic, Jan Peise, Luis Santos, Frank Deuretzbacher, Leibniz Univ. Hannover (Germany); Jan J. Arlt, Aarhus Univ. (Denmark); Carsten Klempt, Leibniz Univ. Hannover (Germany); Augusto Smerzi, Luca Pezze, European Lab. for Non-linear Spectroscopy (Italy); Philipp Hyllus, Univ. del País Vasco (Spain)

The concept of entanglement has evolved from a controversial building block of quantum mechanics to the basic principle of many highly topical applications.

These applications range from quantum computation to fundamental tests of physics and novel metrology concepts. The experimental generation of practically useful entanglement is a challenging task. In optics, parametric down-conversion in nonlinear crystals has become one of the standard methods to generate entangled states of light. The rapid progress in the preparation and manipulation of ultracold neutral atomic gases now allows for the realization of such entangled states with matter waves. Bose-Einstein condensates of atoms with non-zero spin provide a mechanism analogous to parametric down-conversion. The presented process acts as a two-mode parametric amplifier and generates two clouds with opposite spin orientation

consisting of the same number of atoms. At a total of 10000 atoms, we observe a squeezing of the number difference of -7 dB below shot noise, including all noise sources. As a first application, we demonstrate that the created state is useful for precision interferometry. We show that its interferometric sensitivity beats the standard quantum limit, the ultimate limit of unentangled states. The created states of matter can be employed in future atom interferometers to improve the sensitivity of gyroscopes, accelerometers, gravity sensors or atomic clocks.

8637-45, Session PWed

Photocatalytic 3D nano-optical trapping using TiO₂ nanosphere pairs mediated with Mie scattered near-field

Toshiyuki Honda, Mitsuhiro Terakawa, Minoru Obara, Keio Univ. (Japan)

The enhanced localized optical near-field on a nanostructure can drive optical trapping to the nanometer scale. The near-field optical trapping has been studied by using not only metal substrates but also dielectric substrates of silicon slot waveguide (1D trapping) and silicon/silicon nitride photonic crystal resonator (3D trapping). In this paper, we propose a 3D photocatalytic 3D nano-optical trapping using poly-rutile TiO₂ nanosphere pairs mediated with Mie scattered near-field for size-selective trapping. The trapping forces were calculated from optical intensity distribution in 3D nanogap spaces of 20 nm and 50 nm between two 240-nm nanospheres simulated by FDTD method. The system consists of two 240-nm TiO₂ nanospheres placed on a silica substrate in water, excited with 400-nm laser shorter than the bandgap of TiO₂. The polarizability mode in the spheres mainly governs Mie scattered localized near-field intensity between the spheres. The hexapole mode can induce the highest near-field intensities between the spheres. The trapping stiffness for 20-nm polystyrene (PS) sphere in a gap distance of 20 nm was 44 pN/nm/W. The optical force vector shows that the PS is trapped with sufficient forces into the center of the nanogap space, and then driven into the direct surface of the TiO₂ sphere for photocatalytic reaction. This system can work in water biology as a photocatalytic trapping for killing virus, etc. In addition, we propose a new system of using two different incident lasers for optical trapping and for photocatalytic reaction to control separately trapping and photocatalytic reaction.

8637-46, Session PWed

Efficient sorting of Bessel beams

Angela Dudley, Thandeka Mhlanga, Andre McDonald, Filippus S. Roux, CSIR National Laser Ctr. (South Africa); Martin Lavery, Miles Padgett, Univ. of Glasgow (United Kingdom); Andrew Forbes, CSIR National Laser Ctr. (South Africa)

A procedure to efficiently sort orbital angular momentum (OAM) states of light, by performing a Cartesian to log-polar coordinate transformation which translates helically phased beams into a transverse phase gradient, currently exists [1]. We implement this mode transformer, which comprises of two custom refractive optical elements [2], to efficiently sort Bessel beams carrying OAM. Introducing two cylindrical lenses, allows the focusing of each of the input OAM Bessel states to a different lateral position in the Fourier plane and separates the radial wave-vectors in the image-plane. We demonstrate the concept by separating twenty-one OAM states and twenty radial wave-vectors.

[1]. M. P. J. Lavery, D.J. Robertson, G. C. G. Berkhout, G. D. Love, M. J. Padgett, and J. Courtial, "Refractive elements for the measurement of the orbital angular momentum of a single photon," *Opt. Express* 20(3), 2110 (2012).

[2]. G. C. G. Berkhout, M. P. J. Lavery, J. Courtial, M. W. Beijersbergen, and M. J. Padgett, "Efficient sorting of orbital angular momentum states of light," *Phys. Rev. Lett.* 105(15), 153601 (2010).

8637-47, Session PWed

Effect of chemical environment on membrane stiffness of EC cells using optical tweezers

Punam S. Sonar, Univ. degli Studi di Modena e Reggio Emilia (Italy) and Univ. of Pune (India) and AU-KBC Research Ctr. (India); Vivek S. Jadhav, Univ. of Pune (India) and The AU-KBC Research Ctr. (India) and Trinity College Dublin (Ireland); Krishna priya M., Suvro Chatterje, The AU-KBC Research Ctr. (India); B. M. Jaffar Ali, Pondicherry Univ. (India)

Single beam optical tweezers (OT) is an established tool in the field of life sciences and enables to study mechanical properties of single cells. In present study, we used OT system to investigate the membrane stiffness of single endothelial cells (EC) under three different chemical environments; (a) treated with cadmium nanoparticles, (b) spermine NONOate, a nitric Oxide donor, (c) treated with combination of cadmium nanoparticles and spermine NONOate. The results of this study reveal that the membrane stiffness of EC responds differently to various chemical manipulations. It is observed that membrane stiffness decreases when EC are treated with cadmium nanoparticles as compared with control; treating the cadmium treated EC with spermine NONOate recovers the membrane stiffness to normal state of the stiffness of the cells. Since cell membrane stiffness is a reporter of underlying membrane-cytoskeletal connectivity, our results suggests spermine NONOate mediate reversal of cadmium induced membrane-cytoskeletal remodeling.

8637-51, Session PWed

Sorting optical angular momentum from a multimode optical fiber

Thien An Nguyen, Giovanni Milione, The City College of New York (United States); Daniel A. Nolan, Corning Incorporated (United States); Martin P. J. Lavery, Miles J. Padgett, Univ. of Glasgow (United Kingdom); Robert R. Alfano, The City College of New York (United States)

We present an experimental method to sort the optical orbital and spin angular momentum eigenstates, i.e. circular polarized optical vortices, from the output of a multimode optical fiber. This method is based on combining conventional Stokes polarimetry with an orbital angular momentum of light "sorter" to measure, efficiently and dynamically, the fiber's total angular momentum spectrum. The sorter consists of two refractive elements that map orbital angular momentum states at the sorter's input plane to different spatial positions at the output plane. In combination with a Wollaston prism it is possible to monitor all angular momentum states simultaneously in a single imaging plane. Various total angular momentum spectra are created and measured by varying the state of polarization of a beam coupled off axis to the fiber input, demonstrating the applicability of this approach. Applications in mode-division multiplexing and optical fiber sensors will be discussed.

8637-27, Session 7

New horizons for Supercontinuum light sources: from UV to mid-IR (*Invited Paper*)

Carsten L. Thomsen, Frederik D. Nielsen, Jeppe Johansen, Peter M. Moselund, NKT Photonics A/S (Denmark)

Commercially available supercontinuum sources continue to experience a strong growth in a wide range of industrial and scientific applications. In addition, there is a significant research effort focused on extending the wavelength coverage both towards UV and MID IR. Broadband sources covering these wavelength ranges has received significant attention from potential users, as there is a wide array of applications for which there are

few suitable alternatives light sources – if any.

Our developments in the field of MID IR supercontinuum sources have been based on radical approaches; such as soft glasses and novel pumping schemes, whereas shifting the spectrum further towards the UV have been based on advanced microstructure fiber designs.

We will in this talk present our latest developments and give our view on the future of spatially coherent broadband supercontinuum sources.

8637-28, Session 7

Topological ergodic dynamics of optical singularities in laser-induced speckle field following “optical damage” of photorefractive LiNbO₃: Fe crystal

Marat S. Soskin, Vasyil Vasil’ev, Institute of Physics (Ukraine)

Generic developing elliptic polarized speckle-fields were created in laser beam propagating through photorefractive crystal LiNbO₃ by “optical damage” effect. They possess circularly polarized C points and are accompanied by optical diabolos [1]. Topological space-time scenarios of time unlimited chain and short time loop reactions were established. They are mandated by conservation laws of Poincaré index of wavefront [1] and topological charge [2], with minimization of field free energy [3].

Speckle-fields develop mainly by topological chain reactions of connected links (~80%) and short-term loops (~20%) when starting singularities pair annihilates soon. All reactions start and finish by hyperbolic star-monster pairs only. Hyperbolics can transform reversibly to elliptics inside links of chain reactions. Chain and loop reactions exist for accompanied orthogonal polarized OVs, which are topologically much simpler due to absence of morphological forms for C points and two forms for accompanied optical diabolos.

Discovered topological chain reactions differ principally from known nuclear and chemical chain reactions due to obligatory conservation law for singularities total topological charge. They are promising for investigations of nonlinear processes in recording media induced by wave fields with various wavelengths.

1. I. Freund, Opt. Commun., 272, 293 (2007).
2. J.P. Nye, Natural Focusing and Fine Structure of Light (IOP Publ., Bristol, 1999).
3. A.M. Sonnet, E.G. Virga, Dissipative Ordered Fluids (Springer, 2012).

8637-29, Session 7

LC nanocomposites: induced optical singularities, managed nano/micro structure, and electrical conductivity

Vladislav V. Ponevchinsky, Institute of Physics (Ukraine); Andrii I. Goncharuk, F. D. Ovcharenko Institute of Biocolloidal Chemistry (Ukraine); Sergey S. Minenko, Institute for Scintillation Materials (Ukraine); Longin N. Lisetski, Institute for Scintillation Materials (Ukraine); Nikolai I. Lebovka, F. D. Ovcharenko Institute of Biocolloidal Chemistry (Ukraine); Marat S. Soskin, Institute of Physics (Ukraine)

Developed methods of polarization singular optics were applied for investigation of nematic and cholesteric LC matrices doped by multi-walled carbon nanotubes (MWCNTs), actual objects for science and applications. MWCNTs assemble spontaneously to micro scale clusters with inner contacts. They undergo cascade of incubation processes up to stable composites structures. It was shown optically, MWCNTs clusters possess fractal structure. Anchoring of LC molecules to nanotubes side walls creates the stressed cladding of LC matrix on the cluster borders. This generates by-turn system of polarization singularities and inversion walls born under applied electric field between neighbor

clusters. Electrical conductivity of nanocomposites grows on few orders when neighbor clusters contact at appropriate concentration of nanotubes (percolation transition). Cholesteric nematogenic (EBBA) and smectogenic (BBA) matrices diminish quantity of contacts and electrical conductivity of nanocomposites accordingly when their temperature decreases. It was shown by technique of selective reflection from doped cholesteric matrices that nanotubes with nearly direct shape enlarge pitch of cholesteric helices. Mosaic of LC domains, claddings around nanotube clusters and inverse walls between them were realized in cholesteric matrices doped by 0.05 wt. % of MWCNTs. Such composites are promising media for creation of new family of sensors with enlarged sensitivity.

8637-30, Session 7

Measurements on optical transmission matrices of strongly scattering nanowire layers

Duygu Akbulut, Univ. Twente (Netherlands); Tom Strudley, Univ. of Southampton (United Kingdom); Jacopo Bertolotti, Univ. Twente (Netherlands) and Univ. of Florence (Italy); Tilman Zehender, Technische Univ. Eindhoven (Netherlands); Erik P.A. M. Bakkers, Technische Univ. Eindhoven (Netherlands) and Technische Univ. Delft (Netherlands); Willem L. Vos, Univ. Twente (Netherlands); Otto L. Muskens, Univ. of Southampton (United Kingdom); Allard P. Mosk, Univ. Twente (Netherlands)

Light incident on a scattering medium is redistributed over transport channels that either transmit through or reflect from the medium. We perform experiments aiming at finding individual transport channels of extremely strongly scattering materials. A small number of transport channels are open with transmission coefficient close to 1; field transmission takes place through these channels. This means that, even if two very different incident fields are sent to the sample, the corresponding transmitted fields are correlated. As the scattering becomes stronger, these correlations become more pronounced.

One way to investigate these correlations is to construct a transmission matrix by measuring the fields transmitted through the medium in response to pre-determined incident fields. An observation of correlations in the optical transmission matrices of strongly scattering materials have not been reported so far.

We measure transmission matrices of strongly scattering layers of disordered GaP nanowires, one of the strongest scattering materials in the visible regime. The samples under study have thicknesses varying between ~1.5 μm and ~6.5 μm and transport mean free path of ~0.2 μm. We perform singular value decomposition on the measured matrices and investigate effects of correlations on the obtained singular values.

8637-31, Session 7

Higher order mode propagation in ultrathin optical fibers for atom traps

Fredrik K. Fatemi, U.S. Naval Research Lab. (United States); Sylvain Ravets, Lab. Charles Fabry (France); Jonathan E. Hoffman, Joint Quantum Institute (United States) and Univ. of Maryland, College Park (United States) and National Institute of Standards and Technology (United States); Guy Beadie, U.S. Naval Research Lab. (United States); Luis A. Orozco, Steven L. Rolston, Joint Quantum Institute (United States) and Univ. of Maryland, College Park (United States) and National Institute of Standards and Technology (United States)

Ultrathin optical fibers, created by drawing standard optical fiber, provide a practical way of connecting standard photonic equipment to quantum systems. Atoms trapped in evanescent fields of these fibers are

strongly coupled to photons propagating through these subwavelength waveguides. Previously, strong atom-photon interactions have been demonstrated in fibers with submicron diameters, thin enough to admit only the fundamental HE₁₁ mode. Higher order modes in fibers with larger diameters would open additional trapping geometries due to the azimuthal variation of the polarization profile. In this work, we discuss propagation experiments in ultrathin fibers using the first excited TE₀₁, TM₀₁, and HE₂₁ modes. We have currently achieved over 85% transmission of 780 nm light in this family of modes in fibers with 400 nm radius.

To achieve high transmission, the fibers must be drawn adiabatically for the desired mode, but the adiabaticity requirements are significantly more stringent for higher order modes than for the HE₁₁ mode. We investigate adiabaticity by monitoring the transmitted power and beam profiles during the drawing process. Nonadiabatic behavior is marked by lowered transmission and strong oscillations in the throughput due to beating between other excited modes, which we identify analytically and numerically. We discuss the optimization of the drawing process for adiabatic propagation through both the choice of fiber tapering parameters and type of optical fiber used. The observed dynamics are supported by extensive numerical simulations. This work is supported by ONR, ARO, DARPA, the Fulbright Foundation, and the NSF through the PFC at JQI.

8637-32, Session 8

Optical robotics: optimising both light and matter

Jesper Glückstad, Technical Univ. of Denmark (Denmark)

A generic approach for optimizing light-matter interaction involves the combination of optimal light sculpting methods with the use of optimally shaped structures to provide for true light-driven micro-robotics. The optical forces and torques that can be created in this light-matter interaction governs how advanced the light-driven micro-robotics can be taken. The standard requirement of having a tightly focused beams in high-numerical optical tweezing of a spherical object exemplifies the need for optimal light-sculpting (strong focussing in this case) for an object where the shape is given in advance. We will outline our novel approach to this light-matter interaction where contemporary computational models are used on both the light sculpting and the object shaping to optimise the achievable forces and torques necessary for establishing a powerful optical micro-robotics platform of the future.

Specifically we design different three-dimensional micro-structures with submicron features and fabricate them by two-photon photopolymerization. These optimally shaped structures are subsequently handled and controlled using our proprietary BioPhotonics Workstation. We exploit the light shaping capabilities available in the BioPhotonics Workstation to demonstrate a novel strategy for controlling the microstructures and their robotic function that goes beyond conventional optical trapping and manipulation. We will finally propose designing light-driven micro-robots by this approach for so-called structure-mediated access to the nanoscale.

8637-33, Session 8

Optical micro-assembling of non-spherical particles

Sarah Isabelle Ksouri, Reza Ghadiri, Andreas Aumann, Andreas Ostendorf, Ruhr-Univ. Bochum (Germany)

Holographic optical trapping has been developed for the manipulation of polymeric microparticles or biological cells with almost circular shape. As is well known, spherical particles can already be trapped and controlled with simple Gaussian beams. The preassemblies used in the experiments are generated by a two-photon-polymerization (2PP) process in micrometer or nanometer range. This leads to the idea of connecting 2PP-micromanufacturing with an optical tweezer (OT) process in a

bottom-up operation. For manipulation of non-spherical particles specific beam profiles can be used to induce desired three-dimensional movements. To combine the two processes of 2PP-manufacturing and OT-manipulation, external parameters have to be adjusted, because both processes work under unequal ambient conditions. Thus an optimal design integrating a fiber laser for holographic optical trapping is presented as well as important parameters which permit trapping of non-spherical 2PP-particles. The long-term objective is to develop an optical micro-machining tool for contactless manufacturing and manipulation in just one system.

8637-34, Session 8

Optimising forces and torques for optical micromanipulation

Simon Hanna, Stephen H. Simpson, David Phillips, Univ. of Bristol (United Kingdom)

The motion of a colloidal particle in an optical field depends on a complex interplay between the structure of the field, and the geometry and composition of the particle. There are two complementary approaches to generating a particular force field. The first, involving sculpting of the optical field with e.g. a spatial light modulator, has been extensively developed. A second method, highlighted recently [1], involves sculpting of the particles themselves, and has received much less attention. However, as modern two-photon polymerisation methods advance, this avenue becomes increasingly attractive for micromanipulation. In this paper we will show how computational methods may be used to optimise particle geometries in such a way as to produce desirable patterns of forces and torques. These designs are then tested using particles fabricated using the two-photon method. In particular, we will demonstrate the design of a constant force optical spring for use as a passive force clamp, a high efficiency optical wing, and a shape-optimised microtool.

[1] "Optical manipulation: Sculpting the object", J. Glückstad, Nature Photonics, V5, pp7-8, (2011)

8637-35, Session 8

Impedance matching an optical nano-antenna to a waveguided optical (dielectric) waveguide (*Invited Paper*)

Lars Rindorf, Danish Technological Institute (Denmark)

By careful design an optical nanoantenna may be a highly efficient capturer and emitter of light, with a scattering cross section much larger than its physical size (naively) merits. By proper design it may transmit light only in certain wavelength ranges while completely blocking other wavelengths in analogy to electrical pass-band/block band filter caused by impedance matching. This behavior can also be realized for different angles of incidence, different modes in the dielectric waveguides, or different polarizations of light.

Alu et al. (PRL 2008) showed how the methodology of microwave engineering could be adapted to work for optical nanostructures. Using this work as a basis we study the matching of optical nano-antennas to dielectric waveguides. It is shown that the strict definition of the RF (MHz-GHz) impedance notion must be relaxed to be practically adaptable for optical structures as the strict definitions makes it difficult to apply.

In the current work we intend to use the optical nano-antenna to address various functionalities in the recently demonstrated waveguided optical waveguide (WOW) by Palima et al. (Optics Express 2012). Specifically, we intend to study a WOW with an optical nano-antenna which can block the guiding light wavelength while admitting other wavelengths of light which address certain functionalities, e.g. drug release, in the WOW. In particular we study a bow-tie optical nano-antenna to circular dielectric waveguides in aqueous environments.

8637-36, Session 9

Optofluidics for energy applications (*Invited Paper*)

Demetri Psaltis, Ecole Polytechnique Fédérale de Lausanne (Switzerland)

Optofluidics refers to a class of devices and techniques that combine optics and fluidics. Biophotonics has been a major application of optofluidics partially because in biology we normally use light to make measurements of entities suspended in liquids. Therefore biophotonics naturally combines fluids and optics. The same thing is true in the field of solar fuels where generally chemicals in liquid form are exposed to sunlight which catalyzes or thermally accelerates a chemical reaction that generated useful fuels. The design of a solar fuel system requires the simultaneous optimization of the optical and fluidic properties of the system. We will discuss how optofluidic solar fuel systems [1] that rely on microstructured components with dual, optical and fluidic functionality can improve the fuel generation efficiency.

[1] Erickson D, Sinton D, Psaltis D, Optofluidics for energy applications, Nature Photonics, Vol. 5, pp. 583-590, October 2011

8637-37, Session 9

Azimuthal polarization for Raman enhancement in capillary waveguides

Jessica C. Mullen, Michael P. Buric, Steven D. Woodruff, National Energy Technology Lab. (United States)

Hollow, metal-lined capillary waveguides have recently been utilized in spontaneous gas-Raman spectroscopy to improve signal strength and response time. The hollow waveguide is used to contain the sample gases, efficiently propagate a pump beam, and efficiently collect Raman scattering from those gases. Transmission losses in the waveguide may be reduced by using an azimuthally polarized pump beam instead of a linearly or radially polarized pump. This will lead to improved Raman signal strength, accuracy, and response time in waveguide-based Raman gas-composition sensors. A linearly polarized laser beam is azimuthally polarized using passive components including a spiral-phase plate and an azimuthal-type linear analyzer element. Half-wave plates are then used to switch between the azimuthally polarized beam and the radially polarized beam with no change in input pump power. The collected Raman signal strength and laser-throughput are improved when the azimuthally polarized pump is used. Optimization of the hollow waveguide Raman gas sensor is discussed with respect to incident pump polarization.

8637-38, Session 9

Optimized systems for energy efficient optical tweezing

Ronald Kampmann, Roman Kleindienst, Andreas Oeder, Adrian Grewe, Stefan Sinzinger, Technische Univ. Ilmenau (Germany)

Optical tweezers are a powerful tool for analysis and manipulation e.g. in the fields of micro biology, chemistry and physics. However, the requirements on optical tweezers are different in each specific case. In microfluidics or production technologies for example microscopic objects have to be manipulated at large working distances and with best possible trapping forces per photon.

For this purpose we designed and fabricated a customized optical tweezer system. Our integrated design process includes an estimation of the trapping forces per incident photon for a specific field distribution in the focus. We apply algorithms based on geometrical and electromagnetic (Mie theory) force simulations. The optimized field

distributions are the merit functions for the optical design procedure performed in standard ray tracing tools. The optimized optical design combines refractive and reflective optical surfaces. An integrated refractive double axicon generates an annular intensity distribution which is perfectly focused by an annular offaxis parabolic mirror. This results in an aberration minimized high numerical aperture (NA) ring illumination. The high angles of incidence generate an efficient trapping field distribution in the focal plane of the parabolic mirror. For in situ observation it is possible to integrate additional optical elements in the center of the system.

The complete analytical optical design solution is used for the fabrication of the optical components by 5-axis ultraprecision micro machining. Systematic fabrication errors can be taken into account by online monitoring and compensation of the environmental conditions. Our optical design and fabrication procedures are verified by profilometric measurements as well as an investigation of the generated intensity distribution in the focal plane. First experimental results of the trapping performance are presented.

8637-39, Session 9

Single laser beam based passive optical sorter

Oto Brzobohary, Martin Šiler, Vitezslav Karasek, Lukáš Chvátal, Institute of Scientific Instruments of the ASCR, v.v.i. (Czech Republic); Tomáš Jiřmár, Univ. of St. Andrews (United Kingdom); Pavel Zemánek, Institute of Scientific Instruments of the ASCR, v.v.i. (Czech Republic)

We experimentally and theoretically demonstrate sorting of colloidal particle suspension (i.e. mixture of micrometer-sized particles of various diameters or compositions). The sorting is performed in a weakly focused laser beam that is reflected under an oblique angle. This approach is easy to implement while it provides very fast sorting of even dense samples. Moreover, we demonstrate effect of beam polarization on the sorting efficiency.

8637-40, Session 10

Analytical techniques for the study of focused beams (*Invited Paper*)

Miguel A. Alonso, Univ. of Rochester (United States)

Gaussian beams are useful paraxial solutions to the wave equation, and serve as the foundation for the definition of other solutions like Hermite- and Laguerre-Gauss beams. Gaussian beams correspond mathematically to spherical waves focused at a distant complex point. If the imaginary distance of this focus from the real space is not much greater than the wavelength, these complex focus-waves constitute nonparaxial generalizations of Gaussian beams. By using electric and magnetic dipoles instead of spherical waves, vector versions of these fields have been proposed.

In this talk we show several ways in which this technique can be used to study properties of focused fields beyond the paraxial regime. Complex focused dipoles can be used to model nonparaxial versions of Gaussian fields with linear, circular or elliptical polarizations, as well as other interesting polarization distributions like radial, azimuthal, and the recently proposed full Poincaré. Additionally, other interesting beam distributions can also be given analytically, including nonparaxial Airy-Gauss beams. Further, complete orthonormal bases can be generated that allow the efficient expansion of an arbitrary focused field, and that can be regarded as nonparaxial generalizations of Laguerre-Gauss beams. The Mie scattering coefficients for any of these fields is given in closed form, regardless of the angular spread of the field and the position of the particle, allowing analytic calculations of the forces and torques exerted on the particle by these fields. Finally, these analytic expressions lend themselves to the study of the interaction between orbital and spin angular momenta in the nonparaxial regime.

8637-41, Session 10

Mode analysis using the correlation filter method

Daniel Flamm, Christian Schulze, Friedrich-Schiller-Univ. Jena (Germany); Darryl Naidoo, Council for Scientific and Industrial Research (South Africa); Andrew Forbes, Council for Scientific and Industrial Research (South Africa) and Univ. of KwaZulu-Natal (South Africa); Michael Duparré, Friedrich-Schiller-Univ. Jena (Germany)

We introduce the correlation filter method for measuring the modal power spectrum of multi-mode beams. The method is based on an optical filter performing the integral relation of correlation. This filter is realized as a computer-generated hologram with a specifically designed transmission function based on the spatial distribution of the set of modes under test. The beam that is illuminating the hologram is generating a diffraction pattern containing information about modal amplitudes and intermodal phase differences. We will show that a simple single-shot intensity measurement is sufficient to gain the information about modal amplitudes and phases from the diffraction pattern which result in the ability to reconstruct the optical field under test including phase singularities.

The correlation filter method in combination with a Stokes parameter measurement enables to determine the polarization state of modes. This, in turn, allows for the reconstruction of the spatially varying polarization distribution of the beam.

Beside a detailed presentation of the measurement process, the setup and the design of the correlation filters, the major advantage of the method, the ability to perform real-time measurements is introduced. As a test system, we investigate the guided modes of a few mode multi-mode fiber and show fast changing modal coupling processes. Thereby, we show measurement results of online-monitoring the reconstructed optical field of the beam under test.

8637-43, Session 10

Modal decomposition for measuring the orbital angular momentum density of light

Christian Schulze, Daniel Flamm, Friedrich-Schiller-Univ. Jena (Germany); Andrew Forbes, Council for Scientific and Industrial Research (South Africa); Michael Duparré, Friedrich-Schiller-Univ. Jena (Germany)

We present a novel technique to measure the orbital angular momentum (OAM) density of light. The technique is based on modal decomposition, enabling the complete reconstruction of optical fields, including the reconstruction of the beams Poynting vector and the OAM density distribution. The modal decomposition is performed using a computer-generated hologram (CGH), which allows fast and accurate measurement of the mode spectrum. The CGH encodes the modes of interest, whose powers and relative phase differences are measured from the far-field diffraction pattern of the illuminating optical field with the hologram transmission function. In combination with a classical measurement of Stokes parameters, including a polarizer and a quarter-wave plate in front of the hologram, the polarization state of each mode is measured. As a consequence, any arbitrary vector field can be reconstructed, including amplitude, phase, and polarization. Having all information on the optical field, the Poynting vector and the OAM density can be calculated directly.

We applied our method to beams emerging from optical fibers, which allows us to investigate arbitrary coherent superposition of fiber modes with complexly shaped intensity and polarization distributions. The excitation of certain mode mixtures is done by appropriate input coupling and using diffractive phase masks to shape the input beam and hence enhance the excitation efficiency of distinct modes. The accuracy of the achieved results is verified by comparing the reconstructed with the directly measured beam intensity, revealing excellent agreement.

8637-44, Session 10

Polarization singularities and fiber modal decomposition

Nirmal K. Viswanathan, Vijay Kumar, Univ. of Hyderabad (India)

A partially coherent EM wave passing through an inhomogeneous medium (a two-mode optical fiber here) gives rise to different types of polarization singularities (PS) due to the interference of eigen (fundamental and/or vortex) modes of different phase and spatial variation of polarization. Singularities in 2D elliptic polarization fields are C-points (undefined polarization ellipse orientation) and L-lines (undefined polarization ellipse handedness). The generic topological charges are for C-point and for L-lines. The PS can be represented as:

Where, A is the amplitude, φ relative phase, waist of the Gaussian envelope, vortex charge and for linear and for circular bases. An isolated C-point surrounded by Lemon or Star PS pattern of index is formed due to the superposition of orthogonal circular-polarized (CP) Gaussian and vortex modes depending on the sign of l . Vectorial topological dipole is formed due to the superposition of orthogonal linear polarized Gaussian and vortex modes or two orthogonal CP vortex modes of same charge. On the other hand, superposition of orthogonal polarized and opposite charged vortex modes gives rise to two C-points of same indices. The relative amplitude and phase difference between the constituent modes determines the size of the L-contour and orientation of the Lemon, Star, and two C-points respectively. Using these features we propose and demonstrate a novel method for modal decomposition using PSs measured at the fiber output. This is a unique method for modal decomposition which utilizes the polarization and phase of the constituent modes in contrast to the existing techniques.

8637-49, Session 10

Optical tweezers at gigaPascal pressures

Richard W. Bowman, Univ. of Glasgow (United Kingdom); Filippo Saglimbeni, Univ. degli Studi di Roma La Sapienza (Italy); Graham M. Gibson, Univ. of Glasgow (United Kingdom); Roberto Di Leonardo, Univ. degli Studi di Roma La Sapienza (Italy); Miles J. Padgett, Univ. of Glasgow (United Kingdom)

Diamond anvil cells allow us to study the behaviour of materials at pressures up to hundreds of gigaPascals in a small and convenient instrument, however physical access to the sample is impossible once it is pressurised. Optical tweezers use tightly focussed lasers to trap and hold microscopic objects, and their ability to measure nanometric displacements and femtonewton forces makes them ubiquitous across the nano and bio sciences. We show that optical tweezers can be used to hold and manipulate particles in such a cell, in the "macro tweezers" geometry allowing us to use objective lenses with a higher working distance. Traps are structured to overcome the limitations imposed by the sample cell. We demonstrate the effectiveness of the technique by measuring water's viscosity up to 1.2 GPa. The maximum pressure reached was limited by the water crystallising under pressure.

8638-18, Session PWed

Radiative cooling of power LED by silicon photonic cooler

Volodymyr K. Malyutenko, V Lashkaryov Institute of Semiconductor Physics (Ukraine); Viacheslav V. Bogatyrenko, Oleg Y. Malyutenko, V. Lashkaryov Institute of Semiconductor Physics (Ukraine)

When it comes to semiconductors, conventional radiative cooling based on optical up conversion (anti-Stokes luminescence provoked by a laser beam) is difficult to perform. By fundamental reasons, up conversion net cooling could be realized only in direct bandgap semiconductors with internal quantum efficiency close to unity and extremely high extraction efficiency. Both are difficult to realize experimentally.

To bypass these limitations, we developed and experimentally demonstrated recently (JAP 108, 073104, 2010) new approach in radiative cooling by optical down conversion in Si, which is classical indirect bandgap semiconductor with very low internal quantum efficiency. Here we report the latest results on radiative cooling of an active electronic device. More specifically, we demonstrate net cooling of power green LED operating in CW mode ($I=300$ mA), and self heated up to 100-2000 C. The LED sits on and makes thermal contact with a cooler that is a 15 mm x 15 mm x 4 mm FZ Si substrate with carrier lifetime of 3 ms. Remote energy source (light pump) is a 1.09-micron diode laser beam focused on a wafer surface far away from the LED. We measure 50 C cooling/heating in both LED and Si wafer when the pump is on/off. The concept is based on the enhancement of thermal emission in Si (> 3 micron band) with power conversion efficiency well above 100 % provoked by free carrier generated with a light pump (PR B 76, 113201, 2007) and fueled with heat energy.

8638-1, Session 1

Optical refrigeration study of Er-doped oxysulfide crystal powders (*Invited Paper*)

Angel J. Garcia-Adeva, Daniel Sola, Mohammed Al Saleh, Univ. del País Vasco (Spain); Odile Merdrignac-Conanec, Univ. de Rennes 1 (France); Rolindes Balda, Joaquin Fernandez, Univ. del País Vasco (Spain) and Ctr. de Fisica de Materiales (Spain)

In the last years, considerable interest has been focused on the use of upconversion materials doped with trivalent-rare-earth (RE) ions for cooling processes. Most of them have been concerned with the bulk halide host materials with low phonon energies (especially for the chloride, including both single crystals and glasses, with phonon energies smaller than 500 cm^{-1}), which promise high upconversion luminescence efficiency by suppressing the nonradiative multiphonon relaxation. However, relatively little work has been reported on the upconversion luminescence of non-halide host materials. Among them, rare earth oxysulfide materials possess favorable physical properties, such as high chemical durability and thermal stability. They are widely used as the luminescent host materials of several commercially available phosphors, such as the red emitting phosphors for fluorescent lighting and cathode ray tube. In particular, lanthanum oxysulfide crystal matrix, a uniaxial P-3m wide-gap semiconductor material, is known as an excellent host lattice for trivalent RE ions having a maximum phonon energy of about 400 cm^{-1} . In the present investigation we have worked out the upconversion properties of Er^{3+} -doped $\text{La}_2\text{O}_2\text{S}$ crystal powders as well as its potentiality for anti-Stokes cooling. The latter has been studied by using infrared thermography upon excitation in the 800-900 nm infrared band. The wavelength and pumping power dependence of the temperature field across the powder has been investigated for a number of samples of various Er concentrations. It is found that cooling processes in these materials are most efficient upon excitation in resonance with a two or three-phonon anti-Stokes process. The implications of these findings and prospects for future work are discussed.

8638-2, Session 1

Non-radiative decay of holmium-doped laser materials (*Invited Paper*)

Steven R. Bowman, Shawn P. O'Connor, Nicholas J. Condon, E. Joseph Friebele, Richard S. Quimby, U.S. Naval Research Lab. (United States)

Anti-Stokes fluorescent cooling has been previously observed in resonantly pumped Ytterbium, Erbium, and Thulium doped optical materials. We have examined the 2.1 μm transition in trivalent Holmium as another potential eyesafe medium for optical cooling and high power lasers. Resonant optical pumping of the 5I7 \rightarrow 5I8 Ho^{3+} transition has been examined using sensitive room temperature calorimetry for several laser materials. We will report the pumping results and effective quantum defects measured in $\alpha\text{-SiO}_2$, $\text{Y}_3\text{Al}_5\text{O}_{12}$, Lu_2O_3 , YLiF_4 , ZBLAN, and KPb_2Cl_5 . Electron-phonon quenching is enhanced for the low energy 2.1 μm emission. Host materials were selected to provide the widest range of phonon energies for comparison with energy gap scaling.

8638-3, Session 1

Optical refrigeration progress: cooling below NIST cryogenic temperature of 123K (*Invited Paper*)

Seth D. Melgaard, The Univ. of New Mexico (United States); Denis V. Seletskiy, The Univ. of New Mexico (United States) and Air Force Research Lab. (United States); Alberto di Lieto, Mauro Tonelli, Univ. di Pisa (Italy); Mansoor Sheik-Bahae, The Univ. of New Mexico (United States)

We have achieved cryogenic optical refrigeration with a record low temperature in optical refrigeration by cooling 5% wt. $\text{Yb}:\text{YLF}$ crystal to $119\text{K} \pm 1\text{K}$ (≈ 154 C) at $\lambda=1020$ nm corresponding to its E4-E5 Stark manifold resonance with an estimated cooling power is 180 mW. This demonstration confirms the predicted minimum achievable temperature (MAT). Further cooling is achievable as shown by measurements of a doping study where a 10% wt. $\text{Yb}:\text{YLF}$ crystal with reduced parasitic heating has predicted cooling below 100K ($\approx 173\text{K}$).

8638-4, Session 1

Progress towards cryogenic temperatures in intracavity optical refrigeration using a VECSEL

Alexander R. Albrecht, Mohammadreza Ghasemkhani, The Univ. of New Mexico (United States); Jeffrey G. Cederberg, Sandia National Labs. (United States); Denis V. Seletskiy, The Univ. of New Mexico (United States) and Air Force Research Lab. (United States); Seth D. Melgaard, Mansoor Sheik-Bahae, The Univ. of New Mexico (United States)

We report on the use of a high power vertical external-cavity surface-emitting laser (VECSEL) utilizing 12 InGaAs quantum wells emitting around 1020nm for laser cooling. The emission wavelength of the laser can be controlled and stabilized using a birefringent filter. A 5% Yb-doped YLF crystal is placed inside the VECSEL cavity under Brewster angle, the whole cavity is inside a vacuum chamber, to reduce the convective heat load of the cooling sample. Starting from room temperature, a cooling of the YLF crystal by 78K is observed. Similar crystals have now reached temperatures below the NIST-defined cryogenic temperature of 123K when pumped at 1020nm outside of the laser cavity, using a non-resonant, multi-pass pumping scheme. We discuss the progress, advantages, and challenges of laser cooling

inside a VECSEL cavity, including the VECSEL active region design for optimized operating wavelength and power; the design of a compact cavity that can accommodate a birefringent filter for wavelength control, as well as the cooling sample; and the dimensions and doping level of the YLF crystal for optimal cooling. The path towards a compact and efficient, vibration and cryogen free, all solid state cryocooler device is outlined.

8638-5, Session 1

Laser cooling with rare-earth doped direct band gap semiconductors (*Invited Paper*)

Galina A. Nemova, Raman Kashyap, Ecole Polytechnique de Montréal (Canada)

Laser cooling of solids with anti-Stokes fluorescence was proposed in 1929¹ and experimentally realized for the first time in Yb³⁺-doped ZBLANP sample in 1995.² In 2009, the first cryogenic operation was demonstrated in Yb³⁺:LiYF₄ crystal.³ Today laser cooling of solids with anti-Stokes fluorescence has already been observed with Yb³⁺, Tm³⁺, and Er³⁺ rare-earth (RE) ions in wide variety of glass and crystal hosts. In all laser cooling experiments, the hosts are insulating materials and only the ground and excited levels of RE ions are involved in the cooling cycle. The valence as well as conduction bands of the isolator hosts do not participate in cooling process. RE-doped semiconductors have been extensively studied in view of their potential applications in optoelectronics and telecommunication.⁴ Contrary to devices based on RE-doped isolators, in all devices based on RE-doped semiconductors the valence and conduction bands are involved in the operation of the devices. We consider laser cooling with RE-doped semiconductor (Yb³⁺:InP), where the pump source excites electrons from the ground (2F_{7/2}) to the excited level (2F_{5/2}) of the Yb³⁺ ions and the intrinsic thermal quenching of the 4f-shell provides the energy transfer with the generation of the electron-hole pairs at the acceptor-like electron trap. Future thermalization results in electron and hole generation in the bands. During thermal quenching, the phonon absorption process takes place. The electron-hole radiative recombination removes energy from the system leading to its refrigeration. It is shown that the increase in the difference between the energy of the absorbed photon and the radiated one results in an increase in the cooling efficiency of up to 10 times compared with laser cooling in RE-doped isolator hosts. The cooling process can be accelerated considerably by the decreased radiative lifetime.

- [1]. P. Pringsheim, Z. Phys. 57, 739 (1929).
- [2]. R. I. Epstein et al., Nature (London) 377, 500 (1995).
- [3]. D. V. Seletskiy et al., Demonstration of an optical cryocooler CLEO/IQEC 2009 (Post deadline submission).
- [4]. M. A. J. Klik, T. Gregorkiewicz, Phys. Rev. Lett. 89, 227401 (2002).

8638-6, Session 2

Electro-luminescent cooling: light-emitting diodes above unity efficiency (*Invited Paper*)

Rajeev J. Ram, Parthiban Santhanam, Duanni Huang, Dodd Grey, Massachusetts Institute of Technology (United States)

The observation of light emission with photon energy in excess of the electrical input energy per electron (qV) is readily accessible in LEDs at a variety of wavelengths. At these operating points, the electron population is pumped by a combination of electrical work and Peltier heat originating in the semiconductor's lattice. As early as 1953 this phenomenon had been experimentally observed in a SiC emitter and connected physically to the Peltier effect. Nevertheless, net cooling, or equivalently electroluminescence with wallplug efficiency greater than unity, has eluded direct observation for more than five decades.

The primary limitation has been that the overall efficiency of electrical-to-optical energy conversion is small as the likelihood of radiative

recombination (quantum efficiency) is low when $hw/qV > 1$ and decreases as V decreases. Recently, a new regime for electroluminescent cooling of a semiconductor diode was experimentally demonstrated. In this regime application of a forward bias voltage V less than the thermal voltage $kBT = q$ imposes a small deviation from thermodynamic equilibrium on the device. In response, the rates of both radiative and nonradiative recombination in the device's active region have contributions at linear order in V, so that the external quantum efficiency is voltage independent. As a result, the LED's optical output power scales linearly with voltage while the input power scales quadratically, resulting in arbitrarily efficient photon generation accompanied by net electroluminescent cooling of the solid at low bias. Experimental evidence of electro-luminescent cooling will be presented for infrared LEDs over a range of wavelengths and temperatures.

8638-7, Session 2

Laser cooling of a semiconductor by 40 kelvin (*Invited Paper*)

Qihua Xiong, Jun Zhang, Dehui Li, Renjie Chen, Nanyang Technological Univ. (Singapore)

We demonstrated the first net laser cooling in a semiconductor using cadmium sulfide (CdS) nanobelt facilitated by multiple longitudinal optical phonon assisted upconversion. By monitoring the peak shift of Stokes photoluminescence spectra probed by 473 nm laser with a low power, local temperature variation of CdS nanobelts suspended holes etched on SiO₂/Si substrates can be measured with different laser pumping (488, 502, 514 and 532 nm). Under a low power excitation, we have achieved a ~40 K and ~20 K net cooling in CdS nanobelts starting from 290 K pumped by 514 nm and 532 nm lasers, respectively. We have also obtained a ~15 K cooling from 100 K pumped by a 532 nm laser. The cooling effect is critically dependent on the pumping wavelength, the blue shifting parameters and the absorption, the latter of which can be evaluated from photoconductivity measurement on individual nanowire level. Detailed spectroscopy analysis suggests that cooling to even lower temperature is possible in CdS nanobelt if thermal management is optimized. To explain the cooling effect in CdS nanobelts, we propose that multi-phonon resonance play an important role due to enhanced Fröhlich interactions in CdS nanobelts, as such more than one longitudinal optical phonon is destroyed in each cooling cycle leading to significantly enhanced blue shifting parameter. Although the complete theory to explain the up-conversion process of CdS nanobelts still remains to be developed, our findings suggest alternative II-VI semiconductors for laser cooling compared to III-V GaAs-based heterostructures.

8638-8, Session 2

Laser cooling of a thermal load using CdS nanobelts

Qihua Xiong, Dehui Li, Jun Zhang, Renjie Chen, Nanyang Technological Univ. (Singapore)

In this report, we demonstrated the cooling of the silicon on insulator (SOI) using CdS nanobelts dispersed on the SOI substrate. We have realized a 34 K and 43 K net cooling starting from 290 K under a 4.5 mW 514 nm and a 7 mW 532 nm pumping, respectively. In contrast, the heating has been observed while pumped by 502 nm and 488 nm lasers. A net cooling of ~ 50 K for the same nanobelt, which are suspended across holes etched on the SOI, has been achieved as well starting from 290 K. The difference can be attributed to thermal conductive losses.

8638-9, Session 2

Multi-phonon and Raman assisted cooling in semiconductors (*Invited Paper*)

Jacob B. Khurgin, Johns Hopkins Univ. (United States)

In this talk I describe the theory of cooling the semiconductors using the below-the-bandgap excitation. We show that two different processes can contribute to the cooling. The first one is the real process of multi-phonon-assisted absorption followed by Anti-stokes luminescence. The second one is a virtual resonantly-enhanced Anti-Stokes Raman scattering. The cooling efficiency for both cases is limited by phonon-assisted luminescence and Stokes Raman scattering, but in general these processes do show promise of net cooling in polar semiconductors with strong electron-phonon interaction.

8638-10, Session 2

Laser cooling attempts in high-quantum efficiency GaInP/GaAs double heterostructures

Daniel Bender, Jeffrey G. Cederberg, Sandia National Labs. (United States); Chengao Wang, Mansoor Sheik-Bahae, The Univ. of New Mexico (United States)

Optical refrigeration could be a technology to create a next generation cryocooler whose operation would be solid state and free from refrigerants that can leak. Such a cooler would have numerous benefits over existing technology for space-based cryocooling. A semiconductor based optical cooler offers the attraction of direct integration with focal plane array sensor layers and motivates our attempts to cool GaAs. We report on recent attempts to optically cool the GaAs/GaInP semiconductor double heterostructure. By varying the growth conditions at the GaAs/GaInP interface we are able to produce a record external quantum efficiency of $99.5 \pm 0.1\%$ in GaAs. This efficiency is in excess of what is expected to be needed to demonstrate cooling in GaAs; however, cooling has not yet been realized due to background absorption. Experimental cooling attempts will be presented and the issue of background absorption below the band edge will be discussed. Further, will we present ideas for ways to lower the background absorption during the growth process. Through low temperature photoluminescence and fractional heating measurements we show characterization of background absorption for different samples produced by varying constituent gas partial pressure during GaAs growth.

Sandia National Laboratories is a multi-program laboratory managed and operated by Sandia Corporation, a wholly owned subsidiary of Lockheed Martin Corporation, for the U.S. Department of Energy's National Nuclear Security Administration under contract DE-AC04-94AL85000.

8638-11, Session 3

Laser cooling by collisional redistribution of radiation in dense gases (*Invited Paper*)

Martin Weitz, Anne Sass, Rheinische Friedrich-Wilhelms-Univ. Bonn (Germany); Ulrich Vogl, Univ. of Maryland, College Park (United States); Peter Moroshkin, Rheinische Friedrich-Wilhelms-Univ. Bonn (Germany)

Laser cooling of atomic gases via collisional redistribution of radiation is a cooling technique based on laser-induced transitions in a high pressure buffer gas environment demonstrated first in 2009 [1]. The cooled gas has a density of more than ten orders of magnitude above the typical values in Doppler cooling experiments of dilute atomic gases. Here we present further development of that experimental work and new theoretical analysis results of the obtained cooling effect.

Redistribution cooling is observed with a mixture of rubidium atoms

and a rare buffer gas at a few hundred bars pressure. Highly red detuned incident optical radiation can be absorbed when a buffer gas atom approaches a rubidium atom in the dense gas sample. On the other hand, spontaneous decay occurs mostly at larger perturber distances, so that the emitted photons have higher frequencies than the incident radiation and the gas ensemble is cooled. Thermal deflection measurements presently indicate a cooling within the dense gas sample to cryogenic temperatures starting from an initial temperature of few hundred degrees Celsius in the heated gas cell. We have carried out model calculations to solve the heat transport problem in the dense gas cell, showing reasonable agreement between theory and experiment. The new laser cooling technique is suitable for the cooling of "macroscopic" gas ensembles of high density. We are also setting up a new experiment on collisional redistribution cooling of molecular gases.

[1] U. Vogl and M. Weitz, Nature 461, 70 (2009)

8638-12, Session 3

Electrocaloric refrigerator using electrohydrodynamic flows in dielectric fluids (*Invited Paper*)

Markus P. Hehlen, Alexander H. Mueller, Nina R. Weisse-Bernstein, Los Alamos National Lab. (United States); Miad Yazdani, United Technologies Research Ctr. (United States); Richard I. Epstein, ThermoDynamic Films LLC (United States)

The electrocaloric effect (ECE) observed in thin films of ferroelectric polymers or oxides has attracted much interest in recent years for its potential use in refrigerators and electrical generators. Applying an electric field to an electrocaloric material raises its temperature, and removing the electric field lowers its temperature. A refrigerator can be constructed by placing an electrocaloric material between two heat switches. The performance of such an electrocaloric heat pump depends on the ratio K of the effective thermal transport coefficients of the heat switch in the closed and open state. Such a heat engine could outperform thermoelectric coolers if $K > 10$ and vapor-compression refrigerators if $K > 100$. One way to construct a heat switch is to use electrohydrodynamic (EHD) flows in dielectric fluids to enable thermal switching between a closed state (mainly convection) and an open state (mainly conduction). Here we report on thermal transport switching in thin layers of dielectric fluids driven by EHD flows from an array of interdigitated metal electrodes. Biasing the electrode array with 500 V drew a 420 nA ohmic DC current and induced fluid convection. An associated switching of thermal transport coefficients from 70 W/m/K to 300-400 W/m/K was measured. This corresponds to a switching contrast $K \sim 6$ and demonstrates the potential of this thermal switching approach. We will review the physical principles behind electrocaloric refrigeration and explore the application of this technology to solid-state laser refrigeration devices.

8638-13, Session 3

Brillouin cooling (*Invited Paper*)

Tal Carmon, Univ. of Michigan (United States)

Brillouin scattering [1-4] is one of the most important and generic processes in light-matter interaction [1-8] as it couples electromagnetic waves and acoustic waves. A lesser-known capacity of Brillouin scattering is cooling. This is because in bulk materials [1-5] phonon annihilation is inherently accompanied by the competing process of phonon creation. However, by engineering the optical and vibrational properties in confined geometries, we can selectively favor the anti-Stokes process, giving rise to net phonon absorption. Here, we experimentally demonstrate spontaneous anti-Stokes Brillouin cooling, performed in an ultra-high Q microcavity. Our technique exploits efficient scattering between two optical modes to resonantly enhance only the blue side of the Brillouin-scattering spectra, breaking the cooling-heating symmetry of the scattering process. The device allows an acoustic

density wave to transfer energy to light, thereby reversing the energy flow in the Brillouin process [2] demonstrated by laser pioneer Charles Townes half a century ago. We show here that a scattering process in nature has been used to cool solids [9]. Although many challenges exist, our Stokes-filtering technique might be extended to enable the Raman cooling of solids.

8638-14, Session 3

Optomechanical interactions in piezoelectric thin films (*Invited Paper*)

Matt Eichenfield, Sandia National Labs. (United States)

Consider an x-y cut, optically thin film of a piezoelectric material like aluminum nitride and, in that slab, a guided TE plane-wave propagating in the plane of the slab. There always exists a microwave frequency acoustic (Lamb) wave *with the same wavelength*, with a strain that induces a displacement current polarized like the optical wave. These two waves are fundamentally coupled to one another via the piezoelectric effect, and--in fact--renormalize each other, resulting in a modification of the speed of propagation of both waves.

Unfortunately, because of the vastly different acoustic and optical velocities, the MMPOM interaction cannot be resonant both spatially and temporally. Thus, the effect has historically been ignored, as--even in highly piezoelectric materials--it only changes the speed of the waves by a part in 10^8 . However, for 200 THz photons, which would be coupled to ~10 GHz phonons, the MMPOM-induced shift would be 2 MHz. This is twice as large as the largest shift ever demonstrated in a conventional optomechanical system employing 200 THz photons. Moreover, by carefully tailoring the modal dispersion via patterning the film into a piezoelectric optomechanical crystal, one can significantly slow the optical velocity without slowing the acoustic velocity, enhancing the interaction even further.

The MMPOM interaction has a very different Hamiltonian than the conventional, parametric optomechanical interaction, which induces an interaction between the acoustic field and the optical intensity. The MMPOM Hamiltonian is a direct, field-field interaction, which endows these systems significantly different physical properties than their conventional optomechanical counterparts. With this in mind, I will discuss new and interesting phenomena in microfabricatable systems employing MMPOM interactions, as well as potential applications.

8638-15, Session 4

Towards all-fiber optical coolers using Tm-doped glass fibers (*Invited Paper*)

Dan T. Nguyen, Jie Zong, Dan L. Rhonehouse, Andy Miller, NP Photonics, Inc. (United States); Garrett Hardesty, Nai Kwong, College of Optical Sciences, The Univ. of Arizona (United States); Rolf Binder, College of Optical Sciences, The Univ. of Arizona (United States) and The Univ. of Arizona (United States)

Optical cooling in Tm-doped glass fibers is potentially applicable in many device applications due to its light weight, compact, vibrationless and micro-scale design and the potential for long lifetimes even in harsh space conditions. More important, the cooling fiber can be easily integrated to an optical fiber system that can transfer part of the heat to a remote location. However, there are also challenges to be overcome for optical cooling in the fibers such as small absorption/cooling volume, parasitic heat generated from impurities in the glass, and loss in fiber couplings. Also, scattered light can create heat. In this report, we present our investigation of optical cooling in an all-fiber system. We used different wavelengths from 1940nm to 1992nm, single-mode Tm+3-doped fiber lasers with high efficiency and high power to pump a Tm+3-doped glass fiber, which is designed to provide the cooling action on an affixed heat source. The effects of impurities including OH-absorption and transition metals have been investigated systematically using different purified glasses for fiber fabrication. The concept of piping

waste photons to remote heat dumping will be discussed. Experimental results with spectroscopic and thermistor measurements indicate cooling effects in the system, and are simulated theoretically.

8638-16, Session 4

Accurate measurement of external quantum efficiency in semiconductors (*Invited Paper*)

Chengao Wang, The Univ. of New Mexico (United States); Jeffrey G. Cederberg, Daniel Bender, Sandia National Labs. (United States); Mansoor Sheik-Bahae, The Univ. of New Mexico (United States)

The state of current research in laser cooling of semiconductors is reviewed. Record external quantum efficiency (99.5%) is obtained for a GaAs/InGaP heterostructure bonded to a dome lens at 100 K by wavelength-dependent laser-induced temperature change (scanning laser calorimetry).

Power-dependent photoluminescence measurement (PDPL) is proved to be an efficient way to determine the quantum efficiency and screen the sample quality before processing and fabrication. Second harmonic generation (767nm) from a 5ns Er:YAG laser is used as the pump source for the PDPL experiment.

Absorption measurement is also used as a tool to quantitatively determine the quality of wafer bonding, which is a critical step in the manufacture of devices for laser cooling of semiconductors.

8638-17, Session 4

Spectroscopic and life-time measurements of quantum-doped glass for optical refrigeration: a feasibility study

Sébastien Loranger, Antoine Lesage-Landry, Elton Soares de Lima Filho, Galina Nemova, École Polytechnique de Montréal (Canada); Paulo C. Morais, Noelio O. Dantas, Univ. Federal de Uberlândia (Brazil); Raman Kashyap, École Polytechnique de Montréal (Canada)

We show for the first time to our knowledge, measurements of anti-Stokes fluorescence, and show lifetime measurements in quantum dot (QD) doped glass, which has been proposed as a potential material for optical refrigeration¹. It was suggested in Ref. 1 that such dopants would drastically improve the efficiency of optical refrigeration, which would allow cooling in high phonon energy materials, since QDs exhibit a high cross-section and a very short fluorescence life-time in comparison with rare earth ions dopants. The glass host studied here is known as SNAB (SiO₂, Na₂CO₃, Al₂O₃, B₂O₃) and is doped with PbS QDs. We show that when excited at a proposed pump wavelength (1340 nm and 1550 nm) for cooling, anti-Stokes fluorescence is emitted, which is required for laser cooling. We also show fluorescence lifetime measurements of those QDs, which is in the order of 300 ns. Such lifetime is 4-5 orders of magnitudes smaller than the typical lifetime of rare earth dopants. From additional fluorescence spectrum measurements at higher energy (pumping wavelength 1.064 μm), we estimate the quantum efficiency of such a system. The observation of anti-Stokes fluorescence and short lifetime is evidence that QDs could be developed as cooling dopants, however improvements would have to be made in the quantum efficiency as well as the background absorption of the host glass for successful applications.

References:

1. G. Nemova and R. Kashyap, "Laser cooling with PbSe colloidal quantum dots," J. Opt. Soc. Am. B, 29, 676-682 (2012).

Conference 8639: Vertical-Cavity Surface-Emitting Lasers XVII

Wednesday - Thursday 6 -7 February 2013

Part of Proceedings of SPIE Vol. 8639 Vertical-Cavity Surface-Emitting Lasers XVII

8639-1, Session 1

VCSELS for high-speed data networks (*Invited Paper*)

M. V. Ramana Murty, Avago Technologies Ltd. (United States);
Sumon K. Ray, K.-L. Chew, Max V. Crom, Aadi Sridhara, C. Zhao,
Chu Chen, Tom R. Fanning, Avago Technologies Singapore
(Singapore)

Applications of 850 nm VCSELS have bloomed in recent years arising from their low cost, and the ease of forming one- and two-dimensional arrays. In addition to the traditional measures of operation over a wide temperature range, link length and device lifetime, the figures of merit increasingly include power consumption (pJ/bit), footprint (bits/mm²) and cost (\$/Gb/s). As 1 x 12 arrays of 10G VCSELS are widely adopted, there is a clear need for improvement along all these fronts. This is achieved through development of VCSELS operating at higher data rates, and modifications to the VCSEL structure.

In this paper, we will discuss the development of VCSELS operating at 10 - 25 Gb/s. An aperture size of 8 - 9 μ m is sufficient for 10 Gb/s, while smaller apertures are used for operation at the higher data rates. The devices exhibit low threshold current, the emission spectrum shows multiple transverse modes, and the small-signal 3 dB bandwidth exceeds 15 GHz over temperature for the smaller aperture devices. These features provide the bases for devices for the emerging 25 Gb/s applications. The dc, ac, and spectral characteristics of the VCSELS will be discussed in the context of the operation at various data rates.

8639-2, Session 1

The next-generation high-data rate VCSEL development at SEDU (*Invited Paper*)

Chuan Xie, Neinyi Li, Shenghong Huang, Li Wang, Chiyu Liu,
Sumitomo Electric Device Innovations, U.S.A., Inc. (United States)

In May of 2012, Emcore's VCSEL FAB and VCSEL based transceiver business became part of Sumitomo Electric Device Innovations USA (SEDU). After this change of ownership, our high speed VCSEL development effort continues. In this paper, we will first update the VCSEL FAB's transition. We will then report the progress made in the past year in our 25Gbps to 28Gbps VCSEL. This next generation device is targeted for EDR, 32GFC as well as other optical interconnect applications.

8639-3, Session 1

Progress and challenges in industrial fabrication of wafer-fused VCSELS emitting in the 1310-nm band for high-speed WDM applications (*Invited Paper*)

Vladimir Iakovlev, Alexei Sirbu, Zlatko Mickovic, Dalila Ellafi, Eli Kapon, Ecole Polytechnique Fédérale de Lausanne (Switzerland);
Grigore Suruceanu, Alexandru Mereuta, Andrei Caliman, Beam Express S.A. (Switzerland)

Building wavelength-multiplexed transmitter modules like, for example, 4x10 Gbps coarse-wavelength division-multiplexing (CWDM) modules emitting at 1271, 1291, 1311 and 1331 nm based on low power consumption VCSELS has the promise in dramatic decreasing of module power consumption. Wafer fusion approach proved to be very successful in demonstrating state of the art vertical cavity surface emitting lasers

(VCSELS). Standard design comprises InAlGaAs/InP quantum wells, tunnel junction injection of carriers in the active region which determines the device aperture and 2 distributed Bragg reflectors (DBRs). Several issues are being addressed in the work for entering the large-scale applications of such VCSELS in optical communication systems:

- (i) wavelength setting of emission wavelength within (CWDM) grid
- (ii) trade-off between VCSEL bias current for high speed modulation, operation power and voltage.
- (iii) Compatibility with industry standards in VCSEL fabrication and packaging.
- (iv) Reliability in operation conditions of these devices according to industry standards.

Over the last years we have demonstrated continuous improvements of parameters and reliability of wafer fused long-wavelength VCSELS. Progress and challenges in industrial fabrication of "GREEN" wafer-fused VCSELS emitting in the 1310 nm band for high speed WDM applications will be discussed in the talk.

8639-4, Session 2

Progress in extended wavelength VCSEL technology (*Invited Paper*)

Klein Johnson, Matthew Dummer, William Hogan, Mary Hibbs-Brenner, Charles Steidl, Vixar Inc. (United States)

While 850nm VCSELS have a long history of development and are widely available on a commercial basis, VCSELS at other wavelengths are less common and at an earlier stage of maturity. Vixar has been developing VCSELS at both shorter (680nm) and longer (1850nm) wavelengths. This paper reports on advances in technology at both of these wavelengths.

680nm VCSELS based upon the AlGaAs/AlGaInP materials system were designed and fabricated for high speed operation for plastic optical fiber (POF) based links for industrial, automotive and consumer applications. High speed testing was performed in a "back-to-back" configuration, coupling the output of the VCSEL into a short length of glass fiber and then into an 8GHz Picometrix O/E. Eye diagrams were collected at a variety of temperatures up to 90°C, with open eyes observed to 10Gbps. Devices were then coupled into various types and lengths of POF. While testing over various speeds and fiber lengths is still on-going, good performance at 3Gbps has been demonstrated over 15 meters of Partially Chlorinated POF (PCP), 4.25Gbps over 8 meters of PCP, and 1Gbps over 10 meters of standard 1mm diameter step index PMMA. Reliability testing has been performed over a range of temperatures and currents. Preliminary results predict a TT1% failure of at least 200,000 hours at 40°C and an average current modulation of 4mA. In addition, the VCSELS survive 1000 hours at 85% humidity 85°C in a non-hermetic package.

1850nm InP based VCSELS are being developed for optical neurostimulation. The goals are to optimize the output power and power conversion efficiency. 7mW of DC output power has been demonstrated at room temperature, as well as a power conversion efficiency of 12%. Devices operate to 85°C.

8639-5, Session 2

Nonpolar gallium nitride VCSELS (*Invited Paper*)

Casey Holder, Univ. of California, Santa Barbara (United States);
Daniel Feezell, The Univ. of New Mexico (United States);
James S. Speck, Steven P. DenBaars, Shuji Nakamura, Univ. of California, Santa Barbara (United States)

Nonpolar and semipolar orientations of gallium nitride offer several

**Conference 8639:
Vertical-Cavity Surface-Emitting Lasers XVII**

advantages for vertical-cavity surface-emitting lasers (VCSELs). The reduction or absence of the quantum-confined Stark effect in nonpolar and semipolar quantum wells leads to devices with enhanced radiative efficiencies and higher optical gain compared to c-plane oriented VCSELs. Additionally, anisotropic gain within the quantum well plane should result in a consistent and well-defined polarization direction of the emission in nonpolar and semipolar VCSELs.

A major difficulty in fabrication of GaN-based VCSELs is the formation of the bottom facet and DBR mirror. Epitaxial DBR mirrors have been demonstrated on c-plane VCSELs, but these are very difficult to manufacture, especially on non-c-plane orientations where additional relaxation mechanisms are available. Dielectric bottom DBRs have been used to demonstrate GaN-based VCSELs after substrate removal. Substrate removal for c-plane VCSELs grown on sapphire has been achieved using laser liftoff, but this method is precluded with freestanding GaN substrates. Lapping/polishing has been used to thin the substrate for VCSELs fabricated on free-standing GaN, but this method gives little control of cavity length.

We report the first known electrically-injected nonpolar m-plane GaN VCSELs, operating under pulsed injection at room temperature. As predicted, m-plane GaN VCSELs exhibit polarization locking, with the polarization direction consistently oriented along the a-direction of the wurtzite crystal structure. We also report a novel fabrication method, utilizing photoelectrochemical etching of a sacrificial InGaN region for substrate removal and cavity length definition. This method allows for the use of dielectric DBR mirrors with freestanding GaN substrates, while maintaining precise control of cavity length by placement of the sacrificial layer during epitaxial growth.

Initial device results include a wavelength of 411.9 nm with a FWHM of 0.25 nm and a maximum observed power output of 19.5 μ W. Devices have exhibited polarization ratios higher than .7 above threshold (with no additional measures taken to account for spontaneous emission or to reduce collection of scattered light). These initial results and additional results, as well as the fabrication method employed, will be presented and discussed.

8639-6, Session 2

Comprehensive electro-opto-thermal simulation of GaSb-based VCSELs

Zhiqiang L. Li, Simon Li, Crosslight Software Inc. (Canada)

Recently electrically-pumped and continuous-wave operating single-mode VCSELs emitting at 2.3-2.6 μ m have been demonstrated based on GaSb materials. There are several unique features in the design:

- 1) strained AlGaAsSb quantum wells (QWs) offering long wavelength (2-3 μ m) emitting light.
- 2) A buried tunnel-junction is located above the QW region providing lateral electrical and optical confinement by selective etching.
- 3) p-type layers are substituted by n-type ones increasing carrier mobility and reducing the self-heating.
- 4) Lattice-matched n-doped AlAsSb/GaSb superlattice is used as n-DBR.
- 5) Amorphous Si/SiO₂ layers are used as top DBR.
- 6) Intra-cavity contacts feed the current directly into highly conductive layers.

Despite the promising performance of GaSb-based VCSELs, the development has been hindered by the complicated device structure and insufficient knowledge on material data. Accurate device modeling would help to find the optimum design and substantially reduce the cost of experiments.

In Crosslight, we have developed comprehensive advanced models to simulate electric, optical and thermal behaviour of VCSELs. For electric problem, the Poisson equation solves for the potential generated by given carrier distribution, and the continuity equation describes how carriers transport following the potential. It provides the carrier densities in QW region for calculating the material gain by Schrodinger equation. It also provides the refractive index changes to the optical solver, which

solves for the optical modes and feeds the optical mode to the photon-rate equation. The photon-rate equation solves for the photon density which translates to the optical power, and it is coupled to the Poisson and continuity equations by stimulated and spontaneous emission rates.

These models give a comprehensive insight into the physics of the device, such as optical gain and loss, threshold current, current-voltage relation, thermal roll-over, 2D temperature distribution, optical mode and carrier distribution etc.

8639-7, Session 3

Ultra-compact vertical-cavity surface-emitting lasers using a double set of photonic crystal mirrors (*Invited Paper*)

Corrado Sciancalepore, Institut des Nanotechnologies de Lyon (France) and CEA-LETI-Minatec (France); Pierre Viktorovitch, Institut des Nanotechnologies de Lyon (France); Badhise Ben Bakir, CEA-LETI-Minatec (France); Xavier Letartre, Christian Seassal, Institut des Nanotechnologies de Lyon (France)

It is well known that high-contrast metastructures can be exploited to perform a controllable coupling between matter and electromagnetic radiation. At optical frequencies this paves the way toward an arbitrarily adjustable spatio-temporal molding of light at the wavelength scale. In detail, high-index-contrast periodic structures such as photonic crystal membranes (PCMs) can be used for controlling the resonant coupling of radiated light to “heavy photons” states in strongly corrugated waveguides, thus putting photons through a slowed-down transport regime which results in an efficient quasi-3D light harnessing. More recently, one-dimensional Si/silica photonic crystals have been adopted as compact, flexible, and power efficient mirrors in vertical-cavity surface-emitting lasers (VCSELs) emitting in C-band which have been realized within a mass-scale fabrication paradigm by employing standard 200-mm microelectronics pilot lines. The extreme flexibility of such innovative photonic architecture enables to perform a fully-controllable transverse mode filtering, including polarization and far-field control, while the strong near-field mode overlap within mirrors can be exploited to implement unique optical functions such as on-chip optical routing and enhanced sensing capabilities. Furthermore, device compactness ensures a considerable reduction in the device footprint, power consumption and parasitics, adding in required features for broadband modulation and high-speed data processing. High fabrication yields obtained via molecular wafer bonding of III-V alloys on silicon conjugate excellent device performances with cost-effective high-throughput production, addressing industrial needs for a fast research-to-market transfer. In conclusion, double photonic crystal VCSELs constitute thus a robust high-performance building block for the follow-through of semiconductor lasers and VCSEL photonics.

8639-8, Session 3

Heat assisted magnetic recording (HAMR) with nano-aperture VCSELs for 10 Tb/in² magnetic storage density

Sajid Hussain, Shreya Kundu, National Univ. of Singapore (Singapore); Charanjit S. Bhatia, National Univ. of Singapore (Singapore); Hyunsoo Yang, Aaron Danner, National Univ. of Singapore (Singapore)

We have conducted a thorough experimental analysis of nano-aperture VCSELs for use in heat-assisted magnetic recording (HAMR). To the best of our knowledge, this is the first study to both explore the impact of magnetic media proximity on VCSEL aperture power throughput and to use statistical methods to simultaneously characterize thousands of aperture designs.

To achieve areal recording densities beyond 1 Tb/in², high anisotropy

**Conference 8639:
Vertical-Cavity Surface-Emitting Lasers XVII**

magnetic materials are required to overcome the super-paramagnetic effect. These require high switching fields which are not conventionally available. Heat assisted magnetic recording (HAMR) is a potential technology to reduce the coercivity of the media and thus the required switching field by localized heating to enable writing of bits. The challenges being faced by this technology are to develop a precise method of delivering light to a very small, subwavelength bit area with sufficient power through a near field aperture, and the fabrication of a laser source which can be integrated with current write heads used in hard disk drives. The focus of our work is to characterize nano-aperture VCSELs and test their potential application to HAMR. We have fabricated 850 nm VCSELs with large arrays of differently shaped nano-apertures in the gold layer on top of each VCSEL. Unlike previous methods in which a single nano-aperture on a VCSEL has been characterized, our array method allows use of statistical methods to optimize aperture designs with a high degree of accuracy. C-shaped and H-shaped nano-apertures have also been fabricated in a gold layer deposited on a SiO₂ substrate to observe the effect of close proximity of magnetic media (FePt) on the performance of nano-apertures, and polarization effects have also been characterized.

The light coming out of the nano-aperture arrays will be focused on high coercivity FePt material in the presence of available external magnetic field. MFM will be used to observe the switching in the media

8639-9, Session 3

VCSELs with nematic and cholesteric liquid crystal overlays

Krassimir Panajotov, Vrije Univ. Brussel (Belgium); Maciej Dems, Technical Univ. of Lodz (Poland); Carlos Belmonte, Hugo Thienpont, Vrije Univ. Brussel (Belgium); Yi Xie, Jeroen Beeckman, Kristiaan Neyts, Univ. Gent (Belgium)

We study theoretically the spectral and polarization threshold characteristics of Vertical-Surface-Emitting Lasers with nematic (cholesteric) liquid crystal overlay: NLC (CLC) – VCSELs. The NLC-VCSEL is studied in three different configurations of the NLC cell. Our model predicts the possibility of selecting between two orthogonal directions of linear polarization (LP) of the fundamental mode (x or y LP) by choosing appropriate NLC length. It further predicts very strong polarization discrimination with LP mode threshold gain difference as large as several times the threshold gain of the lasing mode. We also numerically demonstrate an active control of light polarization by electro-optically tuning the LC director and show that either polarization switching between x and y LP modes or continuous change of the LP direction is possible. We also numerically demonstrate that NLC-VCSEL is capable of efficient wavelength tuning.

Completely different is the behaviour of the CLC-VCSEL: it becomes a coupled system with different spectral, threshold and polarization characteristics than the ones of the stand-alone VCSEL. Due to the existence of a band gap for circularly polarized light in the liquid crystal, lasing occurs in almost circularly polarized modes at the LC side. The threshold current significantly decreases while the CLC-VCSEL birefringence increases: wavelengths are separated due to the CLC birefringence rather than to the inherent VCSEL birefringence that determines the solitary VCSEL linearly polarized mode wavelength splitting. Lasing can still occur when removing a large part of the VCSEL distributed Bragg mirror.

8639-10, Session 3

An ultra-stable VCSEL light source

John Downing, GreatSpace, LLC (United States); Dubravko Babic, Univ. of Zagreb (Croatia); Mary Hibbs-Brenner, Vixar Inc. (United States)

Sensor users increasingly demand accurate portable devices with semiconductor light emitters for metrology, health monitoring and

environmental testing. The dual requirements for accuracy and low-power consumption are challenging because the performance of all light emitters and detectors as well as the properties of optical materials change with temperature, sometimes by several thousand ppm/°C. Typically, optical power is stabilized with a TEC, however, TECs consume 50 mW or more of electrical power. In this paper, we report the fabrication of a light source that produces one mW of optical power from 30 mW of electrical power with a stability of ±25 ppm/°C over a 50°C temperature range, without a TEC [1, 2]. Our device is based upon a single-mode (SM), polarization-stable VCSEL (Vixar, Inc.) operated in a closed power-control loop. The novel component is an interference coating designed to reflect more or less light at a bipolar (+/-) rate as emission wavelength changes with temperature. The rate depends on the polarization angle of the VCSEL beam, so by simply adjusting the initial angle, the change in coating reflectance can precisely compensate for the combined effects of: 1) VCSEL polarization drift and beam quality, 2) monitor-photodiode responsivity and 3) aging. We found that even polarization-stable VCSELs exhibit polarization drift by up to 0.35 degrees per °C. VCSEL makers rarely, if ever, report this important characteristic. The reflectance of the temperature-compensating coating is extremely sensitive to angle of incidence. It can change by 2% (20,000 ppm) per degree of incidence angle and therefore close attention must be given to collimation and alignment. While many laboratories can deposit the coating, very few of them can measure reflectance at a specified angle of incidence ±0.05° because their spectrophotometers (Agilent, Perkin Elmer and Shimadzu) have light-beam divergences 20 times larger than we can tolerate.

8639-11, Session 4

Widely tunable singlemode surface micro-machined MEMS-VCSELs operating at 1.95µm

Karolina Zogal, Technische Univ. Darmstadt (Germany); Tobias Gruendl, Technische Univ. München (Germany); Christian Gierl, Sujoy Paul, Technische Univ. Darmstadt (Germany); Christian Grasse, Technische Univ. München (Germany); Peter Meissner, Technische Univ. Darmstadt (Germany); Marcus C. Amann, Technische Univ. München (Germany); Franko Kueppers, Technische Univ. Darmstadt (Germany)

Tunable diode laser absorption spectroscopy is of topical interest for environmental monitoring, process control or trace gas detection. Widely tunable vertical-cavity surface-emitting laser (VCSEL) is an ideal light source for those applications, because of its inherent longitudinal single-mode behaviour, narrow linewidth, low power consumption and compactness. In industrial gas sensing applications, a broad tuning range enables to address several molecules with a single laser source facilitating selective concentration analysis in heterogeneous gas compositions. We present a surface micro-machined micro-electro-mechanical system (MEMS) tunable VCSEL predestined for broadband spectroscopy around 1.95µm, where several gases of importance exhibit stronger absorption lines as for lower wavelengths. The presented tunable VCSELs combine an InP-based cavity incorporating five AlGaInAs/GaInAs quantum wells (QW), a buried tunnel junction and a concave surface micro-machined MEMS distributed Bragg reflector (DBR) which can be electro-thermally actuated for wavelength tuning. We compare two VCSELs with rectangular (REC) and triangular (TRI) shaped QWs. We study the lasers static characteristics comprising output power, threshold current and emission spectra as well as dynamic behaviour of the MEMS-DBR. The static characteristics are supported by the simulations. The lasers show single-mode operation and high side-mode suppression-ratio SMSR > 50dB within the whole tuning range of 50 nm (REC) and 35 nm (TRI). We measure 1 mW and 1.76 mW fibre-coupled optical powers, the threshold current of 2.5 mA and 2.0 mA and the threshold voltage of 0.9 V and 0.8 V for the REC and TRI respectively. The 3dB modulation frequency of the DBR-membrane is 110Hz.

8639-12, Session 4

1060 nm tunable monolithic high index contrast subwavelength grating vertical-cavity surface-emitting laser

Thor Ansbæk, Il-Sug Chung, Elizaveta S. Semenova, Ole Hansen, Kresten Yvind, Technical Univ. of Denmark (Denmark)

Fast and widely tunable VCSEL devices are interesting for a variety of sensing applications e.g. swept source optical coherence tomography where a wavelength around 1060nm is used for ophthalmology. We present an electrical pumped tunable vertical-cavity surface emitting laser (VCSEL) where the top distributed Bragg reflector has been completely substituted by an air-cladded high-indexcontrast subwavelength grating (HCG) mirror. In this way an extended cavity design can be realized by reducing the reflection at the intra-cavity semiconductor-air interface using an anti-reflective coating (ARC). Previous monolithic MEMS tunable HCG VCSELs have employed a partial DBR for current spreading and increased reflectivity of the top mirror, but this narrows the mode-hop free tuning range due to the compound cavity formed.

We demonstrate a single growth step device incorporating an n-DBR, InGaAs/GaAsP quantum wells, oxidized AlGaAs AR coating, AlInP sacrificial layer and a MEMS tunable GaAs HCG. The first results using electrostatic tuning shows a 3dB tuning range of 10nm and total continuous tuning range of 16 nm limited by the pull-in instability of the half-wavelength air gap used in the current design. The static emission wavelength is 1070 nm with 0.9 mW output power.

8639-13, Session 4

Vertical cavity surface-emitting laser with tunable polarization and wavelength

Yi Xie, Jeroen Beeckman, Lieven Penninck, Wouter Woestenborghs, Univ. Gent (Belgium); Krassimir Panajotov, Vrije Univ. Brussel (Belgium); Kristiaan Neyts, Univ. Gent (Belgium)

A technological platform for a vertical cavity surface emitting laser (VCSEL) with tunable polarization and wavelength is presented. It is realized by integrating an 850nm VCSEL chip in a liquid crystal (LC) cell that uses photo-alignment to orient the LC. Two kinds of LC, nematic LC and cholesteric LC (cLC), are filled in the cell and form a thin layer over the VCSEL emitter. The VCSEL and the LC layer can be electrically driven with separate electrodes. On the one hand, the polarization state of the laser emission can be controlled by applying an appropriate voltage over the nematic LC layer. The polarization of the emission depends on the emission angle, in particular for voltages close to the LC threshold voltage, which is in agreement with expectations from the extended Jones calculus. On the other hand, the cLC layer has a reflection band in which is the VCSEL emission, so that it acts as an optic feedback and the emission wavelength can be tuned by 2nm by changing the device temperature from 25°C to 50°C. It is confirmed that the wavelength tuning due to the temperature effect of VCSEL itself is less than 1nm. We expect that a larger-range wavelength tuning is possible by improving the technology in the near future.

8639-14, Session 4

Giant wavelength-temperature dependence of 850nm VCSELs with a metal/semiconductor thermally actuated mirror

Masanori Nakahama, Hayato Sano, Takahiro Sakaguchi, Akihiro Matsutani, Fumio Koyama, Tokyo Institute of Technology (Japan)

We demonstrate a giant wavelength-temperature dependence of a micromachined 850nm VCSEL with a thermally actuated metal/semiconductor cantilever mirror for widely tunable lasers. The cantilever

consists of AlGaAs semiconductor DBR and top Cr/Au metal layer. Since the thermal expansion coefficient of Au is 2.5 times larger than that of AlGaAs, the top mirror at the end of the cantilever actuates upward or downward when the cantilever temperature is changed. The cantilever displacement of a VCSEL brings broad and continuous wavelength tuning. The modeling shows a possibility of giant negative temperature dependence of wavelength more than several nm/K, which is determined by a cantilever length and metal thickness. We fabricated the device and experimentally demonstrate the giant temperature dependence. The fabricated device exhibits a temperature dependence of -1.6 nm/K for 130 μm long cantilever, and a wavelength tuning range of 35 nm in 850 nm band was obtained by the device temperature change of only 12K. Although an external temperature controller was used to tune the wavelength at this moment, a metal heater could be integrated into the micro-machined mirror for electro-thermal wavelength tuning. Thanks to the large temperature dependence of wavelength, wide tuning range with small amount of heating power and low tuning voltage can be expected. Our structure will enable widely tunable VCSELs with low power consumption for ultra-high capacity WDM optical links and for high resolution real time OCT imaging.

8639-15, Session 4

Widely tunable MEMS-VCSELs operating at > 70 degrees C

Christian Gierl, Technische Univ. Darmstadt (Germany); Tobias Gründl, Walter Schottky Institut (Germany); Karolina Zogal, Sujoy Paul, Technische Univ. Darmstadt (Germany); Christian Grasse, Gerhard Böhm, Walter Schottky Institut (Germany); Peter Meissner, Technische Univ. Darmstadt (Germany); Markus C. Amann, Walter Schottky Institut (Germany); Franko Küppers, Technische Univ. Darmstadt (Germany)

Tunable VCSEL are attractive tools for applications such as gas spectroscopy, fiber Bragg-sensors and telecommunications, especially for fibre to the home application. Their inherently short cavity enables wide single mode tuning ranges due to their large free spectral range. Especially their low power consumption makes them attractive for the fast growing market of telecommunication.

In this paper we present the first tuneable VCSEL emitting around 1550 nm, which operates at high temperatures up to 70 °C over a broad tuning range. The presented device consists of two main parts: A half-VCSEL consisting of the active semiconductor part with a fixed DBR at the bottom and a movable DBR-membrane on the top. Both parts embed an air-gap with variable thickness. Electro-thermal heating of the movable DBR-membrane increases the air-gap length which shifts the resonant wavelength to higher values. A mode hop free single mode tuning range >80 nm at 20 °C and of 45 nm at 70 °C is demonstrated. The devices show a record high fibre-coupled output power of 3 mW at 20 °C and 0.5 mW at 70 °C. The side mode suppression ratio is larger than 40 dB over the entire tuning and temperature range. This new technology is cost effective and thus capable for mass production. It is applicable for tuneable VCSELs operating in different wavelength regimes, which are limited by the absorption of the DBR materials only.

8639-16, Session 4

Far-field emission characteristics and linewidth measurements of surface micro-machined MEMS tunable VCSELs

Sujoy Paul, Christian Gierl, Technische Univ. Darmstadt (Germany); Tobias Gründl, Walter Schottky Institut (Germany); Karolina Zogal, Peter Meissner, Technische Univ. Darmstadt (Germany); Markus C. Amann, Walter Schottky Institut (Germany); Franko Küppers, Technische Univ. Darmstadt (Germany)

**Conference 8639:
Vertical-Cavity Surface-Emitting Lasers XVII**

Vertical-cavity surface-emitting lasers (VCSELs) with continuous tunability and high purity emission spectrum operating at around 1550 nm are attractive components for many applications such as optical fiber based telecommunications, fiber Bragg-grating sensing and spectroscopy.

In this paper, we demonstrate for the first time the far-field experimental results for this type of widely tunable surface-micromachined VCSELs operating at 1550nm optical wavelength. The laser consists of two parts: the half-VCSEL with fixed bottom mirror and the micro-electro-mechanical system (MEMS) based dielectric DBR mirror. The radius of curvature of top movable mirror along with predefined diameter of circular buried tunnel junctions (BTJs) of the active material are well optimized for single lateral-mode emission. The presence of the sole fundamental Gaussian mode is verified from the far-field measurements. The SiO/SiN based dielectric mirror structure can be well adopted for a wide range of emission wavelength, which is only limited by the absorption regime of the DBR materials. For these particular VCSELs, a mode-hop free continuous tuning over 100nm has been demonstrated, which is achieved by electro-thermal tuning of the MEMS mirror. The fiber coupled power is above 2 mW over the entire tuning range. The singlemode laser emission has more than 40dB of side mode suppression ratio (SMSR). Within the tuning range, we also demonstrate the linewidth characteristics of these newly developed micro- machined MEMS tunable VCSELs.

8639-33, Session PWed

High-frequency signal generation using 1550 nm VCSEL subject to two-frequency optical injection

Antonio Consoli, Univ. Politécnica de Madrid (Spain); Ana Quirce, Angel Valle, Luis Pesquera, Univ. de Cantabria (Spain); Jose Manuel Garcia Tijero, Ignacio Esquivias, Univ. Politécnica de Madrid (Spain)

We report high frequency signal generation using a two-frequency optically injected VCSEL emitting at 1550 nm. Three 1550 nm VCSELs are used in the proposed scheme: the slave laser is optically injected with two VCSELs and frequency locked to one of them. A Radio Frequency signal is generated from the slave VCSEL at the frequency spacing between the two master lasers. Different frequencies (up to 45 GHz) are obtained by varying the polarization current of the detuned master VCSEL and changing its emission wavelength. We report the output signal characteristics as a function of the optical injection parameters.

8639-17, Session 5

The range of VCSEL wearout reliability acceleration behavior and its effects on applications

James K. Guenter, Luke A. Graham, Robert A. Hawthorne, Bobby M. Hawkins, Ralph Johnson, Gary Landry, Jim Tatum, Finisar Corp. (United States)

For nearly twenty years most models of VCSEL wearout reliability have incorporated Arrhenius activation energy near 0.7 eV, usually with a modest current exponent in addition. As VCSEL production extends into more wavelength, power, and speed regimes new active regions, mirror designs, and growth conditions have become necessary. Even at more traditional VCSEL 850-nm wavelengths instances of very different reliability acceleration factors have arisen. In some cases these have profound effects on the expected reliability under normal use conditions, resulting in wearout lifetimes that can vary more than an order of magnitude. These differences enable the extension of VCSELs in communications applications to even greater speeds with reliability equal to or even greater than the previous lower-speed devices. This paper discusses some of the new applications, different wearout behaviors and their implications in real-life operation. The effect of different acceleration behaviors on reliability testing is also addressed.

8639-18, Session 5

25 Gbps and beyond: VCSEL development at Philips

Roger King, Steffan Intemann, Stefan Wabra, Philipp Gerlach, Michael Riedl, Philips Technologie GmbH U-L-M Photonics (Germany)

The exploding demand for high speed transceivers and active optical cables used e.g. in data centers and high performance computers is accelerating the development of next generation VCSEL products designed for transmission speeds of 25, 28, and up to 32 Gbps. Besides the increase in bandwidth, a second major aspect in product development is minimizing the power consumption in an optical link, as this is becoming a predominant issue for power and heat management.

We present the recent status of Philips' product development addressing the demand described above. Device characteristics as well as system design and system performance aspects (e.g. interaction with VCSEL driver IC) are presented and discussed. Production relevant topics like impacts on yields, reliability, and testing are addressed as well. We will also give an outlook on what is expected to be achieved in the next years.

8639-19, Session 5

28 Gb/s 850 nm oxide VCSEL development at Avago

Jingyi Wang, Laura Giovane , Avago Technologies Ltd. (United States); Zheng-wen Feng, Tom Fanning, Chen Chu, Aadi Sridhara, Friedhelm Hopfer, Terry Sale, An-Nien Cheng, Avago Technologies Singapore (Singapore); Bing Shao, Li Ding, Pengyue Wen , Avago Technologies Ltd. (United States)

Avago's 850nm oxide VCSEL, for applications requiring modulation at 25-28G, has been designed for -3dB bandwidths in excess of 18GHz over the temperature range of 0-85C. The VCSEL has been optimized to minimize DBR mirror thermal resistivity, electrical resistance and optical losses from free carrier absorption. The active region is designed for superior differential gain and the device has been engineered for high electrical bandwidths. The small-signal modulation response has been characterized and the large-signal eyes diagrams show excellent high-speed performance over the temperature range of 0-85C. Characterization data on other link parameters such as relative intensity noise and spectral width will also be presented.

8639-20, Session 5

Reliability and degradation of oxide VCSELs due to reaction to atmospheric water vapor

Alexandru Dafinca, Anthony R. Weidberg, Univ. of Oxford (United Kingdom); Steven J. McMahan, Rutherford Appleton Lab. (United Kingdom); Robert W. Herrick, C8 MediSensors, Inc. (United States)

For short-link data communications, 850nm oxide-aperture vertical cavity lasers (VCSELs) dominate the marketplace, with hundreds of millions of channels shipped over the past 15 years. Unfortunately, it has been discovered that such VCSELs are susceptible to premature failure if exposed to atmospheric water vapor. In the past, this has been of limited concern, since most links were packaged in hermetically-sealed cans that were protected from moisture ingress. However, for high data rates, parallel optics will increasingly be used – in such applications, plastic packaging is generally used, which is permeable to moisture. Thus, understanding the chain of failure and the acceleration model is important.

**Conference 8639:
Vertical-Cavity Surface-Emitting Lasers XVII**

Over the past few years, the ATLAS detector in CERN's Large Hadron Collider (LHC) has had approximately 6000 channels of Parallel Optic VCSELs fielded under well-documented ambient conditions similar to what might be expected in future data centers. Exact time-to-failure data has been collected on this large sample, providing for the first time actual failure data at use conditions, as opposed to estimates based on extrapolation. In addition, the same VCSELs were tested under a variety of accelerated conditions to allow us to construct a more accurate acceleration model.

Finally, a variety of new methods were applied to better understand the failure mechanism. Plan view TEM shows evidence of cracks at the edge of the oxide aperture. Furthermore, data on reductions in spectral width, and increases in threshold and far-field before failure can all be combined to create a picture of how cracking modifies device parameters to show signs of immanent failure. We will discuss what we believe the chain of failure is, ending ultimately in fast-growing dark-line defects (climb dislocations) causing sudden failure.

8639-21, Session 6

VCSEL arrays with integrated optics (*Invited Paper*)

Holger Moench, Stephan Gronenborn, Johanna Kolb, Pavel Pekarski, Ulrich Weichmann, Philips Research (Germany); Michael Miller, Philips Technologie GmbH U-L-M Photonics (Germany)

Systems with arrays of VCSELs can realize multi kilowatt output power. The inherent simplicity of VCSELs enables a performance and cost breakthrough in solutions for thermal processing and the pumping of solid state lasers. The use of an array of micro-optics i.e. one micro-lens per VCSEL enables multiple advantages: First it can function as a collimating lens in order to realize a brightness of an array which is similar to the brightness of a single VCSEL. Second the micro-lens can be part of an imaging system for tailored intensity distributions. Last but not least the micro-lens with some feedback into the VCSEL can help to select laser modes in order to increase brightness and mode stability. Wafer-level integrated micro-optics allows keeping the VCSEL advantage of complete and operational lasers on wafer level including the micro-optics. This talk presents our approach to bond a GaAs wafer with a 3" micro-optics wafer. The type of glass used for the optics wafer has been selected to match the coefficient of thermal expansion of GaAs and is suitable for hot pressing of the lens structures. An adjustment strategy with corresponding markers on both wafers is used to allow the adjustment on a standard mask aligner thus realizing many thousand lens adjustments in a single process step. The technology can be combined with VCSEL wafers with thinned substrate as well as with complete substrate removal. The basic technology and illustrative prototype systems are described in this talk.

8639-22, Session 6

Development of a high-power vertical-cavity surface-emitting laser array with ion-implanted current apertures (*Invited Paper*)

Hideyuki Naito, Masahiro Miyamoto, Yuta Aoki, Akira Higuchi, Kousuke Torii, Takehito Nagakura, Takenori Morita, Junya Maeda, Hirofumi Miyajima, Harumasa Yoshida, Hamamatsu Photonics K.K. (Japan)

Vertical-Cavity Surface-Emitting Lasers (VCSELs) are very attractive to high power light sources owing to the advantageous configuration of two-dimensional arrays and being free from catastrophic optical damages [1]. Most of the VCSELs employ oxide-confined current apertures thanks to great success in optical communication systems in which the devices are operated under high frequency conditions at relatively low output powers. By contrast, the requirements to VCSELs for

high power applications must be quite different.

Typical technologies for formation of the current apertures are a selective-oxidation and an ion-implantation. The oxidation technology provides not only the current apertures but also an effective transverse optical confinement which is capable of the reduction of optical diffraction loss. That is the reason why the oxide-confined VCSELs have been employed in most of applications with VCSELs. However, the importance of optical confinement decreases with increasing the aperture diameter. Additionally, the strain and defects generated by the oxidation degrade the reliability for high power devices. And hence, the ion-implantation technique, which is free from the issue, has a potential to be the better method for the high power VCSELs with large aperture configuration.

In spite of that fact, the ion-implanted VCSELs have not been actively researched even in high power applications. Here we report on a high power VCSEL-array with proton-implanted current apertures. A peak output power of over 40 W under pulse operation has been achieved at an emission wavelength of 980 nm from the 7-arrayed VCSEL with 100- μ m-current apertures. This is the first demonstration of ten watt-class output power for an ion-implanted VCSEL. The corresponding power density is estimated to be over 70 kW/cm², which is three times greater than the record power density of the short-pulse operated oxide-confined VCSEL [2]. This result provides a chance to realize high power VCSEL-arrays with ion-implanted current apertures.

References

- [1] J.-F. Seurin et al., Proc. SPIE, 6908, 690808 (2008)
- [2] D. Liu et al., Appl. Phys. Express, 4, 052104 (2011)

8639-23, Session 6

High-power red VCSEL arrays

Jean-Francois Seurin, Viktor Khalfin, Guoyang Xu, Alexander Miglo, Daizong Li, Delai Zhou, Mukta Sundaresh, Wei-Xiong Zou, Chien-Yao Lu, James D. Wynn, Chuni Ghosh, Princeton Optronics, Inc. (United States)

High-power red laser sources are used in many applications such as cosmetics, cancer photodynamic therapy, and DNA sequencing in the medical field, laser-based RGB projection display, and bar-code scanning to name a few.

Vertical-cavity surface-emitting lasers (VCSELs) can be used as high-power laser sources, as efficient single devices can be configured into high-power two-dimensional arrays and scaled into modules of arrays. VCSELs emit in a circular, uniform beam which can greatly reduce the complexity and cost of optics. Other advantages include a narrow and stable emission spectrum, low speckle of the far-field emission, and good reliability.

However, developing efficient red VCSEL sources presents some challenges because of the reduced quantum-well carrier confinement and the increased Aluminum content (to avoid absorption) which increases thermal impedance, and also decreases the DBR index contrast resulting in increased penetration length and cavity losses. We have recently developed VCSEL devices lasing in the visible 6xx nm wavelength band, and reaching 30% power conversion efficiency. We then fabricated high-power 2D arrays by removing the GaAs substrate entirely and soldered the chips on ceramic and diamond submounts. Such arrays have demonstrated several Watts of output power at room temperature, in quasi-continuous-wave (QCW) and continuous-wave (CW) operation. Results and advantages of these visible VCSEL arrays will be discussed.

**Conference 8639:
Vertical-Cavity Surface-Emitting Lasers XVII**

8639-24, Session 6

High-power format-flexible 885-nm vertical-cavity surface-emitting laser arrays

Chad Wang, Fedor Talantov, Henry Garrett, Glen Berdin, David Millenheft, Terri Cardellino, Jonathan Geske, FLIR Electro-Optical Components (United States)

High-power, format flexible, 885 nm vertical cavity surface-emitting laser (VCSEL) arrays have been developed for solid-state pumping and illumination applications. In this approach, a common VCSEL size format was designed to enable tiling into flexible formats and operating configurations. The fabrication of a common chip size on ceramic submount enables low-cost volume manufacturing of high-power VCSEL arrays. This base VCSEL chip was designed to be 5x3.33 mm², and produced up to 50 Watts of peak continuous wave (CW) power. To scale to higher powers, multiple chips can be tiled into a combination of series or parallel configurations tailored to the application driver conditions. In actively cooled CW operation, the VCSEL array chips were packaged onto a single water channel cooler, produced over 1.3 kW of peak power. 1x1, and 1x3 cm² formats, producing 178, 247, and 500 Watts of peak power, respectively, in under 130 A operating current. In QCW operation, the 1x3 cm² VCSEL module, which contains 18 VCSEL array chips packaged on a single water cooler, produced over 1.3 kW of peak power. In passively cooled packages, multiple chip configurations have been developed for illumination applications, producing over 100 Watts of peak power in 60 Hz and 1 kHz operating conditions. These VCSEL chips use a substrate-removed structure to allow for efficient thermal heatsinking to enable high-power operation. This scalable, format flexible VCSEL architecture can be applied to wavelengths ranging from 800 to 1100 nm.

8639-25, Session 7

Numerical analysis of photonic-crystal VCSELs (*Invited Paper*)

Tomasz Czyszanowski, Maciej Dems, Robert P. Sarzala, Technical Univ. of Lodz (Poland); Krassimir Panajotov, Vrije Univ. Brussel (Belgium)

The introduction of a photonic-crystal to the VCSEL produces single mode emission in a very broad range of applied currents. The mechanism responsible for the discrimination of high-order modes originates from two counter-acting phenomena:

The PhC introduces lateral mode confinement through a strong waveguide effect and additionally by the Bragg reflections from a regular net of PhC holes.

The holes of the PhC destroy the vertical periodicity of the DBR and contribute to the selective reduction in reflectivity of the mirror. As a result, the mode which overlaps the holes of the photonic crystal leaks through and becomes discriminated.

We present numerical analysis of the influence of parameters of photonic crystal on the wavelength of emission, modal gain, slope efficiency, emitted power and tuning range in single mode VCSELs. We recognise several mechanisms determining high power emission in the single mode regime, which are: selective leakage, thermal focusing, waveguide effect induced by the photonic-crystal, gain spectrum red shift and its maximum reduction with increase of driving currents. We show that careful design of the photonic crystal allows for 10% increase in the emitted power of a single-mode regime and it allows for broad range of the steering currents from 5 to 50 mA. Such attributes support tuning of the single-mode emission over the 20 nm range of the spectrum.

8639-26, Session 7

Single-mode photonic crystal VCSELs with high modulation bandwidth at record low current density

Kent D. Choquette, Meng Peun Tan, Stewart Fryslye, Univ. of Illinois at Urbana-Champaign (United States); James A. Lott, Technische Univ. Berlin (Germany); Nikolay N. Ledentsov, VI Systems GmbH (Germany)

Data transmission over multimode fiber using single mode VCSELs has been shown to be energy efficient and insensitive to launching condition. Furthermore, transmission distance is expected to increase with reduced chromatic dispersion due to narrow spectral width and lower modal dispersion due to the suppression of higher order modes. To achieve single mode lasing, the oxide aperture diameters must be small so that the higher order modes are cut off, but this typically comes at the expense of a high series resistance and a high operating current density resulting in degradation of device lifetime. The separation of the current and lasing apertures enables us to maintain the single mode waveguide condition with a relatively large current aperture at the same time. We report high modulation speed single mode VCSELs whose current confinement is provided by proton implantation while the waveguiding aperture for the lasing modes is defined by a photonic crystal defect. We achieve small signal bandwidths of approximately 20 GHz/s with at a record low current density. No one will read this but the system requires I put something in.

8639-27, Session 7

Spatial mode discrimination using intra-cavity patterns in long-wavelength wafer-fused vertical-cavity surface-emitting lasers

Nicolas Volet, Lukas Mutter, Ecole Polytechnique Fédérale de Lausanne (Switzerland); Tomasz Czyszanowski, Jarosław Walczak, Technical Univ. of Lodz (Poland); Benjamin Dwir, Vladimir Iakovlev, Alexei Sirbu, Alexandru Mereuta, Andrei Caliman, Elyahou Kapon, Ecole Polytechnique Fédérale de Lausanne (Switzerland)

We report on spatial mode discrimination in long-wavelength wafer-fused vertical-cavity surface-emitting lasers (VCSELs) incorporating ring-shaped air gap patterns at the fused interface between the active region and the top distributed Bragg reflector (DBR). These 70-nm deep patterns were implemented by reactive-ion etching (RIE) with the aim of favoring the fundamental mode while preserving high output power. The VCSELs under consideration emit around 1320 nm and incorporate an InAlGaAs/InP active region, a re-grown circular tunnel junction (TJ) and undoped AlGaAs/GaAs DBRs. A large batch of devices was investigated by on-wafer mapping, allowing drawing conclusions on their typical behavior. We observe experimentally that transverse modes with near-field patterns confined by the TJ structure within the ring diameter are enhanced by the additional optical confinement introduced, whereas the higher order ones are weakened or even suppressed. Numerical simulations of the patterned-cavity VCSELs, based on our fully three-dimensional electrical, thermal and optical VCSEL computational model, support these observations. We can indeed predict that beyond a certain value of inner diameter, ring-shaped patterns confine HE₂₁ and enhance its modal gain. Below that value, HE₂₁ can be pushed out of the optical aperture and suffer large losses. Optimized parameters were found numerically for enhancing the single-mode properties of the devices with negligible penalty on emitted power and threshold current.

8639-28, Session 7

22 Gb/s error-free data transmission beyond 1 km of multi-mode fiber using 850-nm VCSELs

Rashid Safaisini, Krzysztof Szczerba, Erik Haglund, Petter Westbergh, Johan S. Gustavsson, Anders Larsson, Peter Andrekson, Chalmers Univ. of Technology (Sweden)

Long distance transmission (>1 km) over multimode fibers (MMFs) at high bit rates (BRs) (>20 Gb/s) using 850 nm vertical-cavity surface-emitting lasers (VCSELs) is of great importance in applications such as data links in large office areas and data centers. One of the main challenges in achieving long distance transmission via MMFs is their limited bandwidth due to the effects of chromatic and modal dispersion. These effects can be mitigated by improved VCSEL modal properties, for example, by employing VCSELs with narrow spectral width to reduce the effects of chromatic dispersion. The effects of modal dispersion can also be reduced by exciting a reduced number of fiber modes when utilizing single (or quasi-single) mode VCSELs.

Here we report on the first error-free (bit error rate 10^{-12}) data transmission beyond 1 km of OM4 MMF at BRs up to 22 Gb/s using a high modulation bandwidth 850 nm VCSEL. A VCSEL with small $\sim 3\ \mu\text{m}$ aperture diameter defined during the wet oxidation step ensures quasi-single mode (side-mode suppression ratio >20 dB) operation with a RMS spectral width of 0.29 nm. The top distributed Bragg reflector (DBR) reflectivity of the VCSEL is also optimized for high output power by shallow etching. Realizing a quasi-single mode VCSEL with a narrow spectral width and high optical power reduces the effects of fiber dispersion and fiber and connector losses for achieving such a long distance transmission at high BRs.

The paper presents the highest BR-distance product for a link employing MMFs and directly modulated VCSELs.

8639-29, Session 8

Traveling wave electro-optically modulated coupled-cavity surface emitting lasers

Mateusz Zujewski, Hugo Thienpont, Vrije Univ. Brussel (Belgium); Krassimir Panajotov, Vrije Univ. Brussel (Belgium) and Institute of Solid State Physics (Bulgaria)

We present a design of a high speed electro-optically modulated coupled-cavity vertical-cavity surface emitting laser monolithically integrated in a traveling wave electrode structure (TW EOM CC-VCSEL). Such electrical configuration allows to overcome the RC time constant limitation of a traditional lumped electrodes design. We use segmented transmission line to match the impedance of the whole structure to the 50 Ω electrical network [1]. This is done by adding passive sections with high characteristic impedances next to the modulator, which typically has lower than 50 Ω characteristic impedance. We use transmission matrix method to model the response of the device and reflections at the voltage source interface. The CC-VCSEL optical design is based on longitudinal mode switching induced by the electro-optic effect [2], which has been recently experimentally demonstrated [3]. We optimize our structure with respect to the device physical dimensions, frequency response, microwave reflections and modulation efficiency. We propose two different designs that are theoretically able to reach modulation speeds limited only by carrier extraction time from the quantum wells of the modulator and at the same time having lower than -20 dB reflections to the voltage source and modulation efficiency of about 80%. For 1.5 μm long modulator cavity, carrier saturation velocity limits the bandwidth of proposed structures to 330 GHz.

[1] M. Chacinski, et al., J. Lightw. Technol. 27(16), 3410–3415 (2009).

[2] K. Panajotov, et al., Opt. Express 18, 27525–27533 (2010).

[3] T. D. Germann, et al., Opt. Express 20(5), 5099–5107 (2012).

8639-30, Session 8

Impact of the aperture diameter on the energy-efficiency of oxide-confined 850-nm high-speed VCSELs

Philip Moser, James A. Lott, Philip Wolf, Gunter Larisch, Hui Li, Technische Univ. Berlin (Germany); Nikolay N. Ledentsov, VI Systems GmbH (Germany); Dieter Bimberg, Technische Univ. Berlin (Germany)

A new record for energy-efficient oxide-confined 850 nm vertical-cavity surface-emitting lasers (VCSELs) particularly well suited for high-speed optical interconnects is presented. Error-free performance (defined as a bit error ratio of less than 1×10^{-12}) at 25 Gb/s is achieved with only 56 fJ/bit of dissipated energy per quantum of information. Novel current spreading sections and doping profiles are used to reduce the resistance and operating voltage of our devices. We determine the influence of the oxide-aperture diameter on the energy-efficiency of our VCSELs by comparing devices with different aperture diameters all operating at 25 Gb/s. A detailed analysis of the total and dissipated powers versus the modulation bandwidth of devices with different aperture diameters allows us to determine the aperture diameter yielding the most energy-efficient performance. Trade-offs between various parameters such as output power, spectral width, current density, maximum modulation bandwidth, and the energy-efficiency are demonstrated and discussed. We show that our present single-mode VCSELs are more energy-efficient than our multimode VCSELs. We further demonstrate that bias points for maximum wall-plug efficiencies and epitaxial device designs for minimum threshold current density do not necessarily lead toward, or correlate to energy-efficient VCSEL operation.

8639-31, Session 8

Push-pull modulation of lateral coupling of dual VCSEL cavities using a bow-tie shape

Hamed Dalir, Akihiro Matsutani, Fumio Koyama, Tokyo Institute of Technology (Japan)

During the recent years, ultra-high speed and low power consumption VCSELs have been attracting much interest for optical interconnects in data center, supercomputers and etc. In this paper we propose the lateral coupling of dual VCSEL cavities using a bow-tie shape oxide aperture. Lateral optical confinement is formed using an oxide layer and double bit felling axes while the joint region is less than a few micrometer leads to a leaky travelling wave in the lateral direction. The intensity distribution of laterally coupled cavities was calculated by using a three dimensional mode-matching method (FIMMWAVE, Photon Design Co.). The result shows no-noticeable radiation loss when two oxide-defined VCSEL cavities are coherently coupled. The modeled VCSEL structure consists of 25pairs top Al_{0.92}GaAs/Al_{0.16}GaAs DBR and 40 pairs bottom DBR. Increasing width of bow-tie shape will reduce the coupling efficiency of two cavities. We fabricated 980nm laterally coupled cavity VCSELs with a bow-tie shape oxide aperture. We figured out the near-field pattern (NFP) and far-field pattern (FFP) measurements of the fabricated device. According to NFP and FFP measurements we could conclude that two oxide-confined cavities are coherently coupled and the transverse mode was demonstrated with push-pull current modulation scheme.

In addition, the modeling on small-signal modulation show large modulation bandwidth free from relaxation oscillation frequencies with the total photon density unchanged. The modulation bandwidth could be potentially increased by a factor of 3 in comparison with conventional VCSELs. This basic concept is useful for increasing the modulation speed of VCSELs.

8639-32, Session 8

High-speed 850-nm VCSELs with 28 GHz modulation bandwidth for short reach communication

Petter Westbergh, Rashid Safaisini, Erik Haglund, Johan S. Gustavsson, Chalmers Univ. of Technology (Sweden); Anders Larsson, Chalmers Univ. of Technology (Sweden); Andrew Joel, IQE plc (United Kingdom)

We present results from our new generation of high performance, high-speed 850 nm oxide confined vertical cavity surface-emitting lasers (VCSELs). The p- and n-doped distributed Bragg reflector (DBR) mirrors have been optimized to reduce electrical resistance and optical absorption. This aids to delay thermal rollover due to current and absorption induced self-heating and allows for a higher photon density to be reached. In combination with a reduced cavity length for improved transport and increased longitudinal confinement, this results in a higher resonance frequency and modulation bandwidth. After post fabrication processing to fine tune the top contact layer thickness and optimize the cavity photon lifetime through a shallow surface etch, we are able to reach record high 3dB modulation bandwidths: 28 GHz for $\sim 4 \mu\text{m}$ oxide aperture diameter VCSELs, and 27 GHz for devices with a $\sim 7 \mu\text{m}$ oxide aperture diameter. Data transmission experiments demonstrate that these VCSELs are capable of error-free transmission (BER < 10⁻¹²) at bit-rates approaching 50 Gbit/s.

Conference 8640: Novel In-Plane Semiconductor Lasers XII

Monday - Thursday 4 -7 February 2013

Part of Proceedings of SPIE Vol. 8640 Novel In-Plane Semiconductor Lasers XII

8640-1, Session 1

Progress towards GaAs- and InP-based Bismuth-containing efficient semiconductor lasers

Stephen J. Sweeney, Univ. of Surrey (United Kingdom)

Bismuth-containing III-V alloys have attracted interest owing to the fact that adding small amounts of Bi to GaAs strongly decreases the band gap, E_g , while increasing the spin-orbit splitting energy, Δ_{SO} , allowing suppression of fundamental loss processes such as the hot-hole producing Auger recombination process and inter-valence band absorption (IVBA) which plague near-infrared devices. The condition for loss suppression requires that $\Delta_{SO} > E_g$ which is impossible to satisfy with conventional alloys for the near-infrared. We report on the results of spectroscopic investigations of the band-structure of both GaAsBi/GaAs and InGaAsBi/InP, alloys. From these measurements we observe that E_g decreases strongly with increasing Bismuth fraction at $\sim 80\text{meV}/\text{Bi}\%$ in GaAsBi/GaAs and $\sim 56\text{meV}/\text{Bi}\%$ in InGaAsBi/InP, which may be modelled using valence band anti-crossing theory (VBAC). Furthermore, due to VBAC, the temperature dependence of the band gap is reduced suggesting that the temperature dependence of the gain peak in lasers is weaker, confirmed from experiments on GaAsBi/GaAs LEDs. In the GaAsBi/GaAs system, for a Bismuth fraction of $\sim 9\%$ one may achieve a band gap of 800meV , corresponding to a wavelength of $1.55\mu\text{m}$ while satisfying the loss suppression condition that $\Delta_{SO} > E_g$ with less than 1% compressive strain. In the InGaAsBi system, $\Delta_{SO} > E_g$ for $\sim 3\text{-}4\%$ Bismuth at which point $E_g < 0.6\text{eV}$ ($> 2\mu\text{m}$) and provides a route towards efficient lattice-matched InP-based mid-infrared lasers. We also describe how the quaternary GaAsBiN provides further opportunities for mid-infrared devices where E_g , Δ_{SO} , the band offsets and strain can be controlled to produce near- and mid-infrared lasers with reduced Auger and leakage currents.

8640-2, Session 1

High Modal Gain 1.5 μm InP Based Quantum Dot Lasers: Dependence of Static Properties on the Active Layer Design

Vitalii Sichkovskiy, Vitalii Ivanov, Johann P. Reithmaier, Univ. Kassel (Germany)

Self-organized InAs/InAlGaAs/InP(100) quantum dot systems are promising candidates for telecommunication applications at $1.55\mu\text{m}$. Recent progress in epitaxial growth led to the ability to control the geometry and morphology of InAs QDs. Such quantum dot ensembles with nearly circular shapes were grown in an As₂ environment and exhibited record low photoluminescence line widths in comparison with quantum dash structures [C. Gilfert et. al., APL 96, 191903 (2010)]. This enabled much improved $1.55\mu\text{m}$ QD lasers combining a moderately low absorption and high modal gain of 10 cm^{-1} per QD layer [C. Gilfert et. al., APL 98, 201102 (2011)] resulting in high modulation speed and low noise figures [D. Gready et. al., IEEE Phot. Technol. Lett. 24, 809 (2012)].

In this paper, we report on a new set of device structures where the influence of the number of QD layers on static properties, e.g., modal gain, threshold current density and spectral properties of the QDs lasers are investigated. For a large number of QD layers, e.g., 6 QD layers, a very high modal gain of $> 70\text{ cm}^{-1}$ could be obtained. By reducing the number of QD layers, i.e., lowering the modal gain, the wavelength shift with temperature can be reduced to values below $0.2\text{ nm}/\text{K}$, which is 2.5 times less than for QW lasers. Also the influence of the active structure design is studied, e.g., broadened waveguides for reduced internal absorption and narrow waveguides for minimizing the carrier transport time will be compared and discussed.

8640-3, Session 1

Ultrafast phenomena in QD/QDash lasers (Invited Paper)

Amir Capua, Ouri Karni, Gadi Eisenstein, Technion-Israel Institute of Technology (Israel); Johann P. Reithmaier, Univ. Kassel (Germany)

InP QD/QDash gain media have been demonstrated to enable superb practical properties for telecom applications such as multi wavelength amplification, signal processing, signal regeneration and wavelength conversion.

Understanding the basic characteristics of these special gain media requires however experimental investigations with special tools combined with advanced modeling. We have addressed ultrafast dynamical properties of QD/QDash lasers and amplifiers using two unique experimental systems. The first is an ultrafast multi wavelength pump probe system and the second is a X-FROG system. These are accompanied by detailed simulations of the various phenomenon we observe.

The first unique observation we report is an instantaneous gain response occurring all across an inhomogeneously broadened InP QD/QDash gain spectrum as a response to a 150 fs pulse. The response stems from carriers generated by two photon absorption which relax extremely fast within the wire like gain spectrum. Using moderate electronic and optical excitation levels enables to extract energy dependent relaxation rates which yield important information related to the electronic structure and coupling between different dashes within the inhomogeneously broadened gain spectrum.

The nonlinearly induced gain is shown to initiate laser oscillations in a similar QDash medium and finally, a cascaded FWM process occurring between a short pulse and the two CW fields of a QD laser is demonstrated. The special FWM process causes a hole on the pulse spectrum and also an amplitude modification of the pulse trailing edge.

8640-4, Session 1

Effect of optical waveguiding mechanism on the lasing action of chirped InAs/AlGaInAs/InP quantum dash lasers

Mohammed Zahed A. M. Khan, Tien Khee Ng, King Abdullah Univ. of Science and Technology (Saudi Arabia); Chi-Sen Lee, Pallab K. Bhattacharya, Univ. of Michigan (United States); Boon S. Ooi, King Abdullah Univ. of Science and Technology (Saudi Arabia)

We report on the atypical emission dynamics of InAs/AlGaInAs/InP quantum dash (Qdash) lasers employing varying AlGaInAs barrier thickness (multilayer-chirped structure). The analysis is carried out via fabry-perot (FP) ridge (RW) and stripe (SW) waveguide laser characterization corresponding to the index and gain guided waveguiding mechanisms, respectively, and at different current pulse width operations. The laser emissions are found to emerge from the dispersive size Qdash ensembles across the four Qdash-barrier stacks and governed by their overlapping quasi-zero dimensional density of states (DOS). The spectral characteristics demonstrated prominent dependence on the waveguiding mechanism at quasi-continuous wave (QCW) operation (large pulse width). The RW geometry shows unusual spectral split in the emission spectra on increasing current injection while the SW geometry show typical broadening of lasing spectra. These effects have been attributed to the dependence of inhomogeneous broadening on the current injection in the RW geometry as a result of lateral current spreading which recurrently alters the nonequilibrium carrier distribution and the energy exchange between Qdash groups across the Qdash-barrier stacks, and among less dispersive in-plane dashes. Furthermore, the progressive

**Conference 8640:
Novel In-Plane Semiconductor Lasers XII**

redshift of peak emission with injection current is a result of increase in active region junction temperature, which on the other hand is observed to be minimal during the short pulse width (SPW) operation. Our investigation sheds light on the device physics of chirped Qdash laser structure and provides guidelines for further optimization in obtaining broad lasing spectra devices.

8640-5, Session 1

Novel photonic devices formed through etched facets (*Invited Paper*)

Alex Behfar, Norman Kwong, BinOptics Corp. (United States)

Etched facet technology (EFT) allows semiconductor lasers to be manufactured without the need for cleaving. This allows processing and testing in wafer-form, as opposed to bar-form for cleaved facet devices. Given the freedom from the cleavage planes of the semiconductor crystal, EFT has allowed new and novel photonic devices to be formed. In this paper, several devices that take advantage of additional freedom offered by etched facets are discussed: Horizontal-Cavity Surface-Emitting Laser (HCSEL); monolithically integrated laser and monitoring photodetector (MPD); and Single-Longitudinal Mode (SLM) laser.

A HCSEL is fabricated through the use of a facet that is etched at 45-degrees to the laser cavity. The etched facet serves as a total internal reflection surface to emit light perpendicular to the plane of the semiconductor substrate. HCSELs can provide the reliability and power of in-plane lasers with the benefits of laser emission perpendicular to the substrate.

By using EFT, laser facets are formed without cleaving a wafer into bars, therefore, other photonic devices can be integrated with the laser. A monolithically integrated laser and MPD has been demonstrated. Such photonic device integration is an effective way to reduce product cost and improve product performance and uniformity.

Gratings produced using EFT has allowed the fabrication of SLM lasers. These SLM lasers are more cost effective to manufacture compared to conventional Distributed Feedback (DFB) lasers that require gratings and epitaxial regrowth. SLM lasers operating at 1310nm were fabricated that met stringent Telecom requirements. In some material systems, fabricating a DFB laser is very difficult and, as such, SLM lasers become a particularly attractive option for that material system.

8640-6, Session 1

High power pulses at tunable repetition rates from a monolithically integrated mode-locked laser device

Xuhan Guo, Adrian H. Quarterman, Adrian Wonfor, Vojtech Olle, Richard V. Penty, Ian H. White, Univ. of Cambridge (United Kingdom)

Although monolithically mode-locked laser diodes (MMLLDs) have great potential for a wide range of applications due to their low cost, compactness, high efficiency, and unique ability to be directly electrically modulated, they cannot yet compete with mode-locked solid state or fiber lasers in terms of pulse duration or peak power. However, recent advances in the design and fabrication of photonic integrated circuits (PICs) are enabling rapid progress in this field. To address the issues of high repetition rates and low peak powers in MMLLDs we demonstrate an integrated MMLLD-Modulator-MOPA concept designed to achieve simultaneous high peak power and low repetition rate operation.

The device presented here consists of a conventional MMLLD with 3.7 GHz fundamental repetition rate, followed by a Mach-Zehnder modulator, which allows the repetition rate to be reduced, and an SOA to boost the output power. It is assembled purely from generic building blocks, and the design and fabrication of this device therefore addresses the issue of high R&D cost by using the advantages offered by the EuroPIC foundry approach.

Using this device, we demonstrate the generation of 12.3 ps pulses at a wavelength of 1550 nm, and with peak powers up to 90 mW. The Mach-Zehnder modulator allows electronic tuning of the repetition rate from 3.7 GHz to 108 MHz, and the MOPA boosts the peak power by up to 14 dB compared with the MMLLD alone. These results are a significant improvement on those achieved in previous designs using MMLLDs with 14 GHz fundamental repetition rates.

8640-7, Session 2

Monolithic wide tuning laser diodes for gas sensing at 2100 nm

Lars Hildebrandt, Andreas Heger, Johannes Koeth, Marc O. Fischer, nanoplus GmbH (Germany)

Novel monolithic widely tunable laser diodes in the 2.1µm wavelength region based on GaSb / AlGaAsSb are presented. Using the concept of a binary superimposed (BSG) lateral grating structure and multisegment Vernier-tuning, stable single-mode output is realized at discrete wavelength channels in the 2060 nm – 2140 nm region. A total tuning above 80 nm in six channels is demonstrated. In every wavelength channel, the output wavelength can be tuned by current and temperature. Each wavelength channel offers between 1 nm and 6 nm of modehop free tuning, making this novel widely tunable laser highly attractive as a monolithic multiple-gas sensing light source. The wavelength channels can be arbitrarily placed within the material gain allowing BSG lasers to sweep over any gas absorption line within 80nm.

Within a wavelength channel, the widely tunable lasers show DFB like spectral performance with average side-mode suppression-ratios above 40 dB, output power of up to 15 mW at 25°C and comparable temperature and current tuning coefficients in the talk we will present an overview of laser concept, performance data and applications.

8640-8, Session 2

Narrow-linewidth three-electrode regrowth-free semiconductor DFB lasers with uniform surface grating

Kais Dridi, Abdessamad Benhsaien, Akram Akrouf, Univ. of Ottawa (Canada); Jessica Zhang, Canadian Microelectronics Corp. (Canada); Trevor J. Hall, Univ. of Ottawa (Canada)

There has been much interest in developing low-cost laser sources for applications such as photonics integrated circuits and advanced coherent optical communications. The ultimate objectives in this development include a wide wavelength tunability, a narrow linewidth, and an ease of integration with other devices. For this purpose, semiconductor surface grating distributed feedback (SG-DFB) lasers have been introduced. SG-DFB manufacturing consists of a unique sequence of planar epitaxial growth resulting in a major simplification to the fabrication process. SG-DFB lasers are highly monolithically integrate-able with other devices due to their small footprint.

The segmentation of the built-in top electrode helps to alleviate the adverse spatial-hole burning effects encountered in single-electrode devices and brings hence significant enhancements to the laser performance. For the first time, we report here on the design, fabrication, and characterization of InGaAsP/InP multiple-quantum-well (MQW) SG-DFB lasers with uniform third-order surface grating etched by means of stepper lithography and inductively-coupled reactive-ion. The uncoated device reported here is 750 µm-long SG-DFB laser whose central and lateral top electrodes are 244 µm-longs each, separated by two 9 µm-long grooves. The experimental characterization shows stable single mode operation at room temperature under uniform and non-uniform injection. High side mode suppression ratios (SMSRs) (50-55dB) under a wide range of injection current have been discerned as well. A relatively broad wavelength tuning (>4nm) has also been observed. Moreover, a narrow linewidth (<250 kHz) has been recorded for different injection currents.

**Conference 8640:
Novel In-Plane Semiconductor Lasers XII**

8640-9, Session 2

Sub-MHz linewidth of 633-nm diode lasers with internal surface DBR gratings

David Feise, Gunnar Blume, Johannes Pohl, Bernd Sumpf, Katrin Paschke, Ferdinand-Braun-Institut (Germany); Hendrick Thiem, Matthias Reggentin, Thomas Laurent, eagleyard Photonics GmbH (Germany)

Red-emitting diode lasers having a large coherence length and a tunable, narrow spectral line width with an emission power in the 10 mW range are sought for a variety of techniques in applications such as spectroscopy, interferometry and holography. Currently helium-neon lasers or diode lasers with external wavelength stabilization are widely used for these applications.

By integrating a wavelength stabilization element into the ridge waveguide (RW) of the diode laser chip itself a new degree of miniaturization and stability can be reached. To this end, we have developed RW lasers with deeply etched surface distributed Bragg reflector (DBR) gratings in order to achieve a high-yield, single-epitaxy manufacturing process. These DBR lasers consist of a 1.5 mm RW gain section and a 500 μm grating DBR-reflector, which has a reflectivity of about 60%. The facets of the laser were coated to achieve a reflectivity of 30% at the front and smaller than 0.1% at the rear facet.

The diode lasers achieve an output power of 20 mW at 150 mA and 15°C at a wavelength of about 633 nm. The spectral selectivity of the DBR is sufficient to allow single longitudinal operation at selected working points. Self-delayed heterodyne measurements were performed to measure the emission line width of these lasers using a 1 km long fibre, which gives a spectral resolution of about 100 kHz. A line width of less than 1 MHz was obtained. In reliability tests at 14 mW a lifetime of more than 3,000 h could be demonstrated, dedicating these devices for the above mentioned applications.

8640-10, Session 2

Mass production design for a high-speed continuously-tunable and monolithically formed DFB laser

Bob van Someren, Mach8 Lasers (Netherlands); Christian Zimmermann, nanoplus GmbH (Germany)

We are developing an acoustically induced DFB laser where the DFB grating is set up by the index variations caused by a high frequency acoustical field driven in the waveguide layer of a standard side emitting laser stack. The acoustical field is set up by an acoustical resonator, which is formed monolithically on the laser, close to the ridge waveguide. The width of the acoustical resonance is in the order of 2 to 4 μm , depending on design. Thus the tuning range of the laser is also in the range of 2 to 4 % of the center wavelength. The RF frequencies needed to drive the acoustical field are in the order of 2 to 4 GHz and thus the tuning bandwidth is in the order of nano seconds.

8640-11, Session 2

InP quantum dot lasers with temperature-insensitive wavelength

Sam Shutts, Peter M. Smowton, Stella N. Elliott, Cardiff Univ. (United Kingdom); Andrey B. Krysa, The Univ. of Sheffield (United Kingdom)

An emission wavelength that is stable as a function of temperature is a prime requirement of new developments in laser applications such as lab-on-a-chip or optical coherence tomography where room temperature or above, passively cooled and portable operation is required. In edge-emitting lasers, where the lasing wavelength follows the gain peak position, we achieved improvement in the temperature sensitivity by careful cavity design. The two main competing influences on gain peak position are the shift in bandgap of the material as a function of temperature and the degree of pumping. We used detailed measurements of the gain spectra as a function of temperature obtained using the segmented contact method to design the lasing cavity. Control of the length of the cavity and the degree of pumping required to reach threshold enabled us to reduce the temperature sensitivity of the wavelength. A superior improvement is available in quantum dot compared to quantum well based devices because of the broad gain spectrum produced by the distribution of dot sizes obtained with Stranski Krastanov growth. We grew structures consisting of 3 monolayers of InP deposited on a lattice matched $\text{Al}_{0.3}\text{Ga}_{0.7}\text{InP}$ lower confining layer covered with a quantum well upper confining layer of lattice matched GaInP. These layers were repeated 3x and enclosed in an $\text{Al}_{0.3}\text{Ga}_{0.7}\text{InP}/\text{AlInP}$ optical waveguide. The structures were grown by MOVPE on GaAs substrates. We achieved a low figure of 0.03 nm/K, up to 106 °C (380 K) as compared to the 0.17 nm/C due to the bandgap change.

8640-12, Session 3

654-nm broad-area lasers for QCW operation with a maximal facet load of 76 mW/ μm

Bernd Sumpf, Martina Pohl, Wolfgang Pittroff, Ralf Staske, Götz Erbert, Günther Tränkle, Ferdinand-Braun-Institut (Germany)

Compared to diode lasers emitting in the near infrared, the development of high power diode lasers in the red spectral range is more challenging due to the applicable compound semiconductors and the limited stability of the laser facets. At 654 nm, high-power diode lasers operating in QCW mode are needed for the efficient pumping of Q-switched Alexandrite ($\text{Cr}^{3+}:\text{BeAl}_2\text{O}_4$) lasers.

The presented broad area (BA) lasers are based on a GaInP single quantum well embedded in AlGaInP waveguide layers. The structure provides a vertical far field angle of 31° (FWHM). The material data are: transparency current density 220 A/cm², internal efficiency 0.83, internal losses 1.0 cm⁻¹. BA lasers (100 μm x 1.5 mm) were fabricated, facet coated including a passivation procedure, and mounted on AlN, CuW, and CVD diamond submounts.

In QCW operation (100 μs , 35 Hz) at 15°C, devices mounted on AlN had threshold currents of about 600 mA, slope efficiencies up to 1.3 W/A, and conversion efficiencies of 0.36. A maximal output of 6.3 W was measured. At -10°C the maximal peak power was determined to 7.6 W, i.e. a facet load of 76 mW/ μm .

The influence of the overall strain (mounting and QW) for devices mounted on the different submount materials on threshold current, slope efficiency, conversion efficiency, spectra, near and far field width will be discussed. Finally measurements at different duty cycles up to CW operation complete the presentation.

**Conference 8640:
Novel In-Plane Semiconductor Lasers XII**

8640-13, Session 3

Highly-reliable operation of 638-nm broad stripe laser diode with high wall-plug efficiency for display applications

Tetsuya Yagi, Naoyuki Shimada, Takehiro Nishida, Hiroshi Mitsuyama, Motoharu Miyashita, Mitsubishi Electric Corp. (Japan)

Laser based displays, as laser pico to cinema projectors have gathered much attention because of large gamut, low power consumption, and so on. Laser light sources for the displays are operated mainly in CW, and heat management is one of the big issues. Therefore, highly efficient operation is necessitated. And the displays are requested to be highly reliable, meaning the lasers should be highly reliable. In this paper, we will present latest results of latest Mitsubishi 638 nm broad stripe laser diode (LD), which shows highly reliable and highly efficient operation.

The main cause that limits the wall plug efficiency (WPE) in red LDs is an electron over flow from an active layer. To reduce the overflow, large optical confinement with AlInP cladding layers is one of powerful methods, and adopted. Conventional broad stripe LDs have no facet protecting structures as a window-mirror one because the ones have low optical density. We found that catastrophic optical degradation at the facet is a main degradation mechanism in red LDs and the window-mirror is mandatory for highly reliable operation. Our LDs also have a window-mirror structure for highly reliable operation. The LD shows WPE of 35% at 600 mW output, CW, 25°. To the best of our knowledge, the value is the highest record. The LDs have been operated at 400 mW, CW, 45°. The LDs show stable operation up to 7000 hours without any catastrophic optical degradation.

8640-14, Session 3

Continuous-wave operation of green/yellow laser diodes based on BeZnCdSe quantum wells (Invited Paper)

Ryoichi Akimoto, Toshifumi Hasama, Hiroshi Ishikawa, National Institute of Advanced Industrial Science and Technology (Japan); Jun-ichi Kasai, Sumiko Fujisaki, Shigehisa Tanaka, Shinji Tsuji, Hitachi, Ltd. (Japan)

We have demonstrated continuous wave operation of BeZnCdSe quantum well laser diodes at room temperature in the green to yellow spectrum range. The laser diodes structures were grown by molecular beam epitaxy. To overcome low doping ability of p-cladding layer materials such as ZnMgSSe or ZnMgBeSe, a short-period superlattice of BeMgZnSe/ZnSe:N was employed [1]. High-power lasing over 50mW at a peak wavelength of 536 nm was achieved [2]. By employing highly strained BeZnCdSe quantum wells, continuous wave lasing up to 570nm has been achieved. The threshold current densities of 20-?m-wide lasers were found to be sufficiently low (less than 0.85 kA/cm²) in the wavelength range of 545nm to 570nm[3]. It should be noted that ZnSe-based alloy containing beryllium has a much higher degree of covalency than other II-VI compounds. Thus these material systems are expected to overcome a problem of limited lifetime due to weakness inherent to II-VI materials [4].

References

- [1] J. Kasai, R. Akimoto, H. Kuwatsuka, T. Hasama, H. Ishikawa, S. Fujisaki, T. Kikawa, S. Tanaka, S. Tsuji, H. Nakajima, K. Tasai, Y. Takiguchi, T. Asatsuma and K. Tamamura, Applied Phys. Express 3, 091201 (2010).
- [2] S. Fujisaki, J. Kasai, R. Akimoto, S. Tanaka, S. Tsuji, T. Hasama and H. Ishikawa, Applied Phys. Express 5, 062101 (2012).
- [3] J. Kasai, R. Akimoto, T. Hasama, H. Ishikawa, S. Fujisaki, S. Tanaka and S. Tsuji, Applied Phys. Express 4, 082102 (2011).
- [4] A. Waag, F. Fischer, H. J. Lugauer, Th. Litz, J. Laubender, U. Lunz, U.

Zehnder, W. Ossau, T. Gerhardt, M. Moller, and G. Landwehr: J. Appl. Phys. 80792 (1996).

8640-15, Session 3

High-power blue and green laser diodes and their applications (Invited Paper)

Uwe Strauss, Thomas Hager, Jens Müller, Fabian Kopp, Georg Brüderl, Teresa Lermer, Adrian Avramescu, OSRAM Opto Semiconductors GmbH (Germany)

On one side direct green laser of several tens of milliwatt will pave the way for high volume applications like embedded laser projection. In 2011, Osram achieved cw-operation at 50mW output power with good lifetimes. In 2012, several companies announced products for mobile projection with low power consumption. On the other side, there is interest in high power laser projection above 1000lm. In 2012, blue power laser above 1W optical output entered the market. Green light was generated by phosphor conversion reaching luminance above the level of LED based systems. The next steps will be reduction of system costs by an increase of the optical output per device. In this talk, a push of power levels will be presented: direct green R&D lasers are characterized up to 200mW, blue R&D power lasers are tested up to 3W.

8640-16, Session 4

Passive mode-locking in the cavity of monolithic GaN-based multi-section laser diodes

Thomas Weig, Fraunhofer-Institut für Angewandte Festkörperphysik (Germany); Ulrich T. Schwarz, Fraunhofer-Institut für Angewandte Festkörperphysik (Germany) and Albert-Ludwigs-Univ. Freiburg (Germany); Luca Sulmoni, Jean-Michel J. Lamy, Nicolas Grandjean, Ecole Polytechnique Fédérale de Lausanne (Switzerland); Dmitri L. Boiko, Ctr. Suisse d'Electronique et de Microtechnique SA (Switzerland)

GaN-based laser diodes with monolithically integrated saturable absorbers are compact short-pulse, high peak power light sources in the violet and blue spectral range. We demonstrate multi-segment, edge-emitting laser diodes with an absorber section p-contact in the center or at the edge of the cavity. Envisioned applications for these multi-section laser diodes are high-density optical storage systems, high-resolution bioimaging, and nanoprocessing.

The pulse repetition frequency for intra-cavity mode-locking is given by the round trip time in the cavity. For typical cavity lengths of the order of one millimeter, the repetition frequency lies in the several ten GHz range. The carrier lifetime in the absorber section may not exceed a few ten picoseconds in order to stabilize mode-locking at such high frequency. We measure the carrier life time in the absorber as function of reverse bias voltage. For negative bias voltages of -15 V, the measurements provide an upper limit of 40 ps to the carrier life time in the absorber. Tunneling is the dominating process in this regime.

We observe passive mode-locking in laser diodes where the absorber section extends of 20 to 30% of the cavity length. Pulse repetition frequencies and pulse length are measured by a streak camera. For a 1.2 mm long cavity the values are 40 GHz and 7 ps (full width half maximum), respectively. In a laser diode with 0.6 mm cavity length stable mode-locking was observed with a repetition frequency of 90 GHz and pulse width of 4 ps, not taking into account the temporal resolution of about 1.5 ps. These results are consistent with a very fast switching of the saturable absorber between absorption and transparency.

**Conference 8640:
Novel In-Plane Semiconductor Lasers XII**

8640-17, Session 4

Superradiant pulse generation from InGaN heterostructures *(Invited Paper)*

Peter P. Vasil'ev, Univ. of Cambridge (United Kingdom) and P.N. Lebedev Physical Institute (Russian Federation); Vojtech Olle, Richard V. Penty, Ian H. White, Univ. of Cambridge (United Kingdom)

Superradiant (SR) emission in semiconductors can be used for the generation of high power picosecond or sub-picosecond pulses, on-demand, at a variety of wavelengths. This flexible method of pulse production is suited for a wide range of applications, including biological imaging and high density storage. Such applications would particularly benefit from short wavelength SR generation, and therefore following a general introduction to the field, this paper describes recent achievements in the demonstration of SR emission in GaN-based structures.

We have experimentally demonstrated SR emission from 2- and 3-section violet GaN/InGaN semiconductor lasers. The p-contact of commercial single-contact lasers were modified into multiple contact structures by focused ion beam etching. SR pulse evolution and different operating regimes have been measured as a function of temperature and driving conditions varying both the forward pulsed current to the gain section and the reverse bias voltage to the absorber section. Temperature dependence of pulse parameters in the range of from 15 deg C to 90 deg C was studied. The properties of SR emission from tested GaN/InGaN structures are very similar to those reported for infrared AlGaAs/GaAs laser diodes.

8640-18, Session 4

InGaN/GaN quantum dot blue and green lasers *(Invited Paper)*

Pallab K. Bhattacharya, Animesh Banerjee, Thomas Frost, Ethan Stark, Univ. of Michigan (United States)

Compact solid state visible lasers are needed for a variety of applications including full color mobile projectors, heads up displays in automobiles, optical data storage, and medical applications. Visible lasers emitting in the green and shorter wavelengths are generally realized with quantum well active regions. Quantum dots (QDs) provide several critical advantages over quantum wells: (i) 3-D confinement; (ii) smaller piezoelectric field and resulting blue shift with bias current increase; (iii) reduced recombination at dislocations. These advantages were demonstrated by us recently, for the first time, in green- and blue-emitting InGaN/GaN Fabry-Pérot QD lasers. In this talk we will describe the epitaxial growth and optical properties of these lasers.

The InGaN/GaN QD laser heterostructures are grown by plasma-assisted molecular beam epitaxy. With optimized growth, the internal quantum efficiency of the blue (420nm) and green (520nm) QDs are ~60% and 38%, respectively. Tunnel injection heterostructure lasers, for more uniform injection of holes, were also grown. Ridge waveguide lasers with ridge widths varying from 2-15um and cavity lengths of 0.7-1.5mm were fabricated.

The threshold current density is typically ~1.2 kA/cm² for the green lasers, and ~930A/cm² for the blue lasers under pulsed biasing. These values are considerably lower than those reported for equivalent InGaN/GaN quantum well lasers. The measured differential gain of the devices is ~2x10⁻¹⁶cm² and the temperature dependence of the threshold current of the green lasers is characterized by T₀~200K. The small-signal modulation properties of the devices are being characterized and these characteristics will also be described and discussed.

8640-19, Session 4

Optical and polarization properties with staggered AlGaIn quantum wells for mid- and deep-ultraviolet lasers and light-emitting diodes

Jing Zhang, Nelson Tansu, Lehigh Univ. (United States)

Mid- and deep-ultraviolet (UV) lasers and light emitting diodes (LEDs) have applications for biochemical agent identification, and free space communication. Approaches based on novel AlGaIn-based QW active region design with the potential to achieve large gain and spontaneous emissions are of great interest for UV lasers and LEDs. One of the key factors leading to large optical gain in deep-UV AlGaIn QW laser active region is by using the valence subband crossover between the heavy-hole (HH) and crystal-field split off (CH) subbands, which will lead to dominant and large transverse magnetic (TM)-polarized gain.

In this work, we investigate the use of the large overlap design by using staggered AlGaIn QWs in suppressing the charge separation, as well as achieve polarization control of the emission. The staggered AlGaIn QWs can be realized by engineering the step-shaped layers of high and low Al-content AlGaIn. The use of staggered AlGaIn QWs leads to improved optical matrix elements resulting in large TM-polarized optical gain. The use of two-layer staggered AlGaIn QW leads to ~21.5% higher optical gain than that of the conventional QW accompanied by reduction in emission wavelengths, and this improvement is attributed from its suppressed charge separation effect. The enhanced TM-polarized spontaneous emissions are also obtained from the use of two-layer staggered AlGaIn QW, which are applicable for deep-UV LEDs. In addition, by using thinner staggered AlGaIn QW, the polarization control of the gain properties can also be achieved resulting in polarization switching to TE-polarized gain at deep UV spectral regime.

8640-20, Session 5

Mid-infrared quantum cascade frequency combs *(Invited Paper)*

Jérôme Faist, Andreas Hugi, ETH Zurich (Switzerland)

We demonstrate the operation of an electrically injected, quantum cascade laser based mid-infrared frequency comb. Very narrow beatnote linewidth of <200Hz with a comb spanning 60cm⁻¹ are demonstrated. When beaten with a DFB QCL laser, the device shows a linewidth of 1MHz, limited by temperature and thermal drifts. Applications to spectroscopy will be discussed.

8640-21, Session 5

Frequency-modulated quantum cascade lasers for free-space data links *(Invited Paper)*

Sergey Suchalkin, Seungyong Jung, Stony Brook Univ. (United States); Min Jang, The Univ. of Texas at Austin (United States); Richard L. Tober, U.S. Army Research Lab. (United States); Mikhail A. Belkin, The Univ. of Texas at Austin (United States); Gregory Belenky, Stony Brook Univ. (United States)

Several approaches to produce high-speed optical frequency modulation (FM) in mid-infrared quantum cascade lasers (QCLs) by both electrical and optical means will be discussed and compared. Experimental results showing that QCLs can be FM-modulated at >1GHz data bandwidth rates with >10 GHz frequency excursions will be presented together with a proof-of-principle QCL-based optical FM data link.

**Conference 8640:
Novel In-Plane Semiconductor Lasers XII**

8640-22, Session 5

Discrete tuning between the modes of a multiple-wavelength quantum cascade laser using a micro-scale external cavity

Meinrad Sidler, ETH Zurich (Switzerland); Romain Blanchard, Harvard School of Engineering and Applied Sciences (United States); Tobias S. Mansuripur, Harvard Univ. (United States); Patrick Rauter, Stefan Menzel, Harvard School of Engineering and Applied Sciences (United States); Yong Huang, Jae-Hyun Ryou, Russell D. Dupuis, Georgia Institute of Technology (United States); Jérôme Faist, ETH Zurich (Switzerland); Federico Capasso, Harvard School of Engineering and Applied Sciences (United States)

We explore a mechanism allowing for controlled discrete tuning between the modes of a multiple-wavelength QCL, relying on a micro-scale external cavity. By positioning a gold mirror behind the back facet of the laser, we form a variable length Fabry-Perot cavity. There are no focusing optical elements placed in the cavity, so the magnitude of the external feedback decreases quickly with the external cavity length.

When a single-mode distributed feedback (DFB) QCL is used, we observe a periodic modulation (with a periodicity of half a wavelength) of the threshold current (with 25% maximum modulation amplitude) and maximum output power (with 66% maximum amplitude) as a function of the external cavity length. This modulation is a coupled cavity effect: when a given mode is in resonance with the external cavity, high scattering losses increase the threshold and decrease the maximum power output. However, at longer cavity lengths the modulation depth decreases rapidly due to the reduced amount of feedback.

We then use a multi-wavelength DFB-QCL lasing simultaneously at four modes spaced apart by 20 cm⁻¹ in the absence of an external cavity. With the external cavity, we observe a modulation depth close to 100% for each individual mode. This increased modulation depth is the result of gain competition, which amplifies the effects of small cavity loss differences between the modes. MEMS devices could be used to form the tunable external cavity.

8640-23, Session 5

External ring-cavity quantum cascade lasers
(Invited Paper)

Pietro Malara, Istituto Nazionale di Ottica (Italy) and Harvard Univ. (United States); Romain Blanchard, Tobias S. Mansuripur, Harvard Univ. (United States); Paolo de Natale, Istituto Nazionale di Ottica (Italy); Federico Capasso, Harvard Univ. (United States)

A mid-infrared external ring-cavity laser based on a quantum cascade gain medium is demonstrated. Its properties are investigated by a direct comparison to the Fabry-Perot (FP) device represented by the QC waveguide without external cavity.

Above a critical current, the ring QCL undergoes a transition from a perfectly bidirectional regime to an unstable regime, where the power in the clockwise and anticlockwise direction is unbalanced. By further increasing the current, the power oscillations increase, until a fully directional regime is achieved, as shown in the figure below. The clockwise-anticlockwise competition dynamics that give rise to this behavior are similar to those observed in semiconductor and gas ring lasers, and can be modeled by means of a field rate equation approach.

The directional regime of the ring QCL is also of particular interest because spatial hole burning (SHB) is suppressed. A comparison between the FTIR spectra shows that the multimode behavior that characterizes the FP-QCL is suppressed in the directional ring laser, which spontaneously approaches single-mode operation after several round-trips. The existence of SHB-free regimes and the presence of an external intracavity beam path make the presented laser an excellent

candidate for high-energy active mode-locking, and high sensitivity spectroscopic applications in the mid-infrared.

8640-24, Session 6

Broadband mid-infrared wavefront engineering with optical antenna metasurfaces
(Keynote Presentation)

Federico Capasso, Nanfang Yu, Patrice Genevet, Mikhail A. Kats, Harvard School of Engineering and Applied Sciences (United States); Francesco Aieta, Harvard School of Engineering and Applied Sciences (United States) and Univ. Politecnica delle Marche (Italy); Zeno Gaburro, Harvard School of Engineering and Applied Sciences (United States) and Univ. degli Studi di Trento (Italy)

Conventional optical components such as lenses and holograms rely on gradual phase shifts accumulated during light propagation to shape light beam. New degrees of freedom in optical design are attained by introducing in the optical path abrupt phase changes over the scale of the wavelength. In this talk, we will discuss how a two-dimensional array of plasmonic antennas in form of V-shape metallic structures with spatially varying phase response and sub-wavelength separation can imprint such phase discontinuities on propagating light and thereby enable wavefront engineering. The design of these metasurfaces is focused in mid-infrared because of low plasmonic losses and the lack of standard high performance optical components in this wavelength range

We demonstrated that a linear phase variation on the interface between two media leads to anomalously reflected and refracted beams in accordance with generalized laws of reflection and refraction derived from Fermat's principle. If we consider an interface with a phase gradient arbitrarily oriented with respect to the plane of incidence rather than parallel to it, the reflected and refracted beams are non-coplanar with the incident beam, leading to a three-dimensional generalization of the new laws of reflection and refraction. Out of plane refraction has been experimentally demonstrated.

Optical antenna metasurfaces enable wavefront engineering with unprecedented flexibility, which is promising for a wide variety of planar optical components. Optical phase array with subwavelength control of light parameters could lead to a surface optics technology capable of large scale applications including novel spatial wave modulators.

8640-25, Session 6

Recent progress in development of InAs-based interband cascade lasers
(Invited Paper)

Rui Q. Yang, Lu Li, Yuchao Jiang, Lihua Zhao, Robert T. Hinkey, Hao Ye, Tetsuya D. Mishima, Michael B. Santos, Matthew B. Johnson, The Univ. of Oklahoma (United States)

After about 18 years of exploration and development, interband cascade (IC) lasers have now been proven to be capable of continuous wave operation at room temperature and above for a wide wavelength range of 2.9 to 5.7 micron in the mid-infrared spectral region. In contrast to quantum cascade lasers based on intersubband transitions, IC lasers circumvent the fast phonon scattering issue by using the transition between conduction and valence bands for photon emission. As such, the threshold current density is significantly lowered with high voltage efficiency, resulting in low power consumption. Here, we will present our recent progress in InAs-based IC lasers, which use plasmon cladding layers to replace superlattice cladding layers, resulting in improved thermal dissipation and extended lasing wavelengths.

**Conference 8640:
Novel In-Plane Semiconductor Lasers XII**

8640-26, Session 6

Extremely temperature-insensitive continuous-wave broadband quantum cascade lasers

Kazuue Fujita, Masamichi Yamanishi, Shinichi Furuta, Tatsuo Dougakiuchi, Atsushi Sugiyama, Tadataka Edamura, Hamamatsu Photonics K.K. (Japan)

Quantum cascade (QC) lasers are promising light sources for many chemical sensing applications in the mid-infrared spectral range. For industrial applications, broadband wavelength tuning of external-cavity QC lasers with very broad gain-width has been demonstrated. QC lasers based on anti-crossed dual-upper-state (DAU) designs are one of the promising candidates because of its broad bandwidth as well as high device performances. In fact, wide wavelength tuning of external cavity QC lasers with the anti-crossed DAU designs has been exhibited in several wavelengths: the tuning range of ~25% in pulsed mode and >17% in cw mode at room temperature.

Here we report conspicuous temperature performances of continuous wave quantum cascade lasers with broad gain bandwidths. The lasers with the anti-crossed DAU designs, characterized by strong super-linear current-light output curves, exhibit the extremely high characteristic temperature for threshold current density, $T_0 \sim 750$ K above room temperature. In addition, its slope efficiency is growing with increasing temperature (negative T_1 -value). For the pulsed operation of a short 1 mm length laser, the temperature coefficient reaches the surprisingly high value of 2520 K over 340-380 K temperature range, which corresponds to the rate of temperature change, $d(I_{th}/I_{th,300K})/dT = 5 \times 10^{-4} \text{ 1/K}$. The distinctive characteristics of the DAU lasers are attributable to the optical absorption quenching which has been clarified to take place in indirect pumped QC lasers. Such high characteristic temperatures of the DAU-QC lasers provide great advantages for practical applications, in addition to its potential of broadband tuning.

8640-27, Session 6

Mid-infrared electroluminescence from ridge-waveguide devices using hole funneling into the valence band of GaAs/Al(Ga)As quantum cascade structures

Mohammed I. Hossain, Purdue Univ. (United States); Zoran Ikonc, Univ. of Leeds (United Kingdom); John L. Reno, Sandia National Labs. (United States); Oana Malis, Purdue Univ. (United States)

We report mid-infrared electro-luminescence from ridge-waveguide devices using p-doped GaAs/AlGaAs/AIAs quantum cascade (QC) structures. This is the first report of electro-luminescence from full laser devices using intersubband transitions in the valence band of the GaAs/AlGaAs material system and an important step towards hole quantum cascade lasers (QCLs). The novelty of the devices consists in the mechanism of charge injection into the active region and the waveguide geometry. A funnel injector made of Al_{0.2}Ga_{0.8}As quantum wells with AIAs barriers is used to fine tune injection of holes into the GaAs/AIAs active region. The waveguide has a single-metal layer plasmon geometry with a 6- μm thick core. The arsenide materials were grown by molecular-beam epitaxy (MBE) using Carbon for p-type doping. The design and growth take advantage of the virtual lack of strains in arsenide materials as compared to other p-type materials studied in the past (i.e. Si/SiGe). Moreover, the arsenide MBE growth is fairly mature, and, therefore, has the monolayer thickness control and reproducibility necessary for the growth of hole QC structures. The luminescence spectra exhibit a peak at about 150-meV consistent with heavy-to-heavy hole intersubband transitions. The nature of the transition was confirmed with polarization sensitive measurements. The measured energy is in agreement with the designed light emitting transition calculated considering an interdiffusion

length of 4- \AA . Moreover, the I-V characteristics indicated that the field across the active region matches the design field (70-kVcm⁻¹). These results provide insight and valuable information for further device optimization towards a possible hole QCL.

8640-28, Session 7

Advances in electrically pumped Ge-on-Si lasers (Invited Paper)

Jurgen Michel, Rodolfo E. Camacho-Aguilera, Yan Cai, Lin Zhang, Zhaohong Han, Lionel C. Kimerling, Massachusetts Institute of Technology (United States)

Electrically pumped Ge lasers, integrated on a CMOS platform, are promising candidates as integrated light sources for on-chip photonic systems. The wide gain spectrum from 1520 nm to 1700 nm makes the Ge lasers ideal light sources for WDM applications.

There are two main challenges for efficient electrically pumped Ge lasers, high n-type doping concentration and low-loss coupling from Ge waveguides to Si waveguides. The high n-type doping is necessary to overcome the indirect bandgap of Ge and reach gains comparable to other compound semiconductor lasers. We will show that an in-situ delta doping process will yield active Phosphorous concentrations of about $5 \times 10^{19} \text{ cm}^{-3}$.

The first demonstrated lasers were made from Ge waveguides and did not couple light to Si waveguides, commonly used for on-chip photonic systems. Due to the large refractive index difference between Ge (4.0) and Si (3.5) low loss coupling from a Ge waveguide to a Si waveguide is challenging but a requirement for efficient Ge lasers. We will discuss the different device designs to provide low loss coupling for low threshold lasing.

8640-29, Session 7

Optimization of the hybrid silicon photonic integrated circuit platform (Invited Paper)

Martijn J. R. Heck, Michael L. Davenport, Sudharsanan Srinivasan, Jared Hulme, John E. Bowers, Univ. of California, Santa Barbara (United States)

In the hybrid silicon platform, active III/V based components are integrated on a silicon-on-insulator photonic integrated circuit by means of wafer bonding. This is done in a self-aligned back-end process at low temperatures, making it compatible with CMOS-based silicon processing. This approach allows for low cost, high volume, high quality and reproducible chip fabrication.

Such features make the hybrid silicon platform an attractive technology for applications like optical interconnects, microwave photonics and sensors, operating at wavelengths around 1.3 μm and 1.55 μm . For these applications energy efficient operation is a key parameter. In this paper we present our efforts to bring the III/V components in the hybrid silicon platform, such as lasers and optical amplifiers, on par with the far more mature monolithic InP-based integration technology.

We present our development work to increase hybrid silicon laser and amplifier wall-plug efficiency. This is done by careful optimization of III/V mesa geometry and guiding silicon waveguide width. We also discuss current injection efficiency and thermal performance. Furthermore we show the characterization of the low-loss and low-reflection mode converters that couple the hybrid III/V components to silicon waveguides. Reflections below -32 dB and a loss of 0.3 dB per converter were obtained.

**Conference 8640:
Novel In-Plane Semiconductor Lasers XII**

8640-31, Session 7

InAs/GaAs quantum dot lasers on Si substrates by wafer bonding (*Invited Paper*)

Katsuaki Tanabe, Yasuhiko Arakawa, The Univ. of Tokyo (Japan)

No Abstract Available.

8640-32, Session 7

The role of silicon surface orientation on the performance of Ga(NAsP)/(BGa)(AsP) QW lasers on (001) Si

Nadir Hossain, Graham Read, Stephen J. Sweeney, Univ. of Surrey (United Kingdom); Sven Liebich, Martin Zimprich, Kerstin Volz, Bernardette Kunert, Wolfgang Stolz, Philipps-Univ. Marburg (Germany)

Electrical injection laser operation in monolithically integrated Ga(NAsP)/(BGa)P QW lasers on an (001) silicon substrate shows great promise for future integration of photonics with electronics. Lasing has been obtained up to 165K with a Jth of 1.6 kAcm⁻². Achieving room temperature operation with low Jth requires an understanding of the physical origins of the high Jth in these devices. In this work, we investigate the correlation of the silicon substrate miscut with the recombination and loss mechanisms in Ga(N~7%AsP)/(BGa)(AsP)/Si SQW lasers. The devices in this study grown on two different silicon substrates (Device A is on a silicon substrate with 0.1° miscut angle in (110) direction and Device B is on a silicon substrate with 0.1° miscut angle but 30° away from (110) direction). The Jth of device A (device B) is measured to be ~3.2 kAcm⁻² (~0.87 kAcm⁻²) at 80K. The lower Jth in device B compared to device A suggests that device B is grown on a silicon substrate with a miscut angle and direction close to optimum. T0 on device A (device B) to be ~46K (~118K) at 80K. The value of T0 = 2T/3 indicates that the monomolecular current contribution at threshold in device A is significant. T1 on device A (device B) to be ~51 K (~62 K) at 80K. The small T1 values is an indication of optical or recombination losses. The prognosis for room temperature lasing on silicon with this approach will be discussed in more depth at the conference.

8640-33, Session 8

Subwavelength plasmonic lasers (*Invited Paper*)

Hong-Gyu Park, Soon-Hong Kwon, Ju-Hyung Kang, Yoon-Ho Kim, Korea Univ. (Korea, Republic of)

We propose two types of full three-dimensional subwavelength surface-plasmon-polariton (SPP) cavities: a metal-coated dielectric nanowire with an axial heterostructure and a dielectric nanodisk/silver nanopan structure. In the metal-coated dielectric nanowire plasmonic structure, SPPs are strongly confined at the nanowire-metal interface sandwiched by a plasmonic mirror that consists of nanowire core/low-index shell/metal shell. Such confinement is allowed based on the following two properties: controllable frequency of the plasmonic mode by introducing a low-index layer between the dielectric nanowire core and outer metallic shell, and the existence of a cut-off frequency of the plasmonic mode. Numerical simulations show for a cavity $50 \times 50 \times 40 \text{ nm}^3$ that a mode volume of <math><10^{-5} \text{ um}^3</math> and a quality factor of >36000 are achieved at temperature of 20 K. In addition, we report the experimental demonstration of an optically-pumped plasmonic lasing action from a dielectric nanodisk/silver nanopan structure with a subwavelength mode volume. In experiment, a whispering-gallery plasmonic mode with a mode volume of $0.56 (\lambda/2n)^3$ is excited at the bottom of the silver nanopan structure, which is convinced from measurements of the spectrum, mode image, and polarization state, as well as agreement with numerical simulations. Also, our measurement shows that the

significant temperature-dependent lasing threshold of the plasmonic mode contrasts and distinguishes them from optical modes. We believe that these subwavelength plasmonic cavities and lasers represent a significant step towards the realization of faster and smaller coherent light sources which are suitable for an ultracompact nanophotonic integrated circuit.

8640-34, Session 8

Electrical injection schemes for nanolasers

Alexandra Lupi, Il-Sug Chung, Kresten Yvind, Technical Univ. of Denmark (Denmark)

The performance of injection schemes among recently demonstrated electrically pumped photonic crystal nanolasers has been investigated numerically. The computation has been carried out at room temperature using commercial semiconductor simulation software (Crosslight).

For the simulations two electrical injection schemes have been compared: vertical p-i-n junction through a current post structure as in [1] and lateral p-i-n junction with either uniform material as in [2] or with a buried heterostructure (BH) as in [3].

To allow a direct comparison of the three schemes the same active material consisting of 3 InGaAsP QWs with InGaAsP barriers on an InP substrate has been chosen for the modeling.

In the simulations the main focus is on the electrical and optical properties of the nanolasers i.e. electrical resistance, threshold voltage, threshold current and wallplug efficiency.

In the current flow evaluation the lowest threshold current has been achieved with the lateral electrical injection through the BH; while the lowest resistance has been obtained from the current post structure, even though this model shows a higher current threshold because of the lack of carrier confinement.

The advantages and disadvantages of the different electrical injection schemes will be discussed and guidelines for the optimal device design will be presented.

References

- [1] HG. Park et al., IEEE Journal of Quantum Electronics 41(9), 1131-1141, 2005
- [2] B. Ellis et al., Nature Photonics 5(5), 297-300, 2011
- [3] S. Matsuo et al., Optics Express 20(4), 3773-3780, 2012

8640-35, Session 8

Towards a monolithic photonic crystal waveguide mode-locked laser

Kenneth J. Leedle, Altamash Janjua, Seonghyun Paik, Mark J. Schnitzer, James S. Harris, Stanford Univ. (United States)

For a given average power, the energy per pulse of a mode-locked laser increases with increasing cavity length, lowering the repetition rate. Photonic crystal slow light optical waveguides can be used to address the high repetition rates and resulting low pulse energies of conventional semiconductor lasers by substantially increasing the optical cavity length while keeping the device compact. Such a device could enable a semiconductor laser to power two-photon microscopy, an advanced non-linear technique for time-resolved deep-tissue imaging. We present a design for realizing a monolithic two-segment quantum dot passively mode-locked photonic crystal laser. The cavity consists of a novel photonic crystal waveguide designed for low dispersion and wide bandwidth by engineering the slab thickness and manipulating photonic crystal lattice structure. Group velocity dispersion below $5 \times 10^4 \text{ ps}^2/\text{km}$, over an order of magnitude lower than similar dispersion engineered photonic crystal waveguides, is achieved over more than 2% bandwidth, more than sufficient for mode-locking. Gain is achieved by optically pumping epitaxially grown InAs/GaAs quantum dots in part of the photonic crystal waveguide, and the saturable absorber section

**Conference 8640:
Novel In-Plane Semiconductor Lasers XII**

is reversed biased to enable pulse shaping. A cladding scheme is used to apply reverse bias to the saturable absorber and shorten its recovery time. Devices are fabricated using a combination of electron beam lithography, anisotropic etching, and selective under-etching processes, similar to standard photonic crystal waveguides. The low-dispersion, wide bandwidth waveguide, combined with the low self-phase modulation of InAs quantum dots could enable a compact, low repetition rate mode-locked laser to be demonstrated.

8640-36, Session 8

Photonics beyond diffraction limit: Plasmon waveguide, cavities, and integrated laser circuits (*Invited Paper*)

Xiang Zhang, Univ. of California, Berkeley (United States)

I will discuss recent development in scaling down photonics. First I will present theoretical and experimental investigation of passive low loss waveguide using hybrid plasmon design. We propose a new optical cavity design approach using indefinite medium that has a drastically different scaling law than conventional microcavities, and discuss its experimental demonstrations. Finally we will show an active plasmonic laser circuit that integrated with 5 tiny cavities that multiplexed into a single waveguide-an effort towards integrated photonics at nano-scale.

8640-37, Session 9

Application implications of the impressive advances in quantum cascade lasers and needed characteristics of corresponding detectors (*Invited Paper*)

Hui Chun Liu, Shanghai Jiao Tong Univ. (China)

Semiconductor quantum structures have not only enabled discoveries of new phenomena but also realizations of novel photonic devices. In this talk I will discuss two successful examples and more importantly the applications that they have enabled. The first one is the, by now, well-established quantum-well infrared photodetector (QWIP). Large focal plane arrays up to 1k²1k format and multi-spectral imaging sensors have been fabricated and used in space applications. High performance QWIP imagers are sold and used in various systems. On the other hand, single-element QWIPs have not attracted much interest because of their inherent narrow spectral response (???? ~10-20%) and the need for more cooling than the established HgCdTe detectors, with the exception of high-speed/high-frequency applications. With the development of high performance quantum cascade lasers (QCLs), especially in the mid-infrared region of about 4 to 11 μ m, the situation is different. Here I will first outline the current status of QWIPs and QCLs, and then discuss QWIPs being used in laboratories for high-speed/high-frequency infrared detection involving QCLs. I will continue with discussions of potential applications of QWIP-QCL pair for environmental/industrial sensing in the infrared spectrum. QWIPs and QCLs together form a very promising technology base for sensing.

8640-38, Session 9

Optical wavelength conversion in terahertz quantum cascade lasers (*Invited Paper*)

Pierrick Cavalié, Julien Madéo, Joshua R. Freeman, Jean Maysonnave, Kenneth Maussang, Juliette Mangeney, Jérôme Tignon, Sukhdeep S. Dhillon, Ecole Normale Supérieure (France)

The nonlinear optical properties of intersubband and interband transitions in quantum wells has received considerable attention owing to their enhanced nonlinear susceptibilities compared to the bulk characteristics. Indeed efficient non-linear wave mixing between a near-infrared interband probe in presence of an intense terahertz (THz) beam (intersubband resonance) in quantum wells has been previously demonstrated. However, the THz radiation is typically provided by a Free Electron Laser that strongly limits its relevance to applications. Here we demonstrate that these types of high order nonlinear processes can be realized using the resonant nonlinearities within a compact and practical device – the quantum-cascade-laser.

8640-39, Session 9

Direct optical sampling of a mode-locked terahertz quantum cascade laser

Joshua R. Freeman, Jean Maysonnave, Kenneth Maussang, Pierrick Cavalié, Ecole Normale Supérieure (France); Nathan Jukam, Ruhr-Univ. Bochum (Germany); Harvey E. Beere, David A. Ritchie, Univ. of Cambridge (United Kingdom); Juliette Mangeney, Sukhdeep S. Dhillon, Jérôme Tignon, Ecole Normale Supérieure (France)

Quantum cascade lasers (QCLs) operate over a wide range frequencies, from 250 μ m to below 3 μ m. However, the temporal output of QCLs has received relatively little attention. Modelocking of mid-IR QCLs was observed by second-order autocorrelation [1] but for the THz region this is not available. Recently coherent asynchronous sampling was used to make the first measurement of modelocking in THz QCLs [2]. It was found that the modelocked pulses narrowed as the device was driven further above threshold, opposite to the trend found in [1].

Here we take a different approach and use an electrooptic sampling method to directly sample the total time-domain intensity of the THz radiation from an actively modelocked QCL. The advantages of using intensity detection are: (1) we always detect the total intensity emitted by the QCL rather than only the part which is synchronized with the probe pulse, (2) We do not need any seed pulse or stabilization electronics for the detection.

By using this method we are able to unambiguously determine the shape of the THz pulses emitted from the modelocked QCL. In measuring this we find that the pulses tend to broaden as the QCL is driven further above threshold. However, when the QCL is biased around threshold with a strong round-trip modulation we observe Gaussian-shaped transform limited pulses with a FWHM of 19 \pm 2 ps. Furthermore, we examine the initiation of mode-locking in addition to the quasi-steady-state regime.

[1] C. Y. Wang et al. Opt. Express 17,12929(2009)

[2] S. Barbieri et al. Nat Photon 5,306(2011)

**Conference 8640:
Novel In-Plane Semiconductor Lasers XII**

8640-40, Session 9

THz quantum cascade lasers for operation above cryogenic temperatures (*Invited Paper*)

Mikhail A. Belkin, Karun Vijayraghavan, The Univ. of Texas at Austin (United States); Augustinas Vizbaras, Walter Schottky Institut (Germany); Aiting Jiang, The Univ. of Texas at Austin (United States); Frederic Demmerle, Gerhard Boehm, Ralf Meyer, Markus C. Amann, Walter Schottky Institut (Germany); Alpar Matyas, Reza Chashmahcharagh, Paolo Lugli, Christian Jirauschek, Technische Univ. München (Germany); Zbigniew R. Wasilewski, Univ. of Waterloo (Canada)

In this talk, we will discuss novel approaches to produce THz quantum cascade laser sources that can operate at temperatures of 240K and above. We will present the results of our theoretical and experimental investigation of GaAs/AlGaAs terahertz quantum cascade lasers based on the bandstructure that uses variable height barriers. We will also demonstrate the latest design and performance data for room-temperature terahertz quantum cascade laser sources based on efficient intra-cavity difference frequency generation. The latter devices achieve up to 0.5mW/W₂ mid-infrared to terahertz conversion efficiency and provide THz output in nearly the entire 1-5THz spectral range at room temperature.

8640-41, Session 10

Long-wavelength ($[\lambda] \approx 12- 16 \mu\text{m}$) and cascaded transition quantum cascade lasers (*Invited Paper*)

Xue Huang, Yenting Chiu, Jingyuan L. Zhang, Princeton Univ. (United States); William O. Charles, Phononic Devices (United States); Vadim E. Tokranov, Serge Oktyabrsky, Univ. at Albany (United States); Claire F. Gmachl, Princeton Univ. (United States)

Long-wavelength ($\approx 12- 16 \mu\text{m}$) Quantum Cascade (QC) lasers are crucial devices for improving the detection sensitivity of QC-laser based sensing for important gases including BTEX (benzene, toluene, ethylbenzene, and xylenes) or uranium hexafluoride. A brief review on recent progress on long-wavelength QC lasers will be given in the presentation. A high-performance QC laser emitting at $\sim 14 \mu\text{m}$ is demonstrated, optimized by employing a diagonal optical transition and a “two-phonon-continuum” depletion scheme. It shows a low threshold current density of 2.0 kA/cm², a peak power of 336 mW, and a slope efficiency of 375 mW/A, all at 300 K, as well as a high characteristic temperature ~ 310 K over a wide temperature range around room temperature (240- 390 K).

In order to optimize the ridge profile and width for long-wavelength QC lasers, the ridge-width dependence of threshold of $\sim 14 \mu\text{m}$ QC lasers by both wet etching and dry etching is studied. The main challenge for narrowing wet-etched ridges is the high loss caused by mode coupling to surface plasmon modes at the insulator/metal interface of sloped sidewalls. Conversely, dry-etched ridges avoid surface plasmon mode coupling due to the absence of transverse magnetic (TM) polarization for the vertical insulator and metal layers. Therefore, dry-etched QC lasers have a lower threshold for narrow ridge widths, e.g., for $\sim 14 \mu\text{m}$ QC lasers under test here, the threshold current density of a $14 \mu\text{m}$ wide laser by dry etching is 60% lower than that by wet etching.

To further improve the quantum efficiency of QC lasers, we demonstrate a same-wavelength cascaded transition approach, with two cascaded transitions designed at the same wavelength in each stage to enhance the peak gain. This idea is implemented in the two structures. The first one includes a stack of 25-stage same-wavelength cascaded-transition QC structures sandwiched between two stacks of 30-stage conventional single-transition QC structures, from which the ridge lasers emit at $\sim 14.5 \mu\text{m}$.

8640-42, Session 10

Room temperature continuous wave operation of long wavelength (9-11 μm) distributed feedback quantum cascade lasers for glucose detection

Feng Xie, Catherine G. Caneau, Herve P. LeBlanc, Sean Coleman, Ming-Tsung Ho, Lawrence C. Hughes, Chung-en Zah, Corning Incorporated (United States)

Using a range of grating pitches, we obtained distributed feedback (DFB) quantum cascade lasers (QCL) operating CW at room temperature over the 9-11 μm range. Single mode CW operation is demonstrated up to 10.8 μm , and up to 40 °C. To the best of our knowledge, it is the longest CW lasing wavelength reported for a DFB QCL operating above room temperature. The wavelength coverage per wafer is larger than 110 cm⁻¹. DFB QCLs from two wafers which have different gain peaks have lasing wavelengths near optical absorption peaks of glucose.

8640-43, Session 10

Stacked active region THz quantum cascade lasers with improved performance

Martin Brandstetter, Christoph Deutsch, Alexander Benz, Karl Unterrainer, Hermann Detz, Aaron M. Andrews, Werner Schrenk, Gottfried Strasser, Technische Univ. Wien (Austria)

Improving the performance of terahertz (THz) quantum cascade lasers (QCLs) in terms of operating temperature and output power is crucial for the applicability of these devices in industrial and scientific fields. Besides the active region design also the waveguide is essential for high performance devices.

By increasing the waveguide- and active region thickness the waveguide losses are reduced, the generated optical power inside the cavity is increased and the far-field is improved due to a larger output aperture. THz QCLs are typically grown via molecular beam epitaxy (MBE) therefore thick active regions would require unreasonable long growth times.

In order to overcome this issue, we stack two identical THz QCL active regions with a thickness of 15 μm on top of each other by direct wafer bonding. We make use of a double-metal waveguide providing low losses and high confinement of the optical mode. In this way we achieve a total active region/ waveguide thickness of 30 μm .

We show that the optical output power is increased by significantly more than a factor of two compared to devices with single active region thickness and that the far-field is improved while the maximum operating temperature is not reduced. The threshold voltage is increased by a factor of 2 indicating an excellent bonding interface with negligible contact resistance.

The authors acknowledge financial support by the Austrian Scientific Fund FWF (SFB-IRON F2511, and DK CoQuSW1210), the Austrian Nano Initiative project (PLATON) and the Vienna Science and Technology Fund (WWTF).

8640-44, Session 10

Towards nanowire-based terahertz quantum cascade lasers: prospects and technological challenges

Michael Krall, Martin Brandstetter, Christoph Deutsch, Hermann Detz, Tobias Zederbauer, Aaron M. Andrews, Werner Schrenk, Gottfried Strasser, Karl Unterrainer, Technische Univ. Wien (Austria)

A major challenge in the development of terahertz quantum cascade lasers (QCLs) is to increase the maximum operating temperature. The operation at elevated temperatures is fundamentally limited by non-radiative scattering and in order to suppress non-radiative intersubband relaxation processes an additional in-plane confinement has been proposed [1].

In fact, such additional confinement has already been realized using strong magnetic fields, considerably increasing the maximum operating temperature [2]. We discuss the prospects and technological challenges of an alternative approach using the one-dimensional nature of semiconductor nanowires. Using a highly anisotropic reactive ion etching process, we fabricate devices with arrays of pillars ranging from nanowire-dimensions to micrometer-sizes from semiconductor heterostructures grown by standard molecular beam epitaxy. In comparison to bottom-up growth schemes this method naturally gives a very precise control of diameter and positioning. Surface states are of particular importance in nanowire-based devices especially for THz QCLs due to their low doping densities. We, therefore, investigate the use of the aluminum-free $\text{In}_{0.53}\text{Ga}_{0.47}\text{As}/\text{GaAs}_{0.51}\text{Sb}_{0.49}$ material system recently studied for mid-infrared and THz QCLs [3-5]. The nanowires are electrically characterized using double-barrier resonant tunneling structures, showing no significant deterioration of the negative differential resistance behavior for diameters down to 100 nm. For investigating their potential application in THz QCLs arrays of pillars have been integrated into a double-metal waveguide using a planarization technique in order to study device behavior with diameter scaling. Measurements show electroluminescence from pillars with diameters above one micrometer. Below one micrometer surface depletion becomes a major limitation for these devices.

- [1] C.-F. Hsu, J.-S. O, P. Zory, and D. Botez, *IEEE J. Sel. Top. Quantum Electron.* 6, 491 (2000).
- [2] A. Wade, G. Fedorov, D. Smirnov, S. Kumar, B. S. Williams, Q. Hu, and J. L. Reno, *Nature Photonics* 3, 41 (2009).
- [3] M. Nobile, P. Klang, E. Mujagi?, H. Detz, A.M. Andrews, W. Schrenk, and G. Strasser, *Electron. Lett.* 45, 1031 (2009).
- [4] C. Deutsch, A. Benz, H. Detz, P. Klang, M. Nobile, A.M. Andrews, W. Schrenk, T. Kubis, P. Vogl, G. Strasser, and K. Unterrainer, *Appl. Phys. Lett.* 97, 261110 (2010).
- [5] H. Detz, A.M. Andrews, M. Nobile, P. Klang, E. Mujagi?, G. Hesser, W. Schrenk, F. Schäffler, and G. Strasser, *J. Vac. Sci. Technol. B* 28, C3G19 (2010).

8640-45, Session 11

Multiwatt long wavelength quantum cascade lasers based on high strain composition with 70% injection efficiency

Arkadiy A. Lyakh, Richard Maulini, Alexei Tsekoun, Rowel Go, C. Kumar N. Patel, Pranalytica, Inc. (United States)

A strain-balanced, $\text{In}_{0.58}\text{Ga}_{0.42}\text{As}/\text{Al}_{0.64}\text{In}_{0.36}\text{As}/\text{InP}$ quantum cascade laser structure, designed for light emission near $9\mu\text{m}$, was grown by molecular beam epitaxy. Buried heterostructure lasers with cavity dimensions of 3mm by $10\mu\text{m}$ mounted on AlN/SiC composite submounts demonstrated maximum pulsed and continuous wave room temperature optical power of 4.5 and 2W and wallplug efficiency of 16%

and 10%, respectively. The $9\mu\text{m}$ lasers, owing to their compact size, high WPE and optical power should be ideal sources in commercial and defense LWIR applications with strict SWaP requirements. Spontaneous emission electroluminescence of 14meV was measured for round mesas processed from the laser material despite employment of the high strain composition in the active region design. Waveguide losses, transparency current density, differential gain, and injection efficiency for the upper laser level were measured to be 1.6cm^{-1} , $1.3\text{kA}/\text{cm}^2$, $14\text{cm}/\text{kA}$, and 70%, respectively. Pulsed laser characteristics were shown to be self-consistently described by a simple model based on rate equations using measured 70% injection efficiency.

8640-46, Session 11

High-power multi-wavelength quantum cascade laser arrays

Patrick Rauter, Stefan Menzel, Burc Gokden, Federico Capasso, Harvard Univ. (United States)

Recently, the use of quantum cascade lasers (QCLs, [1]) as a source for stand-off detection and spectroscopy in the mid-infrared has increased the demand for high-power single-mode devices with tunable wavelength [2,3]. Due to their independence of mechanical components and bulky gratings, multi-wavelength arrays offer a number of advantages over external cavity QCLs, which have been used for stand-off spectroscopy systems up to now. We report on the demonstration of a monolithic multi-wavelength, high-power array covering the regime between 9.2 and $9.8\mu\text{m}$, which is based on master-oscillator power-amplifier (MOPA) QCLs [4,5].

An array of 16 MOPA QCLs has been fabricated, based on a broadband bound-to-continuum design [6]. MOPAs are two-section devices. The output of a 2 mm long standard single-mode distributed feedback (DFB) QCL of low output power is injected into a 2.4 mm long tapered QCL section, which amplifies the seeded DFB mode while maintaining both its spectral purity and its high beam quality due to adiabatic mode spreading [4]. An anti-reflection coating covering the power amplifier facet suppresses self-lasing of this section at high driving currents. Varying the DFB grating period from device to device allows the operation at 16 different wavelengths. Each device in the array operates at single-mode peak powers in excess of 750 mW, with individual devices reaching 3.9 W at room temperature. All array elements feature longitudinal (spectral) as well as lateral single-mode emission, resulting in excellent far field properties with a full-width-at-half-maximum angle of 6° in chip plane. High peak output power at a series of different wavelengths and excellent beam quality render the demonstrated array highly suitable for stand-off spectroscopy applications.

- [1] J. Faist et al., *Science* 22, 553 (1994).
- [2] C. A. Kendziora et al., *Proc. of SPIE* 8373, 83732H (2012).
- [3] F. Fuchs et al., *Opt. Eng.* 49 (11), 111127 (2010).
- [4] S. Menzel et al., *Opt. Express* 19, 16229 (2011).
- [5] M. Troccoli et al., *Appl. Phys. Lett.* 80, 4103 (2002).
- [6] A. Wittmann et al., *IEEE J. Quantum Elect.* 44, 36 (2008).

8640-47, Session 11

High power quantum cascade lasers with tapered oscillators

Romain Blanchard, Burc Gokden, Harvard School of Engineering and Applied Sciences (United States); Tobias S. Mansuripur, Harvard Univ. (United States); Nanfang Yu, Mikhail A. Kats, Harvard School of Engineering and Applied Sciences (United States); Tadataka Edamura, Masamichi Yamanishi, Hamamatsu Photonics K.K. (Japan); Federico Capasso, Harvard School of Engineering and Applied Sciences (United States)

**Conference 8640:
Novel In-Plane Semiconductor Lasers XII**

Tapered oscillator QCLs with large gain volume are demonstrated. The devices exhibit up to 4.5W peak power output at room temperature with nearly diffraction limited beam quality. A combination of high reflectivity and low reflectivity coatings on the facets, lead to an increased peak power up to 6W at room temperature. In order to correct for the strong astigmatism of the output beam, plasmonic collimators are defined on the facet of these QCLs to reduce the vertical divergence angle, constituting the first demonstration of plasmonic collimators operating at high peak powers up to 3W.

8640-48, Session 11

Widely-tunable quantum cascade lasers using sampled grating reflectors

Tobias S. Mansuripur, Stefan Menzel, Romain Blanchard, Harvard Univ. (United States); Laurent Diehl, Christian J. Pflügl, EOS Photonics (United States); Yong Huang, Jae-Hyun Ryou, Russell D. Dupuis, Georgia Institute of Technology (United States); Marko Loncar, Federico Capasso, Harvard Univ. (United States)

Widely tunable lasers in the mid-infrared are highly desirable for spectroscopy applications. We demonstrate a three-section sampled grating quantum cascade laser (SG-QCL) which consists of a Fabry-Perot (FP) section placed between two sampled grating reflectors (SGR). The reflectivity spectrum of a SGR comprises a comb of evenly spaced peaks near the wavelength of interest. The two SGRs are chosen to have slightly different comb spacings, so that wavelength tuning is achieved by the Vernier principle: the mode with the lowest lasing threshold is determined by which two comb peaks overlap, thereby providing a high reflectivity at both ends of the FP cavity. A small shift in the reflectivity spectrum of one mirror causes two new peaks to align, resulting in a large, discrete jump of the lasing mode. Tuning is achieved experimentally by adjusting the time duration and relative delays of the electrical pulses applied to the various sections of the device, which controls the amount of current-induced Joule heating in each section. We demonstrate a device which can lase at nine single modes spanning a range of 0.36 μm (47 cm^{-1}), from 8.42 to 8.78 μm , or 4.2% of the center wavelength. This tuning range is a factor of twelve greater than that which can be achieved by current-tuning of distributed feedback QCLs. The side mode suppression ratio of each mode is at least 10 dB, and seven of the modes exceed 300 mW in peak optical power per facet.

8640-49, Session 11

Optimization of QCL facet coatings for low-power consumption sensing applications

Ralf Ostendorf, Christian Schilling, Quankui K. Yang, Stefan Hugger, Rolf Aidam, Rachid Driad, Wolfgang Bronner, Fraunhofer-Institut für Angewandte Festkörperphysik (Germany); Frank Fuchs, Fraunhofer-Institut für Angewandte Optik und Feinmechanik (Germany); Joachim H. Wagner, Fraunhofer-Institut für Angewandte Festkörperphysik (Germany)

Quantum cascade lasers (QCLs) become more and more attractive for a wide range of applications, such as gas sensing, detection of hazardous substances and free space communications. This growing demand for mobile and compact QCL based sensing systems which most desirably should be battery powered for handheld operation, calls for QCL chips with low power consumption and high wall plug efficiency.

Most approaches devoted to the improvement of QCL wall plug efficiency focus either on the development of new epitaxial designs or the application of buried heterostructure technology for proper thermal management. On chip level, however, facet coating is an efficient way to optimize a given laser structure with respect to its output power and wall plug efficiency. We examined thoroughly the influences of the facet reflectivity on the lasing characteristics of mid-infrared QCLs. For this, we performed stepwise optical anti-reflection coating of both facets

of a single QCL device with a fixed cavity length. The lasing threshold, slope, efficiency and wall plug efficiency were determined between each coating step. The results allow for an individual optimization of the mirror losses for any given laser cavity length, and thus for an optimized low power consumption in particular for short cavity lasers. In addition, the integration of QCLs in low-footprint sized modules for sensing applications will be presented.

8640-50, Session 11

Single-mode quantum cascade lasers with asymmetric Mach-Zehnder interferometer type Fabry-Perot cavity

Peter Q. Liu, Princeton Univ. (United States); Xiaojun Wang, AdTech Optics, Inc. (United States); Claire F. Gmachl, Princeton Univ. (United States)

Quantum Cascade (QC) lasers are compact and versatile light sources suitable for a broad range of absorption spectroscopy based molecular sensing applications. However, for most of such sensing applications, single-mode operation of QC lasers is a prerequisite. Conventional single-mode QC lasers, e.g., distributed feedback [1] or external cavity QC lasers [2], have much higher cost than multi-mode simple ridge QC lasers, mainly due to their complicated and demanding device fabrication or time-consuming system integration and alignment processes.

In order to achieve more cost-effective single-mode QC lasers, we demonstrate a novel type of laser cavity design which consists of an asymmetric Mach-Zehnder (AMZ) interferometer structure monolithically integrated in a conventional Fabry-Perot (FP) cavity with simple ridge waveguide and as-cleaved facets. Strong wavelength selectivity is introduced by the properly designed AMZ interferometer whose transmission spectrum comprises narrow, equidistantly spaced peaks [3], which in turn selects a specific FP mode associated with the entire cavity near the peak optical gain, effectively facilitating single-mode operation of the laser. Continuously tunable single-mode operation of QC lasers is achieved in pulsed mode from 80 K to room temperature and in continuous-wave mode with high side-mode suppression ratio up to ~35 dB. A model on such cavity structures is also developed which explains the observed laser mode characteristics with satisfying accuracy. Another crucial technological advantage for such AMZ interferometer type cavities is that their fabrication process is identical to that for simple ridge lasers, therefore providing a promising solution to achieving more cost-effective single-mode QC lasers.

[1] J. Faist, C. Gmachl, F. Capasso, C. Sirtori, D.L. Sivco, J.N. Baillargeon, and A.Y. Cho, Appl. Phys. Lett. 70, 2670 (1997).

[2] G. Wysocki, R.F. Curl, F.K. Tittel, R. Maulini, J.M. Billiard, and J. Faist, Appl. Phys. B 81, 769 (2005).

[3] E.L. Wooten, R.L. Stone, E.W. Miles, and E.M. Bradley, J. Lightwave Technol. 14, 2530 (1996).

8640-67, Session PWed

980-nm external-cavity passively mode-locked laser with extremely narrow RF linewidth

Ying Ding, Univ. of Dundee (United Kingdom) and Institute of Semiconductors (China); Wei Ji, Jingxiang Chen, Song Zhang, Xiaoling Wang, Beijing Univ. of Technology (China); Huolei Wang, Haiqiao Ni, Jiaoqing Pan, Institute of Semiconductors (China); Bifeng Cui, Beijing Univ. of Technology (China); Maria Ana Catalana, Univ. of Dundee (United Kingdom)

This paper reports on the mode-locked operation of a 980-nm external cavity passively mode-locked laser with extremely narrow RF linewidth. Optical pulses with 10-ps pulse duration were generated at a repetition

**Conference 8640:
Novel In-Plane Semiconductor Lasers XII**

rate of 955 MHz, with an average output power of 39.3 mW – which corresponds to a peak power of 4.1 W, generated directly from the oscillator. The RF spectrum displays a -3dB RF linewidth of only ~40 Hz, as well as a 60 dB dynamic contrast, revealing the exceptionally low-noise fundamental mode-locked operation of this laser. The external cavity was composed of a 1.5-mm long edge-emitting chip and an output coupler with a ~4% reflectivity. The two-section flared chip incorporated an active region with a dual InGaAs quantum well sandwiched by an asymmetrical waveguide, and was operated at room temperature. By taking advantage of the broad tunability of the repetition rate which external-cavity lasers can afford, we investigated the limits of stable fundamental mode-locked operation at the lowest repetition rates (or maximum external cavity lengths). The results demonstrated in this paper represent a promising first step in the development of compact and high peak-power ultrafast laser systems for biomedical imaging applications – in particular, for those based on nonlinear microscopy techniques, such as Two-Photon Excited Fluorescence (TPEF) and Second Harmonic Generation (SHG), which typically rely on the use of near-infrared ultrashort pulses.

8640-68, Session PWed

Suppression of pointing instability in quantum cascade lasers via transverse mode control

Pierre M. Bouzi, Peter Q. Liu, Nyan L. Aung, Princeton Univ. (United States); Xiaojun Wang, AdTech Optics, Inc. (United States); Claire F. Gmachl, Princeton Univ. (United States)

Quantum Cascade (QC) lasers are semiconductor devices operating in the mid-infrared and terahertz regions of the electromagnetic spectrum. Since their first demonstration in 1994, they have evolved rapidly into high power devices [1][2]. However, they also have intrinsic challenges, such as beam steering at high power. Such phenomenon has been observed in QC lasers operated in CW mode, and attributed to the interaction between the two lowest transverse modes in the laser cavity [3].

In this project, we have utilized focused ion beam (FIB) milling to etch two small trenches from the top of the laser ridge in an attempt to reduce pointing instability in our QC lasers operated in pulsed mode. The initial idea was to perturbate the modes distributed more toward the sides of the laser ridge, while leaving the fundamental mode intact. Initial results showed a slight improvement in the beam far-field distribution and less pulse fluctuations. However, the lateral modes were still present within the cavity, and the pulse instability was not completely eliminated. We, then, filled the afore-mentioned trenches with platinum in an effort to completely suppress the propagation of higher order transverse modes in the cavity. The results obtained show a Gaussian like far-field distribution at various current levels, and a nearly complete elimination of pulse fluctuations, with a 10-fold improvement in standard deviation. This work is supported in part by MIRTH (NSF-ERC).

[1] Y. Bai et. al., APL 98, 181102 (2011)

[2] P. Q. Liu et. al., Nat. Phot. 4, 95-98 (2010)

[3] W. W. Bewley, et. al., IEEE J. Quantum Electron. 41, 833 (2005)

8640-51, Session 12

Analysis of bulk and facet failures in high-power diode lasers (Invited Paper)

Jens W. Tomm, Forschungsverbund Berlin e.V. (Germany)

Although high-power diode lasers are the most efficient man-made light sources, the power not converted into light (about a quarter to half of the total) causes strong heating and even device degradation. Together with other thermal effects, such as filamentation caused by thermal lensing, degradation effects still prevent broad area diode lasers to reach ultrahigh emission powers. The catastrophic optical damage (COD), a sudden degradation mechanism, sets one of the major limits. We unravel

the early stages of COD by monitoring spatio-temporally resolved optical emission pattern and temperatures and correlate them with the observed structural damage. COD occurs in highly localized damage regions on a 10-1000 ns timescale. Catastrophic optical bulk damage follows very similar sequences except for the starting point, which is located in the bulk, e.g., at defects or other 'weak points'. Also here the starting points and courses of action of the process are spatio-temporally resolved and compared with the damage pattern that is observed by subsequent physical inspection. Another limit can be caused by external feedback; i.e. if a fraction of the emission power is returned into the diode laser cavity containing the gain medium. We present experiments on gradual degradation of broad-area diode lasers revealing the quantum well to remain unaffected by degradation. Severe impact, however, is observed on the cladding layers and the waveguide of the device structure. Thus an overview is given on selected mechanisms preventing high-power broad area laser to reach their ultimate limits in terms of output power and reliability.

8640-52, Session 12

Catastrophic degradation in high-power InGaAs-AlGaAs strained quantum well lasers and InAs-GaAs quantum dot lasers

Yongkun Sin, Stephen LaLumondiere, Brendan Foran, Neil Ives, Nathan Presser, William Lotshaw, Steven C. Moss, The Aerospace Corp. (United States)

Reliability and degradation processes in broad-area InGaAs-AlGaAs strained quantum well (QW) lasers are under intensive investigation because these lasers are indispensable as pump lasers for fiber lasers and amplifiers that have found an increasing number of industrial applications in recent years. Extensive efforts by a number of groups to develop InAs-GaAs quantum dot (QD) lasers have recently led to significant improvement in performance characteristics, but due to a short history of commercialization, high power QD lasers lacks studies in reliability and degradation processes.

For the present study, we investigated reliability and degradation processes in MOCVD-grown broad-area InGaAs-AlGaAs strained QW lasers as well as in MBE-grown broad-area InAs-GaAs QD lasers using various failure mode analysis (FMA) techniques. Dots for the QD lasers were formed via a self-assembly process during MBE growth. We employed two different methods to degrade lasers during accelerated life-testing: commercial life-tester and our newly developed time-resolved electroluminescence (TR-EL) set-up. Our TR-EL set-up allows us to observe formation of a hot spot and subsequent formation and progression of dark spots and dark lines through windowed n-contacts during entire accelerated life-tests. Deep-level-transient spectroscopy (DLTS) and time-resolved photoluminescence (TR-PL) techniques were employed to study trap characteristics and carrier dynamics in pre- and post-stressed QW and QD lasers to identify the root causes of catastrophic degradation processes in these lasers. We also employed electron beam induced current, focused ion beam, and high-resolution TEM to study dark line defects and crystal defects in post-aged QW and QD lasers at different stages of degradation.

8640-53, Session 12

Comparison of catastrophic optical damage in InP/(Al)GaInP quantum dot and quantum well diode lasers

Stella N. Elliott, Cardiff Univ. (United Kingdom); Martin Hempel, Max-Born-Institut für Nichtlineare Optik und Kurzzeitspektroskopie (Germany); Ute Zeimer, Ferdinand-Braun-Institut (Germany); Peter M. Smowton, Cardiff Univ. (United Kingdom); Jens W. Tomm, Max-Born-Institut für Nichtlineare Optik und Kurzzeitspektroskopie (Germany)

**Conference 8640:
Novel In-Plane Semiconductor Lasers XII**

Catastrophic damage was induced in InP/(Al)GaInP based MOCVD-grown quantum well and quantum dot red/NIR emitting broad-area diode lasers subjected to single current pulses of 5 A to 20 A. Catastrophic optical bulk damage (COBD) occurred in quantum dot devices in contrast with catastrophic optical mirror damage in quantum well devices, at similar high facet power densities. Subsequent panchromatic cathodoluminescence of the quantum dot active layers showed dark, non-radiative spots, not observed in the comparison quantum well devices. These spots, also present in unprocessed material, had an area density of the order of 10^6 cm^{-2} : five orders of magnitude lower than the densities of the dots themselves. These were measured in uncapped samples by STM and in full structures with absorption measurements to be of the order of 10^{11} cm^{-2} . In devices each subject to one single 12A current pulse of lengths from 100 ns to 10 μs , the number of spots did not increase after the pulse but the average dark spot size increased for pump current pulse lengths of 500 ns and beyond but was not a function of pulse length. Since at this current the lasing action ceased after 100 – 200 ns the size increase was optically mediated. The cathodoluminescence intensity of both the spots themselves and the background areas inside the pumped stripe decreased as a function of pulse length, correlating with duration of applied current. More detailed insight into the nature of the damage can be used to effect improvements in growth and hence laser performance.

8640-54, Session 12

Multi-spectral investigation of bulk and facet failures in high-power single emitters at 980 nm (Invited Paper)

Dan A. Yanson, Moshe Levy, Moshe Shamay, Shalom Cohen, Sarah Geva, Yuri Berk, Renana Tessler, Genady Klumel, Noam Rappaport, Yoram Karni, SCD Semiconductor Devices (Israel)

Failures in high-power InGaAs/AlGaAs single emitters at 980 nm are investigated using laser-ablated windows on the substrate side. Both bulk and facet failures are analyzed with electroluminescence imaging, near-IR and mid-IR spectroscopy, and FIB/SEM microscopy. Presence of branching dark line defects was confirmed in both failure modes. The defects exhibit absorption levels between 0.22 eV – 0.55 eV and have a disordered epilayer structure. We also report an electroluminescence study of a single emitter just before and after failure. In failed emitters, the electroluminescence emission is much stronger and undergoes a blue shift.

8640-55, Session 12

1120nm high-brilliant laser sources for SHG-modules in bio-analytics and spectroscopy

Katrin Paschke, Christian Fiebig, Gunnar Blume, Frank Bugge, Jörg Fricke, Götz Erbert, Ferdinand-Braun-Institut (Germany)

High-brilliant diode lasers at 1120nm with a high optical output power, nearly diffraction limited beam and narrow spectral line width are increasingly important for non-linear frequency conversion to 560nm. Modules at 560nm are key components for many applications, e.g. time resolved fluorescence spectroscopy, atomic spectroscopy, confocal microscopy, photocoagulation in ophthalmology, medical skin treatments, DNA sequencing or high-resolution refractometry. Here the missing direct modulation capability and low efficiency limit the applicability of current laser sources.

This can be avoided by the use of diode lasers with exactly these required properties as well as a certain wavelength tunability to open further application fields. Especially, tapered diode lasers are well suited for applications requiring a high optical output power in combination with a good beam quality. The combination of such devices with monolithic internal gratings led to the development of Distributed Bragg-Reflector tapered diode lasers (DBR-TPL).

At the conference we will show results concerning the development of such a high-brightness single frequency DBR-TPL at 1120nm up to 10 W levels with a conversion efficiency of about 44%. In preliminary reliability tests at 8W a lifetime of more than 1,500 h could be demonstrated. Due to their high brightness and compactness these monolithic diode lasers are paving the way for non-linear frequency conversion and allow the miniaturization of existing laser systems for bio-analytics and spectroscopy, respectively.

8640-56, Session 13

Novel broad area diode lasers with transverse Bragg grating in external resonators

Christof Zink, Mario Niebuhr, Danilo Skoczowsky, Axel Heuer, Ralf Menzel, Univ. Potsdam (Germany)

There have been many approaches to improve the beam quality and spectral characteristics of laser diodes in the last years. One of them integrated a mode selective element in the laser diode itself. We present the realization of such a mode selective element through a refractive index grating at the chip surface. The grating and the material parameters define the resonance angle for a certain wavelength. A beam which propagates at this angle is constructively reflected at particular layers of the grating and thereby enables narrow-bandwidth mode selection.

This kind of transverse Bragg resonance (TBR) grating for diode lasers was first examined by A. Yariv et al. It has been shown that a one dimensional TBR grating is insufficient to obtain transversal and longitudinal single mode emission [2]. To achieve this, a higher dimensional gratings or further selective elements, e.g. an angled front facet, are necessary.

Our approach to obtain single mode emission uses a one dimensional TBR laser diode inside an external optical resonator with a tilted feedback mirror to select the desired TBR mode.

We used on double quantum well laser diodes with a surface etched TBR grating, provided by the Ferdinand-Braun-Institute. The TBR structure has a period of $W_{\text{per}} = 3 \mu\text{m}$ and an average refraction index of $n_{\text{avg}} = 3.3$. The active defect core of the laser diodes have widths of $W_{\text{def}} = 28.5 \mu\text{m}$ and $91.5 \mu\text{m}$, respectively. The laser diode was designed for a wavelength of $\lambda = 975 \text{ nm}$, resulting in a resonance angle of $\theta_{\text{res,cal}} = 9.3^\circ$.

By tilting the feedback mirror, it is possible to select the TBR mode. The TBR mode is characterized by a pronounced local maximum of the output power in one of the far field branches, while the emission spectrum shows a decrease in bandwidth compared to on axis operation. The experimental results for both laser diodes show different far field emission profiles and deviations to the calculated TBR angle $\theta_{\text{res,cal}}$.

The measured TBR angles θ_{res} in comparison to the calculated resonance angle $\theta_{\text{res,cal}}$ were examined with the transfer matrix method. By varying the different parameters the deviation between calculated and experimental resonance angle could be traced back to a change of the refractive index within the defect core. The refractive index in the pumped defect core depends on the charge carrier density. Up to the threshold current the charge carrier density increases with the pump current and therefore the refraction index decreases. Above threshold the refraction index increases with the pump current, explaining the observed discrepancies between experiment and theory. From these investigations design rules for new generations of such TBR chips could be developed.

**Conference 8640:
Novel In-Plane Semiconductor Lasers XII**

8640-57, Session 13

Cryogenically-cooled eyesafe diode laser for resonant pumping of Er-doped gain media

Zhigang Chen, Weimin Dong, Xingguo Guan, Sandrio Elim, Shiguo Zhang, Mike Grimshaw, Mark Devito, Paul O. Leisher, Manoj Kanskar, nLIGHT Corp. (United States)

There is great interest in the development of high-power, high-efficiency InP-based broad area pump diode lasers operating in the 14xx-15xx nm band to be used for resonant-pumping of Er-doped solid state lasers. Cryogenic cooling of diode lasers can provide great benefit to performance, arising from the dramatic reduction in the threshold current and the increase in the diode's slope efficiency. These improvements are attributed to reduction in the non-radiative losses and leakage current associated with thermionic emission of carriers from the quantum well. This is, however, at the expense of a large increase in the diode voltage, limiting the power conversion at cryogenic temperatures. In this work, we report on the development of high-power, high-efficiency diode lasers and stacked arrays operating at 15xx-nm, which are specifically designed and optimized for operation at cryogenic temperatures. We show that the diode voltage defects under cryogenic operation can be greatly reduced through reducing the energy band offsets at the hetero-interface, and through material change to reduce the dopant ionization energy, effectively mitigating carrier freeze-out at low temperatures. Optical cavity designs and band engineering optimization are also explored for low intrinsic optical loss and low carrier leakage. A peak power conversion efficiency of >70% was demonstrated at a temperature of ~100K. Ongoing effort are carried out for implementation of high-power (>500W rated) and high-efficiency (>70%) stacked arrays of at 15xx-nm for use in solid state pumping experiments.

8640-59, Session 13

Dynamic response of a monolithic master-oscillator power amplifier at 1.5 μm

Pawel Adamiec, Borja Bonilla, Antonio Consoli, Jose Manuel Tijero, Ignacio Esquivias, Univ. Politécnic de Madrid (Spain); Julien Javaloyes, Univ. de les Illes Balears (Spain); Salvador Balle, Institut Mediterrani d'Estudis Avançats (Spain)

We study experimentally the dynamic response of a fully integrated high power master-oscillator power-amplifier emitting at 1.5 μm. The tapered amplifier is driven in cw conditions while the DFB master-oscillator is subject to a variety of driving conditions at different frequencies. High peak power (2.7 W) optical pulses with short duration (100 ps) have been generated by gain switching the master-oscillator under optimized driving conditions. In direct modulation of the master-oscillator we observe stable and unstable regimes, attributed to compound cavity effects. The radio-frequency spectra of the optical output have been measured with both sections driven in cw conditions, providing information on the Relative Intensity Noise (RIN) and evidencing a self-pulsation regime. The results are analyzed considering both, the oscillator and amplifier separately, and the compound cavity.

8640-60, Session 13

Dynamics of high power gain switched DFB RW laser under high-current pulse excitation on a nanosecond time scale

Andreas Klehr, Sven Schwertfeger, Hans Wenzel, Thomas Hoffmann, Armin Liero, Ralf Staske, Olaf Brox, Götz Erbert, Günther Tränkle, Ferdinand-Braun-Institut (Germany)

High-power diode lasers capable of generating spectrally stable nearly diffraction-limited optical pulses in the nanosecond range can be used in

a variety of applications including free-space communications, metrology, material processing and frequency doubling. For these applications the knowledge of the temporal and spatial stability of the optical pulses is important.

In this paper we present detailed experimental investigations of the impact of the amplitude and the widths of the current pulses injected into a distributed-feedback (DFB) laser emitting at a wavelength of 1064nm. The nearly rectangular shaped current pulses have a width up to 50ns and an amplitude up to 2.5A. The repetition frequency is 200kHz. The laser has a ridge waveguide (RW) for lateral waveguiding with a ridge width of 3μm and a cavity length of 1.5mm.

Time resolved investigations show, that depending on the amplitude and the duration of the current pulses, the optical power exhibits different types of oscillatory behavior during the pulses, accompanied by changes in the lateral near field intensity profiles and optical spectra. Three different types of instabilities can be distinguished: Mode beating with frequencies between 25GHz and 30GHz, switching between different lateral modes and self-sustained oscillations with a frequency of about 4GHz.

From the experimental results can be deduced, that during the current pulse the carrier density in the active region and in the optical confinement layers increases. On the other hand, due to the very large current density the RW heats up. A temperature increase of about 9K during a 50ns long current pulse with an amplitude of 1.9A can be estimated.

8640-61, Session 13

Tapered multi-section quantum-dot amplifiers and mode locked laser for high-peak power and picosecond pulse generation

Michel Krakowski, Myke Ruiz, Alcatel-Thales III-V Lab. (France); Ying Ding, Daniil Nikitichev, Maria Ana Cataluna, Edik U. Rafailov, Univ. of Dundee (United Kingdom); Lukas Drzewietzki, Stefan Breuer, Wolfgang E. Elsaesser, Technische Univ. Darmstadt (Germany); Charis Mesaritakis, Dimitris Syvridis, Univ. of Athens (Greece); Igor Krestnikov, Innolume GmbH (Germany); Ivo Montrosset, Politecnico di Torino (Italy); Yannick Robert, Eric Vinet, Michel Garcia, Alcatel-Thales III-V Lab. (France)

We present a review on the performances obtained with fully gain guided quantum-dot multi-sections tapered laser and amplifiers emitting at 1260nm. These devices have been developed to produce high optical peak power for application in multi-photon microscopy.

High peak power and ultra short pulse generation under passive mode locking of tapered laser have been achieved, with record values for peak power produced by quantum dot tapered lasers.

Depending on the device geometry or operation conditions, we can point out:

- Pulse duration of 820 fs, pulse repetition frequency of 10Ghz, peak power of 15W
- Pulse duration of 672 fs, pulse repetition frequency of 16GHz, peak power of 3.8W
- Pulse duration of 640 fs, pulse repetition frequency of 13.4Ghz, peak power of 8.03W
- Pulse duration of 616 fs, pulse repetition frequency of 13Ghz, peak power of 7.88W

Tapered SOA have been used in a discrete MOPA configuration, with mode locked lasers in external cavity for pulse repetition frequency lowering, showing record values of peak power produced by all semiconductor quantum dot system.

Depending on the device geometry or operation conditions, we can point out:

- Pulse repetition frequency of 1.1GHz, average power of 294mW, peak power of 26.3W, pulse energy of 267pJ

**Conference 8640:
Novel In-Plane Semiconductor Lasers XII**

- Pulse repetition frequency of 648MHz, average power of 208mW, peak power of 30W, pulse energy of 321pJ

Tapered SOA with a regular mode locked laser have shown similar peak power of around 33W, at a pulse repetition frequency of 16GHz, with a pulse duration of 1.6ps.

8640-62, Session 14

High-power diode lasers between 1.8 μ m and 3.0 μ m

Sascha A. Hilzensauer, Catharina Giesin, Jeanette Schleife, m2k-laser GmbH (Germany); Steve Patterson, DILAS Diode Laser, Inc. (United States); Marc Kelemen, m2k-laser GmbH (Germany)

High-power diode lasers in the mid-infrared wavelength range between 1.8 μ m and 3.0 μ m have emerged new possibilities for solid-state pumping and material applications based on water absorption with favoured wavelengths at 2.9 μ m and 1.94 μ m. GaSb based diode lasers are naturally predestined for this wavelength range and offer clear advantages in comparison to InP based diode lasers in terms of output power and wall-plug efficiency.

We will present results on MBE grown (AlGaIn)(AsSb) quantum-well diode laser single emitters and bars with 20% and 30% fill factor emitting between 1.8 μ m and 3.0 μ m. Different epitaxial and resonator designs have been investigated in cw and pulsed mode in order to meet industrial needs of high wallplug and fiber-coupling efficiencies. Also AuSn soldering of GaSb based lasers has been established instead of traditional Indium soldering. More than 30% maximum wall-plug efficiency in cw operation for single emitters and laser bars has been reached together with output powers for single emitters of 2W (cw) and 9W (pulsed). Single emitters and bars have been tested for lifetime.

The single emitters and bars are all suitable for fiber coupling. For a 1-bar module typical coupling efficiencies between 70% and 80% have been established for 400 μ m core fibers. For single emitter modules coupling efficiencies of more than 85% into 200 μ m core fibers have been demonstrated. In terms of output power, an AuSn soldered laser stack built of 7x 20% fill factor bars emitting at 1870nm, results in a record value of 87W at 50A in qcw condition.

8640-63, Session 14

High-power GaSb laser diodes with reduced beam divergence and enhanced temperature performance

Soile Suomalainen, Jukka Viherfiälä, Antti I. Laakso, Riku Koskinen, Jonna Paajaste, Mervi Koskinen, Tapio Niemi, Mircea Guina, Tampere Univ. of Technology (Finland)

Mid-infrared laser based on (AlGaIn)(AsSb) material system emitting in 2-3 μ m wavelength range have been intensively studied for over a decade in order to improve their high-power performance. High-power GaSb-lasers are attractive sources for various applications such as material processing. Output power exceeding 1 W and divergence of the fast axis of the output beam down to 44° have been reported previously with narrow waveguide structures. [1, 2]

In this paper, we report on a novel narrow waveguide GaSb laser structure, where a Al_{0.3}Ga_{0.7}AsSb layer is inserted into a n-Al_{0.5}Ga_{0.5}AsSb cladding to modify the waveguide mode and thus reduce the divergence of the far field. GaInAsSb quantum wells were embedded into 260 nm thick Al_{0.3}Ga_{0.7}AsSb waveguide layer grown by molecular beam epitaxy. A large optical confinement (LOC) structure with Al_{0.9}Ga_{0.1}AsSb cladding layers and a narrow waveguide structure without waveguide mode modification were fabricated for comparison. Wafers were processed into 130 μ m wide broad area lasers and cleaved to form 0.9 mm long cavities. Chips were mounted p-side up for characterization.

The FWHM of the fast axis reduced from 57° of the LOC structure down to 37° for the narrow waveguide structure. An addition of the 300 nm thick n-Al_{0.3}Ga_{0.7}AsSb layer to the n-cladding layer further decreased the FWHM of the fast axis down to 34°. The slope and the temperature characteristics of the threshold current, T₀, are improved for the narrow waveguide structures compared with the LOC structure. Slope efficiency of 15 % and T₀ of 70 K were observed for the narrow waveguide structures, and only 10 % and 50 K respectively for the LOC structure. The output power of these devices is ~150 mW in pulsed mode with 1 A current due to bonding p-side up. With a proper p-side down bonding and thermal engineering the power level of Watt is expected.

1. M.T. Kelemen, J. Weber, M. Rattunde, G. Kaufel, J. Schmitz, R. Moritz, M. Mikulla, J. Wagner, "High-power 1.9- μ m diode laser arrays with reduced far-field angle," IEEE Photon. Tech. Lett. 18, 628 (2006).
2. C. Pfahler, G. Kaufel, M.T. Kelemen, M. Mikulla, M. Rattunde, J. Schmitz, J. Wagner, "GaSb-Based Tapered Diode Lasers at 1.93 μ m With 1.5-W Nearly Diffraction-Limited Power," IEEE Photon. Tech. Lett. 18, 758 (2006).

8640-64, Session 14

Influence of band offset and auger recombination on the temperature sensitivity of GaInAsSb/GaSb mid-infrared lasers

Barnabas A. Ikyo, Stephen J. Sweeney, Alf R. Adams, Igor P. Marko, Konstanze Hild, Univ. of Surrey (United Kingdom); Markus C. Amann, Shamsul Arafin, Walter Schottky Institut (Germany)

There are numerous applications for lasers in the 2-3 μ m mid-infrared spectral window. Existing interband lasers suffer from increased threshold current density (J_{th}) with increasing temperature due to non-radiative processes such as Auger recombination and carrier leakage which limit their maximum operating temperature. In type-I interband devices, the band gap determines the wavelength, hence investigating the effects of band gap shift on the device properties provides a means of optimisation. In this work, temperature and hydrostatic pressure have been used independently to tune the bandgap of GaInAsSb type-I edge emitting lasers. The dependence of J_{th}, Auger current (J_{Auger}) and radiative current (J_{rad}) on the band gap of these devices is presented. Results show that by applying pressure, the T₀ of the 2.6 μ m device increases from 37 \pm 5K up to ~53 \pm 5K when operating at 2.3 μ m under pressure. This value is similar to the as-grown 2.3 μ m for which T₀ = 59 \pm 5K. However, J_{th} is ~25% higher compared to an as-grown 2.3 μ m device. This difference is due to the fact that the as-grown 2.3 μ m device maintains larger band offsets than the pressure-tuned 2.3 μ m device. Hence, the reduced J_{th} of the as-grown device may be associated with a lower carrier leakage current. Whilst the larger band offset helps reduce J_{th} it makes little difference to its temperature sensitivity in these type-I GaInAsSb/GaSb devices. This indicates that further optimisation of the band offset would bring little benefit in terms of T₀ and that reducing the Auger process would be of much larger benefit.

8640-65, Session 14

Analysis of thermally activated leakage current in a low-threshold-current quantum-cascade laser emitting at 3.9 μ m

Yuri V. Flores, Grygorii Monastyrskyi, Mikaela Elagin, Mykhaylo P. Semtsiv, W. Ted Masselink, Humboldt-Univ. zu Berlin (Germany)

We have recently described the design of a quantum-cascade laser (QCL) active region that is based on taking advantage of the dependence of interface scattering on the conduction band discontinuity [1]. By using low barriers where the upper laser state has its maximum probability and high barriers where the lower laser state has its maximal probability in strain-compensated designs for short wavelength emission, the lifetime of the upper laser state can be increased, while decreasing the lifetime of

Conference 8640:
Novel In-Plane Semiconductor Lasers XII

the lower laser state. First realizations of this design result in $J_{th}=1.7$ kA/cm² at 300 K, slope efficiency $\eta = 1.4$ W/A, $T_0 = 175$ K, and $T_1 = 550$ K.

This talk describes a method to extract the leakage current into higher minibands from the temperature dependence of the threshold current density and to reconstruct the energies of the higher-lying states from this current. The modeling includes the thermal population of LO phonons that drive the leakage. We apply the method to two QCLs emitting near 4 μ m, one of which is based on the interface-scattering engineered low-threshold design. The measured energies are compared with those calculated from a numerical solution of Schrödinger's equation.

[1] M. P. Semtsiv, Y. Flores, M. Chashnikova, G. Monastyrskiy, and W. T. Masselink, Appl. Phys. Lett. 100, 163502 (2012).

8640-66, Session 14

The influence of inter-valley scattering on 3.5 μ m InGaAs/AlAs(Sb) quantum cascade lasers

Shirong Jin, Abdullah Aldukhayel, Igor P. Marko, Univ. of Surrey (United Kingdom); Shiyong Zhang, Engineering and Physical Sciences Research Council (United Kingdom) and The Univ. of Sheffield (United Kingdom); Dmitry G. Revin, John W. Cockburn, The Univ. of Sheffield (United Kingdom); Stephen J. Sweeney, Univ. of Surrey (United Kingdom)

Quantum cascade lasers (QCLs), which cover mid- to far-infrared spectral region are promising for applications including sensing and communications, particularly in the 2.9-5.3 μ m window. Realizing QCLs at short wavelengths is challenging because of the large conduction band offset needed for required high energy intersubband transitions. The InGaAs/AlAsSb material system is particularly interesting because it provides large conduction band offset of ~ 1.6 eV and also offers lattice-matching to InP with its established device fabrication technology. However, the inter-valley scattering between the Gamma- and L- valleys has been a concern since the lowest indirect L minimum becomes very close to the Gamma-upper laser level in this system. Here InGaAs/AlAs(Sb) QCLs of ~ 3.5 μ m with laser operation above room temperature have been investigated using cryogenic and hydrostatic pressure techniques in order to probe the extent to which such scattering processes are important. We find that the characteristic temperature, T_0 , which is a measure of the temperature sensitivity of the device, drops from 260K for $T < 220$ K to 154K for $T > 220$ K. This indicates the occurrence of a loss process at higher temperature. Since hydrostatic pressure varies the relative positions between Gamma-, X- and L-minima, it enables a better understanding of the carrier leakage via inter-valley scattering. From the measured pressure dependence of the threshold current, we found that the carrier leakage to the L-minima is negligible at low temperature but accounts for $\sim 4\%$ of the threshold current at RT. The implications for this on short wavelength QCL performance will be discussed in further detail.

Conference 8641: Light-Emitting Diodes: Materials, Devices, and Applications for Solid State Lighting XVII

Monday - Thursday 4 -7 February 2013 • Part of Proceedings of SPIE Vol. 8641 Light-Emitting Diodes: Materials, Devices, and Applications for Solid State Lighting XVII

8641-1, Session 1

Analytic model for the efficiency droop in light-emitting diodes made of semiconductors with asymmetric carrier-transport properties based on drift-induced reduction of injection efficiency (*Invited Paper*)

E. Fred Schubert, Jaehee Cho, Rensselaer Polytechnic Institute (United States)

An analytic model is developed for the droop in the efficiency-versus-current curve for LEDs made from semiconductors having a strong asymmetry in carrier concentration and mobility. In such semiconductors $n \gg p$ and $\mu_n \gg \mu_p$. GaN is an example of a semiconductor having such strong asymmetry. For pn-junction diodes made of such semiconductors, the high-injection condition needs to be generalized to include mobilities. We show that the high-injection condition can be easily reached. Under high-injection conditions, electron drift in the p-type layer of the diode causes a decrease of the injection efficiency and an associated reduction in internal quantum efficiency. The drift-induced leakage function is shown to have a 3rd-order as well as a 4th-order dependence on the carrier concentration. The third-order coefficient, C-sub-DL is found to be approximately $10^{-29} \text{ cm}^6/\text{s}$. An analytic formula giving the onset-of-droop current density in LEDs is derived. The analytic model very well explains the experimental efficiency-versus-current curves of GaInN LEDs.

8641-2, Session 1

Optimizing the multiple quantum well thickness of an InGaN blue light emitting diode

Bing Xu, Junliang Zhao, Shuguo Wang, Haitao Dai, Tianjin Univ. (China); ShengFu Yu, National Cheng Kung Univ. (Taiwan); Ray-Ming Lin, FuChuan Chu, Chang Gung Univ. (Taiwan); Chou-Hsiung Huang, Chang Gung Univ. (Taiwan); Xiao Wei Sun, Tianjin Univ. (China)

The investigations on ?-materials have been focused for many years due to their widely tunable wavelength from ultraviolet to green. The quality of InGaN multiple quantum wells (MQWs) is very important for the high performance of InGaN based light emitting diodes (LEDs), so it is necessary to study the optimization of the growth parameters of InGaN MQWs. In this study, we prepared InGaN-LEDs with well thickness ranging from 2.4 nm to 3.6 nm and investigated the effect of well thickness on the electrical and optical properties. Our samples are grown on c-plane sapphire substrates by atmosphere pressure metalorganic chemical vapor deposition (AP-MOCVD). The result of X-ray diffraction demonstrates that our samples have same structure and same Indium composition; the only change is well thickness. Based on a band-tail model, the exciton localization effect (ELE) is studied by temperature-dependent photoluminescence (TDPL). It is found that ELE is enhanced by increasing quantum well thickness up to 2.7nm, but with the further increase of quantum well thickness, the ELE becomes weaker. In addition, by investigating an excitation power dependent PL measurement, the result of the wavelength shift can be attributed to quantum confined Stark effect (QCSE), which becomes strong because of strong polarizations in the wide quantum well structure. Our study suggested that the ELE is the main influence in the thin quantum well thickness, while QCSE is the main effect in the wide quantum well thickness. Furthermore, it is found that efficiency droop can be reduced by increasing well thickness. On the other hand, relative internal quantum efficiency (IQE) measurements indicate that a thinner well results to

higher IQEs owing to the greater spatial overlap of electron and hole distribution functions.

8641-3, Session 1

Direct green LED development in nano-patterned epitaxy (*Invited Paper*)

Christian Wetzel, Theeradetch Detchprohm, Rensselaer Polytechnic Institute (United States)

Blue LED progress has laid the ground works of nitride technology to tackle the higher challenge longer wavelength emitters of green, yellow, and orange. Use of bulk GaN substrate allows to leapfrog epitaxy development and offers crystallographic planes that allow higher crystal perfection and a control over piezoelectric polarization. Their combination allows stabilization of emission wavelength with current and reduce discrepancy of absorption and emission energies. Further improvement is found in substrate patterning on the micro and nano-meter length scale where we find roughly equal performance enhancement due to both, enhancement in light extraction and enhanced crystalline perfection.

8641-4, Session 1

Probing the efficiency droop with GaInN light-emitting triode: effect of hole-injection efficiency on droop behavior

Sunyong Hwang, Jun Hyuk Park, Dong-yeong Kim, Jong Kyu Kim, Pohang Univ. of Science and Technology (Korea, Republic of)

The hole-injection efficiency into the active region of GaN-based light emitting diodes (LEDs) is much lower than the electron-injection efficiency due to the asymmetry between electron and hole concentrations and mobilities. Al_xGa_{1-x}N electron-blocking layer (EBL) is implemented in typical GaN-based LEDs to mitigate such asymmetry. However, AlGaIn EBL creates not only the undesirable potential barrier for hole-injection, but also a positive sheet charge at the GaN spacer / AlGaIn EBL interface increasing difficulty of hole-injection, which is considered as one of dominant efficiency-droop-causing mechanisms. In our previous work, we suggested light-emitting triode (LET) structure as a method of probing the effect of hole-injection efficiency on efficiency droop by accelerating holes in p-type GaN region, enabled by additional anode.¹ We suggested that the increased hole-injection efficiency alleviated efficiency droop of the devices.

In this study, we fabricated further advanced LET structure to more efficiently change hole-injection efficiency on conventional GaN-based light-emitting diode (LED) epitaxial structure, LED structure having graded-superlattice electron blocking layer (GSL-EBL), and additional Mg dopant gradation on GSL-EBL embedded LED structure, details of which can be found in the the other work.² Newly designed LET structure utilizes grid-square patterned anodes on p-type GaN, which maximizes the effective hole-accelerated region by introducing regularly patterned grid type anode and individual square anode in it.

Anode-to-anode and anode-to-cathode voltage biases are systemically varied to control the hole-injection efficiency of the devices, and corresponding external quantum efficiencies (EQE) are measured, considering effective emission area, as well as temperature dependent EQE is investigated. Based on those measurements, relation between hole-injection efficiency and efficiency droop will be deeply discussed to elucidate that the major mechanisms responsible for the efficiency droop in GaN-based LEDs.

Conference 8641: Light-Emitting Diodes: Materials, Devices, and Applications for Solid State Lighting XVII

8641-5, Session 2

Native-substrate GaN-based LEDs for solid state lighting (*Invited Paper*)

Michael R. Krames, Soraa, Inc. (United States)

For the last decade or so, GaN-based LEDs have made great strides in performance and cost reduction and have significantly penetrated markets such as LCD Backlighting, Signaling, Automotive, and Specialty Lighting applications. However, the vast General Lighting market is still largely dominated by inefficient, expensive, and/or environmentally questionable technologies such as incandescent, high-intensity discharge, and Hg-based fluorescent lamps. We submit that the primary performance barrier preventing LEDs from supplanting these inferior technologies in commercial markets today, especially the retrofit lamp market, is not the lumens per Watt challenge, but rather the quality of light and total lumen or intensity level achieved by LED products to date. We present a new approach to high quality illumination products from LEDs formed from native GaN substrates. These GaN-on-GaN™ devices offer unprecedented performance at high power density, enabling novel, cost-effective product designs and a quality of light and look and feel that are not achieved employing conventional LEDs formed on foreign substrates like sapphire or silicon.

8641-6, Session 2

LED color mixing with diffractive structures

Theresa Bonenberger, Univ. of Applied Sciences Hochschule Ravensburg-Weingarten (Germany) and Karlsruhe Institute of Technology (Germany); Joerg Baumgart, Univ. of Applied Sciences Hochschule Ravensburg-Weingarten (Germany); Simon Wendel, Cornelius Neumann, Karlsruhe Institute of Technology (Germany)

Lighting solutions with colored LEDs provide many opportunities for illumination. One of these opportunities is to create a color tunable light source. In this way different kinds of white light (color temperature) as well as discrete colors may be realized.

This opens the field for applications as mood lighting.

The spatial separation of the LEDs is converted into an angular separation by any collimating optics. This angular separation causes such problems like color fringes and colored shadows that cannot be accepted in most applications. Conventional methods to solve these problems include e.g. mixing rods or dichroic filters. A new approach is the use of the dispersive effect of a diffractive structure to compensate the angular separation of the different colors.

In this contribution the potential and limitations of diffractive structures in LED color mixing applications are discussed. Ray tracing simulations were performed to analyze such important parameters like efficiency, color performance and the cross section of the color mixing optics. New means for the estimation of color mixing performance were developed. A software tool makes it possible to detect the color distribution within ray trace data and it provides a quality factor to estimate the color mixing performance. It can be shown that LED parameters like chip size and the spectral band width have a large influence on the mixing process.

The ray tracing simulations are compared with results of an experimental setup such that both measured as well as simulated data is presented.

8641-7, Session 2

Highly-reliable vertical InGaN/GaN blue LED on 8-inch Si (111) substrate (*Invited Paper*)

Jun-Youn Kim, Youngjo Tak, Joosung Kim, Jaekyun Kim, Hyun-Gi Hong, Su-Hee Chae, Moonseung Yang, Jung Hoon Park, Yongsoo Park, U-In Chung, InKyeong Yoo, Kinam Kim,

SAMSUNG Advanced Institute of Technology (Korea, Republic of)

The transition layers which consist of AlGaIn layers and the unique epitaxial structures which consist of the dislocation reduction layer and stress compensation layers were grown on AlN nucleation layer to control the stress and reduce the dislocation, simultaneously. After that, over 3.5 μm -thick Si doped GaN layer with $4.5 \times 10^{18} \text{ cm}^{-3}$ doping concentration has been grown successfully without any cracking. The full width at half maximum (FWHM) values of GaN (0002) and (10-12) ω -rocking curves were 250 and 360 arcsec, respectively. On top of n-GaN layer, 5 periods of InGaIn/GaN multi quantum well (MQW) formed the active layers for blue light emission following on 20 InGaIn/GaN short-period superlattices. A 20 nm-thick Mg-doped p-type AlGaIn for electron blocking layer and a 100 nm-thick p-type GaN layers were added for final LED epitaxial structure. Vertical LEDs are fabricated via epilayer transfer.

I-V relations reveal that the reverse leakage current mechanism of LEDs on Si is mainly attributed to the field-enhanced thermionic emission, also known as Poole-Frenkel emission similar to those of commercial-grade LEDs on sapphire. Median values of output powers from LEDs are measured about 500 mW at 350 mA without encapsulation. Median values of reverse leakage current at -5 V and forward voltage @ 1 A are about -6 nA and 2.08 V, respectively, almost comparable to the values of commercial LED or even better. Over 90% of vertical LEDs on whole 8-inch satisfy forward and reverse leakage specification of commercial vertical LEDs on sapphire.

8641-9, Session 2

Satellite to satellite temperature control using a novel 400-nm UV pyrometer

Michael Heuken, Markus Luenenbuerger, Frank Schulte, Ruediger Schreiner, Bernd Schineller, AIXTRON SE (Germany)

In mass production of SSL devices the focus is on yield and process control. In Planetary Reactors the AutoSat temperature controller is capable of independently adjusting the temperature of the individual satellites. Combining this with a near-UV pyrometer capable of measuring the real GaN surface temperature allows further narrowing the wafer to wafer spread.

In the newly developed T400 pyrometer we use a sharp cut-off filter which allows wavelengths below 405 nm to pass to a photo-multiplier with subsequent digital photon counting and digital processing. The tool is capable of measuring more than 30 points across a 4 inch wafer for the temperature range above 650°C. This allows assessing the temperature profile across the wafer and allows computing a stable average for every wafer, which can then be used as input for the AutoSat controller.

In temperature vs. wavelength evaluations of LED structures a value of -1.37 nm per Kelvin growth temperature was found, which corresponds well to the values reported in the literature. This shows the validity of the T400 measurement.

Combining AutoSat and T400 we were able to reduce the total temperature spread from GaN surface to GaN surface for all satellites from 4.5 K to 0.4 K. In a marathon of 10 LED runs in the AIX G5HT in the 14x4 inch configuration the maximum wavelength spread was 4.9 nm peak to peak at an average of 457.2 nm. The on-wafer standard deviation was around 1.3 nm.

8641-10, Session 3

Near-field photometry for organic light-emitting diodes (*Invited Paper*)

Venkat Venkataramanan, Univ. of Toronto (Canada) and Lumentra Inc. (Canada); Rui Li, Univ. of Toronto (Canada)

Organic Light Emitting Diode (OLED) displays are now ubiquitous in mobile devices. With rapidly improving efficacy and reliability, OLED is predicted to become the next generation of light source for general

Conference 8641: Light-Emitting Diodes: Materials, Devices, and Applications for Solid State Lighting XVII

lighting. Currently, the standard photometric methods for solid state lighting are based on point-like emitters. However, OLED devices are extended surface emitters, where spatial uniformity and angular variation of brightness and colour are important. This necessitates advanced test methods to obtain meaningful data for fundamental understanding, lighting product development and deployment.

In this work, a near field imaging goniophotometer was used to characterize white OLED devices, where luminance and colour information of the pixels on the light sources were measured at a certain distance for various angles. Analysis was performed to obtain angular dependent luminous intensity, CIE chromaticity coordinates and correlated colour temperature (CCT) in the far field. Further more, a complete ray set with chromaticity information was generated, so that illuminance at any distance and angle from the light source can be determined. The generated ray set is needed for optical modeling and design of OLED luminaires. Our results show that luminance at two positions of the OLED surface can be different by more than two times and CCT can vary by more than 2000K. This causes the same source being perceived as warm or cold depending on the viewing angle. As OLEDs are becoming commercially available, this could be a major challenge for lighting designers. Near field measurement can provide detailed specifications and quantitative comparison between OLED products for performance improvement.

8641-11, Session 3

Numerical analysis of nanostructures for enhanced light extraction from OLEDs

Lin Zschiedrich, JCMwave GmbH (Germany); Horst J. Greiner, Philips Research (Germany); Jan Pomplun, JCMwave GmbH (Germany); Sven Burger, Frank Schmidt, Konrad-Zuse-Zentrum für Informationstechnik Berlin (Germany) and JCMwave (Germany)

Summary explaining how this research is working towards energy, sustainability and conservation:

First, the object of study, OLED, is a device designed especially for energy efficient lightening. We develop and investigate methods for designing even more efficient OLEDs (through enhanced light extraction, achieved by nanostructures in the device). Further, the numerical methods we develop allow to perform device optimizations on standard PCs or workstations at extremely low computational costs. Therefore, in many cases the use of supercomputers can be avoided which allows for a faster and more energy-friendly design process.

Organic light-emitting diodes (OLED) are key elements for many lighting applications.

However, for planar OLEDs efficiency is reduced due to low light extraction levels.

Nanostructures like photonic crystals or low-index gratings can be used for improved efficiency.

In order to optimize geometrical and material properties of such structures, simulations of the outcoupling process are very helpful [1].

For simulating Maxwell's equations we use the time-harmonic finite-element method (FEM).

Our implementation relies on adaptive, higher-order finite-elements [2], rigorous implementations of transparent boundary conditions [3] and domain-decomposition methods [4].

With this we reach accurate results on relatively large 3D computational domains.

In this contribution we discuss finite-element modelling of light extraction from structured devices and report on numerical convergence studies for state-of-the-art nanostructured OLED setups.

[1] H. Greiner, Light extraction from OLEDs with (high) index matched glass substrates, Proc. SPIE 6999, 69992T (2008).

[2] J. Pomplun, S. Burger, L. Zschiedrich, F. Schmidt, Adaptive finite element method for simulation of optical nano structures, phys. stat. sol. (b) 244, 3419 (2007).

[3] L. Zschiedrich, S. Burger, B. Kettner, and F. Schmidt, Advanced Finite Element Method for Nano-Resonators, Proc. SPIE 6115, 611515 (2006).

[4] L. Zschiedrich, S. Burger, A. Schaedle, F. Schmidt, A rigorous finite-element domain decomposition method for electromagnetic near field simulations, Proc. SPIE 6924, 692450 (2008).

8641-12, Session 3

Extremely efficient flexible organic light-emitting diodes using graphene electrodes for solid state lighting (*Invited Paper*)

Tae-Hee Han, Pohang Univ. of Science and Technology (Korea, Republic of); Youngbin Lee, Sungkyunkwan Univ. (Korea, Republic of); Mi-Ri Choi, Pohang Univ. of Science and Technology (Korea, Republic of); Sang-Hoon Bae, Sungkyunkwan Univ. (Korea, Republic of); Byung Hee Hong, Seoul National Univ. (Korea, Republic of); Jong-Hyun Ahn, Sungkyunkwan Univ. (Korea, Republic of); Tae-Woo Lee, Pohang Univ. of Science and Technology (Korea, Republic of)

Graphene films have a strong potential to replace indium tin oxide anodes in organic light-emitting diodes (OLEDs), to date. However, the luminous efficiency of OLEDs with graphene anodes has been limited by a lack of efficient methods to improve the low work function and reduce the sheet resistance of graphene films to the levels required for electrodes. Here, we fabricate flexible OLEDs by modifying the graphene anode to have a high work function and low sheet resistance, and thus achieve extremely high luminous power efficiencies (37.2 lm/W in fluorescent OLEDs, 102.7 lm/W in phosphorescent OLEDs), which are significantly higher than those of optimized devices with an indium tin oxide anode (24.1 lm/W in fluorescent OLEDs, 85.6 lm/W in phosphorescent OLEDs). We also fabricate flexible white OLED lighting devices using the graphene anode. These remarkable device efficiencies increase the feasibility of using graphene anodes to make extremely high-performance flexible organic optoelectronic devices by overcoming the major drawbacks (low work function and trap formation due to diffusion of indium and tin) of conventional ITO anodes. These results demonstrate the great potential of graphene anodes for use in a wide variety of high-performance flexible organic optoelectronics such as flexible, stretchable full-colour displays and solid-state lighting.

8641-14, Session 3

Light-emitting electrochemical cells: a low-cost alternative for large-area light-emission (*Invited Paper*)

Ludvig Edman, Umeå Univ. (Sweden)

Light-emitting electrochemical cells (LECs) offer a number of important advantages over competing emissive technologies -- notably the utilization of air-stable electrodes and thick and uneven active materials. This unique opportunity opens the door for a recently demonstrated ambient fabrication of low-cost and flexible light-emitting sheets using R2R coating techniques [1], and I will present our recent results in this field.

A critical drawback with LECs has been a short operational lifetime. We have for a long time worked to resolve this problem and also been able to identify a number of lifetime-limiting chemical [2] and electrochemical [3] side reactions. By following motivated and straightforward design principles to minimize the extent of these side reactions, we are now able to repeatedly realize LEC devices that emit with significant brightness (>100 cd/m²) and good efficiency (>2 lm/W for red emission, >10 lm/W for green emission) for several months of uninterrupted operation.[4,5]

In another development, we have performed a parallel optical probing and scanning Kelvin probe microscopy study on planar LEC devices during operation, and the acquired light emission and potential profiles

Conference 8641: Light-Emitting Diodes: Materials, Devices, and Applications for Solid State Lighting XVII

present irrefutable evidence for that electrochemical doping takes place in-situ in the active material, and that a dynamic p-n junction structure can self-assemble in an LEC during operation.[6]

Finally, we have conceptualized and demonstrated a truly metal-free and “all-plastic” LEC device comprising a graphene cathode and a conducting-polymer anode.[7] Both electrodes in this device architecture are transparent and the light emission is accordingly omni-directional. Moreover, all parts of the device can be processed from solution, which — in combination with the elimination of expensive and/or reactive metal materials — promises to pave the way for a low-cost production of functional light-emitting devices.

References

- [1] Sandström, A., Nature Communications, 2012, 3, 1002.
- [2] Wågberg, T., et al., Advanced Materials, 2008, 20, 1744.
- [3] Fang, J., et al., Journal of the American Chemical Society, 2008, 130, 4562.
- [4] Fang, J., et al. Advanced Functional Materials, 2009, 19, 2671.
- [5] Asadpooravarish, et al. Appl. Phys. Lett. 2012, 100, 193508.
- [6] Matyba, P., et al., Nature Materials, 2009, 8, 672.
- [7] Matyba, et al., ACS Nano, 2010, 4, 637.

8641-15, Session 4

Polychromatic white LED using GaN nano pyramid structure (*Invited Paper*)

Taek Kim, Joosung Kim, Moonseung Yang, Yongsoo Park, U-In Chung, SAMSUNG Advanced Institute of Technology (Korea, Republic of); Yongho Ko, Yong-Hoon Cho, Korea Advanced Institute of Science and Technology (Korea, Republic of)

Currently, most white light emitting diodes (LEDs) are made of blue LEDs covered by phosphors which convert the part of blue emission to yellow. In this approach, the luminous efficacy is limited because energy loss is unavoidable when an optical down conversion is involved. Monolithic white LEDs which emit multiple spectra such as blue-yellow or three primary colors have been considered for an ultimate solution. However, a InGaN blue LED efficiency decreases with increasing wavelength while a InGaP red LED efficiency decreases with decreasing wavelength, resulting the absence of efficient green and yellow emitters (called Green Gap). The green gap in nitride LEDs stems from a combination of poor crystal quality and large piezoelectric field in indium-rich InGaN on the c-plane.

We have been exploring selectively grown nano-pyramidal structures to solve the Green Gap and to achieve a monolithic white LED. Selectively grown GaN pyramid is of great interest as an effective way to reduce the piezoelectric field by providing semipolar growth direction on well-established and high quality c-plane substrate¹. In addition, nano scale structure is expected to reduce the strain caused by lattice mismatching. Previously we have reported highly efficient yellow MQWs with a peak wavelength of 570 nm on nano scale GaN pyramid structures.

In this talk, we will characterize the optical properties of InGaN MQWs on nano pyramids and introduce the possibility of monolithic white LED by utilizing planar and nano-pyramid hybrid structure. We will also discuss on the color temperature tunability of the white LED.

8641-16, Session 4

Variations of the dimension and emission wavelength of regularly patterned InGaN/GaN quantum-well nanorod light-emitting diode arrays

Che-Hao Liao, Wen-Ming Chang, Yu-Feng Yao, Hao-Tsung Chen, Chia-Ying Su, Chih-Yen Chen, Chieh Hsieh, Horng-Shyang Chen, Chang-Gan Tu, Yean-Woei Kiang, Chih-Chung Yang, National

Taiwan Univ. (Taiwan)

The cross-sectional sizes of the GaN nanorods (NRs) and quantum-well (QW) NRs of different heights and different hexagon orientations between different template hole patterns, including different hole diameters and pitches, are demonstrated. The cross-sectional size of the GaN NRs is controlled by the patterned hole diameter and has little to do with the NR height and pitch. On the other hand, the cross-sectional size of the QW NRs is mainly determined by the NR height and is slightly affected by the hexagon orientation. The cross-sectional size variation of GaN NRs is interpreted by the three-dimensional nature of the formed catalytic gallium droplet. The cross-sectional size variation of QW NRs is explained by the condition of constituent atom supply in the gap volume between the neighboring NRs. Also, the plan-view and cross-sectional cathodoluminescence emission wavelengths, including the whole scale and local measurements, among those samples are compared. The emission wavelength depends on the NR height, cross-sectional size, pitch of the pattern, and hexagon orientation. It involves in the factors of indium incorporation rate and well layer thickness and shows a complicated combination of various affecting factors. Generally speaking, the QW NRs with a shorter QW NR, a larger cross-sectional size, or a larger pitch have a longer emission wavelength. The NRs with the side-by-side hexagon orientation have longer emission wavelengths, when compared with those with the edge-to-edge hexagon orientation.

8641-17, Session 4

Introduction of the Moth-eye patterned sapphire substrate technology for cost-effective high-performance LED (*Invited Paper*)

Koichi Naniwae, Midori Mori, Toshiyuki Kondo, Atsushi Suzuki, Tsukasa Kitano, EL-SEED Corp. (Japan); Satoshi Kamiyama, EL-SEED Corp. (Japan) and Meijo Univ. (Japan); Motoaki Iwaya, Tetsuya Takeuchi, Isamu Akasaki, Meijo Univ. (Japan)

Light extraction efficiency (LEE) is one of the most crucial issues for high performance nitride-based LEDs fabrication. Since the refractive index of the nitride-based epilayers is much larger than that of air or sapphire, the critical angle for total internal reflection is small, which results in poor LEE values of LEDs. For example, the LEE value of typical blue LEDs on flat sapphire substrates (FSS) without resin encapsulation is usually only around 20%. Patterned sapphire substrates (PSS) are widely used in current commercial LEDs to improve the LEE. By using it, the generated light in the nitride-based active layer is scattered by the micron scale structure of PSS and gets extracted from the device. We have however proposed a new solution using the nano-scale patterning techniques, the so-called “Moth-eye Patterned Sapphire Substrate (MPSS)”. Since the MPSS has an optical wavelength order periodic structure, the diffraction effect enhances the light extraction possibility by reducing the total internal reflection at the GaN/sapphire interface. In addition, since the MPSS consists of only sub-micron scale pattern, it allows us to reduce the GaN template thickness to the same level as that on FSS without sacrificing the GaN quality. Having a thinner GaN layer is beneficial not only in terms of cost but also in terms of wafer size expansion since the reduced GaN thickness results in less wafer bowing. As a result of comprehensive comparisons between MPSS, PSS and FSS, we have come to the conclusion that the introduction of our MPSS does provide the most cost effective solution for high performance LED production.

8641-18, Session 4

NiO as hole transport layers for all-inorganic quantum dot LEDs

Liyuan Tang, Xiao Li Zhang, Haitao Dai, Shuguo Wang, Xiao Wei Sun, Tianjin Univ. (China)

Quantum dot light-emitting diodes (QD-LEDs) have recently attracted much attention due to its highly saturated emission color and the

Conference 8641: Light-Emitting Diodes: Materials, Devices, and Applications for Solid State Lighting XVII

capability of tuning the emission color by means of engineering its size. Although quantum dot LEDs based on organic semiconductor materials can obtain high injection efficiency, the short lifetime caused by the degradation of the organic layers under moisture and oxygen and the instability of the metal contacts limits its advanced application in QLEDs. Recently we found that large-band-gap metal oxides such as NiO and ZnO could be used as charge transport layers to enhance the stability of QD-LED. In this letter, we reported the all-inorganic quantum dot light-emitting diodes, which employ NiO as the hole transport layer. NiO has been used extensively as holes transport layer due to its ease of deposition, and chemical compatibility with the CdSe/ZnS QDs. In our experiment, the luminescent layer were prepared by spin-coating core-shell CdSe/ZnS quantum dots on NiO hole transport layer, which deposited on patterned ITO covered glass plates by means of magnetron sputtering. The light emitting efficiency of QD-LEDs with various NiO films were investigated to obtain the optimized processing procedure for NiO film. In addition, we also discussed the impact of the annealing temperature and the Ar/O₂ ratio on the LED performance. Experimental results showed that the transmittance of NiO films in visible range can be enhanced by increasing the Ar/O₂ ratio.

8641-19, Session 4

Light extraction efficiency enhancement by growing ZnO nanorods on n-GaN emitting surface of vertical GaN-based LEDs

Yen-Ju Wu, Yu Shan Wei, Chih-I Hsieh, Cheng-Yi Liu, National Central Univ. (Taiwan)

To improve the light extraction efficiency of the vertical GaN-based LEDs, the n-GaN emitting surface usually would be textured by either wet-etching or by ICP dry-etching. One of the most common wet-etching processes is the KOH etching. It has been reported that pyramidal morphology would form on the n-GaN surface with KOH etching. In this study, to further enhance the light extraction efficiency of the vertical GaN-based LEDs, we grew ZnO nanorods (NRs) on the n-GaN emitting surface of vertical pyramidal GaN-based LEDs by low temperature hydrothermal method. We found that ZnO NRs can nucleate on the side-planes (r-plane) of pyramids on the n-GaN surface. Interestingly, the ZnO NRs were growing in perpendicular to the n-GaN surface, which is in the (0002) direction. After growing ZnO NRs on the pyramidal n-GaN surface, L-I measurements were done on the LEDs samples with ZnO NRs. We found that the vertical ZnO NRs enhanced the light output of the vertical LED by as much as 10 %. We believe that the ZnO NRs grown on the n-GaN surface serve as a light guides to mitigate the internal total reflection effect on the n-GaN surface. Also, we note that the ZnO NRs on the n-GaN emitting surface affect the light pattern of the LEDs. The detail optical characterization of the vertical thin-GaN LEDs with ZnO NRs would be present and discussed in this talk.

8641-20, Session 4

Fabrication of moth-eye patterned sapphire substrate (MPSS) and influence of height of corns on the performance of blue LEDs on MPSS

Takayoshi Tsuchiya, Shinya Umeda, Motoaki Iwaya, Tetsuya Takeuchi, Meijo Univ. (Japan); Satoshi Kamiyama, Meijo Univ. (Japan) and EL-SEED Corp. (Japan); Isamu Akasaki, Meijo Univ. (Japan); Toshiyuki Kondo, Tsukasa Kitano, Midori Mori, Atsushi Suzuki, Fumiharu Teramae, EL-SEED Corp. (Japan); Hitoshi Sekine, DIC Corp. (Japan)

It was reported that a moth-eye patterned sapphire substrate (MPSS), which has a periodic corn structure with sub-micrometer order pitch, can enhance a light extraction efficiency of nitride-based light emitting diodes (LEDs). Due to light-wave diffraction effect, MPSS has a higher potential

of light extraction than a commonly used patterned sapphire substrate (PSS) with micron-order structure. However, obtaining sufficient height of corns for enhancing the light extraction efficiency is difficult, because of a small etching rate selectivity of resist mask and sapphire. In this paper, a MPSS fabrication method based on ultra-violet (UV) nano-imprinting technique with a thick resist patterning is described to form periodic corn structure with the height of up to 350 nm.

To fabricate an etching mask of MPSS, an UV-nano-imprinting equipment with a 350 nm-thick UV-resist developed by DIC Corporation was used for our experiment. With an optimization of BCl₃ dry etching condition, an etching rate selectivity of sapphire to resist was increased up to 1.5. Then, we fabricated MPSS samples with a fixed pitch of 460 nm, and a height of corns of 250, 300 and 350 nm. Performance of nitride-based blue LEDs grown on a series of MPSS will also be discussed.

8641-21, Session 4

Plasmon-enhanced upconversion for Yb³⁺/Er³⁺ doped in Y₂O₃ and NaYF₄ nanocrystalline hosts

Madhab Pokhrel, Brian G. Yust, Ajith K. Gangadharan, Dhiraj K. Sardar, The Univ. of Texas at San Antonio (United States)

In the recent years, metal-enhanced upconversion fluorescence efforts have focused on glass composites and films. In addition to this, surface plasmonic responses have yielded strong surface-enhanced Raman scattering (SERS), and improvement in solar cell absorption. In this work, we are reporting the synthesis of core/spacer/shell nanocomposites composed of gold nanorods with the plasmonic peak at 980 nm coated with mesoporous SiO₂ and subsequently coated with Er³⁺/Yb³⁺ doped (e. g. Au@SiO₂@Y₂O₃:Er³⁺/Yb³⁺) nanocrystalline host through a facile method. We tuned the plasmonic peak of the gold nanorods to 980 nm, where we systematically design the spacer (SiO₂) thickness to optimize (e. g. Au@SiO₂@Y₂O₃:Er³⁺/Yb³⁺) nanostructure materials. In this work, we also describe the synthesis methods to obtain gold nanorods with different aspect ratio. The detailed optical characterizations such as absorption, emission, and fluorescence decay were performed to explore the emission processes in the VIS-NIR as well as to quantitatively estimate the fluorescence quantum yield. Mechanisms of upconversion by two photon and plasmonic response to upconversion emission and energy transfer processes between the Yb³⁺ to Er³⁺ ions are interpreted and explained. Our studies show that gold nanorod (NPs) can be coated with the upconverting nanoparticles. Preliminary studies show that this upconversion emission enhancements and quenching is shown to be dependent on the dielectric silica spacer thickness thus suggesting that the surface-plasmon-coupled emission plays an important role in the enhancement of upconversion emission.

8641-61, Session 4

ZnO nanowire-based light-emitting diodes with tunable emission from near-UV to blue

Thierry Pauporté, Oleg Lupan, Bruno Viana, Tanguy Le Bahers, Ecole Nationale Supérieure de Chimie de Paris (France)

Nanowires (NWs)-based light emitting diodes (LEDs) have drawn large interest due to many advantages compared to thin film based devices. Markedly improved performances are expected from nanostructured active layers for light emission due to good light extraction. The use of wires avoids the presence of grain boundaries and then limits the non-radiative recombinations. An electrochemical deposition technique has been developed for the preparation of ZnO-NWs based light emitters. Nanowires of high structural and optical quality have been epitaxially grown on p-GaN single crystalline films substrates and the heterojunction has been integrated in LED devices. The fabricated LED exhibited high brightness and low-threshold emission voltage. Moreover, it has been shown that the wires acted as waveguides that favored the directional light extraction. CdCl₂ or CuCl₂ were used as an additive in the

Conference 8641: Light-Emitting Diodes: Materials, Devices, and Applications for Solid State Lighting XVII

deposition bath for ZnO doping. The doping could be tuned by changing their concentration in the bath and yielded to a bandgap narrowing. LEDs prepared with the doped nanowires exhibited low-threshold emission voltage and the single electroluminescence emission peak was shifted from ultraviolet to violet-blue spectral region compared to pure ZnO/GaN LEDs. The emission wavelength could be tuned by changing the Cd or Cu atomic concentration in the ZnO nanomaterial. The shift, due to the bandgap reduction, will be discussed, including insights from DFT computational investigations: the bandgap narrowing has two different origin for Zn_{1-x}Cd_xO and Zn_{1-x}Cu_xO.

8641-63, Session 4

Broadband emission from an ensemble of nano-pillars with multiple diameters

Kwai Hei Li, Hoi Wai Choi, The Univ. of Hong Kong (Hong Kong, China)

Generating white light from monochromatic light sources is commonly achieved via one of two common methods: exciting fluorescence phosphors from a shorter wavelength LED, or mixing light from three or more LED chips, commonly known as RGB LEDs. Phosphor efficiency degrade over time, and have lifetimes shorter than the chip itself. RGB LEDs require turning on three or more p-n junctions and suffer from color mixing issues. We introduce a promising approach towards achieving phosphor-free white light emission, tapping on strain engineering and nanoscale processing.

The proposed approach makes use of a long wavelength chip, which is invariably strained due to the high Indium content. By relaxing the built-in strain in a controllable manner, through the formation of dimension and site-controlled nano-pillars, the emission wavelength of individual pillars of varying sizes will blue-shift towards short wavelengths. The extent of blue-shift (strain relaxation) depends on a number of factors including dimension and lateral ion penetration.

Nano-pillars of a continuum of dimensions are patterned by nanosphere lithography, making use of a nanosphere colloid containing spheres with a wide range of diameters. The resultant structure contains an ensemble of nano-pillars each emitting a slightly different wavelength according to its dimension, producing a continuous broadband spectrum with FWHM of 72.23nm. With the right mix of nano-pillar dimensions, different shades of white light can be generated from a single array, representing a viable single-chip phosphor-free white light generating solution. Most importantly, the strain-relaxed nanostructures offer both high internal quantum efficiencies and light extraction efficiencies.

8641-22, Session 5

MOVPE-grown n-In_xGa_{1-x}N (x>0.5)/p-Si(111) template as a novel substrate *(Invited Paper)*

Akio Yamamoto, Univ. of Fukui (Japan) and JST-CREST (Japan); Naoteru Shigekawa, Osaka City Univ. (Japan)

After the finding of the low band-gap energy (~0.7 eV) for InN, InN-based nitride semiconductor alloys have had much attention as materials for a variety of optical and electronic devices. This is because a wide range of band-gaps, for example from 0.7 to 3.4eV for InGaN, can be realized by changing only composition of the alloys. The use of conductive Si substrates for InGaN growth as well as for GaN growth can expand the freedom of the device design, improve the device performance mainly due to the high thermal conductivity of Si, and reduce device costs. Furthermore, a low resistance ohmic contact predicted at the n-In_{0.45}Ga_{0.55}N/p-Si interface is another advantage for the n-In_xGa_{1-x}N (x>0.5)/p-Si system. This means that an n-In_xGa_{1-x}N (x>0.5)/p-Si template can serve as a unique substrate for a variety of optical and electronic devices. This paper reports the successful preparation of n-InGaN/p-Si structures by MOVPE. A thick (~0.5 μm) InGaN with an intermediate In composition has been successfully grown at around 600°C on Si(111) substrates using an AlN interlayer. No cracks are found

in the InGaN layer because such a low growth temperature results in a small tensile stress in the epilayer. Ohmic I-V characteristics are obtained between n-InGaN and p-Si and the resistance is markedly decreased with increasing In content in InGaN. It is found that the presence of the AlN interlayer does not have a significant contribution to the series resistance.

8641-23, Session 5

Epitaxial growth of nonpolar ZnO and Zn_xMg_{1-x}O on LiAlO₂ and MgO substrates *(Invited Paper)*

Teng-Hsing Huang, Cheng-Ying Lu, Tao Yan, Liuwen Chang, National Sun Yat-Sen Univ. (Taiwan); Jih-Jen Wu, National Cheng Kung Univ. (Taiwan); Mitch M. C. Chou, Klaus H. Ploog, National Sun Yat-Sen Univ. (Taiwan)

Zinc oxide (ZnO) and magnesium oxide (MgO) are both II-VI compound semiconductors but possess different crystal structures, i.e. wurtzite for ZnO and rock-salt for MgO, in thermodynamic equilibrium. In addition, both ZnO and MgO can be substituted by each other to a great extent of ~40 % without losing their structural stability. The resultant ternary oxides have a great importance on band gap engineering for optoelectronic applications. A thorough review on studies of epitaxial growth, defects and optical properties of nonpolar (10 -10) ZnO and Zn_{1-x}Mg_xO epilayers on (100) gamma-LiAlO₂ substrates by chemical vapor deposition is given. Basal stacking faults, threading dislocations and inversion domains were observed in the ZnO epilayer with densities on the order of 10⁻⁵ cm⁻², 10⁻⁹ cm⁻² and 10⁻⁴ cm⁻¹, respectively. On the other hand, only basal stacking faults and threading dislocations were found in the Zn_{0.9}Mg_{0.1}O epilayers with densities of about an order of magnitude lower its ZnO counterpart. Monochromatic cathodoluminescence images revealed the non-radiative nature of the basal stacking faults. In addition, rock-salt Zn_{1-x}Mg_xO epilayers with high substitutions of ZnO (50-80%) in MgO were obtained on the MgO (100) substrate by plasma-assisted molecular beam epitaxy. The epilayers are smooth and possess low FWHM values (0.30o-0.47o) of the (002) rocking curves. The bandgap energy of the Zn_{0.8}Mg_{0.2}O epitaxial layer is measured as low as 4.73 eV. The stability of the epilayer is also discussed.

8641-24, Session 5

Properties of bulk nitride substrates and epitaxial films for device fabrication *(Invited Paper)*

Jaime A. Freitas Jr., U.S. Naval Research Lab. (United States)

The III-V nitride semiconductor material system continues to play a significant and growing role in a wide range of device technologies. The typical low intrinsic carrier density of this material system, leading to low leakage and low dark current, place it as one of the most promising material systems for the fabrication of photodetectors and high-temperature electronic devices.

Despite improved performance of devices fabricated on films deposited on foreign substrates, the properties of thin heteroepitaxial nitride films are still seriously limiting the performance of devices demanding higher material yields. The high growth temperature required to produce these wide bandgap materials exacerbates fundamental material problems such as residual stress, difference in thermal expansion coefficient, low energy defect formation and impurity incorporation. In addition, doping activation and self-compensation are difficult to control at the typically high deposition temperatures. Furthermore, the high concentration of dislocations, resulting mostly from lattice constant mismatch, typically on the order of 10E9 to 10E10 cm⁻², must be reduced to improve device performance. Overcoming these limitations will require the use of native substrates to grow electronic grade homoepitaxial films.

AlN substrates grown by physical vapor transport and sublimation-

Conference 8641: Light-Emitting Diodes: Materials, Devices, and Applications for Solid State Lighting XVII

recondensation processes are insulators, while GaN grown by hydride vapor phase epitaxy or by ammonothermal processes are always n-type conductive with a free carrier concentration typically between $10E17$ to $10E19$ electrons/cm³. High quality epitaxial films with controlled electrical transport properties have been deposited on both substrates by chemical vapor deposition and molecular beam epitaxy. The properties of the state of the art of bulk and thick-freestanding film (quasi-bulk) nitride substrates and homoepitaxial films will be reviewed.

[1] J.A. Freitas, Jr., J. of Physics D: Applied Physics 43 (2010) 073001.

8641-25, Session 6

Proposal of coherent-structure InN/GaN QW-based photonic devices: SMART technology for achieving wavelength tunings up to infrared by novel 1-ML InN / GaN matrix MQWs (*Invited Paper*)

Akihiko Yoshikawa, Song-Bek Che, Kazuhide Kusakabe, Chiba Univ. (Japan); Xinqiang Wang, Peking Univ. (China)

We propose novel III-Nitride-based photonic-devices consisting of ultrathin InN wells coherently embedded in GaN barriers. We have already reported successful fabrication of fine structure MQWs of 1 monolayer (ML) thick InN wells coherently embedded in GaN matrix, and the present proposal is its extension so that we can achieve wavelength tuning in wide range wavelengths covering not only for visible light emitters up to red but also for III-N tandem solar cell applications covering almost whole AM1.5 solar spectrum. In all cases, the thicknesses of InN wells are basically 1-ML, and in fact often fractional-ML, and sometimes 2-ML thick or more under special conditions. Two possible ideas are proposed; the first one is to use asymmetric structure MQWs of 1-ML-InN/InGaN/GaN, and the second is to use (InN)_n/(GaN)_m short-period superlattices as quasi InGaN ternary alloys. Corresponding growth processes are quite unique and the deposition temperatures are higher the critical one for continuously growing thick InN layers. This is necessary to make the quality of resultant MQW structures high. Then we named these novel structures as SMART: (Superstructure Magic Alloys fabricated at Raised Temperatures).

Since all proposed photonic devices are consisting coherent structure InN/GaN-based MQWs and/or quasi InGaN ternary alloys, we believe that these are really plausible ideas not only for extending the LED-emission colors up to red and even infrared, but also at the same time really achieving III-Nitride based high efficiency tandem solar cells covering almost whole AM1.5 solar spectrum.

8641-26, Session 6

Thermal management and light extraction in multi-chip and high-voltage LEDs by cup-shaped copper heat spreader technology (*Invited Paper*)

Ray-Hua Horng, Hung-Lieh Hu, Li-Shen Tang, Sin-Liang Ou, National Chung Hsing Univ. (Taiwan)

For LEDs with original structure and copper heat spreader, the highest surface temperatures of 3?3 array LEDs modules were 52.6 and 42.67 °C (with 1050 mA injection current), while the highest surface temperatures of 4?4 array LEDs modules were 58.55 and 48.85 °C (with 1400 mA injection current), respectively. As the 5?5 array LEDs modules with original structure and copper heat spreader were fabricated, the highest surface temperatures at 1750 mA injection current were 68.51 and 56.73 °C, respectively. The thermal resistance of optimal LEDs array module with copper heat spreader on heat sink using compound solder is reduced obviously. On the other hand, the output powers of 3?3, 4?4 and 5?5 array LEDs modules with original structure were 3621.7, 6346.3 and 9760.4 mW at injection currents of 1050, 1400 and 1750 mA,

respectively. Meanwhile, the output powers of these samples with copper heat spreader can be improved to 4098.5, 7150.3 and 10919.6 mW, respectively.

The optical and thermal characteristics of array LEDs module have been improved significantly using the cup-shaped copper structure. Furthermore, various types of epoxy-packaged LEDs with cup-shaped structure were also fabricated. It is found that the light extraction efficiency of LED with semicircle package has 55% improvement as compared to that of LED with flat package. The cup-shaped copper structure was contacted directly with sapphire to enhance heat dissipation. In addition to efficient heat dissipation, the light extraction of the lateral emitting in high-power LEDs can be improved.

8641-27, Session 6

Improvement of InGaN LED performance with graphene related materials (*Invited Paper*)

Chang-Hee Hong, Chonbuk National Univ. (Korea, Republic of)

Graphene and its derivatives are currently considered to be the most promising materials that could modernize diverse electronic and optical devices by virtue of its remarkable properties. In this study the application of graphene-based materials (graphene grown by chemical vapor deposition and graphene oxide) in InGaN light-emitting diodes (LEDs) for current spreading and heat dissipation is addressed. Flexible, highly transparent graphene sheets are already explored as an alternate electrode to state-of-the-art indium tin oxide (ITO) in solar cells and LEDs. However, modifications in the inherent properties of graphene are highly essential for specific applications. For example, in the case of InGaN LEDs, it is crucial that the graphene-GaN contact ought to have low contact resistance and lowest possible barrier. Thus, interface engineering is becoming a vital part of device fabrication in order to further advance graphene's application in LEDs. First the performances of InGaN LEDs integrated with multi-layer and few-layer graphene electrodes modified by using HNO₃ and AuCl₃ are compared. Enhancement in the work function and reduction in the sheet resistance were observed for graphene treated with either dopants. Graphene treated with HNO₃ preserved its high optical transmittance (over 90% in the visible region) while the AuCl₃ treatment offered a low sheet resistance of ~80 ohm/square for a three layer graphene. The device with modified few-layer graphene electrode offered improved performances over the one made with multilayer graphene. This is attributed to the accessibility offered by the few-layer graphene for effective layer-by-layer modification and the high transparency over that of ITO.

This part describes the enhancement of LED characteristics using reduced graphene oxide (rGO) patterns as an intermediate layer. It is known that direct growth of GaN on graphene is impossible due to the lack of chemical reactivity. Here it is experimentally demonstrated that graphene oxide (GO) pattern acts as a buffer layer for lateral epitaxial overgrowth of high quality GaN and provides a better heat dissipation. The GO was deposited by spray coating method. Thermal reduction of GO and growth of GaN layers were accomplished in a metal-organic chemical vapor deposition system under one-step process. A systematic study showed that the embedded rGO pattern enables the growth of single-crystal high-quality GaN. Consequently, the fabricated device offered a low thermal resistance (down to 28%) and junction temperature (down to 32%), while its electrical and optical properties being superior to those of the conventional device. All possible mechanisms for the improvements in LED characteristics are briefly discussed.

8641-28, Session 6

Economic fabrication of optoelectronic devices with novel nanostructures (*Invited Paper*)

Pei-Wen Lin, Sih-Chen Lu, National Cheng Kung Univ. (Taiwan); Yu-Min Liao, Chin-Yi Chen, Yuh-Renn Wu, National Taiwan Univ. (Taiwan); Yun-Chorng Chang, National Cheng Kung Univ. (Taiwan)

Conference 8641: Light-Emitting Diodes: Materials, Devices, and Applications for Solid State Lighting XVII

Modern optoelectronic devices, such as light-emitting diodes (LEDs) and laser diodes (LDs), have been improved to a record-high efficiency and widely used in various industrial applications. New concepts have to be incorporated in order to further improve their efficiencies. Nanophotonics provides new and novel ways to manipulate the emitted photonics, which has been proved to be able to improve the device's performance. However, the expensive fabrication cost to fabricate the necessary nanostructures has limited the penetration of these nanostructures into current optoelectronic industrial applications.

In this study, several economic nanofabrication methods that have been developed in our group for the last few years will be demonstrated. We were able to fabricate several interesting Nanophotonic nanostructures that can be incorporated into modern industrial factories. Nanodisk and nano-hole arrays can be fabricated using Nanosphere and Nanospherical-Lens Lithography. These nanosphere-related methods use a single-layered nanosphere array as a shadow mask for metal evaporation or photolithography mask for UV exposure. One-dimensional nanowire structures can be fabricated at a pre-determined location using Nano-Crack Lithography, whose electric connections can be easily fabricated due to the known nanowire's location. All these three methods are very cost-effective and only require the most common instruments in current industrial factories. The fabricated nanostructures not only exhibit high fabrication quality but also cover large area. These nanostructures will be embedded into various optoelectronic devices. Optical and electrical characterizations of these devices will also be presented. We believe these economic nanofabrication methods will soon find their roles in current optoelectronic industries.

8641-29, Session 6

CdZnO/ZnO quantum-well light-emitting diodes based on p-GaN

Hong-Shyang Chen, Shao-Ying Ting, Yu-Feng Yao, Che-Hao Liao, Chih-Yen Chen, Chieh Hsieh, Hao-Tsung Chen, Chih-Chung Yang, National Taiwan Univ. (Taiwan)

A CdZnO/n-ZnO multiple-quantum-well (QW) light-emitting diode (LED) with the QWs and n+-ZnO capping layer grown with molecular beam epitaxy (MBE) on p-GaN, which is grown with metalorganic chemical vapor deposition (MOCVD), is fabricated and characterized. Because of the weak carrier localization mechanism in the ZnO-based LED, its defect emission is quite strong and dominates the LED output when injection current is low. The blue shift of LED output spectrum in applying a forward-biased voltage and the large blue-shift range in increasing injection current show the different behaviors of such a ZnO-based LED from those of a nitride LED. Also, a vertical light-emitting diode (VLED) with the same epitaxial structure is fabricated and characterized. Its performances are compared with those of a lateral LED based on the same epitaxial structure to show the significantly lower device resistance, larger spectral blue-shift range in increasing injection current, smaller leakage current, weaker output intensity saturation, and relatively lower defect emission in the VLED. Meanwhile, CdZnO/ZnO QW samples are grown on GaN and ZnO templates with MBE under different conditions of substrate temperature, Cd effusion cell temperature, and O₂ flow rate for emission characteristics comparison. The Cd incorporation on the ZnO template is generally lower, when compared with that on the GaN template, such that the O₂ flow rate needs to be reduced for stoichiometric CdZnO/ZnO QW growth on the ZnO template. Besides the wurtzite CdZnO structure, the rock-salt CdZnO structure exists in the CdZnO well layers when the total Cd content is high.

8641-30, Session 6

Fabrication and device characteristics of GaN-based light emitting diodes with periodic subwavelength structures

Jae Su Yu, Hee Kwan Lee, Kyung Hee Univ. (Korea, Republic of)

Recently, there has been growing interest in enhancing the light extraction of light emitting diodes (LEDs) by applying various structures including surface texturing, photonic crystals, porous films, and nanorods/nanowires. For disordered structures, however, it is somewhat difficult to achieve a good control over their size and morphology, eventually optical properties. For periodic nano patterning, electron beam lithography has disadvantages of expensive process and low throughput. Meanwhile, transparent conducting oxides exhibit high transparency and superior electrical property. The use of TCO films with patterned subwavelength surface structures can provide a continuously graded refractive index profile between the LED surface and air which suppresses effectively the internal Fresnel reflection. In this presentation, we reported the fabrication and device characteristics of InGa_N/Ga_N multiple quantum well LEDs with antireflective periodic aluminum-doped zinc oxide (AZO) subwavelength structures. The AZO subwavelength structures were fabricated on the surface of LEDs by the double exposure laser interference lithography and a subsequent dry etching. For LEDs with AZO subwavelength structures, the light output power and current-voltage curve were compared with those of the conventional LEDs. These results may give a deep understanding into the light extraction technology for high-efficient LEDs.

8641-31, Session 7

Understanding and overcoming doping limits in GaN (Invited Paper)

Joerg Neugebauer, Bjoern I. Lange, Christoph Freysoldt, Max-Planck-Institut für Eisenforschung GmbH (Germany)

The p-type doping of GaN and its alloys with InN and AlN has been notoriously difficult to achieve and presents even today a major challenge when attempting to reach acceptor levels above $\sim 5 \times 10^{19} \text{cm}^{-3}$. Traditionally, the incorporation of Mg in GaN using MOCVD has been explained by a co-doping process with H and a subsequent annealing step to drive the H out. An important consequence of this mechanism is that dopant (Mg) and co-dopant (H) should be incorporated in a 1:1 ratio. Recent experimental studies however show strong deviations from this ratio when going to high Mg concentrations thus indicating that the co-doping model needs to be revised. Using state-of-the-art ab initio calculations we have therefore systematically studied formation energies of native defects, dopants, and hydrogen. In contrast to previous studies we (i) extended these investigations to parasitic phases such as Mg₃N₂ that form at high concentration levels and (ii) apply very recent methodological advances in computing defects energies that largely remove the infamous bandgap problem and the spurious interaction of charged defects in periodic boundary conditions as commonly employed. Our results provide new insight into the complex defect chemistry of these materials systems. Particularly, based on these calculations we are able to explain the underlying mechanisms causing the change in the dopant-H ratio and show that our picture on co-doping needs to be revised. Consequences for practical process conditions will be discussed.

8641-32, Session 7

p-type transparent conductive oxide as ohmic contact for p-GaN

Chih-I Hsieh, Cheng-Yi Liu, National Central Univ. (Taiwan)

In this study, we report a p-type AlN doped SnO₂ thin films, which is processed by co-sputtering with RF magnetron sputtering system. The lowest resistivity is 0.69 $\Omega\text{-cm}$ occurred at 25 wt.% AlN doping with 450 °C annealing for 30 minutes. Using XPS analysis, we found that that the hole-carriers of the p-type AlN doped SnO₂ thin films are caused by the two substitution reactions, which are Al³⁺-Sn⁴⁺ and N₃₋-O₂₋ substitutions. With the developed p-type AlN-doped SnO₂ thin films, we investigate the contact resistance between p-type Al:SnO₂ thin films and p-GaN. The detail electrical characteristics of the contact between p-type Al:SnO₂ thin films and p-GaN will be reported in this talk.

Conference 8641: Light-Emitting Diodes: Materials, Devices, and Applications for Solid State Lighting XVII

8641-33, Session 7

Selective electrochemical etching of GaN-based superlattice layer

Dong-uk Kim, Heonsu Jeon, Hyungrae Cha, Seoul National Univ. (Korea, Republic of)

Superlattice is a periodic layer structure of two or more materials and commonly used to improve the quality of epitaxial GaN LED thin films. We have demonstrated that it is possible to etch such a common GaN-based superlattice selectively. It is found out that the superlattice confines holes well due to its lower bandgap than the surrounding materials and therefore is etched selectively during electrochemical etching. After mesa etching to expose the superlattice sidewalls of a conventional GaN LED epilayer structure and preparing a metal contact for n-GaN around the mesa, sample was immersed in 0.3M oxalic acid electrolyte for electrochemical etching. A carbon stick was also immersed as a cathode, while the GaN wafer itself served as an anode. At an appropriate reverse bias voltage, avalanche breakdown occurred at the interface between the mesa sidewall and electrolyte, and effectively enhanced hole concentration right at the exposed superlattice sidewalls, which is a necessary condition for selective lateral etching. At the optimum reverse bias voltage of 20 V, we were able to etch the superlattice layer laterally and to lift 80 μm x 80 μm square pieces of epilayer off from the substrate. We expect that our selective lateral electrochemical etching of the conventional superlattice layer has an impact on the thin GaN LED processing technology.

8641-34, Session 7

Conduction mechanism of composite multi-layer V: ZnO transparent conduction thin films

Yu Shan Wei, National Central Univ. (Taiwan)

In this study, the electrical properties of the multi-layer V-doped ZnO TCLs (transparent conductive layer) were investigated. Metal V and ZnO targets were alternatively sputtered to produce the V/ZnO multi-layer thin film structure on quartz substrates. Five different multilayer structures were processed, which are 1², 3², 4², 6², 9². The front digit means the layer number of the V metallic layer and the later digit means the layer number of the ZnO layer. We found that the multi-layer sample of 3x4 shows the best electrical conduction among all multi-layer samples. The resistivity of the as-deposited V:ZnO (3²) thin films can reach a fairly good resistivity of $2.98 \times 10^{-2} \Omega\text{-cm}$, which is much lower than the resistivity of the as-deposited ZnO thin film. The lowest resistivity ($3.82 \times 10^{-3} \Omega\text{-cm}$) of V:ZnO (3²) thin film occurred at 300 $^{\circ}\text{C}$ annealing. By the XPS analysis and HR-TEM, we conclude that the hetero-interface of ZnVO₃/ZnO_{1-x} is the main conduction path for free carriers (high carrier-mobility path). And, the major free-carrier source is the oxygen vacancies formed in the ZnO layers. We tend to believe that the substantial oxygen vacancies formed in the ZnO layer are caused by the oxidation of the neighboring V metal layers, which consume the oxygen atoms from the ZnO layers.

8641-35, Session 8

AllnGaN-based deep ultraviolet light-emitting diodes and lamps (*Invited Paper*)

Asif M. Khan, Univ. of South Carolina (United States)

Currently several research teams around the world are developing AllnGaN based Deep Ultraviolet (DUV) solid state light sources. Light emitting diodes (LEDs) with emission at 250-340 nm are an ideal replacement for mercury lamps, which currently are the only deep UV light source for air-water purification, polymer curing and bio-medical diagnostics and treatment.

The recent focus for the 250-280 nm deep UV LED research has been

primarily in increasing the power, wall-plug efficiency (WPE) and device lifetime. To improve the internal quantum efficiency innovative materials growth approaches are being pursued to fabricate low-defect and highly conducting n-p-type Al_xGa_{1-x}N (x > 0.4) layers, heterojunctions and multiple-quantum-wells. In addition to the IQE improvement, research efforts are also targeting improved light extraction by the use of substrate shaping and reflective p-contacts. The increased IQE and light extraction has now yielded 270-280 nm DUV LEDs with WPE values as high as 4-6 % with an external quantum efficiency (EQE) well over 10%. Large area deep UV LED Lamps are also being developed to get higher emitted powers by increasing the pump currents to well over 200 mA while still maintaining a lower current-density and hence increased device lifetimes. Devices with powers as high as 30 mW (200 mA pump) and lifetimes well in excess of 2000 hours have now been reported.

8641-36, Session 8

Deep ultraviolet light-emitting diodes fabricated on AlN substrates prepared by hydride vapor phase epitaxy

Toru Kinoshita, Tokuyama Corp. (Japan) and Kobe Univ. (Japan); Keiichiro Hironaka, Toshiyuki Obata, Toru Nagashima, Tokuyama Corp. (Japan); Rafael F. Dalmau, Raoul Schlessler, Baxter Moody, Jinqiao Xie, HexaTech, Inc. (United States); Shin-ichiro Inoue, Kobe Univ. (Japan); Yoshinao Kumagai, Akinori Koukitsu, Tokyo Univ. of Agriculture and Technology (Japan); Zlatko Sitar, HexaTech, Inc. (United States) and North Carolina State Univ. (United States)

AlGaN-based DUV-LEDs with emission wavelength around 265 nm, which corresponds to the absorption peak of DNA, are expected to replace mercury lamps in applications for air and water purification. In order to adopt AlGaN-based DUV-LEDs as practical and reliable ultraviolet light sources, bulk AlN substrates with low dislocation densities are required to fabricate high-performance DUV-LEDs on them. Several groups have reported that the use of bulk AlN substrate prepared by PVT yielded a remarkable improvement in the reliability of devices. However, significant light absorption in the ultraviolet region was typically observed in PVT-AlN substrates, which markedly decreased the external quantum efficiency. Recently, to overcome this issue, we proposed that thick AlN layers growth by HVPE on PVT substrates may offer a solution with low dislocation density and high transparency in the ultraviolet region.

In this work, we demonstrated AlGaN-based DUV-LEDs fabricated on HVPE-AlN substrates for the first time. The HVPE-AlN substrates for growing the LED structures were prepared by growing 250- μm -thick HVPE-AlN layers on PVT-AlN substrates. After the LED processing, the PVT-substrates were removed by mechanical polishing. The remaining thickness of the HVPE-AlN was approximately 170 μm . The 170- μm -thick HVPE-AlN substrate showed an external optical transmittance of 62% (including reflection) in the deep ultraviolet range of 250-270 nm.

DUV-LEDs mounted on AlN submounts with Au-Sn solder exhibited nearly symmetric single peak with emission wavelength at 268 nm, extracted through the HVPE-AlN substrate. The output power and external quantum efficiency under DC operation at 250 mA were recorded at 28 mW and 2.4 %, respectively.

8641-37, Session 8

Improved-efficiency high-power 260-nm pseudomorphic ultraviolet light-emitting diodes (*Invited Paper*)

Leo J. Schowalter, James R. Grandusky, Jianfeng Chen, Mark C. Mendrick, Shawn R. Gibb, Muhammad Jamil, Crystal IS, Inc. (United States)

Conference 8641: Light-Emitting Diodes: Materials, Devices, and Applications for Solid State Lighting XVII

Ultraviolet-C (UVC) radiation, with wavelengths shorter than 300 nm, is an effective means of disinfecting water, air and surfaces without the use of chemicals. The most efficient disinfection will occur at a wavelength of ~ 265 nm due to a peak in the DNA absorption. Light emitting diodes (LEDs) can be fabricated to emit at this wavelength by tuning the aluminum concentration in Al_xGa_{1-x}N quantum wells sandwiched between p-type and n-type semiconductor. Crystal IS has developed bulk AlN substrates for this application which offer several key advantages including low lattice and thermal mismatch between the substrate and the device layers. Pseudomorphic growth of Al_xGa_{1-x}N with $x > 0.6$ on bulk AlN substrates can be obtained resulting in device layers with low dislocation densities, low resistivities, and atomically smooth surfaces. The low defect density in the active region has led to improved efficiencies and long lifetimes.

The most important parameters for these devices are the wall plug efficiency and output power. The wall plug efficiency is the product of the internal quantum efficiency (IQE), the current injection efficiency internal efficiency, the electrical efficiency, and the extraction efficiency. We have optimized the product of the IQE and the current injection efficiency to achieve internal efficiencies of 70%. At typical operating conditions of 100 mA, electrical efficiencies greater than 75% have been achieved. The extraction efficiency has been the biggest issue with achieving high wall plug efficiencies, but recent advances have pushed this to a typical value over 15%. These improvements, along with improved thermal management, have led to 20 mW of output power at a WPE of 5% at 65 mA and 90 mW at a WPE of 3.2% at 300 mA for a 260 nm LED in CW operation. In addition to the high WPE and output power, the devices emit in a lambertian pattern allowing the source to be imaged as nearly a point source. At 300 mA operating conditions, a radiant exitance of 7 W/cm² and a radiance of 2.2 W/cm²/sr has been achieved which is several orders of magnitude higher than mercury lamps.

This work was supported in part by DARPA under the Compact Mid-Ultraviolet Technology (CMUVT) program and by the Army Research Laboratory under Cooperative Agreement Number W911NF-09-2-0068.

8641-38, Session 8

Transparent electrodes for AlGaIn-based deep-ultraviolet light-emitting diodes

Hee-Dong Kim, Min Ju Yun, Kyeong Heon Kim, Ho-Myoung An, Tae Geun Kim, Korea Univ. (Korea, Republic of)

Deep ultraviolet light-emitting diodes (UV-LEDs) have attracted much attention in areas of air/water sterilization and decontamination, bioagent detection and natural light. However, the maximum external quantum efficiency reported so far is less than 5% at a wavelength of 280 nm due to the difficulty in obtaining Ohmic contact to p-type AlGaIn as well as high-quality p-type AlGaIn growth. Apart from AlGaIn growth issues, it is very important to develop transparent electrodes (TEs) with excellent optical and electrical properties in deep UV regions in view of device fabrication. Although indium tin oxide films are widely used as the TEs for near UV-LEDs (>365 nm), they are no longer available in the deep-UV region due to its large absorption. Therefore, new types of TEs with high optical and electrical properties in the deep UV region must be developed.

In this work, we developed a current flowing process applicable to all kinds of wide-bandgap oxides and nitrides deposited on p-GaN (or p-AlGaIn) layers, in order to obtain both Ohmic contact and high transmittance from infrared to deep UV light bands. As a result, we achieved excellent Ohmic behavior and optical transmittance over 80 % at a wavelength of 280 nm from several wide-bandgap materials such as ZrO₂, Ga₂O₃ and AlN deposited on p-GaN and even p-AlGaIn. More details on the experimental result will be presented at the conference.

8641-39, Session 9

Vertical light-emitting diodes fabricated with photoelectrochemical liftoff (*Invited Paper*)

Chieh Hsieh, Chih-Yen Chen, Che-Hao Liao, Horng-Shyang Chen, Chun-Han Lin, Chih-Chun Lin, Yean-Woei Kiang, Chih-Chung Yang, National Taiwan Univ. (Taiwan)

Because of certain fundamental drawbacks of the laser liftoff technique, the yield of sapphire substrate liftoff based on this technique for fabricating vertical light-emitting diode (LED) is quite low. Here, a low-cost, large-area, effective sapphire substrate liftoff method based on the photoelectrochemical (PEC) etching technique is demonstrated. By preparing patterned sapphire substrate (PSS) with one-dimensional periodic grooves and the epitaxial structure with the grooves preserved to form tunnels, PEC electrolyte can flow along the tunnels to etch the bottom of the GaN layer for separating the PSS from the wafer-bonded epitaxial layer. Assisted by the device isolation procedure, the PSS liftoff of a quarter-wafer sample can be completed in 8 min. After a smoothing process of the exposed N-face surface after liftoff, a vertical LED is fabricated for comparing its characteristics with those of a conventional LED. Also, the combination of PEC etching with phase mask interferometry can provide us with a low-cost method of fabricating LED surface grating for enhancing the light extraction efficiency. However, before we can decide the period of the phase mask, we need to find out the optimized surface grating period on the LED. Based on a Llyod's interferometer, the variations of the output intensity and electrical property of a surface-grating vertical LED with different grating periods on the n-GaN layer are demonstrated. The effects of changing the duty cycle and groove depth in forming the one-dimensional surface grating on the LED light extraction are also discussed.

8641-40, Session 9

Low temperature growth of InGaIn by pulsed sputtering and its applications to long wavelength LEDs (*Invited Paper*)

Hiroshi Fujioka, Univ. of Tokyo (Japan) and CREST-JST (Japan)

It is well known that performance of nitride LEDs are dramatically degraded with the increase in their wavelengths. Although phase separation reactions in the InGaIn layers due to the large miscibility gap are often considered to be responsible for efficient light emission in blue LEDs at least partially, it is also known that it makes crystal growth of high-concentration InGaIn for long wavelength LEDs quite difficult. Obviously, epitaxial growth of this material at very high temperatures by the use of a high pressure CVD apparatus is the most straightforward strategy to avoid this problem. However, synthesis of InGaIn under highly non-equilibrium conditions such as extremely low temperatures also is a promising alternative way. For this purpose, we have recently developed a new growth technique named PSD (pulsed sputtering deposition). In this technique, surface migration of the film precursors is enhanced by the pulsed supply with high kinetic energies and, therefore, the growth temperature can be dramatically reduced. PSD has already attracted much attention of industry engineers because its productivity is much higher than that of MOCVD. We have found that InGaIn films prepared by PSD have intense room temperature photoluminescence in the range from UV to NIR. We have found the intensity ratio of room temperature photoluminescence to low temperature photoluminescence at a long wavelength of 720 nm is as high as 48 %, which is the highest value ever reported. We will also demonstrate successful operation of RGB LEDs with the use of PSD high In concentration InGaIn.

Conference 8641: Light-Emitting Diodes: Materials, Devices, and Applications for Solid State Lighting XVII

8641-41, Session 9

Key issues of vertical thin-GaN LED technology (*Invited Paper*)

Cheng-Yi Liu, Yen-Shuo Liu, National Central Univ. (Taiwan)

Recently, high-power light-emitting diodes (LEDs) with vertical thin-GaN structure attract serious attention because of their excellent thermal dissipation. The main feature of the vertical thin-GaN LED structure is that the metal-organic chemical vapor deposition (MOCVD) grown GaN LED epi-layer is stripped off and transferred onto the better thermal and electrical conduction substrate (such as, high-doped Si or Cu) by wafer bonding and laser lift-off (LLO) techniques. In this talk, we will discuss the four key issues of vertical thin-GaN LED; (1) n-GaN surface texture. (2) DLC thermal layer. (3) KrF laser stripping. (4) stress-relief in the transformed GaN LED epi-layers.

8641-42, Session 9

Analysis of light extraction efficiency enhancement for thin-film-flip-chip InGaN quantum wells light-emitting diodes with GaN micro-domes

Peng Zhao, Hongping Zhao, Case Western Reserve Univ. (United States)

As the promising candidate for the next generation lighting technology, light-emitting diodes (LEDs) play an important role in solid state lighting. The limitation occurred in light extraction efficiency of III-nitride LEDs is attributed to the large refractive index difference between III-nitride semiconductor ($n \sim 2.4$) and free space ($n \sim 1$), which leads to significant total internal reflection at the semiconductor and air interface.

Here, we propose a new method to achieve large enhancement of light extraction efficiency for commercially used thin-film flip-chip (TFFC) InGaN quantum wells (QWs) LEDs by utilizing semiconductor micro-dome structures on n-GaN surface. The extraction efficiency analysis is based on three dimensional finite difference time domain (3D-FDTD) method. In TFFC InGaN QWs LEDs, the p-GaN layer thickness is critical for maximizing the light extraction efficiency due to the interference between original incident light from InGaN QWs and the reflections from bottom mirror. Based on the TFFC InGaN QWs LEDs with optimized p-GaN thickness, the GaN micro-domes will be applied to enhance the light extraction efficiency, which could be formed by reactive ion etching (RIE) of the GaN layer with a self-assembled dielectric microsphere monolayer as mask. The effects of micro-dome diameter and height in the range of submicron to micron on the light extraction efficiency will be comprehensively studied and compared with conventional TFFC InGaN QWs LED with flat surface. Significant enhancement of the light extraction efficiency (2.5-2.7 times for 460nm emission and 2.7-2.8 times for 550nm emission) is achievable from LEDs with GaN micro-domes with optimized micro-dome diameter and height.

8641-43, Session 10

Growth of high-indium InGaN films using a combined deposition technique and its application for long-wavelength light-emitting diodes (*Invited Paper*)

Kun-Ching Shen, Dong-Sing Wu, Tzu-Yu Wang, Ray-Hua Horng, National Chung Hsing Univ. (Taiwan)

High indium content InGaN films were grown on sapphire substrate using low temperature pulse laser deposition (PLD) with nitrogen plasma and a specific target. The controllable target consists of two separate sections: an indium sheet with periodic rectangular-holes and a standard GaN

wafer. By changing the rectangular-hole area, a modulated indium vapor was excited by pulsed laser and introduced into the InGaN deposition reaction, contributing the increase in the incorporation of indium into the InGaN film. The structural and optical stability of the 33 and 60% indium InGaN revealed no differences in the line-shape and peak position even after annealing at 800°C for 75 min from x-ray diffraction and photoluminescence results. Moreover, such high thermal stability of 60% InGaN film was put in metal organic chemical vapor deposition (MOCVD) to regrow GaN layer, the peak position of 860 nm remained unchanged after MOCVD regrowth. The flat and uniform of regrown sample indicates that the PLD method used in this study is indeed promising for the development long wavelength of high indium content InGaN emitters.

8641-44, Session 10

Light quality and efficiency of consumer grade solid state lighting products

Carsten Dam-Hansen, Dennis D. Corell, Anders Thorseth, Peter B. Poulsen, Technical Univ. of Denmark (Denmark)

The rapid development in flux and efficiency of Light Emitting Diodes (LED) has resulted in a flooding of the lighting market with Solid State Lighting (SSL) products. Many traditional light sources can advantageously be replaced by these SSL retrofit products. There are however large variations in the quality of the available products, and some are not better than the ones they are supposed to replace. Here the results of a two year study investigating SSL products on the Danish market are presented. The light sources have been tested for luminous flux and spectral power distribution. Focus has been on SSL products for replacement of incandescent lamps and halogen spotlights. More than 300 SSL replacement lamps have been tested for efficiency and light quality with respect to correlated color temperature and color rendering properties. The warm white light and good color rendering properties of these traditional light sources are a must for lighting in Denmark and the Nordic countries. We compare the test results with the requirements in the EU LED quality charter, and find many products with light inferior light quality and efficiency. The lumen and color maintenance over time has been investigated by non-accelerated lifetime tests and results for products running over 8000 h will be presented. A new internet based SSL product selection tool will be shown. Here the products can be compared on efficiency, light quality parameters and price, thus providing a better basis for the selection of SSL products for consumers.

8641-45, Session 10

GaN-based nanorod technology for solid state lighting (*Invited Paper*)

Andreas Waag, Xue Wang, Johannes Ledig, Milena Erenburg, Jian Dong Wei, Matin Mohajerani, Hergo-Heinrich Wehmann, Technische Univ. Braunschweig (Germany); Uwe Jahn, Henning Riechert, Paul-Drude-Institut für Festkörperelektronik (Germany); Martin Strassburg, Martin Mandl, Hans-Jürgen Lugauer, Ulrich Steegmüller, Osram Opto Semiconductors GmbH (Germany)

GaN nanorods and 3D columns recently attracted a lot of attention since they are expected to be an exciting new route towards solid state lighting. In contrast to a planar thin film technology or pyramid structures, a completely 3-dimensional nanorod approach gives more freedom in the device design. E.g., a core-shell design of LEDs based on 3D GaN offer a dramatically enhanced active area per wafer footprint, since the active area is scaling with height of the 3D structures. High quality core-shell devices will have a tremendous impact on LED technology.

This talk will give an overview on the state of the art of our 3D GaN research, particularly focusing on patterned MOCVD growth and 3D characterization. Electron beam induced current (EBIC) measurements are a suitable tool in order to access the inner electronic structure of the 3D LEDs. The minority carrier diffusion length can be derived from such

Conference 8641: Light-Emitting Diodes: Materials, Devices, and Applications for Solid State Lighting XVII

measurements. A thorough analysis of 3D LED geometry and their optical properties as a function of growth parameters and pattern geometry gives insights into relevant growth mechanisms. Problems during nucleation can give rise to multiple polarity growth.

Potential advantages and challenges of this exciting new strategy towards low cost high efficiency solid state lighting will also be discussed.

8641-46, Session 10

Multispectral CMOS sensors with on-chip nanostructures for wavelength monitoring of LED devices

Stephan Junger, Nanko Verwaal, Wladimir Tschekalinskij, Norbert Weber, Fraunhofer-Institut für Integrierte Schaltungen (Germany)

Lifetime, efficiency, and flexible color output make LEDs the predestined solution for light sources for many lighting applications. However, high-end illumination devices based on LEDs require precise color matching, because the dominant wavelength depends on temperature and changes due to aging effects of the LEDs. A change in junction temperature results in a wavelength drift, and a drift of few nanometers results in a noticeable and therefore unwanted change in the color temperature. Color-sensing feedback achieves greater color accuracy compared to simpler junction-temperature feedback, but typically the added cost of the color sensor is not negligible.

We demonstrate the performance of multispectral sensors fabricated using a complementary metal-oxide semiconductor (CMOS) process. Various metallic nanostructures for color filtering were simulated using the finite-difference time-domain (FDTD) method and layouted using the work flow of integrated circuit design. Sub-wavelength hole arrays as plasmonic filters and nanorod arrays are tailored in order to achieve different band pass and cut-off filters. Together with CMOS photodiodes implemented below the filtering nanostructures, these novel integrated devices for multispectral sensing can be fabricated in high volume for low-cost color-feedback systems of high-end LEDs illumination devices. First measurements indicate that a wavelength change of 3 nm yields a relative signal change of more than 20 % due to the steep-edge characteristics of the filters.

8641-47, Session 10

Three zone Topside Temperature Control (TTC) in a Close Coupled Showerhead (CCS) reactor

Frank Schulte, A. Boyd, O. Feron, P. Lauffer, X. Chen, Markus Luenenbuerger, R. Leiers, AIXTRON SE (Germany); Simon Thomas, AIXTRON Ltd. (United Kingdom); Bernd Schineller, Michael Heuken, AIXTRON SE (Germany)

For MOCVD of GaN based LEDs control of the wafer surface temperature is critical to device yield. Temperature is a main parameter for the process, particularly for the MQW growth step.

In this study a CRIUS® II-XL CCS reactor with a 19x4 inch configuration and 3 independent concentric heater zones was used. To monitor the temperature profile over the entire radius of the wafer carrier we developed the Argus topside pyrometer. It utilizes an array of dual wavelength detectors which delivers a temperature map of the wafers. The surface temperature of each zone was calculated from the mapping and zones were independently closed loop controlled to follow the set-point temperature. The controller was designed for partial as well as full wafer loads.

To assess the reproducibility of control 5 consecutive fully loaded 19x4" LED process runs followed by 6 partially loaded runs (7 prime wafers each) were performed. The wafer carrier was exchanged between each run and zone top side temperature control was used for the entire

process above 500°C.

Thickness uniformity values of 1.0% on-wafer and 0.6% wafer-to-wafer, and PL peak wavelength uniformity of 1.3 nm on-wafer and 0.9 nm wafer-to-wafer at a mean wavelength of 452.1 nm were observed for all fully loaded runs. This demonstrates consistent control of all three heater zones. The spread across all 95 wafers was 5.5 nm.

The 6 partial loaded runs had similar uniformities and only increased the full range of run average wavelengths to 1.7 nm.

8641-48, Session 11

Quantum dot LED phosphors: performance and reliability improvements (*Invited Paper*)

Juanita Kurtin, Pacific Light Technologies (United States)

Quantum dots (QDs) are rare-earth free downconverters which have been demonstrated as ideal phosphor replacement materials from an optical perspective, with the potential to enable a 30% improvement in LED efficiency as compared to today's rare-earth phosphors at the same quality of light. However to date QDs have demonstrated less than ideal reliability under standard LED chip conditions, prohibiting cost-effective integration into conventional luminaire formats. This talk will discuss the present status and future prospects of QDs as LED downconverters, including recent advances in connecting quantum dot structure to high temperature and high intensity performance, an updated look at QD reliability, and the limits of QDs in a variety of phosphor configurations.

8641-49, Session 11

Color tunable green-yellow-orange-red erbium/europium codoped fluoro lead germanate glass phosphor for application in LED illumination technology

Artur S. Gouveia-Neto, Wellington S. Souza, Renata O. Domingues, Ernande B. Costa, Luciano A. Bueno, Univ. Federal Rural de Pernambuco (Brazil)

LED-based lighting technology has drawn much interest recently owing to their wide variety of benefits over daily used incandescent and conventional fluorescent illuminants. Since the realization of white-light-emitting diodes, they are viewed as the next generation solid-state illumination technology. The advantages range from energy consumption to environmental issues. Essentially, there exist two approaches to produce white-light employing LEDs. Color addition using LEDs producing the three primary wavelengths, or visible light emission from UV/blue excited rare-earth doped phosphors. White LEDs produced via a blue-LED and a yellow emitting phosphor, has attracted much interest recently. However, this technique suffers from low color rendering index and the generated white-light changes with excitation power or temperature. Another deficiency is the absence of red components which prevents the generation of light in the red spectral region and the combination of yellow phosphor and blue-LED produces rather high correlated color temperature (CCT > 4500K). To overcome these drawbacks, a white LED fabricated via UV-blue excited red, green, and blue emitting phosphors is required. Recently, several attempts have been made to mix RE3+ multi-doped phosphors to produce either multicolor or white-light emission. Color tunability incorporates functionality to the multicolor phosphor for "smart light" technology. Recently, phosphor color tunability via excitation power, temperature, and active ions concentration has been realized. Color tunable wide gamut light covering the greenish, yellow-green, yellow, orange, and reddish tone chromaticity region in europium/erbium codoped lead-cadmium-germanate PbGeO₃:PbF₂:CdF₂ glass phosphors is presented. The phosphors were synthesized, and their light emission properties examined under UV/blue light-emitting-diode excitation. Luminescence emission around 525, 550, 590, 610, and 660 nm was obtained and analyzed as a function of Eu/Er concentration, excitation wavelength, and glass host composition. The

Conference 8641: Light-Emitting Diodes: Materials, Devices, and Applications for Solid State Lighting XVII

color tunability was actually obtained via proper combination of Er³⁺ and Eu³⁺ active ions concentration. Results indicate that the color-tunable fluorolead germanate erbium/europium codoped glass phosphor herein reported is a promising novel contender for application in LED-based solid-state illumination technology

8641-51, Session 11

The latest phosphor solutions for LED backlighting and general lighting (*Invited Paper*)

Yi-Qun Li, Intematix Corp. (United States)

No Abstract Available.

8641-52, Session 11

Theoretical and experimental analyses of energy transfer mechanisms between Er³⁺ and Yb³⁺ doped in La₂O₂S

Madhab Pokhrel, Ajith K. Gangadharan, Dhiraj K. Sardar, The Univ. of Texas at San Antonio (United States)

In recently years, a great deal of research has focused on finding lanthanide doped nano and micron size phosphors that will undergo near infrared to visible upconversion. Search for finding the efficient upconversion in nano and micron size materials is an on-going issue. One way of increasing the upconversion fluorescence is by co-doping oxysulfide hosts with Er and Yb ions with appropriate concentrations. We would like to report twenty different concentrations of Yb and Er individually doped in La₂O₂S phosphor synthesized by solid state flux fusion method. We study the effects of sensitizer (Yb) concentration on the upconversion fluorescence. The mechanisms of upconversion by two photon and energy transfer processes will be interpreted and explained through the decay analysis of Er and Yb under the indirect and upconversion excitation. In order to compare the efficiency of these phosphors with those of other materials presently in use, it is important to quantify their upconversion efficiencies. It is worth mentioning here that most of the research work on upconversion materials does not quantify any upconversion efficiency. Absolute quantum efficiency of the upconverting particle will be reported for all the Er, Yb doped in La₂O₂S samples depending on the concentrations. Preliminary studies show that intense green emission has been observed for the composition of 9 mol% Yb and 1 mol% Er. The high luminescence output enables the present phosphors to find potential lighting applications such as LED, lasers, displays etc.

8641-53, Session 11

Characterization and endurance study of aluminate/silicate/garnet/nitride phosphors for high-performance SSL

Nicola Trivellini, LightCube SRL (Italy); Matteo Meneghini, Matteo Dal Lago, Diego Barbisan, Marco Ferretti, Gaudenzio Meneghesso, Enrico Zanoni, Univ. of Padova (Italy)

With this work we report on the performance and degradation mechanism of commercially available remote phosphors (RP) for application in LED lighting systems. RP LED systems are very attractive for general illumination, but relatively few information is available regarding their performances and reliability.

Thermal characterization was performed on remote phosphor plates deposited on a Polycarbonate substrate excited by means of 455nm high power LEDs. Thermal analysis indicates that phosphors can reach temperatures above 60°C during operation at an ambient

temperature of 25°C when subjected to an optical power of 316 mW/cm². We demonstrate that temperature is a strong driving force for the degradation of these systems, by means of reliability tests carried out at different temperatures between 85 and 145°C.

Results indicate a gradual reduction in luminous flux output and a decrease of correlated color temperature as a consequence of stress. For the higher stress temperature (145°C) the flux reaches the 20% of its initial value and the CCT decreases from 4000 K to 3200K after 1000h of stress. Degradation rate is strongly correlated with stress temperature resulting in a more prominent degradation at higher temperatures. The Arrhenius plot indicates an activation energy of 1.2 eV for a TTF of 90%.

After the ageing at 145°C for 1000h we have compared the polycarbonate substrate (after removing the phosphors by means of mechanical polishing) with an untreated reference by means of Microscopic optical analysis. Results indicate a clear darkening and decrease of light transmission.

8641-8, Session PWed

Visual susceptibility analysis for solid-state lighting of commercial PC-WLEDs

Cheng-Feng Yue, Chun-Chin Tsai, Far East Univ. (Taiwan); Wood-Hi Cheng, National Sun Yat-Sen Univ. (Taiwan)

Human susceptibility to visual discomfort of solid-state lighting was investigated by statistically analyzing for commercial phosphor-converted white light-emitting diodes (PC-WLEDs) with considering optical characteristics such as correlated color temperature (C.C.T., or T_{cp}), chromaticity, lumen, color rendering Index (C.R.I.), radiation pattern. These statistic analyses of human factor engineering were based on the surveys and visual measurements among 500 male and female volunteers of ages 18 to 22. The levels of these optical parameters were standardized for indication of the discomfort degree or sensitivity to human visual susceptibility. The results showed that, compared to male human eyes, female ones could have 20% more sensitive to color rendering on R985 Index, 15% higher in color temperature; however, 30% less sensitive to lumen, and 30% lower recognition ability to radiation pattern. Consequently, it becomes more important for LED manufacturers and solid-state lighting designers to take consideration of such human factor engineering into their products and services.

8641-13, Session PWed

Fabrication of OLED with a new yellow fluorescent dopant and measurements of photoluminescence and electroluminescence properties

SungNam Lee, Gweon Young Ryu, Dong Myung Shin, Hongik Univ. (Korea, Republic of)

A yellow fluorescent material, BDAT-CP was synthesized for OLEDs. This material designed by changing molecular structure of (2Z)-3-[4,4"-bis(dimethylamino)-1,1':4',1"-terphenyl-2'-yl]-2-phenylacrylonitrile (BDAT-P). The UV-Visible absorption peak of BDAT-CP was measured to be at 329 nm and its photoluminescence (PL) emission spectrum showed red light-emission peaked at 628 nm in chloroform solvent and Solid Powder PL showed yellow emission peaked at 582nm. The device structures were Indium tin oxide (ITO) / N,N'-bis-(1-naphyl)-N,N'-diphenyl-1,1'-biphenyl-4,4'-diamine (NPB, 50 nm) / 2-methyl-9,10-bis(naphthalen-2-yl)anthracene (MADN, 30 nm) : BDAT-CP (5%) / 4,7-diphenyl-1,10-phenanthroline (Bphen, 30 nm) / Liq(2 nm) / Al. The maximum peak of electroluminescence (EL) spectra was measured 14700 cd/m² at 9 V. The device exhibits Luminance efficiency of 7.13 cd/A at 172.13 mA/cm² and quantum efficiency of 2.77 % at 0.56 mA/cm² which shows excellent properties than BDAT-P.

8641-50, Session PWed

Performance enhancement of high-temperature glass-based phosphor-converted white light-emitting diodes employing SiO₂

Chun-Chin Tsai, Cheng-Feng Yue, Far East Univ. (Taiwan); Wood-Hi Cheng, National Sun Yat-Sen Univ. (Taiwan); Min-Ching Lin, Walsin Lihwa (Taiwan); Ching-Jen Pan, HELIO Optoelectronics Corp. (Taiwan)

Considering better stabilities of lumen and chromaticity characteristics, the degradation behavior of innovative encapsulation glass of Ce:YAG phosphor particulate composite coated with sol-gel derived SiO₂ was investigated for high temperature phosphor-converted white light-emitting diodes (PC-WLEDs) through thermal aging tests at various temperatures from 150°C to 350°C, compared with those of silicone phosphor and uncoated Ce:YAG phosphor glasses. The photoluminescence measurements of such new phosphor glass material showed 17% increase in fluorescence intensity of Si-coated phosphor particles, as also 10% raise for phosphor glass and 5% lumen elevation of PC-WLED comparative to those with uncoated Ce:YAG phosphor. These brand new coated phosphor particles in glass matrix could provide widely-pursued applications for high power WLED with excellent reliability.

8641-66, Session PWed

Application of Gabor hologram for designing a new optical imaging system

Mohamed Darwiesh, Military Technical College (Egypt); Ashraf F. El Sherif, Arab Academy for Science, Technology & Maritime Transport (Egypt)

The optical imaging systems are widely spread in recent years in many applications. Since most optical imaging system depends on tracking surface detail, a key discovery was that most modern laminated work surfaces are microscopically embossed, presumably to reduce glare. When this texture is obliquely illuminated by a light source a pattern of highlights and shadows (speckle pattern) is revealed. The performance of the optical imaging systems with different surfaces has been studied.

Optical characteristics of the used surfaces were verified by the utilization of standard diffuse objects using the method of Gabor holography. The obtained single-exposure Gabor holograms were used to produce Gabor circular fringes with different light sources (He-Ne laser, Diode laser, and different colored LEDs).

The Gabor fringes were used to display the relations between the fringes order and its radii. From these relations we have obtained the corrected values of the light sources wavelength.

The measured wavelengths were found to be in good agreement with the real one in the case of laser sources (He-Ne laser and Diode laser). But, for LED sources the experimental verification leads to the conclusion that when using light source (laser diode of $\lambda=697\text{nm}$) give the same performance of (a red LED with central peak at $\lambda=682\text{nm}$ and $\text{BW}=30\text{nm}$), and (laser diode of $\lambda=611\text{nm}$) give the same performance of (an orange LED with central peak at $\lambda=597\text{nm}$ and $\text{BW}=35\text{nm}$), and (laser diode of $\lambda=567\text{nm}$) give the same performance of (a yellow LED with central peak at $\lambda=591\text{nm}$ and $\text{BW}=12\text{nm}$), and (laser diode of $\lambda=556\text{nm}$) give the same performance of (a green LED with central peak at $\lambda=566\text{nm}$ and $\text{BW}=24\text{nm}$), and (laser diode of $\lambda=460\text{nm}$) give the same performance of (a blue LED with central peak at $\lambda=463\text{nm}$ and $\text{BW}=34\text{nm}$).

This means that the electronic sensor can deliver the same accuracy of laser diodes when replacing it by commercial LEDs. So, we can design a new cheaper, high performance optical imaging system using commercial LED sources.

8641-67, Session PWed

Use CCT and lighting distribution control algorithm for optimized energy saving with human factor lighting

Chih-Wei Lin, Jung-Min Hwang, Chin-Ming Shih, Ke-Fang Hsu, Industrial Technology Research Institute (Taiwan)

In this study, a process for optimizing the color temperature and lighting distribution on indoor LED lighting for human factor and energy saving is proposed. Based on the features of LED lighting, the diversified fixture design is more possibilities, such as the fixture with color-temperature and lighting distribution tunable. Therefore, the generalized reduced gradient optimization method is used to calculate the corrected color temperature of the fixture for the seat near the window affected by sun light. This research result could be used in the LED lighting design for more energy saving.

8641-68, Session PWed

Miniaturization of remote phosphor LED packages

Tsung-Xian Lee, Heng-Yu Song, National Taiwan Univ. (Taiwan)

The concept of the remote phosphor is proven to be one of the effective solutions for improving luminous efficiency of white LEDs by solving the problem of phosphor thermal and scattering loss. However, most of them need to use large packaging to keep their performance. Such development is adverse to market trends, which also resulted in higher manufacturing costs and the difficulties in luminaire design. In this paper, we analyze the packaging size effect and search its limitation, so that we can apply to reduce the size of remote phosphor structure. Accordingly, the miniaturization performance of two different remote phosphor packages is further improved, which makes the remote phosphor package valuable for practical application. Besides, spatial color uniformity is also critical index in the evaluation of high-quality white LEDs. Many approaches only consider the performance of luminescence efficiency of remote phosphor, but have often overlooked the effect of spatial color distribution caused by chip, phosphor and packaging structure. A non-optimized white LED light source will induce the increase of spatial color deviation, and influence the actual illumination effects. Base on this point, we also consider the non-uniform phenomenon of color distributions in our design.

8641-69, Session PWed

Characteristics of III-nitride nonpolar LEDs grown by plasma-assisted molecular beam epitaxy

Chen-Yu Lin, Tsung-Yi Chou, Ching-Wen Chang, Yuan-Ting Lin, Li-Wei Tu, National Sun Yat-Sen Univ. (Taiwan)

In the recent years, non-polar III-V nitrides light-emitting diodes (LEDs) with low droop have been fabricated and studied. It has not only high performances in optical output power and wider wavelength range, but also polarized light emission characteristic, which opens up new fields of applications.

The m-plane III-nitrides were grown on m-plane sapphire by plasma-assisted molecular beam epitaxy (PAMBE) without buffer layer. We optimized the growth temperature and V/III flux ratio systematically for each epitaxial layer. The surface morphology and crystal quality were strongly correlated with the narrow optimized growth window. The optical and structural properties were studied in this report. The polarization dependent photoluminescence (PL) for m-plane GaN and m-plane p-GaN/InGaN/n-GaN (p-i-n) structure were investigated at 15K and 300K. The PL intensity of polarization along the a-axis was always stronger than along the c-axis and the polarization ratio was also calculated.

Conference 8641: Light-Emitting Diodes: Materials, Devices, and Applications for Solid State Lighting XVII

The strains of the m-plane nitrides films were deduced by micro-Raman spectroscopy and were related to the degree of the polarization. The m-plane blue LED (432 nm) was fabricated with 14% indium composition of InGaN. A standard diode current-voltage (I-V) curve was obtained with a threshold voltage 4.12 V. The polarization dependent electroluminescence (EL) was also measured at room temperature, which yielded a polarization ratio of 42%. The growth and characteristics of m-plane multiple quantum well (MQW) structure LEDs will also be discussed in this report.

8641-70, Session PWed

Performance of nitride-based light-emitting diodes using an Indium-zinc-oxide transparent electrode with moth-eye structure

Shugo Mizutani, Satoshi Nakashima, Motoaki Iwaya, Tetsuya Takeuchi, Satoshi Kamiyama, Isamu Akasaki, Meijo Univ. (Japan); Toshiyuki Kondo, Fumiharu Teramae, Atsushi Suzuki, Tsukasa Kitano, Midori Mori, EL-SEED Corp. (Japan); Masahito Matsubara, Idemitsu Kosan Co., Ltd. (Japan)

An indium-tin-oxide (ITO) thin film is used as a transparent ohmic contact to p-GaN in general nitride-based light-emitting diodes (LEDs). The properties of ITO such as high transmittance of light, a low sheet resistivity and a low contact resistance are suitable to LEDs. However, the ITO has a chemically stable poly-crystallinity after annealing, so that it makes difficult to form nano-patterning for further improvement of the light extraction efficiency. In this paper, we propose a new transparent electrode material, Indium-zinc-oxide (IZO) in favor of microfabrication.

A 300 nm-thick IZO ($\text{In}_2\text{O}_3 : \text{ZnO} = 91.3 : 10.7$, wt%) film was deposited on p-GaN and sapphire substrates by a reactive sputtering technique. The contact resistance was $9.4 \times 10^{-4} \text{ Ohm cm}^2$, which is comparable to that of ITO. Other physical properties such as a resistivity and a high transmittance were also comparable to those of ITO. These properties show sufficient potentials of IZO as a transparent electrode material to nitride-based LEDs.

Although IZO has a poly-crystallinity, its surface is very flat and can be etched by BCl_3 dry etching. Therefore, an advantage of IZO is easiness of pattern formation. We succeeded to form a moth-eye structure with a pitch of 460 nm to IZO transparent contact on a nitride-based LED. The moth-eye structure on IZO electrode showed a fine nano-scale structure, while that on ITO has rough surface. As a result, light output of IZO-LED was 10% higher than that of ITO-LED. IZO is an excellent alternative to the transparent electrode material in nitride-based LED.

8641-71, Session PWed

Electrical and thermal properties of laser-assisted doped Ti/Al ohmic contacts to N-face n-type GaN

Su Jin Kim, Kyeong Heon Kim, Ho-Myoung An, Korea Univ. (Korea, Republic of); Tak Jeong, Korea Photonics Technology Institute (Korea, Republic of); Tae Geun Kim, Korea Univ. (Korea, Republic of)

GaN based vertical light-emitting diodes (VLEDs) have been considered promising devices for high-power applications due to the advantages such as efficient heat sink and uniform current spreading. In order to fabricate high performance VLEDs, low-resistance and high quality ohmic contacts are required. For Ga-face n-GaN of lateral-type LEDs, the contact resistivity of $10^{-5} \sim 10^{-6} \text{ Ohm cm}^2$ were easily achieved. However, for N-face n-GaN of VLEDs, it is still challenging to achieve effective ohmic contacts since the [000-1] N-face is grown with an opposite polarity to [0001] Ga-face. This difference in the surface structure makes it difficult to obtain low-resistance ohmic contacts to the N-face n-GaN.

In this work, we investigated the effect of laser-assisted Si doping to N-face n-GaN on the electrical and thermal properties of Ti (30 nm)/Al (200 nm) contacts. The N-face n-GaN samples were prepared by using metal organic chemical vapor deposition (MOCVD), along with laser-lift off (LLO) and dry etching processes to expose the N-face n-GaN layer. In the experimental result, the contact resistivity was dramatically reduced from $7.61 \times 10^{-4} \text{ Ohm cm}^2$ to $8.72 \times 10^{-5} \text{ Ohm cm}^2$ by applying laser-assisted Si diffusion process to the GaN surface before the Ti/Al deposition. Also, no degradation in specific contact resistivity was observed for these highly doped samples after annealing at 300 °C. This improvement can be attributed to the reduction in the Schottky barrier height (SBH) via donor-like surface defects such as VN or SiGa formed by the laser-assisted doping. More details on the experimental result will be presented at the conference.

8641-72, Session PWed

Enhancement in external quantum efficiency of UVLED with embedded oxide structure

Kun-Ching Shen, Dong-Sing Wu, Min-Hao Yang, Wen-Yu Lin, Ray-Hua Horng, National Chung Hsing Univ. (Taiwan)

High performance 380 nm ultraviolet vertical light-emitting diodes (LEDs) were developed using an embedded self-textured oxide pattern (STO) with metal-organic chemical vapor deposition (MOCVD). From scanning electron microscopy (SEM) image, the threshold dislocation densities (TDs) of LED epilayer were effectively reduced to 10^7 cm^{-2} by inserting the STO due to the relaxation of residual stress. The vertical-type LEDs are fabricated using a combination technique of wafer bonding and sapphire substrate separation. When the vertical-type LED chips (size: $1.125 \text{ mm} \times 1.125 \text{ mm}$) was driven with a 350 mA injection current, the output powers of the LEDs with and without STO were measured to be 158.6 and 75.4 mW, respectively. The external quantum efficiency of LED with STO exhibits 70% higher than that of LED without STO. As increasing injection current to 1000 mA, a near 450 mW light output was measured from STO-LED sample. This benefit was attributed to the introduction of STO structure which can not only block the propagation of threading dislocations but also intensify the light extraction of LED

8641-73, Session PWed

High-quality quantum-dot-based full-color display technology by pulsed spray method

Kuo-Ju Chen, Hsin-Chu Chen, Kai-An Tsai, National Chiao Tung Univ. (Taiwan); Chien-Chung Lin, National Cheng Kung Univ. (Taiwan); Yung-Jung Hsu, National Chiao Tung Univ. (Taiwan); Min-Hsiung Shih, Academia Sinica (Taiwan); Hao-Chung Kuo, National Chiao Tung Univ. (Taiwan)

We fabricated the colloidal quantum-dot light-emitting diodes (QLEDs) with the $\text{HfO}_2/\text{SiO}_2$ -distributed Bragg reflector (DBR) structure using a pulsed spray coating method. Moreover, pixelated RGB arrays, 2-in. wafer-scale white light emission, and an integrated small footprint white light device were demonstrated. The experimental results showed that the intensity of red, blue, and green (RGB) emissions exhibited considerable enhancement because of the high reflectivity in the UV region by the DBR structure, which subsequently increased the use in the UV optical pumping of RGB QDs. In this experiment, a pulsed spray coating method was crucial in providing uniform RGB layers, and the polydimethylsiloxane (PDMS) film was used as the interface layer between each RGB color to avoid cross-contamination and self-assembly of QDs. Furthermore, the chromaticity coordinates of QLEDs with the DBR structure remained constant under various pumping powers in the large area sample, whereas a larger shift toward high color temperatures was observed in the integrated device. The resulting color gamut of the proposed QLEDs covered an area 1.2 times larger than that of the NTSC standard, which is favorable for the next generation of high-quality display technology.

Conference 8641: Light-Emitting Diodes: Materials, Devices, and Applications for Solid State Lighting XVII

8641-74, Session PWed

Food quality monitoring using LED-induced fluorescence based on multi-wavelength

Chao Feng, Xuan Liu, Zhejiang Univ. (China) and Joint Research Ctr. of Photonics (China); Liang Mei, Zhejiang Univ. (China) and Joint Research Ctr. of Photonics (China) and Lund Univ. (Sweden); Chunsheng Yan, Sailing He, Zhejiang Univ. (China) and Joint Research Ctr. of Photonics (China)

A compact, low-cost and powerful light emitting diode (LED)-induced fluorescence detective system based on multi-wavelength is constructed and described, which is used for monitoring food quality and evaluating food classification, such as the varieties of tea, the freshness of fruit and so on. The LEDs are mounted in a compact and symmetric metal probe (diameter 40mm) with six LEDs in a circle; and in the center, a large core optical fiber is placed to collect the induced fluorescence into a compact Ocean Optics USB 2000 spectrometer, and at the same time the corresponding long pass filter is mounted to eliminate the interference of the excited spectrum. These six LEDs are tilted inward 15° and their wavelengths cover the visible range (400nm-650nm) and extend to UV region (265nm-400nm). By utilizing multiple excited wavelengths, we can obtain much more physical and chemical information from detected samples than single excited wavelength that is used in our previous work, and then the quality of the similar samples can be well separated. What's more, inspite of the complex nature of the samples, with the application of principle components analysis (PCA), it is able to extract the dominant features of the samples with a large signal to noise ratio (SNR), which can be used to classify and characterize the samples into different grades.

8641-75, Session PWed

Experimental observation of enhanced phosphorescence from one-dimensional photonic crystal phosphor structure

Kyungtaek Min, Yun-Kyoung Choi, Heonsu Jeon, Seoul National Univ. (Korea, Republic of)

The importance of phosphor can never be overemphasized, as phosphor-capped white light-emitting diodes (LEDs) find application possibilities almost everywhere. Consequently, a great deal of efforts has been devoted to develop efficient phosphors with tailored optical properties. We have proposed one-dimensional (1D) photonic crystal (PC) as a simple phosphor structure from which phosphorescence can be largely enhanced in comparison with its bulk counterpart. The 1D PC structure considered here is a distributed Bragg reflector consisting of alternately stacked binary materials with different refractive indices. Using the transfer-matrix and plane-wave expansion methods, we investigated various properties of the 1D PC phosphors, such as field distributions of pump photons and phosphorescence enhancement factor as a function of pump photon wavelength. Theoretically, we estimated the phosphorescence enhancement factor as high as 7 when a monochromatic pump wavelength is tuned exactly to a photonic band-edge (PBE). For experimental assessment, we fabricated a 1D PC structure, in which quantum dots (QDs) were embedded as phosphor molecules. Poly(N-vinylcarbazole) ($n \sim 1.683$) and cellulose acetate ($n \sim 1.475$) were spin-coated alternately on a glass substrate, while CdSe/ZnS QDs were embedded only in the Poly(N-vinylcarbazole) layers. The fabricated 1D PC exhibited the central wavelength of photonic band-gap (PBG) at 460 nm (with maximum reflectance of $\sim 90\%$). When QDs in the PC structure were optically pumped by a monochromatic tunable light source, we observed that phosphorescence reached its maximum when the pump photon energy matches with the long wavelength side PBE, which is consistent with the theoretical prediction.

8641-54, Session 12

First-principles studies of loss mechanisms in LEDs (*Invited Paper*)

Chris G. Van de Walle, Daniel Steiauf, Qimin Yan, Univ. of California, Santa Barbara (United States); Emmanouil Kioupakis, Univ. of Michigan (United States)

No Abstract Available.

8641-55, Session 12

InGaN-Delta-InN quantum-well light-emitting diodes with carrier transport effect

Guangyu Liu, Jing Zhang, Chee-Keong Tan, Nelson Tansu, Lehigh Univ. (United States)

III-nitride materials based light-emitting diodes (LEDs) and laser diodes (LDs) have lead to revolutionary development of solid state lighting and display applications. Despite the tremendous progresses achieved in high efficient and high brightness InGaN based LEDs emitting at violet and blue spectrum region, the efficiency of InGaN LEDs suffer from significant reduction as one tries to extend the emission wavelength to green spectral regime and beyond attributed to 1) severe charge separation issue as a result of the strong polarization field in III-nitrides and 2) compromised material quality because of immature growth of high-indium content InGaN layer. The proposed approaches to increase the radiative recombination rate of green InGaN LED include non-polar InGaN/GaN QW and c-plane InGaN QWs with large optical matrix element.

Recently, the use of InGaN-delta-InN QWs structures with emission wavelength in the yellow and red spectral regimes were proposed. In this work, the optical and electrical characteristics of InGaN QW with the insertion of several monolayers of InN as the active region of LEDs were studied using APSYS simulations. The carrier transport effect was taken into consideration in the device simulation. The k.p based quantum mechanical solver was employed for quantum well solution, which is self-consistently coupled with the modified drift-diffusion theory for carrier transport. By taking into account the carrier transport, the device characteristics of the III-Nitride LEDs using InGaN-Delta-InN QW active regions were obtained. The use of delta layer active region resulted in increase in optical matrix element and spontaneous emission rate accompanied by red-shift in the emission wavelength, which in turn leads to improved internal quantum efficiency of the LEDs emitting in the yellow and red spectral regime. The optimization of the delta layer position in the InGaN-Delta-InN QWs also leads to improved spontaneous emission rate by ~ 2.5 times over that of conventional QWs.

8641-57, Session 12

Temperature-dependent efficiency droop in GaInN light-emitting diodes (*Invited Paper*)

Jaehee Cho, David S. Meyaard, Rensselaer Polytechnic Institute (United States); Jong Kyu Kim, Pohang Univ. of Science and Technology (Korea, Republic of); Cheolsoo Sone, Samsung Electro-Mechanics (Korea, Republic of); E. Fred Schubert, Rensselaer Polytechnic Institute (United States)

GaN-based light-emitting diodes (LEDs) have become increasingly prevalent in illumination applications. However, a long standing problem called "efficiency droop" has been impeding the development and future prospects of LEDs as the ultimate illumination source. The efficiency droop can be categorized by using two classifications: current-density droop and temperature droop. The former describes the decrease in radiative efficiency with increasing operating current. The latter is represented by the decrease in radiative efficiency with increasing

Conference 8641: Light-Emitting Diodes: Materials, Devices, and Applications for Solid State Lighting XVII

temperature.

In this study, we will summarize the physical origins and mechanisms that can cause the temperature droop; they include Shockley-Read-Hall (SRH) recombination, carrier leakage (overflow) from the active region, and saturation of the radiative recombination coefficient.

Recombination in LEDs is commonly described by the ABC model. This simplistic model considers A, B, and C to represent the SRH, radiative, and Auger coefficient, respectively. For a quantitative analysis of each loss mechanism, however we utilize the ABC+f(n) model, where f(n) refers to additional non-radiative recombination mechanisms, such as leakage from the active region. We measure temperature-dependent radiative efficiency from GaInN LEDs and extract the contribution of each carrier loss mechanism. This analysis shows that the temperature droop is mainly attributed to two different mechanisms: the increase in SRH recombination and the increase in the f(n) term.

Furthermore, we find that the temperature droop is strongly dependent on current density. That is, regardless of LED chip size, the temperature droop is the same when injecting LEDs having different chip sizes with the same current density. However, as the current density is decreased by increasing the size of LED chips, temperature droop is exacerbated. We believe that at low current densities, SRH recombination is dominant and the non-radiative recombination lifetime decreases with increasing temperature. However, with increasing current density, the effect of SRH recombination becomes smaller in comparison with other high-current loss mechanisms, resulting in alleviation of the temperature droop.

In conclusion, in order to improve the high temperature performance of LEDs two issues must be addressed: Reducing the dislocation density in GaN LEDs to minimize SRH recombination, and reducing the causes of the f(n) term, which we attribute to electron leakage from the active region.

8641-58, Session 12

Reduced efficiency droop of GaInN-based light-emitting diodes by using graded AlGaIn/GaN superlattice electron blocking layers

Jun Hyuk Park, Jong Kyu Kim, Pohang Univ. of Science and Technology (Korea, Republic of)

We present a promising way to reduce efficiency droop as well as to increase internal quantum efficiency (IQE) of GaInN-based high power light-emitting diodes (LEDs). AlGaIn/GaN superlattice (SL) electron-blocking layers (EBLs) have been reported to show higher hole concentration than bulk AlGaIn EBLs¹, reducing the asymmetry of carrier transport that is considered as one of the dominant mechanisms responsible for efficiency droop and low IQE². However, such SL EBLs cause a penalty in operating voltage of LEDs due to the potential barriers at the AlGaIn/GaN hetero-interfaces. In this study, we introduce AlGaIn/GaN SL EBLs with gradually increasing Al composition towards the active region (GSL-EBL) to avoid the operating-voltage penalty while maintaining the high IQE and reduced efficiency droop.

Simulation results predict that LEDs with GSL EBLs show higher hole concentration, lower electron leakage, thus lower efficiency droop, and comparable operating voltage compared to LEDs with SL-EBL and conventional bulk EBL.

In accordance with the simulation, GaInN/GaN multiple quantum well LEDs with 5-period Al_xGa_{1-x}N/GaN GSL EBL (x varies from 0.23 to 0.15 with 0.02 interval) and 9-period Al_xGa_{1-x}N/GaN GSL EBL (x varies from 0.23 to 0.07 with 0.02 interval), grown by metal-organic chemical vapor deposition on c-plane sapphire substrate, show higher external quantum efficiency (EQE), much reduced efficiency droop, and comparable or even lower operating voltage in comparison with conventional LEDs having bulk AlGaIn EBL and AlGaIn/GaN SL EBL.

8641-59, Session 13

Nanowire-based light-emitting diodes (*Invited Paper*)

Lars Samuelson, Lund Univ. (Sweden) and Glo AB (Sweden)

Semiconductor nanowires have emerged as a highly versatile materials system for many kinds of applications, ranging from electronics to photonics and from solar energy to biomedical sensor systems. In this talk I will summarize the status of how III-nitride and III-V nanowires offer a highly promising technology for visible, as well as infrared, LEDs which can be grown either on conventional substrates, like sapphire, or on silicon wafers.

The unique geometry of nanowires has led to the development of a technology for unique control of heterostructures, also for such where planar technology would prevent heterostructure combinations. Our long (> 10 years) experience in this field has created a platform of III-V and III-nitride nanowires with emission wavelengths ranging from mid-IR to deep-UV. A special, and unique, opportunity is offered by the in-situ formation of ultra-thin needles of c-oriented cores which, in a subsequent growth process, serve as ideal and perfectly dislocation-free substrates for growth of device structures on the m-facets, i.e. in directions where piezo-electric effects are negligible.

In a recently started EU-project, called "Nanowires for Solid State Lighting" (NWs4LIGHT), we aim at developing 3 (or 4) color LEDs, emitting the colors Blue, Green and Red (or Blue, Green, Yellow and Red), each driven at ideal LED-conditions and without the use of lossy phosphors. I will describe the status of this effort as well of the general performance status of the technology, with its unique value for display applications as well as for lighting.

8641-60, Session 13

Effects of Ag doping on the ZnO nanometer column array inorganic/organic heterostructure LED

Xiao Li Zhang, Tianjin Univ. (China)

Low-dimensional nanostructural materials have attracted great interest. Electroluminescent devices based on ZnO have been widely reported, but nanostructural ZnO inorganic/organic heterostructure LED is rare. Effects of Ag doped and undoped ZnO nanometer column array inorganic/organic heterostructure are reported. Doped and undoped Ag in ZnO films was fabricated on ITO glass substrate by sol-gel and then annealed in the furnace at 200 °C. 500 nm diameter column arrays were etched on ZnO by lithography. 10% Polyvinyl Alcohol (PVA) was spin-coated with a rotation rate of 2000 rpm (rotations per minute) on ZnO column array to provide a smooth surface for subsequent thin film deposition, and to produce isolation of the individual ZnO column array. Oxygen plasma etching for 15 s was applied to remove PVA coated on the surface of ZnO column array to expose them for junction formation. PEDOT:PSS as hole transport layer was filtered and then spin-coated with 3000 rpm for 30 s. Ag (100 nm) films were deposited subsequently by thermal evaporation in a high vacuum condition of about 3×10⁻⁴ Pa. Surface morphology was observed using field emission scanning electron microscopy (SEM) and atomic force microscopy (AFM). Electroluminescence (EL) of the inorganic/organic heterostructure LED was observed by a Si photodiode attached to a spectrometer. Ag doped and undoped ZnO films were discussed by X-ray diffraction (XRD) and photoluminescence (PL).

8641-62, Session 13

Selective area growth of InGaN/GaN nanostructures for green and white light emission (*Invited Paper*)

Enrique Calleja, Univ. Politécnica de Madrid (Spain)

Although self-assembled NCs are easy to grow with a high crystal quality that favours the study of basic material properties, efficient LEDs based on self-assembled NCs suffer severe limitations derived from a strong dispersion (morphological, electrical) inherent to the self-assembled process.

During the last years, selective area growth (SAG) of GaN [1-3] has been developed to grow NCs with well-controlled position and diameter, resulting in geometrical arrays of NCs with very little morphology dispersion. Successful localized growth on patterned or masked (nanoholes) substrates depends critically on a balance between metal atoms diffusion and desorption, both strongly influenced by the growth temperature, surface roughness, and III/V ratio.

From the nucleation stage, conditions to avoid growth inhibition on r-facets are studied, leading to control the nanostructure topmost geometry (pyramidal or flat). Different approaches will be discussed concerning the structure of the ordered NRs arrays, where the active region (emitting region) can be either InGaN QDisks with different In% or “thick” InGaN portions with constant or graded In% compositions. Efficient red, green and blue (RGB) emission is achieved by optimizing the InGaN active layer in GaN/InGaN NRs arrays.

In this work, ordered GaN and InGaN NCs have been grown by plasma-assisted molecular beam epitaxy (PAMBE) at different temperatures and III/V ratios in order to study the change in morphology and its influence on the optical properties of these nanostructures. By an appropriate selection of optimal growth conditions, InGaN NCs emitting in the red, green, and blue spectral range have been fabricated. Once emission wavelength is controlled, white light emission at room temperature is achieved. Different approaches to achieve either green emission or white emission from InGaN/GaN nanostructures will be shown. The most recent results will also focus on the growth of InGaN/GaN nanostructures and nanoLED arrays on Silicon substrates.

References

- [1] S. Ishizawa, H. Sekiguchi, A. Kikuchi, K. Kishino, *phys. stat sol. (b)* 244, 6, 1815 (2007).
- [2] H. Sekiguchi, K. Kishino, A. Kikuchi, *Appl. Phys. Express* 1, 124002 (2008).
- [3] K. Kishino, H. Sekiguchi, A. Kikuchi, *J. Crystal Growth* 311, 2063 (2009).
- [4] A. Bengochea-Encabo, F. Barbagini, S. Fernandez-Garrido, J. Grandal, J. Ristic, M.A. Sanchez-Garcia, E. Calleja, U. Jahn, E. Luna, and A. Trampert, *J. Crystal Growth* 325, 89 (2011).

8641-64, Session 13

Top-down fabricated III-nitride nanowire LEDs and solar cells

George T. Wang, Qiming Li, Jonathan J. Wierer Jr., Daniel D. Koleske, Jeffrey J. Figiel, Sandia National Labs. (United States)

Although planar heterostructures dominate current optoelectronic architectures, 1D nanowires have distinct and advantageous properties that may enable higher efficiency, longer wavelength, and cheaper devices. We present here a “top-down” approach for fabricating ordered arrays of high quality GaN-based nanowires with controllable height, pitch and diameter. The nanowires are formed via a 2-step etch process from c-plane GaN grown by metal-organic chemical vapor deposition. The process combines a lithographic dry etch followed by a selective, wet chemical etch of the nanowire sidewalls, leading to hexagonally-shaped nanowires with nonpolar m-plane sidewalls. By adjusting the wet etch step, nanowires with diameters from several hundred nanometers

down to tens of nanometers can be fabricated. Importantly, the wet etch step also removes damage caused by the dry-etch, as shown by photoluminescence measurements. Precisely engineered axial nanowire heterostructures can be formed from planar heterostructures, while radial nanowire heterostructures can be formed via regrowth. The fabrication, structure, optical properties, and device performance of the nanowires and InGaN/GaN nanowire LEDs, both axial and radial-type, will be discussed in detail. Using this technique, vertically integrated, radial InGaN/GaN nanowire based solar cells have also been demonstrated and their performance measured for the first time. Sandia National Laboratories is a multi-program laboratory managed and operated by Sandia Corporation, a wholly owned subsidiary of Lockheed Martin Corporation, for the U.S. Department of Energy’s National Nuclear Security Administration under contract DE-AC04-94AL85000.

8641-65, Session 13

Plasmonic-based light-emitting diode: improved emission of solid-state lighting sources

Gabriel Lozano, Said R. K. Rodriguez, FOM Institute for Atomic and Molecular Physics (Netherlands); Marc A. Verschuuren, Philips Research Nederland B.V. (Netherlands); Jaime Gómez-Rivas, FOM Institute for Atomic and Molecular Physics (Netherlands) and Eindhoven Univ of Technology (Netherlands)

Herein, we demonstrate how surface plasmon polariton optics or plasmonics can improve the performance of highly efficient dyes employed in solid-state lighting (SSL). We make use of large area arrays of metallic nanoantennas fabricated by an imprint lithography technology that sustain collective plasmonic resonances. This enables to shape the angular pattern of the emission, beaming most of the light into a very narrow angular range in a defined direction. The enhancement for unpolarized emission reaches a factor of 60 at certain frequency in the forward direction and a factor of 14 when integrated over all the emission range of the dye. This behaviour is the result of the emission of the dye into collective plasmonic resonances known as surface lattice resonances (SLRs) that arise from the coupling of localized surface plasmon polaritons to diffracted orders in the array [1,2]. SLRs have a large spatial extension [3] and can couple very efficiently to free space radiation due to their hybrid photonic-plasmonic character. These features lead to the highly directional emission in defined directions [4]. The possibility to tune the dispersion of SLRs by varying the shape and dimensions of the nanoparticles, the lattice structure and the period of the array, opens the possibility to fully control the emission of different light emitters integrated in plasmonic-based LEDs. In addition, we have investigated the combination of these structures with high power standard blue LED sources, showing that the plasmonic structure acts as an integrated optical component to shape the emission pattern of the dye layer. Plasmonics provides a reliable platform for state-of-the-art lighting applications. These results open a new path for fundamental and applied research in SSL, wherein plasmonic nanostructures can mould the spectral and angular distribution of the emission with unprecedented precision.

References

- [1] G. Vecchi et al., “Shaping the fluorescence emission by lattice resonances in plasmonic crystals of nanoantennas” *Phys. Rev. Lett.* 102, 146807, 2009.
- [2] V. Giannini et al., “Lighting up multipolar surface plasmon polaritons by collective resonances in arrays of nanoantennas” *Phys. Rev. Lett.* 105, 266801, 2010.
- [3] G. Vecchi et al., “Surface modes in plasmonic crystals induced by diffractive coupling of nanoantennas”, *Phys. Rev. B* 80, 201401, 2009.
- [4] S. R. K. Rodriguez et al., “Quantum rod emission coupled to plasmonic lattice resonances: A collective directional source of polarized light”, *Appl. Phys. Lett.* 100, 111103, 2012.

Conference 8642: Emerging Liquid Crystal Technologies VIII

Tuesday - Wednesday 5 -6 February 2013

Part of Proceedings of SPIE Vol. 8642 Emerging Liquid Crystal Technologies VIII

8642-25,

Is blue-phase LCD ready for prime time? (Keynote Presentation)

Shin-Tson Wu, CREOL, The College of Optics and Photonics,
Univ. of Central Florida (United States)

Polymer-stabilized blue-phase liquid crystal (BPLC) has become an increasingly important technology trend for information display and photonic applications. BPLC exhibits several attractive features, such as reasonably wide temperature range, submillisecond gray-to-gray response time, no need for alignment layer, optically isotropic voltage-off state, and large cell gap tolerance when an in-plane switching (IPS) cell is employed. Fast response time not only suppresses image blurs but also enables color sequential display without noticeable color breakup. With sequential RGB LED colors, the spatial color filters can be eliminated so that both optical efficiency and resolution density are tripled. High optical efficiency helps to reduce power consumption while high resolution density is particularly desirable for the future Ultra High Definition Television. However, some bottlenecks such as high operation voltage, hysteresis, residual birefringence, and image sticking, remain to be overcome before widespread application of BPLC can be realized. To reduce operation voltage, both new BPLC materials and new device structures have been investigated. In this paper, we will review the recent advances in BPLC material development and new device structures. Especially, we will focus on new BP LCDs with low operation voltage, and free from hysteresis and residual birefringence. The prime time for BP LCD is near.

8642-1, Session 1

New lyotropic mixtures presenting the biaxial nematic liquid crystalline phase (Invited Paper)

Antonio Figueiredo Neto, Univ. de São Paulo (Brazil); Erol Akpınar, Abant İzzet Baysal Üniv. (Turkey); Dennys Reis, Univ. de São Paulo (Brazil)

After the experimental realization of the biaxial nematic phase (NB) in the lyotropic mixture of potassium laurate (KL)/1-decanol (DeOH)/water by Yu and Saupe in 1980, some research groups reported on new mixtures presenting the NB phase during the last three decades. These studies were useful to the understanding of the physical-chemical characteristics of this remarkable phase, about its chemical stability and the symmetry of the micelles in these mixtures. Some years ago we proposed the intrinsically biaxial micelles (IBM) model, which is based on the different orientational fluctuations of the same type of micelles in the three nematic phases. New lyotropic liquid crystalline quaternary mixtures of potassium laurate (KL), potassium sulphate (K₂SO₄)/alcohol (n-OH)/water, with the alcohols having different number of carbon atoms in the alkyl chain (n), from 1-octanol to 1-hexadecanol, were investigated by optical techniques (optical microscopy and laser conoscopy). The biaxial nematic phase domain is present in a window of values of $n = n_{KL} (+-) 2$, where $n_{KL} = 11$ is the number of carbon atoms in the alkyl chain of KL. The biaxial phase domain got smaller and the uniaxial-to-biaxial phase transition temperatures shifted to the relatively higher temperatures on going from 1-nonanol to 1-tridecanol. Moreover, these new mixtures present high values of the birefringence's comparing to other lyotropic mixtures. This result is expected to be related to the micellar shape anisotropy. Our results are interpreted assuming that alcohol molecules tend to segregate in the micelles in a way that depends on the relative value of n with respect to n_{KL} . The larger the value of n, the more alcohol molecules tend to be located in the curved parts of the micelle, favoring the uniaxial nematic calamitic phase with respect to the biaxial and uniaxial discotic nematic phases.

The Scientific and Technological Research Council of Turkey (Tubitak), the National Institute of Science and Technology on Complex Fluids (INCT-FCx), CNPq and FAPESP from Brazil for supporting this study.

8642-3, Session 1

Engineered complex molecular order in liquid crystals towards unusual optics and responsive mechanics

(Invited Paper)

Carlos Sanchez-Somolinos, Univ. de Zaragoza (Spain); Laurens T. de Haan, Albert P. H. J. Schenning, Technische Univ. Eindhoven (Netherlands); Cees W. M. Bastiaansen, Technische Univ. Eindhoven (Netherlands) and Queen Mary Univ. of London (United Kingdom); Dirk J. Broer, Technische Univ. Eindhoven (Netherlands)

Defects in liquid crystals (LC) have been studied over decades, e.g. to disclose information and knowledge on the structure of LC phases.[1] Despite the rich physics behind, defects have generally been avoided due to the deleterious effects in the optical characteristics of devices such as for example liquid crystal displays (LCDs). Because of this, defect-free systems with good transparency have been usually pursued. More recently, LC defects have been identified as a tool to implement new physical functions. As an example, a LC cell having an azimuthally distributed director field has been used to transform circularly polarized light into light with an helical mode carrying angular orbital momentum.[2] On the other hand, Smalyukh and coworkers have demonstrated the use of such helical beams to induce LC defects in a controlled way. [3]

Besides optical applications, nematic network films with disclination type director profiles have also been predicted to deform into shapes such as cones or anticones upon an appropriate external stimulus.[4] We have implemented a methodology to create different disclination patterns by combining the use of linear photopolymerizable polymers (LPPs) [5] and reactive mesogens. The preparation of these systems and their potential applications in the field of mechanical actuators and optical films will be described in this communication.

Acknowledgments:

We thank Mark Warner and Carl Modes from University of Cambridge (United Kingdom) for helpful discussions. We thank the Dutch NWO (VICI grant), the Spanish MINECO project MAT2011-27978-C02-02, CSIC project i-LINK0394, Gobierno de Aragón, and FEDER funding (EU) for their financial support.

References:

- [1] A. Saupe, *Mol. Cryst. Liq. Cryst.* 21, 211 (1973).
- [2] L. Marrucci, C. Manzo, and D. Paparo, *Phys. Rev. Lett.* 96, 163905 (2006)
- [3] I.I. Smalyukh, Y. Lansac, N.A. Clark & R.P. Trivedi, *Nature Materials* 9, 139-145 (2010).
- [4] C.D. Modes, K. Bhattacharya, M. Warner, *Phys. Rev. E* 81, 060701 (R) (2010).
- [5] M. Schadt, K. Schmitt, V. Kozinkov, V. Chigrinov, *Jpn. J. Appl. Phys.*, 31, 2155 (1992)

8642-4, Session 2

Advanced finite-element methods for design and analysis of nano-optical structures (Invited Paper)

Sven Burger, Konrad-Zuse-Zentrum für Informationstechnik Berlin (Germany) and JCMwave (Germany); Lin Zschiedrich, Jan Pomplun, JCMwave GmbH (Germany); Mark Blome, Konrad-Zuse-Zentrum für Informationstechnik Berlin (Germany); Frank Schmidt, Konrad-Zuse-Zentrum für Informationstechnik Berlin

Conference 8642: Emerging Liquid Crystal Technologies VIII

(Germany) and JCMwave (Germany)

Optical elements with nanometer dimensions are of great importance in many technological fields. Examples are semiconductor device manufacturing (e.g., optical nanolithography), new light sources (e.g., VCSELs), diffractive optical elements (DOEs), photovoltaics (e.g., thin-film solar cells), sensing (e.g., plasmonic bio-sensors), optical communication systems (e.g., integrated optics).

The functionalities of such elements critically depend on geometrical and material properties of the experimental arrangement. For understanding and designing properties of materials and devices numerical simulations of Maxwell's equations are very helpful. Rigorous and accurate simulations of such setups are challenging because (i) structures and field distributions are defined on multi-scale geometries (e.g., nanometer layers extending over microns), (ii) material properties (e.g., permittivity of metal) lead to high field enhancements or singularities at edges and corners of the objects, (iii) typical regions of interest are 3D and large in scales of cubic wavelengths, (iv) structures often are embedded into inhomogeneous exterior domains (e.g., plasmonic particles embedded into the material stack of a solar cell).

For approaching such simulation tasks we develop and use finite-element methods (FEM solver JCMsuite [1]). We discuss simulations of several nanooptical devices, ranging from fundamental research topics to industrial applications.

[1] J. Pomplun, S. Burger, L. Zschiedrich, F. Schmidt. *phys. stat. sol. (b)* 244, 3419 (2007).

8642-5, Session 2

High frequency performance extending to millimeter-waves in inverted-microstrip-line-type LC phase shifter (*Invited Paper*)

Toshiaki Nose, Yusuke Ito, Akita Prefectural Univ. (Japan); Liang-Chy Chien, Otilia C. Catanescu, Andrii Golvin, Kent State Univ. (United States); Yoji Isota, Takayuki Sasamori, Ryouta Ito, Michinori Honma, Akita Prefectural Univ. (Japan)

Various liquid crystal (LC) phase shifters operating for super high frequency electromagnetic waves have been investigated so far by using planar type excellent waveguide such as microstrip line (MSL) and coplanar waveguide (CPW). First invented planar type LC phase shifters were constructed by using MSL which has been most developed excellent planar waveguide in the super high frequency electromagnetic waves. CPW type LC phase shifters are successively gathering attentions, because all of the signal and ground electrodes are on the same surface and it leads to easiness in integration to construct various integrated functional devices. However, there is an essential drawback of degradation of phase shifting magnitude because the propagating electromagnetic waves feel the permittivity both of substrate and LC materials, and then the modulation effect of LC materials is reduced to be less than a half.

In this paper, novel MSL type LC phase shifter is investigated to attain excellent phase shifting performance with maintaining the ease in integration similar to the CPW type phase shifter. Various LC materials are also tested for more improvement of the high frequency operation extending to the millimeter-wave region.

8642-6, Session 2

Submillisecond-response IR spatial light modulators with polymer network liquid crystal

Jie Sun, Yuan Chen, Univ. of Central Florida (United States); Shin-Tson Wu, CREOL, The College of Optics and Photonics, Univ. of Central Florida (United States)

Polymer network liquid crystal (PNLC) is attractive for many photonic applications because of its fast response time and large phase modulation. However, the voltage-on state light scattering caused by multi-domains of LC molecules hinders its applications in the visible and near infrared regions. To reduce domain sizes and eliminate scattering for $\lambda = 1.06 \mu\text{m}$ and $1.55 \mu\text{m}$, we studied the effect of LC viscosity on domain sizes. PNLCs based on five different LC hosts were prepared. The LC host was first mixed with 6% reactive mesogen and then filled into a $12\text{-}\mu\text{m}$ cell with homogeneous alignment. After UV curing, we measured the on-state transmission spectra of these five PNLCs. By fitting the transmission spectra with Rayleigh-Gans-Debye model, we can estimate the average domain sizes. We found that the domain sizes of PNLC are inversely proportional to the rotational viscosity of the LC host. This finding can be explained by the Stokes-Einstein equation. As a result, PNLC with a slower diffusion rate would cause smaller domain sizes, which in turn lead to faster response time. To achieve a slower diffusion rate, we cured the PNLC samples at a lower temperature. By selecting a high viscosity and high η LC host, we demonstrate a scattering-free ($<3\%$) 2π phase modulator at $\lambda = 1.06 \mu\text{m}$ and $\lambda = 1.55 \mu\text{m}$. Temperature affects the PNLC performance significantly. As the operation temperature increases from 25°C to 70°C , the response time drops from $220 \mu\text{s}$ to $30 \mu\text{s}$. 2π operating voltage for $\lambda = 1.06 \mu\text{m}$ slightly increases from 70V to 90V . Meanwhile, hysteresis decreases from 7.7% to 2% . If reflective mode is employed, operating voltage can be reduced. Our fast-response, scattering-free PNLC has potential applications in spatial light modulators and adaptive lenses.

8642-7, Session 2

Enhanced phase manipulation for adaptive optics applications with a 6-Pi Liquid Crystal on Silicon (LCoS) device

Enrique-Josua Fernández, Lab. de Óptica Univ. de Murcia (Spain); Emmanuel Chirre, Pedro M. Prieto, Pablo Artal, Univ. de Murcia (Spain)

Phase modulators based on liquid crystal technologies are currently employed in many fields because of their advantages. Liquid Crystal on Silicon (LCoS) devices have notably improved the performance of this technology. It has reduced the effect of some of the drawbacks, as response speed or diffraction losses. However, those are still present to a certain extent, which can be important for applications involving large aberrations. We present the results obtained with a new type of LCoS device capable for up to 6Pi modulation before performing phase wrapping (Holoeye Photonics AG, Germany), as compared with a regular 2Pi -LCoS system. A dedicated experimental setup was built incorporating the two modulators, so that simultaneous operation and comparison of both could be performed. The apparatus included a Hartmann-Shack wavefront sensor and an optical relay for the recording of experimentally generated point spread functions (PSFs). The system was illuminated with quasi-monochromatic light from a laser source as well as using white light from a thermal source to characterize chromatic effects. The fidelity was found similar in the two devices, while diffraction losses were less in the 6Pi as accounted by the effects in the recorded PSFs. In addition, the range of generation of aberrations was larger in the latter. Response time from changing a given phase to another was found slightly larger in the 6Pi device. Generation of PSFs showed a superior performance of the 6Pi -LCoS. The use of 6Pi -LCoS technology on adaptive optics is promising, surpassing some of the drawbacks of previous state-of-the-art devices.

8642-8, Session 3

Liquid crystal lasers: recent advances (*Invited Paper*)

Juergen Schmidtke, Lu Lu, Heinz S. Kitzerow, Univ. Paderborn (Germany); Eugene M. Terentjev, Univ. of Cambridge (United Kingdom)

**Conference 8642:
Emerging Liquid Crystal Technologies VIII**

During the past decade, photonic band edge lasers based on cholesteric liquid crystals have attracted considerable interest as self-assembling, coherent, tunable light sources. We report on recent progress towards practical applications: (i) PDMS-enclosed LC lasers for lab-on-chip applications; (ii) electrical fine tuning; and (iii) performance improvement by electric fields.

We demonstrate the operation of LC laser confined between optically clear and elastic polydimethylsiloxane (PDMS) rubber substrates. The formation of a planar helical texture in the cholesteric film was supported by microstructuring of the PDMS layer surface. With PDMS being the standard material for the fabrication of microfluidic devices, this opens a simple and flexible route for the integration of microscopic laser sources for lab-on-chip applications like spectroscopy or photochemistry.

We report on high-precision, continuous, electrical tuning of a LC laser. A micro-patterned array of electrodes creates an electric field perpendicular to the cholesteric helix, which distorts the chiral order of the liquid crystal, thus shifting the resonant band edge modes. This configuration allows for smooth, low-voltage tuning of the laser emission in a wavelength range of about 4 nm, using low voltages.

The lasing threshold and slope efficiency of a LC laser can be improved by application of an electric field: Using a dye-doped CLC with negative dielectric anisotropy, emission characteristics improves with increasing ac electric field along the cholesteric helix. Possible reasons are a partial suppression of thermally driven director fluctuations, as well as a stabilization of the planar cholesteric texture against disturbances by the optical pumping process.

8642-9, Session 3

Liquid crystals under high-power nanosecond laser irradiation (*Invited Paper*)

Svetlana G. Lukishova, Univ. of Rochester (United States)

High-damage-threshold liquid-crystal optical elements are used for high-power laser applications as mirrors, waveplates and optical power limiters. Several nonlinear optical effects under high-power, nanosecond laser irradiation of liquid crystals will be outlined: (1) athermal helical pitch dilation and unwinding of cholesteric mirrors by the field of a light wave (in free space and in a laser resonator) [1-4]; (2) dependence of nonlinear refraction of liquid crystal on the laser beam diameter in presence of two-photon absorption [1,4]; (3) cumulative effects in nonlinear absorption and refraction at low repetition rate (5-10 Hz) [1,4]; (4) feedback-free kaleidoscope of patterns in dye-doped liquid crystals (hexagons/stripes) [1,5].

REFERENCES

- [1] S.G. Lukishova, "Liquid crystals under two extremes: (1) high-power laser irradiation, and (2) single-photon level", *Mol. Cryst. Liq. Cryst.*, Vol. 559, 127-157 (2012).
 [2] S.G. Lukishova et al., "Nonlinear "brightening" of a film of nonabsorbing chiral nematic under selective reflection conditions", *JETP Lett.*, Vol. 63, 423-428 (1996). [3] S.G. Lukishova et al., "Behavior of nonlinear liquid-crystal mirrors, made of nonabsorbing cholesteric, in the cavity of an Nd:YAG laser operating in the cw regime and at a high pulse repetition frequency", *Quantum Electronics*, Vol. 26, 796-798 (1996).
 [4] S.G. Lukishova, "Nonlinear optical response of cyanobiphenyl liquid crystals to high-power, nanosecond laser radiation", *J. Nonlinear Opt. Phys. & Mater.*, Vol. 9, 365-411(2000). [5] S.G. Lukishova et al., "Far-field patterns from dye-doped planar-aligned nematic liquid crystals under nanosecond laser irradiation", *Mol. Cryst. Liq. Cryst.*, Vol. 453, 393-401 (2006).

8642-10, Session 3

Micro-second modulation of refractive index and reflection band of cholesteric liquid crystal with nano-pore filled with liquid crystal (*Invited Paper*)

Masanori Ozaki, Yo Inoue, Osaka Univ. (Japan); Hiroyuki Yoshida, Osaka Univ. (Japan) and JST-PRESTO (Japan)

We report a high-speed electrooptic response of cholesteric liquid crystal possessing a rise time of 26 micro seconds and a decay time of 6 micro seconds with holding the clear reflection band. The fast response was demonstrated in a CLC containing nano-sized spaces less than 20 nm inside a sponge-like anisotropic polymer matrix with a helical order. In this composite system, the selective reflection can be controlled by modulating the refractive index with keeping the helical structure.

8642-11, Session 3

Electrically-tunable liquid crystal lenses and applications (*Invited Paper*)

Yi-Hsin Lin, Hung-Shan Chen, Ming-Syuan Chen, National Chiao Tung Univ. (Taiwan)

In this paper, the electrically-tunable liquid crystal (LC) lenses and the applications are reviewed. We introduce the mechanism and design rules first. The different kinds of LC lenses are also introduced. The challenges of LC lenses are discussed and the possible solutions are proposed. Several applications based on LC lenses and operating principles are also introduced, such as cell phones, pico projectors, optical zoom systems, microscopy, solar systems and eyeglasses.

8642-12, Session 3

Multi-domain vertical alignment of nematic liquid crystals for reduced off-axis gamma shift (*Invited Paper*)

Tae-Hoon Yoon, Byung Wok Park, Ki-Han Kim, Pusan National Univ. (Korea, Republic of); Hoon Kim, Ki-Chul Shin, Hee Seop Kim, Samsung Display Co., Ltd. (Korea, Republic of)

Several liquid crystal (LC) modes, such as twisted nematic, vertical alignment (VA), and in-plane switching, have been in competition with each other in the LC display market. Among them, the VA mode has been widely used because of the high contrast ratio. Since the LC molecules are aligned perpendicular to the substrate in the initial state, an excellent dark state can be obtained at normal viewing direction. However, effective phase retardation of LC layer at oblique viewing direction differs greatly from that at normal viewing direction. Thus, gamma distortion phenomenon occurs at oblique view direction. To reduce the gamma shift in the VA mode at oblique viewing direction, multi-domain VA modes were proposed. Gamma shifts of these modes are smaller than that of the single domain VA mode, but the problems still remain. Recently, several technologies for 8-domain alignment were proposed to decrease gamma shift at off-axis. However, additional driving circuits are required to realize the 8-domain structure.

In this paper we report technologies for the multi-domain VA mode with no additional driving circuits. By using the proposed technologies, we can obtain the dual threshold voltage in each sub-pixel to realize the multi-domain VA mode with no decrease of contrast ratio.

8642-13, Session 5

Resonant transfer of light from a planar waveguide into a tunable nematic liquid crystal microcavity (*Invited Paper*)

Igor Muševic, V.S.R. Jampani, Matjaz Humar, Jožef Stefan Institute (Slovenia)

We have recently demonstrated that a microdroplet of a nematic liquid crystal in a radial configuration is a perfect electrically tunable liquid crystal microcavity. Here we demonstrate resonant transfer of light from a planar waveguide into a nematic microcavity, embedded in a carrier fluid. In our experiments, microdroplets of a nematic liquid crystal 4-Cyano-4'-pentylbiphenyl (5CB) were dispersed in a 10mM sodium dodecyl sulfate (SDS) in water that promoted perpendicular surface anchoring of 5CB and radial droplet configuration. Planar waveguides were produced by spinning a high refractive index polymer (1.68 at 632nm) onto a soda lime glass. We used the supercontinuum source to generate a broad spectrum of light from 500nm to 2000nm and launched a band of the spectrum into the thin film waveguide using a prism film coupler. The resonant tunneling of light from the waveguide into the LC microcavities was observed, because the spectrum of light radiated from the microdroplets clearly showed whispering gallery modes (WGM). Furthermore, the tuning of the resonant transfer was achieved by temperature change.

8642-14, Session 5

Bichromatic optical switch of refractive light from a photonic crystal based on HPDLC doped with azo component (*Invited Paper*)

Andy Y. Fuh, Ming-Shian Li, Shing-Trong Wu, National Cheng Kung Univ. (Taiwan)

This study demonstrates all optical switches between four-levels of the refractive light from a body-centered tetragonal photonic crystal based on holographic polymer-dispersed liquid crystals that are fabricated using two-beam interference with multiple exposures. The switching mechanism is due to the effective index modulation of the PC that contain a liquid crystal/azo-dye mixture. The refractive beam can be controlled by two pumping laser beams. The switching time between the blue pumping laser and the combination of blue and green pumping lasers pumped level is fast. The study also discusses the switching times between the various refractive-intensity levels.

8642-15, Session 5

Fabrication of liquid crystal gratings based on photoalignment technology (*Invited Paper*)

Yan-Qing Lu, Wei Hu, Nanjing Univ. (China); Abhishek Srivastava, Vladimir G. Chigrinov, Hong Kong Univ. of Science and Technology (Hong Kong, China)

A series of liquid crystal (LC) gratings are fabricated mainly based on photoalignment, which include (1) Nematic LC grating with alternating 90° twisted nematic (TN) regions and homogeneous alignment (PA). Both 1D and 2D diffraction gratings are demonstrated by periodic photoalignment of sulfonic azo-dye (SD1) films with a linearly polarized light beam. (2) A polarization independent of 1D/2D LC gratings with alternate orthogonal homogeneously aligned regions. No polarizer is employed. (3) A polarizer-free submillisecond response grating employing dual-frequency LC (DFLC) together with patterned hybrid aligned nematic (HAN) structures. To obtain instantly controllable LC microstructures rather than simple gratings, a digital micro-mirror device (DMD) based a micro-lithography system is developed. It may generate arbitrary micro-images on photoalignment layers. Besides normal phase gratings, more complex 2D patterns including quasicrystal structure are demonstrated, which give us

more freedom to develop microstructured LC based photonic devices.

8642-16, Session 5

Theta-2theta diffractometry of anisotropic holographic gratings composed of liquid crystal and polymer phases

Hiroshi Kakiuchida, Kazuki Yoshimura, Masato Tazawa, National Institute of Advanced Industrial Science and Technology (Japan); Akifumi Ogiwara, Kobe-C.C.T. (Japan)

Holographic polymer dispersed liquid crystals (HPDLCs) have great potentialities for electrically, thermally and optically responsive diffractive devices. The present paper proposes an easy and reliable structural analysis method, and the microstructural origins of high-efficient and linearly-polarized optical diffraction from HPDLCs were quantitatively analyzed by establishing a widely useful structural model. The HPDLCs basically consist of spatially periodical distribution of submicron-scale liquid crystal (LC) droplets in polymer matrix, which can be organized by photoinduced polymerization and subsequent phase separation into polymer- and LC-phases during holographic exposure. Furthermore, LC molecules can be uniaxially oriented due to the periodic phase separation. In the present study, four independent Bragg diffraction spectra, which were measured in two orthogonal polarization states at temperatures below and above the nematic-isotropic phase transition point, were analyzed all at once by employing anisotropic diffraction theory under the restraint of the structural model that was established based on a variety of practical HPDLC structures. The anisotropic refractive indices of the spatially periodic LC- and polymer-rich phases were separately determined using Cauchy dispersion formula as a function of optical wavelength in visible to near-infrared ranges. The microscopic structure, including the degree of phase separation into LC and polymer components, morphological anisotropy, LC orientational order, and thermo-optic property, was quantitatively analyzed based on a simple but widely useful structural model. The present diffractometric analysis was examined in validity by comparisons of the analyzed structures with the microscopic observations by scanning electron microscope and polarizing optical microscope. The present method is expected to be an analysis tool widely applicable for various HPDLC structures.

8642-17, Session 5

Beam shaping to improve holography techniques based on spatial light modulators

Alexander V. Laskin, Vadim Laskin, AdlOptica Optical Systems GmbH (Germany)

Modern holographic techniques based on Spatial Light Modulators get serious benefits from providing uniform intensity distribution of a laser beam: more predictable and reliable operation, higher efficiency of laser energy usage, more simple mathematical description of diffraction transformations, etc. Conversion of Gaussian intensity distribution of TEM00 lasers to flat-top one is successfully realized with refractive field mapping beam shapers like piShaper, which operational principle presumes transformation with high flatness of output wavefront, conserving of beam consistency, providing collimated output beam of low divergence, high transmittance, extended depth of field, negligible residual wave aberration, and achromatic design provides capability to work with several laser sources with different wavelengths simultaneously. Applying of these beam shapers brings serious benefits to the Spatial Light Modulator based techniques like Computer Generated Holography or Dot-Matrix mastering of security holograms.

This paper will describe some design basics of refractive beam shapers of the field mapping type and optical layouts of their applying in holographic systems. Examples of real implementations and experimental results will be presented as well.

**Conference 8642:
Emerging Liquid Crystal Technologies VIII**

8642-18, Session 6

**Liquid crystal plasmonic metamaterials
(Invited Paper)**

Toralf Scharf, Ecole Polytechnique Fédérale de Lausanne (Switzerland)

Metamaterials today are often realized as complex structured metasurfaces. Their functionality is based on combination of plasmonic resonances in metallic nanostructures and interferences. Novel concepts of bottom up fabrication using liquid crystal self-organization promise the realization of bulk metamaterials. Only very few view such composite self organizing materials based on liquid crystals are demonstrated up to now.

In detail we use rod like nematic liquid crystal molecules that are grafted onto gold nanoparticles. Structural analysis is done by X-ray scattering experiments that revealed an arrangement of the nanoparticles in chains similar to the ones found in columnar phases. To aspect are of particular importance: The sufficient size of nanoparticles to achieve efficient plasmon resonance effects and the ligands anchored on the particles that control the self-assembling properties. The combined effect of the ligands birefringence and the anisotropic arrangement of the plasmonic nanoparticles lead to a strong polarization dependence of the metamaterial's optical properties. These results demonstrate the ability to fabricate a self ordered and tunable metamaterial by chemical engineering of the nanoparticles with liquid crystalline mesogenic ligands.

In our contribution, we show experimental evidence of coupling resonances of metallic nanoparticles in an entire self-organizing material. We give details on the pathway to design such structures and to adjust their optical and mechanical properties. Theoretically insight of the electromagnetic properties is provided and the approaches to effective material design will be given.

8642-19, Session 6

**Terahertz waves and liquid crystals:
prospects and challenges (Invited Paper)**

Nico Vieweg, TOPTICA Photonics AG (Germany)

The last decades have seen a growing attention among scientists on the terahertz properties of liquid crystals. On the one hand, the dielectric properties of liquid crystals at terahertz frequencies are relatively unexplored and the observed low energy phenomena's are not yet well understood. On the other hand, terahertz technology requires switchable devices, in which liquid crystals potentially could serve as a base material. With this contribution, an overview is given about the research done so far on the properties and applications of liquid crystals in the terahertz frequency range. The way from first liquid crystal terahertz experiments to comprehensive systematic studies of their structure-terahertz property relations is outlined. Furthermore, the evolution from basic concepts to first liquid crystal terahertz devices are emphasized and prospects and future challenges will be discussed. Due to the development of compact and more cost efficient components, terahertz spectrometers matured from room filling laboratory equipment to compact reliable scientific tools. Modern terahertz instruments will thus be highlighted in this report.

Liquid crystal terahertz devices could help terahertz technology to continue this trend and to pave the way to a wider range of application.

8642-20, Session 6

Optically switchable second harmonic generation in a liquid crystal thin film within femtoliter volume

Kuan-chieh Chen, Guan-Yu Zhuo, National Taiwan Univ. (Taiwan); Shi-Wei Chu, National Taiwan Univ. (Taiwan) and National Taiwan

Univ. (Taiwan)

Nematic liquid crystal (NLC) is one of most useful soft matters. Because the molecular orientation can be controlled electrically, NLC is widely applied to display devices. It is known that NLC exhibits strong second-harmonic-generation (SHG) due to its orderly arranged molecules. The strength of SHG is strongly dependent on the angle between the incident beam polarization and the NLC molecular orientation, so the SHG in NLC can be switched on/off by rotating the NLC director. However, it is very difficult to control the orientation of NLC director electrically within a micrometer spatial domain. In this report, we demonstrated the orientation control of NLC with sub-micrometer spatial resolution based on optical Freedericksz transition (OFT) combined with a high-numerical-aperture objective. We have used azo-dye doped NLC to reduce the intensity threshold of OFT to the order of W/cm² with 473-nm excitation. Interestingly, we found that the threshold of OFT increases with tighter focuses. This effect can be explained by the intermolecular forces from the NLC molecules around the focal spot.

By incorporating both the blue laser and a femtosecond near-infrared laser into an optical scanning microscope, we have successfully demonstrated switch of SHG inside a NLC thin film. Note that SHG is confined within femtoliter focal volume due to its intrinsic nonlinearity. That is, we have achieved an ultra-small switch of nonlinear optical signal in NLC. This work will find applications in optical communication as well as imaging fields.

8642-22, Session 7

Functional organic materials based on polymerized liquid crystal monomers (Invited Paper)

Dick J. Broer, Cees W. M. Bastiaansen, Michael G. Debijs, Albert P. H. J. Schenning, Technische Univ. Eindhoven (Netherlands)

Functional organic materials are of great interest for variety of applications. For precise functional properties, well-defined hierarchically ordered supramolecular materials are crucial. The self-assembly of liquid crystals has proven to be an extremely useful tool in the development well-defined nanostructured materials.[1] During my lecture, I will show the example of photopolymerizable hydrogen bonding mesogens to demonstrate that a wide variety of functional materials can be made from a relative simple set of building blocks. Upon mixing these compounds with other reactive mesogens, nematic, chiral nematic, and smectic liquid crystalline materials can be formed that can be applied as actuators [2], sensors [3], and nanoporous membranes [4], respectively.

References:

- [1] D.J. Broer, C.W.M. Bastiaansen, M.G. Debijs, A.P.H.J. Schenning, *Angew. Chem. Int. Ed.*, 51 (2012) 7102–7109.
- [2] K.D. Harris, C.W.M. Bastiaansen, J. Lub, D.J. Broer, *Nano Lett.* 5 (2005).1857.
- [3] N. Herzer, H. Guneyesu, D.J.D. Davies, D. Yildirim, A.R. Vaccaro, D.J. Broer, C.W.M. Bastiaansen A.P.H.J. Schenning, *J. Am. Chem. Soc.* 134 (2012) 7608.
- [4] A.P.H.J. Schenning, Y. Gomez-Gonzalez, I. Shimanova, D.J. Broer, *Liq. Cryst.* 38 (2011) 1627; C. Luengo Gonzalez, C.W.M. Bastiaansen, J. Lub, J. Loos, K. Lu, H.J. Wondergem, D.J. Broer, *Adv. Mater.* 20 (2008).1246.

8642-23, Session 7

Photoalignment studies on azo containing thiophene based acrylates

Gurumurthy Hegde, Univ. Malaysia Pahang (Malaysia); Rasha Atalla, Univ. of Gothenburg (Sweden); David Chambers-Asman, Nottingham Trent Univ. (United Kingdom); Avtar Matharu, The Univ. of York (United Kingdom); Mashitah Yusoff, Univ. Malaysia

Conference 8642: Emerging Liquid Crystal Technologies VIII

Pahang (Malaysia); Lachezar Komitov, Univ. of Gothenburg (Sweden)

The advantages of LC photoalignment technology in comparison with common “rubbing” alignment methods tend to the continuation of the research in this field. Nowadays azo-dye alignment materials can be already used in LCD manufacturing, e.g. for the alignment of monomers in LCP films for new generations of phase retarders, polarizers and color filters. Roll-to-roll process is possible due to the high sensitivity of azo-dye films. Tuning the alignment properties like (anchoring energy, ability of align LC materials, image sticking, light sensitivity, photo stability, reorientation speed etc.) is possible by preparing the suitable materials with the azo-group.

On the other hand, due to their ability to undergo certain changes in their structure under light illumination, thiophenes have attracted a lot of attention. Here we report our findings on a rather unusual and very interesting series of liquid crystalline materials based on a molecular core comprising an azobenzene linkage (-N=N-), lateral fluoro-substituents and a thiophene ring (see figure). The performed study showed that inclusion of fluoro substituents at certain positions enhances the photoalignment properties

8642-24, Session 7

Liquid crystal biosensor for detecting cholic acid

Sihui He, CREOL, The College of Optics and Photonics, Univ. of Central Florida (United States); Wenlang Liang, Jiyu Fang, Univ. of Central Florida (United States); Shin-Tson Wu, CREOL, The College of Optics and Photonics, Univ. of Central Florida (United States)

The concentration level of bile acids is a useful indicator for the diagnosis of liver diseases since individual suffering from liver diseases often has a sharp increase in bile acid concentration. The prevalent measurement method in detecting bile acids is the chromatography coupled with mass spectrometry. Here we present a simple biosensor platform based on LC thin films for the detection of cholic acid. This platform has the advantage of low cost, label-free, solution phase detection, and it only needs an optical microscope for the detection. In the experiment, a thin LC film was hosted by a copper grid supported with a polyimide-coated glass substrate, and then immersed into aqueous solution. The adsorption of sodium dodecyl sulfate (SDS) at the LC/water interface generated homeotropic anchoring. The SDS at the interface can be removed by cholic acid, triggering a transition from homeotropic to homogeneous anchoring. The anchoring transition of the LC thin film allows 8 μ M cholic acid to be detected within 10 min. This result could be further optimized by tuning the LC film thickness, the concentration of SDS and the pH value of the solution.

8642-26, Session 8

Dynamic optical architectures using cholesteric liquid crystals (*Invited Paper*)

Timothy J. Bunning, Air Force Research Lab. (United States); Nelson V. Tabiryan, Svetlana V. Serak, Uladzimir Hrozhyk, BEAM Engineering for Advanced Measurements Co. (United States); Jonathan P. Vernon, Vincent Tondiglia, Lalgudi V. Natarajan, Timothy J. White, Air Force Research Lab. (United States)

We present recent work on novel electro-optical and photo-optical effects in liquid crystal based constructs. These dynamic changes are driven by light induced changes to azo-benzene molecules which have been incorporated either into the LC backbone, as a dopant to a LC fluid, or within the surface boundary layer. Several constructs are presented including a polarizer-free optical switch based on cycloidal diffractive

waveplates, reflective cholesteric cells which can be toggled between a reflective and a scattering state, and reflective systems whose interaction with incident irradiation is autonomous. We also present recent work on novel electro-optical effects of negative dielectric, polymer stabilized cholesteric liquid crystals. Weakly crosslinked systems formed using non-chiral monomers exhibit large scale symmetric broadening of the selective reflection notch at low DC field strengths. Systems which possess more polymer content and formed using chiral monomers exhibit large scale red tuning of the reflection notch. We believe the two observations are related and involve subtle movement of the polymer networks under the applied field.

8642-27, Session 8

Optical properties of field sequential color NTN-LCDS doped with nanoparticles

Shunsuke Kobayashi, Tokyo Univ. of Science (Japan)

We have studied optical output of FSC-LCDs with nanoparticles that exhibit homogeneous and wide viewing angle. We make a suggestion of an index: Luminance / (W/m²) and it is shown that our FSC-NTN-LCD show a high value of figure of 4 in this index.

8642-36, Session 8

Liquid crystals for microwave applications (*Invited Paper*)

Atsutaka Manabe, Merck KGaA (Germany)

Recently liquid crystals (LCs) have attracted a lot of attention as electrically steerable dielectric media for GHz- and THz- applications.

Typical examples are their use in phase shifters, phased array- and reflectarray antennas. In the pioneering study, Dolfi used K15 as liquid crystal medium in his phase shifter. It shows reasonable anisotropy of permittivity from 2GHz to 15GHz, which was sufficient to demonstrate the potential of the device. In order to make the device more attractive, efforts have been made to increase the anisotropy of permittivity in GHz frequencies. So-called “High Dn LC” mixtures have been selected from the conventional portfolio and tried for various types of microwave devices.

These approaches have been quite successful and LC-based phase shifter become competitive to semiconductor equivalents at high operating frequency range of 30GHz and beyond. However, it was found that the dielectric loss is still too high which limit the competitiveness, especially for low microwave frequency. The purpose of this study is therefore to design LC mixtures optimized for microwave application, in concrete, to realize low dielectric loss while maintaining high tunable range. More than 400 LC compounds have been characterized in terms of complex permittivity at 19GHz, and based on the single screening result, new class of mixtures have been successfully designed for microwave application. The best LC mixture shows De of 1.0 and tand of 0.0043 at 19GHz. This will enable electrically steerable, extremely thin, flat antenna design with low production cost.

8642-30, Session PWed

Photo-controlled electrical conductivity in CNT-doped liquid crystal composites

Vijay Kumar Muthu, Ctr. for Soft Matter Research (India); Lakshmi Madhuri, Krishna Prasad, Ctr. for Liquid Crystal Research (India)

Employing optical fields to control the electrical conductivity of materials, especially soft matter, such as liquid crystals (LC) is an attractive proposition. From the LC point of view, photo-isomerization, and consequent change in shape of azobenzene molecules is a handy tool to realize such a feature. In order to achieve high conductivities,

**Conference 8642:
Emerging Liquid Crystal Technologies VIII**

in otherwise insulating materials, we have taken the path of creating composites of LC with carbon nanotubes (CNT). Long term stabilization of CNT in the fluid environment of LC is not trivial and therefore techniques such as slow mixing processes, surface modifications of CNT are to be employed. In this work we have added the photo-isomerizable property to the composite in two different ways: a physical mixing process wherein the photoactive part is present in the system without any chemical bonding, and a second method in which the photoactive part is covalently attached to CNT. The presentation compares the achievable control of the magnitude of conductivity, both in its magnitude and anisotropy by thermal as well as photo-processes. Influence of the actual structure of the LC phase, as well as the chemical nature of the photoactive molecule will also be discussed. Possible means of achieving long term stabilization of the conductivity are suggested.

8642-31, Session PWed

Reverse-mode polymer stabilized cholesteric texture by dual frequency liquid crystal with multi-stable states

Cheng-Che Wu, Che-Syuan Wang, National Taiwan Univ. (Taiwan); Tien-Lung Chiu, Yuan Ze Univ. (Taiwan); Jiunn-Yih Lee, Jiun-Haw Lee, National Taiwan Univ. (Taiwan)

In our device, low transmission is achieved by light scattering with focal conic (FC) state of cholesteric liquid crystal (ChLC). High transmission can be achieved by planar (P) state of long-pitch ChLC. By adding a few amount monomer to construct the fiber-like anisotropic polymer network parallel to the substrate during UV polymerization in the long-pitch ChLC molecules host, it is called the reverse-mode polymer stabilized cholesteric texture (RPST) which is normally at the planar state and looks transparent. By employing dual-frequency LC, it can be switched to FC state upon low frequency voltage driving and stabilized at low transmission. And it can switch back to planar state with high frequency and voltage driving. In such a device, polymer network will be distorted by the LC molecules upon the voltage driving, which in turns to stabilized the LC molecules with the removal of the voltage. Monomer concentration is an important parameter in our RPST. Increasing monomer concentration increases the driving voltage. Lower concentration of monomer cannot provide enough anchoring force to compete with the alignment layer. In our device, multi-stable grayscales were obtained due to the retention of polymer network which can be deformed and stabilized by various LC distributions upon electric field. Hence, each grayscales can be stabilized over two weeks.

8642-32, Session PWed

Colloids mediated liquid crystal blue phases

Everett Rhinehalt, Emine Kemiklioglu, Jeoung-Yeon Hwang, Liang-Chy Chien, Kent State Univ. (United States)

A small amount of colloids was dispersed in a blue phase liquid crystal, and the blue-phases were found to exhibit extended temperature range. The stabilized temperature range of the blue phase was a function of their most effective concentration, different sizes of colloid particles and shape of colloidal particles. The temperature range was probed and determined and the temperature range of the blue phases was found to decrease as the colloidal particle size increased. Additionally, the temperature dependent of Bragg wavelength peak was found to red-shifted in the colloidal-BP mixtures. The electro-optical results, especially the switching voltage and response time suggested that concentration and size of dispersed colloids modified the elastic energy of the blue phase liquid crystal composites and have led to a lower switching voltage.

8642-33, Session PWed

Capacitive-based shear stress sensor using liquid crystal

Alaeddin S. Abu-Abed, Evan C. Lemley, Mohamed Bingabr, Univ. of Central Oklahoma (United States)

For decades, the measurement of the dynamic shear stress has been a topic of great interest for many of fluid dynamics monitoring and diagnostics applications. In particular, shear stress monitoring is of crucial importance in biomedical, aircrafts, gas turbine, turbulent flow, and aerodynamics. The measurement of shear stress is critical in all these applications as it helps in delivering robust system design. In the biomedical field, monitoring and measuring the wall shear stress in blood vessels is critical in studying and diagnosing various disease. Several mathematical and experimental models have been developed as efforts to study the hemodynamic of blood, in particular the blood wall shear stress. Recent studies have shown that wall shear stress is closely related to the development of arteriosclerosis disease which seriously affects the human health.

This paper presents a capacitive liquid crystal-based technique to measure wall shear stress. In this work, the authors have developed an alternative method which utilizes LC film embedded in an interdigital capacitive microstructure. This innovation will transduce the shear force, which deforms the LC profile, into a measurable capacitive quantity via tracking the LC deformation. This promising sensor has strong potential applications in bioengineering systems where monitoring the blood shear stress is critical such as carotid artery experiments. Some of the issues addressed in this work are the impact of the shear stress on the liquid crystal molecular ordering (order parameter) and the influence of electrode geometries and material properties on the measured capacitances.

The proposed mechanism replaces the present optical transduction techniques in LC-based shear stress sensors, and offers remarkable advantages over the conventional visual inspection optical methods. For example, it provides greater insight into the fundamental distortion occurring in the LC film due to the shear stress force, and offers the ability to identify and track the average deformation. In addition, a simpler system with autonomous operation and reduced possible false alarms is achievable.

8642-34, Session PWed

Radial polarizer with continuous optic axis using selective wetting inscription based on a liquid crystalline polymer

Jun-Hee Na, Jiyeon Kim, Se-Um Kim, Sin-Doo Lee, Seoul National Univ. (Korea, Republic of)

Liquid crystalline polymers (LCPs) have attracted much attention for various electro-optic (EO) and biomimetic applications due to the unique optical anisotropy in solid state and the controllability of the optic axis in various geometries. Among a number of the optical components based on the LCPs, the optical retarders play an important role in many optical systems such as 3-dimensional displays, optical data storage, and optical communication systems through the change in the phase or the polarization state of light. Although the LCP retarders with a single unidirectional (or bidirectional) optic axis, defined typically by a rubbing process, have been widely used, more sophisticated components such as a sinusoidal version of a phase retarder and an optical film with multi-optic axes are needed for specific applications.

In this work, we demonstrated a new optical device exhibiting radial polarization with the continuous optic axis which was realized using the wetting transition of the LCPs. It was found that the selective wetting inscription (SWI) technique together with ultraviolet (UV) irradiation was capable of producing circular wrinkle patterns of the LCP by chain ordering. The LCP molecules were well aligned along the interface between the hydrophilic and hydrophobic regions defined by the SWI

Conference 8642:
Emerging Liquid Crystal Technologies VIII

process due to the amphiphilic properties of the LCPs. The resultant radial polarizer showed the perfect continuity of the optic axis and the high optical transmittance. Our approach based on the SWI in combination with the UV exposure is a very simple and versatile method of micro-patterning anisotropic polymers.

8642-35, Session PWed

Fast switching of a nematic liquid crystal cell without alignment layer and alignment process

Tae-Hoon Yoon, Jung-Wook Kim, Dong Han Song, Ki-Han Kim, Pusan National Univ. (Korea, Republic of)

We propose a method for fast-switching of nematic liquid crystals without either alignment materials or alignment process. Three-terminal electrode structure is used to apply in-plane and vertical electric fields to randomly-aligned liquid crystals. A vertical field is applied to align liquid crystals vertically for the dark state, whereas an in-plane field is applied to align liquid crystals homogeneously for the bright state. We obtained the turn-on time of 1.2 ms and turn-off time of 0.5 ms in the three-terminal electrode structure without either alignment materials or alignment process. However, three-terminal electrode structure without either alignment materials or alignment process shows low transmittance. For higher transmittance, we mixed reactive mesogen and nano-particles with anisotropic molecular shape to liquid crystals. As a result, we obtained a transmittance similar to the conventional fringe field switching mode and achieved the total response time of less than 3 ms.

8643-15, Session PWed

Plastic optical touch panel based on vertically directional coupling

Beom-Jun Cheon, Jun-Whee Kim, Min-Cheol Oh, Pusan National Univ. (Korea, Republic of)

Plastic optical waveguide touch panel based on evanescent field coupling in vertical direction between arrayed channel waveguides and flexible planar waveguide is proposed. Channel waveguide with the width of 25 μm and the thickness of 5 μm has a formation of the vertical and horizontal array waveguide on $n \times n$ matrix which has 5 mm intervals between cross points. When the channel waveguide on the glass wafer and the planar waveguide on PMMA are attached, the spacer with the thickness of 5 μm is formed to prevent initial coupling between two waveguides. Index matching liquid fills the gap between arrayed channel waveguides and flexible planar waveguide in order to enhance the transparency of waveguides and increase the evanescent field. When the force is applied in vertical direction, flexible planar waveguide is bent to get close to arrayed channel waveguides so that the guided mode in the channel waveguides is coupled into the flexible planar waveguide. To measure the device performance, a 1550 nm DFB laser was connected to 1X4 splitter and a 4-ch V-groove single mode fiber to make coupling as much lights as possible in waveguide on the input section, while the multi mode fiber is used on the output section to fully detect the light passing through the waveguide. By applying a force of 1 N, the change of light intensity by CCD and output intensity modulation of 23 dB was obtained by virtue of the efficient evanescent field coupling between the waveguides made of the same polymer material.

8643-18, Session PWed

Estimation of true radiance and sub-pixel position of saturated point targets

Erez Avrahamov, Bar-Ilan Univ. (Israel); Shavit Nadav, Elisra Electronic Systems Ltd. (Israel); Zeev Zalevsky, Bar-Ilan Univ. (Israel)

In this paper we present a mathematical model, its numerical simulations as well as preliminary experimental results used for the estimation of the true radiance value as well as the sub pixel position of a point targets that caused to saturation in the specific pixel at the detector where they appeared. The estimation is done by applying the model for the point spread function of the optics and by using the values of the neighbor and the non saturated pixels.

The innovation presented in this paper is that it is possible to obtain an almost absolute reconstruction of all the data that is missing due to this saturation by using mathematical tools, i.e. by taking the additive Gaussian values in the eight neighboring pixels into account. We present two major paths that afford maximal data extraction with minimal assumptions and approximations: improved Gaussian method allowing us obtaining all the missing data through the use of calculations with an accuracy of less than one percent and a method based on computing ratios between samplings of the Gaussian function. Numerical simulations as well as preliminary experimental results will be presented.

8643-19, Session PWed

Scene-based nonuniformity correction algorithm based on optical flow

Chen Peng, Nanjing Univ. of Science and Technology (China)

The performance of infrared imaging system is strongly affected by non-uniformity in infrared focal-plane arrays (FPA). In the classical scene-based nonuniformity correction (NUC) method, errors commonly occur resulting from local motion between two frames. In this paper, a novel

scene-based NUC method is presented. This method calculates robust optical flow between two adjacent frames to get the velocity vector of each pixel in the current frame. In this way, corresponding to the pixel in the current frame, the location of the pixel in previous frame is known, and then these frames can be locally registered easily. Based on the assumption that any two detectors with the same scene would produce the same output value, minimize the mean square error between two local registered images to get the estimation of each detector's gain and offset. With gain and offset parameters, nonuniformity of infrared imaging system can be corrected. One advantage of this scene-based NUC algorithm is that it can adapt to scene with local motion. The performance of the proposed algorithm is studied with infrared image sequences with simulated nonuniformity and infrared imagery with real nonuniformity. It shows that fixed-pattern noise is reduced efficiently even when the scene include local motion.

8643-20, Session PWed

The Influence of pH of the precursor solution on TiO₂ films under hydrothermal synthesis

Lei Xia, Zhihui Feng, Haitao Dai, Shu Guo Wang, Xiao Wei Sun, Tianjin Univ. (China)

As a fine material widely used in solar cells, electrochromic devices and an excellent photocatalyst, Titanium dioxide (TiO₂) has attracted more and more attention. In general, TiO₂ exists in three crystal phases: brookite, anatase and rutile, among which rutile TiO₂ is more suitable for electrochromic devices due to its lower production cost, higher chemical stability and higher refractive index. The performance of the TiO₂ thin films was affected by many factors such as reaction temperature, time and concentration. The influence of the pH of the precursor solution on the formation of TiO₂ thin films, however, has not been studied thoroughly. In this paper, we investigated the formation of TiO₂ films with various pH precursor solutions for electrochromic applications. The pH of the solution was controlled by the ratio of the involved precursors such as Hydrochloric acid (HCl) and urea (CO(NH₂)₂) reagent. Experimental results show that the pH of the solution will change the speed of the reaction rate. Thus the film thickness can be controlled with various pH of the solutions. By exploring the effect of pH of solutions on the formation films, we achieved the optimized TiO₂ film for electrochromic display.

8643-21, Session PWed

Lateral ink mobility and fringe field effects across the porous matrix of an electrophoretic display

Kelly Li Tsui, Manuel Ahumada, San José State Univ. (United States); Mateusz Bryning, Zikon, Inc. (United States); Michelle Hartono, Sang-Joon Lee, San José State Univ. (United States)

This investigation studies lateral mobility of nanodroplet ink in a reverse-emulsion electrophoretic display (REED). The display consists of a stationary porous matrix that serves as the "paper" between planar electrodes. One relative advantage of this type of electronic paper display is that it can be produced with low-cost materials and manufacturing processes. A key component is a porous matrix made of bonded titanium dioxide powder, which can be prepared in a variety of inexpensive thick-film deposition methods. A limiting factor for image resolution, however, is a fringe field effect than occurs at edges between pixels. Ideally the dye-containing nanodroplets in the reverse-emulsion ink move in a direction that is strictly perpendicular between the opposing pairs of electrodes for each distinct pixel. However, diffusion of the nanodroplets and electric fields from neighboring pixels can result in some degree of lateral motion as well. The magnitude and time evolution of this fringe field effect is measured as a function of pixel spacing and field strength, using microscope video capture and post-processing image analysis. The results provide design rules for selection of geometric and operational conditions, according to application-driven resolution requirements.

**Conference 8643:
Advances in Display Technologies III**

8643-1, Session 1

Aerial LED signage by use of crossed-mirror array (*Invited Paper*)

Hirotsugu Yamamoto, Ryousuke Kujime, Hiroki Bando, Shiro Suyama, Univ. of Tokushima (Japan)

In this invited paper, our developed aerial 3D LED signage technique is reviewed.

3D representation of digital signage improves its significance and rapid notification of important points. Real 3D display techniques such as volumetric 3D displays are effective for use of 3D for public signs because it provides not only binocular disparity but also motion parallax and other cues, which will give 3D impression even people with abnormal binocular vision. Our goal is to realize aerial 3D LED signs.

We have specially designed and fabricated a reflective optical device to form an aerial image of LEDs with a wide field angle. The developed reflective optical device composed of crossed-mirror array (CMA). CMA contains dihedral corner reflectors at each aperture. After double reflection, light rays emitted from an LED will converge into the corresponding image point. The depth between LED lamps is represented in the same depth in the floating 3D image.

Floating image of LEDs was formed in wide range of incident angle (at least 15 deg to 80 incident angle) with a peak reflectance at 35 deg. The image size of focused beam (point spread function) agreed to the apparent aperture size.

When LEDs were located three-dimensionally, the focused distances were the same as the distance between the real LED and the CMA. Tiling of three CMAs enlarged viewing angle of the 3D image.

8643-2, Session 1

Real-time pickup and display integral imaging system without pseudoscopic problem

Jonghyun Kim, Jae-Hyun Jung, Byoung-ho Lee, Seoul National Univ. (Korea, Republic of)

Most of pickup methods in integral imaging suffer from pseudoscopic problem, which means 3D reconstruction is reversed in depth. Several approaches are proposed to overcome this problem over decades. However, previous approaches did not provide real-time real orthographic 3D images without special optical devices, which is the crucial base technique for future 3D interactive system. Our objective is to construct real-time pickup and display integral imaging system without pseudoscopic problem. A simple lens array and a high speed CCD can capture 3D information of the object and a commercial LC display panel displays the elemental image in real-time. Reconstructed image is real and orthographic so that the observer can touch the 3D image. Furthermore, applying pixel mapping algorithm proposed by our group recently, elemental image of orthographic 3D image is obtained in real-time. This algorithm, based on image interweaving process, can also change the depth plane of the displayed 3D images in real-time. C++ programming is used for real-time capturing, image processing, and displaying. For real-time high quality 3D video generation, a high resolution and high frame rate CCD (AVT Prosilica GX2300C) and LC display panel (IBM 22inch 3840x2400) are used in proposed system. We present proper simulation and experiment to verify our proposed system. A 1mm spherical lens array is used both at pickup process and display process and ten to hundred millimeter scale 3D object is used in pickup process. As a result, reconstructed 3D image is real and orthographic as expected. Operation time of proposed algorithm with normal personal computer is short enough to show the validity of the proposed real-time algorithm.

8643-3, Session 1

Characterization of different types of 3D displays using viewing angle and imaging polarization measurements (*Invited Paper*)

Pierre M. Boher, Thierry Leroux, Thibault Bignon, ELDIM (France)

No Abstract Available.

8643-4, Session 1

Measurement of the optical characteristics of electro-wetting prism array for three-dimensional display

Yunhee Kim, Yoon-Sun Choi, Samsung Advanced Institute of Technology (Korea, Republic of); Alexander Morozov, Samsung Electronics Co., Ltd. (Korea, Republic of); Kyuwhan Choi, Samsung Advanced Institute of Technology (Korea, Republic of); Yongjoo Kwon, Samsung Electronics Co., Ltd. (Korea, Republic of); Jungmok Bae, Hong-Seok Lee, Sangyoon Lee, Samsung Advanced Institute of Technology (Korea, Republic of)

Recently liquid-based optical devices are emerging as attractive components in three-dimensional (3D) display for its compact structure and fast response time. Among them electro-wetting (EW) prism array is one of the promising 3D devices. It steers the beam, which enables to provide corresponding perspectives to observer. For high quality autostereoscopic 3D displays the important factors are the beam steering angle and the beam profile, the optical characteristics. In this paper, we propose a method to measure the optical characteristics of the EW prism and show experimental results on our prototype EW prism array, which consists of 5 by 5 with 200um by 200um size prisms. A modified 4-f system is adopted for the proposed method. It provides two kinds of information of the optical characteristics of EW prism at image plane and at Fourier plane. First, the proposed measurement setup magnifies the image of the EW micro prism array so that we can observe the status of the each prism array directly with bare eye and align a mask easily for selecting a prism to be examined at image plane. Secondly, the steering angle can be calculated by measuring the displacement of the beam at the Fourier plane, where the angular profiles that have important information on the oil-water interface is observed precisely. The principle of the proposed method will be explained, and the measured optical characteristics from experimental results on EW prism we fabricated will be provided, which proves the validity of the measurement method.

8643-5, Session 1

Curved transreflective holographic screens for head-mounted display

Mickaël Guillaumée, Ctr. Suisse d'Electronique et de Microtechnique SA (Switzerland); Seyed Payam Vahdati, Eric Tremblay, Victor J. Cadarso, Jonas Grossenbacher, Jürgen Brugger, Ecole Polytechnique Fédérale de Lausanne (Switzerland); Randall Sprague, Innovega Inc. (United States); Christophe Moser, Ecole Polytechnique Fédérale de Lausanne (Switzerland)

Wearable augmented reality displays present many potential applications, from industrial to commercial and entertainment usage. State of the art head mounted displays (HMDs) are facing two main challenges: how to obtain a wide displayed field of view and simultaneously maintaining unoccluded through vision. To deal with these challenges, complex optical devices have been developed, resulting in rather bulky systems. Recently, an advanced contact lens approach was

**Conference 8643:
Advances in Display Technologies III**

proposed [1] to circumvent these shortcomings. With this approach, a portion of the contact lens images the information displayed on the spectacle while the surrounding part of the contact lens provides the through vision to the unaided eye. A key part of this system is provided by a transfective holographic film laminated on the curved spectacle surface to redirect each displayed pixels towards the centre of the eye. The resulting size of the HMD is drastically reduced while keeping a large field of view and unoccluded through vision.

This paper presents the design principle, fabrication and tests results of curved transfective holographic films to be used in conjunction with contact lens. The holographic films are written on curved spectacles. These films efficiently diffract the light from a projector mounted on the side of an eyewear towards the eye. Diffraction only occurs at the RGB laser lines used in the projector. At the same time, light from the surrounding environment is transmitted with low aberrations, allowing the wearer to see through.

The imaging properties of such spectacles have been tested with a flat dual-aperture prototype contact lens. We show a prototype demonstration of augmented reality see-through glasses with over 50 degrees field of view and excellent uniformity of the displayed images, thus paving the way for small footprint HMDs.

[1] R. Sprague and J. Schwiegerling, Interservice/Industry Training, Simulation, and Education Conference (I/ITSEC), 10143 (2010).

8643-6, Session 1

High-power red-emitting DBR-TPL for possible 3D holographic or volumetric displays

David Feise, Christian Fiebig, Gunnar Blume, Johannes Pohl, Katrin Paschke, Ferdinand-Braun-Institut (Germany)

Holographic or volumetric displays not only require ever more data to render full 3d images, but also demand much more light to produce images with high contrast in order to compete with current 2d or quasi-3d technology. For environmental reasons, it is highly desirable to move from conventional, filtered projection displays towards direct writing. The only light sources available for such an approach, which requires a high light output with a spatial resolution beyond conventional light sources, are lasers. When adding the market demands for high electro-optical conversion efficiency, direct electrical modulation capability, compactness, reliability and mass-production compliance, this leaves only semiconductor diode lasers.

We present red-emitting diode lasers emitting a powerful, visible beam with a large spatial and spectral coherence, which are ideally suited for 3d holographic and volumetric imaging. The lasers have a tapered design to provide almost diffraction limited radiation ($M^2 < 1.5$) with an optical output power in excess of 500 mW in the wavelength range between 633 nm and 638 nm. The simultaneous inclusion of a distributed Bragg reflector (DBR) surface grating provides additionally wavelength selectivity and hence a spectral purity < 5 pm.

These properties allow dense spectral multiplexing to achieve output powers of several watts, which would be required for 3d volumetric display applications.

8643-7, Session 2

Direct integration of a 4-pixel emissive display into a knit fabric matrix

Jared P. Coyle, Genevieve Dion, Adam K. Fontecchio, Drexel Univ. (United States)

There exists a growing demand for displays in wearable applications. Wearable displays have traditionally been state-of-the-art flexible designs that are subsequently mounted onto clothing fabric. Ideally, such a design would itself be fabric-integrated. Recently, much attention has been placed on work involving the weaving of photonic bandgap and other optical fibers to create a true fabric based display. Little exists in the technical literature concerning knit-based fabric displays.

In this research, a prototype 4-pixel emissive fabric display is demonstrated. Individual conductive silver fibers act as a cathode. The cathode fibers are dip-coated coated first with a transport layer of Poly-3,4-ethylenedioxythiophene poly-styrenesulfonate (PEDOT:PSS). After drying, coated fibers are coated again, but in poly-2-methoxy-5-(2'-ethylhexyloxy)-p-phenylene vinylene (MEH-PPV). When this entire structure is placed in contact with a separate metallic fiber (functions as an anode), a PLED is formed. After drying and annealing, coated fibers are then knit into a fabric matrix using a Shima Seiki SIG123 automated knitting machine. The knit pattern itself provides a passive matrix addressing system similar to that of a more simple weave. Multiple knit patterns are investigated.

The resultant fabric based displays are actuated using an Agilent DC power supply. Electroluminescence spectra at various observation angles are collected under tension using an ocean optics UV-NIR spectrometer, and display intensity is obtained using a spectrophotometer. Current-voltage behavior of individual pixels is obtained using a Keithley 2400 sourcemeter. The performance of individual fiber pixel displays is compared with that of an equivalent planar device and the pixel knit patterns.

8643-8, Session 2

A CMOS microdisplay with integrated controller utilizing improved silicon hot carrier luminescent light sources

Petrus J. Venter, Univ. of Pretoria (South Africa) and INSiAVA (Pty) Ltd. (South Africa); Trudi-Heleen Joubert, Monuko du Plessis, Univ. of Pretoria (South Africa); Antonie C. Alberts, Marius E. Goosen, Pieter Rademeyer, INSiAVA (Pty) Ltd. (South Africa)

Microdisplay technology, the miniaturization and integration of small displays for various applications, is predominantly based on OLED and LCoS technologies. Silicon light emission from hot carrier electroluminescence has been shown to emit light visibly perceptible without the aid of any additional intensification, although the electrical to optical conversion efficiency is not as high as the technologies mentioned above. For some applications, this drawback may be traded off against the major cost advantage and superior integration opportunities offered by CMOS microdisplays using integrated silicon light sources. This work introduces an improved version of our previously published microdisplay by making use of new efficiency enhanced CMOS light emitting structures and an increased display resolution.

Silicon hot carrier luminescence is often created when reverse biased pn-junctions enter the breakdown regime where impact ionization results in carrier transport across the junction. Avalanche breakdown is typically unwanted in modern CMOS processes. Design rules and process design are generally tailored to prevent breakdown, while the voltages associated with breakdown are too high to directly interact with the rest of the CMOS standard library. This work shows that it is possible to lower the operating voltage of CMOS light sources without compromising the optical output power. This results in more efficient light sources with improved interaction with other standard library components.

This work proves that it is possible to create a reasonably high resolution

**Conference 8643:
Advances in Display Technologies III**

microdisplay while integrating the active matrix controller and drivers on the same integrated circuit die without additional modifications, in a standard CMOS process.

8643-9, Session 2

Effect of nanodroplet ink concentration on switching response of reverse-emulsion electrophoretic displays

Winston K. Wang, San José State Univ. (United States); Remy Cromer, Zikon, Inc. (United States); Michel G. Goedert, Maryam Mobed-Miremadi, Sang-Joon Lee, San José State Univ. (United States)

Reverse-emulsion electrophoretic display (REED) technology is based on an electro-responsive ink comprised of self-assembled nanodroplets dispersed in a non-polar liquid. The dye-containing nanodroplets in this reverse emulsion are selectively driven toward or away from the viewing plane by patterned electrodes that define distinct pixels. In this study, experimental measurements are conducted to determine how ink concentration in this reverse emulsion affects display performance with respect to image contrast and switching speed. Of key interest is the optimum concentration level that achieves high contrast without diminishing effectiveness that might be caused by saturation or shielding effects. The experimental observations are compared to predicted behavior based on multiphysics simulation of charged particle motion. The charged particle simulation further explores functional dependencies on electric field strength and characteristic geometric parameters of the stationary porous matrix through which the nanodroplets travel. In order to facilitate parametric simulations, the ink is first characterized in terms of approximate size distribution by dynamic light scattering corroborated by atomic force microscopy. The effective electrophoretic mobility of the nanodroplets through the porous matrix is approximated using microscope video recording of a moving front, which is created as dye-containing nanodroplets move under an electric field through the otherwise transparent solvent.

8643-10, Session 2

Microlens array based LCD projection display with software-only focal distance control

Marcel Sieler, Peter Schreiber, Andreas Bräuer, Fraunhofer-Institut für Angewandte Optik und Feinmechanik (Germany)

State of the art LED pico-projectors using single-channeled optical layouts always require a trade-off between achievable flux and minimum system size. Furthermore, their limited depth of focus require additional mechanically moving components for focusing if variable projection distances are essential for their specific application. We present a novel microlens-array based LCD projector breaking these constraints of conventional LED illuminated systems thus enabling a super compact, robust and bright module while offering new features for electronic focal distance control without additional mechanical components. While the short focal length of each contributing channel maintains a certain system slimmness, the superposition of all individual projections on the screen done by image-preprocessing leads to dramatic flux enhancement without blurring effects. Starting with the working principle of array projection we focus on key properties regarding depth of focus for examining novel image-preprocessing algorithms that enable for software-only focal distance control. Further improved program code enables sharp images even onto free-form screen geometries. The realized prototype utilizes a transmissive LCD microdisplay along with a monolithic array of 45 microlenses directly mounted on top of the display coverglass. While the display is illuminated by a collimated white LED; each channel is assigned to one primary color by applying a color filter array buried below the microlenses to obtain a full color image on the screen. The displayed image content is controlled via PC by a novel

software tool, whose correct operation is visualized by the obtained experimental results.

8643-11, Session 3

Compact laser module with a high-speed liquid crystal attenuator for see-through display applications

Takaaki Takeishi, Masafumi Ide, Shinpei Fukaya, Seiko Kato, Takaaki Nozaki, Citizen Holdings Co. Ltd. (Japan)

At present, many types of head mounted displays (HMDs) have been appeared on the HMD early adaptor market. Many of them have become equipped with see-through capability aiming to be used outside and to realize augmented reality (AR) features. In the near future, we are obtaining eyeglasses with built in displays.

These see-through type displays require dimming capability in response to ambient environmental conditions. One of the candidates of the dimming system for laser diode (LD) based engines is neutral density variable attenuators for all RGB three colors without changing the display's white point. We can control the LD output power by changing the current of each LD; however, each characteristic of the LD varies depending on the operating points and the types of LDs. So if we apply the variable attenuators to the laser sources, the operating schemes of the laser pico-projection system can become very simple. Our proposed system is based on hybrid laser sources which consist of three mono-color LDs and a built in high speed independent liquid crystal attenuator for each color, which works as a neutral density attenuator by synchronizing each attenuator.

In this study, we propose a laser module with a nematic liquid crystal variable attenuator using radially arranged electrodes. The 2.0 μm cell gap and the 50 μm aperture of the lateral electrodes are used. The module is suitable for see-through displays. The attenuator with a less than 2.5 ms gray to gray response time (driven by a 100Vpp) is realized.

8643-12, Session 3

Gas permeable nanowire grid polarizer integrated into contact lenses through nanoimprint lithography

Andrew E. Hollowell, Univ. of Michigan (United States) and Sandia National Labs. (United States); Young Jae Shin, L. Jay Guo, Univ. of Michigan (United States)

Optical components incorporated directly into contact lens materials allow for the realization of advanced projection based display technologies for use in augmented reality and heads up displays^{1,2}. A fabrication process suitable for large scale manufacturing has been developed for encapsulating wire grid polarizers into gas permeable and biocompatible films allowing direct integration into personal contact lenses with high polarization efficiency, wide field of view, and long term stability.

Fabricating nanowire grid polarizers for visible light requires subwavelength features (pitch<180nm) which are difficult to fabricate in a manufacturable manner with conventional lithographic techniques. Electron-beam lithography offers low throughput while interferometric lithography has limitations on exposure area. Here nanoimprint lithography is used as an efficient technology to fabricate a nanostructured etch mask with high throughput and low cost. In contrast to liftoff processes, oblique angled evaporations³, and transfer printing⁴ a single step reactive ion etch is used to etch aluminum thin films through these nanoimprint defined masks offering the potential for manufacturable visible wavelength polarizers with high contrast and wide angle insensitivity. Extremely selective gas etching allows nanoscale thin films to be undercut releasing the wire grid for increased delamination yield when compared to stamping and peeling processes. Full

**Conference 8643:
Advances in Display Technologies III**

encapsulation of these wire grid polarizers into PDMS offers a solution for realizing flexible, gas permeable, and bio compatible wire grid polarizers. The results of this approach will be presented at the conference.

References

1. J. Pandey, Y. Liao, A. Lingley, R. Mirjalili, B. Parviz, and B. Otis, IEEE TBCAS, Vol. 4, No. 6, (2010).
2. H. Ho, E. Saeedi, S. S. Kim, T. T. Shen, and B. A. Parviz, IEEE MEMS 10.1109, (2008).
3. L. Chen, J. J. Wang, F. Walkters, X. Deng, and M. Buonanno, App. Phys. Lett. 90, 063111 (2007).
4. T. Kim, and S. Seo, Nanotechnology 20, 145305, (2009).

8643-13, Session 3

Design concept of an FLC-NLC combined circular polarization switch for 3D laser pico-projectors

Seiko Kato, Takaaki Takeishi, Masafumi Ide, Takaaki Nozaki, Citizen Holdings Co. Ltd. (Japan)

At present, LED-based pico-projectors are still dominant; however, according to the compact size requirement, the demand for pico-projectors using laser light sources is expected to grow in the near future. 3D support is one of the pico-projector's demanding features.

There are two types of 3D systems. One is active shutter system and the other is passive shutter system. We have proposed a novel combined circular polarization switch for 3D laser pico-projectors for passive shutter glasses, which consists of a high speed ferroelectric liquid crystal (FLC) linear polarization switch and a multi-order quarter wave plate for RGB color chromatic compensations using a nematic liquid crystal (NLC).

In this study, we present a design concept of the polarization switch and improved behaviors as bandwidth comparison with an achromatic compensation method using an FLC with low order compensation films. The adjustment for each RGB laser wavelength using an additional polymer film working in the target ranges 445 – 640 nm are also indicated. The novel design can be broaden the low crosstalk range less than 0.5 % from 59 % to 91 % of the target range. In addition, we fabricate a prototype based on the design concept and evaluate the crosstalk and 3D performance, which are crucial for 3D projector attributes, in combination with a MEMS system. The proposed switch can be placed in the path of the combined RGB laser beam and is suitable for both the imager based and the scanning MEMS based systems because its simple structure and compact design.

8643-14, Session 3

A passive cooling system proposal for multifunction and high-power displays

Ilker Tari, Middle East Technical Univ. (Turkey)

Flat panel displays are conventionally cooled by internal natural convection, which constrains the possible rate of heat transfer from the panel. On one hand, during the last few years, the power consumption and the related cooling requirement for 1080p displays have decreased mostly due to energy savings by the switch to LED backlighting and more efficient electronics. However, on the other hand, the required cooling rate recently started to increase with new directions in the industry such as 3D displays, and ultra-high-resolution displays (recent 4K announcements and planned introduction of 8K). In addition to these trends in display technology itself, there is also a trend to integrate consumer entertainment products into displays with the ultimate goal of designing a multifunction device replacing the TV, the media player, the PC, the game console and the sound system. Considering the increasing power requirement for higher fidelity in video processing, these multifunction devices tend to generate very high heat fluxes, which

are impossible to dissipate with internal natural convection. In order to overcome this obstacle, instead of active cooling with forced convection that comes with drawbacks of noise, additional power consumption, and reduced reliability, a passive cooling system relying on external natural convection and radiation is proposed here. The proposed cooling system consists of a heat spreader flat heat pipe and aluminum plate-finned heat sink with anodized surfaces. For this system, the possible maximum heat dissipation rates from the standard size panels (in 26-70 inch range) are estimated by using our recently obtained heat transfer correlations for the natural convection from aluminum plate-finned heat sinks together with the surface-to-surface radiation. With the use of the proposed passive cooling system, the possibility of dissipating very high heat rates is demonstrated, hinting a promising green alternative to active cooling.

8643-16, Session 4

Molecularly controlled interfacial layer strategy toward highly-efficient simple-structured organic light-emitting diodes (Invited Paper)

Tae-Hee Han, Mi-Ri Choi, Pohang Univ. of Science and Technology (Korea, Republic of); Chang-Lyoul Lee, Advanced Photonics Research Institute (Korea, Republic of); Tae-Woo Lee, Pohang Univ. of Science and Technology (Korea, Republic of)

This paper basically presents a fundamental and comprehensive strategy to realize very simplified small-molecule OLEDs with a very high current efficiency (CE), which include only a single emitting layer of small molecules on top of a spin-coated conducting polymer layer. Conventional conducting polymers, poly(3,4-ethylenedioxythiophene):poly(styrenesulfonate) (PEDOT:PSS) or polyaniline doped with polymeric acids have been usually used as the hole injection layer (HIL) or the anode layer; however in OLEDs, most-commonly used PEDOT:PSS has serious problems due to inefficient hole-injection, inefficient electron-blocking, and substantial quenching of excitons close to the PEDOT:PSS. With simplified structures with a conventional HIL (PEDOT:PSS or a small molecule HIL), we observed a significant drop of CE.

Our idea to simplify structure to realize highly efficient small-molecule OLEDs uses a molecularly-controlled, high-performance interfacial polymeric HIL on the anode, which enable efficient blocking of exciton quenching as well as efficient hole-injection and efficient electron-blocking at the same time. Our HILs are composed of PEDOT:PSS and a tetrafluoroethylene-perfluoro-3,6-dioxo-4-methyl-7-octene-sulfonic acid copolymer, one of perfluorinated ionomers (PFI), which develops a gradient work function (WF) by self-organization of the PFI (We call "GraHIL"). This single-layered small molecule OLED has much greater CE (~20 cd/A) than do standard multilayered small molecule OLED devices that use conventional well-known hole injecting small-molecule, 4,4',4"-tris(N-(2-naphthyl)-N-phenyl-amino)triphenylamine as a HIL (CE ~12 cd/A). The dramatic improvement in simplified OLEDs is achieved because that molecularly controlled GraHIL meets all the requirements for realization of simplified small-molecule OLEDs. From our studies regarding exciton quenching, we find that the self-organized surface layer of our GraHIL having efficient hole-injection/electron-blocking capability can prevent the severe quenching of excitons at the HIL/emitting layer interface without needing a hole transporting layer.

8643-17, Session 4

Blue phosphorescent organic light-emitting diode with oxadiazole host

Yu-Hao Liu, National Taiwan Univ. (Taiwan); Yi-Hsin Lan, National United Univ. (Taiwan); Yi-Chi Bai, National Dong Hwa Univ. (Taiwan); Wan-Hsi Yang, National Taiwan Univ. (Taiwan); Pei-Yu Lee, Yuan Ze Univ. (Taiwan); Mao-Kuo Wei, National Dong Hwa Univ. (Taiwan); Chi-Feng Lin, National United Univ. (Taiwan); Tien-Lung Chiu, Yuan Ze Univ. (Taiwan); Man-Kit Leung, Jiun-Haw Lee, National Taiwan Univ. (Taiwan)

Blue phosphorescent organic light-emitting diode (OLED) is one of the most important technical bottlenecks for OLED display and lighting applications. In such a device, a wide bandgap material is needed as the host material for carrier transport and transfer energy to the dopant material. Here, we use an oxadiazole derivative as the host material with electron transporting characteristics in the blue phosphorescent OLED. The structure in our device were ITO glass as anode, N,N'-diphenyl-N,N'-bis(1-naphthyl)-1,10-biphenyl-4,40-diamine (NPB) as the hole-transport layer (HTL), 1,3-bis(carbazol-9-yl)benzene (mCP) as the electron-blocking layer (EBL), OXD derivative material doped with iridium(III) bis[[4,6-difluorophenyl)-pyridinato-N,C2'] picolinate (Flrpic) as the EML, 3-(4-Biphenyl)-4-phenyl-5-tert-butylphenyl-1,2,4-triazole (TAZ) as the electron-transport layer (ETL), LiF as the electron injection layer (EIL), and Al as cathode. The thickness of HTL, EBL, EML, ETL, EIL and cathode are 50 nm, 10 nm, 30 nm, 40 nm, 1.2 nm and 100 nm, respectively. When without Flrpic dopant, the device driving voltage is 9.2 V at 100mA/cm². When Flrpic is doped inside the OXD matrix, driving voltage increases because this OXD has excellent electron mobility that Flrpic acts as electron trap in EML, as shown in Fig. 1. Fig. 2 shows current efficiency versus luminance with various dopant concentrations. The cd/A increased with the Flrpic dopant concentration increased. It can see the maximum cd/A was obtained when Flrpic dopant concentration is at 15%, that maximum current efficiency occurs at luminance 19.1 cd/m² of 39.9 cd/A, respectively. At Flrpic dopant concentration 18%, device efficiency drops down because of triplet-triplet annihilation.

8644-1, Session 1

Non-Bragg diffraction orders in lithium niobate and its application to one-shot phase-shifting holographic interferometry

Partha P. Banerjee, George T. Nehmetallah, Ujitha A. Abeywickrema, Univ. of Dayton (United States); Sergei F. Lyuksyutov, The Univ. of Akron (United States); Nickolai V. Kukhtarev, Alabama A&M Univ. (United States)

Phase shifting digital holography offers the advantage of determining the amplitude and phase of the object through the monitoring of the recorded intensities upon applying different phase shifts between the object wave and the reference. However, for a fast-moving or fast-deforming object, phase shifting holography may not be practical owing to the time involved in physically changing the phase shifts between the object and the reference, and a real-time method would be advantageous. We show in this paper that the appearance of Bragg and multiple non-Bragg orders during two-beam coupling in photorefractive lithium niobate can be used to our advantage in simultaneously recording intensities that contain information about different phase shifts between the object and the reference. Up to 7 non-Bragg orders are observed and their temporal evolution is recorded. We show examples of intensity patterns in Bragg and non-Bragg orders in the near and far-fields during recording of holograms of different objects with a plane wave or spherical wave as a reference. We show that the diffracted intensities should contain information about the amplitude and phase of the object, similar to that obtained from phase shifting holography. Finally, we show examples of reconstruction of the object from the recorded information in the Bragg and non-Bragg orders using our one shot phase shifting holographic interferometry.

8644-2, Session 1

Photopolymer composition with high sensitivity

Nariman Achourbekov, Rouslan Birabassov, Svetlana Peredereeva, LumiStor Inc. (Canada); Ozra Pouraghajani, Univ. Laval (Canada); Arbinder S. Pabla, LumiStor Inc. (Canada)

We investigate a photopolymer composition comprising an inert polyphenyl ether binder capable of supporting radical polymerization and a photopolymerizable component comprising radically polymerizable multifunctional (meth)acrylic oligomers/monomers with improved holographic and optical properties. We have assessed the holographic properties of Urethane acrylates with polyester and polyether backbones such as acrylate trifunctional monomer, hyperbranched polyester acrylates and aliphatic Urethane Acrylate from Sartomer with functionalities up to 18 and molecular weights in the range of 200-2000, different oligomeric polyphenyl ether binders with wide range of initial viscosity such as Six-ring polyphenyl ether (6P5E), Five-ring polyphenyl ether (5P4E) and mixture of isomers such as Santovac 5™. It was shown that the holographic properties are strongly affected by an optimum choice of viscosity and molecular weight of the inert binder, in cooperation with suitable photopolymerizable multifunctional (meth) acrylic oligomers/monomers so as to provide rigidity of the medium while maintaining good diffusion of the inert binder from exposed regions to unexposed regions during recording. The dynamics of the holographic grating build up process were studied using RTIR spectroscopy, differential scanning calorimetry and a holographic technique.

It was further shown that high functionality of used oligomers/monomers has strong influence on the photopolymer holographic properties. This is because a cross-linked polymer network structure with high rate of initial photocuring and dense polymer network could inhibit monomer diffusion. By optimizing these parameters volume gratings of diffraction efficiency

97% and M-number values $M\# = 5.6$ for film thickness of 0.2-0.25mm and average photosensitivity of 30 multiplexed holograms up to 3.4 cm/mJ have been achieved.

8644-3, Session 1

Three dimensional (3D) parallel processing holographic lithography using femtosecond laser pulse

Anas Fauzi, Sung-Jin Kim, Chungbuk National Univ. (Korea, Republic of); Jong Rae Jung, Suwon Science College (Korea, Republic of); Seock-Hee Jun, Univ. of Incheon (Korea, Republic of); Nam Kim, Chungbuk National Univ. (Korea, Republic of)

Holographic three dimensional (3-D) lithography using femtosecond laser pulse were demonstrated in this paper. The 3-D image were created using CAD tools then plotted in to MATLAB coordinates. From this coordinates the computer generated hologram (CGH) will be calculated using kinoform algorithm with Optimal-Rotation-angle (ORA) method. Kinoform is one of CGH algorithm that only depends on the phase distribution of the light incident upon it. It is more suitable for optical trapping as well as lithography because phase modulation provides increased intensity transfer when compared to amplitude modulation, so the maximum amount of light reaches the silicon surface as the sample material in the experiment. In order to achieve high resolution result in parallel processing of several points the ORA method were applied. The ORA method will increase the uniformity of the diffraction peaks, so that the resolution of the reconstructed image also increased.

The phase hologram (CGH) was displayed on reflection type LCoS-SLM, irradiated using femtosecond laser pulse. The reflected beam from the SLM will directed to sample surface. In this research, silicon wafer coated with poly(methyl-methacrylate) or PMMA were used as the sample. The use of femtosecond pulse duration of a Ti:sapphire laser will improve the holograms resolution (~8000 dpi) due to the shorter femtosecond pulse duration and the larger peak powers that generate larger photonics concentrations at the beam focus. And Ti:sapphire laser could enable the single-shot exposure of an entire 3D structure at once. By creating a multi-plexed phase hologram containing feature dimensions at various planes, the laser could provide enough power to simultaneously induce cross-linking/ polymerization at each plane. The result would be the first example of a completely 3D lithography system. A scanning electron microscopy (SEM) was used to verify the result.

8644-4, Session 1

Versatile phase stabilization technique for holographic recording of large aperture volume Bragg gratings

Daniel Ott, Ivan B. Divliansky, CREOL, The College of Optics and Photonics, Univ. of Central Florida (United States); Marc SeGall, Univ. of Central Florida (United States); Leonid B. Glebov, CREOL, The College of Optics and Photonics, Univ. of Central Florida (United States)

Volume Bragg gratings (VBGs) are high precision optical devices with feature sizes as small as fractions of a micrometer. To achieve a consistent high quality recording of such small feature sizes, precision control in the fabrication process is necessary. Of the various fabrication processes used to make VBGs, holographic recording of a two beam interference pattern allows for the largest aperture size. This technique is preferred for creating large aperture gratings for free space applications. For mitigation of the interference pattern smearing during the recording process, it is necessary to implement phase stabilization. This includes

Conference 8644:
Practical Holography XXVII: Materials and Applications

a vibration isolated table, shielding from air fluctuations, and often, an active phase stabilization system to control the position of the fringe pattern within a fraction of the grating period. We present a new method for phase stabilization of a holographic recording system for volume Bragg gratings. The primary feature of this method is that it is extremely flexible and simple to integrate into an existing holographic recording setup. The setup allows for Bragg gratings with arbitrary tilt and resonant wavelength to be recorded. An analysis of the effects of phase stabilization and a method for analyzing the effectiveness of this phase stabilization approach are also introduced and successfully demonstrate its benefits.

8644-5, Session 2

Collimating beam shaper for holography and interferometry

Alexander V. Laskin, Vadim Laskin, AdlOptica Optical Systems GmbH (Germany)

Beam shaping is important technique to improve holographic and interferometric technologies, and refractive field mapping beam shapers like piShaper demonstrate strong capabilities in increasing predictability and reliability as well simplifying the realization of the mentioned technologies. Most often the piShaper are implemented as telescopic systems with collimated beams at entrance and exit. At the same time the fiber-coupled TEM00 laser sources become more popular in holography and interferometry because of their high beam quality, reduced high frequency noise due to spatial filtering in a TEM00 fiber and convenience in usage. Therefore, the beam shapers should be compatible with those fiber-coupled lasers featured with high beam divergence. Basic piShaper design principles allow to implement a system combining the functions of beam shaping and collimation, as result divergent Gaussian laser beam from TEM00 fiber is transformed, almost lossless, to collimated flattop beam with low divergence, flat wave front, extended depth of field, reduced noise; such a beam is optimum for SLM-based technologies of CGH, Dot-Matrix mastering of security holograms, holographic data storage, holographic projection, lithography, interferometric techniques of Volume Bragg Gratings recording, etc. Achromatic design of the telescopic and collimating beam shapers allows working with several laser sources with different wavelengths simultaneously that is, for example, important in multi-colour Denisyuk holography.

This paper will describe some design basics of collimating refractive beam shapers of the field mapping type and optical layouts of their applying in holographic systems. Examples of real implementations and experimental results will be presented as well.

8644-7, Session 2

1-step 3D achromatic transmission holograms digitally printed using a 440nm pulsed laser for embossed applications

Stanislovas J. Zacharovas, Geola Digital uab (Lithuania); David C. Brotherton-Ratcliffe, Geola Technologies Ltd. (United Kingdom); Ramunas J. Bakanas, Andrej Nikolskij, Geola Digital uab (Lithuania)

The pulsed laser Direct-Write Digital Holography (DWDH) technique has been applied to print high resolution digital achromatic and mixed rainbow-full-colour achromatic transmission holograms showing deep images. Such holograms have been successfully used as master-originals for the production of embossed holograms.

Digital image holograms produced by the DWDH process consist of a large ensemble of many small, usually square, elemental holograms. This process is very similar to the way in which a digital photograph is produced by printing a large ensemble of elemental pixels. In the case of the DWDH hologram however, the equivalent of the pixel is a "hogel",

which is a very small hologram capable of projecting a unique pattern of light. The hogel is capable of projecting brightness and colour information which varies over both vertical and horizontal projection angles. By recording each hogel using perspective-view image data derived from either virtual or real cameras, high definition 3D images of great depth may be synthesized. This can be likened to conventional stereography - but digital image holography uses many more perspective-view pictures, thus allowing deep 3D images to be generated over a wide viewing zone. Importantly, digital image holograms produced by the DWDH process can be recorded in one step. This allows the effective generation of an H2 hologram without the need to produce an H1 master first. The price paid for this large convenience is the innate pixelated structure of DWDH holograms. But such pixelisation can be greatly mitigated if the hogel is small enough.

8644-8, Session 2

The effect of aberrated recording beams on reflecting Bragg gratings

Marc SeGall, Univ. of Central Florida (United States); Daniel Ott, Ivan B. Divliansky, Leonid B. Glebov, CREOL, The College of Optics and Photonics, Univ. of Central Florida (United States)

Reflecting Bragg gratings (RBGs) are used in a variety of applications which may require large apertures or narrow spectral selectivity, which requires a uniform period over a range of several millimeters both in depth and across the aperture. While previous work has considered the effect of aberrations assuming that the grating can be treated as a single recording plane, we model the effect of aberrations present in the recording beams of a two-beam interference holographic setup on gratings which are sufficiently large that this is no longer possible. Aberrations up to fourth order are characterized by using their associated Zernike polynomials and the period of the interference pattern produced is generally spatially dependent both across the aperture and along the depth of propagation. Using coupled wave theory to determine the spectral response we find that the reflection spectrum will depend on the size of the beam being reflected, the location of the beam across the grating face, and the length and strength of the grating. In particular we examine a thin, grating with 99% reflectivity and a thick grating with 70% reflectivity. Both gratings demonstrate a spatially dependent resonant wavelength and the contrast of the side lobes are reduced. Spectral broadening and asymmetrical spectra are also observed for certain aberrations. However, these effects are reduced in the case of the highly reflective grating due to its much larger initial spectral width.

8644-9, Session 3

Development of full-color full-parallax digital 3D holographic display system and its prospects (*Invited Paper*)

Xuewu Xu, Xinan Liang, Yuechao Pan, Ruitao Zheng, Abel Z. Lum, Phyu Phyu Mar Yi Lwin, Sanjeev Solanki, A*STAR - Data Storage Institute (Singapore)

In the past five years, we researched on digital 3D holographic display systems, funded by Home2015 Programme of A*STAR, Singapore. In 2009, we had developed a monochrome system by using a single spatial light modulator (SLM) and a red laser diode, which could display 50-Mpixel holograms at 25 Hz refresh rate via an optical scan tiling approach. In 2011, we had developed a full-color system by using five physically tiled SLMs and RGB lasers, which could display 6.5-Mpixel holograms at 1440 Hz with a displayed image size of 3 inch in diagonal. In 2012, we developed a full-color system by using twenty-four physically tiled SLMs and RGB lasers, which could display 378-Mpixel holograms at 60 Hz via an optical scan tiling approach, with a displayed image size of 10 inch in diagonal. Full-color full-parallax 3D holographic videos had been transmitted at 9.44Gbps and 45 Gbps via network and played back with both the systems developed in 2011 and 2012, respectively.

**Conference 8644:
Practical Holography XXVII: Materials and Applications**

In this paper, we will review and compare the above three holographic display systems developed by our group from various aspects, including SLMs, lasers, optics designs, hologram computation, data transmission, and system synchronization. We will also discuss the bottlenecks and prospects of further development of the system for practical applications.

8644-10, Session 3

Study on holographic TV system based on multi-view image and depth map

Takanori Senoh, Kenji Yamamoto, Ryutaro Oi, Yasuyuki Ichihashi, National Institute of Information and Communications Technology (Japan)

Since electronic holography provides ultimate 3D images, it is expected to be an ideal 3D TV method in future. Since fringe patterns for electronic holography are huge amount of data, however they are difficult to broadcast or record electronically. In this paper, we investigated methods to solve this problem. Since Computer Generated Holography (CGH) can generate fringe patterns from a small amount of data of 3D model's coordinates and colors, it half solves the problem. The other half problem is how to get 3D models of natural scenes. For this answer, we used multi-view images and the associated depth maps. In the rest of paper, experimental results of depth map estimation, coding of them, and fringe pattern generation, and the electronic holography image reconstruction are reported. Depth map estimation algorithm improved by introducing an adaptive matching error selection method in the stereo-matching process of multi-view images was used. Encoder improved by Global Depth and View Prediction method (GDVP) was used to encode multi-view images and depth maps. Fringe patterns were generated from decoded multi-view images and depth maps. Electronic holography images were reconstructed from the generated fringe patterns.

8644-11, Session 3

Real-time reconstruction of digital holograms with GPU

Mert Dogar, Hazar A. Ilhan, Meric Ozcan, Sabanci Univ. (Turkey)

Digital holography made it possible to capture and reconstruct holograms in a computer environment. In a conventional CPU, the real-time reconstruction is not possible when the size of the holograms increase to several megapixels range. However, a GPU (the parallel processing unit that is included in commercial graphics cards), can provide the required computational power. The rapid developments in commercial graphics card technology provide an opportunity to process large blocks of data in a very short amount of time which reduces the hologram reconstruction time significantly. In this paper, basics of GPU programming for hologram reconstruction are introduced and the efficiency of CPU and GPU implementations of the three reconstruction algorithms (Fresnel transformation, angular spectrum method, convolution with free space propagation) are compared. Experimental results indicate that an average GPU provides more than 100 times speedup over a high-end multi-core CPU.

8644-12, Session 3

Autofocusing in digital holography

Hazar A. Ilhan, Mert Dogar, Meric Ozcan, Sabanci Univ. (Turkey)

Digital holography allows the acquisition of 3D profiles of objects. Digitally captured holograms are reconstructed at the respective distances of the objects to reveal the phase and the intensity profiles. However, computing an object's 3D profile with only a single reconstruction requires prior knowledge of the distance of the object from the camera. Otherwise, by performing several reconstructions at different distances and by evaluating each image with sharpness estimation, one can determine the in-focus distance of the object. Moreover, it is not practical to perform several reconstructions in real-time systems since reconstruction is the most computationally heavy part in digital holographic imaging. In this paper, we apply common sharpness functions to digitally recorded holograms for autofocus algorithms found in the literature and we compare the accuracy of the estimations. In addition, we show that automatic focus distance search can be done in real-time with scaled-down holograms obtained from the original hologram. This new method improves the speed of autofocus algorithms on the order of square of the scaling ratio. We show that numerical simulations and experimental results are in good agreement.

8644-13, Session 4

Realistic 3D image reconstruction in CGH with Fourier transform optical system

Tsubasa Ichikawa, Kazuhiro Yamaguchi, Yuji Sakamoto, Hokkaido Univ. (Japan)

Computer-generated holograms (CGHs) enable observers to see ideal 3D images without feeling of fatigue. In CGH, peculiar rendering techniques are necessary to express realistic 3D images because CGHs have parallax. We have proposed the calculation method with ray tracing method that expresses hidden surface removal, shading and so on. Ray tracing method is capable of rendering realistic images. However, resolutions of current output devices are not high enough to display CGH, so the size of reconstructed images is restricted and viewing zone and visual field are very narrow. Therefore it is hard to confirm advantageous effects of the proposed method. To enlarge the size of reconstructed images, the Fourier transform optical system is used. Then we introduce the technique to apply calculation method of CGH with ray tracing method to the Fourier transform optical system in this study. The proposed method conducts intersection determinations with ray tracing method every an elementary hologram. By assuming the intersections as sets of point light sources and calculating light waves on elementary holograms, the full-parallax CGHs are implemented. However, since the Fourier transform optical system reverses the depth of images and reconstructs in front of a hologram, pseudo stereoscopic 3D images which hidden surface removal was implemented in the direction opposite to the viewpoint are obtained by above method. We solved this problem by observing conjugate images. We conducted optical reconstructions and computer simulations that show proposed method is able to make realistic CGHs implementing hidden surface removal in the Fourier transform optical system.

**Conference 8644:
Practical Holography XXVII: Materials and Applications**

8644-14, Session 4

Using electronic holography to generate speckle-free and shaded reconstructed images

Takayuki Kurihara, Yasuhiro Takaki, Tokyo Univ. of Agriculture and Technology (Japan)

The elimination of speckles is required for electronic holography to improve reconstructed 3D images. To increase the realism of computer-generated holographic images, we require a shading technique specializing in electronic holography. We previously proposed the speckle reduction technique and the shading technique, separately. We now propose a combination of these techniques which provides speckle-free and shaded reconstructed images.

3D objects are represented by an aggregate of object points, which are divided into multiple object point groups displayed in a time-sequential manner. Each object point group consists of an array of sparsely separated object points, preventing the occurrence of interference between them. Each object point group is generated by displaying a 2D array of zone plates on a high-speed SLM. The amplitude distribution of the zone plates is modulated two-dimensionally to control the angular intensity distribution of light emitted from the object points, so the shading of reconstructed images changes depending on the viewer's eye position. The SLM generates multiple binary images illuminated by different light powers to represent 2D modulated zone plates in a time-sequential manner.

A DMD was used as the high-speed SLM. Its resolution was 1,024 × 768, and the frame rate was 13.333 kHz. Each object point group consists of 16 × 24 object points. The reconstructed image consists of 8 × 4 object point groups to obtain a total of 128 × 96 object points. Eight binary images represented each object point group. The frame rate for 3D image generation was 52 Hz.

8644-15, Session 4

Large-pixel-count hologram data processing for holographic 3D display

Yuechao Pan, Xuewu Xu, Xinan Liang, Abel Z. Lum, Ruitao Zheng, Phyu Phyu Mar Yi Lwin, A*STAR - Data Storage Institute (Singapore)

The pixel count of hologram for a holographic 3D display system increases rapidly with the increase of reconstructed object size and viewing angle. According to our analysis, for 10 inch reconstructed object size with 5° viewing angle, the hologram with a pixel count of 372 Millions is required. Such a large pixel count is a challenge for both hologram computation and hologram data transmission. The computation load is analyzed to be a few hundreds of TFLOP for the object with a few million object points, and the hologram data transmission rate is analyzed to be 22.3 Gbps and 67.0 Gbps for monochrome and color displays at 60 Hz, respectively. A GPU based computing platform with 22.4 TFLOPS computing power was built and a distributed computation method was implemented for computing large-pixel-count holograms. Computation time of 18 seconds was achieved for 372Mpixel hologram for the object with about 800k object points. A hologram data transmission platform was built with high speed network in order to meet the above data transmission requirement. During the playback of holographic video using our holographic 3D display system, the hologram data was read out from SSDs, transmitted over the high speed network, and finally launched onto SLMs for reconstruction. A data transmission rate of 31.8 Gbps was achieved, which corresponded to monochrome reconstruction of 372Mpixel hologram at 84Hz and full-color reconstruction of 186Mpixel hologram at 43Hz. The increasing demand for computation power and data transmission rate of large-pixel-count hologram video displays has been effectively addressed.

8644-16, Session 4

Calculation technique for a holographic stereogram from multi-view images

Kyohei Ikeda, Yasuhiro Takaki, Tokyo Univ. of Agriculture and Technology (Japan)

Because holographic stereograms can be generated from multi-view images captured by ordinary cameras, it is a significant technique to produce holograms of real scenes. However, the calculations for generating computer-generated holographic stereograms, particularly the diffraction calculations for the multiview images, are time consuming. This study proposes a new technique to reduce the calculation time for holographic stereogram generation.

The proposed technique does not involve diffraction calculations. We assume that the 3D image generation by holographic stereograms might be similar to that by multi-view autostereoscopic displays; multiple parallax images are displayed with rays converging to corresponding viewpoints. Therefore, a wavefront whose amplitude is the square root of an intensity distribution of the parallax image and phase is a quadric phase distribution of a spherical wave converging to the viewpoint is considered. Multiple wavefronts are calculated for multiple viewpoints and are summed up to obtain an object wave. Finally, the hologram pattern is calculated by adding the object wave and an appropriate reference wave. The sampling theorem is considered to determine the arrangement of the viewpoints and the resolution of the parallax images.

The proposed technique was verified experimentally. An SLM with a resolution of 1,920 × 1,200 was used. We prepared 10 × 5 viewpoints with an interval of 4.7 mm at a distance of 600 mm from the SLM. The resolution of the parallax images was 192 × 120. The calculation time was less than 0.1 s. We confirmed that appropriate parallax images could be observed at corresponding viewpoints.

8644-17, Session 4

Progress in updatable photorefractive polymer-based holographic displays via direct optical writing of computer-generated fringe patterns

Sundeep Jolly, James Barabas, Daniel E. Smalley, V. Michael Bove Jr., MIT Media Lab. (United States)

We have previously introduced an architecture for updatable photorefractive holographic display based around direct fringe writing of computer-generated holographic fringe patterns. In contrast to interference-based stereogram techniques for hologram exposure in photorefractive polymer (PRP) materials, the direct fringe writing architecture simplifies system design, reduces system footprint and cost, and offers greater affordances over the types of holographic images that can be recorded. In this paper, motivations and goals for employing a direct fringe writing architecture for photorefractive holographic imagers are reviewed, new methods for PRP exposure by micro-optical fields generated via spatial light modulation and telecentric optics are described, and resulting holographic images are presented and discussed. Experimental results are reviewed in the context of theoretical indicators for system performance.

**Conference 8644:
Practical Holography XXVII: Materials and Applications**

8644-18, Session 5

Color holography: recent improvements and applications (Invited Paper)

Hans I. Bjelkhagen, Hansholo Consulting Ltd. (United Kingdom)

A review of recent improvements and applications in color holography is provided. Color holography recording techniques in silver-halide emulsions and photopolymer materials are discussed. Both analogue Denisyuk color holograms and digitally-printed color holograms are described. The light sources used to illuminate the recorded holograms are very important to obtain ultra-realistic 3-D images. In particular the new light sources based on RGB LEDs are significant improvements in displaying color holograms with improved image quality over today's commonly used halogen lights. Color holograms of museum artefacts have been recorded with new mobile holographic equipment.

8644-19, Session 5

Holofos: an optimized LED illumination system for color reflection holograms display

Andreas Sarakinos, Nikos Zervos, Alkis Lembessis, The Hellenic Institute of Holography (Greece)

True color reflection holograms can be successfully recorded by exposing panchromatic holographic plates to 3 or more LASER beams of suitable wavelengths. Traditional halogen spotlight illumination of color holograms relying on reflection holograms' Bragg diffraction sampling capabilities has many drawbacks. This kind of illumination, especially for a broadband hologram, results in heightened levels of chromatic dispersion and blurring of image points far from the hologram's surface. On the other hand, by intensity mixing of selected narrow band LEDs with peak wavelengths matched to those used during recording, high quality reproduction of deep color holograms can be achieved. In this paper we will present the HoLoFos LED RGB and RGBW color hologram illuminating devices. These devices have a wide color gamut achieved by precision, digitally controlled, RGB intensity mixing at pre selected wavelengths. Dichroic and refractive optics combine the RGB or RGBW LEDs' beams into quasi point-source output beam of uniform color cross section. A quantitative spectro-radiometric characterization of the HoLoFos devices and resolution tests results using a series of test holograms will also be presented.

8644-20, Session 5

Quantitative phase noise in a two-color low-coherence digital holographic microscope

Zahra Monemhagdoust, Ecole Polytechnique Fédérale de Lausanne (Switzerland); Frédéric Montfort, Yves Emery, Lyncée Tec SA (Switzerland); Christian D. Depeursinge, Lyncée Tec SA (Switzerland) and Ecole Polytechnique Fédérale de Lausanne (Switzerland); Christophe Moser, Ecole Polytechnique Fédérale de Lausanne (Switzerland)

In digital holographic microscopy, the long coherence length of laser light causes parasitic interferences due to multiple reflections in and by optical components in the optical path of the microscope and thus degrades the image quality. The parasitic effects are greatly reduced by using a short coherence length light source. The main drawback of using a short coherence light source in off-axis digital holographic microscope, is the reduction of the interference fringe contrast occurring in the field of view. A volume diffractive optical element (VDOE) is designed and fabricated to enable single shot full-field imaging in a digital holographic microscope with two low coherence sources in a single reference arm. Single shot image acquisition at both wavelengths allows for high speed imaging and increasing the axial unambiguous range. The VDOE for dual-color operation is composed of two multiplexed slanted transmission

volume gratings recorded on a photopolymer, with mutually orthogonal coherence plane tilts. Each multiplexed grating is designed to the respective wavelength in the reference arm of an off-axis two color DHM. Coherent interferences associated by the VDOE introduce coherent phase noise in the phase measurements which influences the image quality and the vertical accuracy. This effect is numerically analysed and experimentally quantified in a commercial system.

8644-21, Session 5

Holographic elements and holographic techniques used in photonics

Gerald L. Heidt, Dominic Speer, Wasatch Photonics, Inc. (United States)

Since the invention of holography in 1948, most of the attention has been focused on holographic three-dimensional images and displays. This new 3D technology generated a lot of attention in the 70's through the 90's. The work that was being done for manipulating light other than 3D imaging and displays was not as well known. This paper discusses how holographic elements and holographic interference techniques are now being used in the Photonics industry.

8644-22, Session 6

Stacked binary diffractive optical element for generating high-resolution pattern

Ting-Xuan Hua, Cheng-Huan Chen, National Tsing Hua Univ. (Taiwan)

Phase type binary diffractive optical element(DOE) has become popular due to its surface relief can be fabricated with lithography process. The complexity and efficiency of the diffraction pattern is limited by the number of phase level and resolution of the surface relief. Higher phase level and resolution demands higher precision in the process to obtain the desired diffraction pattern. The four level DOE requests two photomasks in the fabrication process, and the alignment as well as the processing parameter has been well developed in our laboratory. However, the number of phase level is not enough for generating sufficiently fine image pattern as desired. The stacking of two four level binary DOEs has been proposed to resolve this issue. Two design methods for the DOE have been exploited and compared with each other on the performance, one is the equivalent eight level model, and the other one is the combinational model of two functional DOEs. The fabrication process of the DOE can be divided into three steps, the first one is the photomasks preparation, and the second one is the lithography process on silicon substrate to make the negative mold such as exposure, development, and etching, and the last one is pressing on UV curing adhesive with silicon mold, exposing to UV light to form solid micro structures, and mold removal. The developed methodology will be useful for enhancing the function or performance of binary DOE with limited phase level and resolution due to the constrain from the available precision in fabrication process.

**Conference 8644:
Practical Holography XXVII: Materials and Applications**

8644-23, Session 6

Modeling and design of grating-assisted semiconductor lasers for biomedical imaging by digital holographic microscopy

Meng-Mu Shih, Univ. of Florida (United States)

The digital holographic microscopy can provide three-dimensional images, which are reconstructed from the light scattering of biomedical samples. Recently red semiconductor lasers were used as the light sources in the early detection of neuronal cell death. Compact semiconductor lasers with integrated metal-gratings can improve the light-source stability and system performance. This presentation demonstrates the theoretical modeling of such lasers by using the photonic and the optical methods. Numerical results about the grating-assisted coupling by these two methods are close when varying structural and material parameters. Qualitative interpretations of quantitative results provide insights into the modeling and design of such lasers.

8644-25, Session 6

Interaction and collaboration in an HOE-based autostereoscopic display

Jonny Gustafsson, Kungliga Tekniska Högskolan (Sweden)

Many applications can benefit greatly from using 3D displays. One of these applications is product development, where 3D viewing can enhance the understanding of a design and the making of a real physical model often would be too slow or expensive. The development of and decision on a design are highly collaborative processes. The tools used for design visualization should therefore also allow for good communication, both between people locally and between different geographical sites.

With these requirements in mind we have been working on an autostereoscopic display that uses a holographic optical element¹. This display technology can be used in many configurations and geometries. For the product development application we have chosen to mount the display as a table top. This image can be displayed over the table top so it can be freely interacted with, by hand or by using haptic devices.

The table top configuration and the fact that the viewer does not need to wear special glasses or some other equipment helps to make communication between the users easier and more natural.

In this presentation we describe a development of the display which can be viewed from two sides of the table. We also describe interaction techniques used on the display and communication between displays of the same or different types.

J. Gustafsson, C. Lindfors, L. Mattsson, T. Kjellberg, "Large-format 3D interaction table", in *Stereoscopic Displays and Virtual Reality Systems XII*, Proc. SPIE 5664, 589-595, (2005)

8644-26, Session 7

Hidden images of holography: wavefront reconstruction of abnormalities within holographic recording

Martin J. Richardson, De Montfort Univ. (United Kingdom)

Unplanned abnormalities within the holographic recording often lead to new areas of research. When recording off-axis pulsed laser transmission holograms, one may observe a number of un-planned visual wavefronts in the form of spurious light which records optics and the presence of individuals captured in the lab during the recording. For example, optical echo, polarization effects and hitherto unexplained coherence elongations result in holograms with astounding depth and the outlines of negative space, or destructive interference, caused by movement

during the pulsed duration. These awkward results can lead to new areas of research because abnormalities add to our knowledge and understanding of the physics of holography. This paper offers an insight of such recordings where unrehearsed abnormalities are observed and reported.

8644-27, Session 7

The hologram as a space of illusion

Rosa M. Oliveira, Univ. de Aveiro (Portugal)

One of the most interesting aspects of art holography is the study of 3D holographic image. Over the centuries, artists have chased the best way to represent the third dimension as similar to reality as possible. Several steps have been given in this direction, first with the perspective, then with the photography, later with the movies, but all of these representations of reality wouldn't reach the complete objective. The realism of a 3D representation on a 2D support (paper, canvas, celluloid) is completely overcome by holography. In spite of the fact that the holographic plate or film is also a 2D support, the holographic image is a recording of all the information of the object contained in light. Our perception doesn't need to translate the object as real. It is real. Though immaterial, the holographic image is real because it exists in light. The same parallax, the same shape. The representation is no more an imitation of the reality but a replacement of the real object or scene.

The space where it exists is a space of illusion and multiple objects can occupy the same place in the hologram, depending on the viewer's time and place. This introduces the fourth dimension in the hologram: the time, as well as the apparent conflict between the presence and the absence of images, which is just possible in holography.

8644-28, Session 7

Time cognition: inside and outside the holographic space

Maria I. Azevedo, Martin J. Richardson, De Montfort Univ. (United Kingdom); Luís Miguel Bernardo, Univ. de Porto (Portugal)

During the Renaissance, man placed himself in a vantage point to organize the sensorial data of the surrounding world that expressed the supremacy of his viewpoint; the man of the twentieth-first century is looking at the world as a whole from its orbit, not from inside like the Renaissance man did with perspective, but from outside, like we do with holography, to have a totalling view and to be able to explore and control it more firmly.

These concepts are examined, and inform a series of Digital Art Holograms and Lenticular technology based on different geometries for image capture, using the HoloCam Portable Light System, with the Canon camera angled toward the floor, according different angles and different heights.

Using concepts of time and space we explore the idea of improve the holographic space, on one hand, trying that the space is down than the floor and in other hand, working the holographic image in a way that the shapes are coming to the plate into the space of the viewer, from back to forward, in a way that the surface of the plate don't seems the frontier.

Further work related these concepts to Virtual and Augmented Reality systems, forging research directions and creating experiences.

**Conference 8644:
Practical Holography XXVII: Materials and Applications**

8644-29, Session 7

Time and space through light

Sandra Oliveira, Martin J. Richardson, De Montfort Univ. (United Kingdom)

The concept of developing artworks using light as a technique has been a subject of different approaches by artists for centuries. Nevertheless, only in the last century have artists been able to go further in exploring different views and forms by contemplating new creations, which personify light as the subject matter. Holographic techniques have been paramount in this evolution due to its specific characteristics that enable the creation of time and space with light on a surface. These elements are fundamental for the development of creativity as the specific instruments used achieve the materialization of a concept. Light with its unique composition became a pencil with which the artists could draw, taking the process of creativity to a new level, opening new doors regarding how art is approached, created and seen.

This paper will explore the relationship between space and time driven by light, and demonstrates the way light covers and embodies space depicting time in holographic conceptions. Light is a fundamental and essential instrument in holography and could be described as the catalyst that brings time and space together. Therefore the inclusion of light with time and space produces a new depth to artistic creativity. The synergy produced by combining the three elements of time, space and light result in a three dimensional image which gives an authentic and genuine replication of the subject matter.

8644-30, Session 7

Time stands still

Yin-Ren Chang, Martin J. Richardson, Chien-Chung Chen, De Montfort Univ. (United Kingdom)

Among traditional painting techniques in fine art, cubists appropriate elements of abstraction by discarding the traditional methods of perspective, in order to represent movement and multiple points of view within two-dimensional images. Moreover, cubists try to approach the sculptural medium in a painterly way by accumulating layers of angular planes and to create a faceted surface in an object. This art style proposes movement of an object in the play of light on its many angles. Holography as a time-based art medium, it opens up fresh opportunity to make spatiotemporal artistic statements in a new sensory experience.

In contemporary holographic art, computer graphic technologies have been the pivotal source of digital holography. "Time stands still" aims to discuss the potential of employing computer geometric shape modelling in holography, and developments from modern art. Exploring how 3D visual language is used by artist and makes the material/immaterial with experimental holographic creative works. This paper tries not only to discuss the relationship between 3D objects and depicting motion, but also to bring to reality the interplay between spatial dimensions and the interaction between a flat surface and a realistic emergent form in the theme of time movement.

8644-31, Session PWed

Short-wave boundary of applicability of relief-phase reflecting holograms on a thin film of a chalcogenide glassy semiconductor

Sergey N. Koreshev, National Research Univ. of Information Technologies, Mechanics and Optics (Russian Federation); Vladislav P. Ratushny, HoloGrate, JSC (Russian Federation)

In the course of carrying out the present work, it was stated that a parasitic surface nano-structurization is peculiar to reflective relief-phase holograms obtained on thin layers of a chalcogenide glassy semiconductor (CGS). The results of experimental researches of the

effect of a relief height for reflective relief-phase holograms on the parameters of their surface parasitic nano-structurization are presented in this paper. With the use of data obtained applying atomic force microscope (AFM) Solver P-47 and software complex "Nova", it was defined a short-wave boundary for applicability of such holograms. In addition to the conventional software complex "Nova", aiming at reducing time necessary for determination of a short-wave boundary for relief-phase hologram applicability, there was developed a software module, which operation is based on the determination of the averaged-out over a basic area (scanning area) relief profile shape of the hologram structure, the definition of root-mean-square roughness (RMSR) values of its surface averaged-out over the same basic area, and on the subsequent computation of the boundary wavelength for the hologram applicability. The determined short-wave boundary value came to 80nm. Starting from this value, the holograms with the relief height optimal from the view of maximal diffraction efficiency meet the Marechal's criterion $\sigma \ll \lambda/27$ (σ - root-mean-square roughness parameter) and the criterion of permitted light diffusion $\sigma \ll \lambda/100$. Thus, the level of light diffusion and aberration permitted for precision optical systems is ensured in a reconstructed with their use image.

8644-32, Session PWed

Direct fringe printer for computer-generated holograms: improvement of printing speed

Hiroshi Yoshikawa, Nihon Univ. (Japan); Takeshi Yamaguchi, Nihon Univ (Japan); Satoshi Kajiro, Nihon Univ. (Japan)

We have been developing direct fringe printer that can output holographic fringe on a photosensitive material. The pixel pitch of the printer is 0.44 micro-meter and the printing speed is 3 GPixels per hour. Although the speed is faster than that of other printing methods, more speed is desired to print over 100 GPixels holograms. In this paper, we use high power laser to reduce the settling time that is required to eliminate vibration after a stepper motor movement. Some other improvements are also discussed.

8644-33, Session PWed

A hologram recording method for 1 Tbit/in²

Shohei Ozawa, Kaito Okubo, Hiroyuki Kurata, Takefumi Yamada, Manabu Yamamoto, Tokyo Univ. of Science (Japan)

Recently, the development of a mass archival memory for the data center is demanded. As an archival memory, the hologram memory is suitable, and several terabit per square inch is demanded as for the memory capacity. In this paper, we studied about a record reproduction method that was able to correspond to 1TB memory capacity. The record reconstruction method is shown as follows. First of all, holograms are written by shift multiplexed recording that uses spherical reference wave

- (1) The angle of incidence degree of spherical reference beams (interference angle between the signal beam and the reference beam) is changed, and two or more holograms are overwritten in the same track.
- (2) Shift multiplexing in a radial direction and multiplexed holograms are overwritten in a same way.

In this method, the multiplexed holograms can be recorded by medium shift because it uses spherical reference beams. Moreover, we can overwrite new holograms by slightly changing the reference beam angle in a shift-multiplexing method. In addition, because it uses spherical reference beam, the shift-multiplexed recording in the radial direction becomes possible. We can verify both shift-multiplexed recording with 5?m shift and overwriting 5 track data in a one same track. Also, the 50?m shift multiplexing can be obtained in a radial direction of a disk. By using these methods, the data capacity can be expected to reach several terabit per square inch.

**Conference 8644:
Practical Holography XXVII: Materials and Applications**

8644-34, Session PWed

The design of ROM-type holographic memory with iterative Fourier transform algorithm

Hideki Akamatsu, Shuhei Yoshida, Unno Noriyuki, Kai Yamada, Manabu Yamamoto, Tokyo Univ. of Science (Japan)

The research of the hologram memory is advanced as one of the high-speed, mass storage systems of the next generation. Especially, it is given priority to the write-once system that uses the photo polymer as a recording medium, and recently the development of a mass ROM type hologram memory that replaces a past optical disk becomes important. In this paper, the repetition Fourier transform algorithm was adopted to make the hologram memory of ROM type by using the element that had the phase distribution like diffractive optics (DOE), and the design and the evaluation were performed.

The sample was made for trial purposes with electron beam cutting based on the simulation result, and the performance of the reproduction image was evaluated.

It was confirmed that the hologram designed by the repetition Fourier transform algorithm had been appropriately reproduced as a result.

In the experiment, first of all, the simulation method was verified with a phase modulation machine. Next, the direction of depth was concretely modulated to multivalued by the electron beam cutting method and DOE was made. The purpose of making of the direction of depth multivalued is to obtain high SNR as for the improvement of the level of the reproduced output of DOE?

The experimental and the simulation results are demonstrated in the conference.

8644-35, Session PWed

Spatial frequency study of holograms with albumins material

Manuel Jorge Ordóñez-Padilla, Arturo Olivares-Pérez, Luis R. Berriel-Valdos, Instituto Nacional de Astrofísica, Óptica y Electrónica (Mexico)

We present the analysis of holographic recording in photosensitive films using albumin matrixes: gallus gallus and Callipepla cali, exposed to a $\lambda = 442\text{nm}$, with ammonium dichromate as a photo-oxidant agent. These simultaneously were performed holographic diffraction gratings with different spatial frequencies. Getting high diffraction efficiencies of holographic gratings as a function of spatial frequency (lines/mm), known as modulo of the transfer function (MTF). We made a comparison of the experimental results between the different bird albumins.

8644-36, Session PWed

Spatial frequency behavior of holograms made with pectin and oxidizing agents

Manuel Jorge Ordóñez-Padilla, Arturo Olivares-Pérez D.D.S., Instituto Nacional de Astrofísica, Óptica y Electrónica (Mexico); Nicolás Grijalva-Ortiz, Benemérita Univ. Autónoma de Puebla (Mexico); Israel Fuentes-Tapia, Instituto Nacional de Astrofísica, Óptica y Electrónica (Mexico)

We present an analysis of photosensitive holographic films with pectin, registered with a wavelength of $\lambda = 442\text{ nm}$, He-Cd laser. These were used as agents of photo-oxidation, two substances: ammonium dichromate and iron ammonium citrate. Simultaneously, experimental procedures were performed for different spatial frequencies of holographic gratings. These were determined experimentally diffraction efficiencies of gratings as a function of spatial frequency (lines/mm)

known as modulo of transfer function (MTF). We show a comparison of results between the matrices prepared with different oxidizing agents.

8644-37, Session PWed

Measurement method for objective evaluation of reconstructed image quality in CGH

Kazuhiro Suzuki, Yuji Sakamoto, Hokkaido Univ. (Japan)

CGH (Computer Generated Hologram) is a hologram generated by simulating the recording process of a hologram in a computer. Various methods have been proposed for generating a hologram in CGH. However, objective evaluation method for comparing the reconstructed images by the hologram created by each method has not been established. To compare the reconstructed images, subjective evaluation is generally performed, however, it is necessary for subjective evaluation to standardize various conditions such as age and vision of the subject. Therefore, the objective evaluation is necessary to compare the quality of reconstructed images.

VSNR (Volume Signal to Noise Ratio) has been proposed for objective evaluation. VSNR is a three-dimensionally extended SNR (Signal to Noise Ratio), and it represents the difference between spatial light distribution of the reconstructed images and real object. Therefore VSNR is usable for quality measuring in the 3D domain. However, measurement and comparison of VSNR have been performed only computer simulation.

In this paper, we propose the measurement method of spatial light distribution using digital camera and determines the VSNR. By taking pictures of the reconstructed images and real objects at various focal lengths, the spatial light distributions are generated. VSNRs of various CGH methods and multi-view 3D display technologies are measured by the distributions. As comparing the VSNRs, we show the relation of VSNRs between different CGH methods, and it is confirmed that the speckle noise deteriorate VSNR of the reconstructed images of holograms.

8644-38, Session PWed

Eyepiece-type full-color electro-holographic display for binocular vision

Takuo Yoneyama, Chanyoung Yang, Yuji Sakamoto, Hokkaido Univ. (Japan); Fumio Okuyama, Suzuka Univ. of Medical Science (Japan)

There are head-mounted type 3-D displays with see-through vision which are expected to be useful with the Augmented Reality technique which provide visible information. However, because they are used stereoscopic method for 3-D vision, observer tends to be tired to see the 3-D image due to the disparity between accommodation and convergence. On the other hand, electro-holography is the technique which displays holograms on electro-devices such as spatial light modulator, and enables observers to see ideal 3-D images without feeling uncomfortable for many hours.

Therefore, we apply the holography technique into eye-piece type display in order to solve the disparity problem. Our system shows larger size of reconstructed image than conventional electro-holographic display by using the Fourier transform optical system. In stereoscopic display, apparent depths of objects are influenced by difference of PD (pupilo distance) but in our system, the influence is eliminated. Moreover, the time sequential method is adopted to reconstruct full-color holographic images. The influence caused by difference of PD, distortion of the reconstructed images due to using lens and different wave length for color are corrected by proposed algorithm to calculate computer-generated hologram.

In this paper, we proposed the calculation algorithm and report fabrication of the eye-piece type full color electro-holographic display for binocular vision. To confirm the effectiveness of the proposed system, the reconstructed images are evaluated objectively and subjectively. Results

**Conference 8644:
Practical Holography XXVII: Materials and Applications**

of experiments show that reconstructed full-color images are located correct depths and have correct parallax.

8644-39, Session PWed

Compound common-path digital holographic microscope

Weijuan Qu, NgeeAnn Polytechnic (Singapore); Zhaomin Wang, Chee Yuen Cheng, Ngee Ann Polytechnic (Singapore); Anand K. Asundi, Nanyang Technological Univ. (Singapore)

A compound digital holographic microscope (with reflection mode and transmission mode) has been build up based on a unique optical configuration of digital holographic microscopy. A cube beam splitter in the optical path both split and combine a diverging spherical wavefront emerging from a microscope objective to give off-axis digital holograms. When a plane numerical reference wavefront is used for the reconstruction, the phase curvature introduced by the microscope objective together with the illuminating wave to the object wave can be physically compensated. Results from surfaces structures on silicon wafer and micro-optics on fused silica demonstrate applications of this compound digital holographic microscope for technical inspection in material science.

8644-40, Session PWed

Holographic diffraction gratings to measure micromovements

Arturo Olivares-Pérez D.D.S., Instituto Nacional de Astrofísica, Óptica y Electrónica (Mexico); Mayra A. Lara-Peña, Janeth A. García-Monge, Pavel A. Valencia-Acuña, Joan M. Villa-Hernández, Univ. de Sonora (Mexico)

Holographic diffraction gratings can measure micro movements, with a system that detects each period of the moving grating. One of the important features of this device is the grating period, which determines the measurement accuracy. The period can be on the order of fractions of micron, with high reproducibility and with an error of half period. One of the qualities of this system is its robustness; the measures are invariant to noise induced by device movements and environment thermal changes.

8644-41, Session PWed

Acrylamide-adhesive as holographic recording medium

Santa Toxqui-López, Benemérita Univ. Autónoma de Puebla (Mexico); Arturo Olivares-Pérez D.D.S., Israel Fuentes-Tapia, Instituto Nacional de Astrofísica, Óptica y Electrónica (Mexico)

In recent years, many types of polymers have been used in different recording holographic medium due their relatively low cost and some of them are be self-developing needing no wet processing or thermal treatment. Therefore, in this research recording materials based on Acrylamide-adhesive polymer layer are prepared by gravity settling method after time drying, the layers are characterized by recording transmission holographic gratings (LSR 445 NL 445 nm) and measuring the first order diffraction efficiency holographic parameter. This recording material has good diffraction efficiency and environmental stability.

8644-42, Session PWed

An optical symmetric cryptographic system with simultaneous encryption and transmission of binary data and secret key by using dual phase-shifting digital holography

Sang Keun Gil, Univ. of Suwon (Korea, Republic of); Seok Hee Jeon, Univ. of Incheon (Korea, Republic of); Jong Rae Jung, Suwon Science College (Korea, Republic of)

We propose a new optical symmetric cryptographic system with simultaneous encryption and transmission of binary data and secret key by using dual phase-shifting digital holography. Dual phase-shifting digital holography contains two inner and outer interferometers which are used for encrypting data and a secret key at the same time. The technique using dual phase-shifting digital holographic interferometry is efficient because this scheme has an advantage of interference fringe data acquiring time. In this system, 2-step phase-shifting digital interferograms are acquired by moving the PZT mirror with phase step of 0 or $\pi/2$ in the reference beam path and are recorded on CCD. The secret key is expressed with random binary amplitude and random phase for convenience. Binary information data is encrypted by the secret key by applying phase-shifting digital holographic method, and this secret key is also encrypted by phase-shifting digital holographic method and transmitted. Encrypted digital hologram in our method is Fourier transform hologram and is recorded on CCD with 256 gray-level quantized intensities. These encrypted digital holograms are able to be stored by computer and be transmitted over a communication network. With this encrypted digital hologram, the original binary data are decrypted by the same secret key. Simulation results show that the proposed method can be used for a cipher and security system.

8644-43, Session PWed

Fast generation of video hologram patterns by use of motion vectors of three-dimensional objects

Seung-Cheol Kim, Xiao-Bin Dong, Min Woo Kwon, Eun-Soo Kim, Kwangwoon Univ. (Korea, Republic of)

Thus far, various approaches to generate the computer-generated holograms (CGHs) of 3-D objects have been suggested but, most of them have been applied to the still images, not to the video images due to their computational complexity. Recently, a method to fast compute the CGH patterns of 3-D video images has been proposed by combined use of data compression and novel look-up table (N-LUT) techniques. In this method, temporally redundant data of 3-D video images are removed with the differential pulse code modulation (DPCM) algorithm and then the CGH patterns for these compressed video images are calculated with the N-LUT method. However, as the 3-D objects move rapidly, image differences between the video frames may increase, which results in a massive growth of calculation time of the video holograms. Therefore, we propose a novel approach to significantly reduce the computation time of 3-D video holograms by employing a new concept of motion-vector of the 3-D object. In the proposed method, 3-D objects are firstly segmented from the 1st frame of the 3-D videos, and the CGH patterns for each segmented object are computed with the N-LUT algorithm. Secondly, motion vectors between each segmented object and the corresponding objects in the consecutive 3-D video frames are calculated. Thirdly, the CGH patterns for each segmented object are shifted with the calculated motion vectors. Finally, all these shifted CGH patterns are added up to generate the hologram patterns of the consecutive 3-D video frames. To confirm the feasibility of the proposed method, experiments are performed and the results are comparatively discussed with the conventional methods in terms of the number of object points and computation time.

8644-44, Session PWed

Holographic optical element for head-mounted display application using photopolymer

Jing-Ai Piao, Mei-Lan Piao, Chungbuk National Univ. (Korea, Republic of); Eun-Seok Kim, EunSung Display Co., Ltd. (Korea, Republic of); Nam Kim, Chungbuk National Univ. (Korea, Republic of)

We studied HOE (Holographic Optical Element) which using photopolymer as the material, and analyzed the optical characteristic for applying it to HMD (Head Mounted Display). HMD is a display device, worn on the head or as part of a helmet that has a small display optic in front of one or each eye. Since the HMD is embedded various optical elements in limited space to display virtual image, reducing size of the optical elements volume is one of the issue. In order to solve this problem, we proposed a novel material: photopolymer, as the HOE for HMD optical element. Photopolymer is one of the hologram recording materials, it has high diffraction efficiency, after recording hologram we don't need any chemical or thermal processing.

The HOE can manufacture various optical elements easily, for example mirror, lens, and optical filter. Comparing with conventional HMD system it will significantly reduce the size and weight of the optical elements. To confirm the possibility of photopolymer application for HMD, we designed the HOE structure using photopolymer to replace two optical system of conventional see-through HMD. One is couple in optics system and the other one is couple out optics system. The couple in optics is an optical system that guiding the beam of display image into LGP (Light Guide Plate), and the couple out optics system receives the beam through LGP to guide it in the pupil of people. We have carried out experiments to verify the validity of the proposed method.

Conference 8645: Broadband Access Communication Technologies VII

Tuesday - Thursday 5 -7 February 2013

Part of Proceedings of SPIE Vol. 8645 Broadband Access Communication Technologies VII

8645-1, Session 1

MIMO - free space optics (*Invited Paper*)

Z. Ghassemlooy, Northumbria Univ. (United Kingdom)

In the past decade, the world has witnessed a dramatic increase in the traffic carried by the telecommunication networks. Optical fibre based systems have a long way to go, before it reaches the customer premises because of very high installation costs. Wireless solutions such as radio frequency are also limited in bandwidth due to the low carrier frequencies used and regulated spectrum. FSO can provide an economically viable, attractive alternative, offering an ultra high bandwidth at much lower cost. Terrestrial FSO is a cost effective way of solving the last mile access network bottleneck by offering end users a huge bandwidth that is comparable to that obtainable from optical fibre. FSO technologies complements existing technologies in a number of applications where there is a need for higher data rates, improved service quality particularly in bandwidth hungry services such as video conferencing, telemedicine among others. Unfortunately, the advantages of FSO are obscured by the strong dependence of its performance on weather conditions. Fog, aerosols, rain and gases and other particles suspended in the atmosphere result in laser irradiance/intensity attenuation. Another factor that accounts for the FSO performance degradation in a clear atmosphere is the irradiance fluctuation (scintillation) and the phase fluctuation due to the atmospheric turbulence. To combat these problems and ensure full link availability the MIMO FSO system is one possible solution. This talk will give an overview of MIMO-FSO systems.

8645-2, Session 2

100-GHz and 300-GHz coherent radio-over-fiber transmission using optical frequency comb source

Atsushi Kanno, Toshiaki Kuri, Iwao Hosako, Tetsuya Kawanishi, National Institute of Information and Communications Technology (Japan); Yoshihiro Yasumura, Yuki Yoshida, Ken-ichi Kitayama, Osaka Univ. (Japan)

Direct and seamless conversion between optical and radio signals with high capacity transmission link has been highly demanded for future access network including home network. In this scenario, millimeter-wave and sub-millimeter-wave radios are promising candidates due to its broad bandwidth and atmospheric attenuation. For example, the attenuation values for 100 and 300 GHz are less than 0.4 and 3 dB/km, respectively. The low attenuation value can extend the transmission distance; thus 100-GHz band is applicable to an access network. On the other hand, at 300 GHz, the attenuation can not only prevent the interference effect but also increase the security due to its short transmission distance. To seamlessly convert between these high-frequency radios and optical signals, radio-over-fiber (RoF) technology is attractive.

We demonstrate 100- and 300-GHz RoF and radio signal transmission using combined RoF and digital coherent technologies. 25-GHz-spaced optical frequency comb source, which is comprised of an optical frequency shifter in an amplified optical fiber loop, set at a transmitter could provide frequency-stabilized 100- and 300-GHz RoF signals. The baseband component was modulated by 10-Gbaud quadrature-phase-shift-keying. The generated 100- and 300-GHz radio signals transmitted over the air were received by radio receivers consisting of all the electronic devices such as a mixer and an oscilloscope worked as an analogue-to-digital converter. Off-line digital signal processing in a similar manner as a conventional optical digital coherent receiver could successfully demodulate these radio signals within a forward error correction limit of a bit error rate of 2×10^{-3} .

8645-3, Session 2

FDMA-PON architecture according to the FABULOUS European project

Silvio Abrate, Istituto Superiore Mario Boella (Italy); Roberto Gaudino, Politecnico di Torino (Italy); Benoit Charbonnier, France Telecom R&D (France)

The FABULOUS Project proposes an NG-PON2 architecture based on:

- A first level of multiplexing on a single optical wavelength by using Frequency Division Multiplexing (FDM), and in particular FDM in downstream and FDMA in upstream.
- A higher level of multiplexing above FDM/FDMA using wavelength division multiplexing (WDM)
- Complete compatibility with currently deployed PON fiber plants, avoiding any active element or WDM filter in the optical distribution network
- A revolutionary reflective ONU (R-ONU) concept that goes beyond the R-SOA scheme and does not require fixed or tunable laser sources at the customer side, while exhibiting modulation format flexibility, polarization insensitivity, and an innovative Faraday rotation effect that helps to greatly simplify the Central Office (OLT) hardware infrastructure. The R-ONU will be designed, manufactured tested and demonstrated at all levels from the component level up to a full system demonstrator in a realistic PON experiment. The R-ONU transceiver will be built onto a single Silicon Photonics chip.
- Self-coherent receiver at the OLT side, allowing much higher performance than direct detection receivers, thus solving the problem of reflective ONU architectures that usually have a very limited power budget available in the upstream path due to transmission impairments. Thanks to the implementation of an innovative Faraday rotation mechanism at the ONU, the self-coherent receiver of the OLT can be realized with a simplified configuration, avoiding the usual complicated and expensive polarization diversity schemes that imply duplication of high-cost resources such as optical hybrids and high-end Digital Signal Processing Units.

8645-4, Session 3

Devices for variation-tolerant low-loss high-index contrast photonic integrated circuits (*Invited Paper*)

Wesley D. Sacher, Joyce K. S. Poon, Univ. of Toronto (Canada)

High-index contrast material systems, such as silicon-on-insulator (SOI), have been the focus of extensive research in recent years with the aim of producing compact and energy-efficient photonic integrated circuits for long-haul, local area network, and even chip-scale communications. The compact device footprints attainable in these material systems come at the cost of substantially increased optical losses and sensitivity to nanoscale dimensional variations compared to low-index contrast planar lightwave circuits. Ultimately, for high index-contrast photonics to be a reliable and competitive alternative to traditional photonic circuits and bulk optics, high-index contrast devices must be low loss and variation tolerant.

In this work, we outline our designs and demonstrations of compact, low-loss, variation-tolerant optical devices in SOI and silicon-nitride-on-SOI (SiN-on-SOI) platforms. We describe our design and modelling strategies. The devices we will present include novel adiabatic polarization-splitters and rotators, polarization controllers, low-loss and high bandwidth grating couplers, and variation-tolerant microcavities for filtering and modulation. Our implementations with foundry partners will be discussed.

8645-5, Session 4

Active devices in next-generation access networks (*Invited Paper*)

Leo Spiekman, Alphion Corp. (United States)

Next generation access networks present many more opportunities and challenges in the optical layer than the present generation of such networks do. I will review the optical components that can be used advantageously in this environment, with an emphasis on optical amplifiers in PON extension and WDM-PON.

8645-6, Session 4

Constellation design for next-generation hierarchically-modulated PON systems

Naotaka Shibata, Noriko Iiyama, Jun-Ichi Kani, Sang-Yuep Kim, Jun Terada, Naoto Yoshimoto, Nippon Telegraph and Telephone Corp. (Japan)

Higher-order modulation and coherent detection are promising techniques for increasing the capacity per wavelength in the next-generation multi-wavelength passive optical network (PON) systems. To realize the capacity increase with accepting the co-existence of legacy optical network units (ONUs) that use on-off keying (OOK) and direct detection, we have proposed a hierarchically-modulated passive optical network (PON) system. In the proposed system, the optical line terminal (OLT) transmits a star quadrature amplitude modulation (QAM) signal in which a phase-shift keying (PSK) signal is multiplexed with an OOK signal. The legacy ONUs receive only the OOK part via direct detection while new ONUs receive the PSK signal in addition via coherent detection.

In this paper, we study the performance of signals with various constellations for the hierarchically-modulated PON systems that overlay an over 20-Gbps PSK signal on a 10-Gbps OOK signal; previous work examined only the performance of an 8-star QAM signal. All these signals consist of a PSK signal with lower amplitude (inner-PSK signal) and a PSK signal with higher amplitude (outer-PSK signal). We propose to decrease the modulation level of the inner-PSK signal and increase that of the outer-PSK signal for improving the bit error rate performance in some conditions. Simulations show the minimum required average received power for the various constellations examined: it is shown that effective design depends on the extinction ratio. For example, 10-star QAM improves the minimum required average received power by 3 dB compared to 8-star QAM when the extinction ratio is 12 dB.

8645-7, Session 4

WDM-PON power budget extension techniques for Nx10 Gbit/s DPSK signals

Ali Emsia, Technische Univ. Darmstadt (Germany); Quang Trung Le, Dieter Briggmann, Franko Küppers, Technical University of Darmstadt (Germany)

This paper shows optical power extension techniques for 10 Gbit/s per channel for WDM-PON DPSK systems. The scheme is based on semiconductor optical amplifiers. We present 56.5 total optical power budget enhancement using our configuration for the downstream scenario. The setup is cost effective in terms of optical components. Only one DLI (Delay Line Interferometer) is used to convert DPSK signals to OOK. We present experimentally as well as through simulations that our scheme has better performance than a single SOA as a power budget extender.

8645-8, Session 4

Next generation PON evolution (*Invited Paper*)

Anand Srivastava, Indian Institute of Technology Mandi (India)

A passive optical network (PON) features a point-to-multi-point (P2MP) architecture to provide broadband access. As full services are provisioned by the massive deployment of PON networks worldwide, operators expect more from PONs. These include improved bandwidths and service support capabilities as well as enhanced performance of access nodes and supportive equipment over their existing PON networks. The direction of PON evolution is a key issue for the telecom industry. Next-generation PONs are divided into two phases: NG-PON1 and NG-PON2. Mid-term upgrades in PON networks are defined as NG-PON1, while NG-PON2 is a long-term solution in PON evolution. Major requirements of NG-PON1 are the coexistence with the deployed GPON systems and the reuse of outside plant. Unlike NG-PON1 that has clear goals and emerging developments, there are many candidate technologies for NG-PON2. However, one thing is clear, NG-PON2 technology must outperform NG-PON1 technologies in terms of ODN compatibility, bandwidth, capacity, energy and cost efficiencies.

There are several types of prospective technologies that can be adopted for NG-PON2. Among the prospective technologies, the first method is to improve the rate to 40G from 10G by following the TDM technology. The second method is the employment of wavelength division multiplexing (WDM) PON to achieve 40G access. The possible multiplexing schemes can be coarse wavelength division multiplexing (CWDM) or dense wavelength division multiplexing (DWDM). The ODSM PON topology based on TDMA+WDMA is also suggested, which dynamically manages user spectrum without modifying the ODN and ONUs. The third prospect is OCDMA-PON. OCDMA-PON uses code division multiple access (CDMA) to encode ONU signals, thereby avoiding the timeslot assignment for data transmission required by a time division multiple access (TDMA) systems. The O-OFDMA PON topology is an option that uses orthogonal frequency division multiple access (OFDMA) technology to differentiate ONUs, thus effectively improving bandwidth usage.

This talk discusses the above prospective technologies for NG-PON2 within the framework of NG-PON recommendations

8645-9, Session 4

Chirp-managed lasers as cost-efficient transmitters for 10-Gbit/s WDM-PONs

Quang Trung Le, Ali Emsia, Dieter Briggmann, Franko Küppers, Technische Univ. Darmstadt (Germany)

This manuscript proposes the use of chirp managed lasers (CML) as cost-effective downstream (DS) transmitters for next generation access networks. As the laser bandwidth is as high as 10 GHz, the CML could be directly modulated at 10 Gbit/s for downstream transmission in future wavelength division multiplexing passive optical networks (WDM PON). The laser adiabatic chirp, which is the main drawback limiting the transmission performance of directly modulated lasers, is now used to generate phase-shift keying (PSK) modulation format by direct modulation. The direct PSK modulation is an attractive alternative to on-off keying format as a smaller modulation current is required, and the signal's spectral width is as narrow as the information bandwidth which is desired to minimize the inter-symbol interference due to fiber chromatic dispersion. The laser chirp analysis is investigated in details, and the relevant modulation scheme for direct differential PSK (DPSK) modulation is presented. The network architecture using CML as downstream transmitter is proposed. At the user premise, the wavelength reuse technique based on reflective colorless upstream transmitter is used. The optical network unit (ONU) reflects and orthogonally remodulates the received light with upstream data. A full-duplex transmission with symmetrical 10-Gbit/s bandwidth is demonstrated. Bit-error-rate measurement showed that an optical power budget of 36 dB could be obtained with direct phase-shift-keying modulation of CML which proves that the proposed solution could be a strong candidate for future WDM-PONs. For the upstream transmission, Rayleigh scattering effects are reported and analyzed in single-pass and bidirectional architectures.

**Conference 8645:
Broadband Access Communication Technologies VII**

8645-10, Session 5

Developments in photonic and mm-wave component technology for fiber radio (*Invited Paper*)

Stavros Iezekiel, Univ. of Cyprus (Cyprus)

A review of photonic component technology for fiber radio applications at 60 GHz will be given. We will focus on two architectures: (i) baseband-over-fiber and (ii) RF-over-fiber. In the first approach, up-conversion to 60 GHz is performed at the picocell base stations, with data being transported over fiber, while in the second both the data and mm-wave carrier are transported over fiber.

For the baseband-over-fiber scheme, we examine techniques to improve the modulation efficiency of directly-modulated fiber links. These are based on traveling-wave structures applied to series cascades of lasers. This approach combines the improvement in differential quantum efficiency with the ability to tailor impedance matching as required. In addition, we report on various base station transceiver architectures based on optically-controlled MMIC self-oscillating mixers, and their application to 60 GHz fiber radio. This approach is that it allows low cost optoelectronic transceivers to be used for the baseband fiber link, whilst minimizing the impact of dispersion.

For the RF-over-fiber scheme, we report on schemes for optical generation of 60 GHz. These use modulation of a Mach-Zehnder modulator at V_{pi} bias in cascade with a Mach-Zehnder driven by 12.5 Gb/s data. One of the issues in RF-over-fiber is dispersion, while reduced modulation efficiency due to the presence of the optical carrier is also problematic. We examine the use of silicon nitride micro-ring resonators for the production of optical single sideband modulation in order to combat dispersion, and for the reduction of optical carrier power in order to improve link modulation efficiency.

8645-11, Session 5

Millimeter-wave band 20-Gbps wireless data transmission using optical carrier suppression and DSP algorithm based on discrete multi-tone

Yong-Yuk Won, Jaeheung Kim, Sang-Kook Han, Yonsei Univ. (Korea, Republic of)

Various researches on broadband wireless data over optical fiber have been done for the high-resolution multimedia services. In this paper, a new scheme is proposed to support broadband wireless services. Based on the optical carrier suppression (OCS) and the discrete multi-tone (DMT), an optical fiber can transmit data higher than 20 Gbps which are wirelessly transmitted over millimeter-wave band. Two optical sidebands obtained by OCS technique are directly modulated on multiple RF subcarriers in the DMT and then transformed into millimeter-wave band carrier by photo-detector with bandwidth of 60 GHz. Multiple RF subcarriers, whose orthogonality is maintained by DMT technique, are also modulated with 20-Gbps data using modulation scheme such as quadrature phase shift keying (QPSK). To transmit wirelessly QPSK-formatted data by the DMT, an antenna should be designed with considering the fact that the DMT-QPSK wireless data are more sensitive to fading effects as well as wireless transmission length.

It also has to have a gain high enough to support data rate higher than 20 Gbps. From the Friis' transmission formula, it is expected that as the wavelength decreases the ratio of received power to transmitted power decreases. Since a high-gain antenna has a narrow beamwidth, it is important that the antenna can perform beamforming depending on the data rate. A new tapered slot antenna array has been also designed to generate narrow beams and its peak gain reaches up to 14 dBi. As a result, the link between transmitting and receiving antennas secure gain up to 24 dBi.

8645-12, Session 5

Seamless integration of 100-G wire line and 100-GHz wireless link system (*Invited Paper*)

Ze Dong, Georgia Institute of Technology (United States) and ZTE USA (United States); Jianjun Yu, ZTE USA (United States); Xinying Li, Nan Chi, Fudan Univ. (China)

We demonstrate how to integrate 100-G wireline signal in a 100-GHz wireless system. Key techniques includes high-performance 100-G polarization-division-multiplexing-16QAM optical signal generation with pre-equalization and post-equalization, all-optical signal up-conversion to 100 GHz and advanced digital signal processing (DSP). This DSP including the frequency domain down-conversion, compensation of chromatic dispersion, polarization de-multiplexing and carrier recovery has been proved valid even if the parallel 2x2 MIMO wireless link is utilized. The BER of the 100G signal over 400-km fiber and 0.5-m wireless at 100 GHz is smaller than FEC limitation.

8645-13, Session 5

Effect of the degree of phase-correlation of laser sources on the transmission and optical coherent detection in radio-over-fibre systems

Ramon Maldonado-Basilio, Ran Li, Sawsan Abdul-Majid, Hamdam Nikkiah, Univ. of Ottawa (Canada); Kin-Wai Leong, Viscore Technologies Inc. (Canada); Trevor J. Hall, Univ. of Ottawa (Canada)

High capacity radio-over-fiber (RoF) systems rely on the capability to efficiently generate, transport, and detect millimeter-wave carriers modulated at high data rates. Heterodyne beating of two independent laser sources has been proposed as an alternative to generate multi-Gbps quadrature phase modulated signals imposed on millimeter wave carriers, which avoids the need for electronic generation of high frequency carriers. Implementing complex modulation formats at the RoF down-link along with the optical coherent detection at the receiver end overcomes some of the issues found in intensity modulation direct detection schemes.

In this work, the performance improvement of a coherent RoF system carrying 10Gbps QPSK signals is numerically analyzed in terms of the degree of phase correlation between the lasers utilised at the down-link (optical heterodyne beating) and at the up-link (optical coherent detection). Relative to phase correlated lasers featuring linewidths of 10MHz, the peak power of the 60GHz carrier generated at the down-link is reduced by 8dB for uncorrelated lasers. In addition, the error vector magnitude of the received signal at the up-link is improved from over 20% (for uncorrelated lasers and linewidths of 5MHz) to around 7% (for correlated lasers) at an optical received power of -30dBm. The results obtained reinforce the idea of using coherent comb laser sources with phase correlated modes located at the Central Office. It also motivates the eventual deployment of techniques to control the degree of phase-correlation between the lasers used as signal and local oscillator at the optical coherent receivers.

**Conference 8645:
Broadband Access Communication Technologies VII**

8645-14, Session 5

Power consumption of communication systems employing radio-over-fiber distributed antenna systems for railway

Tien Dat Pham, Atsushi Kanno, Tetsuya Kawanishi, National Institute of Information and Communications Technology (Japan)

New wireless technologies which can adapt bandwidth requirements for broadband and multimedia services such as WiMAX and LTE have recently developed. To deal with high demands on bandwidth especially in dense population areas, cellular networks have changed towards using smaller cells. However, the needs of fast moving users in the car or on the train have not been paid much attention. Fast moving users are still needed to transfer to large cells, which considerably reduces their available bandwidth. Meanwhile, trains with high speed have been developed rapidly worldwide, and considered as a fast, convenient and green public transportation system. Because high speed trains normally travel over a long distance, there will be a strong demand for broadband wireless communication in high speed trains.

Cellular-based trackside networks with small cells and high carrier frequencies can be a promising solution for railway. In that situation, radio-over-fiber distributed antenna systems utilizing WDM technology can be an attractive means to interconnect remote antenna units along the railway track to the control stations. However, considering a huge number of remote antenna units placed along the track, power consumption will become one of the main concerning factors. In this paper, we propose a model to investigate and optimize power consumption and energy efficiency of a RoF DAS system for railway. Based on the model, optimum system design in terms of remote cell size and number of cells in a WDM ring are derived with respect to minimizing system energy consumption. From the model we also can determine an appropriate approach to upgrade a currently deployed conventional cellular network to a RoF DAS system with least power consumption. The results demonstrate that by using RoF DAS systems, power consumption can be significantly reduced. The results in the paper might give some insights to the planning of broadband communication systems for railway in the future.

8645-15, Session 6

Optical wireless applications: a solution to ease the wireless airwaves spectrum crunch (Invited Paper)

Mohsen Kavehrad, The Pennsylvania State Univ. (United States)

With the increasing popularity of multimedia services supplied over the radio frequency networks, services such as web browsing, audio and video on demand, it is for sure only a matter of time before users will face extreme congestion while trying to connect to avail themselves of these aforementioned services. Advances in displays, battery technology and processing power have made it possible for users to afford and carry around smart phones and tablets. As we are entering a new era of always on connectivity, the expectation from users for not only ubiquitous but also seamless voice and video services presents a significant challenge for today's telecommunications systems. The prospects for the delivery of such multimedia services to these users are crucially dependent on the development of low cost physical layer delivery mechanisms.

According to market research published by Cisco Systems, Inc. [1] the largest manufacturer of networking equipment, mobile data consumption is going to explode in the next 5 years, largely due to the proliferation of mobile video and mobile web applications. Cisco market research includes the Visual Networking Index or VNI. The VNI research predicts mobile data use to expand from 90,000 terabytes to 3,600,000 terabytes monthly. This is an increase of a factor of 40 in 5 years, or more than 100% cumulative annual growth rate (CAGR). This is an enormous growth in mobile data, a very large portion of which is growth due to the proliferation of mobile video (66%). Much of this mobile data growth

(about 70%) will be consumed by laptops and other mobile ready portables such as pico-projectors, wireless reading devices, digital photo frames, and smart phones. These mobile devices can generally be thought of as in-building networked devices which are used to share information (video) within a classroom, conference, or meeting room. The report predicts that a greater amount of traffic will migrate from fixed to mobile networks.

In the past few years, we have witnessed rapid growth in technologies producing low-cost communications devices, using the RF license-free bands: ISM (2.4–2.4835 GHz), UNII (5.15–5.25 & 5.35–5.825 GHz). As the technology advances, the service capability of such devices will strengthen. However, uncontrolled deployment of devices using the same spectrum allocation can generate interference beyond the level systems can afford, thus leading to service quality deterioration. The IEEE 802.15.2 working group was formed to address this growing problem; however, without controlling the number of devices operating within certain areas, the problem cannot be solved, unless more bandwidth becomes available. The 57–64 GHz band has been added to license free bands; however design of communication systems at these extremely high frequencies is very challenging. It will take some years before products of reasonable cost and satisfactory performance will be introduced in the market. Also, adding bandwidth does not address the problem at its root. What is needed is a broadband, interference-free or at least interference-resistant technology, allowing easy frequency reuse made available to the customer at an affordable cost [2]. Considering the rapidly growing wireless consumer devices [1], it is evident that the need for such technology is quite urgent.

It is a known fact that the electromagnetic spectrum has become extremely crowded [3].

The wireless handheld devices require ever-increasing bandwidth, and along with that, explosive growth in inter-device wireless communications is already creating huge demands on spectrum resources which can be resolved only by near zero-sum allocation decisions, made through a mixture of bidding and politics.

As a possible alternative to ease the access to radio spectrum, higher frequency waves above 30 GHz tend to travel only a few miles or less and generally do not penetrate solid materials very well. This offers a sustainable solution for the current Spectrum Crunch in the lower microwave bands. One mission of this paper is to demonstrate practical and usable networks that can select a self-limiting link distance, allowing spectrum reuse. The motivation for operators of such bands to actually choose to self-limit is that by doing so, they improve the signal-to-noise against competing users at a lower cost than trying to overcome interference. These characteristics of wave propagation are not necessarily disadvantageous as they enable more densely packed communications links. Thus, high frequencies can provide very efficient spectrum utilization through "selective spectrum reuse", and naturally increase the security of transmissions.

Optical systems and networks offer a far greater bandwidth. This means new devices and systems have to be developed. Semiconductor Light Emitting Diode (LED) is considered to be the future primary lighting source for buildings, automobiles and aircrafts. LED provides higher energy efficiency compared to incandescent and fluorescent light sources and it will play a major role in the global reduction of carbon dioxide emissions, as a consequence of the significant energy savings. Lasers are also under investigation for similar applications. These core devices have the potential to revolutionize how we use light, including not only for illumination, but as well; for communications, sensing, navigation, positioning, surveillance, and imaging. In this paper we will elaborate on advantageous such networks can offer.

REFERENCES

1. "Cisco Visual Networking Index: Global Mobile Data Traffic Forecast Update, 2009-2014" [Available Online]: http://www.cisco.com/en/US/solutions/collateral/ns341/ns525/ns537/ns705/ns827/white_paper_c11-520862.html.
2. M. Kavehrad, "Sustainable Energy-Efficient Wireless Applications Using Light", IEEE Communications Magazine, pp. 66-73, December 2010.
3. D. Goldman, "Sorry, America: Your wireless airwaves are full", @CNN Money Tech, February 21, 2012.

8645-16, Session 6

Novel 60 GHz CPW array antennas with beam-forming features for indoor wireless over fiber networks

Ioannis Petropoulos, Spiros Mikroulis, Adonis Bogris, Technological Educational Institute of Athens (Greece); Hercules Simos, Technological Educational Institute of Piraeus (Greece); Kostantinos Voudouris, Technological Educational Institute of Athens (Greece)

License-free 60GHz based technology, which offers ultra-high bit rates in order to satisfy new demanding services, suffers from limited coverage due to increased propagation loss. In this case, Radio (Wireless) over Fiber (RoF) technology, can greatly improve the wireless network, in terms of low-cost, reduced power requirements, and improved performance. It is critical, to design high gain, adaptive antennas, integrated on a photonic substrate, in order to overcome physical limitations with a cost-efficient approach for next generation indoor wireless over fiber networks.

In this work, two types of high gain, low cost, 60 GHz coplanar waveguide (CPW) slot linear array antennas are designed using HFSS, for indoor use. The first type incorporates Rogers Duroid 6010 substrate ($\epsilon_r=10.6$) while the second type is based on InP substrate ($\epsilon_r=12.4$). Both antennas can be integrated with optoelectronic devices due to the utilization of high dielectric substrates. A comparison between the two aforementioned array types is performed regarding gain, bandwidth, beam width and scattering parameter (S11). In addition to this, beam-steering properties are investigated, in terms of radiation pattern and side lobe suppression, employing least mean square (LMS) algorithm to estimate the amplitude and phase of the excitation signals. An antenna gain up to 18 dBi for the Duroid substrate, and 16.5 dBi for the InP substrate, is calculated with a bandwidth between 1-1.5 GHz depending on the number of array elements. Finally, a feeding network is designed incorporating typical high-speed photodiode for array excitation, and matching properties are extracted.

8645-17, Session 6

Impact of new RAN architectures on fronthauling (Invited Paper)

Matthias Fricke, Deutsche Telekom AG (Germany)

This presentation provides a brief overview of the current implementation of the different mobile network generations. The issues typically discussed with Radio Access Networks are the effective realization of mobile backhauling and the resulting choice of technologies. The work presented, however, focuses solely on fronthauling. This is the part of RAN resulting from the splitting of the conventional baseband architecture into an RF unit and an actual signal processing unit. This separation, together with the reduction of the number of physical locations, sets new requirements on the access networks. Their impact on the transport, as well as a comparative analysis of advantages and drawbacks of likely future architecture, are presented.

8645-18, Session 6

Investigation on a low-cost single wavelength converged wired-60 GHz wireless OFDM-based system employing a photonic patch antenna

Spiros Mikroulis, Technological Educational Institute of Athens (Greece); Ivan Aldaya, Telecom Paris-Tech, Optical Communications Group (France); Ioannis Petropoulos,

Technological Educational Institute of Athens (Greece); Elias Giakoumidis, Athens Information Technology (Greece); Kostantinos Voudouris, Technological Educational Institute of Athens (Greece); Ioannis Tomkos, Athens Information Technology (Greece)

Wireless-based indoor access technology has been tremendously developed over the last decade, providing a bit rate, limited by the current standards, of up to 100Mbps. Ongoing this, the license-free spectrum at 60GHz, which offers an available bandwidth of 7GHz, can be utilized in order to satisfy the upcoming Giga-bit rate short range indoor networking needs. In addition to this, recent advances in wired broadband access, such as passive optical network (PON)-based fiber-to-the-x (FTTx) tend to resist against the bottleneck in the cable network deployment, known as the "last mile" problem. In this case, Radio (Wireless) over Fiber (RoF) technology, potentially re-using the already deployed PON-FTTx infrastructure, combines mobility and high capacity, through a cost efficient and green telecom approach.

In this work, a low cost converged wireline and 60GHz wireless hybrid system utilizing a single wavelength is proposed, employing two single electrode LiNbO3 modulators for all-optical frequency up-conversion, and baseband modulation. Additionally, a novel 15dBi, broadband, coplanar based, photonic patch array antenna is designed on a high dielectric substrate for application to a low-cost, efficient photonic-wireless transceiver. A microwave/optical/wireless design is utilized, in order to evaluate the system employing 3Gb/s quadrature phase shift keying (QPSK) orthogonal frequency division multiplexing (OFDM) based on IEEE 802.15.3c wireless prestandard and OFDM FTTx-PON co-propagating in a standard single mode fiber (SSMF). An acceptable forward error correction (FEC) aided performance Error Vector Magnitude (EVM) <32% is calculated for a wireless channel of up to 10m and a PON urban scenario of 20km length, respectively.

8645-19, Session 6

Proposal of adaptive wireless cell configuration for RoF-DAS over WDM-PON system

Tatsuhiko Iwakuni, Osaka Univ. (Japan); Kenji Miyamoto, NTT Access Network Service Systems Labs. (Japan); Takeshi Higashino, Nara Institute of Science and Technology (Japan); Katsutoshi Tsukamoto, Osaka Institute of Technology (Japan); Shozo Komaki, Univ. Teknologi Malaysia (Malaysia); Takayoshi Tashiro, Youichi Fukada, Jun-Ichi Kani, Naoto Yoshimoto, NTT Access Network Service Systems Labs. (Japan); Katsumi Iwatsuki, Tohoku Univ. (Japan)

Radio on fiber (RoF) - distributed antenna system (DAS) over wavelength division multiplexing - passive optical network (WDM-PON) with multiple - input multiple - output has been proposed as a next generation radio access network (RAN). This system employs optical time division multiplexing (OTDM) over one WDM channel to multiplex and transmit various types of wireless interfaces such as 3.9G, Wireless LAN and WiMAX. A combination of star and bus topologies has employed to cover a wide service area. The optical transmission loss is caused notably at remote base stations (RBSs) quipped on a WDM bus link. The loss is relatively small, but at the RBS far from the center station (CS), the RBS suffers the large accumulated loss, so the reduction of cell size provides the increasing of the number of RBSs, causes the degradation of the SNR of RoF link. This paper addresses this trade-off problem, and considers the application to the actual service area by the channel capacity investigation of RoF-DAS over WDM-PON with computer simulation. Then, this paper focuses on the flexibility of RoF-DAS over WDM-PON, considers the adaptive radio cell configuration according to population fluctuations of day and night, or densely populated areas and sparsely populated areas, respectively.

8645-24, Session PWed

Sensing RF signals with the optical wideband converter

George C. Valley, George A. Seffler, Thomas J. Shaw, The Aerospace Corp. (United States)

The optical wideband converter (OWC) is a system for measuring properties of RF signals in the GHz band without use of high speed electronics. In the OWC the RF signal is modulated on a repetitively pulsed optical field with a large wavelength chirp, the optical field is diffracted onto a spatial light modulator (SLM) whose pixels are modulated with a pseudo-random bit sequence (PRBS), and finally the optical field is directed to a photodiode and the resulting current integrated. The PRBS is then changed and another measurement is made. When the number of measurements equals the number of SLM pixels, the RF signal can be obtained in principle by multiplying the measurement vector by the inverse of the square matrix given by the PRBSs and the properties of the optics. When the number of measurements is smaller than the number of pixels, a compressive sensing (CS) measurement is performed, and sparse RF signals can be obtained using one of the standard CS recovery algorithms such as the penalized ℓ_1 norm (also known as basis pursuit denoising) or one of the variants of matching pursuit. Accurate reconstruction of RF signals requires good calibration of the OWC. This can be done using RF signals of sparsity 1 (e.g., single short pulses or single frequency sinusoids), or with conventional measurements of optical properties of the SLM and other components. In this talk, we present results using the OWC for several different classes of RF signals recovered using 3 techniques (matrix inversion, basis pursuit, and matching pursuit). We compare recovered waveforms using measurement matrices obtained with conventional calibration to those recovered using measurement matrices obtained by probing the OWC with sparse signals. Applications of the OWC in microwave photonics, test and measurement devices, and telecommunications are discussed.

8645-26, Session PWed

Overview of the performances of PMMA-SI-POF communication systems

Stefano Straullu, Silvio Abrate, Istituto Superiore Mario Boella (Italy)

Poly-Methyl-MethAcrylate based optical fibers with Step-Index profile and 1 mm core diameter (PMMA-SI-POF) are widely deployed in automobile infotainment systems thanks to the MOST standards that adopts them as the preferred physical medium. However, thanks to their mechanical robustness and tolerance and their ease of installation, they make a suitable medium for local networking. However, their good mechanical characteristics have to be paid in terms of performances, since PMMA-SI-POF based systems are severely limited in both bandwidth and attenuation. We will present a review of the best research results that have been obtained at the different speeds that are defined by the Ethernet standard: 10 Mb/s, 100 Mb/s and 1 Gb/s, showing that PMMA-SI-POF can easily overcome copper performances while being smaller, cheaper, easier to install in brownfield environment. To date, the following results have been obtained: 425 m at 10 Mb/s, 275 m at 100 Mb/s and 75 m at 1 Gb/s; these results have been obtained with commercial eye-safe components, and we believe that overcoming them requires in most cases the development of a new class of components.

An overview of the different modulation formats that have been adopted, the most suitable equalization techniques and the best affordable components will be given. In the end, an overview of the current commercial systems performances and the road standardization procedures are taking will be given.

8645-28, Session PWed

Precoding techniques for PAPR reduction in asymmetrically clipped OFDM based optical wireless system

Bilal A. Ranjha, Mohsen Kavehrad, The Pennsylvania State Univ. (United States)

In this paper, we have analyzed different precoding based Peak-to-Average-Power (PAPR) reduction techniques for asymmetrically-clipped Orthogonal Frequency Division Multiplexing (OFDM) optical wireless communication systems using LED. Intensity Modulated Direct Detection (IM/DD) technique is among the popular techniques for optical wireless communication systems. OFDM cannot be directly applied to IM systems because of the bipolar nature of the output signal. Therefore some variants of OFDM systems have been proposed for (IM/DD) optical wireless systems. Among them are DC-biased-OFDM, Asymmetrically-Clipped Optical OFDM (ACO-OFDM) and Pulse Amplitude Modulated Discrete Multitone (PAM-DMT). Both ACO-OFDM and PAM-DMT require low average power and thus are very attractive for optical wireless systems. OFDM systems suffer from high PAPR problem that can limit its performance due to non-linear characteristics of LED. Therefore PAPR reduction techniques have to be employed. This paper analyzes precoding based PAPR reduction methods for ACO-OFDM and PAM-DMT. We have used Discrete Fourier Transform (DFT) coding, Zadoff-Chu Transform (ZCT) and Discrete Cosine Transform (DCT) for ACO-OFDM and only DCT for PAM-DMT since the modulating symbols are real. We have compared the performance of these precoding techniques using different QAM modulation schemes. Simulation results have shown that both DFT and ZCT offer more PAPR reduction than DCT in ACO-OFDM. For PAM-DMT, DCT precoding yields significant PAPR reduction compared to conventional PAM-DMT signal. These precoding schemes also offer the advantage of zero signaling overhead.

8645-29, Session PWed

Performance comparison of beacon-enabled and non-beacon-enabled IEEE 802.15.4 MAC in WSN over fiber systems

Aldo E. Perez-Ramos, Salvador Villarreal-Reyes, Arturo Arvizu-Mondragon, Edwin Martinez-Aragon, Ctr. de Investigación Científica y de Educación Superior de Ensenada (Mexico)

Several studies have shown the feasibility of distributing IEEE 802.11 and IEEE 802.15.4 signals over long distances by using Radio-over-Fiber (RoF) links. The aim of developing such RoF systems is to provide low operational costs, enlarged network coverage, low attenuation, large bandwidth, and electrical interference immunity. These characteristics are important for the deployment of wireless sensor networks (WSN) over large coverage areas, where sharing information between two network clouds separated by several kilometers may be vital. Nevertheless, in order to achieve these aims it is not enough to guarantee the wireless signal integrity over the RoF links. For instance, the delay introduced by the RoF links could adversely affect the performance of IEEE 802.11 and IEEE 802.15.4 medium-access-control (MAC) mechanisms with the consequent drop in overall network performance.

Although the RoF links effects over the IEEE 802.11 MAC have been widely studied, to the best of our knowledge such effects have not been completely analyzed for the IEEE 802.15.4 MAC. Studying these effects is important as the CSMA-CA MAC mechanism implemented in IEEE 802.15.4 is different to that used in IEEE 802.11. Furthermore, two different MAC operation modes are considered within the IEEE 802.15.4 standard namely: beacon enabled and non-beacon enabled. This paper introduces an experimental investigation of the RoF link effects over both IEEE 802.15.4 MAC operating modes. Performance metrics in terms of data throughput are provided for both operation modes and different fiber lengths. Suggestions are provided for the effective deployment of RoF enabled IEEE 802.15.4 WSN.

**Conference 8645:
Broadband Access Communication Technologies VII**

8645-30, Session PWed

Minimalist-design, high-functionality, micro-ring resonator-based optical filter with narrow linewidth and low group delay using Looped Back Over- and Under-coupled Resonator (LOBOUR)

Bo Ye, Binghamton Univ. (United States); Benjamin B. Dingel, Nasfine Photonics, Inc. (United States); Weili Cui, Binghamton Univ. (United States)

We present a minimalist design but high functionality micro-ring resonator based optical filter with narrow linewidth and low group delay using a novel design we called LOBOUR for Looped Back Over- and Under-Coupled Resonator (LOBOUR). The characteristics of both narrow linewidth and low group delay (low chromatic dispersion) generally do not come together especially when using a single ring resonator. The Cascaded Over- and Under-Coupled Resonator (COUR) design was able to achieve this goal with two rings but introduced many fabrication difficulty issues. Here, we present an alternative design to COUR which uses only one ring resonator and without fabrication and manufacturing issues. It can achieve 50 dB extinction ratio and tens of ps performance. We also present important parameter selection mapping for LABOUR.

8645-20, Session 7

QPSK modulation for AC-power-signal-biased visible light communication system

Yu-Feng Liu, National Chiao Tung Univ. (Taiwan); Chien-Hung Yeh, Information and Communications Research Lab. (Taiwan); Chi-Wai Chow, National Chiao Tung Univ. (Taiwan); Yang Liu, Hong Kong Productivity Council (Hong Kong, China)

The long life-time, high efficiency, low-cost of LED has made it an important role in lighting. Due to the large signal power, LED lighting can provides reliable wireless communication link. To provide these LED with bias current, the AC to DC converter is often used for DC LED. In this work, we develop a AC-power-signal-biased system compatible with AC LED. The bias tee circuit is designed to combine AC-power signal and the message signal with QPSK format. This driving scheme needs no AC-to-DC converters and it is suitable for driving AC LED. The bias voltage in the proposed system dynamically changes with the AC power from the outlet. Only in part of the duration can the information-bearing signal be transmitted. Synchronization is completed to avoid threshold effect of LED. The system provides a technique for combining large AC power signal and small information signal, while power-efficiency and maintaining capability of signal transmission. The QPSK format is used, which has a spectral efficiency of 2 bit/Hz and it is a band-pass signal. The transmission data rate achieved is 120Kbps with distances of 2 m.

8645-21, Session 7

Comparison of VLC-based indoor positioning techniques

Weizhi Zhang, Mohsen Kavehrad, Ctr. for Information & Communications Technology Research (United States)

Indoor positioning systems have lots of applications in several research fields, such as location based service (LBS), indoor navigation service, robotic industry, etc. Many techniques have been proposed in this field based on Radio Frequency (RF) wave propagation, such as RFID, UWB, WLAN, Bluetooth, etc. However, these techniques have difficulties in delivering reasonable positioning accuracy due to multipath effects. On the other hand, positioning systems based on IR or Ultrasonic require a sensor network infrastructure which leads to extra cost and

deployment time. In recent years, researchers have been searching the possibility to perform accurate indoor positioning by using Visible Light Communication (VLC) technology.

Several papers have been published on this research interest and the related positioning method presented in each maps into one of the following techniques; Triangulation, Scene analysis and Proximity. Each of these methods has its inherent advantages and drawbacks.

In this paper, we will evaluate localization techniques by the following performance metrics: accuracy, space dimension and complexity. We will further discuss a couple of factors that would affect the performance of each of these positioning systems, including multipath reflections and synchronization.

Finally, future prospects of research in VLC-based indoor positioning are addressed.

8645-22, Session 7

Demonstration of using digital FIR filter and matched filter to increase data rate in visible light communication

Yu-Feng Liu, National Chiao Tung Univ. (Taiwan); Chien-Hung Yeh, Industrial Technology Research Institute (Taiwan); Chi-Wai Chow, Po-Yen Huang, National Chiao Tung Univ. (Taiwan); Yang Liu, Hong Kong Productivity Council (Hong Kong, China)

With the advancing of LED technology, the interest of using visible light to provide communication is increasing. To provide low-cost and high speed communication, the problem of bandwidth limitation of phosphor-based white-light LED is to be solved. The use of digital-filters in time-domain is demonstrated to enhance the transmission data-rate using phosphor-based white-light LED, with a 3-dB bandwidth of 1.28MHz. The previous research shows pre-distortion in time-domain is effective in equalizing the system; thus in this work, the techniques of signal processing at time-domain is further developed with the channel estimation. The digital FIR-filters are used to eliminate channel effect and maximize the system signal to noise ratio. The format used in the experiment is the 4-ASK modulation which represents 2 bit in each of the symbol and the spectrum is band-limited from DC to 10MHz. The matched filtering is achieved by calculating the zero-forcing equalizer (ZFE) and the coefficients are used in the transmitter to reduce the inter-symbol-interference (ISI) caused by channel effect. Without using optical blue-filtering, a data rate of 20 Mbps is achieved by using 4-ASK modulation. In the experiment, a single LED was used to support transmission distance of 1 m. The digital filtering provides flexibility of adaptively change equalizer in different circumstances.

8645-23, Session 7

Recent developments in high-speed optical wireless indoor communications (*Invited Paper*)

Klaus-Dieter Langer, Fraunhofer-Institut für Nachrichtentechnik Heinrich-Hertz-Institut (Germany)

No Abstract Available.

Conference 8646: Optical Metro Networks and Short-Haul Systems V

Tuesday - Thursday 5 -7 February 2013

Part of Proceedings of SPIE Vol. 8646 Optical Metro Networks and Short-Haul Systems V

8646-1, Session 1

Techniques to realize flexible optical terabit-per-second transmission systems (*Invited Paper*)

M. Nölle, Colja Schubert, Ronald Freund, Fraunhofer-Institut für Nachrichtentechnik Heinrich-Hertz-Institut (Germany)

In this paper, we review emerging technologies to build up Tb/s per channel transmission capacity. We discuss the appropriate choice of modulation formats, as well as options for generation and multiplexing of multiple lower bit rate sub-channels. Different multiplexing approaches, mainly based on various implementations of orthogonal frequency division multiplexing and Nyquist wavelength division multiplexing are introduced. Their main strengths and weaknesses are discussed by means of selected experimental demonstrations.

8646-2, Session 2

Cognition-enabling techniques in heterogeneous and flexgrid optical communication networks (*Invited Paper*)

Idelfonso Tafur Monroy, Antonio Cabellero Jambrina, Silvia Saldana Cercos, Robert Borkowski, Technical Univ. of Denmark (Denmark)

This talk will present our recent progress in the introduction of cognition-enabling techniques at the physical layer and in the control plane with the aim to fully exploit the benefits of emerging flex-grid and elastic bit rate optical networks. These activities are performed within the European project CHRON: Cognitive Heterogeneous Reconfigurable Optical Network.

8646-3, Session 2

Towards terabit optical transmission: from coherent 100Gb/s to WDM superchannels (*Invited Paper*)

Julio C. Oliveira, Edson P. da Silva, Luis H. de Carvalho, Vitor B. Ribeiro, Daniel M. Pataca, Fabio D. Simoes, CPqD (Brazil)

Recent advances in high speed optical transmission enables more than 1Tb/s per channel based on advanced modulation formats. Results on dual polarization QPSK, N-QAM and Co-OFDM optical transmission are presented and addressed in a reconfigurable optical transmitters scenario.

8646-4, Session 2

Multicast traffic grooming in flexible optical WDM networks (*Invited Paper*)

Ankitkumar N. Patel, Philip N. Ji, NEC Labs. America, Inc. (United States); Jason P. Jue, The Univ. of Texas at Dallas (United States); Ting Wang, NEC Labs. America, Inc. (United States)

In Metropolitan Area Networks (MANs), point-to-multipoint applications, such as IPTV, video-on-demand, distance learning, and content distribution, can be efficiently supported through light-tree-based multicast-communications instead of lightpath-based unicast-communications. The application of multicasting for such traffic is

justified by its inherent benefits of reduced control and management overhead, and elimination of redundant resource provisioning. Supporting such multicast traffic in Flexible optical WDM (FWDM) networks that can provision light-trees using optimum amount of spectrum within flexible channel spacing lead to higher wavelength and spectral efficiencies compared to conventional ITU-T fixed grid networks. However, in spite of such flexibility, the residual channel capacity of stranded channels may not be utilized if the network cannot offer channels with arbitrary line rates. Additionally, the spectrum allocated to guard bands used to isolate finer granularity channels remains unutilized. These limitations can be addressed by using traffic grooming in which low-rate multicast connections are aggregated and switched over high capacity light-trees. In this paper, we address the multicast traffic grooming problem in FWDM networks, and propose a novel auxiliary graph-based algorithm for the first time. The performance of multicast traffic grooming is evaluated in terms of spectral, cost, and energy efficiencies compared to lightpath-based transparent FWDM networks, lightpath-based traffic grooming-capable FWDM networks, multicast-enabled transparent FWDM networks, and multicast traffic grooming-capable fixed grid networks. Simulation results demonstrate that multicast traffic grooming in FWDM networks not only improves spectral efficiency, but also cost, and energy efficiencies compared to other multicast traffic provisioning approaches of FWDM and fixed grid networks.

8646-5, Session 3

Integrated devices for 100G and higher data rates for the next-generation optical communication systems (*Invited Paper*)

Yoshinori Hibino, NTT Electronics Corp. (Japan); Atul K. Srivastava, NEL America, Inc. (United States)

Low cost integrated components are key to the commercial success of the current 100G and future 400G transmission systems. PLC technology for hybrid integration of transmitters and receivers is attractive for the future selectable modulation format systems ranging from QPSK to 64-QAM for 100G and higher data rates. Moreover, integrated multiport switches for the flexible grid CDC ROADMs with integrated optical amplifier arrays will be critical for the dynamic networks.

This talk will focus on the novel integrated devices enabling the next generation optical networks and highlight the recent standards activity towards smaller and lower cost modules.

8646-6, Session 3

Integrated optical receivers using planar lightwave circuit technology (*Invited Paper*)

Toshikazu Hashimoto, Nippon Telegraph and Telephone Corp. (Japan)

For providing large capacity photonic transport networks, various modulation formats including polarization division multiplexing and multilevel phase shift keying have been investigated extensively. These advanced formats require an integrated receiver composed of an optical passive circuit, photodiodes and trans-impedance amplifiers.

We have been developing such optical passive circuits using planar lightwave circuit technology to achieve excellent receiver performance and realized receivers for several types of advanced format such as DQPSK and DP-QPSK. This paper will give an overview of techniques adopted to those optical circuit and the integration of receiver components focusing on an 100-Gbit/s DP-QPSK coherent receiver.

**Conference 8646:
Optical Metro Networks and Short-Haul Systems V**

8646-7, Session 3

A global standardization trend for high-speed client and line side transceivers (*Invited Paper*)

Hideki Isono, Fujitsu Optical Components (Japan)

Through the recent contents progress in information oriented society, the required information volume is expanding rapidly. Under these circumstances, high-speed and high-capacity optical communication systems are deployed in the industry. Especially high speed optical transceiver is the key device to realize high-speed system, and the practical development is accelerated in the industry. In order to develop these leading edge products timely, the establishment of the global standards is strongly demanded in the industry. Based on these backgrounds, Forum standardization bodies such as OIF/IEEE802.3 are energetically creating the standards in the industry. With regard to 40G/100G standardization activities, OIF leads telecom field and IEEE802.3 leads datacom field, and both activities become important recently. The recent topics of these two standardization bodies are reviewed and its future direction is discussed. Two organizations have completed the 1st gen 40G/100G standards, and soon after they starts creating the 2nd gen 40G/100G standards for targeting more compact size and low power consumption transceivers, mainly because the unexpected huge increase of the information volume. Key factor for the 2nd gen is the low power consumption technology such as new CMOS technology and the design improvement of the heat dissipation. Also from the mechanical point of view, the development of the new electrical interface such as 25G/50G and the brand-new hybrid integration technologies are strongly expected in the industry. New configurations using Silicon-photonics are reported by many organizations in the recent standardization meetings.

8646-21, Session 3

Optical techniques for generating and demultiplexing higher-order modulation formats (*Invited Paper*)

Alan E. Willner, The Univ. of Southern California (United States)

No Abstract Available.

8646-8, Session 4

Energy consumption and traffic scaling of dynamic optical path networks (*Invited Paper*)

Kiyo Ishii, Junya Kurumida, Shu Namiki, Toshifumi Hasama, Hiroshi Ishikawa, National Institute of Advanced Industrial Science and Technology (Japan)

Dynamic path switching in lower layers such as optical or sub-wavelength layer-1 path connections is essential for future networks to provide end-to-end, bandwidth-guaranteed, large-capacity services without energy crunch.

While this is almost generally agreed, the number of ports in optical switches tends to be limited by technological difficulties, severely restraining the scale of the network. However, video-related services, which will occupy the most traffic in future, will significantly alleviate such a limit due to the nature of video usage as it is generally provided through prior reservation in which a relatively high call blocking or long latency for a connection can be tolerated, allowing a limited number of switch ports to accommodate a relatively high number of subscribers.

This paper demonstrates that a network using optical switches with a limited number of ports, multi-granular paths, and a hierarchical network topology can be of a national scale with the number of subscribers being several tens of millions. The purpose of detailing the plausible network topology is to show that such a network offers an energy

benefit of approximately three orders of magnitude compared with that extrapolated from current router-based networks.

We then discuss some important technical aspects of such dynamic optical path networks. They include the reachability of optical signals, the suppression of EDFA transients, and the features of silicon photonics switches. Finally we will briefly introduce our research activities that are vertically integrated from application to device layers to realize the dynamic optical path network we envision here.

8646-9, Session 4

The projects of Disaster-Resistant Information Communication Network at the Research Organization of Electrical Communication, Tohoku University (*Invited Paper*)

Katsumi Iwatsuki, Tohoku Univ. (Japan)

After the East Japan Great Earthquake, Tohoku University has established Research Organization of Electrical Communication to achieve the most advanced disaster-resistant information communication network in the world. In this paper, we will introduce our projects of "Disaster-Resistant Information Communication Network" based on industry-academia-government collaboration.

8646-10, Session 4

Impact of wave propagation delay on latency in optical communication systems

Tetsuya Kawanishi, Atsushi Kanno, National Institute of Information and Communications Technology (Japan); Yuki Yoshida, Ken-ichi Kitayama, Osaka Univ. (Japan)

Latency is an important figure to describe performance of transmission systems for particular applications, such as data transfer for earthquake early warning, transaction for financial businesses, interactive services such as online games, etc. Latency consists of delay due to signal processing at nodes and transmitters, and of signal propagation delay due to propagation of electromagnetic waves. Signal processing delay can be reduced by using parallel processing based on large-scale integration CMOS technologies. However, propagation delay has an absolute limit because any electromagnetic waves should not be faster than the speed of light in vacuum c . Thus, the lower limit of the latency in transmission systems using conventional single mode fibers (SMFs) depends on wave propagation speed in the SMFs which is slower than c . Mobile backhaul connecting small cells via radio-over-fiber systems would be useful to increase the total throughput and improve the spectrum efficiency, but latency should be larger than in large cell systems because of delay in SMFs. Photonic crystal fibers, hollow fibers and large core fibers can have low effective refractive indices, and can transfer light faster than in SMFs. In free-space optical systems, signals propagate with the speed c , so that the latency could be smaller than in optical fibers. For example, LEO satellites would transmit data faster than optical submarine cables, when the transmission distance is longer than a few thousand kilometers. This paper will discuss combination of various transmission media to reduce negative impact of the latency, as well as applications of low-latency systems.

**Conference 8646:
Optical Metro Networks and Short-Haul Systems V**

8646-12, Session 5

Applications of bio-inspired computational intelligence in optical networks *(Invited Paper)*

Joaquim F. Martins Filho, Carmelo J. A. Bastos Filho, Daniel A. R. Chaves, Univ. Federal de Pernambuco (Brazil)

The computational intelligence field has experimented an amazing growth in the last years. Beyond the well known techniques, such as Genetic Algorithms (GA) and Multi-Layer Perceptron Neural Networks (MLPANN), many novel paradigms have been proposed to tackle different types of problems, such as combinatorial permutation problems in high dimensionality, multimodal optimization and multi-objective optimization with many conflicting objectives. In general, these approaches are inspired in the nature. Some examples of these novel algorithms are evolutionary strategies (ES), Differential Evolution (DE), Particle Swarm Optimization (PSO), Ant Colony Optimization (ACO), Artificial Immune Systems (AIS), Artificial Bee Colony optimization (ABC), Fish School Search (FSS), among others. These algorithms have been frequently applied to solve complex problems in many scientific areas since the mid nineties. Furthermore, many researches have proposed to tackle networking problems with bioinspired techniques. Recently, some efforts have been carried out in order to demonstrate that these techniques can be useful to tackle tough problems in optical networks, such as to solve the Routing and Wavelength Assignment (RWA) problem, to design the physical and the logical topology of these networks and to properly place some high cost devices along the network when it is necessary, such as regenerators and wavelength converters. This paper presents some examples of the use of evolutionary computation, swarm intelligence and neurocomputing to solve these optical network problems.

8646-13, Session 5

The benefits of converged packet/TDM/DWDM switching in metro aggregation networks *(Invited Paper)*

Dror Bar On, Nokia Siemens Networks US, LLC (United States); Stefan Voll, Nokia Siemens Networks (Germany); Robert Au Yang, Nokia Siemens Networks US, LLC (United States)

Next generation metro aggregation systems are expected to use integrated lambda, circuit and packet switching platforms. We analyzed a typical North American Tier 1 aggregation scenario using a converged transport platform offering OTN, MPLS-TP and lambda switching. Vertical integration (multiple transport technologies) and horizontal integration (multiple service types) yielded about one third savings over a traditional L3 over DWDM approach. The number of wavelengths needed was roughly halved. The usage of hybrid interfaces which allow to share the wavelength between OTN and MPLS services leads to additional savings which will increase as the line rate shifts from 10G to 40G and 100G

8646-15, Session 5

FMCW-based monitoring and signaling for reconfigurable optical networks

Sebastian Gaede, Marcel Jastram, Helmut-Schmidt-Univ. (Germany); Christian G. Schäffer, Helmut-Schmidt Univ. (Germany)

Future optical networks are a future proof solution for high data rate transmission and would be the last step needed for the all optical network revolution. For an efficient management of such networks health monitoring of the physical network infrastructure and the remote control of network key components like Optical Network Units (ONUs), routers and optical switches plays an important role.

Conventional optical FMCW monitoring systems are based on the

transmission of linearly chirped optical signals into the network under test. The reflection due to fiber irregularities is mixed with the transmitted signal by heterodyne photodetection resulting in a delay dependent beat spectrum representing the impulse response of the system under test.

In conventional FMCW-monitoring systems the spatial resolution is limited by the laser linewidth due to optical phase noise. A simple way to overcome this limitation is to apply phase noise cancellation by using modulation sidebands. The spatial resolution of this approach increases significantly, nevertheless it entails problems regarding multiple target ambiguity. Another possibility to enhance the spatial resolution is the variable chirp rate FMCW-technique. In this approach the change of the beating frequency with respect to the chirp frequency is evaluated leading to a new parameter to determine the reflection distance without being limited by the laser linewidth.

In this paper the above mentioned approaches to increase the spatial resolution are analyzed and their performance is experimentally evaluated. Additionally a simple signaling scheme based on optical FMCW is presented to simultaneously protect and control the network.

8646-29, Session 5

An infrastructure with a unified control plane to integrate IP into optical metro networks to provide flexible and intelligent bandwidth on demand for cloud computing

Wei Yang, Trevor J. Hall, Univ. of Ottawa (Canada)

The Internet is entering an era of cloud computing to provide more cost effective, eco-friendly and reliable services to consumer and business users. With the deployment of public and private clouds, the nature of the Internet traffic will undertake a fundamental transformation. Consequently, the current Internet will no longer suffice for serving cloud traffic in metro areas. Therefore, a more flexible, intelligent and eco-friendly networking infrastructure is in need for cloud-based resources.

In this work, an infrastructure with a unified control plane that integrates simple packet aggregation technology with optical express is proposed. In this infrastructure, while Ethernet switches with OpenFlow capability distribute or aggregate cloud traffic to or from edge metro areas, the optical express technology is adopted to provide flexible and eco-friendly bandwidth on demand to transport data flows in core metro areas. IP routers are pushed out of data paths and only exist in the control plane of the infrastructure. The connection setup or release in optical metro networks for traffic flows to or from edge metro areas is controlled by the interoperation between IP routers and electrical traffic controllers in optical metro networks. IP routers offer intelligent routing for any data flows and signaling for data flows ending at Ethernet edges and going across metro optical cores. The electrical traffic controllers in optical metro networks interoperate with IP routers to reconfigure all-optical switches to allocate or release optical express bandwidth for flow-based IP traffic. With this unified control plane, the infrastructure integrates IP into optical metro networks to provide flexible, intelligent, and eco-friendly bandwidth on demand for cloud computing.

8646-16, Session 6

Polarization studies of GRIN MMF for short haul/access networks *(Invited Paper)*

Scott S. H. Yam, Queen's Univ. (Canada)

Multimode fibre communications systems can generally be found in enterprise networks and data centres, where the span link is short and the traffic load is heavy. As the data rates in these systems scale beyond 10 Gb/s per wavelength, the effect of launch polarization on system performance becomes significant. While much attention has been devoted on the issue throughout the standardization process of the 10 Gb/s multimode fiber Ethernet (10GbE) systems, (e.g. IEEE 802.3aq 10GBASE-LRM), no comprehensive model has been presented

**Conference 8646:
Optical Metro Networks and Short-Haul Systems V**

to describe the behavior. This paper will discuss this polarization dependence and our attempts to model this physical phenomenon.

8646-17, Session 6

Application-specific specialty optical fibers: A new platform for challenging fiber designs (Invited Paper)

Bishnu P. Pal, Indian Institute of Technology Delhi (India)

In this talk we would present our extensive research on designs of a variety of application-specific optical fibers and realization of some of these. These ranged from fibers with large mode effective area dispersion slope compensating fibers for broadband compensation of DWDM signals in the S-, C-, and L-bands, design and realization of inherently gain-flattened erbium-doped fibers, air-core Bragg type of microstructured fibers characterized by huge figure of merit for dispersion compensation, and Bragg fibers for signal transmission in metro networks. We would also present our research on Bragg fiber for exotic applications. For example, solid core Bragg fibers for super-continuum light generation, Bragg-like chirped fibers for loss and dispersion control as well as generation of parabolic pulses. Due to recent interest to tap the IR wavelength region beyond 2 micrometer for optical communication and realization of guided wave optical devices, we would present our recent numerical studies on soft glass based large mode area Bragg like fibers for fiber lasers, and chalcogenide-based holey type of microstructured fibers for a variety of mid-IR applications like fiber-based light source, extremely large mode area fibers, and fiber-based super continuum light source.

8646-19, Session 7A

Advanced techniques and concepts for ultra-high-speed optical networking (Invited Paper)

Milorad Cvijetic, College of Optical Sciences, The Univ. of Arizona (United States)

Sophisticated modulation and coding schemes as well as advanced detection techniques need to be applied to increase the overall spectral efficiency in transmission of optical signals. At the same time, novel networking concepts with griddles and elastic bandwidth allocation have to be employed to increase the network flexibility. In this paper we provide an overview of modulation and coding techniques which have been or may be used in delivering multi-terabit bandwidth in high speed optical networks. Also, advanced networking technologies that enable bandwidth switching at different granularities will be described.

8646-20, Session 7A

Experimental investigation of 100-Gbps transmission over 80-km single mode fiber using discrete multi-tone modulation

Toshiki Tanaka, Masato Nishihara, Tomoo Takahara, Fujitsu Labs., Ltd. (Japan); Lei Li, Zhenning Tao, Fujitsu Research and Development Center Co., Ltd. (China); Jens C. Rasmussen, Fujitsu Labs., Ltd. (Japan)

The demands for capacity of optical communication system are exponentially increasing due to the spread of the broadband mobile communication. To meet these demands, digital coherent technologies are introduced to the core network systems. However, for business access systems, like the mobile back-haul, we also have to consider reduction of the cost and size as essential factors. Discrete multi-tone (DMT) modulation, which is employed in digital subscriber lines, is very attractive because of its high spectral efficiency with simple

configuration. Furthermore, widely used and low cost devices are needed as the elements of the transponder.

In this work, we have experimentally studied the feasibility of the DMT modulation for 100-Gbps transmission over SMF of up to 80 km.

In our experiment, the DMT modulation and demodulation processes were done by off-line processing. We used the direct modulated laser and the single-end photodiode for direct detection because of its low cost and compactness.

We experimentally evaluated the transmission performance at wavelengths in the 1300-nm and 1550-nm regions and analyzed the degradation factors. By using their countermeasures to extend transmission distance, we realized the capacity of 100 Gbps with 2WDM x 50 Gbps over 80 km. To our knowledge, this work is the highest capacity in 80-km transmission system using direct modulation and direct detection.

These results show that the DMT modulation can be used to realize high capacity transceiver with simple and cost effective configuration for the bi-directional transmission system like a passive optical network.

8646-18, Session 7B

Application of digital signal processing in high-speed visible-light communication system (Invited Paper)

Nan Chi, Yiguang Wang, Yuanquan Wang, Rongling Li, Huiliang Shang, Fudan Univ. (China)

In recent years, there has been constantly gaining interest in visible light communication motivated by the dramatic development of LED technologies. In this paper we propose and experimentally demonstrate a novel configuration of a visible light communication system based on subcarrier multiplexing and advanced modulation format. The configuration of the proposed scheme consists of multiple transmitters, multiple subcarriers and one receiver. As LED array or multiple LEDs are implemented in the room, each LED can be used as a transmitter. Multiple RF subcarriers are first modulated with data and then modulated onto the white light. Receiving the mixed signals, the user can down-convert the signals from the specific subcarrier.

Pre-equalization, post-equalization and power allocation are adopted and analyzed in this paper. We also discussed the nonlinearity and channel characteristics of white LEDs. Using this scheme, a 64QAM-OFDM modulation format can be achieved with a spectral efficiency (SE) of 5bit/s/Hz. The over-all data rate is above 400Mb/s. The BER performance can be at least 5dB improved by using digital signal processing.

8646-23, Session 8

Impact of modulator chirp in 100 Gbps class optical discrete multi-tone transmission system

Masato Nishihara, Toshiki Tanaka, Tomoo Takahara, Fujitsu Labs., Ltd. (Japan); Lei Li, Zhenning Tao, Fujitsu Research and Development Center Co., Ltd. (China); Jens C. Rasmussen, Fujitsu Labs., Ltd. (Japan)

Demand on the traffic of optical transmission system is growing continuously and 100 Gbps class system is strongly expected for both core network and short reach application. Especially, for short reach application, the high simplicity and low cost are important as well as the high capacity. Discrete multi-tone (DMT) technique is a multi-carrier modulation technique, which transmits data only by the real part and does not use the imaginary part. DMT technique is widely employed in the DSL system from its simple configuration. Recently, several works introduce DMT technique to the optical transmission to achieve the simple and cost effective system.

**Conference 8646:
Optical Metro Networks and Short-Haul Systems V**

One of the main factors that limit the transmission performance of the 1.5- μ m band DMT system is the chromatic dispersion of the transmission fiber. Interplay between the chromatic dispersion and the chirp generates the “dip” in frequency response of the modulation signal. This “dip” deteriorates the DMT signal, which multiplexes the subcarriers in frequency domain, and degrades the transmission characteristics for the distance over 20 km. This degradation is influenced by the chirp characteristic of the transmitter, which is mainly determined by the modulator configuration.

We experimentally measured and compared the chirp characteristics of various modulator configurations, which are lithium-niobate modulator, directly modulated laser, and electro-absorption modulator, by the frequency discriminator method using Mach-Zehnder interferometer. Measured alpha parameter varied from 0 to 3.5 with modulator configurations and conditions. We also measured the transmission characteristics by using above-mentioned modulators and discuss the suitable transmitter configuration for DMT technology.

8646-24, Session 8

Nyquist-WDM transmission of 7 x 192 Gb/s PDM 16-QAM signals using high-speed DACs operating at 42 GS/s

Shogo Yamanaka, NTT Photonics Labs. (Japan); Takayuki Kobayashi, Akihideo Sano, Akihiko Matsuura, Yutaka Miyamoto, NTT Network Innovation Laboratories (Japan); Munehiko Nagatani, Hideyuki Nosaka, NTT Photonics Laboratories (Japan)

We report on wavelength-division-multiplexed (WDM) seven-channel 192-Gb/s polarization-division-multiplexed (PDM) 16-QAM transmission. The transmitter comprises high-speed digital-to-analog converters (DACs) fabricated by indium phosphide (InP) heterojunction bipolar transistor (HBT) technology, and FPGA-based multi-channel digital signal generator that enables us to perform digital signal processing at the transmitter side at a sampling rate of 42 GS/s. The transmitter generated 24 Gbaud electrical waveforms for optical 16-QAM signals. Using low-loss and low-nonlinear pure silica core fiber (PSCF), we achieved 480-km WDM transmission on 25-GHz grid, and spectral efficiency (SE) of 7.17 b/s/Hz.

8646-25, Session 8

Simulation and experimental validation of OSNR monitoring for different modulation formats using delay-line-interferometer

Wajih A. Daab, Salman Khaleghi, Mohamed R. Chitgarha, Morteza Ziyadi, Alan E. Willner, The Univ. of Southern California (United States)

We simulate and validate an OSNR monitoring technique using a delay-line-interferometer (DLI). We determine the OSNR of a data stream by measuring the output power of DLI ports. We take advantage of the fact that the coherent signal power distribution into the constructive and destructive ports is different from that for non-coherent noise power. We show the performance of the monitor for both amplitude-shift-keyed and phase-shift-keyed signals. The proposed OSNR monitor uses inexpensive optical components and low-speed electronics, including: a DLI, a narrowband optical filter, and two simple power detectors that capture the power variations according to each signal's OSNR.

8646-26, Session 9

Optical regeneration on signals beyond 100Gbps with phase-sensitive amplification (Invited Paper)

Youichi Akasaka, Fujitsu Network Communications Inc. (United States); Jeng-Yuan Yang, Inwoong Kim, Motoyoshi Sekiya, Fujitsu Laboratories of America (United States)

This is the same information above. The chair (Dr. Atul Srivastava) suggested to pur 100 words abstract in.

Capacity demand has continued to increase exponentially. For the system capacity expansion, increasing the spectral efficiency by using multi-level modulation formats may be a good candidate.

One drawback of multi-level formats is the requirement of higher signal-to-noise ratio. This requests more frequent OEO regenerations due to its shorter reach.

Optical regeneration using phase sensitive amplifier (PSA) has a possibility to prolong the reach by suppressing phase noise generated during fiber transmission.

In this paper, we will discuss performance of PSA focusing on its ultra-fast and low-noise operation, and optical regeneration.

8646-27, Session 9

Advances in pulse stabilization schemes for high-repetition rate actively mode-locked fiber lasers (Invited Paper)

Balaji Srinivasan, Anish Bekal, Indian Institute of Technology Madras (India)

Actively mode-locked fiber lasers are attractive for optical communication applications as they are compact, efficient, and require relatively low maintenance. However, the generation of stable ultra-short pulses is a significant challenge due to the inherent high dispersion of the host glass, high non-linearity owing to small waveguide cross-section, and the environmental susceptibility of the fiber laser cavity.

In this talk, we will present an analysis of the pulse stability in actively mode-locked fiber lasers through a detailed study of the pulse breaking behaviour in both positive and negative dispersion regimes. Controlled experiments carried out in a dispersion managed cavity to validate the above simulations will be elucidated. Finally, we will discuss recent results on the generation of stable pulses using a repetition rate-independent regenerative scheme.

8646-28, Session 9

**1.3- μm waveband multiple-wavelength InAs/
InGaAs quantum dot light source for wide
wavelength range of 10 Gb/s transmissions
over 8-km long holey fiber**

Yasuaki Kurata, Aoyama Gakuin Univ. (Japan); Naokatsu Yamamoto, Kouichi Akahane, Tetsuya Kawanishi, National Institute of Information and Communications Technology (Japan); Hideyuki Sotobayashi, Aoyama Gakuin Univ. (Japan); Yuki Yoshioka, Hiroshi Takai, Tokyo Denki Univ. (Japan)

Development of new optical frequency resources in the wavelength range of the T- and O-bands (Thousand-band: 1.000-1.260 μm and O-band: 1.260-1.360 μm) has been investigated extensively for ultra-broadband optical communications. Especially, we have demonstrated low-transmission loss and endlessly single-mode characteristic of a holey fiber (HF) transmission system in the ultra-broadband range between 1.0- and 1.6- μm wavelengths. On the other hands, a self-assembled quantum dot (QD) structure is one of the most promising candidates in the T- and O-bands as the broadband WDM light source. It is known that the QD structure as the nano-structured material have an interesting optical gain property based on the discrete energy state of carriers which confined in the QDs, which realize high-performance and broadband optical gain media in these wavebands.

In this paper, we develop a 1.3- μm waveband QD optical frequency comb laser (QD-CML) as the WDM light source for stable generation of multiple-wavelength peaks from the single and compact QD gain chip. We also demonstrate error-free 10 Gb/s data transmissions over the 8-km long low-loss ultra-broadband holey fiber transmission line by using a newly developed O-band multiple-wavelength InAs/InGaAs QD light source in the wavelength range of 1286-1302 nm. We expect that the developed multiple-wavelength QD light source will be applied to the attractive WDM light source for the flexible access network and the optical interconnect for the data centers.

Conference 8647: Next-Generation Optical Communication: Components, Sub-Systems, and Systems II

Tuesday - Thursday 5 -7 February 2013 • Part of Proceedings of SPIE Vol. 8647 Next-Generation Optical Communication: Components, Sub-Systems, and Systems II

8647-1, Session 1

Progress and prospects for space-division multiplexing (*Invited Paper*)

Guifang Li, Univ. of Central Florida (United States)

Transmission capacity of single-mode fibers will be exhausted in the near future due to exponential growth of the internet traffic. Space is the only degree of freedom yet to be exploited to further increase transmission capacity. The simplest form of space-division multiplexing is to build parallel systems using fiber bundles. Are there benefits of using multimode fibers or multi-core fibers for space-division multiplexing. We present recent progress and future prospect for space-division multiplexing.

8647-2, Session 2

Field trial for the mixed bit rate at 100G and beyond (*Invited Paper*)

Jianjun Yu, Zhensheng Jia, Ze Dong, Hung-Chang Chien, ZTE USA (United States)

Successful joint experiments with Deutsche Telecom (DT) on long-haul transmission of 100G and beyond are demonstrated over standard single mode fiber (SSMF) and inline EDFA-only amplification. The transmission link consists of 8 nodes and 950-km installed SSMF in DT's optical infrastructure with the addition of lab SSMF for extended optical reach. The first field transmission of 8x200-Gb/s Nyquist-WDM signals is reported over 1750-km distance with 21.6-dB average loss per span. Each channel modulated by 54.2-Gbaud PDM-CSRZQPSK signal is on 50-GHz grid, achieving a net spectral efficiency (SE) of 4 bit/s/Hz. We also demonstrate mixed data rate transmission coexisting with 1T, 400G, and 100G channels. The 400G uses four independent subcarriers modulated by 28-Gbaud PDM-QPSK signals, yielding the net SE of 4 bit/s/Hz while 13 optically generated subcarriers from single optical source are employed in 1T channel with 25-Gbaud PDM-QPSK modulation. The 100G signal uses real-time coherent PDMQPSK transponder with 15% overhead of soft-decision forward error correction (SD-FEC). The digital post filter and 1-bit maximum likelihood sequence estimation (MLSE) are introduced at the receiver DSP to suppress noise, linear crosstalk and filtering effects. Our results show the future 400G and 1T channels utilizing Nyquist WDM technique can transmit longhaul distance with higher SE using the same QPSK format.

8647-3, Session 3

Ultrafast optical signal processing and characterization based on fiber/integrated-waveguide technologies (*Invited Paper*)

Jose Azana, Institut National de la Recherche Scientifique (Canada)

This communication will review recent work on the development of fundamental passive all-optical signal processing devices, including ultra-fast photonic time differentiators and integrators, using fiber-optics or integrated-waveguide technologies. The focus will be on devices based on all-fiber/waveguide resonant structures, e.g. long-period gratings, Bragg gratings and micro-ring resonators. The photonic signal processors to be discussed in this talk offer operation speeds (bandwidths) easily in the terahertz range, i.e. well beyond the reach of their electronic counterparts, in very compact designs (on a chip). The developed devices are of specific interest for a wide range of

applications in next-generation ultra-broadband optical communication systems. Applications to be discussed in the talk include (sub-) picosecond optical pulse shaping, real-time intensity and phase measurement of high-speed (GHz-bandwidth) optical signals, group-delay characterization of fiber-optics components, ultra-fast photonic memory and counting devices, and improved all-optical time-domain switching (up to 640Gbps).

8647-4, Session 4

Reconfigurable optical networking functions using orbital angular momentum (*Invited Paper*)

Alan E. Willner, The Univ. of Southern California (United States)

No Abstract Available.

8647-5, Session 4

Optical vortices: an innovative approach to increase spectral efficiency by fiber mode-division multiplexing (*Invited Paper*)

Pierpaolo Boffi, Paolo Martelli, Alberto Gatto, Mario Martinelli, Politecnico di Milano (Italy)

We will show the capabilities of optical modes known as circular vortices in order to perform mode-division multiplexing (MDM) propagation in fiber.

The optical circular vortices are characterized by a definite value of spin and orbital angular momentum: they are circularly polarized and, in case of non-null topological charge, they possess helical phase fronts with a singularity on the fiber axis, where the intensity vanishes. They form an orthogonal set of fiber-optic modes and remain orthogonal during propagation until the fiber maintains its cylindrical symmetry. The possible modal cross-talk originated owing to external perturbations can be strongly limited by choosing a suitable set of multiplexed vortices characterized by a sufficiently high "distance" in terms of propagation constant. Therefore, they can be exploited as a robust basis for MDM communications, in addition to the well-established techniques of multiplexing such as WDM and PDM.

Moreover, we will show how optical vortices can be spatially multiplexed and demultiplexed in an all-optical way by means of an interferometric technique.

Hence, we propose circular vortices not only as an alternative way to increase the fiber capacity by means of MDM, but also as a cost-effective and "green" approach able to reduce power dissipation in high spectral efficient systems with respect to solutions based on coherent detection and computationally complex digital MIMO processing, employed in MDM with usual LP modes.

8647-6, Session 4

Performance analysis of spectrally efficient free-space data link using spatially multiplexed orbital angular momentum beams

Hao Huang, Yongxiong Ren, Yan Yan, Yang Yue, Nisar Ahmed, Amanda Bozovich, The Univ. of Southern California (United States); Samuel J. Dolinar Jr., Jet Propulsion Lab. (United States); Alan E. Willner, The Univ. of Southern California (United States)

An orbital angular momentum (OAM) beam can be described as a light beam whose electrical field contains a spiral phase term $\exp(il\theta)$, where l is the OAM beam charge indicating the number of 2π -phase changes along the angular direction in a circle of the transverse plane [1]. Generally, OAM beams with different charges are orthogonal to each other, so that multiplexing/demultiplexing of OAM beams, while each one is considered as an independent channel, can be used to achieve high spectral efficiency and capacity in a communication system. In this paper, we present the measurement results of a spectrally efficient 2.56Tb/s free-space data link using OAM beams [2]. This link includes 32 independent data streams, each one encode a 20-Gaud/s 16-quadrature-amplitude-modulation signal on a different OAM beam. Consequently, those beams are mode-, polarization-multiplexed as one collinear beam, and further spatially multiplexed as two concentric rings due to the property of ring-shaped intensity profile of OAM beams. We measured the bit-error-rate (BER) curves of all 32 channels, all of which can achieve a BER of $<2 \times 10^{-3}$. The performance degradation due to the spatial multiplexing using concentric ring scheme is analyzed. The crosstalk between the inner ring and outer ring is <-30 dB, which results in an OSNR penalty of <0.5 dB. In addition, the effect of the pre-filtering is investigated, and negligible penalty is observed from the experimental result.

- [1]. A. M. Yao, et al, Adv. Opt. Photon. 3, 161 (2011).
- [2]. J. Wang et al, Nature Photon. 6, 488 (2012).

8647-7, Session 4

Orbital Angular Momentum (OAM) in fibers for scalable optical networks (Invited Paper)

Siddharth Ramachandran, The Boston Univ. Photonics Ctr. (United States)

In the last decade, perhaps the most extensively studied complex beam-shape of light is the class of vortex beams, which possess phase or polarization singularities. These beams have several potential scientific and technological applications, such as laser-based electron and particle acceleration, single-molecule spectroscopy, higher-dimensional quantum encryption, optical tweezers that can apply torques, and metal machining. A recently developed fiber that resembles an anti-guide, which closely mirrors the field profile of optical vortices, has enabled their stable generation and propagation in optical fibers, for distances up to kilometres for the first time. Since fibers are well known for their ability to offer nonlinear and dispersive tailoring of light, this opens the door to studying, and exploiting, nonlinear phenomena with such beams. This talk will discuss these intriguing possibilities enabled by fiber propagation of beams that have long been considered interesting, but hitherto unstable in nature. Specifically, we will consider their ramifications for scaling capacity of networks using orbital angular momentum as a new degree of freedom.

8647-8, Session 4

Few-mode fiber transmission with in-line few-mode erbium-doped fiber amplifier (Invited Paper)

Ezra Ip, NEC Labs. America, Inc. (United States); Ming-Jun Li, Kevin Bennett, Scott R. Bickham, Corning Inc. (United States); Yue-Kai Huang, Akihiro Tanaka, Eduardo Mateo, Junqiang Hu, Ting Wang, NEC Labs. America (United States); Andrey Korolev, Konstantin Koreshkov, Corning Inc. (United States); William Wood, Corning Inc (United States); Jesus Linares, Carlos Montero, Vincente Moreno, Xesus Prieto, Univ. of Santiago de Compostela (Spain); Yutaka Yano, Yoshiaki Aono, Tsutomu Tajima, Kiyoshi Fukuchi, NEC Corp. (Japan)

We are nearing the end of the road for capacity increase in single-mode fiber transmission. To continue sustaining Moore's Law-like growth in capacity, space-division multiplexing (SDM) is required. Solutions for SDM transmission include using parallel strands of single-mode fiber, multicore fibers, multimode fibers, and a combination therefore. Each of these solutions have different cost and complexity scaling, and their relative merits still being hotly debated. Multimode fibers have the advantage of achieving the highest capacity per unit area, due to the parallel channels being collocated. Multimode fiber amplifiers can also have improved efficiency per bit compared with parallel single-mode amplifiers. For multimode transmission to be practical, at least two major challenges need to be overcome: modal gain control and receiver complexity. In a few-mode fiber, higher-order modes typically have higher attenuation and coupling losses, so a functional amplifier will need to preferentially amplify higher order modes. In this talk, we will discuss modal gain control strategies via a combination of doping profile control and multimode pump control. The second challenge is that the propagating modes in a few-mode fiber are expected to mix freely due to splices, connectors and free-spacing coupling. MIMO detection technique is expected to be a requirement at the receiver. For weakly coupling fiber, complexity is reduced by minimizing the difference in propagation velocities of the propagating modes. We will demonstrate experimental results for few-mode fiber transmission with a gain-equalized inline few-mode fiber amplifier.

8647-9, Session 5

Few-mode fiber for optical MIMO transmission with low-computational complexity (Invited Paper)

Taiji Sakamoto, Takayoshi Mori, Takashi Yamamoto, Fumihiko Yamamoto, Nippon Telegraph and Telephone Corp. (Japan)

Internet traffic has been increasing rapidly and we must greatly increase the transmission capacity to accommodate a huge amount of traffic in the near future. To deal with this capacity crunch, newly proposed multiplexing technologies such as a multiple-input multiple-output (MIMO) system using few-mode fiber (FMF) are being intensively investigated.

Although a MIMO system requires no mode multiplexer or demultiplexer to completely combine or separate the modes, the computation needed to recover the signals at the receiver becomes more complex as the differential mode delay (DMD) between the propagation modes increases. Thus, it is desirable to reduce the DMD before the signals are received, and low DMD fiber and DMD compensated fiber line have been proposed to reduce the MIMO processing complexity.

In this paper, we introduce our recent results on mode-division multiplexing transmission with MIMO processing. We have been developing FMFs to reduce the MIMO processing complexity and proposed multi-step index fibers to control the DMD of the fibers and to compensate for the total DMD. We conducted 2x2 WDM-MIMO transmission experiments and showed our technique can reduce

Conference 8647: Next-Generation Optical Communication: Components, Sub-Systems, and Systems II

the MIMO processing complexity to less than 1/80 compared to that without DMD compensation. We also investigated reduced-complexity MIMO (RC-MIMO) processing for a transmission system without DMD compensation, which can reduce the computational complexity even when using FMF with a high DMD. We experimentally verified that computational complexity is independent of the DMD value of the fiber by using RC-MIMO processing.

8647-10, Session 5

Measuring differential group delay and distributed scattering in few mode fibers for mode division multiplexing (*Invited Paper*)

Jeffrey W. Nicholson, OFS Labs. (United States); Lars Grüner-Nielsen, K. Jerspersen, OFS (Denmark); Yi Sun, OFS Fitel LLC (United States); Robert L. Lingle Jr., OFS Fiel LLC (United States); Dan P. Jakobsen, Bera Palsdottir, OFS (Denmark)

Mode division multiplexed systems in few mode fibers has attracted considerable attention as a means to increase the transmission capacity of a single fiber. The optical properties of the few-mode transmission fiber are an integral part of the performance of such communications systems. The fiber should be low attenuation, low nonlinearity and have a high dispersion coefficient. In addition the fiber should support a specific number of well guided modes, have low differential group delay between the modes and have low coupling between the modes.

Because of the importance of the DGD and mode coupling, measurement techniques to characterize the fibers are important for optimizing fiber designs for few mode transmission systems. In this talk we will present results on characterizing DGD and mode coupling in long lengths of fiber using the newly developed measurement technique, S2 imaging. Fibers with both low and high DGD values, as well as different levels of distributed mode coupling will be presented.

8647-11, Session 5

Separation of LP modes using volume holographic demultiplexer with a dual-wavelength method for mode division multiplexing

Kento Kawabata, Atsushi Okamoto, Hokkaido Univ. (Japan); Satoshi Honma, University of Yamanashi (Japan); Yuta Wakayama, Hokkaido Univ. (Japan); Kunihiro Sato, Hokkai-Gakuen University (Japan); Akihisa Tomita, Hokkaido Univ. (Japan)

Mode division multiplexing (MDM) technology has been actively studied to overcome the capacity crunch caused by the rapid growth in network traffic demand. In MDM systems, a mode demultiplexer is required to separate signals modulated over spatial eigenmodes in an optical fiber. In this study, we propose a volume holographic mode demultiplexer incorporating a dual-wavelength method, which enables us to setup the receiving system in MDM easily and flexibly for a large number mode multiplexing. One feature of our method is that it can separate a number of multiplexed modes through angularly hologram multiplexing, which is performed with angular shifting of reference beams and mode field generation using a spatial light modulator. In addition, it is possible to separate multiplexed spatial modes at different wavelengths by appropriate angular difference between the two holographic writing beams for every spatial mode. The dual-wavelength method allows us to use different wavelengths for recording and readout operation of the volume holographic demultiplexer. Thereby, the proposed method can be applicable to wavelength division multiplexing systems. We demonstrated mode separation using the demultiplexer with dual-wavelength within visible region as a preliminary stage. In the experiment, three LP modes at a wavelength of 532 nm were recorded by angular

multiplexing in a photopolymer. Then, the diffraction beams were observed when irradiating these three LP modes at a wavelength of 633 nm on the recorded hologram. The results showed that the separation ratios of three LP modes reached around 90%.

8647-12, Session 6

Novel optical fibers for high-capacity transmission systems (*Invited Paper*)

Ming-Jun Li, Corning Incorporated (United States)

The rapid growth of multi-media and data rich applications has driven the bandwidth demand for long-haul fiber-optic links at unprecedented rates. Major telecommunication service providers all over the world are looking for new technologies that allow cost effective system upgrades. At the same time, growing capacity demands also imposes challenges on interconnections between super computers and data centers. While continuing improvements in conventional fiber optic technologies will increase the system capacity further in a short term, recent studies show that the transmission capacity over single-mode optical fibers is rapidly approaching its fundamental Shannon limit. To overcome this limit, new technologies using space division multiplexing are needed to provide a solution to the future capacity growth.

In this paper, we discuss novel optical fibers for increasing capacity for transmission systems. For conventional fibers, because transmission impairments such as chromatic dispersion, polarization-mode dispersion can be perfectly compensated for by digital signal processing, the only fiber parameters that can be optimized further are fiber attenuation and effective area. We will discuss system figure of merit for the two parameters and present recent results on ultra-low loss and large effective area fibers. For next generation fibers, we will focus on multicore and few mode fibers for space division multiplexing, which has the potential to increase the capacity by an order of magnitude. We will present fiber design considerations and review recent progress on multicore and few mode fibers. Finally, we will discuss major challenges in space division multiplexing applications using multicore and few mode fibers.

8647-13, Session 6

Modeling linear and nonlinear transmission in multi-mode fibers (*Invited Paper*)

Cristian Antonelli, Antonio Mecozzi, Univ. degli Studi dell'Aquila (Italy); Mark Shtaif, Tel Aviv Univ. (Israel)

We discuss the modeling of linear and nonlinear propagation in multi-mode/core optical fibers in the context of optical communications. A generalized Stokes space representation is introduced for handling multi-mode fiber propagation in the presence of mode coupling. Using this formalism, we define the modal dispersion vector and characterize its statistics. We also show that nonlinear propagation in the presence of random mode coupling is described by coupled multi-component Manakov equations, giving rise to interesting new physical phenomena.

8647-14, Session 6

Multicore fiber with one-ring structure (*Invited Paper*)

Shoichiro Matsuo, Yusuke Sasaki, I. Ishida, Katsuhiro Takenaga, Fujikura Ltd. (Japan); Kunimasa Saitoh, Masanori Koshiba, Hokkaido Univ. (Japan)

The characteristics of a multicore fiber with one-ring structure are reviewed. The one-ring structure, which has no center core, can overcome issues on the hexagonal close-pack structure that is the most popular multicore structure. The one-ring structure has flexibility

Conference 8647: Next-Generation Optical Communication: Components, Sub-Systems, and Systems II

in the number of cores and is unrelated to the core pitch limitation due to cutoff wavelength lengthening due to no center core structure. The one-ring structure is effective to suppress the worst case crosstalk that is crosstalk assuming all cores carry equal signal power. In the case of hexagonal close-pack structure, the worst case crosstalk of an inner core is 7.8 dB larger than that between two cores. The different worst crosstalk is observed depending on the number of nearest neighbor cores. The one-ring structure can limit the degradation to 3.0 dB for all cores. Fabricated 12-core fiber with the one-ring structure based on the simulation realized effective core area of 80 μm^2 and very low crosstalk less than -40 dB after 100-km propagation.

8647-15, Session 7

Optical transmission modeling by means of Volterra series (*Invited Paper*)

António L. J. Teixeira, Univ. de Aveiro (Portugal) and Nokia Siemens Networks (Portugal) and Instituto de Telecomunicacoes (Portugal); Jacklyn D. Reis, Univ. de Aveiro (Portugal) and Instituto de Telecomunicacoes (Portugal)

The increased demand for broadband in optical access networks has pushed engineers and scientists around the world to develop new solutions to better exploit the capabilities of Passive Optical Networks (PON). Most of the research works focus on how to maximize the number of users, the users' data rate and reach at minimal cost, complexity and occupied bandwidth. On that sense, coherent communication either based on Orthogonal Frequency-Division Multiple Access (OFDMA) [1] or Wavelength-Division Multiplexing (WDM) [2] is a notorious technological advance for enabling Next-Generation Optical Access Networks (NG-OAN). Particularly, the spectral efficiency is enhanced by the combination of reduced channel spacing, higher order modulation formats such as M-PSK (Phase-Shift Keying) and M-QAM (Quadrature Amplitude Modulation) and high channel count. This solution, sometimes referred as ultra-dense WDM-PON (UDWDM-PON) [3], theoretically exploits the ultimate capacity of the optical fiber, i.e. around 9 bits/s/Hz per polarization over 500 km [4].

It is expected that strong fiber nonlinearities limit the system's performance when the channel spacing is reduced to only a few Gigahertz and the channel count is increased [5]. The feeder fiber power and transmission distance are key variables to describe the nonlinear fiber's performance. Therefore, it is crucial to develop mathematical tools capable of analyzing and simulating the nonlinear propagation over the optical fiber. Split-Step Fourier is the worldwide reference for emulating the light propagation over the optical fiber. As far as the nonlinear performance is concern, perturbation approaches have been used for describing the performance for different fiber optic transmission systems [6][7][8]. Among them, Volterra theory have gained a lot of attention from the optical communication community due to its versatility in modeling the total field propagation [9], weight independently fiber nonlinearities [5] or as a nonlinear filter in the digital domain [10].

As such, in this paper we firstly discuss Volterra series toward the prediction of fiber nonlinearities in NG-OAN scenarios via numerical simulations. The main advantage of Volterra series is the use of transfer functions that take into account the interplay between linear and nonlinear effects for modulated signals. In addition, very fast numerical calculations can be achieved by optimizing the frequency samples points to be evaluated. The most relevant fiber effects, such as cross-phase modulation (XPM) and four-wave mixing (FWM), are identified and their ranges of dominance over distance and power are established. In this case, SNR estimates for SPM, XPM and FWM are calculated based on the Volterra model. Then, analytical expressions are extrapolated to find the evolution of nonlinearities and the overall system's performance.

The second part of the paper points out the directions for fiber nonlinear compensation on future Terabit aggregate PONs. After identifying the most relevant transmission impairments for various users requirements (capacity and reach), nonlinear compensation is addressed based on Volterra series nonlinear equalizers and frequency allocation schemes. As a result, the overall network performance is improved, thereby alleviating the signal-to-noise ratio requirements in the coherent transceivers around

the optical network.

References

- [1] N. Cvijetic, "OFDM for Next Generation Optical Access Networks," *Journal of Lightwave Technology*, vol. 30, no. 4, pp. 384-398, 2012.
- [2] H. Rohde, S. Smolorz, J. S. Wey, and E. Gottwald, "Coherent Optical Access Networks," in *Optical Fiber Communication Conference (OFC)*, 2011, p. OTuB1.
- [3] S. Smolorz, H. Rohde, E. Gottwald, D. W. Smith, and A. Poustie, "Demonstration of a coherent UDWDM-PON with real-time processing," in *Optical Fiber Communication Conference (OFC)*, 2011, p. PDPD4.
- [4] R.-J. Essiambre, G. Kramer, P. J. Winzer, G. J. Foschini, and B. Goebel, "Capacity Limits of Optical Fiber Networks," *Journal of Lightwave Technology*, vol. 28, no. 4, pp. 662-701, Feb. 2010.
- [5] J. D. Reis, D. M. Neves, and A. L. Teixeira, "Analysis of Nonlinearities on Coherent Ultra-Dense WDM-PONs Using Volterra Series," *Journal of Lightwave Technology*, vol. 30, no. 2, pp. 234-241, 2012.
- [6] A. Mecozzi, C. B. Clausen, and M. Shtaif, "System impact of intra-channel nonlinear effects in highly dispersed optical pulse transmission," *IEEE Photonics Technology Letters*, vol. 12, no. 12, pp. 1633-1635, 2000.
- [7] M. Nazarathy et al., "Phased-array cancellation of nonlinear FWM in coherent OFDM dispersive multi-span links," *Optics Express*, vol. 16, no. 20, pp. 15777-15810, Sep. 2008.
- [8] P. Poggolini, A. Carena, V. Curri, G. Bosco, and F. Forghieri, "Analytical Modeling of Nonlinear Propagation in Uncompensated Optical Transmission Links," *IEEE Photonics Technology Letters*, vol. 23, no. 11, pp. 742-744, Jun. 2011.
- [9] K. V. Peddanarappagari and M. Brandt-Pearce, "Volterra series transfer function of single-mode fibers," *Journal of Lightwave Technology*, vol. 15, no. 12, pp. 2232-2241, 1997.
- [10] F. P. Guiomar, J. D. Reis, A. L. Teixeira, and A. N. Pinto, "Mitigation of intra-channel nonlinearities using a frequency-domain Volterra series equalizer," *Optics Express*, vol. 20, no. 2, pp. 1360-1369, Jan. 2012.

8647-16, Session 7

Quasi-phase-matched electro-optic modulators for high-speed signal processing

James E. Toney, SRICO Inc. (United States); Vincent Stenger, James Busch, Peter Pontius, Michael Clabough, Andrea Pollick, Sri Sriram, SRICO Inc (United States)

This paper reports on the design, fabrication and testing of quasi-phase-matched (QPM) lithium niobate electro-optic modulators optimized for the 40-60 GHz frequency range. The device used a single-drive, coplanar-waveguide (cpw) electrode structure that provided a good balance between impedance and RF loss, and a DC Vpi.L product of approximately 10 V.cm. Ferroelectric domain engineering enabled push-pull operation with a single drive, while achieving low chirp. A custom developed pulsed poling process was used to fabricate periodic domain QPM structures in lithium niobate. QPM periods were in the range of 3 mm to 4.5 mm, depending on the design frequency. The pulse method enabled precise domain definition with a minimum of overpoling. Low-loss diffused optical waveguides were fabricated by an annealed proton exchange (APE) process. By operating in both co-propagating and counter-propagating modes, the QPM devices can be used to implement dual band RF bandpass filters simultaneously covering both 10-20 GHz and 40-60 GHz frequency bands. Arrays of QPM device structures demonstrated in this work form the basis for a reconfigurable RF photonic filter. The RF photonic QPM technology enables efficient concurrent antenna remoting and filtering functionality. Applications of the technology include fiber radio for cellular access and finite impulse response filters for wideband electronic warfare receivers.

8647-17, Session 7

Filter-bank based digital sub-banding ASIC architecture for coherent optical receivers
(Invited Paper)

Moshe Nazarathy, Alex Tolmachev, Technion-Israel Institute of Technology (Israel)

Our novel approach to the ASIC signal processing architecture of coherent communication receivers consists of parallelizing the coherent optical receiver digital processing in frequency domain sub-bands rather than in time. We have conceived a method to perform the partitioning into multiple sub-band with high computational efficiency. As the photonic channel impairments grow with bandwidth squared (extremely long channel memory due to optical dispersion over long-haul fiber links), our “divide & conquer” approach, partitioning of the processing into multiple frequency-domain sub-bands, radically simplifies the real-time computational load, enabling efficient and precise post-processing in multiple parallel sub-band receivers following the filter-bank.

The resulting receiver ASICs are estimated to be a factor of up to two less complex than conventional receiver ASICs. At ultra-high transmission rates, the current power consumption of the ASICs performing the receiver signal processing becomes a major bottleneck hindering advent of high speed optical transmission and preventing an “optical Moore’s law”, hence this factor of two savings in complexity is very significant. Moreover, as the processing has been structured in multiple independent sub-bands (e.g., 15 sub-bands of ~1.7 GHz each), the performance of the multiple-parallel sub-band receivers is better than the performance of a reference full band 25 GHz conventional receiver which processes the full wide spectrum at once. In particular, as each sub-band is narrowband and relatively flat in frequency, the adaptive filters equalizing the optical channel impairments converge much more rapidly and more precisely, providing more robust dynamic operation and improved performance.?

8647-18, Session 7

Mathematical and system level HW description DSP algorithms modeling investigation in an experimental 100G optical coherent system

Vitor B Ribeiro, Flávio A. Silva, Julio C. R. F. Oliveira, Lucas V. Franz, Eduardo O. Schneider, Cleber Moretti, CpqD Foundation (Brazil); Stenio M Ranzini, CPqD (Brazil)

Today and next generation optical coherent systems rely more and more in DSP algorithms to improve capacity, spectral efficiency and fiber impairments mitigation. The amount of signal processing is remarkable, and because of that ASICs are preferable in order to comply with cost, power consumption and size, required in OIF 100G optical module standards. One important step in the ASIC development process is the validation of the DSP algorithms mathematical models in a high level language that consider HW characteristics and constrains. In this work we present, compare and evaluate in experimental data the mathematical model developed in Matlab and the SystemC model developed in C++. The DSP algorithms functionalities implemented were orthonormalization, CD equalizer, clock recovery, dynamic equalizer, frequency offset and phase estimation. The SystemC model considers clock signals, reset/enable structures, parallelization, finite fixed-point operations and structures that are closer to the ASIC HW implementation; due to these restrictions the performance is not as good as the mathematical modeling. The DSP algorithms models are evaluated in two 112 Gbit/s DP-QPSK experimental scenarios. In the first scenario the models are evaluated in back-to-back with ASE noise loading; in the second scenario the models are compared in a 226km optical fiber recirculation loop, with 80x112 Gbit/s DP-QPSK channels (8.96 Tbit/s). In the back-to-back experiment the OSNR penalty from the mathematical model to the SystemC model is only 1,5dB and in the recirculation loop the maximum reach is 2,600 km and 2,200 km for the Matlab and SystemC models respectively.

[Return to Contents](#)

8647-19, Session 7

Complexity-reduced digital nonlinear compensation for coherent optical system

Zhenning Tao, Liang Dou, Weizhen Yan, Yangyang Fan, Fujitsu Research and Development Center Co., Ltd. (China); Lei Li, Fujitsu Research and Development Center Co., Ltd. (China); Shoichiro Oda, Yuichi Akiyama, Hisao Nakashima, Takeshi Hoshida, Jens Rasmussen, Fujitsu Labs., Ltd. (Japan)

The major drawback of conventional intra-channel nonlinearity compensation algorithms, such as back-propagation, is the high computational complexity. It usually employs one compensation stage per transmission span, so that the complexity is dozens of times of that for linear compensation.

In a motivation to derive less complex nonlinear compensators, we studied the perturbation analysis of nonlinear propagation. The analysis provided a hint about how to compensate the complex linear/nonlinear distortions in multiple spans of optically amplified transmission link in a nonlinear compensator having smaller number of concatenation of frequency- and temporal- domain operations. Consequently, the required number of FFT/IFFT is dramatically reduced compared with the conventional back-propagation and the computational complexity is accordingly reduced.

In this paper, we firstly review such techniques, namely the perturbation back-propagation (PBP) and the perturbation pre-distortion, and illustrate their common physical foundation. To reduce the computational complexity even further, we propose simplified PBP that replaces the multi-tap finite impulse response filter with one-tap infinite impulse response filter. Experiments show that the performance of the simplified PBP is virtually the same as the original PBP. Next, we propose simplified pre-distortion that can significantly reduce the complexity by combining the perturbation terms that shares approximately equal coefficients. The performance of the simplified algorithm is verified in a real-time 112 Gb/s dual polarization quadrature phase shift keying experiment. The results show little performance degradation whereas the number of terms is reduced from 19732 to 41 in the simplified pre-distortion.

8647-26, Session PWed

Optically-actuated MEMS and Bragg grating-based optical switch design

Anjan K. Ghosh, Dipen Barot, Dhirubhai Ambani Institute of Information and Communication Technology (India); Sagnik Pal, University of Florida (United States)

1. Introduction

Fiber Bragg gratings can be used to fabricate a large variety of sensors [1]. In a recent paper the application of a MEMS Bragg grating sensor in measuring forces is discussed [2]. A laser beam focused on a MEMS structure can exert a force [3]. Combining these two ideas we show that MEMS Bragg grating device can measure power in a laser beam.

2. Design and Analysis

If a fiber Bragg grating with a Bragg wavelength λ_B is subjected to a longitudinal strain s and a temperature change ΔT then the relative Bragg wavelength shift is given by [1,2]

$$\Delta \lambda_B / \lambda_B = (a+z)\Delta T + (1-p)s \tag{1}$$

where a , z and p are the coefficients of thermal expansion, the thermo-optic effect, and the photo-elastic effect of the waveguide with grating, respectively.

In Ref [2], a MEMS structure with waveguide Bragg gratings was reported. This structure consisted of an isosceles triangle in which the two equal sides of the triangle were the Bragg gratings. If a force F is applied to the apex of the triangle it was shown in Ref [1] that the longitudinal strain proportional to the force is developed in the two sides of the triangle. The strain is also dependent on the dimensions of the structure.

If we assume that the material of the waveguide has a negligible amount of absorption at the wavelength λ of an external laser then we can show that the force exerted by the focused beam of that laser on the waveguide is given by [2]

$$F = AI/c \quad (2)$$

where I is the peak intensity of the laser beam, A is the area of the focused spot, R is the reflectivity of the waveguide surface and c is the velocity of light in free space. Thus, an external laser can be used to apply a force to the MEMS Bragg grating structure in Ref [2]. From this force a strain is built up in a MEMS device.

By solving the heat transport equation in the steady state we can show that if a laser beam is focused on a MEMS cantilever we can calculate the temperature increase at the center of the spot. The temperature increase is also proportional to the laser intensity and spot size. Substituting the values of dT and s resulting from the laser intensity in Eqn. (1) we notice that if we focus an external laser beam at the apex of the isosceles triangle with Bragg gratings we can produce a shift in the Bragg wavelength that is almost linearly proportional to the peak laser intensity, I . Calibrating this we can thus develop a sensor for measuring the peak power of the laser. This device can also act as an optically actuated optical switch.

3. Conclusion

Using analysis we have shown that a waveguide Bragg grating based MEMS structure can measure the peak power of a laser beam incident on it. This device can also be used for measuring the spot size of a laser beam.

4. References

- [1] R. Kashyap, Fiber Bragg Gratings (Academic Press, 1999).
- [2] K. Reck, E. Thomas and O. Hansen, "MEMS Bragg grating force sensor", Optics Express, 19, 19190-19197 (2011).
- [3] A. Ghosh and S. Pal, "A MEMS device for measuring laser power and spot-size", in Quantum Sensing and Nanophotonic Devices VI, Vol. 7222 of SPIE Proceedings (SPIE, Bellingham, WA, 2009), 72220N.

8647-20, Session 8

Performance comparison of RZ pulse formats in PDM-16QAM high rates transmissions with optical pre-filtering

Edson P. da Silva, Luis H. de Carvalho, Marcelo L. Lopes, Vitor B. Ribeiro, CpqD Foundation (Brazil); Aldário C. Bordonalli, Univ. Estadual de Campinas (Brazil); Julio C. R. F. Oliveira, CpqD Foundation (Brazil)

The spectral density of digitally modulated signals depends directly on pulse format used for transmission of information symbols. Spectral occupancy of the modulated signal can be modified according to the frequency response of the channel to facilitate the retrieval of information at the receiver. New generation of coherent optical transmission systems operating at high rates are subject to various bandwidth restrictions aspects, such as limitations of electronic components and optical filtering via ROADMs deployed on networks. As noted in technical literature, the RZ pulse formats have some advantages compared to traditional NRZ pulses in optical fiber transmissions. In particular, RZ pulses have a better performance in situations where nonlinear effects of the fiber severely impact the quality of transmission. Among other situations, this occurs in systems that employ modulation formats for high order QAM (16QAM, 64QAM, etc.). Moreover, since RZ pulses have shorter duty cycle, temporal spread of the transmitted symbols cause less performance degradation due to ISI compared with NRZ pulses. This report presents results of experiments carried out in a 226 km recirculation loop, to evaluate the performance of NRZ, RZ 67%, 50% RZ and RZ 33% pulse shapes in a transmission of DP-16QAM. As application it is proposed and experimentally demonstrated a transmission system that employ 28 GBd dual carrier DP-16QAM channels operating with a total line rate of 448 Gb/s each, utilizing RZ pulse format and carrier narrow pre-filtering (25 GHz) to increase spectral efficiency of transmission, aggregating a 400G channel in a 75GHz WDM grid.

8647-21, Session 8

All-optical amplitude regeneration for non-return-to-zero differential-phase-shift-keying signal

Bingrong Zou, Wuhan National Lab. for Optoelectronics (China); Yu Yu, Wuhan National Laboratory for Optoelectronics, Huazhong Univ of Science & Technology (China); Kaisheng Chen, Lei Xiang, Wuhan National Lab. for Optoelectronics (China); Weili Yang, Wuhan National Laboratory for Optoelectronics, Huazhong Univ of Science & Technology (China); Xinliang Zhang, Wuhan National Lab. for Optoelectronics (China)

The phase modulated format has attracted more attentions nowadays, and the relevant all-optical signal processing especially the regeneration for the phase modulated formats is quite desirable to extend the transmission distance and increase the transparency of optical networks. The accumulation of the nonlinear phase noise can be reduced by limiting the intensity fluctuations of the phase modulated signal, and thus the amplitude-only regeneration, which is usually simple and cost-effective, seems to be promising and receives many interests in the long haul transmission. In this paper, we propose and experimentally demonstrate amplitude regeneration for the non-return-to-zero differential-phase-shift-keying (NRZ-DPSK) signal at 40 Gb/s using two cascaded semiconductor optical amplifiers (SOAs) and a subsequent delay interferometer (DI). The regeneration scheme includes three stages, which are the NRZ-DPSK to return-to-zero DPSK (RZ-DPSK) format conversion achieved by the cross phase modulation effect in an SOA, the amplitude regeneration of RZ-DPSK realized by using the gain saturation effect in a second SOA and the format conversion from RZ-DPSK back to NRZ-DPSK based on the constructive interferometer with a DI. The amplitude noise can be significantly reduced while the phase information keeps unchanged. A negative power penalty of 1.2 dB can be obtained through the bit-error-rate measurements. Furthermore, the signal format can be preserved before and after the regeneration. Compared to the fiber based amplitude regenerator, the proposed structure requires a low power assumption and is promising for integration. Moreover, the amplitude regeneration for multi-channel input can be further achieved using an improved scheme.

8647-22, Session 10

High-speed in-line polarimeter with the built-in polarization reference as a sensor in fiber optic transmission systems

Vitaly Mikhailov, Bryan Rabin, Paul Westbrook, OFS Labs. (United States)

Recently we have demonstrated an in-line, high speed, low loss polarimeter based on four 45 degree tilted fiber Bragg gratings, written on high-birefringence (Hi-Bi) fiber. We also demonstrated a robust calibration procedure, without an external polarization reference.

In this paper we demonstrate the use of our polarimeter in sensing applications, related to telecom systems. We show that the polarimeter can be used to detect and locate a fiber disturbance in the fiber link up to 100 km long with accuracy of hundreds meters. This has been done by using intensity modulated auxiliary channels. The polarimeter measures polarization variation to detect the fiber movement while the analysis of the intensity pattern is exploited to pinpoint the movement location. This can be used in 100 Gb/s DP-QPSK transmission systems to locate the source of fast environmentally-caused polarization rotation, as well as preventing illegal tapping into the system. However, it also can be used as a general movement sensor.

Since our polarimeter has a built-in reference - an axis of the HiBi fiber it can also be used to measure the polarization extinction ratio. We demonstrated the ability of the in-line HiBi polarimeter to measure temperature induced polarization extinction ratio degradation of

**Conference 8647: Next-Generation Optical Communication:
Components, Sub-Systems, and Systems II**

hundreds of meters length of PM fiber. Real time extinction ratio monitoring is important to access the performance of PM fiber installed within cell phone towers.

8647-23, Session 10

Supercontinuum generation in dispersion-tailored lead-silicate fiber taper

Hongyu Hu, Wenbo Li, Shaozhen Ma, Niloy K. Dutta, Univ. of Connecticut (United States)

In this paper we theoretically study the broadband mid-IR supercontinuum generation (SCG) in a lead-silicate microstructured fiber (the glass for simulation is SF57). The total dispersion of the fiber can be tailored by changing the core diameter of the fiber so that dispersion profiles with two zero dispersion wavelengths (ZDWs) can be obtained. Numerical simulations of the SCG process in a 4 cm long SF57 fiber/ fiber taper seeded by femto-second pulses at telecommunications wavelength of 1550 nm are presented. The results show that a fiber taper features a continuous shift of the longer zero dispersion wavelength. This extends the generated continuum to longer wavelength region compared to fibers with fixed ZDWs. The phase-matching condition (PMC) is continuously modified in the fiber taper and the supercontinuum generated extends from ~1000 to ~ 5000 nm. We have also studied the coherence properties of the supercontinuum generated. Simulations are conducted by adding quantum noise into the input pulse at 1550 nm, and the complex degree of first-order coherence function and the overall spectral degree of coherence are both calculated. Although the spectral broadening is comparable, the degree of coherence is shown to vary with different pumping conditions. It decreases with higher peak power and longer duration due to the significant competition between the soliton-fission process and the noise-seeded modulational instability. By a suitable choice of the input pulse parameters, it is possible to generate perfectly coherent supercontinuum with a flat broadened spectrum extending to ~5000 nm in this fiber taper.

8647-24, Session 10

A new scheme for novel all-optical wavelength conversion with ultrabroad conversion tunability and modulation-transparency

Yongkang Gong, Nigel J. Copner, Kang Li, Jungang Huang, Juan J. Martinez, Daniel Rees-Whippey, Sara Carver, Univ. of Glamorgan (United Kingdom)

Increasing demands on global delivery of high-performance network-based applications, such as cloud computing and (ultra)high definition video-on-demand streaming, requires wavelength conversion techniques with broad conversion wavelength tuning range and high modulation format transparency. However, so far as we know, none of the existing all-optical wavelength conversion (AOWC) techniques can meet the requirements. Here we propose a novel modulation-format-transparent AOWC scheme which does not require phase matching and therefore has excellent tunability of wavelength conversion.

The new scheme is named “spoof” four wave mixing (SFWM). In the SFWM, a dynamic refractive index grating induced by the beating of the co-propagating pump and signal is able to modulate a BG to create ARPs at either side of the unperturbed BG bandgap. When a probe wave located at the wavelength of ARP is counter-propagating, it is reflected from the induced ARPS while tracking the signal data information but at the new wavelength. In contrast to the well-known FWM, where the induced dynamic refractive index grating modulates photons to create a wave at a new frequency, the SFWM is different in that the dynamic refractive index grating is generated in a nonlinear Bragg Grating (BG) to excite additional reflective peaks at either side of the original BG bandgap in reflection spectrum. This fundamental difference enable the SFWM to avoid the intrinsic shortcoming of stringent phase matching required in the conventional FWM, and allows AOWC with modulation format transparency and ultrabroad conversion range, which represents a major advantage for next generation of all-optical networks.